

TL
521
4563

1925
NASM

AERONAUTICS

ELEVENTH ANNUAL REPORT

OF THE

U.S.
NATIONAL ADVISORY COMMITTEE
FOR AERONAUTICS

1925

INCLUDING TECHNICAL REPORTS

Nos. 210 to 232



WASHINGTON
GOVERNMENT PRINTING OFFICE
1926

ADDITIONAL COPIES
OF THIS PUBLICATION MAY BE PROCURED FROM
THE SUPERINTENDENT OF DOCUMENTS
GOVERNMENT PRINTING OFFICE
WASHINGTON, D. C.
AT
\$1.00 PER COPY (paper covers)

LETTER OF SUBMITTAL

TO THE CONGRESS OF THE UNITED STATES:

In compliance with the provisions of the act of March 3, 1915, establishing the National Advisory Committee for Aeronautics, I submit herewith the eleventh annual report of the committee for the fiscal year ended June 30, 1925.

The statement of the present status of aviation, as outlined in Part V of the committee's report, should dispel the impression that America is lagging in the technical development of aircraft for military purposes. Scientific research on the fundamental problems of flight and the collection of results of research conducted in other progressive nations are official duties of the committee. Their opinion that America is at least abreast of other nations in the technical development of aircraft is commended to the Congress as the most authoritative that can be had. I agree with the committee that substantial progress in aeronautics is dependent largely upon scientific research. I believe that the work of the committee is the most fundamental activity of the Government in connection with the development of aeronautics and that its continuance is essential if America is to maintain its present advanced position in aircraft development.

The condition of the aircraft industry and the prospects for the development of commercial aviation on a sound basis have materially improved during the past year. To encourage the development of commercial aviation I wish especially to indorse the recommendation of the committee for the creation of a Bureau of Air Navigation in the Department of Commerce.

CALVIN COOLIDGE.

THE WHITE HOUSE,
December 10, 1925.

LETTER OF TRANSMITTAL

NATIONAL ADVISORY COMMITTEE FOR AERONAUTICS,
Washington, D. C., November 21, 1925.

MR. PRESIDENT:

In compliance with the provisions of the act of Congress approved March 3, 1915 (Public No. 271, 63d Cong.), I have the honor to transmit herewith the Eleventh Annual Report of the National Advisory Committee for Aeronautics for the fiscal year ended June 30, 1925.

During the past year gratifying progress has been made in improving the performance and reliability of aircraft, and the committee's program of continuous scientific research gives promise of maintaining America's advanced position among progressive nations in the technical development of aircraft for military purposes.

Public interest in aeronautics has greatly increased; and confidence in the ultimate success of commercial aviation in America on a sound basis is warranted. A beginning has been made by the letting of contracts by the Post Office Department for air transportation of the mails. In order, however, to hasten the development of commercial aviation on a broad scale, a bureau of air navigation should be created in the Department of Commerce with broad powers.

The condition of the aircraft industry has been substantially improved by the greater volume of Government orders. With sustained Government business and with the prospect of a growing commercial demand for aircraft, the condition of the aircraft industry may be regarded as no longer acute.

While these factors are encouraging and indicate progress toward a healthy development of commercial aviation on a sound basis, the committee desires to emphasize the importance of the scientific work of this committee as the most fundamental activity of the Government in connection with the development of aeronautics, from both a commercial and a military standpoint.

Respectfully submitted.

CHARLES D. WALCOTT,
Chairman.

The PRESIDENT,
The White House,
Washington, D. C.

CONTENTS

Letter of submittal.....	Page III
Letter of transmittal.....	V
Eleventh annual report.....	1
PART I. ORGANIZATION	
Functions of the committee.....	2
Organization of the committee.....	2
Meetings of the entire committee.....	3
The executive committee.....	4
Subcommittees.....	4
Committee on governmental relations.....	5
Committee on publications and intelligence.....	5
Committee on personnel, buildings, and equipment.....	5
Quarters for committee.....	5
The Langley Memorial Aeronautical Laboratory.....	6
The Office of Aeronautical Intelligence.....	6
Financial report.....	7
PART II. GENERAL ACTIVITIES	
Revision of nomenclature for aeronautics.....	8
The thirteenth Wilbur Wright memorial lecture.....	8
Consideration of aeronautical inventions.....	8
Adoption of standard atmosphere.....	9
Adoption of altimeter calibration standard.....	9
Standard method for determination of high-altitude performance.....	9
Use of nongovernmental agencies.....	10
Standardization of wind-tunnel results.....	10
Cooperation of Army and Navy.....	10
Investigations undertaken for the Army and the Navy.....	11
Special committee on design of Army semirigid airship RS-1.....	11
American Aeronautical Safety Code.....	12
PART III. REPORTS OF TECHNICAL COMMITTEES	
Report of committee on aerodynamics.....	14
Report of committee on power plants for aircraft.....	26
Report of committee on materials for aircraft.....	32
PART IV. TECHNICAL PUBLICATIONS OF THE COMMITTEE	
Summaries of technical reports.....	40
List of technical notes issued during the past year.....	46
List of technical memorandums issued during the past year.....	47
Bibliography of aeronautics.....	49
PART V. THE PRESENT STATUS OF AVIATION	
The present state of technical development.....	50
Aeronautical research in the United States.....	54
Relation of aeronautical research to national defense.....	55
The general problem of aeronautical organization.....	56
Progress in commercial aviation.....	57
The problem of the aircraft industry.....	58
The airship problem.....	58
Summary.....	58
Conclusion.....	59

TECHNICAL REPORTS

	Page
No. 210. "Inertia Factors of Ellipsoids for use in Airship Design," by L. B. Tuckerman	61
No. 211. "Water Model Tests for Semirigid Airships," by L. B. Tuckerman	69
No. 212. "Stability Equations for Airship Hulls," by A. F. Zahm	83
No. 213. "A Résumé of the Advances in Theoretical Aeronautics made by Max M. Munk," by Joseph S. Ames	89
No. 214. "Wing Spar Stress Charts and Wing Truss Proportions," by Edward P. Warner	135
No. 215. "Air Forces, Moments and Damping on Model of Fleet Airship Shenandoah," by A. F. Zahm, R. H. Smith, and F. A. Loudon	153
No. 216. "The Reduction of Airplane Flight Test Data to Standard Atmosphere Conditions," by Walter S. Diehl and E. P. Lesley	185
No. 217. "Preliminary Wing Model Tests in the Variable Density Wind Tunnel of the National Advisory Committee for Aeronautics," by Max M. Munk	203
No. 218. "Standard Atmosphere—Tables and Data," by Walter S. Diehl	219
No. 219. "Some Aspects of the Comparison of Model and Full-Scale Tests," by D. W. Taylor	247
No. 220. "Comparison of Tests on Air Propellers in Flight, With Wind Tunnel Model Tests on Similar Forms," by W. F. Durand and E. P. Lesley	271
No. 221. "Model Tests with a Systematic Series of 27 Wing Sections at Full Reynolds Number," by Max M. Munk and Elton W. Miller	301
No. 222. "Spray Penetration with a Simple Fuel Injection Nozzle," by Harold E. Miller and Edward G. Beardsley	319
No. 223. "Pressure Distribution on the C-7 Airship," by J. W. Crowley, jr., and S. J. DeFrance	327
No. 224. "An Investigation of the Coefficient of Discharge of Liquids Through Small Round Orifices," by W. F. Joachim	369
No. 225. "The Air Forces on a Model of the Sperry Messenger Airplane without Propeller," by Max M. Munk and Walter S. Diehl	379
No. 226. "Characteristics of a Boat Type Seaplane During Take-Off," by J. W. Crowley, jr., and K. M. Ronan	391
No. 227. "The Variable Density Wind Tunnel of the National Advisory Committee for Aeronautics," by Max M. Munk and Elton W. Miller	403
No. 228. "A Study of the Effect of a Diving Start on Airplane Speed," by Walter S. Diehl	421
No. 229. "Pressure Distribution over Thick Tapered Airfoils, N. A. C. A. 81, U. S. A. 27 C Modified and U. S. A. 35," by Elliott G. Reid	431
No. 230. "Description and Laboratory Tests of a Roots Type Aircraft Engine Supercharger," by Marsden Ware	449
No. 231. "Investigation of Turbulence in Wind Tunnels by a Study of the Flow About Cylinders, by H. L. Dryden and R. H. Heald	463
No. 232. "Fuels for High-Compression Engines," by Stanwood W. Sparrow	481

NATIONAL ADVISORY COMMITTEE FOR AERONAUTICS

3341 NAVY BUILDING WASHINGTON D. C.

CHARLES D. WALCOTT, Sc. D., *Chairman*,
Secretary, Smithsonian Institution, Washington, D. C.
DAVID W. TAYLOR, D. Eng., *Secretary*,
Washington, D. C.
JOSEPH S. AMES, Ph. D., *Chairman, Executive Committee*,
Director, Physical Laboratory, Johns Hopkins University, Baltimore, Md.
GEORGE K. BURGESS, Sc. D.,
Director, Bureau of Standards, Washington, D. C.
JOHN F. CURRY, Major, United States Army,
Chief, Engineering Division, Air Service, Dayton, Ohio.
WILLIAM F. DURAND, Ph. D.,
Professor of Mechanical Engineering, Stanford University, California.
EMORY S. LAND, Captain, United States Navy,
Bureau of Aeronautics, Navy Department, Washington, D. C.
CHARLES F. MARVIN, M. E.,
Chief, United States Weather Bureau, Washington, D. C.
WILLIAM A. MOFFETT, Rear Admiral, United States Navy,
Chief, Bureau of Aeronautics, Navy Department, Washington, D. C.
MASON M. PATRICK, Major General, United States Army,
Chief of Air Service, War Department, Washington, D. C.
S. W. STRATTON, Sc. D.,
President, Massachusetts Institute of Technology, Cambridge, Mass.
ORVILLE WRIGHT, B. S.,
Dayton, Ohio.

EXECUTIVE COMMITTEE

JOSEPH S. AMES, *Chairman*.
DAVID W. TAYLOR, *Secretary*.

GEORGE K. BURGESS.	MASON M. PATRICK.
JOHN F. CURRY.	S. W. STRATTON.
EMORY S. LAND.	CHARLES D. WALCOTT.
CHARLES F. MARVIN.	ORVILLE WRIGHT.
WILLIAM A. MOFFETT.	

GEORGE W. LEWIS, *Director of Aeronautical Research*.
JOHN F. VICTORY, *Assistant Secretary*.

During the past year there was no change in the membership of the committee.

The entire committee meets twice a year, the annual meeting being held in October and the semiannual meeting in April. The present report includes the activities of the committee between the annual meeting held on October 16, 1924, and that held on October 22, 1925.

The organization of the committee at the close of the past year was as follows:

Charles D. Walcott, Sc. D., chairman.

David W. Taylor, D. Eng., secretary.

Joseph S. Ames, Ph. D.

George K. Burgess, Sc. D.

Maj. John F. Curry, United States Army.

William F. Durand, Ph. D.

Capt. Emory S. Land, United States Navy.

Charles F. Marvin, M. E.

Rear Admiral William A. Moffett, United States Navy.

Maj. Gen. Mason M. Patrick, United States Army.

S. W. Stratton, Sc. D.

Orville Wright, B. S.

MEETINGS OF THE ENTIRE COMMITTEE

The semiannual meeting of the entire committee was held in Washington on April 23, 1925, and the annual meeting on October 22, 1925. At these meetings the general progress in aeronautical research was reviewed and the problems which should be experimentally attacked were discussed. Administrative reports were submitted by the secretary and by the Director of the Office of Aeronautical Intelligence. Doctor Ames, chairman of the executive committee, made complete reports of the research work being conducted by the committee at the Langley Memorial Aeronautical Laboratory.

At the semiannual meeting on April 23, it was noted that that date was the tenth anniversary of the first meeting of the committee, which had been held in the office of Secretary of War Garrison on April 23, 1915. The chairman remarked that 5 of the original 12 members—namely, Messrs. Ames, Durand, Marvin, Stratton, and Walcott—were still active members of the committee. Doctor Durand then recounted some of the proceedings of the first meeting, and how the original organization was effected.

At this meeting also General Patrick outlined the present purchasing policy of the Air Service and the relation of the Government to the industry, calling attention to the improvement in the latter respect during the past three years. Admiral Moffett addressed the committee on airships and their uses, pointing out particularly the importance of the use of mooring masts in connection with airship operation. Captain Land, of the Bureau of Aeronautics, described the general construction and operation of the aircraft carrier U. S. S. *Saratoga*, pointing out on a model of the ship the plan of arrangements for handling aircraft. He also exhibited photographs showing what the British Navy is doing in the development of aircraft carriers, and photographs of the American Navy's experimental carrier, the U. S. S. *Langley*.

The day following the semiannual meeting, on invitation of Admiral Moffett, members of the committee visited the naval air station at Lakehurst, N. J., and inspected the station and the rigid airships *Shenandoah* and *Los Angeles*.

At the annual meeting Doctor Ames, chairman of the executive committee, in addition to making a comprehensive report of the progress made in the investigation of a number of research problems, emphasized the existing lack of knowledge of the characteristics of aircraft propellers. He stated that the provision of means and the devising of methods for studying the performance and characteristics of air propellers constituted the greatest need at the present time in the field of technical development. He then outlined the plans of the committee for the construction of special propeller research equipment at its laboratory at Langley Field.

At the annual meeting the committee had as its guests Rear Admiral Mark L. Bristol, United States Navy, and Commander John H. Towers, United States Navy, former members

of the committee, who had recently returned to the United States from foreign duty. The committee's technical assistant in Europe, Mr. John Jay Ide, who happened to be in Washington at the time, was also present, and he and Admiral Bristol gave interesting accounts of aeronautical activities and developments in Europe.

At the annual meeting the committee accepted an invitation from General Patrick for the members of the committee to visit the engineering division of the Air Service at McCook Field, Dayton, Ohio, to inspect the field and become directly acquainted with the various engineering activities of the station.

The election of officers was the concluding feature of the annual meeting. The present officers of the committee were elected for another year, as follows: Chairman, Dr. Charles D. Walcott; secretary, Dr. David W. Taylor; chairman executive committee, Dr. Joseph S. Ames.

THE EXECUTIVE COMMITTEE

For carrying out the work of the advisory committee the regulations provide for the election annually of an executive committee, to consist of seven members, and to include further any member of the advisory committee not otherwise a member of the executive committee but resident in or near Washington and giving his time wholly or chiefly to the special work of the committee. The present organization of the executive committee is as follows:

Joseph S. Ames, Ph. D., chairman.
 David W. Taylor, D. Eng., secretary.
 George K. Burgess, Sc. D.
 Maj. John F. Curry, United States Army.
 Capt. Emory S. Land, United States Navy.
 Charles F. Marvin, M. E.
 Rear Admiral William A. Moffett, United States Navy.
 Maj. Gen. Mason M. Patrick, United States Army.
 S. W. Stratton, Sc. D.
 Charles D. Walcott, Sc. D.
 Orville Wright, B. S.

The executive committee, in accordance with the general instructions of the advisory committee, exercises the functions prescribed by law for the whole committee, administers the affairs of the committee, and exercises general supervision over all its activities. The executive committee holds regular monthly meetings, and special meetings when necessary.

The executive committee has organized the necessary clerical and technical staffs for handling the work of the committee proper. General responsibility for the execution of the research program in aeronautics approved by the executive committee is vested in the director of aeronautical research, Mr. George W. Lewis. In the subdivision of general duties he has immediate charge of the scientific and technical work of the committee, being directly responsible to the chairman of the executive committee, Dr. Joseph S. Ames. The assistant secretary Mr. John F. Victory, has charge of administration and personnel matters, property, and disbursements, under the direct control of the secretary of the committee, Dr. David W. Taylor.

SUBCOMMITTEES

The executive committee has organized six standing subcommittees, divided into two classes, administrative and technical, as follows:

ADMINISTRATIVE

Governmental relations.
 Publications and intelligence.
 Personnel, buildings, and equipment.

TECHNICAL

Aerodynamics.
 Power plants for aircraft.
 Materials for aircraft.

The organization and work of the technical subcommittees are covered in the reports of those committees appearing in another part of this report. A statement of the organization and functions of the administrative subcommittees follows:

COMMITTEE ON GOVERNMENTAL RELATIONS

FUNCTIONS

1. Relations of the committee with executive departments and other branches of the Government.
2. Governmental relations with civil agencies.

ORGANIZATION

Dr. Charles D. Walcott, chairman.
Dr. David W. Taylor.
John F. Victory, secretary.

COMMITTEE ON PUBLICATIONS AND INTELLIGENCE

FUNCTIONS

1. The collection, classification, and diffusion of technical knowledge on the subject of aeronautics, including the results of research and experimental work done in all parts of the world.
2. The encouragement of the study of the subject of aeronautics in institutions of learning.
3. Supervision of the Office of Aeronautical Intelligence.
4. Supervision of the committee's foreign office in Paris.
5. The collection and preparation for publication of the technical reports, technical notes, and technical memorandums of the committee.

ORGANIZATION

Dr. Joseph S. Ames, chairman.
Prof. Charles F. Marvin, vice chairman.
Miss M. M. Muller, secretary.

COMMITTEE ON PERSONNEL, BUILDINGS, AND EQUIPMENT

FUNCTIONS

1. To handle all matters relating to personnel, including the employment, promotion, discharge, and duties of all employees.
2. To consider questions referred to it and make recommendations regarding the initiation of projects concerning the erection or alteration of laboratories and offices.
3. To meet from time to time on the call of the chairman, and report its actions and recommendations to the executive committee.
4. To supervise such construction and equipment work as may be authorized by the executive committee.

ORGANIZATION

Dr. Joseph S. Ames, chairman.
Dr. David W. Taylor, vice chairman.
Prof. Charles F. Marvin.
John F. Victory, secretary.

QUARTERS FOR COMMITTEE

The headquarters of the National Advisory Committee for Aeronautics are located in the Navy Building, Seventeenth and B Streets NW., Washington, D. C., in close proximity to the Army and Navy services. The administrative office is also the headquarters of the various subcommittees and of the Office of Aeronautical Intelligence.

Field stations of the committee are the Langley Memorial Aeronautical Laboratory, at Langley Field, Hampton, Va., and the office of the technical assistant in Europe, located in Paris.

The scientific investigations authorized by the committee are not all conducted at the Langley Memorial Aeronautical Laboratory, but the facilities of other governmental laboratories and shops are utilized, as well as the laboratories connected with institutions of learning whose cooperation in the scientific study of specific problems in aeronautics has been secured.

THE LANGLEY MEMORIAL AERONAUTICAL LABORATORY

The greater part of the research work of the committee is conducted at the Langley Memorial Aeronautical Laboratory, which is located at Langley Field, Va., on a plot of ground set aside by the War Department for the use of the committee when Langley Field was originally laid out. Langley Field is one of the most important and best equipped stations of the Army Air Service, occupying about 1,650 acres and having hangar and shop facilities for the accommodation of four bombing squadrons, a service squadron, a school squadron, and an airship squadron.

In the committee's laboratory and on the flying field used in connection therewith the fundamental problems of scientific research are investigated. The laboratory is organized with five subdivisions, as follows: Power plants division, wind-tunnel division, flight test division, technical service division, and property and clerical division. The administration of the laboratory is under the immediate direction of the engineer in charge, under the general supervision of the officers of the committee.

The laboratory consists of six buildings. A research laboratory building, containing the administrative offices, the drafting room, the machine and woodworking shops, and the photographic and instrument laboratories; two aerodynamical laboratories, one containing a wind tunnel of the open type and the other a variable density wind tunnel, each unit being complete in itself; two engine dynamometer laboratories of a semipermanent type, both equipped to carry on investigations in connection with power plants for aircraft; and an airplane hangar equipped with a repair shop, dope room, and facilities for taking care of 16 or 18 airplanes.

On June 25, 1925, the committee authorized the construction of propeller research equipment large enough to investigate full-size propellers. It is expected that the propeller research equipment will be completed and in operation before the end of this fiscal year. The test chamber will be of sufficient size to accommodate the fuselage of an airplane, on which the propeller will be mounted and operated by the airplane engine. The throat of the test chamber will be 20 feet in diameter and the actual air speed will be 100 miles an hour.

Contract has been awarded for a new laboratory building known as the Service Building. Funds for the erection of this building were provided by Congress in the appropriation for 1926. The building will be located in the rear of the main research laboratory and will greatly relieve the congestion in the old building, increasing the efficiency of the organization and providing for a normal expansion for the next few years.

The research flight work was carried on with the aid of 19 airplanes, which made a total of 626 flights, approximating 245 hours' total flying time. No serious accident occurred during the year.

Recognition by the Government of the necessity of satisfying the increasing demand for new and accurate knowledge on the fundamental problems of flight has made possible the development of an efficient research organization numbering 105 employees at Langley Field at the close of the fiscal year 1925.

THE OFFICE OF AERONAUTICAL INTELLIGENCE

The Office of Aeronautical Intelligence was established in the early part of 1918 as an integral branch of the committee's activities. Its functions are the collection, classification, and diffusion of technical knowledge on the subject of aeronautics to the military and naval air services and civil agencies interested, including especially the results of research and experimental work conducted in all parts of the world. It is the officially designated Government depository for scientific and technical reports and data on aeronautics.

Promptly upon receipt, all reports are analyzed and classified, and brought to the special attention of the subcommittees having cognizance, and to the attention of other interested parties through the medium of public and confidential bulletins. Reports are duplicated where practicable, and distributed upon request. Confidential bulletins and reports are not circulated outside of governmental channels.

To efficiently handle the work of securing and exchanging reports in foreign countries, the committee maintains a technical assistant in Europe, with headquarters in Paris. It is his duty to visit personally the Government and private laboratories, centers of aeronautical information, and private individuals in England, France, Italy, Germany, and other European countries, and endeavor to secure for America not only printed matter which would in the ordinary course of events become available in this country, but more especially to secure advance information as to work in progress, and any technical data not prepared in printed form, and which would otherwise not reach this country. John Jay Ide, of New York, is the present incumbent.

The records of the office show that during the past year copies of technical reports were distributed as follows:

Committee and subcommittee members.....	1, 113
Langley Memorial Aeronautical Laboratory.....	2, 302
Paris office of the committee.....	3, 428
Army Air Service.....	2, 225
Naval Air Service, including Marine Corps.....	2, 921
Manufacturers.....	3, 997
Educational institutions.....	4, 397
Bureau of Standards.....	1, 108
Miscellaneous.....	14, 393
Total distribution.....	35, 884

The above figures include the distribution of 14,422 technical reports, 6,980 technical notes, and 8,006 technical memorandums of the National Advisory Committee for Aeronautics. Four thousand eight hundred and sixty written requests for reports were received during the year in addition to innumerable telephone and personal requests, and 18,939 reports were forwarded upon request.

FINANCIAL REPORT

The appropriation for the National Advisory Committee for Aeronautics for the fiscal year 1925, as carried in the independent offices appropriation act approved June 7, 1924, was \$457,000, under which the committee reports expenditures and obligations during the year amounting to \$437,510.62, itemized as follows:

Salaries (including engineering staff).....	\$177, 850. 89
Wages.....	92, 341. 03
Supplies and materials.....	16, 202. 08
Communication service.....	853. 07
Travel.....	10, 429. 93
Transportation of things.....	1, 122. 30
Furnishing of electricity.....	8, 013. 15
Rent.....	784. 74
Repairs and alterations.....	8, 707. 65
Special Investigations.....	33, 600. 00
Equipment.....	87, 605. 78
Expenditures.....	437, 510. 62
Unexpended balance.....	89. 38
Reserves ¹	19, 400. 00
	457, 000. 00

In addition to the above, the committee had a separate appropriation of \$13,000 for printing and binding, of which \$10,657.50 was expended.

¹ In accordance with the practice of all Government establishments, the committee this year set up a general reserve of \$10,000 for emergencies and, upon invitation of General Lord, joined the Budget Bureau's "Two Per Cent Club" which necessitated setting up \$9,400 additional.

PART II

GENERAL ACTIVITIES

REVISION OF NOMENCLATURE FOR AERONAUTICS

Since aeronautics is a progressive science, the need arises from time to time for revision of its official nomenclature. Five reports on this subject have been issued by the committee; the first in 1917, the second in 1918, the third in 1919, the fourth in 1920, and the fifth, known as Report No. 157, in 1923.

In October, 1924, a special conference on aeronautical nomenclature was organized by the committee, its membership including officially designated representatives of the Army Air Service, the Bureau of Aeronautics of the Navy Department, the Bureau of Standards, the Society of Automotive Engineers, the American Society of Mechanical Engineers, and the Aeronautical Chamber of Commerce of America. As the number of terms suggested for inclusion in the official nomenclature had greatly increased since the publication of the last report on the subject, the task of revision was much greater than ever before, and to facilitate its execution the entire nomenclature was divided into four main sections and a subcommittee appointed to study and agree upon the terms for each section. These four subcommittees were as follows: Airship terms, aerodynamic terms, power-plant terms, and airway terms.

The four sections of the nomenclature, after revision by these subcommittees, were submitted to and approved by the conference as a whole, and the entire nomenclature was officially approved by the executive committee on September 19, 1925. The new nomenclature will be published in the near future as a technical report, and will supersede all previous publications of the committee on the subject.

THE THIRTEENTH WILBUR WRIGHT MEMORIAL LECTURE

Upon invitation of the Royal Aeronautical Society, Rear Admiral D. W. Taylor, U. S. N. (retired), secretary of the National Advisory Committee for Aeronautics, prepared the Thirteenth Annual Wilbur Wright Memorial Lecture, which was delivered in London, April 30, 1925, the topic being "Some Aspects of the Comparison of Model and Full Scale Tests." This paper dealt with the general question of laws of dynamic similarity and will be published by the National Advisory Committee for Aeronautics as Technical Report No. 219.

CONSIDERATION OF AERONAUTICAL INVENTIONS

Aeronautical inventions are frequently received by the committee for consideration and advice. Such inventions are examined by the committee, the necessary further correspondence is conducted with the inventors, and the inventions that give promise of being of value are brought to the attention of the Army and Navy Air Services with suitable recommendations.

A formal agreement is in effect with the Navy Department whereby aeronautical inventions of a general character which are received by the Navy Department are referred to the National Advisory Committee for Aeronautics for consideration and proper action. In such cases, when a report is made to the Navy Department a copy is sent to the Army Air Service. In a similar manner, although without formal agreement, the committee also examines inventions referred to it by the Army Air Service, and a copy of the report on any invention which appears to be promising is sent to the Navy.

ADOPTION OF STANDARD ATMOSPHERE

In response to the need for a national standard of certain basic physical constants for use in connection with aeronautical calculations relating to pressure, temperature, and density relations in a normal or standard atmosphere, the committee on aerodynamics took up the question, and, after careful consideration and agreement between representatives of the Army Air Service, the Bureau of Aeronautics of the Navy Department, the United States Weather Bureau, and the United States Bureau of Standards, recommended the adoption of a set of values, known as the standard atmosphere.

On December 2, 1924, this standard was officially approved by the executive committee, and, on recommendation of the committee, has since been adopted for use in aeronautical calculations by the War and Navy Departments, the Weather Bureau, and the Bureau of Standards.

Tables and other reference data based on this standard have been prepared by Lieut. Walter S. Diehl, of the Bureau of Aeronautics, for laboratory use, and are being published as Technical Report No. 218 of the committee, entitled "Standard Atmosphere—Tables and Data."

ADOPTION OF ALTIMETER CALIBRATION STANDARD

On suggestion of the aeronautic instruments section of the Bureau of Standards, this committee organized a special conference on altimeter calibration standards as a subcommittee of the committee on aerodynamics, for the purpose of formulating and recommending a new national standard for the calibration of altimeters. The altitude pressure relation previously in use in this country for the calibration of altimeters was based on the assumption of a constant temperature of $+10^{\circ}$ C. at all altitudes, which differed widely from the average temperatures actually experienced and hence caused altimeter readings to deviate considerably from the true altitude in many cases. It was therefore deemed desirable that a new standard be adopted which would be more nearly in agreement with actual conditions.

The special conference on altimeter calibration standards included in its membership representatives of the engineering division of the Army Air Service, the Bureau of Aeronautics of the Navy Department, the Weather Bureau, the Bureau of Standards, the National Aeronautic Association, and this committee. A meeting of the conference was held on December 6, 1924, at which the new standard was agreed upon for recommendation to the committee on aerodynamics. This standard was approved by the executive committee on February 18, 1925, on recommendation of the committee on aerodynamics, and has since been adopted by the War and Navy Departments, the Weather Bureau, and the Bureau of Standards.

STANDARD METHOD FOR DETERMINATION OF HIGH-ALTITUDE PERFORMANCE

In response to a general feeling among the organizations in this country interested, that the methods used by the Federation Aéronautique Internationale for the determination of altitudes in comparing high-altitude performance of airplanes were not sufficiently accurate, a special conference on standard method of comparing high-altitude performance was organized as a subcommittee of the committee on aerodynamics. The membership of this special conference included representatives of the Army Air Service, the Naval Bureau of Aeronautics, the Weather Bureau, the Bureau of Standards, the National Aeronautic Association, and this committee.

A meeting of this conference was held on June 3, 1925, at which a standard method for the determination of high-altitude performance of aircraft was agreed upon for recommendation to the National Aeronautic Association, which is the official representative in this country of the Federation Aéronautique Internationale. On recommendation of the committee on aerodynamics, this standard was transmitted on June 10, 1925, to the president of the National Aeronautic Association, with a view to its presentation at the annual conference of the Federation Aéronautique Internationale.

USE OF NONGOVERNMENTAL AGENCIES

The various problems on the committee's approved research programs are as a rule assigned for study by governmental agencies. In cases where the proper study of a problem requires the use of facilities not available in any governmental establishment, or requires the talents of men outside the Government service, the committee contracts directly with the institution or individual best equipped for the study of each such problem to prepare a special report on the subject. In this way the committee has marshaled the facilities of educational institutions and the services of specialists in the scientific study of the problems of flight.

STANDARDIZATION OF WIND-TUNNEL RESULTS

For the past several years tests have been conducted in various wind tunnels in this country and abroad on series of standard models with a view to bringing about a standardization of wind-tunnel results by a comparison of the results of these tests.

Three cylinder models having a length ratio of 5:1 and four models of the U. S. A. 16 airfoil having an aspect ratio of 6:0 and lengths varying from 18 to 36 inches have been tested during the past year at the Massachusetts Institute of Technology, and tests are now under way at McCook Field. These models had previously been tested at the Langley Memorial Aeronautical Laboratory, the Washington Navy Yard, and the Bureau of Standards. The tests in all the wind tunnels on these models were conducted over as wide a range of V/L as possible and included the determination of lift, drag, and pitching moment for every 4° from -4° to $+20^\circ$.

Tests have also been conducted at the request of the Aeronautical Research Committee of Great Britain on airship and airfoil models constructed by the National Physical Laboratory. During the past year a joint report on the results of the tests in this country of the National Physical Laboratory, R. A. F., 15 airfoil model has been prepared as the result of a conference between the heads of the various laboratories at which the tests were made. This report, in accordance with a recent agreement with the Aeronautical Research Committee, will probably be published in this country in the near future. An exact copy of the National Physical Laboratory airship model is undergoing test in the variable-density wind tunnel of the committee for comparison of the results with those obtained in the wind tunnels of the atmospheric type.

COOPERATION OF ARMY AND NAVY

Through the personal contact of responsible officers of the Army and Navy serving on the three standing technical subcommittees, a knowledge of the aims, purposes, and needs of each service in the field of aeronautical research is made known to the other. The cordial relations that invariably flow from such personal contact are supplemented by the technical information service of the committee's Office of Aeronautical Intelligence, which makes available the latest technical information from all parts of the world. While a healthy rivalry exists in certain respects between the Army and Navy, there is at the same time a coordination of effort in experimental engineering and a mutual understanding that is productive of the best results.

The Army and Navy Air Services have whenever called upon aided in every practicable way in the conduct of scientific investigations by the committee. Each service has placed at the disposal of the committee airplanes and engines required by the committee for research purposes. The committee desires to record its appreciation of the cooperation given by the Army and Navy Air Services, for without this cooperation the committee could not have undertaken many of the investigations that have already made for substantial progress in aircraft development. The committee desires especially to acknowledge the many courtesies extended by the Army authorities at Langley Field, where the committee's laboratories are located, and by the naval authorities at the Hampton Roads Naval Air Station.

INVESTIGATIONS UNDERTAKEN FOR THE ARMY AND THE NAVY

As a rule research programs covering fundamental problems demanding solution are prepared by the technical subcommittees and recommended to the executive committee for approval. These programs supply the problems for investigation by the Langley Memorial Aeronautical Laboratory. When, however, the Army Air Service and the Naval Bureau of Aeronautics desire special investigations to be undertaken by the committee, such investigations, upon approval by the executive committee, are added to the current research programs.

The investigations thus undertaken by the committee during the past year for the Army and the Navy may be outlined as follows:

FOR THE AIR SERVICE OF THE ARMY

Full-scale investigation of different wings on the Sperry messenger airplane.

Investigation of the behavior of an airplane in landing and in taking off.

Investigation of pressure distribution over the wing section of a VE-7 airplane.

Investigation of pressure distribution and accelerations on a pursuit type airplane.

Investigation of performance characteristics of aeromarine variable-thickness and variable-camber wing.

Acceleration readings on the PW-9 airplane.

FOR THE BUREAU OF AERONAUTICS OF THE NAVY DEPARTMENT

Investigation and development of a solid-injection type of aeronautical engine.

Development of aircraft engine supercharger.

Distribution of loading between wings of biplanes and triplanes.

Investigation of planing angles and get-away speeds of seaplanes.

Flight tests of superchargers.

Investigation of landing speed of TS airplane.

Investigation of aerodynamic loads on the U. S. S. *Los Angeles*.

Investigation of spoiler aileron control for TS airplane.

Investigation of performance characteristics of DT and CS seaplanes.

Investigation in the variable-density wind tunnel of standard propeller sections with various camber ratios.

Investigation of performance of four propellers in flight.

Investigation of water-pressure distribution on seaplane hulls.

Investigation of autorotation.

Investigation of performance of model air propellers in a free air stream and in front of VE-7 model.

Propeller tests on SC-1 airplane.

SPECIAL COMMITTEE ON DESIGN OF ARMY SEMIRIGID AIRSHIP RS-1

At the request of the Army Air Service, the National Advisory Committee for Aeronautics appointed a special subcommittee to examine and report on the design and construction of the Army semirigid airship known as the *RS-1*. This special subcommittee was organized on February 13, 1923. The five members were:

Henry Goldmark, chairman.

W. Hovgaard.

Max M. Munk.

L. B. Tuckerman.

W. Watters Pagon, secretary.

The committee met for the first time on February 23, 1923, and held 20 subsequent meetings. Four of these meetings were held at the works of the Goodyear Tire & Rubber Co., Akron, Ohio; one at Wilbur Wright Field, Dayton, Ohio; one at Scott Field, Belleville, Ill.; one at St. Louis, Mo.; and the remainder in the office of the National Advisory Committee

for Aeronautics, Washington, D. C. At practically all the meetings representatives of the engineering division of the Army Air Service and of the contractor were present and joined in the discussion.

The committee was requested to report and pass upon the design and calculations, including the method of determining the load factors and factors of safety in the design, of the *RS-1*. The committee completed its report in June, 1925, which was accepted by the executive committee and transmitted to the Chief of the Army Air Service.

The *RS-1* is a semirigid type airship, 300 feet in length, and has a capacity of 700,000 cubic feet. The triangular keel is attached with the apex pointed up and is suspended by catenary cables which are attached to three points in the keel at 10-foot intervals. The keel is constructed of aluminum alloy columns, Phoenix type, with a maximum length of 10 feet. These columns are connected by ball and socket joints in forged Lynite housings.

The *RS-1* is the first semirigid airship to be constructed in America. Of the three years spent in bringing the *RS-1* to completion, a large percentage of the time was spent in research and experimentation, which have given data of lasting importance.

One of the most important investigations was the test of a water model representing the airship, on which an elaborate series of tests was conducted by the engineering division of the Army Air Service under the direction of Professor Hovgaard. In these tests the model represented the conditions in the actual airship very closely, a wooden keel having the same relative rigidity as a full-size metallic keel being fitted to the fabric envelope.

This is believed to be the first model test of a semirigid airship in which the effect of the keel on the deflections and stresses has been taken into account. The results of the tests furnished a valuable check on the theoretical computations made by the committee.

At the meeting of the committee at Scott Field, with the *RS-1* in a practically completed condition and inflated with helium, preliminary measurements to determine the changes in the shape of the envelope and the stresses in the keel under different service conditions were made. These measurements, although of a preliminary nature, are of interest, as they seem to confirm the theoretical computations. It is understood that an extended series of measurements will be made on the airship when completed and ready to fly.

The committee devoted much time to a review of the stresses in the *RS-1*, and also made an extended study of the strength of semirigid airships generally, which is probably more complete than any previous study undertaken. In connection with this study, individual members of the committee have made analytical investigations on different points involved, which add materially to the general knowledge on this subject. The individual contributions were added to the report in the form of appendixes, including particularly discussions of the aerodynamic load, of the design of the nose cap, of breathing stresses, and of the static longitudinal stability of semirigid airships.

AMERICAN AERONAUTICAL SAFETY CODE

The final draft of the Aeronautical Safety Code was approved by the sectional committee that is sponsored by the Bureau of Standards and the Society of Automotive Engineers (Inc.), on April 23, 1925, and was subsequently submitted to and approved by the sponsors who referred it to the American Engineering Standards Committee for final approval as a tentative American standard. The code has been prepared in printed form and may be obtained from the society.

The sectional committee is widely representative of the aeronautical interests and functions under the procedure of the American Engineering Standards Committee, the principal organizations represented on the sectional committee being the Aeronautical Chamber of Commerce, American Institute of Electrical Engineers, American Society of Mechanical Engineers, American Society for Testing Materials, American Society of Safety Engineers, Manufacturers Aircraft Association, National Aeronautic Association, National Aircraft Underwriters Association, National Advisory Committee for Aeronautics, National Safety Council, Rubber Association of America, Society of Automotive Engineers (Inc.), Underwriters' Laboratories (Inc.), United

States Bureau of Standards, United States Forest Service, United States Navy Department, United States Post Office Department, United States War Department, United States Weather Bureau.

The committee is a continuing one, subject to call by the sponsors to reconsider the code in part or as a whole whenever it may seem advisable to do so, although it is felt that such revisions should not be necessary for some time because of the care that was taken in preparing the code. It has been the objective of the committee to prepare a code that will promote general agreement and mutual understanding as to acceptable practices for safety in the construction and performance of aircraft but not to prescribe too closely the methods of design, construction, or operation. It is hoped that on this basis the code will prove to be a valuable guide to designers, constructors, and operators of both aircraft and airdromes in advancing the development of commercial aviation, and to constituted authorities in enforcing regulations that may be enacted to govern this branch of the transportation service and industries.

PART III

REPORTS OF TECHNICAL COMMITTEES

REPORT OF COMMITTEE ON AERODYNAMICS

ORGANIZATION

The committee on aerodynamics is at present composed of the following members:

Dr. Joseph S. Ames, Johns Hopkins University, chairman.
Commander H. C. Richardson, United States Navy, vice chairman.
Prof. Edward P. Warner, Massachusetts Institute of Technology, secretary.
Dr. L. J. Briggs, Bureau of Standards.
Capt. Gerald E. Brower, United States Army, engineering division, Air Service, McCook Field.
Lieut. W. S. Diehl, United States Navy.
H. N. Eaton, Bureau of Standards.
George W. Lewis, National Advisory Committee for Aeronautics (ex officio member).
Maj. Leslie MacDill, United States Army, engineering division, Air service, McCook Field.
Prof. Charles F. Marvin, Weather Bureau.
Dr. A. F. Zahm, construction department, Washington Navy Yard.

FUNCTIONS

The functions of the committee on aerodynamics are as follows:

1. To determine what problems in theoretical and experimental aerodynamics are the most important for investigation by governmental and private agencies.
2. To coordinate by counsel and suggestion the research work involved in the investigation of such problems.
3. To act as a medium for the interchange of information regarding aerodynamic investigations and developments, in progress or proposed.
4. To direct and conduct research in experimental aerodynamics in such laboratory or laboratories as may be placed either in whole or in part under its direction.
5. To meet from time to time on the call of the chairman and report its action and recommendations to the executive committee.

The committee on aerodynamics, by reason of the representation of the various organizations interested in aeronautics, is in close contact with all aerodynamical work being carried out in the United States. In this way the current work of each organization is made known to all, thus preventing duplication of effort. Also all research work is stimulated by the prompt distribution of new ideas and new results, which add greatly to the efficient conduction of aerodynamic research. The committee keeps the research workers in this country supplied with information on all European progress in aerodynamics by means of a foreign representative who is in close touch with all aeronautical activities in Europe. This direct information is supplemented by the translation and circulation of copies of the more important foreign reports and articles.

The committee on aerodynamics has direct control of the aerodynamical research conducted at Langley Field, the propeller research conducted at Stanford University under the supervision of Dr. W. F. Durand, and a number of special investigations conducted at the Bureau of

Standards. The aerodynamical investigations undertaken at the Washington Navy Yard, the engineering division of the Army Air Service at McCook Field, the Bureau of Standards, and the Massachusetts Institute of Technology are reported to the committee on aerodynamics.

LANGLEY MEMORIAL AERONAUTICAL LABORATORY

ATMOSPHERIC WIND TUNNEL RESEARCH—*Airfoils.*—Biplane and triplane lift distribution tests have been continued and the results further studied and analyzed. At low-flying speed, the air forces may be considered for all practical design purposes as equally divided among the component wings. At high-flying speed, however, and in the case of a highly maneuverable airplane the distribution of the lift follows a less simple law. This distribution depends then on the wing sections used, and even more on the geometric arrangement of the wing cellule.

The pressure distribution measurements on three thick airfoil models (N. A. C. A. 81, U. S. A. 27C mod., and U. S. A. 35) have been satisfactorily completed. The technique of testing half-span models by the use of a reflecting plane was developed in the course of these experiments. The experience gained will be of great benefit in future work. The information obtained will be valuable in both stress analysis and airfoil design.

As a further result of this research, a new thick wing section has been designed and its air forces have been measured. The results show a considerable gain in aerodynamic efficiency. Furthermore, one very undesirable property common to most tapered wings has been eliminated. Most tapered airfoils have the root section and the tip wing section parallel; occasionally the tip is washed out. This results in an airfoil with a changeable angle of zero lift along the span, and consequently, when the total lift is zero the air force on the tips is downward and that at the middle section is upward. In the new design the wing has been sufficiently washed in to bring all sections simultaneously to zero lift.

A half-span, pressure distribution model of the upper wing, aileron, and overhanging horn balance of a Fokker D-VII airplane is now awaiting test. Interest in this investigation centers around the pressures on the aileron, balance, and that portion of the wing tip which will be affected.

Model airplanes.—Models of two airplanes, one a pursuit landplane and the other a giant twin-boat seaplane, both designed by Mr. J. V. Martin, were given complete tests at the request of the select committee of inquiry into operations of the United States Air Services.

There have also been made tests with the model of a training type airplane. This investigation was one of the most interesting problems of the year. The airplane had exhibited the unusual characteristic of progressing from a normal spin into a flat one from which recovery had sometimes been impossible. Special apparatus was devised to give the model freedom in pitch while spinning in the tunnel. The tests showed that a reduction of gap, accompanied by an upward and forward shift of the center of gravity, serve to eliminate this tendency, and it is believed that under these conditions the controls would be sufficiently effective to prevent entering the flat spinning condition. On completion of the spin tests, the lift, drag, and pitching moment of the model with reduced gap were measured.

Fabric flapping.—A very important problem was an investigation relating chiefly to airship coverings. The factors which control the flapping of a rectangle of fabric supported along its edges and having only one surface exposed to tangential air flow were studied. The air speed at which flapping definitely began was observed, and the data are sufficiently indicative to show the most logical means of suppressing the phenomenon. Prevention of flapping in the covering of an airship would materially reduce the resistance to motion and increase the life of the fabric.

Rotating cylinders.—To clear up some of the questions unanswered by last year's tests, a new investigation of rotating cylinders has been conducted. The reversal of direction of the cross wind force at low-speed ratios has been explained. The air forces observed were far in excess of those of ordinary wings of similar dimensions. The tests show that the air forces on rotating cylinders can not be computed by assuming the circulation to be equal to the circulation of one cylinder's surface, as has been proposed by several authors. The shape of the cylinder ends proved of great influence on the results; end disks had a beneficial influence.

Miscellaneous.—As in the past, the tunnel has been used to calibrate and locate the aerodynamic axes of a number of instruments.

Tests of a "turbulence meter" were made and the results were used to further improve this instrument.

Technique of producing smoke and photographing filaments of the same in the air stream has been materially improved. Through the use of electrical apparatus, it is now possible to obtain these photographs with an exposure of approximately one-millionth of a second.

VARIABLE DENSITY WIND TUNNEL—Research on airfoils.—A series of airfoils has been tested in the variable density wind tunnel at a high Reynolds number. These 27 sections were derived from Doctor Munk's theory of the airfoil such that the travel of the center pressure would be small. The test results showed remarkable agreement with the theory, and in particular demonstrated clearly that the coefficient of pitching moment about a point at 25 per cent of the chord is practically a constant, which is predicted by the theory. There were several good sections in this group, which show excellent characteristics (N. A. C. A. M-4, M-6, and M-12). Further work on similar airfoils is to be done in the near future.

In connection with the research on the Army Air Service (Sperry) messenger airplane, a group of airfoils of the same sections (U. S. A. 5, U. S. A. 27, U. S. A. 35A, U. S. A. 35B, R. A. F. 15, Göttingen 387, and Clark Y) were tested at five different tank pressures from a low to a high Reynolds number. Besides obtaining results comparable with full-scale conditions on these sections, information was obtained as to the variation of the airfoil characteristics with scale or Reynolds number. In general, the minimum drag coefficient decreases as the scale is increased. The maximum lift/drag ratio increases in the same manner, though to a lesser extent. The scale effect of the maximum lift coefficient differs considerably for different airfoils, and as yet no general rule can be stated as to its true scale effect.

Tests are now in progress on a series of biplane cellules, using airfoils of the R. A. F. 15 section with several gap/chord ratios.

Tunnel wall interference tests.—In making corrections for the effect of the wind tunnel walls on data from tests, there was noticed considerable discrepancy in the slope of the lift coefficient curve plotted against angle of attack of observed values compared with the theoretical. Doctor Munk is now analyzing the theoretical corrections and tests are now in progress in the tunnel to determine the experimental corrections. These tests are made with airfoils of the same section and chord, but of various aspect ratios.

A velocity survey across the tunnel close to the walls is to be made, taking into account its influence on the induced drag.

Tests of airplane models.—The United States Army Air Service (Sperry) messenger airplane model with U. S. A. 5 wings was tested at full-scale conditions as received from the engineering division, Air Service, without a propeller. In comparing the results obtained with those of free-air tests on the airplane, the minimum drag of the model was found to be low. As is the case with most atmospheric wind-tunnel models, most of the details were omitted. These were then added, with a subsequent increase of 30 per cent in the minimum drag. In both cases the propeller was omitted. The effect of a rotating propeller is known to be considerable. In further work on this research a propeller will be installed on the model and the condition of operation will be that of zero torque.

A test of a model of the Fokker D-VII was made at a Reynolds number very close to full scale and from a computed performance, remarkable agreement with that of flight tests of the full-size airplane was found.

Miscellaneous.—A new method of support for models was developed in which stream-line wires of a large size are used, both in compression for negative loading and in tension for positive loading. A decrease in tare drag of 90 per cent on the 20-atmosphere tests was obtained.

Adjustments have been made at various times to the balance apparatus, improving its operation and reliability. The air flow has been further improved by minor changes in the walls of the experimental chamber and by covering the outer cone with painted canvas.

Because of the high humidity and operating temperatures some difficulty has been encountered with the separation of the drive-propeller laminations. This was finally overcome by the use of a special glue and by covering the blades with a monel metal sheath.

FLIGHT RESEARCH—Airships.—During the last year the information obtained as a result of the investigation of pressure distribution on the hull and tail surfaces of a nonrigid airship has been studied, analyzed, tabulated, and submitted in report form. The data thus available cover the pressures experienced at the 400 points investigated in nearly all possible maneuvers and are of great value for design purposes, being the only material of this kind that has been obtained in any great quantity on an airship in actual flight. While the results showed that the pressures and loadings resulting from maneuvers were never in excess of those used in design computations, they indicated, however, that those experienced in bumps and gusts were probably very much larger and might exceed the design factors in use at the present time.

As a continuation and an elaboration of the tests on a nonrigid type, considerable time and work has been spent on the preparation of a research program and the construction of apparatus for pressure distribution, turning trials, and acceleration tests on a rigid type, the U. S. S. *Los Angeles*. Some preliminary acceleration tests have already been carried out on this airship, in which it was attempted to measure the accelerations produced by gusts and bumps, in conjunction with strain gauge measurements conducted by the Bureau of Aeronautics. The tests were unsuccessful, however, owing to lack of proper air conditions.

Airplanes.—The air flow about an airplane in flight has received considerable attention within the last year in connection with two flight research problems—namely, angle-of-attack measurements and investigation of ground effect. The former problem, that of obtaining accurate angle-of-attack measurements in flight, is extremely important for flight-test work because of the nearly universal use of angle of attack as a basis for comparing different results. The measurement is very difficult of attainment because of the effect of the interference of the airplane itself upon any instrument used for measuring angle of attack. A survey of the air flow about the wing structure of a biplane in flight has been conducted, which showed that a small region or zone existed where the interference on an angle-of-attack vane was negligible, and consequently an instrument mounted at this place would register angle of attack with sufficient accuracy. The second problem, ground effect, is now being investigated. It is considered that the change of performance of an airplane at an altitude and close to the ground is due to the change of air flow produced by the proximity of the ground. By means of longitudinal smoke flow over the wings and transverse patterns obtained by flying through smoke curtains, together with pressure distribution measurements along a chord of the wing, a study is being made which it is felt will provide information for estimating quantitatively the ground effect.

At the request of the Army Air Service an investigation has been conducted and completed on the landing and take-off characteristics of nine airplanes, comprising all of the service types used by the Army. The material obtained shows the air speed, acceleration, control position, and ground run of each airplane when landing and taking off. It was intended primarily for use in the instruction of student pilots, to enable them to visualize the movement of the controls, the behavior of the airplane, etc., but will also be found of value in the improvement of the landing and take-off characteristics in new design, as well as useful for estimating the proper size of proposed landing fields.

Planing tests conducted for the Bureau of Aeronautics on three representative types of seaplanes—single-float, twin-float, and boat type—have been completed. The complete planing characteristics, including air speed, water speed, angle of attack, length and time of run, etc., have been measured on each type, and a comparison of these full-scale results with similar ones obtained in model-basin tests will be made with a view to improving the methods of the latter. The results obtained are also of direct value to designers of seaplanes and seaplane floats and should be of interest and value to the service pilot in obtaining the best take-off performance of each type. Laboratory tests are now in progress on the development of a method of measuring

the water-pressure distribution on a pontoon while landing, taking off, and taxiing. The maximum pressures occur as a result of the impact at landing or the impact of waves striking the hull, and the forces exist for such a short period of time that the difficulty of recording is considerable.

Because of the higher speed and greater maneuverability of present-day airplanes, the methods of load computations and loading specifications now in use are in need of revision to eliminate the possibility of failure in flight. Although considerable work has been done in the wind tunnel and in flight on pressure distribution, there is little information available on the pressures experienced during accelerated flight which is known to be applicable to modern airplanes. An investigation has been completed on two airplanes, the *VE-7* and the *TS*, in which the pressures over a rib section of the wing and tail surfaces have been measured in violent maneuvers. These pressures and loads will be used for preliminary revision of the load-computation methods now in vogue, but, as a single rib is only indicative of the loads on a complete wing, further work has been planned in which a complete investigation will be made of the pressure distribution over the wings and tail surfaces of a high-speed pursuit airplane. The apparatus and instruments for this latter research are in readiness and an airplane with special alterations to accommodate the apparatus is under construction.

Tests are now in progress on a Sperry messenger airplane equipped with six different sets of wings, the purpose of which is to determine full-scale characteristics which may be compared to the same characteristics of a model of the airplane as determined in an atmospheric and a variable density wind tunnel in order to study and if possible determine the nature and magnitude of the existing scale effect. The experiments have already indicated the necessity of a much closer duplication of the actual airplane for a model used in the variable density tunnel at high Reynolds number than for the same in the atmospheric tunnel, and has necessitated the reconstruction of the Sperry messenger model for use in the variable density tunnel. In connection with these tests a study has been made of the methods of obtaining an airplane's lift and drag characteristics in flight and a paper has been prepared and published describing the various methods, with recommendations for their use, based on the experience of the laboratory in such test work.

In order to find the variation in the wing contour of an airplane from the intended contour due to inaccuracies in construction and to the sag of the covering between the ribs of a fabric-covered wing, measurements are being made on a number of service airplanes. The information is desired principally for use in determining the accuracy necessary in model construction but will also provide data from which the comparison of the aerodynamic qualities of wings with rigid and sagging coverings may be derived.

Propellers.—The methods and apparatus for flight testing of airplane propellers developed last year have been improved upon, so that the laboratory is in position, and has been requested to do an increasing amount of this type of research. At present two propeller researches are in progress, consisting of tests of four propellers for the *VE-7* airplane and four for the *SC-1* seaplane. The former research is a continuation of last year's propeller research program, the flight tests to be compared with wind tunnel tests of similar model propellers to further establish the relation between the two, and the latter is to determine the propeller most suitable for the *SC-1* seaplane.

Performance.—Performance tests are now being conducted on DT and CS airplanes to determine the possible improvements in the performance of these airplanes equipped with Wright T-2 and T-3 engines when the use of (a) overcompression, (b) superchargers, (c) gears, or (d) combination of gears with overcompression or superchargers, is resorted to. In addition to the performance tests of complete airplanes, flight tests have been conducted on various airplane gears and apparatus which are auxiliary to the airplane. In this category were the tests of the spoiler aileron control and the aeromarine variable-camber wing. The former is a flap gear for airplanes, used to supplement the aileron control, which was designed and built by and tested for the Bureau of Aeronautics. The tests of the variable-camber wing were made at the request of the Army Air Service.

INSTRUMENT RESEARCH AND DEVELOPMENT.—The increase in flight research during the past year has made it necessary to duplicate a number of the standard instruments. Opportunity was taken, in constructing these instruments, to incorporate many improvements which were found desirable.

One of the most important pieces of instrumental equipment completed this year was the altitude chamber. In this apparatus an instrument may be subjected to the same pressures and temperatures as those experienced at altitudes, ranging from ground level to over 40,000 feet. It was developed for the purpose of studying the effect of low temperatures and pressures on our various recording instruments with a view to the elimination of errors resulting from the effect. The design of the apparatus is such that it is convenient to operate, is absolutely safe, and requires the minimum of time for making the necessary investigations.

A new type of flight-path air-speed recorder was developed and put into operation. This instrument is used for simultaneous recording of the flight-path angle and the air speed of an airplane, and is far superior to previous models in that its charts are more easily renewed, it is easily installed in various airplanes, has greater accuracy, and is more reliable in operation. The 60-capsule recording manometers under development during the past year for use on airship investigations have been completed but are now being adapted for pressure-distribution tests on the Boeing pursuit airplane. A suspension-type galvanometer has been completed by the Bureau of Standards and will be used in connection with the measurement of control forces. For use in the calibration of altitude instruments a new motor-driven micromanometer has been developed which affords greater accuracy, is more convenient, and reduces the time required for calibrations.

Of the more important instruments under development or construction those described below are typical. There is now being assembled an instrument for recording the air speed and altitude, having a mechanism arranged for many traverses of the altitude chart, resulting in a recorder combining extreme sensitivity with large range. This instrument should prove of value for very accurate determinations of the height of airplanes at high altitudes. An instrument which will prove of value in both the flight research and power plants work is a temperature-revolutions-per-minute recorder. This will combine in one instrument recording on one chart an electric-resistance type thermometer and an electric-type tachometer. For power plant use a fuel-flow recorder is being developed. This instrument will make use of the difference in pressure of a fluid passing through various sections of a Venturi, and will fill an important need in the investigation of engine characteristics during flight. For the more accurate calibration of accelerometers and turn recorders, as well as the study of means of damping for such instruments, a calibrating fixture is being developed. This apparatus will reduce the time required for making such calibrations and also allow the study of proper damping of accelerometers and turn recorders. A model is now being constructed to show the effect of a rotating cylinder in an air stream and will effectively demonstrate the principle of the Flettner rotor.

At the Bureau of Standards an electric-driven turn recorder is being developed along the lines of our standard recording instruments, a three-component galvanometer is being designed, and a very accurate thermometer of the resistance type is being constructed for use at low temperatures, such as are experienced at high altitudes.

Perhaps the most important investigation carried on during the year has been the study of pressure lag and depreciation in tubing. This work was carried on for the purpose of determining the most suitable lengths and sizes of tubing to be used with recording instruments in connection with the study of pressure distribution on aircraft. A complete investigation was made to determine the lag in pressure through long tubes and the reduction or increase in pressure at the far end of such tubes. Much data have been obtained which will allow the use of the proper size and length of tubing in connection with many of our pressure-distribution researches and insure the maximum accuracy of results. A careful study has been made of the temperature effect upon our standard pressure capsules and from this investigation methods of assembly and adjustment have been devised which almost entirely eliminate temperature effect upon these important components of our pressure-recording instruments.

All of these investigations have required special apparatus which has been designed and constructed at the Langley Memorial Aeronautical Laboratory. A Bendemann hub dynamometer which has been received from the Navy Department has been thoroughly investigated, tested, and found satisfactory for use in connection with the flight test of power plants. In connection with some of our wind-tunnel problems the instrument section has developed a method for making very accurate models of propellers. These model propellers are made entirely from metal and are an exact duplicate, except as to size, of the large propellers from which the measurements were taken. The use of these small model propellers in connection with model tests in the variable density wind tunnel will help increase the accuracy of comparison between model tests and full-scale research.

The National Advisory Committee for Aeronautics has cooperated with both the Army and Navy in supplying special recording instruments for various flight problems. At the request of the Bureau of Aeronautics the committee has supplied the Navy with accelerometers and instructed their personnel in their operation for studying the characteristics of the catapult and landing gear on the U. S. S. *Langley* and at the Naval Aircraft Factory in connection with the strength requirements for airplanes.

AERODYNAMIC THEORY

Last year's progress in fundamental aerodynamic theory has been substantiated throughout the present year. Its application to practice has been demonstrated, and further light thrown on its derivation and on its relation to other branches of technical mechanics.

All experiments made to check the important theory were successful and show very good agreement. Within the useful range of angle of attack of an airfoil, the lift and air force moment computed agree in a very satisfactory way with the values observed in experiments.

The theory was used to lay down a series of wing sections all distinguished from ordinary wing sections by a characteristic of great practical value, viz, the absence of travel of the center of pressure. Not only did the wind-tunnel tests confirm this anticipated stability of the wing section, but some of these sections (notably, M-6) also proved to be good wing sections in respects other than stability, so that the new theory has directly led to an improvement of wing section design.

Theory has been advanced in several minor respects. Several tables of important numerical values have been computed and published. Some of these tables are required for the actual application of the airship hull theory and of the wing theory, and give the numerical values of aerodynamic inertia factors. An elaborate investigation refers to pressure distribution tests and gives rules for the distribution of pressure orifices and to compute conveniently the air forces from observations. Standard conditions of the atmosphere have been established to make free flight observations comparable in all cases. Further progress has also been made to improve the interpretation of wind-tunnel experiences. The wind tunnel continues to be the main source of experimental information in aerodynamics, and new insight has been obtained on how to construct the models and how to take care of the influence of the tunnel dimensions on the result.

The variable-density wind tunnel has so far substantiated expectations and has not yet shown any indication of scale effect at tests made at full Reynolds number.

It is expected that the next year will bring further steady progress along all these lines. Furthermore, the fundamental theory will be expanded and worked out in detail to cover a larger portion of the problems and in order to forecast more aerodynamic properties. The first problem to be attacked will be the computation of the pressure distribution over a wing section, and further progress in the wind-tunnel technique is expected.

STANFORD UNIVERSITY

During the year the staff of the aerodynamic laboratory has been occupied in the preparation of four reports based on research and observation work carried on for the most part during the preceding year and noted in the report for 1924. These researches by name are as follows:

- (1) Loss of propulsive efficiency due to operation of air propellers forward of obstructions representing actual airplane structures.

(2) Tests of 13 Navy type propellers.

(3) Tests of 30 model propellers for Army Air Service, engineering division, McCook Field.

(4) Tests of five Navy type model propellers in connection with a model representing the mid-structural part of the Vought airplane and carried out in parallel with tests on the actual airplane in flight, conducted at Langley Field.

The reports of these investigations have been completed and numbers (1), (2), and (4) have been placed in the hands of the committee for examination and publication.

The laboratory is just now beginning two new researches as follows:

1. Tests on a group of metal air-propeller models with adjustable blades and representing 31 different propellers. These tests are to be carried out for the Army Air Service, engineering division, at McCook Field.

2. Tests on the Vought airplane model, as in research (4) referred to above, and in combination with three metal air-propeller models.

In addition, windmill and propeller brake tests have been carried out on a three-bladed model propeller form.

During the year some refinements and minor changes, as indicated by experience, have been made in the propeller dynamometer and instrumental equipment of the laboratory.

WASHINGTON NAVY YARD

Airfoils and wings.—Tests have been made during the past year on 31 models of airfoils and airplane wings. These models include both routine design testing and research. Among the research tests were a series of six airfoils in which the effect of various forms of cut-outs in the center of the span was investigated, the results indicating that the conventional form is probably the most satisfactory aerodynamically. Other research investigations on airfoils included five models with trailing edge flaps.

The study of modifications of standard airfoils is being further extended along the lines previously followed. The immediate purpose of this study is to improve the structural characteristics of certain thin but very efficient sections without seriously affecting their high efficiency.

Control surfaces.—Thirteen model-control surfaces have been tested during the past year. Of these models, eight were tested for design purposes, chiefly to study the effect of plan form, and the remaining models were divided between two research investigations.

A research was made to obtain data on three forms of trailing edge flaps suitable for reducing the landing speed as well as supplying lateral control. The results show that the combination is quite feasible, but that further tests are desirable to develop a better type of flap.

A research on the so-called "dead-center effect" has been partially completed. Pilots have reported the existence on certain airplanes of an angular range about the neutral position, particularly for elevators, for which there was no response to control movements. This research has been laid out to investigate the relation between control angle and controlling force for small angles for six types of controls. Data so far obtained do not indicate any unusual action, the lifting force varying linearly with control angle at and near the neutral position.

Airplane parts.—Testing on the series of fuselage models, long delayed by more urgent work, is now under way. As previously explained, this series consists of 10 models representative of Navy designs.

Comparative tests have been made on two full-scale radiators, one a conventional tubular free-air type, the other a Heinrich stream line fin type. The Heinrich type was found to compare very favorably with the conventional type.

Tests have been completed on two model flying-boat hulls which differed mainly in the fineness of the lines aft. The model with the finer lines had appreciably less resistance in both air and water.

Airplane models.—Routine tests have been made on 10 airplane models during the past year. Most of these models were tested in both land planes and sea plane arrangements and one model was tested with three wing sections. In all, 19 complete routine tests were made.

An unusually extensive investigation was made on the models of the *NB-1* in order to investigate the flat spin peculiar to this type. These tests over the full range of 360° in angle of attack with and without tail surfaces.

There has been a very pronounced tendency to extend the range covered by routine tests. It is estimated that a routine test on an airplane model at the Washington Navy Yard now requires approximately ten times the number of readings taken in a similar test five years ago. However, owing to the improvements which have been made in the testing technique, a routine test now requires considerably less time than it formerly did.

In connection with the routine testing of current airplane designs there are two features of general interest. In 1921 the Navy adopted the method of calculating a correction for all minor parts such as struts, wires, and fittings. Since that time the test data have been uniformly reliable and their use in predicting performance has been very satisfactory. The second feature is the rapidity with which test data are made available to the designer. In order to avoid the delay incident to the preparation of a formal report, a photostatic copy of all test data is forwarded to the Bureau of Aeronautics immediately upon the completion of a test, and becomes available to the designers without further delay.

Miscellaneous tests.—Tests have been made on four full-size target sleeves, two being of the conventional cone type and two of a new stream-line type.

A very extensive series of standardization tests on airfoils and cylinders has been completed on the N. A. C. A. models.

In the course of a study of vibration of tail surfaces in certain types of airplanes a series of tests which shed considerable light on the fundamental causes of vibration and flutter were made. The report on these tests should be of interest to all engineers.

Three tests have been made on the fairing of a nacelle into the upper surface of the lower wing of a biplane. These tests indicate the necessity for a generous fillet if it is desired to reduce interference to a reasonable value.

Calibration tests have been made on 12 Pitot-Venturi tubes and the characteristics of one tube were determined over a wide range of angle in pitch and yaw. A research investigation is now under way to develop a reliable tube which can be made at a low cost.

Lighter than air.—Testing on lighter-than-air models during the past year has been confined to a series of tests on the C-class airship in pitch and yaw with two types of control surfaces. Several projects are now on hand awaiting completion of more urgent work. These tests include damping coefficients on three models and resistance tests on the car of a rigid airship.

BUREAU OF STANDARDS

Wind-tunnel investigations.—The aerodynamical work of the Bureau of Standards during the past year has been carried on in part in the three wind tunnels in Washington and in part, through the courtesy of the Chemical Warfare Service, at the large compressor plant at Edgewood Arsenal. The wind tunnels at the Bureau are 3, $4\frac{1}{2}$, and 10 feet in diameter and have speed ranges of 11 to 150 miles per hour, 17 to 90 miles per hour, and 10 to 70 miles per hour, respectively. The compressor plant at Edgewood is capable of delivering 2,000 cubic feet of free air per minute at any desired pressure up to 100 lbs./in.²

Further studies of expanding nozzles have been made at Edgewood in cooperation with the Ordnance Department of the Army with a view to securing an air stream suitable for measuring the resistance of model projectiles at speeds above the speed of sound. For speeds up to approximately 1.15 times the speed of sound, expanding nozzles have been designed which give an air stream practically free from variations in static pressure at distances from the mouth of the nozzle greater than two diameters. At higher speeds, however, standing pressure waves of approximately sine-wave form are present in the jet to a distance of six diameters or more from the mouth of the nozzle.

In cooperation with the National Advisory Committee for Aeronautics, measurements have been made at Edgewood Arsenal of the pressure distribution over six airfoils ranging in camber ratio from 0.10 to 0.20 at speeds from 0.5 to 1.08 times the speed of sound. The measurements

were made in a free-air stream 2 inches in diameter, using airfoils of 1 inch chord length. An analysis of these results is now in progress.

The study of the design of fins for the stabilization of aircraft bombs has been continued in cooperation with the Ordnance Department of the Army. Tests have been extended to cover a large range of aspect ratio and the results have been analyzed in such a way that it is possible to predict from the drawing of a bomb the position of the center of pressure with a precision of about 3 per cent of the bomb length. In addition it has been possible to suggest certain modifications which lead to more economical use of material in that equal or greater stability can be secured by smaller fins. The utility of these modifications has been confirmed by dropping bombs with the modified fins and comparing their behavior with bombs having fins of the original type.

Measurements of the characteristics of one type of bomb have been carried through a range of 360° and the results utilized in certain step-by-step computations of actual bomb trajectories, which differ considerably from trajectories computed on the assumption that the bomb remains always tangent to its trajectory.

In cooperation with the National Advisory Committee for Aeronautics an investigation has been made of turbulence in wind tunnels. The measurements were made in the $4\frac{1}{2}$ -foot tunnel and consisted of measurements of the drag of cylinders in the turbulent region behind screens of fine and coarse mesh and of measurements of variations in static pressure. The results are described in detail in a technical report of the committee.

Measurements have been completed of the distribution of pressure over the surface of a square-base prism, 8 by 8 by 24 inches, with the wind normal to the axis of the prism but at various angles to the face. The measurements were carried out in the 10-foot wind tunnel at speeds up to 70 miles per hour. The distribution of pressure over a cylinder 8 inches in diameter and 60 inches long with axis normal to the wind has been measured in the same tunnel and measurements on a cylinder 12 inches in diameter are in progress. These studies are parts of an investigation of the wind pressure on structures.

A number of tests were made at the request of the Select Committee of Inquiry into Operations of the United States Air Services.

At the request of the editors of the International Critical Tables, members of the staff have collected the data for the aerodynamics section of the tables.

An investigation of the aerodynamic characteristics of airfoils at high speeds which was carried out in cooperation with the National Advisory Committee for Aeronautics has been published during the year as Technical Report No. 207 of this committee.

Aeronautic instrument investigations.—The aeronautic instruments section of the Bureau of Standards has continued its program of cooperative research and development work on aircraft instruments with the National Advisory Committee for Aeronautics, the Navy, the Army, and other Government departments and private concerns.

A number of special flight-test instruments have been constructed for the National Advisory Committee for Aeronautics. These instruments include an electric resistance-type thermometer for measuring very low air temperatures, a small highly sensitive galvanometer, and a small gyroscope for use in a turn recorder. A camera sextant has been built for the Bureau of Aeronautics for use on the Navy rigid airships. This sextant photographs on a strip of bromide paper images of the sun and of a bubble level and the reference scales. The advantage of the instrument lies in the fact that the images of the sun and bubble need not be brought to coincidence on the central line, but their distances from this line can be measured on the finished print and the necessary corrections applied. A small portable developing tank makes it possible to obtain a finished print within five minutes' time of the exposure.

Theoretical and experimental researches in connection with the improvement of aeronautic instruments have been continued. A catalogue has been prepared for the engineering division of the Army Air Service of various types of aeronautic instrument mechanisms showing diagrammatically the various parts, giving brief descriptions of the mechanisms, and discussing their performance. The analysis of the toggle arm used in many mechanisms has been extended

to air-speed indicators, as well as to altimeters. A new mechanism giving a straight scale, in contrast to the usual circular scale, has been investigated and is being used in two tachometers under construction for the Bureau of Aeronautics. The experimental investigation of the static and running friction of small instrument bearings has been continued with definite progress. A report has been prepared on the investigation of pressure elements, which was undertaken for the engineering division of the Army Air Service. An investigation of the errors of mercurial barometers is also in progress for the purpose of studying the unexplained inaccuracies in the readings of these instruments and the means for their elimination. An investigation of hysteresis in bars of various metals and its relation to the damping of the vibrations of tuning forks is in progress. The theory of the deflection of bimetallic bars has been generalized to include bimetallic plates.

Programs and material for discussion have been prepared for two conferences of representatives of the National Advisory Committee for Aeronautics, the Bureau of Standards, the Army Air Service, the Naval Bureau of Aeronautics, the Weather Bureau, and the National Aeronautic Association, conducted under the auspices of the National Advisory Committee for Aeronautics. The first of these conferences approved and secured the official adoption for use in the United States of a new altimeter calibration standard based on the Toussaint standard atmosphere. The new standard, which constitutes a distinct improvement in the calibration of altimeters, represents quite accurately yearly average atmospheric conditions both in the United States and in Europe, in contrast to the old standard which assumed an isothermal air column whose temperature was $+10^{\circ}$ C. The second conference, made up of representatives of the same organizations as the first, adopted resolutions regarding the determination of altitudes which have been forwarded as United States recommendations to the Federation Aeronautique Internationale with a view to improving the accuracy of the methods now in use for establishing altitudes attained in the attempt to establish new altitude records.

During the past year two publications, National Advisory Committee Technical Reports No. 198, "Astronomical Methods in Aerial Navigation," and No. 206, "Nonmetallic Diaphragms for Instruments," were published.

MASSACHUSETTS INSTITUTE OF TECHNOLOGY

Wind tunnels and instrumental equipment.—The efforts of the wind-tunnel staff during the year have been concentrated on the installation and test of the propeller dynamometer and auxiliary apparatus in the $7\frac{1}{2}$ -foot wind tunnel. The installation of the dynamometer was completed early in the year, and after some calibration it was put into use for regular propeller testing. Propellers have been run up to a tip speed of over 400 feet per second, with continuous measurement of thrust and torque.

The dynamometer was planned for the particular purpose of testing propellers and models in the presence each of the other and measuring the interferences between them, and is so designed as to permit the making of such interference tests at any angle of attack. The model under test is supported on wires, and the three forces and three moments acting are all read simultaneously by six identical automatic balances from which the wires depend. Readings for all forces and moments can be obtained in about five seconds after the model has been adjusted to the correct attitude. The first tests on interference are being made on a $\frac{1}{4}$ -scale model of a DH-4B, the wings being clipped to permit it to enter the tunnel.

Propeller tests.—As already noted, several model propellers representing designs in actual use by the Army have been tested for thrust and torque over the operating range of slip ratios. Tests were run at a number of different rotational speeds for the same slip ratio, and indicated a scale effect considerably larger than had been anticipated, especially for models of wooden propellers designed for high-powered engines and having very thick sections near the boss.

Model tests.—The practice of testing complete models for the Army Air Service has been continued. As in the previous years, special attention has been given to control and stability characteristics.

Miscellaneous.—The small wind tunnel (4-foot diameter) has been employed much of the time for instruction and for researches carried out independently by students. Among the

pieces of work undertaken there have been included an analysis of the elements affecting the longitudinal balance of an airplane and a study of the autorotation characteristics of windmills or helicopter propellers inclined at various angles to the wind stream.

McCOOK FIELD

General.—The routine work at McCook Field during the past year has included complete tests on 13 airplane models, with a rather elaborate investigation of the effect on fuselage, chassis, tail surfaces, etc., determined by successive removal of these parts from the model. The usual number of calibrations were made on aircraft instruments as requested from time to time by the flight or instrument branch. Routine airfoil tests numbered 15; miscellaneous tests, 30; and airfoil tests for wall interference studies, 320.

Wall interference investigation.—A series of seven geometrically similar airfoils was prepared, of differing sizes and having 0.15 cylindrical camber, chosen for the purpose of exaggerating the effects under examination. These surfaces were tested at slow speeds on the N. P. L. balance, and at speeds up to 250 miles per hour on the wire balance. In addition, a series of five C-27 airfoils of differing sizes was tested on the N. P. L. balance.

In connection with this series of tests pressure traverses were made, the laborious nature of these having been lately reduced by the use of improved methods and in particular the development of the "integrating impact tube." Pressure drops due to various models in the tunnel were measured and interpreted to a precision of three-tenths of 1 per cent on the velocity head.

Some rough outdoor tests were conducted to investigate new methods of checking wall interference, using a rotary wind-driven propeller as the most convenient object for test.

Alteration of the air flow of the 5-foot wind tunnel.—The character of air flow has been altered by the installation of an improved form of straightener, and by the elimination of the honey-comb. This alteration was intended for the original layout of the tunnel in 1922, but it was not convenient at that time to install it. A new arrangement of the static plate orifices has been installed, and the whole recalibrated. The previous flow had a turbulence corresponding to about 12 per cent of the velocity head; the new flow has a turbulence corresponding to about $2\frac{1}{2}$ per cent of the velocity head. The new straightener by which this change has been accomplished is a development from the straightener first used in the 14-inch wind tunnel in 1918, and has been the result of various empirical studies since that time, and in particular some model studies in the 14-inch wind tunnel in 1925.

Officers' school.—The usual period required by the McCook Field Officers' School was devoted to instructing 13 officers in wind-tunnel procedure.

Twenty-foot wind tunnel project.—In the summer of 1924 a 20-foot wind-tunnel project for the new McCook Field was brought up, in continuation of earlier studies on large wind-tunnel design commenced by the Air Service in 1917. With the object of corroborating published data on various wind-tunnel structures, four scale models were built and tests started in February, 1924.

Parachute fabrics.—Resistance and air leakage of various parachute fabrics were examined in the wind tunnel, the general conclusions being that the closeness of the weaves examined did not noticeably change resistance.

Effect of bullet holes in wing fabric.—A full-sized portion of an MB-3A wing was put in the wind tunnel for high-speed test of the tearing effect when bullet holes existed in the fabric.

Rotating cylinder.—Stream-line flow around a rotating cylinder was determined in December, 1924, by taking photographs of a simple apparatus using the silk-streamer method. Rough observations were made on the lift and drag of the rotating cylinder.

A method was perfected along lines originated by the General Electric Co. for securing pictures of air flow over a body. The method involves painting the body with a suitable paint, subjecting same to the air flow, and photographing the result after the flow lines have formed.

Test of Carmier gun sight.—The gun sight was mounted in the wind tunnel in the manner actually used on the aircraft gun, and its behavior under various accelerations was noted.

Humidifying apparatus in the 14-inch wind tunnel.—For purposes of visualizing air flow in the high-speed wind tunnel, water-humidifying nozzles were installed in the hangar. Previously it has been customary to await suitable weather humidity conditions when it is desired to make observations of air flow.

Center section type of radiator.—Half-size sections of air foils were tested for comparative resistance with and without radiator.

REPORT OF COMMITTEE ON POWER PLANTS FOR AIRCRAFT

ORGANIZATION

The committee on power plants for aircraft is at present composed of the following members:

Dr. S. W. Stratton, Massachusetts Institute of Technology, chairman.

George W. Lewis, National Advisory Committee for Aeronautics, vice chairman.

Henry M. Crane, Society of Automotive Engineers.

Prof. Harvey N. Davis, Harvard University.

Dr. H. C. Dickinson, Bureau of Standards.

Leigh M. Griffith, Langley Memorial Aeronautical Laboratory.

Edward T. Jones, engineering division, Army Air Service, McCook Field.

Commander E. E. Wilson, United States Navy.

FUNCTIONS

The functions of the committee on power plants for aircraft are as follows:

1. To determine which problems in the field of aeronautic power-plant research are the most important for investigation by governmental and private agencies.

2. To coordinate by counsel and suggestion the research work involved in the investigation of such problems.

3. To act as a medium for the interchange of information regarding aeronautic power-plant research, in progress or proposed.

4. To direct and conduct research on aeronautic power-plant problems in such laboratories as may be placed either in whole or in part under its direction.

5. To meet from time to time on call of the chairman and report its actions and recommendations to the executive committee.

By reason of the representation of the Army, the Navy, the Bureau of Standards, and the industry upon this subcommittee, it is possible to maintain close contact with the research work being carried on in this country and to exert an influence toward the expenditure of energy on those problems whose solution appears to be of the greatest importance, as well as to avoid waste of effort due to unnecessary duplication of research.

The committee on power plants for aircraft has direct control of the power-plant research conducted at Langley Field and also of special investigations authorized by the committee and conducted at the Bureau of Standards. Other power-plant investigations undertaken by the Army Air Service or the Bureau of Aeronautics are reported upon at the meetings of the committee on power plants for aircraft.

SUBCOMMITTEE ON ACCIDENTS

In order to determine, if possible, the exact causes of aircraft accidents, the greater number of which are due to failure of some part of the power-plant installation, a subcommittee on accidents has been organized as a subcommittee of the committee on power plants for aircraft. The functions of this subcommittee are to assemble and analyze data on accidents in the Army, Navy, and Postal Air Services with a view to determining the types of matériel failures which most commonly occur in aircraft. The organization of the subcommittee on accidents is as follows:

G. W. Lewis, National Advisory Committee for Aeronautics, chairman;

Lieut. B. R. Dallas, United States Army;

Lieut. W. H. Dillon, United States Navy;

C. F. Egge, Air Mail Service.

LANGLEY MEMORIAL AERONAUTICAL LABORATORY

FUEL INJECTION ENGINE—*Engine performance.*—The study of the application of fuel injection to the two-cycle engine with spark ignition has been continued and brought to a conclusion. The induction system of the Liberty engine cylinder was further modified, which gave improved results. The study did not include design development necessary to permit satisfactory operation at low speeds and loads. It was found that 53 brake horsepower could be consistently developed with the modified Liberty cylinder at 1,300 revolutions per minute (116 lbs./sq. in. B. M. E. P.), using a scavenging air pressure of $5\frac{1}{2}$ lbs./sq. in. Only 28 brake horsepower is obtained with the standard Liberty engine at the same speed. A report covering this work has been prepared for publication.

The application of fuel injection to four-cycle aeronautic engines operating with Diesel engine fuel oil and using the heat of compression for igniting the fuel has been further studied. A special steel cylinder mounted on the single cylinder Liberty engine base and arranged for the adaptation of separate cylinder heads has been used to study combustion-chamber forms. A precombustion or bulb-type cylinder head has been tested at speeds up to 1,800 revolutions per minute, using an eccentric-operated pump and an automatic diaphragm-type injection valve. Brake mean effective pressures up to 88 lbs./sq. in. and fuel economies comparable to those of present-day aircraft engines have been obtained with an injection advance angle of approximately 27° before top dead center. The low compression pressure of 280 lbs./sq. in., high explosion pressures, and certain features of construction have, however, limited the possibilities of obtaining a higher satisfactory power performance with this cylinder head.

A new cylinder head of the same general type has been designed and is being constructed which will permit compression pressures up to 500 lbs./sq. in. and which provides for various precombustion chamber volumes and shapes and degrees of turbulence.

A second head of slightly concave cross section and arranged for injection of fuel directly into the cylinder is being tested. A cam-operated fuel pump and a spring-loaded type of injection valve are being used in this work. A limited number of tests have been made to determine the effect of variation of the injection rate on the power output and fuel economy. In connection with these tests a simple device for determining maximum explosion pressures has been developed, by the aid of which it has been possible to maintain definite cylinder pressures for comparative purposes. Although the results with these two heads are not exactly comparable, they indicate at this time that the precombustion chamber type of cylinder head is the more promising of the two for aeronautic application.

The Universal test engine has been fitted with an eccentric-operated pump and automatic diaphragm-type valves. An investigation of the influence of compression pressure on the performance of this engine operating as a compression ignition engine has been started. This engine is peculiarly adaptable for such work, since the compression pressure can be changed readily while the engine is in operation by raising or lowering the cylinder head. Preliminary tests at 1,400 revolutions per minute have given fuel consumptions of 0.50 pound per brake horsepower-hour for loads up to 60 lbs./sq. in. brake mean effective pressure. Owing to the form of the combustion chamber combined with lack of effective turbulence, satisfactory performance at higher power was not obtained.

Fuel injection pumps and valves.—The performance of an eccentric-operated injection pump which controls injection by means of a relief valve has been determined with special bench testing equipment, consisting essentially of a motor-driven jackshaft with a flywheel, and provided for attaching fuel pumps, and a deflector and clutch mechanism which permit the passage at will of one or more sprays to a target held on and rotated with the flywheel. By means of this apparatus the effects of speed, injection-valve opening pressure, primary fuel pressure, injection-valve tube length, and closure of the relief valve at various points in the pump cycle on the lag of the spray behind the pump cycle have been determined. The duration of injection, the maximum injection pressures developed, and the fuel weight discharged per cycle for various pump settings were also determined. This work has aided materially the study of the application of injection systems to engine service and the analysis of engine performance.

Two types of automatic diaphragm-type injection valves giving highly atomized fuel sprays have been developed. The first type discharges the fuel at the periphery of the diaphragms and the second through a steel nozzle supported in the center of the diaphragm. Conical sprays, having spray cone angles up to 130° , and obtained by means of either mechanical guides or rotation of the jet, have been studied.

Characteristics of fuel sprays.—Further development of the apparatus for taking a series of pictures at high speed of the growth of a single fuel spray has resulted in the determination of the penetration characteristics of the sprays of several types of injection valves. A description of the apparatus used for this work may be found in the previous annual reports of the committee. A series of tests have been made which give the penetration and development with time of sprays produced by a positively operated injection valve having a 0.015-inch round orifice. Diesel-engine fuel oil was discharged through this orifice at pressures up to 8,000 lbs./sq. in. into a chamber with glass windows containing nitrogen at pressures up to 300 lbs./sq. in. and a series of photographs taken of the spray during discharge. The results provide means for determining the relationships existing between the chamber and fuel pressures, and a report covering this work, entitled "Spray Penetration with a Simple Fuel Injection Nozzle," has been prepared for publication.

Investigations with this apparatus are now under way on the spray characteristics of several automatic injection valves, using chamber pressures up to 600 lbs./sq. in. and controlling the weight of the fuel discharged. The results to date show that under the same conditions the spray from a simple round orifice has greater penetration, smaller cone angles, and lesser atomization than other types of sprays. While mechanically guided wide angle sprays may have initial velocities as high as those having narrow angles, it is found that they atomize more quickly and thoroughly and have less penetration. The effect of chamber pressure on centrifugal sprays is to decrease materially their spray cone angles and tend to maintain their axial penetration.

Fuel characteristics.—The work on the vapor pressure-temperature characteristics of several fuels used in internal combustion engines has been limited to an investigation of the behavior of various mixtures of gasoline and benzol and a study of the reactions and phenomena noted in the experimental work.

A report has been prepared for publication covering the investigation of the effects of fuel pressure, back-air pressure, and temperature on the coefficients of discharge of various fuels discharged through round orifices suitable for use in fuel-injection valves.

SUPERCHARGING—Roots type.—Comparative climb performance tests with and without supercharging of a DT-2 sea plane carrying equivalent military loads up to 2,000 pounds have been completed, and the results have shown that a material improvement in the performance of this type airplane can be obtained by supercharging even when heavily loaded and operating to moderate altitudes. It was found that when maintaining practically sea-level pressure at the carburetor at all times when supercharging the absolute ceiling was increased 90 per cent when operating without military load and 50 per cent when operating with load. The service ceiling was increased about 80 per cent for all loads, while the average rate of climb to the service ceiling was the same. The climb performance when supercharging was inferior at low altitudes, owing to the use of large propellers.

The first successful supercharging of an air-cooled engine at high altitude has been accomplished at this laboratory, using the Roots type supercharger. Further tests with the Lawrance (Wright) J-1 engine with Roots supercharger in a TS land plane have been completed. When using the same propeller and maintaining full supercharging to 16,000 feet, the original service ceiling of 16,100 feet was increased 65 per cent, the absolute ceiling was increased 56 per cent, the time to 16,100 feet was reduced 59 per cent, and the average rate of climb to the new service ceiling was 43 per cent greater than to the original ceiling without supercharging. Additional information of the effect of supercharging on the cylinder head temperatures of each of the nine cylinders has been obtained, giving maximum recorded temperatures for the various cylinders ranging between 500° F. and 560° F. Close examination of the engine revealed no undue wear or other ill effects as a result of supercharging.

In addition to the above investigation with the model J-1 engine, a further study has been made, using a Roots type supercharger and a Wright model J-4 air-cooled engine in a UO-1 land plane, with a view to learning the effects of supercharging on an engine having a somewhat different cylinder construction. With full supercharging maintained to 18,000 feet, a considerable increase in airplane performance was obtained with apparently no detriment to the engine and without encountering excessive cylinder head temperatures. When operating with the above amount of supercharging and using the same propeller, the original service ceiling of 18,300 feet was increased 72 per cent, the original absolute ceiling of 20,000 feet was increased 66 per cent, the time to 18,300 feet was reduced 54 per cent, and the average rate of climb to the service ceiling was 27 per cent greater than to the original service ceiling without supercharging. Cylinder head temperatures measured at corresponding points on each of the nine cylinders showed a variation among the cylinders of about 150° F. The maximum head temperature under supercharged conditions was 530° F. against a maximum of 470° F. for the unsupercharged condition. Investigation with the J-4 engine is being continued using an increased amount of supercharging.

Further study of the Roots type supercharger has been made in the laboratory to obtain additional information on its performance characteristics.

A DH-4 airplane has been reconditioned and equipped especially for continuing the investigation of the flight characteristics of the Roots type supercharger.

Additional Roots superchargers are being constructed in which are incorporated changes in design found desirable from experience with the present machine. As the new machines will be capable of being operated at speeds much higher than the present machine, it will be possible to study the effect of the higher speeds on the performance characteristics, and thus determine the advisability of increasing the speed of operation and reducing the size and weight of the unit.

Problems incidental to supercharging.—An investigation to determine the effect of high carburetor air temperatures, such as encountered when supercharging, on the power output of water-cooled engines has been completed, and information has been obtained for a Wright model E-4 engine and a Liberty-12 engine with carburetor air temperatures as high as 180° F. This study has shown that, for the higher air temperatures, the relation between engine power and air temperature remains substantially the same as found by other investigators for the lower ranges of temperature.

In connection with the study of methods for measuring the power output of supercharged engines operating at altitude, a Bendemann hub dynamometer has been tested on the stand to ascertain its suitability for the purpose.

Supercharged engine versus other types.—A study of the relative performance of the normal compression engine, the high compression engine, and the supercharged normal compression engine has been continued both in the laboratory and in flight. Tests have been continued with the single cylinder Universal test engine to establish the performance attainable with the high-compression engine without encountering serious detonation when using domestic aviation gasoline. Tests have been conducted with normal ignition advance and the engine throttle by means of the usual butterfly valve, with retarded ignition and engine not throttled and with volumetric efficiency of the engine reduced by varying the timing of the inlet valve. Compression ratios from 4 : 1 to 7.5 : 1 and engine speeds from 1,200 to 1,800 revolutions per minute were investigated, and the factors influencing detonation, such as volumetric efficiency, ignition timing, air-fuel ratio, and piston velocity, were studied. The results have shown that the maximum power output of the high compression engine operating on domestic aviation gasoline at sea level is obtained by maintaining full throttle and retarding the ignition timing sufficiently to suppress detonation, although the fuel consumption with this method is high. In order to make the test results comparable during this investigation, it was necessary to restrict the detonation to a definite amount. Consequently, considerable attention was given to the study of laboratory methods of detecting and measuring detonation. Limitations of methods previously used were established and several new methods tried. A simple apparatus, consisting

of a sensitive balanced pressure ball valve, was finally adopted as being best suited to the conditions of these tests.

The results of the above tests will be used in connection with the program of flight tests which is being conducted to determine the relative performance of a service type seaplane of the load-carrying type, equipped with a normal compression engine, a high compression engine, and a supercharged normal compression engine, all engines having the same displacement and being used both with direct and geared propeller drives. Flight tests with a normal compression Wright T-2 engine in a DT-4 seaplane are now in progress.

POWER PLANT LABORATORY EQUIPMENT.—A small gasometer has been installed and used in conjunction with a special surge chamber for measuring the air consumption of single-cylinder test engines. A second gasometer, of larger capacity, is being installed.

Several detail changes have been made in the Universal test engine. This unit has proved very satisfactory for research purposes.

BUREAU OF STANDARDS

Testing of aviation engines under approximate altitude conditions.—Engine tests under approximate altitude conditions have been made by reducing the pressure at the entrance to the carburetor and at the exhaust port exactly as in an altitude laboratory test but allowing the air surrounding the engine to remain at sea-level pressure. Similar tests were made under "true" altitude conditions—that is to say, with the air surrounding the engine reduced to a pressure corresponding to the altitude. It was concluded that with certain precautions satisfactory results would ordinarily be expected with the approximate type of test.

Supercharging of aircraft engines.—Tests of a Curtiss D-12 engine under supercharging conditions have been made for pressures and temperatures up to those corresponding to an altitude of 15,000 feet. Preparations for a more extensive series of tests with another engine are in progress. This work is so planned as to cover the range of pressures to be expected with the exhaust or the mechanically driven superchargers and should furnish a basis for estimating the performance of an engine equipped with any type of supercharger once the power consumed by that particular device in maintaining a given amount of supercharging is known.

Ignition systems.—A rather complete series of comparative tests of ignition systems has been completed, on the basis of which a report on the "Electrical Characteristics of Ignition Systems" has been prepared.

Phenomena of combustion.—This investigation of factors of fundamental importance as regards the rate of explosive gaseous reactions has been in progress for several years. A soap bubble serves as a constant pressure bomb, the record of the explosive reaction being secured automatically by photographic means. During the past year there has been completed and installed a large container within which the soap bubble can be used as a constant pressure bomb at pressures above or below atmospheric. The apparatus has proved very satisfactory and several groups of measurements have been made.

Fuels for high-compression engines.—A report summarizing the work at the bureau on this subject during the past few years has been submitted to the National Advisory Committee for Aeronautics for publication. The report is primarily a general discussion of the properties essential to a satisfactory fuel for high-compression engines, but certain fuels, benzol and alcohol in particular, are discussed in some detail.

Oxidation test for routine testing of mineral oils.—The oxidation test, the development of which was discussed in the report of last year, has been employed to a considerable extent throughout the year at the bureau and at several other laboratories. It appears to have proved as satisfactory as was anticipated. In this test the oil is subjected for two and one-half hours to a temperature of 200° C. in an atmosphere of oxygen.

Investigation of bearing friction.—Several oils have been compared in the journal friction machine and very consistent results have been obtained. Considerable new apparatus has been constructed, including a simple friction machine for investigating the effect of viscosity upon

wear when an abrasive is in the oil. Preliminary tests indicate that this machine will prove to be unusually valuable.

Investigation of piston friction.—This project had as its aim the finding of the relative magnitude of certain factors affecting piston friction in order that the friction of engines, particularly those of the aviation type, might be more accurately estimated. The experimental work has consisted of measurements of the friction of a four-cylinder engine equipped with several groups of pistons, each group differing from the standard pistons in but one respect. The experimental work on this investigation has been completed and a report is in preparation.

Hot wire anemometer.—A technologic paper has been prepared and published describing the hot wire anemometer which was constructed to measure the average flow of air through radiators mounted in different positions on an airplane.

NEW ENGINE TYPES

Both the Bureau of Aeronautics of the Navy Department and the engineering division of the Army Air Service have continued their efforts toward an increase in the dependability of aircraft engines and their accessories and in bringing about a greater life between overhauls. The two organizations have cooperated closely in developments. The Air Service has continued work on the cam engine and barrel type or Almen engine. The Bureau of Aeronautics has been conducting tests on its experimental heavy-oil engine purchased from the Eastern Engineering Co. (Ltd.), Montreal, Canada. This engine has not developed the power anticipated, but it has demonstrated conclusively that heavy oil can be properly burned in high-speed engines of the two-stroke autoignition, solid-injection type. Development is continuing on the project and promising results have been obtained.

A striking piece of work on the part of the Air Service is the new air-cooled Liberty. This engine has demonstrated on test that the air-cooled in-line engine will be one of the important developments of the future.

Of the service types the Wright Model "J" has advanced to the J-4-A model. The Navy has 140 of these on order, of which a large number have been delivered. Contracts will soon be let for an additional order of the model J-5 which involves an improved cylinder construction. Forty-five J-4 engines have been sold to commercial activities in the United States and to foreign countries in the Western Hemisphere. A life between overhauls of about 200 hours is being obtained and very dependable performance has resulted.

The Wright Model T-3A, a 600-horsepower water-cooled engine for the combined scouting-torpedo-bombing airplanes, is now in general service and has given excellent results. This engine has now advanced to the T-3A type, incorporating minor improvements and changes designed to bring about a life between overhauls of 300 hours.

The Wright Model P-2, the 400-horsepower static-radial, air-cooled engine, which incorporates the fan-type supercharger for rotary induction purposes, has passed its acceptance tests with very excellent performance. Twelve of these engines have been ordered for flight testing purposes and for further development looking toward the service application of this engine at a future date.

The Wright Aeronautical Corporation is developing a new engine of 1,200 cubic inches capacity, scaled down from the P-2 model. This will produce a line of three air-cooled engines in 800, 1,200, and 1,600 cubic inches, designed to meet the Navy's needs in all types of aircraft. The model "J" will be used as a training engine, the new R-1200 in the observation and fighter class, and the large P-2 for single and twin-engined bomber installation.

Both the Army and the Navy have continued the development of the Packard 1A-1500 and 1A-2500 engines. The inverted 1500 is being used in the Loening amphibian, the vertical 1500 in fighters, and the geared 1500 in the large patrol airplane. This latter engine was the power plant for the PN-9's used on the San Francisco to Hawaii project. The first PN-9 holds the world's endurance record for sea planes at 28 hours and 35 minutes, and the same airplane on the Honolulu flight had perfect engine performance until the gasoline was exhausted. The Packard 1A-2500, 800-horsepower water-cooled engine geared two to one, was installed

in the Boeing patrol airplane for the same project. The engine performance of this airplane has likewise been satisfactory.

The Curtiss D-12 engine has continued to give excellent results in pursuit-type airplanes and more of these engines are being purchased. The Curtiss radial R-1454, a 400-horsepower air-cooled engine developed by the Air Service, has been delivered at McCook Field and is now undergoing its tests. This engine incorporates the rotary induction and improved cylinder design, from which good performance is anticipated.

The new Curtiss V-1400, a 12-cylinder V-type water-cooled engine, has lately passed its tests and was flown for the first time in the Pulitzer races. This engine has very striking characteristics of high power, light weight, rugged construction, and accessibility.

In the field of accessories the aeromarine inertia type hand starter has become standard in the Navy and has definitely proved its effectiveness. The scintilla magnetos adopted for general Navy use have likewise measured up to all expectations. There has been continued improvement in all accessory equipment and continued improvement in general dependability.

The rise of the air-cooled engine with improved reduction in power-plant weights, due to the elimination of the cooling system, has forced the water-cooled engine to new endeavors. Increased power through higher crankshaft speeds with reduction gearing has brought about a balance on the basis of specific power-plant weights between the two engines. This will undoubtedly force the air-cooled engine into the higher speeds and reduction gearing. Since results indicate that a large percentage of power-plant failures are due to faults in gasoline, oil, and water lines, the air-cooled engine still has important advantages. This fact accounts for the energy which is now being put into development of the three air-cooled engines for the Navy.

The past year has been marked by the entrance into the aircraft engine field of the Pratt & Whitney Aircraft Co., of Hartford, Conn. The formation of this company brings to the industry the wide experience of the officers of the new company and the well-known manufacturing facilities of Pratt & Whitney.

In general, the Bureau of Aeronautics and the Air Service are cooperating very closely in engine development, and this development is taking the form of improved performance, improved dependability, and increased life between overhauls. The development problem has followed a rational line, and has therefore been a healthy one.

REPORT OF COMMITTEE ON MATERIALS FOR AIRCRAFT

ORGANIZATION

The present organization of the committee on materials for aircraft is as follows:

Dr. George K. Burgess, Bureau of Standards, chairman.
 Dr. H. L. Whittemore, Bureau of Standards, vice chairman.
 S. K. Colby, American Magnesium Corporation.
 Henry A. Gardner, Institute of Paint and Varnish Research.
 Dr. H. W. Gillett, Bureau of Standards.
 Prof. George B. Haven, Massachusetts Institute of Technology.
 Zay Jeffries, Aluminum Company of America.
 J. B. Johnson, engineering division, Army Air Service, McCook Field.
 George W. Lewis, National Advisory Committee for Aeronautics (ex officio member).
 Commander H. C. Richardson, United States Navy.
 G. W. Trayer, Forest Products Laboratory, Forest Service.
 Starr Truscott, Bureau of Aeronautics, Navy Department.
 Prof. Edward P. Warner, Massachusetts Institute of Technology.

FUNCTIONS

Following is a statement of the functions of the committee on materials for aircraft:

1. To aid in determining the problems relating to materials for aircraft to be solved experimentally by governmental and private agencies.

2. To endeavor to coordinate, by counsel and suggestion, the research and experimental work involved in the investigation of such problems.

3. To act as a medium for the interchange of information regarding investigations of materials for aircraft, in progress or proposed.

4. To direct and conduct research and experiment on materials for aircraft in such laboratory or laboratories, either in whole or in part, as may be placed under its direction.

5. To meet from time to time on call of the chairman and report its actions and recommendations to the executive committee.

The committee on materials for aircraft, through its personnel acting as a medium for the interchange of information regarding investigations on materials for aircraft, is enabled to keep in close touch with research in this field of aircraft development. Much of the research, especially in the development of light alloys, must necessarily be conducted by the manufacturers interested in the particular problems, and both the Aluminum Co. of America and the American Magnesium Corporation are represented on the committee. In order to cover effectively the large and varied field of research on materials for aircraft, three subcommittees have been formed, as follows:

Subcommittee on metals:

Dr. H. W. Gillett, Bureau of Standards, chairman.

Zay Jeffries, Aluminum Co. of America.

J. B. Johnson, engineering division, Army Air Service, McCook Field.

George W. Lewis, National Advisory Committee for Aeronautics (ex officio member).

Starr Truscott, Bureau of Aeronautics, Navy Department.

Dr. H. L. Whittemore, Bureau of Standards.

Subcommittee on woods and glues:

G. W. Trayer, Forest Products Laboratory, Forest Service, chairman.

H. S. Betts, Forest Service.

George W. Lewis (ex officio member).

Dr. H. L. Whittemore, Bureau of Standards.

Subcommittee on coverings, dopes, and protective coatings:

Henry A. Gardner, Institute of Paint and Varnish Research, chairman

Dr. W. Blum, Bureau of Standards.

Warren E. Emley, Bureau of Standards.

Prof. George B. Haven, Massachusetts Institute of Technology.

Isadore M. Jacobsohn, Bureau of Standards.

George W. Lewis (ex officio member).

P. H. Walker, Bureau of Standards.

E. R. Weaver, Bureau of Standards.

During the past year, Mr. G. W. Trayer, of the Forest Products Laboratory, has replaced Mr. Carlile P. Winslow on the committee on materials for aircraft. Dr. H. W. Gillett, of the Bureau of Standards, has been appointed a member of the committee and chairman of the subcommittee on metals, succeeding Dr. George K. Burgess in the latter capacity. Mr. Starr Truscott, of the Bureau of Aeronautics of the Navy Department, has also been appointed a member of the committee on materials for aircraft and of the subcommittee on metals, and Mr. Warren E. Emley, of the Bureau of Standards, has been appointed a member of the subcommittee on coverings, dopes, and protective coatings.

Most of the research in connection with the development of materials for aircraft is financed directly by the Bureau of Aeronautics of the Navy Department, the engineering division of the Army Air Service, and the National Advisory Committee for Aeronautics.

The Bureau of Aeronautics and the engineering division of the Air Service, in connection with the operation of tests in their own laboratories, apportion and finance research problems on materials for aircraft to the Bureau of Standards, the Forest Products Laboratory, and the Industrial Research Laboratories.

MEETINGS OF THE COMMITTEE

Several very important meetings of the committee were held during the year. One was held at the Naval Aircraft Factory, Philadelphia, at which the subject of the corrosion of duralumin and its embrittlement was very thoroughly discussed by members of the committee and by representatives of the manufacturers of this, the most widely used light alloy. After the meeting the work in progress at the factory was inspected. A great deal of interest was shown in the PN-9 seaplanes, which were later used in the attempted flight from San Francisco to Hawaii.

SUBSTITUTE FOR SILK PARACHUTE FABRIC

The problem of finding a substitute for the silk which is now used in parachute construction is a part of the general program of this committee. An investigation has been under way for the fabrication of a cloth in this country which will prove acceptable for parachute construction. Acceptable silk fabrics have been produced from the raw materials obtained from China and Japan and fabricated in this country. Since it has never proved practical to cultivate silk in the United States, the problem resolves itself into finding some other fiber which can be substituted for the raw silk fiber.

In order to design a cloth as light as the requirements demand for parachute cloth, fine yarns must be used which can be manufactured from cottons only of long staple. The Pima cotton, which is grown in Arizona, will provide this yarn, and the investigation so far has been made with Sakellaridis cotton, which is practically the same.

Using fine yarns, both singles and doubles, a very careful study has been made of the physical properties in comparison with silk yarns of similar size. The characteristics which are most important are strength, stretch, and resiliency. Advantage was taken of previous work done in the textile field showing the reaction which cotton undergoes during mercerization and treatments with dopes and softeners. Seven treatments were tried and the results of the study permitted the selection of one type of treatment for further study, namely, the coating of the previously mercerized cotton with cellulose acetate dopes containing dissolved resins and softeners. Three distinct types of cellulose acetate dopes were used. The yarns used in the investigation had been mercerized commercially and it was found that this mercerization process had a very decided effect on the strength and elasticity of the yarn. A study of the mercerization was made in conjunction with tests of yarns wet treated and dry treated. In the process of mercerization there are three main operations: The premercerization treatment; the formation of alkali cellulose; and the formation of cellulose hydrate. Each of these three operations requires several minor operations, and in this investigation a study was made of the effect of the variations in the conditions under which the operations were carried out on the properties of the finished mercerized cotton. The yarns used in the investigation were 160/1 and 160/2, five different twists for the single and three each for the plied yarns being used.

The successful conclusion of this investigation will depend largely upon the result of the mercerization experiments. The work so far has been very encouraging, and it is hoped that a definite conclusion will be reached toward the end of the present fiscal year.

SUBCOMMITTEE ON METALS

Intercrystalline embrittlement of duralumin.—During the past year the subcommittee on metals recommended a program of research for the study of intercrystalline embrittlement of duralumin. This program was approved by the National Advisory Committee for Aeronautics and recommended to the Army Air Service, the Bureau of Aeronautics, and the Post Office Department for consideration, and has been accepted by the Air Service and the Bureau of Aeronautics.

The outline of this program is as follows:

- (a) The study of acceleration of this type of corrosion for testing purposes.
- (b) The effect of permanent deformation on material hardened by spontaneous aging.

(c) The effect of deformation on fully hardened material, hardened by accelerated aging at a higher temperature.

(d) The effect of protective coatings.

(e) The effect of gas during the casting.

(f) The effect of heating and quenching mediums.

(g) The effect of the composition of the duralumin tested.

Material with a carefully recorded history of its preparation was received from the Baush Machine Tool Co., and since that material and similar material from the Aluminum Co. of America were to be studied together the investigation did not start until the material from the latter company was received, late in August. Specimens for testing were then made from both lots.

Intercrystalline attack and embrittlement in material received from both companies has been produced experimentally, both in aged material and in that cold-rolled after aging. A study of the rate of attack in calcium chloride solutions of varying strength with specimens both submerged and alternately submerged and dried is in progress.

Material which had been greatly deformed by rolling after aging and slightly deformed by stretching is under test. Preliminary results indicate that stretching prior to test hastens the intercrystalline corrosive attack. Specimens are being sent to the Naval Aircraft Factory and to the Industrial Research Laboratories for coating with various protective coatings. Chemical and electrochemical treatments suggested by the Army as additions to the program will be included in the tests.

The Bureau of Standards has continued to examine specimens found in service. These samples all confirm the conclusion that material cold-worked after aging and subjected to corrosion is especially susceptible to embrittlement, although if the conditions are severe material which has not been worked after aging is also attacked. Material which had been attacked in service by calcium chloride, cleaned, and revarnished, was recently examined to see whether the intercrystalline attack had progressed. In making the comparison, the assumption had to be made that before the material was cleaned corrosion had progressed to the same extent as on the specimens which were tested at that time. On this assumption, no proof was found that the attack had progressed further since the previous examination. These results indicate that a coating which is actually impervious to such agents as water vapor and "salt air" prevents the corrosion. The material was in "notch-brittle" condition after cleaning and was still in that condition, although apparently no worse.

The information now in the possession of the committee does not justify a pessimistic outlook in respect to the use of duralumin as a structural material for aircraft, unless in very thin sheets. It is believed that research on the embrittlement problem will ultimately show how to prepare, protect, and use this material to insure reliability in service. It is also believed that the program for the investigation now in progress, which has been outlined above, is entirely satisfactory.

Structures for airships.—The previous tests of girders for the *Shenandoah* showed that the strength of these girders was determined by the elastic properties of the channels and the type of restraint offered by the lattices. The principal elastic constants of the channels are their two flexural stiffnesses (moments of inertia \times Young's modulus) and their torsional stiffness (torsion constant \times shear modulus).

The object of this investigation is to determine by tests the relative importance of these three constants in determining the strength of the girders. For this purpose it was necessary to study accurately and in detail the deformations of the channels under compressive loads, first in the girders alone and then with outside constraints applied which prevented particular types of deformation.

The technique of measurement which has been worked out has been thoroughly tested. Consistent reproducible results were obtained on the measurement of deflection and twist of the channels of a special girder. Since the lateral deflections were always accompanied by twist a series of readings was taken restraining in succession the twist of one, two, and three

channels but leaving them free to deflect laterally. The girder was loaded under these conditions successively to 5,100 (no restraint), 6,740 (one channel restrained), 6,990 (two channels restrained), and 7,500 (three channels restrained) pounds. The final failure was by twist of two of the channels between restraints and by spreading of the third with buckling of the flanges.

The measurements so far made are consistent with the assumption that with the present construction the coefficient of torsional stiffness of the channels is the controlling factor in determining the load these girders will carry. The measurements will be repeated on girders of regular design to see if these confirm the conclusions.

High-speed fatigue testing.—The investigation of the available methods for high-speed fatigue testing has been continued. Two alternative methods of loading the specimen have been used, each producing the stresses by resonant flexural vibrations. In one, the drive is electrical. A method similar to this has been used by Jenkin in England, who reports successful results. In the other the drive is by means of compressed air. This latter, so far as the investigations show, gives promise of greater simplicity and is the cheaper to operate, especially if a large number of specimens are to be run simultaneously. Apparatus of this type has been built and run. The possibility of longitudinal vibrations has not as yet been investigated experimentally.

The data which have been obtained are, however, insufficient to determine whether or not this type of drive will function satisfactorily over long periods of time.

SUBCOMMITTEE ON WOODS AND GLUES

The Forest Products Laboratory of the Department of Agriculture conducts practically all the investigations on the application of woods and glues to aircraft construction. The investigations that have been conducted and reported on were undertaken at the request of the Bureau of Aeronautics of the Navy Department or the engineering division of the Army Air Service. Some of the more important investigations now in progress are outlined below.

Attachment of metal parts and fittings to wooden members.—A study of the effect of the attachment of metal parts and fittings to wooden members was undertaken chiefly to secure more complete information as to the size, number, and spacing of bolts or other fastening mediums. A study on spruce and ash using solid bolts of various lengths up to one-half inch diameter and hollow bolts ranging from five-eighths to 1 inch in diameter has been made. The results of the tests have been presented in the form of charts which give the most efficient size of bolt for given conditions. Although these charts were prepared for spruce and ash, they may be applied to other species by the introduction of an adjustment factor representing the relation of their strength in compression parallel to the grain, to that of spruce or ash.

Determination of acceptance test values.—In the inspection of wood for airplanes, the need has been felt for a simple and expeditious mechanical test which could be applied to each piece to determine its acceptability. To meet this need the Forest Products Laboratory toughness-testing machine was developed.

The toughness value of wood reflects the relation of tensile to compressive strength, while specific gravity gives an indication of the compressive strength as well as most of the other strength properties. The toughness test together with the specific gravity determination is consequently an excellent means of separating material low in strength from that of average or higher strength properties.

Studies have been made to form a satisfactory basis for the inspection and selection of suitable airplane material, and have been completed on white oak, yellow birch, white ash, and Sitka spruce. As a result of the studies an inspection method has been recommended and the Bureau of Aeronautics and the Army Air Service have now acquired a Forest Products Laboratory toughness-testing machine. It has been possible to inspect and select woods of high quality of five species for which minimum values have been established.

Use of plywood in wing beams.—A series of tests has been made on box beams of various dimensions and on I beams using plywood webs. The results lead to the conclusion that in

the design of either plywood box or I beams a web thickness of 25 per cent greater than that calculated to give equal likelihood of failure by shear or compression will give the best results. The results of a series of tests made during the past two years will be issued in the form of a report and a further study will be made of wing beams of several different types and sizes to secure data on the strength and rigidity of beams and to determine the proper relation between the thickness of the web and the depth of flanges for different cross sections.

Detailed study of methods of fastening plywood.—A preliminary study was made on the use of screws for fastening three-ply wood of different species and sizes to spruce and ash frame members. In this investigation screw sizes, margins, and spacings were used which would develop as nearly as possible the full strength of the plywood without special consideration of the effect on the strength of the members receiving the screw point. As a result of these tests a table of screw sizes for different thicknesses of three-ply wood has been prepared for general design use. The investigation will be continued to include tests of plywood fastenings with small screws to secure data on the strength of such fastenings under different conditions. The study will also include the test of plywood with nails as fasteners.

Development of waterproof glues.—A study of waterproof glues includes a study of the resistance of glues under prolonged exposure to dampness. No adequate study has been made of the durability of glued joints under long periods of time. Experience indicates that in many places where glue joints are used any change in strength or water resistance is very slow. Tests will be carried on over a long period of time with different water-resistant glues to determine with some exactness the conditions under which glues will retain their original properties. Considerable information has been accumulated from the various investigations and a bulletin is now in preparation on the general subject of gluing of woods used for aircraft purposes.

Manufacture of casein water-resistant plywood.—An investigation has been carried on during the past year in an effort to produce a Grade A plywood with casein glues. Satisfactory results have been secured thus far on a laboratory scale, and plans are now being developed for one or more demonstrations on a factory scale. It is believed that by proper control of the glue and the gluing conditions it will be practicable to produce a satisfactory product in quantity. This investigation will be completed this year.

Air seasoning of aircraft woods.—The results of this investigation, which has been under way for three seasons, clearly show that the method of piling and handling the stock has a marked effect upon the rate of seasoning and upon the amount of degrade suffered. The investigation also showed that different species require different treatment and that the season of year during which the stock is first piled determines in a large measure what piling system should be used.

In this connection a survey of the seasoning practice at aircraft manufacturing plants will be made.

Effect of fungus infection on the mechanical properties of wood.—In the course of this investigation, which has been under way for a number of years, approximately 7,200 mechanical tests and 15,000 culture tests have been made. Reports have been prepared on the effect of yellow stain on the mechanical properties of white oak and on the relation of color and toughness strength of white ash. The data obtained from studies of Sitkaspruce and Douglas fir are available in preliminary form only. The data that have been obtained will be carefully analyzed before any additional tests are made.

Cause and detection of brashness of wood.—It is known that brashness and low shock-resisting ability are quite generally found in specimens of low specific gravity. Occasionally, however, pieces with acceptable specific gravity which are apparently sound are weak and brash. The need of some means of detecting such weakness by inspection is obvious. In the study of spruce it has been found that compression failures are not infrequently the cause of low toughness values. A thorough analysis will be made of this spruce material which is now being studied to determine, if possible, the cause of brashness.

SUBCOMMITTEE ON COVERINGS, DOPES, AND PROTECTIVE COATINGS

Gas-cell fabrics.—At the Bureau of Standards extensive investigations have been conducted in the development of experimental gas-cell fabrics for rigid airships. Of the many

varied types of fabrics which have been investigated, three have been selected because of their great promise of yielding suitable gas-cell material, and these are being developed for this purpose. Samples of one of these three type fabrics have already been subjected to outdoor exposure, under outer cover cloth, for a period of over 12 months, while samples of a second have been exposed, under similar conditions, for over 10 months. In both cases the exposures were made during periods including the coldest winter and the hottest summer months, and in neither case was there measurable increase in permeability or great decrease in breaking strength after such exposure. Samples of the third type of fabric mentioned above are now being prepared for exposure tests. While the result of such tests can not be definitely predicted in advance, it is believed that this last type of fabric will prove to be the best of the fabrics which have been investigated, and will, when fully developed, be the most satisfactory substitute for the goldbeater's skin fabric now used in rigid airships. All three of the fabrics mentioned above are light in weight, flexible, and have permeabilities well under the limit of 1 liter per square meter per 24 hours. Other types of fabrics are now under investigation. The study of these, however, has not progressed far enough to warrant any statement as to their probable value.

Other miscellaneous problems worked out at the Institute of Paint and Varnish Research are briefly outlined below.

Coatings for gas cells.—It has been suggested that 6 to 8 per cent of aluminum powder be mixed with the spar varnish which is used to coat the outside of gas cells for airships. As the solar radiation of a fabric exposed to the sun is reduced about 40 per cent, it is probable that aluminum powder in the varnish for gas cells would be advantageous, as the bags and the gas they contain would increase in temperature less rapidly.

Coatings for duralumin to prevent corrosion.—A coating for duralumin produced by anodic deposit of the metal in a plating bath has been developed. The deposit is aluminum oxide, which is a distinct protection. The process is patented. Usually the articles are lacquered after the plated coating is applied.

As there is some danger of weakening the metal in the plating bath, it seems preferable to give two coats of Navy aluminum spar varnish, which is cheaper and seems to give as good protection.

At the suggestion of the Bureau of Aeronautics, duralumin sheets such as are used for airplane pontoons were alternately exposed to sea water and to air under tropical conditions. A coating has been developed which will prevent the growth of barnacles and be durable in air. It is made from plastic resin, coal tar, and toxic poisons. The results were very satisfactory although the conditions were very severe.

Excellent results have been obtained at the Naval Aircraft Factory by using an inexpensive bituminous paint for floats and hulls. If the surfaces are inclosed this paint probably gives the best protection against underwater corrosion. The disadvantage is that, as a thick coat must be applied, the coating is heavy. This paint can be greatly improved by the addition of 10 to 20 per cent of asbestine, a crystalline pigment, showing a rod-like structure under the microscope. The rods act much like reinforcing rods in concrete. On exposure to sunlight, unfortunately, this paint breaks down rapidly, showing an alligator-skin surface. The bituminous compound flakes and powders rapidly.

Cotton flannel is often used as a water stop between sheets of duralumin. If the flannel is impregnated with asphaltum, gasoline will dissolve it. It is preferable to impregnate the flannel with a 3-pound cut of shellac in alcohol, which will not dissolve.

Coatings for magnesium to prevent corrosion.—Preliminary exposure tests of magnesium sheets have been made. It was found that uncoated magnesium sheets corrode slightly and the color becomes dark if exposed so that moisture dries off but that they become deeply pitted in six months if the surface does not dry off. Sheets coated with silicate of soda resist corrosion better than the uncoated sheets although if the surface does not dry off, they do corrode.

Two coats of aluminum spar varnish apparently give perfect protection. This coating was the lightest in weight. Doped coatings were very unsatisfactory. Six-month tests showed about equal corrosion in magnesium and in steel sheets.

Airplane dopes and paints.—Wing surfaces of airplane cotton were given one coat of dope and one coat of viscose. The surfaces were very taut. After exposure for six months some of the surfaces showed scaling of the viscose; others were in very good condition, particularly those having an outer coating of spar varnish. Surfaces coated with viscose are very much smoother than the usual doped surface. They should, therefore, offer less wind resistance. Paints containing aluminum and zinc powder for use on wing surfaces should have the powder mixed with the spar varnish just before the paint is applied. If this is done, the colors are much brighter than they are if the powder is mixed with the varnish and allowed to stand for months before the varnish is used.

It has been found that the scaling of the flag colors, which has been found in service, can be prevented by using lightweight pigments of high opacity instead of the heavy pigments of low opacity which have often been used.

Extensive tests are under way at Washington and at Pensacola with 200 frames covered with airplane cotton and doped with different schemes. Lightweight and permanent tautness and strength are sought.

PART IV

TECHNICAL PUBLICATIONS OF THE COMMITTEE

On recommendation of the committee on publications and intelligence, the National Advisory Committee for Aeronautics has authorized the publication of 23 technical reports during the past year. The reports cover a wide range of subjects on which research has been conducted under the cognizance of the various subcommittees, each report having been approved by the subcommittee concerned and recommended to the executive committee for publication. The technical reports presented represent fundamental research in aeronautics carried on at different aeronautical laboratories in this country, including the Langley Memorial Aeronautical Laboratory, the aerodynamical laboratory at the Washington Navy Yard, the Bureau of Standards, the Forest Products Laboratory, the Stanford University, and the Massachusetts Institute of Technology.

To make immediately available technical information on experimental and research problems, the National Advisory Committee for Aeronautics has authorized the issuance in mimeographed form of another series known as "Technical Notes" of which 23 have been issued during the past year.

In addition to issuing technical reports and technical notes the committee has authorized the issuance in mimeographed form of translations and reproductions of important technical articles of a miscellaneous character in a series known as "Technical Memorandums." In accordance with this authorization, the committee has issued 51 technical memorandums on subjects that were of immediate interest not only to research laboratories but also to airplane manufacturers.

Summaries of the 23 technical reports, and lists of the technical notes and technical memorandums prepared during the past year follow.

SUMMARIES OF TECHNICAL REPORTS

The first annual report of the National Advisory Committee for Aeronautics contained Technical Reports Nos. 1 to 7; the second annual report, Nos. 8 to 12; the third annual report, Nos. 13 to 23; the fourth annual report Nos. 24 to 50; the fifth annual report Nos. 51 to 82; the sixth annual report, Nos. 83 to 110; the seventh annual report, Nos. 111 to 132; the eighth annual report Nos. 133 to 158; the ninth annual report Nos. 159 to 185; the tenth annual report Nos. 186 to 209; and since the preparation of the tenth annual report the committee has authorized the publication of the following technical reports, Nos. 210 to 232:

Report No. 210, entitled "Inertia Factors of Ellipsoids for Use in Airship Design," by L. B. Tuckerman, Bureau of Standards.—This report is based on a study made by the writer as a member of the special committee on design of Army semirigid airship *RS-1* appointed by the National Advisory Committee for Aeronautics.

The increasing interest in airships has made the problem of the potential flow of a fluid about an ellipsoid of considerable practical importance. In 1833 George Green, in discussing the effect of the surrounding medium upon the period of a pendulum, derived three elliptic integrals, in terms of which practically all the characteristics of this type of motion can be expressed. The theory of this type of motion is very fully given by Horace Lamb in his "Hydrodynamics," and applications to the theory of airships by many other writers. Tables of the inertia coefficients derived from these integrals are available for the most important special cases. These tables are adequate for most purposes, but occasionally it is desirable to know the values

of these integrals in other cases where tabulated values are not available. For this reason it seemed worth while to assemble a collection of formulæ which would enable them to be computed directly from standard tables of elliptic integrals, circular and hyperbolic functions and logarithms without the need of intermediate transformations. Some of the formulæ for special cases (elliptic cylinder, prolate spheroid, oblate spheroid, etc.) have been published before, but the general forms and some special cases have not been found in previous publications.

Report No. 211, entitled "Water Model Tests for Semirigid Airships," by L. B. Tuckerman, Bureau of Standards.—The design of complicated structures often presents mathematical problems of extreme difficulty which are frequently insoluble. In many cases, however, the solution can be obtained by tests on suitable models. These model tests are becoming so important a part of the design of new engineering structures that their theory has become a necessary part of an engineer's knowledge.

For balloons and airships water models are used. These are models about $1/30$ the size of the airship hung upside down and filled with water under pressure. The theory shows that the stresses in such a model are the same as in the actual airship.

In the design of the Army semirigid airship *RS-1* no satisfactory way was found to calculate the stresses in the keel due to the changing shape of the bag. For this purpose a water model with a flexible keel was built and tested. This paper gives the theory of the design, construction, and testing of such a water model.

Report No. 212, entitled "Stability Equations for Airship Hulls," by A. F. Zahm.—In the text are derived simple formulæ for determining, directly from the data of wind-tunnel tests of a model of an airship hull, what shall be the approximate character of oscillation, in pitch or yaw, of the full-scale airship when slightly disturbed from steady forward motion.

Report No. 213, entitled "A Résumé of the Advances in Theoretical Aeronautics Made by Max M. Munk," by Joseph S. Ames.—In order to apply profitably the mathematical methods of hydrodynamics to aeronautical problems, it is necessary to make certain simplifications in the physical conditions of the latter. To begin with, it is allowable in many problems, as Prandtl has so successfully shown, to treat the air as having constant density and as free of viscosity. But this is not sufficient. It is also necessary to specify certain shapes for the solid bodies whose motion through the air is discussed, shapes suggested by the actual solids—airships or airfoils—it is true, but so chosen that they lead to solvable problems.

In a valuable paper presented by Dr. Max M. Munk, of the National Advisory Committee for Aeronautics, Washington, to the Delft Conference in April, 1924, these necessary simplifying assumptions are discussed in detail. It is the purpose of the present paper to present in as simple a manner as possible some of the interesting results obtained by Doctor Munk's methods.

Report No. 214, entitled "Wing Spar Stress Charts and Wing Truss Proportions," by Edward P. Warner, Massachusetts Institute of Technology.—In order to simplify the calculation of beams continuous over three supports, a series of charts have been calculated giving the bending moments at all the critical points and the reactions at all supports for such members. Using these charts as a basis, calculations of equivalent bending moments, representing the total stresses acting in two bay-wing trusses of proportions varying over a wide range, have been determined, both with and without allowance for column effect. This leads finally to the determination of the best proportions for any particular truss or the best strut locations in any particular airplane. The ideal proportions are found to vary with the thickness of the wing section used, the aspect ratio, and the ratio of gap to chord.

Report No. 215, entitled "Air Forces, Moments, and Damping on Model of Fleet Airship *Shenandoah*," by A. F. Zahm, R. H. Smith, and F. A. Loudon.—To furnish data for the design of the fleet airship *Shenandoah*, a model was made and tested in the 8 by 8 foot wind tunnel for wind forces, moments, and damping, under conditions described in this report. The results are given for air of standard density. $\rho = 0.00237$ slugs per cubic foot without VL/v correction, and with but a brief discussion of the aerodynamic design features of the airship. This account

is a slightly revised form of Report No. 195, prepared for the Bureau of Aeronautics, July 22, 1922, and by it submitted for publication to the National Advisory Committee for Aeronautics.

Report No. 216, entitled "The Reduction of Airplane Flight Test Data to Standard Atmosphere Conditions," by Walter S. Diehl and E. P. Lesley.—This paper was prepared for the National Advisory Committee for Aeronautics in order to supply the need of practical methods of reducing observed performance to standard conditions with a minimum of labor. The first part gives a very simple approximate method of reducing performance in climb, and is particularly adapted to work not requiring extreme accuracy. The second part gives a somewhat more elaborate and more accurate method which is well suited to general flight test reduction. The third part gives the conventional method of calibrating air-speed indicators and reducing the indicated speeds to true air speeds. An appendix gives working tables and charts for the standard atmosphere.

Report No. 217, entitled "Preliminary Wing Model Tests in the Variable-Density Wind Tunnel of the National Advisory Committee for Aeronautics," by Max M. Munk.—This report contains the results of a series of tests with three wing models. By changing the section of one of the models and painting the surface of another, the number of models tested was increased to five. The tests were made in order to obtain some general information on the air forces on wing sections at a high Reynolds number and in particular to make sure that the Reynolds number is really the important factor, and not other things like the roughness of the surface and the sharpness of the trailing edge.

The few tests described in this report seem to indicate that the air forces at a high Reynolds number are not equivalent to respective air forces at a low Reynolds number (as in an ordinary atmospheric wind tunnel). The drag appears smaller at a high Reynolds number and the maximum lift is increased in some cases. The roughness of the surface and the sharpness of the trailing edge do not materially change the results, so that we feel confident that tests with systematic series of different wing sections will bring consistent results, important and highly useful to the designer.

Report No. 218, entitled "Standard Atmosphere—Tables and Data," by Walter S. Diehl.—This report is an extension of National Advisory Committee for Aeronautics Report No. 147. Detailed tables of pressures and densities are given for altitudes up to 20,000 meters and to 65,000 feet. In addition to the tables the various data pertaining to the standard atmosphere have been compiled in convenient form for ready reference.

Report No. 219, entitled "Some Aspects of the Comparison of Model and Full-Scale Tests," by D. W. Taylor.—This paper was delivered before the Royal Aeronautical Society as the 1925 Wilbur Wright Memorial Lecture. It treats the subject of scale effect from the standpoint of the engineer rather than the physicist, in that it shows what compromises are necessary to secure satisfactory engineering model test data and how these test data compare with full scale or with theoretical values. The paper consists essentially of three parts: (1) A brief exposition of the theory of dynamic similarity, (2) application of the theory to airplane model tests, illustrated by test data on airfoils from the National Advisory Committee for Aeronautics variable-density wind tunnel, and (3) application of the theory to propeller testing, illustrated by comparisons of model and full-scale results.

Report No. 220, entitled "Comparison of Tests on Airplane Propellers in Flight with Wind Tunnel Model Tests on Similar Forms," by W. F. Durand and E. P. Lesley.—The purpose of this investigation, which is the subject of this report, was to determine the performance, characteristics, and coefficients of full-sized air propellers in flight and to compare these results with those derived from wind-tunnel tests on reduced scale models of similar geometrical form.

The full-scale equipment comprised five propellers in combination with a VE-7 airplane and Wright E-4 engine. This part of the work was carried out at the Langley Memorial Aeronautical Laboratory, between May 1 and August 24, 1924, and was under the immediate charge of Mr. Lesley. The model or wind-tunnel part of the investigation was carried out at the aerodynamic laboratory of Stanford University and was under the immediate charge of Doctor Durand.

A comparison of the curves for full-scale results with those derived from the model tests shows that while the efficiencies realized in flight are close to those derived from model tests, both thrust developed and power absorbed in flight are from 6 to 10 per cent greater than would be expected from the results of model tests.

Report No. 221, entitled "Model Tests with a Systematic Series of 27 Wing Sections at Full Reynolds Number," by Max M. Munk and Elton W. Miller.—A systematic series of 27 wing sections, characterized by a small travel of the center of pressure, have been investigated at 20 atmospheres pressure in the variable-density wind tunnel of the National Advisory Committee for Aeronautics.

The results are consistent with each other, and indicate that for such "stable" sections a small effective camber, a small effective S-shape and a thickness of 8 to 12 per cent lead to good aerodynamic properties.

Report No. 222, entitled "Spray Penetration with a Simple Fuel Injection Nozzle," by Harold E. Miller and Edward G. Beardsley.—The tests covered by this report form a part of a general investigation of the application of fuel injection engine principles to aircraft engine service. The purpose of these tests was to obtain specific information on the rate of penetration of the spray from a simple injection nozzle, having a single orifice with a diameter of 0.015 inch when injecting into compressed gases.

The fuel was sprayed into a chamber fitted with glass walls and filled with nitrogen at various pressures. Special high-speed photographic apparatus, capable of taking a continuous series of 15 photographs at a rate of 4,000 per second, was used to record the development of single sprays. The effects of fuel pressures from 2,000 to 8,000 pounds per square inch and chamber pressures from atmospheric to 300 pounds per square inch on the rate of penetration and the development of the spray were studied.

The results have shown that the effects of both chamber and fuel pressures on penetration are so marked that the study of sprays by means of high-speed photography or its equivalent is necessary if the effects are to be appreciated sufficiently to enable rational analysis. It was found for these tests that the negative acceleration of the spray tip is approximately proportional to the 1.5 power of the instantaneous velocity of the spray tip.

Report No. 223, entitled "Pressure Distribution on the C-7 Airship," by J. W. Crowley, jr., and S. J. DeFrance.—This investigation was made by the National Advisory Committee for Aeronautics at the request of the Bureau of Aeronautics, Navy Department, for the purpose of determining the aerodynamic pressure distribution encountered on a "C" class airship in flight. It was conducted in two parts: (a) Tests on the tail surfaces in which the pressures at 201 points were measured and (b) tests on the envelope in which 190 points were used, both tests being made under as nearly identical flight conditions as possible, so that the results could be combined and the pressure distribution over the entire airship obtained.

The method of testing consisted of measuring the pressure by means of orifices located at the desired points connected to the tubes of a multiple liquid manometer. Simultaneous readings of all the pressures were obtained by photographing the manometer.

The results as presented in this report are mainly in tabular form and may be very briefly summarized as follows:

- (1) The maximum local pressure encountered on a tail surface was 7.3 lb./sq. ft.
- (2) The maximum total normal force on a complete tail surface was 352 pounds or a C_{NF} of 0.316 occurring on the bottom fin and rudder during a "reversal" of the rudder.
- (3) The maximum moment of the tail surface forces about the center of buoyancy was 37,200 lb.-ft.
- (4) The investigation of the envelope pressures, while showing the general distribution of pressure satisfactorily, is practically useless in the determination of total aerodynamic forces on the airship.
- (5) It is concluded that the pressures set up by a bump are larger than those obtained in maneuvering.

Report No. 224, entitled "An Investigation of the Coefficient of Discharge of Liquids through Small Round Orifices," by W. F. Joachim.—The work covered by this report was

undertaken in connection with a general investigation of fuel injection engine principles as applied to engines for aircraft propulsion, the specific purpose being to obtain information on the coefficient of discharge of small round orifices suitable for use as fuel injection nozzles.

Flow of the liquids tested under high pressure was obtained with an intensifier consisting of a 5-inch piston driving a direct connected 3/4-inch hydraulic plunger. The large piston was operated by compressed air and the time required for the displacement of a definite volume by the hydraulic plunger was measured with an electrically operated stop watch. The coefficients were determined as the ratio of the actual to the theoretical rate of flow where the theoretical flow was obtained by the usual simple formula for the discharge of liquids through orifices.

Values for the coefficient were determined for the more important conditions of engine service such as discharge under pressures up to 8,000 pounds per square inch, at temperatures between 80° and 180° F. and into air compressed to pressures up to 1,000 pounds per square inch. The results show that the coefficient ranges between 0.62 and 0.88 for the different test conditions between 1,000 and 8,000 pounds per square inch hydraulic pressure. At lower pressures the coefficient increases materially.

It is concluded that within the range of these tests and for hydraulic pressures above 1,000 pounds per square inch the coefficient does not change materially with pressure or temperature; that it depends considerably upon the liquid, decreases with increase in orifice size, and increases in the case of discharge into compressed air until the compressed-air pressure equals approximately three-tenths of the hydraulic pressure, beyond which pressure ratio it remains practically constant.

Report No. 225, entitled "The Air Forces on a Model of the Sperry Messenger Airplane Without Propeller," by Max M. Munk and Walter S. Diehl.—This is a report on a scale-effect research which was made in the variable-density wind tunnel of the National Advisory Committee for Aeronautics at the request of the Army Air Service. A $\frac{1}{16}$ -scale model of the Sperry Messenger airplane with USA-5 wings was tested without a propeller at various Reynolds numbers up to the full scale value. Two series of tests were made: The first on the original model which was of the usual simplified construction, and the second on a modified model embodying a great amount of detail.

While this report is of a preliminary nature, the work has progressed far enough to show that the scale effect is almost entirely confined to the drag. In the tests so far conducted, the drag at any given angle of attack within the normal flying range is found to vary as $\left(\frac{VL}{v}\right)^n$. The exponent n is constant for any one angle of attack, and ranges from -0.045 at large angles of attack to -0.17 at small angles.

It was also found that the model should be geometrically similar to the full-scale airplane if the test data are to be directly applicable to full scale. If the condition of geometric similarity be fulfilled, the data obtained at a full-scale value of Reynolds number agree very closely with free-flight data. The variable-density wind tunnel, therefore, appears to be a very promising instrument for procuring test data free from scale effect. It is also admirably suited for studying the scale effect and obtaining information which is necessary in an interpretation of the results obtained in atmospheric wind tunnels at low values of Reynolds number.

Report No. 226, entitled "Characteristics of a Boat-Type Seaplane During Take-Off" by J. W. Crowley, jr., and K. M. Ronan.—This report, on the planing and get-away characteristics of the *F-5-L*, gives the results of the second of a series of take-off tests on three different seaplanes conducted by the National Advisory Committee for Aeronautics at the suggestion of the Bureau of Aeronautics, Navy Department. The single-float seaplane was the first tested and the twin-float seaplane is to be the third.

The characteristics of the boat type were found to be similar to the single float, the main difference being the increased sluggishness and the relatively larger planing resistance of the larger seaplane. At a water speed of 15 miles per hour the seaplane trims aft to about 12° and remains in this angular position while plowing. At 2.25 miles per hour the planing stage is

started and the planing angle is immediately lowered to about 10° . As the velocity increases the longitudinal control becomes more effective but overcontrol will produce instability. At the get-away the range of angle of attack is 19° to 11° with velocities from the stalling speed through about 25 per cent of the speed range.

Report No. 227, entitled "The Variable-Density Wind Tunnel of the National Advisory Committee for Aeronautics," by Max M. Munk and Elton W. Miller.—This report contains an exact description of the new wind tunnel of the National Advisory Committee for Aeronautics. This is the first American type wind tunnel. It differs from ordinary wind tunnels by its being surrounded by a strong steel shell, 35 feet long and 15 feet in diameter. A compressor system is provided to fill this shell—and hence the entire wind tunnel—with air compressed to a density up to 25 times the ordinary atmospheric density.

It is demonstrated in the report that the increase of the air density makes up for a corresponding decrease in the scale of the model. Hence such American type wind tunnel is free from scale effect.

The report is illustrated by many drawings and photographs. All construction details are described, and many dimensions given.

The method of conducting tests is also described and some preliminary results given in the reports. So far, the tests have confirmed the chief feature of this wind tunnel—absence of scale effect.

Report No. 228, entitled "A Study of the Effect of a Diving Start on Airplane Speed," by Walter S. Diehl.—Equations for instantaneous velocity and distance flown are derived for an airplane which crosses the starting line of a speed course at a speed higher than that which can normally be maintained in horizontal flight. A specific case is assumed and calculations made for five initial velocities. Curves of velocity, average velocity, and distance flown are plotted against time for each case and analyzed. It is shown that the increase in average velocity due to a diving start may be very large for short-speed courses.

Report No. 229, entitled "Pressure Distribution over Thick, Tapered Airfoils, N. A. C. A. 81, U. S. A. 27 C Modified, and U. S. A. 35," by Elliott G. Reid.—At the request of the United States Army Air Service, the tests reported herein were conducted in the 5-foot atmospheric wind tunnel of the Langley Memorial Aeronautical Laboratory. The object was the measurement of pressures over three representative thick, tapered airfoils which are being used on existing or forthcoming Army airplanes. The results are presented in the form of pressure maps, cross-plan load and normal force coefficient curves and load contours.

The pressure distribution along the chord was found very similar to that for thin wings, but with a tendency toward greater negative pressures. The characteristics of the loading across the span of the U. S. A. 27 C Modified are inferior to those of the other two wings; in the latter the distribution is almost exactly elliptical throughout the usual range of flying angles.

The form of tip incorporated in these models is not completely satisfactory and a modification is recommended.

Report No. 230, entitled "Description and Laboratory Tests of a Roots Type Aircraft Engine Supercharger," by Marsden Ware.—This report describes a Roots type aircraft engine supercharger and presents the results of some tests made with it at the Langley Field laboratories of the National Advisory Committee for Aeronautics. The supercharger used in these tests was constructed largely of aluminum, weighed 88 pounds and was arranged to be operated from the rear of a standard aircraft engine at a speed of $1\frac{1}{2}$ engine crankshaft speed. The rotors of the supercharger were cycloidal in form and were 11 inches long and $9\frac{1}{2}$ inches in diameter. The displacement of the supercharger was 0.51 cubic feet of air per revolution of the rotors.

The supercharger was tested in the laboratory, independently and in combination with a Liberty-12 aircraft engine, under simulated altitude pressure conditions in order to obtain information on its operation and performance. During an investigation of the influence on the operation of the engine of various types of air-duct connections between the supercharger and the engine, the supercharger was subjected to considerable rough treatment, which it endured very well, so that it seems apparent that the supercharger could well endure service handling. By the

proper portioning of the air-duct system the engine would operate at all speeds as smoothly and free from vibration as the normal engine.

From these tests it seems evident that the Roots blower compares favorably with other compressor types used as aircraft engine superchargers and that it has several features that make it particularly attractive for such use.

Report No. 231, entitled "Investigation of Turbulence in Wind Tunnels by a Study of the Flow about Cylinders," by H. L. Dryden and R. H. Heald.—With the assistance and cooperation of the National Advisory Committee for Aeronautics the Bureau of Standards has been engaged for the past year in an investigation of turbulence in wind tunnels, especially in so far as turbulence affects the results of measurements in different wind tunnels.

Two methods of making such studies are described in this report together with the results of the use in the 54-inch wind tunnel of the Bureau of Standards. The first method consists in measuring the drag of circular cylinders; the second in measuring the static pressure at some fixed point. Both methods show that the flow is not entirely free from irregularities.

Report No. 232, entitled "Fuels for High Compression Engines," by Stanwood W. Sparrow, Bureau of Standards.—From theoretical considerations one would expect an increase in power and thermal efficiency to result from increasing the compression ratio of an internal combustion engine. In reality it is upon the expansion ratio that the power and thermal efficiency depend, but since in conventional engines this is equal to the compression ratio, it is generally understood that a change in one ratio is accompanied by an equal change in the other. Tests over a wide range of compression ratios (extending to ratios as high as 14.1) have shown that ordinarily an increase in power and thermal efficiency is obtained as expected provided serious detonation or preignition does not result from the increase in ratio.

There are marked differences between fuels as regards the conditions under which they detonate or preignite. It follows that the employment of a high compression ratio is contingent upon securing a fuel which is suitable in its resistance to preignition and detonation and which at the same time possesses the other qualities essential to a satisfactory engine fuel.

This report is based very largely upon tests made at the Bureau of Standards during 1922, 1923, and 1924. It emphasizes the fact that there may be a difference between a fuel's ability to resist detonation and its ability to resist preignition. Although this report is primarily a general discussion of the properties essential to a satisfactory fuel for high-compression engines, certain fuels, benzol and alcohol in particular, are discussed in some detail.

LIST OF TECHNICAL NOTES ISSUED DURING THE PAST YEAR

- | | |
|------|---|
| No. | |
| 205. | The Logarithmic Polar Curve—Its Theory and Application to the Predetermination of Airplane Performance. By Val Cronstedt. |
| 206. | Structural Weight of Aircraft as Affected by the System of Design. By Charles Ward Hall. |
| 207. | The Simplifying Assumptions, Reducing the Strict Application of Classical Hydrodynamics to Practical Aeronautical Computations. By Max M. Munk. |
| 208. | Tests on Duralumin Columns for Aircraft Construction. By John G. Lee. |
| 209. | Tests of Rotating Cylinders. By Elliott G. Reid. |
| 210. | The Testing of Aviation Engines under Approximate Altitude Conditions. By R. N. DuBois. |
| 211. | Aircraft Engine Design. By E. E. Wilson. |
| 212. | Simplified Propeller Design for Low-Powered Airplanes. By Fred E. Weick. |
| 213. | Discharge Characteristics of a High Speed Fuel Injection System. By Robertson Matthews. |
| 214. | Note on the Katzmayer Effect on Airfoil Drag. By Shatswell Ober. |
| 215. | The Calculation of Wing-Float Displacement in Single-Float Seaplanes. By Edward P. Warner. |
| 216. | The Velocity Distribution Caused by an Airplane at the Points of a Vertical Plane Containing the Span. By Max M. Munk. |

No.

217. Note on the Air Forces on a Wing Caused by Pitching. By Max M. Munk.
218. The Estimation of Airplane Performance from Wind-Tunnel Tests on Conventional Airplane Models. By Edward P. Warner and Shatswell Ober.
219. The Comparison of Well-Known and New Wing Sections Tested in the Variable-Density Wind Tunnel. By George J. Higgins.
220. The Drift of an Aircraft Guided Toward its Destination by Directional Receiving of Radio Signals Transmitted from the Ground. By Edward P. Warner.
221. Model Tests on the Economy and Effectiveness of Helicopter Propellers. By Max M. Munk.
222. Air Flow Investigation for Location of Angle of Attack Head on a JN-4h Airplane. By R. G. Freeman.
223. Determination of the Lift and Drag Characteristics of an Airplane in Flight. By Maurice W. Green.
224. Pressure Distribution on the Nose of an Airship in Circling Flight. By Karl J. Fairbanks.
225. Propeller Scale Effect and Body Interference. By Fred E. Weick.
226. Wind-Tunnel Tests of Fuselages and Windshields. By Edward P. Warner.
227. Determination and Classification of the Aerodynamic Properties of Wing Sections. By Max M. Munk.

LIST OF TECHNICAL MEMORANDUMS ISSUED DURING THE PAST YEAR

281. Combustion of Liquid Fuels in Diesel Engine. By Otto Alt. Translated from "Zeitschrift des Vereines deutscher Ingenieure," July 14, 1923.
282. Results of Experiments with Slotted Wings. By G. Lachmann. Translated from "Zeitschrift für Flugtechnik und Motorluftschiffahrt," May 26, 1924.
283. Mooring Airships. By G. A. Crocco. Translated from "Note di Tecnica Aeronavale," 1923.
284. Duralumin, Its Properties and Uses. By R. Beck. Translated from "Zeitschrift für Metallkunde," April, 1924.
285. Calculation of the Hull and of the Car-Suspension Systems of Airships. By R. Verduzio. Translated from "Rendiconti Tecnici," March 15, 1924.
286. The American Airship ZR-3. By L. Dürr. Translated from "Zeitschrift des Vereines deutscher Ingenieure," May 31, 1924, Vol. 68, No. 22.
287. Effect of Altitude on Power of Aviation Engines. By Italo Raffaelli. Translated from "Rendiconti Tecnici," July 15, 1924.
288. Stieber Dynamometer Hub for Aircraft Propellers. By W. Stieber. Translated from "Zeitschrift für Flugtechnik und Motorluftschiffahrt," April 26, 1924.
289. Two-Seat Light Airplanes which Participated in Contest held at Lympne, England, Week of September 29, to Oct. 4, 1924. Taken from "Flight," September 25, October 2 and 9, and from "Aeroplane," September 24, October 1, 8, and 15, 1924. Compiled by N. A. C. A.
290. Aviation Engines in the Endurance Contest. By G. Lehr. Translated from "L'Aéronautique," July, 1924.
291. Measuring Vibration and Torque with the Oscillograph. By R. Elsasser. Translated from "Zeitschrift des Vereines deutscher Ingenieure," May 17, 1924.
292. The Aerodynamic Laboratory of the Belgian "Service Technique de L'Aéronautique." Translated from "Bulletin du Service Technique de L'Aéronautique," May, 1924.
293. Nomogram for Correcting Drag and Angle of Attack of an Airfoil Model in an Air Stream of Finite Diameter. Translated from Report A 58 of the "Rijks-Studiedienst voor de Luchtvaart," reprinted from "De Ingenieur," September 20, 1924.
294. Motive Power Required to Operate a Wind Tunnel. By S. Ziembinski. Translated from "L'Aérophile," August and September, 1924.
295. Hulls for Large Seaplanes. By Giulio Magaldi. Translated from "La Technique Aéronautique," October 15, 1924.

No.

296. Experimental Determination of Pressure Drop Caused by Wire Gauze in an Air Stream. Translated from Report A 77 of the "Rijks-Studiedienst voor de Luchtvaart," reprinted from "De Ingenieur," August 9, 1924.
297. Royal Aero Club Light Aeroplane Competition. By J. S. Buchanan. Paper read before the Royal Aeronautical Society, October 30, 1924.
298. Results of Recent Experiments with Slotted Wings. By G. Lachmann. Translated from "Zeitschrift für Flugtechnik und Motorluftschiffahrt," August 26 and September 26, 1924.
299. Determination of Ignition Points of Liquid Fuels Under Pressure. By J. Tausz and F. Schulte. Translated from "Zeitschrift des Vereines deutscher Ingenieure," May 31, 1924.
300. Pressure Distribution on Fuselage of Airplane Model. Translated from Report A 33 of the "Rijks-Studiedienst voor de Luchtvaart," Amsterdam, reprinted from "De Ingenieur," of January 26, 1924.
301. Light Airplanes of France, Germany, Italy, Belgium, Holland, Czechoslovakia and Lithuania. Compiled by the National Advisory Committee for Aeronautics.
302. Effect of Speed on Economy of Airship Traffic. By W. Bleistein. Translated from "Zeitschrift für Flugtechnik und Motorluftschiffahrt," October 28, December 13 and 27, 1924.
303. Pitot-Static Tubes for Determining the Velocity of Air. By H. Kumbruch. Translated from "Forschungsarbeiten aus dem Gebiete des Ingenieurwesens," 1921, No. 240.
304. Suggestions for Courses of Instruction in Aviation. By Professor Poeschel. Translated from "Luftfahrt," December 5, 1924.
305. Calculation of Wing Spars of Variable Cross-Section and Linear Load. By Leon Kirste. Translated from "L'Aéronautique," January, 1925.
306. Altitude of Equilibrium of an Airship. By Umberto Nobile. Translated from "Rendiconti Tecnici," November 15, 1924.
307. Preliminary Investigation of the Effect of a Rotating Cylinder in a Wing. By E. B. Wolff. Translated from Report A 96 of the "Rijks-Studiedienst voor de Luchtvaart," Amsterdam. Reprinted from "De Ingenieur," No. 49, December 6, 1924.
308. Law of Similitude for the Surface Resistance of Laquered Planes Moving in a Straight Line Through Water. By Frederich Gebers. Translated from "Schiffbau," Vol. 22, 1921, Nos. 29, 30, 31, 32, 33, 35, and 37.
309. Light Aeroplane Engine Development. By Lieut. Col. L. F. R. Fell. Paper read at a joint meeting of the Royal Aeronautical Society and of the Institution of Automobile Engineers, February 19, 1925.
310. The "Magnus Effect," the Principle of the Flettner Rotor. By A. Betz. Translated from "Zeitschrift des Vereines deutscher Ingenieure," January 3, 1925.
311. The Light Airplane. By Ivan H. Driggs. Brief Review of the Results Obtained in the Development of Light Airplanes—I. Modern Theoretical Aerodynamics as Applied to Light Airplane Design—II. Reprinted from "The Slipstream Monthly," December, 1924, and January, 1925.
312. Hesselman Heavy-Oil High-Compression Engine. By K. J. E. Hesselman. Translated from "Zeitschrift des Vereines deutscher Ingenieure," July, 1923.
313. Structural Methods Employed by the Schutte-Lanz Airship Company. By Chief Engineer Gentzeke of the S-L Airship Co. Translated from "Zeitschrift für Flugtechnik und Motorluftschiffahrt," May 15, 1924.
314. Alloys Similar to Duralumin Made in Other Countries Than Germany. By K. L. Meissner. Translated from "Zeitschrift für Metallkunde," 1925.
315. The Problem of Fuel Measurement (The Schiske "Konsummeter"). By K. R. H. Praetorius. Translated from "Der Motorwagen," March 31, 1925.
316. European Commercial Aeronautics. By Lieut. J. Parker Van Zandt.

- No.
317. Air Forces on Airfoils Moving Faster than Sound. By J. Ackeret. Translated from "Zeitschrift für Flugtechnik und Motorluftschiffahrt," February 14, 1925.
 318. High-Velocity Wind Tunnels. (Their Application to Ballistics, Aerodynamics, and Aeronautics.) By E. Huguenard. Translated from "La Technique Aéronautique," Nos. 37-38, November 15 and December 15, 1924.
 319. Report on Commercial Air Transportation Activities in England, France, Germany, and Holland. By Lieut. J. Parker Van Zandt. Prepared for the U. S. Army Air Service.
 320. The "Navigraph." By Ives Le Prieur. Translated from "L'Illustration," April 14, 1925.
 321. Increasing the Power of Internal Combustion Engines. By Georg Prayer. Translated from "Der Motorwagen," September 30, 1924.
 322. Airplane Parachutes. By Lieutenant Mazer. Translated from "Bulletin Technique." August, 1924, of the Service Technique de L'Aéronautique, France.
 323. Recent Experiments at the Göttingen Aerodynamic Institute. By J. Ackeret. Translated from "Zeitschrift für Flugtechnik und Motorluftschiffahrt," February 14, 1925.
 324. Relation of "Lilienthal Effect" to Dynamic Soaring Flight. By Roderich Fick. Translated from "Zeitschrift für Flugtechnik und Motorluftschiffahrt," November 28 and December 12, 1924.
 325. Computation of Cantilever Airplane Wings. By K. Thalau. Translated from "Zeitschrift für Flugtechnik und Motorluftschiffahrt," May 26, 1924.
 326. The Light Airplane. By Ivan H. Driggs. Modern Theoretical Aerodynamics as Applied to Light Airplane Design with a Series of Charts—III. Design of an Airplane with Reference to Physical Dimensions, Component Weights and Disposition of Surfaces—IV. Design of an Airplane with Reference to Balance, Distribution of Weights and Moments—V. Reprinted from "The Slipstream Monthly," February, April, and July, 1925.
 327. Latécoère Air Lines. Prepared for U. S. Army Air Service by Lieut. J. Parker Van Zandt.
 328. Preliminary Report on British Commercial Aeronautics. Prepared for U. S. Army Air Service by Lieut. J. Parker Van Zandt.
 329. Atomization of Liquid Fuels. By Dr. R. Kuehn. Part I—Relation Between Atomization and Combustion. Methods Employed for Determining the Size of Particles and Small Drops. Choice of Experimental Method. Translated from "Der Motorwagen," July 10 and 20, 1924.
 330. Atomization of Liquid Fuels. By Dr. R. Kuehn. Part II—Description of Apparatus. Fuels Tested. Atomization Experiments. Discharge Measurements. Atomization. Translated from "Der Motorwagen," October 10 and 20, and November 30, 1924.
 331. Atomization of Liquid Fuels. By Dr. R. Kuehn. Part III—Critical Discussion of Experimental Results. Mixing the Atomized Fuel with Air. Translated from "Der Motorwagen," December 10, 1924, January 20 and February 10, 1925.

BIBLIOGRAPHY OF AERONAUTICS

During the year 1924 the committee issued a bibliography of aeronautics for the years 1920 and 1921 in one volume, and also a bibliography for 1922. It had previously issued bibliographies for the years 1909 to 1916 and 1917 to 1919. Bibliographies for the years 1923 and 1924, which are now in the hands of the printer, will be issued in separate volumes and should be ready for distribution during the coming year. An annual bibliography will be published hereafter by the committee.

Citations of the publications of all nations are included in the language in which the publications originally appeared. The arrangement is in dictionary form, with author and subject entry, and one alphabetical arrangement. Detail in the matter of subject reference has been omitted on account of cost of presentation, but an attempt has been made to give sufficient cross reference to make possible the finding of items in special lines of research.

PART V

THE PRESENT STATUS OF AVIATION

THE PRESENT STATE OF TECHNICAL DEVELOPMENT

AERODYNAMICS.—Satisfactory progress has been made in the science of aerodynamics during the past year. It is gratifying to note that this progress not only includes the development of basic theories of air flow but also the practical applications of these theories. In the latter field the recent progress has been rapid and still further practical applications may confidently be expected. The most notable example of the recent adaptation of theory to practical problems is probably to be found in the Prandtl-Munk equations, which enable the drag of any system of wings to be calculated from monoplane-test data.

The progress which has been made in the technique and interpretation of wind-tunnel tests closely parallels that made in pure and applied theory. In particular, the limitations of the atmospheric wind tunnel, the corrections which must be applied for the interference between the model and the tunnel walls, the requirements which must be met in model construction, and the securing of full-scale data are problems which appear to have been successfully solved, and the solutions will have an important influence on wind-tunnel investigations in the future. One important result of wind-tunnel investigation has been the development of a number of remarkably efficient wing sections of adequate thickness for economical structures. It is desirable that this development continue substantially along the present course.

There has recently been made available through the various research laboratories and organizations a large volume of airplane propeller data obtained from systematic tests in which all of the major elements of design are treated. These tests determine the effects not only of blade interference, blade shape, camber, pitch-diameter ratio, etc., but also of interference between the propeller and objects in its slip stream. The knowledge of interference effects is of value to the propeller designer, since it enables him to obtain satisfactory results from a single design instead of following the cut-and-try methods involving from three to six designs. While the progress in propeller design has been rapid, there is considerable information yet to be obtained. This information is of such nature that it is best obtained from full-scale tests either in free flight or in a suitable wind tunnel. Considerable free-flight work has already been done and arrangements have been made to supply facilities for full-scale wind-tunnel tests.

A careful study of the present state of knowledge in aerodynamics discloses a number of lines along which future investigations must be carried out. The most important of these will be described briefly.

More knowledge must be obtained on the forces on an airplane in various maneuvers in order that an efficient structure may be designed to carry these loads. The distribution of the loading is particularly important. For example, free flight pressure distribution tests have shown the resultant forces to be substantially those used in design, but, owing to surprising irregularities in distribution, the local loadings sometimes are more than twice as great as the maximum values used in design. A large field for research lies along this line.

The subject of control of airplanes in flight is of primary importance, not only from the standpoint of adequate strength of the control surface, but also from the consideration of adequate control. Several cases of failure of control surfaces have occurred in flight during the past three years. Service operation and flight tests have revealed high local loadings in certain maneuvers on airplanes of the pursuit type. This knowledge is now being applied to current designs, but more information is required.

In regard to the inadequacy of control, the limitations imposed by the inherently indefinite nature of the problem make its solution difficult. It is difficult to define adequate control just as it is difficult to define controllability or maneuverability. Every pilot and every engineer can perhaps find a definition which answers his own requirements, but universal agreement can not be expected. However, the problem can be resolved into three general divisions, as follows:

(1) Control and design characteristics, that is, relations between control and the design characteristics such as the span, chord section, and arrangement of the wings, the location of the center of gravity, the size and location of tail surfaces, the size and shape of the fuselage, etc. Valuable work has been done along this line, but a thorough systematic research is needed.

(2) Controllability and maneuverability: Some airplanes are readily maneuvered into any desired position with very slight effort on the part of the pilot. Other airplanes differing but slightly in general appearance either can not be so maneuvered or else require considerable effort on the part of the pilot. A few of the factors which affect controllability and maneuverability are known, but more complete information is necessary unless the design of pursuit airplanes is to remain an art instead of developing into a science.

(3) Control at low speeds: This is a matter of vital importance for commercial aviation. The subject is now receiving concentrated attention abroad and considerable work has been done in this country. Recent progress has been of such a nature that several solutions now appear available. The goal of the engineer is, of course, to free the airplane entirely from the danger of a crash due to loss of control following a stall at low altitudes. Two methods of attack are available—one to prevent the stall, the other to provide adequate control of the airplane in the stalled condition.

The problem of wing or control surface flutter seems to have been satisfactorily solved through wind tunnel tests, both as to causes and as to prevention. The primary cause appears to be one of relative stiffness or flexibility, and by a suitable proportion of stiffness in any particular case, flutter may be prevented. However, its complete elimination is not to be expected until an exhaustive treatment is made available to designers who will take the necessary precautions in design.

Another subject of considerable importance is the limitations imposed on airplane performance by the design requirements. These limitations are not as widely known as they should be. Consequently, some designers may claim unreasonable performance for their designs because they have failed to take into consideration certain very important requirements, such as adequate structural strength and stiffness. A clear and complete statement of design requirements should be prepared for the information of all designers. Under the present arrangement most of the needed information is available but not in a convenient form.

AIRPLANE STRUCTURES.—*Trend of design.*—While neither the monoplane nor biplane has gained complete acceptance for any particular use during the past year, out of an increasingly clearer understanding of the relative advantages of the two types there has grown an increased tendency toward standardization. For high speed, either for racing or for pursuit airplanes, the biplane has steadily gained in favor until it dominates that field almost completely, notwithstanding the fact that a monoplane holds the world's record for straight-away speed. Structural difficulties with the monoplane, and particularly the danger of wing flutter, have been largely responsible for its decreased popularity where great speed range is desired. Experience seems to show that for general pursuit use, having regard to the importance of maneuverability and the minimum obstruction of the pilot's vision, a biplane with the lower wing considerably smaller than the upper has proved most successful.

The larger military airplanes are of the biplane type in most cases, partly because of the greater compactness of the biplane of a given area and weight. For naval service especially the last consideration is of vital importance.

For commercial service both monoplanes and biplanes are used, the latter having, in general, the advantage in maneuverability and in compactness of form, but suffering somewhat in aerodynamic efficiency by comparison with the single-wing type. Where speeds are low and

efficiency is the primary requirement, as on the lines of central and western Europe, the monoplane controls the field. The monoplanes now in use are either of all-metal construction or fitted with wings covered with plywood.

In the light airplane the importance of efficiency is such that monoplanes and biplanes of very high aspect ratio have given the best results, the former being in the majority. Aspect ratios in this type of airplane, although well above the average for military machines, are, because of the importance of weight in the light airplane, much lower than had become common in glider construction. There is a general tendency to increase aspect ratios and use thicker airfoil sections in all types, and, except in England, the airfoil section having a maximum thickness of less than 0.09 of the chord has virtually disappeared.

Structural materials.—Metal construction of airplane wings has developed much less rapidly in America than in European countries. The practice of any nation in the design of military airplanes is largely governed by the nature of the materials readily available. In America, with large native spruce forests, wooden wing spars are used in most instances, although there is a steadily increasing interest in metal. In Great Britain steel is commonly employed, while in France, which has native resources for the production of aluminum, duralumin is almost universally employed for wings and fuselages. In Germany duralumin holds first place. Metal covering is little used outside of Germany, where it is universally used.

Fuselage construction is of metal in practically all cases because of its greater durability and better shock-absorbing qualities in case of a crash. In America, the Netherlands, and some of the smaller European countries fuselages are commonly constructed of steel tubes assembled by welding. British practice has also inclined toward steel tubes, but with assembly by pinned fittings, while most of the important continental manufacturers use duralumin, either in tubes or structural forms.

When metal is used in wing construction it may take the form of simple tubes, or, as is the common practice in Great Britain, the alloy steel of thin sheet may be rolled into somewhat complex forms and assembled into spars by riveting.

In landing-gear construction the outstanding development of the year in America has been the trial and rapid recognition of the value of the Oleo gear for shock absorption. Such gears reduce the liability to bouncing and at the same time increase the efficiency of shock absorption and the violence with which the airplane can be brought into contact with the ground without damage.

Small floats are still commonly made of wood, although duralumin is sometimes used. In flying-boat hulls, metal is steadily increasing in popularity, as it has been found that seaworthiness can be improved and the weight decreased. The *PN-9* flying boat which attempted the Hawaiian flight and had to cruise on the surface of the water for a number of days was fitted with a metal hull.

AIRCRAFT ENGINES.—Progress in aircraft engine development in this country is reflected in the fact that we now have proved engines in horsepowers ranging from 60 to 800. In the 60-horsepower class there is the Lawrance 3-cylinder radial "L" type. In the 200-horsepower class there are available the Wright model "E" water-cooled and the Wright model "J" air-cooled engines.

In the 300–400 horsepower field the Curtiss D-12, a 12-cylinder water-cooled engine, is in production and has given excellent performance, particularly in pursuit type airplanes. In the 400–500 horsepower field we have the Liberty, Packard 1A-1500, and Curtiss V-1400 engines. The two Packard 1A-1500 engines, with a gear ratio of 2 to 1, formed the power plants for the two *PN-9*'s on the west coast-Hawaiian flight project. The Curtiss V-1400 engine was installed in the Pulitzer and Schneider cup racers. It gives every indication of being an extremely light and rugged engine.

The Wright model P-2 is now undergoing its dynamometer trials and is giving very satisfactory results. This is a 9-cylinder radial air-cooled engine of 450 horsepower at 1,800 revolutions per minute.

In the 500–600 horsepower class the 12-cylinder T-3 water-cooled engine meets the present requirements. This engine in the past year has been extensively used by the Navy in the three-purpose scout-torpedo-bombing airplane.

In the 600–800 horsepower class the Packard 1A-2500, a 12-cylinder water-cooled engine, has been flown in the PB-1, the Navy's west coast-Hawaiian airplane built by the Boeing Airplane Co., and in the latest Army and Navy bombers.

The Curtiss radial 400-horsepower 9-cylinder air-cooled engine is undergoing its tests at McCook Field. It gives great promise as a light-weight engine.

In the past year strides have been made in the matter of reliability and increased service between overhauls. A life between overhauls from two to four times as great as has been had in previous engines is now being obtained by the Wright model "J" and T-3 engines.

The aeromarine inertia starter has solved the starting problem and is in wide use in the Navy.

AIRSHIPS.—During the past year there has been no new airship construction started in the United States. The technical development of airships has necessarily been confined to experimental investigations and research looking toward the improvement of existing airships.

With the completion of the *RS-1* semirigid airship, constructed for the Army Air Service by the Goodyear Tire & Rubber Co., the Army Air Service now has in its possession the largest semirigid airship in the world. A special subcommittee on the *RS-1* appointed by the National Advisory Committee for Aeronautics to report on the design and construction of semirigid type airships has made its report.

The technical development of airships lags considerably behind that of airplanes. There appear to be two reasons for this—the higher cost of airships, and the longer time taken for construction of airships.

The arrival in the United States of the *ZR-3*, now the U. S. S. *Los Angeles*, on October 15, 1924, after an epoch-making nonstop voyage of 5,600 miles in 81 hours, made the United States the possessor of two rigid type airships. The *Los Angeles* is a splendid example of modern airship design and construction.

In October, 1924, the U. S. S. *Shenandoah* successfully completed a 9,000-mile voyage from Lakehurst to Seattle and return. The airship remained away from her shed almost 20 days, basing on mooring masts, and during the period encountered unfavorable weather. The successful completion of the voyage proved the efficiency of the mooring masts, the soundness of construction of the *Shenandoah*, and the skill of her operators.

The loss of the *Shenandoah* on September 3, 1925, while on a voyage to the Middle West, was a severe blow to airship development. At this time the cause of the accident has not been determined, and it is hoped that the naval court of inquiry, after sifting all the evidence, will be able to determine the cause of the accident.

In the past few years the United States has led the world in experimental research with reference to improved design and operation of airships. The United States has now lost its position to Great Britain, which during the past year has actively pursued research and experimental problems and started the construction of two 5,000,000-cubic-feet rigid airships, one being built by the Government and one by a private manufacturer.

During the past year, however, progress has been made in determining the magnitude of stresses which may be encountered by airships in flight. In June, 1925, preliminary strain-gauge measurements were made on the *Los Angeles* in conjunction with the use of a rate-of-turn indicator. It is proposed to extend this work and in addition to conduct simultaneous pressure-distribution measurements in an effort to fix some relation between aerodynamic loads, magnitude of stress in important structural members, and acceleration in a horizontal or vertical plane as shown by a rate-of-turn indicator or sensitive accelerometer mounted in the airship's control cabin.

Further confirmation of existing design theories has been found through the extended tests carried out on a photoelastic model of the structure of a rigid airship at the Massachusetts Institute of Technology.

The behavior of duralumin and other light alloys under conditions likely to be encountered in airship practice has been investigated. Special study has been given to corrosion or deterioration of these alloys from various causes and possible means for preventing such corrosion or deterioration.

Water recovery apparatus has been improved in type, and with this improvement has come a considerable reduction in weight.

Study has been continued on substitute materials for the expensive goldbeater's skin heretofore considered necessary in gas-cell construction. One type of substitute fabric gave so much promise of success that the Navy Department constructed an experimental full-sized cell for test.

In accordance with legislation recently enacted, the Bureau of Mines, Department of Commerce, on July 1, 1925, took over the control of all matters affecting the conservation and production of helium, including operation of the helium production plant at Fort Worth, Tex., heretofore operated by the Navy Department. Attention has been given to lowering the cost of helium transportation and the Army Air Service and the Navy Department have each purchased a tank car for transporting helium. Each car will carry about 215,000 cubic feet of helium, and the saving in freight charges for a period of about two years will practically pay the cost of the tank car.

Experimental work has been continued toward the development of better means of handling large airships in and out of their sheds and while near the ground. The progress made promises the further development of methods which will materially reduce the number of men required for a handling crew. The success obtained with mooring airships both to stationary masts and to the floating mast on the U. S. S. *Patoka* has been gratifying.

AERONAUTICAL RESEARCH IN THE UNITED STATES

The National Advisory Committee for Aeronautics is charged by law with the supervision and direction of the scientific study of the problems of flight, with a view to their practical solution. The committee is authorized by law to direct and conduct research and experiment in aeronautics in such laboratories as may be placed under the direction of the committee. The membership of the committee and of its technical subcommittees is drawn from the governmental agencies concerned and from private life. The members of the main committee and of all subcommittees serve as such without compensation. It is a matter of gratification that since the creation of the committee no person has ever declined an invitation to serve as a member of either the main committee or one of its subcommittees. The committee has therefore been able to draw upon the best talent in America for the study of the fundamental problems of aeronautics, and in this way it has wielded an influence for the advancement of the science of aeronautics that could not have been secured in any other way. This has been done at the direct cost to the Government that involved only the traveling expenses of the members and the maintenance of a place for meetings.

The way the influence of the National Advisory Committee for Aeronautics is exerted is through discussion by each subcommittee of the new technical problems that are constantly arising in aeronautics, and the preparation of research programs from time to time, which programs invariably indicate the particular laboratory where each investigation recommended can be conducted to the best advantage of the Government. Investigations are assigned both to public and private laboratories in a way that makes for the most effective utilization of existing facilities and the most effective study of the problems. After approval by the main committee, estimates for the prosecution of the research programs are submitted to the Bureau of the Budget, and after the appropriations are made by Congress the investigations are pursued under the general cognizance of the executive committee. The more fundamental investigations, for which facilities do not exist elsewhere, are undertaken in the committee's own laboratory, known as the Langley Memorial Aeronautical Laboratory, located at Langley Field, Va., on a plot of ground set aside for the purpose by the Secretary of War, and on which the necessary buildings have been erected by the committee with appropriations provided for the

purpose by the Congress. Other investigations are assigned, for example, to the Bureau of Standards, to the Forest Products Laboratory, to the Weather Bureau, to the Engineering Division of the Army Air Service, to the Navy, and to various universities having the requisite facilities for the proper study of the particular problems so assigned. This method has proved practical and successful in operation, and has led to the accomplishment of substantial results with a maximum of economy and efficiency.

The committee was created by Congress with the status of an independent Government establishment. It is a service organization, ministering to the needs of the Army, Navy, and Air Mail Service, as well as to the needs of commercial aviation. By virtue of its status, it has been able to initiate and conduct fundamental scientific investigations while at the same time responding to numerous requests from the War and Navy Departments for special investigations in aeronautics.

The committee enjoys many advantages which have contributed to its success. Chief among these may be mentioned the following:

1. The members of the National Advisory Committee and of its standing subcommittees serve without compensation, thus enabling the Government to obtain the services of men who would not otherwise be available for Government service.

2. The committee has the status of an independent Government establishment, and by virtue of such status reports directly to the President, receives its appropriations direct from Congress, and is enabled to initiate and conduct investigations of a truly scientific character, limited only by the funds available.

3. The research laboratories of the committee are located on a flying field, where all phases of the work, including flight operations, are controlled and actually performed by the committee's own technical staff, thus bringing theory and practice together under ideal conditions.

4. The committee has the confidence and support of the Army and Navy Air Services, and is able at all times to obtain any cooperation desired.

The committee has just completed its tenth full year of activity. While the satisfaction of useful service rendered is ample reward, the committee feels especially grateful to the President for his recognition of its services, expressed in his message to Congress transmitting the tenth annual report of the committee on December 8, 1924. It is therefore with pardonable pride that the committee quotes the following extract from that letter of President Coolidge addressed to the Congress of the United States:

"* * * I concur in the committee's general recommendations, and agree that in the last analysis substantial progress in aviation is dependent upon the continuous prosecution of scientific research.

"When the National Advisory Committee for Aeronautics was established by Congress in 1915, there was a deplorable lack of technical information on aeronautics in this country. In submitting this, the tenth annual report of the committee, I feel that it is appropriate to say a word of appreciation of the high-minded and patriotic services of the men who have faithfully served their country without compensation as members of this committee and of its subcommittees. Through this committee the talent of America has been marshaled in the scientific study of the problems of flight, with the result that to-day America occupies a position in the forefront of progressive nations in the technical development of aeronautics. The status of the committee as an independent Government establishment has largely made possible its success.

CALVIN COOLIDGE."

RELATION OF AERONAUTICAL RESEARCH TO NATIONAL DEFENSE

The relation of aeronautical research to national defense is direct, and its relative importance is increasing. This is necessarily so, because every improvement in the performance of aircraft makes the probable rôle of aviation in warfare greater. As the relative importance of aviation increases, it becomes more and more desirable for America to achieve and maintain leadership. As leadership can not be attained in all respects, it becomes of the greatest importance for America to lead in technical development. For ultimate leadership in time of emergency the United States must depend on the results of continuous research and development.

The National Advisory Committee for Aeronautics therefore believes it to be its duty to emphasize the importance of scientific research as the most fundamental activity of the

Government in connection with the development of aeronautics. Closely associated with this is the problem of engineering development of aircraft to meet the special needs of the military and naval services.

While the committee is of the opinion that there should be no monopoly of engineering development, either by the Government or by the industry, it believes that it is desirable, in order to secure the best results, that the actual users of military and naval aircraft should be in close touch with competent aeronautical engineers. As a practical proposition, this can be done only if there are such engineers in the Army and Navy Air Services who are in such close touch with the operators that the latter are able to offer to them constructive criticisms in regard to engineering problems. This would enable the aeronautical engineers of the industry to thoroughly understand the problems presented to them and would prevent them from wasting their energies in attempting to develop military types of airplanes which would not meet the requirements of the services.

Without attempting to be specific, the committee is of the opinion that the military and naval services should maintain aeronautical engineering divisions which should be charged primarily with the formulation of specifications of military aircraft, their characteristics and performance; with the critical examination and testing of designs and of aircraft offered by the industry; and with such experimental and development work as can be carried on by them most effectively and most economically.

THE GENERAL PROBLEM OF AERONAUTICAL ORGANIZATION

In its tenth annual report, for the year 1924, the National Advisory Committee for Aeronautics presented an outline of the organization and functions of the four governmental agencies directly concerned with the use or development of aeronautics—namely, the Army Air Service, the Naval Bureau of Aeronautics, the Air Mail Service, and the National Advisory Committee for Aeronautics.

During the past year, there have been two major investigations of the aeronautical situation—the first by the Congressional Select Committee of Inquiry into Operations of the United States Air Services, created by Resolution No. 192 of the House of Representatives (68th Cong., 1st sess.), of which Representative Florian Lampert, of Wisconsin, is chairman; the second by the special board appointed by President Coolidge on September 12, 1925, known as “The President’s Aircraft Board,” of which Mr. Dwight W. Morrow is chairman. The investigations of the two bodies referred to have gone deeply into all phases of aeronautical activity and governmental organization in aeronautics, including the major problems of the relation of aircraft to national defense; the organization, morale, and sufficiency of air personnel; the maintenance of the aircraft industry; the regulation and encouragement of commercial aviation; the development of airways, etc.

It is to be hoped that the recommendations of these two investigating bodies will receive careful consideration and lead to a settlement of the controversies in aeronautics that have existed since the war. The continued unrest in aeronautical circles has served to focus attention primarily on organization and administrative matters, but has also indirectly brought about a broader recognition of the increasing relative importance of aircraft for purposes of war and of commerce.

In the judgment of the National Advisory Committee for Aeronautics, however, the people of the United States are not so much concerned with the form and administration of the Government’s activities in aeronautics as they are with the question as to whether practical and efficient results are being secured. It is only fair to say that the best results have not been obtained and will not be obtained as long as the personnel are disturbed and their attention distracted from their real duties. It is most desirable, therefore, that measures to improve the situation be formulated and carried into effect without delay. This will enable all who have the best interests of aeronautics at heart to cooperate and settle down to work in harmony with that full measure of devotion to duty which is necessary to bring about the greatest practicable development of aeronautics in America, for both military and commercial purposes.

PROGRESS IN COMMERCIAL AVIATION

The past year was notable as witnessing what may prove to be a real, substantial beginning of commercial aviation in America. The most encouraging factors were the initiative shown by private companies in establishing air lines and the relatively large number of responsible bidders for the carrying of air mail by contract with the Post Office Department. When it is realized that commercial aviation exists in European countries at this time only by virtue of the support of the various governments given through various plans of direct and indirect subsidies, it should be especially gratifying to all concerned with the advancement of aeronautics in this country to feel that the era of commercial aviation on a sound basis is about to dawn in America.

Although the National Advisory Committee for Aeronautics has long been of the opinion that commercial aviation must largely make its own way in America, it believes at the same time that the Government should aid commercial aviation in certain respects where Government aid is practicable and necessary. If, in recognition of this principle, commercial aviation can be successfully developed in America on a firm basis, its development will not be limited, whereas the development of European commercial aviation on a direct subsidy basis is necessarily limited by the nature and extent of the subsidies given. The committee believes that the American policy is sound and in the long run will be more effective in stimulating the substantial development of commercial aviation than will the European policy of direct subsidy.

In spite of this optimistic note, the facts of the situation that must be faced show a number and variety of problems requiring study and solution before commercial aviation can take its proper place in America. The most pressing needs requiring attention at this time are, first, legislation establishing the fundamental right of flight, creating a bureau of air navigation in the Department of Commerce for the regulation and licensing of aircraft, airports, and aviators, and for the establishment, maintenance, and lighting of adequate national airways, and providing for the necessary meteorological information; and, second, the improvement of airplane design and structure with a view primarily to making airplanes safer, more reliable, more controllable at low speeds incident to taking off and landing, and less expensive in initial cost, as well as in the cost of maintenance and operation. There should also be assistance from the other governmental agencies concerned, such as the Hydrographic Office, the Coast and Geodetic Survey, the Weather Bureau, the Lighthouse Service, and the Army and Navy Air Services.

To accomplish the first purpose, legislation is necessary. This has been repeatedly recommended by the National Advisory Committee for Aeronautics and has been indorsed in principle by all agencies of the Government concerned. This question is discussed at length in the report of the committee on civil aviation of the Department of Commerce and American Engineering Council. To accomplish the second purpose requires continuous prosecution of scientific research on the more fundamental problems of flight. This is the definite prescribed function of the National Advisory Committee for Aeronautics, and in the last analysis is necessarily the most fundamental activity in the whole field of aeronautics.

In the past the committee has devoted its attention primarily to the solution of problems arising from the development and use of military and naval types of airplanes and, to a lesser extent, airships. While the basic problems of aerodynamics and of design are the same for military and commercial airplanes, the service requirements as to performance, efficiency, and safety differ. Up to the present time airplanes used for commercial purposes in America have been largely adaptations of military types. This is best evidenced by the fact that the Air Mail Service is still using up war-time DH 4 airplanes with certain modifications.

The committee is of the opinion that with the advent of commercial aviation, a new series of problems peculiar to commercial aircraft will be presented. The committee has therefore decided to hold one or more meetings annually with the engineering representatives of aircraft manufacturing and operating industries, with a view to ascertaining definitely the problems deemed of most vital importance and to incorporating the same, as far as practicable, into the general research programs prepared by the committee.

THE PROBLEM OF THE AIRCRAFT INDUSTRY

In its tenth annual report, the committee outlined the relation of the aircraft industry to national defense, and emphasized the need of maintaining a satisfactory nucleus of an industry. This was defined as "a number of aircraft manufacturers distributed over the country, operating on a sound financial basis, and capable of rapid expansion to meet the Government's needs in an emergency." The committee presented certain definite suggestions of steps to be taken by the Government and by the industry to meet the situation that existed at that time. There has been substantial progress during the past year along the lines outlined by the committee, and it is believed that the condition of the industry and the relations of the Government to the industry have been much improved. The greatest single factor in bringing about this improved condition has been the increased volume of Government orders for aircraft, made possible by increased appropriations and contract authorizations for the purchase of aircraft. The present situation, on the whole, may be regarded as more satisfactory at this time, and as offering promise of further improvement.

THE AIRSHIP PROBLEM

Airships are of three types: Rigid, semirigid, and nonrigid. The value of airships for military or commercial purposes has not as yet been conclusively demonstrated. It can not be said, however, that they are without value, nor that they have no further possibilities than have already been demonstrated. The fact of the matter is that all types of airships are in the experimental stage of development. The recent regrettable loss of the rigid airship *Shenandoah* has been urged as a reason for the Government's abandoning airship development, or at least rigid airship development, on the theory that rigid airships never will be practicable.

The committee fully appreciates the seriousness of the airship situation and believes that despite all that has been done in many countries to develop airships, they are still rather delicate structures. The conclusions of the naval court of inquiry as to the causes for the destruction of the *Shenandoah* have not yet been made public. Regardless, however, of the actual technical causes, the committee is of the opinion that it would be a serious error at this time to adopt a policy of merely marking time in the development of airships. In the judgment of the committee, the time has come to decide to do one of two things, viz, either to carry on with the development of airships or to stop altogether.

The development of rigid airships in America for military and naval purposes has, by joint agreement between the War and Navy Departments, been entrusted to the Navy. The question of continuing their development, however, is not altogether a war problem, for airships of all types have probable applications also for commercial purposes. The question, therefore, whether the Navy should continue with the development of rigid airships at this time should not be determined solely upon considerations of their probable naval usefulness. The Army is directly concerned and the commercial development of airships in America may be said to be also at stake. The problem is therefore a national one. Viewed as such, the Navy becomes, in a peculiar sense, the agent of the whole people in the development of rigid airships. In the last analysis, however, it is for the Congress to determine America's policy with regard to continuing the development of airships. As between the two alternatives of carrying on or stopping altogether, the National Advisory Committee for Aeronautics, after careful consideration of the matter, is of the opinion that the development of airships should be continued.

SUMMARY

There has been continued gratifying progress in the technical development of aircraft. Performance and reliability have increased. The committee's program of research for the coming year promises to add substantially to the store of technical knowledge. There is nothing in sight at this time to indicate the probability of the discovery of a revolutionary principle contributing any great or sudden improvement in aircraft. While progress must be gradual, there is every reason to believe that there will be steady improvement in the performance, efficiency, reliability, and safety of aircraft.

Aviation has become more generally recognized as a weapon indispensable to war operations and as an instrument that gives promise of taking its place in the immediate future in the commercial life of the Nation.

During the past year alone there were three investigations of the aircraft situation. A special committee of the House of Representatives known as the "Lampert Committee," and a special board appointed by President Coolidge known as "The President's Aircraft Board," inquired into all details of the aircraft situation and the aeronautical organization of the Government. A third investigation, limited to civil and commercial aviation, was made by a special committee on civil aviation of the Department of Commerce and American Engineering Council. The recommendations of these bodies should serve to clarify the public mind and to focus attention on the major problems requiring immediate solution. Measures to meet the situation should be formulated and carried into effect without delay. In this connection the National Advisory Committee for Aeronautics reiterates its recommendations of previous years for the creation of a bureau of air navigation in the Department of Commerce to regulate and encourage commercial aviation.

The state of the aircraft industry is gradually improving. The most substantial factors in improving the situation during the past year were the increase in appropriations and contract authorizations for the purchase of aircraft by the War and Navy Departments and the increasingly close liaison between the industry and the Government engineers. With sustained Government patronage on a continuous production basis and with the prospect of a growing commercial demand for aircraft, the condition of the aircraft industry will steadily improve.

Air mail service is no longer a novelty. It is passing out of the experimental stage and becoming a necessity in the daily business life of the Nation. It has reached the point where it has become practicable for private firms to carry air mail under contracts with the Post Office Department. Air transportation of the mails should therefore be extended gradually to meet the requirements of the people in all parts of the country.

CONCLUSION

The committee is of the opinion that America is at least abreast of other progressive nations in the technical development of aircraft for military purposes. The committee is grateful to the President and to the Congress for the support that has been given to scientific research in aeronautics. The committee feels that the continuous and systematic study and investigation of the basic problems of flight is the most fundamental activity of the Government in connection with the development of aeronautics and that the continuance of this work will serve to keep America at least abreast of other progressive nations in the technical development of aircraft for all purposes.

Respectfully submitted.

NATIONAL ADVISORY COMMITTEE FOR AERONAUTICS,
JOSEPH S. AMES, *Chairman, Executive Committee.*

REPORT No. 210

INERTIA FACTORS OF ELLIPSOIDS FOR USE IN AIRSHIP DESIGN

By L. B. TUCKERMAN
Bureau of Standards

REPORT No. 210

INERTIA FACTORS OF ELLIPSOIDS FOR USE IN AIRSHIP DESIGN

By L. B. TUCKERMAN

This report is based on a study made by the writer as a member of the Special Committee on Design of Army Semirigid Airship RS-1 appointed by the National Advisory Committee for Aeronautics.

The increasing interest in airships has made the problem of the potential flow of a fluid about an ellipsoid of considerable practical importance. In 1833 Green,¹ in discussing the effect of the surrounding medium upon the period of a pendulum, derived three elliptic integrals, in terms of which practically all the characteristics of this type of motion can be expressed. The theory of this type of motion is very fully given by Lamb,² and applications to the theory of airships by many writers.³ Tables of the inertia coefficients derived from these integrals are available for the most important special cases.^{4 5} These tables are adequate for most purposes, but occasionally it is desirable to know the values of these integrals in other cases where tabulated values are not available. For this reason it seemed worth while to assemble a collection of formulæ which would enable them to be computed directly from standard tables of elliptic integrals, circular and hyperbolic functions, and logarithms without the need of intermediate transformations. Some of the formulæ for special cases (elliptic cylinder, prolate spheroid, oblate spheroid, etc.) have been published before, but the general forms and some special cases have not been found in previous publications.

The additional inertia of the translational potential flow of a fluid about triaxial ellipsoid is proportional to the three coefficients

$$K_1 = \frac{4\pi}{3} abc k_1, K_2 = \frac{4\pi}{3} abc k_2, K_3 = \frac{4\pi}{3} abc k_3$$

Here $\frac{4\pi}{3} abc$ is the volume of the ellipsoid and

$$k_1 = \frac{\alpha_0}{2 - \alpha_0}, k_2 = \frac{\beta_0}{2 - \beta_0}, k_3 = \frac{\gamma_0}{2 - \gamma_0}$$

The additional moment of inertia of the rotational potential flow is proportional to the three coefficients

$$K'_1 = \frac{4\pi}{3} abc \frac{b^2 + c^2}{5} k'_1, K'_2 = \frac{4\pi}{3} abc \frac{c^2 + a^2}{5} k'_2, K'_3 = \frac{4\pi}{3} abc \frac{a^2 + b^2}{5} k'_3$$

Here k'_1 , k'_2 , and k'_3 are given as factors of the corresponding moments of inertia of the ellipsoid itself and

$$k'_1 = \left(\frac{b^2 - c^2}{b^2 + c^2} \right)^2 \frac{\gamma_0 - \beta_0}{2 \frac{b^2 - c^2}{b^2 + c^2} - (\alpha_0 - \beta_0)}$$

with symmetrical expressions for k'_2 and k'_3 .

¹ George Green: "Researches on the vibration of pendulums in fluid media." Trans. R. S. Ed. 1833.

² Horace Lamb: "Hydrodynamics" (4th ed. Camb. 1916), pp. 132-147.

³ See, for example, Max M. Munk: "The aerodynamic forces on airship hulls." N. A. C. A., Report No. 184, 1924.

⁴ Horace Lamb: "The inertia coefficients of an ellipsoid moving in fluid." G. B. A. C. A., R. & M. No. 623, 1918.

⁵ H. Bateman: "The inertia coefficients of an airship in a frictionless fluid." N. A. C. A., Report No. 164, 1923.

In the above formulæ α_0 , β_0 , and γ_0 are the special values for $\lambda=0$ of Green's integrals

$$\alpha = abc \int_{\lambda}^{\infty} \frac{d\lambda}{(a^2 + \lambda) \Delta}, \quad \beta = abc \int_{\lambda}^{\infty} \frac{d\lambda}{(b^2 + \lambda) \Delta}, \quad \gamma = abc \int_{\lambda}^{\infty} \frac{d\lambda}{(c^2 + \lambda) \Delta}$$

$$a \geq b \geq c \quad \Delta = \sqrt{(a^2 + \lambda)(b^2 + \lambda)(c^2 + \lambda)}$$

To transform these integrals into the standard Legendre form substitute

$$\operatorname{sn}(u; k) = \operatorname{sn} u = \sqrt{\frac{a^2 - c^2}{a^2 + \lambda}}, \quad k^2 = \frac{a^2 - b^2}{a^2 - c^2} < 1, \quad k'^2 = \frac{b^2 - c^2}{a^2 - c^2} < 1$$

This gives

$$a^2 + \lambda = \frac{a^2 - c^2}{\operatorname{sn}^2 u}, \quad b^2 + \lambda = (a^2 - c^2) \frac{\operatorname{dn}^2 u}{\operatorname{sn}^2 u}, \quad c^2 + \lambda = (a^2 - c^2) \frac{\operatorname{cn}^2 u}{\operatorname{sn}^2 u}$$

and

$$\frac{d\lambda}{\Delta} = -\frac{2}{\sqrt{a^2 - c^2}} du$$

Then

$$\alpha = \frac{2abc}{(a^2 - c^2)^{3/2}} \int_0^u \operatorname{sn}^2 u \, du = \frac{2abc}{(a^2 - c^2)^{3/2}} \frac{1}{k^2} [u - E(u)]$$

$$\beta = \frac{2abc}{(a^2 - c^2)^{3/2}} \int_0^u \frac{\operatorname{sn}^2 u}{\operatorname{dn}^2 u} du = \frac{2abc}{(a^2 - c^2)^{3/2}} \frac{1}{k^2 k'^2} \left[E(u) - k'^2 u - k^2 \frac{\operatorname{sn} u \operatorname{cn} u}{\operatorname{dn} u} \right]$$

$$\gamma = \frac{2abc}{(a^2 - c^2)^{3/2}} \int_0^u \frac{\operatorname{sn}^2 u}{\operatorname{dn}^2 u} du = \frac{2abc}{(a^2 - c^2)^{3/2}} \frac{1}{k'^2} \left[\frac{\operatorname{sn} u \operatorname{dn} u}{\operatorname{cn} u} - E(u) \right]$$

Here

$$\frac{\operatorname{sn} u \operatorname{dn} u}{\operatorname{cn} u} = \sqrt{\frac{(a^2 - c^2)(b^2 + \lambda)}{(a^2 + \lambda)(c^2 + \lambda)}}, \quad \frac{\operatorname{sn} u \operatorname{cn} u}{\operatorname{dn} u} = \sqrt{\frac{(a^2 - c^2)(c^2 + \lambda)}{(a^2 + \lambda)(b^2 + \lambda)}}$$

and

$$u = \operatorname{sn}^{-1} \sqrt{\frac{a^2 - c^2}{a^2 + \lambda}} = F(\varphi; k) \quad \text{where } \varphi = \sin^{-1} \sqrt{\frac{a^2 - c^2}{a^2 + \lambda}}$$

The values of $u = F(\varphi; k)$ and $E(u) = E(\varphi; k)$ can be obtained directly from standard tables of elliptic integrals.

NOTE.—The notation of elliptic integrals is not standardized. Some authors write the elliptic integral of the second kind as a function of the amplitude φ . Some write the argument first and the modulus or modular angle second; some reverse the order, and some use one form at one time and another at another. Thus we may find the following forms:

$$u \equiv F(\varphi; k) \equiv F(k; \varphi) \equiv F(\varphi; \theta) \equiv F(\theta; \varphi)$$

$$E(u) \equiv E(u; k) \equiv E(u; \theta) \equiv E(\varphi; k) \equiv E(\varphi; \theta) \equiv E(k; \varphi) \equiv E(\theta; \varphi)$$

The more usual tables tabulate the functions according to the amplitude φ and the modular angle θ so that

$$u \equiv F(\varphi; \theta) \quad E(u) \equiv E(\varphi; \theta)$$

where

$$\varphi = \sin^{-1} \sqrt{\frac{a^2 - c^2}{a^2 + \lambda}}, \quad \theta = \sin^{-1} \sqrt{\frac{a^2 - b^2}{a^2 - c^2}}$$

However, the latest, and for some purposes the most convenient, tables by R. L. Hippisley⁶ tabulate $u = F\varphi = F(\varphi; \theta)$ and $E(u) = E(r) + eE$ according to r , where $r^0 = 90^\circ e = 90^\circ \frac{u}{K}$.

⁶ Smithsonian Mathematical Formulæ (1923), pp. 260-309.

When $\lambda = 0$ the formulæ simplify to

$$\begin{aligned}\alpha_0 &= \frac{2abc}{(a^2 - b^2)(a^2 - c^2)^{1/2}} [u_0 - E(u_0)] \\ \beta_0 &= \frac{2abc(a^2 - c^2)^{1/2}}{(a^2 - b^2)(b^2 - c^2)} \left[E(u_0) - \frac{b^2 - c^2}{a^2 - c^2} u_0 - \frac{(a^2 - b^2)c}{ab(a^2 - c^2)^{1/2}} \right] \\ \gamma_0 &= 2 \frac{1 - \frac{ac}{b(a^2 - c^2)^{1/2}} E(u_0)}{1 - \left(\frac{c}{b}\right)^2}\end{aligned}$$

Here

$$\begin{aligned}\varphi_0 &= \sin^{-1} \frac{\sqrt{a^2 - c^2}}{a} = \sin^{-1} e_1, u_0 = F(\varphi_0; \theta) \\ \theta &= \sin^{-1} \sqrt{\frac{a^2 - b^2}{a^2 - c^2}} = \sin^{-1} \frac{e_2}{e_1}, E(u_0) = E(\varphi_0; \theta)\end{aligned}$$

where e_1 and e_2 are the eccentricities of the central sections normal to the intermediate (b) and minimum (c) axes of the ellipsoid.

These formulæ are sufficient for the direct evaluation of $k_1, k_2, k_3; k'_1, k'_2$, and k'_3 in the general case. However, in special cases the elliptic integrals degenerate into algebraic, circular, hyperbolic, or other functions, or the coefficients take on indeterminate forms needing special treatment. The results for many of these special cases are more readily obtained by direct integration of the special differential forms, but for uniformity are discussed here as limiting forms of the general elliptic integrals.

1. VERY LONG ELLIPSOID. Limiting case an elliptic cylinder. As a becomes large so that higher powers of both $\frac{c}{a}$ and $\frac{b}{a}$ become negligible $k \doteq 1$ and at the same time $\varphi_0 \doteq \frac{\pi}{2}$.

$$u_0 \doteq \log \frac{2a}{c} \text{ and } E(u_0) \doteq 1$$

In the limit since $x \log x \doteq 0$

$$\alpha_0 = 0, \beta_0 = \frac{2}{1 + \frac{c}{b}}, \gamma_0 = \frac{2}{1 + \frac{c}{b}}$$

These are of course more directly obtained by treating the two dimensional flow around an elliptic cylinder.⁷

2. ELLIPTIC DISK. $c \doteq 0$. To quantities of the first order in c

$$\alpha_0 = \frac{2c}{b(a^2 - b^2)} [b^2 u_0 - b^2 E(u_0)]$$

$$\beta_0 = \frac{2c}{b(a^2 - b^2)} [a^2 E(u_0) - b^2 u_0]$$

$$\gamma_0 = 2 \left[1 - \frac{c}{b} E(u_0) \right]$$

In the limit $c = 0$, $\varphi_0 = \frac{\pi}{2}$, so that $u_0 = K$ and $E(u_0) = E$, the complete elliptic integrals, $\text{mod } \frac{\sqrt{a^2 - b^2}}{a} = e$.

Then in the limit $\alpha_0 = \beta_0 = 0$, $\gamma_0 = 2$, so that $k_1 = k_2 = 0$, but $k_3 = \infty$.

Thus $K_1 = K_2 = 0$ and K_3 needs special evaluation:

$$K_3 = \frac{4\pi}{3} abc k_3 = \frac{4\pi}{3} abc \frac{\gamma_0}{2 - \gamma_0} = \frac{4\pi}{3} abc \frac{1 - \frac{c}{b} E(u_0)}{\frac{c}{b} E(u_0)}$$

⁷ Horace Lamb, l. c., pp. 79-86.

In the limit $c=0$

$$K_3 = \frac{4\pi}{3} \frac{ab^2}{E}, \text{ mod } k = \frac{\sqrt{a^2 - b^2}}{a} = e$$

when $a=b$ (circular plate) $k=e=0$, $E=\frac{\pi}{2}$, so that $K_3 = \frac{8}{3} a^3$.

Again to quantities of the first order in c

$$k'_1 = \frac{\gamma_0 - \beta_0}{2 - (\gamma_0 - \beta_0)}$$

$$k'_2 = \frac{\gamma_0 - \alpha_0}{2 - (\gamma_0 - \alpha_0)}$$

$$k'_3 = \left(\frac{a^2 - b^2}{a^2 + b^2} \right)^2 \frac{\beta_0 - \alpha_0}{\frac{a^2 - b^2}{a^2 + b^2} - (\beta_0 - \alpha_0)}$$

In the limit $c=0$, $k'_3=0$, but k'_1 and k'_2 become infinite as $\frac{1}{c}$. To this order of approximation.

$$2 - (\gamma_0 - \beta_0) = 2 \frac{c}{b(a^2 - b^2)} [(2a^2 - b^2) E(u_0) - b^2 u_0]$$

$$2 - (\gamma_0 - \alpha_0) = 2 \frac{c}{b(a^2 - b^2)} [(a^2 - 2b^2) E(u_0) + b^2 u_0]$$

so that when $c=0$

$$K'_1 = \frac{4\pi}{15} \frac{ab^4 (a^2 - b^2)}{[(2a^2 - b^2) E - b^2 K]}$$

$$K'_2 = \frac{4\pi}{15} \frac{a^3 b^2 (a^2 - b^2)}{[(a^2 - 2b^2) E + b^2 K]}$$

When $a=b$ (circular disk), these become indeterminate, since $k \doteq 0$ and $E \doteq K \doteq \frac{\pi}{2}$. To quantities of the first order in $(a^2 - b^2)$, $(K - E) = \frac{\pi}{4} \frac{a^2 - b^2}{a^2}$, so that $K'_1 = K'_2 = \frac{16}{45} a^5$.

3. OBLATE SPHEROID. $a=b>c$, $k=0$, $k'=1$.

$$E(u) = u = \varphi = \sin^{-1} \sqrt{\frac{a^2 - c^2}{a^2 + \lambda}} = \sin^{-1} \frac{e}{\sqrt{1 + \frac{\lambda}{a^2}}}$$

and $\lim_{k \doteq 0} \frac{1}{k^2} [u - E(u)] = 1/2 (\varphi - \sin \varphi \cos \varphi)$

then $\alpha = \beta = \frac{2a^2 c}{(a^2 - c^2)^{3/2}} \frac{1}{2} (\varphi - \sin \varphi \cos \varphi) = \frac{2\sqrt{1-e^2}}{e^3} \frac{1}{2} \left(\varphi - \frac{e\sqrt{1-e^2}}{1 + \frac{\lambda}{a^2}} \right)$

$$\gamma = \frac{2a^2 c}{(a^2 - c^2)^{3/2}} (\tan \varphi - \varphi) = \frac{2\sqrt{1-e^2}}{e^3} \left(\frac{e}{\sqrt{1-e^2}} - \varphi \right)$$

When $\lambda=0$, $\varphi = \sin^{-1} e$, so that

$$\alpha_0 = \beta_0 = \frac{\sqrt{1-e^2}}{e^3} \left(\sin^{-1} e - e\sqrt{1-e^2} \right)$$

$$\gamma_0 = 2 \frac{\sqrt{1-e^2}}{e^3} \left(\frac{e}{\sqrt{1-e^2}} - \sin^{-1} e \right)$$

In the limiting case $c=0$, $e=1$ (circular plate) these give as before

$$K_1 = K_2 = 0, \quad K_3 = \frac{8}{3} a^3$$

$$K'_1 = K'_2 = \frac{16}{45} a^5, \quad K'_3 = 0$$

4. PROLATE SPHEROID. $a > b = c$, $k=1$, $k'=0$, $\varphi = \text{gd } u$. Then

$$\alpha = \frac{2ac^2}{(a^2 - c^2)^{3/2}} (u - \tanh u)$$

$$\beta = \gamma = \frac{2ac^2}{(a^2 - c^2)^{3/2}} 1/2 (\sinh u \cosh u - u)$$

where

$$\tanh u = \sin \varphi = \frac{\sqrt{a^2 - c^2}}{\sqrt{a^2 + \lambda}} = \frac{e}{\sqrt{1 + \frac{\lambda}{a^2}}}, \quad \frac{ac^2}{(a^2 - c^2)^{3/2}} = \frac{1 - e^2}{e^3}$$

$$\sinh u \cosh u = \frac{\sqrt{(a^2 - c^2)(a + \lambda)}}{c^2 + \lambda} = \frac{e^2 \sqrt{1 + \frac{\lambda}{a^2}}}{1 - e^2 + \frac{\lambda}{a^2}}$$

and

$$u = \log \sqrt{\frac{1 + \sin \varphi}{1 - \sin \varphi}} = \log \tan \left(\frac{\pi}{4} + \frac{\varphi}{2} \right)$$

when $\lambda=0$, these reduce to

$$\alpha = \frac{(1 - e^2)}{e^3} \left[\log \frac{1 + e}{1 - e} - 2e \right]$$

$$\beta = \gamma = \frac{(1 - e^2)}{e^3} \left[\frac{e}{1 - e^2} - 1/2 \log \frac{1 + e}{1 - e} \right]$$

The special cases 3 and 4 are of course more readily obtained by direct integration.

REPORT No. 211

WATER MODEL TESTS FOR SEMIRIGID AIRSHIPS

By L. B. TUCKERMAN
Bureau of Standards

REPORT No. 211

WATER MODEL TESTS FOR SEMIRIGID AIRSHIPS

By L. B. TUCKERMAN

INTRODUCTION

This report is based on a study made by the writer as a member of the Special Committee on Design of Army Semirigid Airship *RS-1* appointed by the National Advisory Committee for Aeronautics.

The semirigid airship such as the *Roma*, the *Forlanini*, the Italian military type, or the *RS-1* now building for the United States Army, depends, for its strength to resist static and aerodynamic forces, partly on the envelope under pressure and partly on the articulated (Italian military type) or "rigid" (*Roma*, *Forlanini*, *RS-1*) keel.

Theoretical considerations show that the interaction of keel and envelope may be partly favorable and partly unfavorable. As a combined beam they unite to resist bending moments, distributing the bending moments between them, but the "breathing" of the envelope, or poor fit of keel to envelope, cause them to act against each other, setting up additional "internal" stresses balanced between keel and envelope.

Obviously an accurate knowledge of the character of the interaction of envelope and keel, and the relative magnitude of these two effects is of importance in the refinement of the design of the semirigid airship.

Although the theory indicates clearly the existence of both these effects, attempts to calculate their magnitude from theoretical considerations have failed on account of mathematical difficulties involved. Mr. Pagon and Professor Hovgaard (of the National Advisory Committee for Aeronautics *RS-1* committee) have both made simplifying assumptions and secured interesting results, but the assumptions they found necessary are such as to place in doubt even the order of magnitude of their numerical results.

A careful study of their work has not shown any feasible way of removing this difficulty. All assumptions tried which seem reasonably definite, lead to a maze of simultaneous equations involving elliptic integrals. As a double differentiation of the solution of these equations, with respect to pressure and distance, is involved in the determination of the shear stresses, it seems doubtful whether existing tables of elliptic integrals are adequate for their computation, and even if the tables were adequate, the computations would be unreasonably time consuming. Crocco's mechanical computer, although satisfactory for laying out the envelope, is similarly inadequate for the computation of these stresses due to interaction of keel and envelope.

It is therefore worth while to inquire what information regarding this interaction of keel and envelope can be gained from a water model.

Water models have frequently been used for determining the shapes and strengths of balloons and airships and their deformations under static load. The model built to scale, of the same fabric as is used in the ship, is hung upside down and filled with water under pressure and its behavior under different water pressures and different applied loads is studied.

The effect of kinetic loads—such as the wind forces acting on airships in flight, can not be directly determined by water-model tests. It is necessary to determine these wind forces independently by theoretical computations, or by observation on airships in flight or on models in a wind tunnel. The effect of these kinetic forces is then determined by subjecting the model

to equivalent static forces. The theory of such model tests can be found in numerous publications,¹ but, so far, I have seen no discussion of models with flexible keels designed to simulate the flexibility of the keel structure in the semirigid airship.

THE FLEXIBLE KEEL WATER MODEL

A flexible-keel water model will of course be subject to all the conditions of size, pressure, loads, etc., which are necessary in balloon and nonrigid airship models and in addition, to conditions specifying the relations which the elastic constants of the keel in the model should bear to those of the ship. The derivation of these additional relations is the primary object of this paper.

BUCKINGHAM'S II THEOREM

The law of physical similitude, or of dynamic similarity (as it is known when the problems are purely mechanical in their nature) first stated by Newton and developed in recent years by Reynolds, Rayleigh, and others, underlies all theories of model tests. Buckingham² has formulated this law in a theorem, the "II theorem," which is especially convenient for the routine handling of these problems. The complete application of the theorem requires the listing of all the physical quantities ($Q_1, \dots, Q_j \dots Q_n$) involved in the dynamic behavior to be studied, together with the dimensions of each in terms of some convenient system of (m) fundamental units. Buckingham's II theorem then states that any equation connecting these (n) quantities, may be written in the form

$$f(\Pi_1, \Pi_2, \Pi_k, \dots, \Pi_{n-m}) = 0$$

where

$$\Pi_1, \Pi_2, \dots, \Pi_k \dots \Pi_{n-m}$$

are any ($n-m$) independent products of the form $Q_1^{a_1}, Q_2^{a_2}, \dots, Q_j^{a_j} \dots Q_n^{a_n}$ dimensionless in terms of the fundamental units chosen,³ a_1, a_2, \dots, a_n being pure numbers. Some of these Π 's are well known in aerodynamic theory, such as the Reynolds Number $\frac{LV\rho}{\mu}$, the lift and drag coefficients of airplanes $\frac{R}{\frac{1}{2}\delta V^2 A}$, the fineness ratios of airfoils and airships $\frac{L}{L'}$, etc.

The advantage of the formulation of the law of dynamic similarity in the form of Buckingham's II theorem lies in the fact that the attention can be concentrated on the purely physical aspects of the problem, that is, on listing, with their dimensions, all of the quantities upon which the particular dynamic behavior under investigation materially depends.

The formation of ($n-m$) independent Π_k 's is then a matter of routine. After any set of ($n-m$) independent Π_k 's has been found, the arrangement of them into physically more significant groupings is a matter of simple inspection.

SCOPE OF DISCUSSION

Although the conditions for the nonrigid water model could be assumed and the additional relations for the flexible keel separately determined it seemed easier to carry through a systematic discussion on the basis of the II theorem.

The following discussion, then, is intended to include all of the essential factors of water-model design and will, therefore, in large part, reproduce the well-known results of previous water-model theories in developing the conditions necessary for a flexible-keel water model.

¹ References: Crocco, *La Technique Aerienne*, June 1, 1911; Haas and Dietzius, N. A. C. A. Report No. 16, 1917. F. D. Swain, Air Service (War Dept.) Engineering Division, McCook Field Report No. 2067, Apr. 22, 1922; J. C. Hunsaker, Navy Dept., Bureau of Aeronautics, Technical Note No. 1; Upson, Unpublished memorandum of Goodyear Tire & Rubber Co.

² E. Buckingham, *Phys. Rev.* Vol. IV, p. 345, 1914; *Journal A. S. M. E.*, 1915; *Phil. Mag.* Vol. 43, p. 696, 1921.

NOTE.—This theorem in a somewhat modified form has recently been used in an extended discussion of model tests by A. H. Gilson—"The Principle of Dynamical Similarity with Special Reference to Model Tests in Engineering (Laud)," Vol. 117, pp. 325, 357, 391, and 422, 1924.

³ For a discussion as to the limitations on the choice of these units the reader is referred to Buckingham's papers.

GROUPING OF PHYSICAL QUANTITIES

In listing these physical quantities, those of the same physical dimensions, which can be conveniently discussed together, will be listed together in a group. There will, in general, be several groups having the same physical dimensions. Thus, for example, the flexural modulus of the fabric, the flexural and torsional strengths of the keel and the bending moments of the load all have the same physical dimensions (FL). Their relations to the behavior of the model are, however, so different that they can not be conveniently discussed together and they are therefore listed in three separate groups in spite of the fact that they have the same dimensions.

COMPLETE GEOMETRICAL SIMILARITY UNNECESSARY

In so far as shape affects the behavior of the airship, dynamical similarity requires that the model be exactly geometrically similar to the full-sized original; but if the action of a certain member such as a wire or girder depends only on its elasticity or strength, its visible external form is a matter of no importance. The fluid forces on the envelope are of vital importance and, since they depend on the form of the envelope, the model must, in this respect, be geometrically similar to the full-sized ship. But if the fluid forces which act *directly* on the keel are of negligible importance in comparison with the forces between the keel and the envelope, the only strictly geometrical condition imposed on the keel is that its points of attachment to the envelope be similarly situated to those in the full-sized keel. All that is required of the model keel is that its elastic and strength constants shall be suitably adjusted, and its actual shape aside from the positions of the envelope attachments is immaterial because it has no effect on what happens.

ASSUMPTIONS CONCERNING FABRIC OF ENVELOPE

Thus, in a water model one-thirtieth the length of an airship, geometrical similarity would demand an envelope one-thirtieth the thickness of the airship envelope. As this is clearly not feasible, it is usual to assume that the thickness of the envelope is geometrically a negligible factor and that the actual envelope could be replaced by an envelope of any other thickness (small in comparison with the other dimensions of the ship) without affecting its dynamical behavior. Experiments show that this assumption is ordinarily reasonable. This other envelope, however, must be dynamically equivalent to the actual envelope, i. e., it must, considered as an elastic surface, offer the same resistance to deformations as the actual surface. This implies that all the elastic constants of the envelope, tension moduli, shear modulus, tensile strength, and flexural resistance, may be sufficiently specified in terms of forces and moments per unit length instead of per unit area. This is, of course, common in textile measurements, where the strength of a fabric is expressed as a force per linear (not square) inch.

FUNDAMENTAL UNITS

Since the water model is subjected only to static loads, only two fundamental units are needed. For convenience we shall adopt length (L) and force (F) as our fundamental units.

FABRIC CONSTANTS

The *fabric* of the envelope will then be characterized dynamically by the following fabric constants:

1. Its weight per unit area, μ dimensions (FL^{-2})
2. $\left. \begin{array}{l} 2 \text{ tension moduli } F_1, F_2 \\ 1 \text{ shear modulus } F_3 \\ 2 \text{ tensile strengths } F_4, F_5 \end{array} \right\} (F_h) \text{ dimensions } (FL^{-1})$
3. A flexural modulus σ dimensions (FL)

The modulus of normal shear is negligible in all practical cases.

FABRIC STRESSES

There will be induced in the fabric certain tensile and shear stresses measured as

4. Force per unit length T_1, T_2, T_3 (T_h) dimensions (FL^{-1})

ASSUMPTIONS CONCERNING KEEL

Similarly it is obviously impossible to reproduce the keel structure in detail. Only the outer surface of the model keel will reproduce the geometrical shape of the airship keel.

It seems reasonable to assume that the keel will be adequately represented dynamically by a thin elastic rod in which shear deformation and shear stresses are not negligible.

This, perhaps, needs a more detailed explanation. In the theory of the deformations of thin elastic rods, it is assumed that any portion of the rod is equivalent to any other, differing in material or distribution of material through the cross section, provided that the curvatures and twists produced in the two by the same bending moments and the same axial torque are identical, and provided that rupture, permanent deformation, or other failure will occur under identical axial loads, bending moments, and torque. Due to its low stiffness in shear the curvature of the keel of the airship at any place will depend appreciably not only upon the bending moments, but also upon the local distribution of shears. These shears are assumed to be of negligible importance in the ordinary theory of thin rods. Consequently, an adequate representation of the characteristics of the keel must include in addition two shear moduli.

KEEL CONSTANTS

The *keel* will then be characterized dynamically by the following keel constants given as functions of the distance along the keel measured as a fraction of its total length:

5. Weight per unit length m dimensions (FL^{-1})
6. 2 flexural moduli K_1, K_2 } (K_h) dimensions (FL^{-2})
1 torsional modulus K_3
7. 2 flexural strengths H_1, H_2 } (H_h) dimensions (FL)
1 torsional strength H_3
8. 2 shear moduli S_1, S_2 (S_h) dimensions (F)
9. 2 shear strengths S_1', S_2' (S_h') dimensions (F)
10. 1 stretch modulus s dimensions (F)
11. 1 stretch strength s' dimensions (F)

It is unnecessary to consider a compressive strength since in airship construction lightness requires large compression members to be so flexible that compressive failure will only occur in flexure.

WIRE CONSTANTS

Since the weight of the *suspender wires* is a very minor element in the design and their strength is always easily made adequate, it seems reasonable to assume that each can be adequately represented dynamically by a single

12. Wire or cordage stretch constant $W_1, W_2, \dots (W_h)$, dimensions (F) .

SUFFICIENCY OF CONSTANTS

These structural constants are thought to include all the dynamical characteristics of the material and the structure which are of significance in the problem. As a matter of fact, some of these given will be shown to be unnecessary for the purpose. Others are almost certainly of negligible importance. Still others impose conditions on the model which are impracticable so that their disturbing influence must be carefully considered. The list was made unnecessarily full merely to insure that no really significant characteristics were omitted. If, however, any significant structural constants have been omitted the conclusions will be uncertain to the extent that such omitted constants are of importance.

LOADS

Aside from these constants of the material and structure, the forces are essential elements in the problem. These can be applied as concentrated loads, including shears (load differences); they represent weights of cars, fuel tanks, and useful load, propeller thrust, etc

13. Loads $P_1, P_2, \dots (P_h)$ dimensions (F). Bending moments can of course be calculated back to the forces from which they arise. It is, however, frequently desirable to treat them as independent load elements especially when studying the effect of forces remote from their point of application, or of aerodynamic moments whose force distributions are not accurately known. It is therefore convenient to introduce

14. Bending moments $M_1, M_2, \dots (M_h)$ dimensions (FL). That these in part duplicate the forces listed under (13) is no objection since a redundant list does not interfere with the validity of the II theorem. The gas and air pressure might also be included under the forces (13) but because of their manner of application they are more conveniently listed separately.

15. Pressures, gas and aerodynamic $p_1, p_2, \dots (p_h)$ dimensions (FL^{-2}).

DEFORMATIONS

The behavior of the ship under these loads may be studied: First, by

16. Deflections $\delta_1, \delta_2, \dots (\delta_h)$ dimensions (L) which measure its deformation under load, and determine the mode of interaction of its various parts. These are what would be determined in deformation or shape tests.

Volume changes could also be separately listed, but as these always change as the cube of a linear dimension (dimensions (L^3)) a separate term seemed unnecessary.

STRENGTH

Second, by its failure in whole or in part due (a) to tensile stresses, T_h , in the fabric exceeding the corresponding tensile strengths, F_4, F_5 ; (b) to bending moments or torques in the keel exceeding the corresponding strengths, H_1, H_2, H_3 , or to shears exceeding its shear strength, S' , or axial forces exceeding its stretch strength, s' . Tests which determine these conditions of failure are strength tests.

ADVANTAGE OF LIMITATION TO DEFORMATION TESTS

Even in structures of this type there is, over a considerable range, approximate proportionality between load and deflections, so that deflection experiments at low loads, where there is no danger of failure of any part, may be expected to give a satisfactory picture of the dynamic interaction of these parts. This is important, because if low-load tests are adequate for the purpose, it is not necessary to specify the strength constants of the model which will greatly simplify its design.

Moreover, if low-load tests give an adequate understanding of the dynamic interaction of the various parts, strength tests may be unnecessary since the strength of individual parts can be sufficiently well estimated by elementary theory if the laws of interaction of the various parts are known.

In this estimation judgment must be used. It would not be safe to calculate strengths directly on an assumption that loads and deflections are proportional up to failure. Allowance must be made for the deviations from proportionality at high loads. It seems probable, however, that the general nature of these deviations can be determined from low-load tests. The problem is similar to that involved in beam design where the stresses are calculated from elastic theory—allowance being made for the known deviation from Hooke's law at high stresses.

SIZE

The size of the ship (and model) may be characterized by its overall

17. Length L dimensions (L). All other significant dimensions are of course proportional to this.

FLUID DENSITIES

The buoyant (or loading) effect of the fluids used is determined by the density differences between internal (gas, water) and external (air) fluids. It is equal to this density difference multiplied by the acceleration of gravity.

18. Buoyancy B dimensions (FL^{-3}).

FORMATION OF THE Π 'S

From any complete list of the (n) physical quantities (Q_J) involved in a physical phenomenon an indefinite number of products (Π) dimensionless in the (m) fundamental units can be found. Only $(n-m)$ of them, however, are independent. From any group of $(n-m)$ independent Π 's any other Π can be formed by multiplication, division, and extraction of roots.

When several of the physical quantities (Q_J) have the same dimensions, and any Π has been found containing one of them as a factor, other Π 's independent of each other can be found directly from this one by replacing this (Q_J) in turn by each of the others of the same dimensions. Thus since $\frac{BL^2}{F_1}$ is dimensionless, so also are $\frac{BL^2}{F_2}$, $\frac{BL^2}{F_3}$, $\frac{BL^2}{F_4}$ and $\frac{BL^2}{F_5}$ and these form a group of five mutually independent Π 's all of the same type. The quantities F_1 , F_2 , F_3 , F_4 , and F_5 have been listed in a group (2) under the general symbol F_h . For convenience in discussing them together we shall represent this group of Π 's which are all of the same type by the single symbol $\Pi_1 = \frac{BL^2}{F_h}$. In what follows then Π_k will represent not a single dimensionless product but the group of all the mutually independent Π 's of the same type formed from the corresponding groups of Q_J 's. Obviously if there are n' groups of Q_J 's there will be $(n'-m)$ independent types of Π 's.

APPLICATION OF THE Π THEOREM

With this notation, if the quantities which are arranged in these 18 groups are an adequate specification of the dynamic characteristics of the ship, the law of dynamic similarity as expressed in Buckingham's Π theorem states that any equation representing a dynamic behavior of the structure can be expressed in the form,

$$f(\Pi_1, \Pi_2, \dots, \Pi_k, \dots, \Pi_{16}) = 0$$

where f is a function characterizing the particular dynamic behavior in question and Π_1, \dots, Π_{16} represent $(n-2)$ Π 's of any 16 independent types, dimensionless in the chosen units (F, L) formed from all the (n) quantities of the 18 types by multiplication and division. For complete dynamic similarity to exist, all except one of these Π 's must be given the same value in the model as in the ship. The other will then necessarily have the same value. Each of the Π 's then represents a condition to be imposed on the model and any Π_k represents a group of such conditions,⁴ including the obvious one that all quantities of the same group should have the same ratio in model as in ship.

The following seem to be the simplest expressions of these conditions. They have been chosen so that the first determines the model length in terms of the buoyancy (B) and the others determine the remaining quantities in terms of the length:

	<i>Determines</i>
$\Pi_1 = BL^2 \frac{1}{F_h}$	Model length.
$\Pi_2 = \frac{P_h}{L} \frac{1}{F_h}$	Model loads.
$\Pi_3 = \frac{M_h}{L^2} \frac{1}{F_h}$	Model moments.
$\Pi_4 = \frac{P_h L}{F_h}$	Model pressures.
$\Pi_5 = \frac{\delta_h}{L}$ or its equivalent $\Pi'_5 = \frac{\text{Volume change}}{L^3}$	Scale of model deformations.
$\Pi_6 = \frac{T_h}{F_h}$	Fabric tensions in model.

These six relations are usually given in the elementary theory of water models.

⁴ For another method of treatment of groups of quantities of the same dimensions, see Buckingham l. c.

$\Pi_7 = \frac{W_h}{L} \frac{1}{F_h}$	<i>Determines</i> Size of model wire or cordage used for suspensions.
$\Pi_8 = \mu L \frac{1}{F_h}$	Fabric counterweight.

Π_8 is considered by Hunsaker (l. c.) but Π_7 has been found only in the unpublished memorandum of Upson.

The next eight, relating to the flexible keel and to a caution with reference to the fabric have not been found in previous discussions.

$\Pi_9 = m \frac{1}{F_h}$	<i>Determines</i> Keel counterweight.
$\Pi_{10} = \frac{K_h}{L^3} \frac{1}{F_h}$	Elastic constants of model keel.
$\Pi_{11} = \frac{S_h}{L} \frac{1}{F_h}$	
$\Pi_{12} = \frac{s}{L} \frac{1}{F_h}$	
$\Pi_{13} = \frac{H_h}{L^2} \frac{1}{F_h}$	Strength constants of model keel.
$\Pi_{14} = \frac{S_h'}{L} \frac{1}{F_h}$	
$\Pi_{15} = \frac{s'}{L} \frac{1}{F_h}$	
$\Pi_{16} = \frac{\sigma}{L^2} \frac{1}{F_h}$	Flexural rigidity of model envelope.

In the following discussion we shall use the subscript s for the ship and m for the model. Dynamic similarity then requires that $\Pi_{km} = \Pi_{ks}$. This, as will be seen, can not be completely realized.

II, DENSITY DIFFERENCE, SIZE, AND FABRIC CONSTANTS

The buoyance, B_s , for the ship varies somewhat with flying conditions. For hydrogen, at present, it is usual to assume 68 pounds per 1,000 cubic feet, and for helium, 64 pounds per 1,000 cubic feet. The (negative) buoyancy B_m for the water model is, for all practical purposes, the buoyancy of water at 0° C, 62.4 pounds per cubic foot. Hence the ratio is

$$\frac{B_s}{B_m} = \begin{cases} 0.00109 & \text{for hydrogen} \\ 0.001025 & \text{for helium} \end{cases}$$

The fabric constants F_1 , F_2 , F_3 , F_4 , and F_5 , should have the same ratio in model as in ship. It is technically impossible to produce two markedly different fabrics for which this is true. Consequently, it is customary to use the *same* fabric in model as in ship, assuming $F_{hs} = F_{hm}$. In practice this is not perfectly realized. Equal strength demands equal overlap at seams in model and in ship. As the seams are a much greater portion of the area of the model, this results in an effectively stiffer model envelope, i. e., $F_{1s} < F_{1m}$, $F_{2s} < F_{2m}$, $F_{3s} < F_{3m}$, while the strength constants $F_{4s} = F_{4m}$, and $F_{5s} = F_{5m}$. This discrepancy, although not great, is still not negligible, amounting to about 15 to 20 per cent in the case of the *RS-1*. So far as deformations are concerned, this could probably be adequately allowed for by correcting F_1 , F_2 , and

F_3 , by the ratio of seam area to total envelope area in model and ship (this is approximately 1 per cent in the *RS-1* and 17 per cent in the water model tested at Akron) and correspondingly increasing the scale of the model. Such a procedure would lead to an underestimate of strength if it were used for a strength test.

If, however, we relinquish strength tests on the model, F_{4m} and F_{5m} may safely be much smaller than F_{4s} and F_{5s} . In a conversation, Mr. Zimmerman of the Goodyear Co. estimated that if we were content with an equivalent of 2 to 2½ inches ship pressure, the width of overlap in the model could probably be reduced to one-fourth that in the ship, making the correction involved less than 4 per cent, which is probably negligible.

As the bursting strength can be fairly well determined from laboratory tests on the fabric, it would seem preferable to do this.

Where suspension patches are used a similar difficulty is involved. Since the strength of their attachment to the envelope depends almost entirely on the shear resistance of the cement film, equal strength requires that this area be approximately one-thirtieth as great in model as in ship instead of one nine-hundredth as required by geometrical similarity. This discrepancy also can be reduced if strength tests are not required, but in any case the shape and stress of the envelope near patches must be expected to differ considerably in model and in ship.

Assuming, with these qualifications

$$F_{hs} = F_{hm}$$

the requirement that $\Pi_{1m} = \Pi_{1s}$ gives

$$\frac{L_m}{L_s} = \sqrt{\frac{B_s}{B_m}} = \begin{cases} 0.033 & \text{for hydrogen} \\ 0.032 & \text{for helium} \end{cases}$$

the well-known ratio of approximately 1:30. The small correction for seam overlap indicated above could readily be made if it seemed desirable. As F_h appears in practically all the Π 's, this would mean a slight correction to nearly all the model constants. For simplicity of discussion, it will be omitted, and $F_{hm} = F_{hs}$ assumed. The factor $\frac{1}{F_h}$ appearing in the succeeding Π 's is then constant and need not be discussed further.

$\Pi_2, \Pi_3, \Pi_4, \Pi_5, \Pi_6$ —PRESSURES, FABRIC TENSIONS, LOADS, MOMENTS, AND DEFLECTIONS

These show pressures varying as $\frac{1}{L}$, fabric tensions independent of L , loads and deflections proportional to L , moments proportional to L^2 and volume changes to L^3 . As these conditions have been fully discussed in previous publications, they do not need further discussion.

II, SUSPENDER WIRES OR CORDS

Since the W_h 's are directly proportional to the cross-sectional area of the wires (nearly so for cords of similar construction) the model wires and cords, if of the same material and construction, will have diameters varying approximately as \sqrt{L} . As the stretch of suspenders usually constitutes only a small portion of the total deflections of the ship, this condition ordinarily need not be accurately fulfilled. It is merely necessary to choose from available standard wires and cords those which fit the conditions most nearly.

Π_6 AND Π_9 COUNTERWEIGHTS OF KEEL AND ENVELOPE

Here the model differs radically from the ship. In the ship the gas inside is less dense than the air outside, so that the weight of keel and fabric (downward) is opposite in direction of the gas lift (upward). To simulate this condition in the water model it would be necessary to immerse the model in a tank of water and fill it with air under pressure. As this would be difficult experimentally the model is turned upside down and filled with water. The weight of the keel and fabric (downward) is now in the same direction as the water load (downward) which is directly opposite to the condition in the ship. To compensate for this counter-

weighting may be employed. Theoretically, each portion of the envelope should be counterweighted by $\left(\frac{L_s}{L_m} + 1\right) = \frac{\mu_s + \mu_m}{\mu_m}$ times its weight and each portion of the keel by $\frac{(m_s + m_m)}{m_m}$ times its own weight.

Where the actual shape of the envelope is sought from the model test, the accurate individual distributed counterweighting of fabric and keel is important. This, however, requires complicated devices. For fabric counterweighting air bags and netting suspensions have been used which give rough approximations. It seems possible that distributed buoyant material sewed to the inside of the bag might be used. Mr. C. P. Burgess has suggested that this compensation might also be effected by making the model proportionally smaller. Any such change, however, should be used with caution and only relied upon after an investigation of all the other relations involved.

If only *changes* of shape under *changing* loads are desired, it would seem that the complications of separate fabric counterweighting might safely be omitted. This would give a model shape differing from the shape of the ship by less than the changes in shape experienced in normal conditions under changing superpressure. This difference would presumably cause only negligible second order differences in the measured changes under changing load.

If accurate distribution of counterweighting be not necessary, the total counterweighting indicated by Π_8 and Π_9 is automatically insured by the static equilibrium of the model.

$\Pi_{13}, \Pi_{14}, \Pi_{15}$ KEEL STRENGTH

These conditions in connection with Π_{10} , Π_{11} , and Π_{12} seem practically impossible of realization. If, however, we confine our attention to deflection tests at low (safe) loads they can be ignored.

Π_{16} FLEXURAL STIFFNESS OF ENVELOPE

Observations of some model tests lead me to believe that this condition may sometimes be of importance in interpreting them. It requires that the flexural stiffness of the model fabric should be only approximately one nine-hundredth part of that of the ship. The flexural stiffness of the fabric in the ship is safely negligible but that does not mean that a fabric 900 times as stiff in flexure (other properties the same) would not take an appreciably different shape. In fact, it seems certain that it would. The general character of the difference is clear. The stiffer fabric would smooth out changes in curvature of the envelope, rounding off more flatly the portions of sharper curvature. In particular the stiffer fabric would tend to iron out wrinkles so that it is not safe to conclude from the absence of wrinkles in the model that they would not appear in the ship under corresponding conditions. These differences have been noted by others but no discussion of their cause has been found.

Π_{12} LONGITUDINAL STRETCH OF KEEL

The longitudinal stretch of the individual portions of the keel is negligible.

Π_{10} AND Π_{11} , KEEL FLEXIBILITY

The three relations contained in the form Π_{10} require that the two flexural moduli K_1 and K_2 (these are sometimes called "flexural rigidities") and the torsion modulus K_3 (sometimes called "torsional rigidity") of the keel all vary as L^3 . For an isotropic solid section

$$K_1 = EI_1 \text{ and } K_2 = EI_2$$

while the torsion modulus K_3 is for a fairly compact isotropic solid section

$$K_3 = M \frac{A^4}{4 \Pi^2 I} \text{ approximately}$$

where M is the shear modulus of the material A the area and I the polar moment of inertia of the cross section.

If the keel were an absolutely similar structure on a smaller scale these constants would vary as L^4 . The requirements evidently call for a relatively somewhat stiffer keel construction in model than in ship. This is, of course, due to the fact that the envelope is proportionately stiffer in model than in ship. The two relations contained in the form Π_{11} require that the two shear moduli of the keel S_1 and S_2 vary as L . For an isotropic solid cross section

$$S_1 = S_2 = MA$$

For absolutely similar structures these would vary as L^2 , so that the requirements demand that the keel of the model be also relatively stiffer in shear than in the ship.

In adequately meeting the conditions imposed by these Π 's on the five keel constants K_1 , K_2 , K_3 , and S_1 and S_2 lies the possibility of satisfactorily studying the dynamic interaction of keel and envelope.

In the articulated keel of the Italian military type it seems easily possible. Here the vertical flexural modulus $K_1=0$ and the vertical shear modulus $S_1=0$. The torsional modulus K_3 is small and can probably be safely assumed to be zero. This leaves only the horizontal flexural (K_2) and shear (S_2) moduli to be fitted to the model conditions. The vertical stiffness of the keel is furnished by the car suspensions which can easily be adjusted to meet the wire stretch conditions of Π_7 .

Whether an adequate approximation to these five constants can be fitted to a model of the "rigid" keel of the *Roma* or *RS-1* is a question. The values for the ship can be adequately computed from the design data. Theoretically it is possible by properly slotting and boring out a solid keel of the requisite external dimensions to fit it to any value and any ratio of these constants. Practically, it can only be done by a series of cut and try operations continually controlled by measurement. How accurately this needs to be done, in order to secure an adequately representative model, can only be determined by experience.

Even if an accurate fitting is impracticable, it may be possible by experimenting with a number of model keels differing sufficiently in their elastic constants, to work out empirical laws in which these constants appear separately and thus compute back to the actual ship. Even in this case reliable results can only be expected if the flexibility of the model keel does not differ too much from the values indicated by the theory.

CONCLUSIONS

SCOPE OF TESTS

A test on a flexible-keel water model seems to promise valuable information concerning the interaction of keel and envelope in the case of a semirigid airship.

The model should, for best results, be constructed solely for the purpose of studying the change of shape under load.

Any attempt to combine strength tests with deformation tests in the same model would lead to many compromises between conflicting requirements, resulting in less certain results.

ENVELOPE CONSTRUCTION

For these deformation tests all seams and patches should be made as small as possible, consistent with sufficient strength to resist the stresses under relatively low pressures (perhaps 2 to 2½ inches ship pressure) and loads not exceeding the actual loads carried by the ship. By this means the envelope of the model can be made to represent more closely the elastic behavior of the ship's envelope.

CAUTION IN INTERPRETATION

Even when this is done it should be remembered that the model envelope is relatively stiffer than the ship envelope and especially so in flexure. Consequently the shape of the model in regions of sharp curvature, or wrinkling, or in the neighborhood of seams or patches, should not be expected to reproduce accurately the corresponding portions in the ship.

Allowance should also be made for the departure from proportionality between loads and deformations, when strengths are estimated from deformation tests.

COUNTERWEIGHTING

It may be desirable to attempt fairly accurate counterweighting of envelope and keel but for the first trials it would seem desirable to avoid this experimental complexity by confining the attention to *changes* of shape under *changing* loads, which would obviate the necessity of accurate envelope counterweighting.

As a supplementary experiment it is suggested that it might be worth while to attempt envelope counterweighting by means of distributed cork floats or similar devices sewed inside the envelope. The suggestion of a smaller model should only be attempted after a more detailed analysis of the problem.

The distributed counterweighting of the keel is not particularly complicated so that it should certainly be included in supplementary tests.

KEEL CONSTRUCTION

From a construction standpoint this will be the most difficult. The following is a suggested procedure:

Construct a solid keel of the requisite shape and dimensions of an easily worked material (probably wood). Subject this to measured bending moments, torques, and shears, measuring at uniformly spaced stations along it, the curvatures, twist, and shear deformations (these last will probably be negligible in the solid model). Calculate the moduli K_{1m} , K_{2m} , K_{3m} , S_{1m} and S_{2m} and plot them as ordinates with distance along the axis (as fractions of total length) as abscissæ. Plot the corresponding moduli calculated for the keel of the ship, K_{1s} , K_{2s} , and K_{3s} on a scale $\left(\frac{L_m}{L_s}\right)^3$ as large and S_{1s} and S_{2s} on a scale $\frac{L_m}{L_s}$ as large. To satisfy the conditions the plotted curves of K_{1m} should be identical with that of K_{1s} , of K_{2m} with that of K_{2s} , etc. Where the bending moduli K_{1m} and K_{2m} are too high, transverse saw cuts should be made. Where the torsion modulus is too high longitudinal saw cuts should be made.

For the solid model keel, S_{1m} and S_{2m} will probably be practically infinite. Transverse holes bored or cut through the model keel will reduce these values. Rectangular holes with sides parallel to the axis will be more effective than round ones in proportion to the amount of material removed. If sufficiently low shear moduli can not be obtained in this way a built-up keel model will be necessary.

These adjustments must be carefully carried out since the types of cut mentioned, although lowering in greatest measure the constants indicated, at the same time lower all of the elastic constants of the keel. Consequently the process of adjustment will be by a series of successive approximations until the desired constants are obtained.

How accurately this can be done practically can hardly be surmised in advance. The adjustment should be carried to the point at which it seems that further labor would be wasted. If only the same order of magnitude is obtained the test should still give useful information.

SUMMARY OF CONSTRUCTION DATA

1. Fabric same as in ship. Seams and patches as small as possible.

2. All lengths $\frac{L_m}{L_s} = \sqrt{\frac{B_s}{B_m}} = \begin{cases} 0.033 & \text{for hydrogen} \\ 0.032 & \text{for helium} \end{cases}$

3. Suspender wires or cords $\frac{W_{hm}}{W_{hs}} = \frac{L_m}{L_s}$

4. Keel constants, flexure, and torsion $\frac{K_{1m}}{K_{1s}} = \frac{K_{2m}}{K_{2s}} = \frac{K_{3m}}{K_{3s}} = \left(\frac{L_m}{L_s}\right)^3$

Shear $\frac{S_{1m}}{S_{1s}} = \frac{S_{2m}}{S_{2s}} = \frac{L_m}{L_s}$

SUMMARY OF TEST DATA

LOADING

5. Fabric counterweighting proportional to $\mu_s \left(\frac{L_s}{L_m} + 1 \right)$

6. Keel counterweighting proportional to $\frac{m_s + m_m}{m_m}$

7. Loads $\frac{P_{hm}}{P_{hs}} = \frac{L_m}{L_s}$

8. Moments $\frac{M_{hm}}{M_{hs}} = \left(\frac{L_m}{L_s} \right)^2$

9. Pressures $\frac{p_{hm}}{p_{hs}} = \frac{L_s}{L_m}$

STRESSES AND DEFLECTIONS

10. Fabric stresses $\frac{T_{hm}}{T_{hs}} = 1$

11. Deflections $\frac{\delta_{hm}}{\delta_{hs}} = \frac{L_m}{L_s}$

The other requirements of the theory are either unnecessary for deflection tests or impracticable. The important effects of the failure to meet these requirements are summarized in the conclusions under the heading "Caution in interpretation."

REPORT No. 212

STABILITY EQUATIONS FOR AIRSHIP HULLS

By A. F. ZAHM
Navy Department

REPORT No. 212

STABILITY EQUATIONS FOR AIRSHIP HULLS

By A. F. ZAHM

SUMMARY

In the text are derived simple formulæ (9), (13), for determining, directly from the data of wind tunnel tests of a model of an airship hull, what shall be the approximate character of oscillation, in pitch or yaw, of the full-scale ship when slightly disturbed from steady forward motion.

OBJECT

It is desired to write the equations of motion for a finned but carless airship, slightly disturbed from swift head-on steady translation, and thence to deduce criteria for stability in pitch and yaw. These criteria may be expressed first in terms of full-scale coefficients; then in terms of model coefficients applied to full-scale craft. Incidentally some other features of the motion will be noticed.

The present treatment, slightly modified, was prepared for the Bureau of Aeronautics, June 30, 1922, and by it was submitted for publication to the National Advisory Committee for Aeronautics.

INITIAL CONDITIONS

To simplify the treatment, assume the hull symmetrical about its long axis; the centers of mass and volume practically coincident; the weight annulled by the buoyancy; the controls neutral; the motion head-on through still air. The second assumption evades the gravity moment, which for a hull at high speed usually is small compared with the tail moment, and is balanced with the stabilizer.

Starting from the centroid, Figure 1, the axes are x running aft, y apart, z upward. In general, the increments of velocity along and about these axes are, respectively, u, v, w, p, q, r ; the increments of the air force and moment are X, Y, Z, L, M, N .¹ Initially all the components of velocity and wrench are zero, except the forward speed U and the resistance X_0 , which latter has a negligible, if any, effect on the movement other than straightforward.

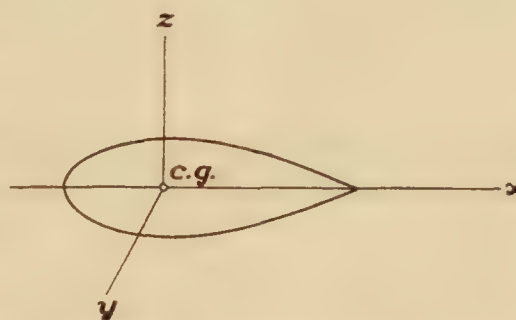


FIG. 1.—Reference axes for airship hull

MOTION IN SIMPLE PITCH

If now the ship with steady speed U is given a slight pitch θ , the entire system of external forces other than X_0 is equivalent to the normal air force Z at the centroid, and the pitching moment M about it. Hence, by d'Alembert's principle, the conditions for kinetic equilibrium are

$$Z = m\dot{w}_1 = m(\dot{w} - U^2q) \text{-----} (1)$$

$$M = B\dot{q} \text{-----} (2)$$

¹ Unless otherwise stated, all components are referred to x, y, z , fixed in the hull and moving with it.

² If θ is not small, U in these equations should be replaced by $u_0 = U \cos \theta$. The difference is immaterial for $\theta < 5^\circ$.

where m is the effective mass of the ship; B its moment of inertia about y ; while the space acceleration of the centroid is \dot{w}_1 if referred to the z axis as instantaneously fixed in space direction, but $\dot{w} - Uq$ if referred to z moving with the ship.³ If m' is the actual mass of the ship, the effective mass m , that is, the ship's actual mass plus its virtual mass due to accelerating the fluid, can be taken as about $1.5 m'$ for transverse accelerated motion whether normal or lateral.

Since both static and damping forces, due to θ and q , are present, it is advantageous to place in evidence the components of Z and M . The part of Z due to θ is θZ_θ , where Z_θ denotes $\partial Z / \partial \theta$; the part due to q is $q Z_q$. They are the usual lift and the damping force; and compose practically the whole of Z . Similarly the static and damping parts of M are θM_θ , $q M_q$. Substituting these four components in (1), (2), gives

$$\theta Z_\theta + q Z_q = m(\dot{w} - q U) \text{-----} (3)$$

$$\theta M_\theta + q M_q = B \dot{q} \text{-----} (4)$$

CONDITIONS FOR STABILITY IN PITCH

The angular velocity is constant for $\dot{q} = 0$, and declines on addition of some restoring moment, due, for example, to the lowering of the centroid. Making $\dot{q} = 0$ reduces (4) to

$$\theta M_\theta + q M_q = 0 \text{-----} (5)$$

Also for such speeds that \dot{w} is small compared with $q U$, one can write (3) more simply

$$\theta Z_\theta + q(Z_q + m U) = 0 \text{-----} (6)$$

These two equations are simultaneous, and taken together represent approximately the conditions essential for dynamically stable motion, i. e., for unamplifying pitch, expressed in familiar aerodynamic quantities.

By (5) the damping moment $q M_q$ rotationally balances the disturbing moment θM_θ ; by (6) the disturbing force θZ_θ , the damping force $q Z_q$, and the inertia force $q m U$, are in translational balance.

CRITERION OF PITCH STABILITY

In (5) and (6) the variables θ and q are the angular displacement and velocity of the small stable oscillation; the other six quantities are specified constants. Eliminating θ , q , gives the stability condition, viz, the relation between these constants which is necessary to satisfy (5), (6), for all small values of θ and q

$$\frac{Z_\theta M_q}{M_\theta(Z_q + m U)} = 1 \text{-----} (7)$$

This criterion can also be written in terms of model data. If s is the scale ratio, u the model speed, and if primes mark the model symbols, the values in (7) are related to the model values thus:

$$\left. \begin{aligned} Z_\theta / M_\theta &= \frac{1}{s} Z'_\theta / M'_\theta \\ M_q / U &= s^4 \mu / u \end{aligned} \right\} \text{-----} (8)$$

where μ is the coefficient of damping moment in pitch for the model with head-on speed u . One may write $Z_q + m U = n m U$, where n is to be found experimentally, since $Z_q \propto U$. Putting these new values in (7), the working criterion for pitch becomes

$$a \frac{\mu}{u} \frac{Z'_\theta}{M'_\theta} = 1 \text{-----} (9)$$

where $a = \frac{s^3}{mn}$. The stability criterion (9) is now in a form convenient to use with familiar wind tunnel data.

³Books on mechanics prove $\dot{w}_1 = \dot{w} - Uq$. See Wilson's Aeronautics §48.

CRITERION OF YAW STABILITY

By a very similar process the yaw velocity proves to be constant when

$$\psi N_\psi + r N_r = 0 \dots\dots\dots (10)$$

$$\psi Y_\psi + r(Y_r - m U) = 0 \dots\dots\dots (11)$$

and decreases when the damping exceeds the disturbing moment; that is when

$$\frac{Y_\psi N_r}{N_\psi (Y_r - m U)} > 1 \dots\dots\dots (12)$$

Hence

$$a \frac{\mu}{u} \frac{Y'_\psi}{N'_\psi} > 1 \dots\dots\dots (13)$$

is the working criterion for yaw stability, and is the analogue of (9). Here $a = \frac{s^3}{mn'}$, where $n' = (Y_r - m U)/m U$, as previously explained for pitch; and the primes indicate model symbols.

By (10) the damping moment $r N_r$ rotationally balances the disturbing moment ψN_ψ ; by (11) the disturbing force ψY_ψ , the damping force $r Y_r$, and the inertia force $-m U$, are in translational balance.

If the yawing velocity is accelerated, and C_r is the opposing moment due to angular inertia, (10) becomes

$$\psi N_\psi + r N_r = C_r \dots\dots\dots (14)$$

which is the analogue of (4), and is simultaneous with (11).

ALTERNATIVE DERIVATIONS

The foregoing treatment fixes the attention upon the chief forces and moments governing the ship's motion under the simple conditions therein assumed. Crocco in 1907, and various British writers some years later, investigated the motion of full-rigged airships with their centroids sufficiently below their buoyancy centers, and obtained approximate criteria which are reducible to forms (9), (13). It is therefore unnecessary to discuss here the practical applicability of the criteria, since that has been done in the writings just cited. Reference may be made to R. & M. Nos. 257 and 361 of the National Physical Laboratory of England.

In passing one may observe that British writers give as stability criteria in pitch and yaw

$$M_q Z_w / M_w (Z_q + U) = 1 \dots\dots\dots (7_1)$$

$$Y_\psi N_r / N_\psi (Y_r - U) > 1 \dots\dots\dots (12_1)$$

in which the symbols are for the ship. On substituting for these symbols their values (in the forms given by those writers) in terms of the model symbols, one readily obtains (9) and (13).

MOMENT ARMS IN YAW

In (12) one may write $N_\psi / Y_\psi = x_1$, which is the arm of the disturbing force, or its distance from the centroid. Hence the other factor must be a length, say $N_r / (Y_r - m U) = x_2$, where x_2 is the distance from the centroid to the resultant of $r Y_r$ and $-m r U$. By (12) therefore

$$x_2 / x_1 = 1 \dots\dots\dots (15)$$

for steady yawing motion. This relation is obvious without the aid of algebra; for (15) merely implies that the lateral disturbing force ψY_ψ is equal and opposite to the resultant $r (Y_r - m U)$ of the reacting forces which kinetically balance it.

In like manner N'_ψ / Y'_ψ is the arm of the disturbing force on the model; hence the other factor $a\mu/u$ in (13) must be the arm of the reacting forces. By dynamical similarity the arms of the forces on the ship are s times as long as those of the model; but equal them when all are expressed as percentages of the length of the major axis of the respective hulls. The stability criterion in either case is the ratio of the reacting to the disturbing arm.

REPORT No. 213

**A RÉSUMÉ OF THE ADVANCES IN THEORETICAL
AERONAUTICS MADE BY MAX M. MUNK**

By JOSEPH S. AMES

National Advisory Committee for Aeronautics

CONTENTS

	Page
General principles of hydrodynamics.....	93
Problems more specially concerning airships.....	96
Introduction.....	96
Moments and forces acting on airships.....	100
Distribution of pressure over the envelope of an airship.....	104
Conclusion.....	105
Problems more specially concerning airfoils and airplanes.....	106
Introduction.....	106
Illustrations of two-dimensional flow.....	107
Angle of attack and lift. Wing section theory.....	115
Conclusion.....	117
Pitching moment and center of pressure.....	118
Conclusion.....	121
Induced drag and induced angle of attack.....	121
Conclusion.....	129
Propeller theory.....	129
Introduction.....	129
Froude's slipstream theory.....	129
The slip curve.....	130
The slip modulus.....	130
Torque.....	132
The torque slip curve.....	133

REPORT No. 213

A RÉSUMÉ OF THE ADVANCES IN THEORETICAL AERONAUTICS MADE BY MAX M. MUNK

By JOSEPH S. AMES

INTRODUCTION

In order to apply profitably the mathematical methods of hydrodynamics to aeronautical problems, it is necessary to make certain simplifications in the physical conditions of the latter. To begin with, it is allowable in many problems, as Prandtl has so successfully shown, to treat the air as having constant density and as free of viscosity. But this is not sufficient. It is also necessary to specify certain shapes for the solid bodies whose motion through the air is discussed, shapes suggested by the actual solids—airships or airfoils—it is true, but so chosen that they lead to solvable problems.

In a valuable paper presented by Dr. Max M. Munk, of the National Advisory Committee for Aeronautics, Washington, before the Delft Conference in April, 1924, these necessary simplifying assumptions are discussed in detail. It is the purpose of the present paper to present in as simple a manner as possible some of the interesting results obtained by Dr. Munk's methods. For fuller details and a discussion of many practical questions reference should be made to Munk's original papers:

1. The Aerodynamic Forces on Airship Hulls. N. A. C. A. Report No. 184, 1924.
2. Elements of the Wing Section Theory and of the Wing Theory. N. A. C. A. Report No. 191, 1924.
3. Remarks on the Pressure Distribution Over the Surface of an Ellipsoid, Moving Translationally Through a Perfect Fluid. N. A. C. A. Technical Note No. 196, 1924.
4. The Minimum Induced Drag of Aerofoils. N. A. C. A. Report No. 121, 1921.
5. General Theory of Thin Wing Sections. N. A. C. A. Report No. 142, 1922.
6. Determination of the Angles of Attack of Zero Lift and of Zero Moment, Based on Munk's Integrals. N. A. C. A. Technical Note No. 122, 1923.
7. General Biplane Theory. N. A. C. A. Report No. 151, 1922.

GENERAL PRINCIPLES OF HYDRODYNAMICS

In all the practical problems to be discussed, only the most general principles of hydrodynamics are used and in practically all cases the problems are reduced to questions involving only energy and momentum. It may be worth while to deduce the few equations necessary, although they are given in every textbook.

Since air is a fluid, the pressure is everywhere perpendicular to any surface through which it is transferred. If u , v , w are components of the velocity of flow at any point,

$$\frac{\partial u}{\partial x} + \frac{\partial v}{\partial y} + \frac{\partial w}{\partial z} = 0,$$

since the density is considered to be constant. The entire energy of the flow is kinetic, and therefore

$$T = \frac{1}{2} \rho \int (u^2 + v^2 + w^2) d\tau$$

where $d\tau$ is an element of volume of the fluid. By Newton's law of motion

$$\rho \frac{du}{dt} dx dy dz = \left[p - \left(p + \frac{\partial p}{\partial x} dx \right) \right] dy dz = - \frac{\partial p}{\partial x} dx dy dz$$

or

$$\rho \frac{du}{dt} = - \frac{\partial p}{\partial x}$$

This may be written

$$\rho du = - \frac{\partial (p dt)}{\partial x}$$

The impulse per unit area in the time dt is, by definition, $p dt$. So the infinitesimal change in velocity du can be considered as produced by the infinitesimal impulse $p dt$, and a finite velocity u may be considered as produced from a state of rest by the finite impulse $P \equiv \int p dt$, where, then

$$\rho u = - \frac{\partial P}{\partial x}$$

or

$$u = \frac{\partial}{\partial x} \left(- \frac{P}{\rho} \right)$$

Similarly, the other two components of the velocity of flow at any point will be defined by

$$v = \frac{\partial}{\partial y} \left(- \frac{P}{\rho} \right), w = \frac{\partial}{\partial z} \left(- \frac{P}{\rho} \right)$$

Flows such as this, where

$$u = \frac{\partial \varphi}{\partial x}, v = \frac{\partial \varphi}{\partial y}, w = \frac{\partial \varphi}{\partial z}$$

are called "potential flows," and φ is called the "velocity potential." In this case, when the flow is considered as produced by an impulse, P ,

$$\varphi = - \frac{P}{\rho} \text{-----} (1)$$

or, the impulse per unit area, equals $-\rho\varphi$.

There are cases of potential flow in which φ is not a single-valued function, and in such

$$P = -\rho (\varphi_1 - \varphi_2) \text{-----} (1a)$$

where φ_1 and φ_2 are the values of φ at the same point. Since $\varphi_2 - \varphi_1 = \int_1^2 (u dx + v dy + w dz)$,

if $_1$ and $_2$ refer to the same point, the integral is called the "circulation," and, if its value is μ , the equation may be written $P = +\rho\mu$, where P is in the direction of the flow.

As an illustration, consider the flow discussed later, equation (41), in which, for any point on the axis of x ,

$$\varphi = A_0 \sin^{-1} x$$

The flow is a two-dimensional one, as shown in the figure. Consider an imaginary surface at x , having a minute length along the axis of x and unit length perpendicular to the plane of the paper. Let the point 1 be on the lower side of the surface and the point 2 on the upper.

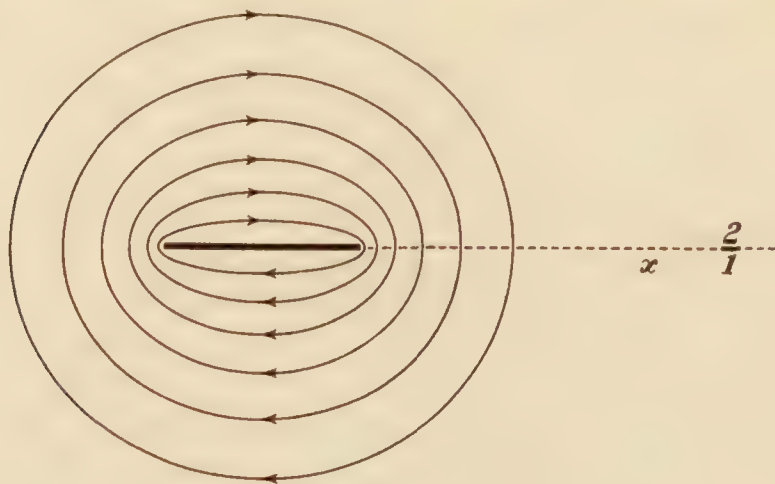


FIG. 1

$$\varphi_2 - \varphi_1 = \int_1^2 d\varphi = 2\pi A_o$$

when the points approach each other indefinitely. The impulse per unit area at the point 1 is $-\rho\varphi_1$ and its action is downward, being perpendicular to the fluid surface below the imaginary surface; at the point 2 the impulse per unit area is $-\rho\varphi_2$, acting upward, since it is perpendicular to the fluid surface above the imaginary surface. Therefore the total impulse per unit area acting downward on the fluid is

$$P = \rho (\varphi_2 - \varphi_1) = \rho 2\pi A_o$$

Again, since

$$\frac{\partial u}{\partial x} + \frac{\partial v}{\partial y} + \frac{\partial w}{\partial z} = 0,$$

φ must satisfy everywhere in the fluid the equation

$$\frac{\partial^2 \varphi}{\partial x^2} + \frac{\partial^2 \varphi}{\partial y^2} + \frac{\partial^2 \varphi}{\partial z^2} = 0$$

Making use again of Newton's equation, and taking into account the fact that, in general, u, v , and w are functions of (t, x, y, z) , the general equations of motion are

$$\frac{du}{dt} = \frac{\partial u}{\partial t} + u \frac{\partial u}{\partial x} + v \frac{\partial u}{\partial y} + w \frac{\partial u}{\partial z} = -\frac{1}{\rho} \frac{\partial p}{\partial x}$$

and two similar ones for $\frac{dv}{dt}$ and $\frac{dw}{dt}$.

But

$$\frac{\partial u}{\partial y} = \frac{\partial v}{\partial x} \text{ and } \frac{\partial u}{\partial z} = \frac{\partial w}{\partial x}$$

since

$$u = \frac{\partial \varphi}{\partial x}, \quad v = \frac{\partial \varphi}{\partial y}, \quad w = \frac{\partial \varphi}{\partial z};$$

therefore

$$\frac{\partial u}{\partial t} + u \frac{\partial u}{\partial x} + v \frac{\partial v}{\partial x} + w \frac{\partial w}{\partial x} = -\frac{1}{\rho} \frac{\partial p}{\partial x}$$

or

$$\frac{\partial}{\partial t} \left(\frac{\partial \varphi}{\partial x} \right) + \frac{1}{2} \frac{\partial}{\partial x} (u^2 + v^2 + w^2) = -\frac{1}{\rho} \frac{\partial p}{\partial x}.$$

with two similar equations for y and z . On integration, these three equations give

$$\frac{\partial \varphi}{\partial t} + \frac{1}{2} (u^2 + v^2 + w^2) = -\frac{p}{\rho} + \text{a constant.}$$

Written differently,

$$p = -\rho \frac{\partial \varphi}{\partial t} + C - \frac{\rho}{2} (u^2 + v^2 + w^2)$$

In the case of a steady state $\frac{\partial \varphi}{\partial t} = 0$, and

$$p = C - \frac{\rho}{2} (u^2 + v^2 + w^2) \dots \dots \dots (2)$$

which is Bernouilli's famous theorem. If there is a portion of space in which the fluid is at rest, the pressure there equals C .

The work done by an impulse is proved in mechanics to be the product of the impulse by the average of the initial and final velocities in the direction of the impulse. If a solid is moving through a fluid otherwise at rest, and if the existing fluid motion is considered as having been produced from rest by impulses applied by the surface of the body, the velocity normal to any element of surface is $\frac{d\varphi}{dn}$ where dn is drawn from the body into the fluid, and the mean value of this and the initial zero velocity is $\frac{1}{2} \frac{d\varphi}{dn}$; further, the impulse, normal to the surface dS , acting on the fluid is $-\rho \varphi \cdot dS$. Therefore, the kinetic energy of the fluid is

$$T = -\frac{\rho}{2} \int \varphi \frac{d\varphi}{dn} dS, \text{ taken over the surface of the solid body} \dots \dots \dots (3)$$

Other general principles will be discussed as the occasion arises.

PROBLEMS MORE SPECIALLY CONCERNING AIRSHIPS

INTRODUCTION

The fundamental problems concerning airships are: (1) the determination of the moments acting on them under varying conditions of flight; (2) the determination of the distribution of transverse forces; (3) the distribution of pressure over the envelope.

These problems can be solved, at least approximately, by the application of certain general theorems.

When a body moves through a fluid otherwise at rest, there is a certain amount of kinetic energy of the fluid caused by the motion of the body. If the latter is moving with a velocity V in a definite direction, if T is the kinetic energy of the fluid due to the motion of the body, and if

ρ is the density of the fluid, by definition $\frac{T}{\frac{1}{2} V^2}$ is called the "apparent additional mass" of the

body for motion in that particular direction, and is written $K \rho$.

As an illustration, consider an infinitely long circular cylinder moving transversely in a definite direction with a velocity V . Choose this direction as the axis for a set of polar coordinates whose origin is on the axis of the moving cylinder. The velocity of any particle of the fluid will be in a plane perpendicular to the axis of the cylinder, so the flow is called two-dimensional, or uniplanar. A particle in contact with the cylinder must have the same component of velocity normal to the cylinder as the wall of the cylinder at that point. So, if r and θ are the polar coordinates of any point of the fluid in a particular transverse plane, and if R is the radius of the cylinder, this condition may be expressed by writing

$$\left(\frac{\partial \varphi}{\partial r} \right)_{r=R} = V \cos \theta_0,$$

if θ_0 denotes the point on the cylinder. This leads at once to the value of φ for any point in the fluid, r , θ , viz

$$\varphi = -\frac{VR^2 \cos \theta}{r}$$

for it may be proved that this satisfies both

$$\frac{\partial^2 \varphi}{\partial x^2} + \frac{\partial^2 \varphi}{\partial y^2} = 0.$$

and the condition just expressed for the surface of the cylinder. Hence the kinetic energy of flow

$$T = -\frac{\rho}{2} \int \varphi \frac{d\varphi}{dn} dS$$

becomes, since at $r=R$, $\varphi = -VR \cos \theta_0$, $\frac{d\varphi}{dn} = V \cos \theta_0$ and $dS = R d\theta_0 h$, where h is any length desired of the cylinder,

$$T = \frac{\rho}{2} V^2 R^2 h \int_0^{2\pi} \cos^2 \theta_0 d\theta_0 = \frac{\rho}{2} V^2 \pi R^2 h$$

Consequently the apparent additional mass is

$$\frac{T}{\frac{1}{2} V^2} = \rho \pi R^2 h$$

i. e., is the mass of the fluid displaced by the cylinder. This is sometimes expressed, with reference to the two-dimensional flow, by saying that the "apparent mass of a circle is $\rho \pi R^2$."

It will be proved later that if a plane lamina infinite in length and of width b is moving transversely with a velocity V , the flow being again two dimensional, the apparent additional mass of a length h of the lamina is $\rho \pi \left(\frac{b}{2}\right)^2 h$ (the same as for a circular cylinder whose diameter

is b .) So the apparent transverse mass of a straight line of length b is $\rho \pi \left(\frac{b}{2}\right)^2$ in a two-dimensional flow, this really being the apparent mass of a portion of length unity of an infinitely long lamina whose width is b .

If a body is moving in a definite direction with a constant velocity, the flow accompanies the body, so that the kinetic energy does not change, therefore there is no drag, which would absorb energy. Further, if the flow gives rise to a single-valued velocity potential, there is no lift. (See a later section.) But although, therefore, the resultant force is zero, there may be a moment acting on the body.

This may best be seen by a consideration of the momentum of the flow. When the body is moving with the velocity V in a definite direction, let there be a component of momentum of flow perpendicular to this direction and let its amount be $A\rho V$. Then, with reference to any axis perpendicular to the plane including the line of velocity and the direction of the component of momentum, there is a certain moment of momentum; and, as the body moves a distance V in a unit time, this moment of momentum increases in that time by an amount $V \cdot A\rho V$. An equal but opposite moment around the specified axis must, therefore, be acting on the body. Hence, moment = velocity of body \times component of momentum of flow perpendicular to the axis of the moment and to the direction of the velocity. The "sense" of the moment is easily seen.

Conversely, if the body does not experience any moment, the momentum of the flow must be entirely in the line of motion of the body.

If a solid body is held stationary in a uniform flow, the kinetic energy of the entire infinite flow is of course infinite, but less than it would be if the body were absent, owing to two reasons: (1) The solid displaces an equal volume of the fluid, which otherwise would be in motion; (2) the velocity of the flow is reduced in front of and behind the body. This decrease in kinetic energy for a definite velocity of flow equals the kinetic energy of the total flow if the solid is moving in a stationary fluid with the same velocity as the velocity of flow in the first case.

When the solid is at rest in a uniform flow, let it be turned slightly through an angle $d\alpha$ about a definite axis; if there is a moment about this axis acting on the body in such a sense that it opposes the rotation $d\alpha$, work will be required to turn the body, and the kinetic energy of the fluid, T' , will increase by an amount equal to the product of this moment and the angular displacement. Similarly, if the moment is in the same sense as $d\alpha$, $-dT' = Md\alpha$. Therefore, if now the body is moving through a stationary fluid, $Md\alpha = dT$, since $dT = -dT'$. Hence

$$M = \frac{dT}{d\alpha} \text{-----} (4)$$

where M is the moment acting on the body around a definite axis, in the same "sense" as $d\alpha$, the angular displacement around this axis.

If, therefore, for a given direction of motion, T is a maximum, a slight change $d\alpha$ would result in a decrease of T , and M would be negative, indicating a moment acting on the body in such a sense as to oppose the change $d\alpha$. Such a direction of motion would therefore be one of stable equilibrium. Similarly, if T is a minimum for a given line of motion, there is unstable equilibrium.

In general, if any motion is generated from rest by an impulse, the work done equals the product of the impulse by half the component of the velocity in the direction of the impulse. The impulse equals the momentum; therefore, the kinetic energy equals one-half the scalar product of the momentum and the velocity. This theorem may be applied to the fluid motions produced by the motion of solids through them.

A body gives rise to a definite kinetic energy of flow if it has a constant velocity in a specified direction; and, if its motion is reversed, it will give rise to the same amount, because the flow at each point of the fluid is reversed. (This is evident because the effect of the presence of the solid body when at rest in a stream of fluid may be duplicated by a certain distribution of sources and sinks, giving rise to the same field of velocity potential as before, outside the space previously occupied by the solid; then, if the stream is reversed and each source is made into a sink of an equal strength and vice versa, the potential field is exactly reversed, so that the velocity at each point is reversed.) The kinetic energy is different for directions of motion other than as specified, but it is always a positive number. Therefore, as the orientation of the line of motion of the body is changed from some definite one to its opposite, there must be two lines of motion—somewhere between—for one of which the kinetic energy is a maximum and for the other of which it is a minimum. For motion in either of these directions, therefore, $\delta T = 0$; that is, for any small angular displacement $\delta\alpha$ around an axis perpendicular to the direction of motion $\delta T = 0$. Consequently there is no moment acting on the body if it is moving in either of these two directions; and the body may therefore be said to be in equilibrium, stable if T is a maximum and unstable if T is a minimum.

Let a body be moving with a velocity V in such a direction that it is in equilibrium; call the direction \bar{A} . The momentum of the flow must be in the same direction, otherwise there



FIG. 2

would be a moment; call its value $K_1\rho V$. Keeping the orientation of the body unchanged, make the line of motion with the velocity V perpendicular to \bar{A} , i. e. along \bar{B} ; let the component along \bar{B} of the momentum of the flow be called $C\rho V$, its component along \bar{A} be called

$D\rho V$, and its component perpendicular to the plane of \overline{A} and \overline{B} be called $E\rho V$. Again, let its line of motion with velocity V be in the plane of \overline{A} and \overline{B} , making an angle α with \overline{A} . Then the momentum along \overline{A} , which may be written G_A , has the value

$$\begin{aligned} G_A &= K_1\rho V \cos \alpha + D\rho V \sin \alpha. \quad \text{Similarly, along } \overline{B} \\ G_B &= C\rho V \sin \alpha; \text{ and, perpendicular to the plane of } \overline{AB}, \\ G_{AB} &= E\rho V \sin \alpha \end{aligned}$$

also

$$\begin{aligned} V_A &= V \cos \alpha \\ V_B &= V \sin \alpha \\ V_{AB} &= 0 \end{aligned}$$

Consequently the kinetic energy of the flow, which equals one-half the scalar product of the momentum and the velocity, is given by the equation

$$T = \frac{\rho}{2} V^2 (K_1 \cos^2 \alpha + C \sin^2 \alpha + D \sin \alpha \cos \alpha)$$

Under these circumstances the moment acting on the body around an axis perpendicular to the plane of \overline{A} and \overline{B} is

$$M = \frac{dT}{d\alpha} = \frac{\rho}{2} V^2 ((C - K_1) \sin 2\alpha + D \cos 2\alpha)$$

But if $\alpha = 0$, $M = 0$, since \overline{A} is a line of equilibrium, therefore $D = 0$. Consequently, when the body is moving in a direction \overline{B} at right angles to \overline{A} —a line of equilibrium, there is a component of momentum $C\rho V$ along \overline{B} and a component $E\rho V$ perpendicular to the plane of \overline{A} and \overline{B} , but none parallel to \overline{A} . If the body is now rotated about the line \overline{A} , through 180° , and again set moving along \overline{B} with a velocity V , the momentum will have a component of momentum $C\rho V$ along \overline{B} , and a component— $E\rho V$ perpendicular to the plane \overline{A} and \overline{B} . Therefore, as the body is rotated about \overline{A} as an axis, there must be some definite orientation such that, for a velocity along \overline{B} , the component of momentum perpendicular to the plane of \overline{A} and \overline{B} is zero. For this orientation, then, the momentum is entirely along \overline{B} . Therefore, the present location of \overline{A} and \overline{B} with reference to the body are what may be called “axes of equilibrium.” They are at right angles to each other. Similarly, it will be possible to find a third axis of equilibrium which is perpendicular to the other two. Every body possesses, therefore, three mutually perpendicular axes of equilibrium, and, in general, no more. Let the apparent additional masses with reference to these three axes be called $K_1\rho$, $K_2\rho$, $K_3\rho$; that is, if V_1 , V_2 , V_3 are the components of V with reference to these same axes, the flow momenta parallel to these axes are $K_1\rho V_1$, $K_2\rho V_2$, $K_3\rho V_3$. Consequently the kinetic energy of the flow is

$$T = \frac{1}{2} \rho (K_1 V_1^2 + K_2 V_2^2 + K_3 V_3^2) \dots\dots\dots (5)$$

The moment acting upon the body is determined by the equations previously given. If the line of velocity is in a plane including two axes of equilibrium, the equations are specially simple. Let the velocity make the angle α with the axis 1; then

$$G_1 = K_1\rho V \cos \alpha; \quad G_2 = K_2\rho V \sin \alpha; \quad G_3 = 0.$$

The component perpendicular to V is

$$K_2\rho V \sin \alpha \cos \alpha - K_1\rho V \cos \alpha \sin \alpha = \frac{\rho}{2} V (K_2 - K_1) \sin 2\alpha$$

and therefore the moment $= \frac{\rho}{2} V^2 (K_2 - K_1) \sin 2\alpha$. This is about an axis perpendicular to the plane of 1 and 2 and is clockwise. (Of course, if $K_2 < K_1$, it is actual counterclockwise.)

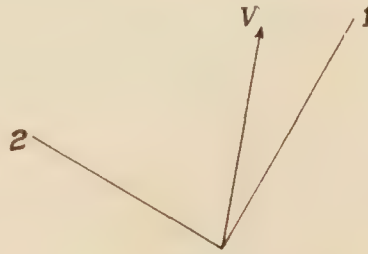


FIG. 3

As stated above, the three "principal" momenta of the flow are $K_1\rho V_1$, $K_2\rho V_2$, $K_3\rho V_3$, where V_1 , V_2 , V_3 are the components of the velocity V . But if the localized vector is formed which represents $K_1\rho V_1$, i. e., the resultant of the parallel vectors representing the components of the momentum along this axis of each individual particle of the fluid; and similarly the localized vectors representing $K_2\rho V_2$ and $K_3\rho V_3$, it will be found that, in general, these three localized vectors do not pass through a common point. Therefore they can not be compounded to form a single localized vector, and we can not in general speak of "the momentum" of the flow. If, however, the moving body is one of revolution, or if it has three mutually perpendicular planes of symmetry, then there is a point common to the three lines of action of the principal momenta, and it is called the "aerodynamic center." In this case we may speak of "the flow-momentum" G , and our previous formulas for moments and kinetic energy may be written

$$\overline{M} = [\overline{G} \cdot \overline{V}] \text{ (6)}$$

$$T = \frac{1}{2} (\overline{G} \cdot \overline{V}) \text{ (7)}$$

MOMENTS AND FORCES ACTING ON AIRSHIPS

Airships may often be considered as having surfaces of revolution described by rotation about the longitudinal axis. The central portion of an airship may be considered as a circular cylinder, and therefore, from what has been proved for circular cylinders, the transverse apparent mass of the airship equals the mass of the fluid displaced, approximately. The longitudinal mass is small, because in longitudinal motion of the airship the air displaced by the bow escapes transversely on the whole and the air flowing in at the stern also flows in transversely, so that the momentum of the air in the direction of motion is small. On the other hand, when the airship moves transversely, the air in a transverse layer perpendicular to the longitudinal axis remains in the layer, so that the flow is a two-dimensional one about a circle. This is true near the central portion of the airship and approximately so elsewhere. Call the longitudinal apparent mass $K_1\rho$, the transverse apparent mass $K_2\rho$.

Let the airship move in a straight line with a velocity V having an angle of yaw (or pitch) φ . The longitudinal momentum $= V \cos \varphi \cdot K_1\rho$; the transverse momentum $= V \sin \varphi \cdot K_2\rho$; hence the component perpendicular to the line of V is $\frac{\rho}{2} V (K_2 - K_1) \sin 2\varphi$, and the moment acting on the airship is

$$M = \frac{\rho}{2} V^2 (K_2 - K_1) \sin 2\varphi \text{ (8)}$$

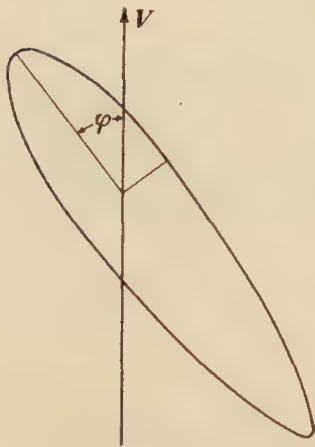


FIG. 4

about an axis perpendicular to the plane including V and the longitudinal axis and is of such a "sense" as to increase φ . It is therefore called the "unstable" moment.

Let the airship move in a horizontal circle of radius r , with a velocity V and at an angle of yaw φ . Call the "apparent moment of inertia" about a transverse axis through the aerodynamic center $K'\rho$. The longitudinal velocity is $V \cos \varphi$; the transverse velocity is $V \sin \varphi$; and the angular velocity is $\frac{V}{r}$. Therefore, the longitudinal momentum is $K_1\rho V \cos \varphi$; the transverse momentum is $K_2\rho V \sin \varphi$, and the angular momentum, which remains constant, is $K'\rho \frac{V}{r}$. Since the aerodynamic center moves in a circle, the resultant force acting on the fluid must always pass through the center of this circle. During the motion the two components of momentum remain constant in amount but their directions rotate with the angular velocity $\frac{V}{r}$. If a vector representing momentum G rotates with an angular velocity ω , a force $G\omega$ must be

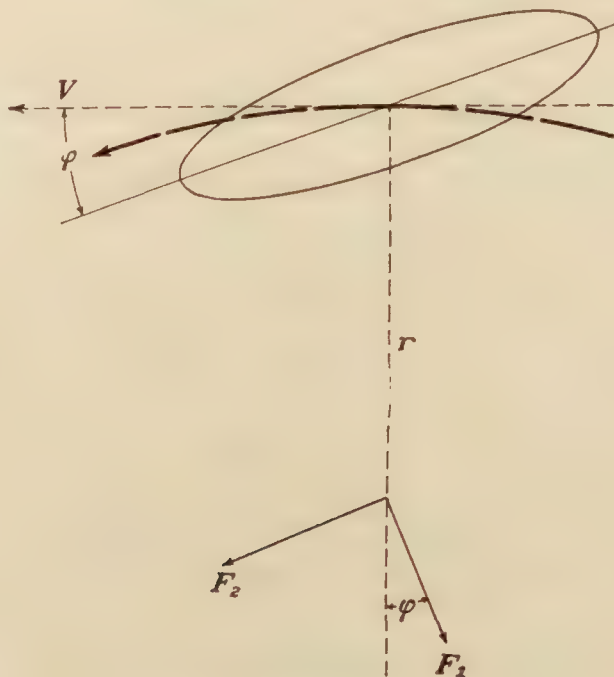


FIG. 5

acting perpendicular to the line of G . Therefore there must be acting on the fluid (1) a transverse force F_1 , opposite in direction to the transverse momentum, equal to $K_1\rho V \cos \varphi \cdot \frac{V}{r}$, (2) a longitudinal force F_2 , in the same direction as the longitudinal momentum, equal to $K_2\rho V \sin \varphi \cdot \frac{V}{r}$. The moment of these forces about an axis through the aerodynamic center, perpendicular to the plane of the motion is $(K_2 - K_1) \frac{\rho}{2} V^2 \sin 2\varphi$. This moment, acting on the fluid, is clockwise (in the drawing); therefore the moment acting on the airship is counterclockwise, tending to increase φ . (There is also a "negative drag.")

This moment is the same in amount as that found for the airship in straight flight with the same angle of yaw; but the distribution of forces along the airship is different in the two cases, as will now be shown by making a closer analysis of the two flows.

Consider an airship flying in a straight line with velocity V , and with an angle of pitch φ downward. In a stationary transverse plane perpendicular to the axis, and therefore approximately vertical, the flow may be regarded as two-dimensional, as explained before. The airship displaces a circle, which changes its size as the ship advances and also its position, owing to the pitch. The apparent mass of the two-dimensional flow in a layer of thickness dx , if S is the area of the circle, is $\rho S dx$, since the apparent transverse mass of a circular cylinder, if the flow is two-dimensional, is known to be equal to the mass of the fluid displaced. The transverse velocity is $V \sin \varphi$, and therefore the transverse momentum upward (in the drawing)

in the layer is $\rho S V \sin \varphi dx$. The rate of change of this is $\rho V \sin \varphi \cdot dx \cdot \frac{dS}{dt}$. But

$$\frac{dS}{dt} = \frac{dS}{dx} \frac{dx}{dt} = + V \cos \varphi \frac{dS}{dx}.$$

Hence at any element of length dx there is a transverse force downward on the airship, given by

$$\frac{\rho}{2} V^2 \sin 2\varphi \frac{dS}{dx} dx$$

This force is in opposite directions at the two ends, and produces the unstable moment.

Now consider the airship flying with constant velocity V , and angle of yaw φ , in a circle of radius r . The transverse momentum of a layer of thickness dx , outward, away from the circle, is, as before, $\rho S v dx$, where v is the transverse velocity. This now varies with the time. So the rate of change of this outward momentum is

$$\rho dx \left(S \frac{dv}{dt} + v \frac{dS}{dt} \right).$$

v is made up of two terms $V \sin \varphi$, due to the translation, and $\frac{V}{r} x$, due to the rotation, where x is measured along the axis from the aerodynamic center. Hence

$$\frac{dv}{dt} = \frac{dv}{dx} \frac{dx}{dt} = \frac{V}{r} V \cos \varphi; \quad \frac{dS}{dt} = \frac{dS}{dx} V \cos \varphi.$$

Thus the rate of change of the transverse fluid momentum outward is

$$\begin{aligned} & \rho dx \left(S \frac{V^2}{r} \cos \varphi + V^2 \frac{dS}{dx} \sin \varphi \cos \varphi + \frac{V^2}{r} x \cos \varphi \frac{dS}{dx} \right) \\ &= \left(V^2 \frac{\rho}{2} \sin 2\varphi \frac{dS}{dx} + V^2 \frac{\rho}{r} S \cos \varphi + V^2 \frac{\rho}{r} \cos \varphi \cdot x \frac{dS}{dx} \right) dx \dots \dots \dots (9) \end{aligned}$$

Therefore this gives the transverse force inward, toward the inside of the circle, on an element of length dx of the airship.

The first of the three terms is the same as found for the case of straight flight. The last two terms combine to form $V^2 \frac{\rho}{r} \cos \varphi \frac{d(xS)}{dx} dx$, and the resultant moment due to this force vanishes. The distribution of these three forces is shown in the accompanying figure.

In discussions of apparent masses it is customary to introduce three constants, defined as follows:

$K_1 \equiv k_1$ volume; $K_2 \equiv k_2$ volume; $K' \equiv k'J$ where J is the moment of inertia of the volume when occupied by matter of density one.

In deducing the transverse forces on an actual airship, it is not correct to assume that the transverse flow is two-dimensional, especially near the ends. A fairly satisfactory formula may be obtained by multiplying each of the three terms in the approximate formula by a definite factor, depending upon the shape of the airship. Munk adduces reasons for multiplying the first term by $k_2 - k_1$ and the other two by k' . (In this discussion there is omitted the transverse component of the centrifugal force produced by the air which is flowing longitudinally and gives rise to the longitudinal mass. It is very small.)

What has been said above applies to airships without fins. • One function of the fins is to counterbalance the unstable moment. If S is the effective area of a pair of fins and b the total span, the lift exerted on them, as proved in a later section, is

$$L = 2\pi \frac{\rho}{2} V^2 \frac{S}{1 + \frac{2S}{b^2}} \cdot \varphi$$

where φ is the angle of attack measured in radians. If the mean distance of the fins from the center of the airship is written a , then, for the lift to balance the unstable moment,

$$La = (k_2 - k_1) \cdot \text{volume} \cdot \frac{\rho}{2} V^2 2\varphi, \text{ since } \varphi \text{ is small.}$$

Hence the area of the fins

$$S = \frac{(k_2 - k_1) \cdot \text{volume}}{a} \frac{1 + \frac{2S}{b^2}}{\pi}$$

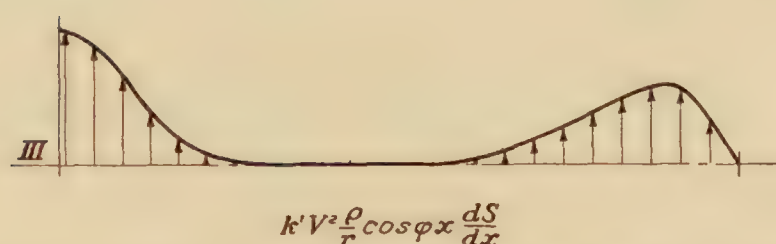
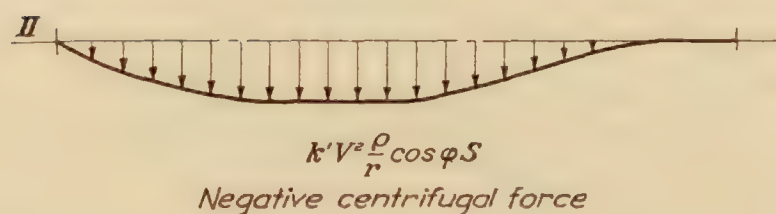
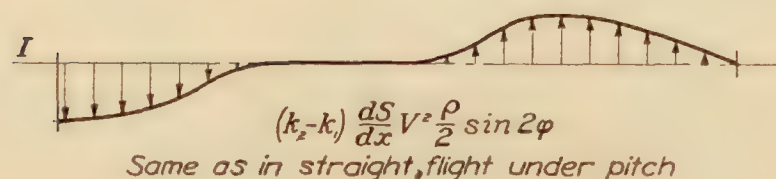
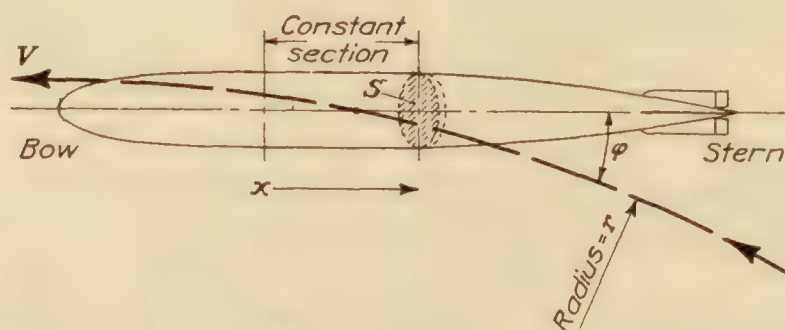


FIG. 6.—Diagram showing the direction of the transverse air forces acting on an airship flying in a turn. The three terms are to be added together

If the ship is flying in a circle of radius r , not simply must the air force on the fins balance the unstable moment, but it must produce the force required to make the airship move in a circle, i. e., $\rho \cdot \text{volume} \cdot \frac{V^2}{r}$. This can therefore be equated to the unstable moment divided by a and hence

$$\rho \cdot \text{volume} \cdot \frac{V^2}{r} = \frac{(k_2 - k_1) \cdot \text{volume} \cdot \frac{\rho}{2} V^2 2\varphi}{a}$$

or

$$\varphi = \frac{a}{r (k_2 - k_1)}$$

and this value may be substituted in the formulas giving the distribution of the transverse forces.

DISTRIBUTION OF PRESSURE OVER THE ENVELOPE OF AN AIRSHIP

It is proved in Lamb's Hydrodynamics, Chapter V, that, if an ellipsoid is moving through a fluid with constant velocity U , parallel to a principal axis, which may be called the x -axis, the velocity potential of the flow at any point of its surface is

$$\varphi = A U x$$

where A is a constant for a given ellipsoid.

This constant A may be expressed in terms of the apparent mass of the ellipsoid for motion parallel to the x -axis. The kinetic energy of the flow is

$$T = -\frac{1}{2} \rho \oint \varphi \frac{d\varphi}{dn} dS \text{ over the ellipsoid.}$$

$$\frac{d\varphi}{dn} dS \text{ may obviously be replaced by } U dy dz.$$

Therefore

$$T = -\frac{1}{2} \rho \oint A U^2 x dy dz = -\frac{\rho}{2} U^2 A \oint x dy dz = -\frac{\rho}{2} U^2 A \cdot \text{volume of ellipsoid.}$$

But by the definition of apparent mass

$$T = \frac{\rho}{2} U^2 k_1 \cdot \text{volume.}$$

Hence

$$A = -k_1, \text{ and } \varphi = -k_1 U x$$

Similarly, if the motion of the ellipsoid is oblique, so that its velocity has the components U, V, W with reference to its principal axes, the velocity potential at any point of the surface is

$$\varphi = -k_1 U x - k_2 V y - k_3 W z \dots\dots\dots (10)$$

the origin of coordinates being at the center of the ellipsoid.

The values of the k 's are given by certain definite integrals. If a, b, c are the semiaxes of the ellipsoid,

$$k_1 = \frac{\alpha}{2 - \alpha} \text{ where } \alpha = abc \int_0^\infty \frac{dp}{(a^2 + p) \sqrt{(a^2 + p)(b^2 + p)(c^2 + p)}}$$

$$k_2 = \frac{\beta}{2 - \beta} \text{ where } \beta = abc \int_0^\infty \frac{dp}{(b^2 + p) \sqrt{(a^2 + p)(b^2 + p)(c^2 + p)}}$$

$$k_3 = \frac{\gamma}{2 - \gamma}, \text{ etc.}$$

For an ellipsoid of revolution

$$b = c, k_1 = \frac{1 - k_2}{2k_2}, k_3 = k_2$$

The following table gives values of k_1 and k_2 for different elongation ratios of an ellipsoid of revolution.

Length (diameters)	k_1 (longitudinal)	k_2 (transverse)	$k_2 - k_1$	k' (rotation)
1	0.500	0.500	0	0
1.50	.305	.621	.316	.094
2.00	.209	.702	.493	.240
2.51	.156	.763	.607	.367
2.99	.122	.803	.681	.465
3.99	.082	.860	.778	.608
4.99	.059	.895	.836	.701
6.01	.045	.918	.873	.764
6.97	.036	.933	.897	.805
8.01	.029	.945	.916	.840
9.02	.024	.954	.930	.865
9.97	.021	.960	.939	.883
∞	.000	1.000	1.000	1.000

Similarly, if the ellipsoid is stationary in a stream of air whose velocity has the components U, V, W , the velocity potential at any point on the surface is

$$\varphi = A' Ux + B' Vy + C' Wz \dots\dots\dots (11)$$

where

$$A' = 1 - A = k_1 + 1, \quad B' = k_2 + 1, \quad C' = k_3 + 1,$$

and are therefore known quantities for a given ellipsoid. Further, the velocity of flow at any point on the surface is along the surface; and points of constant potential lie on parallel ellipses, intersections of the ellipsoid by the family of planes $\varphi = C$.

Consider the intersection of the surface of the ellipsoid by the plane $\varphi = A' Ux + B' Vy + C' Wz = 0$. At these points the gradient of φ is along the surface; hence the velocity of flow has the components $A' U, B' V, C' W$. At any other point on the surface, the direction of the gradient is not along the surface; and, if Δh is the constant perpendicular distance between any two planes whose potentials have a constant difference and if Δs is the shortest distance along the surface between the ellipses in which these planes cut the surface, $\Delta s = \Delta h$ at the first one of the points referred to above, while at any other point $\Delta h = \Delta s \cos \epsilon$, where ϵ is the angle between the normals to the surface at the two points. Consequently the velocity of flow has its maximum at the points first described; and, calling this v_{max} , the magnitude of the velocity at any other point of the surface is $v_{max} \cos \epsilon$.

For the case of an ellipsoid of revolution the velocity at any point on the surface may be found by simple geometry, as follows. Call the plane through the line of general flow and the axis of revolution of the ellipsoid the $X-Y$ plane—in order to have a simple mode of description. Then the transverse axis of the ellipsoid which lies in this plane is the only one which need be considered. The components of the velocity of the general flow are $U, V, 0$; hence the maximum velocity has the components $A' U, B' V, 0$. Let α, β, γ be the direction cosines of the normal to the surface at any point. At a point on the surface where the velocity of flow is a maximum draw a line parallel to this normal, and call the component of v_{max} along it v_1 and that perpendicular to it v_2 . v_2 is, from what has been said before, equal to the velocity of the flow at the point where the normal was originally drawn. But

$$v_{max}^2 = v_1^2 + v_2^2 = (A' U)^2 + (B' V)^2 = (k_1 + 1)^2 U^2 + (k_2 + 1)^2 V^2$$

and

$$v_1 = A' U \cdot \alpha + B' V \cdot \beta = (k_1 + 1) U \cdot \alpha + (k_2 + 1) V \cdot \beta$$

Hence

$$v_2^2 = (k_1 + 1)^2 U^2 + (k_2 + 1)^2 V^2 - ((k_1 + 1) U \alpha + (k_2 + 1) V \beta)^2 \dots\dots\dots (12)$$

Then, by Bernoulli's theorem, viz, $p + \frac{1}{2} \rho V^2 = \text{constant}$, the pressure may be calculated.

With a very elongated ellipsoid, k_1 is small and k_2 nearly equals 1. Hence $A' = 1$ and $B' = 2$, so the components of maximum velocity are U and $2V$. Consequently, while the angle of attack is defined by $\tan \alpha = \frac{V}{U}$, the direction of maximum flow makes an angle φ with the longitudinal axis, where $\tan \varphi = \frac{2V}{U}$. Therefore φ is about twice α .

CONCLUSION

Considering an airship as an ellipsoid of revolution of known volume and elongation ratio, so that k_1, k_2 , and k' (and also K_1 and K_2) are known,

1. The unstable moment, for an angle of yaw φ , in straight or circling flight, is

$$M = \frac{\rho}{2} V^2 (K_2 - K_1) \sin 2\varphi$$

2. The transverse force per unit length is, where S is the cross section at a point x ,

(a) For straight flight,

$$(k_2 - k_1) \frac{\rho}{2} V^2 \sin 2\varphi \cdot \frac{dS}{dx}$$

(b) For circling flight

$$(k_2 - k_1) \frac{\rho}{2} V^2 \cdot \sin 2\varphi \frac{dS}{dx} + k' V^2 \frac{\rho}{r} S \cos \varphi + k' V^2 \frac{\rho}{r} \cos \varphi x \frac{dS}{dx}$$

3. The pressure over the envelope is given by the formula

$$p = C - \frac{1}{2} \rho v^2$$

where, if U and V are the components of flight velocity with respect to the longitudinal and transverse axes,

$$v^2 = (k_1 + 1)^2 U^2 + (k_2 + 1)^2 V^2 - ((k_1 + 1) U \alpha + (k_2 + 1) V \cdot \beta)^2$$

α and β being the direction cosines of the normal to the surface at the point at which the pressure is to be calculated.

PROBLEMS MORE SPECIALLY CONCERNING AIRFOILS AND AIRPLANES

INTRODUCTION

In outlining a theory of an airplane wing it is necessary to show how, assuming certain constructional data, it is possible to calculate, among other things, the lift, the drag due to other causes than viscosity, the pitching moment, and the rolling moment. In the simplest type of wing, that whose chord section is a straight line, flying at a definite angle of attack, the values of the lift and the pitching moment can be calculated immediately. They are seen to depend upon the transverse velocity of the air flow perpendicular to the chord. Similarly, in discussing the properties of a wing whose section is a curved line, if the distribution of the transverse velocity at the points of the chord is known, the lift and pitching moment may be calculated, as will be shown. So the first essential step in the theory of the wing is to discuss mathematical methods of representing arbitrary distributions of transverse velocity over the chord, and to deduce the nature of the consequent flow. It will be shown how the distribution of velocity may be so expressed as to lead to formulas for the lift and pitching moment in terms of quantities known to the designer.

In all this discussion an essential element is the angle of attack; but it is evident that the geometrical angle of attack is not the effective one, owing to the fact that the direction of the relative wind is affected by the presence of the wing. Owing to this modification of the air flow, there is a drag introduced, known as the "induced drag," and the effective angle of attack is the geometrical one diminished by what is called the "induced" angle of attack. The problem is to calculate these and then their effect upon the lift. One method of approach to the problem is to assume as known the distribution of lift along the span, but another and better one is to assume as known the angle of attack at all points along the span and to apply the general method to wings having particular plane forms. It will be seen that all these methods lead back to the discussion of the distribution of the transverse down-wash velocity along the span.

If an airfoil has an infinite span, the flow around it when the air stream is perpendicular to its span may be regarded as two-dimensional. The air particles in a longitudinal plane, i. e., one including the line of flow of the air stream and perpendicular to the span, remain in the plane. Further, if an airfoil of finite span is advancing into a transverse vertical layer of air, it imparts to the air velocity in this plane, so that again one can consider this transverse flow as being two-dimensional about a plane figure which is the projection of the airfoil on this transverse plane. The simplest case of motion in the longitudinal plane is to consider the longitudinal section of the airfoil to be a straight line of a length equal to the chord, and the simplest case of motion

in the transverse plane is to consider the front aspect of an airfoil to be a straight line of a length equal to the span.

The importance of two-dimensional flows requires a brief statement of the properties of conjugate functions which are so useful in all two-dimensional problems. All the cases of flow to be discussed will be those described by a velocity potential, which then satisfies the equation

$$\frac{\partial^2 \varphi}{\partial x^2} + \frac{\partial^2 \varphi}{\partial y^2} = 0$$

Writing $z = x + iy$, if

$$F = f(z) = P(x, y) + iQ(x, y),$$

P and Q are called conjugate functions, because if F is any analytic function

$$\frac{\partial P}{\partial x} = \frac{\partial Q}{\partial y}, \quad \frac{\partial P}{\partial y} = -\frac{\partial Q}{\partial x}.$$

It follows that

$$\frac{\partial^2 P}{\partial x^2} + \frac{\partial^2 P}{\partial y^2} = 0, \quad \frac{\partial^2 Q}{\partial x^2} + \frac{\partial^2 Q}{\partial y^2} = 0$$

to that both P and Q satisfy the fundamental equation for the velocity potential, and, further that

$$\frac{dF}{dz} = \frac{\partial P}{\partial x} - i \frac{\partial P}{\partial y}$$

Consequently, if P is chosen as the velocity potential φ , i. e., if φ is the real part of F , then the real part of $\frac{dF}{dz}$ gives the component of the velocity at any point in the direction of the x -axis, and the imaginary part of $\frac{dF}{dz}$ gives the component of the velocity, at any point, in the negative direction of the y -axis. Therefore the whole motion is defined by the knowledge of F as a function of the single variable z .

ILLUSTRATIONS OF TWO-DIMENSIONAL FLOW

1. Let

$$F = iV(z - i\sqrt{1-z^2}) \dots\dots\dots (13)$$

Then

$$\frac{dF}{dz} = iV \left(1 + \frac{iz}{\sqrt{1-z^2}} \right) = -\frac{Vz}{\sqrt{1-z^2}} + iV \dots\dots\dots (14)$$

There are evidently two singular points $z = \pm 1$, i. e., $x = 1, y = 0$ and $x = -1, y = 0$; and at infinity $\frac{dF}{dz} = 0$.

Along the line joining the two singular points $(-1, 0)$ and $(+1, 0)$, $y = 0$; hence

$$F_o = \pm V\sqrt{1-x_o^2} + iVx_o$$

$$F'_o \equiv \left(\frac{dF}{dz} \right)_o = \mp \frac{Vx_o}{\sqrt{1-x_o^2}} + iV$$

in which the upper signs apply to points on the positive side of the line (i. e., where y is positive), and conversely. Hence, for points on the line

$$\varphi_o = \pm V\sqrt{1-x_o^2} \dots\dots\dots (15)$$

Further, the longitudinal velocity, i. e., the velocity along the x -axis, is

$$v_o = \mp \frac{Vx_o}{\sqrt{1-x_o^2}} \dots\dots\dots (16)$$

and the transverse velocity downward is

$$u_o = V \dots\dots\dots (17)$$

The general function F , which was assumed to begin with, represents, therefore, the two-dimensional flow around a straight line of length 2 moving transversely downward with a velocity V . (Or, the general flow about a lamina, infinite in length and a width 2 , moving transversely with velocity V .)

Near the positive end of the line, i. e., when $x_o = 1 - \epsilon$, ϵ being a small quantity, $v = \mp \frac{V}{\sqrt{2\epsilon}}$,

and therefore v becomes infinite on both sides of the line, but is "outward" on the lower side and inward on the upper.

It should be noted that in defining a function F which leads to a value $\varphi_o = \pm V\sqrt{1-x_o^2}$, the *difference of potential* between two points on opposite sides of the line is $2V\sqrt{1-x_o^2}$. This is at once evident if polar coordinates are used. In that case, writing $z = \cos \delta$, where δ is a complex number,

$$F = iVe^{-i\delta} = V(\sin \delta + i \cos \delta) \dots\dots\dots (13a)$$

$$F' = \frac{dF}{dz} = \frac{dF}{d} \cdot \frac{d\delta}{dz} = -\frac{Ve^{-i\delta}}{\sin \delta} = -\frac{V}{\sin \delta} (\cos \delta - i \sin \delta) \dots\dots\dots (14a)$$

For points on the line $x_o = \cos \delta_o$ where δ_o is real, and

$$\varphi_o = V \sin \delta_o \dots\dots\dots (15a)$$

$$v_o = -\frac{V \cos \delta_o}{\sin \delta_o}, u_o = V$$

hence at

$$\delta_o = 0, v_{edge} = -\frac{V}{(\sin \delta_o)_o} \dots\dots\dots (18)$$

As x_o goes from $+1$ to -1 on the upper side of the line δ increased from 0 to π ; and, as the point returns on the lower side of the line, δ increases from π to 2π . (The flow is shown in the Figure 7.)

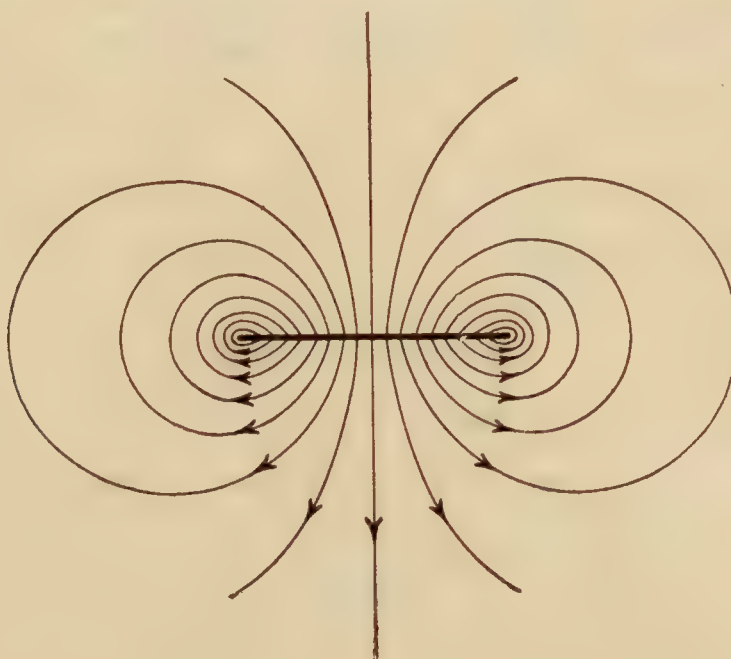


FIG. 7.—Transverse flow, produced by a moving straight line

If the line has the length b , stretching from $\left(-\frac{b}{2}, 0\right)$ to $\left(+\frac{b}{2}, 0\right)$, we may write

$$F = iV \frac{b}{2} \left(\frac{2}{b} z - i \sqrt{1 - \left(\frac{2}{b} z \right)^2} \right) \dots\dots\dots (13')$$

Then

$$F' = - \frac{V \frac{2}{b} z}{\sqrt{1 - \left(\frac{2}{b} z \right)^2}} + iV \dots\dots\dots (14')$$

Thus

$$\varphi_o = \pm V \frac{b}{2} \sqrt{1 - \left(\frac{2}{b} x_o \right)^2} \dots\dots\dots (15')$$

$$v_o = \mp \frac{V \frac{2}{b} x_o}{\sqrt{1 - \left(\frac{2}{b} x_o \right)^2}}, u_o = V \dots\dots\dots (16')$$

Or, using polar coordinates, writing $\frac{2}{b} z = \cos \delta$,

$$F = iV \frac{b}{2} e^{-i\delta} = V \frac{b}{2} (\sin \delta + i \cos \delta) \dots\dots\dots (13'a)$$

$$F' = - \frac{V}{\sin \delta} (\cos \delta - i \sin \delta) \dots\dots\dots (14'a)$$

$$\varphi_o = V \frac{b}{2} \sin \delta_o \dots\dots\dots (15'a)$$

$$v_o = - \frac{V \cos \delta_o}{\sin \delta_o}, u_o = V$$

and

$$v_{edge} = - \frac{V}{(\sin \delta_o)_o} \dots\dots\dots (18')$$

It has been proved that the kinetic energy of the flow is

$$T = - \frac{\rho}{2} \int \varphi \frac{d\varphi}{dn} dS$$

integrated over the moving body, where dn is the normal away from the body. In the case of the line of length b , moving transversely with velocity V

$$\varphi_o = \pm V \frac{b}{2} \sqrt{1 - \left(\frac{2}{b} x_o \right)^2}; \left(\frac{d\varphi}{dn} \right)_o = \mp V; dS = dx_o$$

Hence, integrating over both sides,

$$T = \frac{\rho}{2} V^2 \frac{b}{2} \cdot 2 \int_{-b/2}^{+b/2} \sqrt{1 - \left(\frac{2}{b} x_o \right)^2} dx_o$$

or writing

$$\cos \delta_o = \frac{2}{b} x_o$$

$$T = \frac{\rho}{2} V^2 b \cdot \frac{b}{2} \int_0^\pi \sin^2 \delta_o d\delta_o = \frac{\rho}{2} V^2 \pi \left(\frac{b}{2} \right)^2 \dots\dots\dots (19)$$

But $\pi \left(\frac{b}{2}\right)^2$ is the area of a circle described about the line of length b as a diameter. The apparent transverse mass per unit length, then, of a lamina infinite in length and of width b is $\rho \pi \left(\frac{b}{2}\right)^2$, the same as for a circular cylinder of diameter b moving transversely.

2. A second function, suggested by the first, is

$$F = i A_n e^{-in\delta} = A_n (\sin n\delta + i \cos n\delta) \quad \text{-----} \quad (20)$$

where $z = \cos \delta$.

Therefore

$$F' = -A_n \frac{ne^{-in\delta}}{\sin \delta} = -A_n \frac{n \cos n\delta}{\sin \delta} + i A_n \frac{n \sin n\delta}{\sin \delta} \quad \text{-----} \quad (21)$$

Hence

$$\varphi_o = A_n \sin n\delta_o \text{ [for points on the line joining } (-1, O) \text{ and } (+1, O)] \quad \text{-----} \quad (22)$$

$$v_o = -A_n \frac{n \cos n\delta_o}{\sin \delta_o} \quad \text{-----} \quad (23)$$

$$u_o = A_n \frac{n \sin n\delta_o}{\sin \delta_o} \quad \text{-----} \quad (24)$$

Note that u_o is no longer the same for all points of the line.

For a line of length b , stretching from $\left(-\frac{b}{2}, O\right)$ to $\left(+\frac{b}{2}, O\right)$ we may write, if we wish the same expressions for v_o and u_o as just found,

$$F = A_n \frac{b}{2} (\sin n\delta + i \cos n\delta), \text{ where } \cos \delta = \frac{2}{b} z \quad \text{-----} \quad (20')$$

Therefore

$$F' = -A_n \frac{n \cos n\delta}{\sin \delta} + i A_n \frac{n \sin n\delta}{\sin \delta} \quad \text{-----} \quad (21')$$

$$\varphi_o = A_n \frac{b}{2} \sin n\delta_o \quad \text{-----} \quad (22')$$

$$v_o = -A_n \frac{n \cos n\delta_o}{\sin \delta_o} \quad \text{-----} \quad (23')$$

and

$$u_o = A_n \frac{n \sin n\delta_o}{\sin \delta_o}, \text{ where } \frac{2}{b} x_o = \cos \delta_o \quad \text{-----} \quad (24')$$

In the formula, therefore, for the kinetic energy of the flow

$$\varphi_o = A_n \frac{b}{2} \sin n\delta_o; \left(\frac{d\varphi}{dn}\right)_o = -A_n \frac{n \sin n\delta_o}{\sin \delta_o}$$

and

$$dS = dx_o = -\frac{b}{2} \sin \delta_o d\delta_o,$$

and

$$T = \frac{\rho}{2} A_n^2 \left(\frac{b}{2}\right)^2 n \int_0^{2\pi} \frac{\sin^2 n\delta_o}{\sin \delta_o} \cdot \sin \delta_o d\delta_o = \frac{\rho}{2} A_n^2 \pi \left(\frac{b}{2}\right)^2 n \quad \text{-----} \quad (25)$$

The impulse per unit length required to create the flow is $-\rho\varphi_o$; hence the total impulse is $-\rho\int\varphi_o dx$, taken over both sides of the line, i. e.,

$$P = \rho \int_0^{2\pi} A_n \frac{b}{2} \sin n\delta_o \cdot \frac{b}{2} \sin \delta_o d\delta_o = \rho\pi \left(\frac{b}{2}\right)^2 A_n$$

since $\int_0^\pi \sin n\theta \cdot \sin \theta \cdot d\theta = 0$ unless $n=1$

3. A more general case would then be a superposition of flows like the one last considered, described by

$$F = i \{ A_1 (z - i\sqrt{1-z^2}) + A_2 (z - i\sqrt{1-z^2})^2 + \text{etc.} \} \quad (26)$$

where it is assumed that it is possible to so choose the coefficients as to make the series involved convergent. Obviously, then, for points on the line connecting $(-1, 0)$ and $(+1, 0)$,

$$\varphi_o = A_1 \sin \delta_o + A_2 \sin 2\delta_o + \text{etc.}, \text{ where } \cos \delta_o = x_o \quad (27)$$

$$v_o = - \left\{ \frac{A_1 \cos \delta_o}{\sin \delta_o} + \frac{2A_2 \cos 2\delta_o}{\sin \delta_o} + \text{etc.} \right\} \quad (28)$$

$$u_o = \frac{A_1 \sin \delta_o}{\sin \delta_o} + \frac{2A_2 \sin 2\delta_o}{\sin \delta_o} + \text{etc.} \quad (29)$$

For a line of length b , i. e., making $\cos \delta_o = \frac{2}{b} x_o$

$$\varphi_o = \frac{b}{2} (A_1 \sin \delta_o + A_2 \sin 2\delta_o + \text{etc.}) \quad (27')$$

if v_o and u_o are to have the same forms as before.

In the formula for the kinetic energy, then,

$$\begin{aligned} T &= \frac{\rho}{2} \left(\frac{b}{2}\right)^2 \int_0^{2\pi} (A_1 \sin \delta_o + A_2 \sin 2\delta_o + \dots) (A_1 \sin \delta_o + 2A_2 \sin 2\delta_o + \dots) d\delta_o \\ &= \frac{\rho}{2} \pi \left(\frac{b}{2}\right)^2 (A_1^2 + 2A_2^2 + \dots) \quad (30) \end{aligned}$$

Therefore, not simply are the kinematic properties of the separate flows additive, but the energies also.

The constants in the formula for F may be determined by various physical specifications:

a. Let the distribution of potential be known at all points of the line between $(-1, 0)$ and $(+1, 0)$, the function having equal and opposite values at opposite points.

Then it is possible to so choose coefficients that φ_o may be expressed as follows:

$$\varphi_o = A_1 \sin \delta_o + A_2 \sin 2\delta_o + \text{etc.}$$

for, on multiplying both sides of the equation by $\sin n\delta_o$ and integrating from 0 to π ,

$$\int_0^\pi \varphi_o \cdot \sin n\delta_o d\delta_o = \int_0^\pi (A_1 \sin \delta_o + A_2 \sin 2\delta_o + \dots) \sin n\delta_o \cdot d\delta_o = \int_0^\pi A_n \sin^2 n\delta_o d\delta_o = \frac{\pi}{2} A_n$$

Hence

$$A_n = \frac{2}{\pi} \int_0^\pi \varphi_o \sin n\delta_o d\delta_o \quad (31)$$

and is therefore determined. These values of the A 's may then be substituted in the general function F . (For a line of length b ,

$$A_n = \frac{2}{b} \cdot \frac{2}{\pi} \int_0^\pi \varphi_o \sin n\delta_o d\delta_o \quad (31')$$

in formula 27', etc.)

(A better mode of expression would be to specify that the difference of potential between opposite points is known for each point of the line, i. e., $\Delta\varphi$ is specified. Then expand $\frac{1}{2}\Delta\varphi$ in a series $A_1 \sin \delta_o + A_2 \sin 2\delta_o + \text{etc.}$)

b. Let the distribution of longitudinal velocity be specified at each point of the line of length 2 , being equal and opposite at opposite points.

We may then consider $v_o \sin \delta_o$ as known at each point, and this can be expanded into a series

$$v_o \sin \delta_o = -(A_1 \cos \delta_o + 2A_2 \cos 2\delta_o + \text{etc.})$$

if the A 's are given proper values, viz, since

$$\int_0^\pi v_o \sin \delta_o \cdot \cos n\delta_o d\delta_o = - \int_0^\pi nA_n \cos^2 n\delta_o d\delta_o = -\frac{\pi}{2} nA_n, A_n = -\frac{2}{n\pi} \int_0^\pi v_o \sin \delta_o \cdot \cos n\delta_o d\delta_o \dots (32)$$

and these values may be substituted in the function F in order to determine the flow at all points.

(These same values for the A 's are to be used in the formulas for a line of length b .)

c. Let the transverse velocity be specified at each point of the line, having the same value at opposite points. Then $u_o \sin \delta_o$ is known for each point, and this may be expanded into a series

$$u_o \sin \delta_o = A_1 \sin \delta_o + 2A_2 \sin 2\delta_o + \text{etc.}$$

by giving the coefficients proper values, viz, since

$$\int_0^\pi u_o \sin \delta_o \cdot \sin n\delta_o d\delta_o = \int_0^\pi nA_n \sin^2 n\delta_o d\delta_o = \frac{\pi}{2} nA_n, A_n = \frac{2}{\pi n} \int_0^\pi u_o \sin \delta_o \cdot \sin n\delta_o d\delta_o \dots (33)$$

These values may be substituted in F , etc. (These same values for the A 's are to be used in the formulas for a line of length b .)

The essential thing is that, if specification a , b , or c is made, the flow at all points in space may be deduced.

4. If $f(z)$ is a flow function and contains a parameter x_o , then $f(z, x_o) u_o dx_o$ is also a solution of the equations if u_o is a function of x_o . Hence also

$$F = \int_{-1}^{+1} f(z, x_o) u_o dx_o \dots \dots \dots (34)$$

is a solution, and

$$F' = \int_{-1}^{+1} f'(z, x_o) u_o dx_o, \text{ where } f' = \frac{df}{dz} \dots \dots \dots (35)$$

A value of $f(z, x_o)$ suggested by Munk is

$$f \equiv \frac{1}{\pi} \{ \log (e^{i\delta} - e^{-i\delta_o}) - \log (e^{i\delta} - e^{i\delta_o}) \} \dots \dots \dots (36)$$

where $\cos \delta = z$ and $\cos \delta_o = x_o$.

This solution F may be interpreted physically by deducing the meaning of each elementary term.

$$f' = -\frac{1}{\pi} \frac{\sin \delta_o}{\sin \delta} \frac{1}{\cos \delta - \cos \delta_o} = \mp \frac{1}{\pi} \frac{1}{z - x_o} \sqrt{\frac{1 - x_o^2}{1 - z^2}} \dots \dots \dots (37)$$

where the negative sign is to be taken over the positive side of the line, and the positive sign on the other. There is evidently a singular point at $z = x_o$. For points close to this—not necessarily on the line— $f' = \mp \frac{1}{\pi} \frac{1}{z - x_o}$. Therefore an element of F' , that is, $f' u_o dx_o$, when applied

to these points, has the value

$$\mp \frac{1}{\pi} \frac{1}{z - x_o} u_o dx_o = \mp \frac{1}{\pi} u_o dx_o \frac{x - x_o - iy}{(x - x_o)^2 + y^2}$$

If a small circle of radius r is drawn around the point x_o , and the point x, y lies on it, $r^2 = (x - x_o)^2 + y^2$. The velocity along the x -axis for points on the positive side of the line is $-\frac{1}{\pi} u_o dx_o \frac{x - x_o}{r^2}$, and the velocity along the y -axis is $-\frac{1}{\pi} u_o dx_o \frac{y}{r^2}$; hence there is a radial velocity inward toward x_o , of the value $\frac{1}{\pi} u_o dx_o \cdot \frac{1}{r}$. Therefore the total flow per second in through the semi-circle is $\rho u_o dx_o$. Similarly there is an equal outward flow through the semicircle on the negative side of the line.

This is equivalent, then, to there being a transverse velocity u_o at all points of the element dx_o , toward it on the positive side of the line and away from it on the other. This gives the physical meaning of u_o .

The total function

$$F' = \mp \int_{-1}^{+1} \frac{1}{\pi} \frac{u_o dx_o}{z - x_o} \sqrt{\frac{1 - x_o^2}{1 - z^2}} \quad (38)$$

indicates the effect at a point z of a given distribution of transverse velocity, u_o being the downward velocity at the point x_o , on both sides of the line. The longitudinal velocity, due to this distribution, at a point x on the line is

$$v = \mp \int_{-1}^{+1} \frac{1}{\pi} \frac{u_o dx_o}{x - x_o} \sqrt{\frac{1 - x_o^2}{1 - x^2}}$$

Interchanging symbols, the velocity at a point x_o on the line is

$$v_o = \pm \int_{-1}^{+1} \frac{1}{\pi} \frac{u dx}{x - x_o} \sqrt{\frac{1 - x^2}{1 - x_o^2}} \quad (39)$$

where u is the transverse velocity downward at the point x .

For a point near the positive edge, write $x_o = 1 - \epsilon$ where ϵ is small. Then since $\sin \delta_o = \sqrt{1 - x_o^2} = \sqrt{2\epsilon}$,

$$v_{edge} = -\frac{1}{\pi (\sin \delta_o)_{\delta_o=0}} \int_{-1}^{+1} u \sqrt{\frac{1+x}{1-x}} dx \quad (40)$$

The flow, due to a single element, is shown in Figure 8.

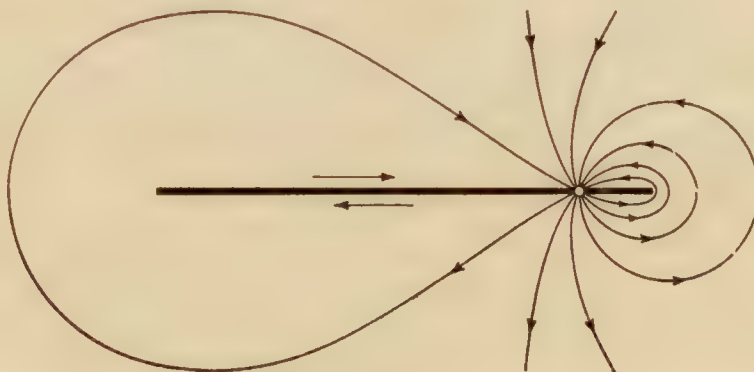


FIG. 8.—Flow around a straight line created by one element of the wing section

If the line has the length b stretching between

$$\left(-\frac{b}{2}, 0\right) \text{ and } \left(+\frac{b}{2}, 0\right) \text{ let}$$

$$F = \int_{-b/2}^{+b/2} f(z, x_o) u_o dx_o$$

where

$$f = \frac{1}{\pi} \{ \log (e^{i\delta} - e^{-i\delta_o}) - \log (e^{i\delta} - e^{i\delta_o}) \}$$

and $\cos \delta = \frac{2}{b} z$ and $\cos \delta_o = \frac{2}{b} x_o$. This leads to a transverse downward velocity u_o at x_o , etc.

Finally

$$v_{edge} = -\frac{2}{b} \frac{1}{\pi (\sin \delta_o)_{\delta_o=0}} \int_{-b/2}^{+b/2} u \sqrt{\frac{1 + \frac{2}{b}x}{1 - \frac{2}{b}x}} dx \dots\dots\dots (40')$$

Two expressions have been deduced, therefore, for the flow due to an arbitrary distribution of transverse velocity over a line of length b :

$$1. \quad \varphi = \frac{b}{2} (A_1 \sin \delta + A_2 \sin 2\delta + \text{etc.})$$

in which

$$A_n = \frac{2}{\pi n} \int_0^\pi u_o \sin \delta_o \cdot \sin n\delta_o \cdot d\delta_o$$

where $\cos \delta = \frac{2}{b} z$ and u_o is the transverse velocity downward at the point x_o .

2. φ is the real part of

$$F = \int_{-b/2}^{+b/2} f(z, x_o) u_o dx_o$$

in which

$$f(z, x_o) = \frac{1}{\pi} \{ \log (e^{i\delta} - e^{-i\delta_o}) - \log (e^{i\delta} - e^{i\delta_o}) \}$$

These are, of course, mathematically identical.

5. A flow of a different kind entirely is given by

$$F = A_o \sin^{-1} z \dots\dots\dots (41)$$

This makes

$$F' = \pm \frac{A_o}{\sqrt{1-z^2}} = \frac{A_o}{\sin \delta}, \text{ where } \cos \delta = z \dots\dots\dots (42)$$

and

$$v_o = \frac{A_o}{\sin \delta} \dots\dots\dots (43)$$

Therefore for points on the line between $(-1, 0)$ and $(+1, 0)$, $u=0$ on both sides of the line and v is positive on the upper side and negative on the other. The flow is as indicated.

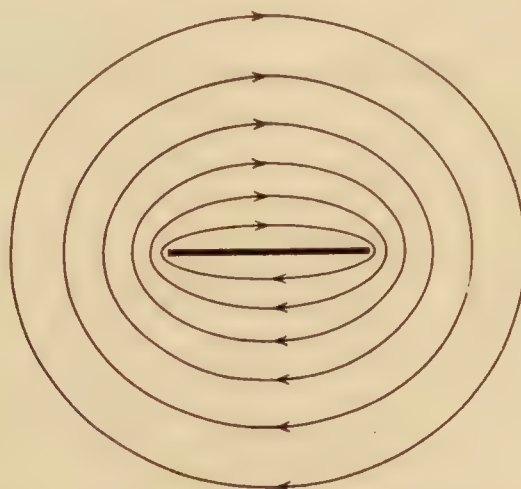


FIG. 9.—Circulation flow around a straight line

F is a multiple valued function, its modulus being $2\pi A_o$. For points on the line $y=0$, beyond $x=-1$ and $x=+1$, $\varphi = A_o \sin^{-1} x$; consequently there is a difference of potential $2\pi A_o$ between two points lying on opposite sides of the line, since each line of flow incloses the origin.

This flow can not be produced by impulsive pressures over the line between $x = -1$ and $x = +1$, because the flow is everywhere parallel to the surface. It can be imagined produced by impulses over all points of the line $y = 0$, extending from one end of the line of length 2 , out to infinity. At all points there is a potential difference $2\pi A_o$; hence the downward impulse per unit length of the line required to generate the motion is $2\pi A_o \rho$. But if the line of length 2 be considered an airplane wing, and if it moves with a velocity V longitudinally, it must deliver to the air per second a momentum downward equal to the lift on the wing, L . Therefore since this momentum is imparted in going a distance V , the momentum imparted per unit length, i. e., the impulse per unit length, is $\frac{L}{V}$. Hence

$$\frac{L}{V} = 2\pi A_o \rho \dots (\text{Kutta's theorem}) \dots \dots \dots (44)$$

or

$$A_o = \frac{L}{2\pi \rho V}$$

and, from (43)

$$v_{edge} = \frac{L}{2\pi \rho V (\sin \delta_o)_{\delta_o=0}} \dots \dots \dots (45)$$

For a line of length b , stretching from $\left(-\frac{b}{2}, 0\right)$ to $\left(+\frac{b}{2}, 0\right)$ write

$$F = A_o \sin^{-1} \left(\frac{2}{b} z \right) \dots \dots \dots (41')$$

Hence

$$F' = \pm \frac{A_o \frac{2}{b}}{\sqrt{1 - \left(\frac{2}{b} z\right)^2}} = \frac{A_o \frac{2}{b}}{\sin \delta} \dots \dots \dots (42')$$

As before,

$$\frac{L}{V} = 2\pi A_o \rho,$$

and therefore

$$v_{edge} = \frac{2}{b} \frac{L}{2\pi \rho V (\sin \delta_o)_{\delta_o=0}} \dots \dots \dots (45')$$

In these formulas L is the lift per unit length along the infinite span, since the problem is treated as a two-dimensional one.

ANGLE OF ATTACK AND LIFT WING SECTION THEORY

In discussing suitable combinations of types of flow for application to airplane wings, it is essential to include a circulation flow so as to secure lift, and also so to choose the types that the total flow divides exactly at the trailing edge. The condition for the latter is that $v_{edge} = 0$. (Kutta was the first to state this condition.)

A. STRAIGHT LINE, ANGLE OF ATTACK α

In order to introduce the angle of attack, consider the problem of the straight line of length 2 moving with a velocity V in a direction making the angle α with the line. The transverse velocity is $V \sin \alpha$, and hence the flow is given by (13a) as

$$F = V \sin \alpha \cdot i \cdot e^{-i\delta} \dots \dots \dots (46)$$

and the longitudinal velocity at the trailing edge is, by (18),

$$-V \sin \alpha \frac{1}{(\sin \delta_o)_{\delta_o=0}} \dots \dots \dots (47)$$

Since α is small, F can also be taken as the flow function for a line inclined to the axis of x by an angle α having a velocity V in the direction of the axis, v and u now referring to the line of flight. (This approximation was proposed and used by Munk.)

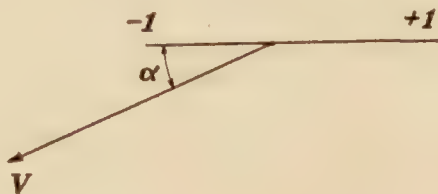


FIG. 10

Due to a circulation flow around the line of length \mathcal{L} , given by $F = A_o \sin^{-1} z$, the longitudinal edge velocity is, from (45),

$$\frac{L}{2\pi\rho V} \frac{1}{(\sin \delta_o)_{\delta_o=0}}$$

Hence, if $v_{edge} = 0$ due to the two flows,

$$\frac{L}{2\pi\rho V} = V \sin \alpha$$

or

$$L = 2\pi\rho V^2 \sin \alpha \dots \dots \dots (48)$$

Introducing the area, $S = \mathcal{L}$ since the span is one, and, writing α in place of $\sin \alpha$,

$$L = 2\pi \frac{\rho}{\mathcal{L}} V^2 S \alpha \dots \dots \dots (48a)$$

giving a lift coefficient

$$C_L = 2\pi\alpha$$

If the line has a length b , the two edge velocities are, by (18') and (45'),

$$-V \sin \alpha \frac{1}{(\sin \delta_o)_{\delta_o=0}} \text{ and } \frac{\mathcal{L}}{b} \frac{L}{2\pi\rho V} \frac{1}{(\sin \delta_o)_{\delta_o=0}}$$

Hence

$$L = 2\pi\rho V^2 \frac{b}{\mathcal{L}} \sin \alpha \dots \dots \dots (48')$$

But $S = b$, and therefore, as before,

$$L = 2\pi \frac{\rho}{\mathcal{L}} V^2 S \alpha \dots \dots \dots (48'a)$$

B. CURVED LINE, ZERO ANGLE OF ATTACK; "APPARENT" ANGLE OF ATTACK

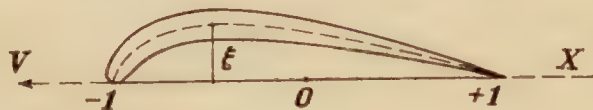


FIG. 11

If the wing is a thin cambered one, it is equivalent to a good approximation, to a curve which is the mean of the upper and lower curves of the wing section. Consider, then, the problem of the motion of such a curved line whose chord is the x -axis, having a velocity V in

the negative direction of the chord. Let ξ be the ordinate of the curve at the point x . Any element of the curve is then moving with the angle of attack whose tangent is $-\frac{d\xi}{dx}$. Therefore, at this element the component of V downward (i. e., as shown above, $V \sin \alpha$, or $V\alpha$) is $-V \frac{d\xi}{dx}$ if the curvature is small. This is to be substituted in the formula previously deduced for the case of a variable transverse velocity along the chord, viz, for a chord of length 2 , from (40),

$$v_{edge} = \frac{V}{\pi (\sin \delta_o)_{\delta_o=0}} \int_{-1}^{+1} \frac{d\xi}{dx} \sqrt{\frac{1+x}{1-x}} dx \dots\dots\dots (49)$$

This leads to a definition of the "mean apparent angle of attack," viz, the angle of attack which a straight line having a chord of equal length would have to possess in order to give this same value of edge velocity and therefore the same lift. Calling this angle α' , the condition, then, is, from (47),

$$-V \sin \alpha' \frac{1}{(\sin \delta_o)_{\delta_o=0}} = \frac{V}{\pi (\sin \delta_o)_{\delta_o=0}} \int_{-1}^{+1} \frac{d\xi}{dx} \sqrt{\frac{1+x}{1-x}} dx$$

Hence

$$\alpha' = -\frac{1}{\pi} \int_{-1}^{+1} \frac{d\xi}{dx} \sqrt{\frac{1+x}{1-x}} dx = \frac{1}{\pi} \int_{-1}^{+1} \frac{\xi dx}{(1-x) \sqrt{1-x^2}} \dots\dots\dots (50)$$

since for $x=1$, $\xi=0$.

For a line of length b , the angle of attack of each element and the component of velocity downward are as before and, from (40'),

$$v_{edge} = \frac{2}{b} \frac{V}{\pi (\sin \delta_o)_{\delta_o=0}} \int_{-b/2}^{+b/2} \frac{d\xi}{dx} \sqrt{\frac{1+\frac{2}{b}x}{1-\frac{2}{b}x}} dx \dots\dots\dots (49')$$

Hence

$$\alpha' = -\frac{2}{b} \frac{1}{\pi} \int_{-b/2}^{+b/2} \frac{d\xi}{dx} \sqrt{\frac{1+\frac{2}{b}x}{1-\frac{2}{b}x}} dx = \left(\frac{2}{b}\right)^2 \frac{1}{\pi} \int_{-b/2}^{+b/2} \frac{\xi dx}{\left(1-\frac{2}{b}x\right) \sqrt{1-\left(\frac{2}{b}x\right)^2}} \dots\dots\dots (50')$$

Since for any given wing section ξ is specified as a $f(x)$, these integrals may be evaluated and α' may be calculated.

CONCLUSION

Considering the wing as one of infinite span, the lift on a cambered wing of chord c and area S , when at zero angle of attack, is

$$L = 2\pi \frac{\rho}{2} V^2 S \alpha'$$

where

$$\alpha' = \left(\frac{2}{c}\right)^2 \frac{1}{\pi} \int_{-c/2}^{+c/2} \frac{\xi dx}{\left(1-\frac{2}{c}x\right) \sqrt{1-\left(\frac{2}{c}x\right)^2}}$$

In this formula ξ is the ordinate from the chord to the mean curve of the upper and lower surfaces of the wing section.

(For simple methods of calculating α' from wing profiles, see N. A. C. A. Technical Note, 122.)

PITCHING MOMENT AND CENTER OF PRESSURE

In the case of a straight line of length 2 moving with a velocity V at an angle of attack α the moment acting on it due to the air forces may be calculated at once from the general theorem already proved, viz: The moment equals the product of the velocity and the component, perpendicular to the velocity, of the momentum of the air flow. Such a line has a transverse

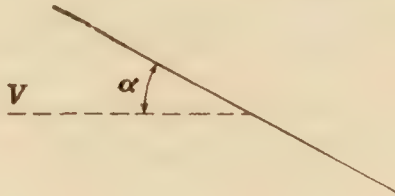


FIG. 12

mass $\pi\rho$, and hence a momentum, perpendicular to the line, of $\pi\rho \cdot V \sin \alpha$. Its component perpendicular to the line of V is then $\pi\rho V \sin \alpha \cdot \cos \alpha$; and therefore the pitching moment (clockwise), for unit span, is

$$M = V^2 \frac{\rho}{2} \pi \sin 2\alpha \dots\dots\dots (51)$$

or

$$= 2\pi \frac{\rho}{2} V^2 \cdot \alpha$$

since α is small.

The lift was found, (48), to have the value, for a wing of unit span,

$$L = 2\pi\rho V^2 \cdot \alpha$$

Hence the distance of the "center of pressure" from the center of the line is

$$\frac{M}{L} = \frac{1}{2} \dots\dots\dots (52)$$

It is therefore independent of α and is 25% of the length of the chord from the leading edge.

For a line of length b the transverse mass is $\pi \left(\frac{b}{2}\right)^2 \rho$, and hence

$$M = 2\pi \left(\frac{b}{2}\right)^2 \frac{\rho}{2} V^2 \alpha \dots\dots\dots (51')$$

Further, from (48'),

$$L = 2\pi \frac{b}{2} \rho V^2 \alpha;$$

Hence

$$\frac{M}{L} = \frac{1}{2} \frac{b}{2} \dots\dots\dots (52')$$

i. e., the center of pressure is "at 25%", and is independent of α .

In the case of a curved line, in order to deduce the center of pressure, it is necessary to calculate the distribution of pressure over the line. By Bernoulli's theorem the pressure at any point equals $C - \frac{\rho}{2} (\text{velocity})^2$ where C is a constant. The general formula for the longitudinal velocity is, (see (28))

$$v_o = - \left(A_1 \frac{\cos \delta_o}{\sin \delta_o} + 2A_2 \frac{\cos 2\delta_o}{\sin \delta_o} + \dots \right)$$

This may be applied to any element of the curve, and is the velocity of the flow toward the right; but since the curved line itself has a velocity V toward the left, the relative velocity between the air and the wing is $V + v_o$ or

$$V - \left(A_1 \frac{\cos \delta_o}{\sin \delta_o} + 2A_2 \frac{\cos 2\delta_o}{\sin \delta_o} + \dots \right)$$

In squaring this, the squares of the A 's may be omitted, since in the integration given below the corresponding terms would disappear. Hence

$$p = C - \frac{\rho}{2} V^2 + \rho V \left(A_1 \frac{\cos \delta_o}{\sin \delta_o} + 2A_2 \frac{\cos 2\delta_o}{\sin \delta_o} + \dots \right) \dots \dots \dots (53)$$

The first two terms are the same for all points on both sides of the line and therefore produce no moment. The second term gives equal and opposite values of p at two opposite points on the line, i. e., if it is a pressure on one side it will be a suction on the other; therefore, the pitching moment (clockwise) for unit span,

$$M = 2 \int_{-1}^{+1} p x dx = 2 \int_{-1}^{+1} p \cos \delta_o \sin \delta_o d\delta_o,$$

where $x = \cos \delta_o$

$$= 2V\rho \int_0^\pi (A_1 \cos \delta_o + 2A_2 \cos 2\delta_o + \dots) \cos \delta_o d\delta_o = 2V\rho \cdot A_1 \frac{\pi}{2} \dots \dots \dots (54)$$

But the value of A_1 in terms of the transverse velocity was found previously, (33), to be

$$A_1 = \frac{2}{\pi} \int_0^\pi u_o \sin^2 \delta_o d\delta_o$$

In the case of an element of the curved line

$$u_o = -V \frac{d\xi}{dx},$$

hence, for a wing of unit span,

$$\begin{aligned} M &= -2\rho V^2 \int_0^\pi \frac{d\xi}{dx} \sin^2 \delta_o d\delta_o \\ &= -2\rho V^2 \int_{-1}^{+1} \frac{d\xi}{dx} \sqrt{1-x^2} dx \\ &= -2\rho V^2 \int_{-1}^{+1} \frac{x\xi}{\sqrt{1-x^2}} dx \dots \dots \dots (55) \end{aligned}$$

For a straight line having the same chord and the angle of attack α , the pitching moment was found to be

$$2\pi V^2 \frac{\rho}{2}$$

so that, in order for the straight line to have the same moment as the curved line at zero angle of attack, the angle of attack of the former must be given by

$$2\pi V^2 \frac{\rho}{2} \alpha'' = -2\rho V^2 \int_{-1}^{+1} \frac{x\xi}{\sqrt{1-x^2}} dx$$

or

$$\alpha'' = -\frac{2}{\pi} \int_{-1}^{+1} \frac{x\xi}{\sqrt{1-x^2}} dx \dots \dots \dots (56)$$

The lift of the straight line was found to be $2\pi\rho V^2\alpha$; hence the lift of the curved line at angle of attack zero is, for unit span,

$$\begin{aligned} L &= 2\pi\rho V^2\alpha', \text{ or on substitution from (50),} \\ &= 2\rho V^2 \int_{-1}^{+1} \frac{\xi dx}{(1-x)\sqrt{1-x^2}} \dots \dots \dots (57) \end{aligned}$$

Hence the distance of the center of pressure from the center of the chord is

$$\frac{M}{L} = - \frac{\int_{-1}^{+1} \frac{x\xi}{\sqrt{1-x^2}} dx}{\int_{-1}^{+1} \frac{\xi dx}{(1-x)\sqrt{1-x^2}}} \dots\dots\dots (58)$$

Writing this fraction equal to h , the position of the center of pressure is given by $\frac{1-h}{2}$ %.

If the length of the chord is b , the moment per unit length of the span is obviously

$$\begin{aligned} M &= 2V\rho\left(\frac{b}{2}\right)^2 A_1 \frac{\pi}{2} \\ &= -2\rho V^2\left(\frac{b}{2}\right) \int_{-b/2}^{+b/2} \frac{d\xi}{dx} \sqrt{1-\left(\frac{b}{2}x\right)^2} dx \\ &= -2\rho V^2 \int_{-b/2}^{+b/2} \frac{\frac{2}{b} x \cdot \xi}{\sqrt{1-\left(\frac{b}{2}x\right)^2}} dx \dots\dots\dots (55') \end{aligned}$$

For a straight line, by (51'),

$$M = 2\pi V^2 \frac{\rho}{2} \cdot \left(\frac{b}{2}\right)^2 \alpha''$$

Therefore,

$$\alpha'' = - \frac{2}{\pi} \left(\frac{2}{b}\right)^2 \int_{-b/2}^{+b/2} \frac{\frac{2}{b} x \cdot \xi}{\sqrt{1-\left(\frac{2}{b}x\right)^2}} dx \dots\dots\dots (56')$$

$$\begin{aligned} L &= 2\pi\rho V^2 \frac{b}{2} \alpha', \text{ per unit length of span, or, from (50'),} \\ &= 2\rho V^2 \left(\frac{2}{b}\right) \int_{-b/2}^{+b/2} \frac{\xi dx}{\left(1-\frac{2}{b}x\right)\sqrt{1-\left(\frac{2}{b}x\right)^2}} \dots\dots\dots (57') \end{aligned}$$

Hence

$$\frac{M}{L} = - \frac{b}{2} \frac{\int_{-b/2}^{+b/2} \frac{\frac{2}{b} x \cdot \xi}{\sqrt{1-\left(\frac{2}{b}x\right)^2}} dx}{\int_{-b/2}^{+b/2} \frac{\xi dx}{\left(1-\frac{2}{b}x\right)\sqrt{1-\left(\frac{2}{b}x\right)^2}}} \equiv h \frac{b}{2} \dots\dots\dots (58')$$

It follows at once that the position of the center of pressure is given by

$$\frac{1}{b} \frac{b}{2} (1-h) = \frac{1-h}{2}$$

The case of two or more wing sections, combined to form a biplane or multiplane, when surrounded by a two-dimensional flow in a longitudinal vertical plane may be treated in the same way as a single section. Each section determines by its slope at each point a distribution of vertical and horizontal velocity. This distribution being known, the resultant moment can be determined; from Kutta's condition for the two trailing edges the lift can be deduced; and finally the center of pressure may be calculated. The mathematical difficulties are, however, great.

CONCLUSION

Considering the wing as one of infinite span, the pitching moment acting on a cambered wing of chord c , per unit length of span, when at zero angle of attack, is

$$M = 2\pi \frac{\rho}{2} V^2 \left(\frac{c}{2}\right)^2 \alpha''$$

where

$$\alpha'' = -\frac{2}{\pi} \left(\frac{2}{c}\right)^2 \int_{-c/2}^{+c/2} \frac{\frac{2}{c} x \cdot \xi \cdot dx}{\sqrt{1 - \left(\frac{2}{c} x\right)^2}};$$

and the ratio of the distance from the leading edge to the center of pressure to the length of the chord is $\frac{1-h}{2}$

$$h = -\frac{\int_{-c/2}^{+c/2} \frac{\frac{2}{c} x \cdot \xi \cdot dx}{\sqrt{1 - \left(\frac{2}{c} x\right)^2}}}{\int_{-c/2}^{+c/2} \frac{\xi dx}{\left(1 - \frac{2}{c} x\right) \sqrt{1 - \left(\frac{2}{c} x\right)^2}}}$$

where

For simple means of calculation, see N. A. C. A. Technical Note No. 122.

INDUCED DRAG AND INDUCED ANGLE OF ATTACK

A. INDUCED DOWNWASH

In what has gone before we have considered only the two-dimensional flow in a vertical longitudinal plane; but this is only part of the motion, for it presupposes a wing of infinite span. If one views a finite wing from the front it is evident that, for many purposes, one may consider again the problem as that of a two-dimensional flow about a straight line, this time in a vertical transverse plane. The wing enters a stationary vertical layer of air and imparts to it a certain energy and momentum, this last giving rise to the lift. While it is passing through the layer it imparts to the air a certain velocity downward, and so is itself moving through air whose relative velocity is not in the direction of flight. This velocity downward, which modifies the direction of the relative velocity of the flow, is called the "induced downwash" u' . Its



FIG. 13

effect is twofold. It evidently decreases the geometrical angle of attack α_g by an angle whose tangent is $\frac{u'}{V}$, or since u' is small compared with V , by an angle $\frac{u'}{V}$. This is called the "induced" angle of attack, i. e.,

$$\alpha_i = \frac{u'}{V} \dots \dots \dots (59)$$

so that $\alpha_e = \alpha_g - \alpha_i \dots$

Again, since the resultant force on the wing is perpendicular to the relative velocity, its direction is changed, thus giving rise to a component parallel to the direction of flight but in an opposite direction. This component therefore opposes the motion of the wing, and is called the "induced" drag, D_i , to distinguish it from the ordinary drag due to the viscosity of the

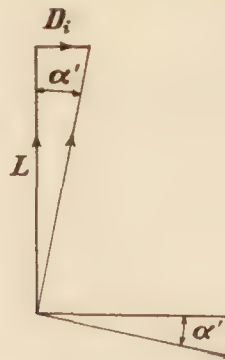


FIG. 14

air. The magnitude of the lift is not much affected by this change in the relative wind. It is evident from the geometry that if dx is an element along the straight line representing the span and dD_i and dL are the corresponding induced drag and lift,

$$dD_i = \frac{u'}{V} dL \text{-----} (60)$$

It is important to determine the connection between u' , the induced down wash, and u , the final downward velocity in the vertical layers of air after the wing has passed through. In one second the wing moves forward a distance V , and therefore the kinetic energy imparted to the air in a layer of thickness V equals the product of the downward impulse (i. e., dL in this case) by the mean of the initial and final downward velocity, viz, $\int \frac{u}{2} dL$. Considered also in terms of the induced drag, this energy equals $\int V dD_i$ which, from (60), equals $\int u' dL$. Therefore

$$u' = \frac{u}{2} \text{-----} (61)$$

B. MINIMUM INDUCED DRAG

An important question in regard to the wing is: Assuming a definite total lift, what distribution of the lift along the span will give rise to a minimum induced drag? Or, calling downward momentum imparted to the air in one second G (i. e., the lift) and the kinetic energy T , what is the distribution of lift such that for a slight modification in the flow $\delta T = 0$ while $G = \text{constant}$? Let there be a slight change in the flow brought about by the addition of a flow defined by a velocity potential φ . The impulse per unit length along the span required to produce this flow is $-\rho\varphi$. Therefore the increase in momentum would be $-\rho \int \varphi dx$ along the span. This must equal zero, since G is constant. The impulse acts upon air already flowing downward with velocity $u' = \frac{1}{2} u$, hence the increase in kinetic energy is the sum of two terms, $-\frac{1}{2} \rho \int u \varphi dx$ and the energy of the added flow itself, which may be neglected since it is proportional to the square of the added velocity, which may be assumed small. Hence, since $\delta T = 0$, $\frac{1}{2} \rho \int u \varphi dx = 0$. Therefore, to satisfy both conditions, $u = \text{const.}$ along the span, and the induced angle of attack is the same at all points. It is easy to see that this is the condition for a minimum (and not a maximum). (In the case of a biplane without stagger, the same condition of $u = \text{const.}$ would be true over both wings.)

In one second the wing advances a distance V and imparts, therefore, a downward velocity u , constant along the span, and a momentum equal to the lift. Let $K\rho$ be the apparent transverse mass of the projection of the wing on a transverse vertical plane due to the flow in the plane (e. g., monoplane wing would give practically a straight line of length b , equal to the span); that is, it is the apparent transverse mass of a surface whose edge is the projection referred to and whose depth is unity. Since the surface described in one second as the wing advances a distance V has as its edge the projection mentioned and a depth V , the apparent

mass set in motion in one second is $K\rho V$, and the momentum imparted in one second is $K\rho Vu$. This must equal the lift. Therefore

$$u = \frac{L}{\rho KV} \quad \text{-----} \quad (62)$$

for the case of minimum induced drag.

The kinetic energy imparted in one second is $\frac{1}{2} K\rho V \cdot u^2$ and this must equal $D_i V$; therefore,

$$\begin{aligned} D_{i\min} &= \frac{1}{2} \rho K u^2 \\ &= \frac{L^2}{4 \cdot \frac{\rho}{2} V^2 \cdot K} \quad \text{-----} \quad (63) \end{aligned}$$

Further

$$\alpha_i = \frac{u'}{V} = \frac{D_{i\min}}{L} = \frac{L}{4 \cdot \frac{\rho}{2} V^2 \cdot K} \quad \text{-----} \quad (64)$$

Since in the neighborhood of a minimum, properties change slowly, these values of $D_{i\min}$ and α_i may be used for other cases of lift distribution also.

The two dimensional flow in the transverse vertical plane about a line of length b equal to the span has already been discussed, viz, for the case of uniform velocity u downward at all points of the line, from (13')

$$F = u \frac{b}{2} i \left(\frac{2}{b} z - i \sqrt{1 - \left(\frac{2}{b} z \right)^2} \right)$$

Hence, for points on the line,

$$\varphi_o = \pm u \frac{b}{2} \sqrt{1 - \left(\frac{2}{b} x \right)^2}$$

The difference in the potential on the two sides of the line at a point x is $2 u \frac{b}{2} \sqrt{1 - \left(\frac{2}{b} x \right)^2}$,

which corresponds to an impulse per unit length (along the chord) of $\rho 2 u \frac{b}{2} \sqrt{1 - \left(\frac{2}{b} x \right)^2}$.

See (1a).

In one second this unit length advances a distance V and communicates a momentum L_1 , where L_1 is the lift per unit length of the span; since this momentum is imparted over a length V , the momentum imparted per unit length is $\frac{L_1}{V}$. Therefore

$$\frac{dL}{dx} = L_1 = 2 V u \rho \frac{b}{2} \sqrt{1 - \left(\frac{2}{b} x \right)^2} = 2 V u \rho \frac{b}{2} \sin \delta_o$$

where

$$\cos \delta_o = \frac{2}{b} x.$$

Hence

$$L = \int_{-b/2}^{+b/2} \frac{dL}{dx} dx = 2 V u \rho \left(\frac{b}{2} \right) \int_0^\pi \sin^2 \delta_o \cdot d\delta_o = V u \rho \pi \left(\frac{b}{2} \right)^2$$

and therefore, on substituting for u its value in terms of L ,

$$\frac{dL}{dx} = \frac{4L \sin \delta_o}{\pi b} \quad \text{-----} \quad (65)$$

This particular distribution of lift along the span, corresponding to minimum induced drag, is called elliptical, because since

$$x = \frac{b}{2} \cos \delta_o \text{ and}$$

$$y \equiv \frac{dL}{dx} = \frac{4L}{\pi b} \sin \delta_o$$

the points (x, y) lie on a semiellipse.

Returning to the values found for D_i and α_i , the value of K may be substituted, viz, $\pi \frac{b^2}{4}$. Therefore

$$D_{i_{min}} = \frac{L^2}{\pi b^2 \frac{\rho}{2} V^2} \dots\dots\dots (66)$$

$$\alpha_i = \frac{L}{\pi b^2 \frac{\rho}{2} V^2} \dots\dots\dots (67)$$

The effective angle of attack varies from point to point along the span. It has been proved that for an element of the wing, of area S , over which α is constant

$$L = 2\pi \frac{\rho}{2} V^2 S \alpha$$

If α_e is the effective angle of attack for an element dx of the span,

$$dL = 2\pi \frac{\rho}{2} V^2 \alpha_e \cdot c \, dx \text{ where } c \text{ is the chord}$$

Hence

$$\alpha_e = \frac{dL}{dx} \frac{1}{2\pi \frac{\rho}{2} V^2 \cdot c}$$

Therefore substituting for $\frac{dL}{dx}$ from (65)

$$\alpha_e = \frac{2L \sin \delta_o}{b \pi^2 c \frac{\rho}{2} V^2} \dots\dots\dots (68)$$

Calling the geometrical angle of attack α_g , it is evident that

$$\alpha_e = \alpha_g - \alpha_i$$

Hence

$$\alpha_g = \frac{2L \sin \delta_o}{b \pi^2 c \frac{\rho}{2} V^2} + \frac{L}{\pi b^2 \frac{\rho}{2} V^2} = \alpha_e \left(1 + \frac{\pi c}{2b \sin \delta_o} \right) \dots\dots\dots (69)$$

C. GENERAL CASE OF CALCULATION OF INDUCED DRAG WHEN DISTRIBUTION OF LIFT ALONG THE SPAN IS KNOWN

In case, however, that the induced downwash is not constant along the span, the induced drag is not a minimum and the distribution of lift is not elliptical; so the formulas just deduced for α_e and α_g do not hold. For the case of a variable transverse velocity along the span use can be made of the general formula (27')

$$\varphi_o = \frac{b}{2} (A_1 \sin \delta_o + A_2 \sin 2\delta_o + \dots), \text{ where } \cos \delta_o = \frac{2}{b} x$$

Hence the difference of potential between opposite points is

$$b (A_1 \sin \delta_o + A_2 \sin 2\delta_o + \dots)$$

and therefore, by the same argument as before,

$$\frac{dL}{dx} = b V \rho (A_1 \sin \delta_o + A_2 \sin 2\delta_o + \dots) \dots \dots \dots (70)$$

Consequently, if $\frac{dL}{dx}$ is specified at all points of the span, $\frac{1}{b V \rho} \frac{dL}{dx}$ may be expanded in a Fourier's series and, the values of the constants being thus determined, the flow is known, etc.

In this general case, by (29),

$$u = A_1 \frac{\sin \delta_o}{\sin \delta_o} + 2A_2 \frac{\sin 2\delta_o}{\sin \delta_o} + \text{etc.}$$

and

$$\alpha_i = \frac{u'}{V} = \frac{\frac{1}{2} u}{V} = \frac{1}{2 V \sin \delta_o} (A_1 \sin \delta_o + 2A_2 \sin 2\delta_o + \text{etc.}) \dots \dots \dots (71)$$

Further, since $\alpha_i = \frac{dD_i}{dL}$,

$$\begin{aligned} D_i &= \int_{-b/2}^{+b/2} \alpha_i \frac{dL}{dx} dx = \rho \left(\frac{b}{2}\right)^2 \int_0^\pi (A_1 \sin \delta_o + 2A_2 \sin 2\delta_o + \text{etc.}) (A_1 \sin \delta_o + A_2 \sin 2\delta_o + \text{etc.}) d\delta_o \\ &= \frac{\pi}{2} \rho \left(\frac{b}{2}\right)^2 (A_1^2 + 2A_2^2 + \dots) \dots \dots \dots (72) \end{aligned}$$

(In the case of minimum induced drag, we found, (66) and preceding, the values

$$D_{i_{min}} = \frac{L^2}{\pi b^2 \frac{\rho}{2} V^2}$$

$$L = V u \rho \pi \left(\frac{b}{2}\right)^2$$

where $u = A_1$ in the general formula, i. e.

$$L = A_1 \rho V \pi \left(\frac{b}{2}\right)^2$$

and therefore

$$D_{i_{min}} = \frac{\pi}{2} \rho \left(\frac{b}{2}\right)^2 A_1^2$$

which shows, since A_2, A_3 , etc., are small compared with A_1 , that $D_{i_{min}}$ —and therefore the corresponding α_i —may be used even in the general case of variable downwash).

D. EFFECT OF INDUCTION UPON LIFT AND ROLLING MOMENTS

The problem of deducing D_i and α_i has been solved, then, for the case when $\frac{dL}{dx}$ is given for all points of the span. Consider now the problem of the angle of attack being known at each point, is there any simple plan form which will permit a solution?

It has been proved that

$$\alpha_e = \frac{\frac{dL}{dx}}{2\pi c \cdot \frac{\rho}{2} V^2}$$

and that $\frac{dL}{dx} = b V \rho (A_1 \sin \delta_o + A_2 \sin 2\delta_o + \dots)$

Hence the general term is

$$\alpha_e = \frac{b A_n \sin n\delta_o}{\pi c V} \dots\dots\dots (73)$$

Further, the general term in α_i , as given in (71), is

$$\alpha_i = \frac{n A_n \sin n\delta_o}{2 V \sin \delta_o} \dots\dots\dots (74)$$

Therefore one is a constant times the other if c is proportional to $\sin \delta_o$ at each point of the span.

For an ellipse of semiaxes $\frac{b}{2}$ and $\frac{C}{2}$ formed as the plan of the wing

$$\frac{\left(\frac{c}{2}\right)^2}{\left(\frac{C}{2}\right)^2} + \frac{x^2}{\left(\frac{b}{2}\right)^2} = 1;$$

hence, since

$$\frac{2}{b} x = \cos \delta_o$$

$$c = C \sin \delta_o$$

Therefore such an elliptical wing makes α_e proportional to α_i .

Further, since the area

$$S = \pi \frac{b}{2} \cdot \frac{C}{2}; \quad \frac{\pi}{4} b c = S \sin \delta_o.$$

The same formula holds for a semiellipse.

For such a plan form, then, the general terms are

$$\alpha_e = \frac{A_n \sin n\delta_o}{2 V \cdot \sin \delta_o \frac{2S}{b^2}}$$

and

$$\frac{\alpha_i}{\alpha_e} = \frac{n\pi c}{2b} = 2n \frac{S}{b^2}$$

For the first term, i. e., $n=1$

$$\alpha_g = \alpha_e + \alpha_i = \alpha_e \left(1 + \frac{2S}{b^2}\right) = \left(1 + \frac{2S}{b^2}\right) \frac{A_1 \sin \delta_o}{2 V \frac{2S}{b^2} \sin \delta_o}$$

and for the general case

$$\alpha_g = \frac{1}{2 V \cdot \frac{2S}{b^2} \sin \delta_o} \left\{ \left(1 + \frac{2S}{b^2}\right) A_1 \sin \delta_o + \left(1 + \frac{4S}{b^2}\right) A_2 \sin 2\delta_o + \dots \right\} \dots\dots\dots (75)$$

or

$$2 V \cdot \frac{2S}{b^2} \sin \delta_o \cdot \alpha_g = \left(1 + \frac{2S}{b^2}\right) A_1 \sin \delta_o + \left(1 + \frac{4S}{b^2}\right) A_2 \sin 2\delta_o + \dots \dots\dots (75a)$$

Therefore, if α_g is specified over the span of an elliptic wing, the Fourier expansion gives values for the A 's, and these may be substituted in the formulas previously found, viz:

$$\frac{dL}{dx} = b V \rho (A_1 \sin \delta_o + A_2 \sin 2 \delta_o + \text{etc.})$$

$$\alpha_t = \frac{1}{2 V \sin \delta_o} (A_1 \sin \delta_o + 2 A_2 \sin 2 \delta_o + \text{etc.})$$

$$D_1 = \frac{\pi}{2} \rho \left(\frac{b}{2}\right)^2 (A_1^2 + 2 A_2^2 + \text{etc.})$$

The entire lift

$$L = \int_{-b/2}^{+b/2} \frac{dL}{dx} dx = \int_0^\pi \frac{dL}{dx} \sin \delta_o d\delta_o.$$

So only the first term has any effect, and

$$L = b V \rho A_1 \int_{-b/2}^{+b/2} \sin \delta_o dx$$

or replacing $\sin \delta_o$ by its value $\frac{\pi}{4} \frac{bc}{S}$ and A_1 by

$$2 V \cdot \frac{2S}{b^2} \frac{1}{1 + \frac{2S}{b^2}} \alpha_g$$

(since only the first term counts),

$$L = \frac{\rho}{2} V^2 \cdot \frac{1}{1 + \frac{2S}{b^2}} \cdot 2\pi \int_{-b/2}^{+b/2} \alpha_g \cdot c dx \dots\dots\dots (76)$$

Expressed in terms of the effective angle of attack,

$$L = \frac{\rho}{2} V^2 \cdot 2\pi \int_{-b/2}^{+b/2} \alpha_e \cdot c \cdot dx$$

hence

$$\alpha_e = \frac{\alpha_g}{1 + \frac{2S}{b^2}} \dots\dots\dots (77)$$

If there were no induction, α_g would equal α_e . So the effect of induction is to reduce α_e in the ratio $1 : 1 + \frac{2S}{b^2}$.

The rolling moment $M = \int_{-b/2}^{+b/2} \frac{dL}{dx} \cdot x \cdot dx$ along the span.

Hence

$$M = - \int_{-b/2}^{+b/2} \frac{dL}{dx} \cos \delta_o \cdot \sin \delta_o \cdot d\delta_o = - \frac{1}{2} \int_{-b/2}^{+b/2} \frac{dL}{dx} \sin 2\delta_o \cdot d\delta_o$$

Therefore only the second term in $\frac{dL}{dx}$, as given in (70), has any effect and, substituting in the original formula for M ,

$$M = b V \rho A_2 \int_{-b/2}^{+b/2} \sin 2\delta_o \cdot x \cdot dx$$

Further, using only the second term in (75a) for α_g ,

$$2V \cdot \frac{2S}{b^2} \sin \delta_o \cdot \alpha_g = \left(1 + \frac{4S}{b^2}\right) A_2 \sin 2\delta_o$$

hence

$$A_2 \sin 2\delta_o = 2V \cdot \frac{2S}{b^2} \sin \delta_o \cdot \frac{1}{1 + \frac{4S}{b^2}}$$

or, since

$$S \sin \delta_o = \frac{\pi}{4} bc, \quad A_2 \sin 2\delta_o = \pi V \frac{c}{b} \frac{1}{1 + \frac{4S}{b^2}} \cdot \alpha_g$$

Consequently

$$M = \frac{\frac{\rho}{2} V^2 \cdot 2\pi}{1 + \frac{4S}{b^2}} \int_{-b/2}^{+b/2} c \cdot x \cdot \alpha_g dx \dots\dots\dots (78)$$

Expressed in terms of effective angle of attack

$$\frac{dL}{dx} = 2\pi \cdot \frac{\rho}{2} V \cdot c \cdot \alpha_e$$

Therefore the rolling moment, by its original definition,

$$M = \frac{\rho}{2} \cdot V^2 \cdot 2\pi \int_{-b/2}^{+b/2} c \cdot x \cdot \alpha_e dx$$

hence

$$\alpha_e = \frac{\alpha_g}{1 + \frac{4S}{b^2}}$$

and it is seen that so far as such moments are concerned, the effect of induction is to reduce α_e in the ratio $1 : 1 + \frac{4S}{b^2}$.

E. NOTE CONCERNING BIPLANES

Since $D_i = \frac{L^2}{4 \frac{\rho}{2} V^2 \cdot K}$ where $K\rho$ is the apparent mass for a two-dimensional flow in the trans-

verse plane; and, since, for a biplane, K is greater than for a single wing, D_i is less, other things being equal. Thus, if K applies to a biplane of a certain total area and span b , and K_1 to a monoplane of the same total area and of span b_1 , the lift is the same for the two, and if the induced drag is to be the same

$$K = K_1 = \pi \left(\frac{b_1}{2}\right)^2$$

or if

$$b_1 = kb, \quad k^2 = \frac{K}{\pi \left(\frac{b}{2}\right)^2}$$

The value of K is known for different combinations of wings, and k may thus be deduced.

CONCLUSION

For a wing of span b and chord c , the area being S , if α_g is the geometrical angle of attack at a point x of the span,

$$L = 2\pi \frac{\rho}{2} V^2 \cdot \frac{1}{1 + \frac{4S}{b^2}} \int_{-b/2}^{+b/2} \alpha_g \cdot c \cdot dx$$

i. e., the effect of induction on the lift is to reduce the effect of the angle of attack in the ratio of $1:1 + \frac{4S}{b^2}$.

The rolling moment

$$M = 2\pi \frac{\rho}{2} V^2 \frac{1}{1 + \frac{4S}{b^2}} \int_{-b/2}^{+b/2} \alpha_g \cdot c \cdot x \cdot dx$$

i. e., the effect of induction on rolling moment is to reduce the effect of the angle of attack in the ratio $1:1 + \frac{4S}{b^2}$.

PROPELLER THEORY

INTRODUCTION

The purpose of a theory of the action of a propeller is to combine with Froude's slip-stream theory a theory of the action of the elements of the blades as airfoils. These elements actually move along spiral paths; but it is possible to simplify the treatment by considering the blades as a single element of area S . Often one can treat the blades as having a definite section, and the blade area as concentrated at one point, say 70 per cent of the radius from the axis. In Munk's treatment of the subject he assumes that, as the flight velocity V and the tip velocity U of the blades are varied, the "shape" of the slip stream does not vary, although its velocity v does. Under these circumstances v is obviously a linear function of V and U so long as the aerodynamic properties of the blade elements remain unchanged.

Under these circumstances, not simply can the efficiency of the propeller be calculated in terms of known quantities, but also a formula for $\frac{dv}{dU}$ which enables one to compute the thrust for any value of $\frac{U}{V}$.

References.—Munk—Analysis of W. F. Durand's and E. P. Lesley's Propeller Tests. N. A. C. A. Technical Report No. 175. Notes on Propeller Design. N. A. C. A. Technical Notes 91, 92, 93, 94.

FROUDE'S SLIPSTREAM THEORY

If the aircraft is moving with a velocity V through air otherwise at rest, the propeller sets in motion backward a slip-stream whose final mean velocity may be called v . The air actually passing through the propeller has already had imparted to it a portion of this velocity, and, by general principles of mechanics, this additional velocity may be proved to be approximately one-half of v . For, imagine the aircraft at rest—as in a wind-tunnel experiment—and placed in a stream of air having the velocity V . Let the propeller be revolving as usual, and let the velocity of the air through the propeller be called $V+w$. Let the final velocity of the slip-stream be called v as above. If m is the mass of air passing per unit time, the thrust of the propeller is mv . This force acts on air moving with velocity $V+w$, hence the work done per unit time is $mv(V+w)$. This is equal to the increase of the kinetic energy of the air, viz.:

$$\frac{1}{2}m(V+v)^2 - \frac{1}{2}mV^2 = mv\left(V + \frac{v}{2}\right)$$

Therefore

$$w = \frac{v}{2} \text{-----} (79)$$

The mass passing the propeller disk per unit time is

$$D^2 \frac{\pi}{4} \left(V + \frac{v}{2} \right) \rho$$

and therefore the thrust

$$T = D^2 \frac{\pi}{4} \left(V + \frac{v}{2} \right) \rho v$$

or

$$\frac{T}{D^2 \frac{\pi}{4} V^2 \frac{\rho}{2}} = \left(1 + \frac{v}{V} \right)^2 - 1 \equiv C_T \text{-----} (80)$$

an absolute coefficient.

If the ratio $\frac{v}{V}$ is small, $C_T = \frac{2v}{V}$, or $\frac{v}{V} = \frac{1}{2} C_T$, but this approximation can be used only for small values of C_T .

THE SLIP CURVE

Since, as explained above, the assumptions made justify one in writing v as a linear function of V , the velocity of flight, and of U ($= \pi n D$), the tip velocity, we may write

$$\frac{v}{V} = m \left\{ \frac{U}{V} - \left(\frac{U}{V} \right)_0 \right\} \text{-----} (81)$$

where $\left(\frac{U}{V} \right)_0$ is the magnitude of the "relative" tip velocity for which the slip-stream velocity, and therefore the thrust, is zero. Therefore, if $\frac{v}{V}$ is plotted against $\frac{U}{V}$, the result is a straight line. (If in any actual propeller test, this plot is not such a straight line, it proves that the assumptions made above do not hold for this test.) This prediction is well supported by actual tests. The curve is called the "slip curve" and $m \left(= \frac{dv}{dU} \text{ for constant } V \right)$ is called the slip modulus. In plotting the curves the experimental values are formed by writing

$$\frac{U}{V} = \pi n \frac{D}{V}$$

$$\frac{v}{V} = \sqrt{1 + \frac{T}{D^2 \frac{\pi}{4} \frac{\rho}{2} V^2}} - 1$$

Munk discusses these actual curves very fully in his papers. One consequence to be noted is that, as a result of tests already made, m is known for propellers of various types and of different blade width, and that its value does not differ greatly from one-eighth for ordinary propellers. Munk also shows how the effective pitch may be calculated.

THE SLIP MODULUS

With certain assumptions, the slip modulus may be calculated. Consider a propeller with narrow blades whose sections are "ideal" and whose pitch ratio is small. With such a propeller the influence of the slip stream on the effective angle of attack may be neglected. Consider the total effective blade area S concentrated at the distance $0.7r$ from the axis.

For small angles of attack, the thrust (i. e., the lift) $T = 2\pi S \frac{\rho}{2} V_1^2 \alpha$, where V_1 is the relative velocity of the air and α is the small angle of attack. This may be calculated as follows:

$$V_1^2 = V^2 + U'^2 = V^2 \left\{ 1 + \left(\frac{U'}{V} \right)^2 \right\}$$

if U' is the tangential velocity of the propeller at the point where S is considered, i. e., $U' = 0.7 U$.

Let U'_0 be such a tangential velocity as causes zero thrust at velocity V . If $\tan \varphi$ equals $\frac{V}{U'}$ and if U is increased slightly, the resulting angle of attack on the blade area S is

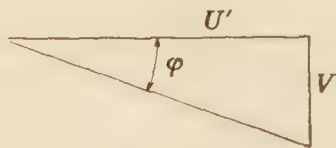


FIG. 15

$$\alpha = -d\varphi = \frac{dU'}{V} \frac{1}{1 + \left(\frac{U'}{V} \right)^2} \quad \text{-----} \quad (82)$$

Therefore

$$T = 2\pi S \frac{\rho}{2} V^2 \frac{dU'}{V}$$

and

$$C_r = 8 \frac{S}{D^2} \frac{dU'}{V}$$

Since C_r is small, it equals $2 \frac{v}{V}$ so that $\frac{v}{V} = 4 \frac{S}{D^2} \frac{dU'}{V}$. But $dU' = 0.7 dU$; and, since before the change dU , the thrust, and therefore v were zero, the slip stream which results from dU is such that $v = m dU = m \frac{dU'}{0.7}$,

$$m = \frac{\frac{v}{V} 0.7}{\frac{dU'}{V}} = 0.7 \frac{4S}{D^2} \quad \text{-----} \quad (83)$$

The fact that m is greater for propellers of greater mean blade width is confirmed by experiment.

In the calculation given above it is assumed that the only change when the tip velocity is increased is dU' ; but, as a matter of fact, there is an additional velocity $\frac{dv}{2}$ at right angles to

U' , which affects the angle of attack. Writing $\cot \varphi = \frac{U'}{V}$,

$$- \left\{ 1 + \left(\frac{U'}{V} \right)^2 \right\} d\varphi = \frac{dU'}{V} - \frac{U'}{V^2} \frac{dv}{2}.$$

Further,

$$dv = m dU = m \frac{U}{U'} dU'$$

Hence the angle of attack

$$\alpha = -d\varphi = \frac{1}{1 + \left(\frac{U'}{V} \right)^2} \frac{dU'}{V} \left(1 - \frac{m}{2} \frac{U}{V} \right) \quad \text{-----} \quad (82a)$$

and

$$m = 0.7 \frac{4S}{D^2} \left(1 - \frac{m}{2} \frac{U}{V} \right)$$

The ratio $\frac{U}{V}$ appearing here is the value at zero thrust, and this should be indicated by writing $\left(\frac{U}{V}\right)_0$. Solving the equation for m ,

$$m = \frac{0.7 \frac{4S}{D^2}}{1 + .35 \frac{4S}{D^2} \left(\frac{U}{V}\right)_0} \text{-----} (83a)$$

The "nominal blade width ratio," $\frac{2S}{D^2}$, is known for a propeller under test, and $\left(\frac{U}{V}\right)_0$ may be determined; so $m = \frac{dv}{dU}$ may be calculated. (In one test, calculation gave 0.13, and observations of the slip curve gave 0.133.)

Since this constant m may thus be considered known, $\frac{v}{V}$ may be calculated for any value of $\frac{U}{V}$ and therefore C_T is known and hence T , the thrust.

TORQUE

The propeller efficiency is the ratio of TV to the power delivered, that is, to the product of the torque Q by ω , the angular velocity.

$$\eta = \frac{TV}{Q\omega} \text{-----} (84)$$

But $T = C_T \cdot D^2 \frac{\pi}{4} \cdot V^2 \frac{\rho}{2}$, and a new coefficient C_Q may be defined such that

$$Q = C_Q \cdot \frac{D}{2} \cdot D^2 \frac{\pi}{4} \cdot V^2 \frac{\rho}{2} \text{-----} (85)$$

Then

$$\pi = \frac{C_T V}{C_Q \omega \frac{D}{2}} = \frac{C_T}{C_Q} \frac{V}{U} \text{-----} (86)$$

The power delivered may be thought of as being spent in three ways: (1) As absorbed in thrust, i. e., $Q_1\omega = TV$, and therefore, since $\eta_1 = 1$, the corresponding $C_{Q_1} = C_T \cdot \frac{V}{U}$; (2) as absorbed in building up the slip stream, i. e., $Q_2\omega = T \frac{v}{2}$, and, since $\eta_2 = \frac{2V}{v}$, the corresponding $C_{Q_2} = C_T \frac{V}{U} \cdot \frac{v}{2V}$; (3) as absorbed by friction, etc. Hence its corresponding $C_{Q_3} = C_Q$ ($C_{Q_1} + C_{Q_2}$), or $C_{Q_3} = C_Q - C_T \left(1 + \frac{v}{2V}\right) \frac{V}{U}$.

This is equivalent to a drag coefficient of the blades which may be calculated as follows: If S is the effective blade area, placed at a distance $0.7r$ from the axis, its tangential velocity is $.7U$; therefore, calling the drag coefficient C_D , the drag is $C_D S \frac{\rho}{2} (.7U)^2$, and the power spent in overcoming this is

$$C_D S \frac{\rho}{2} (.7U)^2 (.7U)$$

This must equal

$$\begin{aligned} Q_3\omega &= C_{Q_3} \left(\frac{D}{2} \omega\right) \cdot D^2 \frac{\pi}{4} V^2 \frac{\rho}{2} \\ &= C_{Q_3} U D^2 \frac{\pi}{4} V^2 \frac{\rho}{2} \end{aligned}$$

Therefore

$$C_D = C_{Q_3} \frac{D^2 \frac{\pi}{4} \cdot 1}{S \cdot \left(\frac{\gamma U}{V} \right)^2 \cdot \gamma} \dots\dots\dots (87)$$

For actual propellers Munk states that $C_D = 0.025$ approximately.

If there were no frictional losses, the efficiency would equal

$$\frac{TV}{(Q_1 + Q_2) \omega} = \frac{TV}{T(V + \frac{v}{2})} = \frac{1}{1 + \frac{1}{2} \frac{v}{V}}$$

Therefore

$$\eta_{max} = \frac{1}{1 + \frac{1}{2} \frac{v}{V}} \dots\dots\dots (88)$$

and, since C_T is known in terms of $\frac{v}{V}$, and T is known in terms of C_T , this maximum efficiency may be expressed in terms of T .

THE TORQUE SLIP CURVE

The slip curve described previously is derived from knowledge of the thrust, and is therefore more useful in the discussion of data obtained from model tests than in the case of tests in actual flight, for in the latter the thrust is an indefinite quantity—so far as theory is concerned. The theoretical value of the slip modulus, m , is derived only by making obvious assumptions, and, rather than trying to improve the theory, it is better to compare the theoretical value with observed values, obtained from the study of actual slip curves for propellers in flight. Again, in studying the properties of different propellers in flight, it is better to start with the knowledge of the torque or power and to deduce a different type of slip curve, because the power is much more definite than the thrust. Further, propellers are designed to absorb a given horsepower at a certain number of revolutions. Consequently, Munk describes a new slip modulus referring to the torque as modified by the interference of the fuselage, etc.

Define a power coefficient

$$C_P = \frac{P}{V \frac{\rho}{2} V^2 D^2 \frac{\pi}{4}} \dots\dots\dots (89)$$

Then, since

$$C_T = \frac{T}{\frac{\rho}{2} V^2 D^2 \frac{\pi}{4}}$$

and, since in the absence of viscosity the efficiency

$$\frac{TV}{P} = \frac{1}{1 + \frac{1}{2} \frac{v}{V}}$$

the "ideal" coefficient would have the value

$$C_T \left(1 + \frac{1}{2} \frac{v}{V} \right)$$

The actual coefficient is of course larger. Then in terms of the actual coefficients C_P and C_T define a slip velocity v' by the equation

$$C_P = C_T \left(1 + \frac{1}{2} \frac{v'}{V} \right) \dots\dots\dots (90)$$

In other words, v' is derived from the knowledge of the torque, as v is from that of the thrust. v' is slightly greater than v .

The curve of $\frac{v'}{V}$ plotted against $\frac{U}{V}$ is called the "torque slip curve," and by studying the two curves, that of $\frac{v}{V}$ and that of $\frac{v'}{V}$, for actual propellers in flight, knowledge may be obtained which will enable the better application of data from model tests.

In order to obtain the values of $\frac{v'}{V}$ from measured quantities, it is necessary to derive a relation between it and C_P . From the two equations

$$C_T = \left(1 + \frac{v'}{V}\right)^2 - 1 \text{ and } C_P = C_T \left(1 + \frac{1}{2} \frac{v'}{V}\right), \quad C_P = \frac{1}{2} \left(\frac{v'}{V}\right)^3 + 2 \left(\frac{v'}{V}\right)^2 + 2 \left(\frac{v'}{V}\right) \dots \dots \dots (91)$$

In N. A. C. A. Report No. 183, Munk gives values of the solution of this equation, so that values of $\frac{v'}{V}$ may be obtained, and then the corresponding torque slip curves,

$$\frac{v'}{V} = m' \left\{ \frac{U}{V} - \left(\frac{U}{V} \right)_o \right\}$$

may be plotted. These may then be compared with the thrust slip curves,

$$\frac{v}{V} = m \left\{ \frac{U}{V} - \left(\frac{U}{V} \right)_o \right\}$$

in which $\frac{v}{V}$ is obtained from a knowledge of T .

Munk made a detailed study of the performance of certain propellers as published in the British R. & M. Nos. 586 and 704, and deduced for comparative purposes the following data:

1. Curves for m and m' .
2. Calculation of m from the theoretical formula, and the value of the correction factor $\frac{m_{obs.}}{m_{calc.}}$. (This varied from 0.97 to 1.13.)

3. Mean effective angle of attack, at 0.7 radius, $\alpha = \cot^{-1} \left(\frac{0.7 U}{V} \right)_o$. Also the observed value. The difference is to be attributed to the effect of the camber of the blade section and to the elastic torsion of the blades.

These formulas and test data are, of course, most important in the study of sets of propellers and of the same propeller when attached to different engines; but they also are of direct use to the engineer who wishes to design a new propeller.

REPORT No. 214

WING SPAR STRESS CHARTS AND WING TRUSS PROPORTIONS

By EDWARD P. WARNER
Massachusetts Institute of Technology

REPORT No. 214

WING SPAR STRESS CHARTS AND WING TRUSS PROPORTIONS

By EDWARD P. WARNER

INTRODUCTION

Although the coming of the thick airfoil section has somewhat decreased the number of airplanes designed with continuous wing spars externally supported at several points, that type of construction has not by any means disappeared. The truss continuous through two or three bays is still commonly used, and the calculation of continuous beams is still making heavy inroads upon the time of the designer. With the objects of reducing the labor involved in such calculations and of deriving some general conclusions on the properties of continuous beams, the curves described in this report have been prepared for publication by the National Advisory Committee for Aeronautics. In presenting them to the public, the writer takes the opportunity of acknowledging the assistance of Mr. Otto C. Koppen, who has done a very considerable proportion of the work of preparation of the material.

SUMMARY

In order to simplify calculation of beams continuous over three supports, a series of charts have been calculated giving the bending moments at all the critical points and the reactions at all supports for such members. Using these charts as a basis, calculations of equivalent bending moments, representing the total stresses acting in two bay wing trusses of proportions varying over a wide range, have been determined, both with and without allowance for column effect. This leads finally to the determination of the best proportions for any particular truss or the best strut locations in any particular machine. The ideal proportions are found to vary with the thickness of the wing section used, the aspect ratio, and the ratio of gap to chord.

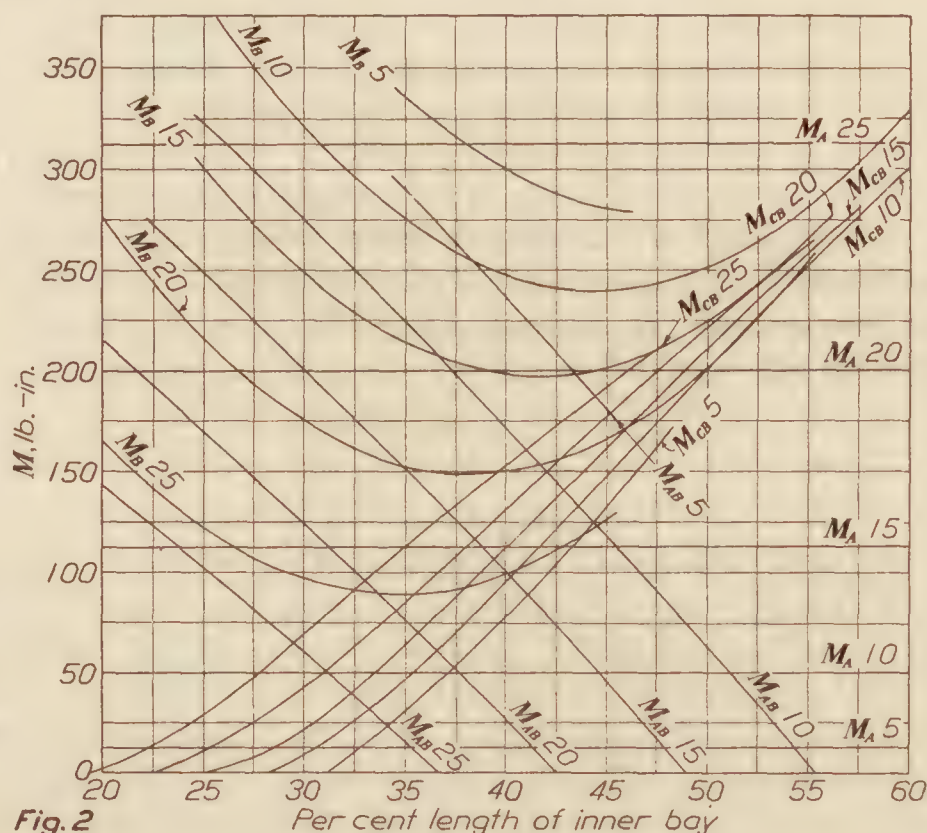
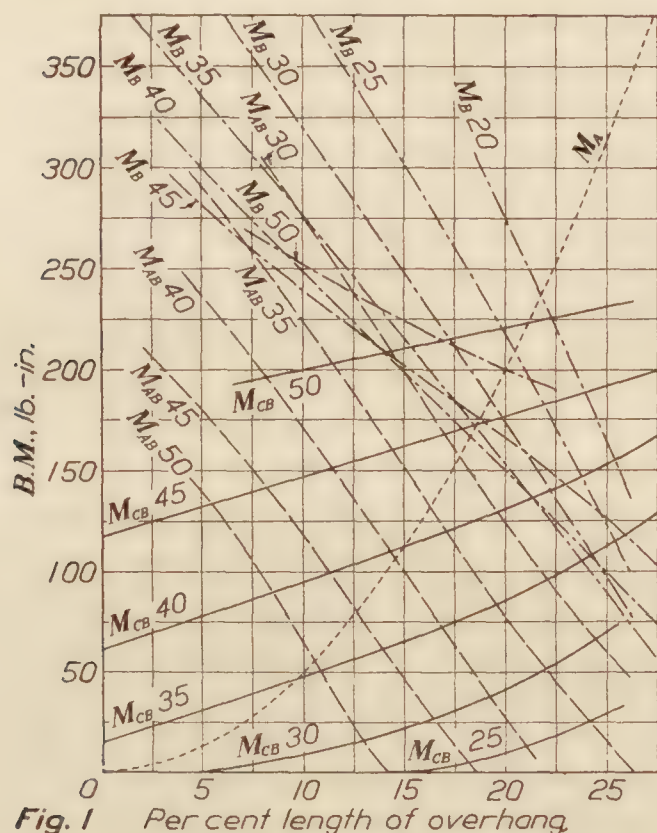
BENDING MOMENT CHARTS

Of all the wing cells built with spars continuous over three or more supports, at least 75 per cent of the total number involve calculation for three supports only. If the loading per unit length of spar be assumed uniform in such a case there are only three variables which affect the bending moments, reactions, and bending stresses for unit loading. Those quantities are dependent only on the length of the inner bay, the length of the outer bay, and the length of the effective overhang, and if all results be reduced to a common total length, as can easily be done, one of these three variables disappears and curves of moment, reaction, and stress can be plotted in terms of the remaining two.

With the object of simplifying the calculation of two-bay continuous trusses and of making it apparent at a glance what gain or loss can be expected from a change of arrangement of the wing bracing, a number of continuous beams have been calculated and curves have been plotted from which it is possible to read off at once the results for any case. The calculations were all based on the assumptions of a uniform loading of 1 pound per inch length of spar and of a total length of spar of 100 inches. The spar was assumed to be held by a horizontal pin at its inner end, so that the bending moment there was zero. The bending moments for all cases on these assumptions are plotted in Figures 1 and 2, the choice between the two sets of curves in any case depend-

ing on their relative convenience for the particular problem in hand. In Figure 1, curves of the absolute values of the bending moments (signs being ignored) at the outer support, at the middle support, and at the point of maximum moment in the middle of each bay have been plotted against the length of overhang, each curve relating to a particular assumed value of the length of the inner bay. In Figure 1, as everywhere else in this text, A denotes the outer support, B the middle one, and C the innermost. M_B therefore represents the bending moment at the inner strut of a two-bay wing truss, M_{CB} that in the middle of the inner bay. In Figure 2 the same thing has been done, but with the length of the inner bay used as the abscissa and with a separate set of curves for each length of overhang (the curves being separated by intervals of 5 per cent of the total length, or 5 inches in a 100-inch spar, in both cases).

The simplicity of the application of these charts can best be illustrated by immediate solution of an illustrative problem. Supposing a spar to have an inner bay 27 inches long, an outer bay 52 inches long, and a 21-inch effective overhang, the bending moments are read off from Figure 1 by going up along an ordinate at the abscissa corresponding to the length of over-



hang until a point two-fifths of the way from the 25 per cent to the 30 per cent curve is reached. The bending moments are found to be:

- 222 lb. ft. at the outer support;
- 179 lb. ft. at the middle support;
- 140 lb. ft. in the outer bay;
- 27 lb. ft. in the inner bay.

The moments in the bays are, of course, of opposite sign from those at the supports. Exactly the same results can be obtained from Figure 2 by running up along the 27 per cent line to an interpolation between the 20 per cent and 25 per cent curves.

As a rule, of course, the loading is not equal to unity, and the length of the beam is not 100 inches. In more general cases the bending moments read from the curves can be corrected by multiplying by the actual intensity of loading and by the square of the ratio of the length to 100 inches.

In Figures 3 and 4 the same work has been done for the reactions at the three supports. Taking again the problem just solved, the reactions can be read off directly as 48 pounds at the outer support, 45 pounds at the middle one, and 7 pounds at the innermost. The corrections to be applied are the same as before, except that the index values of the reactions are multiplied by the direct ratio of the lengths instead of the square of the ratio.

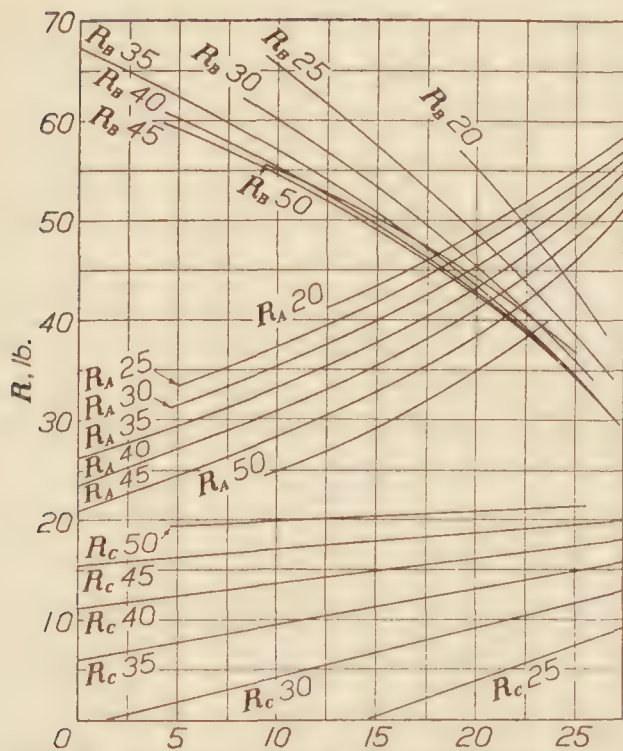


Fig. 3 Per cent length of overhang

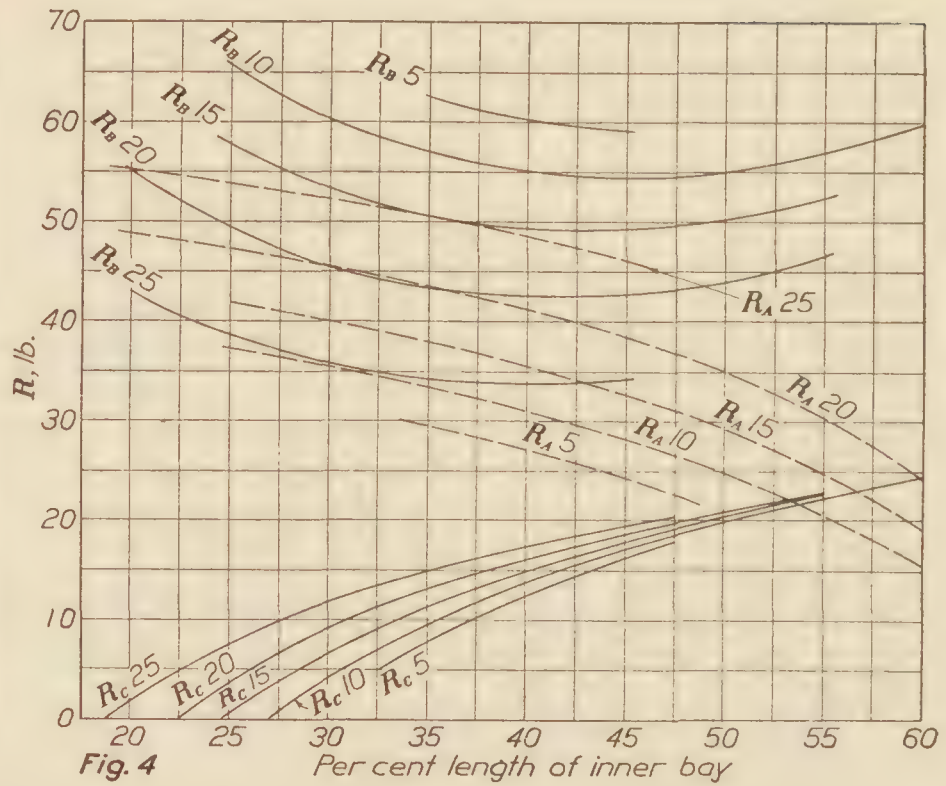


Fig. 4 Per cent length of inner bay

In Figures 5 and 6 the moments and reactions are similarly given for the case of complete fixity of the spar at the inner end. They correspond, in the method of plotting, to Figures 1 and 3. Although it is very rare for a fitting to be used which holds the spar so firmly that the slope is actually unchanged under load, partial fixity is common, and its effect can readily be determined by comparing the figures for complete fixity and complete freedom and taking an intermediate value.

In addition to facilitating the calculation of bending moments and reactions, such charts serve as the basis for calculations of total stress and for a study of the effect of a change in the spacing of interplane struts, as the compressive or tensile stress may readily be thrown in with that due to bending.

TOTAL STRESS CHARTS

The total stress in a spar is given by the familiar formula:

$$f = \frac{My}{I} + \frac{P}{A}$$

which can also be written for sections symmetrical about the neutral axis in the form

$$f = \frac{1}{A} \left(\frac{Md}{2k^2} + P \right)$$

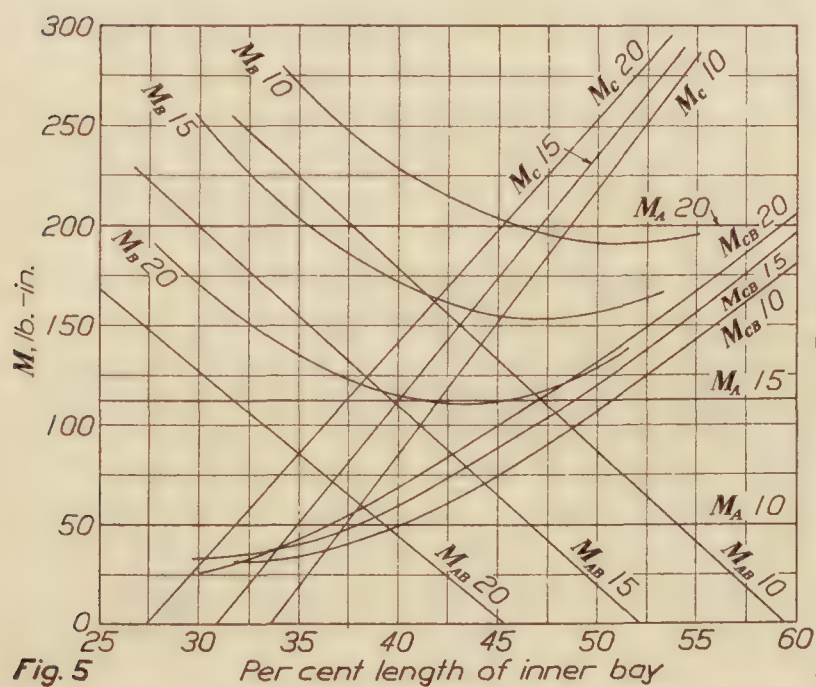


Fig. 5

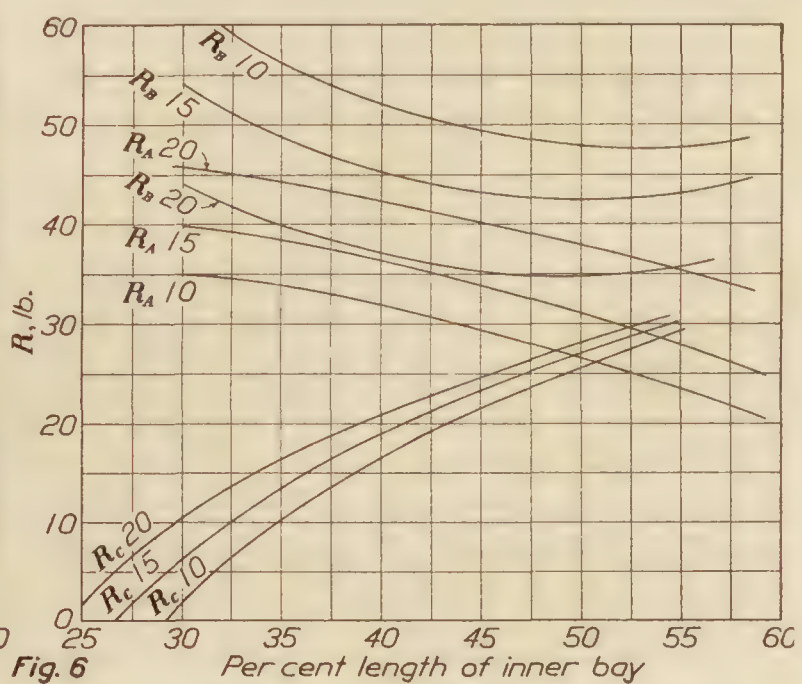


Fig. 6

where d is the total depth of the spar. It has been shown by the writer¹ that the radius of gyration about the neutral axis for a spar of conventional section is in the neighborhood of $.36d$. Substituting that value, the stress equation becomes:

$$f = \frac{1}{A} \left(\frac{M}{.26d} + P \right) = \frac{y}{I} (M + .26Pd)$$

The direct stress in a spar, for any given loading and arrangement of strut locations, is inversely proportional to the gap. The total stress is therefore made up of two components, one of which varies inversely as the spar depth and the other inversely as the gap, and their sum, for any given area of section, strut arrangement, and loading, is a function of the ratio of gap to depth of spar, a ratio which may range in magnitude from 6.5, with a thick airfoil section and a low gap-chord ratio, to 24 at the other extreme of design practice. Usually, however, it lies between 12 and 20. For any given value of that ratio, curves of total stress times section modulus, or of equivalent bending moment, can be plotted as those for actual bending moment have already been plotted without regard to the proportions of the wing truss in any respect other than strut spacing.

As an incident to the calculation of equivalent bending moments the compressions in the spar in the two bays were of course calculated, and the compressions in the outer bay of the upper spar (numerically equal to the tensions in the inner bay of the lower spar if the interplane struts are vertical) are plotted in Figure 7. The figures there given must be multiplied by the total length of the spar, by the ratio of the length of the spar to the gap, and by the unit loading. Furthermore, they are based on an assumption of equal area and similar strut location in the upper and lower wings, and biplane loading correction factors were ignored in calculating them, so that the reactions of the upper and lower spars at a given strut point were

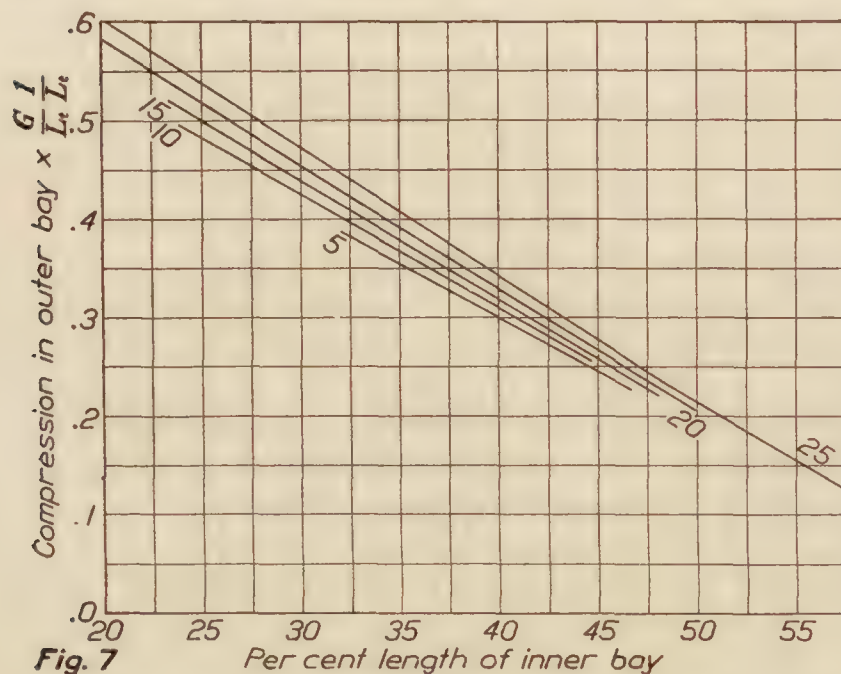


Fig. 7

taken as identical. This method is sound if the struts are vertical and if the unit loading used as a coefficient for the plotted values is the mean of the loadings on the two wings.

It is unnecessary to plot the compression in the inner bay, as its value is independent of strut location if the spars are pin jointed at the inner end. The moment of the compression in the upper spar about the lower hinge pin must be numerically equal to the total moment about the same axis of the air loads applied on the two spars, and it is therefore a constant, wherever the struts may be placed. The compression in the inner bay with a unit loading is always equal to the product of

the length of the spar by the ratio of spar length to gap, the coefficient analogous to that plotted in Figure 7 being unity.

In plotting the equivalent moments, instead of drawing separate curves for the two supports and the two bays, as in the case of the actual moments, only the largest absolute value has been retained for each strut arrangement, and curves of constant value of maximum moment have then been drawn with length of overhang as ordinate and length of inner bay as abscissa. Such curves are more useful, for this particular purpose, than the type previously drawn, for the plots of equivalent moment are intended to serve as a guide to the securing of maximum structural efficiency in design by the choice of an optimum strut location, rather than as a direct aid in routine calculation. The equivalent moment curves for the upper spar

¹ The Design of Wing Spar Sections, by Edward P. Warner, Aviation, May 29, 1922.

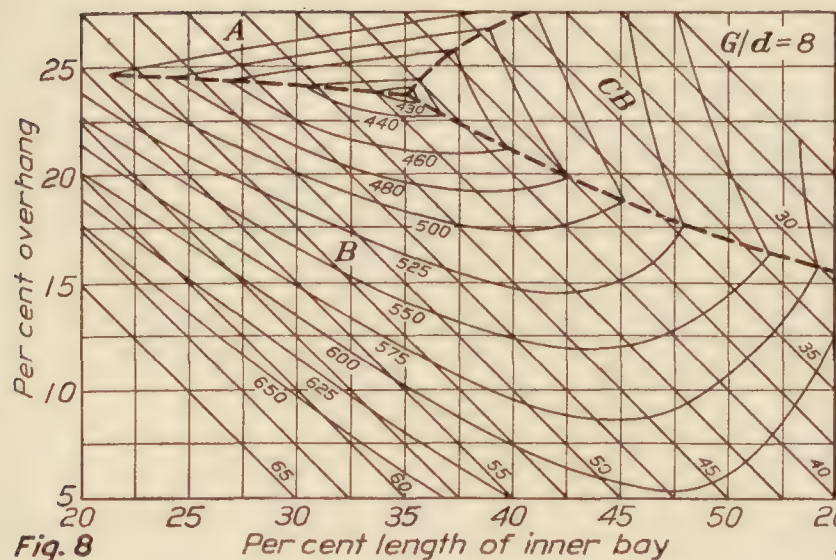


Fig. 8

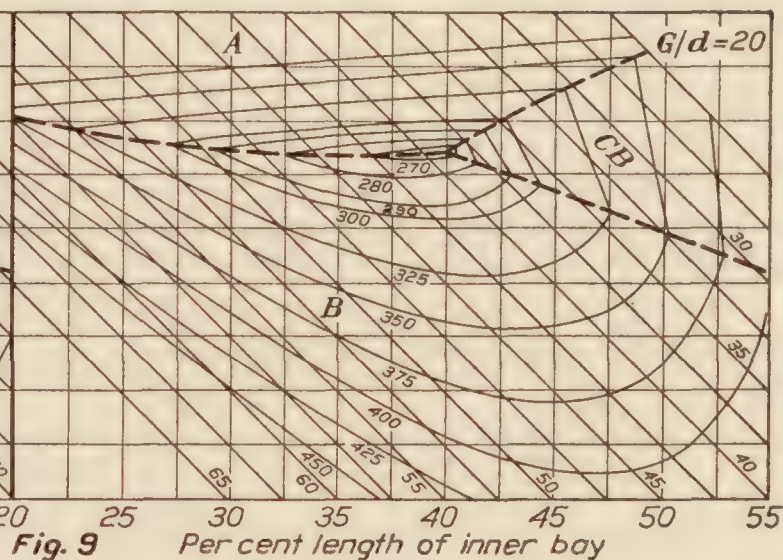


Fig. 9

at two values of G/d are given in Figures 8 and 9, and those for the lower spar for a single value in Figure 10. The diagonals sloping downward and to the right give the length of the outer bay.

It will be observed that each of the three charts of equivalent bending moment is divided into three parts by dotted lines. The lines represent the transfer of worst stress from one point in the spar to another, and the point in the spar at which the worst stress is found is indicated by a symbol in each zone of each chart. An overhang length of 22 per cent combined with an inner bay of 35 per cent, for example, would fall in the zone marked *A* in Figure 9 and in that marked *B* in Figure 8, signifying that the maximum equivalent bending moment in the upper spar falls at the outer strut when G/d is 20 but at the inner strut point when G/d is only 8. There is, of course, an abrupt break in the form and slope of each envelope curve where it passes from one zone to another.

Spruce, the material most commonly used in wing spar construction, shows an exceptionally large difference between ultimate stress in straight compression and modulus of rupture. For rectangular specimens the ratio is about 1.8, the bending strength of course being the larger, but with I and box spars of the proportions ordinarily used the inclusion of a form factor for bending causes the ratio to fall off to about 1.4 on the average. An increase of the proportion of bending stress will then increase the total allowable stress, and an increase of 140 pounds per square inch in bending stress can be balanced by a reduction of 100 pounds per square inch in compression, leaving the factor of safety unchanged. This can be allowed for in drawing charts of equivalent bending moment by multiplying the compressive stress by 1.4, and that has been done in Figures 11 and 12, which otherwise correspond to Figures 8 and 9. Figures 8 and 9 hold most nearly for metal spars; Figures 11 and 12 for spruce.

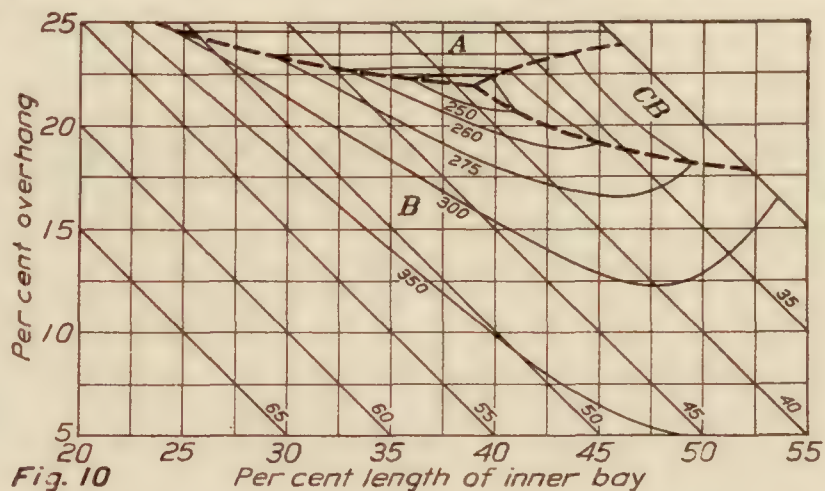


Fig. 10

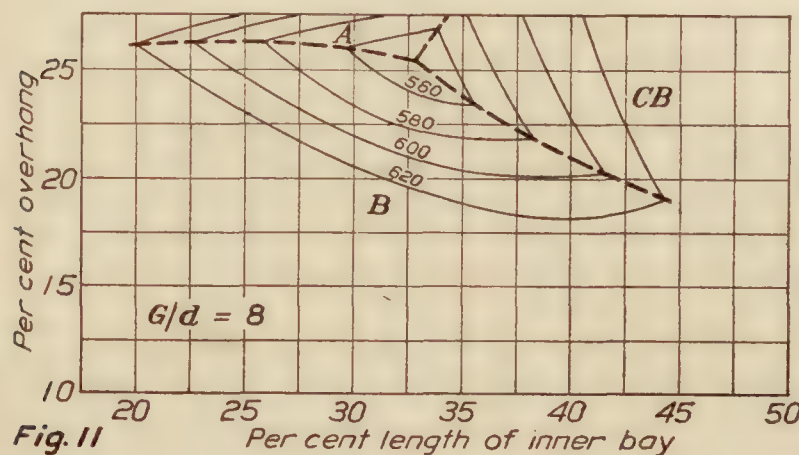


Fig. 11

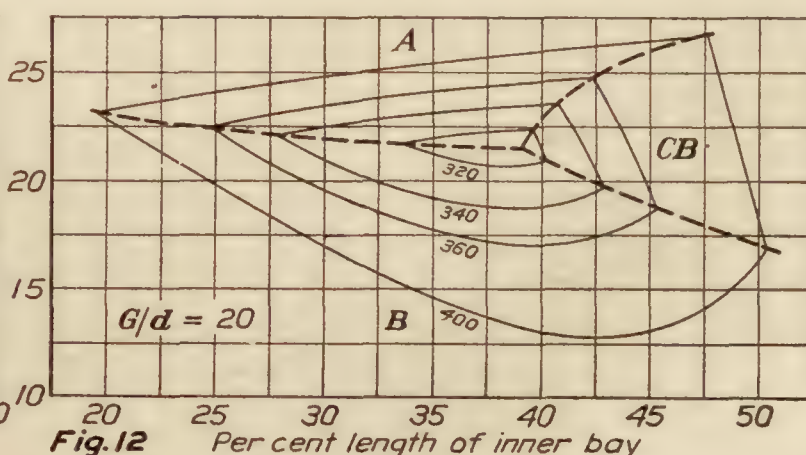


Fig. 12

ALLOWANCE FOR COLUMN EFFECT

In making all these calculations the actual values of all four sets of moments have been taken as on a parity in finding the maximum equivalent moment to enter in the chart. When the distance between bays is great in proportion to the depth of the spar, however, the liability of buckling becomes an important factor, and a bending moment of given magnitude in the middle of a bay is much more serious than one equally large at a strut point. The exact effect of buckling in increasing the liability to failure in the middle of a span is not susceptible of simple treatment, but a satisfactory approximation for most cases can be made by the use of Perry's formula,

$$M' = M \times \frac{P_e}{P_e - P}$$

where M' is the corrected bending moment, M the original bending moment due to lateral loading alone and without allowance for column effect, P the compression in the spar, and P_e the collapsing load under pure compression as calculated by Euler's formula, the length of the column being taken as the distance between points of inflection in the spar and the ends being considered as pin jointed.

The ratio of distance between points of inflection to total length of bay and the ratio of compression stress to total stress both vary widely with interplane strut spacings. Taking account of these variations, the formula for corrected bending moment can be written

$$M' = M \times \frac{1}{1 - \frac{f_c}{f'_t} \times \frac{f'_t}{\pi^2 E k^2} A l^2} = \frac{M}{1 - \frac{f_c}{f'_t} \times \frac{f'_t}{\pi^2 E k^2} l^2} \quad (A)$$

where l is the length between the points of inflection, A the cross-sectional area of the spar, k the radius of gyration of the spar section, f_c the compressive stress in the material due to direct compressive load, and f'_t the total stress. In the case of a spruce spar the total stress may be assumed to be 5,500 pounds per square inch at failure, taking a form factor of approximately .8, assuming a 15 per cent moisture content, and on the further assumption that the ratio of bending stress to compressive stress is approximately two to one. The ultimate stress in the material will of course vary with this ratio, but if the attempt is made to deal separately with the strengths in compression and bending the expression becomes somewhat complex. If a value of 5,500 then be assumed, and E be taken as 1,600,000, the expression for corrected bending moment can be reduced to

$$M' = \frac{M}{1 - \frac{f_c \left(\frac{l}{L}\right)^2 L^2}{f'_t \left(\frac{k}{d}\right)^2 d^2}}$$

where L is the total length of bay, d the depth of the spar, and the other symbols have the same significance as before. The writer has previously shown² that $\frac{k}{d}$, for typical spar sections, is about .36. If this value be used, the expression becomes

$$M' = M \times \frac{1}{1 - \frac{f_c \left(\frac{l}{L}\right) \left(\frac{L}{d}\right)^2}{f'_t \frac{375}{375}}}$$

The total stress as used in these formulas is, of course, that due to the final corrected value of the bending moment, so that

$$f'_t = \frac{M'y}{I} + \frac{P}{A}$$

² Aviation, loc. cit.

It is desirable, however, that the solution for M'/M should be direct and simple, and should involve only quantities dependent on the geometrical properties of the spar alone. M' should appear only in the final result. This end could be attained if it were assumed that $f'_t = f_t \frac{M'}{M}$ where f_t is the total stress which would exist in the spar if there were no buckling effect, or

$$f_t = \frac{My}{I} + \frac{P}{A}$$

The general equation for column effect correction would then become

$$\frac{M'}{M} = \frac{1}{1 - \frac{f_c}{f_t} \frac{M'}{M} \frac{f'_t}{\pi^2 E k^2} l^2}$$

or

$$\frac{M'}{M} = 1 + \frac{f_c}{f_t} \frac{f'_t}{\pi^2 E k^2} l^2$$

The correction factors given by this formula are somewhat too low, while those obtained from the form (A), using $\frac{f_c}{f_t}$ in place of $\frac{f_c}{f'_t}$, are too high, in some cases very much too high. The obvious solution is to use a formula intermediate between the two, such as

$$\frac{M'}{M} = \frac{1 + \frac{f_c}{f_t} \frac{f'_t}{2\pi^2 E k^2} l^2}{1 - \frac{f_c}{f_t} \frac{f'_t}{2\pi^2 E k^2} l^2}$$

The mathematical justification of this procedure need not be given. It is sufficient to say that the compromise formula finally arrived at, although admittedly only an approximation, is found by trial to give results satisfactorily close to the truth in the typical cases to which it has been applied, and for which its results have been directly compared with those obtained by actual calculation from a particular set of figures. Such error as does exist is almost always in the direction of safety, the formula giving too large a correction factor.

In the particular case of a spruce spar, the formula becomes

$$\frac{M'}{M} = \frac{750 + \left\{ \frac{f_c}{f_t} \left(\frac{l}{L} \right)^2 \left(\frac{L}{d} \right)^2 \right\}}{750 - \left\{ \frac{f_c}{f_t} \left(\frac{l}{L} \right)^2 \left(\frac{L}{d} \right)^2 \right\}}$$

The values of $\frac{f_c}{f_t}$ and of $\frac{l}{L}$ have been worked out for all of the cases of interplane strut spacings covered by the extent of Figures 1 to 4 and have been found to vary through exceedingly wide limits. When the ratio of gap to spar depth is 8, for example, the value of $\frac{f_c}{f_t}$ at the worst

stressed point in the middle of a bay in the upper spar ranges from .33 to .93, while, when the gap is twenty times the depth of spar, the corresponding spread is from .16 to .65. The ratio $\frac{l}{L}$ varies as shown by Figure 13, reaching a maximum value of about .86.

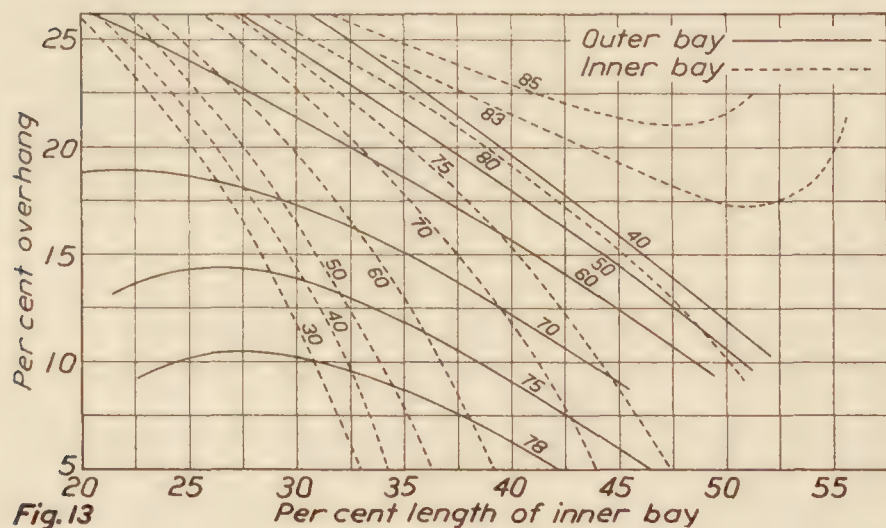


Fig. 13

f_c = compressive stress.

f_t = total stress.

l = distance between points of inflection.

L = distance between supports.

Fortunately, however, it happens that the variation of $\frac{f_c}{f_t} \times \left(\frac{l}{L}\right)^2$ is no larger than that of one factor alone. When $\frac{G}{d}$ is 8 the product for the worst stressed bay ranges from .18 to .55, with the highest values reached when the overhang is long and the inner and outer

bays are of equal length. The products are plotted in Figure 14. Similar curves are given in Figure 15 for a gap/depth ratio of 20, the extreme range in that case being from .09 to .41. The division of the curves of each sheet into two seemingly independent groups, separated by dotted lines, corresponds to the transition of the point of worst stress from one bay to the other (the worst stress being in the outer bay for points to the left of the dotted lines). While it is, of course, possible that the worst stress with allowance for buckling may come in the bay other than that in which it would occur when no such allowance had to be made, that is unlikely except when the truss is so proportioned that the equivalent stresses in the two bays are very nearly equal in any case, so that it will make little difference which one is used. The dotted line was located without reference to any difference between compressive and bending strengths of the spar material.

The ratio of L to d is limited by the necessity of keeping the angle between the lift wires and the wing spars above a certain minimum to provide rigidity to the structure. Neither in a Pratt nor in a Warren truss is it likely that the length of any single bay of a two-bay arrangement will ever exceed twice the gap. When G/d is 8, therefore, the maximum probable value of L/d will be 16. The equation of equivalent moment would then become approximately

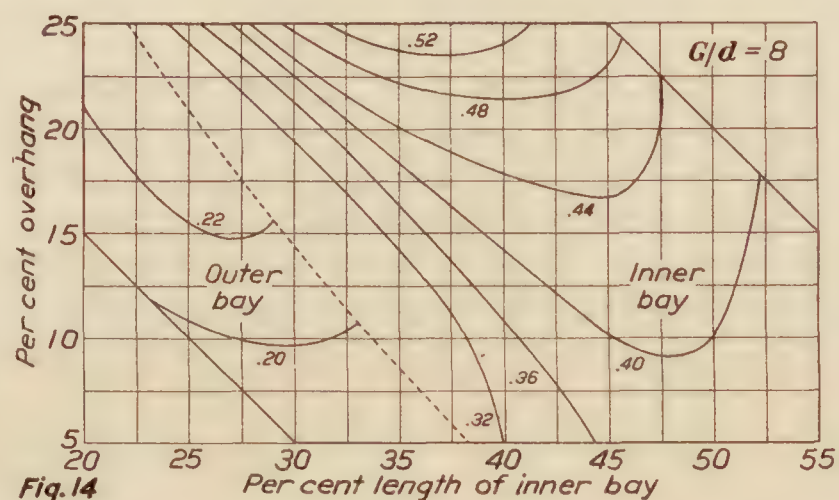


Fig. 14

$$M' = M \frac{1 + \frac{1}{3} \frac{f_c}{f_t} \left(\frac{l}{L}\right)^2}{1 - \frac{1}{3} \frac{f_c}{f_t} \left(\frac{l}{L}\right)^2}$$

For the largest value of the product plotted in Figure 14, this would give $M' = 1.45M$. The corresponding maximum when G/d is 20 is about $14M$, a value so large as merely to signify the impracticability of designing a spar with the length of a single bay equal to forty times the

spar depth. In fact, it seems unlikely, with a spar so shallow in proportion to the gap, that the value of $\frac{M'}{M}$ will ever fall below 1.35 for the worst stressed bay in actual practice.

These figures, of course, relate only to the inner bay, where the values of $\frac{f_c}{f_t} \times \left(\frac{l}{L}\right)^2$ reach their maximum because of the high compressions. If the values for the outer bay be lifted from the sections of Figures 12 and 13 to the left of the dotted lines $\frac{M'}{M}$ when the worst conditions are in that bay is found never to exceed 1.17 with G/d equal to 8, or 1.90 when G/d is 20. As already noted, however, it is unlikely that the actual percentage correction for buckling in a given truss, the proportions of which bring it near to the dotted line of transition, would be materially larger for the inner than for the outer bay, and it is correspondingly unlikely that the introduction of the buckling correction would appreciably shift the transition line. The actual extent of the change can best be shown by a couple of examples. Suppose, for instance, that a wing truss for which G/d is 20 has its spar length divided into an inner bay of 36 per cent, an outer bay of 49 per cent, and an overhang of 15 per cent, proportions which correspond to a point on the dotted line in Figure 15. The values of $\frac{f_c}{f_t} \times \left(\frac{l}{L}\right)^2$ (found by interpolation from the curves) are then .30 in the inner bay and .12 in the outer. If the length of the outer bay be taken as twice the gap, that of the inner bay will be 1.47 times the gap. The values of L/d are 40.0 and 29.4, and those of

$$\frac{\frac{f_c}{f_t} \times \left(\frac{l}{L}\right)^2 \times \left(\frac{L}{d}\right)^2}{750}$$

are .26 and .35 for the outer and inner bays, respectively, corresponding to correction factors of 1.70 and 2.08 to be applied to the bending moments. While the difference between these quantities is considerable, the problem is based on a truss of extreme proportions, and the correction factors would hardly be likely ever to reach such values in practice. If the length of the outer bay had been taken as one and a half, instead of two, times the gap, the corrections would have been only 1.32 and 1.47.

A similar problem for a point on the dotted line in Figure 14, G/d being 8 and the lengths being 33 per cent in the inner bay, 57 in the outer, and 10 in the overhang, gives correction factors of 1.15 in the outer bay and 1.06 in the inner if the outer length be twice the gap. Furthermore, the basic bending moment in the inner bay will be smaller than that in the outer if the proportions of the spar are chosen for uniform stress at the supports as the direct compression is largest in the inner bay, and the larger relative correction applied to M in the inner bay may therefore be little or no larger in its absolute effect on total stress. In general, therefore, it appears that the difference in the factors along the transition line is not great and that no shift of that line need be made. In almost all cases the worst stress in the middle of a bay with made allowance for buckling effect will occur in the same bay where it would be found if buckling were nonexistent or neglected.

The equivalent bending moments with allowance for buckling have been calculated for both gap-spar depth ratios used in the preceding work and for two ratios of length of spar to gap, and envelope curves have been plotted, just as they were plotted in Figures 8 and 9, without the allowance for column effect. Figures 16 and 17 give the equivalent moments for the two spar depths on the assumption that the total effective length of spar is 4.5 times the gap

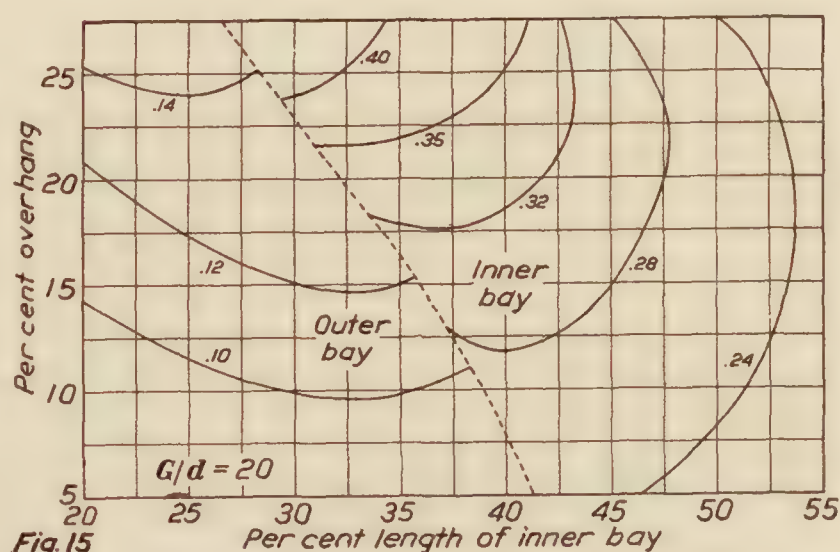


Fig. 15

(surely as large a ratio as would ever be reached in a two-bay machine in practice), while Figure 18 presents similar data for a spar length of 3 times the gap and a gap-spar depth ratio of 20. When L_t/G is 3 and G/d is 8 the column effect is so small as to be negligible. In calculating these curves both bays have been taken into account in all cases. Any shifting of the transition lines of worst conditions from the positions shown in Figures 12 and 13 has therefore been allowed for.

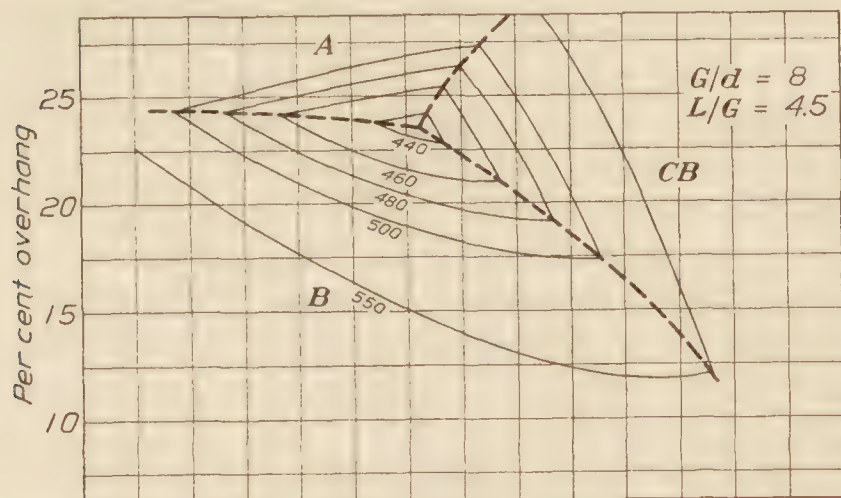


Fig. 16

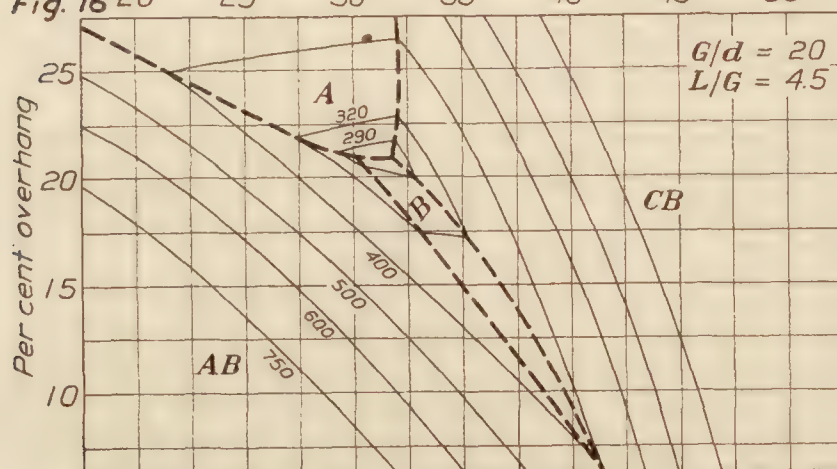


Fig. 17

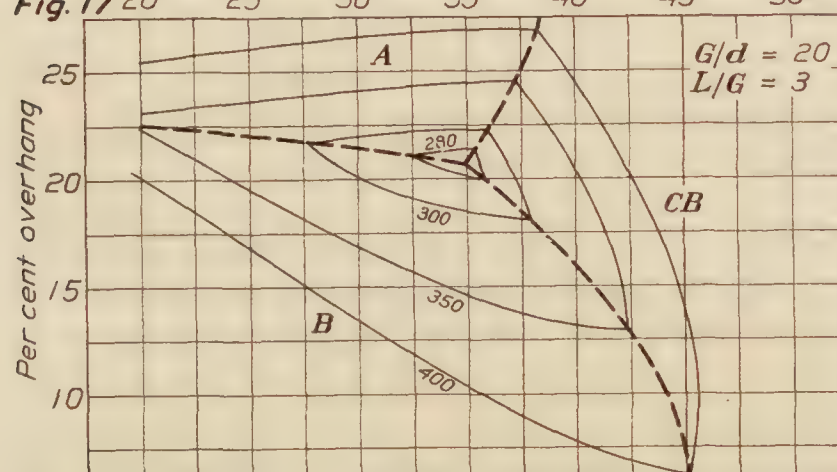


Fig. 18

Per cent length of inner bay.

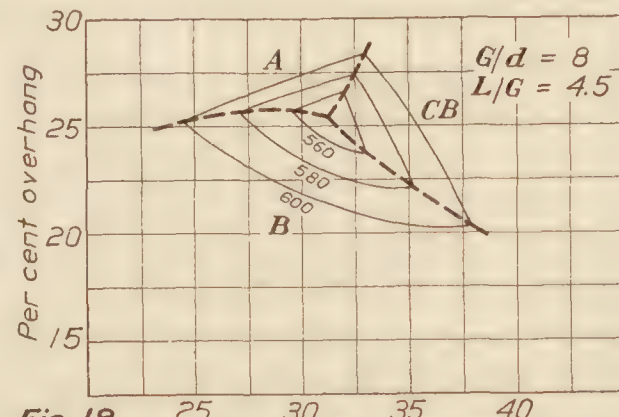


Fig. 19

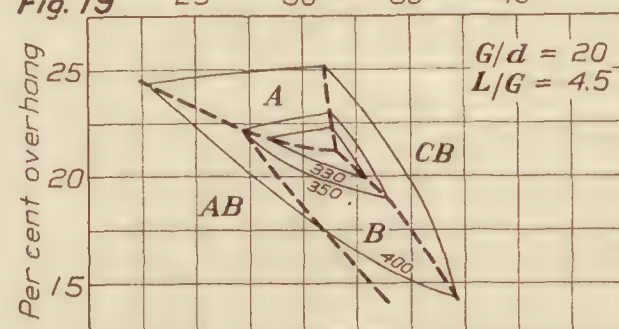


Fig. 20

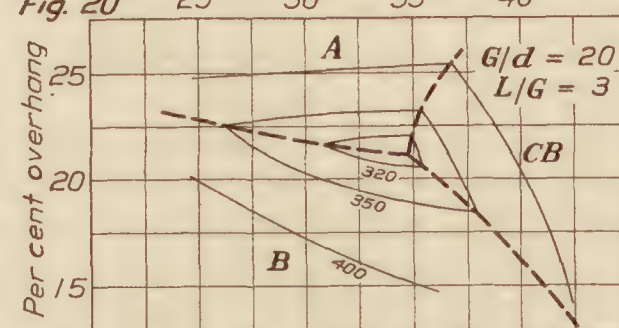


Fig. 21

Per cent length of inner bay

Figures 19, 20, and 21 stand in the same relation to those just discussed as do Figures 11 and 12 to 8 and 9. They are drawn to include allowance for the difference between the bending and compressive strengths of spruce and for the change in allowable stress with variation in the proportion of direct compressive stress to total stress.

DISCUSSION OF CURVES—BENDING MOMENTS

Inspection of the curves in Figures 1 and 2 reveals certain interesting characteristics of the variation of bending moment with the proportions of the truss which are not at once evident from the three-moment equation, nor even from a consideration from a purely physical point of view of the conditions under which the beam works. The first point of interest is the behavior of the moment at the middle support, which has a minimum value for each length

of overhang, the minimum being very nearly a linear function of the three-halves power of the length of overhang.

$$M_{B_{min.}} = 296 - 1.66 (l_3)^{3/2}$$

where l_3 is the length of effective overhang as a percentage of the total effective length of spar. Furthermore, it appears that the minimum value of M_B , for a given overhang is reached when the outer bay is longer than the inner by approximately one-sixth the length of the overhang. If either the inner or the outer bay be held to a fixed length M_B decreases steadily, and roughly along a straight line, as the overhang is lengthened at the expense of the other bay, but that, of course, is what would have been expected.

As for the moments in the middle of the bays, when the overhang is held constant the variation in both bays is almost exactly linear, the maximum in each bay, of course, increasing as the length of that bay itself is increased. The rate of change is approximately 10 pounds inches of moment for every inch of length of the bay in which that moment occurs, the total effective length of the two bays and overhang still being taken as 100 inches.

When the outer bay is held constant, instead of the overhang, both M_{AB} and M_{CB} increase as the inner bay increases. The variation still approximates to the linear, but only roughly, the moment in the inner bay tending toward a minimum as that bay becomes very short, while that in the outer bay appears to approach a maximum as the overhang approaches zero. With the inner bay held constant, linear relationships are again comparatively roughly observed, the moment going up in the outer bay and down in the inner as the outer bay is lengthened at the expense of the overhang.

Since all the variations of bending moments in the bays with changing distribution of the points of support follow straight-line laws at least approximately, it is possible to express them to a first approximation by a pair of very simple equations

$$M_{AB} = 708 - 10l_1 - 14l_3$$

or alternatively,

$$M_{AB} = 10l_2 - 4l_3 - 292$$

and

$$M_{CB} = 9l_1 + 3.6l_3 - 296$$

where l_1 , l_2 , and l_3 are the percentages of total spar length in the inner bay, outer bay, and overhang, respectively. The equation for M_{AB} gives results correct within 7 pounds inches for every point within the range of the curves, while that for M_{CB} is good within 9 pounds inches except under the most extreme conditions. Either is useful as an approximation when the curves are not available. For the sake of completeness a similar equation, necessarily somewhat more complex in form but fitting the curves even more accurately, has been obtained for the bending moment at the middle support.

$$M_B = 292 - 1.66 (l_3)^{3/2} + .39 (l_1 - 50 + \frac{\gamma}{12} l_3)^2.$$

This is considerably more simple than the direct solution from the three-moment equation and gives a result correct within 5 pounds inches at every point. The last moment, that at the outer support, of course, depends only on the effective length of the cantilevered overhang, and is given rigorously by

$$M_A = \frac{l_3^2}{2}$$

REACTIONS

Although the variation of the reactions is comparatively simple in form, it does not lend itself to elementary analytic representation so well as does that of the moments, the curves not running parallel to each other. When the overhang length is kept constant and the bays varied, the reactions at the outer and inner supports of course change in magnitude in the same sense as the lengths of the bays to which they are adjacent. The middle reaction remains virtually constant, reaching a minimum when the inner bay is longer than the outer by about one-eighth

the length of the overhang and increasing very gradually with change from that distribution in either direction. The curves for reaction at the middle support with fixed overhang are, in fact, very similar in form to the curves of bending moment at the same point under the same conditions.

With the inner bay fixed in length the reactions at both the outermost and the innermost supports increase with increasing overhang, the former rapidly and substantially uniformly, the latter very slowly, especially when the inner bay is long. The reaction at the middle support drops off as the overhang grows. For all proportions within the range of ordinary design practice, the outer and middle reactions are within 25 per cent of the same magnitude and the inner reaction is less than half as large as either of the others.

EFFECT OF FIXITY AT THE INNER END

As already remarked, a hinge fitting with a vertical pin puts partial restraint on the change of slope of the spar at its inner end, a degree of fixity which may conceivably lie anywhere between zero and 100 per cent, but which in practice probably is seldom less than 20 per cent or more than 60. (This, of course, does not apply to cantilever wings of thick section, where the fixity must necessarily be complete.)

Comparisons of Figures 2 and 5 show little alteration in the general form of the moment curves but considerable changes in detail. As would be expected, the minimum bending moment at the middle support is obtained with a considerably longer inner bay when the inner end is fixed than when it is free. Whatever the length of overhang, the length of the outer bay for a minimum value of M_B remains virtually constant at 38 per cent. By the time this point of minimum M_B has been reached, however, the inner support has become the critical location, M_C increasing approximately lineally and very rapidly as the inner bay is lengthened. For a fixed length of inner bay, M_C goes up with increasing overhang.

The bending moments in the middle of the inner bay are much decreased, while those in the outer bay are slightly increased, by fixity. Since it is in the inner bay, where the largest compressions are found, that failure by buckling is most likely to occur, the use of a fitting giving partial fixity would be particularly useful when a long inner bay has to be used with a shallow spar. So far as maximum moment at a support is concerned, however, fixity is of comparatively little use, since, for a given overhang, the value of M_B and M_C at the point where they are equal is only about 18 per cent less than the minimum reached by M_B with the inner end of the spar perfectly free in slope. If the comparison of the two conditions be made on the basis of the strut location which gives the lowest value for the bending moment at a support (this is equivalent to making M_B and M_C equal when the inner end is fixed) keeping the overhang fixed, the average decrease of M_{CB} by the fixity is 40 per cent, while M_{AB} is increased by an average of only 5 per cent, and is actually slightly decreased if the overhang be short. It is interesting to note, also, that the proportions which make M_C and M_B equal when there is complete fixity at the end also make M_{CB} and M_{AB} very nearly the same. This of course means that the inner bay would always be the critical one, as the larger compression there makes the column effect much more serious than it can be in the outer bay.

The effect of fixity on reactions is comparatively slight. The minimum reaction at the middle support occurs, in the case of complete fixity, with the length of the inner bay in excess of that of the outer by approximately 16 per cent, and the minima are lower than with a freely hinged end by an average of 7 pounds, or 15 per cent of the mean reaction. The reaction at the inner support is increased by an average of 3 pounds, while that at the outer support goes up about a pound. The compression in the outer bay, for a truss of given proportions is therefore almost entirely independent of the degree of fixity, but fixity will obviously reduce the inner bay compression very materially. That affords another reason, additional to the shortening of the distance between points of inflection in the inner bay, for using a hinge which will fix the spar at least partially when there is danger of trouble from buckling because of the use of a long bay in a shallow spar. Complete fixity may easily have the effect, everything taken into account, of more than doubling the factor of safety in the inner bay considered as a column.

DIRECT LOADS IN SPARS

The compression in the outer bay of the upper spar is primarily a function of the length of the inner bay, being almost entirely independent of the distribution of the remaining length between the outer bay and the overhang. The effect of a given shift in the location of the inner strut has approximately five times as much effect as a corresponding change in the position of the outer.

The change of compression with a change in the position of either strut, the other being held fixed, is very nearly linear. The straight lines tend to diverge when plotted, however, and the single equation which expresses the force for all proportions has therefore to be complicated to the form

$$F_t \times \frac{G}{L_t^2} = .7 - .015l_1 + .000107(60 - l_1)l_3$$

which gives the compression in the outer bay (always on the assumption that the upper and lower wings are similarly supported, with struts at the same points, and that the mean loading of the two is used in calculation) to within .006 for every condition, L_t being the total effective length of the spar.

The compression in the inner bay is, as has already been noted, quite independent of the proportions of the truss if the spars are freely hinged at their inner ends, but is reduced by fixity there, the amount of the reduction being directly proportional to the fixing moments and so being largest when the inner bay is longest and there is most need for some cutting down of the compression and stiffening of the spar.

The tension in the inner bay of the lower spar is of course numerically equal to the compression in the outer bay of the upper member for the type of truss to which these curves relate.

LOCATION OF POINTS OF INFLECTION

The distances between the two points of inflection within a bay have been given, both for the inner and the outer bays, by the curves of Figure 13. It should be noted in using these values that they were calculated without taking into account the effect of buckling in increasing the bending moment within the bay. The effect of increasing that moment while leaving the values at the supports constant is, of course, to shift the points of inflection outward toward the supports. The effective length of column is therefore a function of the depth of the spar and of the amount of compression, as well as of the distribution of the interplane struts, but the shift of the points of zero bending moment is not likely to be great enough to be of serious importance except in spars which would approach very closely to failure by pure lateral instability in any case, and when spars answer to that description no approximations such as these can be of much avail. It is necessary then to apply the generalized theorem of three moments rigorously.

In general, lengthening one bay at the expense of the other tends to increase the relative separation of the points of inflection in that bay, as would be expected. There are, however, exceptions to this general rule. The relative separation in the inner bay of a spar with a long overhang decreases when the length of the inner bay is increased beyond about 50 per cent of the total, and the same holds true in the outer bay when the overhang is short and the outer bay forms more than 60 per cent of the whole effective length of the spar. The diagonal lines representing constant lengths of outer bay have been omitted, to avoid confusion of the figure, but can readily be inserted if desired. With a constant length of inner bay the points of inflection in that section of the spar shift constantly farther apart as the overhang is increased, while for the outer bay the reverse is true and the largest separations always correspond to short overhangs.

EQUIVALENT BENDING MOMENTS AND SPAR PROPORTIONS

The curves in Figures 8 and 9 relate to the case of a spar in a wing of small aspect ratio, in which the column effect is of practically no importance. Specifically, they can be considered as applying with sufficient accuracy to all spars having a total length of less than thirty times their depth, a condition which is sometimes complied with in using thick airfoils. With a

Göttingen 387, for example, a section in which the mean spar depth is likely to be about 9 per cent of the chord, this permits an aspect ratio (figured on the total length of wing, including the part dropped off for tip loss correction) of about 5.8, while with an R. A. F. 15 the corresponding limit is about 3.7. Such proportions are of course unusual, and Figures 8 and 9 are useful as defining a limit rather than as applying directly to actual airplanes.

It will be observed in both figures that the minimum equivalent bending moment is found under the conditions which give equal moments at the two struts and in the middle of the inner bay. The proportions of the truss which give equality of these three moments change somewhat with G/d , the ideal length of inner bay, as shown by Figures 8 and 9, being 35 and 40 per cent, respectively, when G/d is 8 and when the ratio rises to 20, while the outer bay is 41 and 39 per cent and the effective overhang 24 and 21 per cent under the same sets of conditions. It is rather astonishing to find that the outer bay should actually be shorter than the inner for best results if a thin section is used with a large gap and a small aspect ratio. The effect of the location of the inner strut in a truss of that form is, however, small; and a reduction of the length of inner bay from 40 to 32 per cent, the overhang being held constant and G/d being 20, increases the equivalent moment only 5 per cent from its minimum. A reduction

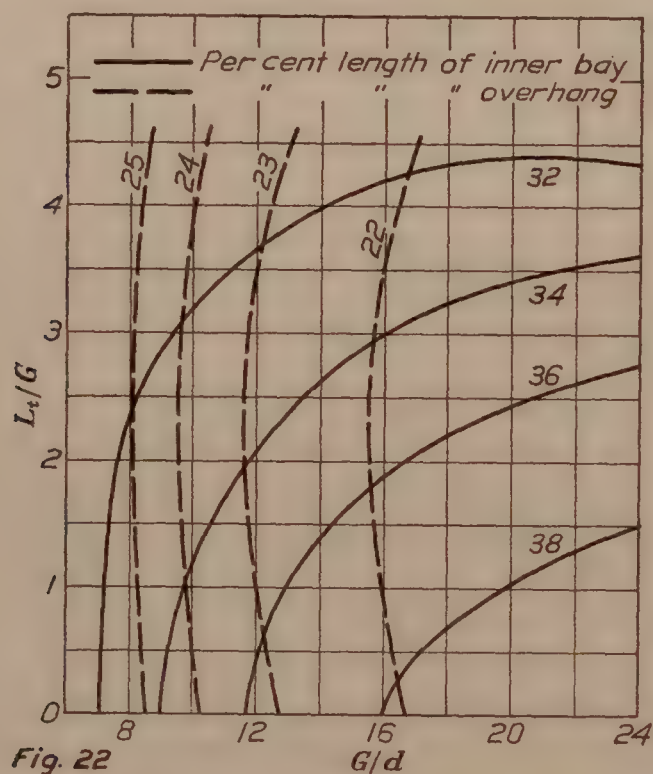


Fig. 22

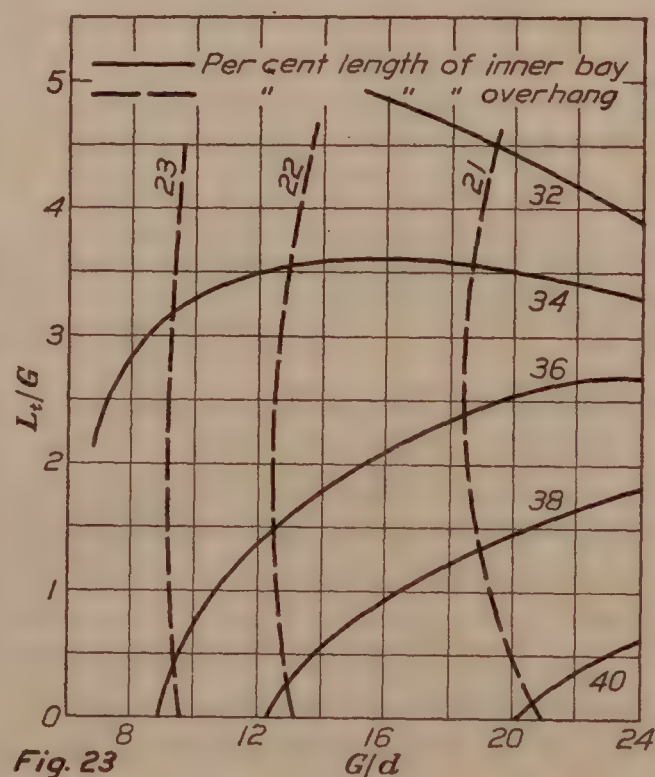


Fig. 23

of only 1 per cent, or an increase of one-half of 1 per cent, in overhang has as much effect. When G/d is 8, the triangular figures of equal moment are more nearly equilateral, and the locations of inner and outer struts are of more nearly equal importance.

Comparing Figures 9, 17, and 18, all of which relate to the same value of G/d and to materials capable of sustaining equal maximum stresses in bending and compression, it is apparent that the minimum equivalent moment is relatively little affected by column action, but that the ideal proportions for the truss are considerably modified. That is shown in the tabulation below, and the result of a comparison of Figures 12, 20, and 21, relating to spruce spars, would be much the same.

$\frac{L_t}{G}$	0	3	4.5
	(No column effect.)		
Minimum equivalent moment,	269	275	285
Inner bay,	40	35	32
Outer bay,	39	44	47
Overhang,	21	21	21

When G/d is only 8 the effect is still less. The column effect with L_t/G equal to 4.5, corresponding to an aspect ratio of nearly 10 if the gap is equal to the chord, increases the minimum

equivalent moment only from 429 to 436, while making it advisable to shorten the inner bay from 35 per cent to 33, leaving the overhang unchanged.

Curves of best length for inner bay and overhang have been plotted in Figure 22 for spruce and in Figure 23 for materials of equal compressive strength and modulus of rupture. The length of inner bay for minimum equivalent bending moment decreases steadily as L_t/G goes up in both cases, and in general it falls off with increasing thickness of airfoil section. With the aspect ratios and gap-chord ratios most commonly used at the present time, however, the thickness of the section has but little effect on the ideal location of the inner strut.

The best overhang, on the other hand, is independent of aspect ratio, being a function only of wing thickness.

If there is to be any departure from the ideal dimensions, or if there is any doubt about what they are, it is better to err in the direction of making the inner bay too short rather than too long, especially when the spars are long and slender. When L_t/G is 4.5 and G/d is 20, for example, the equivalent bending moment is increased 33 per cent by making the inner bay 3 per cent too long, only 12 per cent by making it too short by a like amount. When L_t/G is 3, the inner bay can be shortened 3 per cent at the expense of an increase of less than 4 per cent in the equivalent bending moment.

The proportions here suggested as best are not in exact agreement with those arrived at in previous investigations, but the difference is small. The United States Army Air Service, Engineering Division, for instance, recommends² in all cases an inner bay length of 32 per cent and an overhang of 19½ per cent of the effective spar length. If a single set of proportions were to be picked from this work, on the other hand, as the best average for all conditions, 34 per cent in the inner bay and 21 per cent overhang would appear to be the best choice in metal, 33 per cent and 22 per cent in spruce.

SPAR WEIGHT

If the equivalent bending moment in the spar is known, the sectional area needed in a given material can easily be calculated. The equivalent bending moment is given by the formula

$$M_e = K \left(\frac{L_t}{100} \right)^2 w$$

where K is the quantity plotted in Figures 8 and 9 and elsewhere, L_t the total effective spar length, as before, and w the load per unit length of spar.

On the assumption that $k = 0.36d$, $f = \frac{M_e}{0.26dA}$, d being the depth of the spar and A the sectional area. Then

$$A = \frac{Kw \left(\frac{L_t}{100} \right)^2}{0.26 df} = \frac{Kw \left(\frac{L_t}{100} \right)^2 G}{0.26 Gf}$$

Taking the density of spruce as 26 pounds per cubic foot and the allowable bending stress as 6,400 pounds per square inch, the weight of a spruce spar becomes

$$W_s = \frac{A L_t \times 26}{1,728} = \frac{Kw \left(\frac{L_t}{100} \right)^2 G}{17.28 \times 0.26 \times 6,400 G} = \frac{KW' \left(\frac{L'_t}{100} \right) G L_t}{11,060,000}$$

W' being the total load carried by the spar and L'_t the true length of the spar.

As a general rule, the front spar in a wing with two spars carries about two-thirds of the total load on the wing when the center of pressure is in its farthest forward position, while the rear spar carries all the load at the angle of attack arbitrarily chosen for a low-angle analysis.

² Structural Analysis and Design of Airplanes, Engineering Division, Air Service, U. S. Army, p. 49. The figures there are given in terms of the actual, not the effective, spar length, and they accordingly differ slightly in absolute value from those quoted in this text.

The ratio of total spar weight to total weight of the airplane, exclusive of the wing structure, is therefore approximately

$$\frac{W_s}{W_N} = \frac{\left(\frac{L'_t}{100}\right)}{11,060,000} \left\{ \left(K \frac{G}{d}\right)_R F_L + \frac{2}{3} \left(K \frac{G}{d}\right)_F F_H \right\} \frac{L_t}{G}$$

where W_N is the weight without the wings, W_s the weight of the spar as before, F_L and F_H are the load factors used in the low angle and high-angle analyses, respectively, and the subscripts R and F relate to the characteristics of the rear and front spars, respectively.

Since F_L is usually very nearly two-thirds of F_H , and since W_N is roughly 85 per cent of the total weight, it is possible to simplify further to the form

$$\frac{W_s}{W} = \frac{\left(\frac{L'_t}{100}\right) F_H \frac{L_t}{G}}{9,780,000} \times \frac{\left\{ \left(K \frac{G}{d}\right)_R + \left(K \frac{G}{d}\right)_F \right\}}{2}$$

Values of the product $K \times \frac{G}{d} \times \frac{L_t}{G}$ based on the assumption that the best strut location is used in every case and that the front and rear spars are of the same depth, have been calculated and are tabulated below. The variation of the product with $\frac{G}{d}$, $\frac{L_t}{G}$ being kept equal to unity, is plotted in Figure 24.

$\frac{G}{d}$	$\frac{L_t}{G}$	$K \frac{G}{d} \frac{L_t}{G}$	$K \frac{G}{d}$
8	1	4,300	4,300
8	4.5	19,500	4,340
20	1	6,240	6,240
20	3	18,800	6,280
20	4.5	28,900	6,420

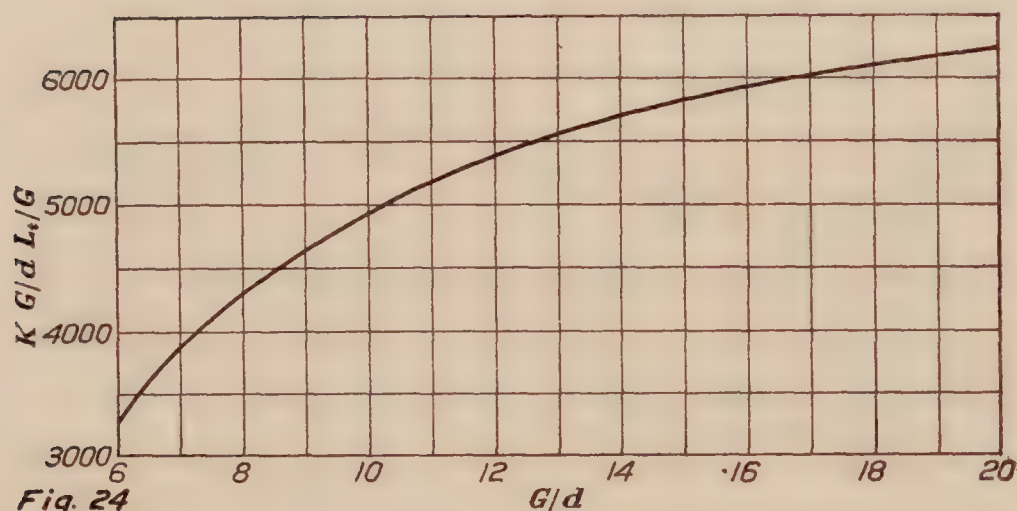


Fig. 24

It will be observed from these figures that both the gap and spar depth have important effect on the weight of the spars. If, for example, the depth of a spar is one-thirty-second of its total length and the gap is reduced from 20 to only 8 times the spar depth the spar weight will be increased by 74 per cent. If the gap be held constant at one-third of the spar length and the spar depth cut from one-

eighth to one-twentieth of the distance between the wings the increase of weight will be 45 per cent.

To illustrate the use of the weight formula, it may be applied to the case of a pursuit airplane with a span of 30 feet, a gap of 5 feet, a spar depth of 3.5 inches, and designed for a load factor of 10. L_t , the effective length of a single spar, is then approximately 13 feet allowing for tip correction and for the length of the center section, and L'_t 14 feet. $\frac{L_t}{G}$ is 2.6 and $\frac{G}{d}$ is 17.1, and the product of K , $\frac{G}{d}$, and $\frac{L_t}{G}$ is given by Figure 24 as 15,800. The ratio $\frac{W_s}{W}$ is then:

$$\frac{W_s}{W} = \frac{\frac{14 \times 12}{100} \times 10 \times 15,800}{9,780,000} = .0272$$

REPORT No. 215

AIR FORCES, MOMENTS AND DAMPING ON MODEL OF FLEET AIRSHIP SHENANDOAH

By A. F. ZAHM, R. H. SMITH, and F. A. LOUDEN

Aerodynamical Laboratory, Bureau of Construction and Repair, U. S. Navy

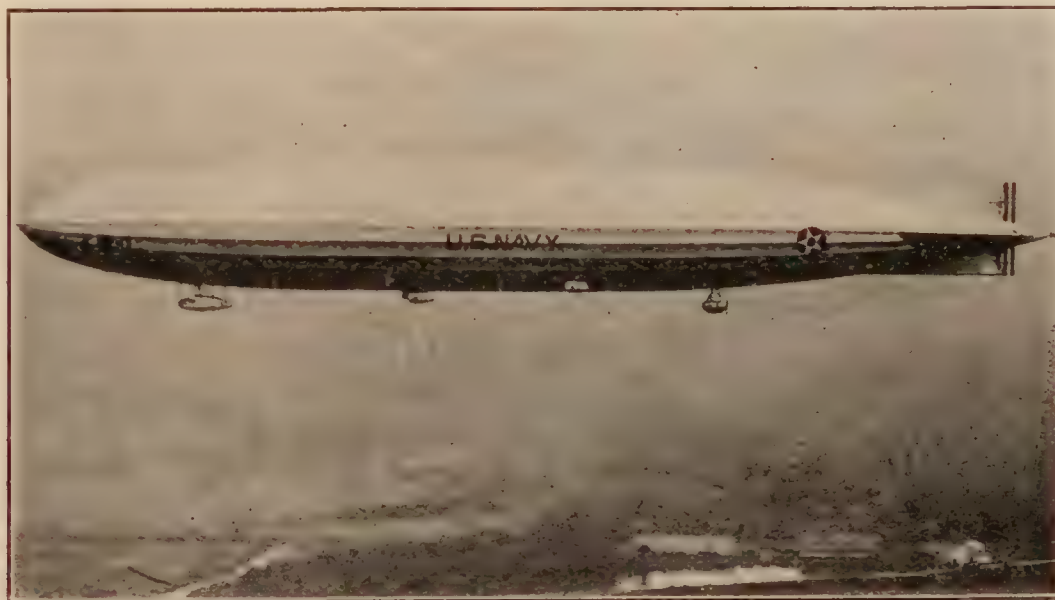
REPORT No. 215

AIR FORCES, MOMENTS, AND DAMPING ON MODEL OF FLEET AIRSHIP SHENANDOAH

By A. F. Zahm, R. H. Smith, and F. A. Loudon

INTRODUCTION

To furnish data for the design of the fleet airship *Shenandoah*, a model was made and tested in the 8 by 8 foot wind tunnel for wind forces, moments, and damping, under conditions described in this report. The results are given for air of standard density, $\rho = .00237$ slugs per cubic foot without VL/v correction, and with but a brief discussion of the aerodynamic design features of the airship. This account is a slightly revised form of Report No. 195, prepared for the Bureau of Aeronautics, July 22, 1922, and by it submitted for publication to the National Advisory Committee for Aeronautics.



Fleet airship Shenandoah of which two models were made and used in these tests

DESCRIPTION OF THE MODEL

The model during its first tests was 67.75 inches long, and was then shortened 3.28 inches by removal of a cylindric midship section to receive further tests. The external appearance of the shorter hull is given in Figure 1; the dimensions of both are given in Figure 2. During the test the long hull was first bare, then fitted successively with the controls 1, 2, 3, 4, 5, shown in Figures 4, 5, 6; the short hull was first bare, then fitted successively with controls 5, 6A, 6B, 6C, 6D; the latter shown in Figure 7. The bodies were of dry pine and varnished; the movable controls all were of brass; the thin fins Nos. 1, 3, were of brass; the thick ones of wood. The cross sections of the fins at their thickest point is given in Figure 3, and the areas of the various fins and controls are given in Table I.

The following classification of the controls has been furnished by the Bureau of Aeronautics:

- Type 1.—Original L-49 controls, flat surfaces.
- Type 2.—Similar to Type 1, but surface double-cambered.
- Type 3.—Flat surfaces, cantilever balance, area approximately 20 per cent greater than Type 1.
- Type 4.—Similar to Type 3, but surfaces double-cambered.
- Type 5.—Internally braced fins, "Handley Page" balance. Area approximately the same as Type 3.
- Type 6.—Movable surfaces A, B, C, D with common fins slightly larger than fins 5.

Dimensions	Short size		Long size	
	Model	Full size	Model	Full size
Length	64.468 inches	196.5 meters=644.7 feet	67.748 inches	206.5 meters=677.5 feet.
Surface of hull	1,253.205 square inches.	11,643 square meters=125,321 square feet.	1,334.136 square inches.	12,395 square meters=133,414 square feet.
Air volume of hull	2,131.598 cubic inches.	60,363 cubic meters=2,131,598 cubic feet.	2,289.736 cubic inches.	64,843 cubic meters=2,289,736 cubic feet.
Maximum sectional area.	48.220 square inches.	448 square meters=4,822 square feet.	48.220 square inches.	448 square meters=4,822 square feet.
Mass of hull	0.00292 slugs	5,051.89 slugs	0.00314 slugs	5,426.67 slugs.

Hinge of elevator and rudder, long model, is at station 41.
Hinge of elevator and rudder, short model, is at station 39.

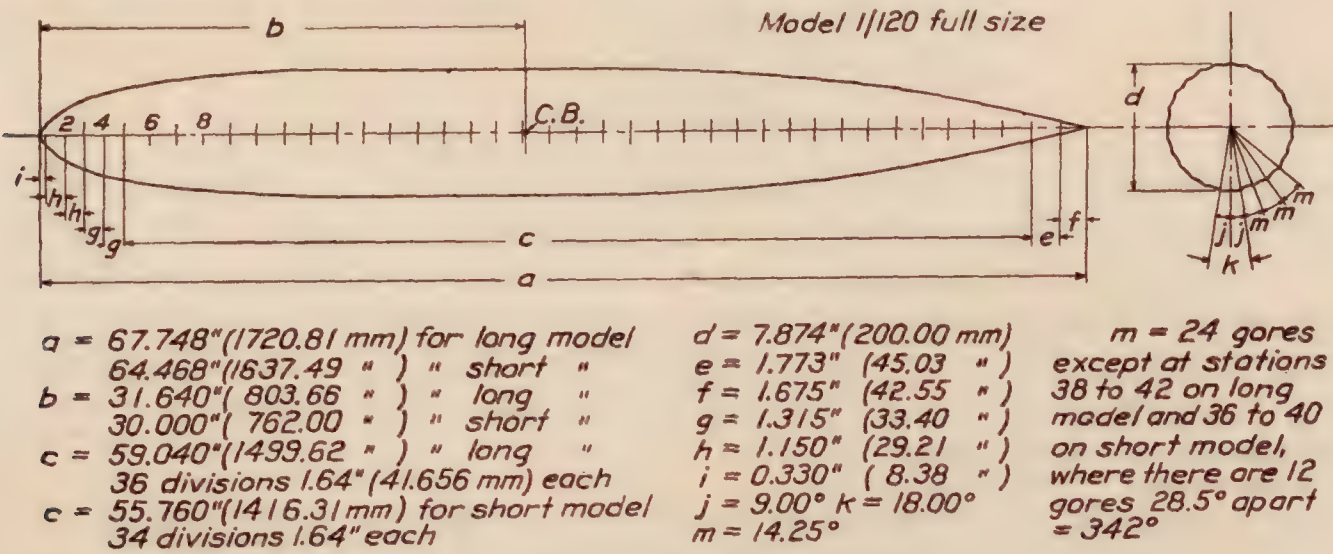


FIG. 2.—Models used in tests for Shenandoah

SHORT MODEL

	Station No.																
	1	2	3	4	5	6	7	8	9	10	11	12	13	14	15-21	22	23
Diameter of circumscribing circle specified	1.454	3.248	4.248	5.062	5.686	6.280	6.726	7.070	7.332	7.526	7.668	7.768	7.828	7.858	7.874	7.854	7.818
Width of all gores except keel specified	.180	.403	.527	.628	.705	.779	.834	.877	.909	.933	.951	.964	.971	.975	.977	.974	.970
Width of keel specified	.229	.510	.666	.793	.891	.984	1.054	1.108	1.149	1.179	1.201	1.217	1.226	1.231	1.233	1.230	1.225

	Station No.																
	24	25	26	27	28	29	30	31	32	33	34	35	36	37	38	39	40
Diameter of circumscribing circle specified	7.762	7.660	7.516	7.332	7.110	6.848	6.542	6.190	5.800	5.368	4.892	4.376	3.810	3.208	2.536	1.802	0.988
Width of all gores except keel specified	.963	.950	.932	.909	.882	.849	.811	.768	.719	.666	.607	.539	.438	.379	.324	.243	.243
Width of keel specified	1.216	1.200	1.177	1.149	1.114	1.072	1.025	.970	.909	.841	.767	.686	.597	.504	.398	.283	.000

LONG MODEL

	Station No.																
	1	2	3	4	5	6	7	8	9	10	11	12	13	14	15-23	24	25
Diameter of circumscribing circle specified	1.454	3.248	4.248	5.062	5.686	6.280	6.726	7.070	7.332	7.526	7.668	7.768	7.828	7.858	7.874	7.854	7.818
Width of all gores except keel specified	.180	.403	.527	.628	.705	.779	.834	.877	.909	.933	.951	.964	.971	.975	.977	.974	.970
Width of keel specified	.229	.510	.666	.793	.891	.984	1.054	1.108	1.149	1.179	1.201	1.217	1.226	1.231	1.233	1.230	1.225

	Station No.																
	26	27	28	29	30	31	32	33	34	35	36	37	38	39	40	41	42
Diameter of circumscribing circle specified	7.762	7.660	7.516	7.332	7.110	6.848	6.542	6.190	5.800	5.368	4.892	4.376	3.810	3.208	2.536	1.802	0.988
Width of all gores except keel specified	.963	.950	.932	.909	.882	.849	.811	.768	.719	.666	.607	.539	.438	.379	.324	.243	.243
Width of keel specified	1.216	1.200	1.177	1.149	1.114	1.072	1.025	.970	.909	.841	.767	.686	.597	.504	.398	.283	.000

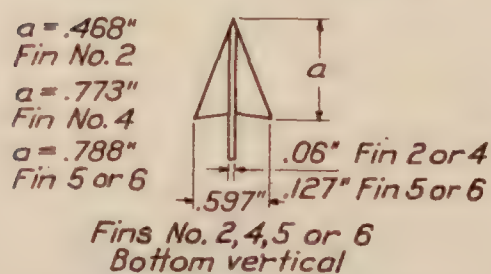
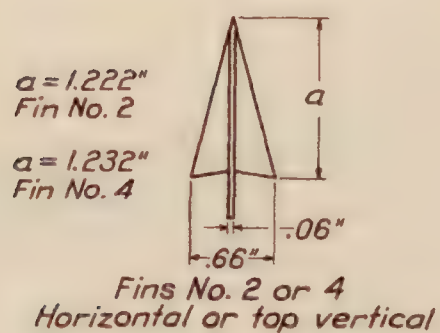
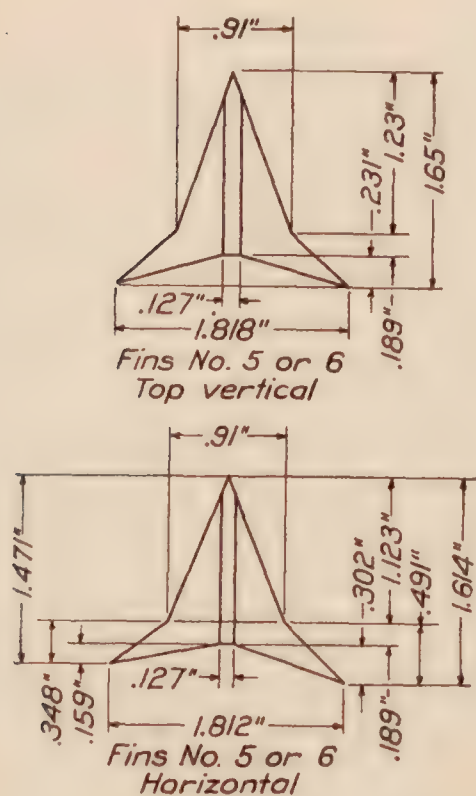


FIG. 3.—Cross section of fins at maximum thickness

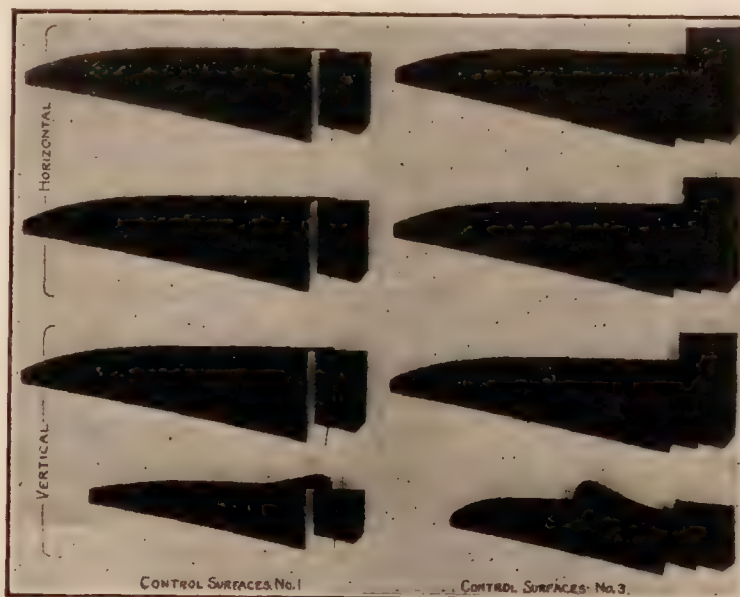


FIG. 4

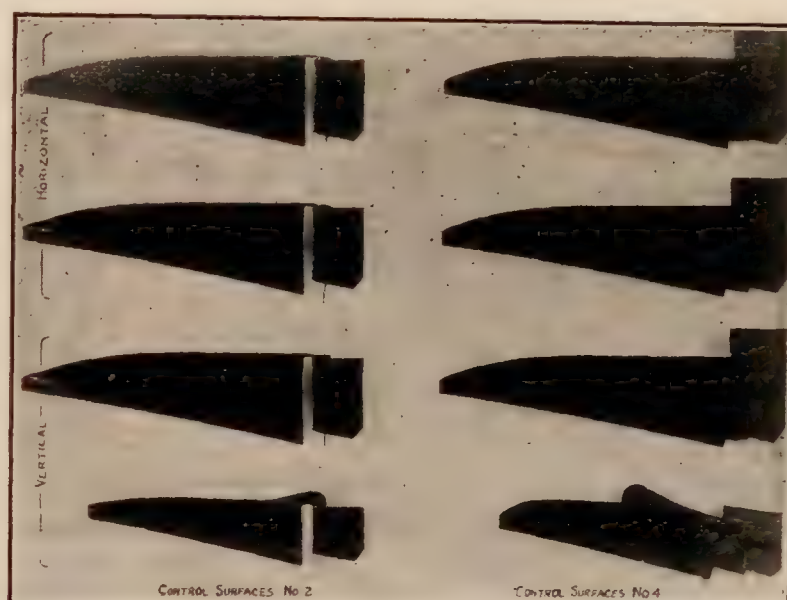


FIG. 5

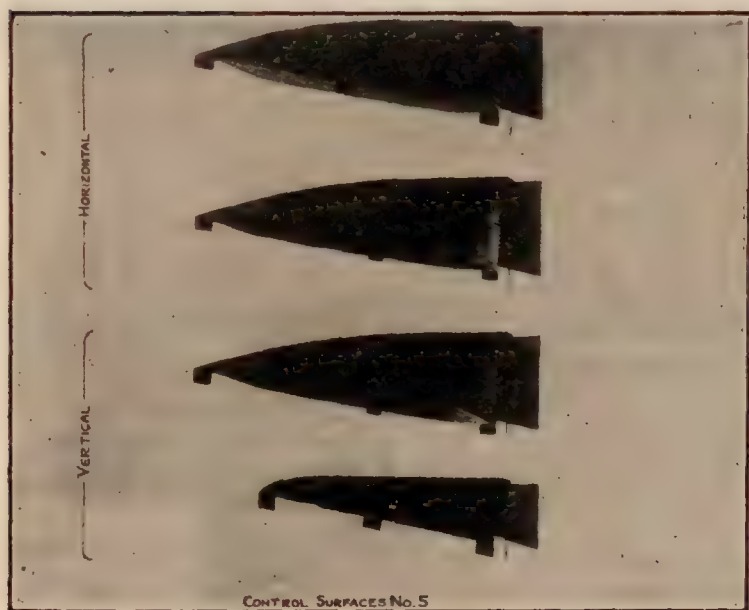


FIG. 6

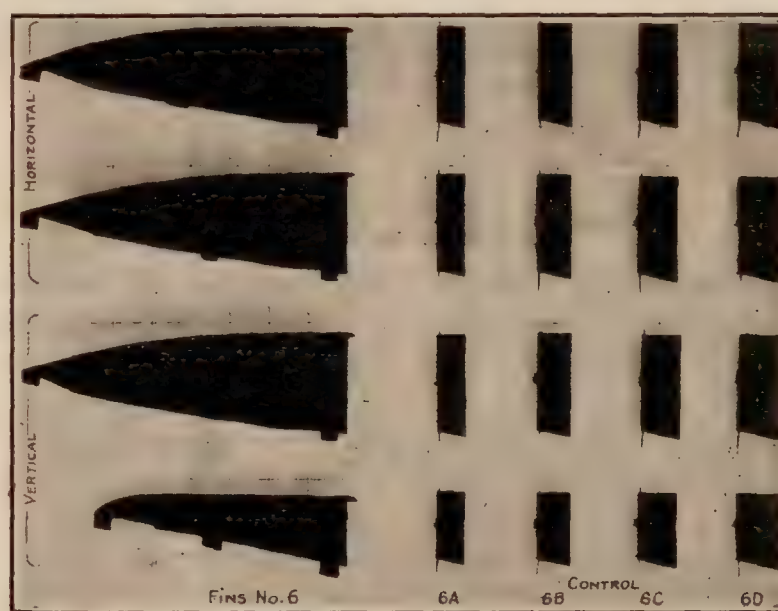


FIG. 7

METHODS OF TEST

During the tests for forces and moments the models were supported from the flange at the bottom of the wind balance shank, as shown in Figure 1, by means of a horizontal frame, from which fine wires ran to suspension points on the hull before and after its center. The mechanism and operation of this balance are described in Report No. 146 of the National Advisory Committee for Aeronautics. The head-on net drag so obtained was checked by measurements on the bifilar balance. In the part of the tunnel under the first named balance the wind has no static pressure gradient, hence correction for horizontal buoyancy for that region was not necessary, as it was for the space under the bifilar balance.

During some of the tests five components of the air force,¹ i. e., the lift, drag, cross-wind force, pitching and yawing moments, were measured simultaneously.

The damping coefficients were determined with the aerodynamic oscillator shown in Figure 8. The oscillator axle had a counterweight at one end, and at the other ran squarely into the hull at its buoyancy center.

The wind speeds and model settings for the various tests are sufficiently disclosed in the tables and diagrams accompanying this text. The oscillation values in the tables are faired from three or four sets of observations made for each condition of model and wind.



FIG. 1.—Model of fleet airship No. 1 suspended on wind balance

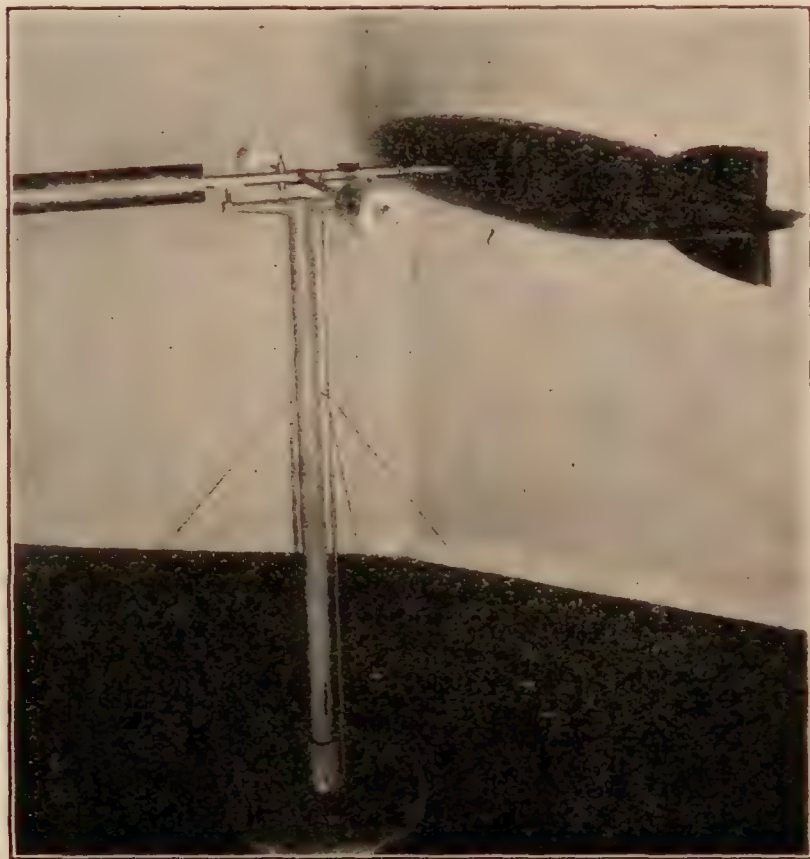


FIG. 8

DRAG OF BARE HULLS

Tables II and III give the head-on drag and the shape coefficient for the bare hulls, long and short, as found for speeds of 20, 30, 40, 50, and 60 miles an hour; also the head-on drag and shape coefficient for 40 miles an hour, with control surfaces 1, 2, 3, 4, and 5. Figs. 9 and 10 show familiar graphs of the head-on drag and shape coefficients for the two bare hulls, at speeds of 20 to 60 miles an hour. At speeds of 40 to 60 miles the long hull has 2 to 3 per cent more drag than the short one, but has a perceptibly smaller shape coefficient, due to its greater volume.

¹ "Dyne" may be used as the exact term for the entire urge of the air on the model. The dyne can have three components of force, and three of moment; for example X, Y, Z, L, M, N. See Routh, *Analytical Statics*, Vol. I

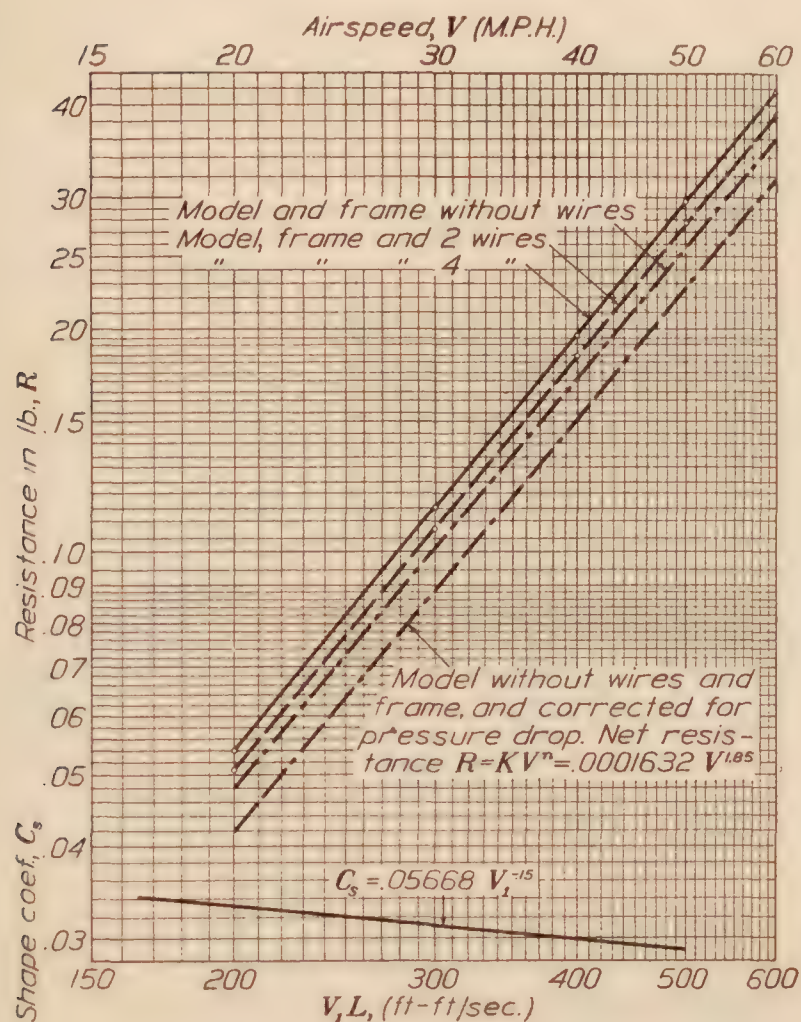


FIG. 9.—Resistance and shape coefficient for long model, bare hull, at 0° pitch and 0° yaw

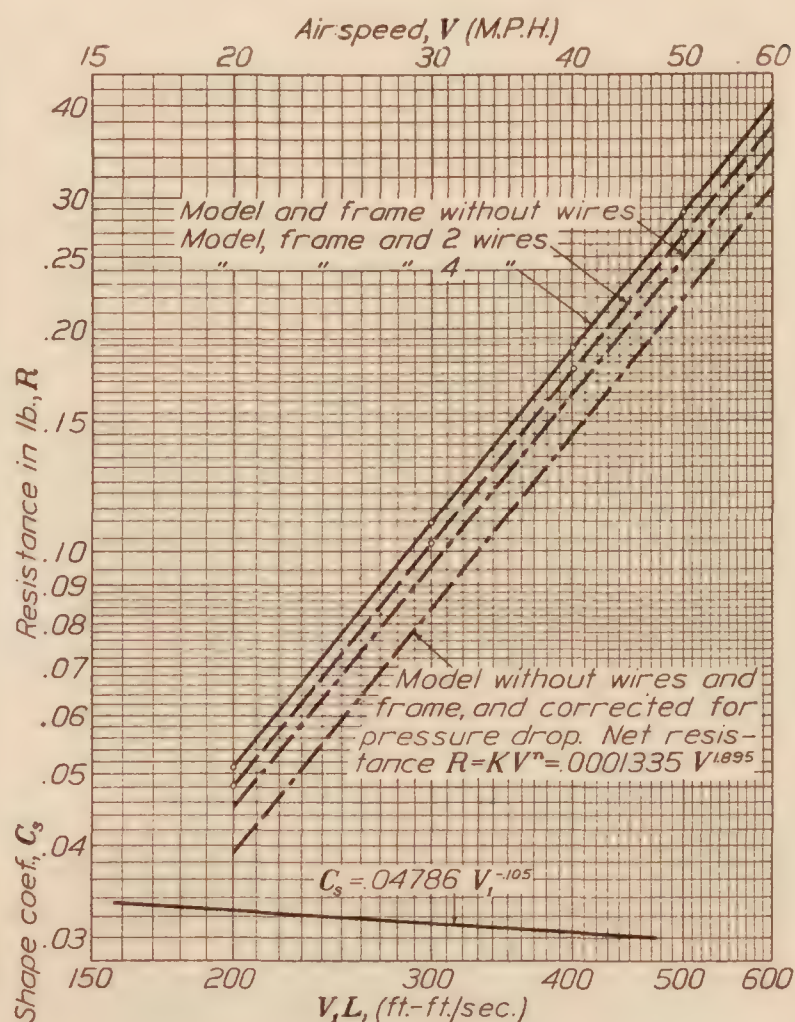


FIG. 10.—Resistance and shape coefficient for short model, bare hull, at 0° pitch and 0° yaw

The disk ratio and shape coefficient, as found at 40 miles an hour, are given for these two bare hulls and some earlier ones in the following table. The drag of a hull's major section, normally exposed as a thin disk, is taken as $0.00283 SV^2$ pounds at V miles an hour, and the ratio of this force to the actual head-on drag of the hull is called the "disk ratio."

Comparison of various bare hulls

Model	Disk ratio	Shape coefficient C_s $= \frac{2R}{\rho(\text{Vol.})^{2/3} V_1^2}$
Short Shenanhoah.....	10.51	0.03122
Long Shenandoah.....	10.16	.03077
Goodrich B.....	15.4	.03090
E. P.....	17.2	.02932
C class.....	16.9	.02872

FORCES FOR VARIOUS ADJUSTMENTS

Tables IV to XV, inclusive, give, for numerous settings, the lift, drag, and side drag on the models, at 40 miles an hour, measured parallel to the axes of the tunnel and balance. Tables XVI to XXIII give the X , Y , Z forces thence derived by simple analysis. Figures 11 to 18 contain plots of the Y , Z forces against angles of pitch and yaw. The X force is too nearly constant from model to model to justify plotting. Figures 14 and 18 show that the forces on the long hull can be closely estimated from the measured forces found with the short hull, thus obviating the need for repeating with the long hull many of the tests first made on the short one. In this estimate it is assumed that any air force increment due to adding the midship segment is the same when the hulls are bare as when furnished with either type of control.

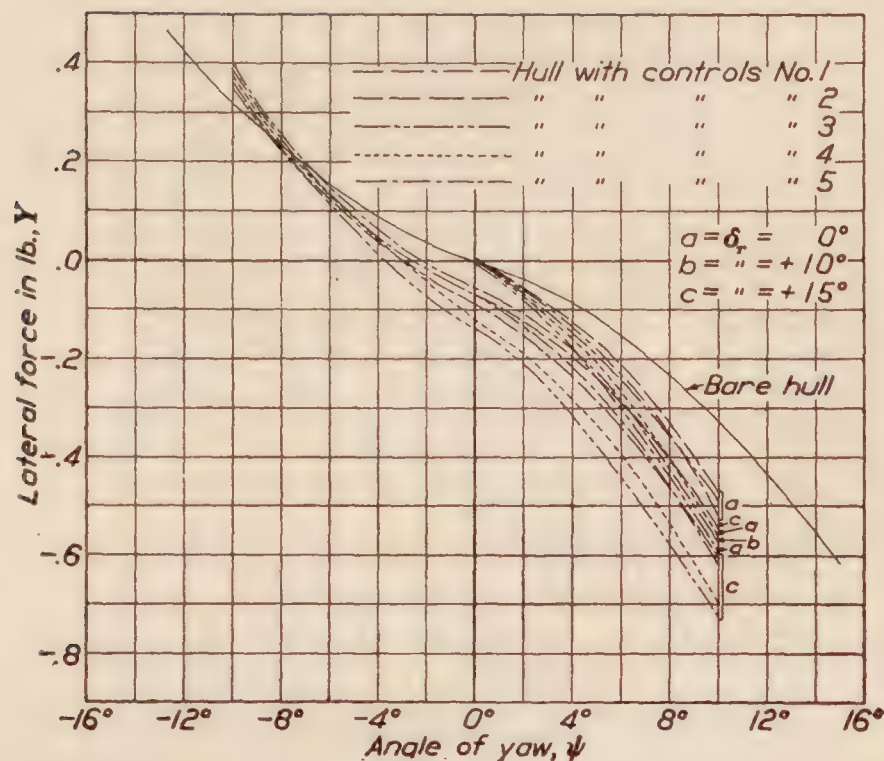


FIG. 11.—Y force for long model with controls Nos. 1 to 5. Model at 0° pitch and elevators neutral. Air speed 40 M. P. H.

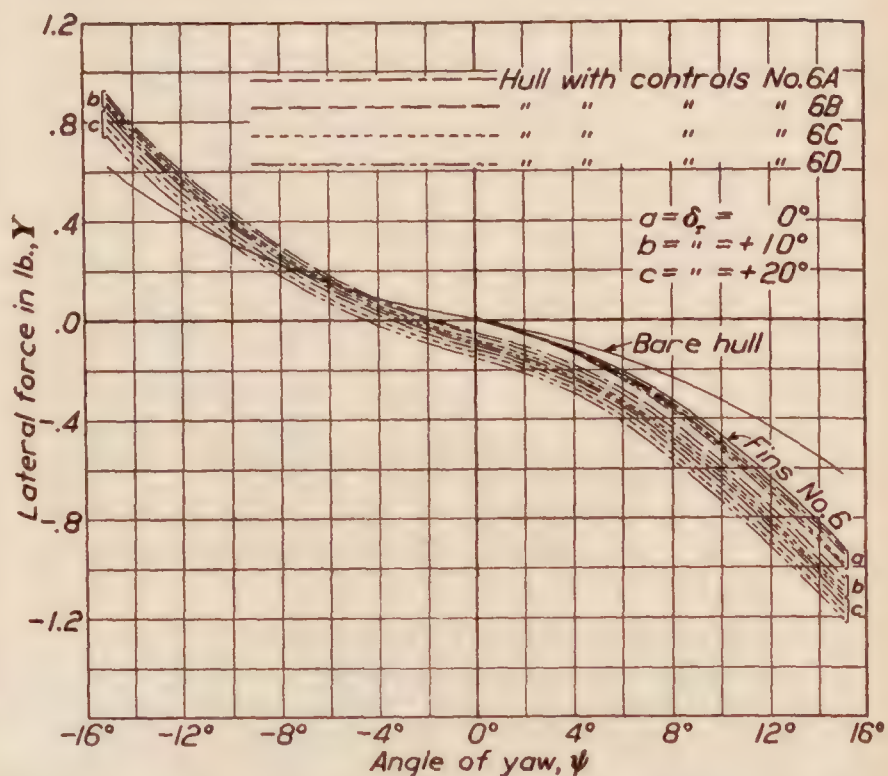


FIG. 12.—Y force for long model with controls No. 6. Model at 0° pitch and elevators neutral. Air speed 40 M. P. H.

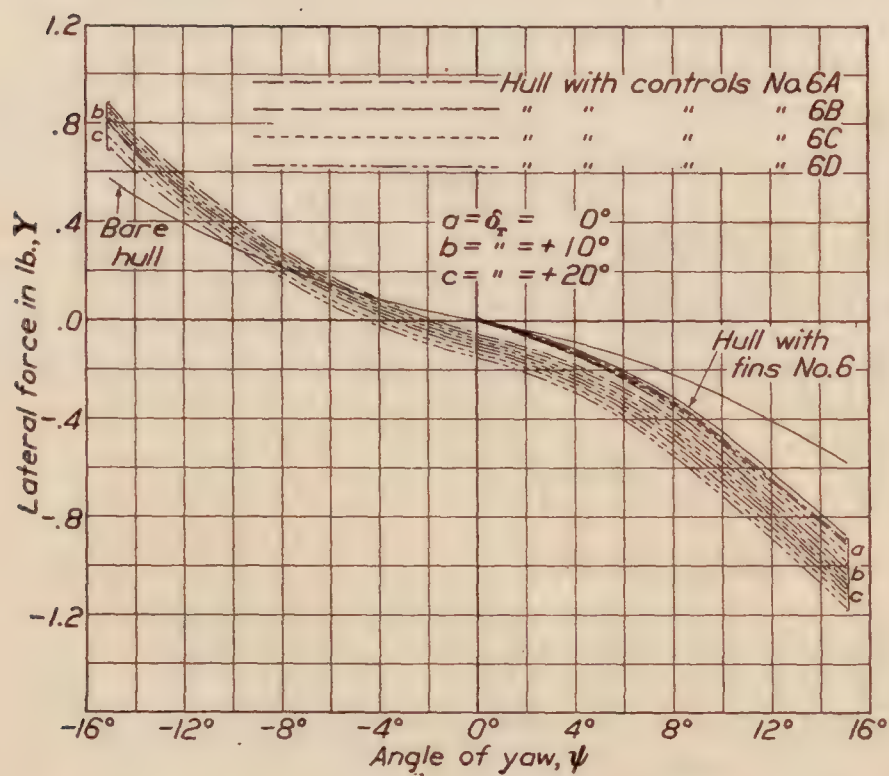


FIG. 13.—Y force for short model with controls No. 6. Model at 0° pitch and elevators neutral. Air speed 40 M. P. H.

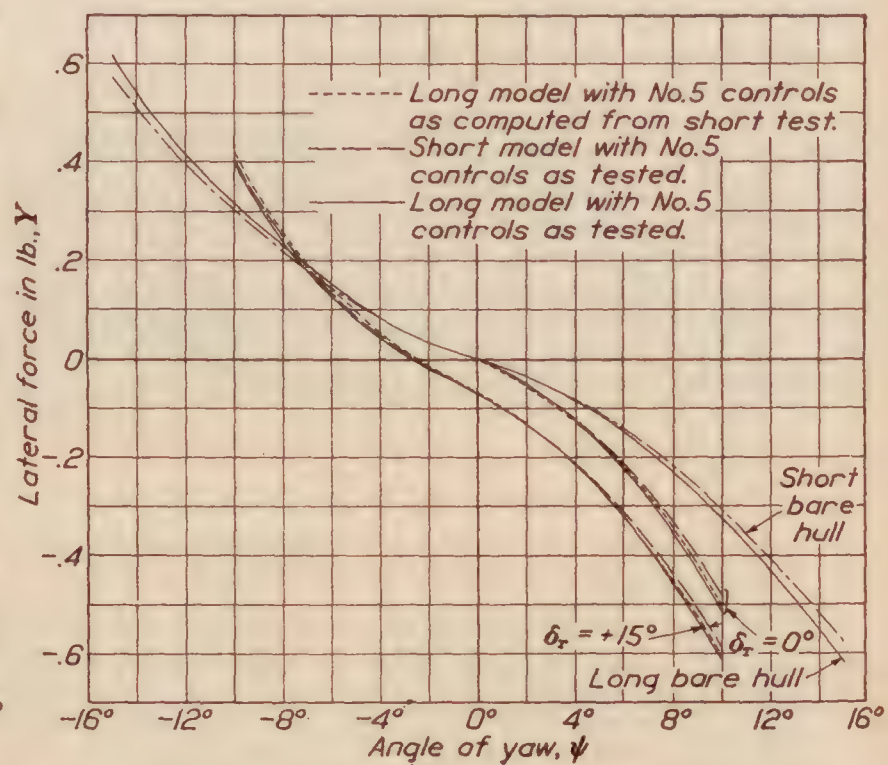


FIG. 14.—Comparison of tested and computed Y force. Model at 0° pitch and elevators neutral. Air speed 40 M. P. H.

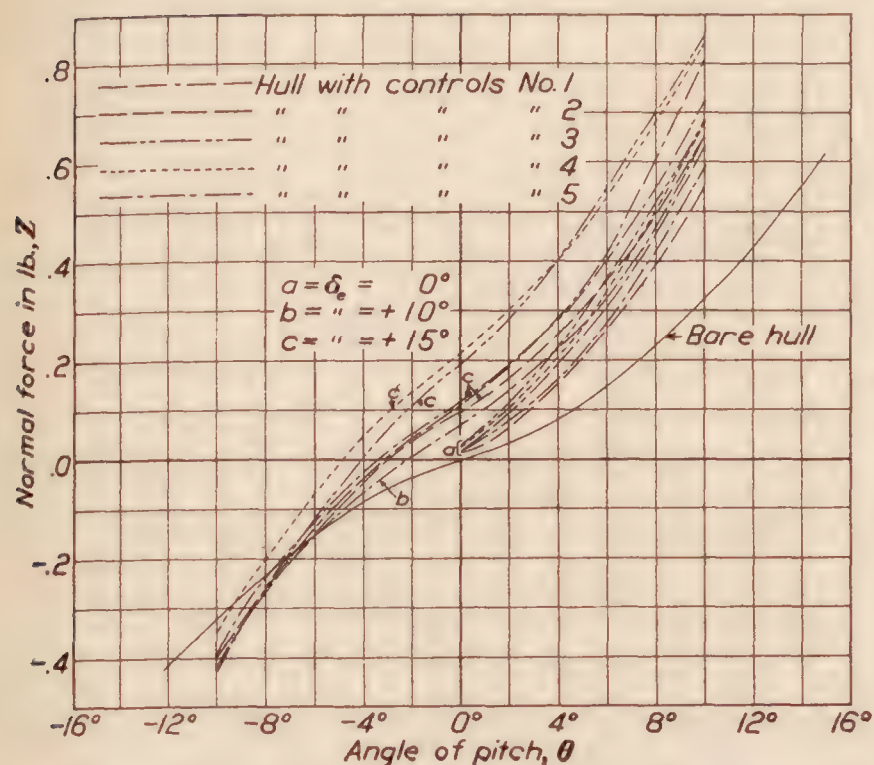


FIG. 15.—Z force for long model with controls No. 1 to 5. Model at 0° yaw and rudders neutral. Air speed 40 M. P. H.

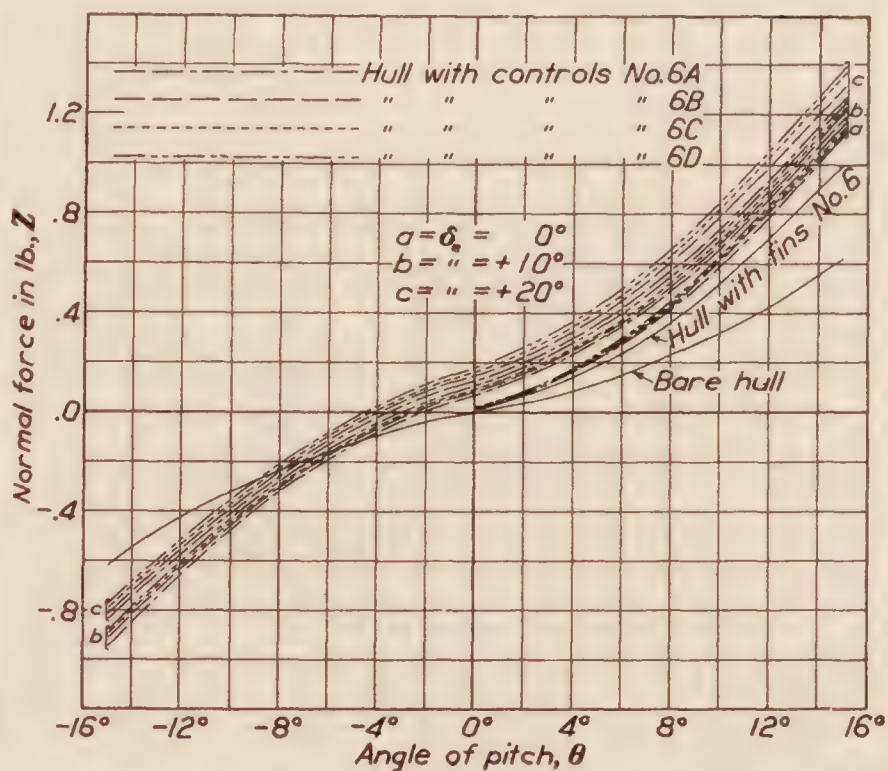


FIG. 16.—Z force for long model with controls No. 6. Model at 0° yaw and rudders neutral. Air speed 40 M. P. H.

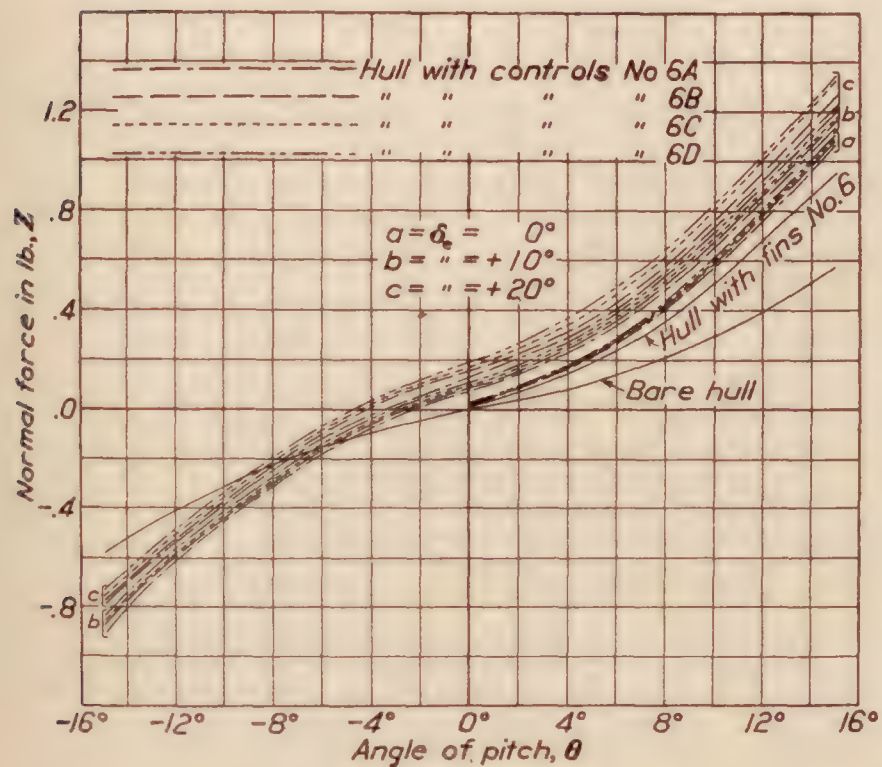


FIG. 17.—Z force for short model with controls No. 6. Model at 0° yaw and rudders neutral. Air speed 40 M. P. H.

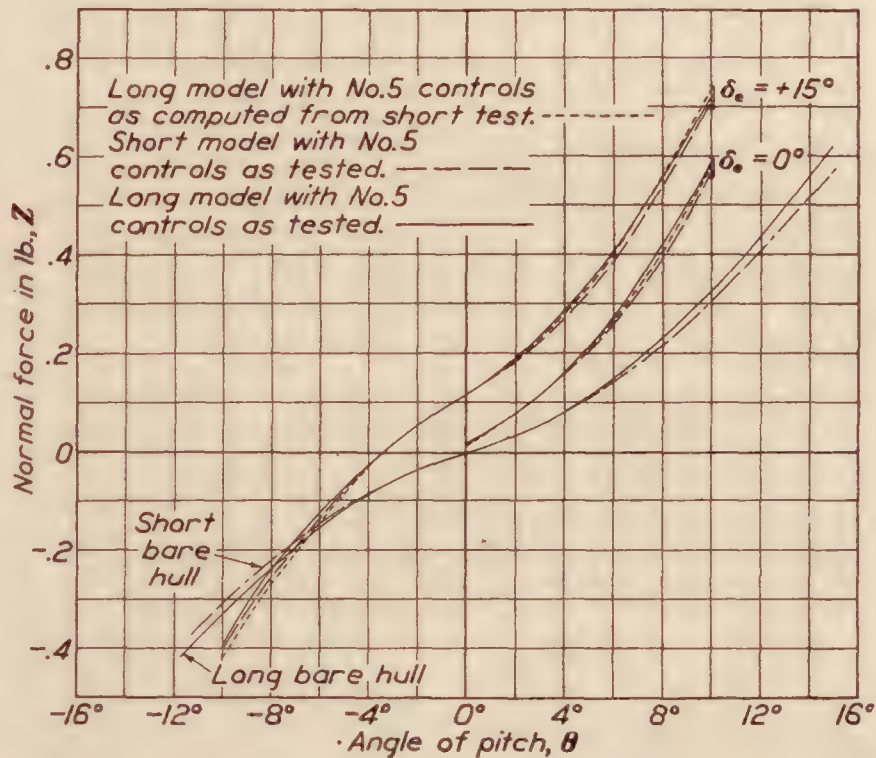


FIG. 18.—Comparison of tested and computed Z force. Model at 0° yaw and rudders neutral. Air speed 40 M. P. H.

MOMENTS FOR VARIOUS ADJUSTMENTS

Tables XXIV to XXX, inclusive, give the pitching and yawing moments, at 40 miles an hour, for the manifold conditions therein specified. Figures 19 to 25 contain plots of these moments against angles of pitch and yaw. Figures 22 and 26 show that the moments on the long model can be accurately estimated from measurements with the short one.

In this estimate the distance of the control force from the center of buoyancy of the short hull is computed as $\Delta M / \Delta Z$, where ΔM , ΔZ are the increments of moment and force due to adding either type of control. This distance plus half the length of the midship segment is the arm of the control surface of the long hull. The product of this arm by the force on the control, plus the moment on the long bare hull, gives the total moment for the hull and control.

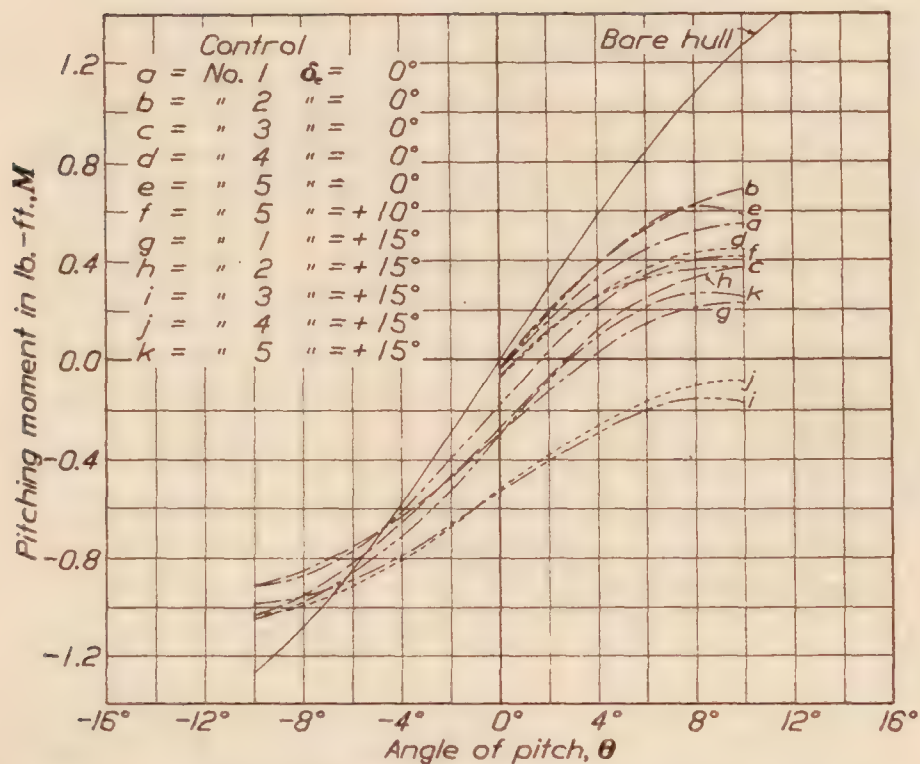


FIG. 19.—Pitching moment for long model about C. B. Bare hull and hull with controls, Nos. 1 to 5. Model at 0° yaw and rudders neutral. Air speed 40 M. P. H.

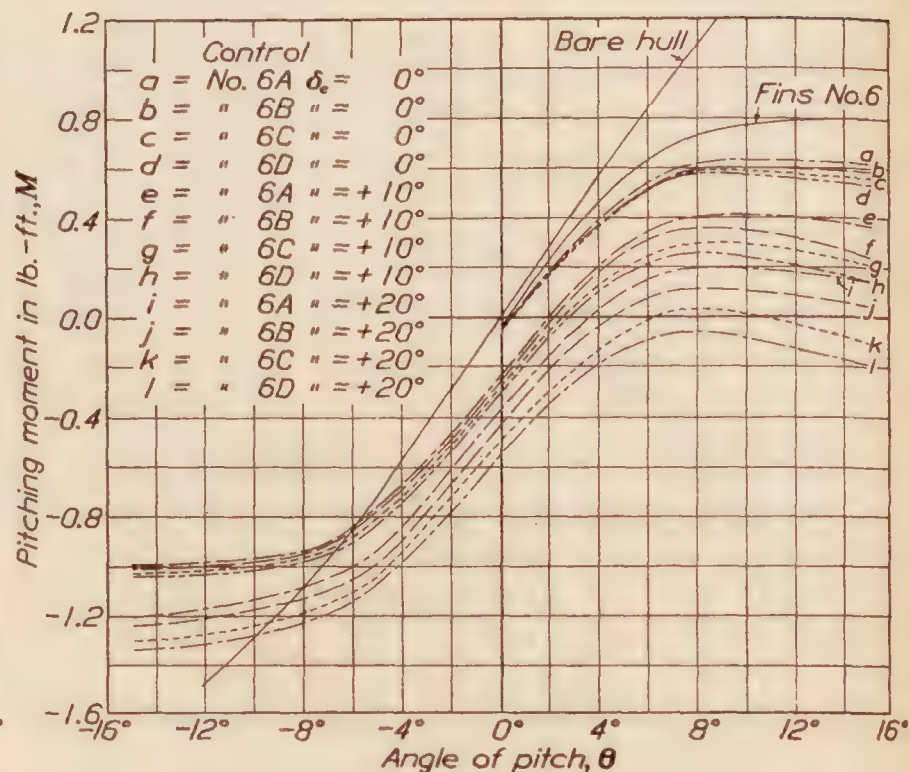


FIG. 20.—Pitching moment for long model about C. B. Bare hull and hull with controls, No. 6. Model at 0° yaw and rudders neutral. Air speed 40 M. P. H.

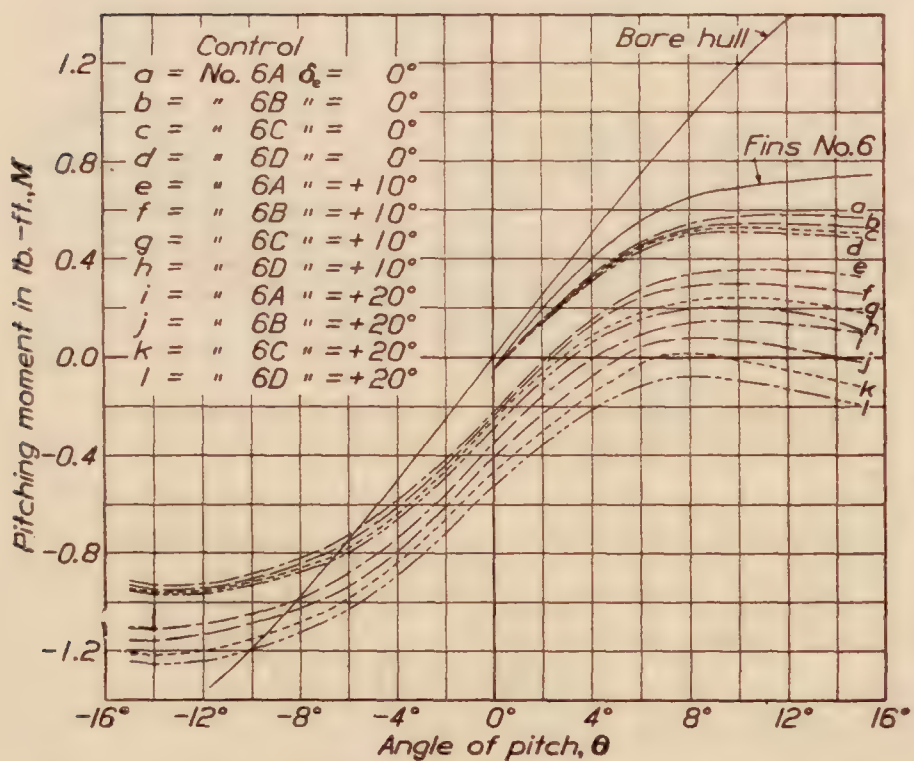


FIG. 21.—Pitching moment for short model about C. B. Bare hull and hull with controls No. 6. Model at 0° yaw and rudders neutral. Air speed 40 M. P. H.

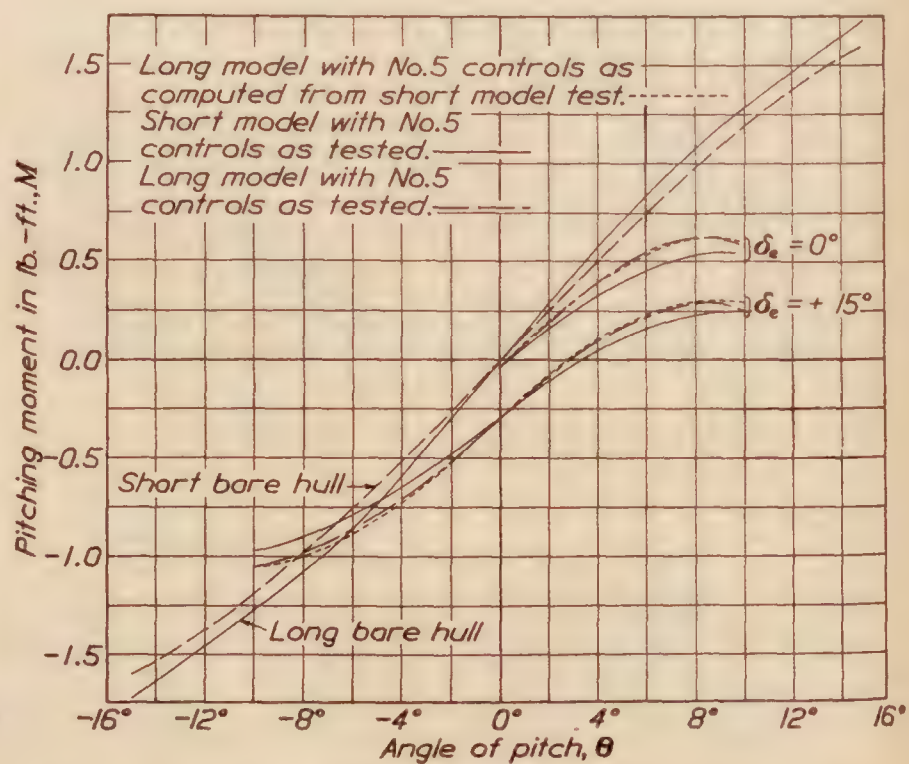


FIG. 22.—Comparison of tested and computed pitching moments. Model at 0° yaw and rudders neutral. Air speed 40 M. P. H. Moment axis at C. B.

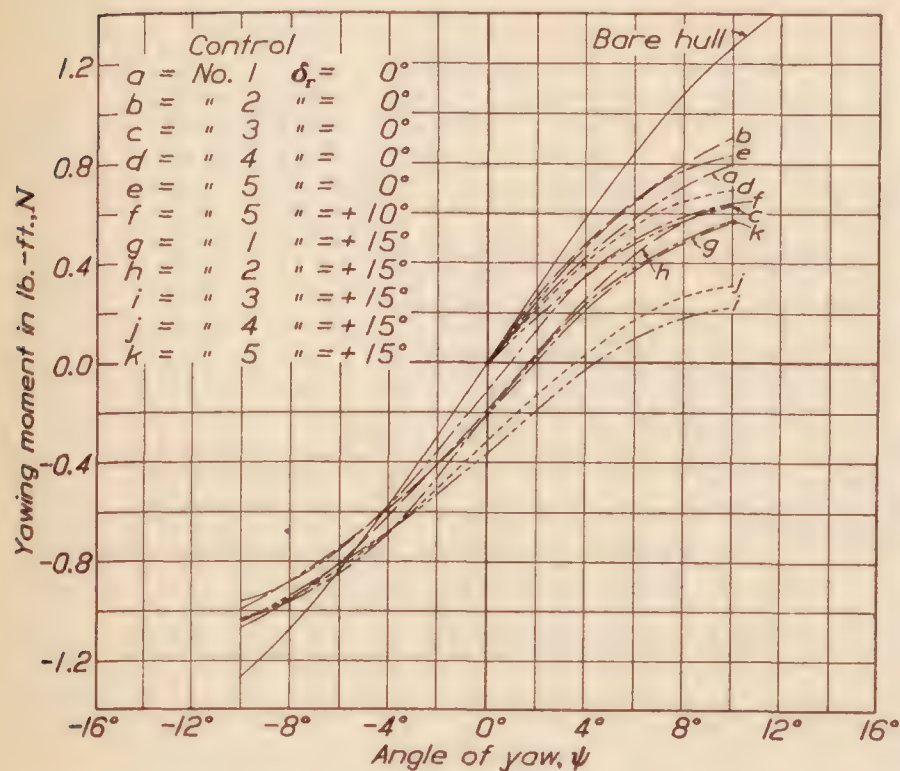


FIG. 23.—Yawing moment for long model about C. B. Bare hull and hull with controls, Nos. 1 to 5. Model at 0° pitch and elevators neutral. Air speed 40 M. P. H.

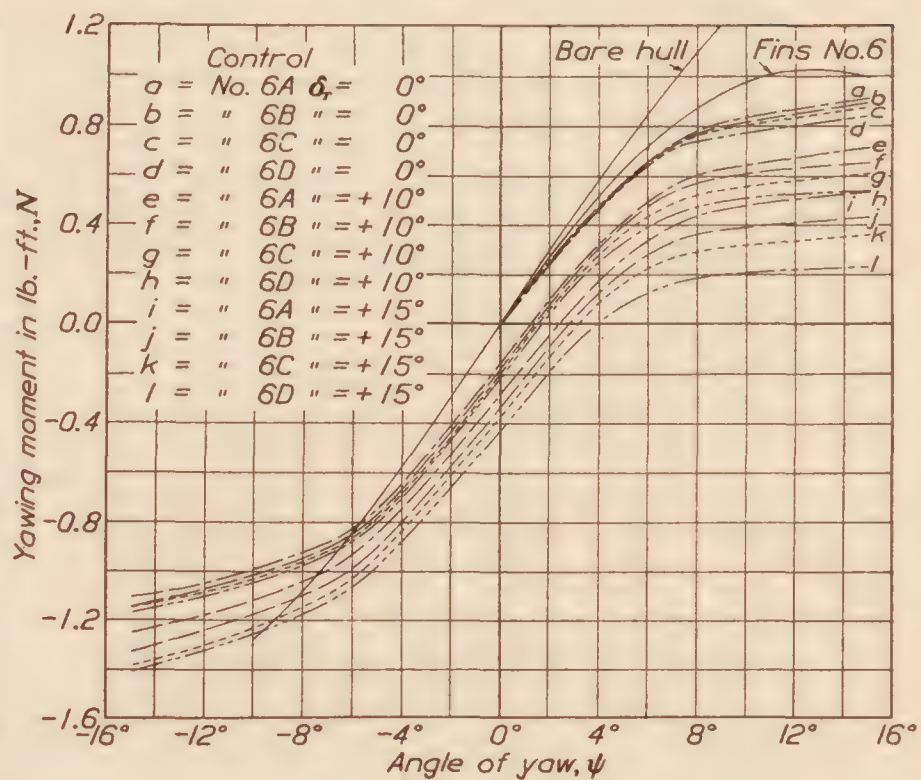


FIG. 24.—Yawing moment for long model about C. B. Bare hull and hull with controls No. 6. Model at 0° pitch and elevators neutral. Air speed 40 M. P. H.

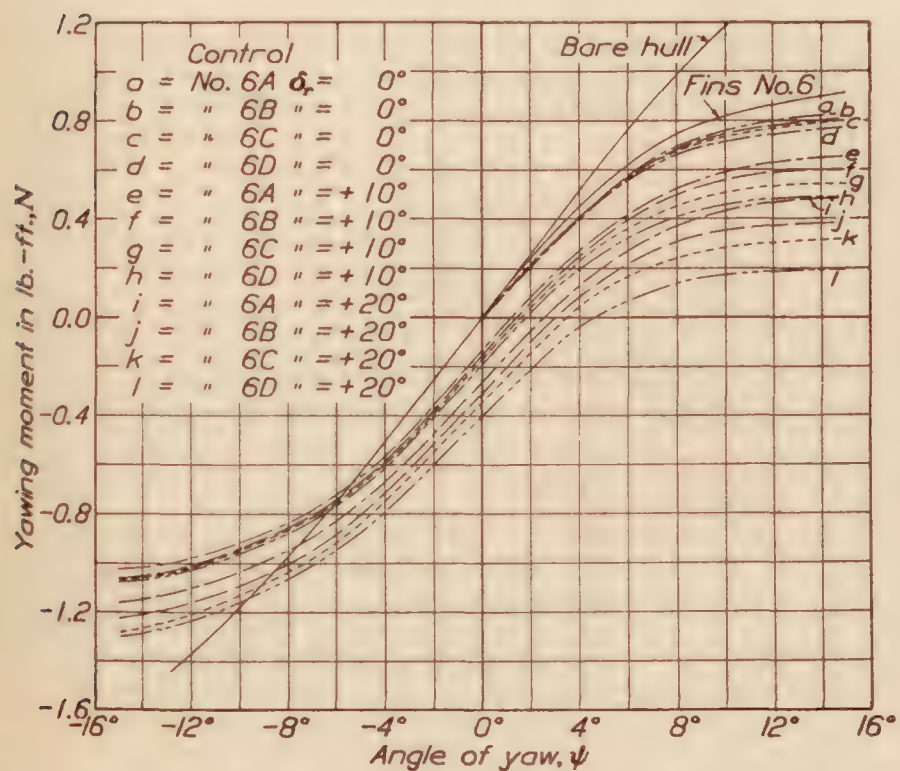


FIG. 25.—Yawing moment for short model about C. B. Bare hull and hull with controls No. 6. Model at 0° pitch and elevators neutral. Air speed 40 M. P. H.

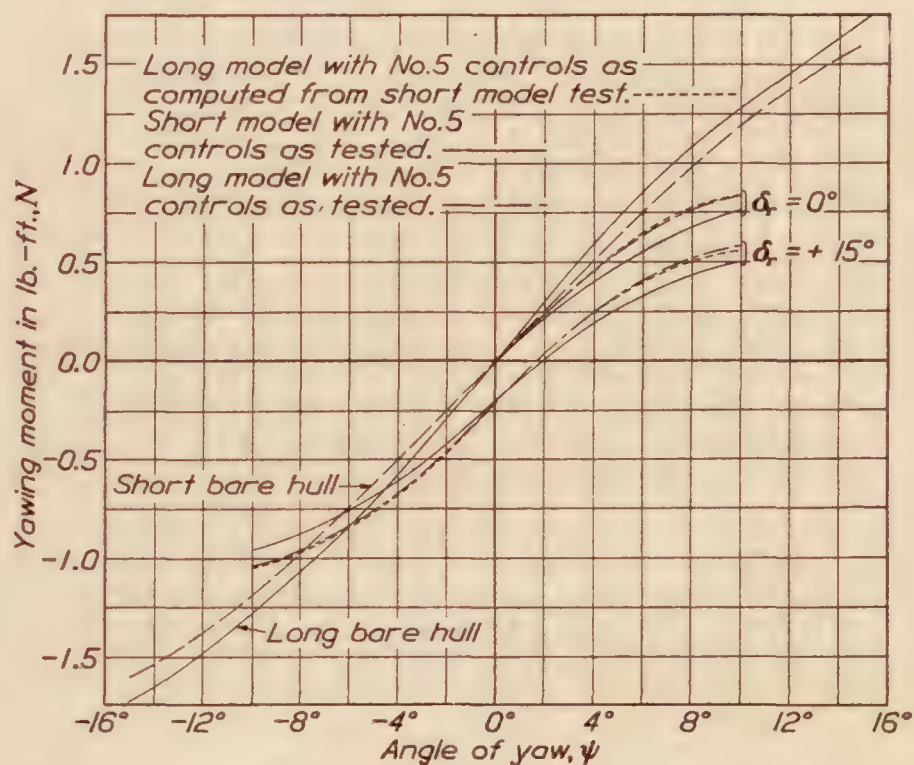


FIG. 26.—Comparison of tested and computed moments. Model at 0° pitch and elevators neutral. Air speed 40 M. P. H. Moment axis at C. B.

FORCES AND MOMENTS AT LARGE ANGLES

Table XXXI gives, for the long hull with No. 5 controls all neutral, the drag, cross-wind force, and yawing moment in a 30-mile wind, on the model set at 0° pitch, and at yaw angles of 0° to 90°. The values of X , Y , N , derived from these data, are plotted against ψ in Figure 27. The vector diagram for this test is given in Figure 28. It shows that when the model is pivoted about the Z axis, as a weather vane, it is unstable in yaw at all angles below 70°. It is noteworthy that X becomes a propulsive force at large angles of attack, as has been observed in similar tests.

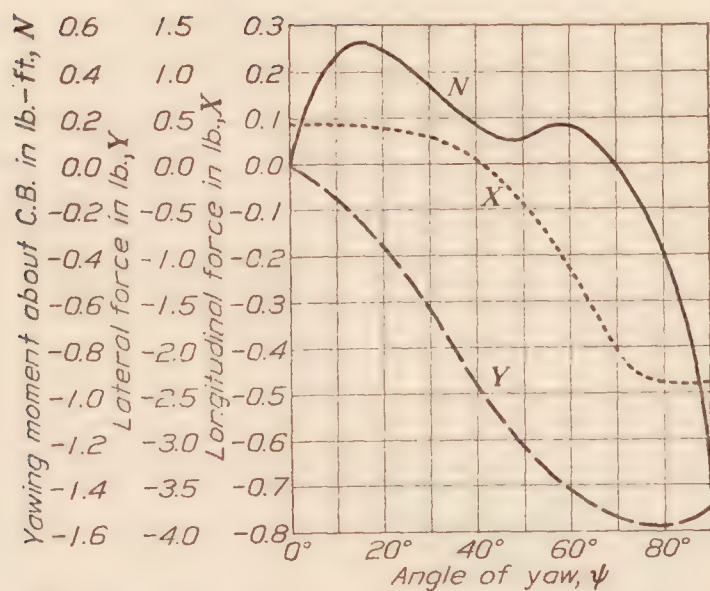


FIG. 27.—X and Y forces and yawing moments N for long model with No. 5 control surfaces. Model at 0° pitch. Elevators and rudders neutral. Air speed 30 M. P. H.

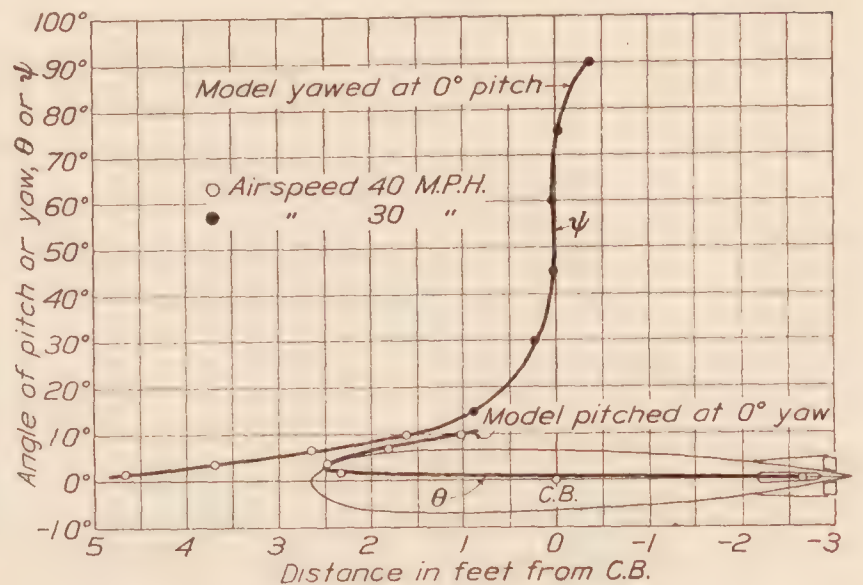


FIG. 29.—Center of pressure travel of long hull with No. 5 control surfaces. Elevators and rudders neutral. Air speed 30 and 40 M. P. H.

CENTER OF PRESSURE

Figure 29 delineates the center of pressure in yaw for the data in Tables XXXI, XX, XXIX, also the center of pressure in pitch for the data in Tables XXII, XXV. As the yaw angle falls below 10° , the center of pressure runs rapidly forward, and travels even beyond the nose of the hull. The same effect is not observed in pitch because the fins are adjusted to give a negative pitching moment at zero pitch.

The forward travel of the center of pressure at small angles of yaw is further illustrated by Figure 30, giving the line of resultant air force on the long hull with Nos. 3 and 4 controls.

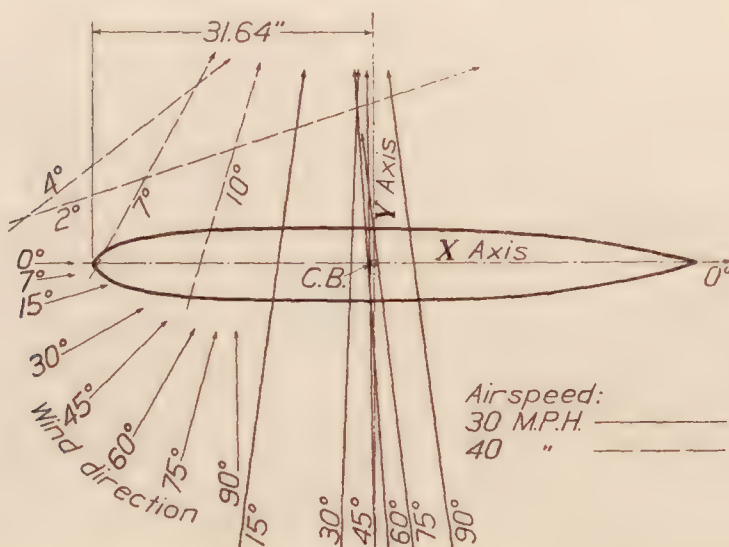


FIG. 28.—Line of resultant air force on long hull with No. 5 controls. Model at 0° pitch. Elevators and rudders neutral. Scale of model 1/120 full size

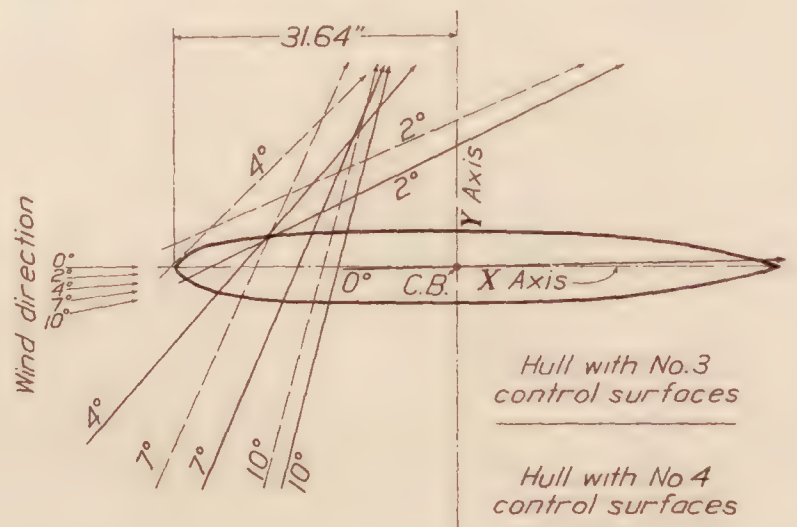


FIG. 30.—Line of resultant air force on long hull with Nos. 3 and 4 controls. Model at 0° pitch. Elevator and rudders neutral. Air speed 40 M. P. H. Scale of model 1/120 full size

COEFFICIENTS OF DAMPING MOMENT

Tables XXXII to XXXIV give the data and derived values for finding the damping coefficient, and Table XXXV the net damping coefficient itself, for the long hull, first bare then with controls 1, 2, 3, 4, 6A, 6D. In Figure 32 these net values are plotted against speed, giving straight-line diagrams, as usual.

The logarithmic decrement, λ , used in computing the damping coefficients, was computed from faired plots of the oscillation data, made in pencil, for all the tests, during the individual runs. Some typical plots on semilog paper are shown in Figure 31.

The structure and theory of the aerodynamic oscillator used in these tests are well known, hence the method of finding the coefficient, μ , of damping moment in the present work is omitted.

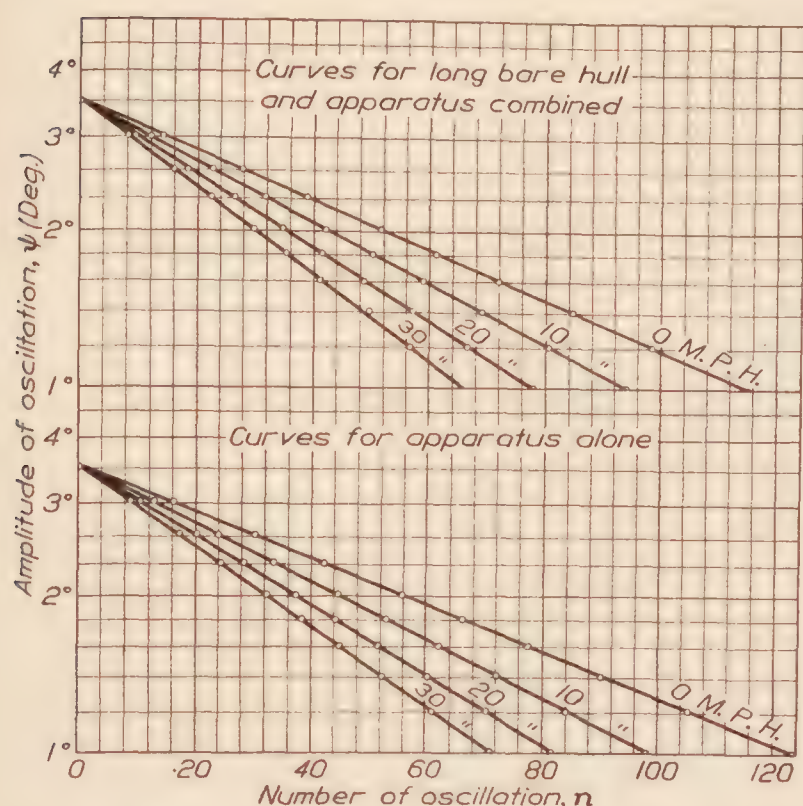


FIG. 31.—Oscillations at various air speeds. Model at 0° pitch. Bare hull

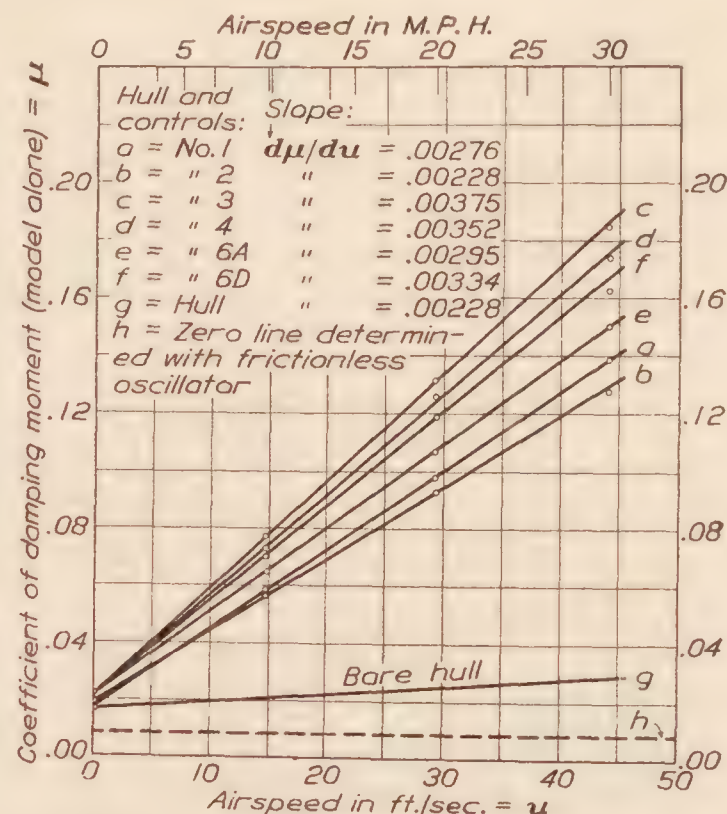


FIG. 32.—Coefficient of damping moment in yaw vs. various air speeds. Model at 0° pitch. Elevators and rudders neutral

STABILITY CRITERIA

By (13), Report No. 212 of the National Advisory Committee for Aeronautics, an airship is stable in yaw if

$$a \frac{\mu}{u} \frac{Y_{\psi}}{N_{\psi}} > 1 \quad \text{-----} (1)$$

where all the symbols but a refer to the model conventionally. Following the earlier usage in aerodynamics, one may write $a = s^3/m$, where s is the scale ratio of airship to model, and m is the natural mass of the ship.

In the present case $a = 120^3/5427 = 318.4$, the denominator being slugs. The working yaw criterion then is

$$318.4 \frac{\mu}{u} \frac{Y_{\psi}}{N_{\psi}} \quad \text{-----} (2)$$

and gives for the full-scale hull the values listed in Table XXXVI.

The last column indicates that the airship is sufficiently stable with some of the types of controls, notably 3, 4. For experience with this kind of craft teaches that satisfactory stability may be expected when the yaw criterion here used somewhat exceeds $1/3$.²

Report No. 212, National Advisory Committee for Aeronautics, derives a in the form $a = s^3/mn$, where n is a constant peculiar to the model. For motion at small angles in yaw it appears that for this model n is less than $1/2$, and hence that the values of the criterion in the last column of Table XXXVI should be at least doubled. The value $n = 1$ was used in computing this table merely to make the values of the criterion directly comparable to those given in other publications, such as the one here cited. On the other hand, if one takes $m = 1.5 \times$ natural mass of the airship, and $n = 1/2$, the value of a becomes $1/3$ greater; and the given criteria must be increased by that amount.

² British R. & M. (new series) No. 361, p. 61.

CONCLUSION

It is believed the designing staff, which initiated the program for the present measurements, will not require a detailed discussion of the data and diagrams, since these are of familiar form and very numerous. The stability criterion, presented in somewhat novel form in Table XXXVI, is derived and discussed in Report No. 212, National Advisory Committee for Aeronautics. If the numerical equations of motion for one or more of the present airship types be required, they can be developed subsequently in such fullness as may seem necessary.

TABLE I
AREA OF MODEL CONTROL SURFACES
[In square inches]

Control member	Number of control surface						
	1 or 2	3 or 4	5	6A	6B	6C	6D
Horizontal fin.....	9.59	10.89	11.44	12.15	12.15	12.15	12.15
Elevator for horizontal fins.....	2.86	3.34	2.72	1.83	2.18	2.61	3.01
Top vertical fin.....	9.59	10.89	11.80	12.40	12.40	12.40	12.40
Rudder for top vertical fin.....	2.86	3.34	2.72	1.83	2.18	2.61	3.01
Bottom vertical fin.....	4.80	7.20	6.43	6.85	6.85	6.85	6.85
Rudder for bottom vertical fin.....	1.78	1.95	1.87	1.28	1.55	1.84	2.12

NOTE: Ratio model to full size=1:120.
1 sq. in. on model=100 sq. ft. on full size.
=9.29 sq. meters on full size.

TABLE II
RESISTANCE OF BARE HULL AND HULL WITH CONTROLS NOS. 1 TO 5

Air speed	Displacement due to model and four wires	Corresponding resistance	Displacement due to model and two wires	Corresponding resistance	Resistance of model without wires	Resistance due to frame	Resistance due to pressure drop	Net total resistance
Bare hull, long model								
M. P. H.	Inches	Pounds	Inches	Pounds	Pounds	Pounds	Pounds	Pounds
20	0.310	0.054	0.290	0.051	0.048	0	0.006	0.042
30	.656	.115	.615	.108	.101	0	.013	.088
40	1.115	.196	1.040	.184	.172	0	.022	.150
50	1.685	.297	1.580	.278	.259	-.001	.032	.228
60	2.358	.414	2.215	.388	.362	-.002	.044	.320
Bare hull, short model								
20	0.298	0.051	0.278	0.048	0.045	0	0.006	0.039
30	.635	.110	.594	.103	.096	0	.012	.084
40	1.090	.189	1.017	.177	.165	0	.020	.145
50	1.655	.287	1.555	.269	.251	-.001	.030	.222
60	2.325	.403	2.178	.378	.353	-.002	.041	.314
Control surface No.	Long model hull with control surface at 40 M. P. H.							
1	1.143	0.206	1.074	0.194	0.182	0	0.022	0.160
2	1.139	.206	1.070	.194	.182	0	.022	.160
3	1.155	.209	1.086	.197	.185	0	.022	.163
4	1.150	.209	1.085	.197	.185	0	.022	.163
5	1.120	.209	1.057	.197	.185	0	.022	.163
Short model hull with control surface at 40 M. P. H.								
1	1.132	0.201	1.064	0.189	0.177	0	0.020	0.157
2	1.119	.200	1.052	.188	.176	0	.020	.156
3	1.140	.204	1.073	.192	.180	0	.020	.160
4	1.135	.204	1.069	.192	.180	0	.020	.160
5	1.110	.205	1.045	.193	.181	0	.020	.161

R=Resistance of model in pounds.
L=Length of model in feet.
Vol.=Volume of model in cubic feet.

TABLE III
SHAPE COEFFICIENT AND CORRESPONDING VALUES OF VL
[Symbols defined below]

Air speed	Shape coefficient $\frac{C_n}{2R} = \frac{C_n}{\rho(Vol.)^{2/3} V_1^2}$	$V_1 L$ (ft.ft./sec.)	VL (ft.mi./hr.)
Bare hull, long model			
M. P. H.			
20	0.03442	165.0	112.6
30	.03205	247.7	169.0
40	.03077	330.0	225.1
50	.02994	412.8	281.6
60	.02917	495.4	337.9
Bare hull, short model			
20	0.03355	157.1	107.1
30	.03216	235.7	160.7
40	.03122	314.2	214.3
50	.03062	392.9	267.8
60	.03004	471.5	321.4
Control surface No.	Long model hull with control surface at 40 M. P. H.		
1	0.03260	330.0	225.1
2	.03260	330.0	225.1
3	.03321	330.0	225.1
4	.03321	330.0	225.1
5	.03321	330.0	225.1
Short model hull with control surface at 40 M.P.H.			
1	0.03361	314.2	214.3
2	.03340	314.2	214.3
3	.03425	314.2	214.3
4	.03425	314.2	214.3
5	.03445	314.2	214.3

V_1 =Air speed in feet per second
 V =Air speed in miles per hour.
 ρ =Air density=.00237 slugs per cubic foot.

TABLE IV

NET MEASURED LIFT IN POUNDS FOR BARE HULLS AND HULLS WITH CONTROL SURFACES NOS. 1 TO 5

[Model at 0° yaw and rudders neutral. Air speed, 40 miles per hour]

Elevator setting δ_e	Angle of pitch θ	Long bare hull	Short bare hull	Long hull with control No.—				Short hull, control No. 5	Long hull, control No. 5	Long hull, control No. 5, computed from short
				1	2	3	4			
Degrees 0	Degrees 0	−0.001	−0.001	+0.014	+0.012	+0.027	+0.025	+0.015	+0.017	+0.015
	+2	+ .029	+ .031	+ .088	+ .057	+ .109	+ .108	+ .075	+ .074	+ .075
	+4	+ .073	+ .072	+ .182	+ .153	+ .214	+ .194	+ .146	+ .146	+ .147
	+7	+ .173	+ .163	+ .351	+ .301	+ .413	+ .400	+ .305	+ .324	+ .315
	+10	+ .294	+ .276	+ .590	+ .516	+ .648	+ .645	+ .532	+ .552	+ .548
	−10								− .398	
	−7								− .190	
	−4								− .052	
	−2								+ .013	
	0								+ .070	
+10	+2								+ .130	
	+4								+ .212	
	+7								+ .381	
	+10								+ .627	
	−10			− .390	− .356	− .365	− .316	− .370	− .365	− .386
	−7			− .178	− .168	− .170	− .110	− .172	− .160	− .183
	−4			− .022	− .015	+ .021	+ .061	− .012	− .011	− .015
	−2			+ .089	+ .045	+ .116	+ .143	+ .057	+ .058	+ .056
	0			+ .110	+ .097	+ .192	+ .216	+ .115	+ .116	+ .115
	+2			+ .178	+ .159	+ .280	+ .299	+ .180	+ .183	+ .181
+15	+4			+ .272	+ .242	+ .389	+ .394	+ .262	+ .278	+ .266
	+7			+ .487	+ .400	+ .598	+ .585	+ .439	+ .455	+ .450
	+10			+ .764	+ .613	+ .812	+ .796	+ .672	+ .685	+ .688

TABLE V

NET MEASURED LIFT FOR SHORT MODEL AND COMPUTED LIFT IN POUNDS FOR LONG MODEL HULL WITH NO. 6 CONTROL SURFACES

[Model at 0° yaw and rudders neutral. Airspeed, 40 miles per hour]

Elevator setting δ_e	Angle of pitch θ	Fins No. 6 (without elevators or rudders) on—		Control No. 6A on—		Control No. 6B on—		Control No. 6C on—		Control No. 6D on—	
		Short hull	Long hull	Short hull	Long hull	Short hull	Long hull	Short hull	Long hull	Short hull	Long hull
Degrees 0	Degrees 0	+0.017	+0.017	+0.018	+0.018	+0.017	+0.017	+0.019	+0.019	+0.018	+0.018
	+2	+ .073	+ .074	+ .078	+ .079	+ .079	+ .080	+ .081	+ .082	+ .078	+ .079
	+4	+ .136	+ .139	+ .152	+ .155	+ .152	+ .155	+ .154	+ .157	+ .157	+ .160
	+7	+ .268	+ .279	+ .316	+ .327	+ .320	+ .331	+ .325	+ .336	+ .330	+ .341
	+10	+ .482	+ .498	+ .538	+ .554	+ .548	+ .564	+ .557	+ .573	+ .564	+ .580
	+15	+ .877	+ .915	+ .992	+1.030	+1.001	+1.039	+1.005	+1.043	+1.019	+1.057
	−15			− .840	− .878	− .802	− .840	− .783	− .821	− .768	− .806
	−10			− .416	− .432	− .405	− .421	− .393	− .409	− .382	− .398
	−7			− .213	− .224	− .203	− .214	− .197	− .208	− .187	− .198
	−4			− .059	− .062	− .048	− .051	− .018	− .021	− .029	− .032
+10	−2			+ .020	+ .019	+ .031	+ .030	+ .036	+ .035	+ .048	+ .047
	0			+ .075	+ .075	+ .085	+ .085	+ .092	+ .092	+ .105	+ .105
	+2			+ .143	+ .144	+ .152	+ .153	+ .164	+ .165	+ .173	+ .174
	+4			+ .218	+ .221	+ .233	+ .236	+ .242	+ .245	+ .265	+ .268
	+7			+ .387	+ .398	+ .403	+ .414	+ .415	+ .426	+ .432	+ .443
	+10			+ .607	+ .623	+ .627	+ .643	+ .644	+ .660	+ .662	+ .678
	+15			+1.062	+1.100	+1.080	+1.118	+1.092	+1.130	+1.114	+1.152
	−15			− .723	− .761	− .608	− .646	− .690	− .728	− .664	− .702
	−10			− .353	− .369	− .339	− .355	− .320	− .336	− .291	− .307
	−7			− .157	− .168	− .137	− .148	− .127	− .138	− .108	− .119
+20	−4			+ .005	+ .002	+ .019	+ .016	+ .031	+ .028	+ .096	+ .093
	−2			+ .080	+ .079	+ .104	+ .103	+ .111	+ .110	+ .131	+ .130
	0			+ .133	+ .133	+ .154	+ .154	+ .172	+ .172	+ .195	+ .195
	+2			+ .198	+ .199	+ .215	+ .216	+ .239	+ .240	+ .247	+ .248
	+4			+ .280	+ .283	+ .302	+ .305	+ .327	+ .330	+ .354	+ .357
	+7			+ .459	+ .470	+ .489	+ .500	+ .514	+ .525	+ .539	+ .550
	+10			+ .681	+ .697	+ .730	+ .746	+ .747	+ .763	+ .779	+ .795
	+15			+1.137	+1.175	+1.169	+1.207	+1.228	+1.266	+1.244	+1.282

TABLE VI

NET MEASURED LIFT IN POUNDS FOR BARE HULLS AND HULLS WITH CONTROL SURFACES NOS. 1 TO 5
[Model at 0° pitch and elevators neutral. Air speed, 40 miles per hour]

Rudder setting δ_r	Angle of yaw ψ	Long bare hull	Short bare hull	Long hull with control No. —				Short hull, control No. 5	Long hull, control No. 5	Long hull, control No. 5, computed from short
				1	2	3	4			
Degrees 0	Degrees 0	+0	+0.001	+0.013	+0.013	+0.019	+0.017	+0.020	+0.019	+0.020
	+2	+0.001	+0.002	+0.013	+0.010	+0.019	+0.018	+0.021	+0.019	+0.021
	+4	+0.001	+0.001	+0.014	+0.011	+0.020	+0.018	+0.020	+0.021	+0.020
	+7	+0.001	0	+0.012	+0.010	+0.020	+0.019	+0.021	+0.020	+0.021
	+10	+0.001	0	+0.013	+0.010	+0.021	+0.017	+0.019	+0.020	+0.019
	+15	0	0							
	-10								+0.021	
	-7								+0.020	
	-4								+0.022	
	-2								+0.020	
+10	0								+0.019	
	+2								+0.021	
	+4								+0.022	
	+7								+0.020	
	+10								+0.019	
	+15									
	-10			+0.013	+0.010	+0.019	+0.017	+0.019	+0.020	+0.019
	-7			+0.011	+0.012	+0.020	+0.018	+0.019	+0.020	+0.019
	-4			+0.013	+0.012	+0.020	+0.017	+0.021	+0.021	+0.021
	-2			+0.011	+0.011	+0.020	+0.017	+0.021	+0.021	+0.021
+15	0			+0.012	+0.012	+0.021	+0.018	+0.019	+0.021	+0.019
	+2			+0.013	+0.011	+0.021	+0.018	+0.020	+0.020	+0.020
	+4			+0.012	+0.011	+0.020	+0.017	+0.020	+0.018	+0.020
	+7			+0.013	+0.012	+0.021	+0.017	+0.018	+0.020	+0.018
	+10			+0.012	+0.011	+0.020	+0.017	+0.013	+0.020	+0.018
	+15									
	-10									
	-7									
	-4									
	-2									

TABLE VII

NET MEASURED LIFT FOR SHORT MODEL AND COMPUTED LIFT IN POUNDS FOR LONG MODEL WITH NO. 6 CONTROL SURFACES
[Model at 0° pitch and elevators neutral. Air speed, 40 miles per hour]

Rudder setting δ_r	Angle of yaw ψ	Short or long hull and fins No. 6, without elevators or rudders	Short or long hull with control No. —			
			6A	6B	6C	6D
Degrees 0	Degrees 0	+0.020	+0.021	+0.020	+0.017	+0.022
	+2	+0.018	+0.019			
	+4	+0.022	+0.019			
	+7	+0.020	+0.018			
	+10	+0.019	+0.018			
	+15	+0.018	+0.019	+0.018	+0.017	+0.017
	-15		+0.016	+0.021	+0.017	+0.017
	-10		+0.018			
	-7		+0.018			
	-4		+0.019			
+10	-2		+0.020			
	0		+0.017	+0.018	+0.019	+0.021
	+2		+0.019			
	+4		+0.020			
	+7		+0.019			
	+10		+0.019			
	+15		+0.018	+0.021	+0.021	+0.023
	-15		+0.021	+0.021	+0.020	+0.023
	-10		+0.018			
	-7		+0.019			
+20	-4		+0.018			
	-2		+0.019			
	0		+0.019	+0.019	+0.019	+0.021
	+2		+0.018			
	+4		+0.020			
	+7		+0.015			
	+10		+0.018			
	+15		+0.018	+0.019	+0.018	+0.020
	+15					
	+15					

TABLE VIII

NET MEASURED DRAG IN POUNDS FOR BARE HULLS AND HULLS WITH CONTROL SURFACES NOS. 1 TO 5

[Model at 0° yaw and rudders neutral. Air speed, 40 miles per hour]

Elevator setting δ°	Angle of pitch θ	Long bare hull	Short bare hull	Long hull with control No. —				Short hull, control No. 5	Long hull, control No. 5	Long hull, control No. 5, computed from short
				1	2	3	4			
<i>Degrees</i>	<i>Degrees</i>									
0	0	0. 146	0. 144	0. 158	0. 157	0. 160	0. 159	0. 155	0. 160	0. 155
	+2	. 146	. 145	. 159	. 158	. 162	. 159	. 157	. 160	. 158
	+4	. 147	. 147	. 165	. 165	. 169	. 165	. 162	. 165	. 164
	+7	. 156	. 153	. 197	. 194	. 204	. 200	. 195	. 190	. 198
	+10	. 188	. 184	. 254	. 249	. 272	. 264	. 256	. 258	. 260
	+15	. 271	. 261							
	-10								. 218	
+10	-7								. 174	
	-4								. 161	
	-2								. 161	
	0								. 162	
	+2								. 166	
	+4								. 175	
	+7								. 210	
+15	+10								. 280	
	-10			. 230	. 224	. 230	. 216	. 208	. 213	. 212
	-7			. 178	. 176	. 187	. 175	. 165	. 175	. 168
	-4			. 163	. 162	. 170	. 170	. 162	. 165	. 164
	-2			. 163	. 162	. 170	. 171	. 165	. 165	. 162
	0			. 164	. 163	. 174	. 175	. 161	. 166	. 161
	+2			. 173	. 169	. 189	. 187	. 165	. 171	. 166
	+4			. 183	. 183	. 215	. 209	. 179	. 182	. 181
	+7			. 231	. 219	. 266	. 261	. 217	. 217	. 220
	+10			. 295	. 284	. 339	. 321	. 278	. 295	. 282

TABLE IX

NET MEASURED DRAG FOR SHORT MODEL AND COMPUTED DRAG IN POUNDS FOR LONG MODEL WITH NO. 6 CONTROL SURFACES

[Model at 0° yaw and rudders neutral. Airspeed, 40 miles per hour]

Elevator setting δ_e	Angle of pitch θ	Fins No. 6 (with- out elevators or rudders) on—		Control No. 6A on—		Control No. 6B on—		Control No. 6C on—		Control No. 6D on—	
		Short hull	Long hull	Short hull	Long hull	Short hull	Long hull	Short hull	Long hull	Short hull	Long hull
Degrees	Degrees										
0	0	0. 155	0. 155	0. 155	0. 155	0. 155	0. 155	0. 155	0. 155	0. 155	0. 155
	+2	. 156	. 157	. 156	. 157	. 157	. 158	. 157	. 158	. 161	. 162
	+4	. 159	. 161	. 165	. 167	. 168	. 170	. 169	. 171	. 175	. 177
	+7	. 181	. 184	. 198	. 201	. 205	. 208	. 210	. 213	. 215	. 218
	+10	. 233	. 237	. 260	. 264	. 270	. 274	. 274	. 278	. 282	. 286
	+15	. 382	. 388	. 430	. 436	. 439	. 445	. 444	. 450	. 454	. 460
	-15			. 376	. 382	. 372	. 378	. 369	. 375	. 372	. 378
	-10			. 220	. 224	. 218	. 222	. 220	. 224	. 218	. 222
	-7			. 174	. 177	. 177	. 180	. 178	. 181	. 181	. 184
	-4			. 160	. 162	. 158	. 160	. 159	. 161	. 160	. 162
+10	-2			. 158	. 159	. 158	. 159	. 159	. 160	. 161	. 162
	0			. 158	. 158	. 158	. 158	. 159	. 159	. 161	. 161
	+2			. 162	. 163	. 164	. 165	. 164	. 165	. 169	. 170
	+4			. 175	. 177	. 175	. 177	. 176	. 178	. 181	. 183
	+7			. 207	. 210	. 215	. 218	. 218	. 221	. 223	. 226
	+10			. 274	. 278	. 281	. 285	. 292	. 296	. 300	. 304
	+15			. 450	. 456	. 466	. 572	. 478	. 484	. 489	. 495
	-15			. 350	. 356	. 324	. 330	. 346	. 352	. 338	. 344
	-10			. 216	. 220	. 219	. 223	. 215	. 219	. 220	. 224
	-7			. 175	. 178	. 175	. 178	. 178	. 181	. 180	. 183
+20	-4			. 163	. 165	. 158	. 160	. 164	. 166	. 165	. 167
	-2			. 162	. 163	. 158	. 159	. 164	. 165	. 164	. 165
	0			. 164	. 164	. 163	. 163	. 166	. 166	. 165	. 165
	+2			. 167	. 168	. 170	. 171	. 173	. 174	. 173	. 174
	+4			. 178	. 180	. 184	. 186	. 192	. 194	. 200	. 202
	+7			. 219	. 222	. 231	. 234	. 241	. 244	. 254	. 257
	+10			. 295	. 299	. 309	. 313	. 324	. 328	. 340	. 344
	+15			. 477	. 483	. 500	. 506	. 529	. 535	. 548	. 554

TABLE X

NET MEASURED DRAG IN POUNDS FOR BARE HULLS AND HULLS WITH CONTROL SURFACES NOS. 1 TO 5

[Model at 0° pitch and elevators neutral. Air speed, 40 miles per hour]

Rudder setting δ_r	Angle of yaw ψ	Long bare hull	Short bare hull	Long hull with control No.—				Short hull, control No. 5	Long hull, control No. 5	Long hull, control No. 5 computed from short
				1	2	3	4			
Degrees	0	0.146	0.144	0.158	0.157	0.160	0.160	0.155	0.160	0.155
	+2	.146	.145	.158	.158	.161	.160	.157	.161	.158
	+4	.147	.147	.160	.162	.164	.163	.161	.165	.163
	+7	.156	.153	.183	.183	.198	.185	.182	.188	.185
	+10	.188	.184	.236	.234	.250	.244	.231	.240	.235
	+15	.271	.261							
	-10								.234	
	-7								.178	
	-4								.163	
	-2								.161	
+10	0								.162	
	+2								.164	
	+4								.169	
	+7								.199	
	+10								.250	
	-10			.217	.209	.221	.221	.218	.233	.222
	-7			.171	.172	.186	.178	.177	.178	.180
	-4			.163	.161	.170	.170	.163	.166	.165
	-2			.162	.161	.169	.170	.160	.165	.161
	0			.164	.162	.171	.172	.159	.164	.159
+15	+2			.174	.168	.176	.177	.161	.166	.162
	+4			.180	.178	.191	.192	.170	.173	.172
	+7			.213	.208	.231	.227	.199	.206	.202
	+10			.269	.260	.304	.298	.258	.264	.262

TABLE XI

NET MEASURED DRAG FOR SHORT MODEL AND COMPUTED DRAG IN POUNDS FOR LONG MODEL WITH NO. 6 CONTROL SURFACES

[Model at 0° pitch and elevators neutral. Air speed, 40 miles per hour]

Rudder setting δ_r	Angle of yaw ψ	Fins No. 6 (without elevators or rudders) on—		Control No. 6A on—		Control No. 6B on—		Control No. 6C on—		Control No. 6D on—	
		Short hull	Long hull	Short hull	Long hull	Short hull	Long hull	Short hull	Long hull	Short hull	Long hull
Degrees	0	0.155	0.155	0.155	0.155	0.156	0.156	0.155	0.155	0.155	0.155
	+2	.155	.156	.156	.157	.157	.158	.159	.160	.159	.160
	+4	.158	.160	.159	.161	.162	.164	.165	.167	.167	.169
	+7	.175	.178	.182	.185	.186	.189	.191	.194	.195	.198
	+10	.221	.225	.231	.235	.239	.241	.240	.244	.248	.252
	+15	.365	.371	.384	.390	.389	.395	.404	.410	.410	.416
	-15			.362	.368	.360	.366	.364	.370	.367	.373
	-10			.216	.220	.214	.218	.214	.218	.212	.216
	-7			.179	.182	.178	.181	.178	.181	.179	.182
	-4			.162	.164	.162	.164	.161	.163	.163	.165
+10	-2			.160	.161	.158	.159	.158	.159	.159	.160
	0			.160	.160	.159	.159	.159	.159	.160	.160
	+2			.161	.162	.163	.164	.163	.164	.163	.164
	+4			.170	.172	.170	.172	.175	.177	.177	.179
	+7			.195	.198	.203	.206	.214	.217	.219	.222
	+10			.251	.255	.260	.264	.269	.273	.281	.285
	+15			.409	.415	.425	.431	.436	.442	.442	.448
	-15			.363	.369	.351	.357	.342	.348	.332	.338
	-10			.222	.226	.214	.218	.214	.218	.216	.220
	-7			.177	.180	.177	.180	.178	.181	.179	.182
+20	-4			.162	.164	.160	.162	.163	.165	.163	.165
	-2			.160	.161	.159	.160	.162	.163	.163	.164
	0			.160	.160	.161	.161	.163	.163	.164	.164
	+2			.162	.163	.169	.170	.174	.175	.177	.178
	+4			.172	.174	.182	.184	.191	.193	.199	.201
	+7			.205	.208	.223	.226	.237	.240	.251	.254
	+10			.268	.272	.290	.294	.310	.314	.328	.332
	+15			.431	.437	.461	.467	.478	.484	.494	.500

TABLE XII

NET MEASURED CROSS-WIND FORCE IN POUNDS FOR BARE HULLS AND HULLS WITH CONTROL SURFACES NOS. 1 TO 5
[Model at 0° yaw and rudders neutral. Air speed, 40 miles per hour]

Elevator setting δ_e	Angle of pitch θ	Long bare hull	Short bare hull	Long hull with control No.—				Short hull, control No. 5	Long hull, control No. 5	Long hull, control No. 5, computed from short
				1	2	3	4			
Degrees 0	Degrees 0	0	-0.001	0	-0.001	0	0	-0.001	+0.002	-0.001
	+2	-.001	-.002	-.001	0	-.001	0	-.001	+0.004	-.001
	+4	-.001	-.001	-.001	-.001	-.001	-.002	0	+0.002	0
	+7	-.001	0	0	-.002	-.003	-.003	-.001	+0.001	-.001
	+10	-.001	0	0	-.001	-.001	0	-.002	+0.001	-.002
	+15	0	0							
	-10								-.001	
	-7								-.001	
	-4								+0.001	
	-2								0	
+10	0								+0.002	
	+2								0	
	+4								0	
	+7								+0.001	
	+10								0	
	-10			-.001	-.003	-.002	-.001	-.001	0	-.001
	-7			-.001	-.002	-.001	-.003	-.001	0	-.001
	-4			+0.001	-.002	-.002	-.001	-.001	0	-.001
	-2			+0.002	+0.001	+0.001	+0.001	-.001	+0.001	-.001
	0			+0.002	-.001	-.001	0	+0.001	+0.005	+0.001
+15	+2			+0.001	-.001	0	+0.001	0	+0.005	0
	+4			+0.001	-.002	+0.001	-.001	0	+0.004	0
	+7			-.002	-.002	-.001	-.002	-.001	+0.001	-.001
	+10			-.001	-.002	-.001	-.002	-.002	+0.001	-.002

TABLE XIII

NET MEASURED CROSS-WIND FORCE FOR SHORT MODEL AND COMPUTED CROSS-WIND FORCE IN POUNDS FOR LONG MODEL WITH NO. 6 CONTROL SURFACES
[Model at 0° yaw and rudders neutral. Air speed, 40 miles per hour]

Elevator setting δ_e	Angle of pitch θ	Short or long hull and fins No. 6, without elevators or rudders	Short or long hull with control No. —			
			6A	6B	6C	6D
Degrees 0	Degrees 0	-0.002	0	-0.001	-0.002	+0.001
	+2	-.002	0	0		
	+4	-.003	-.002	-.002		
	+7	0	-.004	-.001		
	+10	-.001	-.001	-.002		
	+15	-.002	-.002	-.003	0	+0.003
	-15		-.001	-.002	-.002	+0.002
	-10		-.003			
	-7		-.002			
	-4		-.003			
+10	-2		-.003			
	0		-.001	+0.001	-.004	+0.002
	+2		-.002			
	+4		-.001			
	+7		-.002			
	+10		-.002			
	+15		-.003	-.003	+0.002	+0.001
	-15		-.002	-.002	-.005	+0.002
	-10		-.003			
	-7		-.002			
+20	-4		-.003			
	-2		+0.002			
	0		+0.002	-.001	-.002	+0.002
	+2		-.004			
	+4		-.004			
	+7		-.003			
	+10		-.002			
	+15		-.002	-.001	-.003	+0.003

TABLE XVI

X FORCE IN POUNDS FOR BARE HULLS AND HULLS WITH CONTROL SURFACES NOS. 1 TO 5

[Model at 0° yaw and rudders neutral. Air speed, 40 miles per hour]

Elevator setting δ_e	Angle of pitch θ	Long bare hull	Short bare hull	Long hull with control No. —				Short hull, control No. 5	Long hull, control No. 5	Long hull, control No. 5, computed from short
				1	2	3	4			
Degrees 0	Degrees 0	0.146	0.144	0.158	0.157	0.160	0.159	0.155	0.160	0.155
	+2	.144	.143	.156	.156	.158	.155	.154	.157	.154
	+4	.141	.142	.152	.154	.154	.151	.151	.154	.152
	+7	.134	.132	.152	.156	.153	.149	.154	.149	.156
	+10	.134	.133	.147	.156	.155	.148	.159	.154	.161
	+15	.115	.117							
	-10								.145	
	-7								.149	
	-4								.157	
	-2								.161	
	0								.162	
	+2								.161	
	+4								.157	
	+7								.162	
	+10								.166	
+10	-10			.159	.159	.162	.158	.141	.147	.143
	-7			.155	.154	.165	.161	.143	.154	.145
	-4			.161	.162	.171	.174	.160	.163	.161
	-2			.166	.163	.174	.176	.163	.166	.163
	0			.164	.163	.173	.175	.163	.166	.163
	+2			.166	.163	.177	.176	.158	.164	.158
	+4			.164	.167	.186	.181	.160	.162	.161
	+7			.170	.168	.191	.187	.162	.160	.164
	+10			.158	.173	.193	.188	.157	.171	.159
+15	-10									
	-7									
	-4									
	-2									
	0									
	+2									
	+4									
	+7									
	+10									
	+15									
	-10									
	-7									
	-4									
	-2									
	0									

TABLE XVII

X FORCE IN POUNDS FOR HULLS WITH NO. 6 CONTROL SURFACES

[Model at 0° yaw and rudders neutral. Air speed, 40 miles per hour]

Eleva- tor setting δ_e	Angle of pitch θ	Fins No. 6 (with- out elevator or rudders) on—		Control No. 6A on—		Control No. 6B on—		Control No. 6C on—		Control No. 6D on—	
		Short hull	Long hull	Short hull	Long hull	Short hull	Long hull	Short hull	Long hull	Short hull	Long hull
Degrees 0	Degrees 0	0.155	0.155	0.155	0.155	0.155	0.155	0.155	0.155	0.155	0.155
	+2	.153	.153	.153	.153	.154	.154	.154	.154	.158	.158
	+4	.150	.151	.154	.155	.157	.158	.158	.159	.163	.164
	+7	.147	.149	.157	.159	.162	.164	.168	.170	.173	.175
	+10	.146	.148	.162	.164	.170	.172	.173	.175	.179	.181
	+15	.143	.146	.158	.161	.165	.168	.169	.172	.174	.177
	-15			.146	.149	.151	.154	.154	.157	.161	.164
	-10			.144	.146	.145	.147	.148	.150	.149	.151
	-7			.147	.149	.151	.153	.152	.154	.157	.159
	-4			.156	.157	.154	.155	.157	.158	.157	.158
	-2			.158	.158	.159	.159	.160	.160	.162	.162
	0			.158	.158	.157	.157	.159	.159	.161	.161
	+2			.157	.157	.158	.158	.158	.158	.163	.163
	+4			.159	.160	.158	.159	.159	.160	.162	.163
	+7			.158	.160	.164	.166	.166	.168	.168	.170
+10	+10			.163	.165	.167	.169	.176	.178	.179	.181
	+15			.159	.162	.171	.174	.178	.181	.184	.187
	-15			.152	.155	.156	.159	.156	.159	.155	.158
	-10			.152	.154	.156	.158	.155	.157	.155	.157
	-7			.153	.155	.156	.158	.162	.164	.160	.162
	-4			.163	.164	.159	.160	.166	.167	.171	.172
	-2			.165	.165	.161	.161	.167	.167	.168	.168
	0			.164	.164	.163	.163	.166	.166	.164	.164
	+2			.160	.160	.163	.163	.164	.164	.164	.164
	+4			.156	.157	.163	.164	.169	.170	.175	.176
	+7			.161	.163	.169	.171	.176	.178	.186	.188
	+10			.172	.174	.177	.179	.192	.194	.199	.201
	+15			.168	.171	.179	.182	.194	.197	.206	.209

TABLE XVIII

X FORCE IN POUNDS FOR BARE HULLS AND HULLS WITH CONTROL SURFACES NOS. 1 TO 5

[Model at 0° pitch and elevators neutral. Air speed, 40 miles per hour]

Rudder setting δ_r	Angle of yaw ψ	Long bare hull	Short bare hull	Long hull with control No.—				Short hull, control No. 5	Long hull, control No. 5	Long hull, control No. 5, computed from short
				1	2	3	4			
0	Degrees									
	0	0.146	0.144	0.158	0.157	0.160	0.160	0.155	0.160	0.155
	+2	.144	.143	.156	.156	.158	.158	.155	.159	.155
	+4	.141	.142	.150	.153	.152	.153	.153	.157	.154
	+7	.134	.132	.148	.152	.155	.146	.151	.155	.153
	+10	.134	.133	.150	.155	.151	.150	.149	.153	.151
	+15	.115	.117							
	-10								.167	
	-7								.155	
	-4								.159	
	-2								.161	
	0								.162	
	+2								.161	
	+4								.157	
	+7								.157	
	+10								.154	
+10	-10			.154	.150	.158	.158	.151	.165	.153
	-7			.150	.151	.165	.156	.155	.163	.157
	-4			.160	.158	.169	.170	.160	.163	.161
	-2			.163	.162	.172	.172	.160	.165	.160
	0			.164	.162	.171	.172	.159	.164	.159
	+2			.169	.164	.169	.170	.156	.162	.156
	+4			.164	.165	.170	.173	.155	.158	.156
	+7			.167	.167	.171	.173	.155	.160	.157
	+10			.167	.167	.180	.180	.158	.160	.160
+15	-10									
	-7									
	-4									
	-2									
	0									
	+2									
	+4									
	+7									
	+10									
	+15									
	-10									
	-7									
	-4									
	-2									
	0									

TABLE XIX

X FORCE IN POUNDS FOR HULLS WITH NO. 6 CONTROL SURFACES

[Model at 0° pitch and elevators neutral. Air speed, 40 miles per hour]

Rudder setting δ_r	Angle of yaw ψ	Fins No. 6 (without elevators or rudders) on—		Control No. 6A on—		Control No. 6B on—		Control No. 6C on—		Control No. 6D on—	
		Short hull	Long hull	Short hull	Long hull	Short hull	Long hull	Short hull	Long hull	Short hull	Long hull
0	Degrees										
	0	0.155	0.155	0.155	0.155	0.156	0.156	0.155	0.155	0.155	0.155
	+2	.154	.154	.154	.154	.155	.155	.157	.157	.157	.157
	+4	.150	.151	.151	.152	.154	.155	.156	.157	.158	.159
	+7	.146	.148	.152	.154	.155	.157	.160	.162	.162	.164
	+10	.145	.147	.150	.152	.155	.157	.157	.159	.163	.165
	+15	.145	.148	.156	.159	.155	.158	.167	.170	.168	.171
	-15			.141	.144	.144	.147	.153	.156	.160	.163
	-10			.143	.145	.145	.147	.149	.151	.149	.151
	-7			.155	.157	.154	.156	.154	.156	.158	.160
	-4			.156	.157	.157	.158	.157	.158	.159	.160
	-2			.160	.160	.158	.158	.159	.159	.160	.160
	0			.167	.167	.159	.159	.159	.159	.160	.160
	+2			.158	.158	.159	.159	.159	.159	.160	.160
	+4			.158	.159	.157	.158	.161	.162	.162	.163
+10	+7			.156	.158	.160	.162	.169	.171	.173	.175
	+10			.155	.157	.159	.161	.166	.168	.177	.179
	+15			.156	.159	.160	.163	.171	.174	.174	.177
	-15			.156	.159	.155	.158	.156	.159	.157	.160
	-10			.157	.159	.155	.157	.159	.161	.166	.168
	-7			.158	.160	.160	.162	.163	.165	.166	.168
	-4			.159	.160	.160	.161	.164	.165	.164	.165
	-2			.161	.161	.161	.161	.165	.165	.166	.166
	0			.160	.160	.161	.161	.163	.163	.164	.164
	+2			.156	.156	.163	.163	.177	.177	.170	.170
	+4			.157	.158	.166	.167	.172	.173	.179	.180
	+7			.156	.158	.183	.185	.183	.185	.195	.197
	+10			.160	.162	.178	.180	.193	.195	.207	.209
	+15			.155	.158	.182	.185	.189	.192	.201	.204

Z FORCE IN POUNDS FOR BARE HULLS AND HULLS WITH CONTROL SURFACES NOS. 1 TO 5

[Model at 0° yaw and rudders neutral. Air speed, 40 miles per hour]

Elevator setting δ_e	Angle of pitch θ	Long bare hull	Short bare hull	Long hull with control No.—				Short hull, control No. 5	Long hull, control No. 5	Long hull, control No. 5, computed from short
				1	2	3	4			
Degrees	Degrees									
0	0	−0.001	−0.001	+0.014	+0.012	+0.027	+0.025	+0.015	+0.017	+0.015
	+2	+0.035	+0.036	+0.093	+0.062	+0.114	+0.113	+0.080	+0.079	+0.081
	+4	+0.083	+0.082	+0.193	+0.164	+0.226	+0.203	+0.157	+0.157	+0.160
	+7	+0.191	+0.179	+0.372	+0.322	+0.435	+0.421	+0.318	+0.345	+0.330
	+10	+0.322	+0.304	+0.625	+0.552	+0.681	+0.681	+0.567	+0.587	+0.585
	+15	+0.619	+0.574							
	−10								−.428	
	−7								−.210	
	−4								−.063	
	−2								+0.007	
+10	0								+0.070	
	+2								+0.136	
	+4								+0.224	
	+7								+0.402	
	+10								+0.666	
	−10			−.425	−.389	−.399	−.349	−.401	−.396	−.419
	−7			−.198	−.188	−.192	−.130	−.191	−.180	−.203
	−4			−.033	−.040	+0.009	+0.049	−.023	−.022	−.026
	−2			+0.045	+0.039	+0.110	+0.137	+0.051	+0.052	+0.050
	0			+0.110	+0.097	+0.192	+0.216	+0.116	+0.116	+0.116
+15	+2			+0.184	+0.165	+0.286	+0.305	+0.185	+0.188	+0.186
	+4			+0.284	+0.256	+0.435	+0.407	+0.273	+0.290	+0.276
	+7			+0.512	+0.421	+0.624	+0.612	+0.462	+0.477	+0.474
	+10			+0.803	+0.653	+0.857	+0.840	+0.710	+0.726	+0.728

Z FORCE, IN POUNDS, FOR HULLS WITH NO. 6 CONTROL SURFACES

[Model at 0° yaw and rudders neutral. Air speed, 40 miles per hour]

Elevator setting δ_e	Angle of pitch θ	Fins No. 6 (without elevators or rud- ders) on—		Control No. 6A on—		Control No. 6B on—		Control No. 6C on—		Control No. 6D on—	
		Short hull	Long hull	Short hull	Long hull	Short hull	Long hull	Short hull	Long hull	Short hull	Long hull
Degrees	Degrees										
0	0	+0.017	+0.017	+0.019	+0.019	+0.017	+0.017	+0.019	+0.019	+0.015	+0.015
	+2	+0.078	+0.079	+0.083	+0.084	+0.084	+0.085	+0.087	+0.088	+0.083	+0.084
	+4	+0.147	+0.150	+0.163	+0.166	+0.163	+0.166	+0.165	+0.168	+0.169	+0.172
	+7	+0.287	+0.299	+0.337	+0.349	+0.337	+0.349	+0.348	+0.360	+0.353	+0.365
	+10	+0.516	+0.534	+0.574	+0.592	+0.587	+0.605	+0.595	+0.613	+0.603	+0.621
	+15	+0.946	+0.988	+1.068	+1.110	+1.080	+1.122	+1.085	+1.127	+1.102	+1.144
	-15			-0.907	-0.949	-0.871	-0.913	-0.850	-0.892	-0.838	-0.880
	-10			-0.447	-0.465	-0.437	-0.455	-0.425	-0.443	-0.414	-0.432
	-7			-0.232	-0.244	-0.223	-0.235	-0.218	-0.230	-0.202	-0.214
	-4			-0.071	-0.074	-0.059	-0.062	-0.028	-0.031	-0.034	-0.037
+10	-2			+0.015	+0.014	+0.025	+0.024	+0.031	+0.030	+0.042	+0.041
	0			+0.074	+0.074	+0.085	+0.085	+0.092	+0.092	+0.105	+0.105
	+2			+0.148	+0.149	+0.157	+0.158	+0.170	+0.171	+0.179	+0.180
	+4			+0.230	+0.233	+0.245	+0.248	+0.254	+0.257	+0.277	+0.280
	+7			+0.410	+0.422	+0.426	+0.438	+0.438	+0.450	+0.456	+0.468
	+10			+0.645	+0.663	+0.666	+0.684	+0.684	+0.702	+0.704	+0.722
	+15			+1.140	+1.182	+1.163	+1.205	+1.178	+1.220	+1.201	+1.243
	-15			-0.788	-0.830	-0.671	-0.713	-0.754	-0.796	-0.730	-0.772
	-10			-0.385	-0.403	-0.371	-0.389	-0.352	-0.370	-0.330	-0.348
	-7			-0.177	-0.189	-0.158	-0.170	-0.148	-0.160	-0.129	-0.141
+20	-4			+0.006	+0.003	+0.008	+0.005	+0.020	+0.017	+0.084	+0.081
	-2			+0.074	+0.073	+0.099	+0.098	+0.105	+0.104	+0.125	+0.124
	0			+0.133	+0.133	+0.154	+0.154	+0.172	+0.172	+0.195	+0.195
	+2			+0.204	+0.205	+0.221	+0.222	+0.245	+0.246	+0.253	+0.254
	+4			+0.287	+0.290	+0.314	+0.317	+0.340	+0.343	+0.367	+0.370
	+7			+0.483	+0.495	+0.514	+0.526	+0.549	+0.561	+0.566	+0.578
	+10			+0.721	+0.739	+0.773	+0.791	+0.800	+0.818	+0.826	+0.844
	+15			+1.221	+1.263	+1.269	+1.311	+1.323	+1.365	+1.341	+1.383

TABLE XXX

NET MEASURED YAWING MOMENT FOR SHORT MODEL AND COMPUTED YAWING MOMENT IN POUND-FEET FOR LONG MODEL WITH NO. 6 CONTROL SURFACES

[Model at 0° pitch and elevators neutral. Moment axis at C. B. Air speed, 40 miles per hour]

Rudder setting δ_r	Angle of yaw ψ	Fins No. 6 (without elevators or rudders) on—		Control No. 6A on—		Control No. 6B on—		Control No. 6C on—		Control No. 6D on—	
		Short hull	Long hull	Short hull	Long hull	Short hull	Long hull	Short hull	Long hull	Short hull	Long hull
0	Degrees	0	0	0	0	0	0	0	0	0	0
	0	0	0	0	0	0	0	0	0	0	0
	+2	+.234	+.277	+.207	+.249	+.204	+.246	+.208	+.249	+.207	+.248
	+4	+.450	+.535	+.402	+.468	+.400	+.466	+.404	+.470	+.403	+.469
	+6	+.695	+.789	+.646	+.739	+.638	+.730	+.633	+.724	+.617	+.707
	+8	+.812	+.984	+.758	+.826	+.745	+.812	+.733	+.799	+.712	+.777
	+10	+.812	+.984	+.758	+.826	+.745	+.812	+.733	+.799	+.712	+.777
	+12	+.910	+.993	+.830	+.906	+.811	+.890	+.800	+.872	+.767	+.836
	+14			+.830	+.906	+.811	+.890	+.800	+.872	+.767	+.836
	+16			+.830	+.906	+.811	+.890	+.800	+.872	+.767	+.836
	+18			+.830	+.906	+.811	+.890	+.800	+.872	+.767	+.836
	+20			+.830	+.906	+.811	+.890	+.800	+.872	+.767	+.836
	+22			+.830	+.906	+.811	+.890	+.800	+.872	+.767	+.836
	+24			+.830	+.906	+.811	+.890	+.800	+.872	+.767	+.836
	+26			+.830	+.906	+.811	+.890	+.800	+.872	+.767	+.836
+10	Degrees	0	0	0	0	0	0	0	0	0	0
	0	0	0	0	0	0	0	0	0	0	0
	+2			+.074	+.109	+.054	+.087	+.033	+.065	+.017	+.049
	+4			+.263	+.322	+.250	+.306	+.225	+.280	+.192	+.245
	+6			+.478	+.561	+.456	+.536	+.414	+.492	+.372	+.446
	+8			+.584	+.640	+.551	+.605	+.502	+.554	+.458	+.508
	+10			+.651	+.716	+.592	+.651	+.544	+.604	+.485	+.539
	+12			+.651	+.716	+.592	+.651	+.544	+.604	+.485	+.539
	+14			+.651	+.716	+.592	+.651	+.544	+.604	+.485	+.539
	+16			+.651	+.716	+.592	+.651	+.544	+.604	+.485	+.539
	+18			+.651	+.716	+.592	+.651	+.544	+.604	+.485	+.539
	+20			+.651	+.716	+.592	+.651	+.544	+.604	+.485	+.539
	+22			+.651	+.716	+.592	+.651	+.544	+.604	+.485	+.539
	+24			+.651	+.716	+.592	+.651	+.544	+.604	+.485	+.539
	+26			+.651	+.716	+.592	+.651	+.544	+.604	+.485	+.539
+20	Degrees	0	0	0	0	0	0	0	0	0	0
	0	0	0	0	0	0	0	0	0	0	0
	+2			+.130	+.181	+.083	+.133	+.042	+.086	+.038	+.004
	+4			+.328	+.401	+.275	+.340	+.202	+.267	+.106	+.167
	+6			+.426	+.475	+.352	+.393	+.282	+.320	+.171	+.207
	+8			+.426	+.475	+.352	+.393	+.282	+.320	+.171	+.207
	+10			+.426	+.475	+.352	+.393	+.282	+.320	+.171	+.207
	+12			+.426	+.475	+.352	+.393	+.282	+.320	+.171	+.207
	+14			+.426	+.475	+.352	+.393	+.282	+.320	+.171	+.207
	+16			+.426	+.475	+.352	+.393	+.282	+.320	+.171	+.207
	+18			+.426	+.475	+.352	+.393	+.282	+.320	+.171	+.207
	+20			+.426	+.475	+.352	+.393	+.282	+.320	+.171	+.207
	+22			+.426	+.475	+.352	+.393	+.282	+.320	+.171	+.207
	+24			+.426	+.475	+.352	+.393	+.282	+.320	+.171	+.207
	+26			+.426	+.475	+.352	+.393	+.282	+.320	+.171	+.207

TABLE XXXI

YAW FORCES AND MOMENTS ON LONG MODEL HULL WITH NO. 5 CONTROL SURFACES

[Model at 0° pitch. Elevators and rudders neutral. Air speed, 30 miles per hour]

Angle of yaw ψ	Net measured cross-wind force C	Net measured drag D	Yawing moment N , axis 0.61" aft C. B.	X force	Y force	Yawing moment N , axis at C. B.
Degrees	Pounds	Pounds	Pound-inches	Pounds	Pounds	Pound-feet
0	0	0.090	0	+.090	0	0
+15	-.560	.237	+6.72	+.085	-.602	+.529
+30	-1.342	.847	+5.06	+.062	-1.585	+.341
+45	-1.980	1.936	+3.02	-.032	-2.769	+.111
+60	-1.975	2.962	+4.16	-.230	-3.553	+.166
+75	-1.457	3.665	+.35	-.461	-3.916	-.169
+90	-.477	3.738	-14.69	-.477	-3.738	-1.415

TABLE XXXII

OSCILLATION DATA FOR LONG MODEL AND APPARATUS AT VARIOUS AIR SPEEDS

[Model at 0° pitch. Elevators and rudders neutral]

Air speed, miles per hour	Number of oscillations to reduce amplitude from 3.5 to ψ									
	Amplitude ψ (degrees)									
	3.5	3.0	2.6	2.3	2.0	1.8	1.6	1.4	1.2	1.0
Apparatus and bare hull combined										
0	0	14.0	27.5	39.0	51.5	61.0	72.0	84.5	98.5	115.0
10	0	12.0	22.5	31.5	42.0	50.0	59.0	69.0	80.5	94.0
20	0	9.5	18.5	26.5	34.5	41.5	48.5	57.0	66.5	78.0
30	0	8.5	16.0	22.5	29.5	35.0	41.0	49.5	56.5	65.5
Apparatus and hull with control No. 1 combined										
0	0	14.5	28.0	39.0	52.5	62.0	73.0	85.5	99.5	116.5
10	0	7.5	15.0	21.0	27.5	32.5	38.5	45.0	52.5	61.0
20	0	5.5	10.0	14.0	19.0	22.5	26.5	31.0	36.0	42.0
30	0	4.0	7.5	10.5	14.0	17.0	20.0	23.0	27.0	31.5
Apparatus and hull with control No. 2 combined										
0	0	15.0	28.5	40.0	53.5	63.0	74.0	87.0	101.0	119.0
10	0	8.0	15.5	22.0	29.0	35.0	41.0	48.0	56.0	65.5
20	0	5.5	11.0	15.0	20.0	24.0	28.0	33.0	38.5	45.0
30	0	4.0	8.0	11.5	15.0	18.0	21.0	25.0	29.0	34.0
Apparatus and hull with control No. 3 combined										
0	0	14.0	27.5	39.0	51.5	61.0	72.5	85.0	99.0	116.0
10	0	6.5	12.5	17.5	23.5	28.0	33.0	38.5	45.0	53.0
20	0	4.5	8.5	12.0	16.0	19.0	22.5	26.5	31.0	36.0
30	0	3.0	6.5	9.0	11.5	14.0	16.5	19.0	22.5	26.0
Apparatus and hull with control No. 4 combined										
0	0	14.0	27.5	39.0	51.5	61.5	72.0	84.5	98.5	115.0
10	0	7.0	14.0	19.5	25.5	31.0	36.0	42.5	49.5	58.0
20	0	5.0	9.0	12.5	17.0	20.0	23.5	27.5	32.0	37.5
30	0	3.5	7.0	9.0	12.5	15.0	17.5	20.5	24.0	28.0
Apparatus and hull with control No. 6A combined										
0	0	15.0	28.5	40.0	53.0	63.0	74.0	86.0	100.0	117.5
10	0	8.0	15.0	21.0	28.0	34.0	40.0	46.5	54.0	64.0
20	0	5.0	9.5	13.5	18.0	21.5	25.0	29.5	34.5	40.0
30	0	3.5	7.0	10.0	13.5	16.0	19.0	22.0	26.0	30.5
Apparatus and hull with control No. 6D combined										
0	0	14.0	27.5	39.0	52.0	61.5	72.0	85.0	99.0	116.0
10	0	7.5	14.0	20.0	26.5	31.5	37.0	43.5	51.0	59.5
20	0	5.0	9.5	13.0	17.5	21.0	25.0	29.0	34.0	40.0
30	0	3.5	7.0	10.0	13.0	16.0	19.0	22.0	26.0	30.0
Apparatus alone (taken after test on bare hull)										
0	0	16.0	30.0	42.0	55.5	66.0	77.5	90.0	105.0	123.0
10	0	12.5	23.5	33.0	44.5	53.0	62.0	72.0	84.0	98.0
20	0	10.5	20.0	28.0	37.0	44.0	51.5	60.0	70.0	81.5
30	0	9.0	17.0	24.0	32.0	38.0	44.5	52.0	61.0	71.0
Apparatus alone (taken after test on hull with No. 2 control)										
0	0	16.0	30.0	43.0	57.0	67.5	79.5	92.5	108.0	126.0
10	0	13.0	24.5	34.5	46.0	55.0	64.5	75.5	88.0	103.0
20	0	10.8	20.0	28.0	37.5	44.0	51.5	61.0	70.5	82.0
30	0	8.5	16.5	24.0	32.0	38.5	45.0	53.0	62.0	72.0

TABLE XXXIII

COEFFICIENT OF DAMPING MOMENT FOR LONG MODEL AND APPARATUS AT VARIOUS AIR SPEEDS

[Model at 0° pitch. Elevators and rudders neutral]

Air speed, miles per hour	Number of oscillations to damp amplitude from 3° to 2° = n	Duration of damping t (seconds)	Period of complete oscillation $T = t/n$ (seconds)	Logarith- mic decrement $\lambda = \frac{1}{n} \log_2 \frac{3^\circ}{2^\circ}$ = .405/ n	Coefficient of damping moment μ_0 or $\mu_a = \frac{2I\lambda}{T}$ (slug-ft. ² / sec.)
Bare hull and apparatus combined					
0	37.5	61.6	1.643	0.0108	0.055
10	30.0	49.5	1.650	.0135	.069
20	25.0	42.8	1.671	.0162	.082
30	21.0	35.9	1.708	.0193	.095
Hull with control No. 1 and apparatus combined					
0	38.0	64.3	1.692	0.0107	0.056
10	20.0	34.3	1.713	.0203	.107
20	13.5	23.3	1.727	.0300	.155
30	10.0	17.6	1.763	.0405	.205
Hull with control No. 2 and apparatus combined					
0	38.5	66.5	1.728	0.0105	0.057
10	21.0	36.4	1.732	.0193	.104
20	14.5	25.4	1.749	.0279	.149
30	11.0	19.6	1.780	.0368	.193
Hull with control No. 3 and apparatus combined					
0	37.5	64.8	1.727	0.0108	0.058
10	17.5	30.4	1.737	.0231	.124
20	11.5	20.1	1.750	.0352	.187
30	8.5	15.1	1.777	.0477	.250
Hull with control No. 4 and apparatus combined					
0	37.5	65.4	1.743	0.0108	0.059
10	18.5	32.2	1.741	.0219	.119
20	12.0	21.1	1.762	.0338	.182
30	9.0	16.1	1.786	.0450	.239
Hull with control No. 6A and apparatus combined					
0	38.0	66.4	1.747	0.0107	0.058
10	20.0	35.0	1.748	.0203	.110
20	13.0	22.9	1.765	.0300	.162
30	10.0	17.9	1.790	.0405	.216
Hull with control No. 6D and apparatus combined					
0	38.0	66.6	1.751	0.0107	0.058
10	19.0	33.3	1.750	.0213	.117
20	12.5	22.1	1.770	.0324	.175
30	9.5	17.0	1.790	.0426	.228
Apparatus alone (taken after test on bare hull)					
0	39.5	47.8	1.211	0.0103	0.039
10	32.0	38.8	1.213	.0127	.048
20	26.5	32.2	1.214	.0153	.058
30	23.0	28.0	1.215	.0176	.066
Apparatus alone (taken after test on hull with control No. 2)					
0	41.0	49.6	1.211	0.0099	0.037
10	33.0	40.0	1.213	.0123	.046
20	27.5	33.4	1.214	.0147	.056
30	23.5	28.6	1.215	.0172	.065

¹ For values of I see Table XXXIV. μ_0 = Coefficient of damping moment for model and apparatus combined. μ_a = Coefficient of damping moment for apparatus alone.

TABLE XXXIV
COMPUTATIONS FOR MOMENT OF INERTIA $I=K_o T^2/4\pi^2$
[$K_o=M/\psi=61.60$ lb.-ft./rad. $4\pi^2=39.47$]

Oscillating system	<i>T</i> (seconds)	<i>I</i> (slug- feet. ²)
Bare hull and apparatus combined.....	1.643	4.213
Hull with control No. 1 and apparatus combined.....	1.692	4.467
Hull with control No. 2 and apparatus combined.....	1.728	4.661
Hull with control No. 3 and apparatus combined.....	1.727	4.655
Hull with control No. 4 and apparatus combined.....	1.743	4.740
Hull with control No. 6A and apparatus combined.....	1.747	4.763
Hull with control No. 6D and apparatus combined.....	1.751	4.785
Apparatus alone.....	1.211	2.288

TABLE XXXV
COEFFICIENT OF DAMPING MOMENT FOR LONG MODEL ALONE AT VARIOUS AIR SPEEDS
[Model at 0° pitch. Elevators and rudders neutral]

Air speed, miles per hour	Apparatus and model combined, $\frac{2I\lambda}{T}$ $\mu_c = \frac{2I\lambda}{T}$ (Slug-ft. ² /sec.)	Oscillating apparatus alone, $\frac{2I_a\lambda_a}{T_a}$ $\mu_a = \frac{2I_a\lambda_a}{T_a}$ (Slug-ft. ² /sec.)	Model alone, $\mu = \mu_c - \mu_a$ (Slug-ft. ² /sec.)
Bare hull			
0	0.055	0.039	0.016
10	.069	.048	.021
20	.082	.058	.024
30	.095	.066	.029
Hull with control surfaces No. 1			
0	0.056	0.039	0.017
10	.107	.048	.059
20	.155	.058	.097
30	.205	.066	.139
Hull with control surfaces No. 2			
0	0.057	0.037	0.020
10	.104	.046	.058
20	.149	.056	.093
30	.193	.065	.128
Hull with control surfaces No. 3			
0	0.058	0.037	0.021
10	.124	.046	.078
20	.187	.056	.131
30	.250	.065	.185
Hull with control surfaces No. 4			
0	0.059	0.037	0.022
10	.119	.046	.073
20	.182	.056	.126
30	.239	.065	.174
Hull with control surfaces No. 6A			
0	0.058	0.037	0.021
10	.110	.046	.064
20	.162	.056	.106
30	.216	.065	.151
Hull with control surfaces No. 6D			
0	0.059	0.037	0.021
10	.117	.046	.071
20	.175	.056	.119
30	.228	.065	.163

TABLE XXXVI

STABILITY CRITERION FOR LONG MODEL IN YAW

[Model at 0° pitch. Elevators and rudders neutral. Test speed, 40 miles per hour]

Condition of model	Moment arms ³		Criterion ² = ratio of arms= $\frac{\mu^1 Y_\psi}{a \frac{N_\psi}{u}}$
	Disturbing	Reacting	
	N_ψ/Y_ψ	$a\mu/u^1$	
	<i>Per cent</i>	<i>Per cent</i>	
Bare hull.....	-145.7	1.58	-0.011
Hull with No. 1 controls.....	-58.8	15.57	-.265
Hull with No. 2 controls.....	-82.2	12.86	-.156
Hull with No. 3 controls.....	-38.9	21.15	-.544
Hull with No. 4 controls.....	-56.8	19.86	-.350
Hull with No. 6A controls.....	-76.4	16.63	-.218
Hull with No. 6D controls.....	-73.2	18.83	-.257

¹ Here, μ/u denotes slopes of lines in Figure 32.
² This criterion = $Y_\psi N_\psi / UN_\psi$, see Report No. 212, National Advisory Committee for Aeronautics.
 (Y_ψ, N_ψ) = ($\partial Y/\partial \psi, \partial N/\partial \psi$) at $\psi=0^\circ$.
 $a=s^3/m$ =scale ratio³/mass of ship.
 = 120³/5426.67 slugs=318.4.
³ Given in percentage of airship length=644.68 feet.

REPORT No. 216

THE REDUCTION OF AIRPLANE FLIGHT TEST DATA TO STANDARD ATMOSPHERE CONDITIONS

By WALTER S. DIEHL
Bureau of Aeronautics, Navy Department

and

E. P. LESLEY
Stanford University

REPORT No. 216

THE REDUCTION OF AIRPLANE FLIGHT TEST DATA TO STANDARD ATMOSPHERE CONDITIONS

By WALTER S. DIEHL and E. P. LESLEY

SUMMARY

This paper was prepared for the National Advisory Committee for Aeronautics in order to supply the need of practical methods of reducing observed performance to standard conditions with a minimum of labor. The first part gives a very simple approximate method of reducing performance in climb, and is particularly adapted to work not requiring extreme accuracy. The second part gives a somewhat more elaborate and more accurate method which is well suited to general flight test reduction. The third part gives the conventional method of calibrating air-speed indicators and reducing the indicated speeds to true air speeds. An appendix gives working tables and charts for the standard atmosphere.

PART I

THE REDUCTION OF TEST DATA IN CLIMB TO STANDARD CONDITIONS—A SIMPLE APPROXIMATE METHOD

By WALTER S. DIEHL

SUMMARY

This paper was prepared for the National Advisory Committee for Aeronautics to illustrate a simplified method of reducing observed airplane performance data to standard conditions. The method is based on the assumption that under any normal conditions of pressure and temperature, that is, at any given air density, the instantaneous climb (or speed) has the same value that it would have at the same density in standard atmosphere. This assumption allows the corrections to be made to the altitude rather than to a rate of climb deduced from successive altimeter or aneroid readings. As a result, the calculations are reduced to approximately 25 per cent of the amount required by the old method. The results by both methods are in substantial agreement.

The principle of correcting to altitude in the standard atmosphere is also applied to the reduction of air-speed meter readings to true air speeds.

INTRODUCTION

The performance of an airplane must depend on the relations between the power required and the power available. Consequently, in a study of the variations of performance due to changes in atmospheric conditions we must consider the variations of each factor. For any given airplane, at a given air speed, the power required will vary as the square root of the air density. The power available from a conventional airplane engine varies with both pressure and temperature, according to the relations given in National Advisory Committee for Aeronautics Technical Report No. 171. The propeller efficiency at a given slip is probably independent of the pressure and slightly dependent on temperature (i. e., in so far as the viscosity is concerned). The resultant effect of the variations is very difficult to predict unless we assume

a standard atmosphere in which there are definite relations between pressure, temperature, density, and altitude. For the same reasons the observed performance of a given airplane is variable from day to day, so that it is necessary to reduce the observations to standard conditions in order to obtain comparable values.

Unfortunately the reduction of performance data to standard conditions is a tedious process when the usual methods are employed; so tedious, in fact, that few engineers have had the patience to master the methods, and so uncertain that the final results by different methods are not always in accordance with each other. It is the purpose of this paper to present a very simple method based on the assumptions that the rate of climb decreases uniformly with increase in altitude and that the instantaneous climb for normal pressures and temperatures; that is, for any given density, has the same value that it would have at the same density in standard atmosphere. The former assumption is verified by test data and is frequently taken as an accepted fact. The second assumption not only seems to be justified in view of the very small average value of the corrections which must be made for strict accuracy, but it also leads to a great simplification in the method of reduction to standard conditions.

In Part III of this report the conventional method for reducing air-speed meter readings to true airspeeds has been developed along the same lines followed in reducing performance in climb. When these methods are used it will be found that the data from a complete performance test may be quickly reduced to standard conditions. As will be shown later, the results are in substantial agreement with those obtained by the use of the more complicated methods.

For the information of the reader who wishes to compare the new method with the conventional methods reference is made to Chapter IX of Bairstow's *Applied Aerodynamics*, or to the various reports of the British Advisory Committee for Aeronautics, R. & M. 324, 474, 608, etc.

OUTLINE OF THE METHOD

The following brief outline will indicate the steps taken to reduce an observed performance in climb to standard conditions: First, obtain the atmospheric pressures p , either from aneroid readings or from the altimeter readings Z_1 . Next there is found the altitude in standard atmosphere Z_e , at which the density is the same as that determined by each pressure p , and the corresponding observed air temperature t . A time-of-climb curve is then plotted with the equivalent altitudes Z_e as ordinates and the corresponding times T as abscissas. The rates of climb are determined at any desired number of points along this curve by the corresponding tangents. The values so found are plotted as abscissas to some convenient scale against Z_e as ordinates and a straight line is drawn through the points which will give the most probable climb at each altitude. In most cases this line will be well defined. From it the corrected time-of-climb curve is calculated. A table may now be made giving, according to requirements, a series of altitudes in standard atmosphere with the corresponding rate of climb and time of climb. This completes the reduction of the climb data to standard conditions.

The data required for this method of reduction are: Either aneroid pressure readings or the initial pressure p_0 (i. e., the barometric pressure at which the altimeter reads zero), and the altimeter readings Z_1 , time of climb T , and corresponding air temperatures t . Obviously such data as weight of airplane, type and condition of engines, characteristics of propeller, weather conditions, etc., should be taken for general information. R.P.M. and air-speed meter readings are also desirable and should be taken along with the test data.

Whenever possible an aneroid which reads pressure directly should be used. This will eliminate the conversion of altimeter readings to pressures and thus give somewhat greater accuracy to the reduction.

CONVERSION OF ALTIMETER READINGS TO PRESSURES

Standard altimeters in use in the United States are constructed and graduated to read altitudes corresponding to pressures given by the modified Halley's equation

$$Z_1 = 62,900 \log_{10} \left(\frac{29.90}{p} \right) \quad (1)$$

where Z_i is the altimeter reading in feet and p the barometric pressure in inches. The constant 62,900 in this equation corresponds to a mean air temperature of $+10^\circ \text{C}$. and to the average humidity. Only when these conditions are fulfilled does an altimeter read the true altitude. However, the instrument is actuated by pressure, and owing to its uniformly divided scale the barometric pressure corresponding to any reading may readily be obtained from equation (1) written in the form

$$Z_i = 62,900 \log_{10} \left(\frac{p_0}{p} \right) \quad (2)$$

where p_0 is the barometric pressure at which the instrument reads zero. p may be calculated from (2) or read directly from the curve in Figure 1, which is a plot of the data in Table I.

Specimen calculations of p will be found in columns 4 and 5 of Table II, using actual test data taken from Table 10, Chapter IX, of Applied Aerodynamics (Baird). The value of

$\frac{p}{p_0}$ corresponding to each altimeter reading has been read from the curve in Figure 1. The next step is to find the altitude in standard atmosphere having the density determined by p and t . This altitude will be called the "equivalent altitude" and denoted by the symbol Z_e .

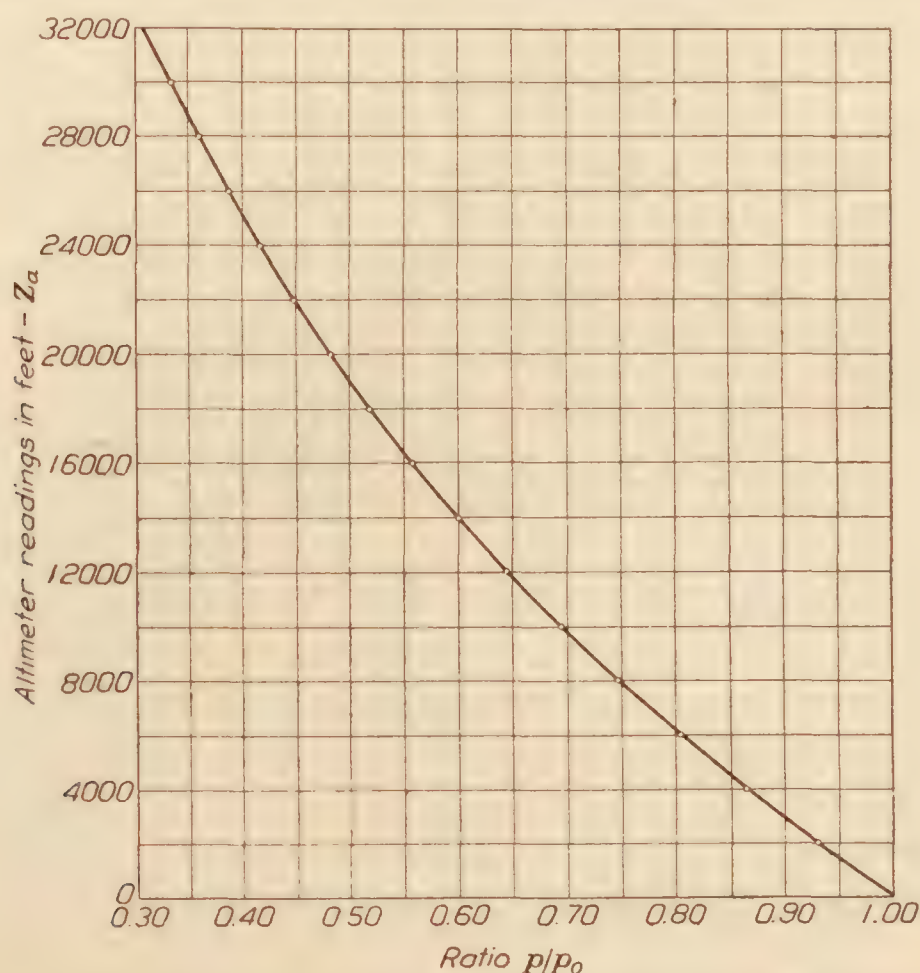


FIG. 1.—Relation between pressure ratio and altimeter reading. (Altimeter reading zero when $p=p_0$)

EQUIVALENT ALTITUDE IN STANDARD ATMOSPHERE

In the standard atmosphere there are definite relations between p , t , ρ , and Z , but we may, without appreciable error, neglect the deviations from normal in p and t and say that the altitude in standard atmosphere corresponding to the density determined by actual values of p and t is an "equivalent altitude" for the observed conditions. That is, the equivalent altitude in standard atmosphere Z_e for any given p and t is that altitude in the standard atmosphere at which the density is that determined by the given values of p and t .

Z_e may be calculated from the equations in National Advisory Committee for Aeronautics Technical Note No. 99, or read directly from the chart in Figure 2. The values in column 6 of Table II were read from Figure 2.

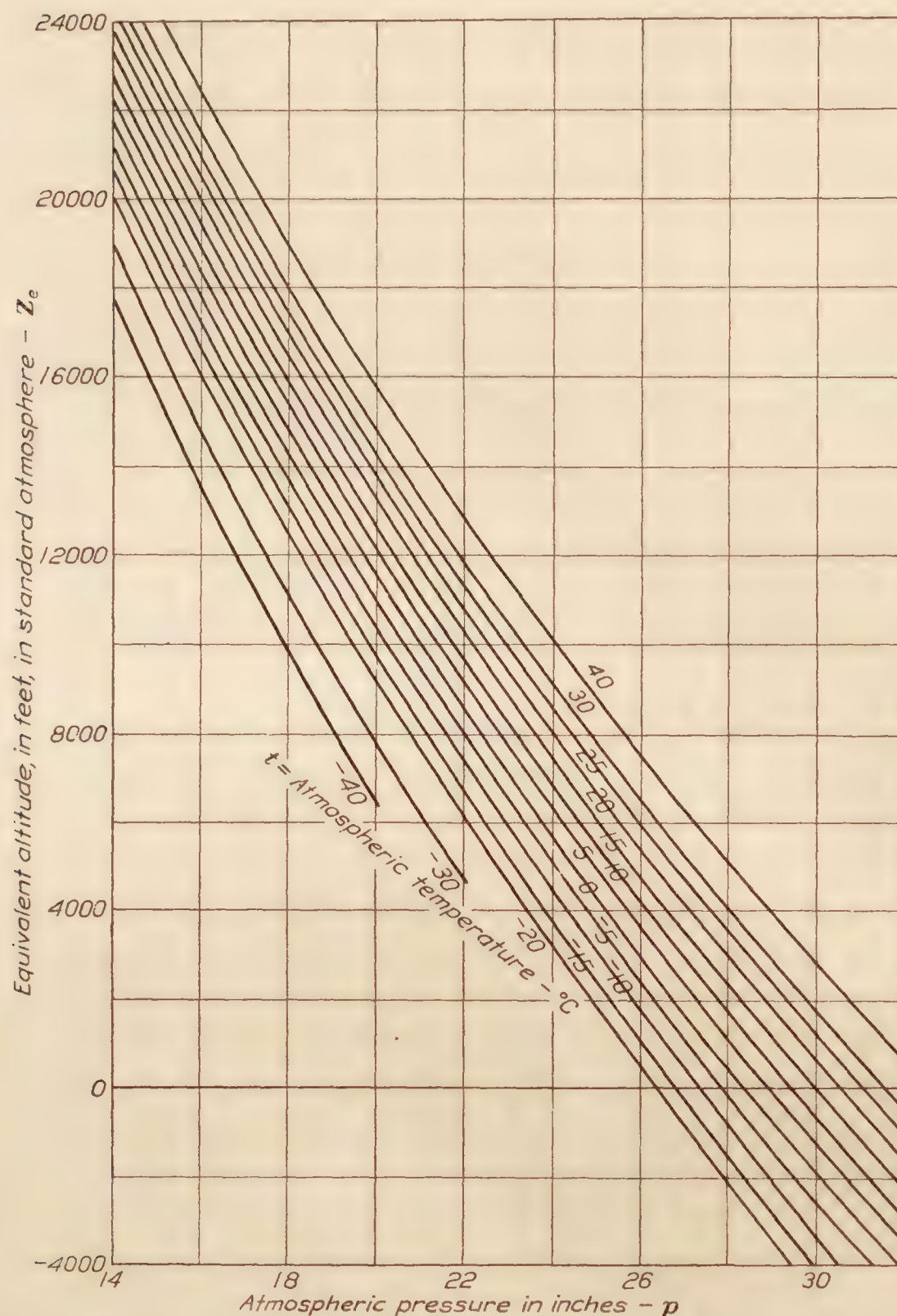


FIG. 2.—Equivalent altitude in standard atmosphere for any given pressure and temperature for use in reducing observed performance to standard conditions

RATE OF CLIMB IN STANDARD ATMOSPHERE

A plot is now made of Z_e against the recorded time T , as in Figure 3, which employs the data from Table II. It is desirable to adopt the largest convenient scale for both variables in this plot, since an open scale enables the slope of the tangent which determines the rate of climb to be read with greater accuracy. When drawing in the curve of Z_e against T great care must be taken in order that it may truly represent the observed data. Some judgment is required to draw it correctly. The curve should pass through every point if practicable, although points which are obviously high or low may be ignored.

The rate of climb at any desired altitude is obtained directly from the slope of tangent at that altitude. The tangent may be obtained in several ways, but the most satisfactory method seems to be the old one in which two transparent triangles are used, one being held fixed and the other slid along it until the parallel to the tangent passes through the origin. This line then intersects the 10-minute abscissa at an altitude which is obviously 10 times the desired rate of climb.

Fortunately, the errors, which are cumulative in time readings, do not affect the rate of climb obtained from the slope of any portion of the climb curve, which is a "true climb." For example, it frequently happens that a cautious pilot does not obtain the maximum climb until an altitude of several thousand feet is reached, or an inexperienced pilot may not obtain the best climb at high altitudes. In either case, if the best climb be obtained and held for a few thousand feet, it will be sufficient to determine the straight line which represents the best rate of climb plotted against altitude. Consequently, the rates of climb as determined by the slopes of the tangents are plotted against altitude and a straight line drawn through the values which give the most probable climb. Scattered high or low values in rate of climb may be neglected entirely, although the rate of climb is more often low than high when incorrect.

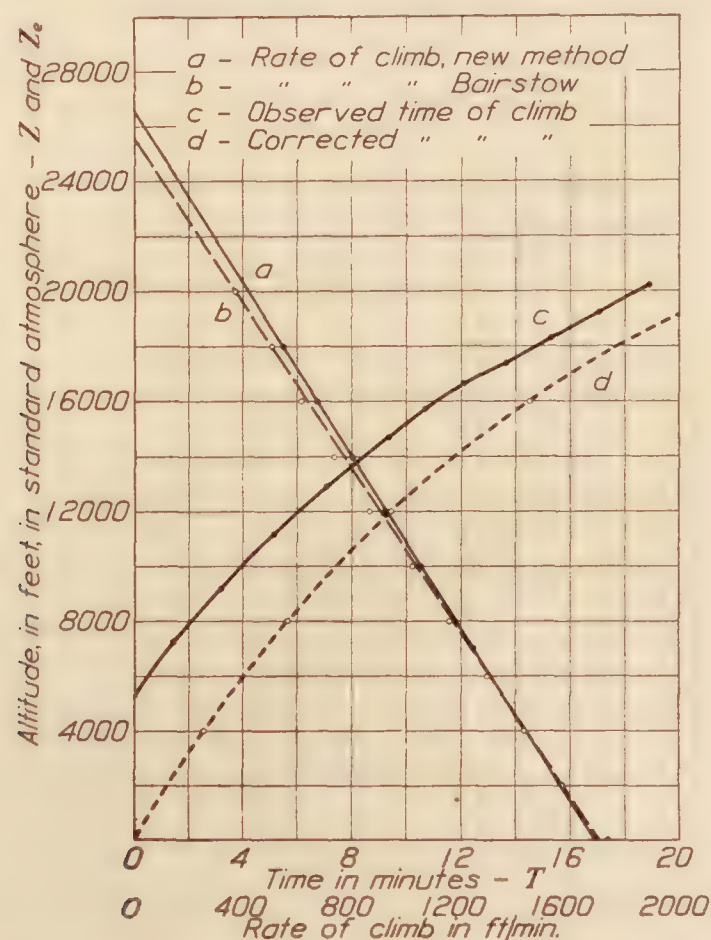


FIG. 3.—Reduction of test data in climb to standard conditions with comparison of results by old and new methods

NOTE.—Observed time of climb is from test data given in Table 10, Chapter IX, "Applied Aerodynamics."

The correct time-of-climb curve may be constructed from the rate-of-climb line either by the use of average rate of climb over short intervals of altitude, or better, by the use of the equation

$$T \text{ minutes} = 2.304 \left(\frac{Z_a}{C_o} \right) \log_{10} \left(\frac{Z_a}{Z_a - Z} \right) \quad (3)$$

where Z_a is the absolute ceiling, Z the altitude to which the time of climb T is desired, and C_o the initial rate of climb. Note that C_o and Z_a are given by the intersections of the rate-of-climb line with the rate-of-climb axis and the altitude axis, respectively.

COMPARISON OF METHODS

The test data used in Table II to illustrate the simplified method of reduction was taken from Chapter IX, Applied Aerodynamics, where it is reduced to standard conditions according to the British method. Unfortunately the ground pressure is not given with this data and must be assumed. The altitudes are given by Bairstow as "aneroid height" without qualification. It is therefore probable that the instrument had a fixed instead of an adjustable scale. Assuming this to be the case, the initial pressure must be $p_o = 29.92$ inches, the value here adopted.

When these data are reduced by the simplified method, the time-of-climb curve plots as in Figure 3. The tangents to this curve give the rates of climb indicated by dots. Bairstow's values for rate of climb are indicated by circles. Assuming that the rate of climb is a linear function of altitude, a straight line has been drawn through each set of reduced rates of climb. It will be noted that the difference is comparatively small and that it is greatest at high altitudes when the corrections are most difficult to apply. The difference in the indicated absolute ceiling is 1,000 feet in 26,000 feet, about 4 per cent. This is ordinarily less than the precision of the test data.

In order that the differences between the two methods may be made more clear, Table III has been prepared. In this table the rate of climb and time of climb are given at a series of altitudes for three cases: (1) The actual figures obtained from reduction of the test data by the old method; (2) the same figures corrected on the assumption that the rate of climb is linear with altitude; and (3) the corresponding results obtained by the simplified method of reduction.

TABLE I

RELATION BETWEEN ALTIMETER READING AND ATMOSPHERIC PRESSURE

$$Z_a = 62,900 \log_{10} \left(\frac{p_0}{p} \right)$$

Z_a	$\frac{p}{p_0}$
Feet	
0	1.0000
1,000	.9640
2,000	.9294
3,000	.8954
4,000	.8638
5,000	.8327
6,000	.8028
7,000	.7735
8,000	.7461
9,000	.7193
10,000	.6935
12,000	.6445
14,000	.5990
16,000	.5567
18,000	.5174
20,000	.4809
22,000	.4469
24,000	.4154
26,000	.3861
28,000	.3588
30,000	.3335

TABLE II

REDUCTION OF PERFORMANCE TEST DATA ON HIGH-SPEED SCOUT

[Test data. $p_0 = 29.92$]

T	Z_a	t oC	p p_0	p	Z_e
Min., sec.	Alti- meter feet			Inches	Feet
0	0	27	1.000	29.92	+1,500
1.28	4,000	18	.864	25.85	5,300
3.12	6,000	15	.803	24.05	7,250
5.07	8,000	11	.746	22.32	9,150
7.04	10,000	7	.693	20.72	11,150
9.22	12,000	3	.644	19.27	12,900
10.41	14,000	-1	.600	17.95	14,700
12.03	15,000	-2	.518	17.30	15,750
13.38	16,000	-4	.557	16.68	16,650
15.18	17,000	-6	.538	16.10	17,400
17.04	18,000	-8	.518	15.50	18,300
18.50	19,000	-10	.499	14.93	19,200
	20,000	-10	.481	14.41	20,250

Test data in columns 1-3 are taken from Table X, Chapter IX of Applied Aerodynamics, Bairstow.

TABLE III

COMPARISON OF PERFORMANCE REDUCED TO STANDARD CONDITIONS BY OLD AND NEW METHODS

Z	Bairstow ¹		Bairstow ²		New method	
	$\frac{dZ}{dt}$	T	$\frac{dZ}{dt}$	T	$\frac{dZ}{dt}$	T
Feet	Feet per minute	Minutes	Feet per minute	Minutes	Feet per minute	Minutes
0	1,740	0	1,705	0	1,690	0
2,000	1,570	1.21	1,510	1.21	1,565	1.21
4,000	1,430	2.54	1,435	2.55	1,435	2.58
6,000	1,295	4.02	1,305	4.00	1,310	4.00
8,000	1,160	5.75	1,170	5.63	1,180	5.63
10,000	1,020	7.49	1,035	7.43	1,050	7.40
12,000	865	9.63	905	9.52	925	9.43
14,000	735	12.15	770	11.90	800	11.70
16,000	615	15.12	640	14.72	675	14.50
18,000	505	18.70	505	18.23	550	17.60
20,000	370	23.30	370	22.80	420	21.90

¹ Table 18, Chapter IX, Applied Aerodynamics. (Actual reduced values.)

² Same data, assuming $\left(\frac{dZ}{dt} \right)$ linear with Z .

PART II

REDUCTION OF AIRPLANE PERFORMANCE IN CLIMB TO STANDARD CONDITIONS

By E. P. LESLEY

SUMMARY

This is a description of the method proposed and used by the staff of the Langley Memorial Aeronautical Laboratory for the reduction of data secured in flight tests to the conditions of the standard atmosphere. It is assumed that, for the moderate changes of pressure and temperature generally encountered in passing from conditions of the actual atmosphere to those of the standard, the power and R. P. M. of the engine, as well as the thrust of the propeller and the lift and drag of the airplane, depend only upon the density, or upon the specific weight, of the air. Under this assumption, a simple method for transforming observed or recorded altitudes and times to altitudes and times for the standard atmosphere is described and illustrated. Rates of climb are determined by drawing tangents to the time-altitude curve.

INTRODUCTION

Experience with several methods of reducing flight-test data to the conditions of the standard atmosphere has led to the formulation and adoption of the following, which, while in some respects not new, and in others possibly not as accurate as might be desired, yet offers the advantages of simplicity, the reduction of the original barograph to the time-altitude curve for the standard atmosphere without preliminary plotting of rates of climb or other curves, and sufficient accuracy for any purpose such reduced data serve.

While the evidence of tests indicates that engine performance varies with air pressure and temperature, even though density remains constant, the introduction of corrections for such variation complicates the problem of reduction very considerably; and since these corrections are usually small, generally within the probable error in the original data, and not determinate without preliminary test of the engine, it appears that they may be neglected without serious consequences. Therefore it is assumed that the power and R. P. M. of the engine are constant for constant density, and do not change with temperature and pressure in passing from the encountered to the standard atmosphere, provided only that the density remains the same. This assumption being granted, it follows that air speed and rate of climb are constant for constant density.

STANDARD ATMOSPHERE

The air of the standard atmosphere is considered dry. The pressure at zero altitude is 760 mm. of mercury and the temperature is 15° centigrade. The specific weight is 1.2255 kg./m.³ The temperature gradient is -6.5° centigrade per thousand meters to an altitude of 10,769 meters, at which a temperature of -55° centigrade is reached. From this point upwards the temperature is assumed constant. Boyle's law, that density, or specific weight, varies directly as the absolute pressure and inversely as the absolute temperature, is assumed to apply throughout.

Using metric notation, in which

- Z = altitude, meters,
- t = temperature, degrees centigrade,
- T_m = harmonic mean temperature, degrees centigrade, absolute,
- p = pressure, millimeters of mercury,
- ρ = density, mass per unit volume, kg.-m.-sec.,
- $g\rho$ = specific weight, kg./m.,³

the conditions of the standard atmosphere may be formulated as follows:

For altitudes up to 10,769 meters

$$t = 15 - 0.0065Z \text{-----} 1$$

$$g\rho = 0.4644 \frac{p}{t + 273} \text{-----} 2$$

$$p = \left(\frac{44,308 - Z}{12,540} \right)^{5.256} \text{-----} 3$$

For altitudes above 10,769 meters

$$t = -55^\circ \text{-----} 4$$

$$g\rho = 0.0021303 p \text{-----} 5$$

$$\text{Log}_{10} p = 2.880814 - \frac{Z}{67.4072 T_m} \text{-----} 6$$

For all altitudes

$$dZ = \frac{-13.59 dp}{g\rho} \text{-----} 7$$

Using English notation, in which

- Z = altitude, feet,
 t = temperature, degrees Fahrenheit,
 T_m = harmonic mean temperature, degrees Fahrenheit, absolute.
 p = pressure, inches of mercury,
 ρ = density, mass per unit volume, lb.-ft.-sec.,
 $g\rho$ = specific weight, lb./cu. ft.,

For altitude up to 35,332 feet

$$t = 59 - 0.003566Z \text{ -----} 8$$

$$g\rho = \frac{1.3256p}{t + 459.4} \text{ -----} 9$$

$$p = \left(\frac{145,365 - Z}{76,140} \right)^{5.256} \text{ -----} 10$$

For altitudes above 35,332 feet

$$t = -67 \text{ -----} 11$$

$$g\rho = 0.003378p \text{ -----} 12$$

$$\log_{10} p = 1.475976 - \frac{Z}{122.862 T_m} \text{ -----} 13$$

For all altitudes

$$dZ = \frac{-70.67 dp}{g\rho} \text{ -----} 14$$

From formulas 1 to 14 the temperature, pressure, and specific weight or density at any altitude in the standard atmosphere are readily calculated. In the appendix, Tables VI and VII show the above quantities for metric and English units, respectively, while the associated Figures 7 and 8 show the specific weight altitude relations as tabulated.

The altitude in the standard atmosphere for specific weight equal to that of the air encountered in flight may be either read directly from the charts or interpolated from the tables, the specific weight of the encountered air having been first computed by formula (2) or (9). The charts are found to be more convenient but the tables more accurate. The former are, however, sufficiently accurate in the usual case.

REDUCTION OF FLIGHT DATA TO STANDARD CONDITIONS

The observed or recorded data consist essentially of time, air pressure, and air temperature. Indicated air speed, revolutions per minute, various engine pressures and temperatures, angle of attack, and any other desired data may be added to these. The pressure is often recorded in terms of indicated altitude, but this is, by a calibration of the instrument, readily converted into pressure in millimeters or inches of mercury.

The essential observed data, together with computations for the time-altitude relation for the standard atmosphere, are conveniently arranged under column headings as follows:

COLUMN NO.	SYMBOL	QUANTITY
1	T_o	Time, observed.
2	ΔT_o	Increment of time, observed.
3	p_o	Pressure, observed.
4	Δp_o	Increment of pressure, observed.
5	t_o	Temperature, observed.
6	$g\rho$	Specific weight (computed from observed temperature and pressure).
7	$g\rho_m$	Mean specific weight for altitude increment.
8	ΔZ_a	Increment of altitude, absolute.
9	Z_s	Altitude in standard atmosphere for equal specific weight.
10	ΔZ_s	Increment of altitude, standard atmosphere.
11	ΔT_s	Increment of time, standard atmosphere.
12	T_s	Time, standard atmosphere.

In the above it is to be noted that the observed times, pressures, and temperatures are presumed to have the correct values, or values determined from calibration curves of instruments used.

ΔT_o is the interval of time between two consecutive observations and equals

$$T_{o_2} - T_{o_1}, T_{o_3} - T_{o_2}, T_{o_4} - T_{o_3}, \text{ etc.}$$

In like manner Δp_o is equal to $p_{o_2} - p_{o_1}$, $p_{o_3} - p_{o_2}$, $p_{o_4} - p_{o_3}$, etc., being consequently negative if observed pressures are decreasing.

$g\rho$ is determined from the equation

$$g\rho = \frac{0.4644p}{t + 273}$$

if metric units are used, or from

$$g\rho = \frac{1.3256p}{t + 459}$$

if the English system is employed,

$$g\rho_m \text{ is equal to } \frac{g\rho_1 + g\rho_2}{2}, \frac{g\rho_2 + g\rho_3}{2}, \frac{g\rho_3 + g\rho_4}{2}, \text{ etc.}$$

ΔZ_a , the increment of absolute altitude, is determined from equation (7) or (14), it being assumed that the relation as expressed for the differentials holds true for the finite increments ΔZ and Δp , and that the change in specific weight from $g\rho_1$ to $g\rho_2$, $g\rho_2$ to $g\rho_3$, etc., is rectilinear. Consequently

$$\Delta Z_a = \frac{-13.59\Delta p_o}{g\rho_m} \text{ for metric units,}$$

$$\Delta Z_a = \frac{-70.67\Delta p_o}{g\rho_m} \text{ for English units.}$$

ΔZ_a is thus positive for decreasing values of p_o , since Δp in such case is negative.

Z_s is read directly from Figure 7 or Figure 8, or is interpolated from Table VI or Table VII for the various values of $g\rho$,

$$\Delta Z_s = Z_{s_2} - Z_{s_1}, Z_{s_3} - Z_{s_2}, \text{ etc.}$$

ΔT_s is deduced from ΔT_o through the relation

$$\frac{\Delta Z_a}{\Delta T_o} = \frac{\Delta Z_s}{\Delta T_s},$$

which arises from the assumption that the engine power is constant for constant density, and that therefore rates of climb are the same for the encountered atmosphere as for the standard atmosphere of equal density. Therefore

$$\Delta T_s = \Delta T_o \frac{\Delta Z_s}{\Delta Z_a}.$$

T_s is the summation of ΔT_s .

Table IV shows the reduction of data from an actual flight test by the above method. As may be noted, the altitude in the standard atmosphere at the start is not zero. This will generally be the case, for although the flight test may be started at near to sea level, it will be the very rare exception that the density encountered at the start will be that of zero altitude in the standard atmosphere.

If it is desired that the time-altitude curve for the standard atmosphere pass through the origin, an initial time increment ΔT_{s_0} , must be included at the beginning of column ΔT_s .

$$\Delta T_{s_0} = \Delta T_{s_1} \frac{Z_{s_1}}{\Delta Z_{s_1}}.$$

ΔT_s is thus positive if Z_{s_1} is positive, and negative if Z_{s_1} is negative.

It sometimes arises that the altitudes of the standard atmosphere for two or more of the observations near the start are negative. In such case it is found most convenient to neglect all but the last of such observations, making the starting point at that observation nearest to zero altitude standard atmosphere. Table IV has the time increment, ΔT_{s_0} , included at the top of column for ΔT_s . The final reduced data, altitude in standard atmosphere Z_s , and time for standard atmosphere T_s , are plotted in Figure 4. The resulting rate of climb curve, determined by taking tangents of the altitude-time curve, is shown.

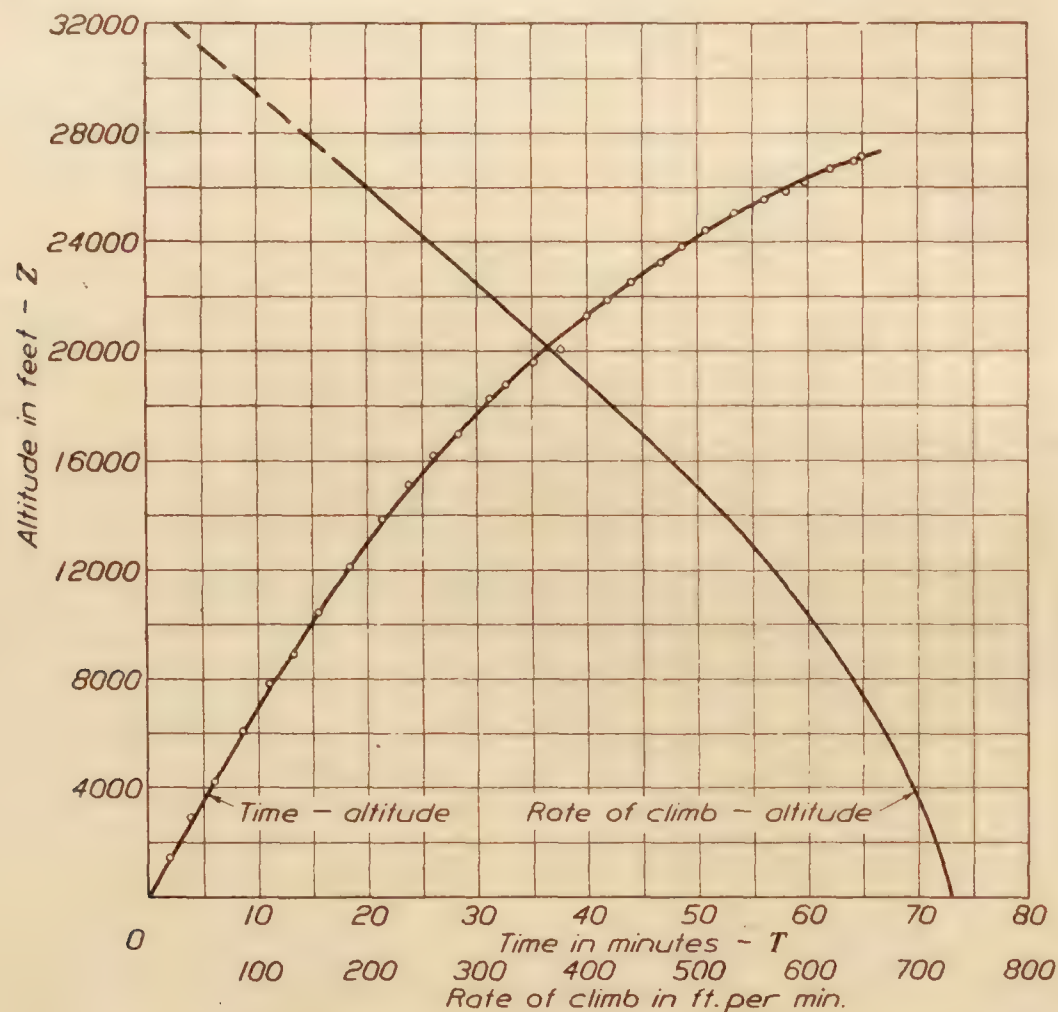


FIG. 4.—DH 4B airplane. Roots supercharger. Flight 18 B standard atmosphere. Reduction of data by Langley Memorial Aeronautical Laboratory Method

DISCUSSION

It may be noted that in the example given the points for time altitude in the standard atmosphere do not all lie upon a smooth, fair curve. The dispersion from such a curve is however, not greater than would be prevalent for points of absolute altitude and observed time, since the slope between corresponding consecutive points is, from the method of reduction, the same for the two cases. The result of this method is that the time-altitude curve for the standard atmosphere has, at altitudes of equal density and if corresponding points are given equal value, the same slope as the curve for observed time versus absolute altitude. Rates of climb in the standard atmosphere are thus the same as rates of climb in the encountered atmosphere of equal density.

It does not generally seem possible to draw through all of the points for altitude and time, whether these be absolute altitude and observed time or altitude in the standard atmosphere and time for the standard atmosphere, what may be properly called a smooth curve, particularly if the observations are made at short time intervals. This is true even if the test flight has been conducted with the best endeavor of the pilot to secure a smooth barograph. If, however, the observations are at comparatively long intervals, a smooth, fair curve is more readily drawn through all points. In the example given the data were recorded at 17-second intervals by means of photograph apparatus. The pressures and temperatures given in Table IV were taken at 2½-minute intervals from the carefully plotted but irregular line drawn through all observations.

TABLE IV
COMPUTATIONS FOR REDUCTION TO THE STANDARD ATMOSPHERE
DH-4B ROOTS SUPERCHARGER
Flight 18 B, September 27, 1923

1	2	3	4	5	6	7	8	9	10	11	12
T_0	ΔT_0	p_0	Δp_0	t_0	$g\rho$	$g\rho_m$	ΔZ_a	Z_a	ΔZ_s	ΔT_s	T_s
0		30.09		80	0.0739			1,130		¹ 1.40	1.40
2.5	2.5	28.05	-2.04	72	.0700	0.0720	2,020	2,940	1,810	2.24	3.64
5.0	2.5	26.67	-1.38	66	.0673	.0686	1,423	4,250	1,310	2.30	5.94
7.5	2.5	24.97	-1.70	60	.0637	.0655	1,837	6,100	1,850	2.52	8.46
10.0	2.5	23.50	-1.47	56	.0604	.0621	1,675	7,800	1,700	2.54	11.00
12.5	2.5	22.50	-1.00	50	.0585	.0594	1,190	8,880	1,080	2.27	13.27
15.0	2.5	21.25	-1.25	46	.0557	.0581	1,588	10,500	1,620	2.55	15.82
17.5	2.5	20.10	-1.15	45	.0528	.0542	1,501	12,100	1,600	2.66	18.48
20.0	2.5	19.00	-1.10	43	.0501	.0515	1,510	13,800	1,700	2.71	21.19
22.5	2.5	18.05	-.95	39	.0479	.0490	1,371	15,200	1,400	2.55	23.74
25.0	2.5	17.25	-.80	34	.0463	.0471	1,202	16,250	1,050	2.18	25.92
27.5	2.5	16.72	-.53	30	.0452	.0457	820	17,000	750	2.28	28.20
30.0	2.5	15.95	-.77	30	.0432	.0442	1,233	18,350	1,350	2.73	30.93
32.5	2.5	15.60	-.35	26	.0425	.0428	578	18,750	400	1.73	32.66
35.0	2.5	15.15	-.45	24	.0415	.0420	757	19,500	750	2.42	35.14
37.5	2.5	14.80	-.35	22	.0407	.0411	602	20,100	600	2.50	37.64
40.0	2.5	14.06	-.74	19	.0389	.0398	1,315	21,350	1,250	2.38	40.02
42.5	2.5	13.75	-.31	15	.0383	.0386	568	21,800	450	1.98	42.00
45.0	2.5	13.26	-.49	11	.0373	.0378	916	22,550	750	2.04	44.04
47.5	2.5	12.90	-.36	9	.0364	.0368	692	23,300	750	2.71	46.75
50.0	2.5	12.50	-.40	5	.0357	.0360	786	23,900	600	1.91	48.66
52.5	2.5	12.10	-.40	0	.0348	.0353	802	24,500	600	1.83	50.49
55.0	2.5	11.87	-.23	-1	.0342	.0345	471	25,100	600	3.18	53.67
57.5	2.5	11.67	-.20	-2	.0337	.0339	418	25,500	400	2.39	56.06
60.0	2.5	11.50	-.17	-3	.0333	.0335	359	25,800	300	2.09	58.15
62.5	2.5	11.30	-.20	-5	.0330	.0331	427	26,100	300	1.76	59.91
65.0	2.5	11.03	-.27	-7	.0323	.0326	586	26,650	550	2.34	62.25
67.5	2.5	10.88	-.15	-9	.0319	.0321	332	27,000	350	2.64	64.88
68.0	0.5	10.80	-.08	-10	.0318	.0318	178	27,100	100	0.28	65.16

¹ 1.40 is an initial time increment equal to the time required to climb from zero altitude in the standard atmosphere to the starting point, which is at 1,130 feet.

PART III
THE CONVERSION OF AIR-SPEED INDICATOR READINGS INTO TRUE AIR SPEEDS
THE AIR-SPEED INDICATOR

By WALTER S. DIEHL

SUMMARY

This part describes the conventional method of calibrating air-speed indicators and reducing indicated air speeds to true air speeds in the standard atmosphere.

INTRODUCTION

In order that the method of converting air-speed indicator readings into true air speeds may be fully understood, a brief explanation of the functioning of the instrument will be given.

An air-speed indicator consists essentially of two parts, the head and the indicator. The head, when placed in a relatively moving fluid, provides a differential pressure p , which is directly proportional to the density of the fluid ρ and to the square of relative velocity V . That is,

$$p = p_0 - p_1 = K\rho V^2 \dots\dots\dots 1$$

For any given type and size of head, K is constant over the usual range of flight velocities and its value may readily be determined by simple tests. When K is known, the value of the differential pressure p may be calculated for any desired values of V and ρ . The indicators, or gauges, are designed to operate on the differential pressure produced by the head. The scale is graduated to read directly the relative velocity corresponding to each differential pressure when ρ has the fixed value 0.00237 (lb.-ft.-sec. units), known as the standard density. If the instrument be properly constructed and graduated, the relative velocities or air speeds will be correctly indicated in air of standard density. When the air density differs from the standard value the readings will be indicated air speeds, V_i , and not true air speeds, V . More properly, the reading of the instrument is always an indicated air speed, which is a true air speed only when the air density has the standard value used in the design of the gauge. The relation between V_i and V is obviously

$$V_i = \sqrt{\rho/\rho_0} V \text{-----} 2$$

since p/K will be constant at any given reading.

Owing to the effects of interference from the parts of the airplane surrounding the head, and to variations in the construction of instruments and in the methods of installation, an air-speed indicator very rarely registers the true indicated air speed. In order to reduce an air-speed indicator reading V_a to the true indicated air speed, V_i , it is therefore necessary to calibrate the installation over the entire range of speeds employed and thus obtain a curve of true indicated air speed against air-speed indicator reading. Note that we are using three speeds, (1) the air-speed indicator reading, V_a , (2) the true indicated air speed, V_i , and (3) the true air speed, V . The ground speed does not enter into readings of air speed except in calibration tests.

The curve of V_i against V_a is known as the calibration curve, and once established for any particular installation it may be used to convert any normal air-speed indicator reading into the corresponding true air speed, as will be shown later. The conventional method of deriving the calibration curve will first be explained.

AIR-SPEED INDICATOR CALIBRATION

The calibration of an air-speed indicator is simply a determination of the true indicated air speeds, V_i , and corresponding air-speed indicator readings, V_a , at a sufficient number of points to determine the curve of V_i against V_a . Since V_i is the speed that should be indicated and V_a is the speed actually indicated, any method which will determine the value of V_i corresponding to V_a will be satisfactory. The usual method is to make timed runs with and against the wind over a measured course. In this method the wind must be approximately parallel to the course, or of comparatively low velocity. The flights should be made at a low and uniform altitude, the pilot using a statoscope if necessary. The timing must be accurate, and only high-grade, properly regulated stop watches or chronographs should be used. Particular care must be taken if the timing is done by the pilot or an observer to see that the starting and stopping of the watch are made under the same conditions. Obviously the length of the course must be accurately known and the ends well defined.

Five sets of runs are usually sufficient, a set being understood to consist of two runs at constant air-speed indicator reading, one with and one against the wind. These runs should be so made that one set is at high speed, one set at the lowest safe flying speed, and the three remaining sets at approximately equal intermediate intervals.

In all calibration tests the following data must be taken: (a) Length of course, barometric pressure, air temperature; (b) altimeter reading, average air-speed indicator reading for each run, time over the course for each run, and air temperature. Note that the readings in group (a) are as necessary as the actual flight data in group (b). These data are reduced to a calibration curve, first by calculating the ground speed over the course with the wind and against the wind, and taking the average of the two as the true air speed at the given meter reading. Note

that this true air speed must be obtained from the average of the two speeds and not from the average time over the course. The next step is to calculate the true indicated air speed, V_i ; that is, the air speed which would have been indicated had the instrument read correctly, according to equation 2.

$$V_i = V \sqrt{\rho/\rho_0} \dots\dots\dots 2$$

The values of $\sqrt{\rho/\rho_0}$ may be read directly from Figure 5 when the barometric pressure and air temperature are known. The barometric pressure should be corrected for the flight altitude. The observed air temperature is used.

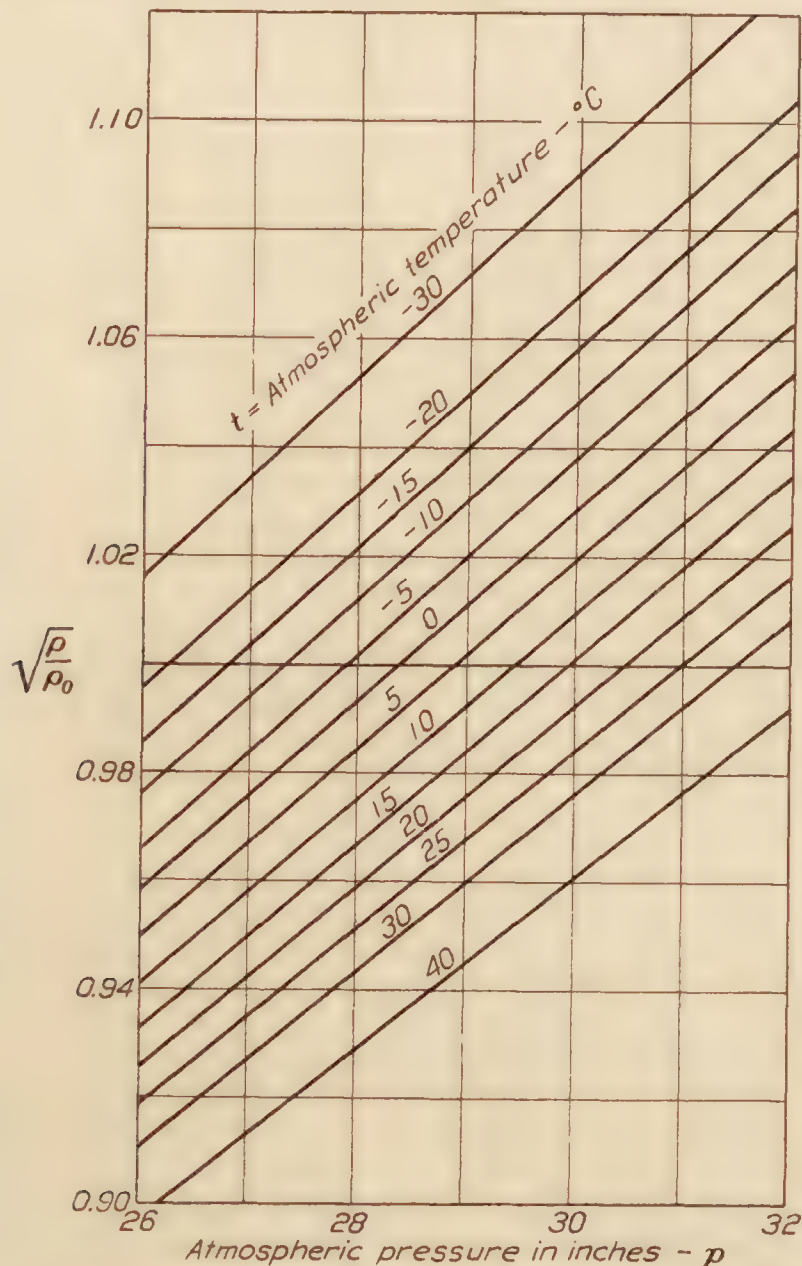


FIG. 5.—Variation of $\sqrt{\frac{\rho}{\rho_0}}$ with p and t for use in calibrating air-speed indicators

The plot of V_i against V_a is usually a straight line. Even in extreme cases the curvature is so slight that the calibration curve may be extended considerably beyond the observed limits without introducing appreciable error, except at very low speeds.

Table V illustrates a convenient method of tabulating the calculations necessary to derive a calibration curve from test data.

REDUCTION OF AIR-SPEED INDICATOR READINGS TO TRUE AIR SPEEDS

The reduction of air-speed indicator readings V_a to true air speeds consists of two steps. The true indicated air speed, V_i , corresponding to V_a , is first read from the calibration curve. V_i is then converted to the true airspeed by the use of equation 2. That is,

$$V = V_i \sqrt{\frac{\rho_0}{\rho}} \dots\dots\dots 2a$$

A convenient method of tabulating the calculations is given in Table V. The following steps are taken in the order given: The test data are put down in three columns, (1) altimeter reading, Z_1 , (2) average air-speed meter reading, V_a , and (3) air temperature, t . The value of $\left(\frac{p}{p_o}\right)$ corresponding to Z_1 is then read from Figure 1 and placed in column 4. $\frac{p}{p_o}$ determines p , since p_o is known. The equivalent altitude in standard atmosphere, Z_s , corresponding to p and t , is read from Figure 2. The value of $\sqrt{\frac{\rho_o}{\rho}}$ is read from Figure 6 and the value of V_i corresponding to V_a is read from the calibration curve. V , the true air speed, is the product of V_i and V , and is plotted against Z_e to obtain the variation of velocity with altitude.

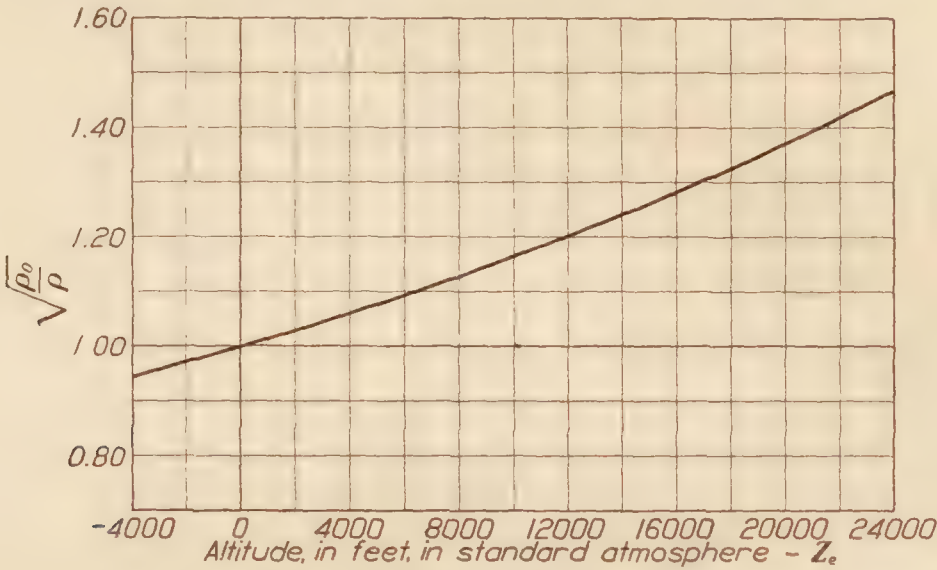


FIG. 6.—Variation of $\sqrt{\frac{\rho_o}{\rho}}$ with Z in standard atmosphere

TABLE V

AIR-SPEED METER CALIBRATION

Airplane type:

No.

Gross weight:

Place:

Date:

Pilot:

Weather: Wind velocity { Miles per hour

Direction:

Barometer:

Temperature:

{ Knots

Length of course L { Land miles

Air-speed meter: Type

{ Nautical miles

Readings in { Miles per hour

{ Knots

1	2	3	4	5	6	7	8	9	10	11	12	
Run	Altitude reading Z_1	Average air-speed meter reading V_a	Time over course		Speed over course		Average air speed V	Air tempera- ture, °C.	Air pressure, p , inches	$\sqrt{\frac{\rho}{\rho_o}}$	Cor- rected indicated air speed, V_i , (11) by (8)	Remarks
			Against wind T_1	With wind T_2	Against wind V_1	With wind V_2						
1												
2												
3												
4												
5												

NOTE.—

$V_1 = \frac{3600L}{T_1 \text{ sec.}}$

$V_2 = \frac{3600L}{T_2 \text{ sec.}}$

$V = \frac{V_1 + V_2}{2}$

Plot V_a (col. 3) against V_1 (col. 12) for correction curve.

APPENDIX
TABLE VI

STANDARD ATMOSPHERE TABLES AND CURVES
STANDARD ATMOSPHERE METRIC UNITS

Altitude, Z, meters	t °C	T To	p po	ρ ρo	Pressure, p, mm.	Specific weight, gp, kg./m. ³
-1,000	21.50	1.0226	1.1244	1.0996	854.58	1.3476
-800	20.20	1.0181	1.0986	1.0791	834.94	1.3325
-600	18.90	1.0135	1.0733	1.0589	815.67	1.2977
-400	17.60	1.0091	1.0484	1.0390	796.75	1.2733
-200	16.30	1.0045	1.0240	1.0193	778.20	1.2492
0	15.00	1.0000	1.0000	1.0000	760.00	1.2255
+200	13.70	.9955	.9765	.9809	742.12	1.2021
400	12.40	.9910	.9534	.9621	724.62	1.1791
600	11.10	.9865	.9308	.9436	704.45	1.1564
800	9.80	.9820	.9087	.9254	690.60	1.1340
1,000	8.50	.9775	.8870	.9074	674.09	1.1120
1,200	7.20	.9729	.8656	.8897	657.89	1.0903
1,400	5.90	.9684	.8448	.8723	642.00	1.0690
1,600	4.60	.9639	.8243	.8551	626.44	1.0480
1,800	3.30	.9594	.8042	.8382	611.19	1.0272
2,000	2.00	.9549	.7845	.8216	596.23	1.0068
2,200	0.70	.9504	.7652	.8052	581.56	.9868
2,400	-0.60	.9459	.7463	.7891	567.19	.9670
2,600	-1.90	.9413	.7278	.7732	553.10	.9475
2,800	-3.20	.9368	.7097	.7575	539.32	.9283
3,000	-4.50	.9323	.6918	.7420	525.79	.9094
3,200	-5.80	.9278	.6744	.7269	512.56	.8908
3,400	-7.10	.9233	.6574	.7120	499.58	.8726
3,600	-8.40	.9188	.6406	.6972	486.88	.8545
3,800	-9.70	.9143	.6242	.6828	474.44	.8368
4,000	-11.00	.9097	.6082	.6686	462.26	.8193
4,200	-12.30	.9052	.5925	.6545	450.32	.8022
4,400	-13.60	.9007	.5771	.6408	438.64	.7853
4,600	-14.90	.8962	.5621	.6273	427.22	.7687
4,800	-16.20	.8917	.5474	.6139	416.02	.7523
5,000	-17.50	.8872	.5330	.6008	405.09	.7363
5,200	-18.80	.8827	.5187	.5879	394.36	.7205
5,400	-20.10	.8781	.5051	.5752	383.88	.7049
5,600	-21.40	.8736	.4916	.5627	373.61	.6897
5,800	-22.70	.8692	.4784	.5505	363.59	.6746
6,000	-24.00	.8646	.4655	.5384	353.77	.6598
6,200	-25.30	.8601	.4528	.5265	344.17	.6453
6,400	-26.60	.8556	.4405	.5149	334.80	.6310
6,600	-27.90	.8511	.4284	.5034	325.62	.6169
6,800	-29.20	.8466	.4166	.4921	316.65	.6031
7,000	-30.50	.8420	.4051	.4810	307.87	.5896
7,200	-31.80	.8375	.3937	.4702	299.29	.5762
7,400	-33.10	.8330	.3828	.4595	290.90	.5632
7,600	-34.40	.8285	.3720	.4490	282.72	.5503
7,800	-35.70	.8240	.3614	.4384	274.71	.5377
8,000	-37.00	.8195	.3512	.4285	266.89	.5252
8,200	-38.30	.8149	.3411	.4185	259.26	.5130
8,400	-39.60	.8104	.3312	.4088	251.79	.5010
8,600	-40.90	.8059	.3217	.3992	244.52	.4893
8,800	-42.20	.8014	.3123	.3898	237.40	.4777
9,000	-43.50	.7969	.3032	.3806	230.45	.4664
9,200	-44.80	.7924	.2942	.3715	223.68	.4552
9,400	-46.10	.7879	.2856	.3625	217.06	.4443
9,600	-47.40	.7833	.2771	.3538	210.62	.4336
9,800	-48.70	.7788	.2688	.3452	204.30	.4230
10,000	-50.00	.7743	.2606	.3367	198.16	.4127
10,200	-51.30	.7698	.2528	.3285	192.16	.4026
10,400	-52.60	.7653	.2451	.3204	186.31	.3926
10,600	-53.90	.7608	.2377	.3124	180.61	.3828
10,800	-55.00	.7569	.2303	.3044	175.06	.3729
11,000	-55.00	.7569	.2232	.2950	169.66	.3614
11,200	-55.00	.7569	.2164	.2859	164.43	.3502
11,400	-55.00	.7569	.2096	.2770	159.34	.3394
11,600	-55.00	.7569	.2032	.2684	154.43	.3290
11,800	-55.00	.7569	.1970	.2601	149.67	.3188
12,000	-55.00	.7569	.1909	.2521	145.05	.3090
12,200	-55.00	.7569	.1849	.2443	140.57	.2995
12,400	-55.00	.7569	.1792	.2368	136.24	.2902
12,600	-55.00	.7569	.1737	.2295	132.04	.2813
12,800	-55.00	.7569	.1683	.2224	127.96	.2726
13,000	-55.00	.7569	.1632	.2155	124.01	.2642
13,200	-55.00	.7569	.1581	.2089	120.19	.2560
13,400	-55.00	.7569	.1532	.2024	116.48	.2481
13,600	-55.00	.7569	.1485	.1961	112.90	.2404
13,800	-55.00	.7569	.1440	.1901	109.41	.2331
14,000	-55.00	.7569	.1395	.1843	106.02	.2259
14,200	-55.00	.7569	.1352	.1786	102.75	.2188
14,400	-55.00	.7569	.1311	.1731	99.58	.2121
14,600	-55.00	.7569	.1270	.1677	96.50	.2056
14,800	-55.00	.7569	.1230	.1625	93.52	.1993
15,000	-55.00	.7569	.1193	.1576	90.65	.1931

TABLE VII

STANDARD ATMOSPHERE ENGLISH UNITS

Altitude, Z, feet	t °F	t °C	T T ₀	p p ₀	ρ ρ ₀	Pressure, p, inches	Specific weight, γ _p , lb./ft. ³
-4,000	73.27	22.93	1.0275	1.1533	1.1225	34.51	0.08588
-3,500	71.48	21.93	1.0241	1.1333	1.1066	33.91	.08466
-3,000	69.70	20.94	1.0206	1.1134	1.0909	33.31	.08346
-2,500	67.92	19.95	1.0172	1.0938	1.0753	32.72	.08227
-2,000	66.13	18.96	1.0138	1.0745	1.0599	32.15	.08109
-1,500	64.35	17.97	1.0103	1.0552	1.0446	31.58	.07993
-1,000	62.57	16.98	1.0069	1.0367	1.0296	31.02	.07878
-500	60.78	15.99	1.0034	1.0182	1.0147	30.47	.07764
0	59.00	15.00	1.0000	1.0000	1.0000	29.92	.07651
+500	57.22	14.01	.9966	.9821	.9855	29.38	.07540
1,000	55.43	13.02	.9931	.9644	.9710	28.86	.07430
1,500	53.65	12.03	.9897	.9469	.9568	28.33	.07321
2,000	51.87	11.04	.9862	.9298	.9428	27.82	.07213
2,500	50.09	10.05	.9828	.9129	.9288	27.31	.07107
3,000	48.30	9.06	.9794	.8962	.9151	26.81	.07001
3,500	46.52	8.07	.9759	.8798	.9015	26.32	.06897
4,000	44.74	7.08	.9725	.8636	.8881	25.84	.06794
4,500	42.95	6.09	.9690	.8477	.8748	25.36	.06693
5,000	41.17	5.09	.9656	.8320	.8616	24.89	.06592
5,500	39.39	4.10	.9622	.8165	.8487	24.43	.06493
6,000	37.60	3.11	.9587	.8013	.8358	23.98	.06395
6,500	35.82	2.12	.9553	.7863	.8232	23.53	.06298
7,000	34.04	1.13	.9518	.7716	.8106	23.09	.06202
7,500	32.25	0.14	.9484	.7571	.7982	22.65	.06107
8,000	30.47	-0.85	.9450	.7427	.7859	22.22	.06013
8,500	28.69	-1.84	.9415	.7286	.7738	21.80	.05920
9,000	26.90	-2.83	.9381	.7147	.7619	21.38	.05829
9,500	25.12	-3.82	.9346	.7011	.7501	20.98	.05739
10,000	23.34	-4.81	.9312	.6876	.7384	20.58	.05649
10,500	21.56	-5.80	.9278	.6743	.7269	20.18	.05561
11,000	19.77	-6.79	.9243	.6614	.7154	19.79	.05474
11,500	17.99	-7.78	.9209	.6486	.7042	19.40	.05388
12,000	16.21	-8.77	.9175	.6359	.6931	19.03	.05303
12,500	14.42	-9.77	.9140	.6234	.6821	18.65	.05219
13,000	12.64	-10.76	.9106	.6112	.6712	18.29	.05136
13,500	10.86	-11.75	.9071	.5992	.6605	17.93	.05054
14,000	9.07	-12.74	.9037	.5873	.6499	17.57	.04973
14,500	7.29	-13.73	.9003	.5757	.6394	17.22	.04893
15,000	5.51	-14.72	.8968	.5642	.6291	16.88	.04814
15,500	3.72	-15.71	.8934	.5530	.6189	16.54	.04736
16,000	1.94	-16.70	.8899	.5418	.6088	16.21	.04658
16,500	0.16	-17.69	.8865	.5309	.5988	15.89	.04583
17,000	-1.63	-18.68	.8831	.5202	.5891	15.56	.04507
17,500	-3.41	-19.67	.8796	.5097	.5793	15.25	.04433
18,000	-5.19	-20.66	.8762	.4992	.5698	14.94	.04359
18,500	-6.97	-21.65	.8727	.4891	.5603	14.63	.04287
19,000	-8.76	-22.64	.8693	.4790	.5509	14.33	.04216
19,500	-10.54	-23.63	.8659	.4691	.5418	14.03	.04145
20,000	-12.32	-24.62	.8624	.4594	.5327	13.75	.04075
20,500	-14.10	-25.62	.8590	.4498	.5237	13.47	.04007
21,000	-15.89	-26.61	.8555	.4405	.5148	13.18	.03938
21,500	-17.67	-27.60	.8521	.4313	.5061	12.90	.03872
22,000	-19.46	-28.59	.8487	.4222	.4974	12.63	.03806
22,500	-21.24	-29.58	.8452	.4133	.4899	12.36	.03740
23,000	-23.02	-30.57	.8418	.4045	.4805	12.10	.03676
23,500	-24.81	-31.56	.8383	.3959	.4721	11.84	.03612
24,000	-26.59	-32.55	.8349	.3874	.4640	11.59	.03550
24,500	-28.37	-33.54	.8315	.3791	.4559	11.34	.03488
25,000	-30.15	-34.53	.8280	.3709	.4480	11.10	.03427
25,500	-31.94	-35.52	.8246	.3629	.4401	10.86	.03367
26,000	-33.72	-36.51	.8211	.3550	.4323	10.62	.03308
26,500	-35.50	-37.50	.8177	.3473	.4247	10.39	.03249
27,000	-37.29	-38.49	.8143	.3397	.4171	10.16	.03192
27,500	-39.07	-39.48	.8108	.3322	.4097	9.94	.03134
28,000	-40.85	-40.47	.8074	.3248	.4023	9.72	.03078
28,500	-42.64	-41.46	.8039	.3176	.3951	9.50	.03023
29,000	-44.42	-42.46	.8005	.3106	.3869	9.29	.02968
29,500	-46.20	-43.45	.7971	.3035	.3820	9.09	.02914
30,000	-47.99	-44.44	.7936	.2968	.3740	8.88	.02861
30,500	-49.77	-45.43	.7902	.2900	.3671	8.68	.02809
31,000	-51.55	-46.42	.7867	.2834	.3603	8.48	.02757
31,500	-53.33	-47.41	.7833	.2770	.3537	8.29	.02706
32,000	-55.12	-48.40	.7799	.2707	.3472	8.10	.02656
32,500	-56.90	-49.39	.7764	.2645	.3407	7.91	.02606
33,000	-58.68	-50.38	.7730	.2583	.3343	7.73	.02558
33,500	-60.47	-51.39	.7695	.2524	.3280	7.55	.02510
34,000	-62.25	-52.36	.7661	.2465	.3218	7.38	.02463
34,500	-64.03	-53.35	.7627	.2408	.3157	7.21	.02416
35,000	-65.82	-54.34	.7592	.2352	.3098	7.04	.02369
35,500	-67.00	-55.00	.7569	.2296	.3033	6.87	.02321
36,000	-67.00	-55.00	.7569	.2242	.2962	6.71	.02265
37,000	-67.00	-55.00	.7569	.2137	.2824	6.39	.02160
38,000	-67.00	-55.00	.7569	.2037	.2692	6.10	.02059
39,000	-67.00	-55.00	.7569	.1943	.2566	5.81	.01963
40,000	-67.00	-55.00	.7569	.1852	.2447	5.54	.01872
41,000	-67.00	-55.00	.7569	.1765	.2332	5.28	.01785
42,000	-67.00	-55.00	.7569	.1683	.2224	5.04	.01701
43,000	-67.00	-55.00	.7569	.1605	.2120	4.80	.01622
44,000	-67.00	-55.00	.7569	.1530	.2021	4.58	.01546
45,000	-67.00	-55.00	.7569	.1458	.1926	4.36	.01474
46,000	-67.00	-55.00	.7569	.1391	.1837	4.16	.01405
47,000	-67.00	-55.00	.7569	.1325	.1751	3.97	.01339
48,000	-67.00	-55.00	.7569	.1264	.1669	3.781	.01277
49,000	-67.00	-55.00	.7569	.1205	.1591	3.60	.01217
50,000	-67.00	-55.00	.7569	.1149	.1517	3.44	.01161

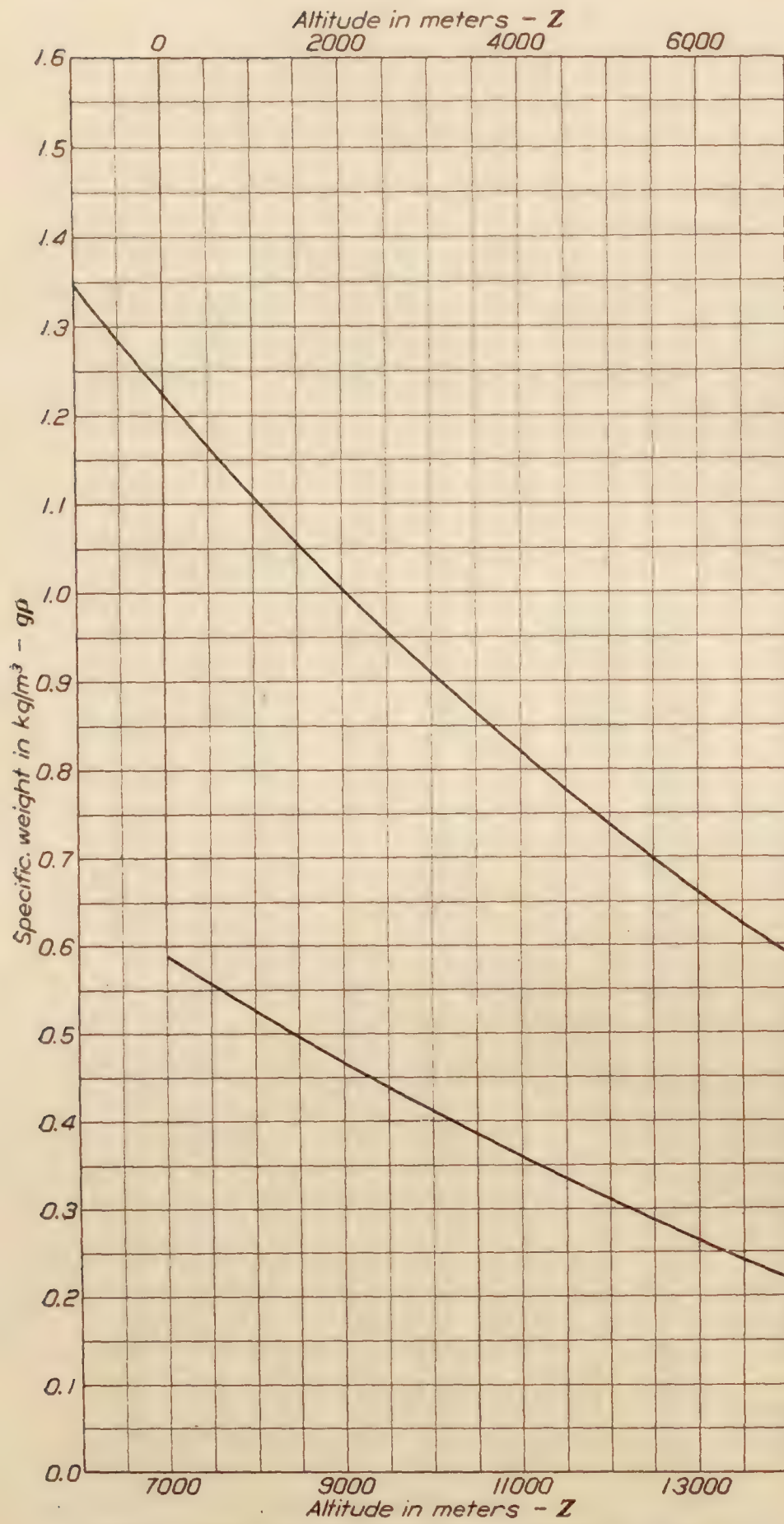


FIG. 7.—Altitude—Specific weight. Standard atmosphere. Metric units

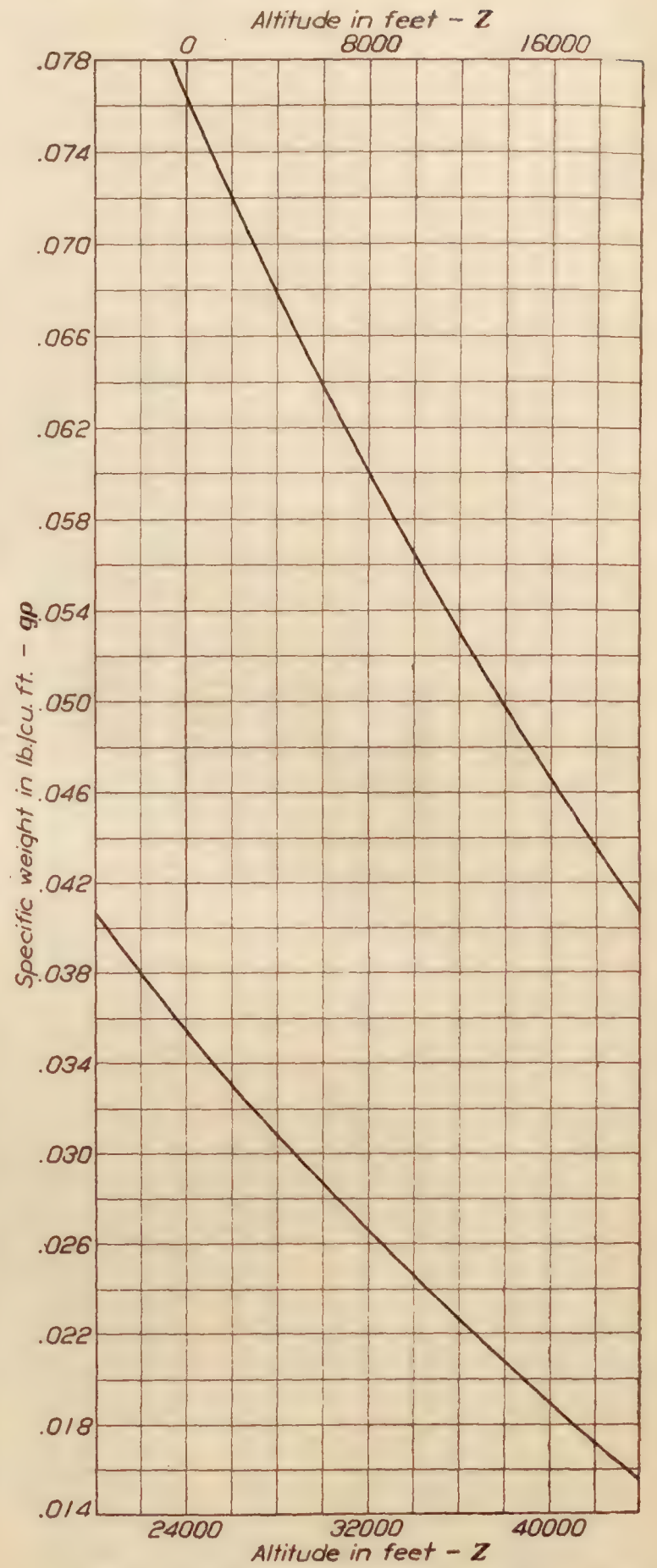


FIG. 8.—Altitude—Specific weight. Standard atmosphere. English units

REPORT No. 217

PRELIMINARY WING MODEL TESTS IN THE VARIABLE DENSITY WIND TUNNEL OF THE NATIONAL ADVISORY COMMITTEE FOR AERONAUTICS

By MAX M. MUNK
National Advisory Committee
for Aeronautics

REPORT No. 217

PRELIMINARY WING MODEL TESTS IN THE VARIABLE DENSITY WIND TUNNEL OF THE NATIONAL ADVISORY COMMITTEE FOR AERONAUTICS

By MAX M. MUNK

SUMMARY

The following report contains the results of a series of tests with three wing models. By changing the section of one of the models and painting the surface of another, the number of models tested was increased to five. The tests were made in order to obtain some general information on the air forces on wing sections at a high Reynolds Number and in particular to make sure that the Reynolds Number is really the important factor, and not other things like the roughness of the surface and the sharpness of the trailing edge.

The few tests described below seem to indicate that the air forces at a high Reynolds Number are not equivalent to respective air forces at a low Reynolds Number (as in an ordinary atmospheric wind tunnel). The drag appears smaller at a high Reynolds Number and the maximum lift is increased in some cases. The roughness of the surface and the sharpness of the trailing edge do not materially change the results, so that we feel confident that tests with systematic series of different wing sections will bring consistent results, important and highly useful for the designer.

ARRANGEMENT OF TESTS

The models used in the tests described in this report were made of aluminum and were smoothly cut to shape, without any polishing.

The chord was 5 in., the span 30 in., which latter is half the throat diameter of the wind tunnel. This ratio is so large that the influence of the tunnel walls begins to be perceptible. The actual aspect ratio of the wing models, which were square and not warped, was 6; but the influence of the walls theoretically changes the air forces as if the aspect ratio had been 6.85.

This report contains all forces and angles of attack as actually observed, making no allowance for the influence of the tunnel walls. We have inserted in the diagrams the parabola of the induced drag for an aspect ratio of 6.85. (References 1 and 2.)

Figure 1 shows diagrammatically how the models were attached to the balance ring. It is a combination of wire attachment and rigid

connection. A pair of vertical wires *A* are stretched from top to bottom of the balance ring. These wires are connected to the wing at one quarter of the chord behind the leading edge. Furthermore, one skid *B*, screwed to the wing, is hinged to a vertical bar *C*, which runs across the air stream and can be moved up and down. The bar is well shielded from the air stream by a tube in which it slides and its motion is used to change the angle of attack.

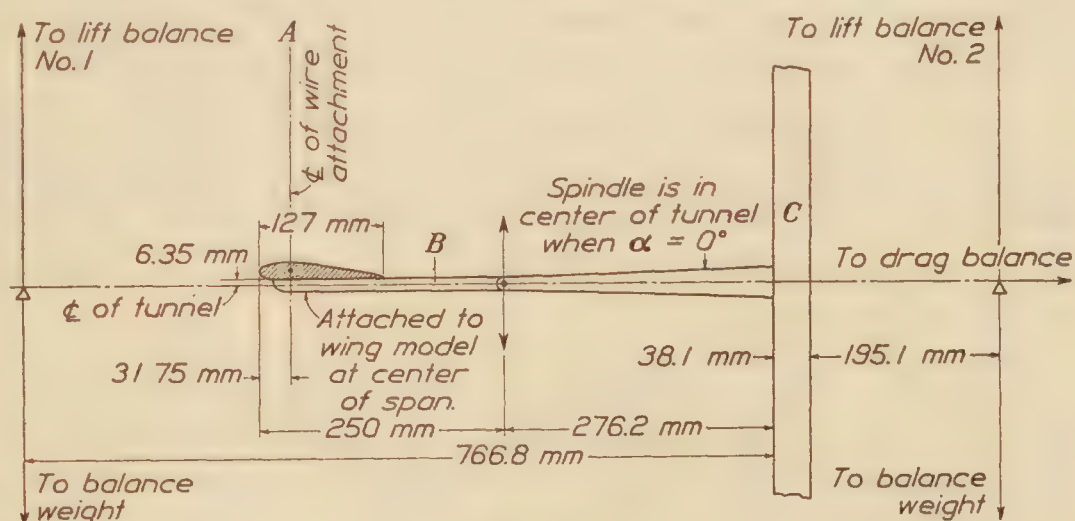
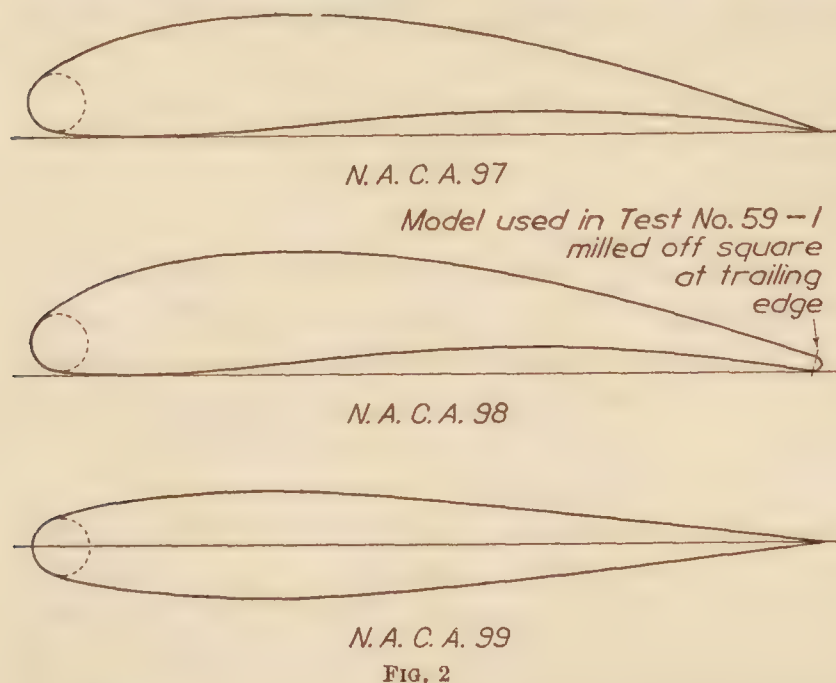


FIG. 1

RESULTS

The results are given in the figures and tables, both of which contain the conditions of each test. There is also a table of ordinates of the three wing sections Nos. 97, 98, and 99. Moreover, the cambered section 98 with round rear edge was milled off to obtain a square end, and the cambered section No. 97 (with a sharp trailing edge), Figure 2, was covered with oil paint after the test had been finished, to study the influence of the surface roughness.



We have, therefore, 5 different models, each of which could be measured at different density of the air. All in all, we have made 18 different runs, each time varying the angle of attack within a large range and determining the lift and drag. In some of the tests we have also determined the pitching moment with respect to a point on the chord and at one quarter of the chord behind the leading edge. The moment is considered positive if it makes the leading edge rise. This reference point is of special importance; the theory of thin wing section gives a pitching moment with respect to this point independent of the angle of attack. This makes it more convenient for practical use. (Reference 2.)

The coefficient of the component of the air force at right angles to the chord is

$$C_N = C_L \cos \alpha + C_D \sin \alpha.$$

Hence the center of pressure can be computed from the moment coefficient, the lift coefficient and the drag coefficient by means of the formula

$$C.P. = 25\% - \frac{C_M}{C_L \cos \alpha + C_D \sin \alpha} \cdot 100\%.$$

$C.P.$ denotes here the distance in per cent of the chord from the leading edge. The moment coefficient is derived from the moment itself by dividing it by the dynamical pressure $V^2 \frac{\rho}{2}$ and by the product of the wing area and the mean chord of the wing.

In the figures the lift coefficient $\frac{L}{Sq}$ is plotted upward. The induced drag coefficient for an aspect ratio of 6.85, the observed drag coefficient, and the moment coefficient $\frac{M}{cSq}$ are plotted against the lift coefficient to the right. The value of the angle of attack is inserted along the lift-drag curve.

Figures 3 to 8 refer to the strut section. The moment is expected to be zero and is nearly so in the figures. The small difference can be explained by taking into account the effect of the finite curvature at the leading edge. The reader will observe that at high pressure the wing shows a marked improvement; the minimum and the mean drag coefficient decreases, while the lift coefficient increases from 0.79 to 1.1. Figures 9 to 14 are corresponding tests with a cambered section of the same thickness. Here we observe the same decrease of the drag coefficient when the Reynolds Number increases, but the maximum lift keeps about constant. It just happens to be slightly larger at 16 atmospheres but resumes its old value at 20.9 atmospheres. The moment curve in Figure 12 coincides with the theoretical vertical straight line quite closely. Figure 14 gives the results for the same model not painted. The increase of roughness was easily felt by touching the model. The difference in the result is, however, of no important magnitude.

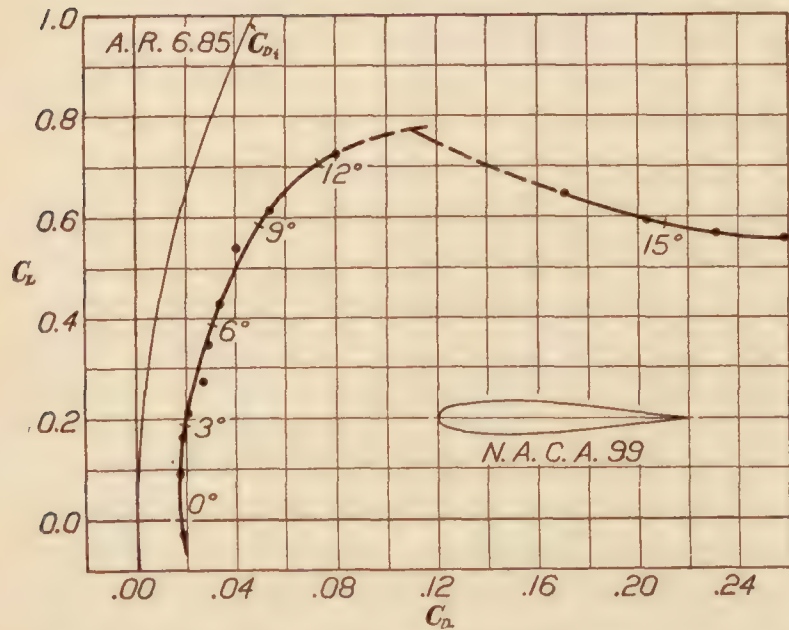


FIG. 3.—Test No. 56-1. Tank pressure 1 atmosphere. Dynamic pressure, $q=27.5 \text{ kg/m}^2$. Reynolds Number 175,000

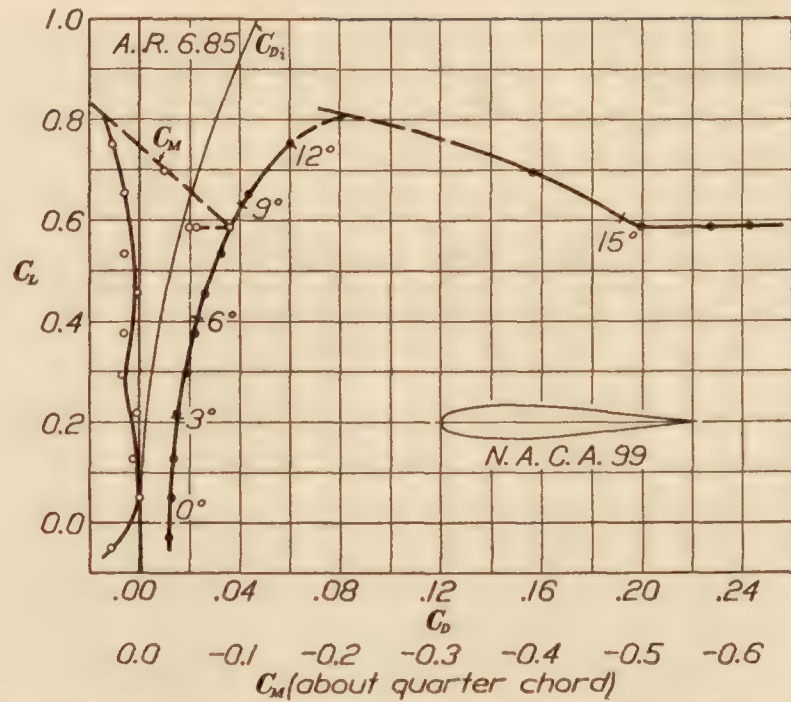


FIG. 4.—Test No. 56-3. Tank pressure 2.03 atmospheres. Dynamic pressure $q=57.3 \text{ kg/m}^2$. Reynolds Number 352,000

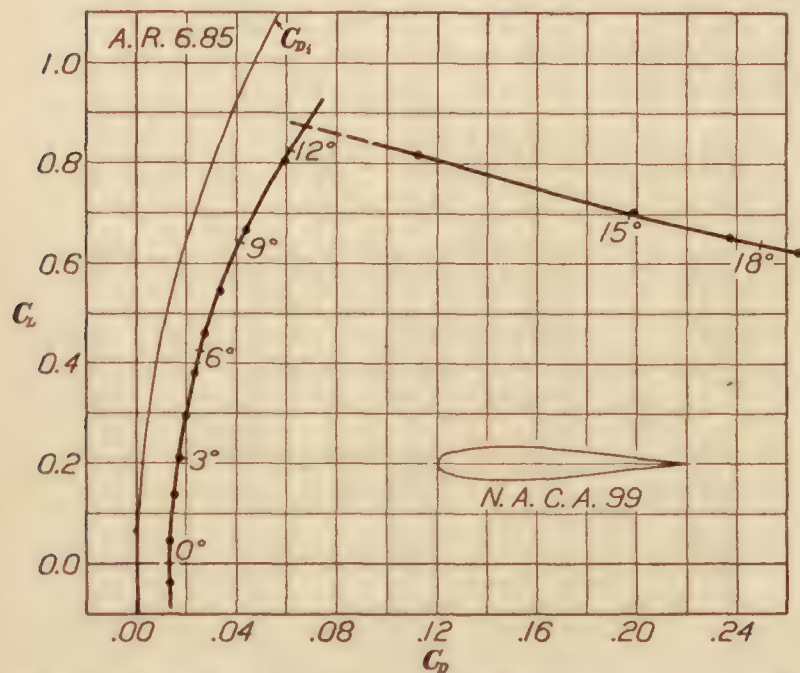


FIG. 5.—Test No. 56-5. Tank pressure 4.05 atmospheres. Dynamic pressure $q=120 \text{ kg/m}^2$. Reynolds Number 719,000

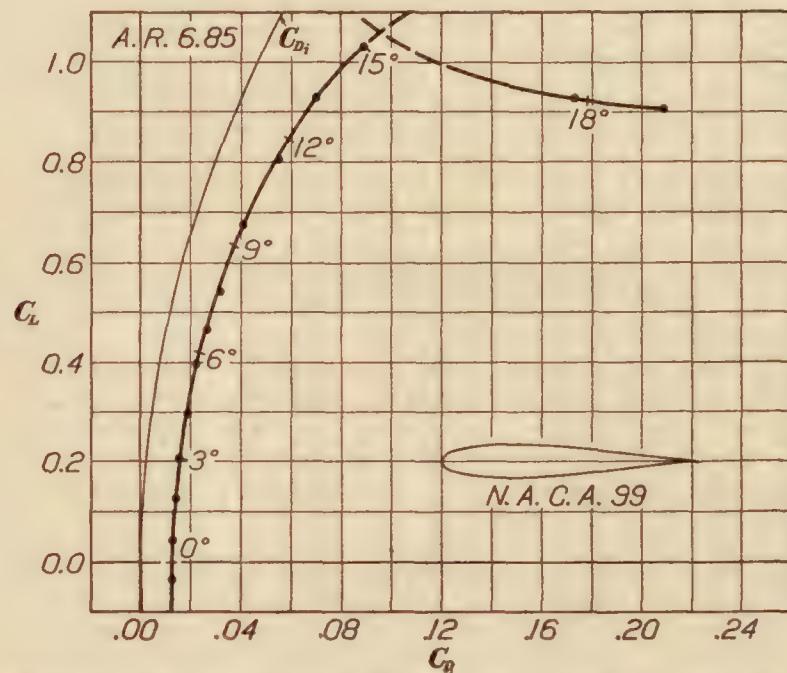


FIG. 6.—Test No. 56-7. Tank pressure 6.0 atmospheres. Dynamic pressure $q=183 \text{ kg/m}^2$. Reynolds Number 1,070,000

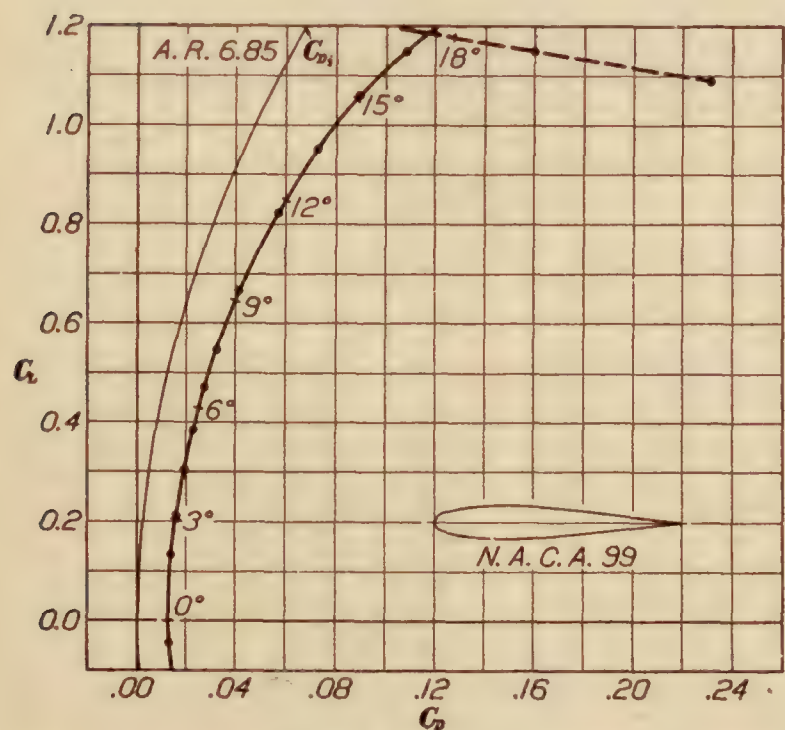


FIG. 7.—Test No. 56-9. Tank pressure 8.3 atmospheres. Dynamic pressure $q=256 \text{ kg/m}^2$. Reynolds Number 1,440,000

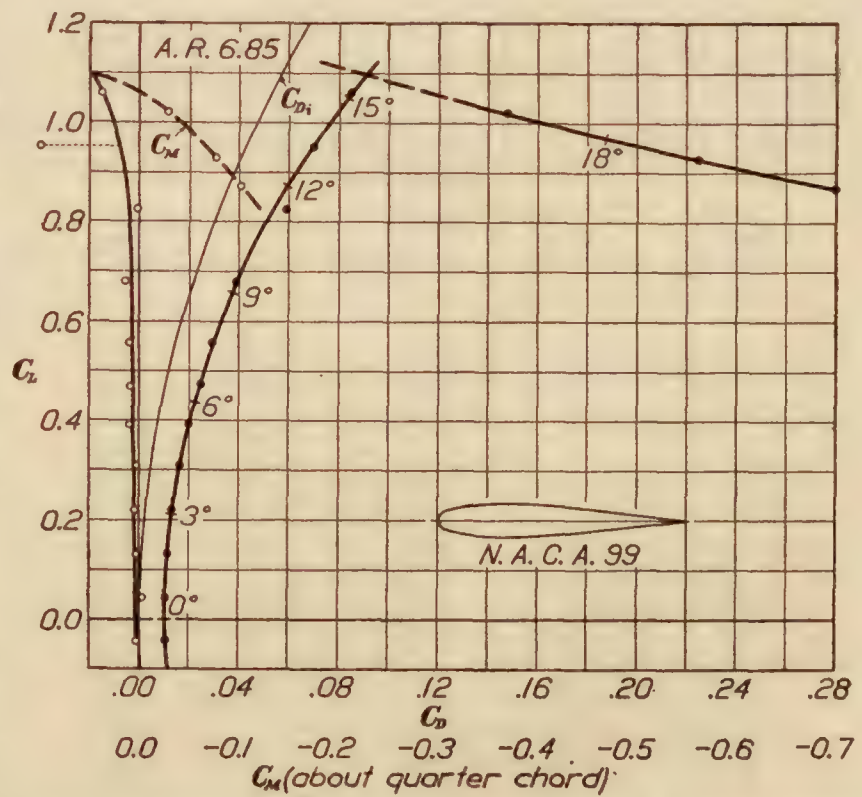


FIG. 8.—Test No. 56-11. Tank pressure 16.24 atmospheres. Dynamic pressure $q=543 \text{ kg/m}^2$. Reynolds Number 2,950,000

The remaining tests, Figures 15 to 19, were made on the cambered section with different trailing edges. The thick rounding of the rear edge of course increases the drag but does not otherwise change the character of the result. The same holds true for Figure 20 with the square trailing edge.

DISCUSSION OF RESULTS

The tests suggest the general rule that at a full Reynolds Number the cambered wing has a smaller drag, the symmetrical section both a smaller drag and a larger maximum lift than in the old type wind tunnel. The roughness of the surface and the sharpness of the trailing edge, if reasonably chosen, have no influence on the results. The results, as those in any wind tunnel should not be scrutinized too closely and not too literally interpreted. The new tunnel will show the direction and the way to the improvement of aircraft, but the results with a square wing alone in an airflow without fuselage and propeller can not give absolute information regarding the air forces on the wings of a real airplane. However, the results obtained give us the right to expect confidently consistent and qualitative results from the investigation of a systematic series of wing models now to be taken up, as likewise from later studies of wings with ailerons and of combinations of several parts of the airplane at full-size Reynolds Number.

TABLE I

SECTION NO. N. A. C. A. 97. FICTITIOUS ASPECT RATIO, 6.85.
MODEL NO. 9. AVERAGE TEMPERATURE, 27° C.
SPAN 30 IN., 76.2 cm PRESSURE, 1 ATMOSPHERE.
CHORD 5 IN., 12.7 cm REYNOLDS NUMBER, 175,000.
AREA, 0.0968 m²

Angle of attack, degree	q kg m ²	Lift L kg	Lift coef. C_L	Drag coef. C_D	Moment coef. C_M
-11.6	27.4	-0.18	-0.068	0.0353	-0.063
-9.2	27.5	-.04	-.015	.0795	-.106
-6.7	27.5	.50	.186	.0242	-.202
-4.1	27.5	.95	.357	.0237	-.156
-2.8	27.5	1.23	.462	.0272	-.197
-1.7	27.5	1.47	.551	.0322	-.179
-.4	27.5	1.76	.661	.0389	-.180
.8	27.5	1.95	.773	.0440	-.200
2.1	27.5	2.18	.820	.0529	-.159
3.2	27.5	2.40	.904	.0601	-.127
5.6	27.5	2.81	1.05	.0806	-.133
7.9	27.5	3.21	1.21	.0981	-.117
10.5	27.5	3.51	1.32	.1242	-.050
13.4	27.5	3.62	1.36	.1585	-.048
14.7	27.5	3.63	1.37	.1781	-.024
15.9	27.5	3.60	1.36	.1970	-.037
17.0	27.5	3.58	1.36	.2160	-.005
18.4	27.5	3.56	1.34	.2340	.024

TABLE II

SECTION NO. N. A. C. A. 97. FICTITIOUS ASPECT RATIO, 6.85.
MODEL NO. 9. AVERAGE TEMPERATURE, 30° C.
SPAN 30 IN., 76.2 cm PRESSURE, 4.1 ATMOSPHERES.
CHORD 5 IN., 12.7 cm REYNOLDS NUMBER, 740,000.
AREA, 0.0968 m²

Angle of attack, degree	q kg m ²	Lift L kg	Lift coef. C_L	Drag coef. C_D
-11.6	122	-1.42	-0.119	0.0154
-9.2	122	-.14	-.012	.0141
-6.7	122	1.91	.161	.0121
-4.2	122	4.15	.349	.0154
-2.8	122	5.32	.445	.0195
-1.6	122	6.47	.544	.0257
-.4	122	7.47	.627	.0309
.8	122	8.59	.722	.0378
2.1	122	9.56	.805	.0460
3.2	122	10.61	.892	.0535
5.6	122	12.53	1.06	.0735
7.9	122	13.99	1.17	.0933
10.6	122	15.16	1.27	.1215
13.4	122	15.62	1.32	.1607
14.7	122	15.77	1.33	.1827
15.9	122	15.74	1.33	.2027
17.0	122	15.67	1.33	.2240
18.4	122	15.50	1.31	.2480
19.8	122	15.29	1.29	.2735
21.1	122	15.00	1.27	.2953
22.3	120	14.77	1.27	.3200

TABLE III

SECTION NO. N. A. C. A. 97. FICTITIOUS ASPECT RATIO, 6.85.
MODEL NO. 9. AVERAGE TEMPERATURE, 35° C.
SPAN 30 IN., 76.2 cm PRESSURE, 8 ATMOSPHERES.
CHORD 5 IN., 12.7 cm REYNOLDS NUMBER, 1,430,000.
AREA, 0.0968 m²

Angle of attack, degree	q kg m ²	Lift L kg	Lift coef. C_L	Drag coef. C_D
-11.6	246	-5.03	-0.211	0.0182
-9.2	246	-.80	-.033	.0137
-6.7	246	3.61	.151	.0139
-4.2	246	7.59	.318	.0173
-2.8	246	10.24	.429	.0214
-1.6	246	12.40	.511	.0264
-.4	246	14.48	.608	.0323
.8	246	16.77	.705	.0395
2.1	246	18.50	.778	.0463
3.2	246	20.56	.864	.0546
5.6	246	24.39	1.03	.0740
7.9	246	27.22	1.14	.0956
10.5	246	29.98	1.26	.1250
13.4	246	31.77	1.34	.1658
14.7	246	32.21	1.36	.1869
15.9	246	32.31	1.36	.2023
17.0	246	32.33	1.36	.2276
18.4	246	31.96	1.35	.2514
19.8	244	31.64	1.35	.2800
21.1	244	31.07	1.32	.3060
22.3	243	30.62	1.31	.3286

TABLE IV

SECTION NO. N. A. C. A. 97. FICTITIOUS ASPECT RATIO, 6.85.
MODEL NO. 9. AVERAGE TEMPERATURE, 37° C.
SPAN 30 IN., 76.2 cm PRESSURE, 16 ATMOSPHERES.
CHORD 5 IN., 12.7 cm REYNOLDS NUMBER, 2,810,000.
AREA, 0.0968 m²

Angle of attack, degree	q kg m ²	Lift L kg	Lift coef. C_L	Drag coef. C_D	Moment about $c/4$ kg-cm	Moment coef. C_M
-11.6	524	-11.64	-0.230	0.0156	139.0	0.217
-9.2	522	-2.43	-.048	.0105	-88.9	-.138
-6.6	525	6.23	.123	.0102	-90.9	-.141
-4.2	525	16.39	.323	.0150	-88.9	-.138
-2.8	525	21.06	.415	.0186	-86.6	-.133
-1.6	523	24.37	.481	.0212	-20.2	-.032
-.4	523	28.57	.565	.0281	-50.8	-.079
.8	523	33.65	.665	.0339	-18.6	-.029
2.1	523	38.71	.765	.0416	-80.6	-.125
3.2	524	43.29	.855	.0525	-83.7	-.136
5.6	524	51.98	1.025	.0743	-87.8	-.136
7.9	524	58.79	1.16	.0966	-82.5	-.128
10.5	528	65.38	1.28	.1285	-63.8	-.098
12.3	528	68.28	1.34	.1428	-67.6	-.104
13.4	526	69.00	1.35	.1660	-89.5	-.139
14.7	530	70.65	1.38	.1908	-83.8	-.129
15.9	528	70.63	1.38	.2147	-84.7	-.131
17.0	527	69.92	1.37	.2339	-86.0	-.133
18.4	527	68.65	1.34	.2630	-92.6	-.143
19.8	524	67.25	1.33	.2881	-84.6	-.131
21.1	523	65.65	1.30	.3169	-96.4	-.150

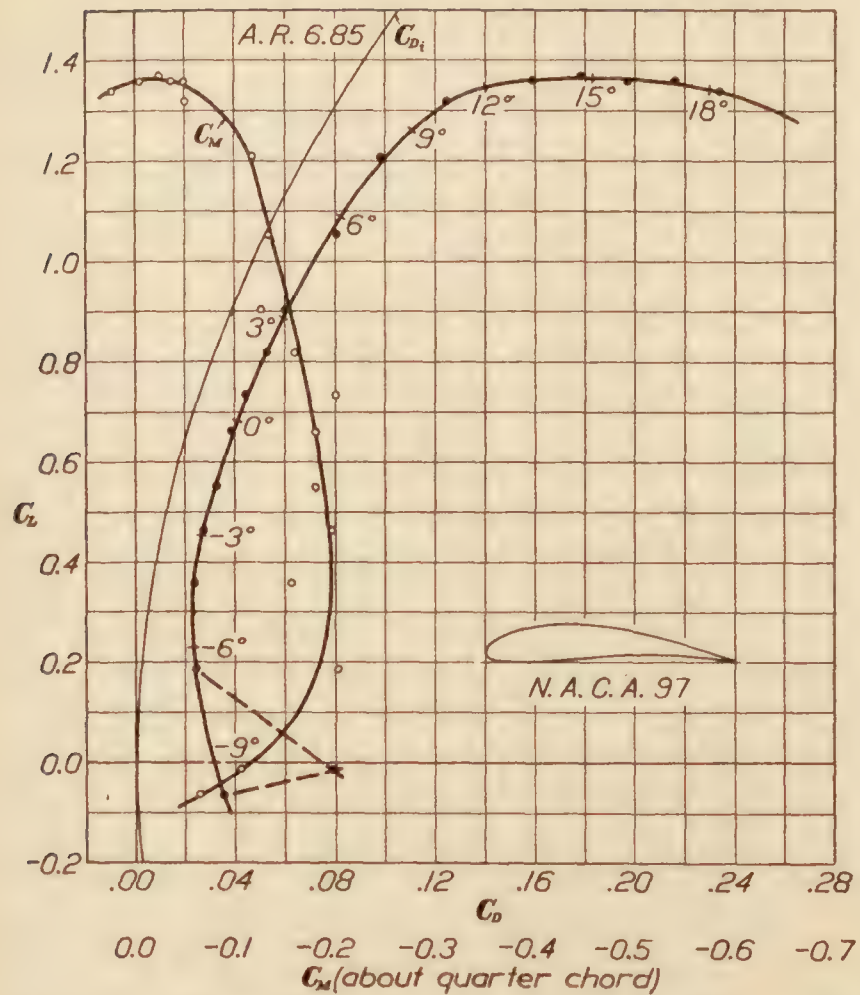


FIG. 9.—Test No. 58-1. Tank pressure 1.0 atmosphere. Dynamic pressure $q=27.5 \text{ kg/m}^2$. Reynolds Number 175,000

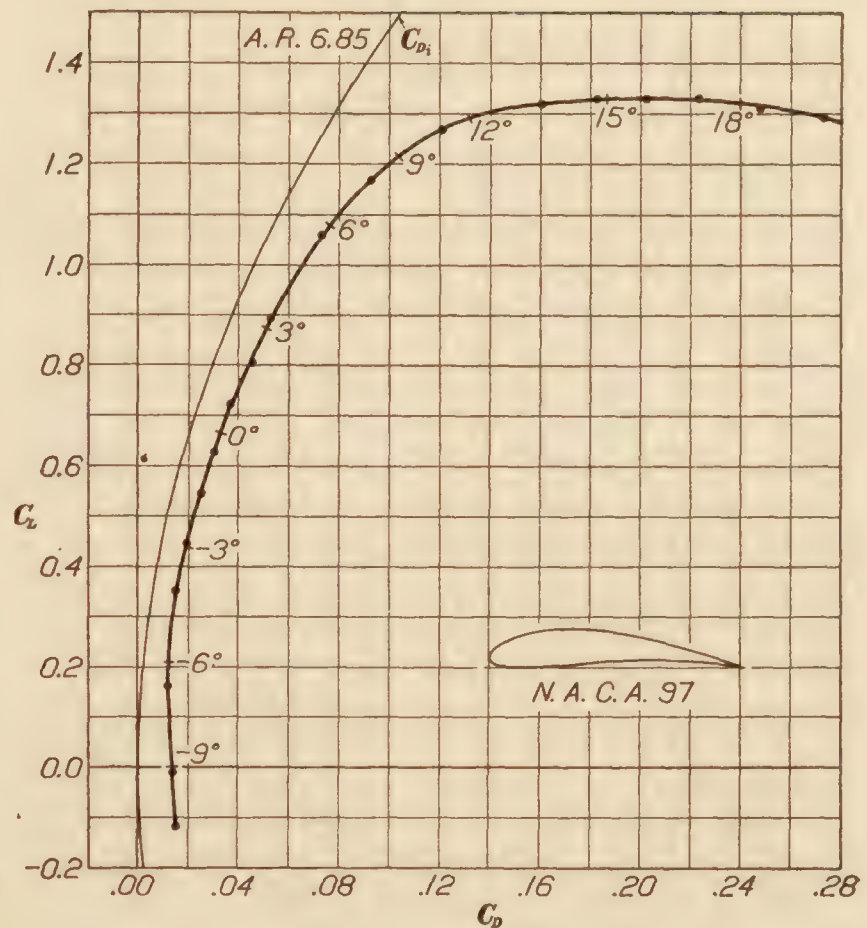


FIG. 10.—Test No. 58-2. Tank pressure 4.1 atmospheres. Dynamic pressure $q=122 \text{ kg/m}^2$. Reynolds Number 740,000

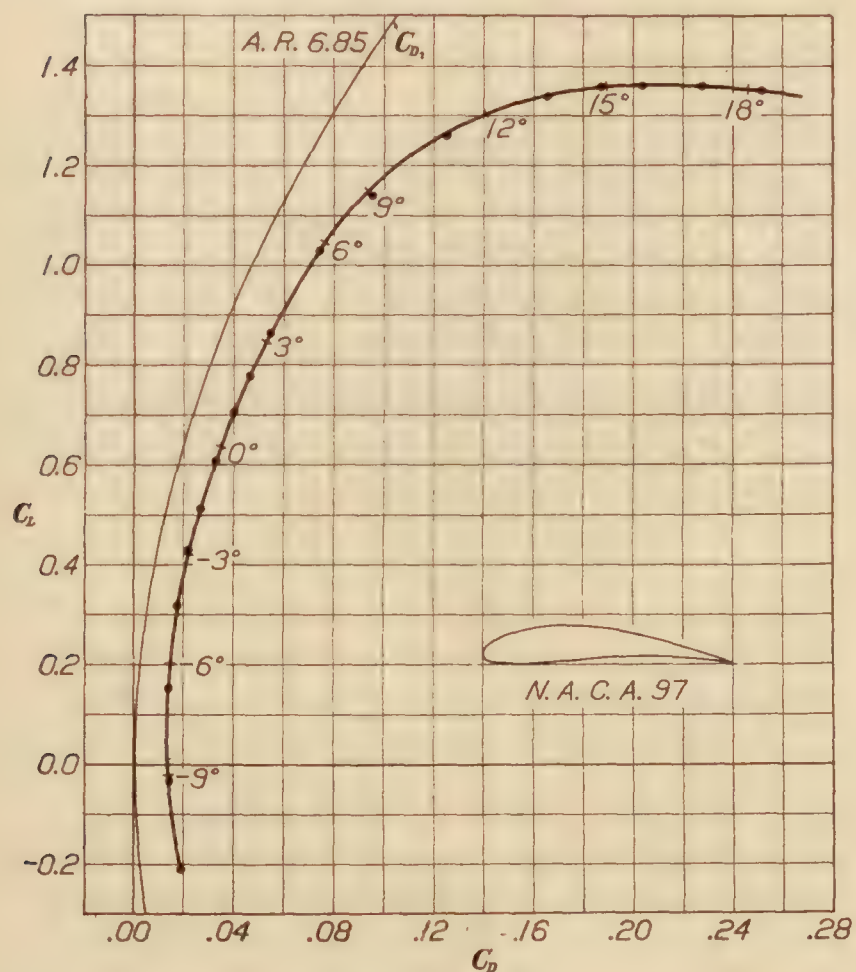


FIG. 11.—Test No. 58-3. Tank pressure 8 atmospheres. Dynamic pressure $q=246 \text{ kg/m}^2$. Reynolds Number 1,430,000

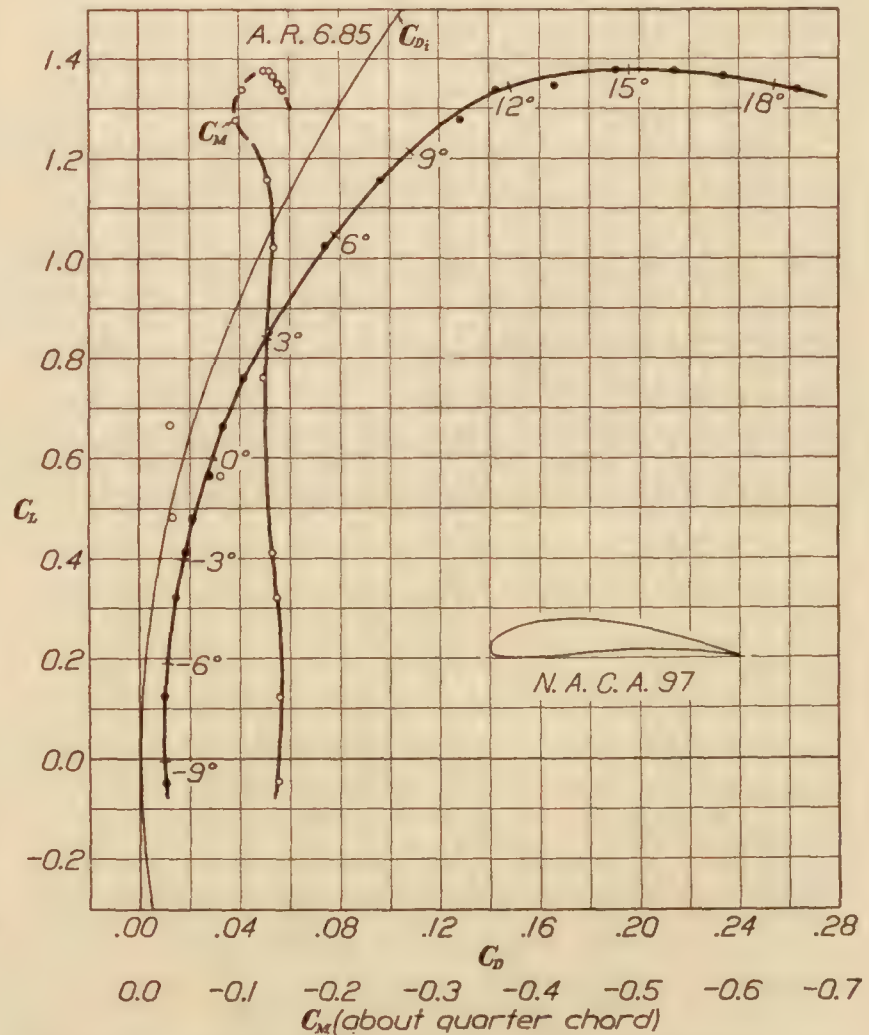


FIG. 12.—Test No. 58-4. Tank pressure 16 atmospheres. Dynamic pressure $q=524 \text{ kg/m}^2$. Reynolds Number 2,810,000

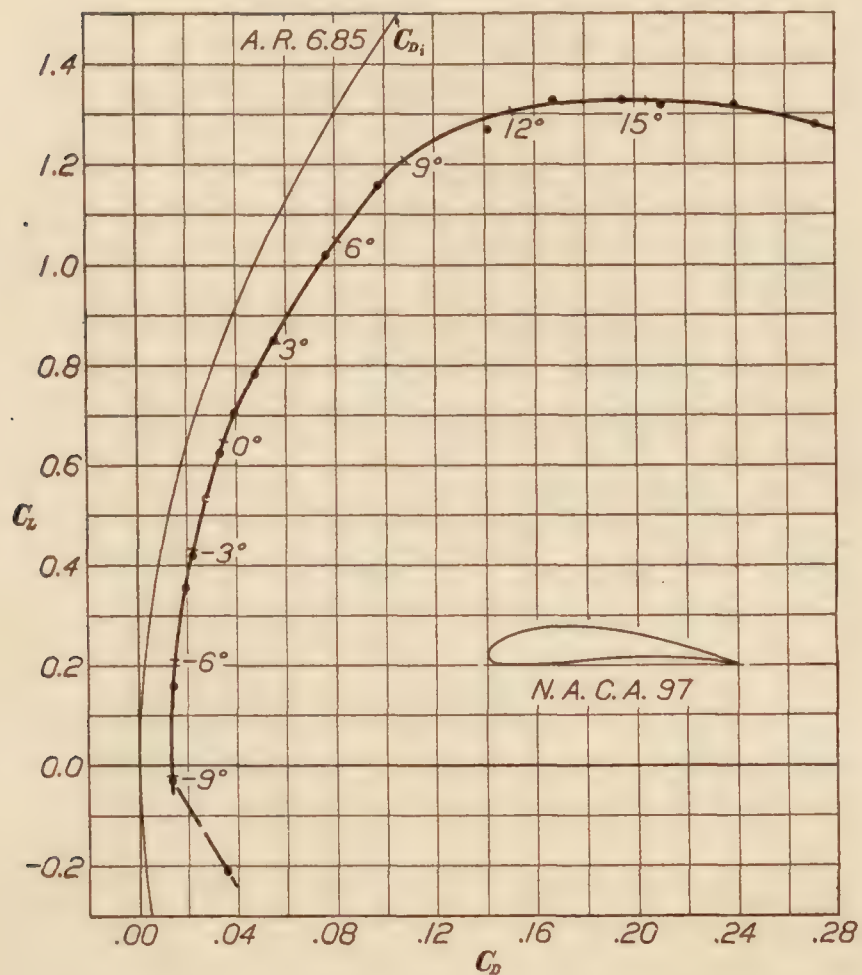


FIG. 13.—Test No. 58-5. Tank pressure 20.9 atmospheres. Dynamic pressure $q=705 \text{ kg/m}^2$. Reynolds Number 3,850,000

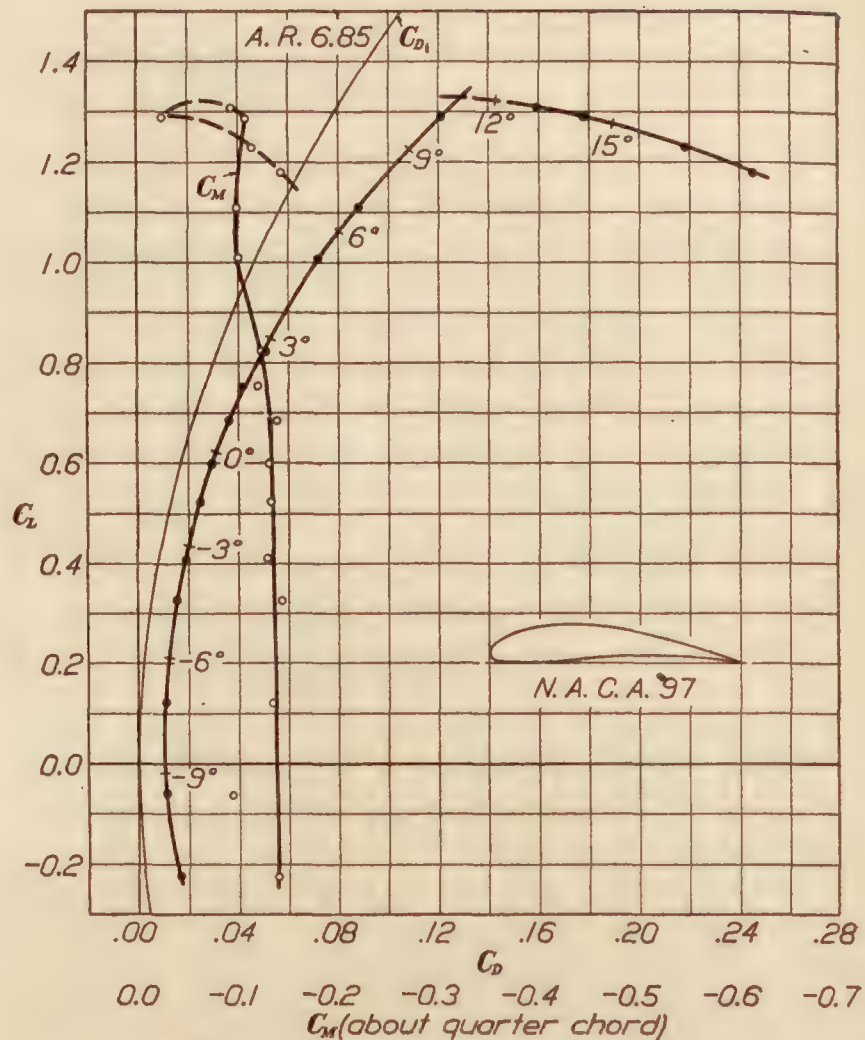


FIG. 14.—Test No. 61-3. Tank pressure 16.7 atmospheres. Dynamic pressure $q=567 \text{ kg/m}^2$. Reynolds Number 3,080,000. Airfoil painted

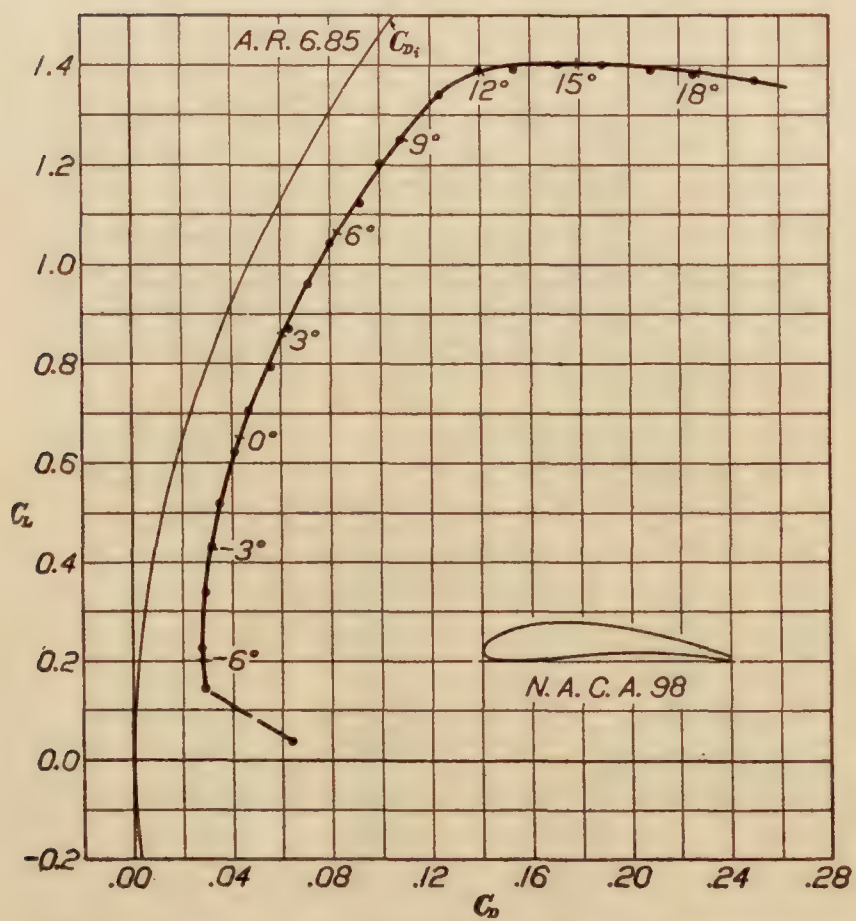


FIG. 15.—Test No. 57-1. Tank pressure 1.0 atmosphere. Dynamic pressure $q=27.8 \text{ kg/m}^2$. Reynolds Number 176,000

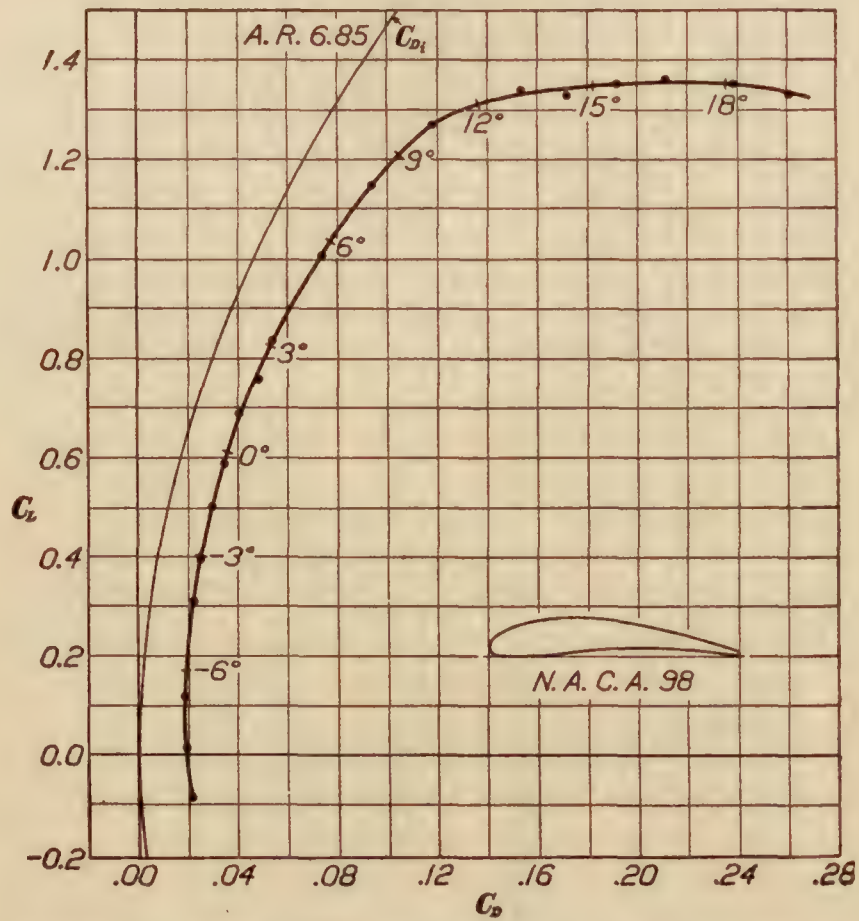


FIG. 16.—Test No. 57-2. Tank pressure 4.15 atmospheres. Dynamic pressure $q=123 \text{ kg/m}^2$. Reynolds Number 755,000

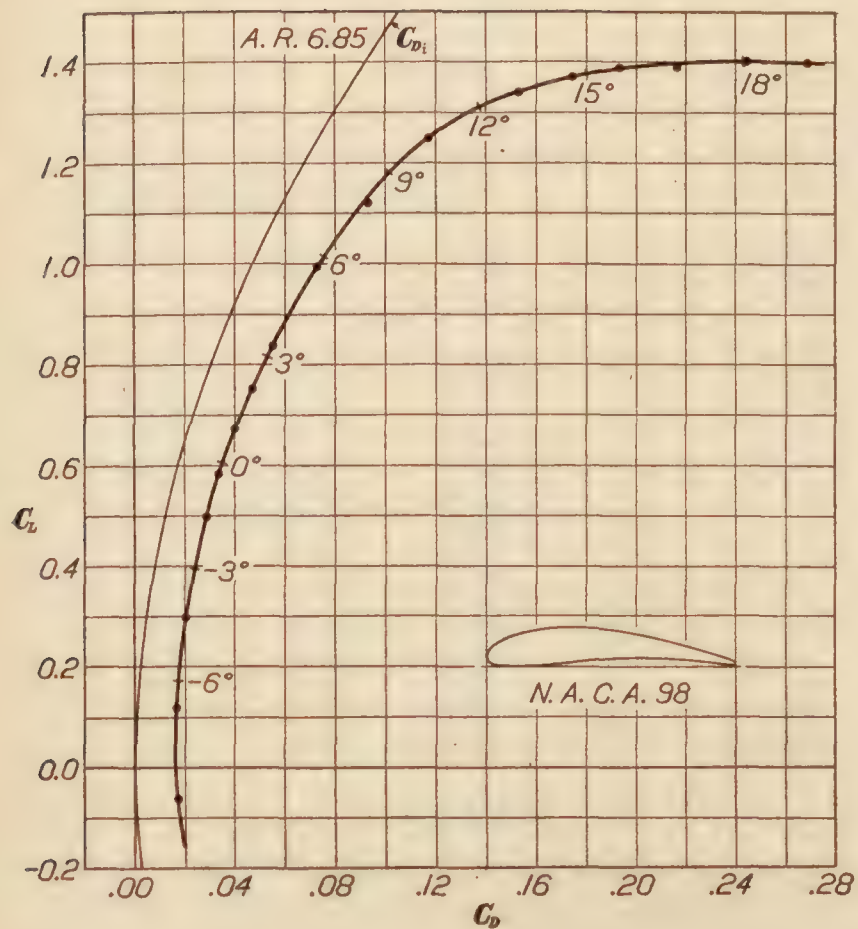


FIG. 17.—Test No. 57-3. Tank pressure 8.2 atmospheres. Dynamic pressure $q=258 \text{ kg/m}^2$. Reynolds Number 1,490,000

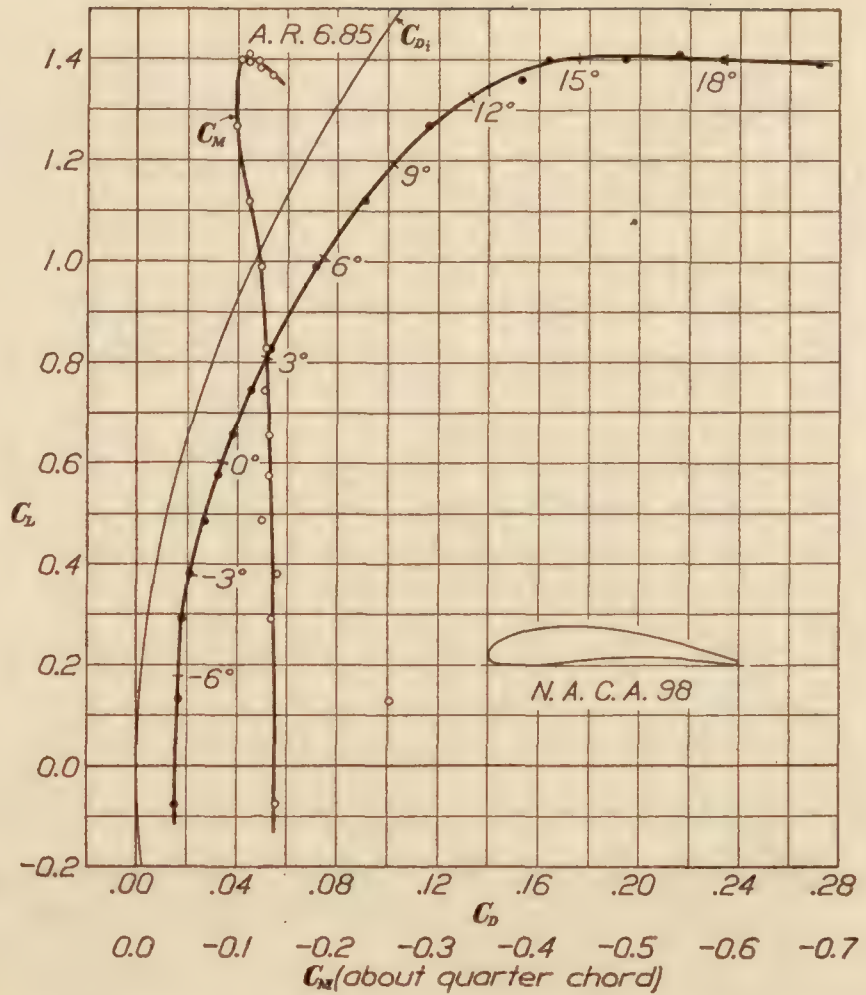


FIG. 18.—Test No. 57-4. Tank pressure 16.44 atmospheres. Dynamic pressure $q=531 \text{ kg/m}^2$. Reynolds Number 2,880,000

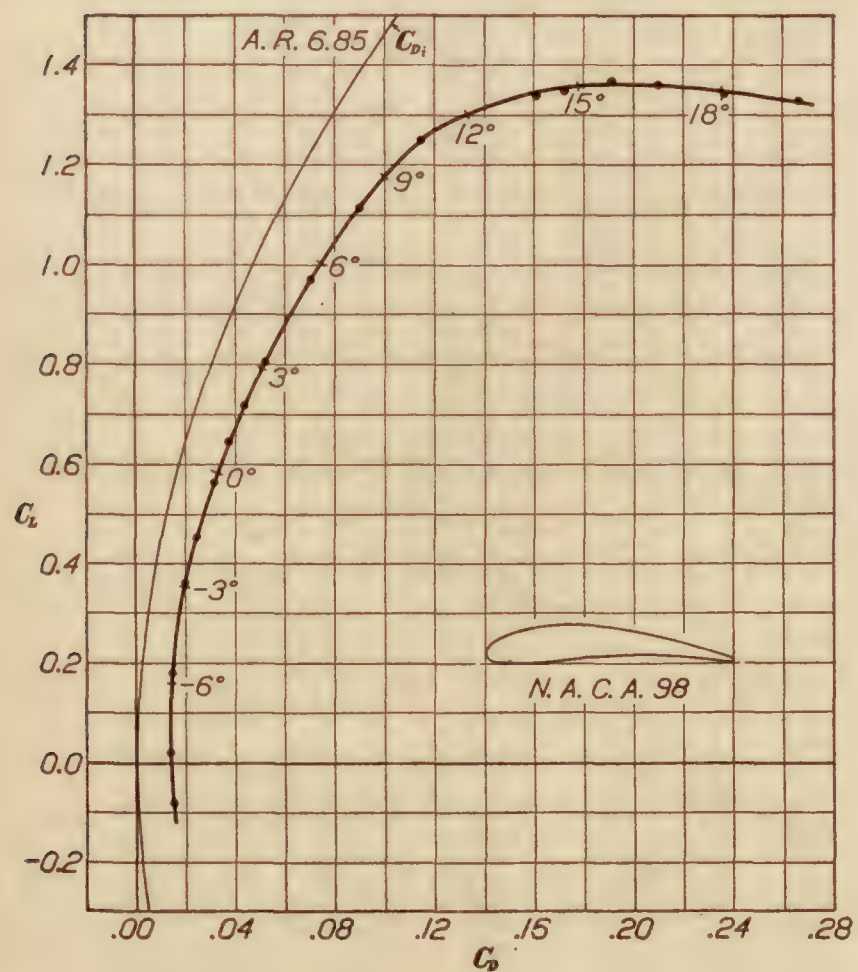


FIG. 19.—Test No. 57-5. Tank pressure 20.4 atmospheres. Dynamic pressure $q=699 \text{ kg/m}^2$. Reynolds Number 3,780,000

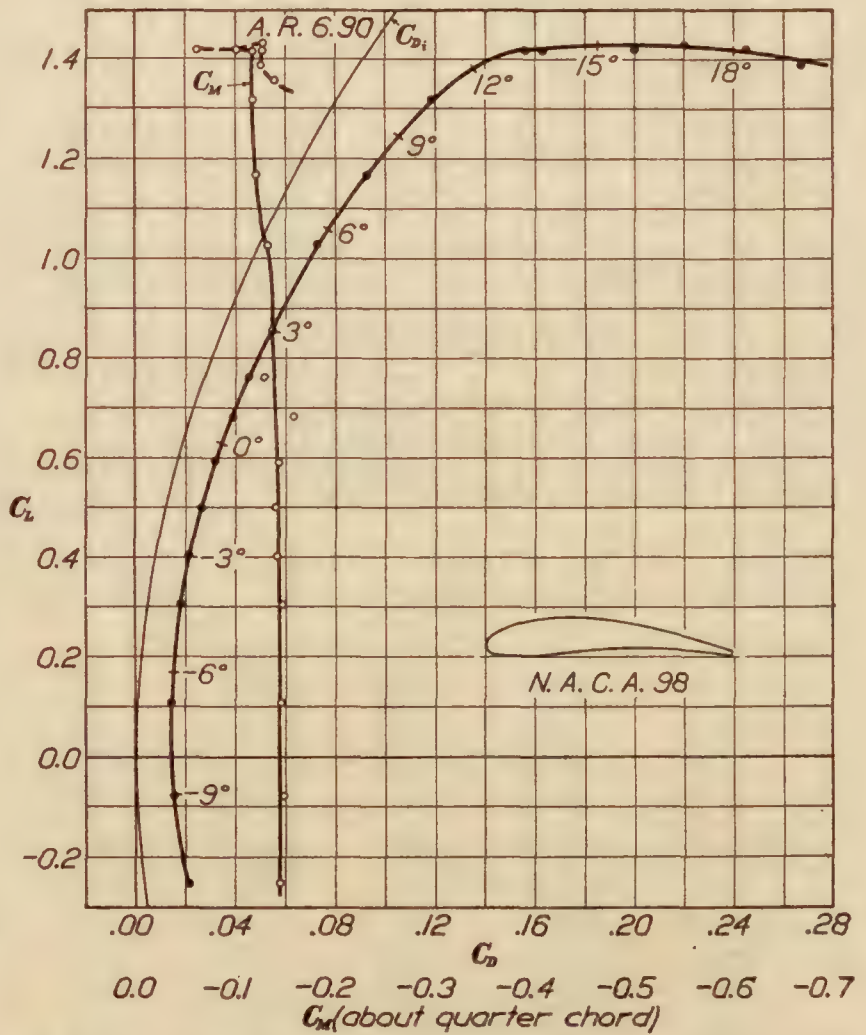


FIG. 20.—Test No. 59-1. Tank pressure 16.2 atmospheres. Dynamic pressure $q=575 \text{ kg/m}^2$. Reynolds Number 2,470,000. Trailing edge milled off square

TABLE V

SECTION NO. N. A. C. A. 97. FICTITIOUS ASPECT RATIO, 6.85.
 MODEL NO. 9. TEMPERATURE, 38° C.
 SPAN 30 IN., 76.2 cm PRESSURE, 20.9 ATMOSPHERES.
 CHORD 5 IN., 12.7 cm REYNOLDS NUMBER, 985,000.
 AREA, 0.0968 m²
 ASPECT RATIO, 6.

Angle of attack, degree	q kg m ²	Lift L kg	Lift coef. C_L	Drag coef. C_D
-11.6	700	-14.1	-0.209	0.0354
-9.2	706	-2.05	.030	.0134
-6.7	705	10.76	.158	.0136
-4.1	713	23.42	.354	.0198
-2.8	711	28.82	.419	.0220
-1.6	711	36.65	.533	.0275
-.4	710	42.75	.623	.0332
.8	709	48.13	.702	.0396
2.1	704	53.38	.784	.0472
3.2	704	58.12	.855	.0556
5.6	704	69.94	1.02	.0760
7.9	704	79.03	1.16	.0971
11.1	704	86.48	1.27	.1412
13.4	704	90.23	1.33	.1672
14.3	704	90.64	1.33	.1948
15.4	704	90.07	1.32	.2107
16.4	704	89.55	1.32	.2397
17.6	704	87.48	1.28	.2720

TABLE VI

SECTION NO. N. A. C. A. 97 FICTITIOUS ASPECT RATIO, 6.85.
 (PAINTED). TEMPERATURE, 37° C.
 MODEL NO. 9. PRESSURE, 16.7 ATMOSPHERES.
 SPAN 30 IN., 76.2 cm REYNOLDS NUMBER, 3,080,000.
 CHORD 5 IN., 12.7 cm
 AREA, 0.0968 m²
 ASPECT RATIO, 6.

Angle of attack, degree	q kg m ²	Lift L kg	Lift coef. C_L	Drag coef. C_D	Moment about c/4	Moment coef. C_M
-11.9	565	-12.36	-0.226	0.0161	-96.8	-0.139
-9.4	569	-3.26	-.059	.0117	-68.4	-.098
-7.2	569	6.71	.122	.0111	-94.5	-.135
-4.5	568	17.96	.327	.0158	-100.3	-.144
-3.2	566	22.33	.406	.0196	-90.8	-.130
-1.9	568	28.71	.523	.0249	-93.6	-.134
-.4	568	32.96	.599	.0300	-92.4	-.132
.7	569	37.77	.688	.0367	-97.2	-.139
1.8	568	41.31	.753	.0421	-84.1	-.120
3.0	569	45.97	.822	.0516	-86.4	-.124
5.4	569	55.45	1.01	.0723	-71.3	-.102
7.6	565	61.53	1.11	.0884	-69.4	-.100
10.3	570	70.51	1.29	.1212	-76.7	-.109
13.2	565	72.37	1.31	.1599	-64.5	-.093
14.4	564	70.23	1.29	.1783	-17.4	-.025
15.6	564	66.89	1.23	.2186	-79.7	-.115
16.8	564	64.52	1.18	.2458	-101.2	-.146

TABLE VII

SECTION NO. N. A. C. A. 98 FICTITIOUS ASPECT RATIO, 6.85.
 MODEL NO. 10. AVERAGE TEMPERATURE, 25.5° C.
 SPAN 30 IN., 76.2 cm PRESSURE, 1 ATMOSPHERE.
 CHORD 5 IN., 12.7 cm REYNOLDS NUMBER, 176,000.
 AREA, 0.0968 m²
 ASPECT RATIO, 6.

Angle of attack, degree	q kg m ²	Lift L kg	Lift coef. C_L	Drag coef. C_D
-8.1	27.8	0.01	0.037	0.0632
-6.8	27.8	.38	.141	.0282
-5.7	27.8	.60	.223	.0273
-4.4	27.8	.90	.336	.0290
-2.9	27.8	1.15	.429	.0314
-1.6	27.8	1.38	.515	.0347
-.4	27.8	1.66	.621	.0413
.8	27.8	1.89	.704	.0463
2.1	28.0	2.14	.792	.0557
3.2	28.1	2.35	.869	.0630
4.5	28.1	2.59	.961	.0708
5.6	28.1	2.80	1.04	.0799
6.6	28.1	3.03	1.12	.0920
7.8	27.6	3.20	1.20	.0995
9.1	27.6	3.35	1.25	.1078
10.5	27.6	3.58	1.34	.1238
11.8	27.6	3.68	1.39	.1396
13.2	27.6	3.72	1.39	.1536
14.5	27.6	3.75	1.40	.1710
15.7	27.6	3.74	1.40	.1895
16.8	27.6	3.71	1.39	.2083
18.1	27.6	3.69	1.38	.2258
19.5	27.6	3.65	1.37	.2502

TABLE VIII

SECTION NO. N. A. C. A. 98. FICTITIOUS ASPECT RATIO, 6.85.
 MODEL NO. 10. AVERAGE TEMPERATURE, 27° C.
 SPAN 30 IN., 76.2 cm AVERAGE PRESSURE, 4.15 ATMOSPHERES.
 CHORD 5 IN., 12.7 cm REYNOLDS NUMBER, 155,000.
 AREA, 0.0968 m²
 ASPECT RATIO, 6.

Angle of attack, degree	q kg m ²	Lift L kg	Lift coef. C_L	Drag coef. C_D
-9.2	122	-0.96	-0.081	0.0212
-8.1	124	.23	.019	.0192
-6.8	125	1.49	.123	.0185
-4.4	125	3.77	.313	.0225
-2.9	122	4.75	.398	.0255
-1.6	122	6.02	.505	.0298
-.4	122	7.06	.591	.0353
.8	122	8.21	.690	.0410
2.1	124	9.11	.761	.0484
3.2	124	10.09	.837	.0548
5.6	125	12.24	1.01	.0747
7.8	125	13.95	1.15	.0945
10.5	125	15.29	1.27	.1188
13.2	125	16.11	1.34	.1544
14.5	125	16.10	1.33	.1731
15.7	124	16.09	1.35	.1933
16.8	122	16.03	1.36	.2125
18.1	122	15.99	1.35	.2396
19.5	122	15.79	1.33	.2619

TABLE IX

SECTION NO. N. A. C. A. 98. FICTITIOUS ASPECT RATIO, 6.85.
 MODEL NO. 10. AVERAGE TEMPERATURE, 32° C.
 SPAN 30 IN., 76.2 cm AVERAGE PRESSURE, 8.2 ATMOSPHERES.
 CHORD 5 IN., 12.7 cm REYNOLDS NUMBER, 1,490,000.
 AREA, 0.0968 m²
 ASPECT RATIO, 6.

Angle of attack, degree	q kg m ²	Lift L kg	Lift coef. C_L	Drag coef. C_D
-9.2	258	-0.16	-0.063	0.0177
-6.8	258	2.91	.117	.0168
-4.4	259	7.44	.297	.0200
-1.6	259	12.42	.496	.0285
-.4	258	14.63	.586	.0336
.8	258	16.81	.674	.0401
2.1	258	18.78	.752	.0470
3.2	258	20.87	.837	.0552
5.6	258	24.85	.995	.0733
7.8	258	28.02	1.12	.0930
10.5	258	31.33	1.25	.1170
13.2	258	33.41	1.34	.1531
14.5	256	33.92	1.37	.1743
15.7	257	34.35	1.39	.1938
16.8	256	34.47	1.39	.2162
18.1	257	34.82	1.40	.2440
19.5	257	34.64	1.40	.2688
20.7	257	34.51	1.39	.2941

TABLE X

SECTION NO. N. A. C. A. 98. FICTITIOUS ASPECT RATIO, 6.85.
 MODEL NO. 10. TEMPERATURE, 42.5° C.
 SPAN 30 IN., 76.2 cm PRESSURE, 16.44 ATMOSPHERES.
 CHORD 5 IN., 12.7 cm REYNOLDS NUMBER, 2,880,000.
 AREA, 0.0968 m²
 ASPECT RATIO, 6.

Angle of attack, degree	q kg m ²	Lift L kg	Lift coef. C_L	Drag coef. C_D	Moment about c/4 kg-cm	Moment coef. C_M
-9.2	526	-3.95	-0.078	0.0157	-90.6	-0.140
-6.8	527	6.64	.130	.0168	-163.0	-.251
-4.4	527	14.73	.289	.0182	-87.5	-.135
-2.9	529	19.44	.380	.0208	-91.0	-.140
-1.6	534	25.10	.486	.0271	-82.3	-.125
-.4	534	29.70	.575	.0325	-86.5	-.132
.8	534	33.92	.656	.0383	-87.3	-.133
2.1	534	38.48	.744	.0455	-84.2	-.128
3.2	531	42.41	.825	.0534	-85.2	-.130
5.6	533	51.07	.990	.0718	-81.7	-.125
7.8	534	58.12	1.12	.0907	-73.1	-.112
10.4	532	65.31	1.27	.1168	-65.4	-.100
13.2	533	70.23	1.36	.1533	-7.8	.012
14.5	532	72.06	1.40	.1640	-69.6	-.106
15.7	531	72.20	1.40	.1945	-73.2	-.112
16.8	531	72.38	1.41	.2160	-72.9	-.112
18.1	531	71.99	1.40	.2340	-79.5	-.122
19.5	530	71.27	1.39	.2721	-79.8	-.123
20.7	530	70.44	1.37	.2972	-89.2	-.137

TABLE XI

SECTION NO. N. A. C. A. 98. FICTITIOUS ASPECT RATIO,
MODEL NO. 10. 6.85.
SPAN 30 IN., 76.2 cm TEMPERATURE, 38° C.
CHORD 5 IN., 12.7 cm PRESSURE, 20.4 ATMOS-
AREA, 0.0968 m² PHERES.
ASPECT RATIO 6. REYNOLDS NUMBER, 3,780,000.

Angle of attack, degree	q kg m ²	Lift L kg	Lift coef. C_L	Drag coef. C_D
-9.2	697	-5.41	-0.080	0.0152
-8.1	698	1.33	.020	.0137
-5.7	698	12.06	.178	.0150
-2.9	697	24.24	.359	.0200
-1.6	697	30.44	.451	.0241
-.4	696	37.98	.563	.0317
.8	695	43.35	.645	.0374
2.1	695	48.26	.718	.0436
3.2	697	54.19	.802	.0516
5.6	698	65.50	.970	.0701
7.8	698	75.30	1.115	.0895
10.5	703	85.06	1.25	.1146
13.2	703	91.10	1.34	.1610
14.5	704	91.95	1.35	.1725
15.7	696	92.19	1.37	.1914
16.8	696	91.59	1.36	.2100
18.1	701	91.32	1.34	.2366
19.5	699	89.89	1.33	.2666
20.7	697	86.63	1.28	.2924

TABLE XIV

SECTION NO. N. A. C. A. 99. FICTITIOUS ASPECT RATIO,
MODEL NO. 11. 6.85.
SPAN 30 IN., 76.2 cm AVERAGE TEMPERATURE,
CHORD 5 IN., 12.7 cm 27° C.
AREA, 0.0968 m² AVERAGE PRESSURE, 2.03
ASPECT RATIO, 6. ATMOSPHERES.
REYNOLDS NUMBER, 352,000.

Angle of attack, degree	q kg m ²	Lift L kg	Lift coef. C_L	Drag coef. C_D	Moment coef. C_M
-0.4	56.9	-0.16	-0.030	0.0117	0.0285
.7	56.9	.28	.050	.0130	.0001
1.9	56.9	.70	.127	.0137	.0070
3.0	57.5	1.20	.217	.0149	.0042
4.2	57.5	1.64	.295	.0189	.0195
5.5	57.3	2.08	.375	.0221	.0150
6.6	57.3	2.50	.452	.0264	.0015
7.7	57.3	2.95	.533	.0333	.0150
9.4	57.3	3.62	.653	.0439	.0150
11.5	57.3	4.18	.752	.0604	.0260
13.6	57.3	3.86	.695	.1572	-.0250
15.2	57.5	3.26	.587	.2000	-.0920
16.9	57.2	3.26	.589	.2278	-.0560
19.0	57.2	3.26	.589	.2430	-.0510

TABLE XII

SECTION NO. N. A. C. A. 98 FICTITIOUS ASPECT RATIO,
(MILLED T. E.). 6.90.
MODEL NO. 10. TEMPERATURE, 39° C.
SPAN 30 IN., 76.2 cm PRESSURE, 16.2 ATMOS-
CHORD 4.95 IN., 12.57 cm PHERES.
AREA, 0.0958 m² REYNOLDS NUMBER, 2,470,000.
ASPECT RATIO, 6.05.

Angle of attack, degree	q kg m ²	Lift L kg	Lift coef. C_L	Drag coef. C_D	Moment about c/4 kg-cm	Moment coef. C_M
-11.7	577	-14.39	-0.260	0.0211	-101.0	-0.146
-9.0	577	-4.25	-.077	.0154	-104.0	-.149
-6.7	578	6.04	.109	.0142	-102.0	-.147
-4.4	578	17.10	.308	.0180	-103.0	-.148
-3.0	578	22.41	.404	.0217	-99.1	-.143
-1.6	575	27.60	.501	.0265	-97.8	-.141
-.4	575	32.74	.594	.0321	-99.6	-.144
.8	573	37.51	.682	.0396	-110.0	-.159
1.8	576	42.37	.766	.0455	-90.5	-.130
3.0	576	47.25	.856	.0543	-95.7	-.138
5.6	577	56.69	1.03	.0735	-93.5	-.134
7.7	577	64.90	1.17	.0931	-84.2	-.121
10.4	579	73.18	1.32	.1192	-83.0	-.119
13.2	579	78.67	1.42	.1564	-82.1	-.118
14.4	566	76.99	1.42	.1634	-42.3	-.062
15.7	579	78.87	1.42	.2004	-72.0	-.103
16.8	577	79.29	1.43	.2203	-90.6	-.130
18.1	577	78.29	1.42	.2454	-89.0	-.128
19.4	577	76.85	1.39	.2676	-88.1	-.127
20.7	562	72.80	1.36	.2998	-95.2	-.140

TABLE XIII

SECTION NO. N. A. C. A. 99. FICTITIOUS ASPECT RATIO,
MODEL NO. 11. 6.85.
SPAN 30 IN., 76.2 cm AVERAGE TEMPERATURE,
CHORD 5 IN., 12.7 cm 26° C.
AREA, 0.0968 m² PRESSURE, 1 ATMOSPHERE.
ASPECT RATIO, 6. REYNOLDS NUMBER, 175,000.

Angle of attack, degree	q kg m ²	Lift L kg	Lift coef. C_L	Drag coef. C_D
-0.4	27.6	-0.08	-0.032	0.0186
.7	27.6	.24	.089	.0173
1.9	27.6	.43	.161	.0186
3.0	27.5	.56	.209	.0207
4.2	27.5	.72	.273	.0266
5.4	27.6	.92	.346	.0290
6.6	27.6	1.14	.427	.0341
7.7	27.6	1.44	.539	.0403
9.4	27.6	1.62	.612	.0536
11.5	27.4	1.92	.722	.0800
13.6	27.4	1.72	.645	.1705
15.2	27.4	1.57	.591	.2034
16.8	27.4	1.50	.565	.2316
19.0	27.4	1.48	.557	.2594

TABLE XVI

SECTION NO. N. A. C. A. 99. FICTITIOUS ASPECT RATIO,
MODEL NO. 11. 6.85.
SPAN 30 IN., 76.2 cm AVERAGE TEMPERATURE,
CHORD 5 IN., 12.7 cm 31° C.
AREA, 0.0968 m² AVERAGE PRESSURE, 6
ASPECT RATIO, 6. ATMOSPHERES.
REYNOLDS NUMBER, 1,070,-
000.

Angle of attack, degree	q kg m ²	Lift L kg	Lift coef. C_L	Drag coef. C_D
-0.4	183	-0.66	-0.037	0.0124
.7	183	.70	.040	.0129
1.9	183	2.22	.126	.0140
3.0	183	3.61	.204	.0156
4.2	183	5.21	.295	.0188
5.4	183	7.04	.396	.0226
6.6	183	8.18	.462	.0270
7.7	183	9.56	.541	.0320
9.4	183	11.92	.672	.0413
11.5	183	14.26	.805	.0558
13.6	183	16.42	.928	.0705
15.2	182	18.28	1.03	.0892
16.8	184	16.14	.906	.1738
19.0	183	16.04	.906	.2087

TABLE XVII

SECTION NO. N. A. C. A. 99. FICTITIOUS ASPECT RATIO, 6.85.
MODEL NO. 11. AVERAGE TEMPERATURE, 38° C.
SPAN 30 IN., 76.2 cm. AVERAGE PRESSURE, 8.3 ATMOSPHERES.
CHORD 5 IN., 12.7 cm. REYNOLDS NUMBER, 1,440,000.
AREA, 0.0968 m².

Angle of attack, degree	q kg m²	Lift L kg	Lift coef. C_L	Drag coef. C_D
-0.4	257	-1.18	-0.047	0.0129
1.9	256	3.25	.131	.0135
3.0	256	5.20	.209	.0157
4.2	257	7.55	.302	.0193
5.4	258	9.59	.385	.0222
6.6	257	11.80	.473	.0266
7.7	257	13.66	.547	.0320
9.4	255	16.35	.662	.0409
11.5	255	20.34	.822	.0566
13.6	257	23.68	.952	.0723
15.2	258	26.50	1.06	.0889
16.8	257	28.71	1.15	.1078
19.0	256	28.50	1.15	.1595
20.7	256	27.26	1.09	.2310

TABLE XVIII

SECTION NO. N. A. C. A. 99. FICTITIOUS ASPECT RATIO, 6.85.
MODEL NO. 11. AVERAGE TEMPERATURE, 40° C.
SPAN 30 IN., 76.2 cm. AVERAGE PRESSURE, 16.24 ATMOSPHERES.
CHORD 5 IN., 12.7 cm. REYNOLDS NUMBER, 2,950,000.
AREA, 0.0968 m².

Angle of attack, degree	q kg m²	Lift L kg	Lift coef. C_L	Drag coef. C_D	Moment coef. C_M
-0.4	544	-2.21	-0.042	0.0109	0.0028
.7	544	2.16	.041	.0106	-.0034
1.9	544	6.77	.129	.0117	.0012
3.0	544	11.51	.218	.0138	.0029
4.2	547	16.34	.309	.0165	.0030
5.4	545	20.49	.389	.0201	.0100
6.6	544	24.82	.471	.0246	.0080
7.7	538	28.83	.555	.0292	.0100
9.4	543	35.63	.678	.0390	.0130
11.5	543	43.19	.823	.0592	.0010
13.6	540	49.81	.950	.0702	.0990
15.2	540	55.82	1.06	.0845	.0390
16.8	541	53.39	1.02	.148	-.0290
19.0	540	48.55	.928	.225	-.0780
20.7	537	45.08	.868	.280	-.1150

TABLE XIX

TABLE OF ORDINATES OF AIRFOIL SECTIONS. NOS. 97, 98 AND 99

Station	Airfoil No. 97		Airfoil No. 98		Airfoil No. 99	
Per cent of chord	Upper	Lower	Upper	Lower	Upper	Lower
0	4.17	4.17	4.00	4.00	0.00	-0.00
2.5	7.93	.73	8.00	.73	3.50	-3.50
5.0	9.50	.33	9.60	.30	4.33	-4.33
7.5	10.80	.10	10.85	.10	4.90	-4.90
10	11.80	.03	11.93	.00	5.33	-5.33
15	13.30	.00	13.40	.00	6.03	-6.03
20	14.28	.17	14.38	.23	6.43	-6.43
25	14.82	.47	14.96	.56	6.66	-6.66
30	15.15	.83	15.37	1.07	6.99	-6.99
40	15.00	1.73	15.30	2.06	6.36	-6.36
50	13.94	2.50	14.28	2.87	5.63	-5.63
60	12.20	2.86	12.60	3.23	4.63	-4.63
70	9.77	2.80	10.30	3.13	3.50	-3.50
80	6.87	2.30	7.70	2.47	2.33	-2.33
90	3.60	1.33	4.87	1.33	1.23	-1.23
95	1.87	.67	3.27	.56	.67	-.67
100	.13	.00	.90	.90	.00	-.00
Radius of leading edge.	3.57		3.57		3.57	
Radius of trailing edge.	---		0.93		---	

REFERENCES

1. Max M. Munk: The Modification of Wind Tunnel Results by the Wind Tunnel Dimensions. Journal of Franklin Institute, August, 1923.
2. Max M. Munk: Elements of the Wing Section Theory and of the Wing Theory. N. A. C. A. Technical Report No. 191. 1924.
3. Max M. Munk: The Determination of the Angles of Attack of Zero Lift and Zero Moment, Based on Munk's Integrals. N. A. C. A. Technical Note No. 122. 1923.

APPENDIX

COMPARISON WITH THEORY

By George J. Higgins

In this appendix, the aerodynamic properties of the N. A. C. A. airfoil No. 97 are computed as far as the present theory allows. This comprises the computation of the lift and the moment characteristics at any angle of attack.

The lift characteristics.—The angle of attack, at which the lift force is zero, is first computed. The method employed is obtained from the N. A. C. A. Technical Note No. 122 (Reference 3). The five-point method is used because of its greater accuracy.

$$-\alpha_{L_0} = F_1 \frac{\xi_1}{c} + F_2 \frac{\xi_2}{c} + \dots + F_n \frac{\xi_n}{c} + \dots$$

in degrees where,

α_{L_0} = angle of attack at which the lift is zero.

ξ = ordinate of the mean camber line at a point (x) on the chord line, minus the ordinate of the trailing edge.

c = the chord of the airfoil.

$$\alpha_{L_0} = \sum f \xi = f_1 \xi_1 + f_2 \xi_2 + f_3 \xi_3 + f_4 \xi_4 + f_5 \xi_5 \quad (\text{Reference 3})$$

$x_1 = 99.458\%c$	$f_1 = 1252.24$	$\xi_1 = 0.13\%c$
$x_2 = 87.426\%c$	$f_2 = 109.048$	$\xi_2 = 2.91\%c$
$x_3 = 50.000\%c$	$f_3 = 32.596$	$\xi_3 = 8.16\%c$
$x_4 = 12.574\%c$	$f_4 = 15.684$	$\xi_4 = 6.31\%c$
$x_5 = 0.542\%c$	$f_5 = 5.978$	$\xi_5 = 3.71\%c$

$$-\alpha_{L_0} = \sum f \xi = 1.63 + 3.17 + 2.66 + 0.989 + 0.222$$

$$\alpha_{L_0} = -8.671^\circ \sim 8^\circ 40'$$

This value agrees well with the observed value. A graphical determination is also made by the two methods shown in the accompanying diagram (Fig. 21).

The angles determined there are:

One-point method,
 $\alpha_{L_0} = -9^\circ 15'$

Two-point method,
 $\alpha_{L_0} = -8^\circ 50'$

The lift force and the lift coefficient for any other angle of attack are obtained from the following expressions (Reference 2):

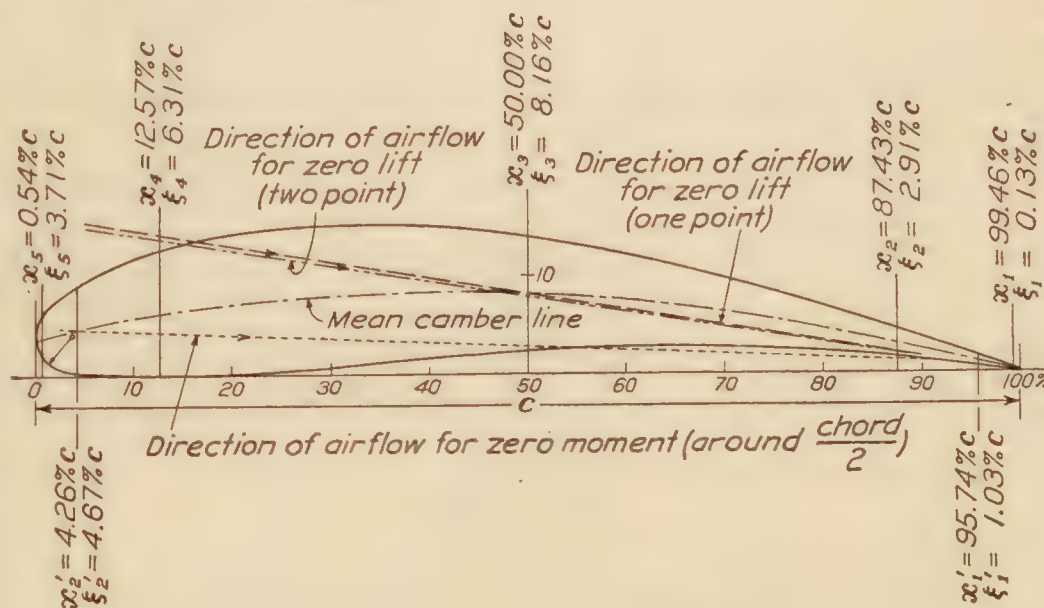


FIG. 21.—Angles of zero lift and zero moment (around $\frac{\text{chord}}{2}$). Airfoil N. A. C. A. No. 97. Found by computation

$$L = 2\pi\alpha \text{ (radians)} \frac{\rho}{2} V^2 S \frac{1}{1 + \frac{2S}{b^2}}$$

$$= \frac{2\pi\alpha \text{ (degrees)} qS}{57.3 \left[1 + \frac{2S}{b^2} \right]}$$

$$C_L = \frac{L}{qS} = \frac{2\pi\alpha \text{ (degrees)}}{57.3 \left[1 + \frac{2S}{b^2} \right]}$$

where

L = lift force
 α = angle of attack
 ρ = density
 V = velocity
 S = surface area
 b = span
 q = dynamic pressure

For the N. A. C. A. No. 97 airfoil,

$S = 0.0968 \text{ m}^2$
 $b = 0.762 \text{ m}$

$$C_L = \frac{2\pi\alpha \text{ (degrees)}}{57.3 \left[1 + \frac{2 \times .0968}{(.762)^2} \right]}$$

$$= .0822 \alpha \text{ (degrees)}$$

$$\frac{dC_L}{d\alpha \text{ (degrees)}} = .0822$$

The slope of the observed lift coefficient curve has a magnitude that is about 86 per cent of that computed.

$$\frac{dC_L}{d\alpha} \text{ (observed)} = .0710$$

The moment characteristics.—The angle of attack, at which the moment about the 50 per cent point of the chord is zero, is computed first in determining the moment. The method is also obtained from the N. A. C. A. Technical Note No. 122 (Reference 3).

$$\alpha_{M_0} = 62.634 \left[\frac{\xi_1}{c} - \frac{\xi_2}{c} \right]$$

where,

α_{M_0} = angle of attack, at which the moment about the 50 per cent point of the chord is zero.

ξ = ordinate of the mean camber line at a point (x) on the chord, minus the ordinate of the trailing edge.

$$\begin{aligned} x_1 &= 95.74\% c. & \xi_1 &= 1.03\% c. \\ x_2 &= 4.26\% c. & \xi_2 &= 4.67\% c. \\ \alpha_{M_0} &= 62.634 (1.03 - 4.67) \\ &= -2.28^\circ \sim -2^\circ 17' \end{aligned}$$

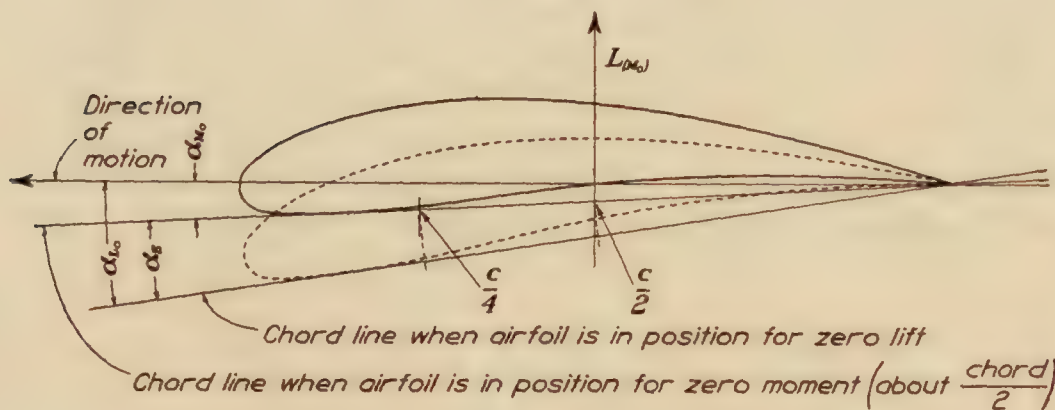


FIG.—22

The graphical construction shown in the diagram (Fig. 21), gives:

$$\alpha_{M_0} = -2^\circ 20'$$

The effective angle, corresponding to the lift at the angle for zero moment, is next determined from the values of the angles for zero lift and zero moment (Fig. 22).

$$\begin{aligned} \alpha_{L_0} &= \text{angle of attack for zero lift} = 8^\circ 40' \\ \alpha_{M_0} &= \text{angle of attack for zero moment} = 2^\circ 17' \\ \alpha_E &= \text{effective angle.} \\ \alpha_E &= \alpha_{L_0} - \alpha_{M_0} \\ &= 8^\circ 40' - 2^\circ 17' \\ &= 6^\circ 13' \sim 6.216^\circ \end{aligned}$$

When the airfoil is in the position such that the moment about the 50 per cent point of the chord is zero, the resultant force passes through this point. Neglecting the moment due to the drag force, which is very small, the moment about any other point on the chord can be computed by obtaining the product of the lift force and its lever arm about that point. By this method, the magnitude of the moment about a point at 25 per cent of the chord is determined. This moment is theoretically constant for all angles of attack and values of lift. When plotted against the lift, the curve will be a straight line parallel to the lift axis.

$$M = L \times l = \frac{2\pi\alpha_E q S}{57.3 \left(1 + \frac{2S}{b^2}\right)} \times \frac{-c}{4}$$

where:

M = moment about 25 per cent of chord

L = lift

l = lever arm = $-\frac{c}{4}$

c = chord = 12.7 cm

α_E = effective angle of attack = 6.216°

q = dynamic pressure = 530 kg/m^2

S = surface area = $.0968 \text{ m}^2$

b = span = .762 m

$$M = \frac{2\pi \times 6.216 \times 530 \times .0968 \times (-12.7) \times .994}{57.3 \left[1 + \frac{2 \times .0968}{(.762)^2}\right] \times 4} = -83.0 \text{ kg cm}$$

$$C_M = \frac{M}{qSc} = \frac{-83.0}{530 \times .0968 \times 12.7} = -0.1275$$

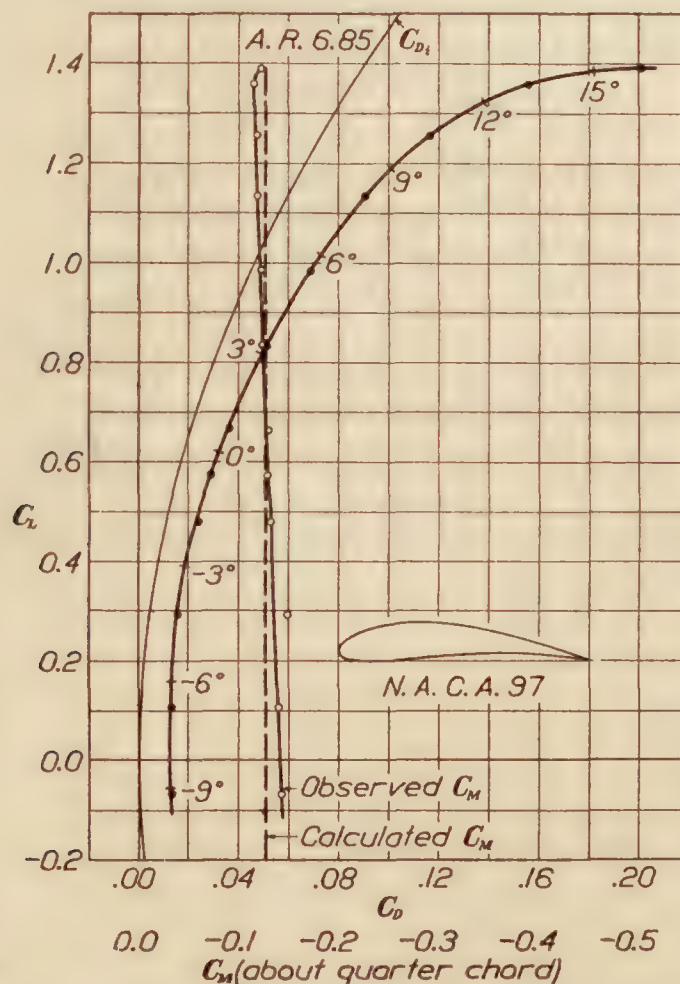


FIG. 23.—Test 60-7. Tank pressure 15.9 atmospheres. Dynamic pressure $q=530 \text{ kg/m}^2$. Reynolds Number 2,920,000. Airfoil with two skids

The computed and the observed values of moment coefficient are shown in the chart of observed values for the N. A. C. A. No. 97 airfoil, Figure 23, for purposes of comparison.

REPORT No. 218

STANDARD ATMOSPHERE—TABLES AND DATA

By WALTER S. DIEHL

Bureau of Aeronautics, Navy Department

REPORT No. 218

STANDARD ATMOSPHERE—TABLES AND DATA

By WALTER S. DIEHL

SUMMARY

This report is an extension of National Advisory Committee for Aeronautics Report No. 147. Detailed tables of pressures and densities are given for altitudes up to 20,000 meters and to 65,000 feet. In addition to the tables the various data pertaining to the standard atmosphere have been compiled in convenient form for ready reference.

INTRODUCTION

A full account of the research conducted by the United States Weather Bureau in laying the foundation for a standard atmosphere is given in Mr. W. R. Gregg's paper on "Standard Atmosphere" (Reference 1). Briefly, the Weather Bureau found that the average annual conditions for latitude 40° in the United States were closely represented by Toussaint's formula for linear decrease in temperature with altitude,

$$T = T_0 - .0065Z \text{ ----- (1)}$$

where T is the temperature in °C. at the altitude Z in meters. The maximum altitude at which this formula can be applied is determined by the temperature of the isothermal atmosphere. This point will be discussed later.

Toussaint's formula not only fulfilled the requirements of simplicity and reasonable accuracy but also had the advantage of being extensively used in Europe. It was therefore adopted by the National Advisory Committee for Aeronautics as the basis of a standard atmosphere for aeronautical work in the United States.

In addition to the aerological observations which led to the recommendation and adoption of a linear decrease in temperature with altitude, Report No. 147 contained brief tables of pressures and densities in the standard atmosphere. These tables were not carried beyond an altitude of 10,000 meters or 33,000 feet although provision was made for extension when required. Subsequent general use has indicated the need of more detailed tables carried up to altitudes of 20,000 meters or 65,000 feet. It is the purpose of this report to supply such tables together with miscellaneous data on the standard atmosphere compiled in a form convenient for ready reference.

OFFICIAL ADOPTION OF BASIC PHYSICAL CONSTANTS

At a regular meeting of the executive committee of the National Advisory Committee for Aeronautics held on December 2, 1924, Dr. Joseph S. Ames, chairman of the committee on aerodynamics, submitted the following letter, dated November 26, 1924, from the committee on aerodynamics:

The EXECUTIVE COMMITTEE,

National Advisory Committee for Aeronautics,

Washington, D. C.

GENTLEMEN: The committee on aerodynamics, by resolution adopted at its meeting held on October 11 1924, recommended that the National Advisory Committee for Aeronautics adopt the following basic physical

constants for use in connection with aeronautical calculations relating to pressure, temperature, and density relations in a normal or standard atmosphere, to be effective on and after January 1, 1925:

For conversion from meters to inches the relation fixed by the United States Statute of 1866 should govern,

$$\begin{aligned} 1 \text{ m} &= 39.3700 \text{ in.} \\ 1 \text{ lb.} &= 453.5924277 \text{ g,} \end{aligned}$$

determined by International Bureau of Weights and Measures in July, 1893.

Force of gravity,

$$\begin{aligned} g &= 9.80665 \text{ m/sec.}^2 \\ &= 32.1740 \text{ ft/sec.}^2 \end{aligned}$$

Weight of cubic centimeter of dry air with normal content CO_2 at temperature of $0^\circ \text{ C. (32}^\circ \text{ F.)}$ and pressure 76 cm. (29.921 in.).

$$\begin{aligned} W &= 0.0012930 \text{ g/cm.}^3 \\ &= 0.08072 \text{ lb/ft.}^3 \end{aligned}$$

The standard temperature for working conditions for both standard density and standard atmosphere to be the same, viz. $15^\circ \text{ C. (59}^\circ \text{ F.)}$.

Coefficient of expansion of air,

$$\begin{aligned} \alpha &= 0.00367 \text{ per degree C.} \\ &= 0.00204 \text{ per degree F.} \end{aligned}$$

Where temperatures on the absolute scale are employed, the approximate scale may be defined by

$$T_{aa} = 273^\circ + t^\circ \text{ C. (459.4}^\circ + t^\circ \text{ F.)}$$

RESULTING VALUES

The foregoing basic constants and assumptions result in the following working values:

Weight of standard air at $15^\circ \text{ C. (59}^\circ \text{ F.)}$, standard pressure,

$$\begin{aligned} W &= 1.2255 \text{ kg/m}^3 \\ &= 0.07651 \text{ lb./ft.}^3 \end{aligned}$$

Standard density at $15^\circ \text{ C. (59}^\circ \text{ F.)}$ and standard pressure,

$$\begin{aligned} \rho &= \frac{W}{g} = 0.12497 \text{ kg.-sec.}^2\text{-m.}^{-4} \\ &= 0.002378 \text{ lb.-sec.}^2\text{-ft.}^{-4} \end{aligned}$$

Respectfully,

COMMITTEE ON AERODYNAMICS,
JOSEPH S. AMES, *Chairman*.

After consideration by the executive committee, and on motion duly seconded and carried, it was

Resolved, That the basic physical constants for use in connection with aeronautical calculations relating to pressure, temperature, and density relations in a normal or standard atmosphere, as recommended by the committee on aerodynamics in its letter referred to, dated November 26, 1924, be, and the same are hereby approved, to be effective on and after January 1, 1925.

STANDARD VALUES

Particular attention has been given to the choice of standard values for the standard atmosphere, and so far as practicable, international standards have been followed. Instead of the density $.001225 \text{ g/cm}^3$ recommended by Toussaint, the value of $.0012255 \text{ g/cm}^3$ has been adopted as conforming to the universally accepted standard of $.0012930 \text{ g/cm}^3$ for dry air of average CO_2 content at 0° C. and 760 mm. In this connection Toussaint's value corresponds to $.0012923 \text{ g/cm}^3$ at 0° C. and 760 mm. The difference between the two values is exceedingly small and entirely negligible in comparing performance data.

The standard atmosphere has been based on approximate absolute temperatures, $T = 273 + t^\circ \text{ C.}$ or $T = 459.4 + t^\circ \text{ F.}$ The absolute temperature corresponding to zero on Fahrenheit scale has here been taken at 459.4° F. , instead of the usual value 459.6° F. , since $(459.4^\circ + 32^\circ \text{ F.})$ corresponds to 273° C. The metric and English values are thereby made directly comparable.

Since the standard atmosphere is used almost entirely by engineers, the engineering units, kilogram-meter-second in the metric system, and pound-foot-second in the English system are used.

The following standard values have been adopted by the National Advisory Committee for Aeronautics for use in the standard atmosphere:

Standard pressure	$p_o = 760$ mm	$= 29.921$ in.
Standard temperature	$t_o = 15^\circ\text{C.}$	$= 59^\circ\text{F.}$
Standard absolute temperature	$T_o = 288^\circ\text{C.}$	$= 518.4^\circ\text{F.}$
Standard specific weight	$g\rho = 1.2255$ kg/m ³	$= 0.07651$ lb./ft. ³
Standard gravity	$g = 9.80665$ m/sec. ²	$= 32.1740$ ft./sec. ²
Standard density ¹	$\rho = 0.12497$	$= 0.002378$
Standard temperature gradient	$a = 0.0065^\circ\text{C/m}$	$= 0.003566^\circ\text{F./ft.}$

The standard conversion factors are:

$$\begin{aligned} 1 \text{ meter} &= 39.3700 \text{ in.} = 3.280833 \text{ ft.} \\ 1 \text{ kilogram} &= 2.204622 \text{ lb.} \end{aligned}$$

The values given above are those ordinarily used; more exact values may be found in Table I.

BASIC ASSUMPTIONS

In addition to the linear decrease in temperature with altitude

$$T = T_o - aZ \text{ ----- (1)}$$

certain basic assumptions are necessary to define the Standard Atmosphere. These assumptions are as follows:

That (a) the air is dry,

(b) air is a perfect gas, obeying the laws of Charles and Boyle, i. e.,

$$p = Rg\rho T \text{ ----- (2)}$$

or

$$\left(\frac{p}{p_o}\right) = \left(\frac{\rho}{\rho_o}\right) \left(\frac{T}{T_o}\right) \text{ ----- (2a)}$$

(c) gravity is constant at all altitudes with the standard value,

(d) the temperature of the isothermal atmosphere is -55°C. or -67°F.

(e) equation (1) holds true for altitudes up to the isothermal atmosphere; the gradient vanishing at the lower limit of the isothermal atmosphere.

The last assumption not only simplifies the standard atmosphere but it also appears to be a very close approximation to actual conditions at any given time. The altitude of the lower limit of the isothermal atmosphere is found from Equation (1) by substituting the isothermal temperature:

$$Z_i = \frac{288 - 218}{.0065} = 10769 \text{ meters}$$

$$Z_i = \frac{518.4 - 392.4}{.00356617} = 35332 \text{ feet.}$$

Since the air is assumed to be a perfect gas, the difference in pressure between two levels is due to the weight of a column of air of unit cross section between the two levels or

$$dp = -g\rho dZ \text{ ----- (3)}$$

This differential equation is of considerable importance, since it is the basis for the formulæ used in computing pressures at altitudes.

¹ Specific weight of mercury at 0°C. $= 13595.1$ kg/m³ $= 848.7149$ lb./ft.³

CALCULATION OF PRESSURES AND DENSITIES IN THE STANDARD ATMOSPHERE

At any altitude in the standard atmosphere the air temperature is known from equation (1) (or from the isothermal temperature). The corresponding pressure is calculated by the well-known modified form of Laplace's equation

$$Z = \frac{p_o}{\rho_o g M} \left(\frac{T_m}{T_o} \right) \log_{10} \left(\frac{p_o}{p} \right) \dots \dots \dots (4)$$

where M is the modulus for the common logarithms, i. e.,

$$M = \log_{10} e = .4342945$$

Letting

$$K = \frac{p_o}{\rho_o g M}$$

and substituting the standard values

$$\begin{aligned} K &= \frac{0.760 \times 13595.1g}{1.2255g \times .434294} \\ &= 19413.28 \text{ m or } 63691.72 \text{ ft.} \end{aligned}$$

A further simplification may be made by setting

$$K' = \frac{K}{T_o}$$

so that

$$\begin{aligned} K' &= \frac{19413.28}{288} = 67.4072 \text{ metric} \\ &= \frac{63691.72}{518.4} = 122.862 \text{ English} \end{aligned}$$

Equation (4) may now be written

$$\log_{10} \left(\frac{p_o}{p} \right) = \frac{Z}{K' T_m} \dots \dots \dots (4a)$$

from which $\frac{p_o}{p}$ is readily obtained.

The corresponding density is given by

$$\frac{\rho}{\rho_o} = \left(\frac{p}{p_o} \right) \left(\frac{T_o}{T} \right) \dots \dots \dots (2a)$$

Since both $\left(\frac{p}{p_o} \right)$ and $\left(\frac{T}{T_o} \right)$ are known.

The foregoing equations are sufficient to determine any of the solutions commonly required. As an example, take the case of pressure corresponding to a given altitude. Equation (4a) may be written

$$\log_{10} p = \log_{10} p_o - \frac{Z}{K' T_m} \dots \dots \dots (4b)$$

which upon substitution of the values for $\log_{10} p_o$ and K' becomes

$$\log_{10} p = 2.880814 - \frac{Z}{67.4072 T_m}$$

for p in mm, Z in m, and T_m in °C,

$$\text{or } \log_{10} p = 1.475976 - \frac{Z}{122.862 T_m}$$

for p in in., Z in ft., and T_m in °F.

CALCULATION OF MEAN TEMPERATURE

The mean temperature T_m which appears in equation (4) is a *harmonic mean* given by

$$T_m = \frac{\int_0^Z dZ}{\int_0^Z \frac{dZ}{T}} = \frac{aZ}{\log_e \frac{T_o}{T_o - aZ}} \quad (5)$$

where a is the temperature gradient.

Equation (5) can not be used above the isothermal level, owing to the discontinuity in the lapse rate, a . However, it may be written in the form

$$T_m = \frac{\sum \Delta Z}{\sum \frac{\Delta Z}{T_m}} = \frac{\Delta Z_1 + \Delta Z_2 + \dots}{\frac{\Delta Z_1}{T_{m_1}} + \frac{\Delta Z_2}{T_{m_2}} + \dots} \quad (6)$$

where T_{m_1} , T_{m_2} , \dots are the average temperatures for the altitude increments ΔZ_1 , ΔZ_2 , \dots as actually used equation (6) is

$$T_m = \frac{Z}{\frac{Z_1}{T_{m_1}} + \frac{(Z - Z_1)}{T}} \quad (6a)$$

where Z_1 is the isothermal level (10769 m or 35332 ft.), T_{m_1} the harmonic mean temperature at Z_1 , and T the isothermal temperature. Substituting for Z_1 , T_{m_1} , and T gives

$$T_m = \frac{Z}{\frac{10769}{251.378} + \frac{Z - 10769}{218.0}} \quad \begin{array}{l} \text{Metric units} \\ Z > 10769 \text{ m} \end{array}$$

$$T_m = \frac{Z}{\frac{35332}{452.680} + \frac{Z - 35332}{392.4}} \quad \begin{array}{l} \text{English units} \\ Z > 35332 \text{ ft.} \end{array}$$

RELATIONS BETWEEN p , ρ , T AND Z

Below the isothermal level certain interesting and useful relations exist between pressure, temperature, density, and altitude. Dividing equation (3) by (2)

$$\frac{dp}{p} = -\frac{dZ}{RT} = -\frac{dZ}{R(T_o - aZ)}$$

Integrating

$$aR \log \left(\frac{p}{p_o} \right) = \log \left(\frac{T}{T_o} \right)$$

or

$$\frac{T}{T_o} = \left(\frac{p}{p_o} \right)^{aR}$$

The value of the exponent aR is independent of the system of units. In the metric system

$$R = \frac{p_o}{g\rho_o T_o} = \frac{.760 \times 13595.1}{1.2255 \times 288} = 29.2708$$

$$\therefore aR = .0065 \times 29.2708 = 0.19026$$

$$\therefore \frac{T}{T_o} = \left(\frac{p}{p_o} \right)^{.19} \quad (7)$$

and

$$\frac{p}{p_o} = \left(\frac{T}{T_o} \right)^{5.256} \quad (8)$$

From equations (2a), (5) and (6) the following equations may be derived:

$$\left(\frac{\rho}{\rho_o}\right) = \left(\frac{p}{p_o}\right)^{.81} \text{-----} (9)$$

$$\left(\frac{p}{p_o}\right) = \left(\frac{\rho}{\rho_o}\right)^{1.235} \text{-----} (10)$$

$$\left(\frac{T}{T_o}\right) = \left(\frac{\rho}{\rho_o}\right)^{0.235} \text{-----} (11)$$

$$\left(\frac{\rho}{\rho_o}\right) = \left(\frac{T}{T_o}\right)^{4.256} \text{-----} (12)$$

$$\left(\frac{\rho}{\rho_o}\right)^{0.235} = \left(1 - \frac{a}{T_o} Z\right) \text{-----} (13)$$

$$\left(\frac{\rho}{\rho_o}\right) = \left(1 - \frac{a}{T_o} Z\right)^{4.256} \text{-----} (14)$$

$$\left(\frac{p}{p_o}\right)^{.19} = \left(1 - \frac{a}{T_o} Z\right) \text{-----} (15)$$

$$\left(\frac{p}{p_o}\right) = \left(1 - \frac{a}{T_o} Z\right)^{5.256} \text{-----} (16)$$

These formulae do not hold true above the lower level of the isothermal atmosphere, i. e., Z must be less than 10769 meters or 35332 feet.

ACKNOWLEDGMENT

All of the important assumptions and standard values used in this report have been officially adopted by the National Advisory Committee for Aeronautics. Certain minor assumptions and standard values not officially adopted previous to the preparation of this report, but considered necessary for a complete statement of the standard atmosphere, have been unanimously selected by Mr. W. R. Gregg of the Weather Bureau and Dr. H. N. Eaton and Dr. W. G. Brombacher of the Bureau of Standards, who have also given great assistance in checking equations, methods of calculation and constants.

A large part of the mechanical work of calculating and checking the tables has been carried out in the National Advisory Committee for Aeronautics offices.

TABLE I
STANDARD ATMOSPHERE—STANDARD VALUES

	Symbol	Metric	English
Standard temperature.....	t	15° C.....	59° F.
Standard temperature absolute.....	T	288° C.....	518.4° F.
Standard pressure.....	p	760 mm of Hg.....	29.92117 in. of Hg.
Standard pressure.....	p	10332.276 kg/m ²	2116.229 lb./ft. ²
Standard gravity.....	g	9.80665 m/s ²	32.1740 ft./sec. ²
Standard specific weight.....	$g\rho$	1.2255 kg/m ³	0.07651 lb./ft. ³
Standard density.....	ρ	0.124966 kg/m/sec.....	0.002378 lb./ft./sec.
Standard temperature gradient.....	a	0.0065 C.....	0.00356617 F.
Standard isothermal temperature.....	t_i	—55° C.....	—67° F.
Standard gas constant for air.....	R	29.2708.....	53.33089.

REFERENCES

1. Standard Atmosphere. W. R. Gregg. N. A. C. A. Technical Report No. 147, 1922.
2. Smithsonian meteorological tables, fourth revised edition.
3. Physics of the Air. W. J. Humphreys. (J. B. Lippincott Co.)
4. Notes on the standard atmosphere. W. S. Diehl. N. A. C. A. Technical note No. 99, 1922.
5. The Determination of the Altitude of Aircraft. W. G. Brombacher, "Journal of the Optical Society of America and Review of Scientific Instruments." Vol. VII, No. 9, September, 1923.

**STANDARD ATMOSPHERE
METRIC UNITS**

Z m	t °C.	T °C. aa	T_m °C. aa	T T_o	p p_o	$\frac{p}{p_o}$	p mm	ρ	$g\rho$ K_g/m^3	t °F.	Z ft
-1000	21.500	294.500	291.235	1.0226	1.1244	1.0996	854.58	.1374	1.3476	70.70	-3280.8
-950	21.175	294.175	291.075	1.0214	1.1179	1.0945	849.63	.1368	1.3413	70.12	-3116.8
-900	20.850	293.850	290.913	1.0203	1.1115	1.0893	844.71	.1361	1.3350	69.53	-2952.7
-850	20.525	293.525	290.752	1.0192	1.1050	1.0842	839.82	.1355	1.3287	68.95	-2788.7
-800	20.200	293.200	290.590	1.0181	1.0986	1.0791	834.94	.1349	1.3325	68.36	-2624.7
-750	19.875	292.875	290.429	1.0170	1.0922	1.0740	830.08	.1342	1.3162	67.78	-2460.6
-700	19.550	292.550	290.267	1.0158	1.0859	1.0690	825.25	.1336	1.3100	67.19	-2296.6
-650	19.225	292.225	290.106	1.0147	1.0796	1.0639	820.45	.1330	1.3038	66.61	-2132.5
-600	18.900	291.900	289.944	1.0135	1.0733	1.0589	815.67	.1323	1.2977	66.02	-1968.5
-550	18.575	291.575	289.783	1.0124	1.0670	1.0539	810.91	.1317	1.2916	65.44	-1804.5
-500	18.250	291.250	289.621	1.0113	1.0607	1.0489	806.16	.1311	1.2854	64.85	-1640.4
-450	17.925	290.925	289.459	1.0102	1.0545	1.0439	801.44	.1305	1.2793	64.27	-1476.4
-400	17.600	290.600	289.297	1.0091	1.0484	1.0390	796.75	.1298	1.2733	63.68	-1312.3
-350	17.275	290.275	289.136	1.0079	1.0422	1.0341	792.09	.1292	1.2672	63.10	-1148.3
-300	16.950	289.950	288.974	1.0068	1.0361	1.0291	787.44	.1286	1.2612	62.51	-984.2
-250	16.625	289.625	288.812	1.0056	1.0300	1.0242	782.81	.1280	1.2552	61.93	-820.2
-200	16.300	289.300	288.650	1.0045	1.0240	1.0193	778.20	.1274	1.2492	61.34	-656.2
-150	15.975	288.975	288.488	1.0034	1.0109	1.0145	773.62	.1268	1.2433	60.76	-492.1
-100	15.650	288.650	288.325	1.0023	1.0119	1.0096	769.06	.1262	1.2373	60.17	-328.1
-50	15.325	288.325	288.163	1.0011	1.0059	1.0048	764.52	.1256	1.2314	59.59	-164.0
0	15.000	288.000	288.000	1.0000	1.0000	1.0000	760.00	.12497	1.2255	59.00	0
50	14.675	287.605	287.873	.9989	.9941	.9952	755.50	.12437	1.2196	58.42	164.0
100	14.350	280.350	287.675	.9978	.9882	.9904	751.03	.12377	1.2137	57.83	328.1
150	14.025	287.025	287.513	.9966	.9823	.9856	746.57	.12317	1.2079	57.25	492.1
200	13.700	286.700	287.350	.9955	.9765	.9809	742.12	.12258	1.2021	56.66	656.2
250	13.375	286.375	287.187	.9944	.9707	.9762	737.73	.12199	1.1963	56.08	820.2
300	13.050	286.050	287.024	.9933	.9649	.9715	733.35	.12141	1.1905	55.49	984.2
350	12.725	285.725	286.861	.9921	.9592	.9668	728.97	.12082	1.1848	54.91	1148.3
400	12.400	285.400	286.697	.9910	.9534	.9621	724.62	.12023	1.1791	54.32	1312.3
450	12.075	285.075	286.534	.9899	.9478	.9575	720.30	.11965	1.1734	53.74	1476.4
500	11.750	284.750	286.371	.9887	.9421	.9528	715.99	.11907	1.1677	53.15	1640.4
550	11.425	284.425	286.208	.9876	.9364	.9482	711.71	.11849	1.1620	52.57	1804.5
600	11.100	284.100	286.044	.9865	.9308	.9436	707.45	.11792	1.1564	51.98	1968.5
650	10.775	283.775	285.881	.9854	.9253	.9390	703.21	.11735	1.1508	51.40	2132.5
700	10.450	283.450	285.717	.9842	.9197	.9345	698.98	.11678	1.1452	50.81	2296.6
750	10.125	283.125	285.554	.9831	.9142	.9299	694.78	.11621	1.1396	50.23	2460.6
800	9.800	282.800	285.390	.9820	.9087	.9254	690.60	.11564	1.1340	49.64	2624.7
850	9.475	282.475	285.227	.9808	.9031	.9208	686.43	.11507	1.1285	49.06	2788.7
900	9.150	282.150	285.063	.9797	.8977	.9163	682.30	.11451	1.1230	48.47	2952.8
950	8.825	281.825	284.900	.9786	.8923	.9119	678.18	.11395	1.1175	47.89	3116.8
1000	8.500	281.500	284.736	.9775	.8870	.9074	674.09	.11340	1.1120	47.30	3280.8
1050	8.175	281.175	284.572	.9763	.8816	.9030	670.01	.11285	1.1065	46.72	3444.9
1100	7.850	280.850	284.408	.9752	.8762	.8985	665.95	.11229	1.1011	46.13	3608.9
1150	7.525	280.525	284.245	.9741	.8709	.8941	661.91	.11174	1.0957	45.55	3773.0
1200	7.200	280.200	284.080	.9729	.8656	.8897	657.89	.11119	1.0903	44.96	3937.0
1250	6.875	279.875	283.916	.9718	.8604	.8853	653.88	.11064	1.0849	44.38	4101.0
1300	6.550	279.550	283.752	.9707	.8551	.8810	649.90	.11010	1.0796	43.79	4265.1
1350	6.225	279.225	283.589	.9696	.8499	.8766	645.94	.10955	1.0743	43.21	4429.1
1400	5.900	278.900	283.424	.9684	.8448	.8723	642.00	.10901	1.0690	42.62	4593.2
1450	5.575	278.575	283.261	.9673	.8396	.8680	638.08	.10847	1.0637	42.04	4757.2
1500	5.250	278.250	283.096	.9662	.8345	.8637	634.18	.10794	1.0584	41.45	4921.3
1550	4.925	277.925	282.932	.9650	.8293	.8594	630.30	.10740	1.0532	40.87	5085.3
1600	4.600	277.600	282.767	.9639	.8243	.8551	626.44	.10687	1.0480	40.28	5249.3
1650	4.275	277.275	282.603	.9628	.8192	.8509	622.59	.10634	1.0428	39.70	5413.4
1700	3.950	276.950	282.438	.9617	.8142	.8467	618.77	.10581	1.0376	39.11	5577.4
1750	3.625	276.625	282.274	.9605	.8092	.8424	614.97	.10528	1.0324	38.53	5741.5
1800	3.300	276.300	282.109	.9594	.8042	.8382	611.19	.10475	1.0272	37.94	5905.5
1850	2.975	275.975	281.945	.9583	.7992	.8340	607.42	.10423	1.0221	37.36	6069.5
1900	2.650	275.650	281.779	.9571	.7943	.8299	603.67	.10371	1.0170	36.77	6233.6
1950	2.325	275.325	281.615	.9560	.7894	.8257	599.94	.10319	1.0119	36.19	6397.6
2000	2.000	275.000	281.450	.9549	.7845	.8216	596.23	.10267	1.0068	35.60	6561.7
2050	1.675	274.675	281.286	.9538	.7797	.8175	592.54	.10215	1.0018	35.02	6725.7
2100	1.350	274.350	281.120	.9526	.7748	.8133	588.86	.10164	.9968	34.43	6889.8
2150	1.025	274.025	280.956	.9515	.7700	.8092	585.19	.10113	.9918	33.85	7053.8
2200	0.700	273.700	280.790	.9504	.7652	.8052	581.56	.10062	.9868	33.26	7217.8
2250	0.375	273.375	280.625	.9492	.7605	.8011	577.94	.10012	.9818	32.68	7381.9
2300	0.050	273.050	280.459	.9481	.7557	.7971	574.34	.09961	.9768	32.09	7545.9
2350	-0.275	272.725	280.295	.9470	.7510	.7931	570.74	.09910	.9719	31.51	7710.0
2400	-0.600	272.400	280.129	.9459	.7463	.7891	567.19	.09861	.9670	30.92	7874.0
2450	-0.925	272.075	279.964	.9447	.7417	.7851	563.64	.09811	.9621	30.34	8038.0

Z m	t °C.	T °C. aa	T _m °C. aa	T T _o	$\frac{p}{p_0}$	ρ ρ_0	P mm	ρ	$\rho\rho$ kg/m ³	t °F	Z ft.
2500	-1.250	271.750	279.798	.9436	.7370	.7811	560.11	.09761	.9572	29.75	8202.1
2550	-1.575	271.425	279.633	.9425	.7324	.7771	556.60	.09711	.9523	29.17	8366.1
2600	-1.900	271.100	279.466	.9413	.7278	.7732	553.10	.09662	.9475	28.58	8530.2
2650	-2.225	270.775	279.301	.9402	.7231	.7691	549.62	.09614	.9427	28.00	8694.2
2700	-2.550	270.450	279.125	.9391	.7186	.7652	546.17	.09565	.9379	27.41	8858.3
2750	-2.875	270.125	278.969	.9380	.7141	.7613	542.73	.09516	.9331	26.83	9022.3
2800	-3.200	269.800	278.803	.9368	.7097	.7575	539.32	.09467	.9283	26.24	9186.3
2850	-3.525	269.475	278.638	.9357	.7052	.7536	535.91	.09419	.9236	25.66	9350.4
2900	-3.850	269.150	278.471	.9346	.7007	.7497	532.53	.09371	.9189	25.07	9514.4
2950	-4.175	268.825	278.305	.9334	.6962	.7459	529.16	.09322	.9141	24.49	9678.5
3000	-4.500	268.500	278.138	.9323	.6918	.7420	525.79	.09274	.9094	23.90	9842.5
3050	-4.825	268.175	277.972	.9312	.6874	.7382	522.46	.09227	.9047	23.32	10006.5
3100	-5.150	267.850	277.805	.9301	.6831	.7344	519.14	.09179	.9001	22.73	10170.6
3150	-5.475	267.525	277.639	.9289	.6787	.7307	515.84	.09132	.8955	22.15	10334.6
3200	-5.800	267.200	277.472	.9278	.6744	.7269	512.56	.09085	.8908	21.56	10498.7
3250	-6.125	266.875	277.306	.9267	.6701	.7231	509.28	.09038	.8862	20.98	10662.7
3300	-6.450	266.550	277.139	.9255	.6658	.7194	506.04	.08991	.8817	20.39	10826.8
3350	-6.775	266.225	276.972	.9244	.6616	.7157	502.80	.08945	.8771	19.81	10990.8
3400	-7.100	265.900	276.805	.9233	.6574	.7120	499.58	.08899	.8726	19.22	11154.8
3450	-7.425	265.575	276.638	.9222	.6532	.7083	496.37	.08851	.8679	18.64	11318.9
3500	-7.750	265.250	276.470	.9210	.6490	.7046	493.19	.08805	.8634	18.05	11482.9
3550	-8.075	264.925	276.303	.9199	.6447	.7009	490.03	.08760	.8590	17.47	11647.0
3600	-8.400	264.600	276.136	.9188	.6406	.6972	486.88	.08714	.8545	16.88	11811.0
3650	-8.725	264.275	275.969	.9176	.6365	.6936	483.75	.08669	.8501	16.30	11975.0
3700	-9.050	263.950	275.801	.9165	.6324	.6900	480.62	.08623	.8456	15.71	12139.1
3750	-9.375	263.625	275.634	.9154	.6283	.6864	477.53	.08578	.8412	15.13	12303.1
3800	-9.700	263.300	275.466	.9143	.6242	.6828	474.44	.08534	.8368	14.54	12467.2
3850	-10.025	262.975	275.299	.9131	.6202	.6792	471.37	.08488	.8324	13.96	12631.2
3900	-10.350	262.650	275.131	.9120	.6162	.6757	468.32	.08444	.8281	13.37	12795.3
3950	-10.675	262.325	274.964	.9109	.6122	.6721	465.28	.08399	.8236	12.79	12959.3
4000	-11.000	262.000	274.796	.9097	.6082	.6686	462.26	.08355	.8193	12.20	13123.3
4050	-11.325	261.675	274.628	.9086	.6043	.6651	459.25	.08311	.8150	11.62	13287.4
4100	-11.650	261.350	274.460	.9075	.6004	.6616	456.25	.08267	.8107	11.03	13451.4
4150	-11.975	261.025	274.293	.9064	.5964	.6580	453.28	.08224	.8065	10.45	13615.5
4200	-12.300	260.700	274.125	.9052	.5925	.6545	450.32	.08181	.8022	9.86	13779.5
4250	-12.625	260.375	273.957	.9041	.5886	.6511	447.38	.08136	.7980	9.28	13943.5
4300	-12.950	260.050	273.788	.9030	.5848	.6476	444.46	.08093	.7938	8.69	14107.6
4350	-13.275	259.725	273.621	.9018	.5809	.6442	441.54	.08050	.7895	8.11	14271.6
4400	-13.600	259.400	273.452	.9007	.5771	.6408	438.64	.08007	.7853	7.52	14435.7
4450	-13.925	259.075	273.284	.8996	.5734	.6374	435.77	.07965	.7811	6.94	14599.7
4500	-14.250	258.750	273.115	.8985	.5696	.6340	432.90	.07923	.7770	6.35	14763.8
4550	-14.575	258.425	272.947	.8973	.5659	.6306	430.04	.07881	.7728	5.77	14927.8
4600	-14.900	258.100	272.778	.8962	.5621	.6273	427.22	.07839	.7687	5.18	15091.8
4650	-15.225	257.775	272.610	.8951	.5584	.6238	424.40	.07796	.7646	4.60	15255.9
4700	-15.550	257.450	272.440	.8939	.5547	.6205	421.59	.07754	.7605	4.01	15419.9
4750	-15.875	257.125	272.271	.8928	.5510	.6172	418.80	.07713	.7563	3.43	15584.0
4800	-16.200	256.800	272.102	.8917	.5474	.6139	416.02	.07672	.7523	2.84	15748.0
4850	-16.525	256.475	271.934	.8906	.5437	.6106	413.27	.07631	.7483	2.26	15912.0
4900	-16.850	256.150	271.764	.8894	.5401	.6073	410.52	.07590	.7443	1.67	16076.1
4950	-17.175	255.825	271.596	.8883	.5365	.6041	407.79	.07549	.7403	1.09	16240.1
5000	-17.500	255.500	271.425	.8872	.5330	.6008	405.09	.07508	.7363	.50	16404.2
5050	-17.825	255.175	271.257	.8860	.5295	.5975	402.38	.07467	.7323	-.09	16568.2
5100	-18.150	254.850	271.089	.8849	.5259	.5943	399.69	.07427	.7283	-.67	16732.3
5150	-18.475	254.525	270.918	.8838	.5224	.5911	397.02	.07387	.7244	-1.26	16896.3
5200	-18.800	254.200	270.749	.8827	.5189	.5879	394.36	.07347	.7205	-1.84	17060.3
5250	-19.125	253.875	270.580	.8815	.5155	.5847	391.71	.07307	.7166	-2.43	17224.4
5300	-19.450	253.550	270.410	.8804	.5119	.5815	389.07	.07267	.7127	-3.01	17388.4
5350	-19.775	253.225	270.241	.8793	.5085	.5784	386.46	.07227	.7088	-3.60	17552.5
5400	-20.100	252.900	270.071	.8781	.5051	.5752	383.88	.07188	.7049	-4.18	17716.5
5450	-20.425	252.575	269.901	.8768	.5017	.5720	381.29	.07149	.7010	-4.77	17880.5
5500	-20.750	252.250	269.730	.8759	.4983	.5689	378.71	.07110	.6972	-5.35	18044.6
5550	-21.075	251.925	269.561	.8748	.4950	.5658	376.15	.07071	.6934	-5.94	18208.6
5600	-21.400	251.600	269.391	.8736	.4916	.5627	373.61	.07032	.6897	-6.52	18372.7
5650	-21.725	251.275	269.221	.8725	.4882	.5596	371.09	.06993	.6859	-7.11	18536.7
5700	-22.050	250.950	269.050	.8714	.4850	.5566	368.58	.06955	.6821	-7.69	18700.8
5750	-22.375	250.625	268.880	.8703	.4817	.5535	366.08	.06917	.6783	-8.28	18864.8
5800	-22.700	250.300	268.709	.8692	.4784	.5505	363.59	.06879	.6746	-8.86	19028.8
5850	-23.025	249.975	268.539	.8680	.4751	.5474	361.11	.06841	.6709	-9.45	19192.9
5900	-23.350	249.650	268.368	.8669	.4719	.5444	358.65	.06803	.6672	-10.03	19356.9
5950	-23.675	249.325	268.198	.8657	.4687	.5414	356.20	.06765	.6635	-10.62	19521.0

Z m	t °C.	T °C. aa	T _m °C. aa	T T ₀	p p ₀	p p ₀	p mm	p	ρρ kg/m ³	t °F.	Z ft.
6000	-24.000	249.000	268.027	.8646	.4655	.5384	353.77	.06728	.6598	-11.20	19685.0
6050	-24.325	248.675	267.856	.8635	.4622	.5354	351.35	.06691	.6561	-11.79	19849.0
6100	-24.650	248.350	267.684	.8624	.4591	.5325	348.94	.06654	.6525	-12.37	20013.1
6150	-24.975	248.025	267.514	.8612	.4559	.5294	346.55	.06617	.6489	-12.96	20177.1
6200	-25.300	247.700	267.342	.8601	.4528	.5265	344.17	.06579	.6453	-13.54	20341.2
6250	-25.625	247.375	267.172	.8590	.4497	.5236	341.81	.06543	.6417	-14.13	20505.2
6300	-25.950	247.050	267.000	.8578	.4466	.5207	339.47	.06507	.6380	-14.71	20669.3
6350	-26.275	246.725	266.830	.8567	.4436	.5178	337.13	.06471	.6345	-15.30	20833.3
6400	-26.600	246.400	266.658	.8556	.4405	.5149	334.80	.06435	.6310	-15.88	20997.3
6450	-26.925	246.075	266.487	.8545	.4374	.5119	332.49	.06398	.6275	-16.47	21161.4
6500	-27.250	245.750	266.315	.8533	.4344	.5091	330.18	.06362	.6240	-17.05	21325.4
6550	-27.575	245.425	266.145	.8522	.4314	.5062	327.90	.06326	.6204	-17.64	21489.5
6600	-27.900	245.100	265.973	.8511	.4284	.5034	325.62	.06291	.6169	-18.22	21653.5
6650	-28.225	244.775	265.802	.8499	.4255	.5006	323.36	.06255	.6135	-18.81	21817.5
6700	-28.550	244.450	265.630	.8488	.4225	.4977	321.11	.06220	.6101	-19.39	21981.6
6750	-28.875	244.125	265.459	.8477	.4195	.4949	318.87	.06185	.6066	-19.98	22145.6
6800	-29.200	243.800	265.286	.8466	.4166	.4921	316.65	.06150	.6031	-20.56	22309.7
6850	-29.525	243.475	265.115	.8454	.4137	.4893	314.43	.06116	.5997	-21.15	22473.7
6900	-29.850	243.150	264.942	.8443	.4108	.4866	312.23	.06080	.5964	-21.73	22637.8
6950	-30.175	242.825	264.771	.8432	.4079	.4838	310.04	.06046	.5930	-22.32	22801.8
7000	-30.500	242.500	264.598	.8420	.4051	.4810	307.87	.06012	.5896	-22.90	22965.8
7050	-30.825	242.175	264.427	.8409	.4022	.4783	305.71	.05978	.5862	-23.49	23129.9
7100	-31.150	241.850	264.254	.8398	.3993	.4756	303.56	.05943	.5827	-24.07	23293.9
7150	-31.475	241.525	264.083	.8387	.3965	.4729	301.42	.05909	.5796	-24.66	23458.0
7200	-31.800	241.200	263.910	.8375	.3937	.4702	299.29	.05876	.5762	-25.24	23622.0
7250	-32.125	240.875	263.738	.8364	.3910	.4674	297.18	.05843	.5729	-25.83	23786.0
7300	-32.450	240.550	263.565	.8353	.3883	.4648	295.08	.05809	.5697	-26.41	23950.1
7350	-32.775	240.225	263.393	.8341	.3855	.4621	292.99	.05776	.5664	-27.00	24114.1
7400	-33.100	239.900	263.219	.8330	.3828	.4595	290.90	.05743	.5632	-27.58	24278.2
7450	-33.425	239.575	263.046	.8319	.3800	.4569	288.84	.05710	.5599	-28.17	24442.2
7500	-33.750	239.250	262.872	.8308	.3773	.4542	286.79	.05676	.5567	-28.75	24606.2
7550	-34.075	238.925	262.700	.8296	.3746	.4516	284.75	.05644	.5535	-29.34	24770.3
7600	-34.400	238.600	262.527	.8285	.3720	.4490	282.72	.05612	.5503	-29.92	24934.3
7650	-34.725	238.275	262.355	.8274	.3693	.4464	280.69	.05580	.5471	-30.51	25098.4
7700	-35.050	237.950	262.182	.8262	.3667	.4439	278.69	.05547	.5440	-31.09	25262.4
7750	-35.375	237.625	262.010	.8251	.3640	.4412	276.70	.05515	.5408	-31.68	25426.5
7800	-35.700	237.300	261.836	.8240	.3614	.4386	274.71	.05483	.5377	-32.26	25590.5
7850	-36.025	236.975	261.663	.8229	.3588	.4361	272.74	.05451	.5345	-32.85	25754.5
7900	-36.350	236.650	261.489	.8217	.3563	.4336	270.78	.05419	.5314	-33.43	25918.6
7950	-36.675	236.325	261.315	.8206	.3537	.4310	268.83	.05388	.5283	-34.02	26082.6
8000	-37.000	236.000	261.140	.8195	.3512	.4285	266.89	.05356	.5252	-34.60	26246.7
8050	-37.325	235.675	260.967	.8183	.3486	.4260	264.97	.05324	.5221	-35.19	26410.7
8100	-37.650	235.350	260.792	.8172	.3461	.4235	263.06	.05293	.5191	-35.77	26574.7
8150	-37.975	235.025	260.619	.8161	.3436	.4211	261.16	.05262	.5161	-36.36	26738.8
8200	-38.300	234.700	260.444	.8149	.3411	.4185	259.26	.05232	.5130	-36.94	26902.8
8250	-38.625	234.375	260.271	.8138	.3386	.4161	257.38	.05201	.5100	-37.53	27066.9
8300	-38.950	234.050	260.096	.8127	.3362	.4137	255.51	.05170	.5070	-38.11	27230.9
8350	-39.275	233.725	259.922	.8116	.3337	.4113	253.65	.05140	.5040	-38.70	27395.0
8400	-39.600	233.400	259.746	.8104	.3312	.4088	251.79	.05109	.5010	-39.28	27559.0
8450	-39.925	233.075	259.571	.8093	.3288	.4063	249.96	.05079	.4981	-39.87	27723.0
8500	-40.250	232.750	259.395	.8082	.3265	.4040	248.13	.05049	.4952	-40.45	27887.1
8550	-40.575	232.425	259.221	.8071	.3241	.4016	246.32	.05019	.4922	-41.04	28051.1
8600	-40.900	232.100	259.046	.8059	.3217	.3992	244.52	.04989	.4893	-41.62	28215.2
8650	-41.225	231.775	258.871	.8048	.3193	.3968	242.73	.04960	.4864	-42.20	28379.2
8700	-41.550	231.450	258.696	.8037	.3170	.3945	240.94	.04931	.4834	-42.79	28543.2
8750	-41.875	231.125	258.521	.8025	.3146	.3921	239.17	.04901	.4805	-43.37	28707.2
8800	-42.200	230.800	258.346	.8014	.3123	.3898	237.40	.04872	.4777	-43.96	28871.3
8850	-42.525	230.475	258.171	.8003	.3101	.3874	235.65	.04843	.4749	-44.55	29035.4
8900	-42.850	230.150	257.995	.7992	.3078	.3851	233.91	.04813	.4720	-45.13	29199.4
8950	-43.175	229.825	257.820	.7980	.3054	.3828	232.18	.04784	.4692	-45.72	29363.5
9000	-43.500	229.500	257.644	.7969	.3032	.3806	230.45	.04756	.4664	-46.30	29527.5
9050	-43.825	229.175	257.468	.7958	.3009	.3782	228.74	.04727	.4625	-46.89	29691.5
9100	-44.150	228.850	257.291	.7946	.2987	.3759	227.05	.04699	.4607	-47.47	29855.6
9150	-44.475	228.525	257.116	.7935	.2965	.3737	225.37	.04671	.4580	-48.06	30019.6
9200	-44.800	228.200	256.940	.7924	.2942	.3715	223.68	.04642	.4552	-48.64	30183.7
9250	-45.125	227.875	256.765	.7913	.2921	.3692	222.01	.04614	.4525	-49.23	30347.7
9300	-45.450	227.550	256.588	.7901	.2899	.3669	220.35	.04586	.4498	-49.81	30511.7
9350	-45.775	227.225	256.414	.7890	.2877	.3647	218.69	.04558	.4470	-50.40	30675.8
9400	-46.100	226.900	256.237	.7879	.2856	.3625	217.06	.04531	.4443	-50.98	30839.8
9450	-46.425	226.575	256.061	.7867	.2835	.3603	215.44	.04503	.4416	-51.57	31003.9

Z m	t °C.	T °C. aa	T_m °C. aa	T T_o	p p_o	ρ ρ_o	p mm	ρ	$g\rho$ kg/m ³	t °F.	Z ft.
9500	-46.750	226.250	255.884	.7856	.2813	.3580	213.82	.04475	.4388	-52.15	31167.9
9550	-47.075	225.925	255.709	.7845	.2792	.3559	212.22	.04448	.4362	-52.74	31332.0
9600	-47.400	225.600	255.533	.7833	.2771	.3538	210.62	.04421	.4336	-53.32	31496.0
9650	-47.725	225.275	255.357	.7822	.2750	.3517	209.02	.04394	.4309	-53.91	31660.0
9700	-48.050	224.950	255.181	.7811	.2730	.3495	207.44	.04368	.4283	-54.49	31824.1
9750	-48.375	224.625	255.006	.7800	.2708	.3473	205.86	.04341	.4257	-55.08	31988.1
9800	-48.700	224.300	254.829	.7788	.2688	.3452	204.30	.04313	.4230	-55.66	32152.2
9850	-49.025	223.975	254.652	.7777	.2667	.3431	202.75	.04287	.4204	-56.25	32316.2
9900	-49.350	223.650	254.473	.7766	.2647	.3409	201.21	.04261	.4178	-56.83	32480.2
9950	-49.675	223.325	254.295	.7754	.2627	.3388	199.68	.04234	.4152	-57.42	32644.3
10000	-50.000	223.000	254.116	.7743	.2606	.3367	198.16	.04208	.4127	-58.00	32808.3
10100	-50.650	222.350	253.762	.7721	.2567	.3323	195.14	.04156	.4075	-59.17	33136.4
10200	-51.300	221.700	253.408	.7698	.2528	.3279	192.16	.04105	.4026	-60.34	33464.5
10300	-51.950	221.050	253.053	.7675	.2490	.3235	189.22	.04054	.3976	-61.51	33792.6
10400	-52.600	220.400	252.698	.7653	.2451	.3291	186.31	.04003	.3926	-62.68	34120.7
10500	-53.250	219.750	252.342	.7630	.2414	.3147	183.45	.03953	.3876	-63.85	34448.7
10600	-53.900	219.100	251.985	.7608	.2377	.3104	180.61	.03904	.3828	-65.02	34776.8
10700	-54.550	218.450	251.627	.7585	.2339	.3061	177.82	.03855	.3775	-66.19	35104.9
10769	-55.000	218.000	251.378	.7569	.2314	.3058	175.91	.03820	.3747	-67.00	35331.3
10800	-55.000	218.000	251.274	.7569	.2303	.3018	175.06	.03802	.3723	-67.00	35433.0
10900	-55.000	218.000	250.921	.7569	.2268	.2975	172.34	.03746	.3669	-67.00	35761.1
11000	-55.000	218.000	250.572	.7569	.2232	.2932	169.66	.03689	.3614	-67.00	36089.2
11100	-55.000	218.000	250.237	.7569	.2097	.2890	167.03	.03628	.3558	-67.00	36417.2
11200	-55.000	218.000	249.907	.7569	.2164	.2848	164.43	.03571	.3502	-67.00	36745.3
11300	-55.000	218.000	249.582	.7569	.2130	.2806	161.86	.03516	.3448	-67.00	37073.4
11400	-55.000	218.000	249.264	.7569	.2096	.2765	159.34	.03462	.3394	-67.00	37401.5
11500	-55.000	218.000	248.959	.7569	.2064	.2724	156.87	.03408	.3342	-67.00	37729.6
11600	-55.000	218.000	248.653	.7569	.2032	.2683	154.43	.03355	.3290	-67.00	38057.7
11700	-55.000	218.000	248.353	.7569	.2001	.2642	152.04	.03303	.3239	-67.00	38385.7
11800	-55.000	218.000	248.060	.7569	.1970	.2601	149.67	.03252	.3188	-67.00	38713.8
11900	-55.000	218.000	247.774	.7569	.1939	.2561	147.34	.03201	.3138	-67.00	39041.9
12000	-55.000	218.000	247.491	.7569	.1909	.2521	145.05	.03151	.3090	-67.00	39370.0
12100	-55.000	218.000	247.217	.7569	.1878	.2482	142.79	.03101	.3042	-67.00	39698.1
12200	-55.000	218.000	246.948	.7569	.1849	.2443	140.57	.03053	.2995	-67.00	40026.2
12300	-55.000	218.000	246.681	.7569	.1821	.2405	138.39	.03006	.2948	-67.00	40354.2
12400	-55.000	218.000	246.418	.7569	.1792	.2368	136.24	.02960	.2902	-67.00	40682.3
12500	-55.000	218.000	246.161	.7569	.1764	.2331	134.12	.02914	.2857	-67.00	41010.4
12600	-55.000	218.000	245.909	.7569	.1737	.2295	132.04	.02869	.2813	-67.00	41338.5
12700	-55.000	218.000	245.661	.7569	.1710	.2259	129.99	.02824	.2769	-67.00	41666.6
12800	-55.000	218.000	245.417	.7569	.1683	.2224	127.96	.02780	.2726	-67.00	41994.7
12900	-55.000	218.000	245.178	.7569	.1657	.2189	125.97	.02737	.2684	-67.00	42322.7
13000	-55.000	218.000	244.942	.7569	.1632	.2155	124.01	.02694	.2642	-67.00	42650.8
13100	-55.000	218.000	244.710	.7569	.1606	.2122	122.09	.02652	.2601	-67.00	42978.9
13200	-55.000	218.000	244.482	.7569	.1581	.2089	120.19	.02611	.2560	-67.00	43307.0
13300	-55.000	218.000	244.258	.7569	.1556	.2056	118.32	.02570	.2520	-67.00	43635.1
13400	-55.000	218.000	244.039	.7569	.1532	.2024	116.48	.02530	.2481	-67.00	43963.2
13500	-55.000	218.000	243.823	.7569	.1508	.1992	114.67	.02491	.2442	-67.00	44291.2
13600	-55.000	218.000	243.611	.7569	.1485	.1961	112.90	.02452	.2404	-67.00	44619.3
13700	-55.000	218.000	243.403	.7569	.1462	.1931	111.14	.02415	.2368	-67.00	44947.4
13800	-55.000	218.000	243.198	.7569	.1440	.1901	109.41	.02377	.2331	-67.00	45275.5
13900	-55.000	218.000	242.996	.7569	.1417	.1872	107.71	.02340	.2295	-67.00	45603.6
14000	-55.000	218.000	242.798	.7569	.1395	.1843	106.02	.02303	.2259	-67.00	45931.7
14100	-55.000	218.000	242.602	.7569	.1373	.1814	104.37	.02267	.2223	-67.00	46259.7
14200	-55.000	218.000	242.413	.7569	.1352	.1786	102.75	.02232	.2188	-67.00	46587.8
14300	-55.000	218.000	242.220	.7569	.1332	.1758	101.15	.02198	.2154	-67.00	46915.9
14400	-55.000	218.000	242.034	.7569	.1311	.1731	99.58	.02164	.2121	-67.00	47244.0
14500	-55.000	218.000	241.851	.7569	.1290	.1704	98.02	.02130	.2088	-67.00	47572.1
14600	-55.000	218.000	241.671	.7569	.1270	.1677	96.50	.02097	.2056	-67.00	47900.2
14700	-55.000	218.000	241.492	.7569	.1250	.1651	95.00	.02064	.2024	-67.00	48228.2
14800	-55.000	218.000	241.316	.7569	.1230	.1625	93.52	.02032	.1993	-67.00	48556.3
14900	-55.000	218.000	241.143	.7569	.1211	.1601	92.07	.02000	.1962	-67.00	48884.4
15000	-55.000	218.000	240.971	.7569	.1193	.1576	90.65	.01969	.1931	-67.00	49212.5
15100	-55.000	218.000	240.804	.7569	.1175	.1551	89.24	.01939	.1901	-67.00	49540.6
15200	-55.000	218.000	240.638	.7569	.1156	.1527	87.84	.01909	.1872	-67.00	49868.7
15300	-55.000	218.000	240.475	.7569	.1138	.1504	86.48	.01879	.1843	-67.00	50196.7
15400	-55.000	218.000	240.314	.7569	.1120	.1480	85.13	.01850	.1814	-67.00	50524.8
15500	-55.000	218.000	240.155	.7569	.1103	.1457	83.80	.01821	.1785	-67.00	50852.9
15600	-55.000	218.000	239.999	.7569	.1086	.1434	82.49	.01793	.1758	-67.00	51181.0
15700	-55.000	218.000	239.845	.7569	.1070	.1412	81.22	.01764	.1730	-67.00	51509.1
15800	-55.000	218.000	239.693	.7569	.1053	.1390	79.96	.01736	.1703	-67.00	51837.2
15900	-55.000	218.000	239.543	.7569	.1036	.1369	78.71	.01710	.1677	-67.00	52165.2

<i>Z</i> <i>m</i>	<i>t</i> °C.	<i>T</i> °C. <i>aa</i>	<i>T_m</i> °C. <i>aa</i>	<i>T</i> <i>T₀</i>	<i>p</i> <i>p₀</i>	<i>ρ</i> <i>ρ₀</i>	<i>p</i> <i>mm</i>	<i>ρ</i>	<i>gρ</i> <i>kg/m³</i>	<i>t</i> °F.	<i>Z</i> <i>ft.</i>
16000	−55.000	218.000	239.394	.7569	.10200	.1347	77.48	.01683	.1651	−67.00	52493.3
16100	−55.000	218.000	239.248	.7569	.10040	.1326	76.28	.01657	.1625	−67.00	52821.4
16200	−55.000	218.000	239.105	.7569	.09885	.1306	75.09	.01632	.1600	−67.00	53149.5
16300	−55.000	218.000	238.962	.7569	.09731	.1285	73.92	.01606	.1576	−67.00	53477.6
16400	−55.000	218.000	238.822	.7569	.09580	.1265	72.77	.01581	.1551	−67.00	53805.7
16500	−55.000	218.000	238.683	.7569	.09441	.1245	71.64	.01556	.1526	−67.00	54133.7
16600	−55.000	218.000	238.547	.7569	.09284	.1226	70.53	.01532	.1503	−67.00	54461.8
16700	−55.000	218.000	238.413	.7569	.09140	.1207	69.44	.01508	.1479	−67.00	54790.0
16800	−55.000	218.000	238.280	.7569	.08997	.1188	68.35	.01484	.1456	−67.00	55118.0
16900	−55.000	218.000	238.150	.7569	.08858	.1170	67.30	.01462	.1433	−67.00	55446.1
17000	−55.000	218.000	238.020	.7569	.08720	.1151	66.26	.01439	.1412	−67.00	55774.2
17100	−55.000	218.000	237.892	.7569	.08584	.1134	65.23	.01416	.1390	−67.00	56102.2
17200	−55.000	218.000	237.766	.7569	.08450	.1116	64.21	.01395	.1368	−67.00	56430.3
17300	−55.000	218.000	237.641	.7569	.08319	.1098	63.22	.01373	.1347	−67.00	56758.4
17400	−55.000	218.000	237.518	.7569	.08190	.1081	62.24	.01351	.1325	−67.00	57086.5
17500	−55.000	218.000	237.396	.7569	.08063	.1065	61.28	.01330	.1304	−67.00	57414.6
17600	−55.000	218.000	237.276	.7569	.07937	.1048	60.32	.01310	.1285	−67.00	57742.7
17700	−55.000	218.000	237.157	.7569	.07813	.1032	59.37	.01289	.1265	−67.00	58070.8
17800	−55.000	218.000	237.040	.7569	.07692	.1016	58.45	.01269	.1245	−67.00	58398.8
17900	−55.000	218.000	236.925	.7569	.07572	.1000	57.55	.01250	.1226	−67.00	58726.9
18000	−55.000	218.000	236.812	.7569	.07454	.09848	56.65	.01230	.1207	−67.00	59055.0
18100	−55.000	218.000	236.699	.7569	.07339	.09694	55.77	.01211	.1188	−67.00	59383.1
18200	−55.000	218.000	236.587	.7569	.07225	.09542	54.91	.01193	.1169	−67.00	59711.2
18300	−55.000	218.000	236.477	.7569	.07111	.09393	54.06	.01174	.1152	−67.00	60039.2
18400	−55.000	218.000	236.368	.7569	.07001	.09248	53.22	.01155	.1134	−67.00	60367.3
18500	−55.000	218.000	236.261	.7569	.06892	.09104	52.39	.01138	.1116	−67.00	60695.4
18600	−55.000	218.000	236.154	.7569	.06785	.08962	51.58	.01120	.1099	−67.00	61023.5
18700	−55.000	218.000	236.049	.7569	.06678	.08823	50.77	.01102	.1082	−67.00	61351.6
18800	−55.000	218.000	235.944	.7569	.06575	.08686	49.97	.01085	.1065	−67.00	61679.7
18900	−55.000	218.000	235.842	.7569	.06472	.08551	49.20	.01069	.1049	−67.00	62007.7
19000	−55.000	218.000	235.741	.7569	.06372	.08418	48.43	.01052	.1032	−67.00	62335.8
19100	−55.000	218.000	235.640	.7569	.06273	.08286	47.68	.01035	.1016	−67.00	62663.9
19200	−55.000	218.000	235.541	.7569	.06176	.08158	46.95	.01020	.1000	−67.00	62992.0
19300	−55.000	218.000	235.443	.7569	.06080	.08031	46.21	.01004	.0985	−67.00	63320.1
19400	−55.000	218.000	235.345	.7569	.05985	.07906	45.49	.00988	.0969	−67.00	63648.2
19500	−55.000	218.000	235.250	.7569	.05892	.07784	44.79	.00973	.0954	−67.00	63976.2
19600	−55.000	218.000	235.155	.7569	.05801	.07663	44.09	.00958	.0940	−67.00	64304.3
19700	−55.000	218.000	235.061	.7569	.05711	.07545	43.40	.00943	.0925	−67.00	64632.4
19800	−55.000	218.000	234.969	.7569	.05622	.07427	42.72	.00928	.0910	−67.00	64960.5
19900	−55.000	218.000	234.877	.7569	.05534	.07312	42.05	.00914	.0897	−67.00	65288.6
20000	−55.000	218.000	234.786	.7569	.05449	.07198	41.41	.00900	.0883	−67.00	65616.7

**STANDARD ATMOSPHERE
ENGLISH UNITS**

Z ft.	t °F.	T °F. aa	T _m °F. aa	T T _o	p p _o	ρ ρ _o	p in.	ρ	gρ lb./ft. ³	t °C.	Z m
-4000	73.265	532.665	525.500	1.0275	1.1533	1.1225	34.51	0.002669	0.08588	22.925	-1219.2
-3800	72.551	531.951	525.148	1.0261	1.1453	1.1161	34.27	.002654	.08539	22.529	-1158.2
-3600	71.838	531.238	524.795	1.0248	1.1373	1.1098	34.03	.002639	.08491	22.132	-1097.3
-3400	71.125	530.525	524.439	1.0234	1.1293	1.1035	33.79	.002624	.08442	21.736	-1036.3
-3200	70.412	529.812	524.086	1.0220	1.1213	1.0972	33.55	.002609	.08394	21.340	-975.4
-3000	69.699	529.099	523.731	1.0206	1.1134	1.0909	33.31	.002594	.08346	20.944	-914.4
-2800	68.985	528.385	523.378	1.0193	1.1055	1.0844	33.08	.002579	.08298	20.547	-853.4
-2600	68.272	527.672	523.024	1.0179	1.0977	1.0784	32.84	.002564	.08251	20.151	-792.5
-2400	67.559	526.959	522.669	1.0165	1.0899	1.0722	32.61	.002550	.08203	19.755	-731.5
-2200	66.846	526.246	522.317	1.0151	1.0822	1.0660	32.38	.002535	.08156	19.359	-670.6
-2000	66.132	525.532	521.962	1.0138	1.0745	1.0599	32.15	.002520	.08109	18.962	-609.6
-1800	65.419	524.819	521.607	1.0124	1.0668	1.0538	31.92	.002506	.08062	18.566	-548.6
-1600	64.706	524.106	521.250	1.0110	1.0592	1.0477	31.69	.002491	.08016	18.170	-487.7
-1400	63.992	523.392	520.895	1.0096	1.0516	1.0416	31.47	.002477	.07970	17.774	-426.7
-1200	63.279	522.679	520.538	1.0083	1.0442	1.0356	31.24	.002463	.07924	17.377	-365.8
-1000	62.566	521.960	520.181	1.0069	1.0367	1.0296	31.02	.002448	.07878	16.981	-304.8
-800	61.853	521.253	519.825	1.0055	1.0293	1.0237	30.80	.002434	.07832	16.585	-243.8
-600	61.140	520.540	519.469	1.0041	1.0219	1.0177	30.58	.002420	.07787	16.189	-182.9
-400	60.426	519.826	519.112	1.0027	1.0146	1.0118	30.36	.002406	.07741	15.792	-121.9
-200	59.713	519.113	518.757	1.0014	1.0073	1.0059	30.14	.002392	.07696	15.396	-61.0
0	59.000	518.400	518.400	1.0000	1.0000	1.0000	29.92	.002378	.07651	15.000	0
100	58.643	518.043	518.222	.9993	.9964	.9971	29.81	.002371	.07628	14.802	30.5
200	58.287	517.687	518.043	.9986	.9928	.9942	29.71	.002364	.07606	14.604	61.0
300	57.930	517.330	517.865	.9979	.9892	.9913	29.60	.002357	.07584	14.406	91.4
400	57.574	516.974	517.686	.9972	.9856	.9884	29.49	.002350	.07562	14.208	121.9
500	57.217	516.617	517.507	.9966	.9821	.9855	29.38	.002343	.07540	14.009	152.4
600	56.860	516.260	517.328	.9959	.9785	.9826	29.28	.002336	.07518	13.811	182.9
700	56.504	515.904	517.150	.9952	.9749	.9797	29.17	.002330	.07496	13.613	213.4
800	56.147	515.547	516.972	.9945	.9714	.9768	29.07	.002323	.07474	13.415	243.8
900	55.791	515.191	516.793	.9938	.9679	.9739	28.96	.002316	.07452	13.217	274.3
1000	55.434	514.834	516.615	.9931	.9644	.9710	28.86	.002309	.07430	13.019	304.8
1100	55.077	514.477	516.437	.9924	.9609	.9682	28.75	.002302	.07408	12.821	335.3
1200	54.721	514.121	516.258	.9917	.9574	.9653	28.65	.002295	.07386	12.623	365.8
1300	54.364	513.764	516.080	.9911	.9539	.9625	28.54	.002289	.07364	12.424	396.2
1400	54.008	513.408	515.901	.9904	.9504	.9596	28.44	.002282	.07342	12.226	426.7
1500	53.651	513.051	515.722	.9897	.9469	.9568	28.33	.002275	.07321	12.028	457.2
1600	53.294	512.694	515.544	.9890	.9434	.9540	28.23	.002269	.07299	11.830	487.7
1700	52.938	512.338	515.366	.9883	.9400	.9512	28.13	.002262	.07277	11.632	518.2
1800	52.581	511.981	515.187	.9876	.9366	.9484	28.02	.002255	.07256	11.434	548.6
1900	52.225	511.625	515.008	.9869	.9332	.9456	27.92	.002249	.07234	11.236	579.1
2000	51.868	511.268	514.830	.9862	.9298	.9428	27.82	.002242	.07213	11.038	609.6
2100	51.511	510.911	514.651	.9856	.9264	.9400	27.72	.002235	.07192	10.839	640.1
2200	51.154	510.554	514.470	.9849	.9230	.9372	27.62	.002229	.07170	10.641	670.6
2300	50.798	510.198	514.291	.9842	.9196	.9344	27.52	.002222	.07149	10.443	701.0
2400	50.441	509.841	514.112	.9835	.9162	.9316	27.41	.002215	.07128	10.245	731.5
2500	50.085	509.485	513.931	.9828	.9129	.9288	27.31	.002209	.07107	10.047	762.0
2600	49.728	509.128	513.755	.9821	.9095	.9261	27.21	.002202	.07085	9.849	792.5
2700	49.371	508.771	513.573	.9814	.9062	.9233	27.11	.002196	.07064	9.651	823.0
2800	49.015	508.415	513.392	.9807	.9028	.9206	27.01	.002189	.07043	9.453	853.4
2900	48.658	508.058	513.213	.9800	.8995	.9178	26.91	.002183	.07022	9.255	883.9
3000	48.301	507.701	513.033	.9794	.8962	.9151	26.81	.002176	.07001	9.056	914.4
3100	47.945	507.345	512.853	.9787	.8929	.9124	26.72	.002170	.06980	8.858	944.9
3200	47.588	506.988	512.674	.9780	.8896	.9096	26.62	.002163	.06959	8.660	975.4
3300	47.232	506.632	512.494	.9773	.8863	.9069	26.52	.002157	.06939	8.462	1005.8
3400	46.875	506.275	512.315	.9766	.8830	.9042	26.42	.002150	.06918	8.264	1036.3
3500	46.518	505.918	512.135	.9759	.8798	.9015	26.32	.002144	.06897	8.066	1066.8
3600	46.162	505.562	511.955	.9752	.8765	.8988	26.23	.002137	.06876	7.868	1097.3
3700	45.805	505.205	511.776	.9745	.8733	.8961	26.13	.002131	.06856	7.670	1127.8
3800	45.449	504.849	511.596	.9739	.8701	.8934	26.03	.002125	.06835	7.471	1158.2
3900	45.092	504.492	511.416	.9732	.8668	.8907	25.94	.002118	.06815	7.273	1188.7
4000	44.735	504.135	511.237	.9725	.8636	.8881	25.84	.002112	.06794	7.075	1219.2
4100	44.379	503.779	511.056	.9718	.8604	.8854	25.74	.002105	.06774	6.877	1249.7
4200	44.022	503.422	510.876	.9711	.8572	.8827	25.65	.002099	.06754	6.679	1280.2
4300	43.665	503.065	510.696	.9704	.8540	.8801	25.55	.002093	.06734	6.481	1310.6
4400	43.309	502.709	510.515	.9697	.8509	.8774	25.46	.002086	.06713	6.283	1341.1
4500	42.952	502.352	510.335	.9690	.8477	.8748	25.36	.002080	.06693	6.085	1371.6
4600	42.596	501.996	510.155	.9684	.8445	.8722	25.27	.002074	.06673	5.886	1402.1
4700	42.239	501.639	509.975	.9677	.8414	.8695	25.17	.002068	.06652	5.688	1432.6
4800	41.882	501.282	509.794	.9670	.8382	.8669	25.08	.002061	.06632	5.490	1463.0
4900	41.526	500.926	509.614	.9663	.8351	.8643	24.99	.002055	.06612	5.292	1493.5

Z ft.	t °F.	T °F. aa	T_m °F. aa	$\frac{T}{T_0}$	p p_0	ρ ρ_0	P in.	ρ	$g\rho$ lb./ft. ³	t °C.	Z m
5000	41.169	500.569	509.434	.9656	.8320	.8616	24.89	.002049	.06592	5.094	1524.0
5100	40.813	500.213	509.253	.9649	.8289	.8590	24.80	.002043	.06572	4.896	1554.5
5200	40.456	499.856	509.073	.9642	.8258	.8564	24.71	.002037	.06552	4.698	1585.0
5300	40.099	499.499	508.892	.9635	.8227	.8538	24.61	.002030	.06532	4.500	1615.4
5400	39.743	499.143	508.711	.9629	.8196	.8512	24.52	.002024	.06513	4.301	1645.9
5500	39.386	498.786	508.531	.9622	.8165	.8487	24.43	.002018	.06493	4.103	1676.4
5600	39.029	498.429	508.351	.9615	.8135	.8461	24.34	.002012	.06473	3.905	1706.9
5700	38.673	498.073	508.170	.9608	.8104	.8435	24.25	.002006	.06453	3.707	1737.4
5800	38.316	497.716	507.990	.9601	.8074	.8409	24.16	.002000	.06434	3.509	1767.8
5900	37.960	497.360	507.810	.9594	.8043	.8383	24.07	.001994	.06414	3.311	1798.3
6000	37.603	497.003	507.629	.9587	.8013	.8358	23.98	.001988	.06395	3.113	1828.8
6100	37.246	496.646	507.448	.9580	.7983	.8333	23.89	.001982	.06375	2.915	1859.3
6200	36.890	496.290	507.268	.9573	.7953	.8307	23.80	.001975	.06356	2.717	1889.8
6300	36.533	495.933	507.086	.9567	.7923	.8282	23.71	.001969	.06337	2.518	1920.2
6400	36.177	495.577	506.905	.9560	.7893	.8257	23.62	.001963	.06317	2.320	1950.7
6500	35.820	495.220	506.723	.9553	.7863	.8232	23.53	.001957	.06298	2.122	1981.2
6600	35.463	494.863	506.542	.9546	.7834	.8206	23.44	.001951	.06279	1.924	2011.7
6700	35.107	494.507	506.360	.9539	.7804	.8181	23.35	.001945	.06259	1.726	2042.2
6800	34.750	494.150	506.179	.9532	.7775	.8156	23.26	.001939	.06240	1.528	2072.6
6900	34.393	493.793	505.998	.9525	.7745	.8131	23.17	.001934	.06221	1.330	2103.1
7000	34.037	493.437	505.816	.9518	.7716	.8106	23.09	.001928	.06202	1.132	2133.6
7100	33.680	493.080	505.635	.9512	.7687	.8081	23.00	.001922	.06183	.933	2164.1
7200	33.324	492.724	505.455	.9505	.7657	.8057	22.91	.001916	.06164	.735	2194.6
7300	32.967	492.367	505.272	.9498	.7628	.8032	22.82	.001910	.06145	.537	2225.0
7400	32.610	492.010	505.091	.9491	.7599	.8007	22.74	.001904	.06126	.339	2255.5
7500	32.254	491.654	504.910	.9484	.7571	.7982	22.65	.001898	.06107	.141	2286.0
7600	31.897	491.297	504.729	.9477	.7542	.7958	22.56	.001892	.06088	-.057	2316.5
7700	31.540	490.940	504.547	.9470	.7513	.7933	22.48	.001886	.06070	-.255	2347.0
7800	31.184	490.584	504.366	.9463	.7484	.7909	22.39	.001881	.06051	-.453	2377.4
7900	30.827	490.227	504.185	.9457	.7456	.7884	22.31	.001875	.06032	-.652	2407.9
8000	30.471	489.871	504.002	.9450	.7427	.7859	22.22	.001869	.06013	-0.850	2438.4
8100	30.114	489.514	503.820	.9443	.7398	.7835	22.14	.001863	.05994	-1.048	2468.9
8200	29.757	489.157	503.637	.9436	.7370	.7811	22.05	.001858	.05976	-1.246	2499.4
8300	29.401	488.801	503.455	.9429	.7342	.7786	21.97	.001852	.05957	-1.444	2529.8
8400	29.044	488.444	503.273	.9422	.7314	.7762	21.89	.001846	.05939	-1.642	2560.3
8500	28.688	488.088	503.091	.9415	.7286	.7738	21.80	.001840	.05920	-1.840	2590.8
8600	28.331	487.731	502.908	.9408	.7258	.7714	21.72	.001835	.05902	-2.038	2621.3
8700	27.974	487.374	502.727	.9402	.7230	.7690	21.64	.001829	.05884	-2.236	2651.8
8800	27.618	487.018	502.545	.9395	.7202	.7666	21.55	.001823	.05865	-2.435	2682.2
8900	27.261	486.661	502.363	.9388	.7175	.7643	21.47	.001818	.05847	-2.633	2712.7
9000	26.904	486.304	502.180	.9381	.7147	.7619	21.38	.001812	.05829	-2.831	2743.2
9100	26.548	485.948	501.998	.9374	.7119	.7595	21.30	.001806	.05811	-3.029	2773.7
9200	26.191	485.591	501.816	.9367	.7092	.7571	21.22	.001801	.05793	-3.227	2804.2
9300	25.835	485.235	501.634	.9360	.7065	.7548	21.14	.001795	.05775	-3.425	2834.6
9400	25.478	484.878	501.452	.9353	.7038	.7524	21.06	.001789	.05757	-3.624	2865.1
9500	25.121	484.521	501.270	.9346	.7011	.7501	20.98	.001784	.05739	-3.821	2895.6
9600	24.765	484.165	501.087	.9340	.6984	.7477	20.90	.001778	.05721	-4.020	2926.1
9700	24.408	483.808	500.906	.9333	.6957	.7454	20.82	.001773	.05703	-4.218	2956.6
9800	24.052	483.452	500.724	.9326	.6930	.7431	20.74	.001767	.05685	-4.416	2987.0
9900	23.695	483.095	500.541	.9319	.6903	.7407	20.66	.001762	.05667	-4.614	3017.5
10000	23.338	482.738	500.359	.9312	.6876	.7384	20.58	.001756	.05649	-4.812	3048.0
10100	22.982	482.382	500.177	.9305	.6849	.7361	20.50	.001751	.05632	-5.010	3078.5
10200	22.625	482.025	499.995	.9298	.6823	.7338	20.42	.001745	.05614	-5.208	3109.0
10300	22.268	481.668	499.812	.9291	.6796	.7315	20.34	.001740	.05596	-5.406	3139.4
10400	21.912	481.312	499.630	.9285	.6770	.7292	20.26	.001734	.05579	-5.605	3170.0
10500	21.555	480.955	499.448	.9278	.6743	.7269	20.18	.001728	.05561	-5.803	3200.4
10600	21.199	480.599	499.265	.9271	.6717	.7246	20.10	.001723	.05544	-6.001	3230.9
10700	20.842	480.242	499.083	.9264	.6691	.7223	20.02	.001718	.05526	-6.199	3261.4
10800	20.485	479.885	498.900	.9257	.6665	.7200	19.95	.001713	.05509	-6.397	3291.8
10900	20.129	479.529	498.717	.9250	.6639	.7177	19.87	.001707	.05491	-6.595	3322.3
11000	19.772	479.172	498.535	.9243	.6614	.7154	19.79	.001702	.05474	-6.793	3352.8
11100	19.416	478.816	498.353	.9236	.6588	.7132	19.71	.001696	.05457	-6.991	3383.3
11200	19.059	478.459	498.170	.9230	.6562	.7109	19.64	.001691	.05440	-7.189	3413.8
11300	18.702	478.102	497.987	.9223	.6537	.7086	19.56	.001686	.05422	-7.388	3444.2
11400	18.346	477.746	497.805	.9216	.6511	.7064	19.48	.001680	.05405	-7.586	3474.7
11500	17.989	477.389	497.623	.9209	.6486	.7042	19.40	.001675	.05388	-7.784	3505.2
11600	17.632	477.032	497.439	.9202	.6460	.7019	19.33	.001670	.05371	-7.982	3535.7
11700	17.276	476.676	497.257	.9195	.6435	.6997	19.25	.001664	.05354	-8.180	3566.2
11800	16.919	476.319	497.075	.9188	.6410	.6975	19.18	.001659	.05337	-8.378	3596.6
11900	16.563	475.963	496.892	.9181	.6384	.6953	19.10	.001654	.05320	-8.576	3627.1

Z ft.	t °F.	T °F. aa	T _m °F. aa	T T _o	p p _o	ρ ρ _o	p in.	ρ	ρρ lb./ft. ³	t °C.	Z m
12000	16.206	475.606	496.710	.9175	.6359	.6931	19.03	.001648	.05303	-8.774	3657.6
12100	15.849	475.249	496.527	.9168	.6333	.6909	18.95	.001642	.05286	-8.973	3688.1
12200	15.493	474.893	496.341	.9161	.6309	.6887	18.88	.001637	.05270	-9.171	3718.6
12300	15.136	474.536	496.157	.9154	.6284	.6865	18.80	.001632	.05253	-9.369	3749.0
12400	14.779	474.179	495.973	.9147	.6259	.6843	18.73	.001627	.05236	-9.567	3779.5
12500	14.423	473.823	495.787	.9140	.6234	.6821	18.65	.001622	.05219	-9.765	3810.0
12600	14.066	473.466	495.603	.9133	.6210	.6799	18.58	.001616	.05203	-9.963	3840.5
12700	13.710	483.110	495.418	.9126	.6185	.6778	18.51	.001611	.05186	-10.161	3871.0
12800	13.353	472.753	495.234	.9119	.6161	.6756	18.43	.001606	.05170	-10.359	3901.4
12900	12.996	472.396	495.049	.9113	.6136	.6733	18.36	.001601	.05153	-10.558	3931.9
13000	12.640	472.040	494.865	.9106	.6112	.6712	18.29	.001596	.05136	-10.756	3962.4
13100	12.283	471.683	494.680	.9099	.6088	.6690	18.21	.001591	.05120	-10.954	3992.9
13200	11.927	471.327	494.495	.9092	.6064	.6669	18.14	.001586	.05104	-11.152	4023.4
13300	11.570	470.970	494.310	.9085	.6040	.6647	18.07	.001580	.05087	-11.350	4053.8
13400	11.213	470.613	494.125	.9078	.6016	.6626	18.00	.001575	.05070	-11.548	4084.3
13500	10.857	470.257	493.941	.9071	.5992	.6605	17.93	.001570	.05054	-11.746	4114.8
13600	10.500	469.900	493.757	.9064	.5968	.6583	17.85	.001565	.05037	-11.944	4145.3
13700	10.143	469.543	493.572	.9058	.5945	.6562	17.78	.001560	.05021	-12.142	4175.7
13800	9.787	469.187	493.386	.9051	.5921	.6541	17.71	.001555	.05005	-12.341	4206.2
13900	9.430	468.830	493.202	.9044	.5897	.6520	17.64	.001550	.04989	-12.539	4236.7
14000	9.074	468.474	493.017	.9037	.5873	.6499	17.57	.001545	.04973	-12.737	4267.2
14100	8.717	468.117	492.833	.9030	.5850	.6478	17.50	.001540	.04957	-12.935	4297.7
14200	8.360	467.760	492.648	.9023	.5827	.6457	17.43	.001535	.04941	-13.133	4328.2
14300	8.004	467.404	492.463	.9016	.5804	.6436	17.36	.001530	.04925	-13.331	4358.6
14400	7.647	467.047	492.278	.9009	.5781	.6416	17.29	.001525	.04909	-13.529	4389.1
14500	7.291	466.691	492.093	.9003	.5757	.6394	17.22	.001520	.04893	-13.727	4419.6
14600	6.934	466.334	491.908	.8996	.5734	.6373	17.15	.001515	.04877	-13.926	4450.1
14700	6.577	465.977	491.723	.8989	.5711	.6352	17.09	.001510	.04861	-14.124	4480.6
14800	6.221	465.621	491.537	.8982	.5688	.6332	17.02	.001506	.04846	-14.322	4511.0
14900	5.864	465.264	491.353	.8975	.5665	.6311	16.95	.001501	.04830	-14.520	4541.5
15000	5.507	464.907	491.168	.8968	.5642	.6291	16.88	.001496	.04814	-14.718	4572.0
15100	5.151	464.551	490.982	.8961	.5620	.6270	16.81	.001491	.04798	-14.916	4602.5
15200	4.794	464.194	490.797	.8954	.5597	.6250	16.75	.001486	.04783	-15.114	4633.0
15300	4.438	463.838	490.612	.8947	.5575	.6230	16.68	.001481	.04767	-15.312	4663.4
15400	4.081	463.481	490.426	.8941	.5552	.6209	16.61	.001476	.04752	-15.511	4693.9
15500	3.724	463.124	490.242	.8934	.5530	.6189	16.54	.001472	.04736	-15.709	4724.4
15600	3.368	462.768	490.057	.8927	.5507	.6169	16.48	.001467	.04720	-15.907	4754.9
15700	3.011	462.411	489.873	.8920	.5485	.6149	16.41	.001462	.04704	-16.105	4785.4
15800	2.655	462.055	489.687	.8913	.5463	.6129	16.34	.001457	.04689	-16.303	4815.8
15900	2.298	461.698	489.501	.8906	.5441	.6109	16.28	.001453	.04673	-16.501	4846.3
16000	1.941	461.341	489.317	.8899	.5418	.6088	16.21	.001448	.04658	-16.699	4876.8
16100	1.585	460.985	489.130	.8892	.5396	.6068	16.15	.001443	.04643	-16.897	4907.3
16200	1.228	460.628	488.944	.8886	.5374	.6048	16.08	.001438	.04628	-17.096	4937.8
16300	0.871	460.271	488.759	.8879	.5352	.6028	16.02	.001434	.04613	-17.294	4968.2
16400	0.515	459.915	488.573	.8872	.5331	.6008	15.95	.001429	.04598	-17.492	4998.7
16500	0.158	459.558	488.387	.8865	.5309	.5988	15.89	.001424	.04583	-17.690	5029.2
16600	-0.198	459.202	488.202	.8858	.5287	.5968	15.82	.001419	.04567	-17.888	5059.7
16700	-0.555	458.845	488.015	.8851	.5266	.5949	15.76	.001415	.04552	-18.086	5090.2
16800	-0.912	458.488	487.830	.8854	.5245	.5930	15.69	.001410	.04537	-18.284	5120.7
16900	-1.268	458.132	487.644	.8837	.5223	.5910	15.63	.001406	.04522	-18.482	5151.1
17000	-1.625	457.775	487.459	.8831	.5202	.5891	15.56	.001401	.04507	-18.680	5181.6
17100	-1.982	457.418	487.272	.8824	.5181	.5871	15.50	.001396	.04492	-18.879	5212.1
17200	-2.338	457.062	487.087	.8817	.5160	.5852	15.44	.001392	.04477	-19.077	5242.6
17300	-2.695	456.705	486.901	.8810	.5139	.5832	15.37	.001387	.04462	-19.275	5273.1
17400	-3.051	456.349	486.714	.8803	.5118	.5812	15.31	.001383	.04447	-19.473	5303.5
17500	-3.408	455.992	486.529	.8796	.5097	.5793	15.25	.001378	.04433	-19.671	5334.0
17600	-3.765	455.635	486.343	.8789	.5076	.5774	15.19	.001373	.04418	-19.869	5364.5
17700	-4.121	455.279	486.157	.8782	.5055	.5755	15.12	.001369	.04403	-20.067	5395.0
17800	-4.478	454.922	485.971	.8776	.5034	.5736	15.06	.001364	.04389	-20.265	5425.5
17900	-4.834	454.566	485.785	.8769	.5013	.5717	15.00	.001360	.04374	-20.464	5455.9
18000	-5.191	454.209	485.598	.8762	.4992	.5698	14.94	.001355	.04359	-20.662	5486.4
18100	-5.548	453.852	485.411	.8755	.4972	.5679	14.88	.001351	.04344	-20.860	5516.9
18200	-5.904	453.496	485.225	.8748	.4951	.5660	14.82	.001346	.04330	-21.058	5547.4
18300	-6.261	453.139	485.038	.8741	.4931	.5641	14.75	.001342	.04316	-21.256	5577.9
18400	-6.618	452.782	484.851	.8734	.4911	.5622	14.69	.001337	.04302	-21.454	5608.3
18500	-6.974	452.426	484.664	.8727	.4891	.5603	14.63	.001333	.04287	-21.652	5638.8
18600	-7.331	452.069	484.478	.8720	.4870	.5584	14.57	.001329	.04272	-21.850	5669.3
18700	-7.687	451.713	484.290	.8714	.4850	.5565	14.51	.001324	.04258	-22.049	5699.8
18800	-8.044	451.356	484.103	.8707	.4830	.5546	14.45	.001320	.04244	-22.247	5730.3
18900	-8.401	450.999	483.917	.8700	.4810	.5528	14.39	.001315	.04230	-22.445	5760.7

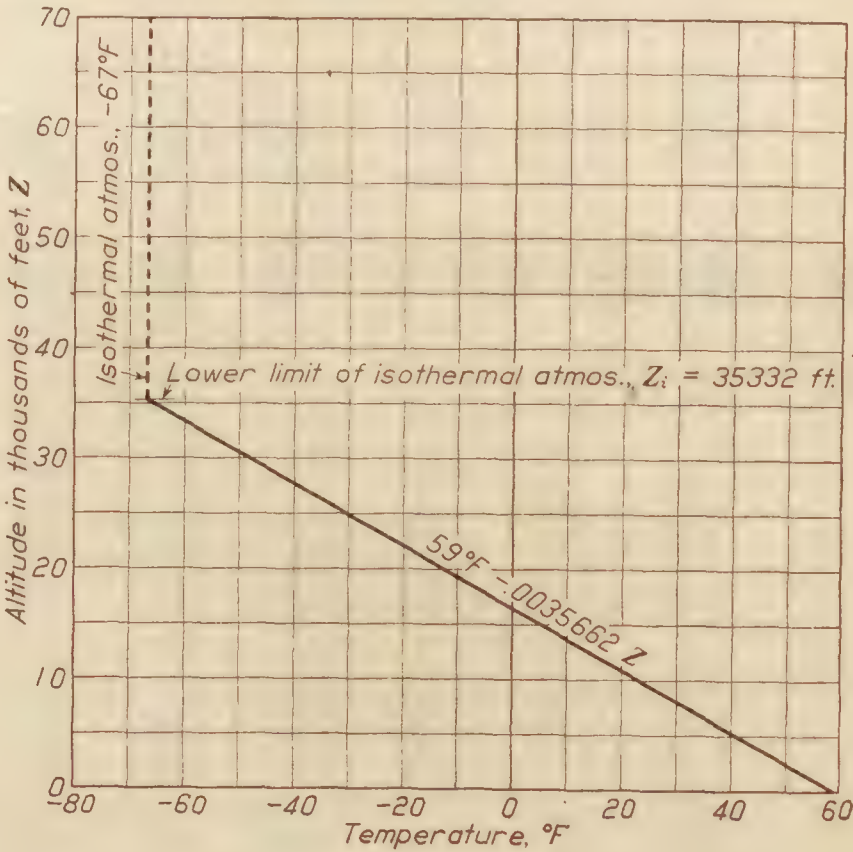
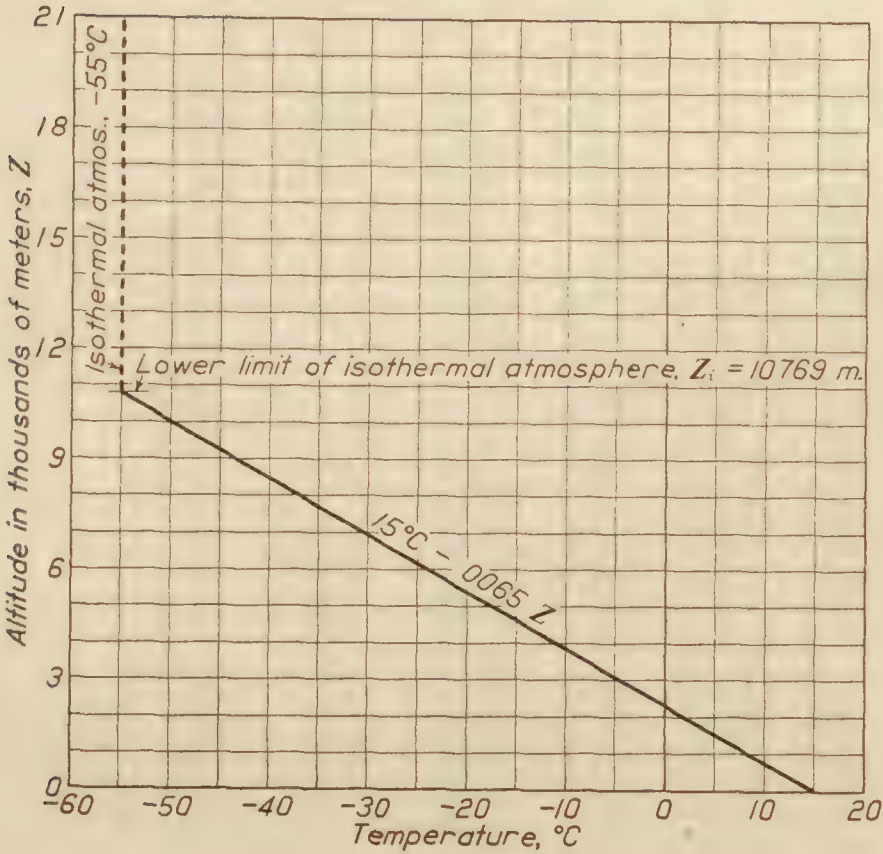
<i>Z</i> ft.	<i>t</i> °F.	<i>T</i> °F. <i>aa</i>	<i>T_m</i> °F. <i>aa</i>	<i>T</i> <i>T₀</i>	<i>p</i> <i>p₀</i>	<i>ρ</i> <i>ρ₀</i>	<i>p</i> in.	<i>ρ</i>	<i>gρ</i> lb./ft. ³	<i>t</i> °C.	<i>Z</i> m
19000	-8.757	450.643	483.729	.8693	.4790	.5509	14.33	.001311	.04216	-22.643	5791.2
19100	-9.114	450.286	483.541	.8686	.4770	.5491	14.27	.001306	.04201	-22.841	5821.7
19200	-9.470	449.930	483.355	.8679	.4750	.5473	14.21	.001302	.04187	-23.039	5852.2
19300	-9.827	449.573	483.168	.8672	.4730	.5454	14.15	.001298	.04173	-23.237	5882.7
19400	-10.184	449.216	482.981	.8665	.4711	.5436	14.09	.001293	.04159	-23.435	5913.1
19500	-10.540	448.860	482.794	.8659	.4691	.5418	14.04	.001289	.04145	-23.633	5943.6
19600	-10.897	448.503	482.608	.8652	.4672	.5400	13.98	.001285	.04131	-23.832	5974.1
19700	-11.254	448.146	482.421	.8645	.4652	.5381	13.92	.001281	.04118	-24.030	6004.6
19800	-11.610	447.790	482.234	.8638	.4633	.5363	13.86	.001276	.04103	-24.228	6035.1
19900	-11.967	447.433	482.047	.8631	.4614	.5345	13.80	.001272	.04089	-24.426	6065.5
20000	-12.323	447.077	481.859	.8624	.4594	.5327	13.75	.001267	.04075	-24.624	6096.0
20100	-12.680	446.720	481.672	.8617	.4575	.5308	13.69	.001263	.04061	-24.822	6126.5
20200	-13.037	446.363	481.484	.8610	.4557	.5290	13.63	.001259	.04048	-25.020	6157.0
20300	-13.393	446.007	481.296	.8604	.4537	.5272	13.57	.001255	.04034	-25.218	6187.5
20400	-13.750	445.650	481.108	.8597	.4517	.5255	13.52	.001250	.04020	-25.417	6218.0
20500	-14.106	445.294	480.921	.8590	.4498	.5237	13.46	.001246	.04007	-25.615	6248.4
20600	-14.463	444.937	480.732	.8583	.4480	.5219	13.40	.001242	.03993	-25.813	6278.9
20700	-14.820	444.580	480.545	.8576	.4461	.5201	13.35	.001238	.03980	-26.011	6309.4
20800	-15.176	444.224	480.357	.8569	.4442	.5183	13.29	.001234	.03966	-26.209	6339.9
20900	-15.533	443.867	480.169	.8562	.4423	.5165	13.24	.001229	.03952	-26.407	6370.3
21000	-15.890	444.510	479.980	.8555	.4405	.5148	13.18	.001225	.03938	-26.605	6400.8
21100	-16.246	443.154	479.793	.8549	.4386	.5130	13.13	.001220	.03925	-26.803	6431.3
21200	-16.603	442.797	479.605	.8542	.4368	.5113	13.07	.001216	.03912	-27.002	6461.8
21300	-16.959	442.441	479.417	.8535	.4350	.5095	13.01	.001212	.03898	-27.200	6492.3
21400	-17.316	442.084	479.229	.8528	.4331	.5078	12.96	.001208	.03885	-27.398	6522.7
21500	-17.673	441.727	479.042	.8521	.4313	.5061	12.90	.001204	.03872	-27.596	6553.2
21600	-18.029	441.370	478.853	.8514	.4294	.5043	12.85	.001199	.03859	-27.794	6583.7
21700	-18.386	441.014	478.666	.8507	.4276	.5025	12.80	.001195	.03846	-27.992	6614.2
21800	-18.743	440.657	478.478	.8500	.4258	.5008	12.74	.001191	.03832	-27.190	6644.7
21900	-19.099	440.301	478.289	.8493	.4240	.4991	12.69	.001187	.03819	-28.388	6675.1
22000	-19.456	439.944	478.100	.8487	.4222	.4974	12.63	.001183	.03806	-28.586	6705.6
22100	-19.812	439.588	477.912	.8480	.4204	.4957	12.58	.001179	.03792	-28.785	6736.1
22200	-20.169	439.231	477.723	.8473	.4186	.4940	12.52	.001175	.03779	-28.983	6766.6
22300	-20.526	438.874	477.534	.8466	.4169	.4923	12.47	.001171	.03766	-29.181	6797.1
22400	-20.882	438.518	477.345	.8459	.4151	.4906	12.42	.001167	.03753	-29.379	6827.5
22500	-21.239	438.161	477.156	.8452	.4133	.4889	12.36	.001163	.03740	-29.577	6858.0
22600	-21.595	437.805	476.966	.8445	.4115	.4872	12.31	.001159	.03727	-29.775	6888.5
22700	-21.952	437.448	476.777	.8438	.4097	.4855	12.26	.001155	.03715	-29.973	6919.0
22800	-22.309	437.091	476.589	.8432	.4080	.4838	12.20	.001151	.03702	-30.171	6949.5
22900	-22.665	436.735	476.399	.8425	.4062	.4821	12.15	.001147	.03689	-30.370	6980.0
23000	-23.022	436.378	476.210	.8418	.4045	.4805	12.10	.001143	.03676	-30.568	7010.4
23100	-23.379	436.021	476.021	.8411	.4028	.4788	12.05	.001139	.03663	-30.766	7040.9
23200	-23.735	435.665	475.831	.8404	.4010	.4772	12.00	.001135	.03650	-30.964	7071.4
23300	-24.092	435.308	475.642	.8397	.3993	.4755	11.95	.001131	.03638	-31.162	7101.9
23400	-24.448	434.952	475.453	.8390	.3976	.4739	11.90	.001127	.03625	-31.360	7132.3
23500	-24.805	434.595	475.265	.8383	.3959	.4721	11.84	.001123	.03612	-31.558	7162.8
23600	-25.162	434.238	475.075	.8377	.3942	.4705	11.79	.001119	.03600	-31.756	7193.3
23700	-25.518	433.882	474.887	.8370	.3925	.4689	11.74	.001115	.03587	-31.955	7223.8
23800	-25.875	433.525	474.698	.8363	.3907	.4672	11.69	.001111	.03574	-32.153	7254.3
23900	-26.231	433.169	474.508	.8356	.3891	.4656	11.64	.001107	.03562	-32.351	7284.7
24000	-26.588	432.812	474.320	.8349	.3874	.4640	11.59	.001103	.03550	-32.549	7315.2
24100	-26.945	432.455	474.131	.8342	.3857	.4624	11.54	.001099	.03538	-32.747	7345.7
24200	-27.301	432.099	473.941	.8335	.3841	.4608	11.49	.001096	.03526	-32.945	7376.2
24300	-27.658	431.742	473.751	.8328	.3824	.4591	11.44	.001092	.03512	-33.143	7406.7
24400	-28.015	431.385	473.561	.8321	.3808	.4575	11.39	.001088	.03500	-33.341	7437.1
24500	-28.371	431.029	473.370	.8315	.3791	.4559	11.34	.001085	.03488	-33.539	7467.6
24600	-28.728	430.672	473.181	.8308	.3775	.4543	11.29	.001081	.03476	-33.738	7498.1
24700	-29.084	430.316	472.991	.8301	.3758	.4527	11.24	.001077	.03464	-33.936	7528.6
24800	-29.441	429.959	472.801	.8294	.3741	.4511	11.20	.001073	.03451	-34.134	7559.1
24900	-29.798	429.602	472.609	.8287	.3725	.4496	11.15	.001069	.03439	-34.332	7589.5
25000	-30.154	429.246	472.420	.8280	.3709	.4480	11.10	.001065	.03427	-34.530	7620.0
25100	-30.511	428.889	472.230	.8273	.3693	.4463	11.05	.001061	.03415	-34.728	7650.5
25200	-30.867	428.533	472.039	.8266	.3677	.4447	11.00	.001057	.03403	-34.926	7681.0
25300	-31.224	428.176	471.850	.8260	.3661	.4432	10.96	.001053	.03391	-35.124	7711.5
25400	-31.581	427.819	471.660	.8254	.3645	.4416	10.91	.001049	.03379	-35.323	7741.9
25500	-31.937	427.463	471.469	.8246	.3629	.4401	10.86	.001046	.03367	-35.521	7772.4
25600	-32.294	427.106	471.279	.8239	.3613	.4385	10.81	.001042	.03355	-35.719	7802.9
25700	-32.651	426.749	471.090	.8232	.3597	.4370	10.77	.001039	.03343	-35.917	7833.4
25800	-33.007	426.393	470.899	.8225	.3581	.4355	10.72	.001035	.03331	-36.115	7863.9
25900	-33.364	426.036	470.709	.8218	.3566	.4339	10.67	.001031	.03320	-36.313	7894.3

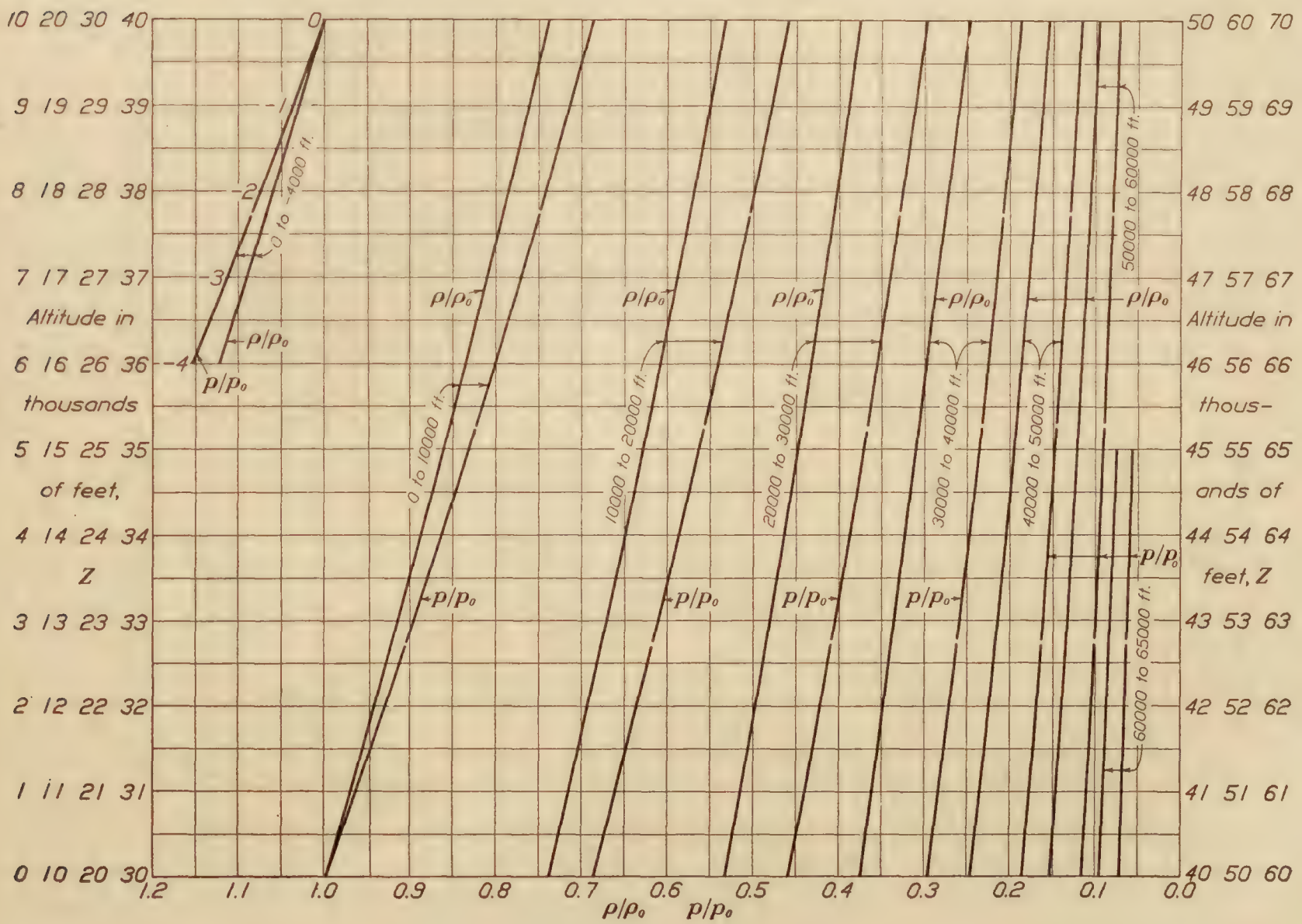
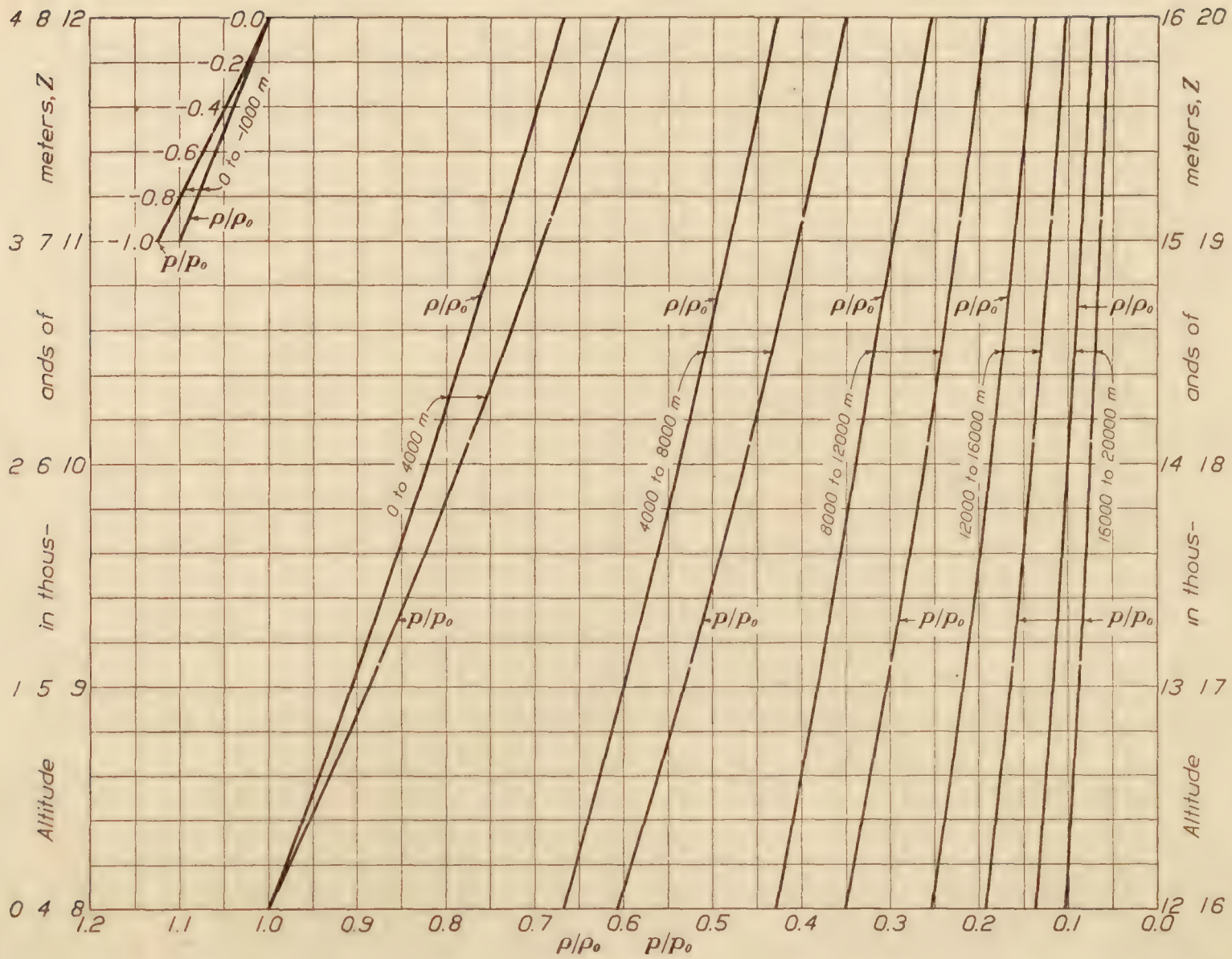
Z ft.	°F.	T °F. aa	T _m °F. aa	T T _o	p p _o	ρ ρ _o	p in.	ρ	gρ lb./ft. ³	t °C.	Z m
26000	−33.720	425.680	470.518	.8211	.3550	.4323	10.62	.001028	.03308	−36.511	7924.8
26100	−34.077	425.323	470.327	.8205	.3535	.4308	10.58	.001024	.03296	−36.709	7955.3
26200	−34.434	424.966	470.136	.8198	.3519	.4292	10.53	.001020	.03284	−36.908	7985.8
26300	−34.790	424.610	469.946	.8191	.3504	.4277	10.48	.001017	.03282	−37.106	8016.3
26400	−35.147	424.253	469.755	.8184	.3488	.4262	10.44	.001013	.03260	−37.304	8046.7
26500	−35.504	423.896	469.563	.8177	.3473	.4247	10.39	.001010	.03249	−37.502	8077.2
26600	−35.860	423.540	469.372	.8170	.3458	.4232	10.34	.001006	.03237	−37.700	8107.7
26700	−36.217	423.183	469.181	.8163	.3442	.4216	10.30	.001002	.03226	−37.898	8138.2
26800	−36.573	422.827	468.989	.8156	.3427	.4201	10.25	.000999	.03214	−38.096	8168.7
26900	−36.930	422.470	468.798	.8150	.3412	.4186	10.21	.000995	.03203	−38.294	8199.1
27000	−37.287	422.113	468.607	.8143	.3397	.4171	10.16	.000992	.03192	−38.493	8229.6
27100	−37.643	421.757	468.415	.8136	.3382	.4156	10.12	.000988	.03180	−38.691	8260.1
27200	−38.000	421.400	468.224	.8129	.3367	.4142	10.07	.000985	.03168	−38.889	8290.6
27300	−38.356	421.044	468.033	.8122	.3352	.4127	10.03	.000981	.03157	−39.087	8321.1
27400	−38.713	420.687	467.841	.8115	.3337	.4111	9.980	.000978	.03145	−39.285	8351.5
27500	−39.070	420.330	467.651	.8108	.3322	.4097	9.939	.000974	.03134	−39.483	8382.0
27600	−39.426	419.974	467.460	.8101	.3307	.4082	9.895	.000971	.03123	−39.681	8412.5
27700	−39.783	419.617	467.269	.8094	.3292	.4067	9.852	.000967	.03112	−39.879	8443.0
27800	−40.140	419.260	467.078	.8088	.3277	.4053	9.808	.000964	.03101	−40.077	8473.5
27900	−40.496	418.904	466.887	.8081	.3263	.4038	9.764	.000960	.03090	−40.276	8503.9
28000	−40.853	418.547	466.695	.8074	.3248	.4023	9.720	.000957	.03078	−40.474	8534.4
28100	−41.209	418.191	466.503	.8067	.3234	.4008	9.676	.000953	.03067	−40.672	8564.9
28200	−41.566	417.834	466.311	.8060	.3219	.3994	9.633	.000950	.03056	−40.870	8595.4
28300	−41.923	417.477	466.119	.8053	.3205	.3979	9.590	.000946	.03045	−41.068	8625.9
28400	−42.279	417.121	465.926	.8046	.3190	.3965	9.547	.000943	.03034	−41.266	8656.3
28500	−42.636	416.764	465.734	.8039	.3176	.3951	9.504	.000940	.03023	−41.464	8686.8
28600	−42.992	416.408	465.542	.8033	.3162	.3937	9.462	.000936	.03012	−41.662	8717.3
28700	−43.349	416.051	465.349	.8026	.3148	.3923	9.420	.000933	.03001	−41.861	8747.8
28800	−43.706	415.694	465.157	.8019	.3134	.3908	9.377	.000930	.02990	−42.059	8778.2
28900	−44.062	415.338	464.966	.8012	.3120	.3893	9.335	.000926	.02979	−42.257	8808.7
29000	−44.419	414.981	464.773	.8005	.3106	.3879	9.293	.000922	.02968	−42.455	8839.2
29100	−44.776	414.624	464.580	.7998	.3092	.3865	9.251	.000919	.02957	−42.653	8869.7
29200	−45.132	414.268	464.388	.7991	.3078	.3851	9.209	.000915	.02946	−42.851	8900.2
29300	−45.489	413.911	464.196	.7985	.3063	.3837	9.168	.000912	.02935	−43.049	8930.7
29400	−45.845	413.555	464.003	.7978	.3049	.3823	9.127	.000909	.02925	−43.247	8961.1
29500	−46.202	413.198	463.811	.7971	.3035	.3809	9.085	.000906	.02914	−43.446	8991.6
29600	−46.559	412.841	463.619	.7964	.3022	.3794	9.044	.000902	.02903	−43.644	9022.1
29700	−46.915	412.485	463.427	.7957	.3008	.3780	9.003	.000899	.02892	−43.842	9052.6
29800	−47.272	412.128	463.235	.7950	.2995	.3767	8.962	.000896	.02881	−44.040	9083.1
29900	−47.628	411.772	463.043	.7943	.2981	.3754	8.921	.000892	.02871	−44.238	9113.5
30000	−47.985	411.415	462.849	.7936	.2968	.3740	8.880	.000889	.02861	−44.436	9144.0
30100	−48.342	411.058	462.656	.7929	.2954	.3725	8.840	.000886	.02850	−44.634	9174.5
30200	−48.698	410.702	462.463	.7923	.2940	.3712	8.800	.000883	.02840	−44.832	9205.0
30300	−49.055	410.345	462.270	.7916	.2927	.3698	8.760	.000879	.02829	−45.030	9235.5
30400	−49.412	409.988	462.075	.7909	.2914	.3685	8.720	.000876	.02819	−45.229	9265.9
30500	−49.768	409.632	461.882	.7902	.2900	.3671	8.680	.000873	.02809	−45.427	9296.4
30600	−50.125	409.275	461.689	.7895	.2887	.3658	8.641	.000870	.02799	−45.625	9326.9
30700	−50.481	408.919	461.495	.7888	.2874	.3644	8.601	.000867	.02788	−45.823	9357.4
30800	−50.838	408.562	461.302	.7881	.2861	.3630	8.562	.000863	.02778	−46.021	9387.9
30900	−51.195	408.205	461.108	.7874	.2848	.3617	8.522	.000860	.02767	−46.219	9418.3
31000	−51.551	407.849	460.914	.7867	.2834	.3603	8.483	.000857	.02757	−46.417	9448.8
31100	−51.908	407.492	460.721	.7861	.2821	.3590	8.444	.000854	.02747	−46.615	9479.3
31200	−52.265	407.135	460.528	.7854	.2808	.3577	8.406	.000851	.02737	−46.814	9509.8
31300	−52.620	406.779	460.334	.7847	.2795	.3564	8.367	.000848	.02726	−47.012	9540.3
31400	−52.978	406.422	460.140	.7840	.2783	.3551	8.329	.000845	.02716	−47.210	9570.7
31500	−53.334	406.066	459.947	.7833	.2770	.3537	8.290	.000842	.02706	−47.408	9601.2
31600	−53.691	405.709	459.754	.7826	.2758	.3524	8.252	.000838	.02696	−47.606	9631.7
31700	−54.048	405.352	459.560	.7819	.2745	.3511	8.214	.000835	.02686	−47.804	9662.2
31800	−54.404	404.996	459.367	.7812	.2732	.3498	8.176	.000832	.02676	−48.002	9692.7
31900	−54.761	404.639	459.174	.7806	.2719	.3485	8.138	.000829	.02666	−48.200	9723.1
32000	−55.117	404.283	458.980	.7799	.2707	.3472	8.101	.000826	.02656	−48.399	9753.6
32200	−55.831	403.569	458.591	.7785	.2682	.3445	8.026	.000820	.02636	−48.795	9814.6
32400	−56.544	402.856	458.201	.7771	.2657	.3419	7.952	.000814	.02616	−49.191	9875.5
32600	−57.257	402.143	457.812	.7757	.2632	.3394	7.878	.000807	.02596	−49.587	9936.5
32800	−57.970	401.430	457.423	.7744	.2607	.3368	7.805	.000801	.02577	−49.983	9997.5
33000	−58.684	400.716	457.034	.7730	.2583	.3343	7.732	.000795	.02558	−50.379	10058.4
33200	−59.397	400.003	456.645	.7716	.2560	.3318	7.660	.000789	.02539	−50.776	10119.4
33400	−60.110	399.290	456.255	.7702	.2536	.3293	7.589	.000783	.02520	−51.172	10180.3
33600	−60.823	398.577	455.867	.7689	.2512	.3268	7.518	.000776	.02501	−51.568	10241.3
33800	−61.537	397.863	455.477	.7675	.2489	.3243	7.447	.000770	.02482	−51.965	10302.3

Z ft.	°F.	T °F. aa	T _m °F. aa	$\frac{T}{T_0}$	$\frac{p}{p_0}$	ρ ρ_0	P in.	μ	ρ lb./ft. ³	t °C.	Z m
34000	-62.250	397.150	455.087	.7661	.2465	.3218	7.377	.000765	.02463	-52.361	10363.2
34200	-62.963	396.437	454.696	.7647	.2442	.3194	7.308	.000759	.02444	-52.757	10424.2
34400	-63.676	395.724	454.305	.7634	.2419	.3170	7.239	.000753	.02425	-53.153	10485.1
34600	-64.389	395.011	453.914	.7620	.2397	.3145	7.171	.000748	.02406	-53.550	10546.1
34800	-65.103	394.297	453.523	.7606	.2374	.3121	7.103	.000742	.02387	-53.946	10607.1
35000	-65.816	393.584	453.132	.7592	.2352	.3098	7.036	.000736	.02369	-54.342	10668.0
35200	-66.529	392.871	452.740	.7579	.2330	.3074	6.970	.000731	.02351	-54.738	10729.0
35332	-67.000	392.400	452.680	.7569	.2314	.3058	6.925	.000727	.02339	-55.000	10759.5
35400	-67.000	392.400	452.351	.7569	.2307	.3048	6.904	.000725	.02332	-55.000	10789.9
35600	-67.000	392.400	451.962	.7569	.2285	.3019	6.838	.000718	.02310	-55.000	10850.9
35800	-67.000	392.400	451.578	.7569	.2264	.2991	6.773	.000711	.02287	-55.000	10911.9
36000	-67.000	392.400	451.198	.7569	.2242	.2962	6.708	.000704	.02265	-55.000	10972.8
36200	-67.000	392.400	450.824	.7569	.2221	.2934	6.644	.000698	.02244	-55.000	11033.8
36400	-67.000	392.400	450.454	.7569	.2199	.2906	6.581	.000691	.02223	-55.000	11094.7
36600	-67.000	392.400	450.087	.7569	.2178	.2878	6.518	.000685	.02201	-55.000	11155.7
36800	-67.000	392.400	449.727	.7569	.2158	.2851	6.456	.000678	.02180	-55.000	11216.7
37000	-67.000	392.400	449.369	.7569	.2137	.2824	6.395	.000671	.02160	-55.000	11277.6
37200	-67.000	392.400	449.016	.7569	.2117	.2797	6.334	.000664	.02139	-55.000	11338.6
37400	-67.000	392.400	448.667	.7569	.2097	.2770	6.274	.000658	.02119	-55.000	11399.5
37600	-67.000	392.400	448.322	.7569	.2078	.2744	6.214	.000652	.02099	-55.000	11460.5
37800	-67.000	392.400	447.981	.7569	.2058	.2718	6.155	.000646	.02078	-55.000	11521.5
38000	-67.000	392.400	447.648	.7569	.2037	.2692	6.096	.000640	.02059	-55.000	11582.4
38200	-67.000	392.400	447.320	.7569	.2018	.2667	6.038	.000634	.02039	-55.000	11643.4
38400	-67.000	392.400	446.997	.7569	.1999	.2642	5.981	.000628	.02020	-55.000	11704.3
38600	-67.000	392.400	446.676	.7569	.1980	.2616	5.924	.000622	.02001	-55.000	11765.3
38800	-67.000	392.400	446.361	.7569	.1961	.2591	5.868	.000616	.01982	-55.000	11826.3
39000	-67.000	392.400	446.049	.7569	.1943	.2566	5.812	.000610	.01963	-55.000	11887.2
39200	-67.000	392.400	445.741	.7569	.1925	.2542	5.757	.000604	.01944	-55.000	11948.2
39400	-67.000	392.400	445.435	.7569	.1906	.2518	5.702	.000598	.01926	-55.000	12009.1
39600	-67.000	392.400	445.133	.7569	.1887	.2494	5.648	.000593	.01908	-55.000	12070.1
39800	-67.000	392.400	444.836	.7569	.1869	.2471	5.595	.000587	.01890	-55.000	12131.1
40000	-67.000	392.400	444.537	.7569	.1852	.2447	5.541	.000582	.01872	-55.000	12192.0
40200	-67.000	392.400	444.244	.7569	.1834	.2424	5.488	.000576	.01854	-55.000	12253.0
40400	-67.000	392.400	443.954	.7569	.1817	.2401	5.436	.000571	.01836	-55.000	12313.9
40600	-67.000	392.400	443.669	.7569	.1799	.2377	5.384	.000565	.01819	-55.000	12374.9
40800	-67.000	392.400	443.384	.7569	.1782	.2355	5.333	.000560	.01802	-55.000	12435.9
41000	-67.000	392.400	443.104	.7569	.1765	.2332	5.283	.000554	.01785	-55.000	12496.8
41200	-67.000	392.400	442.825	.7569	.1749	.2310	5.233	.000549	.01768	-55.000	12557.8
41400	-67.000	392.400	442.551	.7569	.1732	.2288	5.183	.000544	.01751	-55.000	12618.7
41600	-67.000	392.400	442.280	.7569	.1716	.2266	5.134	.000539	.01734	-55.000	12679.7
41800	-67.000	392.400	442.010	.7569	.1699	.2245	5.085	.000534	.01718	-55.000	12740.7
42000	-67.000	392.400	441.742	.7569	.1683	.2224	5.036	.000529	.01701	-55.000	12801.6
42200	-67.000	392.400	441.479	.7569	.1667	.2202	4.988	.000523	.01685	-55.000	12862.6
42400	-67.000	392.400	441.219	.7569	.1651	.2181	4.941	.000518	.01669	-55.000	12923.5
42600	-67.000	392.400	440.963	.7569	.1636	.2160	4.894	.000513	.01653	-55.000	12984.5
42800	-67.000	392.400	440.707	.7569	.1620	.2140	4.848	.000509	.01638	-55.000	13045.5
43000	-67.000	392.400	440.455	.7569	.1605	.2120	4.802	.000504	.01622	-55.000	13106.4
43200	-67.000	392.400	440.206	.7569	.1589	.2100	4.757	.000500	.01606	-55.000	13167.4
43400	-67.000	392.400	439.959	.7569	.1574	.2080	4.712	.000495	.01591	-55.000	13228.3
43600	-67.000	392.400	439.715	.7569	.1559	.2060	4.667	.000491	.01576	-55.000	13289.3
43800	-67.000	392.400	439.472	.7569	.1544	.2040	4.622	.000486	.01561	-55.000	13350.3
44000	-67.000	392.400	439.232	.7569	.1530	.2021	4.578	.000481	.01546	-55.000	13411.2
44200	-67.000	392.400	438.995	.7569	.1515	.2001	4.534	.000477	.01531	-55.000	13472.2
44400	-67.000	392.400	438.760	.7569	.1501	.1982	4.491	.000472	.01517	-55.000	13533.1
44600	-67.000	392.400	438.528	.7569	.1486	.1963	4.448	.000468	.01502	-55.000	13594.1
44800	-67.000	392.400	438.299	.7569	.1472	.1945	4.406	.000463	.01488	-55.000	13655.1
45000	-67.000	392.400	438.071	.7569	.1458	.1926	4.364	.000459	.01474	-55.000	13716.0
45200	-67.000	392.400	437.844	.7569	.1444	.1908	4.323	.000455	.01460	-55.000	13777.0
45400	-67.000	392.400	437.622	.7569	.1431	.1890	4.282	.000450	.01446	-55.000	13837.9
45600	-67.000	392.400	437.401	.7569	.1418	.1872	4.241	.000446	.01432	-55.000	13898.9
45800	-67.000	392.400	437.182	.7569	.1404	.1854	4.200	.000441	.01418	-55.000	13959.9
46000	-67.000	392.400	436.964	.7569	.1391	.1837	4.160	.000437	.01405	-55.000	14020.8
46200	-67.000	392.400	436.750	.7569	.1377	.1819	4.121	.000433	.01391	-55.000	14081.8
46400	-67.000	392.400	436.537	.7569	.1364	.1802	4.082	.000429	.01378	-55.000	14142.7
46600	-67.000	392.400	436.326	.7569	.1351	.1785	4.043	.000425	.01365	-55.000	14203.7
46800	-67.000	392.400	436.118	.7569	.1338	.1768	4.004	.000421	.01352	-55.000	14264.7
47000	-67.000	392.400	435.912	.7569	.1325	.1751	3.966	.000417	.01339	-55.000	14325.6
47200	-67.000	392.400	435.707	.7569	.1314	.1734	3.928	.000413	.01326	-55.000	14386.6
47400	-67.000	392.400	435.504	.7569	.1301	.1718	3.891	.000409	.01313	-55.000	14447.5
47600	-67.000	392.400	435.303	.7569	.1289	.1702	3.854	.000405	.01301	-55.000	14508.5
47800	-67.000	392.400	435.104	.7569	.1276	.1686	3.817	.000401	.01289	-55.000	14569.5

Z ft.	t °F.	T °F. aa	T _m °F. aa	T T _o	p p _o	ρ ρ _o	p in.	ρ	g _o lb./ft. ³	t °C.	Z m
48000	-67.000	392.400	434.906	.7569	.1264	.1669	3.781	.000397	.01277	-55.000	14630.4
48200	-67.000	392.400	434.712	.7569	.1252	.1653	3.745	.000393	.01265	-55.000	14691.4
48400	-67.000	392.400	434.518	.7569	.1240	.1638	3.709	.000390	.01253	-55.000	14752.3
48600	-67.000	392.400	434.326	.7569	.1228	.1622	3.674	.000386	.01241	-55.000	14813.3
48800	-67.000	392.400	434.136	.7569	.1216	.1606	3.639	.000382	.01229	-55.000	14874.3
49000	-67.000	392.400	433.948	.7569	.1205	.1591	3.604	.000379	.01217	-55.000	14935.2
49200	-67.000	392.400	433.760	.7569	.1194	.1577	3.570	.000375	.01205	-55.000	14996.2
49400	-67.000	392.400	433.575	.7569	.1183	.1562	3.536	.000372	.01194	-55.000	15057.2
49600	-67.000	392.400	433.391	.7569	.1171	.1547	3.502	.000368	.01182	-55.000	15118.1
49800	-67.000	392.400	433.210	.7569	.1160	.1532	3.469	.000364	.01171	-55.000	15179.1
50000	-67.000	392.400	433.030	.7569	.1149	.1517	3.436	.000361	.01161	-55.000	15240.0
50200	-67.000	392.400	432.851	.7569	.1138	.1503	3.403	.000358	.01149	-55.000	15301.0
50400	-67.000	392.400	432.673	.7569	.1127	.1488	3.371	.000354	.01138	-55.000	15362.0
50600	-67.000	392.400	432.497	.7569	.1116	.1475	3.339	.000351	.01127	-55.000	15422.9
50800	-67.000	392.400	432.324	.7569	.1106	.1461	3.308	.000347	.01117	-55.000	15483.9
51000	-67.000	392.400	432.151	.7569	.1095	.1447	3.276	.000344	.01106	-55.000	15544.8
51200	-67.000	392.400	431.981	.7569	.1085	.1433	3.245	.000341	.01095	-55.000	15605.8
51400	-67.000	392.400	431.812	.7569	.1075	.1419	3.214	.000337	.01085	-55.000	15666.8
51600	-67.000	392.400	431.644	.7569	.1065	.1405	3.183	.000334	.01075	-55.000	15727.7
51800	-67.000	392.400	431.476	.7569	.1055	.1392	3.153	.000331	.01065	-55.000	15788.7
52000	-67.000	392.400	431.312	.7569	.1044	.1380	3.123	.000328	.010550	-55.000	15849.6
52200	-67.000	392.400	431.148	.7569	.1034	.1366	3.093	.000324	.010450	-55.000	15910.6
52400	-67.000	392.400	430.985	.7569	.1024	.1353	3.064	.000321	.010350	-55.000	15971.6
52600	-67.000	392.400	430.824	.7569	.1015	.1340	3.035	.000318	.010250	-55.000	16032.5
52800	-67.000	392.400	430.665	.7569	.1005	.1327	3.007	.000315	.010154	-55.000	16093.5
53000	-67.000	392.400	430.507	.7569	.09955	.1314	2.978	.000312	.010057	-55.000	16154.4
53200	-67.000	392.400	430.349	.7569	.09866	.1303	2.950	.000310	.009961	-55.000	16215.4
53400	-67.000	392.400	430.193	.7569	.09767	.1290	2.922	.000307	.009857	-55.000	16276.4
53600	-67.000	392.400	430.037	.7569	.09674	.1278	2.894	.000304	.009775	-55.000	16337.3
53800	-67.000	392.400	429.885	.7569	.09582	.1266	2.867	.000301	.009682	-55.000	16398.3
54000	-67.000	392.400	429.734	.7569	.09491	.1253	2.839	.000298	.009591	-55.000	16459.2
54200	-67.000	392.400	429.583	.7569	.09401	.1241	2.812	.000296	.009500	-55.000	16520.2
54400	-67.000	392.400	429.433	.7569	.09312	.1230	2.786	.000293	.009410	-55.000	16581.2
54600	-67.000	392.400	429.285	.7569	.09224	.1218	2.759	.000290	.009320	-55.000	16642.1
54800	-67.000	392.400	429.137	.7569	.09136	.1207	2.733	.000287	.009231	-55.000	16703.1
55000	-67.000	392.400	428.991	.7569	.09049	.1195	2.707	.000284	.009143	-55.000	16764.0
55200	-67.000	392.400	428.847	.7569	.08962	.1184	2.682	.000282	.009056	-55.000	16825.0
55400	-67.000	392.400	428.703	.7569	.08877	.1172	2.656	.000279	.008970	-55.000	16886.0
55600	-67.000	392.400	428.560	.7569	.08793	.1162	2.631	.000276	.008885	-55.000	16946.9
55800	-67.000	392.400	428.419	.7569	.08709	.1151	2.606	.000274	.008801	-55.000	17000.9
56000	-67.000	392.400	428.279	.7569	.08626	.1140	2.581	.000271	.008718	-55.000	17068.8
56200	-67.000	392.400	428.139	.7569	.08544	.1129	2.556	.000268	.008634	-55.000	17129.8
56400	-67.000	392.400	428.001	.7569	.08463	.1118	2.532	.000266	.008551	-55.000	17190.8
56600	-67.000	392.400	427.863	.7569	.08382	.1107	2.508	.000263	.008470	-55.000	17251.7
56800	-67.000	392.400	427.727	.7569	.08302	.1097	2.484	.000261	.008390	-55.000	17312.7
57000	-67.000	392.400	427.592	.7569	.08223	.1087	2.460	.000258	.008310	-55.000	17373.6
57200	-67.000	392.400	427.459	.7569	.08145	.1076	2.437	.000256	.008228	-55.000	17434.6
57400	-67.000	392.400	427.326	.7569	.08067	.1066	2.414	.000253	.008152	-55.000	17495.6
57600	-67.000	392.400	427.193	.7569	.07990	.1056	2.391	.000251	.008074	-55.000	17556.5
57800	-67.000	392.400	427.063	.7569	.07914	.1046	2.369	.000248	.007998	-55.000	17617.5
58000	-67.000	392.400	426.933	.7569	.07839	.1035	2.346	.000246	.007922	-55.000	17678.4
58200	-67.000	392.400	426.804	.7569	.07764	.1025	2.324	.000243	.007847	-55.000	17739.4
58400	-67.000	392.400	426.676	.7569	.07690	.1017	2.302	.000241	.007773	-55.000	17800.4
58600	-67.000	392.400	426.549	.7569	.07617	.1007	2.280	.000239	.007699	-55.000	17861.3
58800	-67.000	392.400	426.423	.7569	.07545	.09969	2.258	.000237	.007626	-55.000	17922.3
59000	-67.000	392.400	426.297	.7569	.07473	.09870	2.237	.000234	.007553	-55.000	17983.2
59200	-67.000	392.400	426.173	.7569	.07402	.09782	2.215	.000233	.007481	-55.000	18044.2
59400	-67.000	392.400	426.049	.7569	.07331	.09687	2.194	.000231	.007410	-55.000	18105.2
59600	-67.000	392.400	425.927	.7569	.07262	.09594	2.173	.000229	.007339	-55.000	18166.1
59800	-67.000	392.400	425.806	.7569	.07193	.09504	2.152	.000226	.007269	-55.000	18227.1
60000	-67.000	392.400	425.685	.7569	.07125	.09413	2.132	.000224	.007201	-55.000	18288.0
60200	-67.000	392.400	425.565	.7569	.07057	.09323	2.112	.000222	.007132	-55.000	18349.0
60400	-67.000	392.400	425.446	.7569	.06990	.09235	2.092	.000220	.007064	-55.000	18410.0
60600	-67.000	392.400	425.328	.7569	.06923	.09147	2.072	.000218	.006997	-55.000	18470.9
60800	-67.000	392.400	425.210	.7569	.06857	.09060	2.053	.000216	.006931	-55.000	18531.9
61000	-67.000	392.400	425.093	.7569	.06792	.08974	2.033	.000214	.006865	-55.000	18592.8
61200	-67.000	392.400	424.978	.7569	.06728	.08888	2.013	.000211	.006800	-55.000	18653.8
61400	-67.000	392.400	424.863	.7569	.06664	.08804	1.994	.000209	.006735	-55.000	18714.8
61600	-67.000	392.400	424.749	.7569	.06601	.08720	1.975	.000207	.006671	-55.000	18775.7
61800	-67.000	392.400	424.635	.7569	.06539	.08638	1.956	.000205	.006609	-55.000	18836.7

<i>Z</i> ft.	<i>t</i> °F.	<i>T</i> °F. <i>aa</i>	<i>T_m</i> °F. <i>aa</i>	<i>T</i> <i>T₀</i>	<i>p</i> <i>p₀</i>	$\frac{p}{p_0}$	<i>p</i> in.	ρ	<i>gρ</i> lb./ft. ³	<i>t</i> °C.	<i>Z</i> m
62000	-67.000	392.400	424.522	.7569	.06476	.08555	1.938	.000203	.006546	-55.000	18897.6
62200	-67.000	392.400	424.410	.7569	.06414	.08473	1.920	.000201	.006483	-55.000	18958.6
62400	-67.000	392.400	424.299	.7569	.06353	.08392	1.901	.000199	.006421	-55.000	19019.6
62600	-67.000	392.400	424.189	.7569	.06293	.08313	1.883	.000198	.006360	-55.000	19080.5
62800	-67.000	392.400	424.080	.7569	.06233	.08235	1.865	.000196	.006299	-55.000	19141.5
63000	-67.000	392.400	423.972	.7569	.06173	.08156	1.847	.000194	.006239	-55.000	19202.4
63200	-67.000	392.400	423.864	.7569	.06114	.08078	1.830	.000192	.006180	-55.000	19263.4
63400	-67.000	392.400	423.756	.7569	.06056	.08001	1.813	.000190	.006121	-55.000	19324.4
63600	-67.000	392.400	423.649	.7569	.05999	.07925	1.796	.000188	.006063	-55.000	19385.3
63800	-67.000	392.400	423.543	.7569	.05942	.07850	1.779	.000186	.006006	-55.000	19446.3
64000	-67.000	392.400	423.439	.7569	.05886	.07775	1.761	.000185	.005949	-55.000	19507.2
64200	-67.000	392.400	423.334	.7569	.05830	.07702	1.745	.000183	.005892	-55.000	19568.2
64400	-67.000	392.400	423.229	.7569	.05774	.07628	1.729	.000181	.005836	-55.000	19629.2
64600	-67.000	392.400	423.126	.7569	.05719	.07555	1.712	.000179	.005780	-55.000	19690.1
64800	-67.000	392.400	423.024	.7569	.05665	.07483	1.696	.000177	.005725	-55.000	19751.1
65000	-67.000	392.400	422.922	.7569	.05611	.07412	1.680	.000176	.005671	-55.000	19812.0







Density-Altitude chart prepared by F. B. Newell, Engineering Division of the Air Service, McCook Field, from Tables and data of this report

REPORT No. 219

SOME ASPECTS OF THE COMPARISON OF MODEL AND FULL-SCALE TESTS

By D. W. TAYLOR

National Advisory Committee for Aeronautics

REPORT No. 219

SOME ASPECTS OF THE COMPARISON OF MODEL AND FULL-SCALE TESTS ¹

By D. W. TAYLOR

Secretary National Advisory Committee for Aeronautics

Aeronautics now covers a large field. The bibliography alone, compiled and published annually by the United States National Advisory Committee for Aeronautics, requires something like 200 pages of a book 7 inches by 10 inches. Needless to say, I am not undertaking to review the whole field.

Owing to the difficulties of conducting free flight tests of performance and the fact that we can not afford to make many mistakes in an appliance whose operation involves the risk of human life, it is peculiarly desirable that we may be able to predict the performance of the completed airplane from small-scale experiments; and probably in no other branch of mechanical science have we at present so many research laboratories.

In view, then, of the universal use of models and wind tunnel tests to obtain results upon which are based predictions of performance of full-sized airplanes, it appears worth while to give some consideration to the foundation, as it were, of such methods. The mathematical basis of the law of mechanical similitude has been traced back as far as Sir Isaac Newton, but it is believed that the first serious practical application was that made by Mr. William Froude, when, some 65 years ago, with the aid of the Admiralty, he built in his garden at Torquay a long tank filled with water, in which he tested models of vessels. Froude's methods have been universally accepted by naval architects as of great value, and they are able to predict performances of full-sized ships with accuracy adequate to the purposes of the engineer. Nevertheless, they are not exact, and in the last analysis their justification is due to the fact that the results they predict for the full-sized ship are substantially verified in practice. However, Froude separated the frictional resistance of the model from its wave-making resistance, or the resistance absorbed in the production of waves, and it is to the latter only that Froude's law of comparison applies. Frictional resistance is calculated from coefficients originally determined by Froude upon the basis of tests with comparatively small plane surfaces at low speeds, and it is generally recognized now by naval architects that large-scale experiments would be desirable to give us greater assurance of accuracy when dealing with present-day ships.

The most fundamental and instructive method of covering this whole question of the value of model experiments is based upon the principle of dimensional homogeneity first fully enunciated, I believe, some 15 years ago by a Russian, Riabouchinski. In the United States, Doctor Buckingham has taken up the matter and done much work to amplify, clarify, and apply the principle. In a paper in 1915 before the American Society of Mechanical Engineers he gave a number of illuminating applications. In the mathematical treatment below I follow essentially Buckingham's methods.

Instead of considering the general formula, which may be of a beautiful simplicity to the mathematical physicist but is not too easy to follow for us who are not mathematical physicists, I will consider only the general case applying to motion of objects in a fluid medium. The

¹ The thirteenth annual Wilbur Wright memorial lecture, read in London before the Royal Aeronautical Society of Great Britain Apr. 30, 1925, by Commander J. C. Hunsaker for Dr. D. W. Taylor and published by permission of that society.

first thing to establish is the quantities involved; that is, the physical quantities present which can affect the case. Let us denote by R the resistance of the object; by V its speed; by L its size, or some linear dimension; by ρ the density of the fluid; by μ the viscosity of the fluid; by C the compressibility of the fluid; and by g the acceleration of gravity. In addition there are certain ratios present which I will denote by r_1, r_2 , etc. These ratios express certain physical facts, such as aspect ratio of an airfoil, its angle of attack, etc. They are all independent of size.

It may be that the quantities enumerated above do not comprise all of the quantities we should consider, but they do comprise the most obvious ones and are sufficient in number to illustrate the point desired to be made. Now all these quantities can be expressed in terms of three units, and we will choose the simplest and most commonly used units, namely, those of mass, m ; length, l ; and time, t . Each of these physical quantities also has well-known dimensions. The table below gives the quantities enumerated above and their dimensions in m, l , and t .

Quantities involved		Dimensions in m, l , and t
R	Resistance.....	$m l t^{-2}$
V	Speed.....	$l t^{-1}$
L	Size.....	l
ρ	Density of fluid.....	$m l^{-3}$
μ	Viscosity of fluid.....	$m l^{-1} t^{-1}$
C	Compressibility of fluid.....	$m^{-1} l^{-1} t^2$
g	Acceleration of gravity.....	$l t^{-2}$
r_1, r_2 , etc.	Ratios.....	Dimensionless.

Now if the quantities above have a relation connecting them it may be written as follows:

$$F(L, \rho, V, R, \mu, C, g, r_1, r_2, \dots) = 0 \quad (1)$$

This equation, of course, teaches us nothing except that there is some relation between the seven physical quantities entering the case. Now let us choose three of the above quantities (this is because we have three units to express them all), and, instead of writing the relation symbolically between the seven simple quantities, let us use the following, involving the seven quantities in four compound quantities or variables:

$$F(L^a \rho^b V^c R, L^d \rho^e V^f \mu, L^g \rho^h V^k C, L^l \rho^m V^n g, r_1, r_2, \dots) = 0 \quad (2)$$

By the principle of dimensional homogeneity, since the physical relations or facts expressed by the above do not change with change of units, the compound variables or quantities above must be dimensionless; that is, of zero dimensions. By expressing their dimensions in terms of the dimensions of the three fundamental units, we have for each quantity three equations to determine the exponents a, b, c , etc. Let us take the first quantity. Our dimensional equation is

$$\begin{aligned} L^a \rho^b V^c R &= l^a m^b l^{-3b} l^c t^{-c} m l t^{-2} \\ &= l^{a-3b+c+1} m^{b+1} t^{-c-2} \end{aligned}$$

In order that the expression may be dimensionless, we must have the index of l , for instance, equal to zero; that is, $a-3b+c+1$ equal to zero; similarly, the indices of m and t must equal zero. This gives us the three equations below, whose solution is obvious:

$$\left\{ \begin{array}{l} a-3b+c+1=0 \\ b+1=0 \\ -c-2=0 \end{array} \right\} \text{whence } \begin{array}{l} a=-2 \\ b=-1 \\ c=-2 \end{array}$$

So, our first quantity is $\frac{R}{\rho L^2 V^2}$

Proceeding to the second quantity and treating it in exactly the same manner, we have the following:

$$\begin{aligned} L^d \rho^e V^f \mu &= l^d m^e t^{-3e} l^f t^{-f} m l^{-1} t^{-1} \\ &= l^{d-3e+f-1} m^{e+1} t^{-f-1} \end{aligned}$$

Whence—

$$\begin{aligned} d-3e+f-1 &= 0 \\ e+1 &= 0 \\ f-1 &= 0 \\ d &= -1 \\ e &= -1 \\ f &= -1 \end{aligned}$$

Then our second expression is $\frac{\mu}{L \rho V}$. Of course in practice it makes no difference whether we use the above expression or its reciprocal. The ratio $\frac{\mu}{\rho}$ is a quantity a good deal used in physical parlance, called the kinematic viscosity, and denoted by ν . So our second variable will be $\frac{\nu}{L V}$.

Proceeding in just the same manner for the third and fourth quantities we finally reduce the general equation to

$$F_1\left(\frac{R}{\rho L^2 V^2}, \frac{\nu}{L V}, \rho L^2 V^2 C \frac{Lg}{V^2}, r_1, r_2, \dots\right) = 0 \quad (3)$$

Now $\rho L^2 C$ has of course the dimensions of $\frac{1}{V^2}$, and since the velocity of sound in air is proportional to $\frac{1}{\sqrt{\rho C}}$, if we denote by V_s the velocity of sound in air we may use instead of the variable $\rho L^2 V^2 C$ the variable $\frac{V^2}{V_s^2}$.

Now we can solve the above symbolically for any one of the compound variables. Solving for the first, we have

$$\frac{R}{\rho L^2 V^2} = F_3\left(\frac{\nu}{L V}, \frac{V^2}{V_s^2}, \frac{Lg}{V^2}, r_1, r_2, \dots\right)$$

Since we are interested primarily in the resistance, R , let us transform the above as below:

$$R = \rho L^2 V^2 \times F_3\left(\frac{\nu}{L V}, \frac{V^2}{V_s^2}, \frac{Lg}{V^2}, r_1, r_2, \dots\right) \quad (4)$$

The ratios r_1, r_2 , etc., express such things as aspect ratio, angle of attack, etc., and hence are obviously the same for the model as for the full-sized object, so that for purposes of comparison between model and full-sized object they affect the case only as constants or fixed coefficients, to be determined by experiment or some other independent method, and can be eliminated from the equation above. This reduces us finally to the general equation:

$$R = \rho L^2 V^2 F_3\left(\frac{\nu}{L V}, \frac{V^2}{V_s^2}, \frac{Lg}{V^2}\right) \quad (5)$$

This, then, is a relation which follows if all of the factors which we originally assumed enter into the case and affect our results. We do not know whether, as a matter of fact, all these factors do affect them as indicated by the general expression for R above. But, obviously, if all of the factors enumerated materially affect our results, producing the preceding equation (5), model experiments are of no value for predicting the performance of the full-sized object. In the model experiment, we make an object differing in scale from the full-sized object, and test it at a speed different from that of the full-sized object. If this method is to be of value in

practice, as a general thing models should be smaller and tested at a lower speed than for the full-sized object. From equation (5) above, however, we see, considering the first combined variable, which we must have constant in proceeding from model to full-sized object, that LV must be constant, since we know that ν is practically constant for standard air. Considering the second term, however, since the velocity of sound in air is constant, if $\frac{V^2}{V_s^2}$ is to be constant V must be constant. Considering the third term, g is constant, and if $\frac{Lg}{V^2}$ is to be constant we must have $\frac{L}{V^2}$ constant. These three requirements evidently reduce to the single one, namely, that neither L nor V can change. In other words, we can not use the model and obtain results for the full-sized object.

However, the equation (5) does not necessarily apply to the case unless it is confirmed by theoretical demonstration, experience, or practical tests. We do not know that as a matter of fact, the compound quantities which we originally considered as possibly affecting the case do all affect it. Suppose none of these quantities has any effect. We then have the exceedingly simple formula

$$R = \rho L^2 V^2 \text{ times a coefficient}$$

If this expresses the facts, a single experiment at a single speed of a model gives us complete information on the resistance at all speeds for all sizes of similar objects.

There is a theoretical basis for regarding this as a basic expression for resistance, the departures from it being, if appreciable, of secondary importance. If the disturbance of a fluid by an object moving through it, or, what is simpler to grasp, if the lines of flow of a fluid past a submerged object do not change with speed, then all forces vary as the square of the speed. For any force is measured by the momentum generated in unit time in the opposite direction, and, taking momentum at such a distance that pressure is not affected, the momentum generated in unit time is proportional to the square of the velocity. Similarly, if the lines of flow are similar as we change size, the momentum generated must vary as L^2 . From consideration of a perfect nonviscous fluid we reach similar conclusions, but, as it happens, in a theoretical perfect fluid objects have theoretically no resistance. Concluding, then, that the expression

$$R = \rho L^2 V^2 \text{ times a coefficient}$$

is a correct first approximation, let us see what we can do to reach a closer approximation.

Suppose that only one of the terms of F_3 in (5) is significant, the rest having no bearing. If the first term is the only significant one, we have

$$R = \rho L^2 V^2 F_3 \left(\frac{\nu}{LV} \right)$$

Similarly, if the second and third terms are the only significant ones, we have

$$R = \rho L^2 V^2 F_3 \left(\frac{V^2}{V_s^2} \right)$$

$$R = \rho L^2 V^2 F_3 \left(\frac{Lg}{V^2} \right)$$

Now, it is obvious that if only one term is significant, we may or may not have a possible basis for model experiment, depending upon the nature of the term. Consider first the expression

$$R = \rho L^2 V^2 F_3 \left(\frac{\nu}{LV} \right)$$

Here the requirement is that $\frac{\nu}{LV}$ should be constant, or, what is the same thing, that $\frac{LV}{\nu}$

should be constant. This results in the undesirable condition that if ν is constant LV must be constant as we pass from model to full-sized object, so that the smaller the model the higher the speed at which it must be tested. This is not a very desirable condition.

Consider now the second requirement:

$$R = \rho L^2 V^2 F_3 \left(\frac{V^2}{V_s^2} \right)$$

If $\frac{V^2}{V_s^2}$ is constant, since V_s itself is constant, V must be constant, and we can not use a low-speed model.

Consider now the third condition. Here our requirement is that $\frac{Lg}{V^2}$ is constant. This is the form found so useful in testing ships' models. The relation that speeds shall be as the square root of linear dimensions results in the test speed for the model being low, so that tests can be easily made. Evidently, however, for a body completely submerged in and surrounded by a fluid, the action of gravity can have practically no effect until the proposed speeds approach the point where vacuua are formed in the fluid. Hence we can confidently eliminate from our general equation above the variable $\frac{Lg}{V^2}$ as the one to govern our second approximation.

Consider next the variable $\frac{V^2}{V_s^2}$. Practically all the speeds with which we are concerned in airplane work, except some propeller speeds, are far below the velocity of sound through air, and there is little reason to believe that the compressibility of the air has a material effect, because the compression is so small. Also, experiments with projectiles indicate the same conclusion. Hence we can eliminate the second term as the one that we must keep when we seek a second approximation. When we come to the first term, however, the case is different. We know that air has viscosity, and we know that the viscosity must have some action at all speeds. Hence the first term can not be argued away on general principles. Also, it may be remarked in passing that the expression

$$R = \rho L^2 V^2 F_3 \left(\frac{\nu}{LV} \right)$$

can be derived independently of considerations of dimensional homogeneity from the equations of motion of a viscous fluid. However, these equations of motion necessarily assume in the first place that there is no other factor, such as compressibility, gravity, etc., involved. We might have originally assumed some more physical quantities present and affecting matters such as nature of surface, or sizes of turbulent vortices in the wind tunnel, but we seem to be restricted to one variable in our F_3 function if we are to profit by model experiments and the viscosity variable seems the one we should choose. The wisdom, or otherwise, of the choice will be shown if model experiments in accordance with the formula do or do not predict full scale performance.

Having then reduced our original broad formula to

$$R = \rho L^2 V^2 F_3 \left(\frac{LV}{\nu} \right) \quad (6)$$

involving the density, the size, the speed, and some unknown function of $\frac{LV}{\nu}$, the well-known Reynolds Number, we need to form some conception of the effect of Reynolds Number, commonly called the scale effect. While we do not know the form of the function, we do know for the flow of water, oil, and air in pipes the relative experimental values. The original wonderful experiments by Reynolds have been repeated and amplified by others since 1880, and it seems established that at low speeds where the fluid flows smoothly F_3 has one set of values, and at high speeds when the motion is completely turbulent there is another well-defined set of

values, while for intermediate speeds values are rather indeterminate. Wind tunnel investigations on such objects as cylindrical wires, struts, and streamline wires show that the resistance departs appreciably from the law of the square with variation of Reynolds Number.

When we come to such objects as an airplane, however, we have difficulty with the ordinary wind tunnel. For constant Reynolds Number to test a model, say, one-twentieth scale, would require wind tunnel speed 20 times the actual flying speed, and there are no wind tunnels that can come in sight of this performance. Such speeds would be greater than the velocity of sound. There appears to be only one practicable solution of the difficulty, namely, the use of a testing tunnel where we vary the density of the air and hence the value of ν .

The kinematic viscosity coefficient ν for air varies inversely as the pressure, and decreases with temperature according to a somewhat complicated relation. Table I below gives numerical values when the unit of length is the centimeter and the unit of time the second.

TABLE I
KINEMATIC VISCOSITY COEFFICIENTS ν IN $\text{cm}^2/\text{sec.}$

Temperature, centi- grade	Pressure in atmospheres				
	1/10	1	5	10	20
50	1.284	0.1284	0.02568	0.01284	0.00642
40	1.292	.1292	.02584	.01292	.00646
30	1.300	.1300	.02600	.01300	.00650
20	1.308	.1308	.02616	.01308	.00654
10	1.318	.1318	.02636	.01318	.00659
0	1.329	.1329	.02658	.01329	.00665
-10	1.340	.1340	.02680	.01340	.00670
-20	1.351	.1351	.02702	.01351	.00676
-30	1.364	.1364	.02728	.01364	.00682
-40	1.378	.1378	.02756	.01378	.00689
-50	1.392	.1392	.02784	.01392	.00696

The variable-density wind tunnel of the National Advisory Committee for Aeronautics, as originally suggested by Doctor Munk of our staff, was described to the society two years ago, and a few sample results given. A good deal of experience has been had since then with the appliance. One lesson of experience has been that when we are working under a pressure of 20 atmospheres it takes but a small electrical spark to kindle a substantial fire. However, these little practical difficulties have been overcome, and experience in testing a number of different airfoils, etc., indicates that this apparatus, or the equivalent, is essential if we are to make a thoroughly reliable second approximation to the performance of an airplane from model tests.

Reynolds Number $\frac{LV}{\nu}$ is a compound ratio whose numerical value in the case of any given object depends upon the ratios between the actual values of LV and ν and their unit values. Unfortunately, each type of object has its own series of Reynolds Numbers because as a rule the values of L are not comparable for dissimilar objects. Thus for an airplane wing we naturally use for L in Reynolds Number the length of the chord. For an airship we would use the length or the diameter or any linear function of the two. But L for the airship would not be comparable with L for the airplane.

Considering airplanes as they are, using the chord of the wing in inches as L , and speeds in statute miles per hour, the Reynolds Numbers come out fairly large. Thus for an airplane of 5-foot chord, at 100 miles per hour in a normal atmosphere, the Reynolds Number will be some 4,800,000. For its model of 6-inch chord, in a wind tunnel at 100 miles per hour with normal air, the Reynolds Number will be 480,000.

Attention is invited now to figures 1 to 3, giving in condensed form results of recent tests of three airfoils of well-known form in the variable-density wind tunnel. Necessary data as to the conditions and the airfoil section to which they apply are shown on each figure. Results are plotted as curves of lift and drag coefficients as ordinates over angles of attack— α —as abscissae, following the standard practice of the United States National Advisory Committee

for Aeronautics. Figure 1 shows results for an American section, U. S. A. 27; Figure 2 shows results for a British section, R. A. F. 15; Figure 3 shows results for a German section, Göttingen 387. It happens that these three typify the medium, the thin, and the thick sections.

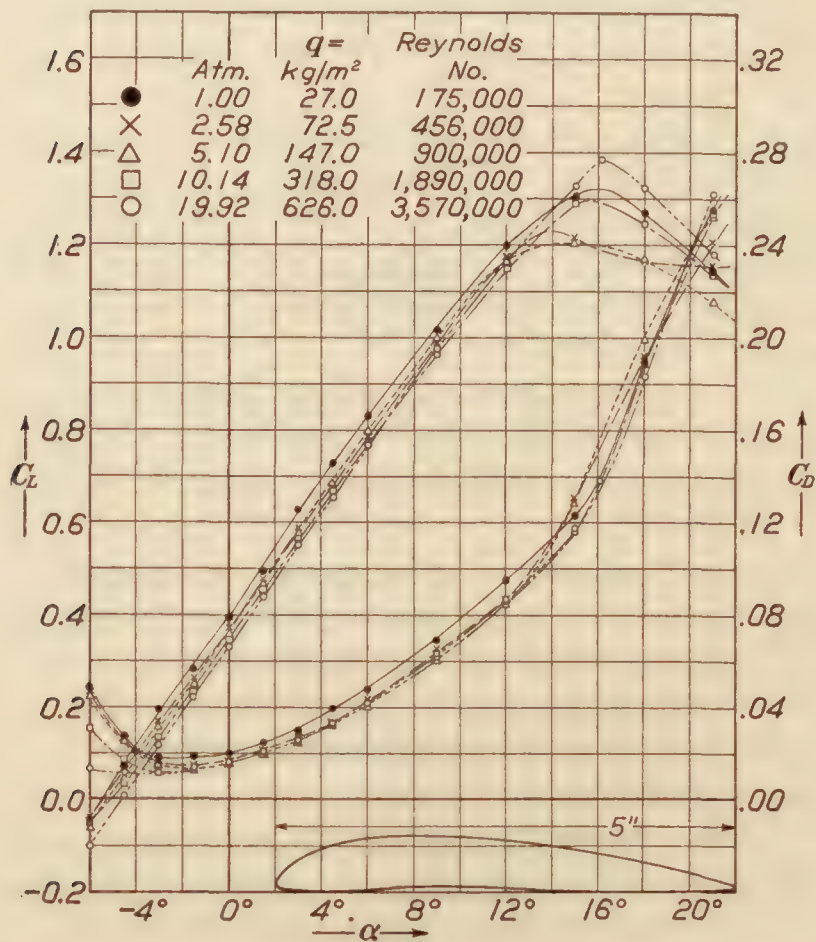


FIG. 1.—Lift and drag characteristics of USA 27 as tested in the Variable Density Wind Tunnel

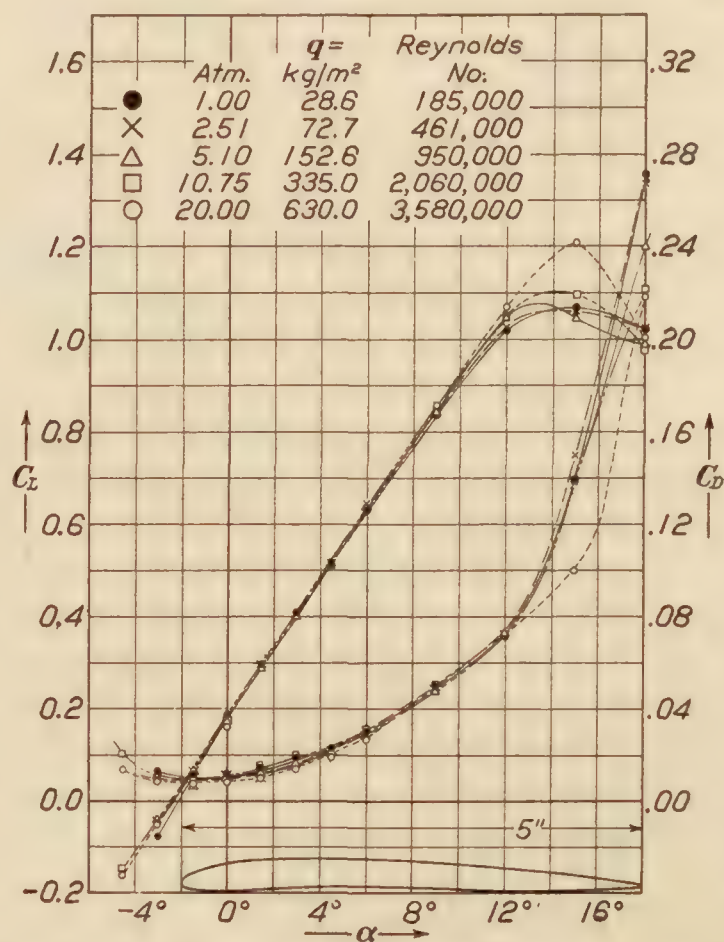


FIG. 2.—Lift and drag characteristics of RAF 15 as tested in the Variable Density Wind Tunnel

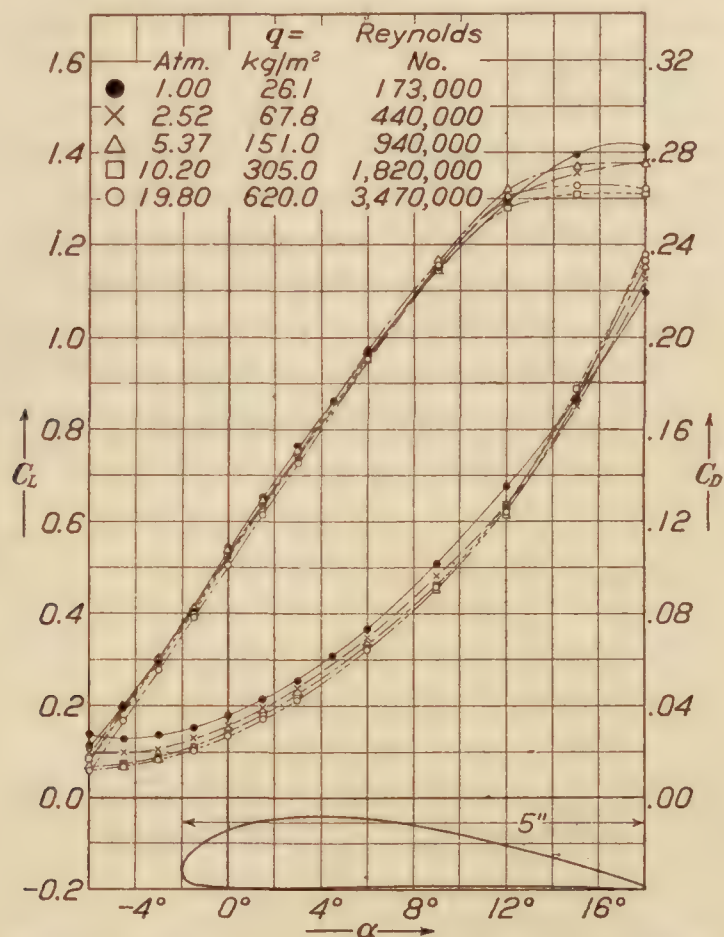


FIG. 3.—Lift and drag characteristics of Göttingen 387 as tested in the Variable Density Wind Tunnel

Ignoring minor eccentricities due to accidental causes, unavoidable experimental error, etc., these curves seem to warrant a few broad conclusions, which, by the way are in agreement with other results too numerous to include.

In the first place, the scale effect appears to have more influence upon the drag than upon the lift. This may be explained upon theoretical grounds.

In the second place, the scale effect increases more and more slowly as the Reynolds Number increases, so that conclusions drawn from experiments with airfoils within the Reynolds Number range of ordinary wind tunnels can not safely be extended to much larger Reynolds Numbers.

In third place, the consistency of the results gives us reason to think that for present-day airplanes we are justified in ignoring the effect of other factors than Reynolds Number in reaching our second approximation to aerodynamic properties of airfoils.

In the fourth place, the thin airfoil appears to show less scale effect than the thick airfoil.

In the fifth place, so far as airfoil action is concerned, the scale effect is, after all, secondary, though by no means negligible when we undertake to estimate closely.

The comments above apply only to airfoils. They do not necessarily apply to wires, struts, etc. Such appendages can be tested separately in the ordinary wind tunnel at Reynolds Numbers much closer to the numbers on the full-sized airplane than is possible with the airplane structure proper.

When we enter the somewhat vexed field of aircraft propellers, model experiment is unquestionably our surest guide. Here, as in all other cases where we utilize model experiment, we must finally assure ourselves by experience or full-scale experiment that we have a safe law of comparison, but the difficulty of accurate full-scale propeller tests in free flight renders it almost essential for the present that we investigate laws of propeller action by model experiment.

This has been done with good results in the marine field and air propellers are even more favorably circumstanced. For instance, for propellers in water we can not apply our law of comparison when cavitation is present. Cavitation does not trouble air propellers as yet. The propeller driving a vessel, assuming the atmospheric pressure as equivalent to 34 feet of water, is working in an inelastic fluid under a total head to the center of propeller of, say, from 35 to 60 feet. The airplane propeller is working in an elastic fluid under a total head, when near the ground, of something like 6 miles. This not only eliminates cavitation but enables us to adopt efficient blade sections that would be impossible in water. The airplane propeller designer is fortunate in this fact and in the further fact that he can use two-bladed propellers. These are capable of more efficiency than three or four bladed propellers, but can seldom be used for marine propellers because when working in an irregular stream, as they must at the stern of a ship, they are liable to cause excessive vibration of the ship.

Models in water act very much as in air, and experiments with thin, narrow two-bladed propellers in water show efficiencies fully as good as those of models of airplane propellers. Table II below gives maximum efficiencies in water of some two-bladed model propellers. They had ogival blade sections, straight faces of uniform pitch, and circular arcs for backs, the edges being sharp, not rounded.

TABLE II
MAXIMUM EFFICIENCIES OF 2-BLADED 16-INCH MODEL PROPELLERS IN WATER

Camber ratio at 0.75 radius	Mean width ratio	Pitch ratios					
		0.4	0.6	0.8	1.0	1.2	1.5
		Maximum efficiencies					
0.1241	0.075				0.85		
.0744	.125				.84		
.0465	.200	0.58	0.71	0.78	.82	0.83	0.84
.0338	.275				.79		

From "Some Results of Tests of Model Propellers," by A. V. Curtis and L. F. Hewins, *Transactions Society of Naval Architects and Marine Engineers*, Vol. 13, 1905.

The airplane propeller designer labors under one disadvantage. There is no doubt that as propeller tip speeds in air approach the velocity of sound, we may expect radical departures from the laws of action at lower speeds. That is a complication I shall not attempt to unravel.

Before taking up the model experiment end of propeller action, it may be as well to take up one general consideration.

Since thrust of a propeller is proportional to the sternward momentum per second generated by its action upon the fluid in which it works, it follows that there must be a certain energy carried off in the fluid to which velocity is communicated. Hence, no propeller can show an efficiency of 100 per cent, and the actual efficiency of an ideal propeller at a given speed of advance must always diminish as its thrust increases. Following the treatment proposed by McEntee in 1906 for propellers operating in water, we can gain some idea of limits in air.

Suppose we have an ideal frictionless propelling apparatus which takes hold of the air and discharges it directly aft without change of pressure and with uniform absolute velocity u feet per second, the velocity of advance of our ideal apparatus with reference to undisturbed air being v feet per second. Then, if A denotes the area in square feet of the slipstream, the mass of the air acted upon per second is

$$\left(\frac{w}{g}\right) A (v+u).$$

The thrust T in pounds from Newton's third law is equal to the sternward momentum generated per second, or

$$T = \left(\frac{w}{g}\right) A (v+u) u$$

Useful work equals

$$Tv = \left(\frac{w}{g}\right) A (v+u) uv$$

The lost work, or kinetic energy, of the air discharged equals

$$\left(\frac{w}{g}\right) A (v+u) \left(\frac{u^2}{2}\right)$$

Whence gross work equals

$$\left(\frac{w}{g}\right) A (v+u) uv + \left(\frac{w}{g}\right) A (v+u) \left(\frac{u^2}{2}\right)$$

Efficiency e equals

$$\frac{\text{Useful work}}{\text{Gross work}} = \left(\frac{v}{v + \frac{u}{2}}\right)$$

If we solve for u in the expression for thrust, we have

$$u = \sqrt{\left(\frac{v^2}{4} + \frac{gT}{wA}\right)} - \frac{v}{2}$$

Substituting in the expression for efficiency, we have

$$e = \frac{4}{\left\{ 3 + \sqrt{\left(\frac{4g}{w} \frac{T}{Av^2} + 1\right)} \right\}}$$

This, then is the general formula for the efficiency of an ideal frictionless propelling apparatus, discharging the fluid passing through it without increase of pressure and accompanying loss of efficiency.

Applying to an air propeller of diameter d feet, substitute $\frac{\pi d^2}{4}$ for A . Also give g its standard value of 32.174 foot/seconds², w the value for standard air of 0.07651 pound/feet³, and express v in miles per hour V instead of feet per second.

When this is done our formula for air becomes

$$e = \frac{4}{\left\{ 3 + \sqrt{\left[\frac{(16 \times 32.174)}{(0.07651 \times 2.15\pi)} \frac{T}{d^2 V^2} + 1 \right]} \right\}} = \frac{4}{\left\{ 3 + \sqrt{\left(\frac{99.56 T}{d^2 V^2} + 1 \right)} \right\}}$$

Figure 4 shows contours of ideal efficiency derived from the above equations plotted upon values of d and $\frac{T}{V^2}$.

It is seen that curves of constant efficiency are parabolas, with values of $\frac{T}{V^2}$ as ordinates and values of diameter as abscissae; also, once we have fixed the diameter and the value of $\frac{T}{V^2}$ we fix the efficiency. It is obvious also that if, for a given diameter, we increase thrust without changing speed, or if, for a given diameter, we decrease speed without changing thrust, the efficiency necessarily falls off.

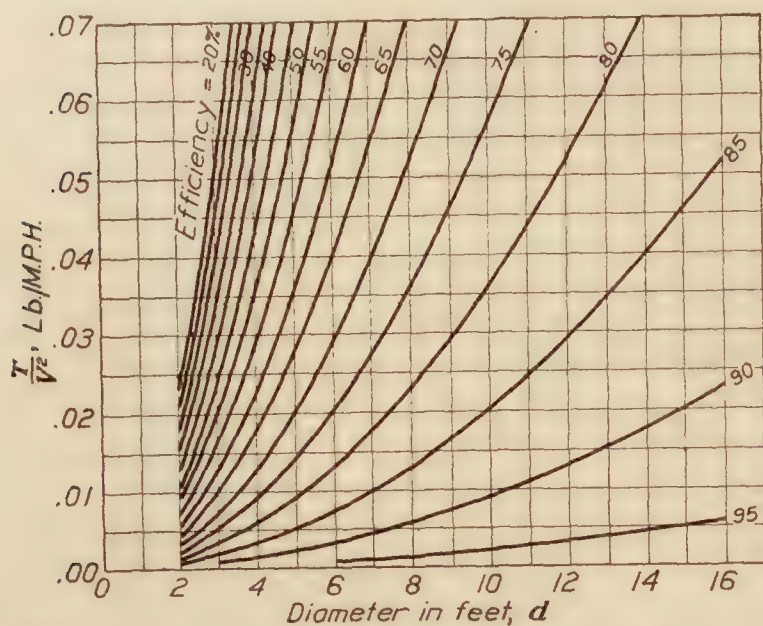


FIG. 4.—Ideal propeller efficiency in air as affected by thrust in pounds— T , speed in M. P. H.— V , and diameter in feet— d

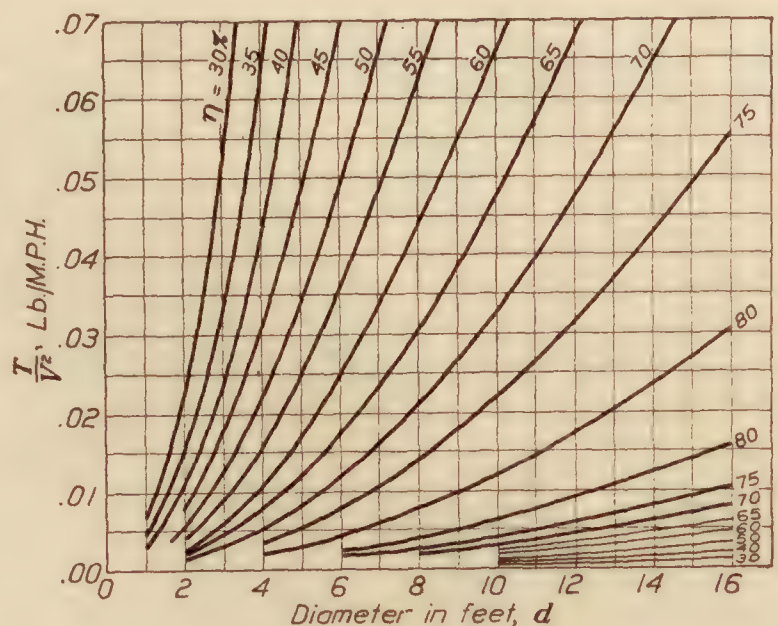


FIG. 5.—Actual propeller, efficiency in air derived from model propeller tests—propeller E Table III

While the above conclusions can be legitimately drawn from Figure 4, we must not forget that this refers to an ideal propeller of the best possible efficiency. Actual propellers in operation lose not only by the energy carried off in the wake, but by their friction and the energy due to transverse motion in the wake, both tending to reduce efficiency. If we assume a law of comparison, which will be discussed later, we can, from tests of a model propeller, draw a diagram similar to Figure 4, covering the performance of all propellers similar to the model. This is done in Figure 5 for a propeller of 0.9 pitch ratio, propeller "E" of Table III tested by Doctor Durand. It will be observed that in its general features Figure 5 corresponds fairly well with the ideal diagram of Figure 4. However, the efficiency contours, instead of increasing indefinitely as we increase the diameter and decrease the values of $\frac{T}{V^2}$, reach a maximum, and then for smaller values of $\frac{T}{V^2}$ the efficiency falls off very rapidly. Above the maximum line the agreement with the ideal diagram is better. We still have the feature that the efficiency of this family of propellers is dependent upon the diameter and the value of $\frac{T}{V^2}$. If in level flight we are operating above the parabola of maximum efficiency and undertake to climb, the value of $\frac{T}{V^2}$ necessarily increases and the efficiency necessarily falls off. If we are operating in level flight in the region below the contour of maximum efficiency and then

undertake to climb, the efficiency increases for a time and then falls off as before. In any case, however, the efficiency of a given propeller varies with the flight conditions.

A propeller is an object moving through air and our general equation (4) applies. Rewriting this with T to denote thrust instead of R to denote any resistance, and diameter D in place of L , we have

$$T = \rho V^2 D^2 F_3 \left(\frac{\nu}{DV}, \frac{V^2}{V_s^2}, \frac{Dg}{V^2}, r_1, r_2, \dots \right) \quad (4)$$

As before, we can confidently eliminate the gravity variable $\frac{Dg}{V^2}$. When it comes to the compression variable $\frac{V^2}{V_s^2}$, we are not upon such sure ground as for the airplane, because tip speeds are much greater than airplane speeds. Probably some types of blade section can approach much more closely than others the velocity of sound in the air without it being necessary to take account of the compression variable. When that does become necessary the problem can be met by testing propeller models in high speed wind tunnels, V being airplane speed. It would seem from this point of view that even now model propellers should be tested at full speed. Eliminating the compression variable as not yet important, we come to the same general expression as for the airplane or

$$T = \rho V^2 D^2 F_3 \left(\frac{\nu}{DV} \right)$$

Here we meet the same Reynolds Number complication. Now, we have seen in dealing with airfoils that the scale effect correction for them was secondary. We know, too, that in propeller action, where a blade is attacking air already somewhat disturbed by its previous passage or the passage of another blade, we may expect great turbulence in the action and we know that the greater the turbulence the less the scale effect correction for viscosity.

So we conclude that if we drop the Reynolds Number variable we have left a first approximation sufficiently close to exactness for practical present-day engineering purposes.

This leads us to the simple expression

$$T = \rho V^2 D^2 F_3 (r_1, r_2, \dots)$$

If this were exact, a model of any size at any speed would tell us all we need know, but bearing in mind that our expression is approximate and the nature of the quantities ignored, we should make our models as large as possible and test them at as high a speed as possible.

The quantities r_1, r_2 , etc., are characteristic ratios and it is very important if we are to utilize model propeller tests to best advantage that we use ratios that are truly and adequately characteristic. Systematic treatment is necessary here. Much progress has been made in connection with aeronautic propellers by regarding their blades as composed of sections of airfoils, and this is essentially a fruitful method of procedure in our search for more efficient forms. It is interesting to note that the underlying idea is the same as that of Mr. William Froude, when for the marine propeller, in 1878, he put forward his blade theory, in which the propeller blades were regarded as made up of plane elements advancing through the water. Mr. Froude at that time said, with much justice:

No theoretical treatment of the action of an actual screw can be sound which does not incorporate and mainly rest on the principles embodied in the treatment of the problem of the plane, and, indeed, the character of the results must, in their most essential features, be the same in both cases.

The fundamental difficulty with the Froude blade theory was that propeller blades are not a plane of no thickness. This fact has been fully recognized by aeronautic designers in treating them as made up of airfoil elements, but after all the model propeller and the full-sized propeller must each be treated in the end as a whole, and our ratios must be based upon that fact.

It is obviously desirable to have diameter appear in all ratios if possible, since diameter is our basic dimension.

The first thing we need to consider is the most desirable ratio by which to express the obliquities of the blades, or the angles which they make with the axis of the propeller. This is sometimes done by stating the angles, but the best plan appears to be to adhere to the idea of pitch. This tends to become absurd in propellers with blades relatively as thick as those used on airplanes, but after all it is always possible at any section to establish a line making a definite angle with the axis. If the propeller has a working face with any material portion of it flat or straight in section on the driving face, this is naturally the line used to express pitch. However that may be, for the family of propellers derived from a given model, the ratio between pitch and diameter is always constant, and as a rule the whole family may be characterized by the extreme pitch ratio. This is about the simplest quantity we can use which gives an idea of the general features of the propeller with reference to the pitch, or blade obliquity if we prefer that expression. Then one of our ratios is the ratio between pitch and diameter, denoted by a .

We need something expressing relative blade width. Aspect ratio will do it, but there seems no necessity for departing from what is frequently called in marine propellers the mean width ratio, namely, the ratio between the mean or average width of the blade and the diameter. If we were always dealing with blades of the same developed outline, it would be simpler and better to use the ratio between the maximum width, a thing we need always to know and use, and the diameter. This would quite well characterize the propeller, but does not seem to be quite so good for universal use in view of variations in blade outline.

We come now to the most difficult ratio to express in practice. We need something to characterize the blade thickness. If propellers all had radially straight faces and straight backs, the simplest and obvious plan would be to extend the line of the face to the axis, the line of the back at maximum thickness to the axis, and express the characteristics of the propeller as regards blade thickness by the ratio between the intercept on the axis thus obtained and the diameter. This is a method which has come into a good deal of use for marine propellers of late years, but the backs of aeronautical propellers vary so much that it is doubtful if we are yet ready to adopt this as a standard ratio. I suggest tentatively for this last ratio the camber ratio at three-fourths of the radius.

It is now necessary to consider what to do with results of model tests.

These results, such as curves of thrust and torque or dimensionless coefficients derived from them, including curves of efficiency of propeller, are usually plotted initially upon the dimensionless quantity $\frac{V}{nD}$ when V is speed of advance of the propeller with reference to undisturbed air in feet per second, n denotes revolutions per second, and D is diameter of the propeller in feet. Now $\frac{V}{nD}$ is a natural coefficient and excellent as a basic variable when we are dealing with one propeller, but when dealing with systematic propeller research and making diagrams for design purposes it is somewhat lacking. For a single propeller, when we plot upon $\frac{V}{nD}$ we are virtually plotting upon the slip ratio s , since if a denote pitch ratio $\frac{V}{nD} = a(1 - s)$.

The question of the basic variable to be used in plotting experimental data for design purposes is a very important one and worthy of a little examination. In the first place this basic variable must be dimensionless since we wish to use model results for dealing with full-sized propellers. There are any number of dimensionless functions available and they are readily converted one to another.

In the second place, looking at the matter from the design point of view, our basic variable should take account of or involve all the quantities known or assumed upon which a propeller design depends. Here we meet the fact that we do not necessarily base a propeller design always upon the same quantities. However, considering airplane, propeller, and motor separately, let us see what quantities we have.

For the airplane we have speed, drag or resistance, and effective or useful power used in overcoming the drag at the speed of the airplane. For the propeller we have speed, revolutions, torque, thrust, power absorbed by torque and power delivered by thrust. For the motor we have revolutions, torque, and power delivered to and absorbed by the propeller.

Now, the propeller is the middleman, as it were, and may be considered as driving the airplane or as absorbing the motor power. From the first point of view we need a basic variable involving speed, revolutions, and either thrust or power delivered by thrust. From the second point of view our basic variable should involve speed, revolutions, and either torque or power absorbed by the propeller.

It appears then that to meet all contingencies we really need two basic variables and obviously they should be readily convertible or connected by a simple relation. This indicates that our two basic variables should both involve speed and revolutions and then one should involve torque and the other thrust, or one should involve power absorbed by the propeller and the other power delivered by the propeller or useful power. Each set has its advantages but the set involving power seems preferable for two reasons. When we deal with motors we normally deal with power not torque, and the relation between power delivered to and delivered by the propeller is very simple, being the efficiency of the propeller with no intervening factor.

Having settled upon the quantities to enter into our basic variable, its form is readily determined by applying the principle of dimensional homogeneity. Consider the variable $P^x R^y V^z \rho$ where P denotes power; R , revolutions; and V , speed; and the exponents x , y , and z are to be determined. The dimensions of P are $m l^2 t^{-3}$; of R , t^{-1} ; and of V , lt^{-1} . Then dimensionally $P^x R^y V^z = m^x l^{2x} t^{-3x} t^{-y} l^z t^{-z} l^{-z}$.

$$\begin{array}{rcl} X+1=0 & 2X+Z-3=0 & -3X-Y-Z=0 \\ X=-1 & Y=-2 & Z=5 \end{array}$$

Our expression is $\frac{\rho V^5}{PR^2}$. This or the equivalent is well known and has been used more or less for many years. Of course we can use the reciprocal or any power. For marine propellers a very convenient expression is

$$1/\sqrt{\left(\frac{\rho V^5}{PR^2}\right)}$$

or calling

$$\rho = 1, \quad \frac{(R\sqrt{P})}{V^{2.5}}$$

For aeronautic work we need to keep ρ and from a practical point of view there seem to be some advantages, as in marine work, in using expressions where R appears in the numerator and in the first power.

These considerations lead us to the expressions below for basic variables.

Based on motor power

$$\frac{R\sqrt{P}}{\rho^{.5} V_m^{2.5}}$$

Based on useful power

$$\frac{R\sqrt{U}}{\rho^{.5} V_m^{2.5}}$$

Now we must select the essential things to be plotted upon our basic variable. Efficiency is one, of course. The other quantity that we need is some dimensionless function involving diameter—our primary dimension—and preferably it should involve diameter in the first power and in the numerator.

Such a function is $\frac{DR}{V}$, which we may call δ . When we come to plot efficiency and δ upon our basic variable we find it desirable to use logarithmic scales to keep curves within manageable limits.

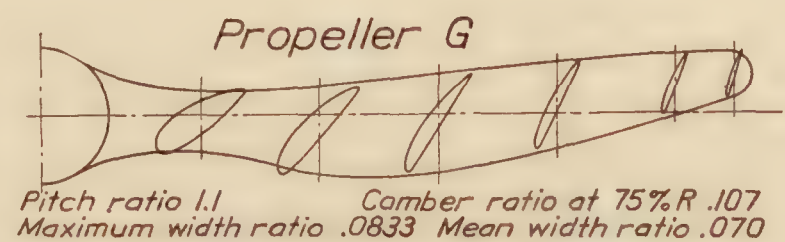
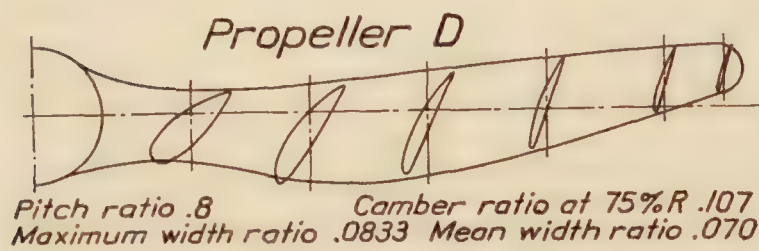
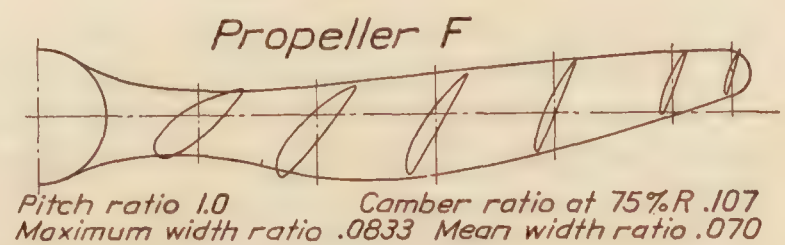
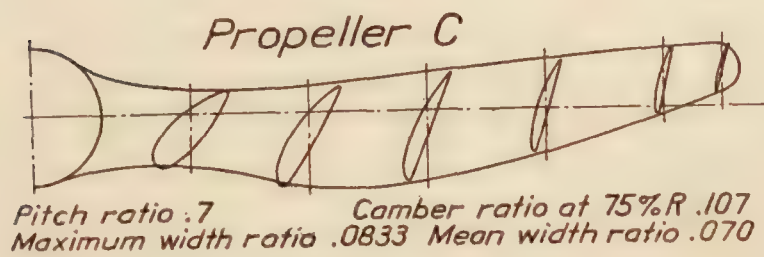
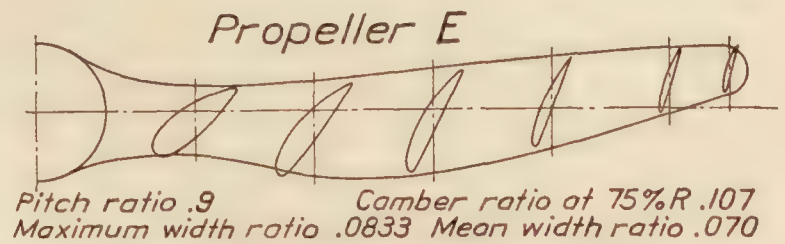
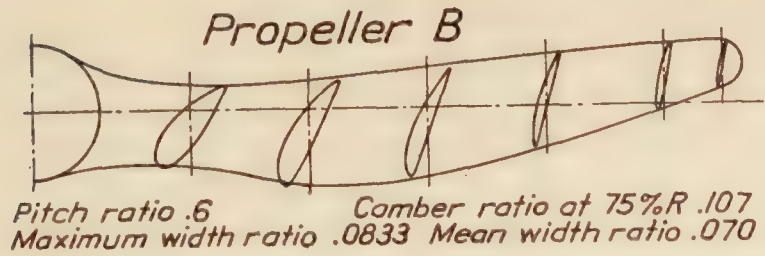
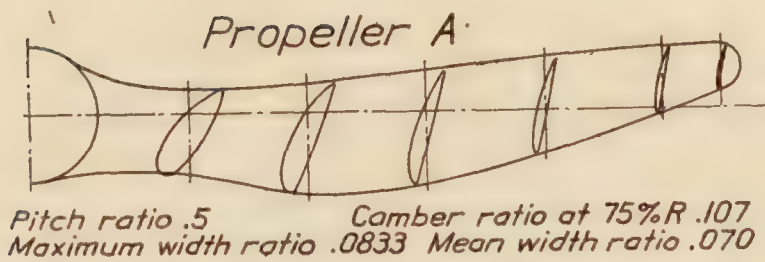


FIG. 6

FIG. 7

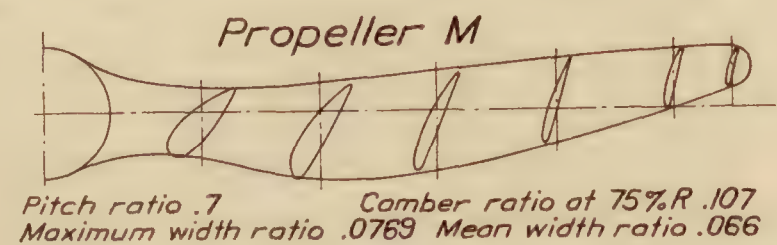
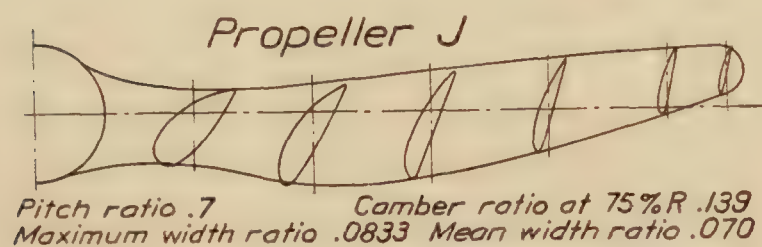
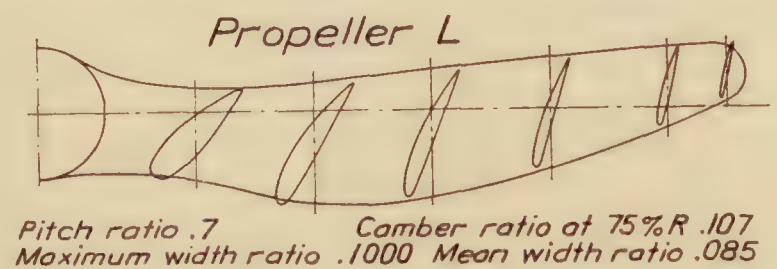
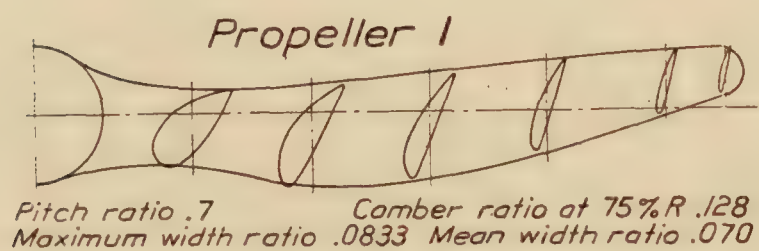
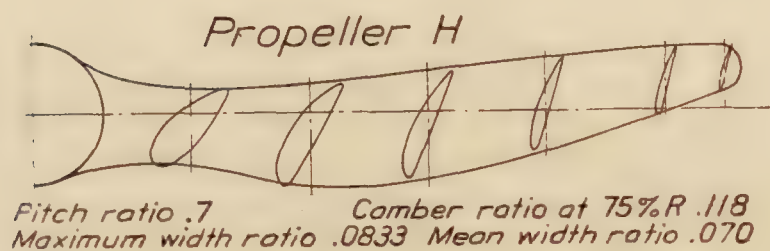


FIG. 8

FIG. 9

The most fruitful model propeller experiments are those made with series of propellers changing one variable at a time. The field is too vast to cover fully in this way, but experiment soon shows that some of our variables are primary in their effects, while others are rather secondary, and may be mainly taken account of in a first approximation without special experiments. Experiments made with a group of propeller models varying systematically were recently completed by Doctor Durand for the United States National Advisory Committee for Aeronautics, and illustrate the points referred to above. Thirteen propellers, "A" to "M," were tested. They are shown by projection and sections in Figures 6 to 9 inclusive, and Table III below gives their essential characteristics.

TABLE III
MODEL PROPELLERS TESTED BY DURAND

Designation	Pitch ratio	Maximum width ratio	Mean width ratio	Camber ratio at 0.75 radius
A	0.5	0.0833	0.070	0.107
B	.6	.0833	.070	.107
C	.7	.0833	.070	.107
D	.8	.0833	.070	.107
E	.9	.0833	.070	.107
F	1.0	.0833	.070	.107
G	1.1	.0833	.070	.107
H	.7	.0833	.070	.118
I	.7	.0833	.070	.128
J	.7	.0833	.070	.139
K	.7	.0666	.046	.107
L	.7	.1000	.085	.107
M	.7	.0769	.066	.107

It will be observed that propellers A to G, inclusive, have essentially the same blade sections similarly distributed radially, but differ in pitch, the pitch ratios running from 0.5 to 1.1. This makes seven propellers with variation in pitch as the primary characteristic. Propellers H to M, inclusive, and also C, all have the same pitch ratio, the differences being in mean width ratio and thickness, expressed by camber ratio at 0.75 radius.

Figures 10 and 11 show the results for the propellers of varying pitch plotted as non-dimensional coefficients upon the basic variable deduced above. Figure 12 shows the seven propellers of uniform pitch but varying blade sections plotted in the same manner upon the basic characteristic or power only. We see from Figures 10 and 11 that the possible efficiency of an airplane propeller is essentially a question not of propeller design but of the requirements to be met by the propeller. Given the power to be absorbed or delivered, the speed, and the revolutions per minute for this family of propellers, and the maximum efficiency attainable is fixed, and it may well happen that it will fall below the 80 per cent efficiency, which is sometimes regarded as normal. Of course Figures 10 and 11 refer to only one family of propellers, but it will be found that almost any family will plot in the same general way. The efficiencies may be a little higher or a little lower, but the variations of efficiency will follow closely the variations of Figures 10 and 11.

Studying these figures, it will be found that for a given combination of power, speed, and revolutions a definite pitch ratio shows the maximum efficiency, but there is a relatively wide range of pitch ratio on each side of that for maximum efficiency where the falling off is slight. Keeping revolutions, power, and speed the same, we may use a smaller propeller of coarser pitch or a larger propeller of finer pitch without a reduction in efficiency of more than a point or so, an amount which could hardly be detected in service.

In view of Figures 10 and 11, inspection of the propellers of the original Wright plane produces admiration of the engineering genius of the pioneers of the air. This low speed plane has two relatively very large propellers of coarse pitch. These characteristics are essential to the best efficiency under the conditions to be met. Fast planes of the present day may obtain good efficiency with single propellers of high revolutions and fine pitch, but if the Wrights had fitted such a propeller their plane probably would not have flown at all.

Coming now to Figure 12 it will be observed that the variation of efficiency is remarkably small for the variations of blade section of all seven propellers, C and H to M inclusive. The differences are almost within the limits of error to be expected in such experiments. As regards diameter, the variation resulting from change of section is normal, the thicker blades requiring smaller diameter because their virtual pitch ratio is greater. Thin blades and narrow blades, similarly, act as normal blades of slightly greater diameter. The efficiency curves in all three

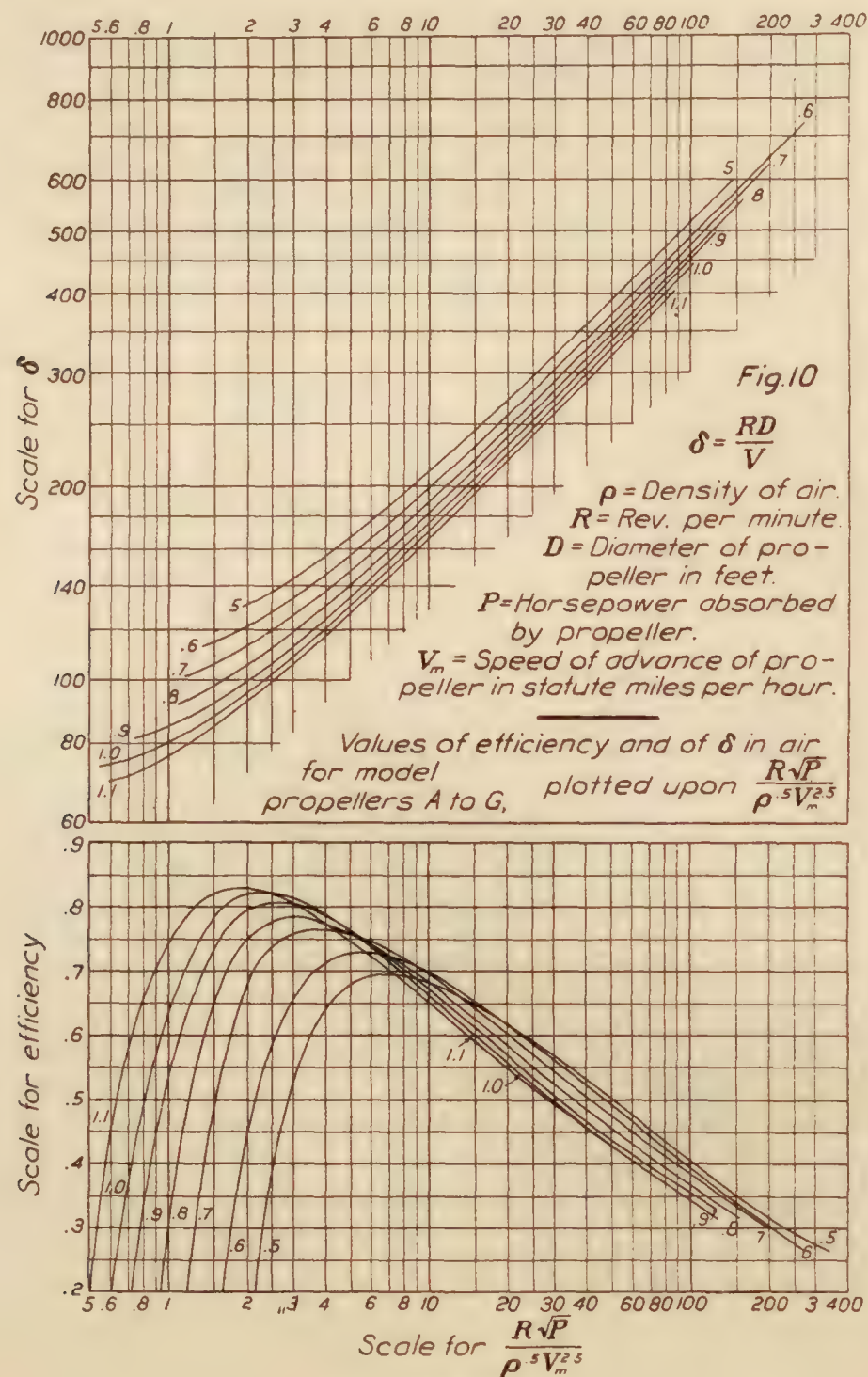


FIG. 10

figures show minor inconsistencies which could readily be faired out. They were taken from curves plotted on entirely different variables.

In concluding this part of my subject, it might be pointed out that systematic diagrams such as Figures 10 and 11, from one family of propellers, may be used to extrapolate with a good deal of accuracy the results to be expected from propellers of another blade type when but one of the type has been tested. If, for instance, the one tested has a pitch ratio of 0.7, we will say, and its δ line falls 3 per cent above or below the δ line for the 0.7 pitch ratio in Figures 10 and 11 we may conclude with good approximation that the same relation will hold for pitch ratios of 0.6 and 0.8. It is rather remarkable at first sight to see how δ lines for propellers of quite different

blade sections tend to parallel one another when plotted upon the basic variables used and how little efficiency is affected by variations of blade sections, etc.

But after all when we go back to first principles these results are perfectly natural.

In air the pressure in the slipstream can not differ much from the undisturbed pressure of the air. Then the thrust is proportional to the sternward momentum, and as shown in Figure 4, there is a certain unavoidable loss or waste of power associated with it, even if we had a perfect propelling instrument. With actual propellers, that are not perfect, we have two further losses

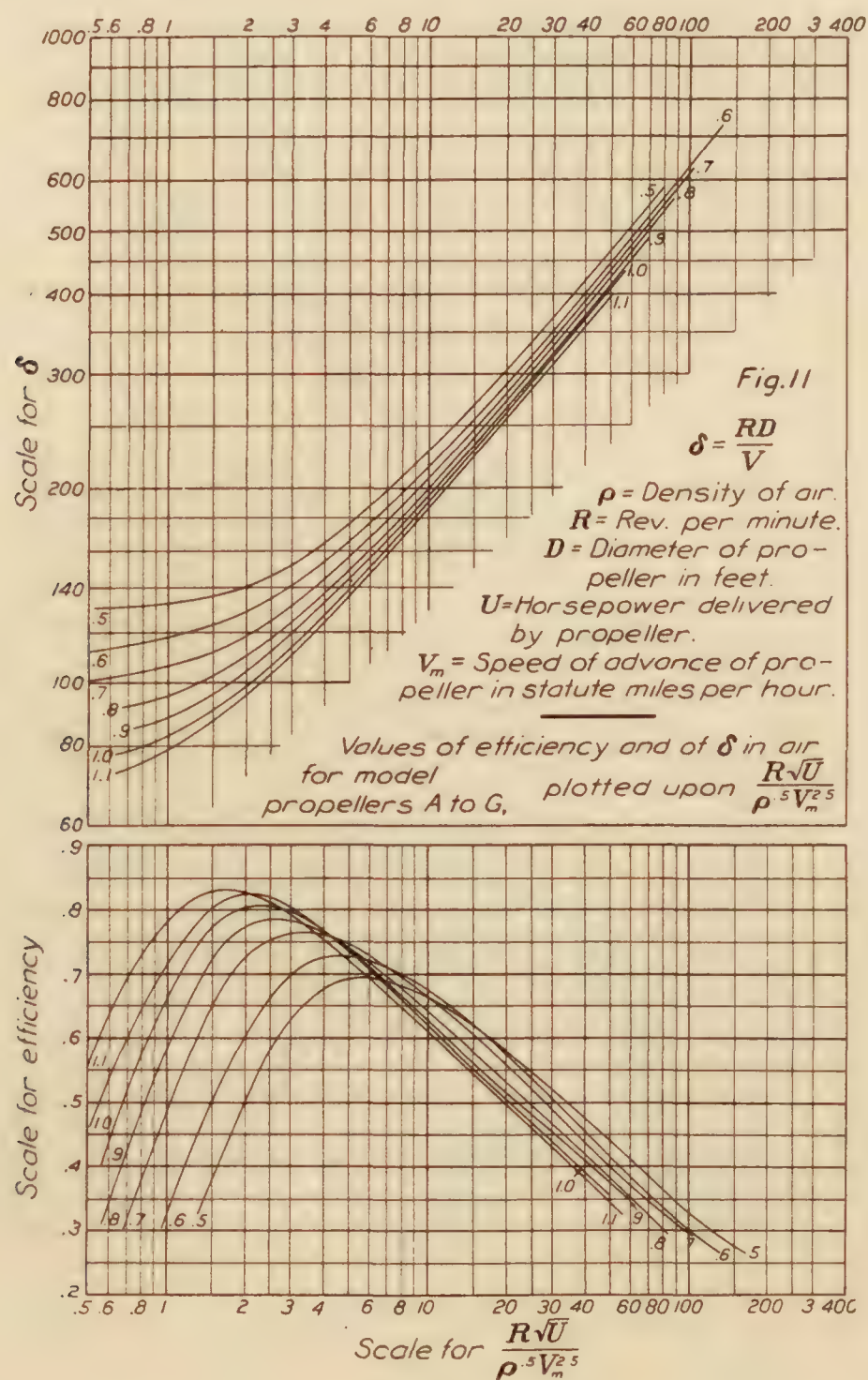


FIG. 11

due to edge or frictional resistance of the blades and to the transverse momentum communicated to the air involving energy. Neither of these two further losses can be eliminated, and from the nature of the case it does not seem that there is a large field for reducing them, though there is plenty of opportunity to increase them.

As tip speeds increase it will be more and more important to develop types of blade section to avoid the quasi cavitation that must be guarded against.

It may be recalled that several times reference has been made to the difficulties of satisfactory full-scale trials. However, we can never rely absolutely upon model experiments until they have been checked by corresponding full-scale trials. During the last year the National

Advisory Committee for Aeronautics has attempted such a comparison, the model experiments and the full-scale tests being both carried out by Prof. E. P. Lesley. The full-scale experiments with five airplane propellers on a VE-7 airplane with a Wright E-4 engine, were conducted at the Langley Memorial Aeronautical Laboratory between May 1 and August 30, 1924. The model experiments were carried out subsequently with models of the same propellers and also a partial model of that part of the airplane exposed to the slip stream, the model being on the scale of 0.3674.

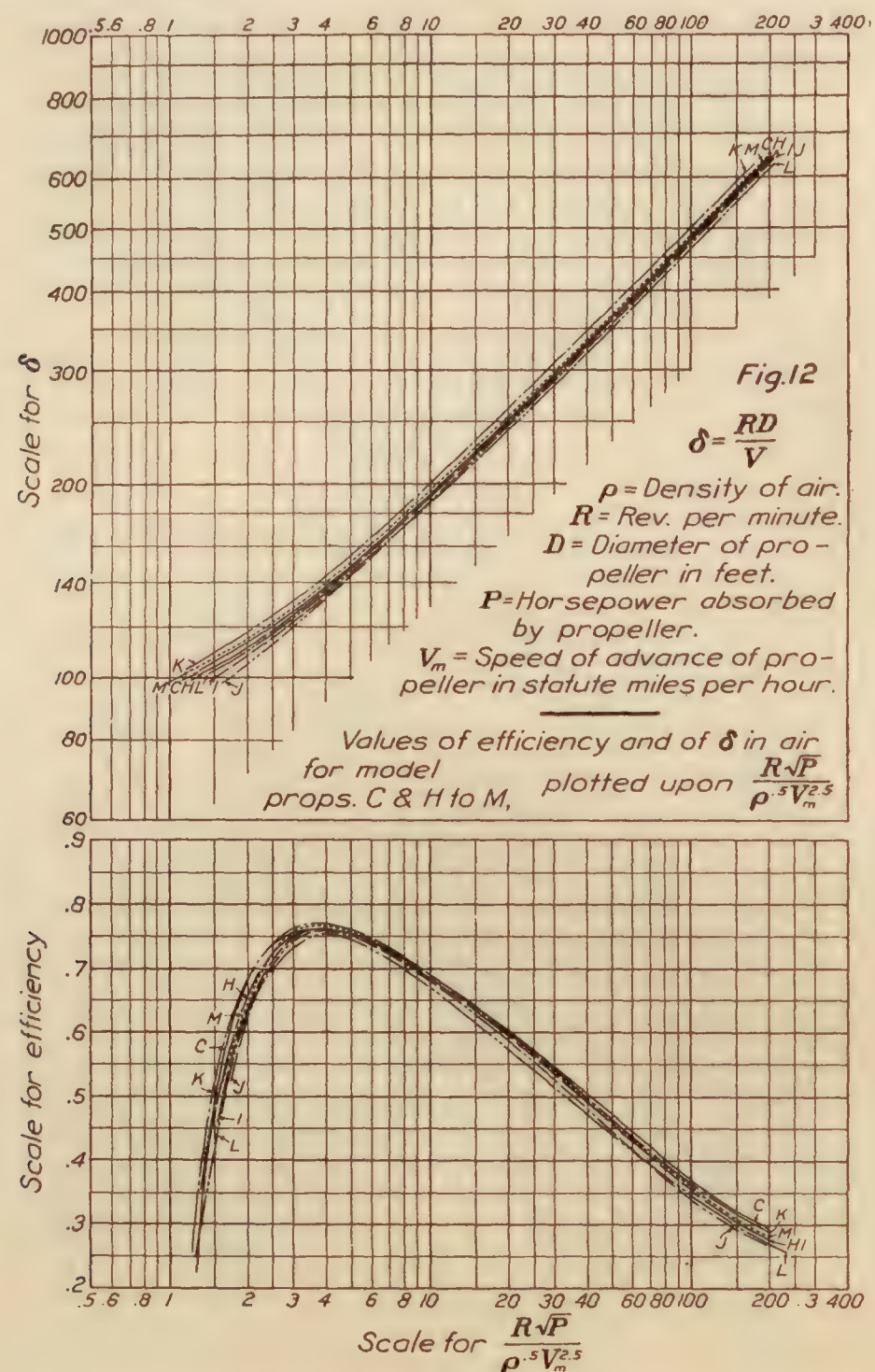


FIG. 12

Heretofore we have considered propeller performance alone. When we come to combine the propeller and its airplane, we meet the complication that each reacts upon and affects the performance of the other. The slip stream from the propeller affects its airplane for tractor propellers, increasing the resistance and somewhat disturbing the balance. This can usually be expressed as regards propulsion matters as an augment of the drag. Furthermore, the disturbance set up in the air by the airplane extends to the air around the propeller, the net result being that the propeller, instead of moving uniformly through the air at the speed of the airplane, moves through air variously disturbed. For the tractor propeller the net result is that the air acted upon by the propeller has already had its relative velocity more or less checked by the reaction from the airplane.

About the only practical way to deal with this matter is to regard this disturbance as equivalent to a uniform slowing up of the air, so that a propeller, instead of behaving as if it were passing through still air with velocity V of the airplane, behaves as if it were passing through still air with a velocity V_1 , less than that of the airplane.

When we come to consider the efficiency of the combination, it is unfortunately necessary to make a clear distinction between the efficiency of the propeller and the "efficiency of propulsion." The efficiency of propulsion is best regarded as the ratio between the power delivered to the propeller and the power necessary to propel the airplane under the circumstances if there were no propeller acting. The efficiency of the propeller, however, is the ratio between the useful power which it delivers and the power delivered to it. The power which it delivers depends upon its actual thrust and its speed, V_1 , through the air upon which it acts. The thrust is normally greater than the drag of the airplane without the propeller, and V_1 is normally less than V . These two factors affect efficiency in opposite directions, and the result is that the efficiency of propulsion may be greater or less than that of the propeller, according to circumstances. In practice we may usually expect to find it somewhat less.

In the free flight experiments at Langley Field it was necessary first to determine the drag of the airplane. This was done over a range of speed from 50 to 135 miles per hour by making steady glides at various steady angles, the propeller being throttled until the thrust was very close to zero, correction being subsequently made for its departure from zero. This being done, it was possible, from the angle of glide and velocity through the air during the glide, both of which were carefully measured, to determine the drag and the ratio between lift and drag. The power could be determined only indirectly, by means of careful calibration runs of the airplane engine on the testing stand with full throttle. The power flights which were used for reduction were made at full throttle, consisting of runs at air speeds from 50 to 135 miles per hour in level flight, climb, or power dive, as determined by the speed. It being impracticable in the full-scale trials to determine the effect of the slip stream upon the airplane or the airplane upon the propeller, the efficiency in the air was regarded as the efficiency of propulsion, not the efficiency of the propeller.

The model tests were made with models of the same five propellers used in the air, and, in order to make them comparable with the free flight test, they also were reduced to an efficiency of propulsion; that is to say, a thrust coefficient was obtained by using the net thrust, which was the actual thrust less the difference between the drag of the airplane model with the propeller working and its drag without the propeller, all being plotted upon the basis of the speed through the air. The five propellers used had the dimensions and coefficients given in Table IV.

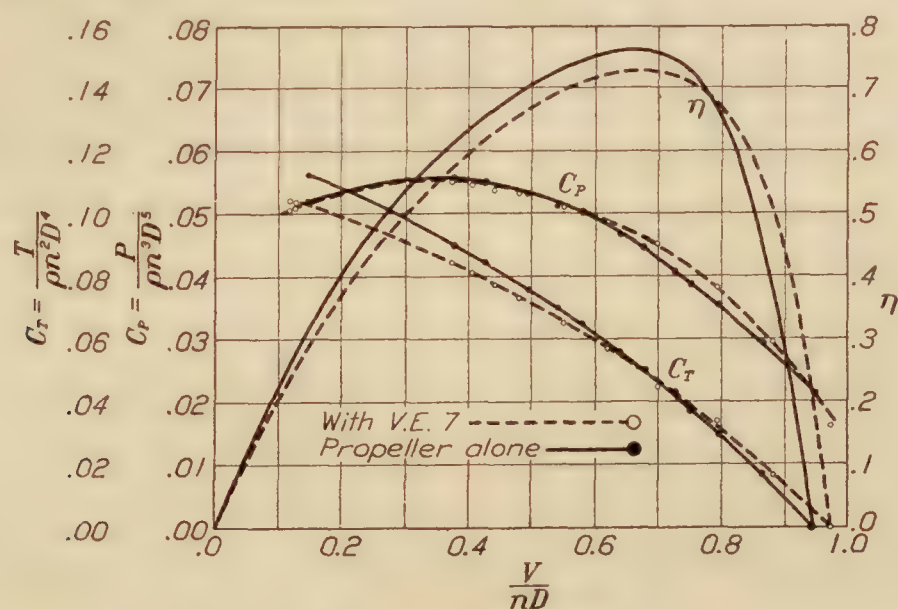


FIG. 13.—Model Propeller I

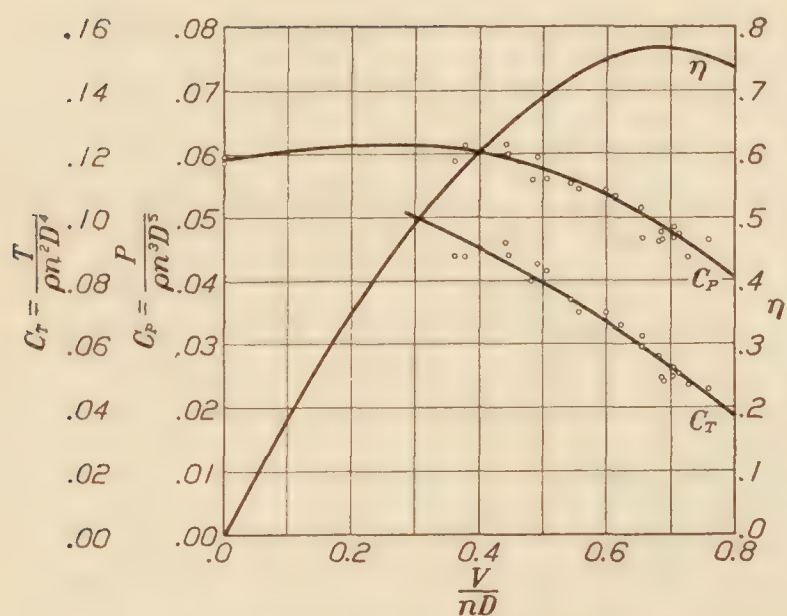


FIG. 14.—Propeller I full scale with VE 7 airplane

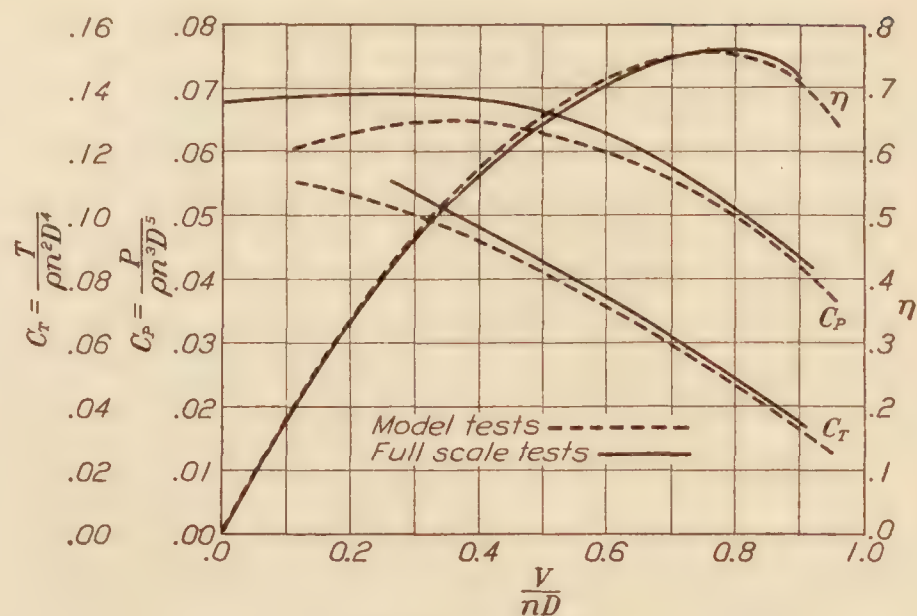


FIG. 16.—Propeller D'

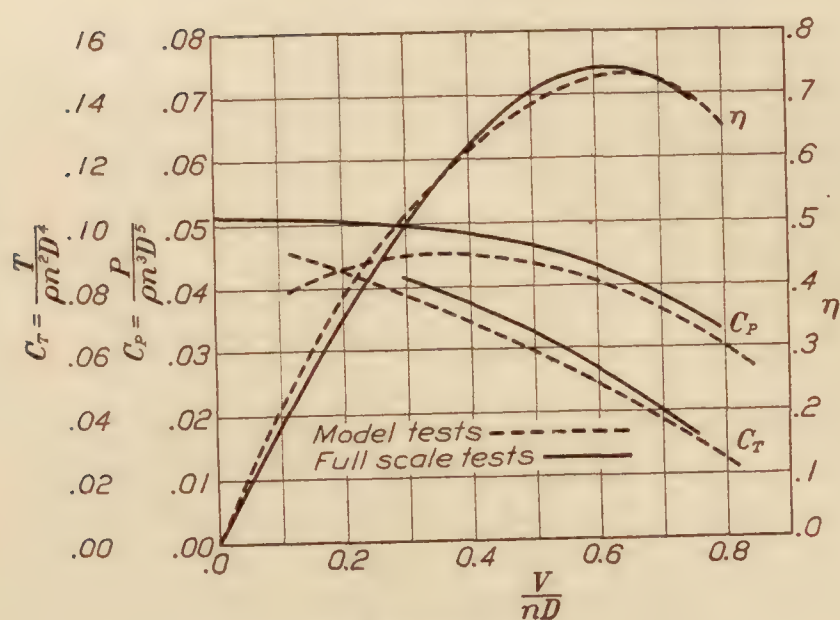


FIG. 15.—Propeller B'

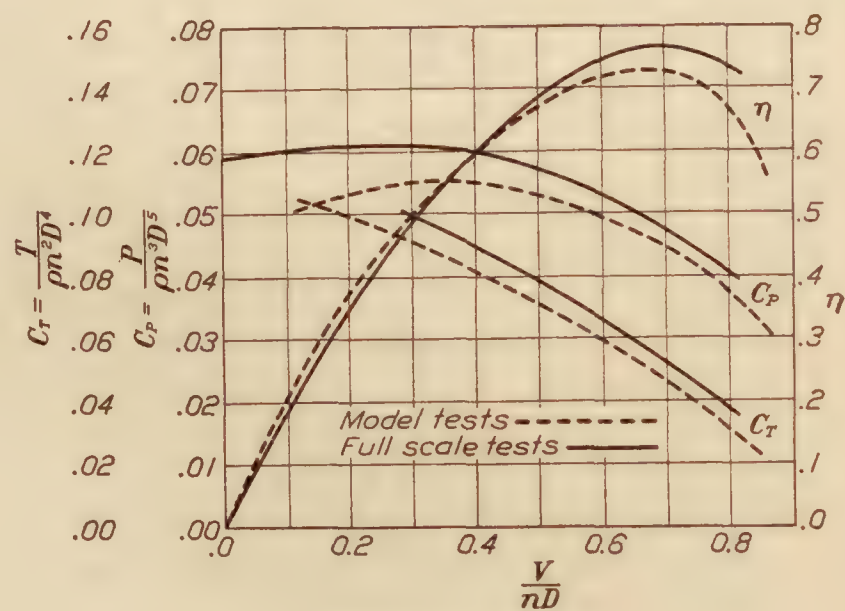


FIG. 17.—Propeller I

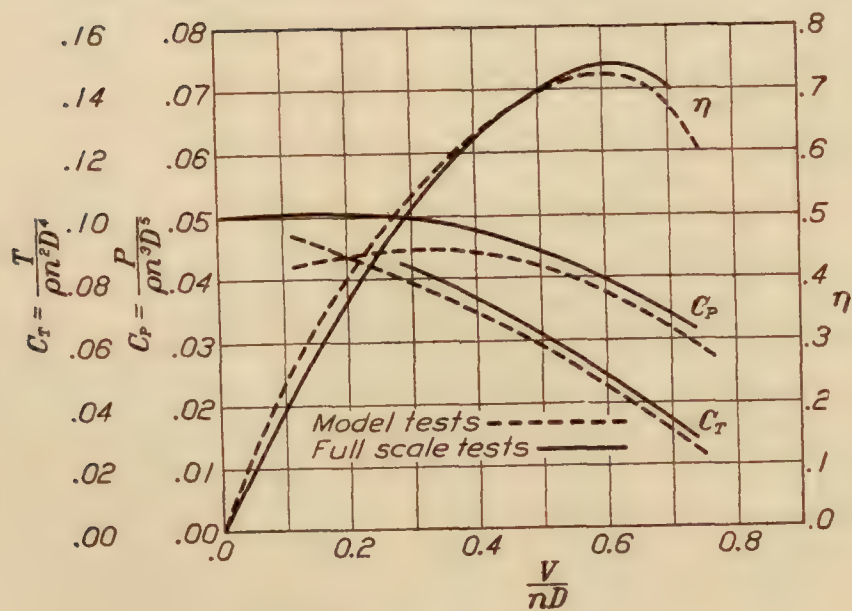


FIG. 18.—Propeller K'

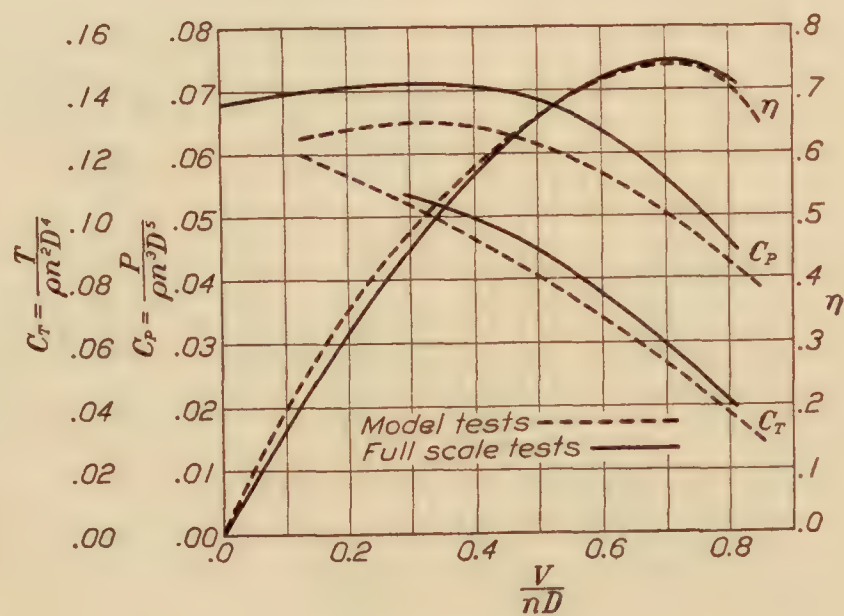


FIG. 19.—Propeller L'

TABLE IV
DATA OF FIVE PROPELLERS USED IN FREE FLIGHT TESTS

Designation	Diameter		Pitch		Pitch ratio	Maximum width ratio	Mean width ratio	Camber ratio at 0.75 radius
B'	8	6	5	1.5	0.6	0.0833	0.070	0.128
D'	7	10	6	3.2	.8	.0833	.070	.128
I	8	2	5	8.6	.7	.0833	.070	.128
K'	8	2	5	8.6	.7	.0666	.046	.128
L'	8	2	5	8.6	.7	.1000	.085	.128

The model results generally were quite consistent.

Figure 13 shows the results of model propeller I with the partial VE-7 model in place, compared with the model results of the propeller alone. In Figures 13 to 19, inclusive, P , upon which values of C_P depend, does not mean power, but foot-pounds per second. T denotes thrust in pounds. Of course, as regards the propeller, abscissae of $\frac{V}{nD}$ mean something slightly different according as the airplane model is or is not present. With the propeller alone it refers to the true slip; with the propeller and model it refers to the apparent slip, and the case is also affected by the use of the net thrust instead of the actual thrust. In the full-scale work we can not determine the actual drag and the air speed relative to the propeller.

Figure 14 shows for propeller I in free flight the curves of C_T , C_P , and corresponding efficiency of propulsion on the basis already explained. Finally, in Figures 15 to 19 there are brought together the results of the model tests with model of plane in place, and the free flight tests in the shape of curves of C_T , C_P , and efficiency. It will be observed that in each case the coefficients are larger in free flight than as estimated from the model results. While the differences vary, as is to be expected, they are consistently too great to be accidental, averaging somewhat on the order of 8 per cent, although for propeller D' they are very small. It is significant that the efficiency differences are very small indeed. Without entering too much into the realm of speculation, it may be pointed out that there are several more or less constant perturbing causes. One is the scale effect; another is the fact that in the model propeller tests the propeller shaft is always parallel to the direction of the flight, whereas in the flight tests the angle made by the propeller shaft with the flight path varied between zero and ten degrees. Inspection of Figures 15 to 19, however, indicates that the perturbation, broadly speaking, increases with the thrust; that is to say, it increases as $\frac{V}{nD}$ decreases. This points to a third cause of perturbation, namely, the elastic deformation of the blades of the propeller under stress, a deformation that would be much greater on the full-sized propeller than on the model tested at less than full speed. A moderate deformation of the full-sized propellers would account for all the discrepancies in Figures 15 to 19.

There are, however, too many uncertainties in such a complicated series of experiments to enable us to fix positively the causes of the discrepancies. In their general features the model and full-scale curves agree very well. It should be pointed out also that, although a difference of, say, 8 per cent of C_P looks large on a diagram, for practical purposes it is not of primary importance. For constant pitch ratio, revolutions, and speed the diameter of the proper propeller varies as the sixth root of C_P , so that a discrepancy of 8 per cent in the value of C_P means a discrepancy of only about 1 per cent in propeller diameter. This is an approximation adequate for the purposes of the engineer. Full-scale tests, where torque and thrust are determined by measurement instead of inference, are of course very desirable, but as far as they go, those to which I have invited your attention are encouraging to those of us who believe that model experiment properly interpreted is not only valuable but indispensable to aeronautical development.

REPORT No. 220

COMPARISON OF TESTS ON AIR PROPELLERS IN FLIGHT WITH WIND TUNNEL MODEL TESTS ON SIMILAR FORMS

By W. F. DURAND and E. P. LESLEY
Stanford University

REPORT No. 220

COMPARISON OF TESTS ON AIRPLANE PROPELLERS IN FLIGHT WITH WIND TUNNEL MODEL TESTS ON SIMILAR FORMS

BY W. F. DURAND AND E. P. LESLEY

INTRODUCTION

The purpose of the investigation, which is the subject of the present report, was to determine the performance characteristics and coefficients of full-sized air propellers in flight and to compare these results with those derived from wind-tunnel tests on reduced scale models of similar geometrical form.

The full-scale equipment comprised five propellers in combination with a VE-7 airplane and Wright E-4 engine. This part of the work has been carried out at the Langley Memorial Aeronautical Laboratory, between May 1 and August 24, 1924, and was under the immediate charge of Mr. Lesley. The model or wind-tunnel part of the investigation was carried out at the aerodynamic laboratory of Stanford University and was under the immediate charge of Mr. Durand.

For the full-scale work power absorbed was determined from calibration curves of the engine, derived both before and after the flight tests were made. Useful work is defined as drag of airplane, without influence of slip stream, times velocity, plus weight times rate of climb; efficiency as useful work divided by power absorbed.

The derived coefficients,

$$C_T = \left(\frac{\text{Thrust}}{\rho n^2 D^4} \right), \quad C_P = \left(\frac{\text{Power}}{\rho n^3 D^5} \right), \text{ and } \eta \text{ (efficiency)}$$

are plotted on $\frac{V}{nD}$, and curves are drawn representing the average of plotted spots.

For the model investigation, the corresponding coefficients and elements of the performance were determined by direct measurement of resistance, thrust, torque, air speed, and revolutions, as described in detail in Part II of the report.

A comparison of the curves for full-scale results with those derived from the model tests shows that while the efficiencies realized in flight are close to those derived from model tests both thrust developed and power absorbed in flight are from 6 to 10 per cent greater than would be expected from the results of model tests.

The more detailed description of the equipment employed, the methods of carrying out the observations, and of analyzing and reducing the results will be found in Parts I and II of the report as below.

PART I

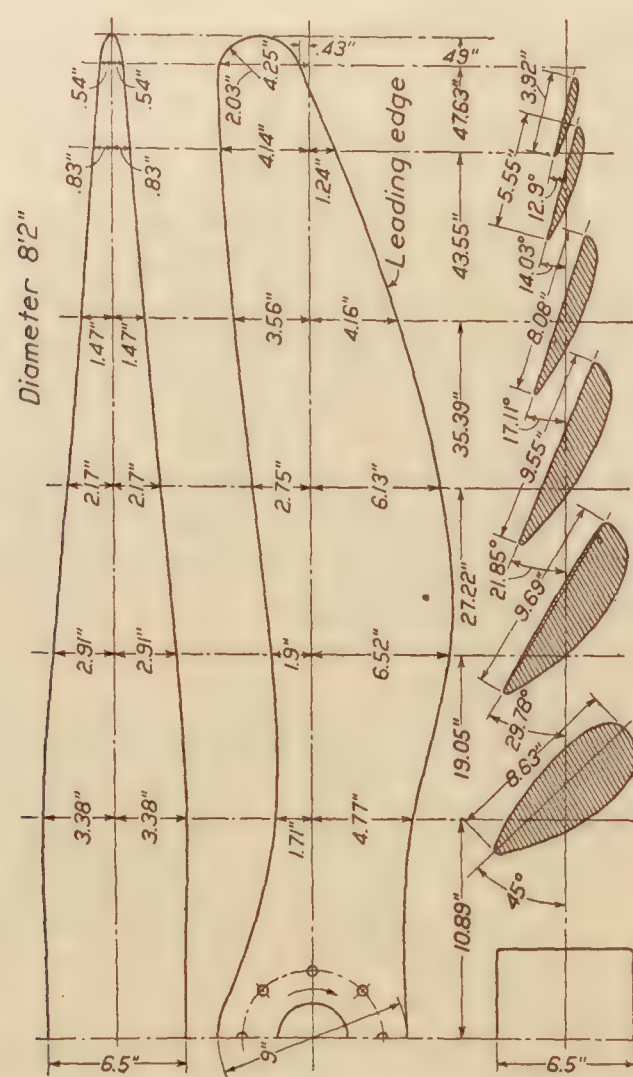
FULL-SCALE TESTS

TEST PROPELLERS

The dimensions of the propellers tested are shown in Figures 1 to 5 and Table VIII.

The propellers are of the United States Navy standard plan form. They were made of birch in the usual laminated construction and covered with cotton fabric. The blade angles were measured before tests, and no appreciable difference was found between such measurements and those made by the Navy inspector at the works of the Hartzel Walnut Propeller Co., the angles being found correct within the tolerance allowed by the Navy specifications. At the close of the tests the pitch angles were again measured and the following determined:

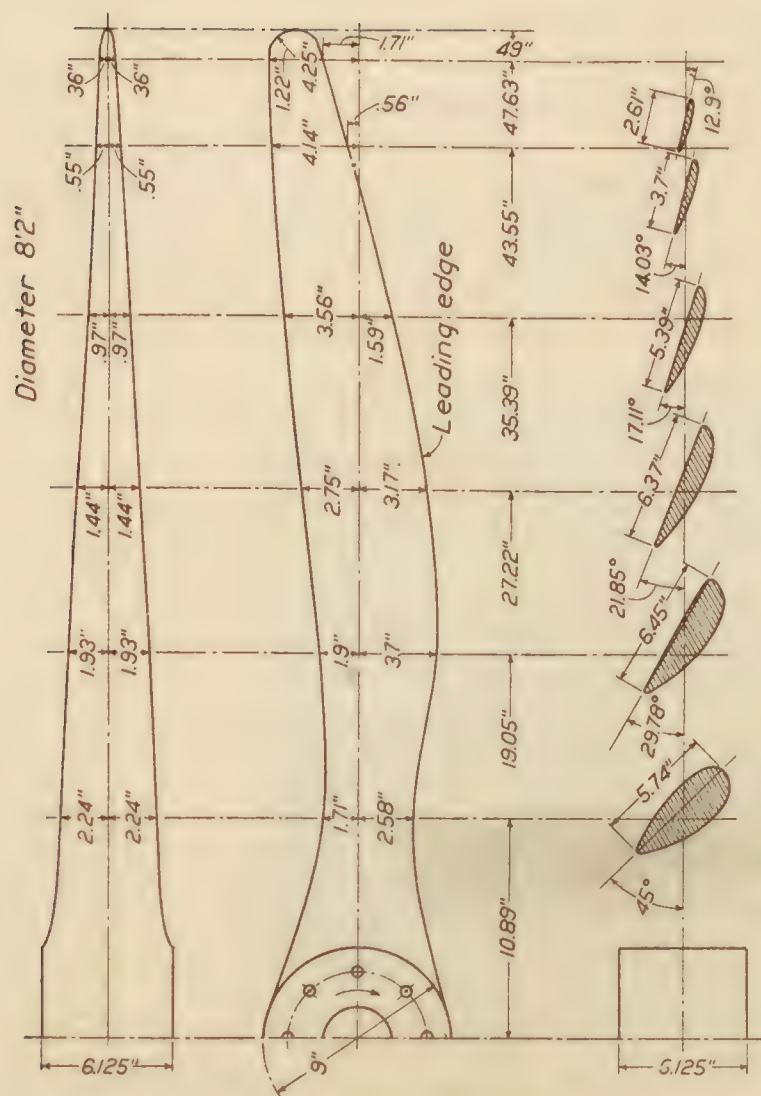
Propeller	Mean geometrical pitch
B'-----	5' - 0.4''
D'-----	6' - 2.8''
I-----	5' - 8.5''
K'-----	5' - 8.5''
L'-----	5' - 8.6''



Pitch: 5' 8.6''. Pitch ratio: 0.7. Aspect ratio: 5.
Camber ratio: Minimum + 20 per cent. Rotation:
Right hand.

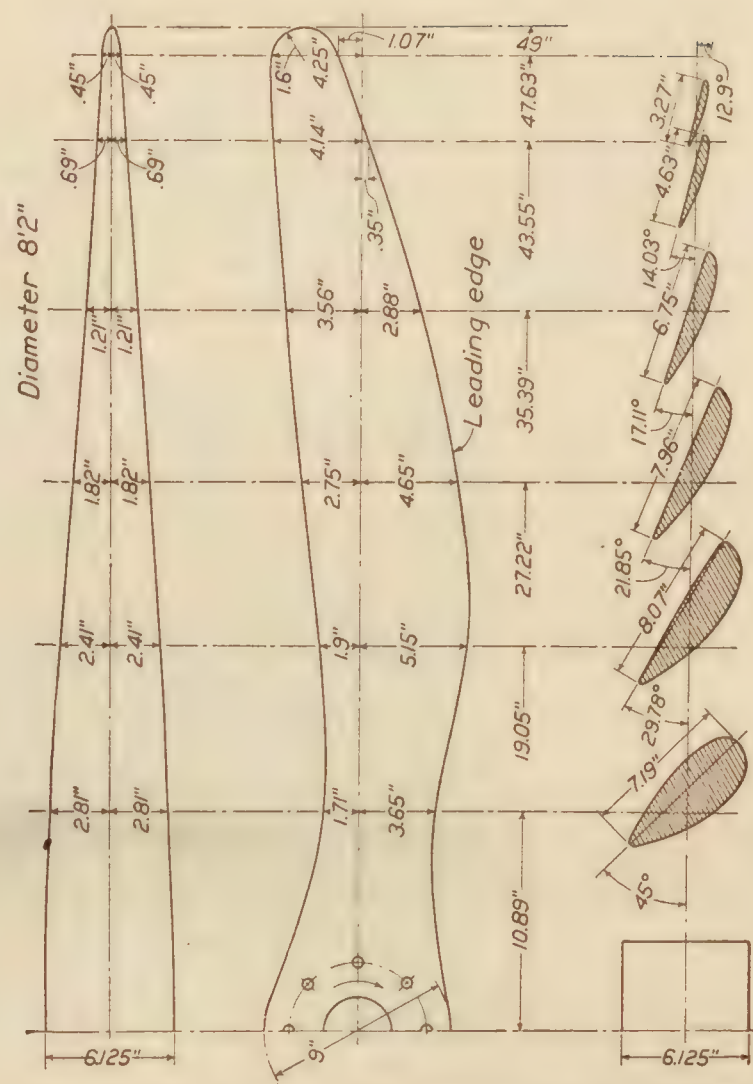
FIG. 1.—Experimental propeller L' for VE-7 airplane

Propeller B' is thus seen to have had at the close of the tests appreciably less than the designed pitch of 5' - 1.2''. All are believed to have been as nearly geometrically similar to the models, which were made from the same drawings by the application of a linear scale ratio, as is practicable of realization with wood construction.



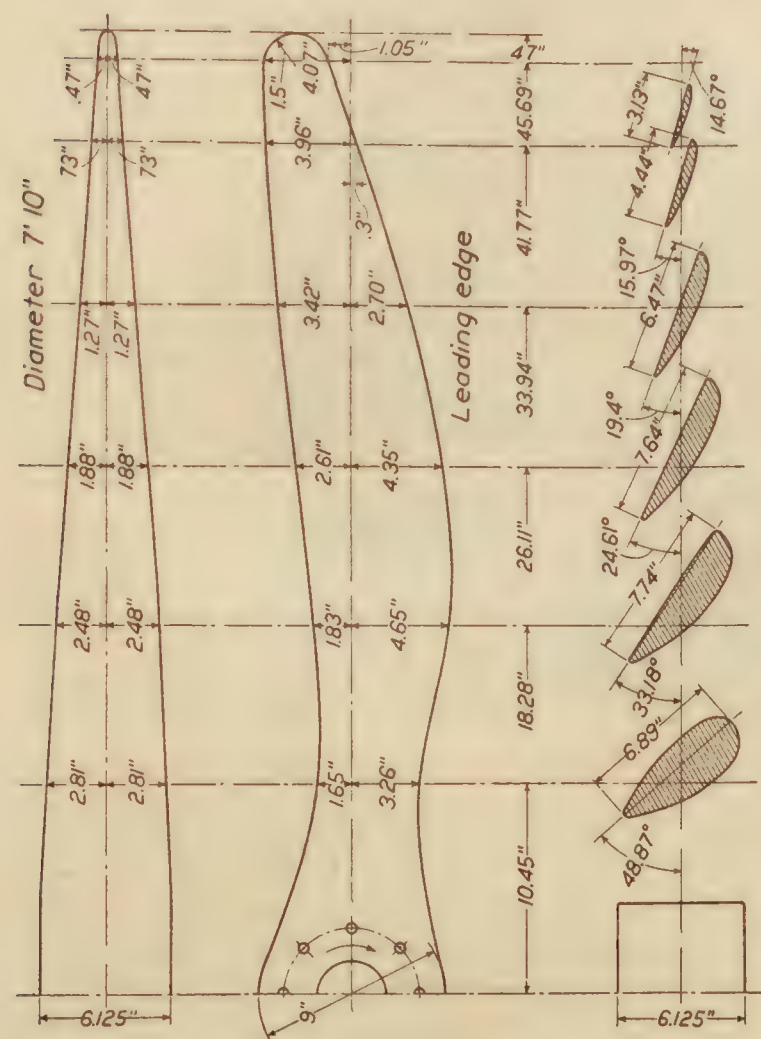
Pitch: 5' 8.6". Pitch ratio: 0.7. Aspect ratio: 7.5. Camber ratio: Minimum + 20 per cent. Rotation: Right hand.

FIG. 2.—Experimental propeller K' for VE-7 airplane



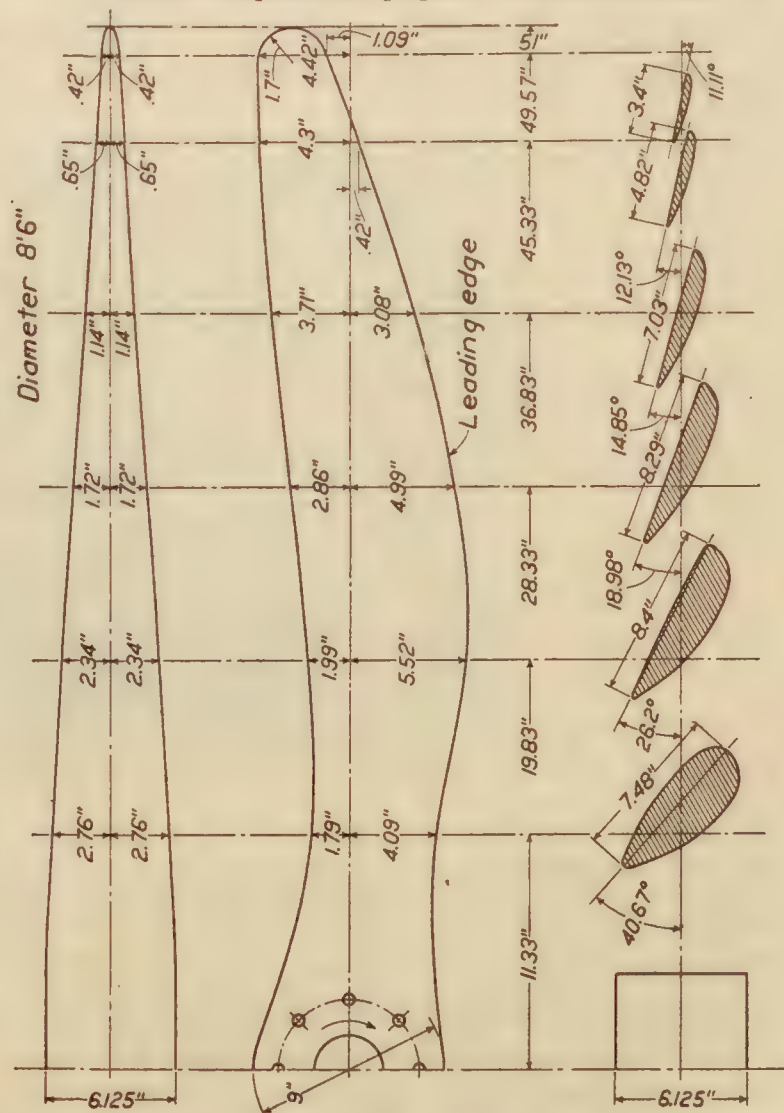
Pitch: 5' 8.6". Pitch ratio: 0.7. Aspect ratio: 6. Camber ratio: Minimum + 20 per cent. Rotation: Right hand.

FIG. 3.—Experimental propeller I for VE-7 airplane



Pitch: 6' 3.2". Pitch ratio: 0.8. Aspect ratio: 6. Camber ratio: Minimum + 20 per cent. Rotation: Right hand.

FIG. 4.—Experimental propeller D' for VE-7 airplane



Pitch: 5' 1.2". Pitch ratio: 0.6. Aspect ratio: 6. Camber ratio: Minimum + 20 per cent. Rotation: Right hand.

FIG. 5.—Experimental propeller B' for VE-7 airplane

INSTRUMENTS AND APPARATUS

The instruments and apparatus used in these tests were as follows:

(1) *N. A. C. A. recording altimeter.*

(2) *N. A. C. A. recording pendulum inclinometer and airspeed meter.*—This instrument was fitted with a heavy diaphragm capsule, used for recording the intake manifold depression, in place of the usual airspeed capsule. The pendulum inclinometer, the instrument being rigidly secured to a shelf in the observer's cockpit, gave records of the angle of the wing to the horizontal.

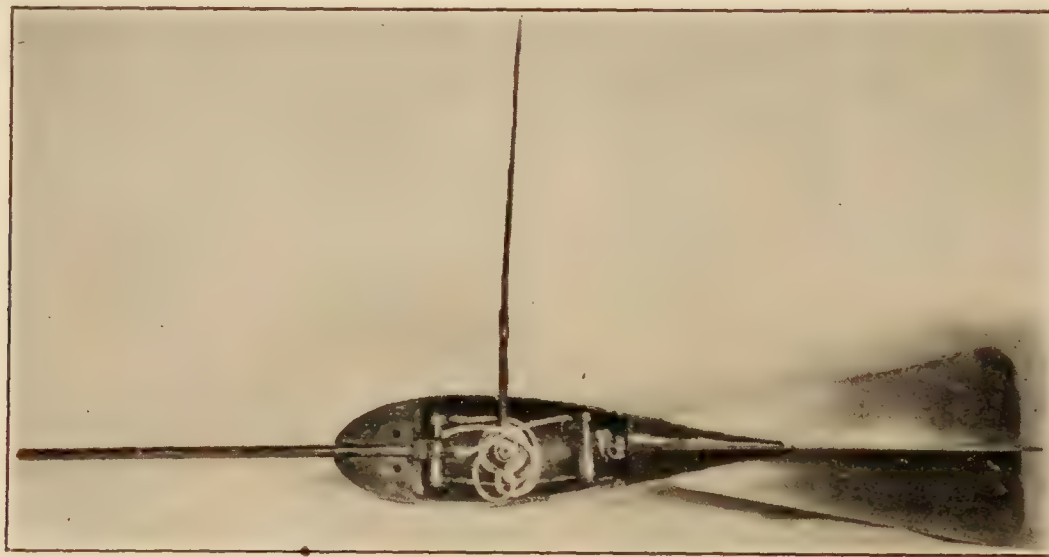


FIG. 6

(3) *A trailing bomb inclinometer and airspeed meter.*—The trailing bomb of this instrument, with cover removed, is shown in Figure 6. It consists essentially of a streamline-form case with stabilizing tail, fitted with a mercury U tube and a Pitot tube. The mercury U tube and Pitot tube are connected, through small rubber tubing and through brass capillary tubing forming the suspending cable, to a pressure diaphragm-type recording instrument placed inside the drum on which the suspending cable is wound. The bomb is suspended from small self-

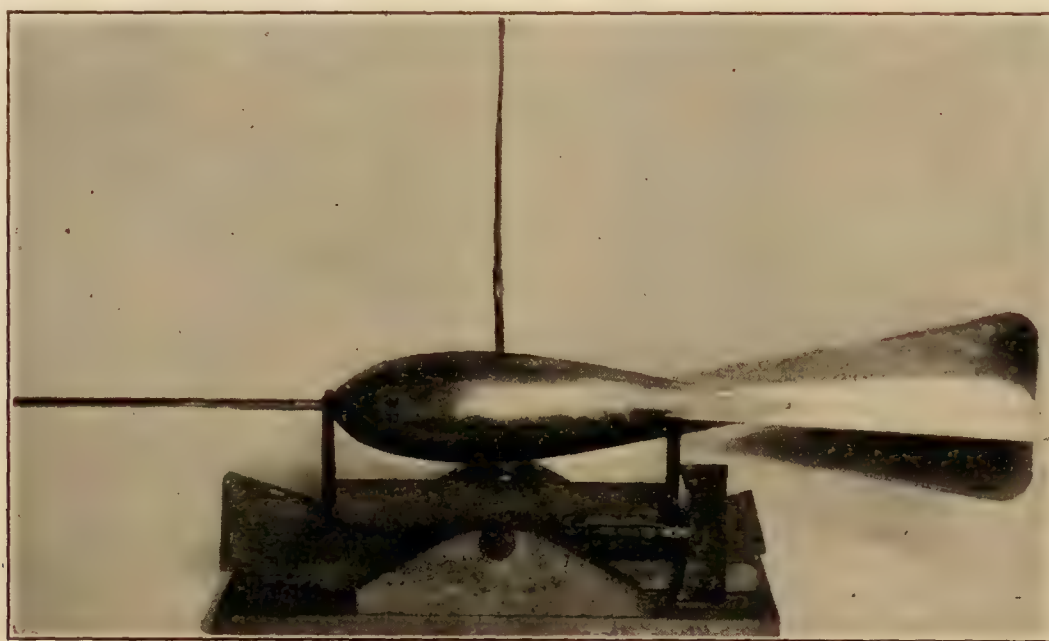


FIG. 7

aligning ball bearings, the bail passing through a longitudinal slot at the top, and is thus free to assume the direction of the air stream flowing by it. Inclination of the bomb from the initial position results in a difference of pressure on the two sides of the diaphragm capsule, to which the mercury U tube is connected, with only a slight displacement of the mercury. The moment of the displacement mercury is balanced by a small righting moment of bomb itself. Thus the bomb remains in any attitude it is placed unless disturbed by some external force. The inclinometer feature is calibrated by placing the bomb in a jig, as shown in Figure 7, tilting

to various positions, and making records of the pressures developed at the capsule of the recording manometer.

An equalizing valve is provided in the system, which permits equalizing the pressures on the two vertical legs of the U tube in any desired initial attitude of the bomb. The range of the instrument, with a diaphragm capsule of given sensitivity, is thus doubled. As used in these tests it was provided that a range of 16° could be covered, the instrument being adjusted to record from 0° to 16° of glide, from 0° to 16° of climb, or from 8° climb to 8° glide as desired.

From the record made the angle of flight path is estimated to 0.1° , but the possible error, due to oscillation in flight, inconstancy of recording capsule, and to error in measuring record, appears to be $\pm 0.5^\circ$.

A sample record, for gliding flight, is shown in Figure 8. The mean distance of the lighter wavy lines from the base is, from a calibration curve, a measure of the angle of flight path, and the distance of the heavier wavy lines from the same base is a measure of velocity head.

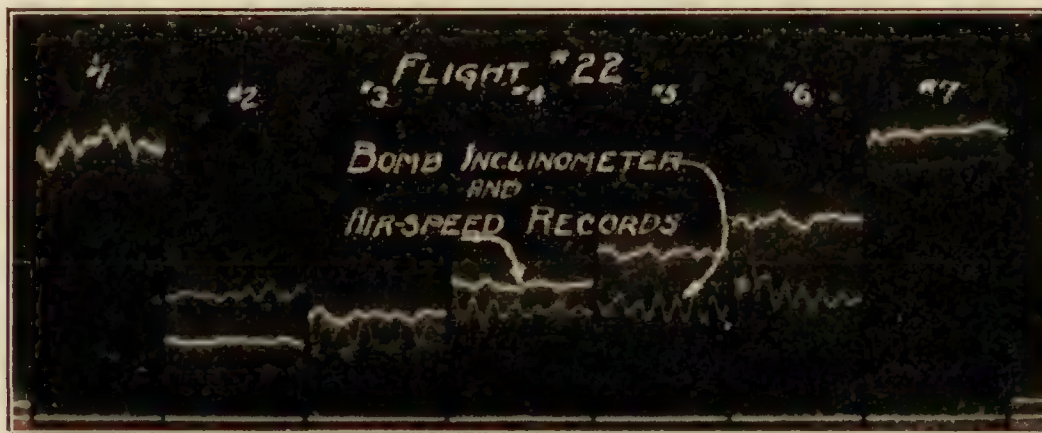


FIG. 8

(4) *Veeder counter*.—This instrument, connected to the engine cam shaft through a simple mechanical clutch, was used to determine engine speed.

(5) *Thermometers*.—Distance-type indicating thermometers were used to determine strut temperature and carbureter intake temperature.

Besides the above, the regular equipment of navigating instruments, such as tachometer, air-speed meter, indicating altimeter, water and oil thermometers, and oil-pressure gage, was installed.

CALIBRATION OF ENGINE

The engine was set up on a Sprague dynamometer test stand for calibration before flight tests, as shown in Figure 9.

During the calibration a 30-70 mixture of benzol and aviation gasoline was used as fuel, the purpose being to avoid danger of incipient detonation at full throttle. In the flight tests, however, it was proposed to use straight gasoline, since this work was to be conducted at such altitudes that the danger of detonation would not exist. This procedure was considered allowable, as it was believed that equal powers would be developed by the mixed and straight fuels under the conditions of flight.

Two carburetor intake temperatures were employed—about 10° and 26° centigrade. On comparison of the brake horsepower developed in the two cases it was found that, for constant speed and barometric pressure, brake horsepower varied closely as $\frac{1}{\sqrt{T}}$, T being the absolute temperature at the carburetor intake. The mixture control was adjusted, in this calibration, to the full rich position.

Some slight troubles were experienced with one magneto, which finally failed due to breaking of the distributor ring. This magneto, a Splitdorf SS-8, was replaced by a Splitdorf Dixie 800.

After installation in the airplane it was noted that the engine appeared to be rather rough, missing considerably at part throttle, and that, with the airplane on the ground and held stationary, it did not drive the propellers at the speeds expected from model tests, if the power as indicated on the dynamometer were being developed. The fuel used in calibration was substituted for aviation gasoline, but no appreciable improvement in performance could be

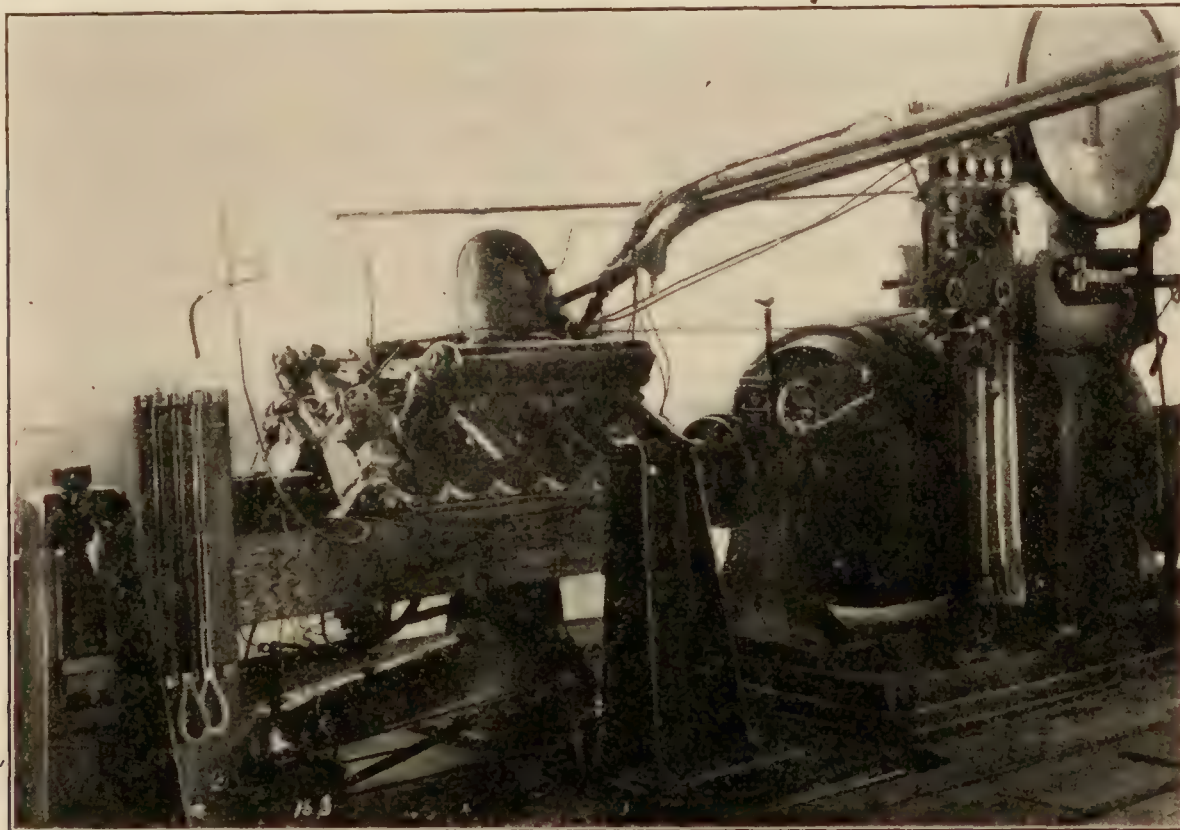


FIG. 9

detected. The installation was therefore checked over, a minor intake manifold leak corrected, the two magnetos used in the calibration replaced by tested accessories (Dixie 800), and the mixture control adjustment wired fast in the full rich position. With these changes the missing was eliminated and the standing R. P. M. at full throttle and with propeller I were observed to be 1,580. The performance with this propeller (standing R. P. M. at full throttle) was thereafter used as an index of engine condition. At no time during the flight tests, which in all occupied about 20 hours running time, was there a change, as shown by the indicating tachometer, of more than 20 R. P. M., the performance being generally consistent.

At the end of the flight tests the engine was subjected to two further calibrations—first, with aviation gasoline as fuel, and second, with the original 30-70 mixture of benzol and aviation gasoline.

The results of the full-throttle runs of the three calibrations, reduced to the conditions of standard air, are shown in Figure 10. The reduction of the observed data to the conditions of standard air (barometer=760 mm., temperature=15.6° centigrade) is accomplished through the assumed relation $B.H.P. = C \frac{p}{\sqrt{T}}$, in which p is the barometric pressure, T the absolute temperature at the carbureter intake, and C a constant.

It may be noted that the calibration after flight tests, with aviation gasoline as fuel, shows B.H.P. about 6½ per cent less than that before flight tests with the mixed fuel, and that the second calibration with mixed fuel is about 3½ per cent below the first. It appears, then,

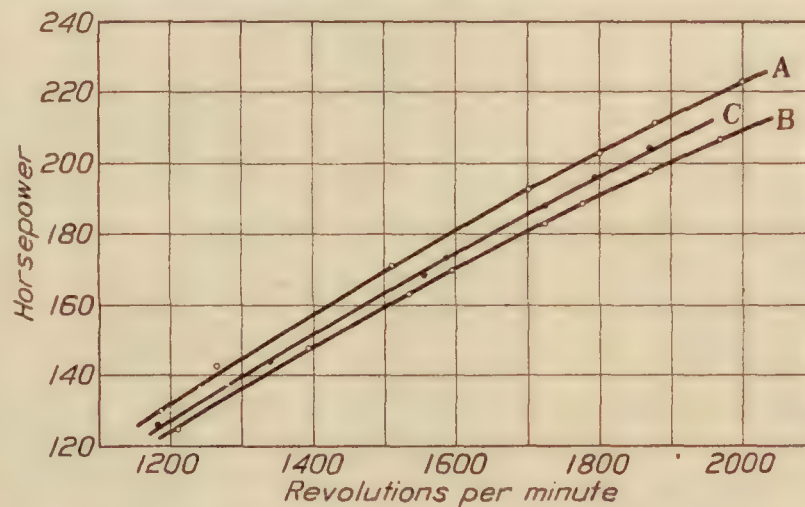


FIG. 10.—Wright E-4 engine calibration reduced to standard air

Curve A—Fuel 30-70 benzol gasoline. Feb. 18, 1924.

Curve B—Fuel gasoline. July 15, 1924.

Curve C—Fuel 30-70 benzol gasoline. July 18, 1924.

that between the calibrations, before and after flight tests, the engine deteriorated about $3\frac{1}{2}$ per cent. Since aviation gasoline was used for fuel in the flight tests and many of these were conducted at moderate altitudes (1,500 to 3,000 feet), it also appears that toward the end of the flight tests the power developed by the engine at full throttle may have been little more than that indicated by the lowest calibration curve, while at the start it may have been close to that indicated by the highest curve.

FLIGHT TESTS

The flight tests consisted of, first, a series of glides, with the propeller at approximate R. P. M. for zero thrust, to determine the lift and drag of the airplane at various speeds; and second, power flights with each propeller at speeds covering the practicable range of the airplane, viz, from 50 to 135 miles per hour.

In the glide tests, after climbing to an altitude of about 3,500 feet, the airplane was jockeyed to a condition of steady glide at about 3,000 feet, where the records were started. The range of speed covered was from 50 to 135 miles per hour. The time occupied by each glide, during making of records, was about 40 seconds. In each glide the throttle was closed until the indicating tachometer showed about the R. P. M. for zero thrust at a particular air speed employed, this R. P. M. being determined from a model test of the propeller.

The recording and indicating instruments gave for the gliding flights:

1. True air speed—as determined from the velocity head recorded from the Pitot tube of the trailing bomb and from density of air as derived from altimeter record and strut temperature.
2. Angle of flight path—as recorded by the trailing bomb inclinometer.
3. Angle of wing—as determined from record of pendulum inclinometer.
4. R. P. M.—as determined from Veeder counter attached to engine.

In the glide tests only one propeller (I) was used.

The power flights were made mainly at full throttle and consisted of runs at air speeds from 50 to 135 miles per hour with each propeller; climbing, level flight, or power dives as determined by the speed.

In addition to the full-throttle runs a number of trials at part throttle were made. These were found generally unsatisfactory, however, because of difficulty in maintaining steady conditions, and were discarded. The intake-manifold pressure, from which it was expected to deduce engine power, was found to fluctuate considerably with the slight throttle adjustment necessary to maintain uniform engine speed at a given speed of flight. Then, too, it was found that the range of $\frac{V}{nD}$ that could be covered in level flight was very small, and that at the lower speeds the power required for level flight was so small as to be below the range of the engine calibration.

In the power flights the instruments provided data for:

- (a) True air speeds—from trailing bomb Pitot and air density as in gliding flight.
- (b) Angle of flight path.
- (c) Angle of wing.
- (d) R. P. M.
- (e) Intake manifold depression (not used except as indication of throttle opening).
- (f) Carburetor intake temperature as determined from indicating thermometer.
- (g) Air density as determined from barometric pressure and strut temperature.

REDUCTION OF DATA

No thrust gliding flights.—The essential observed and computed data for the glide tests are shown in Table I.

The angle of attack is found by subtracting the angle of the flight path from the angle of wing.

The airplane, with fuel, oil, and water and with pilot and observer, was weighed before tests. Allowance is made for fuel, oil, and water consumed in each flight.

Lift is taken as equal to $W \cos \alpha$, α being the angle of the flight path.

The apparent drag is numerically equal but opposite in sign to $W \sin \alpha$.

True drag is apparent drag plus thrust, and thrust is derived from the thrust coefficient of a model propeller for the value of $\frac{V}{nD}$ attained in the glide test, it being rarely possible to realize the exact $\frac{V}{nD}$ for zero thrust (0.972 for propeller I).

$\frac{1}{2} \rho V^2$ is given in the table in pounds per square foot and is derived directly from the record and calibration of the pressure capsule connected to the pitot tube of the trailing bomb.

C_L and C_D are $\frac{\text{Lift}}{\frac{1}{2} \rho V^2 S}$ and $\frac{\text{Drag}}{\frac{1}{2} \rho V^2 S}$ respectively; S being taken as 284.5 square feet.

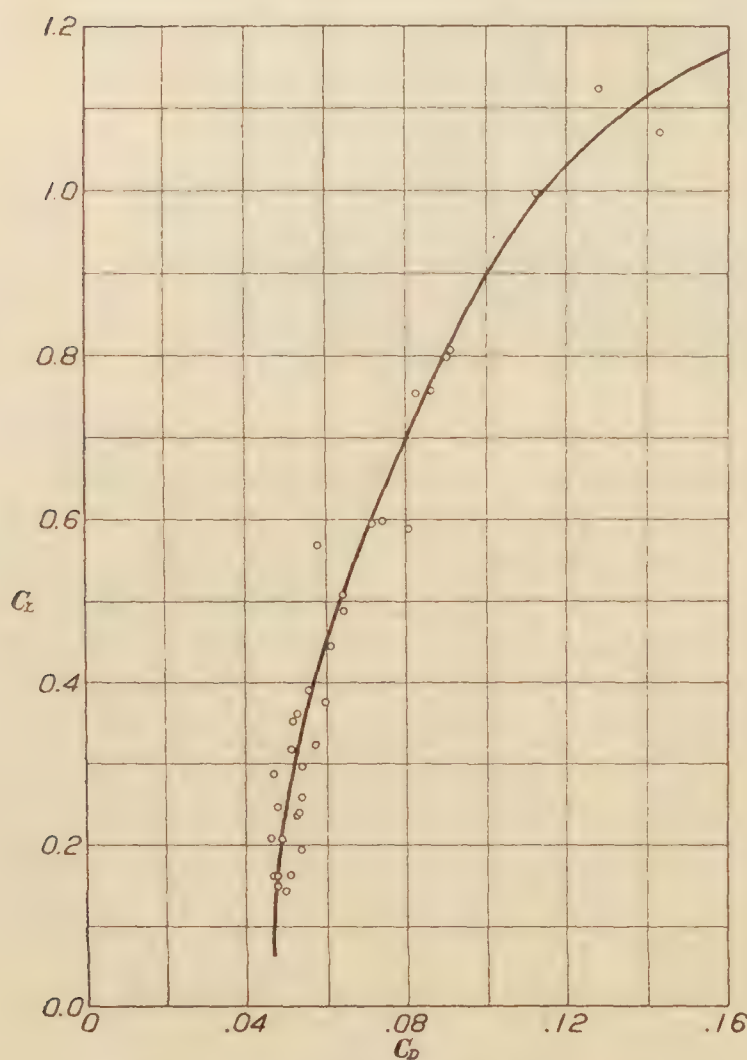


FIG. 11.—Polar diagram of Vought VE-7 airplane

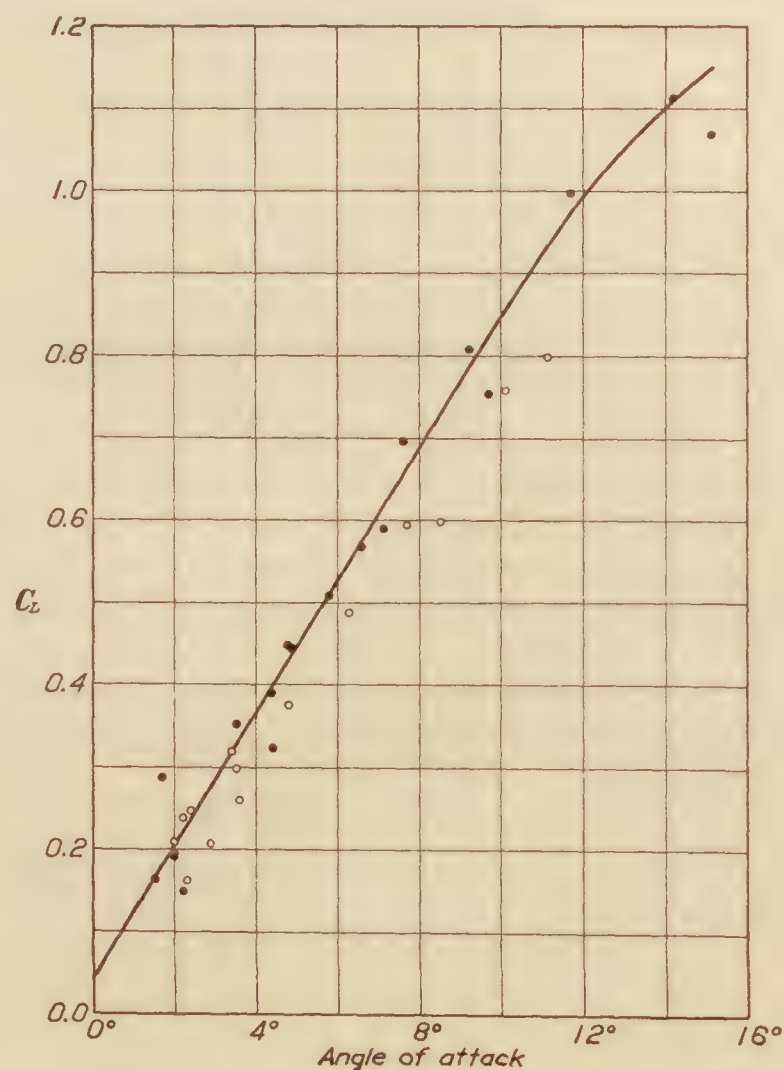


FIG. 12.—Lift characteristic of Vought VE-7 airplane

The final coefficients C_L and C_D , plotted as a polar diagram, are shown in Figure 11, a curve representing a reasonable estimate of the average of points being drawn.

In addition the points for C_L plotted against angle of attack are shown in Figure 12. In drawing a curve for this plot the preference has been given to points determined in the later glides, it being found that in the first flights the pendulum inclinometer was out of adjustment (loose pivots) and the calibration somewhat doubtful.

Power flights.—The essential observed and computed data for the power flights are shown in Table II.

As in the glides, the specific weight of the encountered air is computed from the recorded barometric pressure and the observed strut temperature, the air being regarded as dry. It is realized that the specific weights thus derived are generally somewhat in excess of the correct

values, as the air at Langley Field is usually very humid even at an altitude of two or three thousand feet. However, since at ordinary temperatures the difference in weight between dry and saturated air is less than 1 per cent and since the air encountered was obviously intermediate in weight between dry and saturated air, it was felt that regarding the air as dry involved no error of consequence.

Velocity is computed from specific weight and from the velocity head as recorded by the pressure capsule connected to the trailing bomb Pitot.

R. P. M. are found from observations of the Veeder counter.

Angle of flight path is recorded by the trailing bomb inclinometer and angle of wing by the pendulum inclinometer. Angle of attack may be found by taking the difference between the two angles recorded. Because of difficulty in securing consistent records from the pendulum inclinometer, a different method of determining the angle of attack, described later, was used.

Weight is determined as in the no-thrust gliding flights.

Lift, drag, and thrust are determined as follows:

A first approximation or tentative lift L' ($= W \cos \alpha$) is assumed, thus neglecting the lift component of the propeller thrust. From this tentative lift the observed velocity head and the area of the wing surface C'_L (a tentative lift coefficient) is computed. A corresponding C'_D is read from the polar diagram, Figure 11, and a tentative angle of attack from Figure 12. From C'_D a tentative drag is computed. A tentative thrust T' , equal to tentative drag plus $W \sin \alpha$, is then deduced. A second approximation of lift is then determined by deducting $T' \sin B$, the lift component of tentative thrust, from the tentative lift. B is the angle of the propeller axis to the flight path and is 2° less than the angle of attack. From this second approximation of lift a new lift coefficient, angle of attack, drag coefficient, and drag are derived.

A second approximation of thrust is determined by adding, as before, $W \sin \alpha$ to the drag.

Trials for a third approximation of drag, deduced in a similar manner, gave values differing from the second approximation by too small an amount to be of practical consequence.

Lift and drag as given in Table II are thus second approximations, and angle of attack is that read from Figure 12 for a lift coefficient derived from the second approximation of lift. Likewise, the thrust of Table II is second approximation of drag + $W \sin \alpha$.

Horsepower is derived from the calibration curves of Figure 10 as follows:

It is first assumed that during the tests the engine changed from the condition as represented by the highest calibration curve to that as represented by the lowest; that such change was gradual and that therefore at any time between the first and last flight the condition would be represented by a calibration curve intermediate between A and B, the space being divided by 32 intermediate lines and these with A and B representing 34 calibrations, each of which would show the condition of the engine for the test flight of the corresponding number. Thus test flight 17 would have a calibration curve halfway between A and B. The early test flights would have calibration curves close to A and the later ones curves close to B. It is found that this method results in less dispersion of points from a smooth power curve than if a single calibration curve is used. In other words, two tests of a given propeller, one conducted at the beginning of the flights and the other at the end, appear more consistent if to the first a calibration curve near to A (fig. 10) is applied and to the second one near to B than they do if a single calibration curve is used for both.

The horsepower for standard air and at the observed R. P. M. is thus determined from the calibration assumed for each flight, and the horsepower for the conditions of flight is derived from this through the assumed relation: $HP. = C \frac{p}{\sqrt{T}}$, p being barometric pressure, T absolute temperature at carbureter intake, and C a constant.

We then have the coefficients as previously defined:

$$C_T = \frac{\text{thrust}}{\rho n^2 D^4}$$

$$C_P = \frac{\text{power}}{\rho n^3 D^5}$$

$$\eta = \text{efficiency}$$

$$= \frac{\text{thrust} \times \text{velocity}}{\text{power}}$$

$$= \frac{C_T}{C_P} \times \frac{V}{nD}$$

Any homogeneous system of units may be employed in deriving the above coefficients.

In Figures 13 to 17 the values of C_T , C_P , and η , derived from the flight tests, are shown as ordinates on abscissas of $\frac{V}{nD}$. Curves are drawn which represent, as nearly as practicable, the average of the experimental spots, while, at the same time, indicating a continuous and consistent relation. Table III shows the values of C_T , C_P , and η , finally chosen as best representing the average of experimental points and through which the curves of Figures 13 to 17 are drawn.

Figures 18 to 22 show the coefficients as derived both from model tests and from full-scale tests, the model tests being those of model propeller in combination with a model plane.

DISCUSSION

At the time these tests were started it was believed that the least reliable data would be those resulting from the estimated performance of an engine under conditions somewhat different from those of calibration. It was thought that thrust, as determined from addition of drag of the airplane and component of weight along the flight path, would be subject to little error. It appears, however, assuming that accurate measurements would result in points falling on smooth curves, as in the case of model tests, that there is little difference in the possible error of the power and thrust determinations, the advantage being somewhat in favor of the former. It is evident from the dispersion of spots that the possible error in a single spot is considerable but it seems likely that the curves drawn in Figures 13 to 17, representing as they do the average of many determinations, should show the performance of the full-scale propellers tested within a very moderate error.

With reference to the apparent greater possible error in thrust, it may be here noted that the thrust as determined is composed of two parts, one due to drag and the other due to component of weight along the flight path. Since the angle of the flight path is uncertain within 0.5 degree, the weight component of thrust may be in error as much as 17 pounds, in some cases amounting to 4 per cent of the total. If to this is added an error in drag, due to initial error in the polar diagram or to observation, the final error in thrust may be considerable.

If the efficiencies given in Table II are plotted, it will be found that the efficiency curves as drawn represent a fair average of the points. The dispersion from a smooth curve is, however, generally greater than for thrust or power. The three curves as drawn are consistent; efficiency being determined by

$$\eta = \frac{C_T}{C_P} \frac{V}{nD}$$

Referring to Figures 18 to 22, it may be seen that both thrust and power coefficients as determined from the flight tests are from 6 to 10 per cent more than those derived from model tests, the mean difference being about 8 per cent. The difference appears too consistent and of too great an amount to be chargeable to experimental or accidental error. In the case of

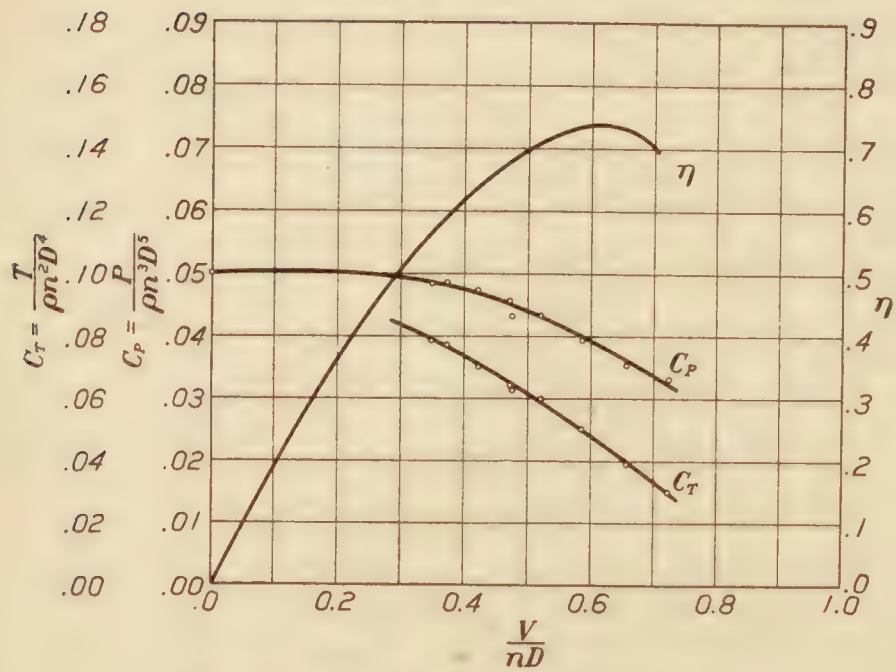


FIG. 13.—Propeller B' full scale with VE-7 airplane

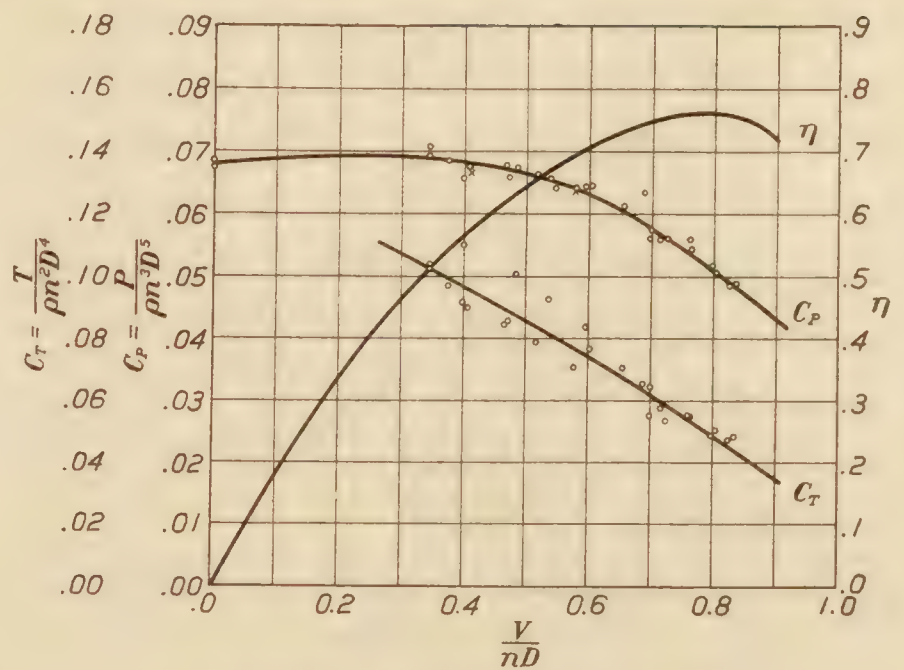


FIG. 14.—Propeller D' full scale with VE-7 airplane

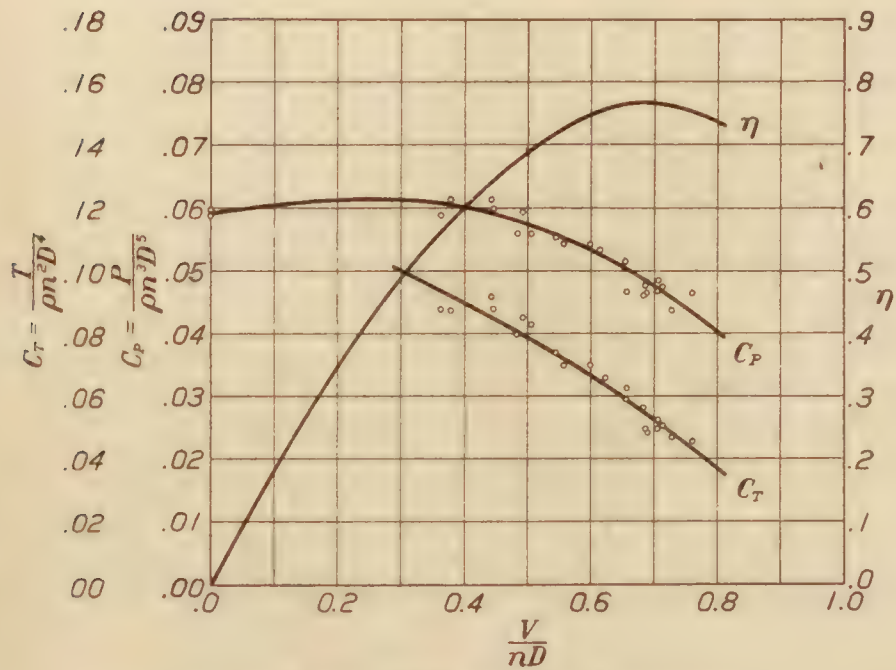


FIG. 15.—Propeller I full scale with VE-7 airplane

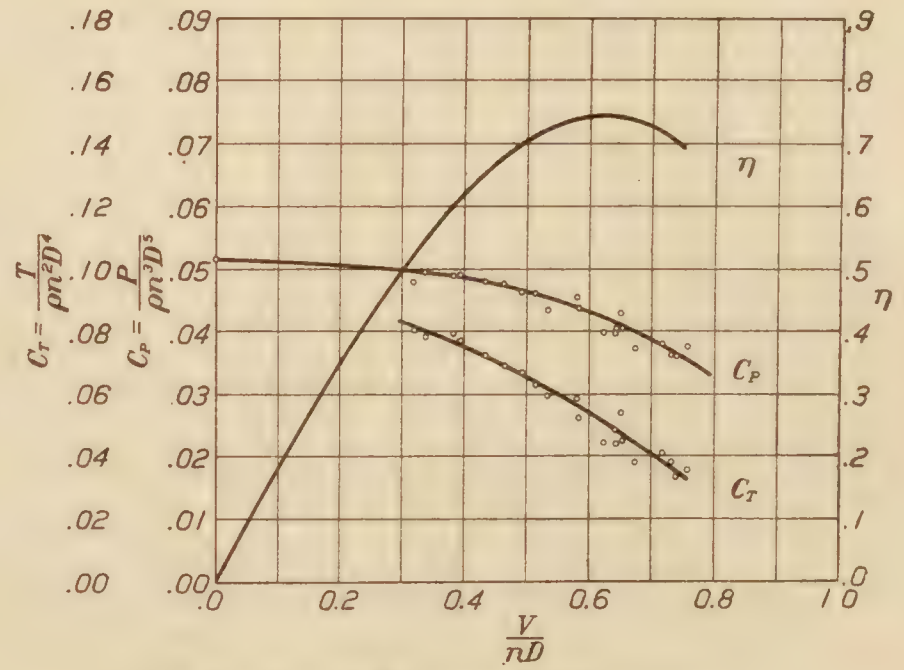


FIG. 16.—Propeller K' full scale with VE-7 airplane

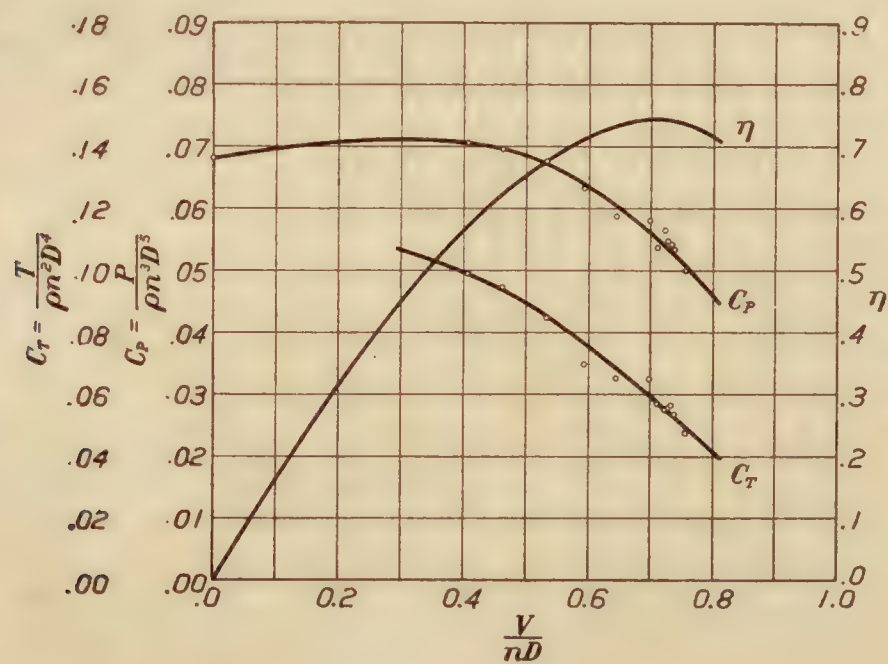


FIG. 17.—Propeller L' full scale with VE-7 airplane

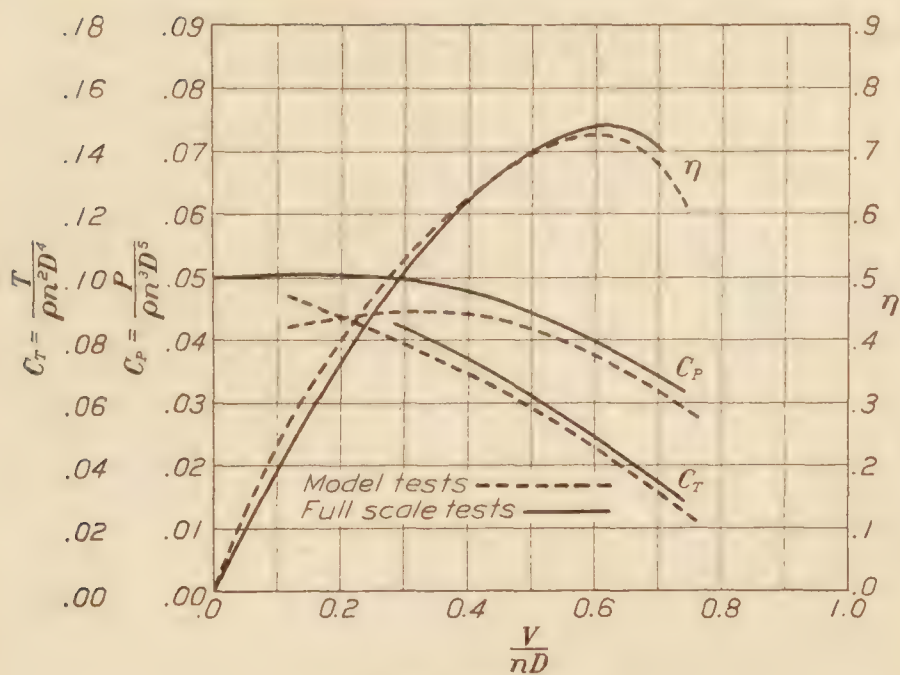


FIG. 18.—Propeller B'

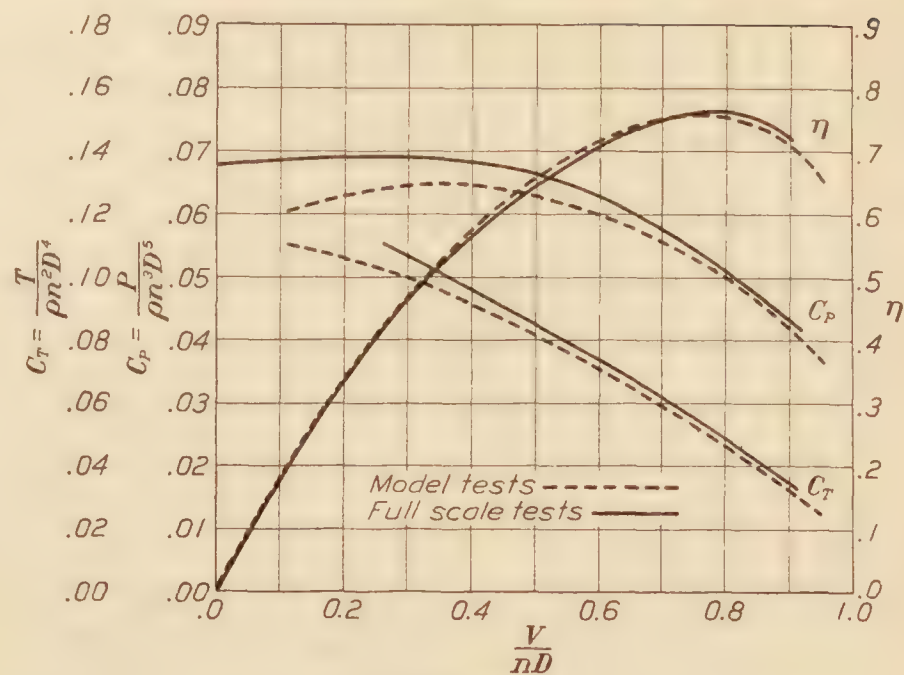


FIG. 19.—Propeller D'

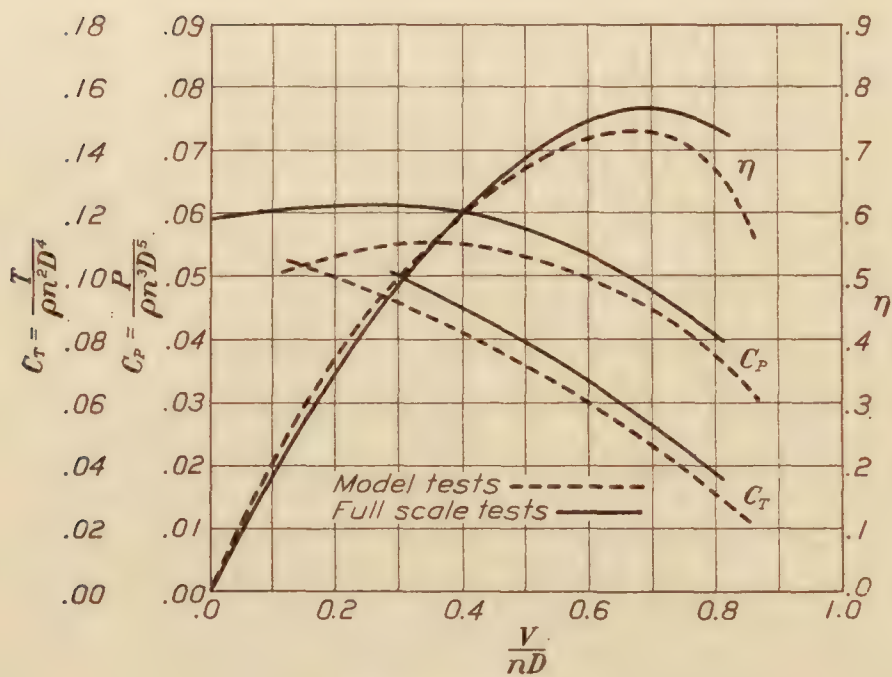


FIG. 20.—Propeller I

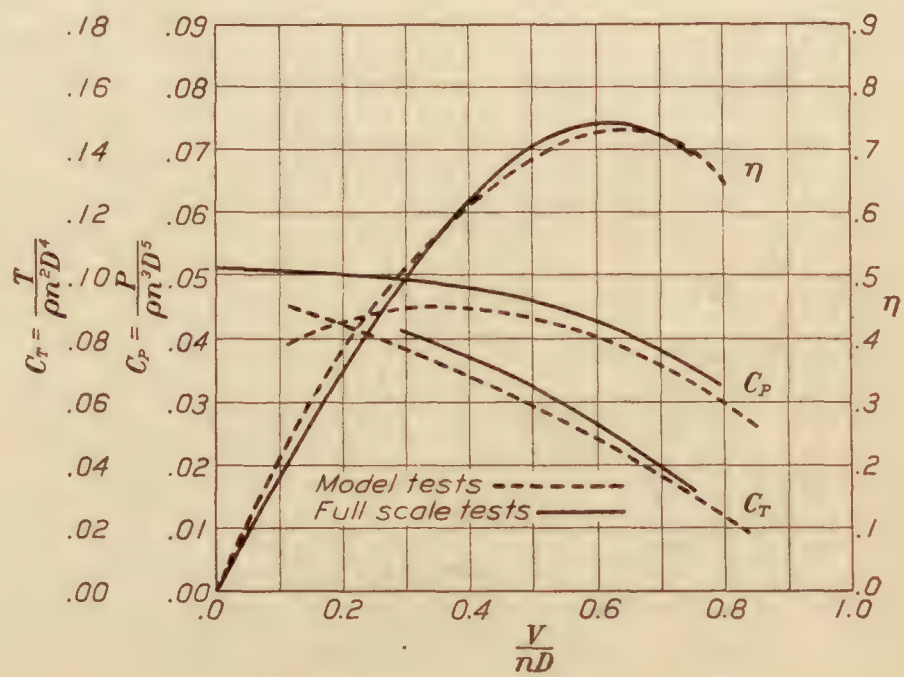


FIG. 21.—Propeller K'

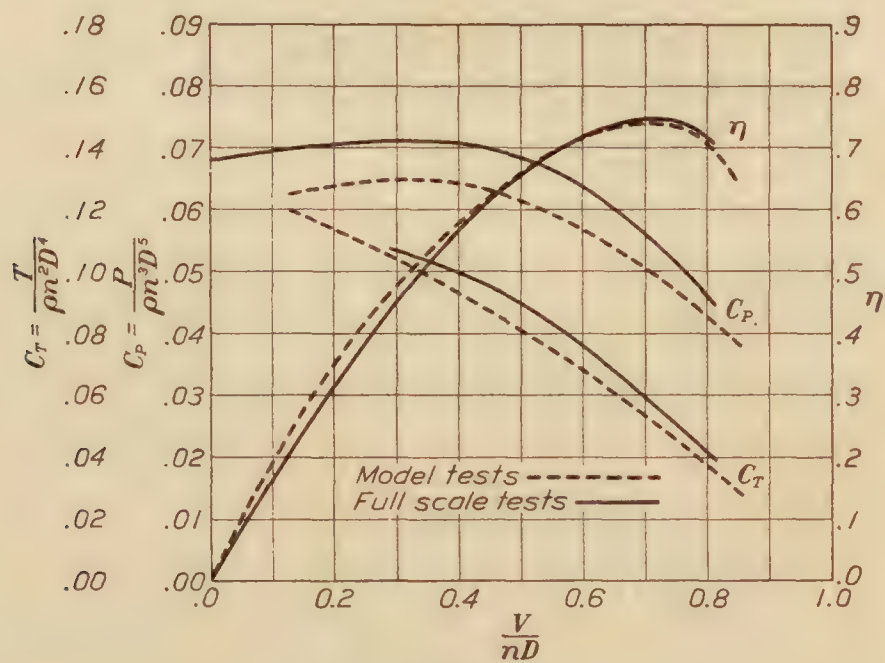


FIG. 22.—Propeller L'

efficiency the difference is considerably less but is also generally consistent. The full-scale propellers show slightly higher peak efficiency than the models and slightly lower efficiency at large slip. The difference is generally less than 3 per cent, in one case only, propeller I, being 4 per cent or more.

There appear to be three possible causes for a somewhat consistent difference between the results of these full-scale and model tests.

1. *Scale effect.*—The linear scale ratio of the full-size propellers and the models is 2.72. The velocity of advance for the flight tests is generally about three times that for the models. The VL for the sections of the full-size propellers is thus about eight times that for the models, the mean model value being about 50 (ft.-sec. units). If the formula

$$L_{c_2} = L_{c_1} + .057 \log_{10} \frac{v_2 l_2}{v_1 l_1} \text{ (Ref. 1)}$$

is applicable, the increase in lift coefficient for the full-scale propeller sections, due to the higher VL , would be such as to increase the thrust and power about the 8 per cent experienced.

2. *Difference in the geometry of the full-scale and model tests.*—In the case of the model propellers the propeller shaft is parallel to the direction of flight. The angle of attack is constant at 2° .

In the flight tests the angle of attack varies between 2° and 12° and the angle of the propeller shaft to the flight path between 0° and 10° . The propeller is thus generally in yaw; only a little at small slip (near peak efficiency) but appreciably at large slip. From such data as are available it appears that the effect of yaw should be to increase both power absorbed and thrust developed. The wider difference between the model and full-scale tests at extreme slip (greater yaw on full-scale) may thus be explained.

3. *Lack of complete similarity of full-scale and model airplanes.*—It will be noted by reference to Figure 24 that in the model airplane the tail surfaces and rear portion of the fuselage are omitted. This was unavoidable with the model propeller dynamometer as constructed. It appears, with respect to power absorbed, that tail surfaces and completed fuselage would have a qualitative effect similar to that of the model as used, but much less in amount. A slight increase in power for small slip and a slight decrease for large slip might thus be expected, as is shown in Part II. However, a considerable body of observation with other models goes to show the very rapid falling off of influence on the propeller with increase of distance between the propeller and the obstructing surface or body, and points definitely to the conclusion that the influence of surfaces giving generally a frictional drag and at distances of one and one-half diameters of the propeller or more would produce an effect on the propeller, presumably within the error of observation.

Likewise it seems unlikely that the slipstream interference offered by the tail surfaces would have any considerable effect upon the shaft thrust as exerted by the model propeller. As is shown in Part II, the thrust credited to the model propeller is equal to the shaft thrust minus the increase or augment of model drag. The shaft thrust might be expected to be larger for the complete model than for the partial model, perhaps by the same order of quantity as with the power. It is not clear what would be the result with regard to the augment of drag, since the slight degree of truncation of the fuselage would tend to offset the influence of the lacking parts of the model, thus perhaps leaving the augment but little changed.

In any case, however, and as noted above, there seems good observational ground for considering the influence of the omitted portions of the model on the propeller performance as presumably within the limit of observational error and in no case apparently sufficient to account for the measurable and consistent difference between model and full-scale results.

Further flight tests and corresponding tests with model propellers and airplanes should be conducted. For the flight tests it is most desirable that simple and reliable thrust and torque meters be developed. The shaft thrust in flight, although not directly applicable to the determination of useful work and consequently of efficiency, would be comparable with a like quan-

tity determined from a model test. The scale effect factor would thus be given a more definite value than if the indirect method of determining thrust, employed in the tests described, is used. The advantage of using a simple and dependable torque meter over relying upon a calibrated engine is obvious.

Indications of somewhat closer agreement between model and full-scale test results are given by model tests conducted at a later date. These tests were too few in number and of insufficient extent to be conclusive and were made too late for inclusion in this report, which was in page proof. They give, however, practically the same power coefficients as previous tests, but thrust coefficients generally somewhat greater, resulting in efficiencies over the working range, from 1 to 3 per cent higher.

It is obvious, in view of the uncertainty in the power developed by the engine, that the power coefficients for the full-scale tests might be made measureably less, and thus the efficiencies for the full-scale propellers also somewhat increased.

The increase in thrust coefficients for the model tests, the decrease in power coefficients for the full-scale tests, and the increase in efficiency for both would tend to bring the full-scale and model results somewhat closer together, and possibly make them as nearly the same as could be expected, considering the experimental errors necessarily involved.

PART II

MODEL TESTS

INTRODUCTION

The model research part of this general investigation was carried on, as noted, at the Aerodynamic Laboratory of Stanford University. There were supplied to the laboratory

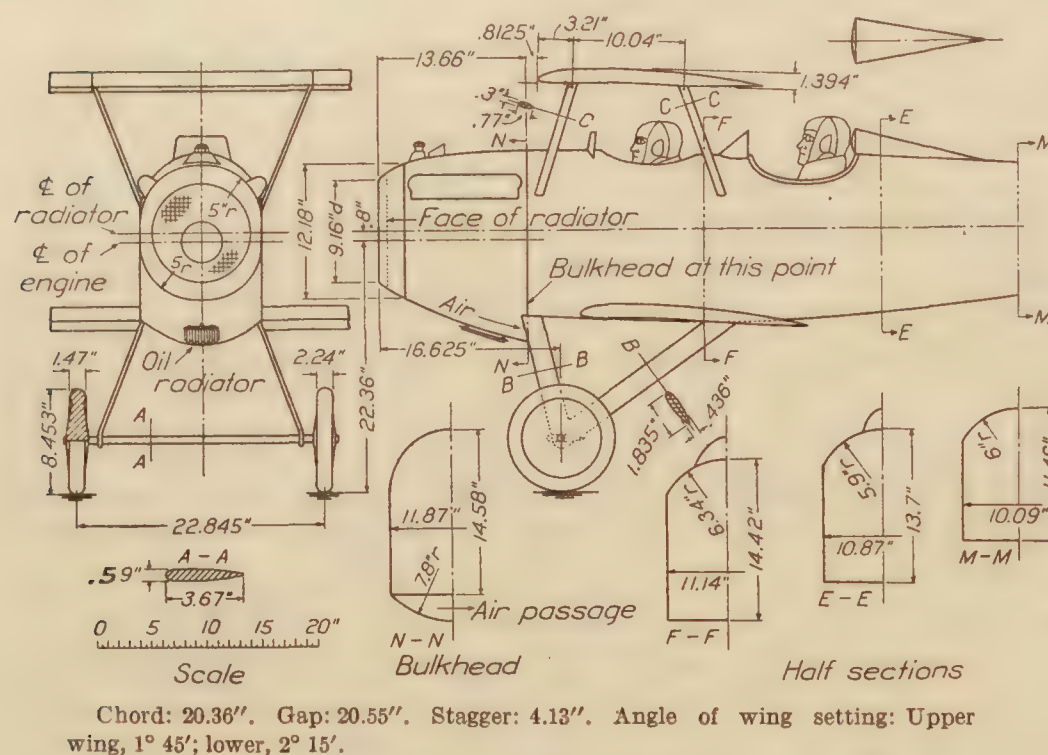


FIG. 23.—Wing tunnel model of VE-7 airplane

the propeller or be influenced by it. It will also be noted from the scale ratio that this 6 feet of model wing spread represents about 16 feet on the airplane, or some 47 per cent of the total wing spread.

A cut of the model with one of the propellers in position is shown in Figure 24.

Due to the construction of the dynamometer and wind tunnel, the rear extension of the fuselage and tail surfaces were necessarily omitted. The fuselage was faired into the body of the dynamometer with only such clearance as to insure complete freedom under observation.

drawings and specifications for five propellers with dimensions and characteristics as shown in Figures 1 to 5, together with a drawing (fig. 23) showing the central portion of the Vought airplane. The scale ratio between model and full size was 0.3674, thus giving a diameter of close to about 3 feet for the model propellers and of 21 inches for the wing chord of the model plane. The model wings were extended in span on each side approximately 18 inches beyond the blade tips of the propellers, and thus included beyond any question all parts of the model which could in any direct way react with

The fuselage was also hollow, with air entering through the mesh representing the radiator and streaming aft between fuselage and dynamometer body, thus reducing the effect of the truncation at the rear end.

For some comment as to the possible or probable influence of the omitted portions of the model, see Part I, "Discussion."

In an investigation of the character proposed it is clear that the airplane structure, viewed as an obstruction in the wake of the propeller, must also be viewed as a necessary part of the airplane and not as an appendage which might be installed or removed at will.

From this point of view we may develop as follows the form of analysis suited to these conditions.

Assume the model and the propeller in operative relation. The propeller under specified conditions, as determined by a given value of V/nD , develops an actual thrust (pull) T . In so doing, however, it increases the wind reaction of the air on the model by some amount A , which may thus be termed the augment of resistance due to the operation of the propeller. If then from the total thrust T there be subtracted the augment A , there will remain a residual or net thrust $(T-A)$, which alone can be credited to the propeller as a useful final product.

Then if the relative air speed of the airplane is V , the net or useful power will be measured by the product $(T-A)V$. Again, if, in order to realize these conditions, the actual torque and revolutions per second required are Q and n , the input or shaft power will be measured by $2\pi nQ$.

We may then define "propulsive efficiency" as the quotient $(T-A)V \div 2\pi nQ$, and if we denote this efficiency by η we shall have

$$\eta = \frac{(T-A)V}{2\pi nQ}$$

From a slightly different viewpoint we may imagine the propeller at the extremity of a shaft, say 1,000 feet in length, extended out ahead of the airplane. In such case we may assume the interaction between airplane and propeller as nonexistent. Both propeller and airplane will operate as in free air, and the resistance of the latter will be the towed or free-air resistance at the given speed. Likewise the thrust (pull) will equal the resistance, and the propulsive efficiency as defined above (with $A=0$) will be the same as the true propeller efficiency in free air. If then we imagine the shaft to be gradually shortened in, there will begin to develop in due time an interaction between the airplane and the propeller, as a result of which both the thrust (pull) developed and the resistance to be overcome will increase. Finally, with the propeller and airplane in their normal operative relation, we shall find a notable increase in both, and if the engine is driven at such speed as will serve to give the same air speed of the airplane as before, then we may consider that the same net result is accomplished. This useful power will evidently be $(T-A)V$ and the input power to accomplish this will be $2\pi nQ$, the power resulting from the actual n and the actual Q . The ratio between the two will then give the propulsive efficiency under the given conditions of operation as defined by the actual value of V/nD . It should be noted that the value of n and hence of V/nD for a given air speed with the propeller and airplane interacting will not, in general, be the same as that for the ideal case without interaction. The attempt to compare the propulsive efficiency at the value of V/nD in the

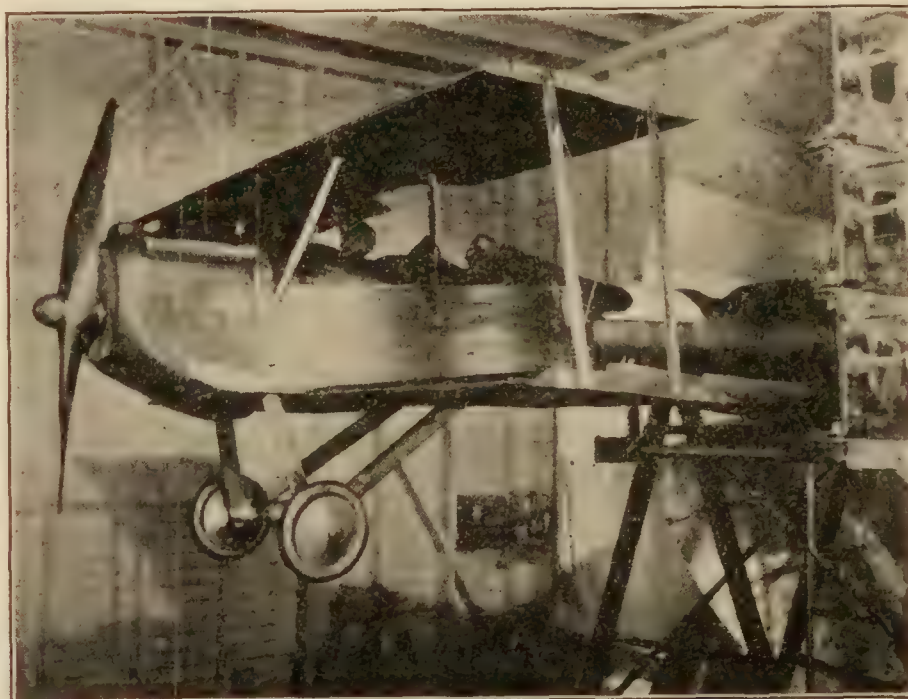


FIG. 24.—Model propeller with model of VE-7 airplane showing method of support

actual case with interaction with the propeller efficiency at different value of V/nD without interaction greatly complicates the problem, however, and it is believed that for present purposes the comparison of the curve of propulsive efficiency on an axis of V/nD with the corresponding curve of propeller efficiency (free) on its axis of V/nD will show sufficiently well the character and extent of the interaction between the airplane and the propeller in its effect on the efficiency of operation.

In order to realize the condition outlined in the preceding analysis, the program of measurements to be made on the model airplane and propeller must comprise the following:

- (1) Wind resistance tests of the model airplane alone.
- (2) The usual tests of the propeller alone, giving for a series of values of V/nD values of thrust, torque, and efficiency.
- (3) Tests of the combination, including resistance measurements on the model and the usual measurements for the propeller. In the set-up for the test in combination the propeller and model are maintained in their proper geometrical relation but with complete independence of suspension and control, so that all measurements may be made independently and thus give values for the propeller as influenced by the model and for the model as influenced by the propeller.

SET-UP OF APPARATUS AND MODEL

In order to realize this program of measurements, the general character of the apparatus employed with the set-up of the model may be briefly indicated as follows:

It will be recalled that the wind tunnel at Stanford University is of the Eiffel type, with a throat diameter of 7.5 feet and an experiment chamber with a length of 12 feet.

The dynamometer as indicated in the cut of Figure 24 consists essentially of a slender tapering barrel some 9 feet long mounted on knife-edges as a cradle dynamometer and with the model propeller motor located in the larger, down-wind end of the barrel, faired in as a part of the barrel form. The motor is connected to the propeller through a special form of drive which transmits torque with longitudinal freedom. This general arrangement provides for the direct measurement of thrust and torque which are weighed on beam scales graduated, respectively, in hundredths of kilograms and in thousandths of kilogram-meters.

In order to provide for the independent measure of forces on the propeller model and on the airplane model, the latter was suspended by piano wires from the ceiling of the experiment chamber, the length of suspension being about 7 feet. This arrangement is shown in the cut of Figure 24.

For the direct measurement of air forces on the model, a piano-wire bridle was attached to the two sides of the model at shaft level and thus accommodating the propeller between the two sides of the bridle leads. From the apex of the triangle thus formed a single piano wire was led forward (up wind) through the honeycomb baffle, through and beyond the tunnel inlet to the end wall of the building, and over a carefully fitted-up pulley down to a gross weight on the plate of a beam scale weighing to hundredths of a pound. Thus by subtraction the pull on the model due to air flow may be directly weighed on the scale.

In order, however, that the reading of the scale may be made to indicate air forces and nothing else, it is necessary that the model, when in the observing condition, should hang in the free gravity position; otherwise there will be a gravity component, plus or minus, included in the scale reading. In order to eliminate any such component, the following operative routine was followed.

The model, without wind and disconnected from the piano wire leading to the scale, was allowed to hang freely under gravity, and while so hanging a transit instrument, set up abreast of the model and at the side of the experiment chamber entirely out of the wind stream, was adjusted with vertical cross hair on a reference mark on a paper scale attached to the model. Then, during the observations, the model was brought, by suitable fine-motion adjustments, exactly to this initial or zero position, with the mark on the vertical cross hair. Under these conditions the scale readings may be properly interpreted as giving (by subtraction from the gross) the actual wind forces on the model.

It is obvious, furthermore, that this arrangement may be used either with or without the propeller, and thus provide for a measurement of air forces on the model, either in a homogeneous air stream or as influenced by the operation of the propeller placed with any desired clearance between itself and the forward edge or plane of the model.

OBSERVATIONS

In accordance with the general methods indicated in the preceding section, observations were made covering the various elements of the problem. These observations, with the resulting values of the various coefficients, are given in Tables IV and V.

In the reduction of these observations, the following coefficients have been employed:

$$\begin{aligned}
 C_T &= \text{thrust coefficient (propeller alone)} \text{ -----} = \frac{T}{\rho n^2 D^4} \\
 C_T &= \text{thrust coefficient (propeller with plane)} \text{ -----} = \frac{T - A}{\rho n^2 D^4} \\
 C_P &= \text{power coefficient} \text{ -----} = \frac{P}{\rho n^3 D^5} \\
 \eta &= \text{efficiency (propeller alone) or propulsive efficiency (propeller with plane)} \text{ -----} = \frac{C_T}{C_P} \frac{V}{nD}
 \end{aligned}$$

Graphical representations of these results are shown in the diagram of Figures 25 to 29.

In these diagrams the individual values of the various coefficients are represented by the plotted points. A smooth curve as best indicating a continuous and consistent law is then drawn through and among these spots, and such curve is accepted as the best indication of the law relating the values of the coefficient to varying V/nD . The values of the efficiency η are then derived from the smooth curves of these coefficients and are plotted as shown in the various diagrams. Tables VI and VII give, for various values of V/nD , the values of the coefficients and resulting efficiencies finally chosen as best representing the continuous and consistent law above referred to.

DISCUSSION

(1) It will be noted in all cases that the presence of the obstruction behind the propeller has the effect of moving to the right on the axis of V/nD the point for zero thrust. This condition is readily seen to follow as a result of the slowing down of the column of air actually operative on the propeller as compared with the air passing freely at the side of the obstruction. For any given value of wind velocity as based on the latter the air column acting on the propeller will be slowed down, the value of n for zero thrust will be decreased, and the value of V/nD correspondingly increased.

As will be noted from the diagram, the amount of this shift on the V/nD scale is 0.05 or less for the various propellers employed and for the amount of obstruction represented by the VE-7 model.

(2) From this shift of the point for zero thrust it naturally results that the curve for thrust or thrust coefficient for the combined case as compared with the propeller alone starts farther to the right and near the start lies above that for the propeller alone.

This means that for large values of V/nD the curves for propeller with model will be above that for propeller alone, as noted in the various diagrams. (Figs. 25 to 29.)

As the slip becomes greater, however, and the values of V/nD become less, this excess decreases, and the two curves ultimately meet and cross. For the conditions represented by the present research this point of crossing is seen to be not far from the value of V/nD for best efficiency.

Beyond this point the curve for thrust coefficient lies below that for the propeller alone, thus showing, for this part of the range, a definite loss in value for the propeller in operative position forward of the model.

(3) It thus appears that for large values of V/nD the presence of the model results in a definite increase in the net propulsive effort derived from the propeller, while for moderate and small values the reverse is the case, and, furthermore, that in general the latter condition (loss of net propulsive effort) obtains over that part of the range which must be employed in practical cases.

(4) Similarly, as for the thrust coefficient, the torque, and hence the shaft power coefficient for the propeller with model, is increased for large values of V/nD and decreased for small values, with a crossing point usually at a smaller value of V/nD than for the thrust coefficient. These conditions are plainly seen in the diagrams of Figures 25 to 29.

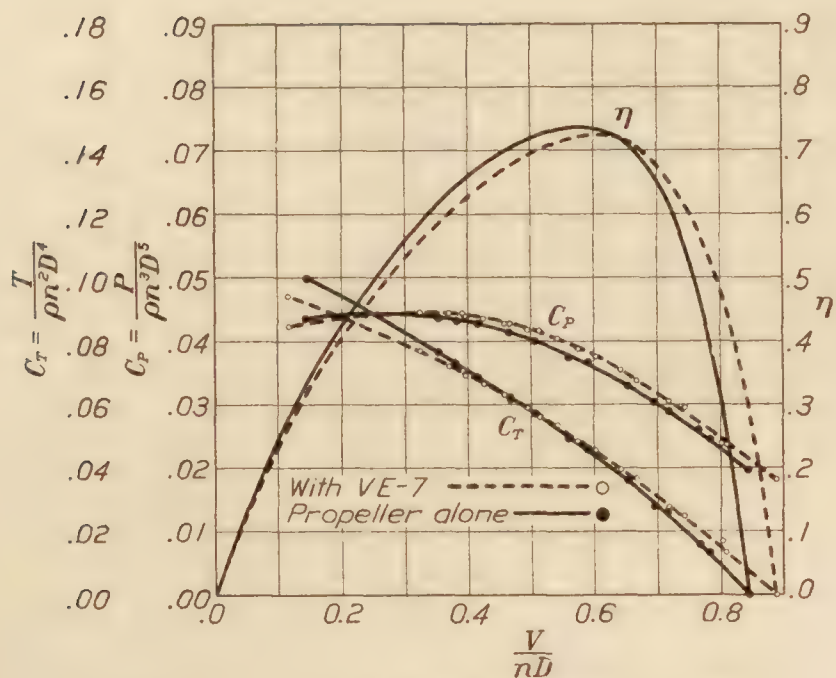


FIG. 25.—Model propeller B

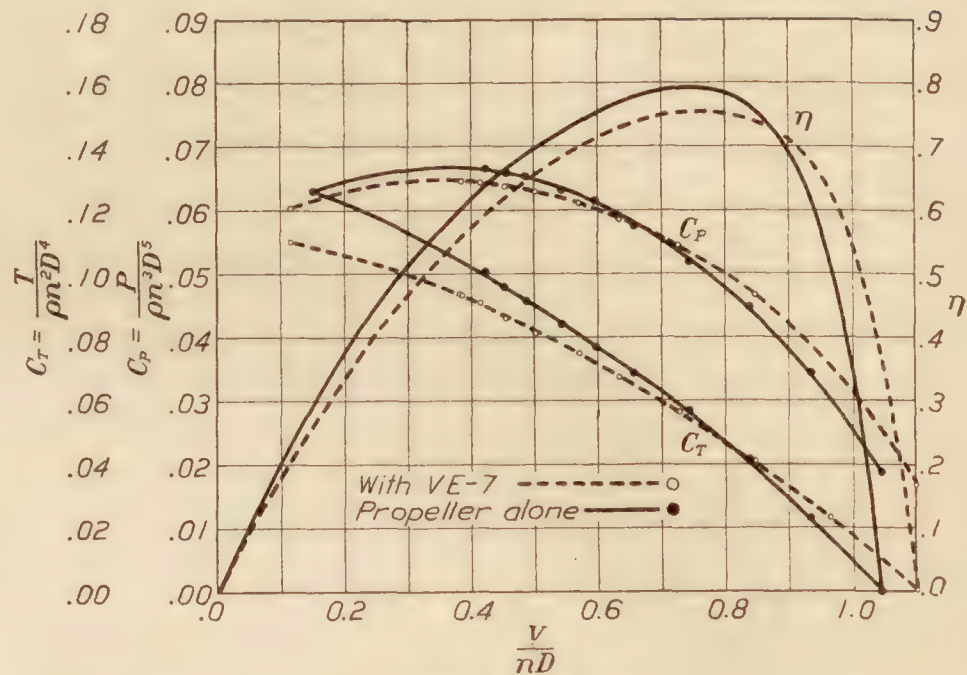


FIG. 26.—Model propeller D'

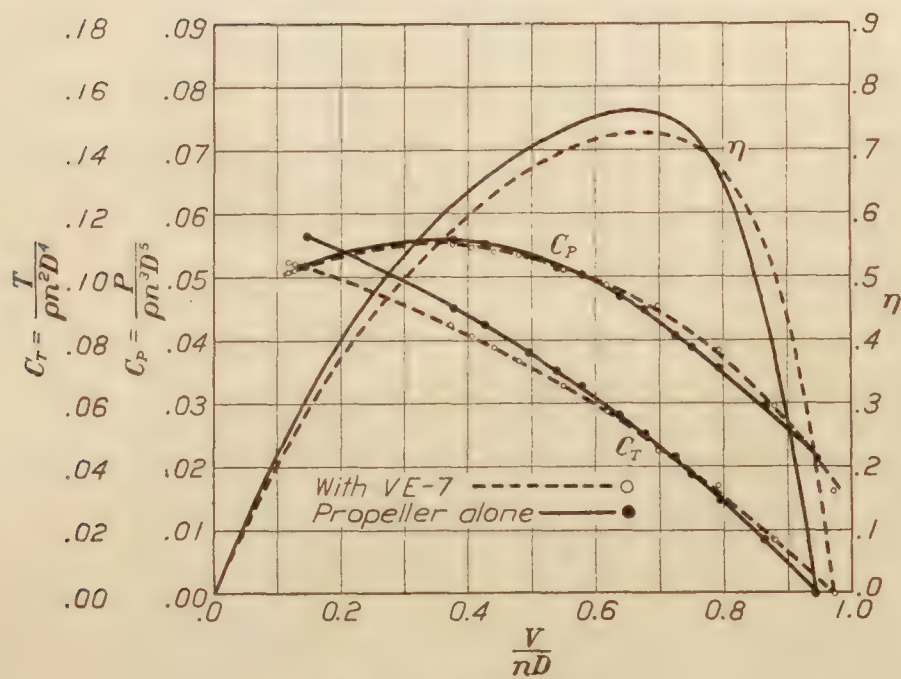


FIG. 27.—Model propeller I

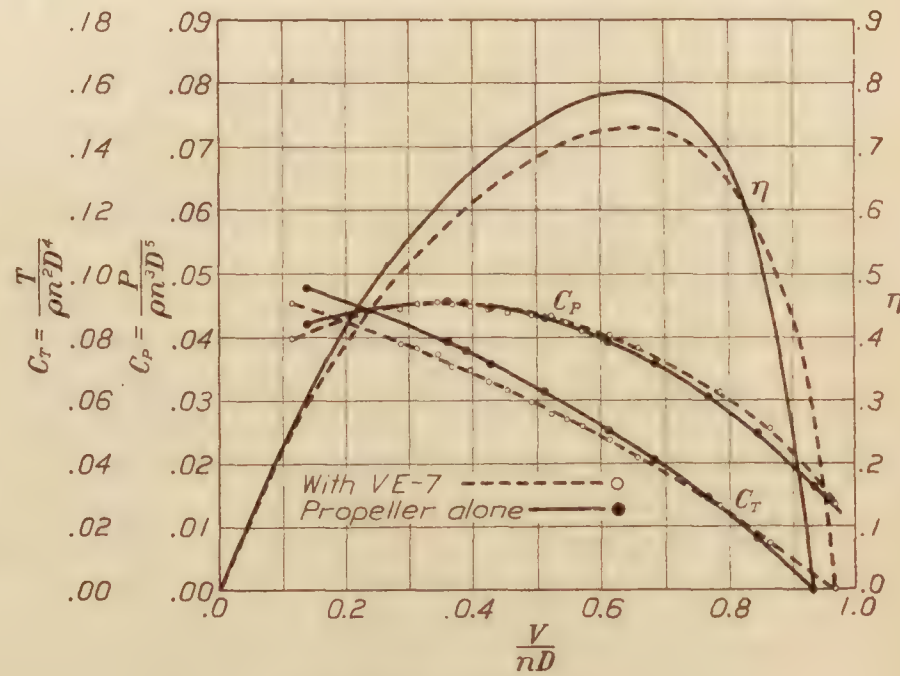


FIG. 28.—Model propeller K'

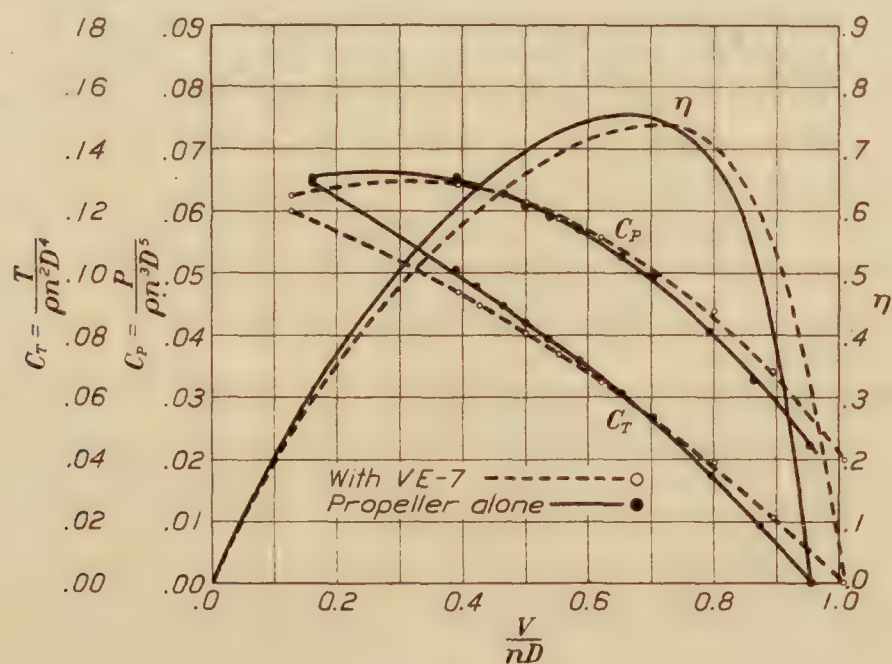


FIG. 29.—Model propeller L

(5) In consequence of these relative changes in the values of the thrust and power coefficients, it results that on the axis of V/nD the point of zero efficiency (for large values of V/nD) is carried to the right (larger values of V/nD) for operation with the model and that generally for large values of V/nD the propulsive efficiency is greater with the obstruction than with the propeller alone. On the other hand, for small or medium values of V/nD the propulsive efficiency for operation with the model is less than that for the propeller alone.

The two curves of efficiency thus cross and the point of equal values is seen to be, in general, at a value of V/nD somewhat larger than that for the maximum value on either curve.

Likewise it is seen that the maximum values of the propulsive efficiency for operation with the model are in all cases less than those for the propeller alone, and in particular that this loss in efficiency is carried over the range of values of V/nD from those for maximum value of efficiency along the direction of decreasing values (increasing slip). Due to limitations in diameter, it results in the normal case that propellers must be used over a range of values of V/nD , beginning with a large value somewhat less than that for maximum efficiency and extending over a small range in the direction of decreasing values. It thus follows that the air propeller in the normal practical case must be used over a segment of the efficiency curve beginning near but somewhat to the left (as here plotted) of the maximum value and extending to the left over a range of decreasing values of efficiency and hence over a range where the effect of an obstruction, as represented by the nose of the fuselage or other part of the airplane structure, will be to decrease the propulsive efficiency as compared with that for the propeller alone at the same value of V/nD .

(6) The amount of the loss in propulsive efficiency over the working range is seen to vary between some 3 and 5 per cent, and so far as these present observations indicate such loss is greater with high pitch ratio than with low and with narrow blades than with wide.

While these conclusions are in general agreement with those drawn from other similar investigations, the number of variant forms in the present research is too small to warrant the drawing of any final or definite general conclusions regarding the character of the relation between such loss in propulsive efficiency and the detailed characteristics of the propeller form.

TABLE I
GLIDE TESTS

Flight and run No.	Angle of glide path	Angle of wing	Angle of attack	Weight	Lift	Apparent drag	$1/2\rho V^2$	Specific weight of air	Velocity ft/sec.	R. P. M.	V/nD	Thrust	True drag	C_L	C_D
1-2	-6.2	3.9	10.1	2,070	2,053	223.6	9.60	0.0688	94.8	745	0.935	10.0	234	0.757	0.0861
1-3	-6.6	1.1	7.7	2,063	2,049	237.0	12.20	.0688	106.9	830	.946	9.1	246	.594	.0712
1-4	-6.6	-0.3	6.3	2,056	2,042	236.3	14.80	.0688	117.7	965	.896	34.7	271	.487	.0646
1-5	-7.6	-2.8	4.8	2,049	2,031	271.1	19.10	.0688	133.6	1,110	.892	48.9	320	.376	.0591
1-6	-9.2	-5.7	3.5	2,042	2,016	326.5	23.90	.0688	149.6	1,200	.916	39.6	366	.297	.0540
1-7	-10.0	-7.6	2.4	2,035	2,004	353.3	28.80	.0688	164.1	1,300	.928	35.7	389	.246	.0476
1-8	-11.2	-9.2	2.0	2,028	1,989	393.9	33.80	.0688	177.9	1,415	.924	47.7	442	.208	.0462
1-9	-13.2	-11.2	2.0	2,020	1,967	461.1	35.80	.0688	183.0	1,500	.897	83.3	544	.194	.0536
2-1	-6.0	-5.1	11.1	2,070	2,059	216.3	9.10	.0691	92.0	740	.914	15.8	232	.798	.0900
2-2	-6.8	1.7	8.5	2,063	2,049	244.3	12.10	.0702	105.3	820	.945	9.2	253	.598	.0739
2-3	-8.5	-4.1	4.4	2,056	2,033	303.9	22.30	.0702	142.9	1,180	.890	56.7	361	.322	.0571
2-4	-9.8	-6.2	3.6	2,049	2,019	348.7	27.50	.0714	157.5	1,300	.891	69.6	419	.259	.0538
2-5	-11.6	-8.7	2.9	2,042	2,000	410.7	34.30	.0714	175.9	1,420	.910	63.7	475	.206	.0489
2-6	-14.3	-12.0	2.3	2,035	1,972	502.6	43.20	.0725	195.7	1,580	.910	78.6	581	.161	.0475
22-2	-7.4	7.7	15.1	2,070	2,053	266.6	6.76	.0695	79.1	624	.932	7.5	274	1.070	.1430
22-3	-5.8	3.9	9.7	2,066	2,055	208.9	9.62	.0700	94.0	752	.919	15.1	224	.754	.0822
22-4	-6.7	-0.1	6.6	2,062	2,048	204.6	12.74	.0702	108.1	828	.959	4.4	209	.568	.0579
22-5	-6.9	-2.1	4.8	2,058	2,043	247.2	16.11	.0702	121.5	976	.915	27.0	274	.447	.0600
22-6	-7.1			2,054	2,038	253.9	19.91	.0705	134.8	1,100	.900	43.6	298	.361	.0528
23-2	-10.0			2,069	2,037	359.2	25.50	.0701	153.0	1,192	.943	21.0	380	.282	.0526
23-3	-11.3			2,064	2,024	404.3	30.20	.0700	166.6	1,336	.917	48.5	452	.236	.0528
23-4	-13.5			2,059	2,002	480.6	36.60	.0702	183.2	1,436	.938	35.6	516	.193	.0498
23-5	-15.4			2,054	1,981	545.8	43.40	.0717	197.4	1,532	.947	31.0	577	.161	.0469
24-2	-7.1	7.1	14.2	2,070	2,054	255.8	6.45	.0697	77.2	576	.985	-22.2	234	1.123	.1280
24-3	-6.1	5.6	11.7	2,066	2,054	219.6	7.28	.0695	82.1	656	.920	11.1	231	.996	.1120
24-4	-5.9	3.3	9.2	2,062	2,051	212.2	8.99	.0695	91.2	744	.901	19.2	231	.806	.0909
24-5	-6.0	1.6	7.6	2,058	2,047	215.1	10.39	.0698	97.9	792	.908	20.0	235	.696	.0799
24-6	-7.1	0.0	7.1	2,054	2,038	253.7	12.20	.0698	106.1	860	.907	23.6	278	.589	.0805
25-2	-6.9	-1.1	5.8	2,070	2,055	248.6	14.30	.0697	114.9	892	.946	10.6	259	.507	.0640
25-3	-7.4	-2.5	4.9	2,066	2,049	266.1	16.30	.0698	122.5	960	.938	15.8	282	.444	.0611
25-4	-7.6	-3.2	4.4	2,062	2,044	272.8	18.50	.0698	130.6	1,024	.937	18.6	291	.390	.0555
25-5	-8.0	-4.5	3.5	2,058	2,038	286.5	20.50	.0699	137.4	1,064	.949	13.1	300	.351	.0517
25-6	-8.8	-5.4	3.4	2,054	2,030	314.3	22.50	.0703	143.5	1,108	.952	12.6	327	.318	.0513
26-2	-8.1	-6.4	1.7	2,070	2,049	291.6	25.20	.0709	151.3	1,216	.914	41.5	333	.287	.0466
26-3	-11.2	-9.0	2.2	2,066	2,027	401.2	29.90	.0711	164.5	1,316	.918	46.9	448	.239	.0529
26-4	-13.1	-11.1	2.0	2,062	2,008	467.3	36.90	.0714	182.4	1,436	.934	39.6	507	.192	.0485
26-5	-15.0	-13.5	1.5	2,058	1,988	532.6	42.90	.0718	196.1	1,592	.905	86.1	619	.163	.0509
26-6	-15.4	-13.2	2.2	2,054	1,980	545.8	47.00	.0710	206.3	1,664	.911	90.6	637	.149	.0478

TABLE II
POWER FLIGHT DATA
PROPELLER B'

Flight and run No.	Specific weight, pounds per ft. ³	V feet per second	R. P. M.	α Angle of flight path	Angle of attack	W	L	D	T	HP.	V/nD	C _T	C _P	η
6-2	0.0748	84.4	1,604	12.6	9.6	2,069	1,916	214	666	174	0.372	0.0771	0.0487	0.589
6-3	.0748	97.0	1,627	11.1	7.3	2,064	1,953	228	625	175	.421	.0702	.0468	.632
6-4	.0746	111.5	1,672	9.7	5.5	2,059	1,994	259	603	181	.471	.0641	.0447	.675
8-2	.0744	125.4	1,704	8.2	4.3	2,054	2,011	290	582	185	.521	.0600	.0435	.719
6-5	.0724	79.1	1,608	12.5	11.3	2,069	1,901	212	661	168	.348	.0785	.0484	.565
8-3	.0721	113.8	1,688	9.4	6.3	2,064	1,992	243	581	175	.476	.0628	.0433	.691
8-4	.0720	146.5	1,764	4.5	3.3	2,059	2,032	354	515	184	.587	.0505	.0401	.739
8-5	.0728	174.9	1,872	0	2.1	2,054	2,046	481	481	197	.658	.0395	.0356	.730
8-6	.0718	197.0	1,928	-5.1	1.5	2,049	2,044	589	400	198	.724	.0307	.0333	.667
8-7	.0765	0	1,620							180	0		.0477	0

PROPELLER D'

11-2	0.0733	874.1	1,648	12.6	12.9	2,070	1,860	218	670	174	0.345	0.1038	0.0687	0.521
11-3	.0737	7.7	1,684	11.2	9.1	2,066	1,945	218	618	178	.399	.0911	.0656	.554
11-4	.0739	102.4	1,664	9.6	5.8	2,062	1,983	238	582	177	.471	.0877	.0674	.613
11-5	.0737	121.4	1,670	7.2	4.7	2,058	2,015	280	588	178	.557	.0806	.0672	.668
11-6	.0742	134.4	1,704	5.6	3.7	2,054	2,027	320	520	182	.603	.0765	.0643	.718
31-2	.0741	72.4	1,608	14.9	13.8	2,070	1,817	229	761	168	.345	.1026	.0707	.501
31-3	.0747	86.2	1,612	13.3	12.3	2,065	1,862	214	690	169	.410	.1095	.0700	.641
31-4	.0745	103.7	1,640	11.5	6.4	2,060	1,970	240	651	171	.484	.1001	.0672	.720
31-5	.0747	116.9	1,660	9.7	4.9	2,055	1,992	269	615	173	.539	.0922	.0657	.756
31-6	.0747	131.1	1,688	7.5	3.9	2,050	2,012	310	578	177	.595	.0837	.0641	.777
31-8	.0765	0.0	1,650	0.0						178	0		.0675	.00
32-1	.0762	167.5	1,800	0.0	2.2	2,075	2,073	464	464	192	.713	.0579	.0559	.738
32-2	.0746	148.0	1,724	4.3	3.2	2,070	2,052	352	507	180	.657	.0704	.0611	.757
32-3	.0749	162.6	1,780	1.7	2.3	2,065	2,040	433	494	187	.700	.0642	.0571	.787
32-4	.0745	179.5	1,808	-2.0	1.9	2,060	2,049	513	441	188	.761	.0551	.0557	.761
32-5	.0792	199.5	1,888	-5.0	1.6	2,055	2,051	582	403	182	.804	.0504	.0505	.802
32-6	.0707	205.2	1,908	-6.5	1.4	2,050	2,041	626	394	187	.824	.0471	.0494	.786
32-7	.0698	206.4	1,896	-6.8	1.3	2,045	2,034	634	392	184	.835	.0481	.0501	.802
32-8	.0757	171.2	1,808	0.0	2.0	2,040	2,039	480	480	193	.726	.0598	.0560	.775
9-2	.0709	81.5	1,660	11.0	11.7	2,069	1,914	216	611	172	.375	.0964	.0684	.528
9-3	.0714	88.6	1,670	10.1	9.3	2,064	1,953	218	580	174	.407	.0898	.0674	.542
9-4	.0710	102.0	1,680	8.9	7.5	2,059	1,978	229	547	175	.466	.0841	.0677	.580
9-5	.0715	114.7	1,700	7.5	5.5	2,054	2,005	259	527	177	.517	.0786	.0653	.622
9-6	.0715	130.0	1,720	5.2	4.2	2,049	2,021	298	484	179	.579	.0705	.0640	.638
12-2	.0735	155.2	1,728	1.9	2.7	2,070	2,063	395	464	185	.689	.0655	.0632	.714
12-3	.0734	166.8	1,828	0.0	2.3	2,065	2,062	437	437	193	.699	.0549	.0560	.685
12-4	.0734	184.5	1,850	-2.4	1.8	2,062	2,044	532	446	194	.764	.0548	.0542	.772
12-5	.0731	197.0	1,892	-4.8	1.5	2,058	2,053	600	428	197	.798	.0504	.0516	.779
12-6	.0765	0.0	1,640							182	0		.0699	0

PROPELLER I

4-2	0.0734	95.7	1,590	12.1	7.7	2,063	1,951	228	660	171	0.442	0.0915	0.0611	0.662
4-3	.0738	108.3	1,622	10.8	5.9	2,056	1,973	247	632	175	.491	.0847	.0582	.714
4-4	.0742	123.9	1,680	8.5	4.4	2,049	2,000	286	589	183	.543	.0732	.0551	.722
4-5	.0749	137.9	1,682	6.8	3.4	2,042	2,015	332	575	186	.599	.0699	.0549	.762
4-6	.0748	156.0	1,747	4.0	2.6	2,035	2,024	403	545	192	.657	.0622	.0506	.808
4-7	.0752	169.0	1,825	1.8	2.1	2,028	2,025	469	531	200	.682	.0562	.0460	.832
4-8	.0765	0	1,580							177	0		.0617	0
5-2	.0744	79.4	1,615	12.7	12.5	2,074	1,872	217	663	174	.361	.0876	.0586	.540
5-3	.0750	108.7	1,660	10.6	5.8	2,068	1,987	251	631	181	.481	.0794	.0558	.684
5-4	.0739	183.7	1,852	-2.0	1.8	2,062	2,062	530	458	195	.729	.0470	.0438	.781
20-1	.0740	167.5	1,796	0	2.2	2,074	2,072	450	450	192	.686	.0492	.0475	.710
20-2	.0707	81.5	1,580	10.6	11.1	2,069	1,927	215	595	161	.381	.0881	.0607	.553
20-3	.0705	96.1	1,584	10.3	8.0	2,064	1,965	225	594	160	.445	.0876	.0598	.652
20-4	.0700	111.3	1,616	9.2	5.9	2,058	1,989	249	578	162	.505	.0823	.0577	.720
20-5	.0701	126.2	1,664	6.6	4.5	2,054	2,011	284	520	167	.557	.0698	.0542	.717
20-6	.0704	140.5	1,680	4.9	3.5	2,049	2,025	327	502	170	.614	.0658	.0531	.760
20-7	.0740	169.5	1,808	-0.3	2.1	2,044	2,043	461	450	193	.689	.0485	.0463	.722
20-8	.0765	0	1,600							175	0		.0588	0
21-1	.0725	171.0	1,784	-0.6	2.2	2,074	2,072	459	437	184	.712	.0504	.0486	.738
21-2	.0704	155.9	1,720	2.4	2.7	2,069	2,061	384	471	175	.665	.0589	.0513	.752
21-3	.0704	170.5	1,776	0	2.3	2,064	2,062	446	446	180	.706	.0522	.0483	.763
21-4	.0704	187.0	1,808	-3.3	1.7	2,059	2,055	523	405	183	.760	.0458	.0463	.752
21-7	.0720	173.0	1,804	-0.6	2.1	2,044	2,043	467	446	187	.704	.0496	.0467	.747

COMPARISON OF TESTS ON AIR PROPELLERS

TABLE II—Continued
POWER FLIGHT DATA—Continued

PROPELLER K'

Flight and run No.	Specific weight, pounds per ft. ³	V feet per second	R. P. M.	α Angle of flight path	Angle of attack	W	L	D	T	HP.	V/nD	C_T	C_P	η
14-2	0.0694	79.5	1,736	11.3	11.8	2,069	1,908	218	623	169	0.337	0.0775	0.0491	0.532
14-3	.0678	93.0	1,732	10.5	8.8	2,064	1,953	220	596	164	.394	.0763	.0488	.616
14-4	.0673	111.5	1,768	8.5	6.2	2,059	1,994	246	550	167	.464	.0681	.0474	.666
14-5	.0684	125.3	1,792	7.0	4.7	2,054	2,002	277	527	171	.514	.0625	.0459	.700
14-6	.0679	142.5	1,808	4.7	3.6	2,049	2,028	326	494	172	.580	.0580	.0452	.744
14-7	.0765	0	1,740							192	.0		.0501	.0
15-2	.0677	164.0	1,852	2.0	2.6	2,069	2,063	404	477	175	.650	.0535	.0427	.814
15-4	.0667	192.0	1,964	-3.4	1.8	2,069	2,066	525	402	182	.7175	.0407	.0379	.770
15-5	.0692	204.5	1,984	-6.8	1.4	2,064	2,054	610	367	192	.7575	.0351	.0374	.710
29-1	.0760	167.8	1,916	0	2.2	2,074	2,072	465	465	204	.643	.0434	.0402	.694
29-2	.0745	145.2	1,832	3.8	3.1	2,069	2,054	359	496	190	.582	.0517	.0435	.692
29-3	.0738	163.0	1,924	0.8	2.4	2,064	2,061	430	459	197	.623	.0439	.0396	.695
29-4	.0729	181.0	1,972	-2.9	1.9	2,059	2,043	511	407	198	.674	.0374	.0371	.680
29-5	.0732	195.0	1,960	-5.1	1.5	2,054	2,050	595	412	189	.731	.0378	.0361	.766
29-6	.0728	201.5	2,004	-7.0	1.4	2,049	2,038	622	372	199	.739	.0331	.0359	.681
29-7	.0760	170.0	1,916	0	2.1	2,044	2,043	476	476	204	.652	.0444	.0404	.716
30-1	.0764	168.0	1,916	0	2.2	2,075	2,073	468	468	205	.645	.0434	.0403	.694
30-2	.0748	76.7	1,768	14.2	11.5	2,070	1,871	210	718	186	.319	.0800	.0476	.536
30-3	.0746	90.6	1,744	13.1	8.3	2,065	1,928	219	687	182	.382	.0788	.0486	.620
30-4	.0751	104.9	1,772	11.4	6.2	2,060	1,970	243	650	187	.434	.0718	.0471	.662
30-5	.0756	120.0	1,788	9.4	4.6	2,055	1,998	279	615	189	.492	.0664	.0460	.710
30-6	.0756	134.0	1,848	7.2	3.6	2,050	2,017	322	579	195	.533	.0584	.0431	.722
30-7	.0763	169.5	1,940	0	2.1	2,045	2,044	474	474	206	.641	.0478	.0389	.788
13-1	.0765	0	1,720							191	.0		.0518	.0

PROPELLER L'

18-1	0.0744	161.1	1,640	0.0	2.4	2,074	2,070	426	426	176	0.722	0.0554	0.0567	0.705
18-2	.0734	80.8	1,460	10.6	10.8	2,069	1,933	215	595	153	.406	.0990	.0706	.568
18-3	.0727	92.7	1,476	9.8	8.3	2,064	1,967	223	574	155	.462	.0944	.0697	.626
18-4	.0726	108.1	1,492	8.0	6.1	2,059	2,000	247	534	155	.532	.0844	.0675	.665
18-5	.0726	124.6	1,544	6.0	4.5	2,054	2,025	286	465	161	.593	.0699	.0632	.656
18-6	.0735	140.0	1,595	4.1	3.3	2,049	2,032	336	482	167	.645	.0671	.0588	.736
18-7	.0743	164.5	1,660	0	2.3	2,044	2,042	438	439	177	.728	.0559	.0549	.741
18-8	.0765	0	1,490							163	.0		.0680	.0
19-1	.0742	162.5	1,684	0.8	2.4	2,074	2,071	431	460	181	.710	.0570	.0537	.754
19-2	.0723	155.1	1,632	2.4	2.7	2,069	2,061	390	477	170	.699	.0648	.0569	.796
19-3	.0729	170.1	1,692	-0.3	2.2	2,064	2,062	458	447	179	.739	.0558	.0532	.775
19-4	.0742	179.5	1,746	-2.7	1.9	2,059	2,057	510	413	188	.756	.0475	.0500	.718
19-7	.0739	167.5	1,680	0	2.2	2,044	2,042	450	450	180	.732	.0562	.0541	.760

TABLE III
FINAL ADJUSTED COEFFICIENTS, FULL SCALE TESTS

PROPELLER B'

V/nD	C_T	C_P	η
0.30	0.0839	0.0493	0.510
.35	.0790	.0486	.568
.40	.0737	.0475	.620
.45	.0678	.0461	.662
.50	.0617	.0441	.700
.55	.0553	.0420	.723
.60	.0485	.0395	.737
.65	.0418	.0370	.735
.70	.0340	.0340	.700

PROPELLER D'

V/nD	C_T	C_P	η
0.30	0.1070	0.0690	0.465
.35	.1013	.0687	.517
.40	.0960	.0680	.564
.45	.0906	.0673	.605
.50	.0850	.0662	.642
.55	.0798	.0648	.677
.60	.0740	.0630	.705
.65	.0679	.0605	.728
.70	.0615	.0576	.746
.75	.0550	.0545	.757
.80	.0485	.0510	.760
.85	.0416	.0471	.750

PROPELLER I

V/nD	C_T	C_P	η
0.30	0.0999	0.0611	0.490
.35	.0948	.0608	.545
.40	.0900	.0600	.600
.45	.0842	.0588	.644
.50	.0786	.0573	.685
.55	.0728	.0555	.720
.60	.0663	.0532	.748
.65	.0595	.0507	.762
.70	.0520	.0475	.765
.75	.0447	.0443	.756
.80	.0372	.0404	.736

PROPELLER K'

V/nD	C_T	C_P	η
0.30	0.0822	0.0495	0.498
.35	.0783	.0490	.560
.40	.0744	.0482	.618
.45	.0698	.0472	.665
.50	.0649	.0462	.703
.55	.0593	.0447	.730
.60	.0530	.0430	.740
.65	.0466	.0409	.739
.70	.0400	.0385	.727
.75	.0329	.0357	.690

PROPELLER L'

V/nD	C_T	C_P	η
0.30	0.1060	0.0710	0.450
.35	.1030	.0710	.508
.40	.0995	.0705	.565
.45	.0950	.0698	.612
.50	.0896	.0685	.655
.55	.0829	.0662	.688
.60	.0755	.0634	.715
.65	.0678	.0600	.735
.70	.0596	.0560	.744
.75	.0504	.0512	.738

TABLE IV
TEST DATA—MODEL PROPELLERS ALONE

PROPELLER B'

No.	$\frac{1}{2} \rho V^2$	V	R. P. M.	T	Q	V/nD	C _T	C _{P₁}
1-----	2.642	47.71	1085	0.0	0.705	0.844	0.0	0.0196
2-----	3.106	51.90	1273	1.323	1.207	.782	.0134	.0245
3-----	2.610	47.42	1188	1.323	1.124	.766	.0153	.0260
4-----	3.114	52.02	1391	2.977	1.694	.718	.0260	.0289
5-----	2.638	47.73	1320	2.977	1.618	.694	.0279	.0304
6-----	3.200	52.59	1550	5.292	2.394	.651	.0362	.0329
7-----	3.218	52.88	1722	8.269	3.275	.590	.0458	.0365
8-----	2.714	48.45	1664	8.269	3.131	.559	.0488	.0371
9-----	2.764	48.95	1856	11.907	4.187	.506	.0565	.0399
10-----	2.894	50.10	2071	16.207	5.371	.464	.0619	.0412
11-----	3.578	55.79	2569	26.790	8.550	.417	.0686	.0428
12-----	3.074	51.63	2613	26.790	8.925	.380	.0728	.0430
13-----	3.164	52.39	2841	33.075	10.620	.354	.0762	.0434
14-----	.281	15.63	2101	26.790	5.807	.143	.0998	.0435

PROPELLER D'

1-----	3.096	51.90	1035	0.0	0.395	1.045	0.0	0.0184
2-----	3.083	51.78	1157	1.323	.922	.932	.0226	.0343
3-----	3.083	51.79	1285	2.977	1.482	.839	.0411	.0447
4-----	3.128	52.17	1463	5.292	2.229	.742	.0564	.0519
5-----	3.178	52.58	1665	8.269	3.182	.656	.0681	.0572
6-----	3.335	53.89	1885	11.907	4.357	.596	.0766	.0612
7-----	3.440	54.75	2106	16.207	5.605	.542	.0835	.0630
8-----	3.367	54.14	2319	21.474	7.054	.486	.0909	.0652
9-----	3.456	54.86	2532	26.790	8.445	.452	.0955	.0657
10-----	3.538	55.50	2745	33.075	10.037	.422	.1003	.0664
11-----	.360	17.70	2444	33.075	7.555	.151	.1260	.0629

PROPELLER I

1-----	2.435	45.28	959	0.0	0.504	0.945	0.0	0.0215
2-----	3.213	52.28	1210	1.323	1.094	.864	.0171	.0296
3-----	3.510	54.75	1377	2.977	1.651	.795	.0298	.0346
4-----	2.502	45.96	1225	2.977	1.479	.750	.0372	.0387
5-----	3.569	55.21	1524	5.292	2.373	.725	.0433	.0406
6-----	2.669	48.20	1423	5.292	2.243	.678	.0506	.0449
7-----	3.352	53.48	1674	8.268	3.290	.639	.0560	.0466
8-----	3.402	53.87	1864	11.910	4.397	.578	.0650	.0502
9-----	2.768	49.00	1813	11.910	4.173	.540	.0698	.0513
10-----	3.816	57.22	2317	21.170	7.137	.494	.0752	.0531
11-----	3.948	58.26	2729	33.070	10.203	.427	.0849	.0548
12-----	2.907	49.61	2630	33.070	9.704	.377	.0900	.0553
13-----	.353	17.42	2363	33.070	7.470	.147	.1132	.0535

PROPELLER K'

1-----	3.191	50.85	1090	0.0	0.515	0.933	0.0	0.0163
2-----	3.245	52.96	1252	1.323	.963	.846	.0162	.0247
3-----	3.366	53.94	1403	2.977	1.498	.768	.0290	.0306
4-----	3.348	53.90	1574	5.292	2.197	.684	.0410	.0357
5-----	3.411	54.30	1777	8.269	3.070	.611	.0503	.0390
6-----	3.479	55.10	2156	14.920	4.909	.511	.0622	.0429
7-----	3.042	51.28	2389	21.168	6.308	.429	.0712	.0445
8-----	2.992	50.86	2618	26.790	7.710	.389	.0751	.0452
9-----	3.051	51.29	2850	33.075	9.252	.360	.0781	.0455
10-----	.377	18.02	2577	33.075	6.965	.140	.0953	.0420

PROPELLER L'

1-----	3.042	50.31	1053	0.0	0.633	0.956	0.0	0.0221
2-----	2.992	49.94	1143	1.323	1.096	.874	.0188	.0326
3-----	3.065	50.53	1268	2.977	1.670	.796	.0343	.0403
4-----	3.141	51.22	1418	5.292	2.613	.722	.0488	.0505
5-----	3.092	51.55	1458	5.960	2.646	.704	.0531	.0493
6-----	3.227	51.91	1590	8.269	3.416	.653	.0607	.0525
7-----	3.227	51.92	1766	11.790	4.544	.588	.0717	.0567
8-----	3.339	52.87	1964	16.207	5.824	.538	.0782	.0588
9-----	3.533	54.38	2174	21.168	7.334	.500	.0833	.0605
10-----	3.582	54.83	2366	26.790	8.933	.464	.0893	.0624
11-----	3.645	55.31	2620	35.278	11.169	.422	.0959	.0636
12-----	3.686	55.81	2862	44.000	13.590	.390	.1009	.0653
13-----	.368	17.63	2188	33.075	7.955	.161	.1287	.0651

TABLE V
TEST DATA—MODEL PROPELLERS WITH MODEL VE-7

PROPELLER B'

No.	$\frac{1}{2}\rho V^2$	V	R. P. M.	T	Aug.	Q	V/nD	C _T	C _{P1}
1-----	2.535	46.24	998	0.0	0.0	0.562	0.889	0.0	0.0180
2-----	2.937	50.16	1192	1.323	.160	1.026	.808	.0132	.0235
3-----	2.526	46.20	1107	1.323	.214	.948	.801	.0144	.0248
4-----	3.020	50.87	1317	2.977	.320	1.564	.742	.0248	.0293
5-----	2.500	45.96	1227	2.977	.358	1.436	.719	.0278	.0304
6-----	3.002	50.72	1457	5.292	.530	2.200	.668	.0363	.0337
7-----	2.530	46.26	1387	5.292	.570	2.120	.641	.0393	.0354
8-----	3.024	50.91	1627	8.269	.850	3.046	.601	.0454	.0374
9-----	2.600	46.98	1571	8.269	.908	2.956	.574	.0482	.0386
10-----	3.041	51.05	1806	11.910	1.150	4.042	.542	.0533	.0403
11-----	2.591	46.89	1751	11.910	1.221	3.951	.514	.0559	.0415
12-----	3.116	51.72	1909	16.210	1.610	5.167	.494	.0585	.0416
13-----	2.639	47.40	1955	16.210	1.663	5.033	.466	.0612	.0426
14-----	3.273	52.97	2221	21.170	2.120	6.457	.458	.0625	.0426
15-----	2.655	47.56	2153	21.170	2.121	6.215	.424	.0662	.0434
16-----	2.779	48.74	2370	26.790	2.729	7.612	.395	.0691	.0440
17-----	3.339	53.50	2629	33.070	3.340	9.284	.391	.0704	.0444
18-----	2.910	49.88	2588	33.070	3.307	9.128	.370	.0717	.0442
19-----	2.364	45.08	2670	37.490	3.754	9.728	.324	.0765	.0444
20-----	.137	11.12	1844	22.050	2.240	4.412	.116	.0940	.0421

PROPELLER D'

1-----	2.640	47.89	905	0.0	0.0	0.274	1.105	0.0	0.0166
2-----	2.714	48.61	1050	1.322	.204	.701	.965	.0232	
3-----	2.709	48.68	1198	2.978	.409	1.335	.847	.0409	.0465
4-----	2.648	48.08	1378	5.293	.638	2.057	.728	.0563	.0543
5-----	2.613	47.75	1576	8.269	.985	2.898	.632	.0672	.0583
6-----	2.766	49.21	1798	11.910	1.418	3.929	.571	.0746	.0609
7-----	2.692	48.53	2015	16.210	1.873	5.074	.502	.0810	.0626
8-----	2.718	48.81	2243	21.170	2.420	6.375	.454	.0858	.0637
9-----	2.718	48.81	2453	26.800	3.040	7.688	.415	.0909	.0642
10-----	2.810	49.64	2686	33.080	3.859	9.284	.386	.0932	.0646
11-----	2.788	49.46	2688	33.080	3.808	9.273	.384	.0933	.0644
12-----	.181	12.54	2236	27.310	3.240	7.075	.117	.1100	.0602

PROPELLER I

1-----	2.455	45.80	942	0.0	0.0	0.360	0.972	0.0	0.0161
2-----	2.591	47.83	1087	1.323	.299	.851	.880	.0170	.0296
3-----	2.609	48.01	1213	2.977	.434	1.371	.792	.0340	.0383
4-----	2.639	48.34	1385	5.291	.698	2.100	.699	.0471	.0451
5-----	2.705	48.91	1582	8.270	1.012	2.956	.619	.0570	.0486
6-----	2.714	48.96	1783	11.910	1.365	3.944	.550	.0652	.0510
7-----	2.535	46.80	1949	16.210	1.735	5.037	.480	.0731	.0533
8-----	2.639	47.71	2170	21.170	2.231	6.301	.440	.0771	.0538
9-----	2.688	48.13	2379	26.790	2.763	7.708	.405	.0813	.0546
10-----	2.723	48.44	2591	33.070	3.441	9.236	.374	.0846	.0552
11-----	.086	8.55	1418	12.130	1.248	2.546	.127	.1040	.0510
12-----	.181	12.50	2094	26.680	2.775	5.545	.119	.1046	.0507

PROPELLER K'

1-----	3.037	51.61	1068	0.0	0.0	0.375	0.966	0.0	0.0134
2-----	2.644	47.34	1096	1.323	.402	.778	.864	.0145	.0256
3-----	3.098	52.16	1326	2.977	.613	1.343	.787	.0262	.0312
4-----	2.709	47.92	1455	5.513	.814	2.044	.659	.0418	.0381
5-----	3.138	52.53	1714	8.269	1.150	2.887	.613	.0474	.0402
6-----	2.548	47.08	1652	8.270	.982	2.752	.570	.0516	.0408
7-----	3.146	52.41	1917	11.690	1.483	2.812	.547	.0539	.0421
8-----	2.736	48.28	1855	11.910	1.478	3.745	.522	.0574	.0432
9-----	3.216	53.18	2165	16.210	2.045	4.971	.491	.0591	.0434
10-----	2.639	47.92	2105	16.260	1.813	4.793	.455	.0630	.0438
11-----	2.845	49.23	2317	21.170	2.569	5.987	.425	.0656	.0442
12-----	2.985	50.42	2545	26.900	3.093	7.340	.396	.0696	.0449
13-----	3.129	52.37	2848	33.070	3.843	8.969	.368	.0702	.0451
14-----	3.339	53.35	3094	41.900	4.268	11.003	.345	.0745	.0456
15-----	2.635	48.14	3091	41.900	4.624	10.530	.312	.0763	.0451
16-----	2.141	43.82	3062	41.900	4.579	10.181	.286	.0777	.0444
17-----	.217	12.83	2193	28.460	2.870	5.408	.117	.0903	.0397

PROPELLER L'

1-----	2.574	47.72	944	0.0	0.0	0.428	1.010	0.0	0.0198
2-----	2.399	45.16	1009	1.323	.191	.874	.895	.0210	.0340
3-----	2.447	45.67	1141	2.977	.314	1.437	.801	.0387	.0438
4-----	2.452	45.72	1304	5.292	.544	2.129	.701	.0529	.0497
5-----	2.447	45.78	1475	8.268	.889	3.033	.621	.0645	.0556
6-----	2.460	45.95	1660	11.910	1.272	4.037	.553	.0736	.0585
7-----	2.526	46.55	1857	16.210	1.713	5.274	.501	.0802	.0611
8-----	2.714	48.31	2270	26.790	2.784	8.180	.426	.0891	.0636
9-----	2.718	48.35	2466	33.070	3.395	9.722	.392	.0933	.0640
10-----	.177	12.37	1957	26.680	2.837	5.928	.127	.1199	.0623

TABLE VI
FINAL ADJUSTED COEFFICIENTS—
MODEL PROPELLERS ALONE

PROPELLER B'			
V/nD	C_T	C_P	η
0.30	0.0822	0.0441	0.559
.35	.0766	.0438	.612
.40	.0705	.0429	.658
.45	.0642	.0416	.697
.50	.0575	.0400	.718
.55	.0508	.0381	.733
.60	.0438	.0357	.735
.65	.0362	.0331	.711
.70	.0280	.0300	.653
.75	.0186	.0266	.525
.80	.0090	.0230	.313

PROPELLER D'			
V/nD	C_T	C_P	η
0.30	0.1128	0.0662	0.510
.35	.1073	.0665	.565
.40	.1020	.0665	.615
.45	.0960	.0658	.657
.50	.0896	.0646	.694
.55	.0832	.0630	.726
.60	.0761	.0607	.752
.65	.0696	.0584	.774
.70	.0623	.0553	.788
.75	.0547	.0518	.791
.80	.0468	.0478	.783
.85	.0382	.0430	.752
.90	.0291	.0380	.690

PROPELLER I			
V/nD	C_T	C_P	η
0.30	0.0988	0.0554	0.534
.35	.0934	.0557	.587
.40	.0875	.0554	.633
.45	.0814	.0545	.672
.50	.0749	.0532	.704
.55	.0683	.0513	.722
.60	.0616	.0492	.751
.65	.0540	.0462	.760
.70	.0460	.0426	.756
.75	.0377	.0388	.728
.80	.0288	.0349	.660
.85	.0192	.0304	.536
.90	.0093	.0261	.321

PROPELLER K'			
V/nD	C_T	C_P	η
0.30	0.0833	0.0451	0.554
.35	.0790	.0452	.611
.40	.0743	.0449	.659
.45	.0690	.0444	.700
.50	.0636	.0433	.734
.55	.0578	.0417	.762
.60	.0519	.0398	.780
.65	.0454	.0375	.786
.70	.0386	.0349	.774
.75	.0315	.0318	.742
.80	.0237	.0282	.672
.85	.0150	.0241	.528
.90	.0058	.0196	.266

PROPELLER L'			
V/nD	C_T	C_P	η
0.30	0.1110	0.0659	0.505
.35	.1045	.0654	.560
.40	.0979	.0642	.610
.45	.0912	.0628	.656
.50	.0843	.0608	.693
.55	.0770	.0586	.723
.60	.0692	.0558	.744
.65	.0612	.0527	.755
.70	.0523	.0490	.748
.75	.0434	.0448	.726
.80	.0339	.0400	.678
.85	.0237	.0347	.582
.90	.0127	.0294	.392

TABLE VII
FINAL ADJUSTED COEFFICIENTS—
MODEL PROPELLERS WITH MODEL VE-7

PROPELLER B'			
V/nD	C_T	C_P	η
0.30	0.0787	0.0444	0.531
.35	.0740	.0444	.583
.40	.0688	.0440	.627
.45	.0639	.0432	.666
.50	.0580	.0417	.695
.55	.0517	.0398	.714
.60	.0452	.0375	.724
.65	.0383	.0349	.714
.70	.0306	.0316	.678
.75	.0228	.0283	.606
.80	.0151	.0248	.487

PROPELLER D			
V/nD	C_T	C_P	η
0.30	0.1000	0.0644	0.466
.35	.0961	.0646	.521
.40	.0918	.0642	.572
.45	.0870	.0636	.616
.50	.0821	.0629	.653
.55	.0768	.0615	.687
.60	.0713	.0599	.714
.65	.0655	.0579	.735
.70	.0595	.0556	.749
.75	.0531	.0519	.753
.80	.0469	.0500	.750
.85	.0401	.0463	.736
.90	.0328	.0419	.708

PROPELLER I			
V/nD	C_T	C_P	η
0.30	0.0912	0.0550	0.498
.35	.0855	.0553	.548
.40	.0818	.0550	.595
.45	.0764	.0541	.636
.50	.0710	.0529	.671
.55	.0652	.0514	.698
.60	.0593	.0496	.717
.65	.0530	.0473	.728
.70	.0462	.0446	.725
.75	.0386	.0412	.709
.80	.0309	.0372	.666
.85	.0223	.0324	.586
.90	.0134	.0271	.445

PROPELLER K'			
V/nD	C_T	C_P	η
0.30	0.0774	0.0450	0.514
.35	.0730	.0451	.566
.40	.0687	.0450	.611
.45	.0640	.0443	.650
.50	.0590	.0432	.683
.55	.0541	.0420	.709
.60	.0489	.0406	.723
.65	.0430	.0383	.730
.70	.0373	.0361	.723
.75	.0310	.0333	.697
.80	.0241	.0301	.641
.85	.0172	.0263	.556
.90	.0102	.0217	.425

PROPELLER L'			
V/nD	C_T	C_P	η
0.30	0.1034	0.0648	0.478
.35	.0980	.0647	.530
.40	.0925	.0640	.578
.45	.0868	.0630	.620
.50	.0806	.0613	.658
.55	.0742	.0592	.689
.60	.0675	.0568	.713
.65	.0604	.0538	.729
.70	.0532	.0505	.737
.75	.0454	.0465	.732
.80	.0378	.0429	.705
.85	.0289	.0382	.643
.90	.0200	.0335	.537

TABLE VIII
ORDINATES FOR SECTIONS OF PROPELLER L'

Radius	10.89''		19.05''		27.22''	35.39''	43.55''	47.63''
Camber	Upper	Lower	Upper	Lower	Upper	Upper	Upper	Upper
Rad. L. E.....	0.980''		0.32''		0.161''	0.104''	0.059''	0.038''
2.5.....	0.856	0.516	0.914	0.059	.660	.425	.245	.157
5.....	1.235	.738	1.316	.082	.947	.614	.350	.229
10.....	1.650	.986	1.761	.111	1.271	.820	.470	.304
20.....	1.990	1.192	2.117	.134	1.529	.986	.565	.366
30.....	2.088	1.251	2.228	.140	1.604	1.039	.594	.385
40.....	2.068	1.241	2.208	.140	1.594	1.029	.588	.382
50.....	1.990	1.192	2.117	.134	1.529	.986	.565	.366
60.....	1.816	1.091	1.940	.121	1.398	.905	.516	.336
70.....	1.548	.928	1.650	.104	1.189	.768	.441	.284
80.....	1.173	.702	1.248	.078	.901	.581	.333	.216
90.....	.732	.438	.781	.049	.562	.362	.209	.134
Rad. T. E.....	0.361''		0.16''		.123''	.080''	.045''	.029''

All ordinates in inches.
Stations in per cent of chord.

ORDINATES FOR SECTIONS OF PROPELLER K'

Radius	10.89''		19.05''		27.22''	35.39''	43.55''	47.63''
Camber	Upper	Lower	Upper	Lower	Upper	Upper	Upper	Upper
Rad. L. E.....	0.784''		0.261''		0.108''	0.068''	0.039''	0.026''
2.5.....	0.571	0.343	0.611	0.036	.441	.248	.163	.106
5.....	.820	.493	.879	.055	.634	.408	.232	.153
10.....	1.101	.660	1.173	.072	.846	.549	.314	.205
20.....	1.323	.794	1.411	.088	1.019	.657	.376	.247
30.....	1.388	.836	1.483	.091	1.072	.692	.395	.259
40.....	1.379	.830	1.470	.091	1.062	.686	.392	.258
50.....	1.323	.794	1.411	.088	1.019	.657	.376	.247
60.....	1.209	.728	1.294	.078	.931	.604	.343	.226
70.....	1.029	.621	1.101	.068	.794	.513	.294	.192
80.....	.781	.467	.833	.052	.601	.389	.222	.145
90.....	.487	.294	.519	.033	.376	.242	.137	.091
Rad. T. E.....	0.170''		0.120''		.082''	.052''	.029''	.020''

All ordinates in inches.
Stations in per cent of chord.

ORDINATES FOR SECTIONS OF PROPELLER I

Radius	10.89''		19.05''		27.22''	35.39''	43.55''	47.63''
Camber	Upper	Lower	Upper	Lower	Upper	Upper	Upper	Upper
Rad. L. E.....	0.844''		0.272''		0.133''	0.087''	0.049''	0.033''
2.5.....	0.719	0.427	0.762	0.049	.556	.357	.204	.133
5.....	1.032	.615	1.097	.068	.789	.512	.291	.193
10.....	1.380	.822	1.470	.092	1.056	.686	.392	.259
20.....	1.661	.991	1.767	.112	1.271	.825	.471	.310
30.....	1.742	1.040	1.856	.117	1.337	.866	.495	.327
40.....	1.729	1.032	1.840	.117	1.326	.860	.490	.324
50.....	1.661	.991	1.767	.112	1.271	.825	.471	.310
60.....	1.522	.906	1.617	.109	1.165	.757	.430	.283
70.....	1.293	.770	1.377	.087	.991	.642	.367	.242
80.....	.980	.582	1.042	.065	.748	.487	.278	.182
90.....	.612	.365	.650	.041	.468	.305	.174	.114
Rad. T. E.....	0.245''		0.120''		.103''	.068''	.038''	.024''

All ordinates in inches.
Stations in per cent of chord.

TABLE VIII—Continued
ORDINATES FOR SECTIONS OF PROPELLER D'

Radius.....	10.45"		18.28"		26.11"	33.94"	41.77"	45.69"
Camber.....	Upper	Lower	Upper	Lower	Upper	Upper	Upper	Upper
Rad. L. E.....	0.877"		0.282"		0.128"	0.083"	0.047"	0.031"
2.5.....	0.686	0.410	0.730	0.047	.526	.338	.194	.128
5.....	.987	.589	1.053	.066	.758	.489	.279	.185
10.....	1.322	.790	1.410	.088	1.015	.655	.373	.247
20.....	1.588	.949	1.692	.106	1.222	.786	.448	.298
30.....	1.664	.996	1.777	.113	1.285	.830	.473	.313
40.....	1.654	.990	1.764	.113	1.275	.821	.470	.310
50.....	1.588	.949	1.692	.106	1.222	.786	.448	.298
60.....	1.454	.868	1.551	.097	1.118	.720	.410	.272
70.....	1.238	.739	1.319	.085	.952	.614	.351	.232
80.....	.937	.558	.996	.063	.720	.464	.266	.175
90.....	.586	.351	.623	.041	.451	.291	.166	.110
Rad. T. E.....	0.26"		0.125"		.098"	.064"	.036"	.024"

All ordinates in inches.
Station in per cent of chord.

ORDINATES FOR SECTIONS OF PROPELLER B'

Radius.....	11.33"		19.83"		28.33"	36.83"	45.33"	49.57"
Camber.....	Upper	Lower	Upper	Lower	Upper	Upper	Upper	Upper
Rad. L. E.....	0.952"		0.306"		0.139"	0.090"	0.051"	0.034"
2.5.....	0.745	0.445	0.792	0.051	.571	.367	.211	.139
5.....	1.071	.639	1.142	.071	.823	.530	.303	.201
10.....	1.435	.857	1.530	.095	1.102	.710	.405	.269
20.....	1.724	1.030	1.836	.115	1.326	.854	.486	.323
30.....	1.806	1.081	1.928	.122	1.394	.901	.513	.340
40.....	1.795	1.075	1.915	.122	1.384	.891	.510	.337
50.....	1.724	1.030	1.836	.115	1.326	.854	.486	.323
60.....	1.578	.942	1.683	.105	1.214	.782	.445	.296
70.....	1.343	.802	1.432	.092	1.034	.667	.381	.252
80.....	1.017	.605	1.081	.068	.782	.503	.289	.190
90.....	.636	.381	.676	.044	.490	.316	.180	.119
Rad. T. E.....	0.280"		0.115"		.106"	.071"	.039"	.026"

All ordinates in inches.
Stations in per cent of chord

REFERENCE

1. W. S. DIEHL: The Variation of Aerofoil Lift and Drag Coefficients with Changes in Size and Speed. N. A. C. A. Technical Report 111. 1921.

REPORT No. 221

MODEL TESTS WITH A SYSTEMATIC SERIES OF 27 WING SECTIONS AT FULL REYNOLDS NUMBER

By MAX M. MUNK and ELTON W. MILLER
National Advisory Committee for Aeronautics

REPORT No. 221

MODEL TESTS WITH A SYSTEMATIC SERIES OF 27 WING SECTIONS AT FULL REYNOLDS NUMBER

By MAX M. MUNK and ELTON W. MILLER

SUMMARY

A systematic series of 27 wing sections, characterized by a small travel of the center of pressure, has been investigated at 20 atmospheres pressure in the variable density wind tunnel of the National Advisory Committee for Aeronautics.

The results are consistent with each other, and indicate that for such "stable" sections a small effective camber, a small effective S-shape and a thickness of 8 to 12 per cent lead to good aerodynamic properties.

PURPOSE OF THE INVESTIGATION

This report contains the results of the investigation of the first systematic series of wing sections, 27 all together, made in the variable density wind tunnel of the National Advisory Committee for Aeronautics at about 20 atmospheres pressure. It was desired to obtain information about those aerodynamical properties of the wing sections which can not be computed. These are the drag at several angles of attack, and the two values of the lift coefficient when (a) the lift coefficient has its maximum and (b) when the air forces change irregularly, commonly known as the "burble point." Without additional work, there was also obtained a check on the aerodynamic properties open to computation, namely, the lift and the moment.

PROGRAM OF THE INVESTIGATION

In this first systematic series the measurements were confined to one tank pressure, about 20 atmospheres. This gives approximately a full size Reynolds Number, for the model scale is about one-tenth, the velocity about one-half of the actual velocity.

The investigation was confined to such wing sections as have a very small travel of the center of pressure. The rate of the travel of the center of pressure is certainly an aerodynamic property of great practical importance, affecting the usefulness of the section for design purposes; it is not wise to compare the performance of several wing sections without taking the different rates of travel of the center of pressure, if any, into account. Within the useful range of the angle of attack, the wing sections described in this report have their center of pressure at about 25 per cent of the chord. Their rate of travel of the center of pressure is accordingly small, and the comparison of their performance is all that remains to be done. Wing sections with a larger rate of travel of the center of pressure may be taken up in a later research.

ARRANGEMENT OF THE TESTS

The 27 models were made of duralumin and were rectangular and not warped. The span is 30 inches; the aspect ratio is 6. The 27 wing sections form a systematic series. The series begins with three symmetrical sections of different thicknesses, M1, M2, and M3. The curves are affine—i. e., the three sets of ordinates can be obtained from each other by multiplying

each ordinate by a constant. Three more sections are then obtained by adding to each of the sets of ordinates M1, M2, M3 the set of ordinates of a certain camberline, say "a," so chosen that theoretically its center of pressure does not travel. The series is further increased by substituting double the ordinates, 2a for a; then another camber line "b," with the same stability characteristics, and then combinations of the two camber lines. The camber lines "a" and "b" will be most easily recognized in wing sections M4 and M10. This process of obtaining the shapes of the wing sections leads to their classification in Table XXVIII. The ordinates of the sections are given in Table XXIX in per cent of the chord. Each figure contains a drawing of the section.

Each airfoil was exposed to the air stream of the variable density wind tunnel of the National Advisory Committee for Aeronautics. It was fastened by thin wires to the balance of this tunnel. Moreover, a skid rigidly fastened to the airfoil was hinged to a vertical bar, forming a part of the balance. This bar extends across the air stream in rear of the model; it is shielded from the air stream and can be moved up and down. When moved thus, the angle of attack of the airfoil is changed. After the airfoil was put in, the tank was closed and the air pressure increased up to about 20 atmospheres. The air forces of the airfoil were then determined over a range of several angles of attack. The drag of the wires and of other attachments were determined in a separate test under the same conditions of flow. The measured drag has been corrected for this drag of the fastening parts in the usual way.

RESULT OF THE TESTS

The results of the tests are given in Tables I to XXVII and are illustrated in the 27 figures. The angle of attack always refers to a line fixed with respect to the section as shown in each diagram. In the tables the air forces are represented by the lift coefficients, the drag coefficients, and the moment coefficients. The lift and drag coefficients are obtained by dividing the lift or drag by the wing area and by the dynamic pressure $V^2 \frac{\rho}{2}$, where V denotes the velocity of the air stream and ρ the mass density of the air. The diagrams are so-called polar curves. The lift coefficient is plotted vertically up, and against it to the right, the drag coefficient, and to the left, the moment coefficient. This latter refers to the moment of the air forces with respect to a point of the chord, one quarter chord from the leading edge. This point is chosen because it gives the least variation of the moment coefficient. The moment is divided by the wing area, by the dynamic pressure, and by the length of the chord. The Reynolds Number is computed with the chord as the characteristic length.

The parabola of the induced drag coefficient for the aspect ratio 6 has been inserted in each diagram. No correction has been made for the influence of the tunnel walls, which may be perceptible, as the wing span is half the tunnel throat diameter. This question is not yet sufficiently cleared up.

In Table XXX, a survey of the series and of the results obtained is given. The first column gives the number of the wing section. The next three columns contain the minimum drag coefficient, the lift coefficient at the "burble point," and the maximum lift coefficient, if any. The last column gives the average moment coefficient, which is always small for the wing sections considered in this investigation.

DISCUSSION OF THE RESULTS

The main results of this test lie in the presentation of new information about the properties of the wing sections given in the tables and in the diagrams.

It seems that a small travel of the center of pressure is generally combined with a smaller maximum lift coefficient. Good sections are in the neighborhood of M6.

The test charts show that at full size Reynolds Number, the minimum drag is much smaller than we are accustomed to obtain in the ordinary atmospheric wind tunnel. The maximum lift is not necessarily larger at a larger Reynolds Number.

One remark concerning the results seems pertinent. As shown by mathematical reasoning in Technical Report No. 191 of the National Advisory Committee for Aeronautics, the moment curves in the diagrams should theoretically be straight vertical lines. Most of them have approximately this shape, but not all of them. The small discrepancies can often be explained by taking the second approximation of the computations into account. For instance, with actual sections of a finite thickness, the theoretical leading edge is situated halfway between the actual one and the center of curvature of the leading edge, giving a shorter effective chord than the actual one. A very thick section, besides, is slightly more stable than a thin section of the same mean curve. Quite irregular moment curves can only be explained by sudden changes of the character of the flow just as at the burble point.

CONCLUSION

Looking at the results obtained in the variable density tunnel (including Technical Report No. 217) from a broader point of view, it is now established that the results obtained at the full size Reynolds Number do not agree with the results at a diminished Reynolds Number. Furthermore, tests now under way show that the variable density tunnel operated at one atmosphere gives results with a given wing section similar to the results obtained in other wind tunnels.

We conclude from these facts that the results obtained at full size Reynolds Number will give better information to the designer than tests run at largely reduced Reynolds Number. The information from the new tunnel will become more and more useful in the same degree as more results are obtained from it, so that results of new tests can be compared with results of similar older tests made under the same conditions.

TABLE I

Section No. M1.
Span 30 in. (76.2 cm).
Area 0.0968 m².
Average temperature 40.5° C.
Average Reynolds No. 3,600,000.

Model No. 21
Chord 5 in. (12.7 cm).
Aspect ratio 6.
Average pressure 20 atmos.

Angle of attack degrees	Dynamic pressure q kg/m ²	Lift coefficient C_L	Drag coefficient C_D	Moment coefficient C_M
-3.0	659	-0.208	0.0093	0.008
-1.5	665	-.104	.0075	.006
0.0	665	-.006	.0072	.005
1.5	665	.120	.0077	.012
3.0	665	.231	.0106	.007
4.5	667	.341	.0145	.011
6.0	664	.458	.0199	.008
9.0	666	.667	.0344	.085
12.0	665	.782	.1012	-.017
15.0	661	.805	.1962	-.065
18.0	660	.788	.2574	-.100
21.0	659	.742	.2967	-.094

TABLE III

Section No. M3.
Span 30 in. (76.2 cm).
Area 0.0968 m².
Average temperature 30.0° C.
Average Reynolds No. 3,670,000.

Model No. 23
Chord 5 in. (12.7 cm).
Aspect ratio 6.
Average pressure 20.15 atmos.

Angle of attack degrees	Dynamic pressure q kg/m ²	Lift coefficient C_L	Drag coefficient C_D	Moment coefficient C_M
-3.0	660	-0.197	0.0096	0.015
-1.5	662	-.095	.0082	.013
0.0	662	.014	.0089	.014
1.5	662	.128	.0096	.017
3.0	662	.236	.0126	.021
4.5	662	.343	.0162	.026
6.0	661	.471	.0214	.052
9.0	662	.675	.0379	.019
12.0	662	.883	.0591	.019
15.0	661	1.069	.0843	.014
18.0	660	1.059	.1628	-.033
21.0	659	.882	.3495	-.081

TABLE II

Section No. M2.
Span 30 in. (76.2 cm).
Area 0.0968 m².
Average temperature 37.0° C.
Average Reynolds No. 3,620,000.

Model No. 22.
Chord 5 in. (12.7 cm).
Aspect ratio 6.
Average pressure 19.95 atmos.

Angle of attack degrees	Dynamic pressure q kg/m ²	Lift coefficient C_L	Drag coefficient C_D	Moment coefficient C_M
-3.0	659	-0.236	0.0105	0.010
-1.5	660	-.125	.0086	.003
0.0	660	-.015	.0078	.010
1.5	660	.097	.0087	.010
3.0	657	.207	.0100	.009
4.5	656	.315	.0145	.015
6.0	655	.428	.0185	.007
9.0	654	.652	.0337	.015
12.0	653	.860	.0591	.015
15.0	652	.903	.1181	-.009
18.0	651	.881	.2436	-.026
21.0	650	.835	.3031	-.095

TABLE IV

Section No. M4.
Span 30 in. (76.2 cm).
Area 0.0968 m².
Average temperature 33.0° C.
Average Reynolds No. 3,680,000.

Model No. 24.
Chord 5 in. (12.7 cm).
Aspect ratio 6.
Average pressure 20.0 atmcs.

Angle of attack degrees	Dynamic pressure q kg/m ²	Lift coefficient C_L	Drag coefficient C_D	Moment coefficient C_M
-4.5	668	-0.279	0.0286	0.005
-3.0	672	-.180	.0146	.008
-1.5	672	-.087	.0075	.014
0.0	672	.025	.0071	.015
1.5	672	.138	.0067	.016
3.0	668	.248	.0108	.021
4.5	669	.359	.0141	.022
6.0	669	.472	.0199	.023
9.0	668	.700	.0369	.021
12.0	667	.905	.0602	.022
15.0	666	.941	.1340	-.006

TABLE V

Section No. M5.
Span 30 in. (76.2 cm).
Area 0.0968 m².
Average temperature 41.5° C.
Average Reynolds No. 3,600,000.

Model No. 25.
Chord 5 in. (12.7 cm).
Aspect ratio 6.
Average pressure 20.1 atmos.

Angle of attack degrees	Dynamic pressure q kg/m ²	Lift coefficient C_L	Drag coefficient C_D	Moment coefficient C_M
-1.5	655	-0.108	0.0076	0.018
0.0	655	.004	.0073	.021
1.5	655	.117	.0082	.020
3.0	656	.231	.0108	.021
4.5	662	.338	.0145	.015
6.0	665	.452	.0190	.025
9.0	662	.681	.0356	.021
12.0	663	.888	.0581	.016
15.0	663	1.076	.0864	.020
18.0	662	1.132	.1625	-.020
21.0	656	1.077	.2526	-.046

TABLE VI

Section No. M6.
Span 30 in. (76.2 cm).
Area 0.0968 m².
Average temperature 38.0° C.
Average Reynolds No. 3,660,000.

Model No. 26.
Chord 5 in. (12.7 cm).
Aspect ratio 6.
Average pressure 20.3 atmos.

Angle of attack degrees	Dynamic pressure q kg/m ²	Lift coefficient C_L	Drag coefficient C_D	Moment coefficient C_M
-3.0	662	-0.202	0.0108	0.009
-1.5	663	-.097	.0093	.011
0.0	663	.016	.0080	.012
1.5	663	.126	.0097	.014
3.0	662	.237	.0111	.015
4.5	663	.340	.0147	.026
6.0	665	.456	.0212	.018
9.0	664	.665	.0356	.021
12.0	661	.875	.0565	.025
15.0	663	1.073	.0816	.033
18.0	662	1.222	.1188	.014
21.0	661	1.169	.1891	-.022

TABLE VII

Section No. M7.
Span 30 in. (76.2 cm).
Area 0.0968 m².
Average temperature 36.0° C.
Average Reynolds No. 3,640,000.

Model No. 27.
Chord 5 in. (12.7 cm).
Aspect ratio 6.
Average pressure 20.0 atmos.

Angle of attack degrees	Dynamic pressure q kg/m ²	Lift coefficient C_L	Drag coefficient C_D	Moment coefficient C_M
-3.0	657	-0.155	0.0372	0.008
-1.5	657	-.051	.0246	.007
0.0	659	.054	.0088	.018
1.5	653	.167	.0101	.021
3.0	655	.279	.0129	.019
4.5	660	.387	.0161	.019
6.0	659	.505	.0227	.024
9.0	658	.738	.0407	.022
12.0	657	.973	.0654	.018
15.0	656	1.139	.0983	.022
18.0	655	1.123	.1983	-.014
21.0	654	1.011	.2708	-.086

TABLE VIII

Section No. M8.
Span 30 in. (76.2 cm).
Area 0.0968 m².
Average temperature 44.0° C.
Average Reynolds No. 3,450,000.

Model No. 28.
Chord 5 in. (12.7 cm).
Aspect ratio 6.
Average pressure 20.0 atmos.

Angle of attack degrees	Dynamic pressure q kg/m ²	Lift coefficient C_L	Drag coefficient C_D	Moment coefficient C_M
-3.0	624	-0.166	0.0100	0.016
0.0	626	.056	.0088	.017
1.5	627	.171	.0101	.016
3.0	627	.283	.0133	.017
6.0	629	.505	.0229	.017
9.0	629	.729	.0393	.029
12.0	628	.949	.0620	.026
15.0	629	1.138	.0921	.015
18.0	625	1.183	.1589	-.037
21.0	624	1.170	.2275	-.085

TABLE IX

Section No. M9.
Span 30 in. (76.2 cm).
Area 0.0968 m².
Average temperature 37.5° C.
Average Reynolds No. 3,620,000.

Model No. 29.
Chord 5 in. (12.7 cm).
Aspect ratio 6.
Average pressure 20.1 atmos.

Angle of attack degrees	Dynamic pressure q kg/m ²	Lift coefficient C_L	Drag coefficient C_D	Moment coefficient C_M
-3.0	650	-0.148	0.0113	0.009
0.0	650	.077	.0101	.014
3.0	656	.294	.0148	.018
4.5	655	.404	.0183	.015
6.0	655	.514	.0249	.028
9.0	654	.739	.0428	.025
12.0	654	.947	.0648	.021
15.0	653	1.096	.0920	.015
18.0	651	1.137	.1450	-.004
21.0	645	1.112	.2015	-.022

TABLE X

Section No. M10.
Span 30 in. (76.2 cm).
Area 0.0968 m².
Average temperature 41.0° C.
Average Reynolds No. 3,630,000.

Model No. 30.
Chord 5 in. (12.7 cm).
Aspect ratio 6.
Average pressure 20.4 atmos.

Angle of attack degrees	Dynamic pressure q kg/m ²	Lift coefficient C_L	Drag coefficient C_D	Moment coefficient C_M
-6.0	654	-0.345	0.0179	-0.007
-3.0	664	-.132	.0080	-.044
-1.5	617	-.020	.0068	-.034
0.0	667	.089	.0071	-.006
1.5	665	.203	.0094	-.008
3.0	665	.313	.0130	-.010
4.5	611	.451	.0194	-.092
6.0	662	.545	.0241	-.002
9.0	661	.771	.0437	-.021
12.0	660	.965	.0728	-.008
15.0	659	1.004	.1472	.000
18.0	656	.962	.2425	-.012
21.0	650	.907	.3053	-.029

TABLE XI

Section No. M11.
Span 30 in. (76.2 cm).
Area 0.0968 m².
Average temperature 36.0° C.
Average Reynolds No. 3,860,000.

Model No. 31.
Chord 5 in. (12.7 cm).
Aspect ratio 6.
Average pressure 20.3 atmos.

Angle of attack degrees	Dynamic pressure q kg/m ²	Lift coefficient C_L	Drag coefficient C_D	Moment coefficient C_M
-3.0	717	-0.120	0.0091	-0.018
-1.5	724	-.018	.0078	-.019
0.0	717	.094	.0089	-.018
1.5	715	.208	.0110	-.017
3.0	720	.313	.0137	-.006
4.5	719	.428	.0186	-.014
6.0	719	.544	.0256	-.012
9.0	721	.762	.0435	-.014
12.0	721	.969	.0682	-.020
15.0	728	1.080	.1135	-.082
18.0	710	1.028	.2159	-.146
21.0	708	.998	.3095	-.184

TABLE XIV

Section No. M14.
Span 30 in. (76.2 cm).
Area 0.0968 m².
Average temperature 41° C.
Average Reynolds No. 3,600,000.

Model No. 34.
Chord 5 in. (12.7 cm).
Aspect ratio 6.
Average temperature 20.3 atmos.

Angle of attack degrees	Dynamic pressure q kg/m ²	Lift coefficient C_L	Drag coefficient C_D	Moment coefficient C_M
-4.5	660	-0.118	0.0106	-0.040
-3.0	660	-.004	.0097	-.002
-1.5	661	.101	.0096	-.040
0.0	660	.217	.0119	-.035
1.5	662	.332	.0149	-.048
3.0	661	.444	.0200	-.030
4.5	656	.560	.0263	-.030
6.0	656	.671	.0347	-.027
9.0	656	.897	.0575	-.039
12.0	654	1.100	.0856	-.051
15.0	654	1.224	.1241	-.034
18.0	652	1.244	.1982	-.073
21.0	651	1.150	.2850	-.121

TABLE XII

Section No. M12.
Span 30 in. (76.2 cm).
Area 0.0968 m².
Average temperature 34.0° C.
Average Reynolds No. 3,800,000.

Model No. 32.
Chord 5 in. (12.7 cm).
Aspect ratio 6.
Average pressure 19.86 atmos.

Angle of attack degrees	Dynamic pressure q kg/m ²	Lift coefficient C_L	Drag coefficient C_D	Moment coefficient C_M
-3.0	706	-0.118	0.0097	-0.049
-1.5	706	-.017	.0089	-.005
0.0	706	.096	.0091	-.005
1.5	705	.207	.0120	-.005
3.0	705	.318	.0156	-.008
4.5	713	.417	.0191	-.003
6.0	710	.537	.0261	+.003
9.0	706	.760	.0441	-.002
12.0	708	.971	.0662	-.000
15.0	707	1.155	.0934	-.008
18.0	706	1.293	.1277	-.025
21.0	706	1.165	.2203	-.072

TABLE XV

Section No. M15.
Span 30 in. (76.2 cm).
Area 0.0968 m².
Average temperature 38° C.
Average Reynolds No. 3,580,000.

Model No. 35.
Chord 5 in. (12.7 cm).
Aspect ratio 6.
Average pressure 19.95 atmos.

Angle of attack degrees	Dynamic pressure q kg/m ²	Lift coefficient C_L	Drag coefficient C_D	Moment coefficient C_M
-4.5	640	-0.108	0.0101	-0.032
-3.0	635	.002	.0091	-.032
-1.5	635	.112	.0103	-.029
0.0	641	.227	.0129	-.022
1.5	646	.339	.0166	-.016
3.0	645	.456	.0213	-.035
4.5	644	.566	.0283	-.020
6.0	648	.671	.0367	-.030
9.0	648	.895	.0582	-.022
12.0	645	1.097	.0845	-.019
15.0	645	1.243	.1147	-.034
18.0	651	1.250	.1697	-.081
21.0	639	1.170	.2467	-.141

TABLE XIII

Section No. M13.
Span 30 in. (76.2 cm).
Area 0.0968 m².
Average temperature 40.0° C.
Average Reynolds No. 3,630,000.

Model No. 33.
Chord 5 in. (12.7 cm).
Aspect ratio 6.
Average pressure 20.2 atmos.

Angle of attack degrees	Dynamic pressure q kg/m ²	Lift coefficient C_L	Drag coefficient C_D	Moment coefficient C_M
-4.5	658	-0.127	0.0408	-0.043
-3.0	657	-.000	.0236	-.011
-1.5	661	.091	.0116	-.038
0.0	658	.209	.0127	-.036
1.5	661	.324	.0167	-.029
3.0	660	.437	.0214	-.014
4.5	658	.549	.0280	-.019
6.0	657	.670	.0378	-.023
9.0	657	.897	.0602	-.021
12.0	661	1.104	.0903	-.029
15.0	661	1.229	.1324	-.033
18.0	660	1.083	.2500	-.112
21.0	658	1.044	.3210	-.128

TABLE XVI

Section No. M16.
Span 30 in. (76.2 cm).
Area 0.0968 m².
Average temperature 38° C.
Average Reynolds No. 3,640,000.

Model No. 36.
Chord 5 in. (12.7 cm).
Aspect ratio 6.
Average pressure 20.05 atmos.

Angle of attack degrees	Dynamic pressure q kg/m ²	Lift coefficient C_L	Drag coefficient C_D	Moment coefficient C_M
-4.5	648	-0.197	0.0332	-0.011
-3.0	651	-.089	.0145	-.015
-1.5	651	.018	.0080	-.010
0.0	650	.135	.0094	-.008
1.5	652	.247	.0119	-.003
3.0	653	.367	.0159	-.013
4.5	658	.478	.0217	-.010
6.0	662	.597	.0295	-.002
9.0	655	.830	.0510	+.002
12.0	654	1.040	.0767	-.004
15.0	652	1.119	.1310	-.017
18.0	648	1.095	.2172	-.045
21.0	641	1.040	.3116	-.088

TABLE XVII

Section No. M17.
Span 30 in. (76.2 cm).
Area 0.0968 m².
Average temperature 37° C.
Average Reynolds No. 3,600,000.

Model No. 37.
Chord 5 in. (12.7 cm).
Aspect ratio 6.
Average pressure 19.93 atmos.

Angle of attack degrees	Dynamic pressure q kg/m ²	Lift coefficient C_L	Drag coefficient C_D	Moment coefficient C_M
-4.5	640	-0.191	0.0307	-0.010
-3.0	641	-.092	.0095	-.014
-1.5	639	.017	.0092	-.011
0.0	640	.133	.0103	-.008
1.5	648	.244	.0126	-.006
3.0	645	.360	.0163	-.001
4.5	644	.476	.0236	-.003
6.0	644	.588	.0300	+.010
9.0	643	.823	.0495	+.003
12.0	641	1.029	.0745	-.019
15.0	640	1.221	.1064	-.001
18.0	640	1.233	.1783	-.045
21.0	638	1.230	.2513	-.040

TABLE XX

Section No. M20.
Span 30 in. (76.2 cm).
Area 0.0968 m².
Average temperature 51° C.
Average Reynolds No. 3,350,000.

Model No. 40.
Chord 5 in. (12.7 cm).
Aspect ratio 6.
Average pressure 20.0 atmos.

Angle of attack degrees	Dynamic pressure q kg/m ²	Lift coefficient C_L	Drag coefficient C_D	Moment coefficient C_M
-4.5	613	-0.078	0.0531	-0.037
-3.0	614	+.029	.0404	-.038
-1.5	622	.136	.0287	-.038
0.0	616	.252	.0173	-.035
1.5	622	.369	.0175	-.002
3.0	622	.487	.0233	-.034
4.5	624	.592	.0310	-.023
6.0	624	.713	.0408	-.030
9.0	616	.946	.0652	-.036
12.0	617	1.156	.0945	-.036
15.0	626	1.311	.1310	-.068
18.0	625	1.300	.1884	-.088
21.0	620	1.256	.2488	-.133

TABLE XVIII

Section No. M18.
Span 30 in. (76.2 cm).
Area 0.0968 m².
Average temperature 45° C.
Average Reynolds No. 3,530,000.

Model No. 38.
Chord 5 in. (12.7 cm).
Aspect ratio 6.
Average pressure 20.08 atmos.

Angle of attack degrees	Dynamic pressure q kg/m ²	Lift coefficient C_L	Drag coefficient C_D	Moment coefficient C_M
-4.5	630	-0.175	0.0111	-0.002
-3.0	635	-.055	.0093	-.015
-1.5	633	.052	.0096	-.012
0.0	633	.164	.0117	-.009
1.5	639	.282	.0149	-.007
3.0	636	.393	.0188	.000
4.5	635	.520	.0250	-.084
6.0	645	.614	.0322	+.003
9.0	640	.823	.0542	.000
12.0	639	1.018	.0769	-.005
15.0	638	1.123	.1220	-.007
18.0	635	1.188	.1717	-.035
21.0	635	1.194	.2315	-.051

TABLE XXI

Section No. M21.
Span 30 in. (76.2 cm).
Area 0.0968 m².
Average temperature 40° C.
Average Reynolds No. 3,530,000.

Model No. 41.
Chord 5 in. (12.7 cm).
Aspect ratio 6.
Average pressure 20.09 atmos.

Angle of attack degrees	Dynamic pressure q kg/m ²	Lift coefficient C_L	Drag coefficient C_D	Moment coefficient C_M
-4.5	632	-0.088	0.0132	-0.029
-3.0	632	.019	.0115	-.030
-1.5	631	.131	.0119	-.029
0.0	633	.250	.0147	-.029
1.5	635	.365	.0180	-.021
3.0	635	.472	.0233	-.020
4.5	635	.589	.0305	-.019
6.0	634	.697	.0393	-.021
9.0	633	.913	.0609	-.024
12.0	633	1.097	.0882	-.025
15.0	629	1.176	.1365	-.049
18.0	624	1.212	.1927	-.072
21.0	628	1.217	.2376	-.073

TABLE XIX

Section No. M19.
Span 30 in. (76.2 cm).
Area 0.0968 m².
Average temperature 43° C.
Average Reynolds No. 3,500,000.

Model No. 39.
Chord 5 in. (12.7 cm).
Aspect ratio 6.
Average pressure 20.2 atmos.

Angle of attack degrees	Dynamic pressure q kg/m ²	Lift coefficient C_L	Drag coefficient C_D	Moment coefficient C_M
-4.5	639	-0.115	0.0570	-0.031
-3.0	636	.030	.0441	+.015
-1.5	642	.123	.0341	-.032
0.0	642	.249	.0257	-.031
1.5	649	.384	.0189	-.023
3.0	637	.496	.0240	-.015
4.5	642	.598	.0297	-.021
6.0	639	.719	.0389	-.023
9.0	641	.946	.0633	-.011
12.0	641	1.153	.0940	-.031
15.0	641	1.258	.1392	-.052
18.0	636	1.171	.1984	-.079
21.0	634	1.137	.2999	-.168

TABLE XXII

Section M22.
Span 30 in. (76.2 cm).
Area 0.0968 m².
Average temperature 38° C.
Average Reynolds No. 3,510,000.

Model No. 42.
Chord 5 in. (12.7 cm).
Aspect ratio 6.
Average pressure 19.6 atmos.

Angle of attack degrees	Dynamic pressure q kg/m ²	Lift coefficient C_L	Drag coefficient C_D	Moment coefficient C_M
-4.5	633	-0.184	0.0616	+0.006
-3.0	637	-.058	.0483	-.013
-1.5	633	.056	.0370	-.013
0.0	637	.179	.0273	-.013
1.5	630	.298	.0165	-.006
3.0	635	.417	.0187	-.001
4.5	634	.529	.0250	-.005
6.0	633	.649	.0340	-.003
9.0	632	.882	.0582	-.002
12.0	631	1.080	.0908	-.028
15.0	631	1.206	.1368	-.031
18.0	630	1.221	.1901	-.065
21.0	625	1.183	.2751	-.103

TABLE XXIII

Section No. M23.
Span 30 in. (76.2 cm).
Area 0.0968 m².
Average temperature 48° C.
Average Reynolds No. 3,370,000.

Model No. 43.
Chord 5 in. (12.7 cm).
Aspect ratio 6.
Average pressure 19.94 atmos.

Angle of attack degrees	Dynamic pressure q kg/m ²	Lift coefficient C_L	Drag coefficient C_D	Moment coefficient C_M
-4.5	611	-0.148	0.0614	-0.001
-3.0	613	-.033	.0467	-.007
-1.5	617	.073	.0361	-.009
0.0	617	.192	.0206	+.004
1.5	620	.308	.0160	.000
3.0	620	.425	.0201	+.004
4.5	620	.531	.0278	+.017
6.0	611	.665	.0355	+.004
9.0	612	.880	.0573	-.008
12.0	607	1.100	.0859	-.004
15.0	610	1.232	.1264	-.018
18.0	606	1.236	.1850	-.070
21.0	606	1.234	.2392	-.080

TABLE XXV

Section No. M25.
Span 30 in. (76.2 cm).
Area 0.0968 m².
Average temperature 35° C.
Average Reynolds No. 3,640,000.

Model No. 45.
Chord 5 in. (12.7 cm).
Aspect ratio 6.
Average pressure 20.0 atmos.

Angle of attack degrees	Dynamic pressure q kg/m ²	Lift coefficient C_L	Drag coefficient C_D	Moment coefficient C_M
-4.5	657	-0.114	0.0662	+0.005
-3.0	653	-0.008	.0543	-.014
-1.5	652	.111	.0470	-.025
0.0	652	.251	.0424	-.030
1.5	653	.381	.0381	-.028
3.0	653	.502	.0364	-.023
4.5	647	.630	.0388	-.017
6.0	650	.745	.0460	-.032
9.0	650	.920	.0790	-.045
12.0	645	1.111	.1114	-.049
15.0	648	1.234	.1496	-.064
18.0	645	1.232	.2029	-.078
21.0	645	1.220	.2455	-.080

TABLE XXIV

Section No. M24.
Span 30 in. (76.2 cm).
Area 0.0968 m².
Average temperature 40° C.
Average Reynolds No. 3,500,000.

Model No. 44.
Chord 5 in. (12.7 cm).
Aspect ratio 6.
Average pressure 20.0 atmos.

Angle of attack degrees	Dynamic pressure q kg/m ²	Lift coefficient C_L	Drag coefficient C_D	Moment coefficient C_M
-4.5	641	-0.133	0.0150	-0.027
-3.0	640	-.019	.0126	-.021
-1.5	635	.087	.0123	-.001
0.0	635	.204	.0143	-.014
1.5	635	.320	.0181	-.013
3.0	638	.431	.0221	+.002
4.5	638	.533	.0282	+.035
6.0	637	.653	.0367	+.025
9.0	637	.875	.0583	-.014
12.0	636	1.055	.0866	-.011
15.0	640	1.126	.1294	-.036
18.0	632	1.133	.1868	-.067
21.0	631	1.155	.2293	-.064

TABLE XXVI

Section No. M26.
Span 30 in. (76.2 cm).
Area 0.0968 m².
Average temperature 41° C.
Average Reynolds No. 3,510,000.

Model No. 46.
Chord 5 in. (12.7 cm).
Aspect ratio 6.
Average pressure 20.0 atmos.

Angle of attack degrees	Dynamic pressure q kg/m ²	Lift coefficient C_L	Drag coefficient C_D	Moment coefficient C_M
-4.5	636	-0.082	0.0684	-0.011
-3.0	633	.039	.0571	-.023
-1.5	633	.159	.0484	-.033
0.0	632	.283	.0410	-.032
1.5	632	.402	.0293	-.023
3.0	629	.532	.0294	-.021
4.5	632	.634	.0359	-.026
6.0	630	.753	.0459	-.026
9.0	630	.976	.0702	-.029
12.0	630	1.133	.1114	-.051
15.0	626	1.186	.1654	-.066
18.0	628	1.197	.2012	-.114
21.0	627	1.185	.2486	-.119

TABLE XXVII

Section No. M27.
Span 30 in. (76.2 cm).
Area 0.0968 m².
Average temperature 35° C.
Average Reynolds No. 3,630,000.

Model No. 47.
Chord 5 in. (12.7 cm).
Aspect ratio 6.
Average pressure 20.2 atmos.

Angle of attack degrees	Dynamic pressure q kg/m ²	Lift coefficient C_L	Drag coefficient C_D	Moment coefficient C_M
-4.5	640	-0.011	0.0497	-0.030
-3.0	640	.081	.0300	-.036
-1.5	641	.182	.0203	-.034
0.0	640	.295	.0189	-.029
1.5	645	.411	.0232	-.023
3.0	644	.519	.0285	-.026
4.5	643	.624	.0358	-.020
6.0	642	.737	.0457	-.019
9.0	642	.929	.0707	-.027
12.0	641	1.007	.1100	-.042
15.0	640	1.048	.1508	-.044
18.0	637	1.081	.1913	-.079
21.0	631	1.086	.2380	-.072

TABLE XXVIII
CLASSIFICATION OF THE SECTIONS

Section	Camber line	Thickness	Section	Camber line	Thickness	Section	Camber line	Thickness
M1	Straight	I	M10	b	I	M19	(2b)	I
M2	Straight	II	M11	b	II	M20	(2b)	II
M3	Straight	III	M12	b	III	M21	(2b)	III
M4	a	I	M13	a+b	I	M22	(a+2b)	I
M5	a	II	M14	a+b	II	M23	(a+2b)	II
M6	a	III	M15	a+b	III	M24	(a+2b)	III
M7	2a	I	M16	(2a+b)	I	M25	2(a+b)	I
M8	2a	II	M17	(2a+b)	II	M26	2(a+b)	II
M9	2a	III	M18	(2a+b)	III	M27	2(a+b)	III

TABLE XXIX
ORDINATES FOR N. A. C. A. AIRFOILS M1 TO M27
[U=Upper camber. L=Lower camber]

No.		Per cent of chord																	
		0	1.25	2.50	5.0	7.5	10	15	20	25	30	40	50	60	70	80	90	95	100
M1	U	0.00	1.03	1.36	1.80	2.10	2.34	2.67	2.88	3.01	3.08	3.05	2.85	2.53	2.08	1.54	0.91	0.57	0.20
	L	.00	-1.03	-1.36	-1.80	-2.10	-2.34	-2.67	-2.88	-3.01	-3.08	-3.05	-2.85	-2.53	-2.08	-1.54	-.91	-.57	-.20
M2	U	.00	1.30	1.74	2.33	2.74	3.05	3.49	3.78	3.95	4.03	4.00	3.74	3.30	2.71	1.99	1.15	.69	.20
	L	.00	-1.30	-1.74	-2.33	-2.74	-3.05	-3.49	-3.78	-3.95	-4.03	-4.00	-3.74	-3.30	-2.71	-1.99	-1.15	-.69	-.20
M3	U	.00	1.86	2.51	3.39	4.00	4.47	5.14	5.57	5.83	5.95	5.89	5.50	4.85	3.96	2.88	1.62	.93	.20
	L	.00	-1.86	-2.51	-3.39	-4.00	-4.47	-5.14	-5.57	-5.83	-5.95	-5.89	-5.50	-4.85	-3.96	-2.88	-1.62	-.93	-.20
M4	U	1.10	2.32	2.86	3.67	4.31	4.83	5.61	6.16	6.51	6.67	6.56	6.05	5.24	4.30	3.39	2.59	2.29	2.09
	L	1.10	.19	.07	.01	.02	.07	.20	.33	.38	.39	.33	.18	.05	.01	.21	.71	1.09	1.60
M5	U	1.89	3.28	3.93	4.87	5.63	6.23	7.14	7.77	8.15	8.34	8.26	7.69	6.80	5.77	4.73	3.78	3.38	3.13
	L	1.89	.59	.34	.09	.02	.00	.04	.07	.11	.13	.07	.02	.02	.17	.59	1.33	1.89	2.50
M6	U	.00	1.97	2.81	4.03	4.94	5.71	6.82	7.55	8.01	8.22	8.05	7.26	6.03	4.58	3.06	1.55	.88	.26
	L	.00	-1.76	-2.20	-2.73	-3.03	-3.24	-3.47	-3.62	-3.71	-3.79	-3.90	-3.94	-3.82	-3.48	-2.83	-1.77	-1.08	-.26
M7	U	.76	2.05	2.77	3.92	4.87	5.68	6.89	7.74	8.26	8.49	8.25	7.32	5.99	4.51	3.13	2.13	1.87	1.79
	L	.76	.00	.04	.32	.65	.99	1.58	1.98	2.23	2.31	2.06	1.53	.85	.27	.00	.30	.71	1.32
M8	U	.95	2.66	3.52	4.82	5.86	6.73	8.08	9.00	9.57	9.82	9.60	8.80	7.22	5.63	4.12	2.94	2.56	2.31
	L	.95	.06	.01	.13	.37	.64	1.09	1.43	1.63	1.72	1.55	1.05	.51	.10	.04	.59	1.12	1.91
M9	U	1.81	4.08	5.14	6.76	8.03	9.08	10.69	11.74	12.38	12.73	12.51	11.43	9.83	7.98	6.11	4.52	3.94	3.53
	L	1.81	.44	.15	.00	.05	.16	.42	.63	.75	.80	.66	.40	.09	.01	.32	1.25	2.03	3.06
M10	U	1.34	2.49	2.97	3.68	4.24	4.71	5.40	5.87	6.16	6.31	6.25	5.82	5.13	4.28	3.35	2.40	1.92	1.42
	L	1.34	.41	.19	.04	.01	.01	.04	.08	.11	.12	.09	.03	.01	.09	.27	.58	.79	1.03
M11	U	2.13	3.59	4.24	5.12	5.78	6.31	7.11	7.66	7.99	8.16	8.10	7.61	6.83	5.83	4.73	3.57	2.97	2.39
	L	2.13	.93	.67	.39	.23	.15	.08	.04	.02	.01	.02	.07	.21	.46	.87	1.43	1.76	2.15
M12	U	.00	2.03	2.86	4.01	4.89	5.59	6.61	7.30	7.74	7.95	7.86	7.25	6.27	4.98	3.50	1.89	1.07	.20
	L	.00	-1.65	-2.14	-2.72	-3.07	-3.31	-3.60	-3.80	-3.92	-3.98	-3.96	-3.82	-3.50	-3.00	-2.31	-1.37	-.81	-.20
M13	U	.84	2.11	2.76	3.77	4.58	5.24	6.28	6.98	7.43	7.65	7.51	6.86	5.81	4.55	3.22	1.87	1.23	.60
	L	.84	.02	.01	.15	.35	.55	.93	1.21	1.38	1.44	1.34	1.05	.66	.30	.07	.00	.05	.16
M14	U	1.28	2.80	3.56	4.70	5.63	6.37	7.51	8.31	8.78	9.01	8.89	8.15	6.99	5.56	4.02	2.42	1.62	.80
	L	1.28	.16	.05	.04	.13	.25	.51	.74	.87	.93	.83	.58	.30	.06	.01	.05	.18	.38
M15	U	2.41	4.47	5.44	6.89	8.04	8.97	10.33	11.28	11.87	12.17	12.03	11.20	9.86	8.16	6.29	4.33	3.35	2.39
	L	2.41	.78	.42	.13	.02	.00	.03	.09	.14	.17	.11	.03	.00	.14	.41	1.02	1.44	1.94
N16	U	.83	2.04	2.71	3.81	4.69	5.42	6.56	7.34	7.82	8.03	7.85	7.06	5.83	4.48	3.14	1.96	1.49	1.16
	L	.83	.01	.04	.25	.51	.78	1.24	1.59	1.80	1.88	1.71	1.30	.72	.26	.01	.13	.35	.68
M17	U	1.16	2.72	3.51	4.75	5.74	6.54	7.70	8.52	9.14	9.37	9.23	8.37	7.05	5.55	4.01	2.64	2.06	1.57
	L	1.16	.08	.01	.07	.23	.43	.78	1.06	1.26	1.30	1.15	.80	.38	.07	.02	.33	.68	1.16
M18	U	2.20	4.25	5.25	6.78	7.99	8.94	10.47	11.48	12.12	12.42	12.26	11.33	9.82	8.09	6.23	4.45	3.66	2.95
	L	2.20	.56	.25	.03	.00	.03	.17	.31	.41	.46	.41	.19	.03	.05	.40	1.17	1.75	2.51
M19	U	.75	2.04	2.88	4.30	5.39	6.39	7.81	8.88	9.50	9.80	9.54	8.50	6.94	5.16	3.37	1.87	1.24	.71
	L	.75	.03	.20	.68	1.21	1.71	2.54	3.12	3.48	3.63	3.43	2.74	1.84	.96	.30	.02	.10	.33
M20	U	.98	2.64	3.57	5.13	6.32	7.41	8.95	10.04	10.77	11.07	10.81	9.70	8.04	6.10	4.16	2.40	1.66	1.05
	L	.98	.00	.03	.39	.82	1.25	1.95	2.46	2.78	2.92	2.72	2.11	1.32	.58	.11	.06	.24	.58
M21	U	1.68	3.89	5.04	6.86	8.30	9.50	11.33	12.58	13.34	13.70	13.46	12.23	10.36	8.17	5.89	3.70	2.73	1.92
	L	1.68	.17	.02	.83	.30	.55	1.03	1.42	1.66	1.75	1.57	1.11	.54	.12	.03	.41	.81	1.44
M22	U	.72	2.11	2.98	4.45	5.60	6.66	8.22	9.31	9.96	10.25	9.94	8.75	7.06	5.14	3.36	1.97	1.53	1.32
	L	.72	.02	.22	.79	1.38	1.92	2.84	3.48	3.87	4.00	3.73	2.88	1.85	.84	.16	.06	.33	.79
M23	U	.87	2.60	3.63	5.23	6.51	7.60	9.28	10.44	11.15	11.48	11.19	9.95	8.14	6.08	4.09	2.53	1.98	1.66
	L	.87	.01	.12	.54	1.01	1.49	2.30	2.86	3.21	3.34	3.06	2.30	1.40	.53	.04	.17	.54	1.12

TABLE XXIX—Continued

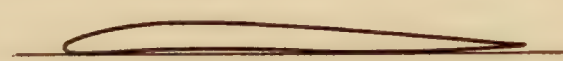
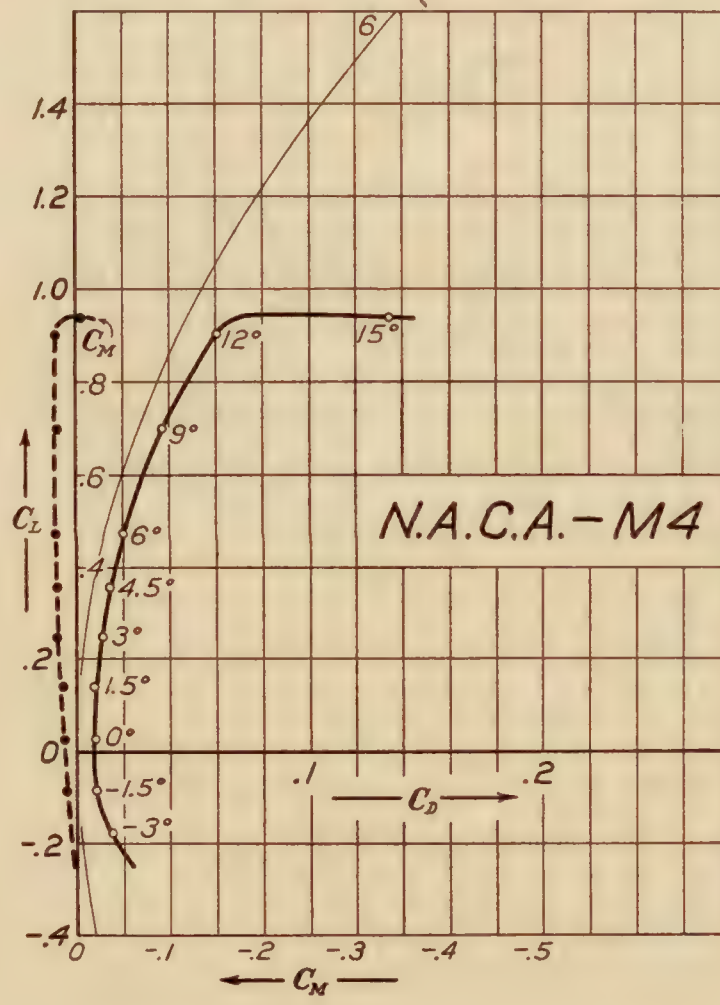
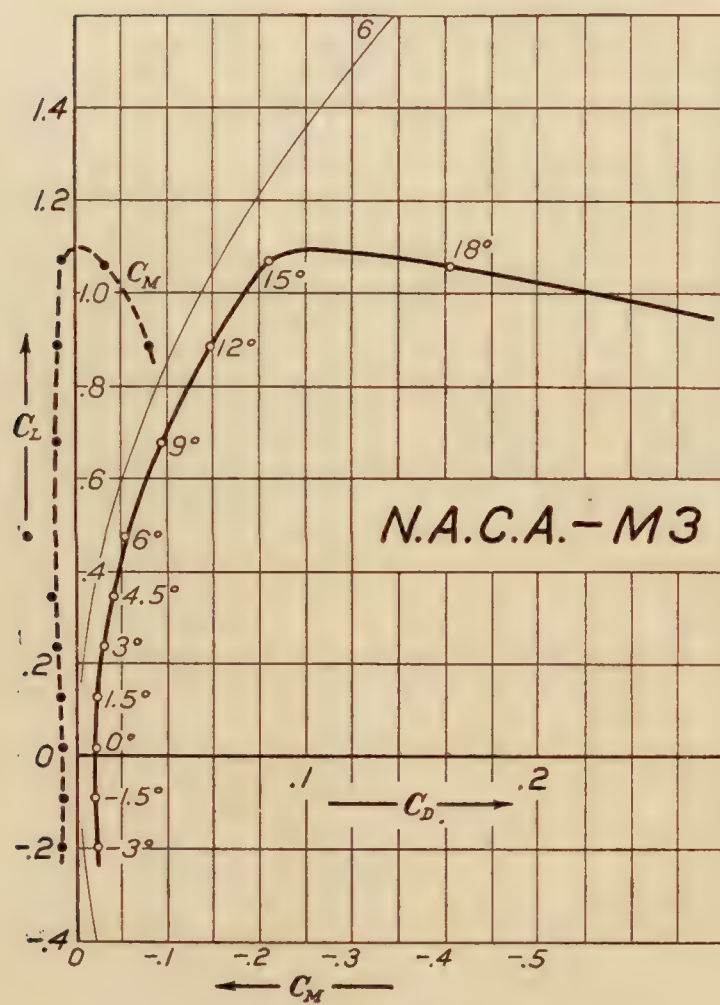
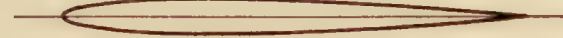
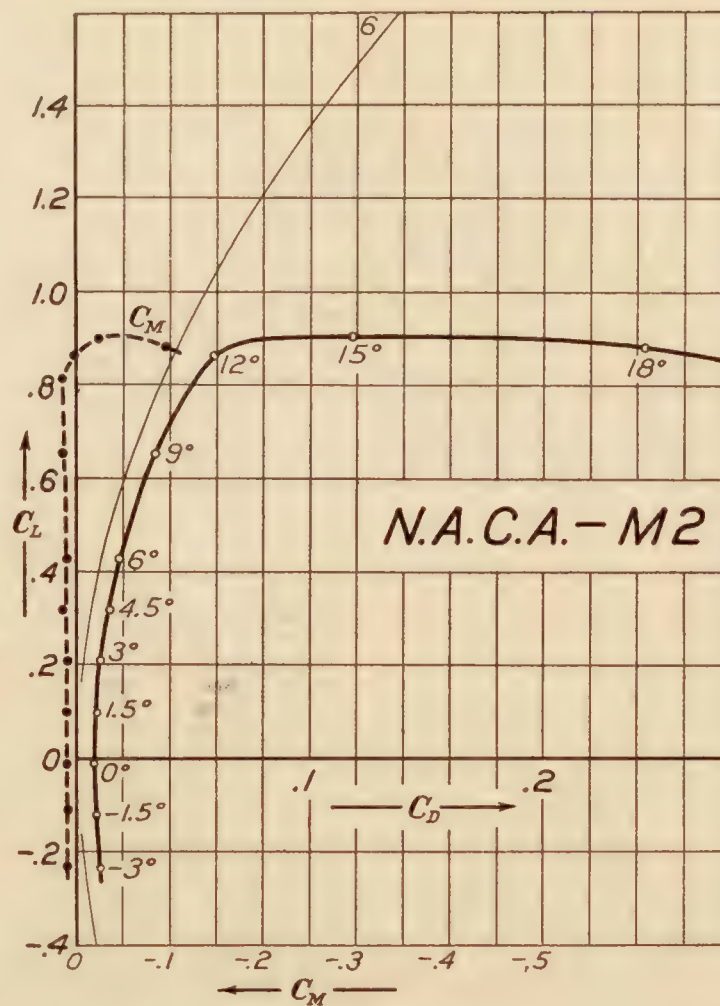
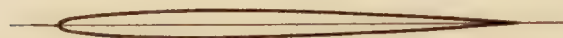
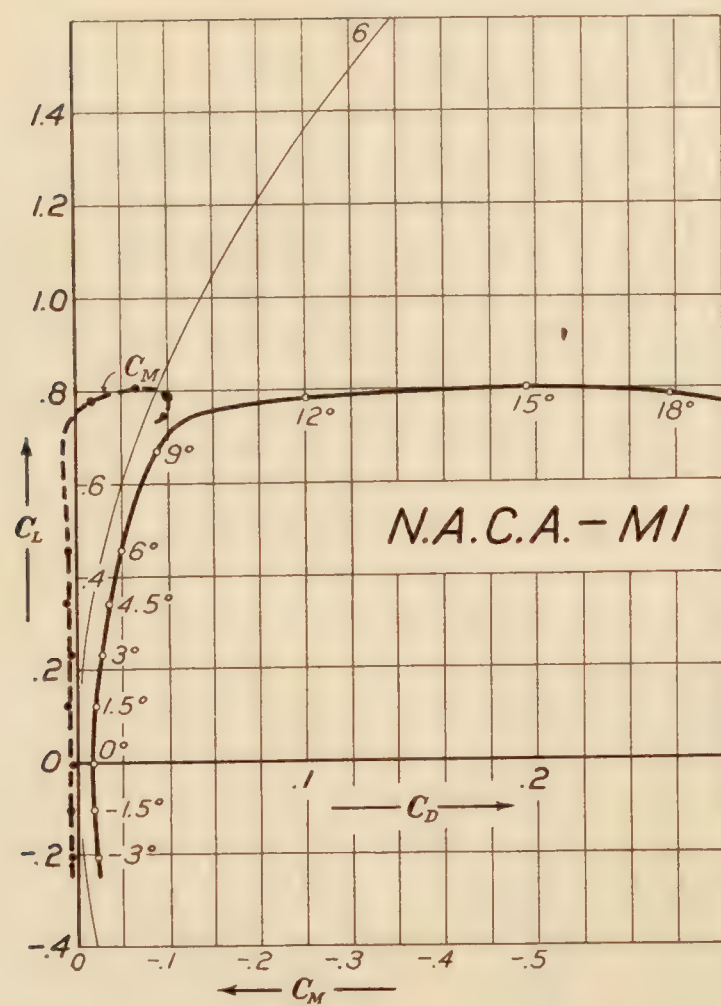
No.	Per cent of chord																	
	0	1.25	2.50	5.0	7.5	10	15	20	25	30	40	50	60	70	80	90	95	100
M24 U	1.50	3.80	5.00	6.92	8.38	9.66	11.59	12.93	13.72	14.08	13.76	12.40	10.39	8.11	5.82	3.85	3.09	2.48
L	1.50	.12	.01	.13	.40	.72	1.31	1.77	2.04	2.13	1.92	1.33	.64	.13	.04	.63	1.26	2.13
M25 U	.67	2.28	3.24	5.04	6.39	7.60	9.52	10.89	11.69	12.05	11.68	10.22	8.16	5.86	3.66	1.90	1.31	.93
L	.67	.09	.45	1.28	2.15	2.91	4.14	5.04	5.54	5.78	5.44	4.36	2.96	1.54	.47	.00	.11	.48
M26 U	.82	2.60	3.71	5.66	7.11	8.41	10.47	11.96	12.80	13.19	12.82	11.32	9.11	6.68	4.32	2.35	1.66	1.20
L	.82	.02	.25	.94	1.68	2.39	3.54	4.35	4.84	5.04	4.72	3.73	2.44	1.19	.29	.02	.26	.72
M27 U	1.22	3.67	5.06	7.23	9.00	10.47	12.72	14.28	15.24	15.69	15.33	13.72	11.36	8.65	5.93	3.56	2.64	1.91
L	1.22	.04	.05	.44	1.00	1.55	2.47	3.17	3.57	3.74	3.45	2.59	1.53	.59	.04	.23	.68	1.39

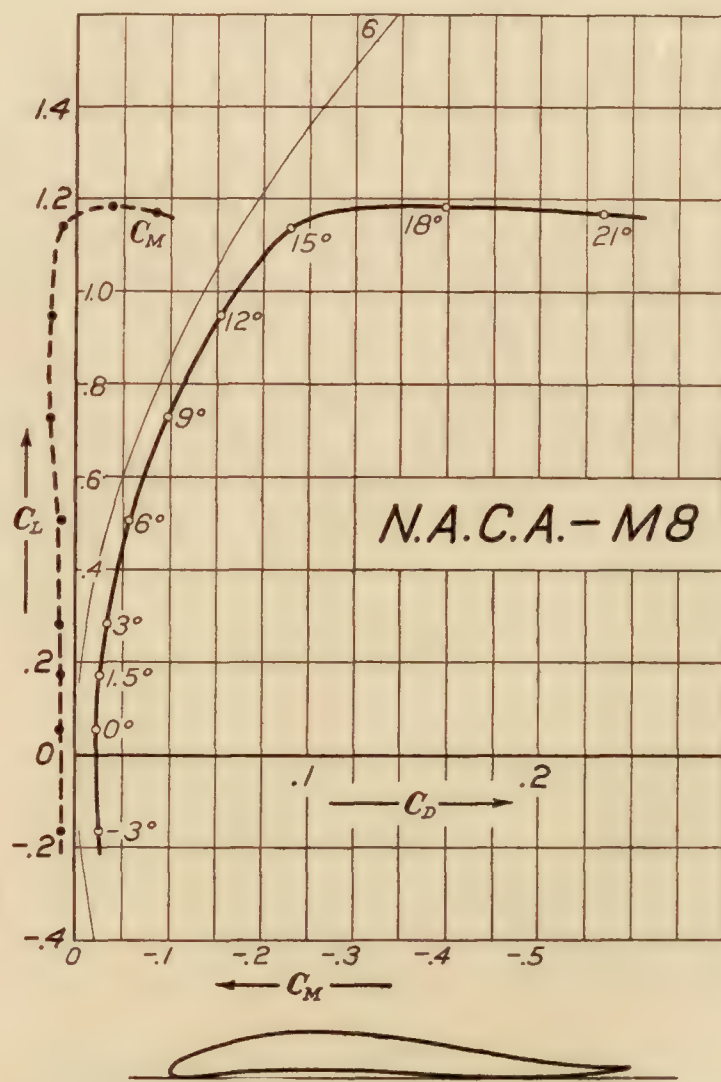
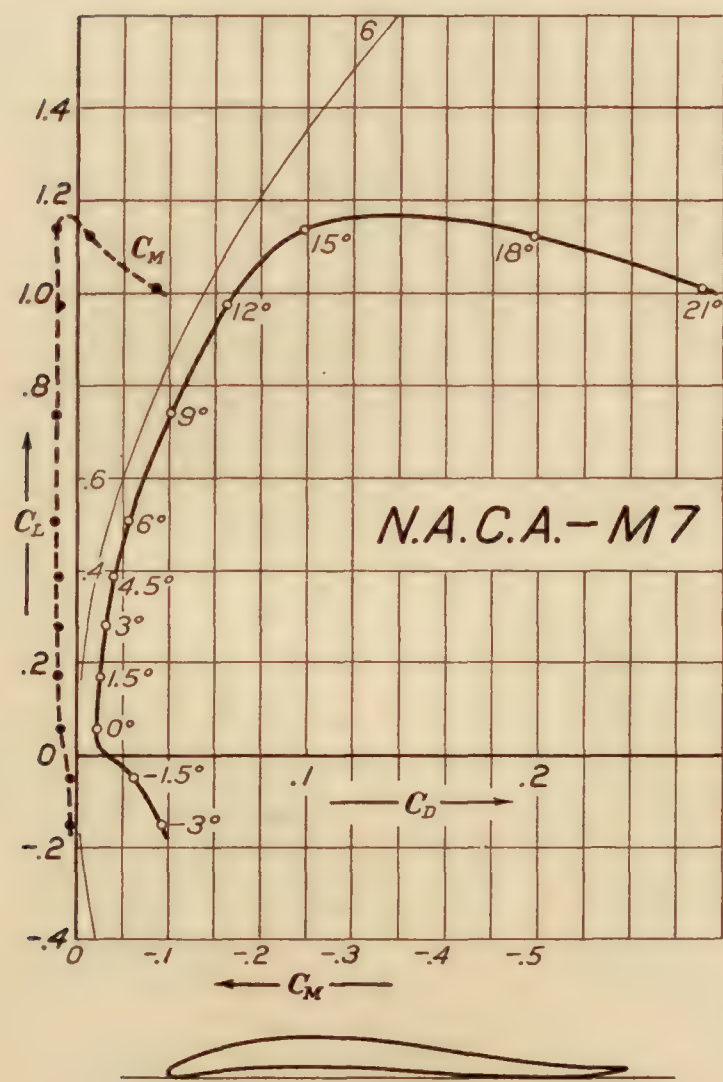
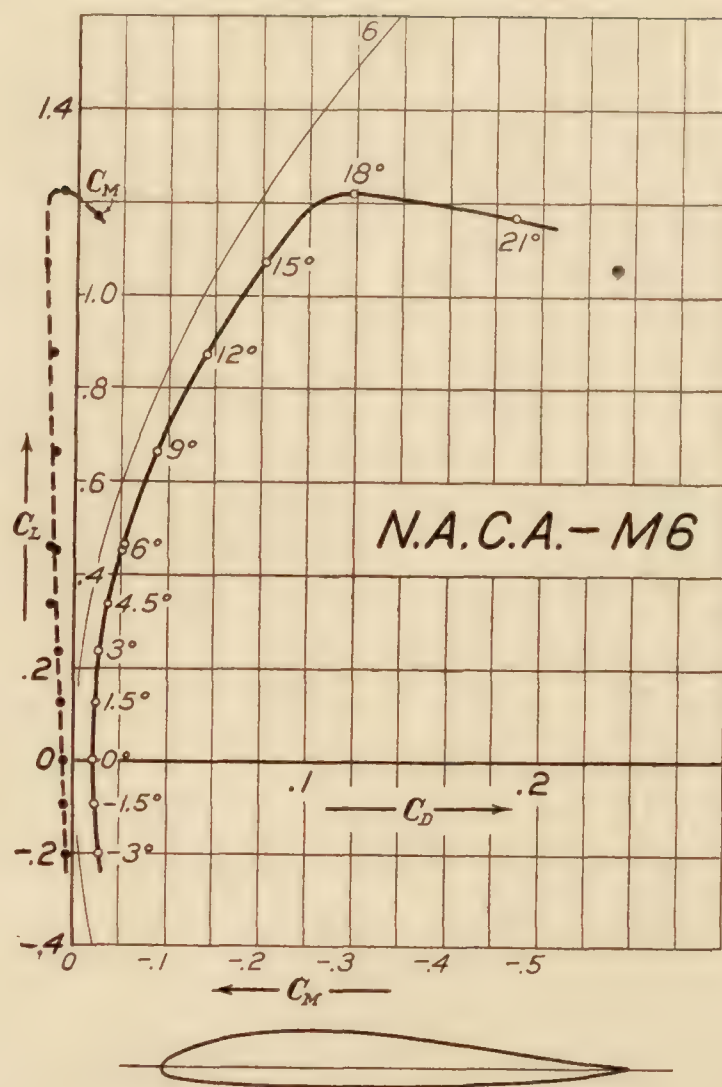
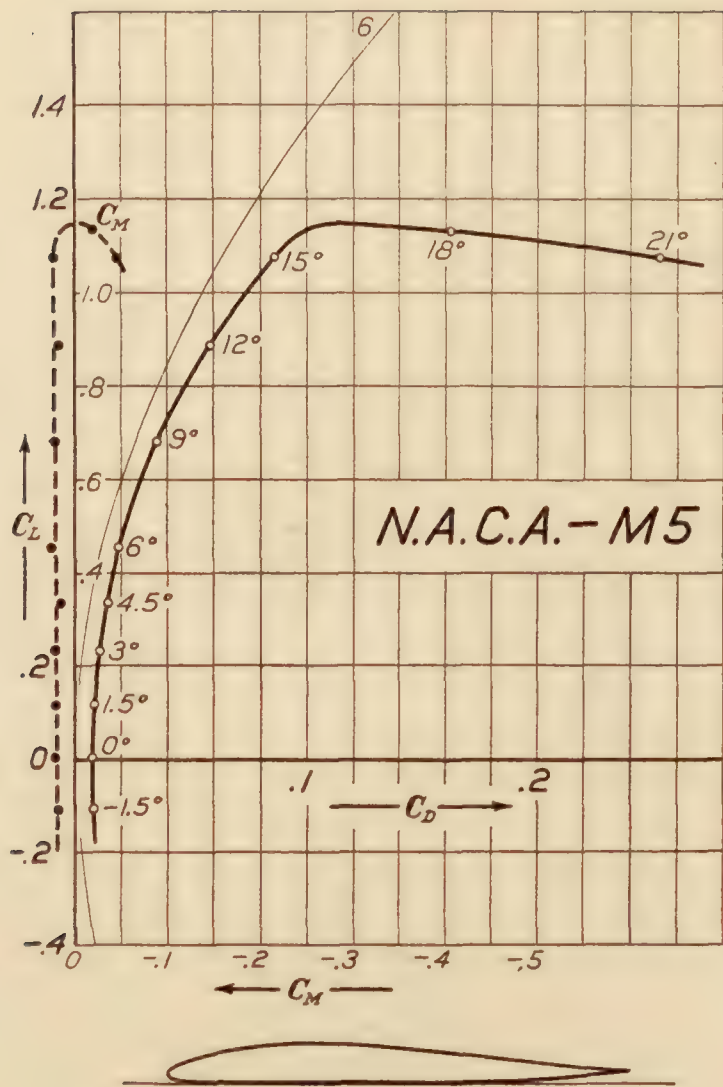
TABLE XXX

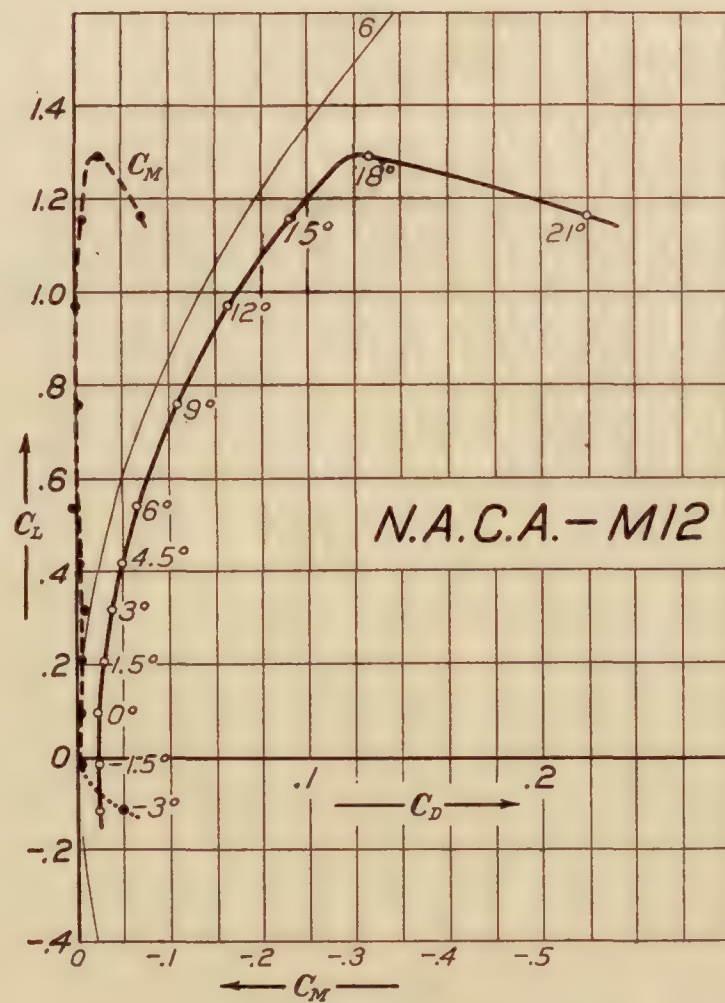
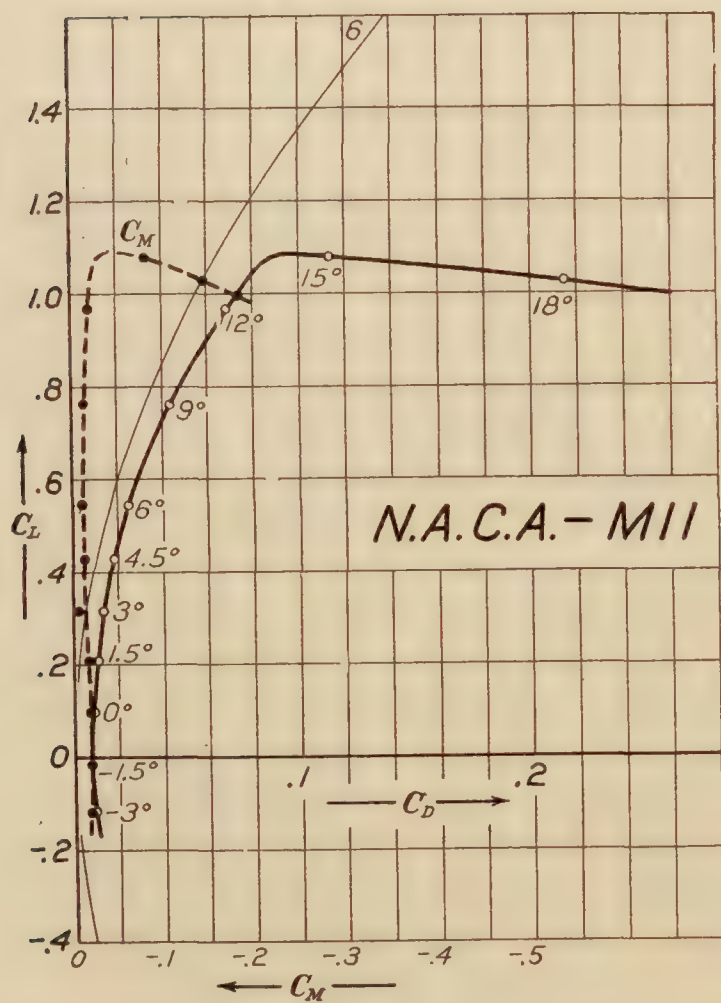
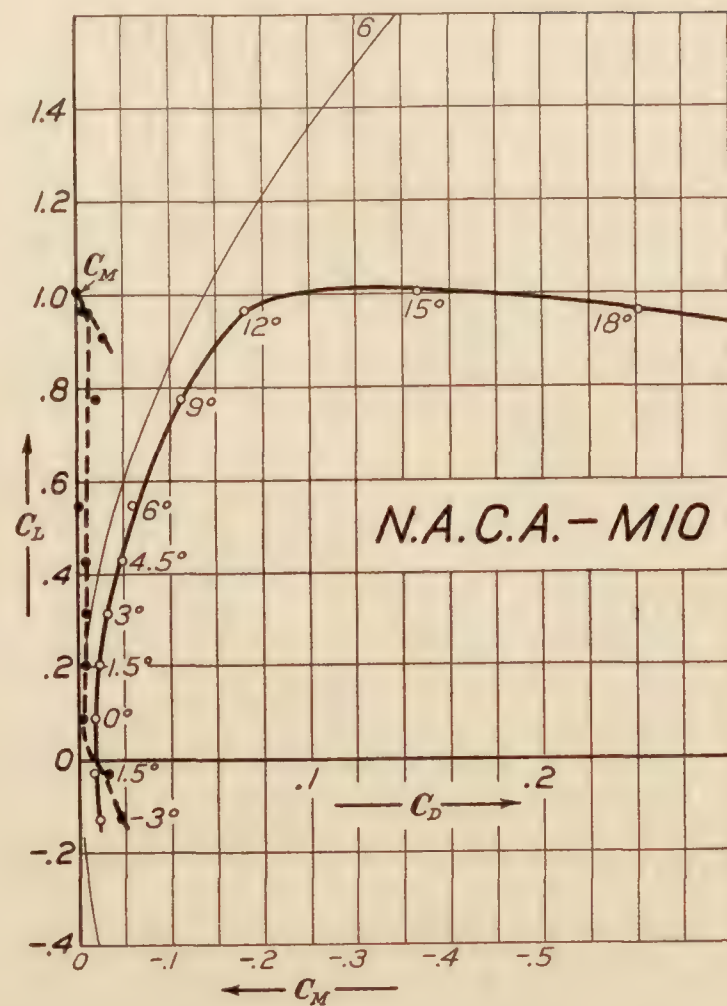
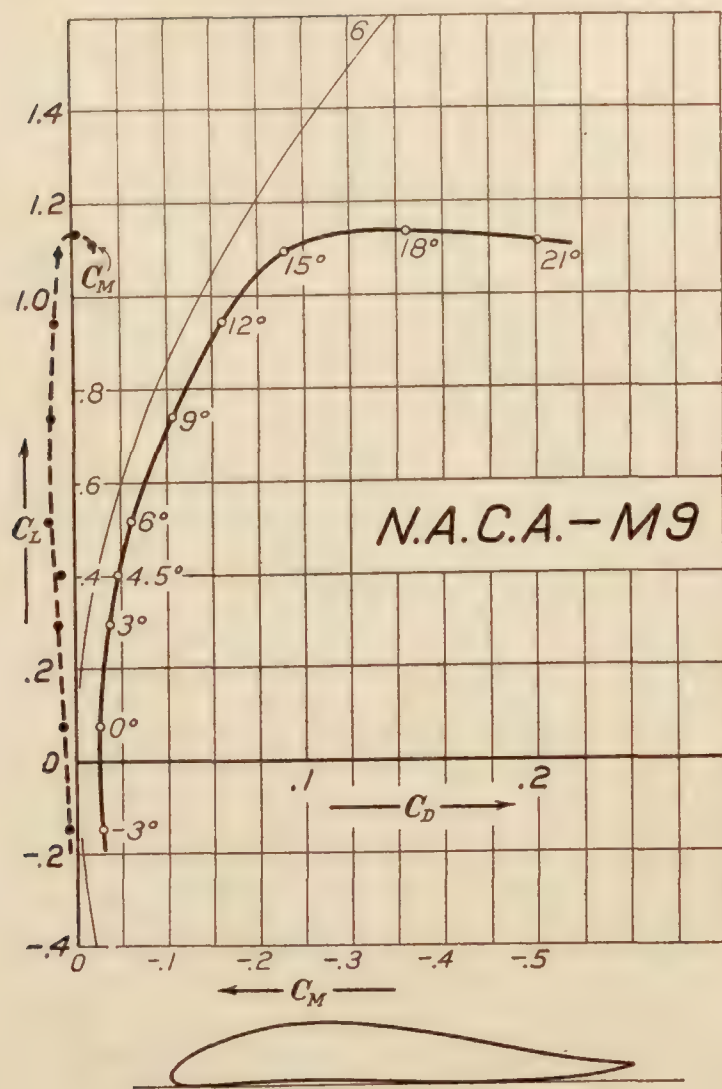
AERODYNAMIC PROPERTIES OF THE SECTIONS¹

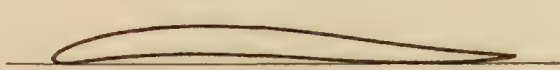
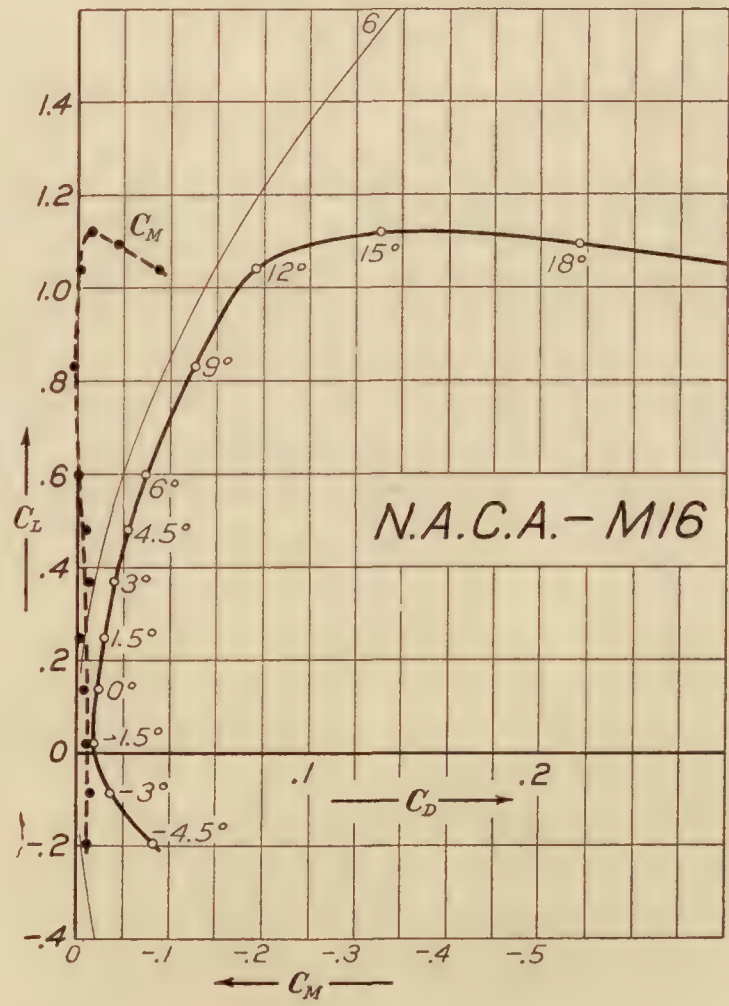
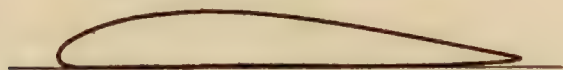
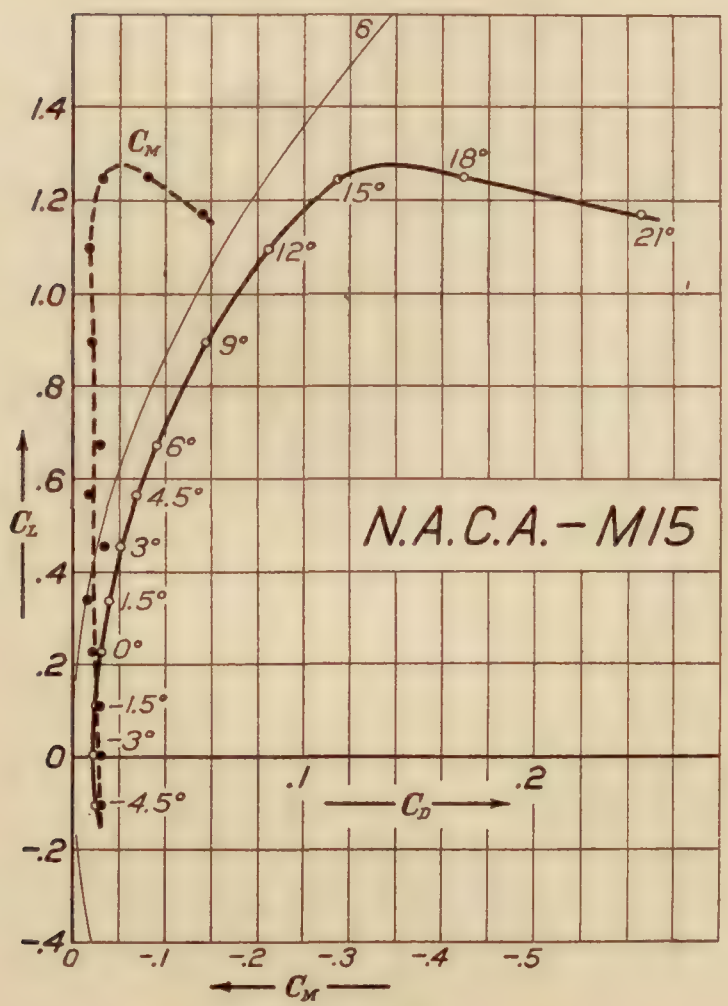
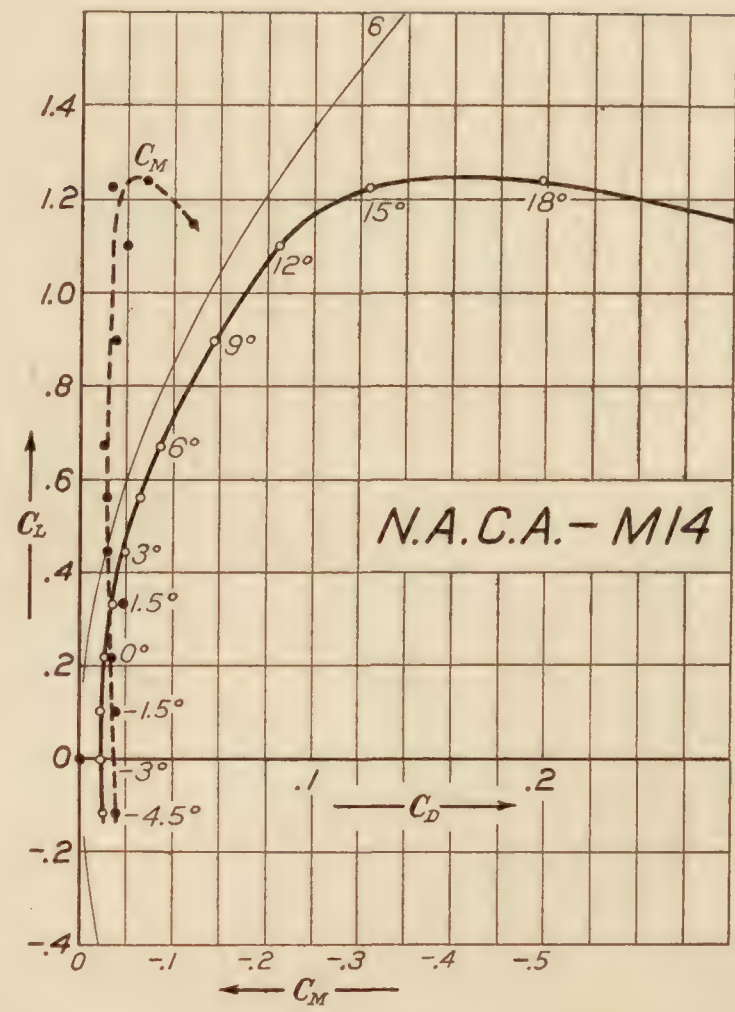
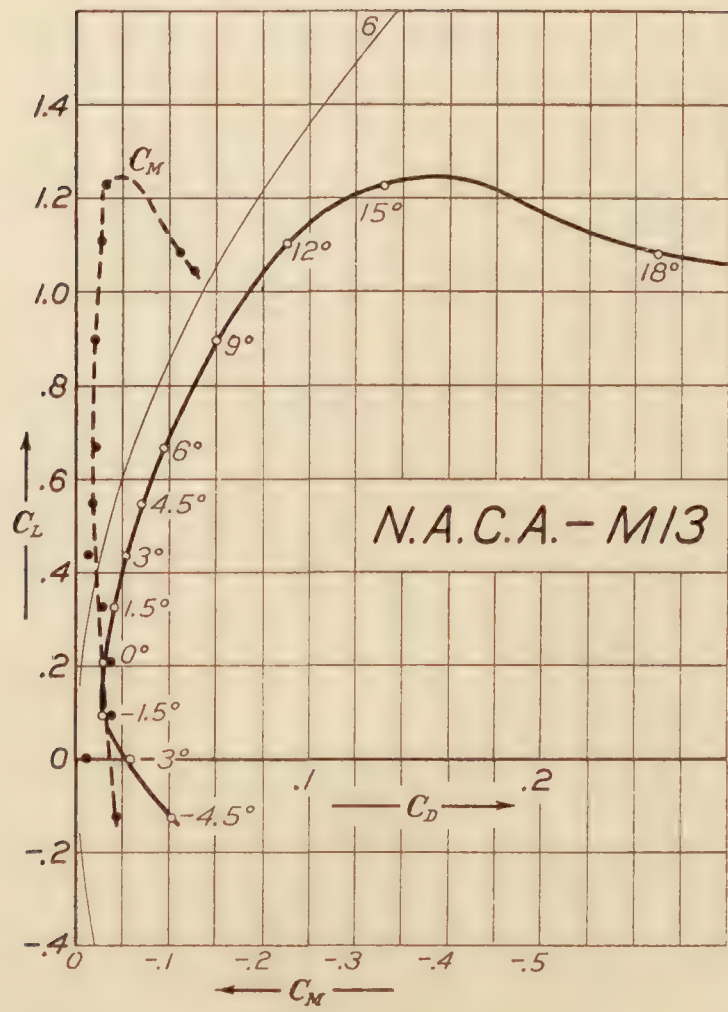
Section No.	Minimum drag coefficient	Maximum lift coefficient	Burble lift coefficient	Average moment ² coefficient
1	0.0072	0.805	0.75	0.008
2	.0078	.903	.85	.010
3	.0082	1.069	1.05	.018
4	.0067	-----	.95	.020
5	.0073	1.132	1.15	.020
6	.0080	1.222	1.20	.025
7	.0088	1.139	-----	.022
8	.0089	1.183	1.15	.020
9	.0101	1.137	1.10	.020
10	.0068	1.004	1.00	-.010
11	.0078	1.080	1.05	-.015
12	.0089	1.293	1.30	.000
13	.0116	1.299	-----	-.025
14	.0096	1.244	1.20	-.035
15	.0091	1.250	1.20	-.025
16	.0080	1.119	1.10	-.005
17	.0092	-----	1.20	-.002
18	.0093	-----	1.00	-.005
19	.0189	1.258	1.20	-.025
20	.0173	1.311	1.30	-.035
21	.0115	-----	1.10	-.025
22	.0165	1.221	-----	-.010
23	.0160	1.236	1.20	-.002
24	.0123	-----	1.10	.000
25	.0364	1.234	-----	-.030
26	.0293	1.197	-----	-.030
27	.0189	-----	.90	-.030

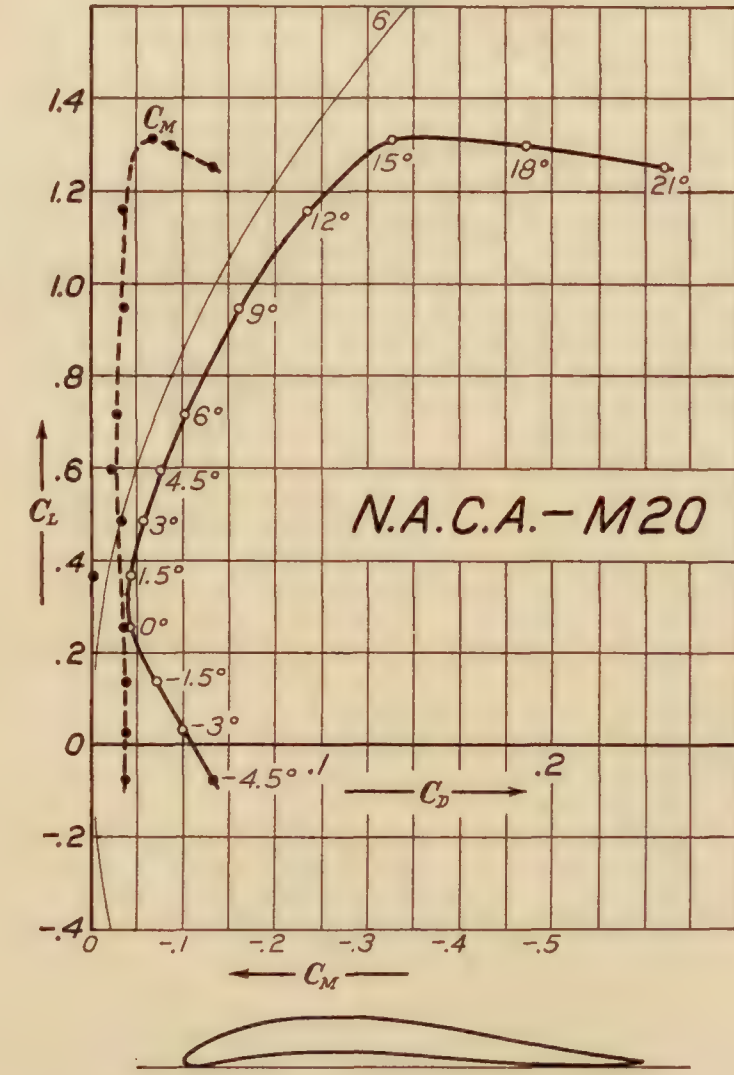
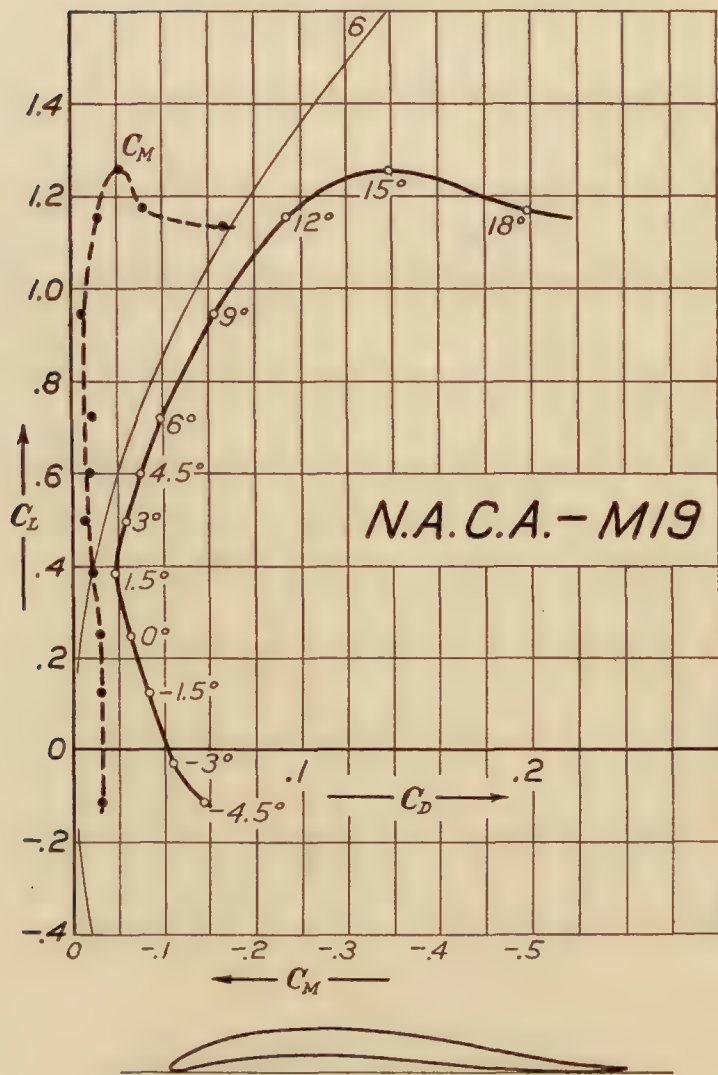
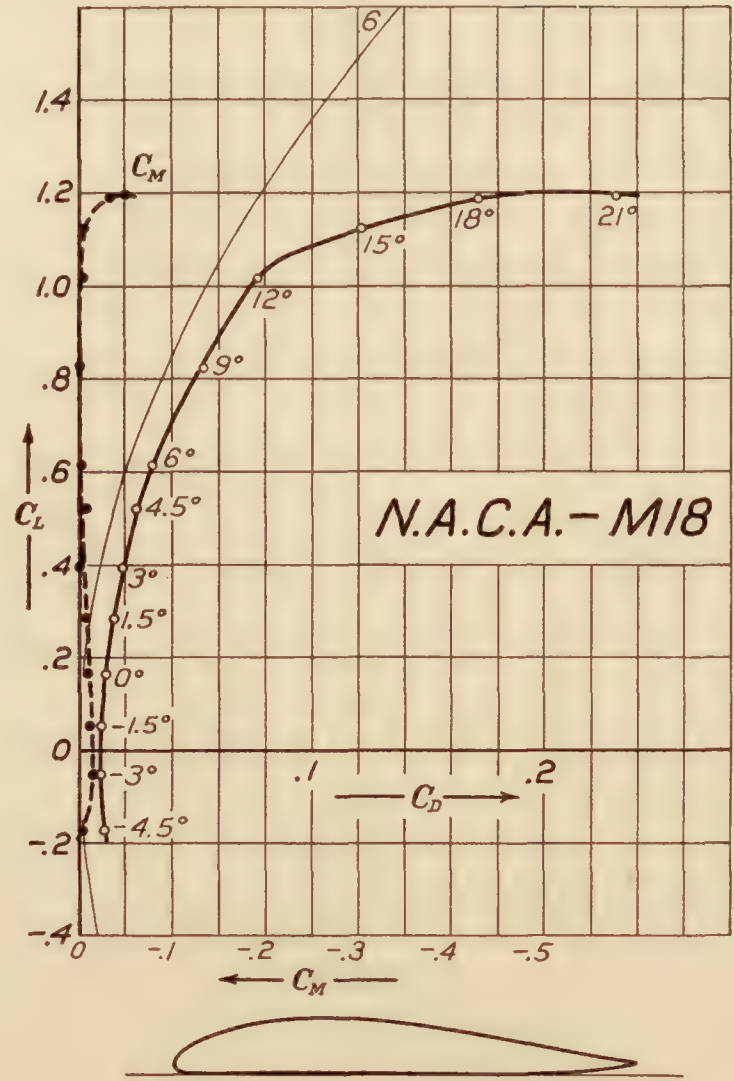
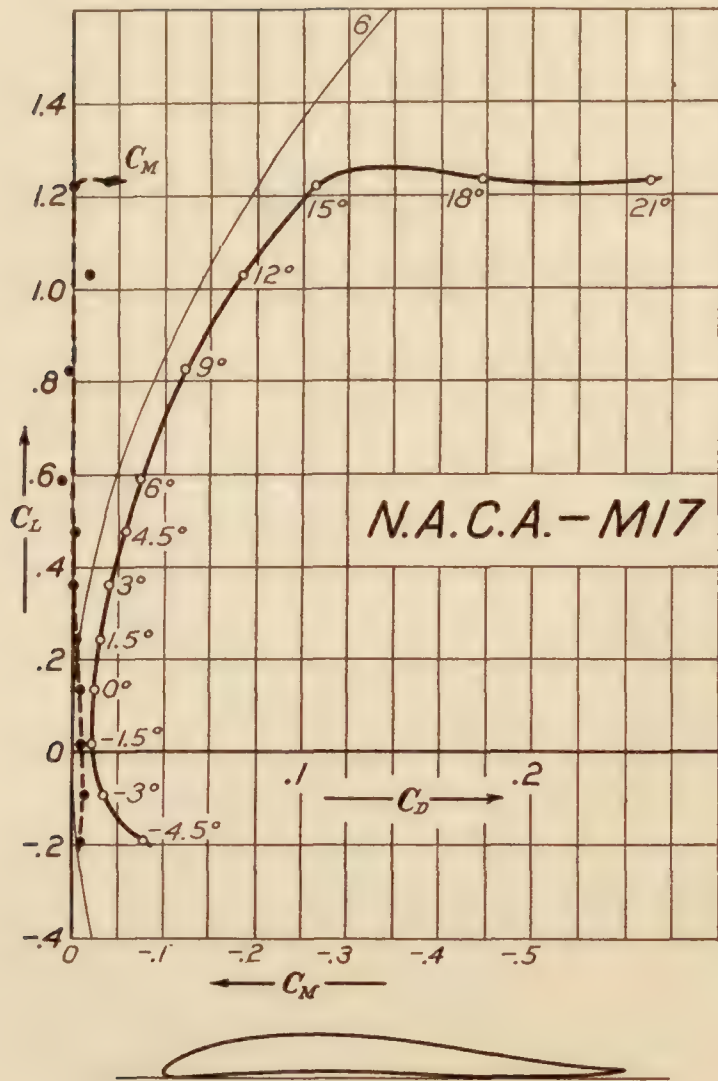
¹ Moments taken about a point at 25 per cent of the chord.² The last column gives the average moment coefficient, which is always small for the wing sections considered in this investigation.

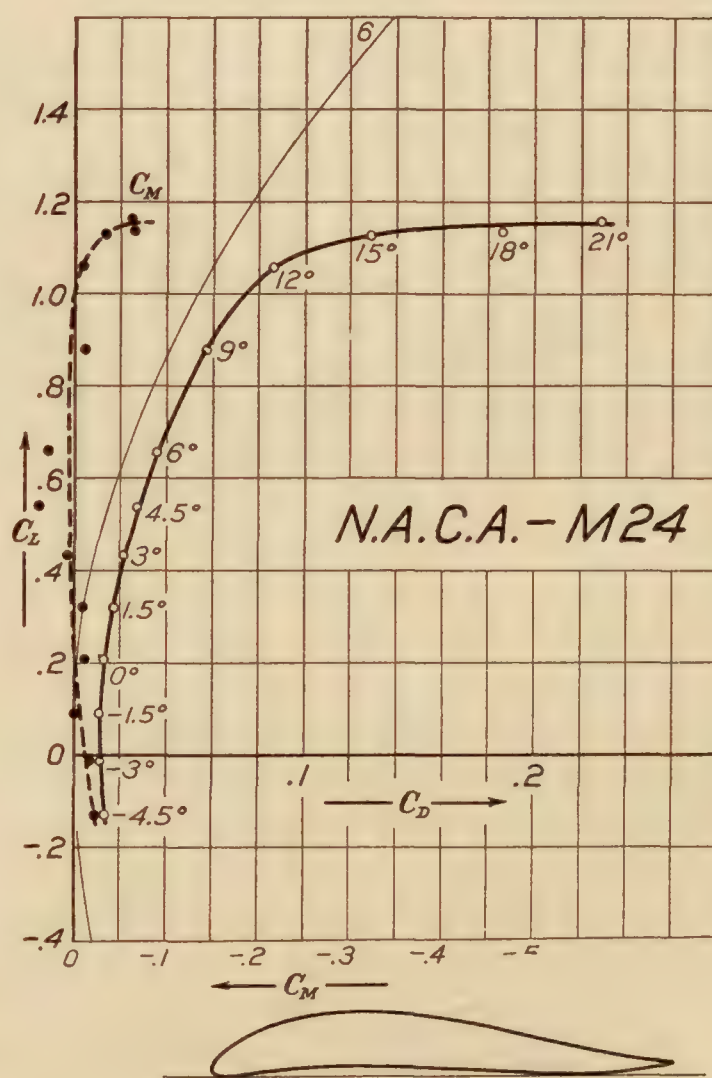
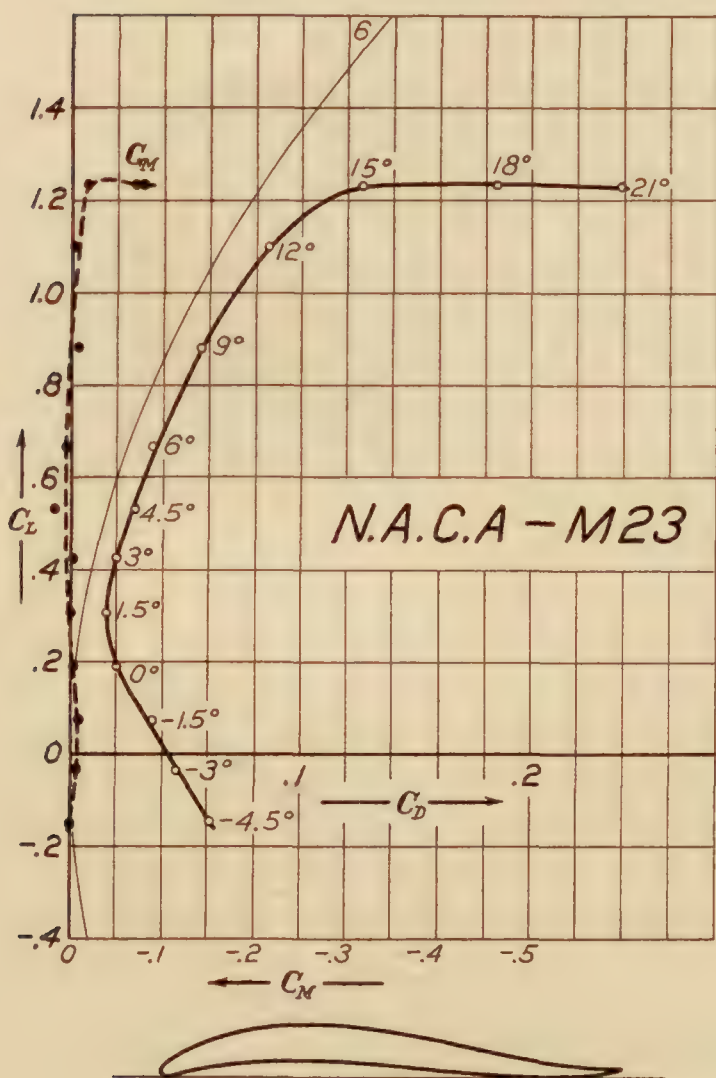
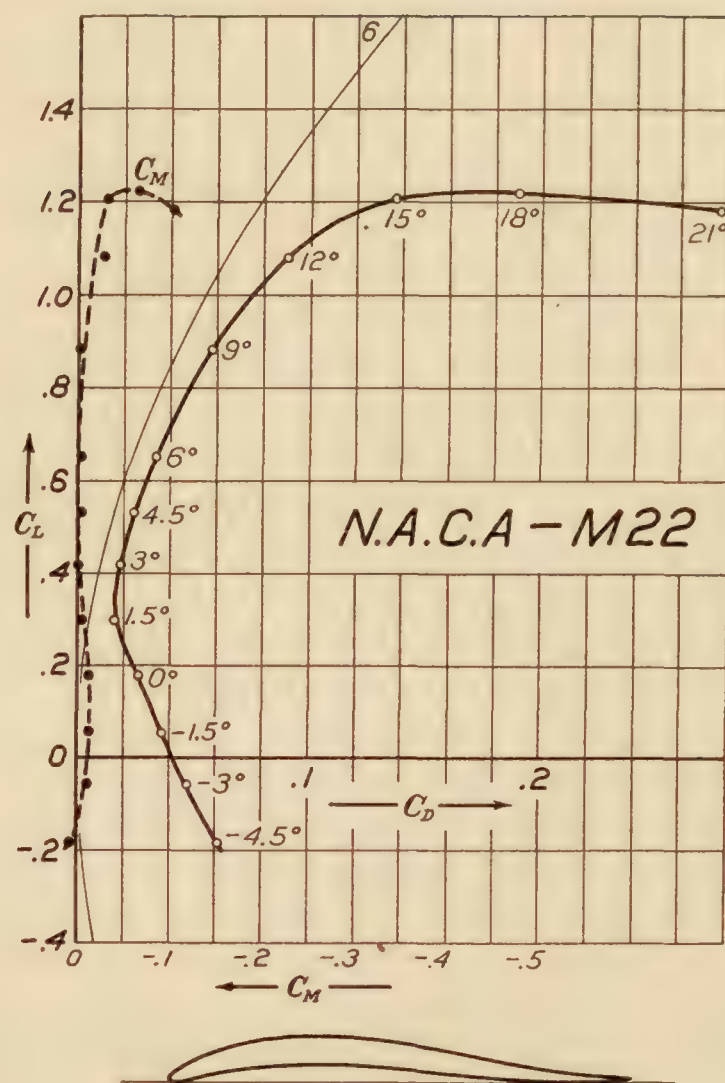
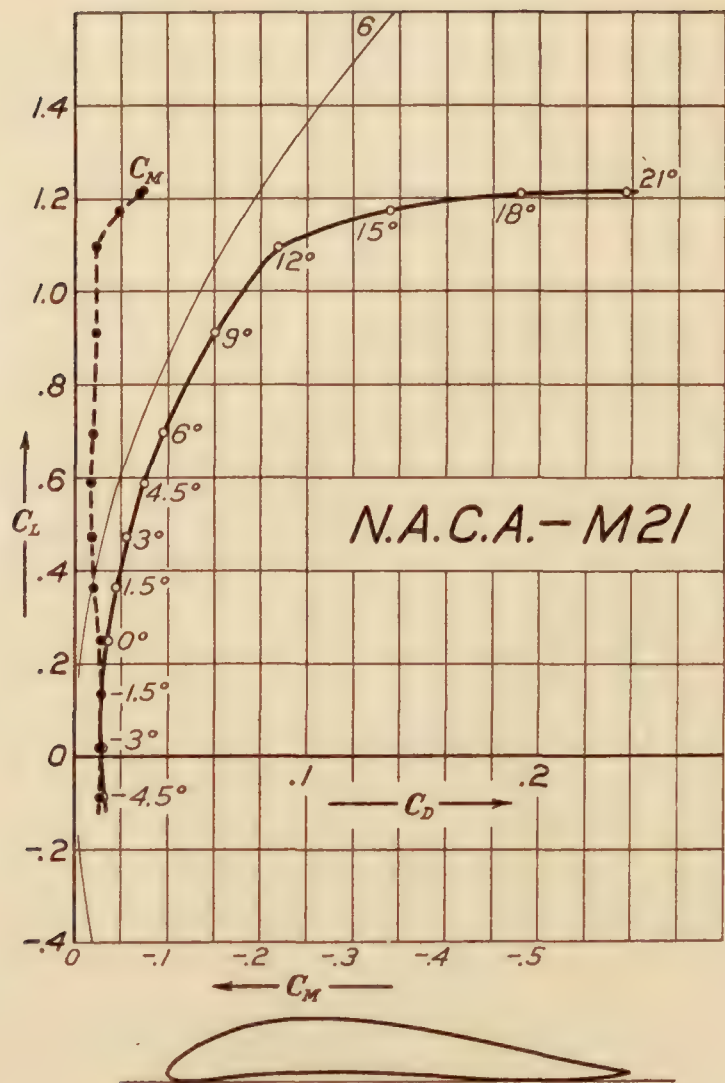


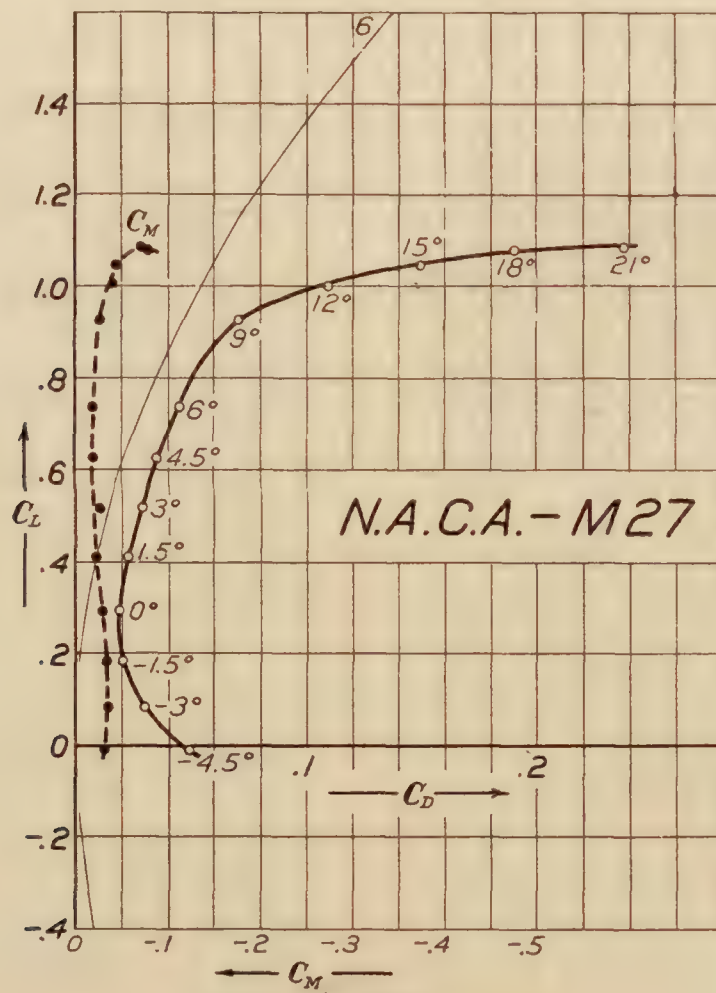
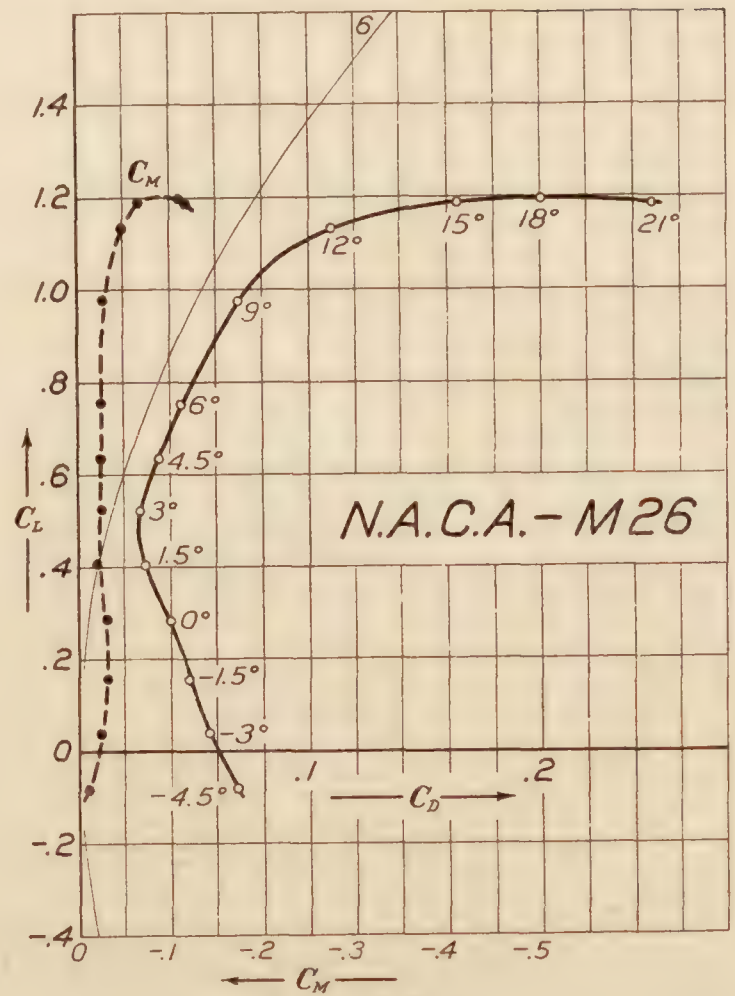
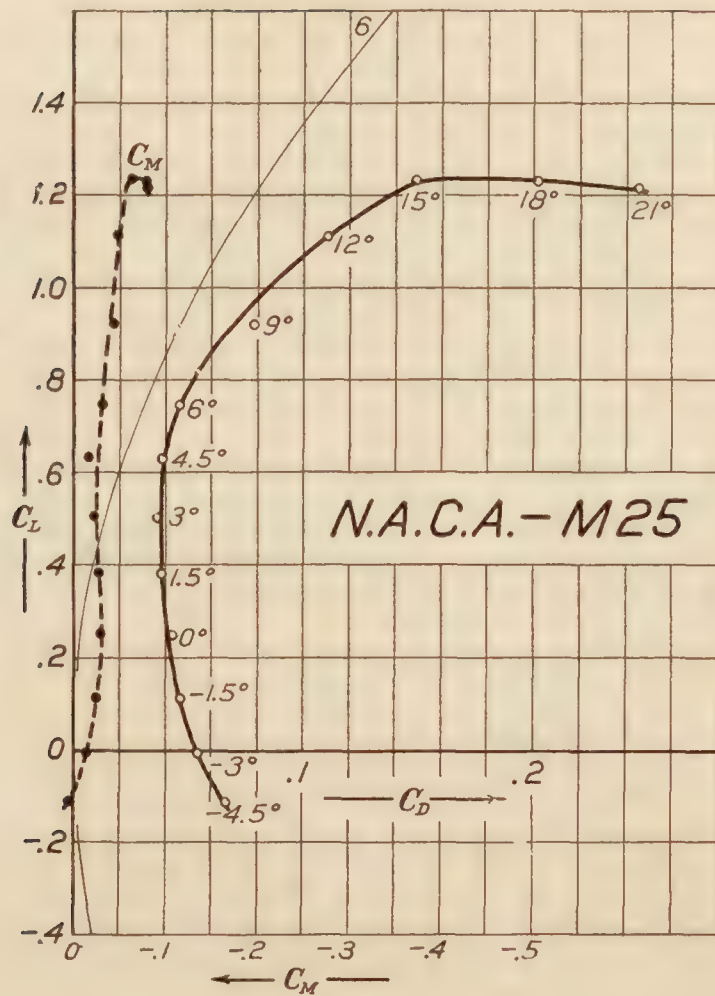












REPORT No. 222

SPRAY PENETRATION WITH A SIMPLE FUEL INJECTION NOZZLE

By HAROLD E. MILLER and EDWARD G. BEARDSLEY
Langley Memorial Aeronautical Laboratory

REPORT No. 222

SPRAY PENETRATION WITH A SIMPLE FUEL INJECTION NOZZLE

By Harold E. Miller and Edward G. Beardsley

SUMMARY

The tests covered by this report form a part of a general investigation of the application of fuel injection engine principles to aircraft engine service. The purpose of these tests was to obtain specific information on the rate of penetration of the spray from a simple injection nozzle, having a single orifice with a diameter of .015 inch when injecting into compressed gases.

The fuel was sprayed into a chamber fitted with glass walls and filled with nitrogen at various pressures. Special high-speed photographic apparatus, capable of taking a continuous series of 15 photographs at a rate of 4,000 per second, was used to record the development of single sprays. The effects of fuel pressures from 2,000 to 8,000 pounds per square inch and chamber pressures from atmospheric to 300 pounds per square inch on the rate of penetration and the development of the spray were studied.

The results have shown that the effects of both chamber and fuel pressures on penetration are so marked that the study of sprays by means of high-speed photography or its equivalent is necessary if the effects are to be appreciated sufficiently to enable rational analysis. It was found for these tests that the negative acceleration of the spray tip is approximately proportional to the 1.5 power of the instantaneous velocity of the spray tip.

INTRODUCTION

It is usual to study the characteristics of sprays produced by fuel injection engine fuel nozzles by spraying into liquids or the atmosphere. While such tests are easily made, they are not entirely satisfactory, since the test conditions are far different from the actual conditions met in the engine cylinder.

Lack of information regarding the effect of the compressed gases on the spray handicaps the analysis of the action inside the engine cylinder. This fundamental information is especially desirable when applying fuel injection to aviation engines, since the conditions in this field are so different from those existing in low-speed engines now in use that commercial experiences can serve only as a very rough guide.

An item of major importance is the rate of penetration of the spray. Kuehn (Reference 1) gives information on the penetration of single drops of various diameters, but these data depend primarily on theoretical calculations and have little value for predicting the action of a fuel spray composed of a comparatively large quantity of liquid in different form. A complete theoretical analysis for the action of sprays necessitates assumptions that lead to uncertain results, so that direct experimental determinations are desirable. Since investigations of this nature have apparently not been made heretofore, this work was undertaken to provide some definite information for a simple nozzle.

PHASES OF PROBLEM CONSIDERED

A simple injection valve, opened by a cam and closed by a compression spring, was used for the present work. A cylindrical nozzle having a diameter of 0.015 inch was used, and the valve needle lift was 0.007 inch.

Due to limitations of the apparatus, it was necessary to confine the study to spray lengths of less than 6 inches and to time periods of less than 0.005 second. While interesting data undoubtedly would have been obtained if the scope could have been extended to include greater spray lengths and longer time periods, the information was desired primarily as an aid in applying fuel injection to aviation engines where the conditions do not demand greater spray lengths or longer

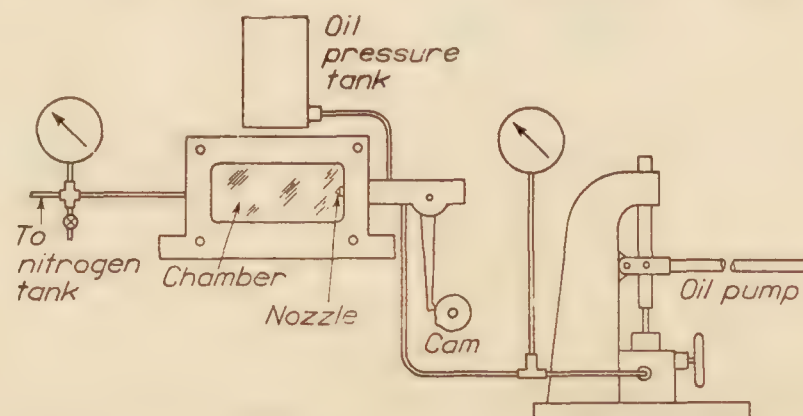


FIG. 1.—Diagrammatic arrangement of apparatus for production and control of spray

time periods. Fuel pressures between 2,000 and 8,000 pounds per square inch at 1,000 pounds per square inch intervals were investigated while injecting into a chamber filled with gas at atmospheric pressure and at 100, 200, and 300 pounds per square inch gauge. Due to strength limitations of the present chamber, greater chamber pressures were not investigated.

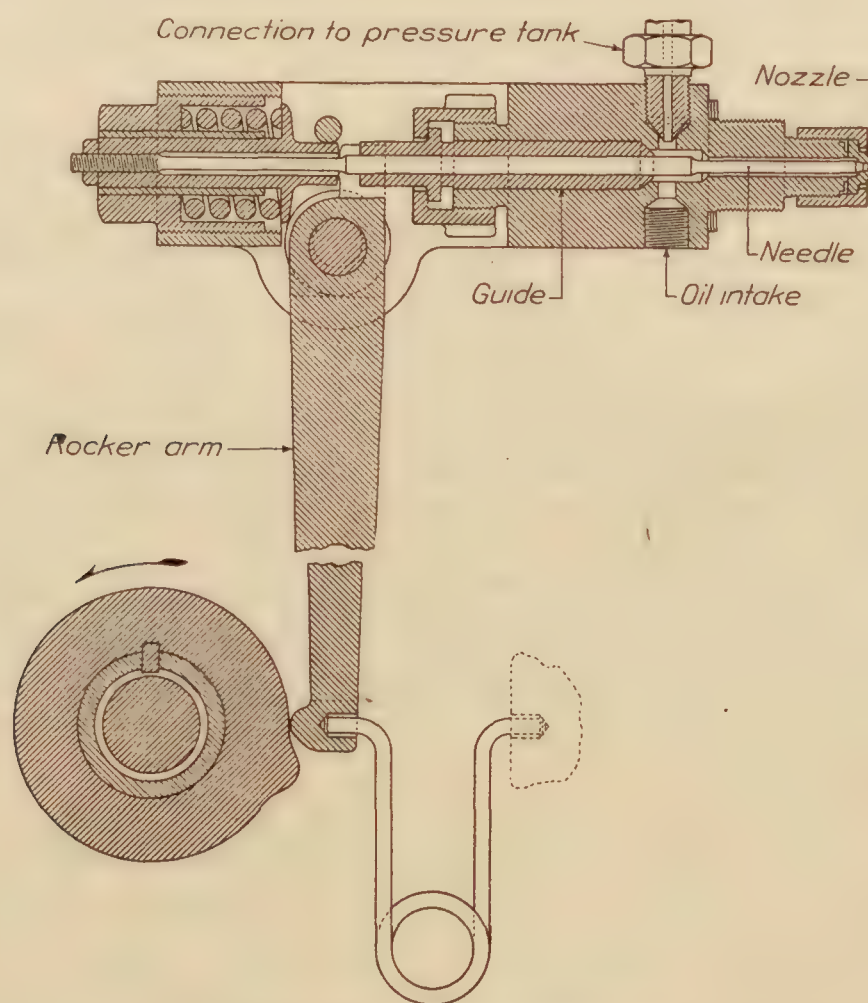


FIG. 2.—Fuel injection valve mechanism

APPARATUS AND METHOD OF OPERATION

The apparatus used for producing and controlling the fuel sprays is shown diagrammatically by Figure 1. The valve mechanism is shown in more detail in Figure 2. The cam shown in these two figures was arranged to make a single revolution at a speed of 900 revolutions per minute by means of a clutch mechanism such as is used on punch presses. A control lever engaged the clutch and thus connected the cam to a shaft rotated by an electric motor at 900

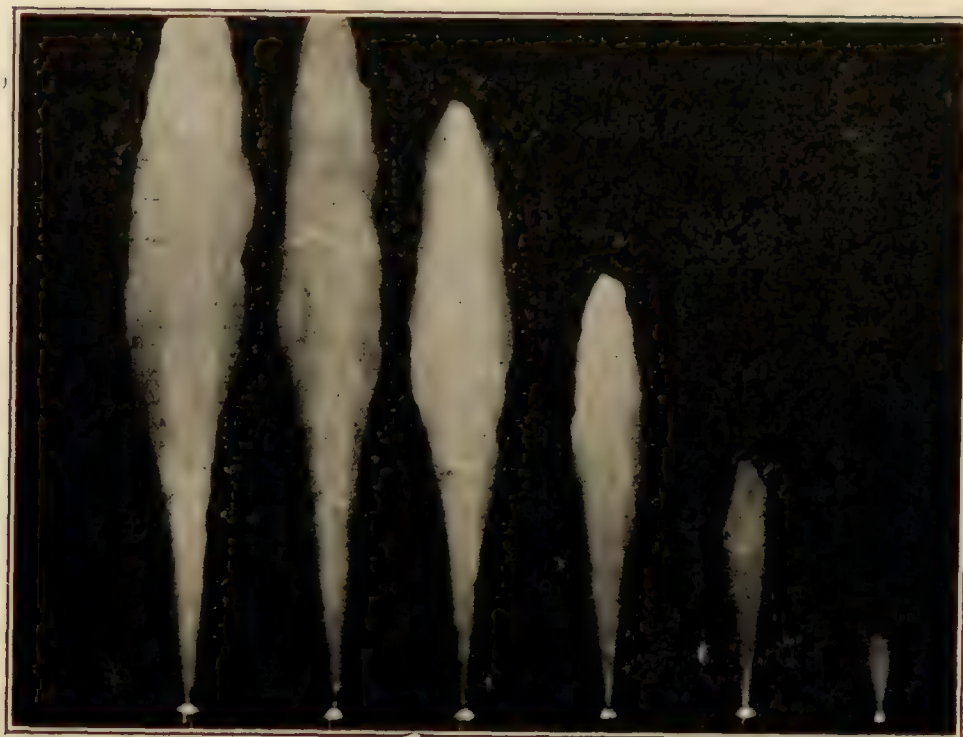


FIG. 3.—Injection pressure, 3,000 lb./sq. in. Chamber pressure, atmospheric



FIG. 4.—Injection pressure, 3,000 lb./sq. in. Chamber pressure, 100 lb./sq. in.



FIG. 5.—Injection pressure, 3,000 lb./sq. in. Chamber pressure, 200 lb./sq. in.
The original photographs for figures 3 to 8 inclusive were retouched for reproduction purposes



FIG. 6.—Injection pressure, 3,000 lb./sq. in. Chamber pressure, 300 lb./sq. in.



FIG. 7.—Injection pressure, 5,000 lb./sq. in. Chamber pressure, 300 lb./sq. in.



FIG. 8.—Injection pressure, 8,000 lb./sq. in. Chamber pressure, 300 lb./sq. in.
The original photographs for figures 3 to 8 inclusive were retouched for reproduction purposes

revolutions per minute. The cam made one revolution and the clutch was then automatically disengaged. The cam lifted the spring-loaded injection-valve needle from its seat through the rocker arm, permitting the discharge of the fuel. The lift of the steel valve needle could be varied by rotating the eccentric rocker arm pin, but, for the present work, it was not changed.

The fuel system was of the constant pressure type, fuel being supplied to the injection valve by means of a hydraulic hand pump at the point shown in Figure 2. The pressure tank just above the nozzle was filled with air before hydraulic pressure was applied and served to minimize the pressure drop during an injection.

The nozzle was mounted at one end of a pressure chamber fitted with glass walls on two sides to permit visual and photographic observation of the spray. This chamber was filled with nitrogen from a pressure tank.

Special high-speed photographic apparatus, capable of taking a continuous series of fifteen photographs at a rate of 4,000 per second was used to record the development of single sprays. Illumination was obtained from a spark gap located near the focus of a parabolic reflector which directed the light into the spray chamber. A camera lens, mounted on the opposite side of the chamber, focused the spray image on a film fastened around a circular drum. This drum was rotated at 3,700 revolutions per minute in a plane perpendicular to the axis of the spray.

Fifteen glass plate condensers, charged to about 30,000 volts each, were arranged to discharge in sequence across the spark gap by means of a rotary switch. The time between condenser discharges, and hence between pictures, was regulated by varying the speed of the rotary switch. Discharge through the rotary switch and spark gap could not occur, until a master switch was closed. This master switch was operated simultaneously with the nozzle valve cam by the same clutch mechanism which controlled the cam.

The duration of a single exposure was estimated to be of the order of 0.000005 seconds. When injecting into gases at 300 pounds pressure, it was necessary to employ a rate of 2,000 exposures per second in order to show the travel of the spray tip across the chamber. When injecting into gas at atmospheric pressure, the rate was increased to 4,000 per second in order to obtain a complete series of pictures before the spray impinged on the opposite chamber wall. Intermediate rates were used for the intermediate chamber pressures.

By striking the control lever which engaged the clutch the injection of fuel and discharge of the condensers took place simultaneously and a record was obtained on the exposed film. All operation was carried out in a darkened room.

A high-grade Diesel engine fuel oil was used for all experiments.

DISCUSSION OF RESULTS

The results given here are for single sprays produced by a single revolution of the cam. It was not feasible to permit continuous operation of the injection system as in actual engines, as the fuel cloud formed in the chamber would obscure the spray. Although differences may exist between sprays under these conditions, visual observation has shown that when injecting into the atmosphere with the chamber removed, continuous operation gave less than 10 per cent greater penetration than obtained with a single spray.

Figures 3 to 8, inclusive, are reproductions of actual photographs taken during the investigation. There was not sufficient contrast in the original photographs to enable intelligible half-tones to be made so that it was necessary to retouch the photographs by increasing the depth of the background and accentuating the nozzle. Much care was taken to alter as little as possible the original outline of the spray. Figures 3 to 6, inclusive, compose a series in which the injection pressure is 3,000 pounds per square inch and the chamber pressure is varied from atmospheric to 300 pounds per square inch gage. Figures 6, 7, and 8 compose another series in which the chamber pressure is 300 pounds per square inch and the injection pressure is varied from 3,000 to 8,000 pounds per square inch.

From such photographs measurements were made of the lengths of the spray images and the distances between images. Figures 9 to 14, inclusive, were plotted from these measurements after taking into account the photographic reduction and the speed of film travel. While

data for figures were taken from a single series of photographs, these were checked by additional photographs and were shown to be representative.

The data given by Figure 15, showing the effect of fuel pressure on spray tip velocity, were obtained from Figure 12. The influence of the chamber and injection pressures on the development of the spray is shown quite markedly by these figures.

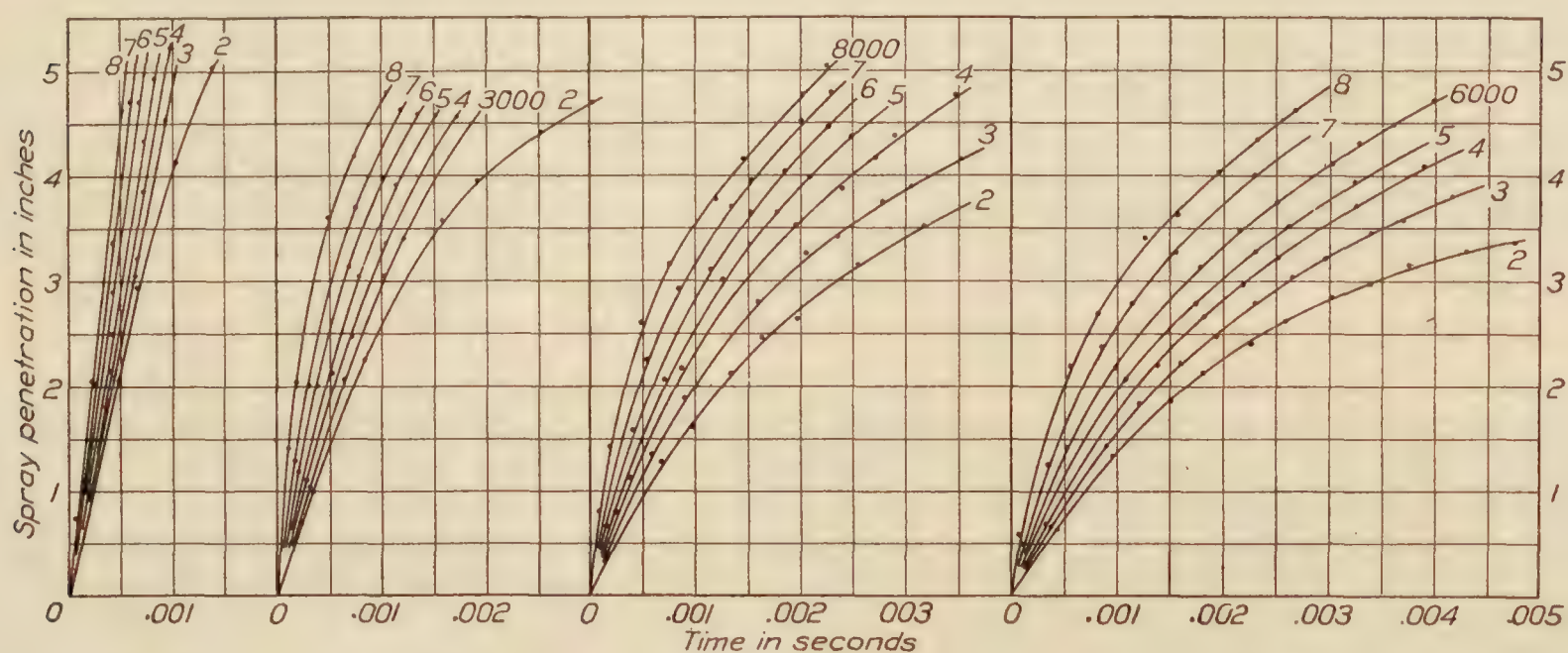


FIG. 9. Chamber pressure, atmospheric. Fuel pressure, 2,000 to 8,000 lb./sq. in. FIG. 10. Chamber pressure, 100 lb./sq. in. gauge. Fuel pressure, 2,000 to 8,000 lb./sq. in. FIG. 11. Chamber pressure, 200 lb./sq. in. gauge. Fuel pressure, 2,000 to 8,000 lb./sq. in. FIG. 12. Chamber pressure, 300 lb./sq. in. gauge. Fuel pressure, 2,000 to 8,000 lb./sq. in.

Effect of fuel pressure on penetration

Figure 16 shows that injection would have been completed in about 0.003 second if the valve needle followed the cam. None of the pictures taken included the entire period of injection, and since time intervals of nearly 0.005 second were recorded it is evident that the cam

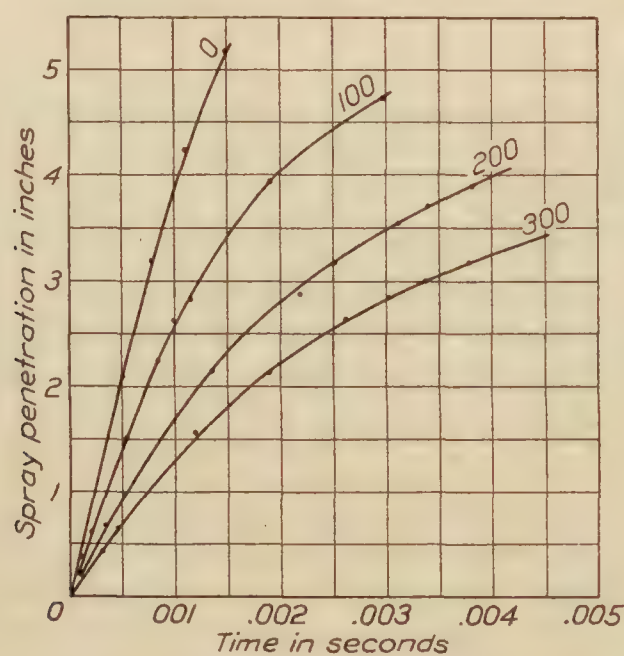


FIG. 13.—Effect of chamber pressure on penetration. Fuel pressure, 2,000 lb./sq. in. Chamber pressure 0 to 300 lb./sq. in. gauge

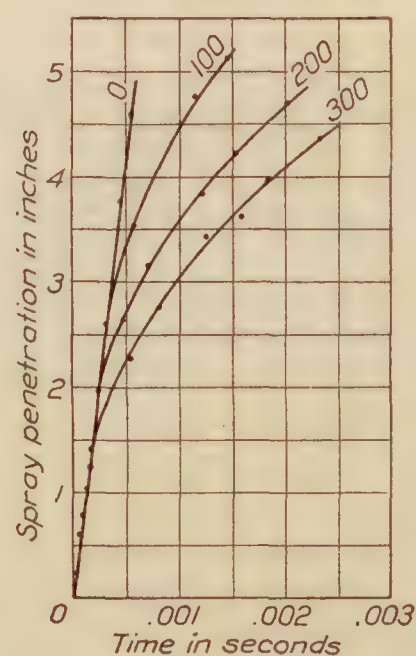


FIG. 14.—Effect of chamber pressure on penetration. Fuel pressure, 8,000 lb./sq. in. Chamber pressure, 0 to 300 lb./sq. in. gauge

did not control the closing of the valve. This action is an explanation of the character of the nozzle calibration curve, Figure 17. Several series of calibrations were made at atmospheric and at 300 pounds per square inch chamber pressure, none of which differed perceptibly from those given on the curve.

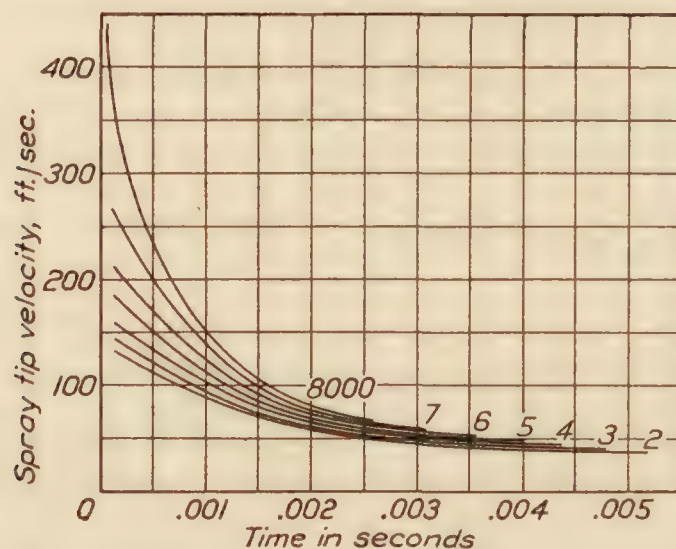


FIG. 15.—Effect of fuel pressure on spray tip velocity. Chamber pressure, 300 lb./sq. in. Fuel pressure, 2,000 to 8,000 lb./sq. in.

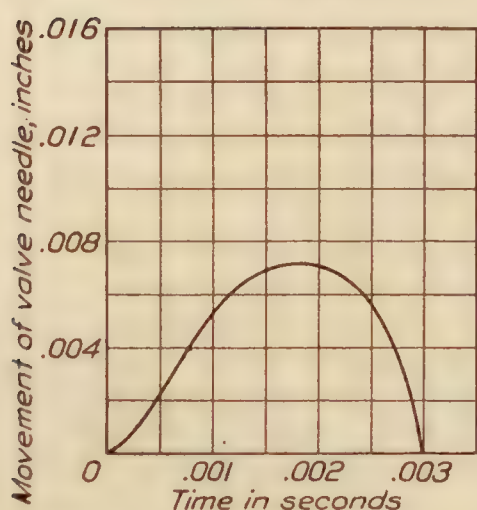


FIG. 16.—Valve lift diagram

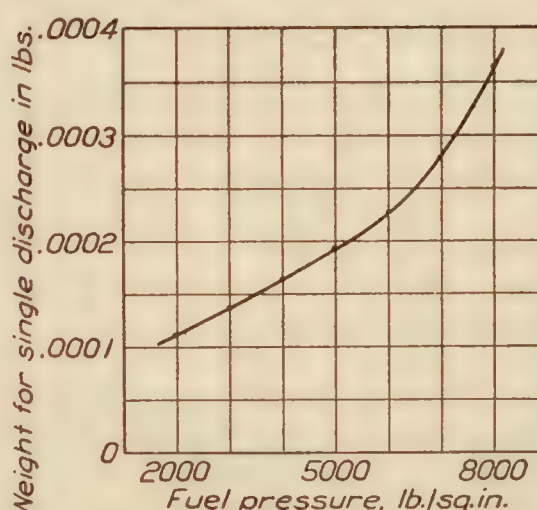


FIG. 17.—Weight of fuel discharged by nozzle

MATHEMATICAL CONSIDERATIONS

The formulation of the mathematical relationships governing the action of liquids injected into compressed gases is considerably involved because of the large number of variables and a lack of knowledge of the true action. Analysis of the experimental results revealed that for the present tests the negative acceleration of the spray tip is approximately proportional to the 1.5 power of the instantaneous velocity of the spray tip.

The applicability of this relation can be readily shown. Assuming such a relation to apply, the mathematical equation will be:

$$-\frac{dv}{dt} = 2k V^{1.5} \quad (1)$$

This may be expressed as:

$$s = \frac{V_o t}{k V_o^{.5} t + 1} \quad (2)$$

where s = spray length or penetration in feet.

t = time in seconds.

k = coefficient.

V_o = initial velocity in feet per second.

Equation (2) may be verified by differentiation. From this equation is derived

$$\frac{t}{s} = \frac{k V_o^{.5} t}{V_o} + \frac{1}{V_o} \quad (3)$$

which is an equation of a straight line for $\frac{t}{s}$ as a function of t . Values of these variables taken

from Figures 9 to 12, inclusive, give the data plotted on Figures 18 to 20. Since the divergence from straight lines is not very great, equation (1) closely represents the physical conditions within the limits of the experiments.

It is interesting to note that equation (3) may be arranged as in equation (4).

$$s = \frac{V_o}{k V_o^{.5} + \frac{1}{t}} \quad (4)$$

From this equation it becomes apparent that $s = \frac{V_o}{k V_o^{.5}}$ when $t = \infty$ so that this equation gives the penetration that would be obtained if discharge never ceased or the limiting value of penetration for the chamber and fuel pressures under consideration. It is evident from equation (3) that $\frac{V_o}{k V_o^{.5}}$ is the reciprocal of the slope of the lines in Figures 18 to 20, and thus a means is obtained of estimating the limiting value of the penetration. Since the condition was not examined experimentally, there is no assurance that the straight lines may be extended, and this operation has little practical utility at the present time. Nevertheless, it probably constitutes the best way to extrapolate the present data. It is interesting to note that, if it is assumed that the data may be extended in this way, the penetration increases with

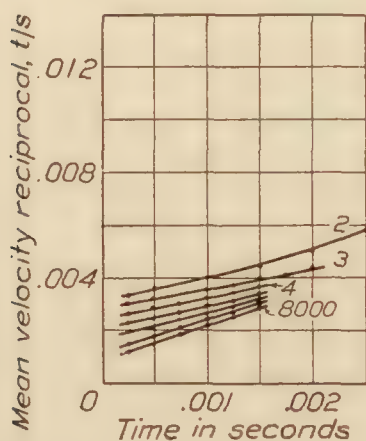


FIG. 18.—Chamber pressure, 100 lb./sq. in.

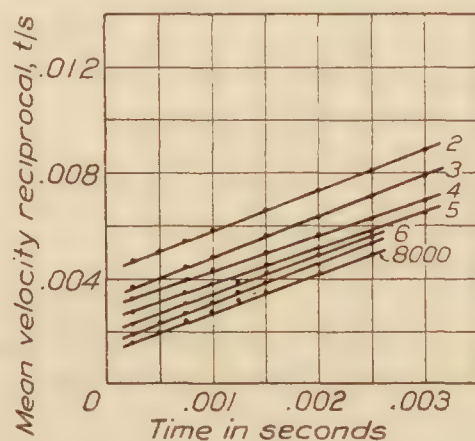


FIG. 19.—Chamber pressure, 200 lb./sq. in.

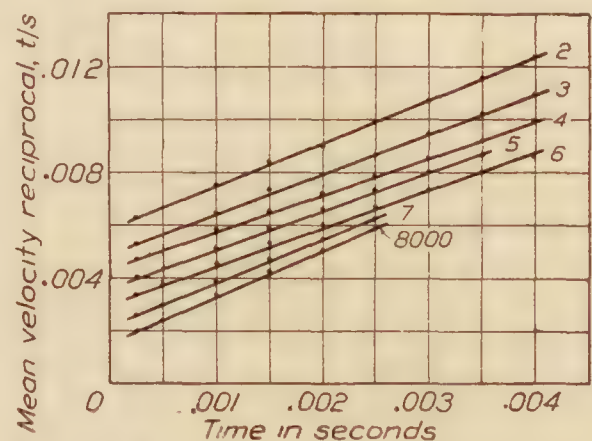


FIG. 20.—Chamber pressure 300 lb./sq. in.

Fuel pressure, 2,000 to 8,000 lb./sq. in. Relation of mean velocity reciprocal (t/s) to time.

fuel pressure to a certain maximum value, after which it decreases with further increases of fuel pressure.

Figure 15 shows that the higher fuel pressures are accompanied by higher initial velocities, but after a certain time interval the spray-tip velocity is nearly the same over a wide range of fuel-pressure variation. The higher initial velocities are probably accompanied by greater atomization, as is indicated by other experiences, and thus the higher pressures would have other beneficial effects besides their influence on penetration.

CONCLUSIONS

These tests have given definite information on the rate of spray penetration from a simple nozzle and on the variation of this rate with various fuel and gas pressures. The extent to which the present results depend on the particular characteristics of the present injection apparatus can only be determined by tests with other types.

Records of the development of fuel sprays injected into compressed gases, obtained by means of high-speed photography, provide a good basis for the analysis of the behavior of sprays produced by various injection nozzles, and therefore should aid materially in considering the influence that the nozzles would have on engine performance.

REFERENCE

1. Ueber die zerstaubung flussiger Brennstoffe, by Dr. Ing. R. Kuehn, Der Motorwagen, January 20, 1925.

REPORT No. 223

PRESSURE DISTRIBUTION ON THE C-7 AIRSHIP

By J. W. CROWLEY, JR., and S. J. DEFRANCE
Langley Memorial Aeronautical Laboratory

REPORT No. 223

PRESSURE DISTRIBUTION ON THE C-7 AIRSHIP

By J. W. Crowley, jr., and S. J. DeFrance

SUMMARY

This investigation was made by the National Advisory Committee for Aeronautics at the request of the Bureau of Aeronautics, Navy Department, for the purpose of determining the aerodynamic pressure distribution encountered on a "C" class airship in flight. It was conducted in two parts (a) tests on the tail surfaces in which the pressures at 201 points were measured and (b) tests on the envelope in which 190 points were used, both tests being made under as nearly identical flight conditions as possible, so that the results could be combined and the pressure distribution over the entire airship obtained.

The method of testing consisted of measuring the pressures by means of orifices located at the desired points connected to the tubes of a multiple liquid manometer. Simultaneous readings of all the pressures were obtained by photographing the manometer.

The results as presented in this report are mainly in tabular form and may be very briefly summarized as follows:

- (1) The maximum local pressure encountered on a tail surface was 7.3 lb./sq. ft.
- (2) The maximum total normal force on a complete tail surface was 352 pounds or a C_{NF} of 0.316 occurring on the bottom fin and rudder during a "reversal" of the rudder.
- (3) The maximum moment of the tail surface forces about the center of buoyancy was 37,200 lb. ft.
- (4) The investigation of the envelope pressures, while showing the general distribution of pressure satisfactorily, is practically useless in the determination of total aerodynamic forces on the airship.
- (5) It is concluded that the pressures set up by a bump are larger than those obtained in maneuvering.

INTRODUCTION

The available data concerning the aerodynamic forces experienced by an airship in flight are very scarce. The British have made some pressure distribution measurements on the tail surfaces of the rigid airships, R-26 and R-32, but only comparatively few points were investigated, and the results, consequently, are not at all complete. So far as is known, there has been no previous complete investigation of pressures on an airship envelope in flight. About the time that these tests were being carried out, an investigation was being made on the hull of the ZR-3 at Friedrichshafen, but the results have not been published.

In these experiments, covering both the envelope and tail surfaces, pressures were recorded at both high and low speeds for each control setting. The maneuvers were: Steady turns, steady climbs and descents, starting of turns and climbs, reversals from left turn to right turn, rising light, flying horizontally while light, and flying through gusts. The airship was flown under all of these conditions in order to make sure that the maximum pressures encountered in normal flight were obtained or exceeded.

METHODS AND APPARATUS

Apparatus.—Pressure pads of the type developed and calibrated in the United States Navy Aerodynamical Laboratory (Reference 1, fig. 1) were cemented directly opposite each

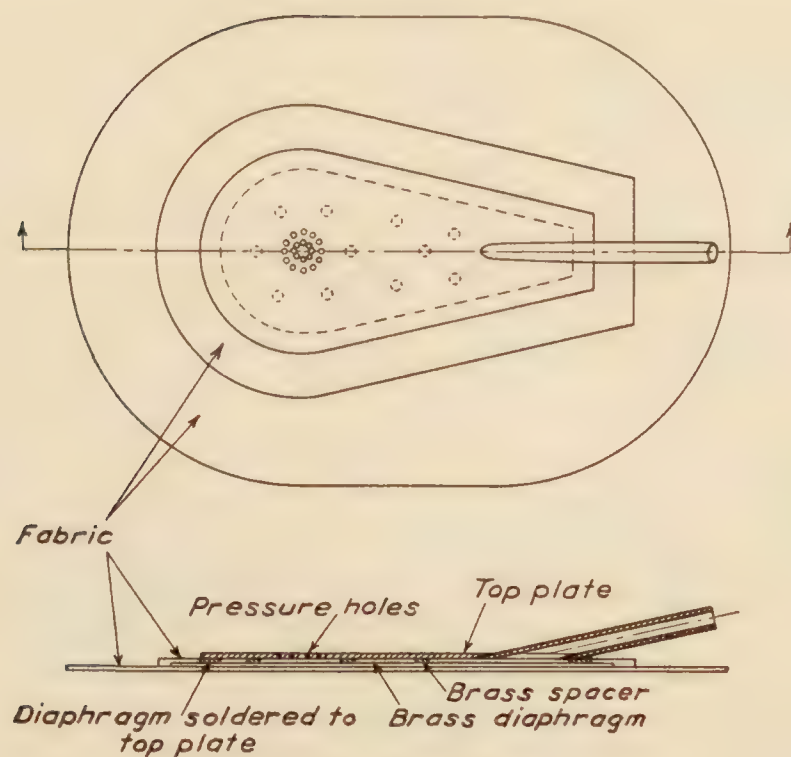


FIG. 1.—Static pressure pad

other on the two sides of the tail surfaces at the points indicated in Figure 2 and on the envelope as shown in Figure 4. In securing the pressure pads to the airship, the connecting tube (fig. 1) was placed to the rear so as to eliminate the influence of the tube on the air flow about the orifice. The orifices were connected by rubber and aluminum tubing to a multiple liquid manometer located in the control car. Each aluminum tube on the tail surfaces was laid next to the fabric (fig. 3), so as to avoid bunching of tubes, which would have caused a great disturbance in the flow.

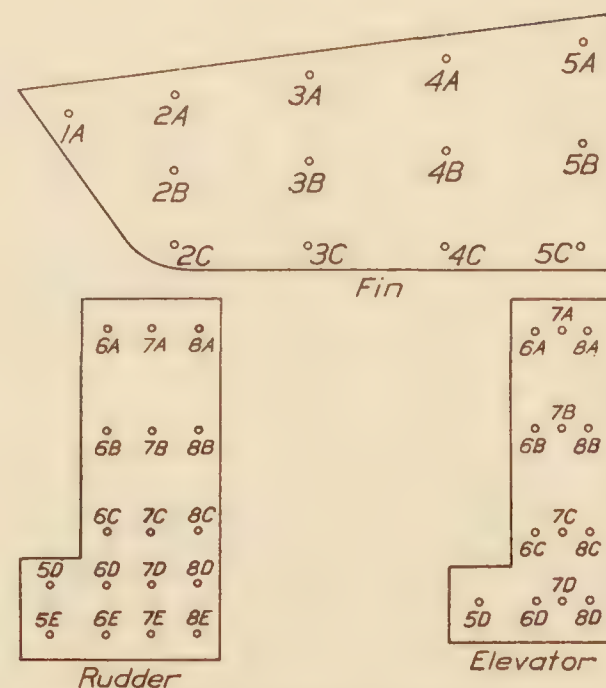


FIG. 2.—Location of pressure pads on tail surfaces



FIG. 3.—Arrangement of tubing on tail surfaces

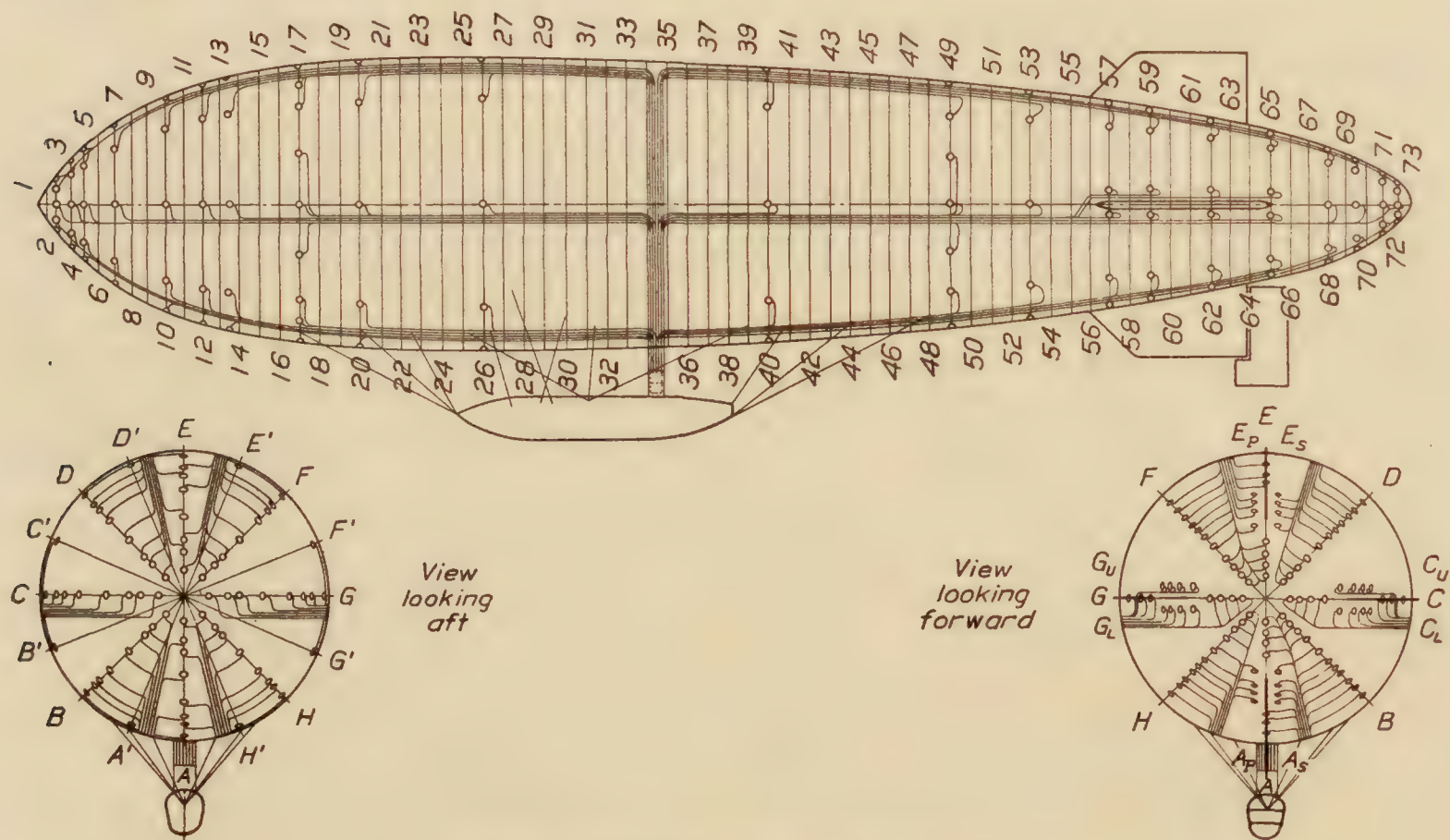


FIG. 4.—Location of pads and tubing on envelope

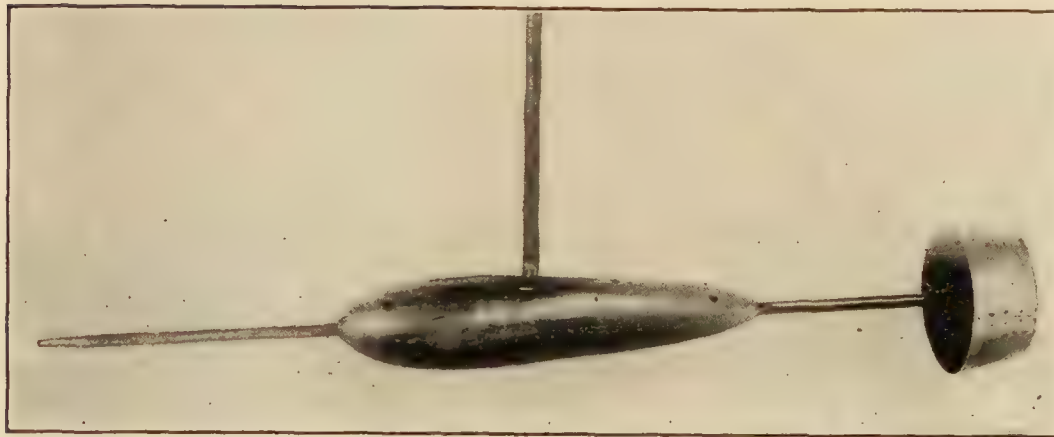


FIG. 5.—Pitot-static head

and the fourth to the trailing static head (fig. 5). The line connecting the level of liquid in the three tubes provided a datum line, in accordance with the roll of the airship, from which pressures could be measured, while that in the fourth tube gave the true static pressure outside of the flow caused by the airship.

The four manometer units were mounted together in one box, and to obtain records (fig. 6) the complete assembly was photographed by a specially designed camera (fig. 7). The camera consisted of a light-tight box and a film container which was removable in daylight. The capacity of the container was a roll of film sufficient for 27 exposures, 6 inches by 6 inches. The spool on which the exposed film was wound was turned by a handle, which in turn, by means of a tripping device, operated the shutter once every revolution, thereby making the record. At each operation of the shutter an electrical contact was made which caused a light to flash and make a timing line on all records being made on drum type instruments. In this investigation an N. A. C. A. recording air-speed meter (Reference 2) and a recording statoscope and inclinometer were used, and by means of the timing lines all records were synchronized.

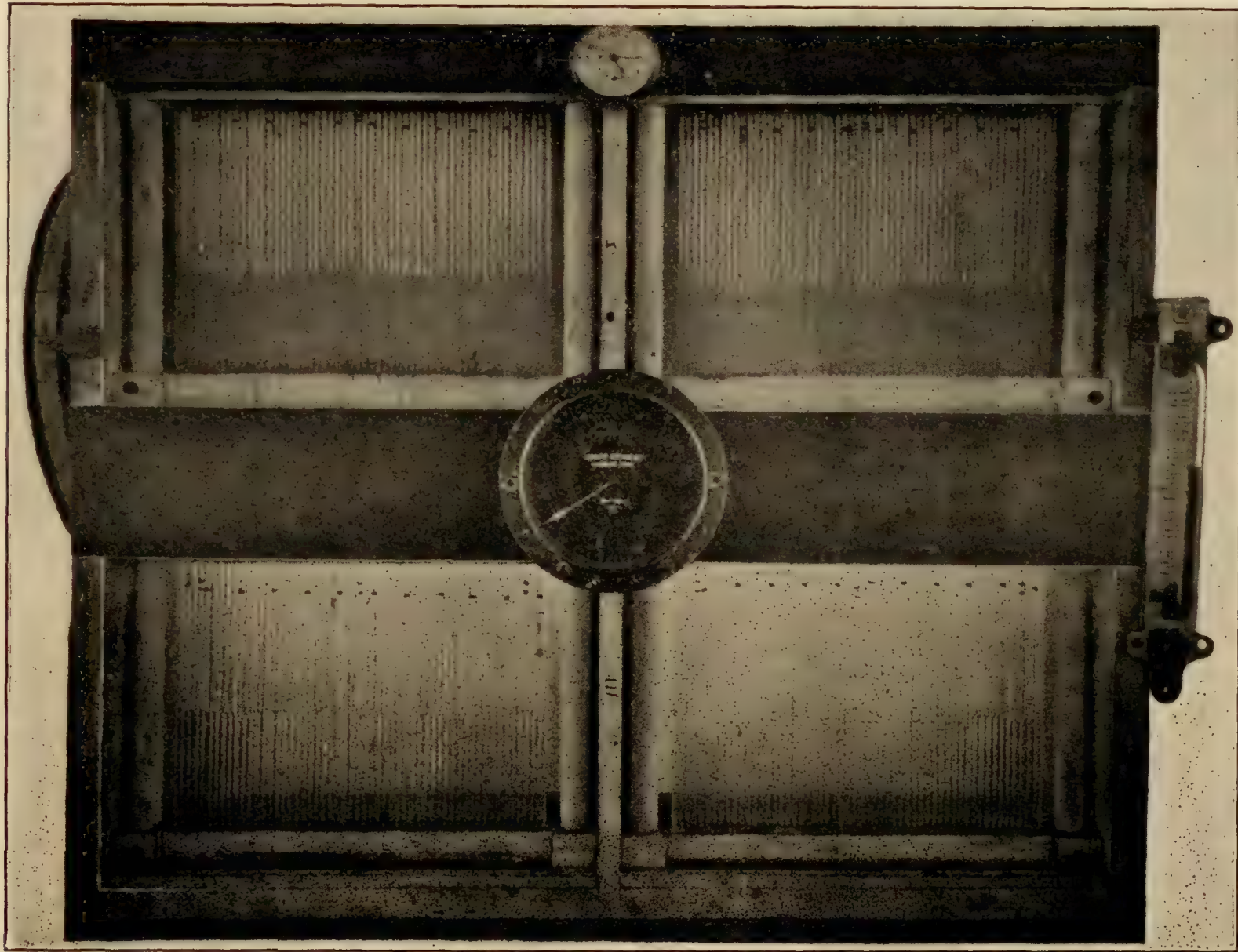


FIG. 6.—Manometer record

Other instruments used in these tests were: rudder position indicator, low range precision altimeter, yaw indicator, stop watch, and thermometer. The rudder position indicator, altimeter, and stop watch were mounted on the manometer box and were photographed with the pressure tubes. The recording air-speed meter and the recording statoscope were connected, respectively, to a trailing Pitot-static head and a trailing static head (fig. 5). Both of these heads were suspended 25 feet below the car so as to be outside of the disturbed flow caused by the airship. The recording statoscope consisted of a recording air pressure capsule, a vacuum bottle, and a by-pass valve connected as shown in Figure 8. The yaw indicator consisted of a protractor mounted on the side of the car. By sighting on the trailing Pitot-static head, the angle of yaw at the car was read on the scale. The rudder position indicator consisted of a graduated disk, which was connected to the rudder control cables. The thermometer was attached to the outside of the car so as to obtain the air temperature for computing the air density.

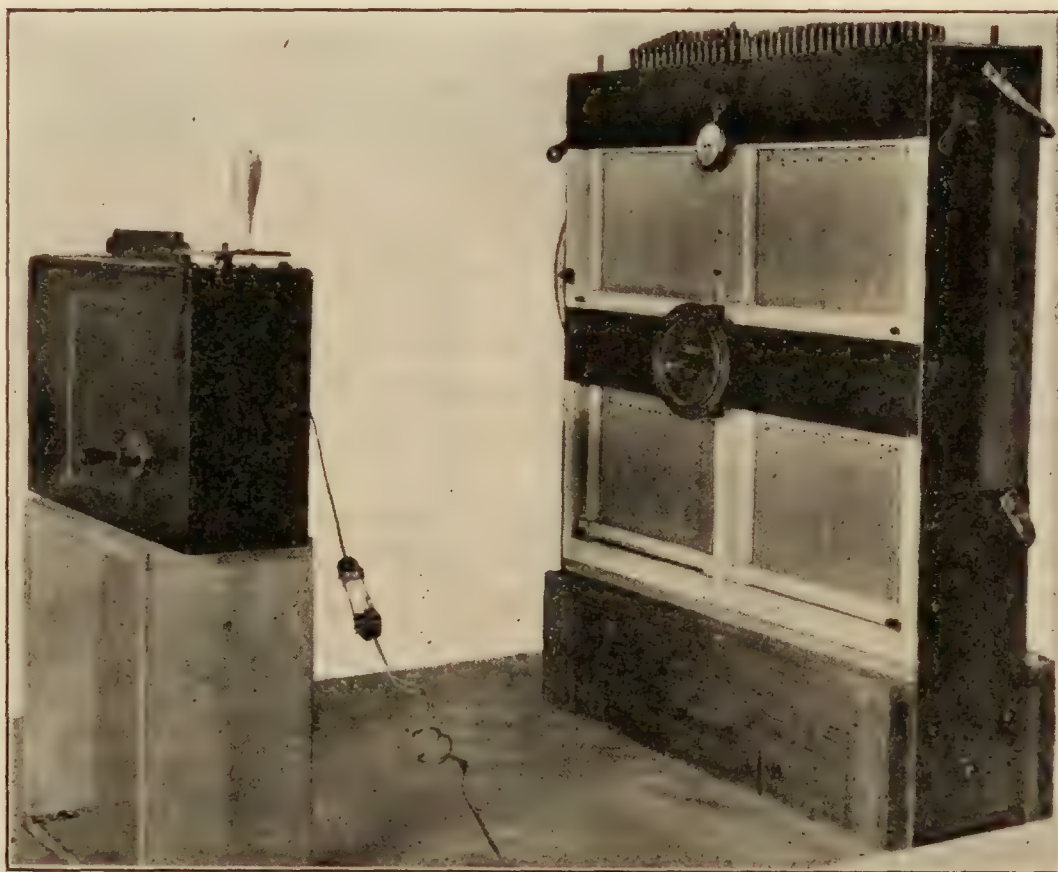


FIG. 7.—Manometer and camera as set up on the ship

The position of the control surfaces was indicated to the pilot by two telautograph instruments, which measure the angles between the stabilizers and movable surfaces and then electrically communicate the readings to an indicator in the cockpit.

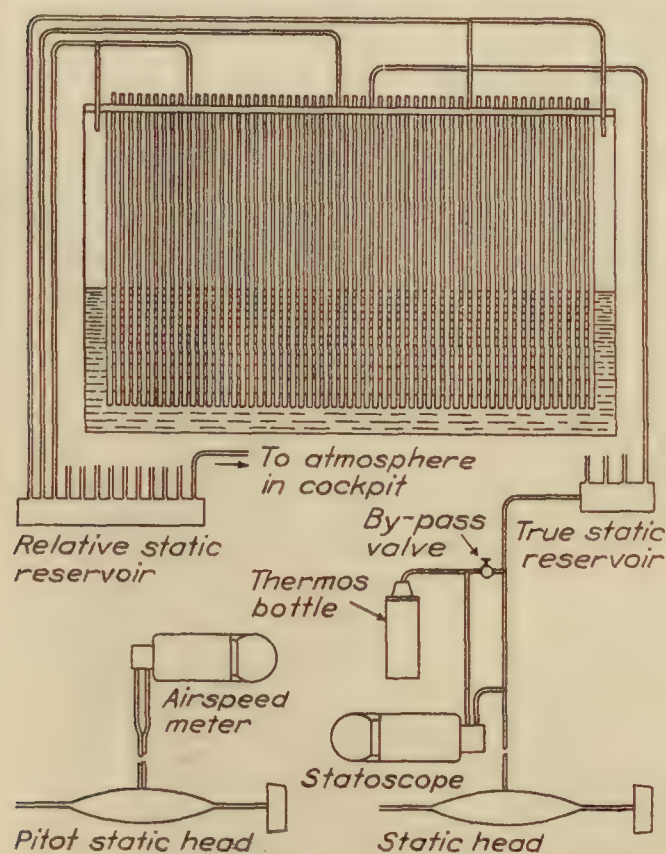


FIG. 8.—Diagram of manometer and instrument connections

Method of tests.—Before the flight tests were made all the connecting tubes were tested for leaks and stoppages. This was accomplished by blowing through the tubes from the orifice end of the line. A manometer at this end and the reading indicated on the multiple manometer were observed at the same time and compared. The same procedure was carried out at the completion of the set of tests and any lines which indicated leaks were discarded. The helm angle indicator was calibrated and the zero reading of the yaw protractor noted for an angle of zero yaw relative to the longitudinal axis of the car.

Before each flight the pilot was supplied with a list of the conditions desired and the camera and recording instruments were loaded. Two observers were required and their first operation was to lower the two trailing bombs. Both observers then gave their attention to the pilot and awaited his signal that the desired condition had been reached. For steady flight conditions simultaneous records of all the instruments were made on receipt of this signal. In changing flight conditions two records were obtained, the first immediately after the movement of the controls and the second as soon after that as possible. With the camera used

the interval between pictures was three seconds. In the reversal condition four photographs were obtained in the above manner. The readings of the helm angle and revolutions per minute were recorded by the pilot.

The maneuvers in which pressures were recorded are tabulated in Table I, which is self-explanatory with the exception of the "light" conditions (runs 22 to 25, inclusive). To obtain these flights while statically light, the airship was brought to equilibrium at a definite altitude and 500 pounds of ballast released. In this condition a horizontal flight was made, maintaining a constant altitude by aid of the elevators (runs 22 and 23) and also a flight with the airship on an even keel but rising due to excess lift (runs 24 and 25).

Reduction and presentation of data.—The data were all obtained from photographic records, except the angle of yaw, temperature, and revolutions per minute, which were tabulated from indicated readings. To facilitate reading of the manometer records, the negatives were placed in a projection lantern and the enlarged image thrown on a screen. The magnification was so chosen that the head of alcohol could be scaled off directly in pounds per square foot. A wire over the screen was shifted so as to run through the images of the menisci of the three tubes, which were connected to the air reservoir in the cockpit. This gave the angle of roll of the ship and a base line to work from. A second wire was shifted into parallelism with the first and passed through the image of the meniscus in the tube connected to the trailing static head. The height of liquid in the various tubes above the latter wire gave directly the pressures relative to the true static condition outside of the disturbed flow.

The rate of change of static pressure, as recorded by the statoscope, was converted into rate of change of altitude by the use of the atmospheric tables. This rate of change of altitude divided by the air speed along the line of flight, gave the sine of the angle of inclination of the flight path. By subtracting this angle of inclination from the angle of inclination of the car as recorded by the inclinometer, the angle of pitch was obtained.

The maneuvers in which the pressures were investigated are given in Table I, while the conditions under which each maneuver was made is tabulated in Tables II and V. Due to flight difficulties the desired rudder and elevator angles given in Table I were not always obtained. The actual angles measured in flight are given in Tables II and V. The pressures over the tail surfaces are given in Table III, while those over the envelope are in Table VI. The resultant forces on the tail surfaces are given in Table IV and those on the envelope in Table VII.

In Table IV the resultant normal forces have been expressed in the coefficient form

$$C_{NF} = \frac{P}{1/2 \rho V^2 A}$$

where C_{NF} = absolute normal force coefficient.

P = load.

A = area of surface.

ρ = air density.

V = true air speed.

The pressures over the tail surfaces were plotted for all runs along each row of holes at right angles to the longitudinal axis of the airship, as shown in Figures 9, 10, 11, 12, 13, 14, 15, and 16. As may be noted in these figures, at each row a curve was drawn of the pressures on each side of the surface and the resultant pressure curve for the row determined from the algebraic sum of these. The areas under these latter curves were measured and used as ordinates in drawing a resultant load curve for each surface. The center of area under each load curve was determined, and with the distance from that point to the center of buoyancy as an arm, the tail surface moment was computed. In all cases a positive load was considered to be acting from bottom to top on the horizontal surfaces and from starboard to port on the vertical surfaces.

To present the distribution of pressure over the hull, the values were plotted upon longitudinal cross sections of the envelope as shown in Figures 17, 19, 21, and 23, and also upon

circular cross sections at each station as in Figures 18, 20, 22, and 24. The resultant vertical and horizontal transverse forces at each station were obtained by numerical integration of the pressures around the envelope. These forces were plotted along the axis of the hull, giving one curve of horizontal forces and one of vertical forces. To these were added the horizontal and vertical loads upon the tail surfaces, thereby giving the total aerodynamic forces acting horizontally and vertically along the axis of the ship. These combined curves were drawn for each maneuver in the same manner as shown in Figures 25a, 25b, 26a, 26b, 27a, 27b, 28a, and 28b.

PRECISION

Experiments made by the National Advisory Committee on an airplane wing during the summer of 1921 and tests made in the United States Navy's Aerodynamical Laboratory showed that the type of pressure pads, Figure 1, used in this investigation gave the same reading of static pressure as a single hole orifice just flush with the surface. More recent experiments made in the National Advisory Committee wind tunnel to find the effect of the position of the connecting nipple showed that there was no change in pressure by moving the pad around from a position with the nipple directly aft to an angle of 90° to the air flow.

Tail surfaces.—The inertia effects in the pressure tubes were eliminated in these tests since only pressure differences, as measured through tubes of the same length and running side by side were used. The manometer was mounted close to the center of gravity of the airship and the vertical accelerations affecting the height of the liquid columns were neglected. The individual pressures are probably accurate to 0.10 lb./sq. ft. The accuracy of the figures given for the total forces is limited by the number of points investigated, because a curve was drawn connecting the individual pressures and the total forces were obtained by integrating the area under this curve. For this reason the total forces on the tail surfaces can not be assumed to be correct to better than ± 5 lb., because the changes in pressure between points were great.

Envelope.—The precision of results on the tail surfaces can not be applied to the pressures or total transverse forces on the envelope. The pressures over the envelope were of small magnitude and the distance between points of investigation was large. So that with the difficulty of measuring the small pressures and because of the fact that they were considered as acting over large areas, great errors might enter into the computation of the total forces.

It should be noted that the angles of pitch and yaw were measured relative to the car, and if applied to the envelope may be in slight error because of the flexibility of the suspension system. There was some difficulty experienced in measuring the angle of yaw because of the swinging of the suspended Pitot-static head on which sightings were taken. However, the readings obtained for steady conditions were correct to the nearest 0.2° . For nonsteady conditions the error may have been slightly greater, because it was difficult to observe the angle at exactly the same instant that the records were made. In determining the angle of flight path from the slope of the statoscope record and the air speed, the assumption was made that there were no vertical air currents or gusts, which was probably the case in all runs, except where the effects of a gust were desired, since the other tests were made over the water.

DISCUSSION OF RESULTS

The discussion of the results of this investigation is confined to a consideration of the actual pressures and total forces encountered in the different maneuvers. While all of the conditions enumerated in Table I were investigated, only those of each maneuver showing the greatest forces are tabulated here. However, the pressures encountered in all of the runs have been tabulated and these data are available at the National Advisory Committee for Aeronautics for reference.

Tail surfaces.—The results of the pressure distribution tests on the tail surfaces are given in Tables II, III, and IV, in which are tabulated the data recorded in flight, the pressures at each orifice, and the total resulting forces on the tail surfaces, respectively. It will be noted in the latter table that in circling flight the loads have been divided into the load on the fin and load on the movable surface only for bottom fin and rudder, and, conversely, in climbing

and descending flight only the horizontal surfaces have been so divided. Graphical presentation of the tail surface data for four runs is shown in Figures 9, 10, 11, 12, 13, 14, 15, and 16, which are representative of the manner in which all of the pressures were plotted for the determination of the resultant normal forces.

From the pressures at each orifice as tabulated in Table III the resultant force at each station may be obtained by the algebraic sum of the pressures on each side of each station. Local loads thus determined show that the largest value recorded for a horizontal surface was 5.7 lb./sq. ft. on the port elevator while flying through a gust. This value exceeded the largest pressure caused by any specific maneuver, which was 5.2 lb./sq. ft. near the leading edge of the starboard fin encountered during a steady descent at 46 M. P. H. Much larger values than these were recorded for the vertical surfaces where the peak pressures ranged from 5 to 7 lb./sq. ft. with a maximum of 7.3 lb./sq. ft. on the top fin during a steady circle at 35 M. P. H. (fig. 11). The largest local pressures were usually found at the leading edge of the fins close to the envelope and on the balancing portion of the rudder and elevators.

Examination of the results in Table IV shows that the greatest resultant forces were experienced on the vertical surfaces. This was to be expected, because more violent maneuvers were made in the horizontal plane than in the vertical. However, the loads recorded for the horizontal surfaces were much greater than those which would be experienced in normal flight, because the tests were made as severe as possible, without increasing the gas pressure in the envelope to a point where the fabric might fail. The greatest total normal force experienced on a complete tail surface was 352 pounds on the bottom fin and rudder in run 27-b, a reversal. Expressed in the coefficient form this becomes 0.316, which is also the largest C_{NF} obtained for a complete tail unit. In comparison with these the maximum normal force on a complete horizontal tail surface was 181 pounds with a maximum C_{NF} of 0.162. As would be expected, the same relation is true for the fixed surfaces where the largest force is found on the top fin, 311 pounds, or C_{NF} 0.554, while the largest on a horizontal fin was 200 pounds, or C_{NF} 0.210. Comparatively large forces were encountered on the rudder. A total force of 250 pounds was obtained in run 9-b and normal force coefficients of 0.550 to 0.570 were found on three different occasions. The maximum C_{NF} encountered on a complete tail unit, 0.316, is less than the value generally used in airship tail surface design, indicating that they are on the safe side.

Large horizontal moments of forces on the tail surfaces about the center of buoyancy were expected as a result of reversing the rudder from 24° port to 18° starboard and were found in the first and second records of the maneuver. In the case of the second, the value reached was 35,100 lb. ft. (Table VIII). The resultant force causing this moment was the largest found during the tests, 352 pounds on the lower fin and rudder and 180 pounds on the top fin, Figure 9.

The gust, which was encountered in run No. 28, apparently came from directly below and the pressures recorded are not those caused by the bump but those due to restoration of the ship to an attitude of normal flight. With the apparatus then available it was impossible to record the full effect of a bump because it was necessary to wait until the gust was felt and then make the record. However, the resultant forces 181 and 152 pounds and the normal force coefficients, 0.162 and 0.136 encountered on the port fin and elevator and starboard fin and elevator respectively, were the largest found on the horizontal surfaces. These forces, together with the observations made at the time of the test, indicate that there is a very great probability that the loads imposed by a bump or gust exceed those obtained in any maneuver.

One of the chief difficulties in these tests was caused by the inability, with the apparatus used, to obtain continuous records of the pressures and the subsequent doubt in regard to the maximum pressures. This limitation is brought out rather forcibly by the above discussion of the bump and is met with in many of the unsteady maneuvers as in the start of a turn. In the latter, runs 9-a and 9-b, it is evident from an inspection of the results in Table IV that the first run, 9-a, was made before the airship had started to turn and possibly before the rudder had moved an appreciable amount because the forces on both the vertical fin and the rudder were small. However, the second run, 9-b, shows greatly increased forces and indicates that the airship was turning. Because of the three seconds interval between records it is impossible to

say exactly when the maximum forces were encountered and whether or not the forces obtained were the actual maximum forces. This, of course, would be eliminated by continuous records.

A further analysis of the results in Table IV shows a peculiar condition in that the load on the tail surfaces was not equally divided between the port and starboard surfaces, or the top and bottom surfaces. An example of this is run 21, where the starboard surfaces have a down load of 73 pounds, while the port surfaces have 146 pounds. This same thing is noted to a greater or less extent throughout the whole series of tests and is only explainable by the possibility that the pressures were obtained while the airship was rolling. It was observed during the flights that most of the maneuvers were accompanied by a rolling motion of the airship.

Envelope.—The results of the pressure distribution tests on the envelope are given in Tables V, VI, and VII, and a graphical presentation of the pressures for four runs, a reversal of controls from 24° port to 18° starboard, a steady circle at 37.5 M. P. H. with 8° starboard rudder, start of a circle at 41.5 M. P. H. with 44° starboard rudder, and a bump at 45 M. P. H. is given in Figures 17 to 24, inclusive. These figures are representative of the manner in which all of the data were plotted.

The curve of the pressure distribution over the envelope did not change greatly with the different maneuvers. The values of pressure were positive in all cases from the nose back about 7 per cent of the length of the airship, where they became negative and remained so along the hull to a region about 10 per cent of the airship's length from the tail. Here again the pressure became positive and continued so to the end of the airship. This is about the same general pressure distribution that was obtained on a model of the *C-2* at 0° yaw in the wind tunnel at the Bureau of Standards. The only radical departure from this general distribution was found in run No. 5 in the region close to the nose. In this region the values changed sign several times and as the photographic record was poor, making it difficult to read the values, these data are considered doubtful.

When the envelope results are considered for the purpose of determining the total aerodynamic loading of the airship they are found to be very unsatisfactory. There are several causes which contribute to the inaccuracy of the envelope results, the chief of these being the relatively small number of points investigated on such a large area as that of the envelope. This, of course, causes each orifice to be considered as representative of the pressure over a considerable area and magnifies the inherent errors of such an investigation which are imposed by the irregularities of the envelope and the interference of wires, pads, tubing, and nose battens that undoubtedly produces disturbances at some of the orifices. This could only be eliminated by a much greater number of orifices which would probably run into prohibitive weight and resistance.

That the aerodynamic forces as measured are not representative of the forces encountered is shown in Figures 29 and 30 in which the transverse forces as measured in Runs 4 and 1 are plotted, together with the theoretical forces for the same runs as computed according to Munk's formula (Reference 3):

$$dF = dx \left[(k_2 - k_1) \frac{dS}{dx} V^2 \frac{\rho}{2} \sin 2\varphi + k' V \frac{\rho}{r} S \cos \varphi + k' V^2 \frac{\rho x}{r} \frac{dS}{dx} \cos \varphi \right]$$

where $k_2 - k_1$ = difference of transverse and longitudinal apparent mass coefficients.

S = cross sectional area

φ = angle of yaw

k' = inertia coefficient

r = radius of turn

x = distance to the aerodynamic center.

NOTE.—The radius of turn, r , was computed from the time for a complete turn as clocked by a stop watch, and the air speed. This value was checked by using the equation given in the British Advisory Committee Report No. 749,

$$r \sin \varphi = 0.9l$$

where l is the distance from the center of pressure on the fins to the *c. g.* of the airship.

The computed forces as plotted in Figures 29 and 30 are not expected to agree exactly with those measured because motion in a perfect fluid was assumed for the computations, but no great discrepancies as are shown could exist and this is a further indication of the unreliability of the aerodynamic loading obtained on the envelope.

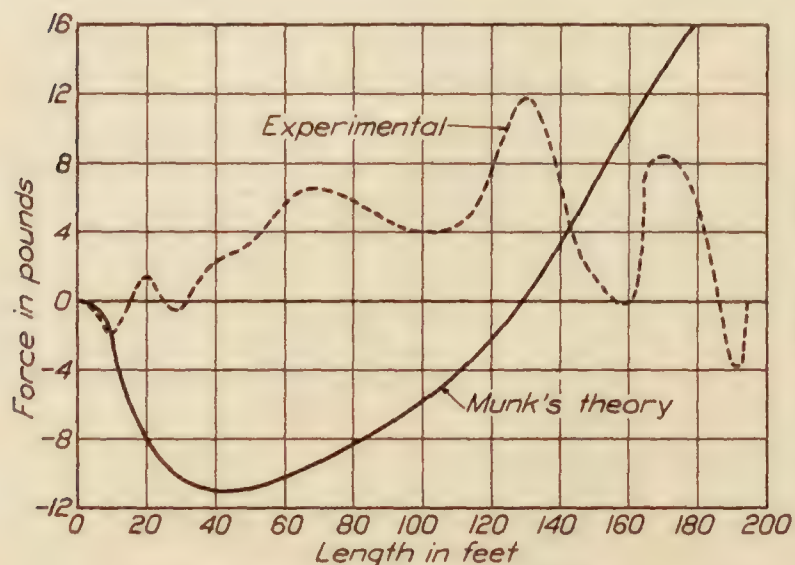


FIG. 29.—Steady circular flight, run No. 4

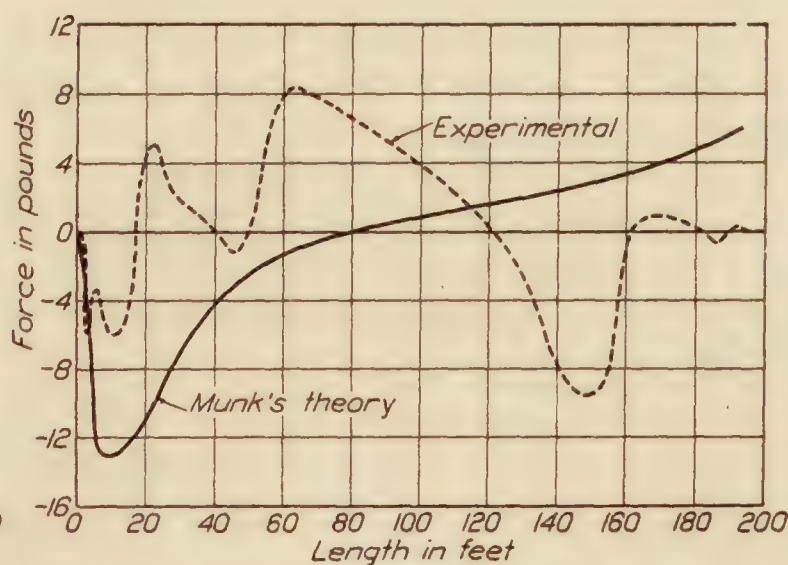


FIG. 30.—Horizontal flight, run No. 1

Theoretical and experimental pressure distribution on the "C-7" airship

CONCLUSIONS

Since the results are scattered throughout such extensive tables, it is thought advisable in conclusion to again summarize some of the more important of them, as follows:

(1) The maximum total load on a complete tail surface was 352 pounds, occurring on the bottom fin and rudder (fig. 9), during a reversal at 40.5 M. P. H., when the rudder was moved from 24° port to 18° starboard. The corresponding normal force coefficient, C_{NF} was 0.316.

(2) The maximum total load on a fixed surface was found to be 311 pounds, and occurred on the top fin (fig. 11) during a steady circle at 35 M. P. H. with the rudder 44° to starboard. This resulted in a normal force coefficient, $C_{NF}=0.554$.

(3) The maximum total load on a movable surface was 250 pounds, and occurred on the rudder (fig. 13) at the start of a turn at 45 M. P. H. with the rudder 44° to starboard. The average pressure over the surface in this case was 2.9 lb./sq. ft. or $C_{NF}=0.565$, and was the largest encountered on any surface during any maneuver.

(4) Large local pressures, ranging from 3 to 7 lb./sq. ft., were encountered, usually on the leading edge of the top fin close to the envelope and on the balancing portion of the rudder and elevators. The largest pressure of this kind was 7.3 lb./sq. ft. on the top fin during a steady circle at an air speed of 45 M. P. H. with the rudder 44° to starboard.

(5) The maximum moment of the tail surface loads about the center of buoyancy was 37,200 lb. ft. and occurred in a steady circle at 35 M. P. H. with the rudder 44° to starboard.

(6) The loads on the envelope were relatively small, the maximum loads ranging from 16 to 18 pounds per running foot along the axis of the ship.

(7) Due to the large areas and small pressures encountered, any irregularity in the hull or slight error in the reading of the pressures would cause a large error in the load per running foot on the envelope. This fact tends to make a complete investigation of the envelope pressures for the purpose of finding aerodynamic forces impracticable, because it is obvious that sufficient points to eliminate this difficulty could not be taken without running into excessive weight and resistance. It is felt, therefore, that the results of the tests on the envelope while showing the general distribution of pressure sufficiently well are practically useless in the determination of total aerodynamic forces on the airship.

(8) Although the pressures actually measured in a bump (figs. 15, 16, 23, 24, 27a, and 27b) were of the same general magnitude as in the other conditions it is felt that the pressures set up by a bump are larger than those obtained in maneuvering.

In general, the tests on the tail surfaces produced valuable data covering the loads and coefficients encountered in flight which confirm the theoretical values used in design.

The investigation of the pressures on the hull, while producing some interesting information relative to general distribution of the pressures, was unsatisfactory for the purpose of finding the aerodynamic loading on the airship. It would seem that such an investigation is unlikely to produce any results of particular value unless possibly on a rigid ship where the resistance of the necessary tubing would be avoided by securing it inside of the envelope. Even with a rigid ship it is felt that such an investigation is impracticable because of the great number of points that it is necessary to investigate and the expense, bulk, and weight of the apparatus required.

For further tests of this nature a pressure recorder giving continuous records is recommended.

BIBLIOGRAPHY

Reference 1. Construction Department, Navy Yard, Report No. 177, "Calibration of Brass Static Pad, C. & R. Sample No. 3," 1921.

Reference 2. F. H. Norton, "N. A. C. A. Recording Airspeed Meter," N. A. C. A. Technical Note, No. 64, 1921.

Reference 3. N. A. C. A. Technical Report, No. 184, "Aerodynamic Forces on Airship Hulls." By Max M. Munk.

N. A. C. A. Technical Note No. 192, "Note on the Pressure Distribution Over the Hull of Elongated Airships with Circular Cross Section." By Max M. Munk.

Reports and Memoranda No. 749, "The Equilibrium of Airships in Curvilinear Flight." By R. Jones.

Reports and Memoranda No. 779, "Experiments on a Model of Rigid Airship R-32, Together with a Comparison with the Results of Full Scale Turning Trials and a Consideration of the Stability of the Ship." By R. Jones, D. H. Williams, and A. H. Bell.

Reports and Memoranda No. 780, "Aerodynamic Pressures on an Airship Hull in Curvilinear Flight." By R. Jones.

Reports and Memoranda No. 794, "The Aerodynamic Loading of Airships." By T. Bairstow.

Reports and Memoranda No. 808, "Pressure Plotting on Fin and Rudder of a Model R-32." By D. H. Williams and A. H. Bell.

Reports and Memoranda No. 811, "Experiments on Rigid Airship R-32, Part I. Pressures on Upper Fin and Rudder." By J. B. Pannell, R. A. Frazer, and H. Bateman.

Bureau of Standards Report, "Pressure Distribution Over the Surface of RS-1 Airship."

TABLE I
LIST OF MANEUVERS INVESTIGATED FOR PRESSURE DISTRIBUTION

Run No.	Maneuver	R. P. M.	Rudder angle (degrees)	Elevator angle (degrees)	Run No.	Maneuver	R. P. M.	Rudder angle (degrees)	Elevator angle (degrees)
1	Horizontal flight	1,250			15	Start climb	1,000		19 U.
2	Steady circle	1,000	8 R.		16	do	1,250		12 U.
3	do	1,000	44 R.		17	do	1,250		19 U.
4	do	1,250	8 R.		18	Steady descent	1,000		11 D.
5	do	1,250	44 R.		19	do	1,000		18 D.
6	Start circle	1,000	8 R.		20	do	1,250		11 D.
7	do	1,000	44 R.		21	do	1,250		18 D.
8	do	1,250	8 R.		22	Horizontal flight light	1,000		
9	do	1,250	44 R.		23	do	1,250		6 D.
10	Steady climb	1,000		12 U.	24	Rising light	1,000		
11	do	1,000		19 U.	25	do	1,250		
12	do	1,250		12 U.	26	Reversal	1,000	24 L. to 18 R.	
13	do	1,250		19 U.	27	do	1,250	24 L. to 18 R.	
14	Start climb	1,000		12 U.	28	Bump	1,250		

TABLE II
PRESSURE DISTRIBUTION TESTS ON TAIL SURFACES
[Table of Data]

	Run No. 1	Run No. 2	Run No. 4	Run No. 5	Run No. 9a	Run No. 9b	Run No. 13	Run No. 17a	Run No. 17b
Wind direction	SE.	SE.	SE.	WNW.	WNW.	WNW.	SE.	SE.	SE.
Wind velocity (M. P. H.)	13	13	13	4	4	4	13	9	9
Air in balloonets (cu. ft.)	3,500	3,500	4,000	1,000	1,500	1,500	4,500	2,000	2,000
Static condition (lb. light)	30	30	Equilib.	50	Equilib.	Equilib.	Equilib.	Equilib.	Equilib.
R. P. M. starboard	1,250	1,000	1,250	1,250	1,250	1,250	1,250	1,250	1,250
R. P. M. port	1,250	1,000	1,250	1,250	1,250	1,250	1,250	1,250	1,250
Gas pressure (inches of water)	1½	1¼	1½	1½	1½	1½	1½-2	1¼-2	1¼-2
Rudder angle (degrees)	0	5 R.	5 R.	18 R.	18 R.	18 R.	0	0	0
Elevator angle (degrees)	0	0	0	0	0	0	12 U.	12 U.	12 U.
Air speed (knots)	45.5	31	41	35	45	45	39.5	45	45
Compass course (degrees)	130	Various.	Various.	Various.	Various.	Various.	135		
Inclination (degrees)	0	0	-1.0	-1.0	0	0	13 U.	0	0
Barometric pressure (at manometer)	29.92	29.94	29.90	29.73	29.70	29.71	29.95	29.86	29.81
Temperature (° F.)	48	48	48	46	46	46	48	53	53
Air density	0.00242	0.00243	0.00243	0.00242	0.00241	0.00241	0.00243	0.00240	0.00240
Corrected rudder angle (degrees)	0	8 R.	8 R.	44 R.	44 R.	44 R.	0	0	0
Corrected elevator angle (degrees)	0	0	0	0	0	0	19 U.	19 U.	19 U.
Corrected air speed (M. P. H.) (N. A. C. A. recording instrument)	47.0	36.5	41.0	35	45.5	45.5	42.0	48.0	46.5
Angle of yaw (degrees)	2.9 R.	5.9 R.	7.4 R.	6.0 R.	4.5 R.	4.5 R.	2.1 L.	1.5 R.	1.5 R.
Fore and aft inclination (degrees)	-5.2	+2.4	-3.2	-1.4	-3.6	-4.2	+10.2	+0.6	+6.0
Inclination of flight path (degrees)	-1.4	+2.6	00	+1.7	00	0	+7.8	+2.2	+7.2
Angle of pitch (degrees)	-3.8	-2	-3.2	-3.1	-3.6	-4.2	+2.4	-1.6	-1.2
Time of complete turn (minutes)		2.52	1.03	1.11					

	Run No. 21	Run No. 23	Run No. 25	Run No. 27a	Run No. 27b	Run No. 27c	Run No. 27d	Run No. 28
Wind direction	WNW.	W.	W.	WNW.	WNW.	WNW.	WNW.	WNW.
Wind velocity (M. P. H.)	4	8	8	4	4	4	4	4
Air in balloonets (cu. ft.)	1,500	1,000	1,000	1,500	1,500	1,500	1,500	1,500
Static condition (lb. light)	Equilib.	525	525	Equilib.	Equilib.	Equilib.	Equilib.	Equilib.
R. P. M. starboard	1,250	1,250	1,250	1,250	1,250	1,250	1,250	1,250
R. P. M. port	1,250	1,250	1,250	1,250	1,250	1,250	1,250	1,250
Gas pressure (inches of water)	1¾-1¼	1½	1½-1½	1½	1½	1½	1½	1¼-2
Rudder angle (degrees)	0	0	0	10L.-10R.	10L.-10R.	10L.-10R.	10L.-10R.	3L.-8 R.
Elevator angle (degrees)	12 D.	4 D.	0	0	0	0	0	3 D.
Air speed (knots)	41	42	44	38	38	38	38	43-45
Compass course (degrees)	280	270	270	Various.	Various.	Various.	Various.	220
Inclination (degrees)	17 D.	8 D.	1	1	1	1	1	10 D.-4 U.
Barometric pressure (at manometer)	29.78	29.78	29.78	29.70	29.70	29.70	29.70	29.83
Temperature (° F.)	45	49	49	46	46	46	46	45
Air density	0.00243	0.00241	0.00241	0.00242	0.00242	0.00242	0.00242	0.00244
Corrected rudder angle (degrees)	0	0	0	24L.-18R.	24L.-18R.	24L.-18R.	24L.-18R.	5½L.-13R.
Corrected elevator angle (degrees)	18D.	6 D.	0	0	0	0	0	4 D.
Corrected air speed (M. P. H.) (N. A. C. A. recording instrument)	46	43	47	40.0	40.5	41.5	42	42.5
Angle of yaw (degrees)	1.5 R.	1.8 L.	2.2 R.	0-7 R.	0-7 R.	0-7 R.	0-7 R.	
Fore and aft inclination (degrees)	-5.0	-3.2	-2.2	-0.2	-1.6	-3.2	-4.4	-5.8
Inclination of flight path (degrees)	-3.3	0	+2.2	+2.45	0	0	0	-3.9
Angle of pitch (degrees)	-1.7	-3.2	-4.4	-2.65	-1.6	-3.2	-6	-2.1

TABLE III

PRESSURE DISTRIBUTION ON THE TAIL SURFACES

[Pressures lb./sq. ft.]

Surface	Pad	Run No. 1	Run No. 2	Run No. 4	Run No. 5	Run No. 9a	Run No. 9b	Run No. 13	Run No. 17a	Run No. 17b	Run No. 21	Run No. 23	Run No. 25	Run No. 27a	Run No. 27b	Run No. 27c	Run No. 27d	Run No. 28
Starboard fin and elevator, upper side-----	1-A	-1.30	-0.60	-0.65	-0.45	-1.10	-0.30	-2.75	-3.20	-----	+0.80	-0.65	-0.90	-0.85	-0.60	-0.40	-0.80	+0.10
	2-A	-.40	-.20	.00	-.10	-.20	+.30	-.45	-.50	-0.10	.00	-.10	.00	-.30	-.15	.00	-.20	+.10
	2-B	-.65	-.30	-.15	-.10	-.60	+.10	-1.00	-1.20	-.40	+.10	-.30	-.40	-.40	-.30	-.25	-.35	+.05
	2-C	-1.00	-.55	-.45	-.20	-1.00	-.20	-1.70	-1.90	-.85	.00	-.80	-.90	-1.00	-.90	-.40	-.70	-.10
	3-A	-.35	-.20	-.10	+.10	-.40	+.35	-.20	-.15	-.30	-.35	-.30	.00	-.30	-.20	.00	-.20	.00
	3-B	-.40	.00	+.10	.00	-.35	+.40	-.20	-.30	-.20	-.45	-.30	-.20	-.40	-.10	.00	.00	-.05
	3-C	-.50	-.15	.00	-.10	-.60	-.50	-.90	-.70	-.55	-.55	-.40	-.40	-.55	-.40	-.25	-.20	-.80
	4-A	+.10	.00	.00	+.10	-.05	+.50	+.15	+.20	-.10	.00	-.10	+.10	-.20	-.10	+.10	.00	+.30
	4-B	+.10	.00	+.20	+.25	-.10	+.70	+.15	+.10	-.10	.00	-.10	+.20	-.20	-.10	.00	.00	+.40
	4-C	+.10	+.05	+.35	-----	-.05	+.70	-.60	-.40	.00	-.10	.00	+.10	-.40	-.10	+.20	.00	+.25
	5-A	+.10	+.15	+.20	+.35	-.10	+.60	+.40	+.50	-.20	-.65	.00	+.10	-.30	-.20	.00	.00	+.20
	5-B	.00	.00	+.20	+.10	-.40	+.40	+.25	+.50	-.85	-1.10	-.30	-.10	-.40	-.30	-.10	.00	+.30
	5-C	-.30	-.25	-.15	+.10	-.70	+.45	-.70	-.60	-1.60	-1.00	-.40	-.60	-.85	-.70	-.25	-.10	+.70
	5-D	+.65	-.15	-.10	-.20	-.40	+.20	-.30	+.60	-2.70	-1.30	+.10	-.20	-.70	-.70	-.20	-.50	+1.40
	6-A	+.10	-.10	.00	.00	-.40	+.40	-.55	+.70	-1.40	-2.00	-.40	-.30	-.70	-.60	-.30	-.20	+.30
	6-B	-1.10	-.70	-.80	-.50	-----	-.30	-.20	-1.50	-2.00	-----	-1.40	-1.50	-----	-.90	-.80	-.80	
	6-C	.00	-.10	-.20	-.10	-.65	+.10	-.45	-.10	-1.90	-2.00	-.60	-.50	-1.10	-.90	-.60	-.60	-----
	6-D	-.85	-.55	-.50	-.40	-1.15	-.40	-.80	-.50	-1.80	-1.80	-1.00	-.90	-1.25	-1.10	-.85	-1.10	+.10
	7-A	-.20	-.20	.00	-.10	-.40	+.50	+.30	+.45	-.80	-1.10	-.50	-.30	-.60	-.40	.00	-.10	+.10
	7-B	-.10	.00	+.10	+.20	-----	+.50	+.30	+.40	-.50	-----	-.25	-.20	-.40	-----	-.05	-.10	+.20
	7-C	-.10	-.10	+.10	+.15	-.60	+.40	-.45	-.50	-1.20	-1.40	-.35	-.40	-.70	-.60	-.30	-.10	+.10
	7-D	-.70	-.15	-.10	+.15	-.65	+.20	-.30	-.40	-1.20	-1.00	-.55	-.50	-1.00	-.70	-.60	-.50	+.10
	8-A	-.50	+.10	+.20	+.20	-.25	+.60	+.20	+.20	-.30	-.90	-.20	.00	-.40	-.20	+.10	.00	-.20
	8-B	-.60	-.10	.00	-.15	-.40	+.40	+.10	.00	-.40	-.80	-.50	-.20	-.40	-.20	-.20	-.10	-----
	8-C	-.45	-.10	+.15	+.20	-.30	+.50	+.60	-.70	-.75	-.70	-.45	-.20	-.60	-.40	-.10	-.10	-.20
	8-D	-.80	+.15	.00	-.10	-.50	+.80	+.10	-.20	-.90	-1.00	-.45	-.50	-1.00	-.60	-.50	-.40	-.45
Starboard fin and elevator, lower side-----	1-A	-1.70	-.55	-.60	-.35	-1.60	-.50	+.50	+.50	-1.80	-4.50	-2.10	-1.10	-1.90	-1.70	-1.20	-.40	-1.50
	2-A	-.65	.00	-.20	-.20	-.40	+.30	+.35	+.20	-.70	-1.75	-.90	-.10	-1.10	-.50	-.50	-----	-.50
	2-B	-1.00	-.30	-.35	-.25	-1.00	-.10	+.20	+.20	-1.20	-2.30	-1.20	-.60	-1.30	-.90	-.60	+.70	-.50
	2-C	-1.70	-.35	-.45	-.30	-1.75	-.30	+.30	-.50	-1.50	-3.00	-1.60	-.85	-1.45	-1.30	-.90	-.80	-1.20
	3-A	-.40	.00	.00	-.10	-.20	+.50	+.20	+.25	-.30	-.80	.00	-.60	-.30	.00	+.10	+.30	
	3-B	-.50	.00	.00	+.10	-.40	+.55	+.50	-.10	-.20	-1.10	-.60	.00	-.75	-.40	+.10	+.10	-.10
	3-C	-1.10	.00	-.20	-.10	-.55	+.50	.00	-.30	-.80	-1.85	-.95	-.10	-.95	-.60	-.20	-----	-.05
	4-A	-.60	-.10	-.10	.00	-.30	+.70	+.15	.00	-.20	-.60	-.50	.00	-.50	-.05	+.10	+.20	-.10
	4-B	-.30	+.10	+.20	+.15	.00	+.70	+.60	-----	-----	-.50	-.20	+.30	-.50	-.10	+.15	-----	-.10
	4-C	-1.00	.00	.00	+.20	.00	+.70	.00	+.30	.00	-2.00	-.35	+.20	-.40	-.20	+.15	+.40	-.25
	5-A	-.70	-.10	-.15	-.20	-.25	+.45	-.20	-.40	-.10	-.30	-.35	+.20	-.60	-.20	.00	.00	.00
	5-B	-.60	.00	.00	.00	-.30	+.40	-.30	-.40	+.50	-.25	-.45	-.20	-.70	-.40	+.10	+.10	-.50
	5-C	-1.50	-.35	-.30	-.20	-.90	+.10	-.20	-.50	.00	-1.50	-1.15	-.80	-1.30	-.70	-.40	.00	-1.40
	5-D	+.90	-1.10	+1.10	+.20	-.15	+.45	+.65	-.30	+1.90	-.10	-1.10	-.80	+.95	+1.10	+1.10	+1.80	-2.10
	6-A	-.90	-.35	-.30	-.20	-.60	+.45	-.80	-1.00	+.60	+.10	-.70	-.50	-.80	-.40	+.10	+.10	-.80
	6-B	-1.50	-.45	-.30	-.40	-1.00	+.20	-1.30	-1.35	+.70	+.10	-1.30	-.85	-.90	-.50	-.10	-.20	-1.30
	6-C	-----	-.40	+.50	-.40	-1.00	+.50	-----	-1.40	+1.00	-1.35	-1.30	-.90	-.85	-.60	-.10	.00	-1.50
	6-D	-2.10	-.65	-.60	-.30	-1.50	-.50	-.80	-1.20	-.10	-1.55	-1.80	-1.10	-1.40	-1.00	-.75	-.70	-1.00
	7-A	-.80	-.30	-.25	.00	-.30	+.50	-.60	-.55	+.15	-.10	-.40	-.35	-.60	-.40	.00	+.25	-.30
	7-B	-.80	-.20	.00	.00	-.60	+.50	-.40	-.70	+.30	-.20	-.45	-.35	-.70	-.20	.00	+.10	-.50
	7-C	-.70	.00	+.15	.00	-.40	+.50	-.60	-----	-----	-1.40	-.60	-.15	-.70	-.30	+.20	+.10	-1.50
	7-D	-1.20	-.30	-.25	.00	-.60	+.20	-.40	-.50	.00	-.90	-.90	-.50	-1.00	-.50	-.20	.00	-.85
	8-A	-.40	-----	.00	.00	-.10	+.85	-.25	-.30	-.20	+.80	-.20	+.20	-.60	-.20	+.30	+.20	+.75
	8-B	-.30	.00	+.10	+1.00	-.85	+.30	-1.00	-.80	+.65	-.20	-1.15	-.90	+1.50	+1.90	+2.10	+1.30	+.80
	8-C	+1.50	-.65	+2.20	+.60	-.80	-.20	+.45	-.70	+.60	+.20	+.15	-.50	+1.10	+1.20	+1.20	+1.10	+.40
	8-D	-.20	-.70	+2.90	+1.10	-.80	-.40	+.10	-.60	+1.00	-.35	-.35	-.20	+1.30	+1.00	+.70	+1.20	+.55

TABLE III—Continued

PRESSURE DISTRIBUTION ON THE TAIL SURFACES—Continued

[Pressure lb./sq. ft.]

Surface	Pad	Run No. 1	Run No. 2	Run No. 4	Run No. 5	Run No. 9a	Run No. 9b	Run No. 13	Run No. 17a	Run No. 17b	Run No. 21	Run No. 23	Run No. 25	Run No. 27a	Run No. 27b	Run No. 27c	Run No. 27d	Run No. 28
Port fin and elevator, upper side-----	1-A	-----	-1.70	-2.00	-1.85	-1.25	-1.50	-2.80	-----	-0.90	-0.10	-0.60	-1.10	-0.20	-0.45	-0.60	-1.85	-0.70
	2-A	-0.70	-.70	-.70	+.65	-.40	-.60	-.60	-0.85	-.20	-.30	-.40	-.20	+.10	-.25	-.50	-1.00	-.50
	2-B	-.80	-.80	-.90	-.90	-.45	-.65	-.80	-1.20	-.40	.00	-.45	-.30	+.30	-.10	-.30	-.70	-.30
	2-C	-1.00	-1.30	-1.40	-1.40	-1.00	-1.40	-1.60	-2.20	-.85	-.50	-.95	-1.00	-----	-.80	-.70	-1.45	-.70
	3-A	-.40	-.60	-.50	-.50	-.20	-.30	-.10	-.10	.00	-.25	-.30	+.10	+.15	-.15	-.30	-1.00	-.10
	3-B	-.50	-.60	-.50	-.55	-.30	-.50	-.15	-.30	-.10	-.30	-.30	-.20	+.35	-.20	-.30	-.80	-.30
	3-C	-----	-.95	-1.10	-1.05	-.60	-1.00	-.85	-1.10	-.55	-1.10	-.50	-.40	+.10	-.65	-.70	-1.10	-.80
	4-A	-----	-.50	-.40	-.50	-.20	-.50	+.30	.00	+.20	-1.05	-.25	.00	.00	-.40	-.30	-.65	-.45
	4-B	-.40	-.50	-.60	-.55	-.10	-.40	+.30	+.10	.00	-.30	-.10	-.10	+.20	-.10	-.25	-.40	-.05
	4-C	.00	-.35	-.50	-.70	+.25	-.10	-.50	-.90	+.20	-.35	-.05	+.30	+.15	-.40	-.20	-1.30	+.10
	5-A	-1.10	-.90	-1.00	-.90	-.90	-1.20	-.05	-.35	-.75	-1.70	-.75	-.50	-.55	-.90	-.90	-1.00	-.60
	5-B	-----	-.50	-.65	-.60	-.40	-.70	+.30	+.35	-.50	-1.40	-1.50	-.10	+.10	-.60	-.65	-.70	.00
	5-C	-.10	-1.00	-1.10	-1.40	-.35	-1.00	.00	-.10	-1.20	-1.00	-.30	-.50	.00	-.70	-.70	-1.20	-.20
	5-D	+.60	-.60	-.85	-.80	.00	-.30	+.35	+.40	-2.10	-1.30	+.20	-.10	+.25	-.40	-.25	-.80	+1.60
	6-A	-.40	-.70	-.90	-1.00	-.60	-1.10	+.55	+.70	-1.30	-2.20	-.60	-.40	-.50	-1.00	-.90	-1.10	+.05
	6-B	+.10	-.60	-.80	-.70	-.40	-.90	+1.00	+1.10	-1.80	-2.15	-.50	-.30	-.30	-1.00	-1.20	-1.00	+.40
	6-C	-.90	-1.00	-1.25	-1.60	-.65	-1.10	-1.25	.00	-1.90	-2.45	-.65	-.75	-.40	-1.20	-1.40	-1.30	+.55
	6-D	-.85	-.90	-1.50	-1.55	-1.00	-1.10	+.55	-.70	-2.10	-1.40	-1.40	-1.20	-.70	-.40	-1.10	-1.60	+.50
	7-A	-.20	-.55	-.60	-.70	-.40	-.80	+.65	+.70	-.55	-1.30	-.30	-.20	-.10	-.70	-.80	-.80	+.05
	7-B	.00	-.50	-.60	-.70	-.10	-.70	+.75	+.85	-.80	-1.40	-.50	-.10	-.20	-.65	-.60	-----	+.20
	7-C	.00	-.75	-.85	-1.40	-.45	-.90	-.30	-.50	-1.40	-1.70	-.65	-.30	-.40	-.90	-.90	-.90	+.30
	7-D	-.40	-.90	-1.20	-1.20	-.30	-1.00	+.40	+.20	-1.00	-1.30	-.60	-.50	-.20	-.90	-.70	-1.10	-.20
	8-A	-.70	-.75	-.70	-.95	-.30	-.90	+.20	+.30	-.60	-1.10	-.50	-.15	-.35	-.80	-.60	-.80	-.45
	8-B	-.70	-.65	-.65	-.80	-.30	-.80	+.10	.00	-.90	-1.30	-.70	-.20	-.10	-.80	-.55	-.80	-.75
	8-C	-.50	-.60	-.65	-.90	-.20	-.80	-.05	-.60	-.80	-1.20	-.40	-.20	-.10	-.70	-.70	-.80	-.50
	8-D	-.40	-.70	-.90	-1.00	-.20	-.80	+.35	+.30	-.70	-.90	-.50	-.20	-.10	-.60	-.70	-.80	-.30
Port fin and elevator, lower side-----	1-A	-1.10	-.65	-.75	-.60	-1.25	-1.90	+.85	+1.30	-1.20	-4.45	-2.00	-1.00	-.90	-1.50	-2.00	-1.00	-1.20
	2-A	-.50	-.35	-.40	-.30	-.50	-.70	+.40	+.50	-.60	-1.30	-.90	-.40	-.20	-.50	-.60	-.50	-.40
	2-B	-.10	-.60	-.65	-.50	-1.00	-1.10	+.30	+.50	-1.10	-1.95	-1.30	-.70	-.60	-.95	-1.10	-.70	-.90
	2-C	-1.20	-.55	-.60	-.40	-.90	-1.30	+.25	+.50	-.80	-2.65	-1.50	-1.00	-.70	-1.30	-1.35	-1.00	-1.20
	3-A	-.60	-.40	-.35	-.30	-.30	-.50	+.15	+.30	-.20	-.90	-.75	-.30	-.20	-.45	-.45	-.50	-.30
	3-B	-.70	-.50	-.55	-.50	-.55	-.70	+.15	+.20	-.40	-.10	-.80	-.30	-.30	-.55	-.75	-.70	-.50
	3-C	-.90	-.60	-.60	-.40	-.65	-1.00	.00	.00	-.50	-1.90	-1.00	-.50	-.40	-.75	-.90	-.80	-.80
	4-A	-.70	-.60	-.50	-.60	-.45	-.80	+.10	+.20	-.10	-.60	-.70	-.40	-.20	-.40	-.60	-.60	-.40
	4-B	-.60	-.40	-.40	-.45	-.10	-.60	+.45	+.50	+.30	-.90	-.55	.00	-.10	-.40	-.50	-.40	-.40
	4-C	-.10	-.20	-.20	-.20	.00	-.40	+.50	+.40	+.10	-1.75	-.30	+.10	+.10	-.35	-.40	-.35	-.20
	5-A	-.60	-.60	-.65	-.75	-.35	-.90	-.10	-.30	+.10	-.30	-.50	-.20	-.20	-.60	-.50	-.70	-.45
	5-B	-1.40	-.70	-.80	-1.15	-.40	-.90	+.15	-.40	+1.00	-1.00	-1.20	-.60	-.10	-.50	-1.00	-.90	-.95
	5-C	-1.40	-.70	-.70	-.90	-.70	-1.30	.00	-.10	+.50	-1.00	-1.20	-.60	-.40	-.90	-1.30	-1.00	-2.00
	5-D	-1.60	-.80	-.50	-.60	-.90	-1.40	-.30	-.45	+1.80	-.90	-1.60	-.40	-.70	-1.00	-1.10	-.70	-4.10
	6-A	-1.00	-.90	-1.00	-1.10	-.60	-1.25	-.60	-.90	+.20	-.10	-.90	-.45	-.40	-.70	-.80	-1.00	-1.10
	6-B	-2.00	-1.20	-1.25	-1.45	-1.05	-1.60	-1.25	-1.20	+1.00	+.10	-1.40	-1.15	-.50	-.90	-1.00	-1.20	-1.75
	6-C	-2.30	-1.40	-1.45	-1.60	-1.40	-2.00	-1.20	-1.45	+.40	-.70	-2.00	-1.30	-.80	-1.50	-1.60	-2.10	-1.90
	6-D	-----	-1.40	-1.50	-1.30	-1.65	-2.10	-1.00	-1.15	-.50	-1.60	-2.00	-1.60	-1.00	-1.40	-1.70	-1.70	-1.50
	7-A	-1.00	-.75	-.80	-.90	-.55	-1.00	-.40	-.50	.00	-.40	-.70	-.40	-.45	-.80	-.85	-1.10	-.80
	7-B	-.80	-.70	-.70	-.90	-.50	-.80	-.20	-.50	+.30	-.10	-.75	-.35	-.10	-.60	-.70	-.90	-1.00
	7-C	-1.20	-.80	-.80	-1.05	-.50	-1.10	-.35	-.60	+.30	-1.15	-1.00	-.70	-.30	-1.00	-.90	-1.00	-1.40
	7-D	-.80	-.60	-.20	-.90	-.50	-1.10	-.25	-.50	+.40	-.90	-1.00	+.20	+.15	-.90	-1.10	-.80	-1.10
	8-A	-.50	-.70	-.75	-.90	-.30	-.50	+.60	-.20	+1.00	-.90	-.20	-.20	+.10	-.20	-.70	-1.00	-.60
	8-B	-.70	-.55	-.70	-1.10	-.15	-.60	+.30	-.35	-.10	-.90	-.50	+.10	-.40	-.70	-.80	-.90	-.70
	8-C	-.50	-.50	-.65	-.85	-.15	-.70	+.25	-.20	-.10	-1.40	-.50	-.25	.00	-.70	-.80	-.80	-1.05
	8-D	-.90	-.85	-.90	-1.00	-.50	-1.30	.00	-.30	-.30	-.70	-.90	-.50	-.30	-.80	-1.00	-1.10	-1.00
Lower fin and rudder, port side-----	1-A	-1.10	+.70	+.75	+1.20	-.50	+1.40	-1.30	-.85	-1.80	-.95	-1.20	-.60	+1.30	-.80	+.35	+1.10	-.45
	2-A	-.90	.00	-.20	+.20	-.30	+.10	-.40	-.40	-1.00	-.70	-.80	-.40	+1.10	-.70	-.25	+.05	-.60
	2-B	-.80	+.10	+.10	-.35	-.40	+.55	-.60	-.70	-1.10	-.60	-.85	-.50	-1.90	-.80	-.10	+.30	-.40
	2-C	-1.50	-.10	-.10	+.40	-1.00	+.15	-.65	-1.15	-1.20	-.95	-1.10	-.80	-2.30	-1.50	-.50	-.05	-.75
	3-A	-.10	-.15	-.10	-.20	-.40	-.15	+.45	-.50	-.70	-.60	-.75	-.40	-.90	-.90	-.50	-.30	-.60
	3-B	-.90	-.30	-.25	.00	-.30	-.10	-.45	-.40	-.85	-.50	-.45	-.25	-1.00	-.60	-.50	-.40	-.35
	3-C	-1.30	-.40	-.40	-.30	-.50	-.20	-.55	-.80	-.90	-.65	-.80	-.60	-1.75	-1.10	-.50	-.20	-.55
	4-A	-.70	-.20	-.25	-.10	-.30	-.25	-.40	-.30	-.65	-.40	-.35	-.10	-.80	-.80	-.40	-.20	-.30
	4-B	-.50	-.20	-.10	-.10	-.30	-.05	-.35	-.40	-.60	-.20	-.50	-.10	-1.00	-.70	-.40	-.25	-.20
	4-C	-.50	-.20	-.25	-.10	-.10	+.20	-.25	-.10	-.40	-.20	-.30	.00	-1.90	-.65	-.10	.00	-.20
	5-A	-.70	-.40	-.50	-.80	-.50	-.90	-.35	-.40	-.40	-.10	-.20	+.10	-.70	-.90	-.70	-.70	-.20
	5-B	-.80	-.50															

TABLE III—Continued

PRESSURE DISTRIBUTION ON THE TAIL SURFACES—Continued

[Pressures lb./sq. ft.]

Surface	Pad	Run No. 1	Run No. 2	Run No. 4	Run No. 5	Run No. 9a	Run No. 9b	Run No. 13	Run No. 17a	Run No. 17b	Run No. 21	Run No. 23	Run No. 25	Run No. 27a	Run No. 27b	Run No. 27c	Run No. 27d	Run No. 28
Lower fin and rudder, starboard side.....	1-A	+0.15	-2.90	+1.45	-0.20			-0.70	-3.30	-1.50			-1.00	-2.40			+2.00	
	2-A	-.80	-.95	-1.30	-1.40	-0.20	-0.90	-.25	-.30	-.50	0.00	-0.35	-.10	-.40	-0.30	-0.50	-1.00	-0.45
	2-B	-.70	-1.45	-2.20	-2.10	-.20	-1.80	-.30	-.15	-.35	.00	-.40	.00	+.10	-.15	-1.05	-2.10	-.40
	2-C	-1.60	-2.30	-2.90	-2.40	-.90	-2.90	-1.00	-1.00	-1.10	-.30	-.80	-1.60	-.35	-.90	-2.05	-2.90	-1.00
	3-A	-.30	-.50	-.80	-.50	+.10	.00		-.20	+.30	-.10	.00	+.20	-.30	-.10	-.40	-.65	
	3-B	-.50	-.65	-.95	-.85	-.05	-.40		-.20	-.40	+.10		.00	-.30	-.10	-.25	-.70	-.40
	3-C	-1.40	-1.65	-2.10			+2.00		-.90	-.80							-1.80	
	4-A		-.55	-.65	-.15	-.15		-.25		-.20	-1.40		-.40	.00		-1.20	-.35	
	4-B	-.50	-.55	-.80	-.50		+.25	-.05	-.20	-.10	+.10	-.20	.00	-.30	.00	+.25	-.20	-.30
	4-C	-.25	-1.10	-2.10	-1.40	+.40	-.85	+.15	.00	+.10	+.30	+.10	+.30	-.40	+.10	-.15	-1.10	-.40
	5-A	-.60	-.50	-.60	+.65	-.10	+.50	-.70	-.50	-.30	-.50	-.60	-.60	-.10	+.25	-.20	-.20	-.60
	5-B	-.60	-.35	-.55	+.60	+.20	+1.90	-.40	-.35	-.20	+.20	-.45	-.10	-.50	+.40	+.40	+.50	-.50
	5-C	-1.30	-1.25	-1.80	.00	+.50	+.90	-.50	-1.05	-.30	-.20	-.80	-.50	+.50	+.1.05	-.40	-.50	-1.20
	5-D	-1.40	-1.20	-1.80	+.1.50	+.1.40	+2.80	+.45	-.15	+.30	+.20	-.60	-.20	+.50	+.1.20	+2.50	+.50	-1.65
	5-E	-1.00	-1.00	-1.20	+.1.00		+2.00	+.50	-.25	.00	+.20	-.50	.00	+.65	+2.60	+2.70	+.50	-1.50
	6-A	-.50	-1.10	-1.60	-.10	-1.40	-.75	-2.50	-1.80	-1.50	-1.20	-1.10	-1.70	-1.40	-1.10	-1.40	-1.40	-1.00
	6-B	-1.20	-.20	-.15	+.1.10	+.85	+2.20	-.50	-.60	-.40	+.20	-.50	-.30	-.10	+.1.10	+1.15	+1.30	-.90
	6-C	-1.40	-.90	-1.40	+.30	+.1.20	+1.50	-.60	-.90	-.70	.00	-.90	-.60	.00	+.1.30	+.90	+.20	-1.60
	6-D	-1.70	-.80	-1.25	-.20	-.20	+.70	-.70	-1.00	-.70	-.20	-1.10	-.80	-.40	+.50	.00	-.10	-1.50
	6-E	-1.20	-.70	-.80	-.10	+.65	+.75	.00	-.45	-.35	-.10	-.70	-.40	-.40	+.55	+.40	-.05	-1.40
	7-A	-.60	-.10	-.30	+.65	+.20	+.35	-.35	-.30	+.30	.00	-.20	-.10	+.15	-.30	+.10	+.20	-.40
	7-B	-1.00	-.30	-.50	+.50	+.25	+.90	-.15	-.30	.00	+.20	-.95	.00	-.30	.00	+.30	+.30	-.30
	7-C	-1.80	-1.30	-1.65	-.80	-.90	-.75	-1.00	-1.15	-1.30	-1.00	-1.40	-1.10	-1.20	-.50	-.70	-1.00	-1.50
	7-D	-1.70	-.85	-1.00	-.70	-.70	-.20	-1.00	-.90	-1.10	-.50	-1.20	-1.00	-.90	-.50	-.60	-.50	-1.60
	7-E	-.90	-.50	-.70	+.10	+.30	+.65	.00	-.40	.00	-.10	-.50	-.30	-.45	+.10	+.20	-.05	-1.00
	8-A	-.50	-1.00	-.70	+.40	-.20	+.50	.00	-1.30	-.80	-.95	-1.00	-1.20	+.20	-.35	+.20	-2.80	-.70
	8-B	-.50	-.40	-.60	-.10	-.10		.00	-1.70	-.35	-.55	-1.25	-.50	-.20	-.50	-.90	-.50	-.50
	8-C	-.85	-.80	-1.10	-1.25	-.50	-.80	-.55	-.50	-.40	-.20	-.70	-.40	-1.10	-.85	-.70	-.80	-.50
	8-D	-.70	-.45	-.45	-.80	-.10	-.20	-.20	-.30	-.10	+.10	-.50	-.20	-.75	-.40	-.20	-.15	-.50
	8-E	-1.50	-.50	-.60	-.10	-.60	.00	-.30	-.75	-.30	-.50	-1.15	-.85	-.25	-.35	-.20	-.40	-1.35
Top fin, starboard side.....	1-A	-1.80	-2.70	-4.10	-5.90	-1.25	-4.40	-.20	-.50	-.80	-1.85	+1.15	-.70	+1.00	-.55	-2.90	-4.70	-1.90
	2-A	-1.20	-.80	-1.25	-1.40	-.70	-1.25	+1.35	.00	+.15	-.75	+.60	-.30	+.35	-.30	-1.00	-1.60	-.70
	2-B	-1.00	-.90	-1.40	-2.80	-.60	-1.20	+.85	-.30	+1.10	-1.60	-.70	-.30		+.20	-.95	-1.60	-1.00
	2-C	-1.50	-1.90	-2.60		-1.10	-2.80	.00	-.99	-.70	-1.30	-1.10	-.50	+.35	-.30	-2.00	-3.40	-1.30
	3-A	-.50	+.10	-.40	.00	-.50	-.60	+1.40	+.10	+1.45	-1.30	-.05	-.20		+.50	-.25	-.60	-.30
	3-B	-.70	-.40	-.80	-.80	-.65	-.60	+.20	+.10	-.60	-.80	-.60	-.40	-.10	-.50	-.90	-1.20	-.40
	3-C		-1.50	-2.90	-3.45	-1.10	-2.10	-.20	-.40	-.75	-1.60	-1.00	-.55	-.70	-.60	-1.35	-3.50	-1.10
	4-A	-.50	-.40	-.50	-.50	-.60	-.30	+.35	+.35	-.30	-1.25	-.50	.00	-.20	-.40	-.60	-.75	-.30
	4-B	-.85	-.05	-.45	-.40	-.70	-.60	-1.00	-.40	+1.10	-1.00	-1.50	-.30	+.35	.00	-.75	-1.00	-.40
	4-C	-1.20	-.10	-2.50	-1.85	-1.20	-3.30	-1.70	-.55	-1.50	-.60	-1.75	-1.00	-.60	-.50	-2.20	-3.00	-.40
Top fin, port side.....	5-A	-.80	-.40	-.50	-.50	-.80	-.40	+.10	+.10	-.80	-2.00	-.80	-.30	-.60	-.50	-.90	-.60	-.50
	5-B	-1.10	-.90	-.90	-1.10	-1.00	-1.10	-.20	-.00	1.00	-1.70	-1.10	-.70	-.15	-.90	-1.10	-1.20	-.70
	5-C	-1.20	-1.40	-1.60	-1.40	-1.00	-2.30	.00	+.15	-.75	+.80	-1.10	-.40	-.40	-.50	-2.00	-2.10	-.90
	1-A	-1.10	+.30	+1.20	+1.45	-1.10	+1.35	-.50	.00	+.65		-1.70	-1.00	-3.80	-1.95	+.20	+.80	-.70
	2-A	-.30	+.10	+.50	+.70	-.20	+.50	+.20	+.50	-.35	-1.10	-.65	-.20	-.95	-.55	+.20	.00	-.30
	2-B	-.40	+.15	+.70	+.95	-.25	+.85	+.10	+.20	-.20	-1.10	-.75	-.30	-1.20	-.60	+.40	+.55	-.20
	2-C	-.85	-.10	+.30	+.45	-.80	+.30	-.35	+.15	-.30	-1.70	-1.25	-.55	-2.30	-1.15	-.10	.00	-.50
	3-A	-.30	-.10	+.15	+1.10	-.20	+.20	+.20	+.50	-.50	-.90	-.60	.00	-.60	-.50	.00	-.20	-1.20
	3-B	-.60	-.30	.00	+.05	-.50	-.20	+.10	+.30	-.30	-1.25	-.80	-.20	-.80	-.50	-.20	-.40	-.50
	3-C	-1.00	-.65	-.70	-.70	-.75	-.70	-.20	+.10	-.65	-1.60	-1.20	-.40	-2.80	-1.00	-.40	-.90	-.70
	4-A	-.30	-.25	+.10	+.30	-.05	+.20	+.40	+.50	-.40	-1.00	-.50	.00	-.30	-.50	-.15	-.20	-.20
	4-B	-.40	-.20	+.20	+.30	-.10	+.20	+.55	+.65	+.20	-1.10	-.40	+.10	-.40	-.30	-.20	-.20	-.40
	4-C	-.40	.00	+.20	-.05	-.55	+.25	+.10	+.30	-1.00	-1.85	-1.35	-.50	-2.50	-.90	-.20	-.20	-.60
	5-A	-.90	-.60	-.40	-.45	-.60	-.60	+.20	+.35	-.20	-1.55	-.90	-.30	-1.00	-.60	-.85	-.80	
	5-B	-.80	-.45	-.30	-.30	-.50	-.40	+.20	+.30	-.60	-1.40	-.85	-.20	-.55	-.70	-.35	-.70	-.80
	5-C	-1.10	-.35	-.50	-.50	-1.00	-.70	-.20	+.10	-1.30	-2.10	-1.50	-.70	-1.70	-1.25	-.60	-1.00	-.80

TABLE IV
LOADS ON TAIL SURFACES

Run No.	Condition	Air speed (M. P. H.)	Control angle (degrees)		Top fin				Bottom fin and rudder							
					Total load		Maximum local load		Total load		Load on fin		Load on rudder		Maximum local load	
			Rudder	Elevator	Lb.	CNF	Lb. per sq. ft.	Sta.	Lb.	CNF	Lb.	CNF	Lb.	CNF	Lb. per sq. ft.	Sta.
1	Horizontal flight	47.0			-59	-0.059	-0.9	2A	-5	-0.004	+22	+0.021	-27	-0.055	+1.3	1
2	Steady circle	36.5	8 R.		-101	-0.163	-3.0	1	-204	-0.225	-189	-0.316	-15	-0.054	-3.6	1
4	do	41.0	8 R.		-249	-0.318	-5.3	1	-234	-0.206	-207	-0.276	-27	-0.077	-2.9	2C
5	do	35.0	44 R.		-311	-0.554	-7.3	1	+91	+0.101	-60	-0.106	+151	+0.570	+6.6	5E-5D
9a	Start circle	45.5	44 R.		-74	-0.077	-1.7	4B-4C	+216	+0.155	+102	+0.110	+115	+0.260	+5.2	5D-5E
9b	do	45.5	44 R.		-284	-0.299	-5.7	1	+263	+0.190	+13	+0.014	+250	+0.565	+6.5	5D
13	Steady climb	42.0		19 U.	-10	-0.011	-2.1	4B-4C	+36	+0.031					-1.6	6A
17a	Start climb	48.0		19 U.	-82	-0.078	-1.1	4B	-17	-0.010					-2.4	1
17b	do	46.5		19 U.	+35	+0.036	+2.0	3A	-78	+0.054					+1.1	5D
21	Steady descent	46.0		21 D.	+20	+0.022	+1.2	4C	+84	+0.059					-1.2	6A
23	Horizontal flight (light)	43.0			+35	+0.040	+2.8	1	+23	+0.019					-1.2	8B
25	Rising flight (light)	47.0			+33	+0.032	-0.6	5B	+3	+0.002	-13	-0.013	+16	+0.032	-1.3	6A
27a	Reversal first exposure	40.0	24L-18 R.		+207	+0.280	+4.8	1	+226	+0.207	+114	+0.159	+111	+0.328	+6.0	5D
27b	Reversal second exposure	40.5	24L-18 R.		+71	+0.095	+1.4	1	+352	+0.316	+159	+0.214	+193	+0.552	+7.2	6E
27c	Reversal third exposure	41.5	24L-18 R.		-180	-0.227	-3.2	1	+239	+0.206	+97	+0.125	+143	+0.388	+5.9	5D-5E
27d	Reversal fourth exposure	42.0	24L-18 R.		-267	-0.326	-5.6	1	+4	+0.004	-94	-0.120	+99	+0.262	+3.6	6B
28	Bump	42.5	24L-18 R.		-18	-0.021	-1.2	1	-92	-0.076	-34	-0.042	-58	-0.151	-2.6	5D

Run No.	Condition	Port fin and elevator								Starboard fin and elevator							
		Total load		Load on fin		Load on elevator		Maximum local load		Total load		Load on fin		Load on elevator		Maximum local load	
		Lb.	CNF	Lb.	CNF	Lb.	CNF	Lb. per sq. ft.	Sta.	Lb.	CNF	Lb.	CNF	Lb.	CNF	Lb. per sq. ft.	Sta.
1	Horizontal flight	-83	-0.062	-31	-0.032	-51	-0.148	-2.1	6B	-101	-0.075	-90	-0.089	-10	-0.030	+2.0	8C
2	Steady circle	+27	+0.032	+34	+0.057	-7	-0.033	+1.1	1	-18	-0.023	-3	-0.006	-15	-0.079	-1.0	5D
4	do	+41	+0.039	+41	+0.055	0	0	+1.3	1	+6	+0.005					+3.0	8D
5	do	+39	+0.051					+1.3	1	-7	-0.010					+1.3	8D
9a	Start circle	-49	-0.040					-0.9	5D	-27	-0.021					-0.9	2C
9b	do	-60	-0.047					+1.0	5D	-2	-0.002					-1.3	8D
13	Steady climb	+69	+0.064	+104	+0.133	-34	-0.131	+3.7	1	+95	+0.086	+125	+0.158	-30	-0.115	+3.3	1
17a	Start climb	+80	+0.058	+132	+0.126	-52	-0.150	+2.7	2C	+24	+0.017	+69	+0.065	-45	-0.129	+3.8	1
17b	do	+127	+0.097	+24	+0.024	+102	+0.306	+3.9	5D	+116	+0.087	+20	+0.020	+96	+0.294	+4.7	5D
21	Steady descent	-73	-0.057	-125	-0.132	+52	+0.165	-4.3	1	-147	-0.113	-200	-0.210	+54	+0.170	-5.3	1
23	Horizontal flight (light)	-121	-0.108	-86	-0.102	-35	-0.128	-1.9	5D	-108	-0.095	-81	-0.098	-26	-0.095	-1.4	1
25	Rising flight (light)	-40	-0.030	-35	-0.034	-6	-0.018	-0.9	6B	-12	-0.009	-5	-0.005	-7	-0.020	-0.8	8B
27a	Reversal first exposure	-89	-0.090					-1.3	2B-2C	-30	-0.032					-2.3	8D
27b	Reversal second exposure	-46	-0.045					-1.0	1	+4	+0.005					+2.1	8B
27c	Reversal third exposure	-82	-0.077					-1.5	1	+13	+0.011					+2.3	8B
27d	Reversal fourth exposure	+42	+0.040					+1.0	4C	+106	+0.097					+2.4	5D
28	Bump	-181	-0.162	-87	-0.105	-94	-0.329	-5.7	5D	-152	-0.136	-114	-0.129	-39	-0.142	-3.5	5D

+Indicates load acting from bottom to top on horizontal surfaces.
+Indicates load acting from starboard to port on vertical surfaces.
* Indicates maximum load encountered.
Areas: Fixed surfaces, 180 sq. ft. each; elevators, 60 sq. ft. each; rudder, 85 sq. ft.

$CNF = \frac{p}{\frac{1}{2}\rho V^2}$
CNF = Absolute coefficient.
p = Pressure per unit area.
ρ = Air density.
V = True air speed.

TABLE V
PRESSURE DISTRIBUTION TESTS ON ENVELOPE

Table of data

	Run No. 1	Run No. 2	Run No. 4	Run No. 5	Run No. 9a	Run No. 9b	Run No. 13	Run No. 17a	Run No. 17b
Wind direction	Variable.	Variable.	Variable.	Variable.	ENE.	ENE.	Variable.	Variable.	Variable.
Wind velocity (M. P. H.)	12	6	6	12	9	9	6	12	12
Air in balloonets (cu. ft.)	None.	None.	None.	None.	2,000	2,000	None.	None.	None.
Static condition (lb. light)	75	25	Equilib.	75	Equilib.	Equilib.	Equilib.	75	75
R. P. M. starboard	1,250	1,000	1,250	1,250	1,250	1,250	1,250	1,250	1,250
R. P. M. port	1,250	1,000	1,250	1,250	1,250	1,250	1,250	1,250	1,250
Gas pressure (inches of water)	1½	1½	1½	1½	1½	1½	1½-2¼	1½-2	1½-2
Rudder angle (degrees)	0	5 R.	5 R.	18 R.	18 R.	18 R.	0	0	0
Elevator angle (degrees)	0	0	0	0	0	0	12 U.	12 U.	12 U.
Air speed (knots)	45	33	39	35	45	45	39	45	45
Compass course (degrees)	210	Various.	Various.	Various.	Various.	Various.	25	210	210
Inclination (degrees)	0	0	0	0	0	0	12.5 U.	13 U.	13 U.
Barometric pressure (at manometer)	29.93	30.12	30.04	29.94	30.15	30.15	30.16	29.91	29.82
Temperature (°F.)	63	77	77	64	73	73	77	64	64
Air density	0.00236	0.00231	0.00230	0.00235	0.00233	0.00233	0.00231	0.00235	0.00234
Corrected rudder angle (degrees)	0	8 R.	8 R.	44 R.	44 R.	44 R.	0	0	0
Corrected elevator angle (degrees)	0	0	0	0	0	0	19 U.	19 U.	19 U.
Corrected air speed (M. P. H.) (N. A. C. A. recording instrument)	43.0	35.0	37.5	32.5	41.5	42.0	40.0	45.0	45
Angle of yaw (degrees)	2.0 L.	6 R.	5 R.	6.5 R.	7.8 R.	7.8 R.	2.0 L.	2.5 R.	2.5 R.
Fore and aft inclination (degrees)		-5.4	+1.2		+1.1	-0.2	+10.5	+5.0	+5.0
Inclination of flight path (degrees)		-2.8	-0.7	-2.8	+0.5	+0.5	+8.0	+2.3	+2.3
Angle of pitch (degrees)		-2.6	+0.5		+0.6	-0.7	+2.5	+2.7	+2.7
Time of complete turn (minutes)		2.32	1.42	1.22					

	Run No. 21	Run No. 23	Run No. 25	Run No. 27a	Run No. 27b	Run No. 27c	Run No. 27d	Run No. 28
Wind direction	ENE.	NE.	Variable.	Variable.	Variable.	Variable.	Variable.	Variable.
Wind velocity (M. P. H.)	9	13	12	12	12	12	12	12
Air in balloonets (cu. ft.)	2,000	None.	None.	None.	None.	None.	None.	None.
Static condition (lb. light)	Equilib.	525	525	75	75	75	75	525
R. P. M. starboard	1,250	1,250	1,250	1,250	1,250	1,250	1,250	1,250
R. P. M. port	1,250	1,250	1,250	1,250	1,250	1,250	1,250	1,250
Gas pressure (inches of water)	1½-1¼	1½	1½-2	1½	1½	1½	1½	1½-2¼
Rudder angle (degrees)	0	0	0	10 L-10 R.	10 L-10 R.	10 L-10 R.	10 L-10 R.	10 L-14 R.
Elevator angle (degrees)	12 D.	5½ D.	3 D.	0	0	0	0	4 U-16 D.
Air speed (knots)	40	39	45	38½	38½	38½	38½	43
Compass course (degrees)	67	45	210	Various.	Various.	Various.	Various.	210
Inclination (degrees)	0-15	3 D.	0	0	0	0	0	3 U-18 D.
Barometric pressure (at manometer)	30.02	30.03	29.82	30.14	30.14	30.14	30.14	29.91
Temperature (°F.)	73	73	63	74	74	74	74	63
Air density	0.00232	0.00232	0.00235	0.00233	0.00233	0.00233	0.00233	0.00235
Corrected rudder angle (degrees)	0	0	0	24 L-18 R.	24 L-18 R.	24 L-18 R.	24 L-18 R.	24 L-28 R.
Corrected elevator angle (degrees)	18 D.	8 D.	4 D.	0	0	0	0	7 U-25 D.
Corrected air speed (M. P. H.) (N. A. C. A. recording instrument)	43	46	45	38	38.5	40.0	42.0	45.0
Angle of yaw (degrees)	2.7 L.	2.6 R.	0.5 L.	0-7 R.	0-7 R.	0-7 R.	0-7 R.	
Fore and aft inclination (degrees)	-5.0		0					-4
Inclination of flight path (degrees)	-2.6	+1.4	+2.5	-0.6	-0.6	-0.6	-0.7	0
Angle of pitch (degrees)	-2.4		-2.5					-4
Time of complete turn (minutes)								

TABLE VI
PRESSURE DISTRIBUTION ON THE ENVELOPE

Pressure lb./sq. ft.

Station No.	Distance to nose, ft.	Diameter, ft.	Pad	Run No. 1	Run No. 2	Run No. 4	Run No. 5	Run No. 9a	Run No. 9b	Run No. 13	Run No. 17a	Run No. 17b	Run No. 21	Run No. 23	Run No. 25	Run No. 27a	Run No. 27b	Run No. 27c	Run No. 27d	Run No. 28
3-----	2.7	8.0	A	+2.90	+2.00	+3.00	+2.00	+3.15	+2.90	+3.40	+3.25	+3.50	+2.90	+3.35	+3.15	+2.50	+2.50	+2.50	+3.00	+3.40
			B	+2.70	+2.00	+3.05	+2.40	+3.20	+3.40	+3.20	+3.40	+3.35	+2.65	+3.40	+3.20	+2.65	+2.40	+2.70	+3.20	+3.45
			C	+2.35	+2.00	+3.00	+2.10	+3.35	+3.45	+2.85	+3.50	+3.60	+3.30	+3.80	+3.40	+2.60	+2.70	+2.85	+3.10	+3.45
			D	+2.35	+2.20	+3.10	+2.10	+2.95	+3.50	+3.40	+3.25	+3.40	+3.10	+3.75	+3.50	+2.60	+2.40	+2.60	+2.90	+3.50
			E	+2.30	+2.05	+3.15	+2.60	+3.45	+3.60	+2.95	+3.20	+3.60	+3.50	+4.10	+3.40	+2.40	+2.70	+2.10	+3.10	+3.45
			F	+2.35	+2.35	+3.30	+2.50	+3.35	+3.35	+3.10	+3.05	+3.45	+3.30	+4.20	+3.40	+2.55	+2.30	+2.30	+2.60	+3.45
			G	+2.60	+2.05	+3.00	+2.20	+3.25	+3.25	+2.95	+3.10	+3.60	+3.20	+3.70	+3.60	+3.15	+2.60	+3.10	+3.30	+3.45
			H	+2.60	+2.00	+3.10	+2.40	+3.20	+3.10	+3.20	+3.35	+3.70	+2.90	+3.60	+3.30	+2.70	+3.00	+2.70	+3.30	+3.45
4-----	4.7	12.8	A	+1.70	+1.60	+2.60	+2.10	+2.65	+2.50	+2.60	+2.50	+2.65	+2.00	+2.50	+2.60	+1.85	+2.00	+2.10	+2.40	+2.60
			B	+1.70	+1.55	+2.40	+2.20	+2.45	+2.65	+2.45	+2.60	+2.40	+2.00	+2.55	+2.50	+2.05	+2.00	+2.25	+2.45	+2.45
			C	+1.70	+1.60	+2.40	+1.70	+2.65	+2.80	+2.40	+2.85	+2.85	+2.50	+3.05	+2.75	+2.05	+2.20	+2.30	+2.65	+2.60
			D	+1.60	+1.75	+2.60	+1.80	+2.65	+3.00	+2.80	+2.60	+2.30	+2.30	+3.30	+2.90	+2.10	+1.80	+1.70	+2.25	+2.60
			E	+1.55	+1.95	+2.60	+2.50	+2.70	+2.90	+2.55	+2.55	+2.90	+3.05	+3.30	+3.00	+1.80	+2.35	+1.60	+2.40	+2.75
			F	+2.00	+1.80	+2.60	+2.30	+2.45	+2.55	+2.40	+2.70	+3.00	+2.50	+3.10	+3.00	+2.35	+2.00	+1.85	+2.25	+3.10
			G	+2.00	+1.30	+2.55	+2.00	+2.35	+2.35	+2.30	+2.20	+2.70	+2.20	+2.80	+2.70	+2.40	+1.90	+2.20	+2.40	+2.80
			H	+2.05	+1.85	+2.55	+2.20	+2.40	+2.65	+2.65	+2.60	+2.85	+1.80	+2.70	+2.70	+2.20	+2.30	+2.00	+2.60	+2.85
5-----	6.5	16.5	A	+1.25	+1.15	+1.75	+2.10	+1.80	+1.90	+2.35	+1.90	+2.00	+1.00	+1.80	+2.00	+1.30	+1.40	+1.50	+2.00	+1.90
			B	+1.05	+1.15	+1.75	+2.00	+1.85	+2.00	+1.90	+1.90	+1.85	+1.20	+1.70	+1.80	+1.45	+1.50	+1.60	+1.95	+1.80
			C	+1.65	+1.15	+1.55	+1.50	+2.00	+2.00	+1.80	+2.15	+2.10	+1.80	+2.10	+1.80	+1.75	+1.80	+1.70	+2.00	+2.05
			D	+1.80	+1.35	+2.10	+1.50	+2.00	+2.30	+1.95	+1.55	+1.60	+2.10	+2.55	+2.25	+1.50	+1.30	+0.60	+1.80	+1.75
			E	+1.10	+1.45	+2.20	+2.50	+2.15	+2.30	+1.95	+1.90	+2.10	+2.40	+2.65	+2.40	+1.25	+1.85	+1.20	+2.00	+1.90
			F	+1.70	+1.45	+2.15	+2.30	+1.90	+2.05	+2.00	+2.05	+2.55	+1.80	+2.50	+2.40	+2.00	+1.60	+1.50	+1.75	+2.60
			G	+1.30	+1.25	+1.95	+1.90	+1.80	+1.80	+1.80	+1.65	+2.10	+1.60	+2.15	+1.85	+1.90	+1.40	+1.30	+1.70	+2.15
			H	+1.10	+1.10	+1.65	+2.10	+1.65	+1.70	+1.85	+1.55	+1.85	+1.15	+1.80	+1.75	+1.50	+1.20	+1.20	+1.60	+1.85
7-----	11.0	23.5	A	+1.20	+1.40	+1.95	+2.10	+1.75	+1.80	+1.05	+1.65	+1.75	+1.15	+1.50	+1.80	+1.60	+1.50	+1.50	+1.85	+1.65
			B	+1.10	+1.35	+1.80	+1.65	+1.70	+1.75	+1.90	+1.65	+1.70	+1.75	+1.50	+1.70	+1.50	+1.70	+1.50	+1.75	+1.55
			C	+1.10	+1.30	+1.90	+1.75	+1.80	+1.80	+1.65	+1.80	+1.80	+1.70	+1.80	+1.80	+1.70	+1.90	+1.65	+1.10	+1.70
			D	+1.75	+1.45	+1.10	+1.75	+1.50	+1.85	+1.80	+1.50	+1.80	+1.30	+1.85	+1.00	+1.60	+1.60	+1.00	+1.05	+1.65
			E	+1.80	+1.75	+1.20	+2.10	+1.00	+1.05	+1.85	+1.05	+1.15	+1.90	+1.45	+1.35	+1.25	+1.90	+1.60	+1.90	+1.80
			F	+1.90	+1.40	+1.95	+2.30	+1.50	+1.50	+1.65	+1.60	+1.75	+1.45	+1.80	+1.85	+1.75	+1.45	+1.35	+1.45	+1.75
			G	+1.40	+1.45	+1.00	+1.80	+1.65	+1.60	+1.70	+1.65	+1.80	+1.35	+1.65	+1.90	+1.70	+1.50	+1.30	+1.60	+1.80
			H	+1.05	+1.45	+1.00	+1.50	+1.65	+1.70	+1.00	+1.55	+1.80	+1.25	+1.60	+1.65	+1.75	+1.40	+1.45	+1.50	+1.65
10-----	18.3	31.2	A	+1.75	+1.70	+1.50	+1.70	+1.60	+1.65	+1.70	+1.60	+1.60	+1.00	+1.10	+1.90	+1.45	+1.60	+1.40	+1.10	+1.95
			B	+1.00	+1.50	+1.40	+1.40	+1.50	+1.70	+1.40	+1.60	+1.15	+1.30	+1.80	+1.00	+1.50	+1.60	+1.50	+1.20	+1.10
			C	+1.15	+1.95	+1.40	+1.50	+1.50	+1.60	+1.50	+1.60	+1.60	+1.00	+1.70	+1.10	+1.50	+1.50	+1.40	+1.85	+1.90
			D	+1.65	+1.70	+1.30	+1.40	+1.70	+1.65	+1.35	+1.70	+1.75	+1.00	+1.55	+1.50	+1.35	+1.65	+1.55	+1.70	+1.75
			E	+1.65	+1.75	+1.45	+1.70	+1.90	+1.70	+1.70	+1.05	+1.10	+1.70	+1.80	+1.90	+1.65	+1.10	+1.00	+1.10	+1.10
			F	+1.50	+1.75	+1.25	+1.70	+1.60	+1.75	+1.60	+1.70	+1.10	+1.00	+1.00	+1.90	+1.65	+1.80	+1.10	+1.25	+1.00
			G	+1.10	+1.90	+1.60	+1.00	+1.20	+1.10	+1.00	+1.10	+1.45	+1.25	+1.20	+1.10	+1.55	+1.70	+1.40	+1.25	+1.30
			H	+1.25	+1.50	+1.40	+1.70	+1.80	+1.85	+1.70	+1.60	+1.75	+1.90	+1.10	+1.80	+1.50	+1.75	+1.00	+1.90	+1.90
12-----	23.5	34.7	A	+1.00	+1.55	+1.30	+1.80	+1.75	+1.70	+1.25	+1.75	+1.00	+1.50	+1.00	+1.60	+1.45	+1.50	+1.60	+1.55	+1.00
			B	+1.15	+1.80	+1.45	+1.80	+1.85	+1.75	+1.60	+1.80	+1.05	+1.40	+1.05	+1.90	+1.55	+1.65	+1.70	+1.55	+1.10
			C	+1.40	+1.60	+1.45	+1.00	+1.80	+1.85	+1.50	+1.95	+1.90	+1.30	+1.00	+1.00	+1.65	+1.85	+1.60	+1.70	+1.00
			D	+1.50	+1.65	+1.35	+1.10	+1.80	+1.75	+1.80	+1.35	+1.90	+1.00	+1.80	+1.40	+1.10	+1.40	+1.50	+1.30	+1.30
			E	+1.90	+1.55	+1.15	+1.00	+1.80	+1.70	+1.70	+1.60	+1.90	+1.00	+1.50	+1.35	+1.15	+1.50	+1.70	+1.50	+1.65
			F	+1.00	+1.80	+1.45	+1.70	+1.90	+1.15	+1.90	+1.90	+1.10	+1.20	+1.10	+1.80	+1.45	+1.85	+1.90	+1.00	+1.00
			G	+1.20	+1.75	+1.45	+1.70	+1.10	+1.00	+1.90	+1.20	+1.40	+1.60	+1.20	+1.00	+1.75	+1.85	+1.00	+1.95	+1.60
			H	+1.30	+1.70	+1.35	+1.60	+1.10	+1.00	+1.80	+1.95	+1.00	+1.30	+1.05	+1.80	+1.60	+1.85	+1.10	+1.90	+1.00
13½----	27.3	36.5	A	+1.00	+1.55	+1.25	+1.85	+1.85	+1.80	+1.00	+1.70	+1.80	+1.40	+1.95	+1.60	+1.30	+1.60	+1.70	+1.50	+1.90
			B	+1.20	+1.70	+1.35	+1.90	+1.90	+1.70	+1.60	+1.80	+1.00	+1.30	+1.95	+1.80	+1.25	+1.60	+1.80	+1.60	+1.05
			C	+1.70	+1.05	+1.50	+1.90	+1.85	+1.90	+1.40	+1.05	+1.90	+1.60	+1.20	+1.00	+1.65	+1.95	+1.90	+1.65	+1.10
			D	+1.40	+1.75	+1.50	+1.50	+1.00	+1.95	+1.75	+1.50	+1.90	+1.10	+1.95	+1.40	+1.50	+1.30	+1.60	+1.60	+1.50
			E	+1.00	+1.75	+1.50	+1.00	+1.00	+1.10	+1.95	+1.65	+1.90	+1.30	+1.95	+1.40	+1.40	+1.60	+1.85	+1.60	+1.70
			F	+1.15	+1.80	+1.45	+1.70	+1.00	+1.30	+1.80	+1.00	+1.10	+1.35	+1.10	+1.80	+1.30	+1.75	+1.85	+1.80	+1.05
			G	+1.30	+1.75	+1.45	+1.60	+1.15	+1.25	+1.90	+1.00	+1.20	+1.80	+1.20	+1.90	+1.40	+1.90	+1.85	+1.80	+1.10
			H	+1.10	+1.75	+1.40	+1.70	+1.90	+1.00	+1.70	+1.90	+1.05	+1.35	+1.05	+1.80	+1.30	+1.60	+1.90	+1.60	+1.00
17-----	37.4	39.9	A	+1.00	+1.80	+1.45	+1.40	+1.90	+1.10	+1.80	+1.70	+1.00	+1.00	+1.00	+1.80	+1.30	+1.70	+1.00	+1.65	+1.05
			B	+1.10	+1.80	+1.45	+1.40	+1.00	+1.90	+1.80	+1.75	+1.95	+1.00	+1.00	+1.75	+1.25	+1.65	+1.00	+1.70	+1.00
			C	+1.40	+1.05	+1.75	+1.35	+1.25	+1.35	+1.00	+1.10	+1.30	+1.30	+1.30	+1.10	+1.55	+1.90	+1.95	+1.90	+1.05
			D	+1.50	+1.00	+1.60	+1.35	+1.90	+1.90	+1.65	+1.80	+1.00	+1.80	+1.00	+1.50	+1.40	+1.50	+1.75	+1.75	+1.90
			E	+1.90	+1.75	+1.40	+1.75	+1.40	+1.10	+1.80	+1.20	+1.45	+1.95	+1.35	+1.15	+1.80	+1.90	+1.80	+1.10	+1.90
			F	+1.00	+1.90	+1.60	+1.50	+1.15	+1.30	+1.55	+1.90	+1.00	+1.70	+1.10	+1.90	+1.45	+1.55	+1.00	+1.55	+1.10
			G	+1.05	+1.95	+1.70	+1.40	+1.25	+1.15	+1.10	+1.00	+1.15	+1.55	+1.30	+1.10	+1.50	+1.05	+1.90	+1.85	+1.20
			H	+1.00	+1.90	+1.65	+1.40	+1.10	+1.10	+1.00	+1.65	+1.00	+1.10	+1.10	+1.10	+1.70	+1.25	+1.50	+1.80	+1.55

TABLE VI—Continued
 PRESSURE DISTRIBUTION ON THE ENVELOPE—Continued
 Pressure lb./sq. ft.

Station No.	Distance to nose, ft.	Diameter, ft.	Pad	Run No. 1	Run No. 2	Run No. 4	Run No. 5	Run No. 9a	Run No. 9b	Run No. 13	Run No. 17a	Run No. 17b	Run No. 21	Run No. 23	Run No. 25	Run No. 27a	Run No. 27b	Run No. 27c	Run No. 27d	Run No. 28
17-----	37.4	39.9	A'	-0.75	-0.55	-0.40	-0.40	-0.80	-0.90	-0.70	-0.65	-0.80	-0.90	-0.90	-0.80	-0.15	-0.40	-0.75	-0.75	-0.95
			B'	-0.70	-0.75	-0.60	-0.35	-1.00	-1.00	-0.65	-0.80	-1.10	-1.15	-1.00	-0.80	-0.20	-0.50	-0.90	-0.90	-0.90
			C'	-0.70	-0.75	-0.50	-0.25	-0.85	-1.10	-0.90	-0.85	-1.20	-1.05	-1.00	-0.80	-0.30	-0.50	-0.90	-0.90	-0.95
			D'	-0.60	-0.83	-0.60	-0.40	-1.00	-1.20	-0.90	-1.05	-1.20	-1.05	-0.95	-0.80	-0.20	-0.55	-0.70	-0.95	-0.90
			E'	-0.70	-0.80	-0.65	-0.50	-1.30	-1.10	-0.65	-1.15	-1.30	-1.85	-1.10	-1.10	-0.70	-0.80	-0.95	-0.90	-0.75
			F'	-1.00	-0.60	-0.45	-1.20	-1.30	-1.40	-0.60	-0.95	-1.10	-1.70	-1.25	-1.15	-0.50	-1.00	-0.90	-0.70	-1.30
			G'	-0.65	-0.85	-0.70	-0.45	-1.10	-1.05	-1.20	-0.95	-1.25	-1.30	-1.10	-0.95	-0.30	-0.60	-1.00	-0.85	-1.15
			H'	-0.90	-0.50	-0.40	-0.40	-0.90	-0.75	-0.65	-0.60	-0.95	-1.20	-0.80	-0.85	0.00	-0.50	-0.65	-0.55	-0.80
20-----	46.3	41.3	A	-0.80	-0.60	-0.25	-0.50	-0.75	-0.65	-0.70	-0.65	-0.90	-0.70	-0.80	-0.80	-0.70	-0.40	-0.65	-0.80	-0.95
			B	-0.85	-0.60	-0.45	-0.60	-0.80	-0.90	-0.90	-0.80	-1.20	-0.95	-0.85	-0.95	-0.40	-0.80	-0.95	-0.85	-1.05
			C	-0.95	-0.60	-0.40	-0.50	-0.60	-1.10	-0.90	-0.70	-1.00	-1.00	-0.90	-1.00	-0.90	-0.60	-0.80	-0.70	-1.00
			D	-0.55	-0.45	-0.15	-0.30	-0.30	-0.40	-0.20	-0.40	-0.65	-0.45	-0.25	-0.25	-0.20	-0.10	-0.45	-0.55	-0.40
			E	-0.80	-0.75	-0.50	-0.40	-0.65	-0.70	-0.75	-0.65	-0.85	-0.60	-0.80	-0.45	-0.30	-0.60	-0.70	-0.70	-0.65
			F	-0.75	-0.70	-0.50	-0.50	-0.90	-1.00	-1.00	-0.90	-1.00	-1.10	-0.90	-0.75	-0.50	-0.70	-0.80	-0.55	-1.00
			G	-0.75	-0.60	-0.35	-0.50	-0.60	-0.70	-0.90	-0.40	-1.00	-0.90	-0.70	-0.75	-0.20	-0.40	-0.75	-0.75	-0.75
			H	-0.75	-0.55	-0.35	-0.40	-0.65	-1.00	-0.90	-0.60	-0.90	-1.00	-0.85	-0.60	-0.30	-0.45	-0.65	-0.55	-0.70
26-----	63.7	42.0	A	-0.70	-0.75	-0.15	-0.20	-0.55	-0.15	-0.20	-0.35	-0.60	-0.65	-0.30	-0.20	-0.25	-0.40	-0.55	-0.30	-0.40
			B	-0.80	-0.70	-0.15	-0.25	-0.50	-0.35	-0.40	-0.50	-0.60	-0.55	-0.50	-0.50	0.00	-0.30	-0.55	-0.50	-0.60
			C	+0.15	-0.20	+0.25	+0.35	+0.20	+0.30	0.00	+0.15	+0.15	-0.85	+0.30	+0.20	+0.35	+0.25	0.00	+0.20	-0.50
			D	-0.40	-0.60	+0.15	-0.30	-0.40	-0.40	-0.10	-0.40	-0.40	-0.50	-0.40	-0.15	-0.20	-0.30	-0.50	-0.40	-0.35
			E	-0.60	-0.95	-0.15	-0.40	-0.50	-0.35	-0.10	-0.40	-0.75	-1.00	-0.55	-0.30	-0.20	-0.60	-0.35	-0.45	-0.45
			F	-0.65	-0.90	-0.05	-0.35	-0.55	-0.10	-0.20	-0.50	-0.75	-0.95	-0.60	-0.45	-0.10	-0.10	-0.60	-0.20	-0.65
			G	-0.40	-0.45	+0.05	-0.30	-0.60	-0.10	-0.30	-0.20	-0.60	-0.50	-0.30	-0.20	+0.10	+0.05	-0.30	-0.10	-0.40
			H	-0.60	-0.75	-0.20	-0.65	-0.70	-0.40	-0.60	-0.45	-0.70	-0.90	-0.50	-0.40	-0.30	-0.35	-0.50	-0.40	-0.50
40-----	104.2	39.7	A	-0.40	-0.30	+0.05	-0.45	+0.10	+0.15	-0.10	+0.10	-0.15	+0.05	+0.10	-0.05	+0.15	+0.10	-0.20	-0.05	-0.05
			B	-0.55	-0.25	+0.15	+0.05	-0.30	-0.15	-0.10	-0.20	-0.20	-0.30	-0.15	-0.10	0.60	-0.10	-0.40	-0.10	-0.25
			C	-0.60	-0.35	+0.15	-0.10	-0.25	0.00	-0.15	-0.20	-0.20	-0.50	-0.35	-0.10	0.00	-0.30	-0.45	-0.35	-0.30
			D	-0.60	-0.40	+0.15	-0.40	-0.30	0.00	0.00	-0.25	-0.20	-0.70	-0.30	-0.15	-0.15	-0.25	-0.40	-0.25	-0.35
			E	-0.50	-0.40	0.00	-0.60	-0.30	-0.35	-0.10	-0.20	-0.60	-0.60	-0.30	-0.40	-0.10	-0.20	-0.50	-0.30	-0.30
			F	-0.60	-0.40	+0.05	-0.25	-0.10	-0.20	-0.10	-0.15	-0.60	-0.25	-0.30	-0.20	0.00	-0.10	-0.30	+0.05	-0.10
			G	-0.85	-0.25	+0.05	-0.20	-0.20	-0.20	-0.20	-0.10	-0.10	-0.75	-0.20	-0.35	0.00	-0.05	-0.45	+0.05	-0.45
			H	-0.55	-0.40	+0.05	-0.40	-0.25	-0.15	-0.25	-0.10	-0.30	-0.40	-0.20	-0.25	+0.20	+0.10	-0.40	-0.15	-0.20
49-----	130.0	35.7	A	-0.50	-0.20	+0.15	-0.30	-0.10	0.00	0.00	+0.10	0.00	-0.10	+0.10	-0.05	+0.10	+0.10	-0.25	0.00	+0.05
			B	-0.45	-0.15	+0.20	+0.10	0.00	+0.10	-0.10	0.00	0.00	-0.15	0.00	-0.05	0.00	0.00	-0.25	0.00	0.00
			C	-0.45	-0.15	+0.40	+0.05	-0.05	+0.40	-0.05	-0.05	0.00	-0.25	0.00	0.00	0.00	-0.05	-0.15	-0.05	0.00
			D	-0.60	-0.35	+0.15	-0.30	-0.25	0.00	-0.10	-0.20	-0.15	-0.60	-0.30	-0.30	-0.20	-0.20	-0.30	-0.20	-0.30
			E	-0.50	-0.40	-0.05	-0.85	-0.30	-0.40	+0.20	-0.05	-0.40	-0.80	-0.25	-0.30	-0.10	-0.10	-0.50	-0.20	-0.25
			F	-0.50	-0.40	-0.35	-0.45	-0.25	-0.50	-0.40	-0.20	-0.45	-0.70	-0.25	-0.50	-0.05	-0.30	-0.50	-0.30	-0.30
			G	-0.45	-0.40	+0.05	-0.30	0.00	-0.05	-0.05	0.00	-0.25	-0.55	-0.05	-0.20	+0.35	+0.15	-0.25	-0.10	-0.20
			H	-0.40	-0.25	+0.05	-0.30	+0.10	+0.05	0.00	+0.20	-0.10	-0.10	+0.10	0.00	+0.30	+0.20	-0.15	0.00	0.00
49-----	130.0	35.7	A'	-0.40	-0.20	+0.05	-0.25	+0.15	0.00	-0.20	+0.05	-0.30	0.00	+0.25	-0.20	+0.10	-0.20	-0.30	-0.20	-0.15
			B'	-0.45	-0.20	+0.15	0.00	0.00	0.00	-0.10	-0.20	-0.05	-0.15	0.00	-0.20	-0.15	0.00	-0.60	-0.40	0.00
			C'	-0.65	-0.35	-0.05	-0.20	-0.65	-0.25	-0.25	-0.60	-0.65	-0.55	-0.40	-0.50	-0.50	-0.70	-0.75	-0.60	-0.30
			D'	-0.45	-0.30	-0.10	-0.40	-0.20	0.00	+0.30	-0.15	+0.10	-0.60	-0.15	-0.15	-0.30	-0.20	-0.20	-0.15	0.00
			E'	-0.25	-0.45	-0.65	-0.85	-0.40	-0.60	-0.50	-0.25	-0.70	-0.80	-0.35	-0.40	-0.25	-0.30	-0.70	-0.40	-0.30
			F'	-0.15	-0.40	-0.30	-0.40	-0.50	-0.40	-0.35	0.00	-0.45	-0.80	-0.10	-0.30	+0.25	+0.20	-0.50	-0.10	-0.30
			G'	-0.20	-0.20	+0.05	-0.30	-0.20	0.00	-0.10	+0.20	-0.10	-0.40	+0.20	-0.10	+0.30	+0.20	-0.20	0.00	0.00
			H'	-0.30	-0.20	-0.15	-0.40	-0.15	-0.20	-0.30	+0.15	-0.15	-0.10	+0.15	-0.15	0.00	+0.15	-0.60	0.00	-0.10
53-----	141.2	33.0	A	-0.25	-0.10	+0.15	-0.30	+0.15	+0.20	+0.20	+0.30	+0.15	+0.15	+0.25	+0.05	+0.20	+0.15	-0.05	+0.05	+0.40
			B	-0.25	-0.15	+0.20	-0.10	+0.15	+0.30	+0.20	+0.35	+0.25	0.00	+0.10	+0.15	+0.15	+0.20	0.00	+0.20	+0.30
			C	-0.50	-0.15	+0.25	-0.10	0.00	+0.40	+0.10	-0.10	-0.10	-0.60	-0.50	-0.15	+0.10	0.00	-0.35	-0.15	-0.20
			D	-0.90	-0.50	0.00	-0.60	-0.20	0.00	-0.20	0.00	0.00	-0.60	-0.30	-0.30	-0.25	0.00	-0.30	-0.20	-0.20
			E	-0.70	-0.55	-0.25	-0.90	-0.15	-0.15	+0.30	0.00	+0.15	-0.80	-0.30	0.00	-0.25	-0.10	-0.10	-0.10	0.00
			F	-0.40	-0.45	-0.20	-0.80	-0.20	-0.45	-0.40	+0.20	-0.30	-0.85	-0.25	-0.40	-0.15	-0.50	-0.40	-0.35	+0.30
			G	-0.25	-0.20	0.00	-0.50	-0.10	-0.15	-0.35	+0.25	0.00	-1.00	0.00	0.00	+0.25	+0.30	0.00	+0.10	+0.20
			H	-0.30	-0.15	+0.15	-0.45	+0.05	-0.10	-0.10	+0.30	0.00	-0.10	0.00	-0.05	+0.15	+0.20	-0.20	0.00	+0.10
57-----	152.5	30.0	A _s	-0.60	-0.45	-1.35	-1.00	-0.15	-1.15	0.00	+0.15	-0.15	-0.30	-0.10	-0.20	+0.55	+0.30	-0.30	-0.55	0.00
			A _p	0.00	+0.25	+0.65	+0.70	-0.10	+0.70	-0.50	0.00	-0.15	-0.30	0.00	-0.10	-1.05	-0.60	-0.35	+0.45	0.00
			B	-0.35	-0.35	-0.05	-0.40	-0.10	-0.10	-0.10	+0.10	0.00	-0.35	-0.05	-0.10	+0.15	0.00	-0.25	0.00	+0.05
			C _L	-0.80	-0.35	+0.05	-0.15	-0.60	-0.10	-0.05	-0.05	-0.15	-1.30	-0.10	-0.55	-0.15	-0.20	-0.55	-0.35	-0.45
			C _U	-1.05	-0.15	0.00	0.00	-0.35	-0.25	-1.00	-1.30	-0.95	0.00	-0.10	-0.60	-1.05	-1.00	-1.60	-0.50	0.00
			D	-0.70	-0.40	+0.05	-0.50	-0.20	-0.20	-0.15	-0.10	+0.15	-0.60	-0.20	-0.20	-0.30	-0.20	-0.20	-0.20	-0.10
			E _s	-0.55	-0.95	-1.30	-2.55	-0.10	-1.15	+0.10	+0.30	+0.15	-0.55	-0.15	-0.10	+0.75	+0.40	-0.35	-0.75	0.00
			E _p	-0.25	+0.25	+1.20	+0.90	-0.40	+0.75	+0.40	-0.15	0.00	-1.25	-0.20	-0.20	-1.35	-0.85	-0.30	+0.65	+0.10
			F	-0.35	-0.55	-0.30	-0.75	-0.10	-0.40	-0.20	0.00	-0.30	-0.55	-0.20	-0.30	0.00	+0.05	-0.45	-0.10	-0.10
			G _L	-0.15	-0.25	+0.20	-0.40	-0.30	-0.30	-0.40	+0.45	+0.20	-1.00	-0.10	-0.40	+0.40	+0.05	-0.35	0.00	-0.40
			G _U	-0.75	-0.40	-0.40	-0.55	-0.50	-0.50	-0.90	-0.40	-1.15	-0.30	-0.10	-0.40	-0.20	-0.30	-0.30	0.00	0.00
			H	-0.20	0.0															

TABLE VI—Continued
PRESSURE DISTRIBUTION ON THE ENVELOPE—Continued

Pressure lb./sq. ft.

Station No.	Distance to nose, ft.	Diameter, ft.	Pad	Run No. 1	Run No. 2	Run No. 4	Run No. 5	Run No. 9a	Run No. 9b	Run No. 13	Run No. 17a	Run No. 17b	Run No. 21	Run No. 23	Run No. 25	Run No. 27a	Run No. 27b	Run No. 27c	Run No. 27d	Run No. 28
59-----	158.3	28.3	A _s	-0.55	-0.55	-0.80	-0.85	-0.15	-0.50	-0.35	+0.10	-0.30	-0.15	-0.25	+0.35	+0.10	-0.15	-0.20	+0.15	
			A _p	+0.20	+0.20	+0.50	+0.50	-0.20	+0.40	-0.30	+0.10	+0.05	-0.30	-0.00	+0.10	-0.50	-0.20	-0.40	+0.20	+0.15
			B	-0.40	-0.45	-0.10	-0.30	-0.15	+0.05	-0.40	0.00	0.00	-0.40	-0.25	-0.20	0.00	0.00	-0.30	0.00	+0.10
			C _L	-0.65	-0.40	-0.05	-0.40	-0.25	+0.35	-0.40	-0.30	-0.35	-0.60	-0.05	-0.50	-0.70	-0.35	-0.40	-0.40	-0.70
			C _U	-0.60	+0.15	+0.40	+0.25	-0.20	+0.30	-0.10	-0.30	-0.25	0.00	-0.15	-0.10	-0.50	-0.50	-0.30	-0.10	+0.25
			D	-0.60	-0.65	0.00	-0.50	-0.30	-0.20	-0.30	-0.55	0.00	-0.55	-0.10	-0.40	-0.35	-0.30	-0.45	-0.40	-0.25
			E _s	-0.70	-0.60	-0.55	-1.60	+0.05	-0.35	+0.20	-0.25	-0.15	-0.70	-0.40	+0.10	-0.35	-0.30	-0.10	-0.25	-0.30
			E _p	+0.05	+0.15	+0.35	+0.10	-0.35	+0.20	-0.25	+0.05	-0.40	-0.75	+0.10	-0.35	-0.30	-0.40	-0.50	0.00	-0.30
			F	-0.30	-0.45	0.00	-0.50	-0.20	-0.15	-0.30	+0.20	-0.15	-0.55	-0.15	-0.25	+0.05	+0.10	-0.30	+0.10	+0.05
			G _L	-0.25	-0.45	-0.05	-0.70	-0.20	-0.40	-1.00	+0.20	-0.10	-0.65	-0.25	-0.35	+0.25	+0.05	-0.40	-0.15	-0.25
			G _U	-0.30	0.00	+0.10	-0.20	-0.30	-0.20	-0.15	-0.15	-0.40	-0.60	-0.05	-0.30	-0.10	-0.10	-0.40	-0.20	+0.10
			H	-0.30	-0.25	+0.10	-0.60	-0.15	-0.15	-0.40	+0.10	-0.15	-0.40	0.00	-0.25	-0.05	-0.05	-0.40	-0.10	-0.20
62-----	166.7	25.4	A _s	-0.55	-0.40	-0.35	-0.30	-0.10	0.00	-0.50	+0.05	-0.30	-0.20	-0.10	-0.25	-0.10	+0.40	0.00	+0.10	+0.25
			A _p	+0.15	-0.05	+0.05	+0.20	-0.10	0.00	-0.30	+0.05	-0.10	-0.50	0.00	+0.15	0.00	-0.35	-0.50	-0.10	-0.20
			B	-0.50	-0.55	-0.20	-0.40	-0.15	+0.05	-0.40	-0.10	-0.25	-0.30	-0.15	-0.30	-0.30	-0.15	-0.30	-0.05	0.00
			C _L	-0.50	-0.35	+0.05	-0.25	-0.20	+0.35	-0.30	-0.30	-0.15	-0.40	-0.20	-0.35	0.00	-0.30	-0.55	-0.25	-0.20
			C _U	-0.60	0.00	+0.50	+0.25	-0.05	+0.50	0.00	+0.10	+0.20	-0.25	+0.15	-0.10	-0.40	-0.35	-0.20	0.00	-0.30
			D	-0.60	-0.85	-0.35	-0.50	-0.50	-0.55	-0.55	-0.50	-0.40	-0.55	0.00	-0.55	-0.20	-0.30	-0.60	-0.50	-0.50
			E _s	-0.40	-0.60	-0.45	-0.50	-0.40	-0.40	-0.40	-0.20	-0.20	-0.65	-0.20	-0.10	-0.10	-0.25	-0.35	-0.50	-0.25
			E _p	+0.25	+0.20	+0.25	-0.50	-0.20	+0.15	+0.15	+0.40	+0.10	-0.85	+0.05	0.00	0.00	0.00	-0.20	+0.30	0.00
			F	-0.45	-0.35	-0.15	-0.60	-0.10	-0.30	-0.30	+0.10	0.00	-0.75	-0.10	-0.40	-0.15	-0.20	-0.20	-0.15	-0.55
			G _L	-0.45	-0.65	-0.30	-1.00	-0.35	-0.60	-0.30	-0.20	-0.40	-0.70	-0.30	-0.40	0.00	-0.30	-0.65	-0.30	-0.40
			G _U	-0.60	-1.00	-0.80	0.00	-0.10	-0.50	-0.30	-0.20	-0.40	-0.70	-0.30	-0.30	0.00	-0.40	-0.20	-0.10	-0.50
			H	-0.70	-0.70	-0.55	-1.10	-0.40	-0.80	-0.60	-0.50	-0.50	-0.65	-0.40	-0.50	-0.40	-0.60	-1.00	-0.55	-0.60
65-----	175.2	21.7	A _s	-0.65	-0.20	+0.40	-1.45	+0.10	-0.70	0.00	-0.15	-0.30	-0.50	+0.10	0.00	-0.90	-0.50	-0.40	-0.30	+0.15
			A _p	-0.40	-0.70	-0.00	+1.55	-0.20	+0.35	-0.70	+0.40	-0.70	-1.20	+0.50	0.00	+0.90	+0.70	+0.30	+0.50	+0.05
			B	-0.35	-0.10	+0.25	0	+0.30	+0.50	+0.10	+0.05	-0.10	-0.10	+0.30	+0.25	-0.20	+0.20	+0.10	+0.20	+0.20
			C _L	-0.65	-0.15	+0.30	0	+0.10	+0.85	+0.15	-0.30	0.00	-0.40	+0.10	+0.05	-0.30	-0.10	0.00	+0.20	+0.45
			C _U	+0.05	0.00	+0.20	+0.20	+0.05	0.00	-0.35	-0.10	-0.10	-0.35	-0.10	-0.10	+0.45	+0.05	-0.40	-0.10	0.00
			D	0.00	+0.05	+0.20	-0.35	0.00	0.00	+0.20	0.00	0.00	-0.70	+0.20	-0.10	0.00	-0.40	-0.15	0.00	
			E _s	0.00	+0.20	+0.50	-0.30	0.00	+0.50	+0.65	+0.50	+0.30	-1.00	+0.45	+0.15	+0.20	+0.20	+0.05	+0.30	+0.25
			E _p	+0.45	+0.15	+0.30	-0.40	0.00	0.00	+0.85	+0.65	+0.65	-1.20	+0.45	+0.35	+0.40	+0.30	0.00	+0.50	+0.40
			F	-0.20	-0.05	+0.40	-0.35	0.00	0.00	+0.10	+0.35	+0.20	-0.80	+0.45	-0.10	+0.15	+0.20	-0.10	+0.15	-0.10
			G _L	-0.35	-0.35	-0.10	-0.75	-0.20	-0.35	+0.20	-0.15	-0.25	-0.80	0.00	-0.05	0.00	-0.10	-0.50	-0.30	-0.05
			G _U	-0.45	-0.15	-0.15	-0.65	-0.60	-0.20	-0.25	-0.35	-1.10	-0.90	-0.45	-0.50	0.00	-0.70	-0.50	-0.30	-0.40
			H	-0.15	-0.20	+0.10	-0.60	+0.15	-0.20	0.00	0.00	0.00	-0.80	+0.20	+0.15	0.00	-0.25	-0.40	-0.15	0.00
68-----	183.4	16.9	A	0.00	+0.15	+0.50	0	+0.65	+0.75	+0.60	+0.40	+0.35	0.00	+0.70	+0.40	+0.15	+0.55	+0.10	+0.40	+0.60
			B	+0.20	+0.25	+0.75	+0.10	+0.65	+0.90	+0.70	+0.50	+0.75	+0.20	+0.80	+0.70	+0.25	+0.45	+0.45	+0.50	+0.85
			C	+0.20	+0.30	+0.50	+0.10	+0.60	+1.30	+0.95	+0.25	+0.40	-0.15	+0.70	+0.50	+0.20	+0.20	-0.10	+0.10	+0.40
			D	+0.30	+0.30	+0.55	-0.10	+0.45	+0.50	+0.70	+0.30	+0.50	-0.30	+0.70	+0.50	+0.15	+0.15	-0.05	+0.15	+0.45
			E	+0.20	+0.35	+0.70	-0.10	+0.40	+0.50	+0.75	+0.70	+0.50	-0.60	+0.75	+0.45	+0.40	+0.30	+0.10	+0.40	+0.40
			F	+0.20	+0.35	+0.65	-0.10	+0.40	+0.40	+0.85	+0.60	+0.40	-0.30	+0.75	+0.40	+0.35	+0.30	-0.05	+0.35	+0.40
			G	+0.15	+0.05	+0.30	-0.35	+0.45	+0.10	+0.50	+0.25	+0.20	-0.15	+0.60	+0.45	+0.30	+0.20	-0.10	+0.10	+0.40
			H	+0.30	+0.25	+0.40	-0.35	+0.50	+0.25	+0.80	+0.30	+0.70	-0.10	+0.65	+0.50	+0.15	+0.10	-0.05	+0.15	+0.45
69½---	187.4	13.9	A	+0.25	+0.35	+0.80	+0.20	+0.70	+1.00	+0.90	+0.55	+0.70	+0.20	+0.90	+0.80	+0.25	+0.70	+0.40	+0.55	+1.15
			B	+0.25	+0.45	+0.75	+0.20	+0.70	+1.00	+1.00	+0.60	+0.85	+0.25	+0.90	+0.80	+0.20	+0.60	+0.50	+0.55	+1.05
			C	+0.50	+0.35	+0.55	+0.10	+0.60	+1.25	+1.00	+0.60	+0.85	+0.15	+0.85	+0.70	+0.25	+0.30	+0.20	+0.45	+0.80
			D	+0.50	+0.40	+0.80	+0.15	+0.55	+0.70	+0.75	+0.80	+0.70	+0.20	+1.00	+0.50	+0.25	+0.30	+0.20	+0.50	+0.90
			E	+0.45	+0.60	+0.90	+0.30	+0.80	+0.95	+0.70	+1.05	+0.85	+0.10	+1.05	+0.70	+0.50	+0.50	+0.30	+0.55	+0.80
			F	+0.40	+0.65	+1.00	0.00	+0.80	+0.75	+0.90	+0.85	+0.75	+0.10	+1.00	+0.70	+0.45	+0.40	+0.20	+0.60	+0.85
			G	+0.50	+0.40	+0.60	0.00	+0.60	+0.30	+1.00	+0.60	+0.70	+0.10	+0.75	+0.70	+0.25	+0.30	+0.20	+0.45	+0.80
			H	+0.50	+0.45	+0.80	-0.20	+0.70	+0.65	+1.30	+0.80	+1.00	-0.10	+0.95	+0.70	+0.25	+0.25	+0.20	+0.50	+0.90
71-----	191.2	10.0	A	+0.60	+0.65	+1.20	+0.30	+0.90	+1.25	+1.35	+1.00	+1.25	+0.25	+1.15	+1.00	+0.45	+0.75	+0.75	+0.85	+1.30
			B	+0.60	+0.55	+0.70	+0.25	+0.70	+1.05	+1.00	+0.75	+0.90	+0.30	+1.00	+0.90	+0.40	+0.65	+0.55	+0.60	+1.30
			C	+0.60	+0.60	+0.65	0.00	+0.70	+1.30	+1.05	+1.05	+0.95	+0.35	+1.00	+1.00	+0.50	+0.50	+0.35	+0.85	+1.20
			D	+0.50	+0.75	+1.00	+0.25	+0.75	+0.95	+1.05	+1.05	+0.95	+0.45	+1.10	+0.80	+0.50	+0.45	+0.35	+0.75	+1.20
			E	+0.70	+0.65	+1.15	+0.45	+1.00	+1.15	+1.00	+1.40	+0.90	+0.45	+1.35	+1.05	+0.70	+0.65	+0.50	+0.90	+1.25
			F	+0.60	+0.65	+1.15	+0.50	+0.85	+0.95	+0.90	+1.00	+1.00	+0.30	+1.10	+0.90	+0.50	+0.60	+0.40	+0.70	+1.30
			G	+0.65	+0.75	+1.20	+0.45	+0.90	+1.00	+1.10	+1.05	+1.00	+0.30	+1.10	+1.10	+0.50	+0.50	+0.35	+0.85	+1.20
			H	+0.50	+0.60	+1.20	+0.10	+0.75	+0.90	+1.35	+1.05	+1.20	+0.20	+1.00	+0.80	+0.50	+0.45	+0.40	+0.75	+1.20
72-----	193.5	6.8	A	+0.80	+0.75	+1.10	+0.30	+1.00	+1.30	+1.30	+1.25	+1.40	+0.25	+1.20	+1.00	+0.60	+0.85	+0.70	+0.95	+1.20
			B	+1.00	+0.75	+0.70	+0.30	+0.80	+1.10	+1.10	+0.70	+1.10	+0.35	+1.10	+1.00	+0.65	+0.70	+0.60	+0.65	+1.20
			C	+0.80	+0.80	+0.70	+0.25	+0.85	+1.30	+1.00	+1.10	+1.10	+0.40	+1.00	+1.10	+0.60	+0.70	+0.60	+0.70	+1.20
			D	+0.80	+0.75	+1.00	+0.40	+0.85	+1.15	+1.15	+1.20	+1.10	+0.65	+1.10	+0.95	+0.65	+0.65	+0.50	+0.90	+1.20
			E	+0.90	+0.70	+1.20	+0.50	+1.00	+1.20	+1.10	+1.50	+1.10	+0.60	+1.35	+1.20	+0.70	+0.75	+0.60	+0.95	+1.20
			F	+0.90	+0.80	+1.20	+0.60	+0.90	+1.00	+0.95	+1.00	+0.95	+0.40	+1.10	+1.00	+0.55	+0.70	+0.50	+0.80	+1.20
			G	+0.80	+0.85	+1.30	+0.65	+0.85	+1.15	+1.15	+1.25	+1.10	+0.50	+1.20	+1.10	+0.65	+0.			

TABLE VII

PRESSURE DISTRIBUTION ON THE ENVELOPE

TABLE OF RESULTANT VERTICAL AND HORIZONTAL LOADS AT EACH STATION

Number of station-----	3	4	5	7	10	12	13½	17	20	26	40
Diameter of envelope at station (ft.)-----	8.0	12.8	16.5	23.5	31.2	34.7	36.5	39.9	41.3	42.0	39.7
Distance of station from nose (ft.)-----	2.7	4.7	6.5	11.0	18.3	23.5	27.3	37.4	46.3	63.7	104.2
VERTICAL LOAD IN LB. PER FT. OF LENGTH											
Run No. 1-----	+3.20	0.00	-1.14	-13.40	-12.50	-12.15	-9.13	-9.17	-4.13	-6.30	+2.78
Run No. 2-----	-1.60	-2.05	-4.78	-3.06	-26.20	+6.69	+4.02	+2.00	+2.06	+3.78	+3.18
Run No. 4-----	-1.01	-1.02	-7.10	-3.78	-3.12	-1.74	+5.47	+4.40	+1.24	-6.30	+4.40
Run No. 5-----	-1.04	-.77	-.49	+.71	.00	-6.94	-9.14	+5.19	-4.13	-.84	+5.96
Run No. 9a-----	-.56	-1.28	-4.18	+.70	+3.12	-2.43	+4.37	+6.00	-4.55	-4.20	+3.17
Run No. 9b-----	-2.80	-2.56	-5.75	-1.17	-.93	+1.73	+10.60	+3.60	-6.19	-.84	+9.13
Run No. 13-----	+.96	.00	+.99	+4.94	-1.56	+12.10	+14.60	-7.98	-7.47	-11.35	-3.18
Run No. 17a-----	+1.28	-.64	-.83	-2.35	+6.86	-7.29	-2.92	+10.76	-1.24	.00	+5.16
Run No. 17b-----	+.32	-1.28	-2.97	-3.53	+.31	-1.74	+.73	+6.79	-8.26	.00	+9.93
Run No. 21-----	-3.84	-8.71	-16.17	-4.00	-6.24	-11.45	-3.65	+17.95	-6.61	+5.04	+11.90
Run No. 23-----	-4.56	-8.32	-13.20	-11.75	-4.72	-7.98	+.73	+4.79	-7.44	+3.78	+8.74
Run No. 25-----	-1.68	-4.73	-8.25	-8.24	-4.05	-8.67	-7.30	+3.99	-11.15	-2.94	+4.76
Run No. 27a-----	+.80	-.64	-2.64	+2.12	+2.18	-10.40	+4.38	+11.18	-7.02	-.42	+7.94
Run No. 27b-----	+1.28	+.64	-3.47	-2.82	+6.24	-3.12	-1.83	+1.19	-6.62	-6.30	+8.34
Run No. 27c-----	+2.40	+5.12	+5.45	+3.75	+10.30	-3.47	-1.10	-3.18	-6.20	+1.68	+2.80
Run No. 27d-----	+2.40	+2.31	.00	-2.35	-2.50	-2.43	+3.65	+6.75	-5.37	-3.36	+2.78
Run No. 28-----	-.32	-2.43	-4.10	-2.59	-.94	-13.30	-8.40	+.80	-9.10	-.84	+3.18
HORIZONTAL LOAD IN LB. PER FT. OF LENGTH											
Run No. 1-----	-.40	-5.76	-3.30	-6.10	+.62	+5.21	+2.92	+.80	-1.24	+8.40	+3.57
Run No. 2-----	-.48	-.25	-.83	-1.41	.00	+2.43	-2.19	-1.20	+2.89	+8.40	+.79
Run No. 4-----	-.64	-1.28	-1.98	-1.18	+1.56	.00	-.73	+1.99	+2.89	+6.30	+3.97
Run No. 5-----	-1.36	-3.84	-7.10	-11.75	+11.54	+10.41	+15.70	+2.39	.00	+15.10	+5.16
Run No. 9a-----	-.88	+2.43	+2.81	+1.64	+9.36	+7.30	+3.65	+4.80	+6.20	+16.40	+3.97
Run No. 9b-----	+1.84	+3.80	+4.12	+4.70	+7.80	+9.37	+12.20	+4.40	+4.13	+2.10	+9.13
Run No. 13-----	+.56	+2.18	-.16	+.94	+7.80	+5.90	+6.57	.00	+6.61	+5.88	+1.98
Run No. 17a-----	+1.68	+2.31	+1.98	+1.18	+5.30	+11.10	+6.90	-1.20	.00	+5.46	-5.16
Run No. 17b-----	-1.04	-4.22	-5.28	-.24	+8.42	+7.64	+6.95	-1.20	+.83	+16.80	+5.16
Run No. 21-----	-.88	+1.28	+2.97	+5.41	-1.56	+4.86	+6.21	+16.75	+11.56	+6.30	-1.19
Run No. 23-----	-1.44	+1.28	-.49	+.94	+13.10	+5.90	+3.29	+2.79	+6.20	+11.32	-1.59
Run No. 25-----	-.48	-1.02	-.82	+.71	+1.86	+3.47	+3.65	+4.79	-1.24	+8.40	+5.96
Run No. 27a-----	-1.44	-3.20	-3.80	-3.06	+3.78	+5.90	-5.11	.00	-1.65	+6.30	-4.76
Run No. 27b-----	-1.04	-.90	+2.15	+6.58	+5.30	+7.64	+4.75	+.79	+.83	+.42	-7.94
Run No. 27c-----	+.16	+.77	-.49	+.23	+18.70	+13.90	+3.65	.00	.00	+5.05	-1.59
Run No. 27d-----	.00	+.38	+3.96	+10.60	+7.80	+14.90	+4.02	-5.17	-3.31	.00	-8.34
Run No. 28-----	+.16	-4.73	-5.43	-2.35	+4.60	+13.85	+6.40	+2.00	.00	+1.68	-2.00

+ Indicates load acting from bottom to top for vertical loads.

+ Indicates load acting from starboard to port for horizontal loads.

TABLE VII—Continued
PRESSURE DISTRIBUTION ON THE ENVELOPE—Continued
TABLE OF RESULTANT VERTICAL AND HORIZONTAL LOADS AT EACH STATION

Number of station.....	49	53	57	59	62	65	68	69½	71	72
Diameter of envelope at station (ft.).....	35.7	33.0	30.0	28.3	25.4	21.7	16.9	13.9	10.0	6.8
Distance of station from nose (ft.).....	130.0	141.2	152.5	158.3	166.7	175.2	183.4	187.4	191.2	193.5
VERTICAL LOAD IN LB. PER FT. OF LENGTH										
Run No. 1.....	+2.85	+13.20	+6.00	+2.83	-2.29	-7.16	-1.02	-1.67	-0.30	-0.27
Run No. 2.....	+6.78	+12.20	+8.40	+4.25	-1.02	-6.73	-1.86	-1.95	-.80	+.20
Run No. 4.....	+7.50	+10.46	+2.70	-.56	-2.54	-3.25	-1.35	-1.67	-.70	-.68
Run No. 5.....	+12.86	+16.17	+12.00	+6.51	+.25	+3.69	+.85	-2.09	-1.80	-1.16
Run No. 9a.....	+9.64	+9.90	+2.70	+1.42	+2.03	+2.82	+3.04	-.28	-.90	-.34
Run No. 9b.....	+13.2	+10.90	+4.50	+2.83	+2.54	-.43	+2.70	+1.11	+.50	+.07
Run No. 13.....	+2.50	+6.60	-4.20	-4.80	-3.56	-9.35	-1.18	+4.03	+2.50	+1.22
Run No. 17a.....	+8.92	+8.25	+4.50	+6.23	-2.03	-4.78	-2.20	-3.48	-2.20	-1.36
Run No. 17b.....	+10.71	+5.94	.00	+1.42	-3.81	-9.33	+2.19	+1.11	+1.70	+1.22
Run No. 21.....	+20.70	+25.40	+11.70	+6.51	+6.35	+6.30	+6.25	-.14	-1.50	-1.40
Run No. 23.....	+12.12	+13.20	+5.40	+.28	-3.30	-2.17	-.17	-1.39	-1.30	-.20
Run No. 25.....	+12.10	+9.24	+3.30	+2.26	+1.27	+2.39	+1.35	+1.95	-.20	-.48
Run No. 27a.....	+8.92	+12.87	+7.50	+4.25	-3.05	-4.77	-2.03	-2.36	-1.20	.00
Run No. 27b.....	+10.71	+12.56	+5.40	+4.24	-.76	-2.82	+2.15	+1.67	+.50	+.136
Run No. 27c.....	+7.48	+6.30	+2.70	+8.50	-4.32	+.65	+2.37	+1.95	-1.50	+.48
Run No. 27d.....	+8.20	+9.90	+5.10	+3.40	+1.27	-1.74	+.84	-.28	-.50	-.34
Run No. 28.....	+10.71	+7.90	+3.60	+5.36	+5.08	+.86	+3.60	+2.50	+.20	.00
HORIZONTAL LOAD IN LB. PER FT. OF LENGTH										
Run No. 1.....	-1.79	-7.60	-9.60	-6.51	+.76	+.65	+.17	-.70	-.10	+.48
Run No. 2.....	+4.64	.00	-.90	-2.83	+3.05	+2.60	+1.69	-1.39	-.37	-.48
Run No. 4.....	+11.80	+5.61	+.60	-.28	+8.38	+7.80	+2.54	-1.39	-4.00	-3.30
Run No. 5.....	+10.71	+10.23	+5.70	+6.22	+10.92	+10.20	+5.07	+2.08	-1.80	-1.56
Run No. 9a.....	-1.79	+1.98	-2.40	-1.12	-1.00	+4.56	+2.03	-1.10	-1.10	-.14
Run No. 9b.....	+12.50	+16.50	+3.00	+7.66	+13.45	+10.20	+11.00	+5.70	+1.50	+.89
Run No. 13.....	+3.57	+6.93	+2.40	+2.83	+.76	+.87	+1.01	-2.08	-.90	-.48
Run No. 17a.....	-2.86	-5.61	-9.00	-10.75	-.76	-2.17	-.51	-1.11	-.80	-1.02
Run No. 17b.....	+7.86	+4.95	+2.70	+2.26	+2.03	+2.17	+2.07	-1.25	-1.00	+.14
Run No. 21.....	+4.29	+8.25	-1.80	+2.83	+8.13	+9.55	+1.69	+2.36	+1.00	+.25
Run No. 23.....	-1.07	.00	-1.50	-1.41	+5.59	+.43	+1.01	+.28	-.40	-.54
Run No. 25.....	+3.93	+1.65	-.30	-.85	+1.78	+2.60	+2.03	-.42	-.30	.00
Run No. 27a.....	-9.64	-2.64	-11.10	-9.90	-1.27	-1.73	-1.18	-1.25	-.30	+.07
Run No. 27b.....	-2.14	+1.98	-8.70	-6.52	+3.31	+3.91	+1.18	+1.11	+.10	+.07
Run No. 27c.....	+2.50	-.66	-6.00	.00	+2.79	+3.48	+2.88	+1.40	+.40	+.61
Run No. 27d.....	+1.79	+.99	-7.50	-4.80	+1.78	+2.82	+.84	-.28	-.40	-.34
Run No. 28.....	+2.50	-7.60	-1.20	-1.42	+7.10	+5.64	+2.54	+.97	.00	.00

+ Indicates load acting from bottom to top for vertical loads.
+ Indicates load acting from starboard to port for horizontal loads.

TABLE VIII
MOMENTS OF FORCES ON TAIL SURFACES ABOUT THE C. B.

Run No.	Moment of horizontal forces (lb. ft.)	Moment of vertical forces (lb. ft.)	Run No.	Moment of horizontal forces (lb. ft.)	Moment of vertical forces (lb. ft.)
1.....	-5,275	15,380	21.....	8,000	14,120
2.....	-22,589	-165	23.....	3,608	17,900
4.....	-37,200	-3,735	25.....	-2,670	4,240
5.....	-12,370	-2,365	27a.....	34,577	8,450
9a.....	12,640	6,020	27b.....	35,100	2,270
9b.....	2,940	5,058	27c.....	6,810	4,700
13.....	1,669	-10,642	27d.....	-17,848	-11,760
17a.....	-7,620	-5,624	28.....	-9,095	27,440
17b.....	8,700	-21,890			

- Indicates counterclockwise moment. Horizontal forces viewed from top; vertical forces viewed from port.

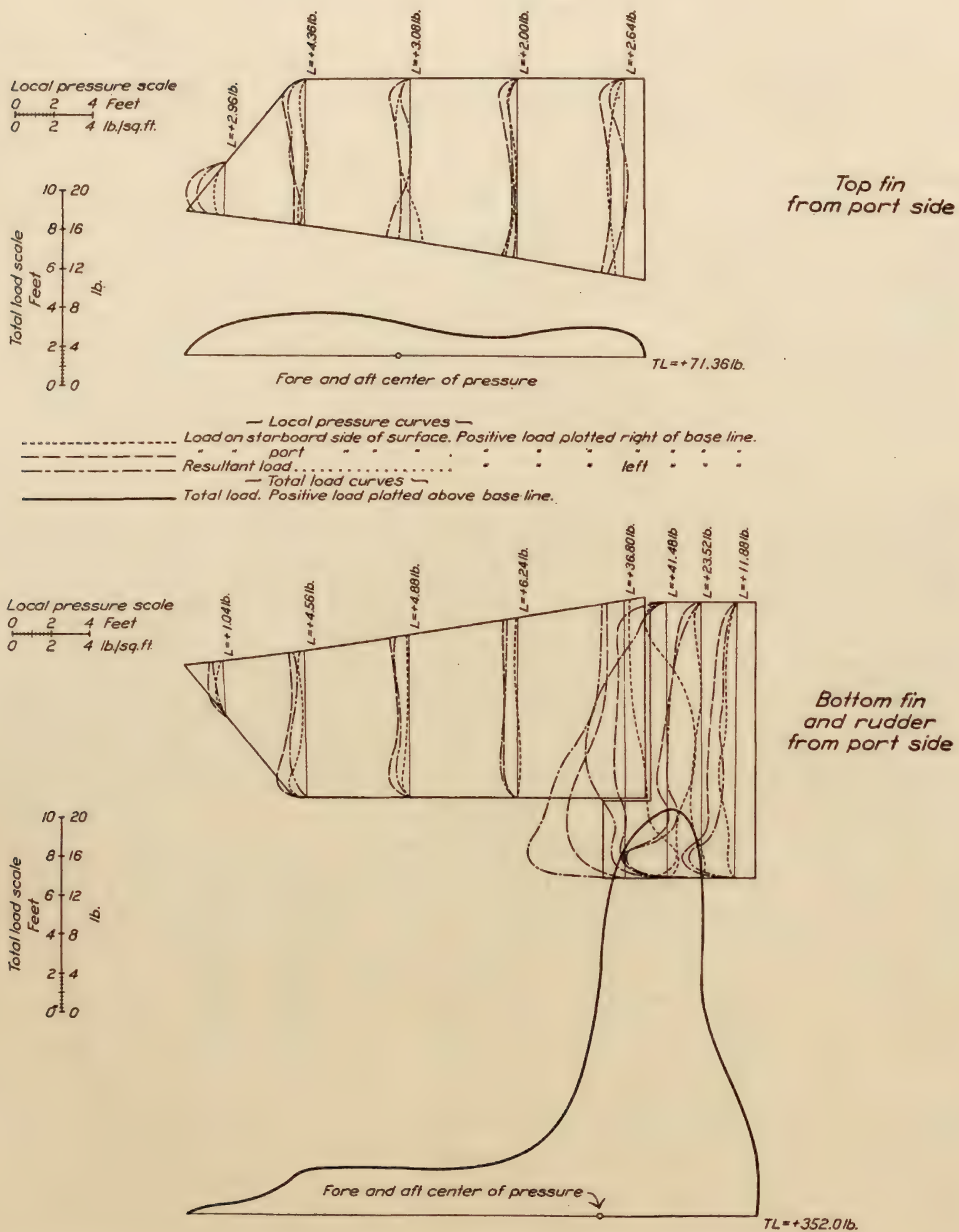


FIG. 9.—Tail surface load curves. Run No. 27b, reversal. Rudder angle 24° left to 18° right. 1,250 R. P. M. Positive loads are those acting from starboard to port

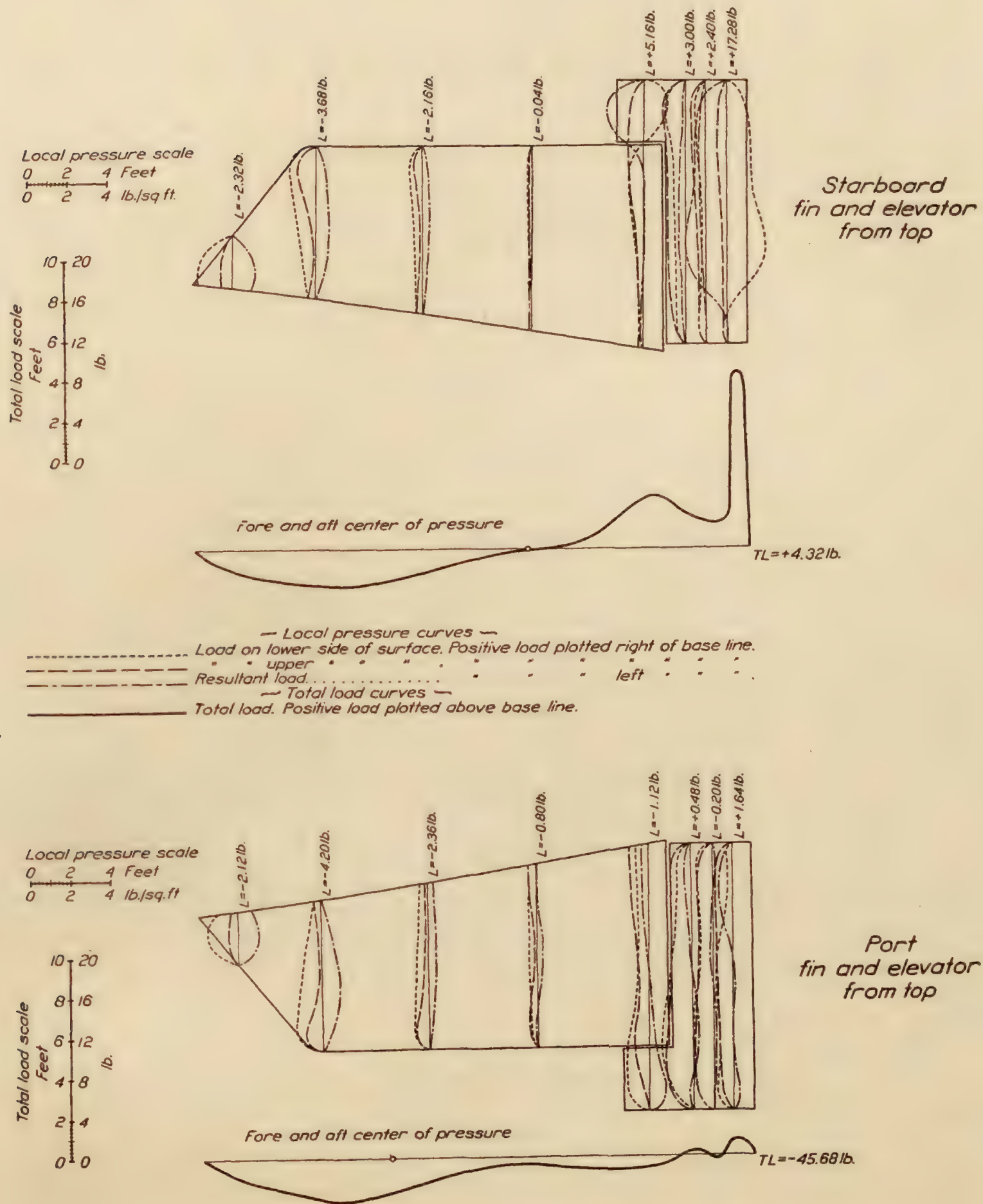


FIG. 10.—Tail surface load curves. Run No. 27b, reversal. Rudder angle 24° left to 18° right. 1,250 R. P. M. Positive loads are those acting from lower side to upper

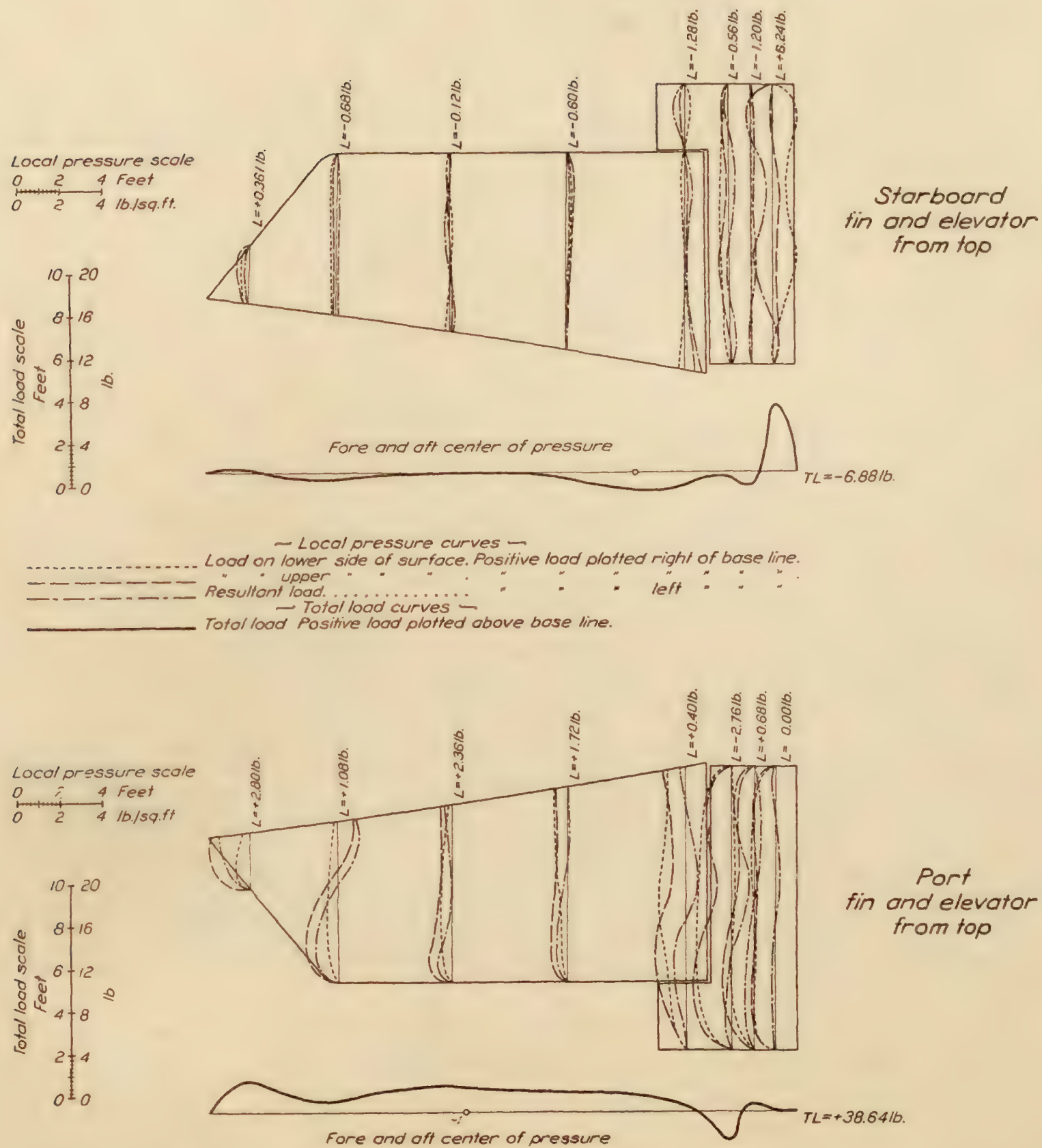


FIG. 12.—Tail surface load curves. Run No. 5, steady circle. Rudder angle 44° right. 1,250 R. P. M. Positive loads are those acting from lower side to upper

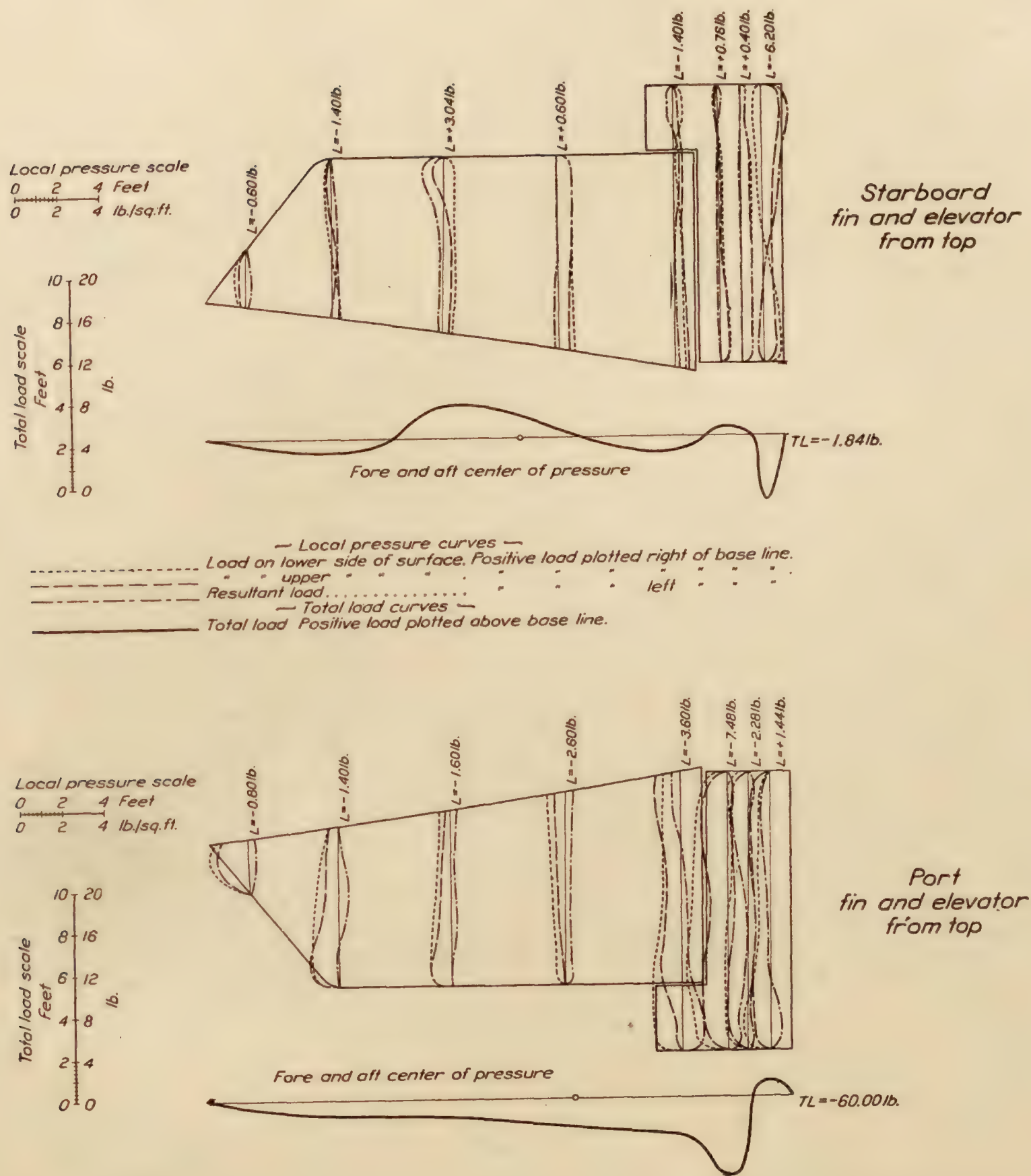


FIG. 14.—Tail surface load curves. Run No. 9b, start circle. Rudder angle 44° right. 1,250 R. P. M. Positive loads are those acting from lower side to upper

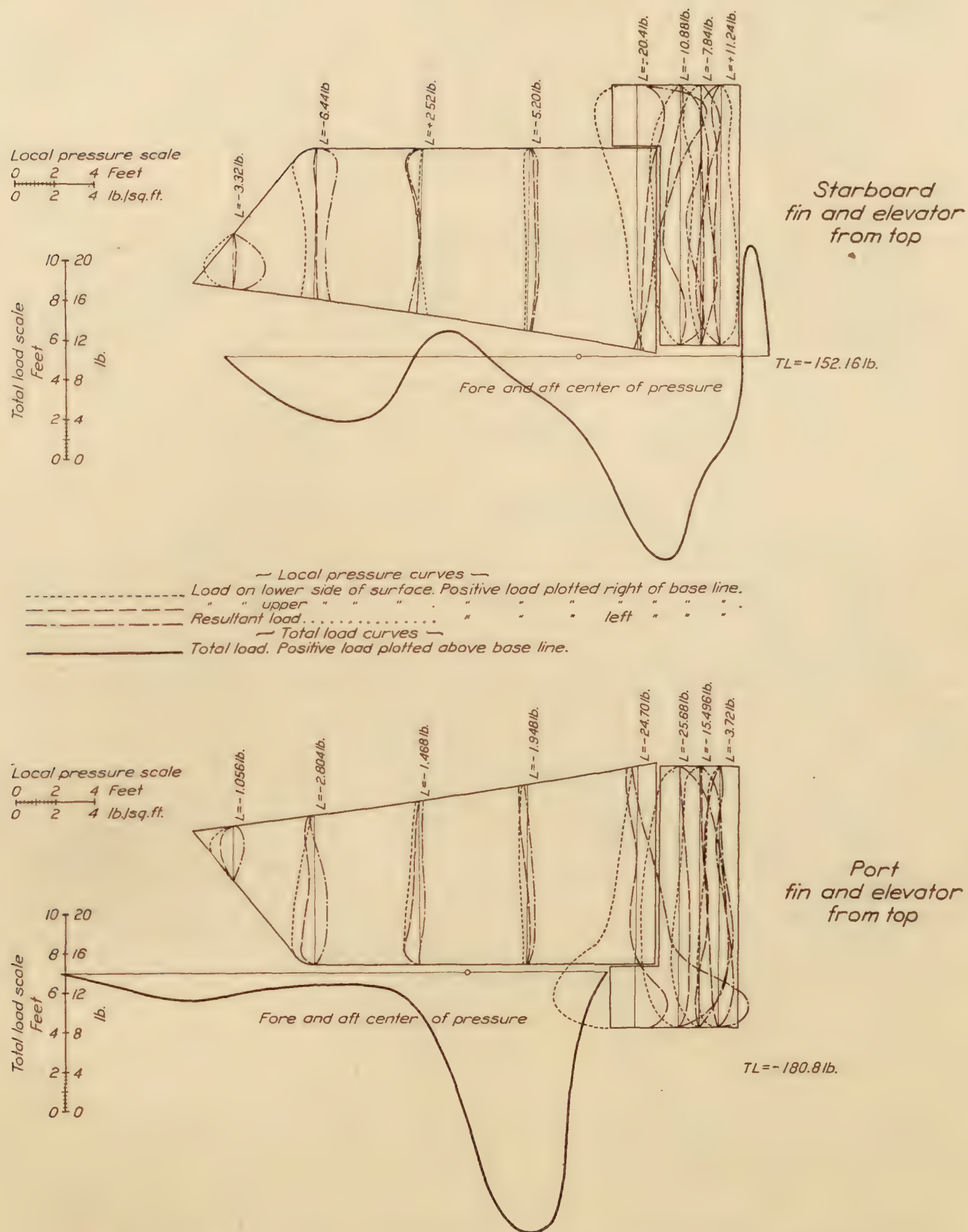
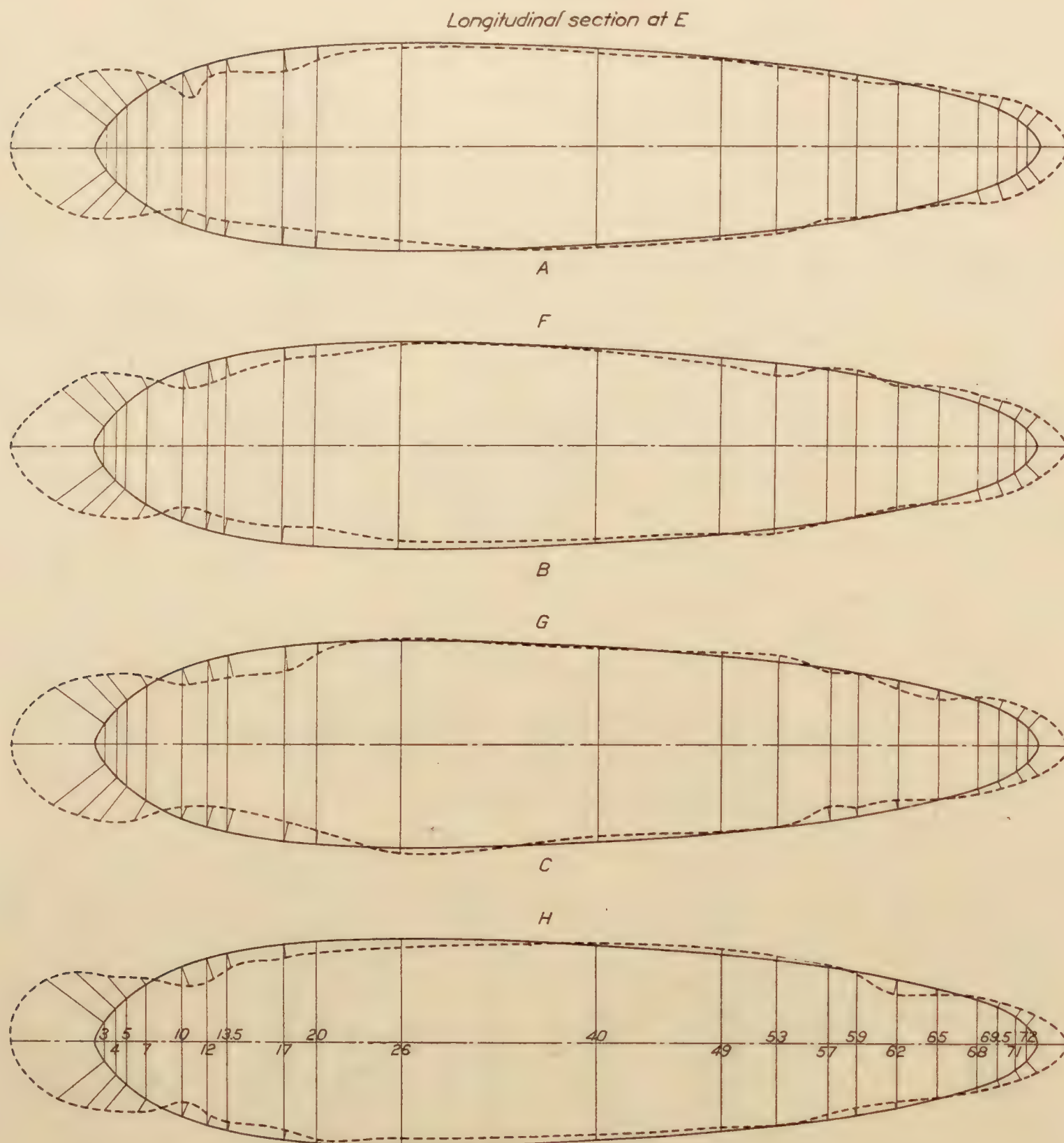


FIG. 16.—Tail surface load curves. Run No. 28, bump. 1,250 R. P. M. Positive loads are those acting from lower side to upper

348—26†——24



Longitudinal section at D
Positive pressure plotted outside, negative pressure inside, of contour.

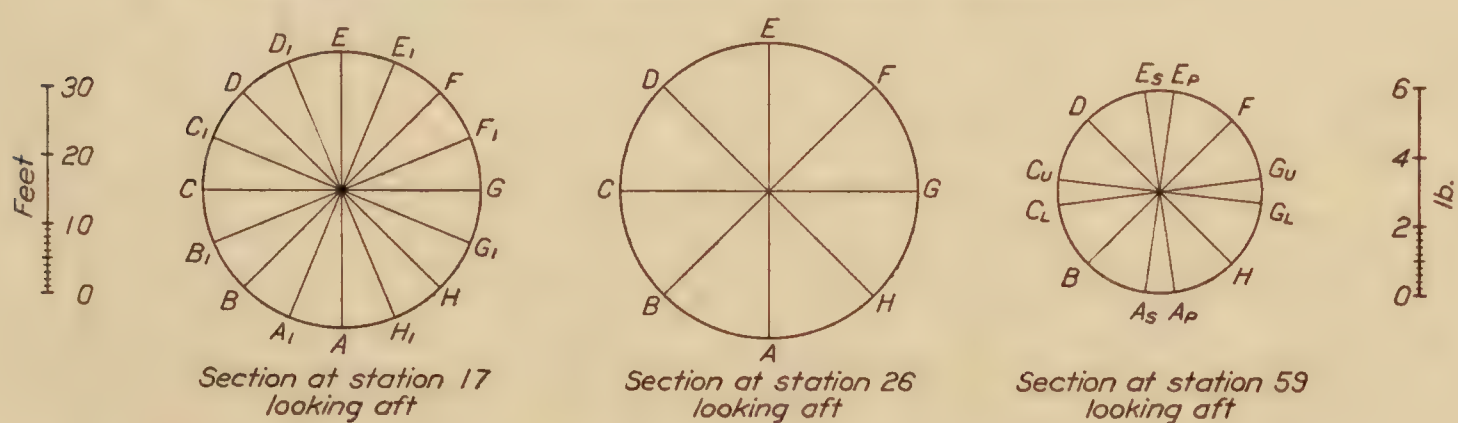
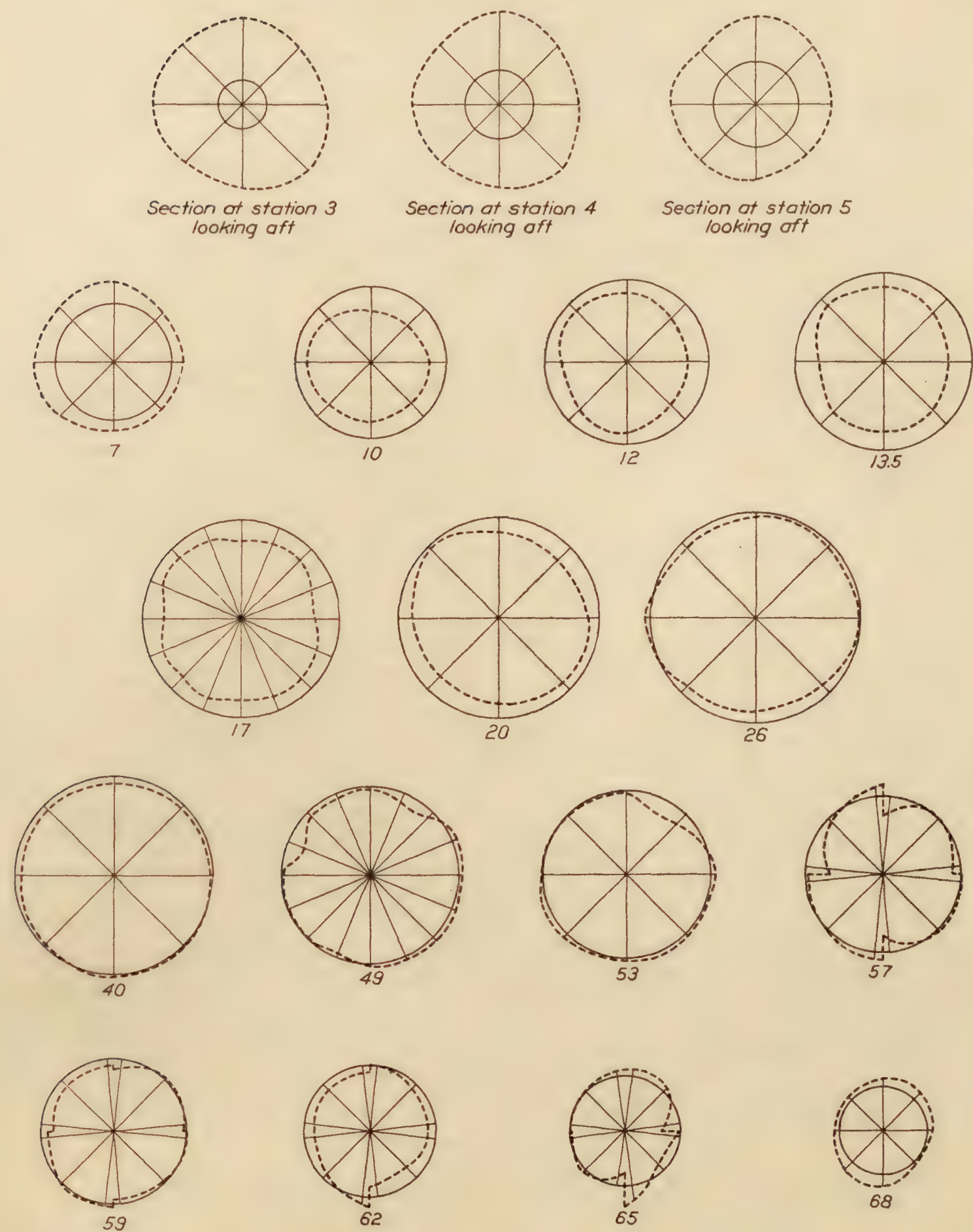


FIG. 17.—Pressure distribution on envelope. Run 27b, reversal. Rudder angle 24° left to 18° right. 1,250 R. P. M.



Positive pressure plotted outside, negative pressure inside, of circumference



FIG. 18.—Circumferential pressure distribution on envelope. Run 27b, reversal. 1,250 R. P. M.

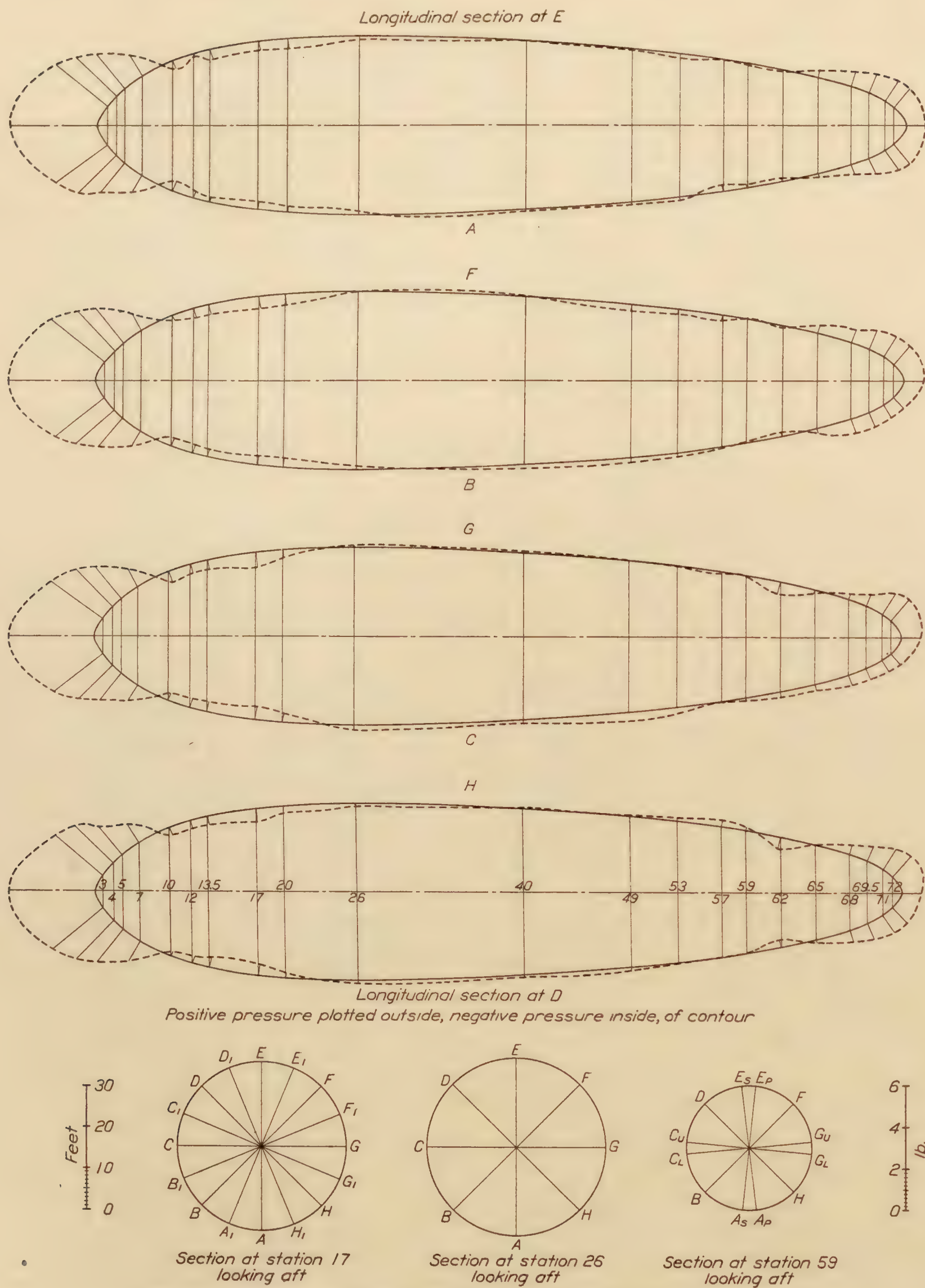
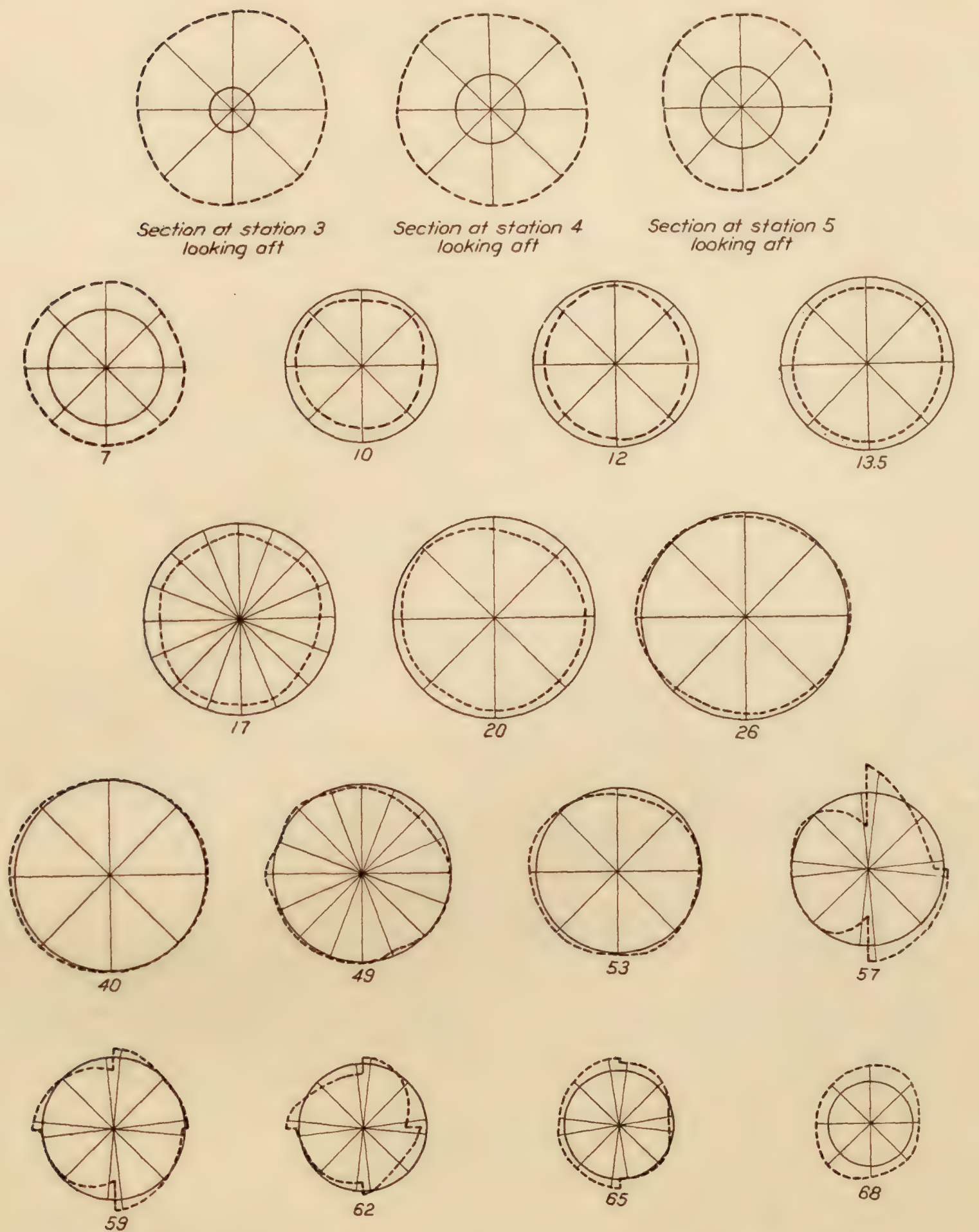


FIG. 19.—Pressure distribution on envelope. Run 4, steady circle. Rudder angle 8° right. 1,250 R. P. M.



Positive pressure plotted outside, negative pressure inside, of circumference



FIG. 20.—Circumferential pressure distribution on envelope. Run 4, steady circle. Rudder angle 8° right. 1,250 R. P. M.

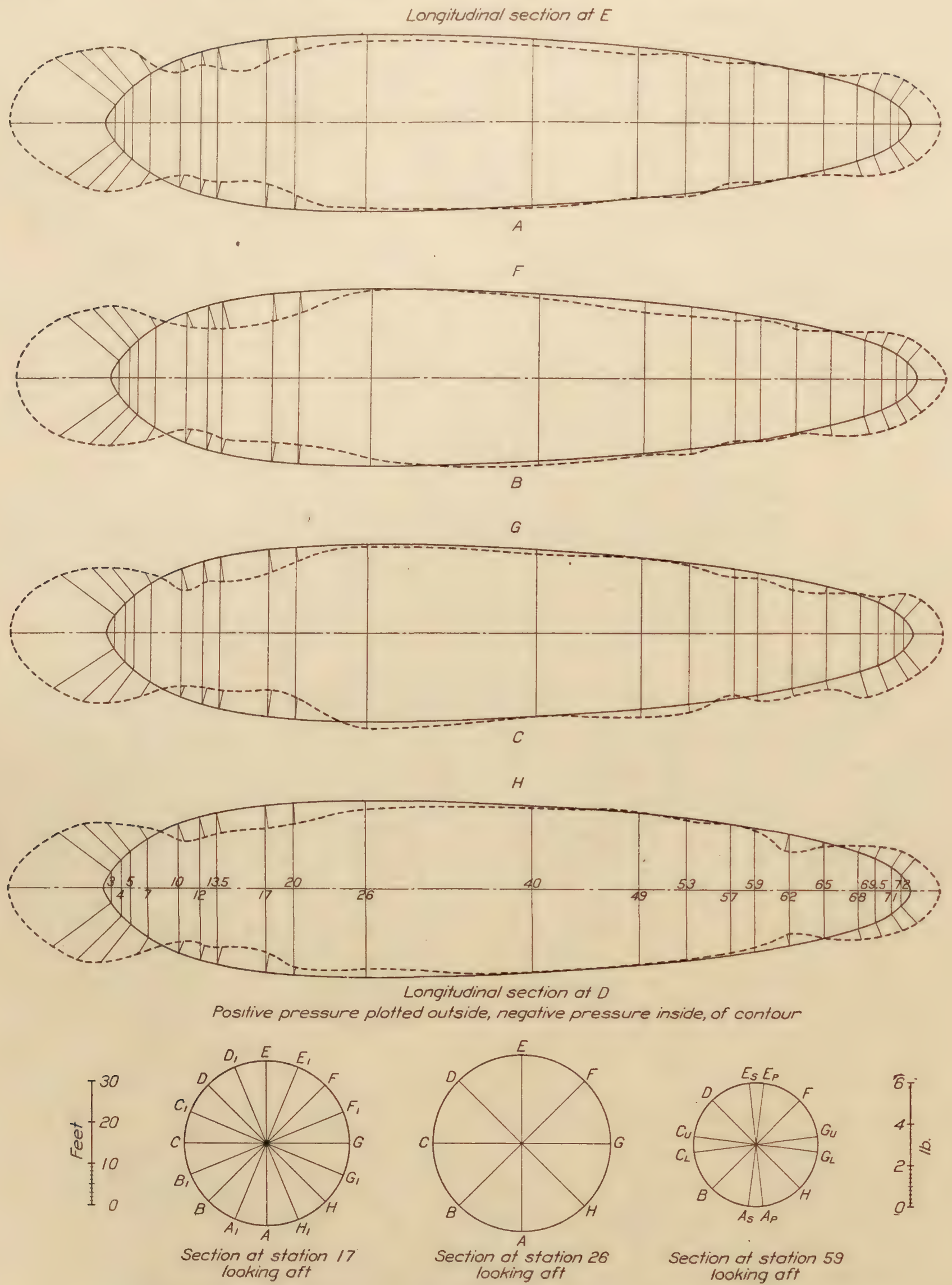
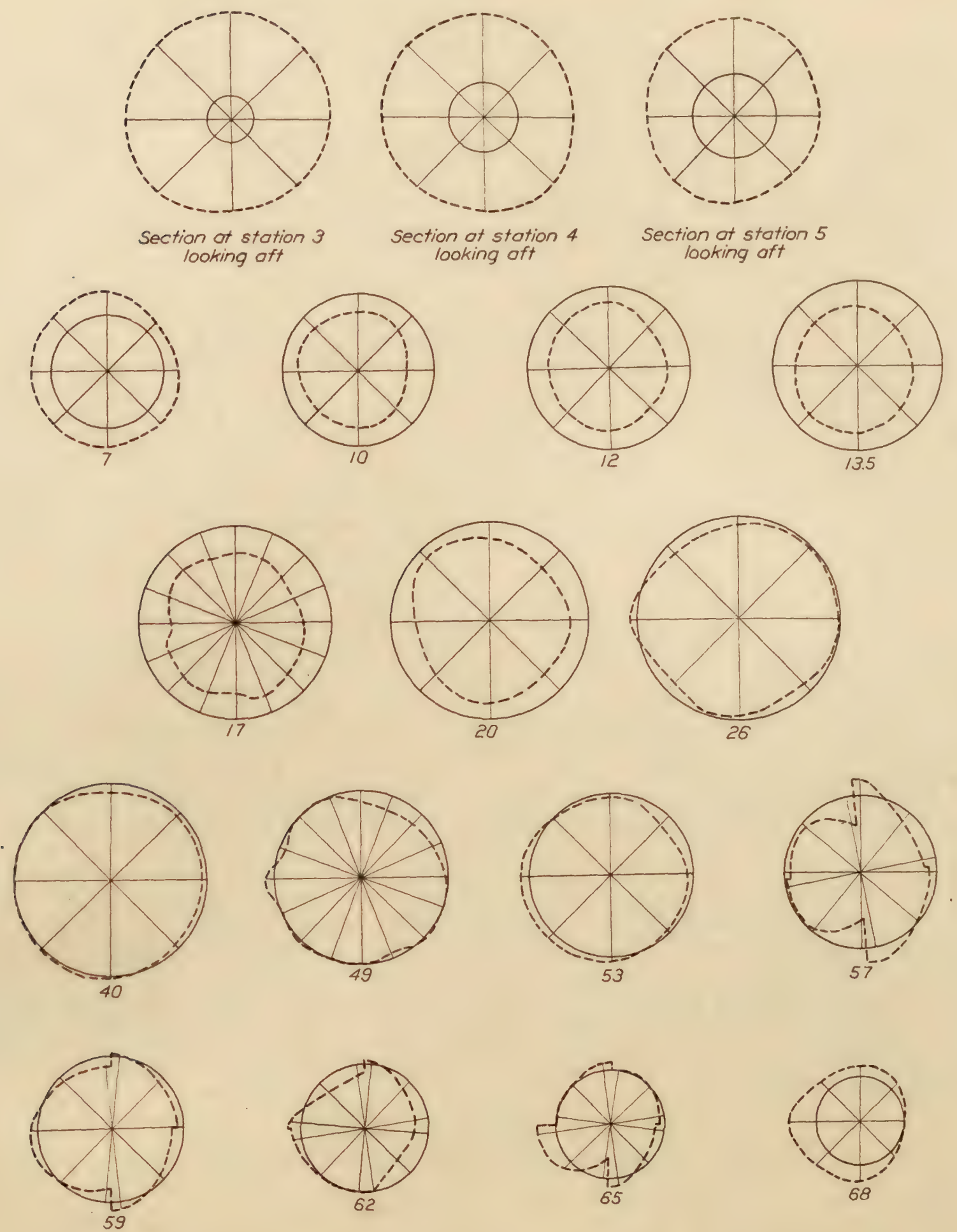


FIG. 21.—Pressure distribution on envelope. Run 9b, start circle. Rudder angle 44° right. 1,250 R. P. M.



Positive pressure plotted outside, negative pressure inside, of circumference



FIG. 22.—Circumferential pressure distribution on envelope. Run 9b, start circle. Rudder angle 44° right. 1,250 R. P. M.

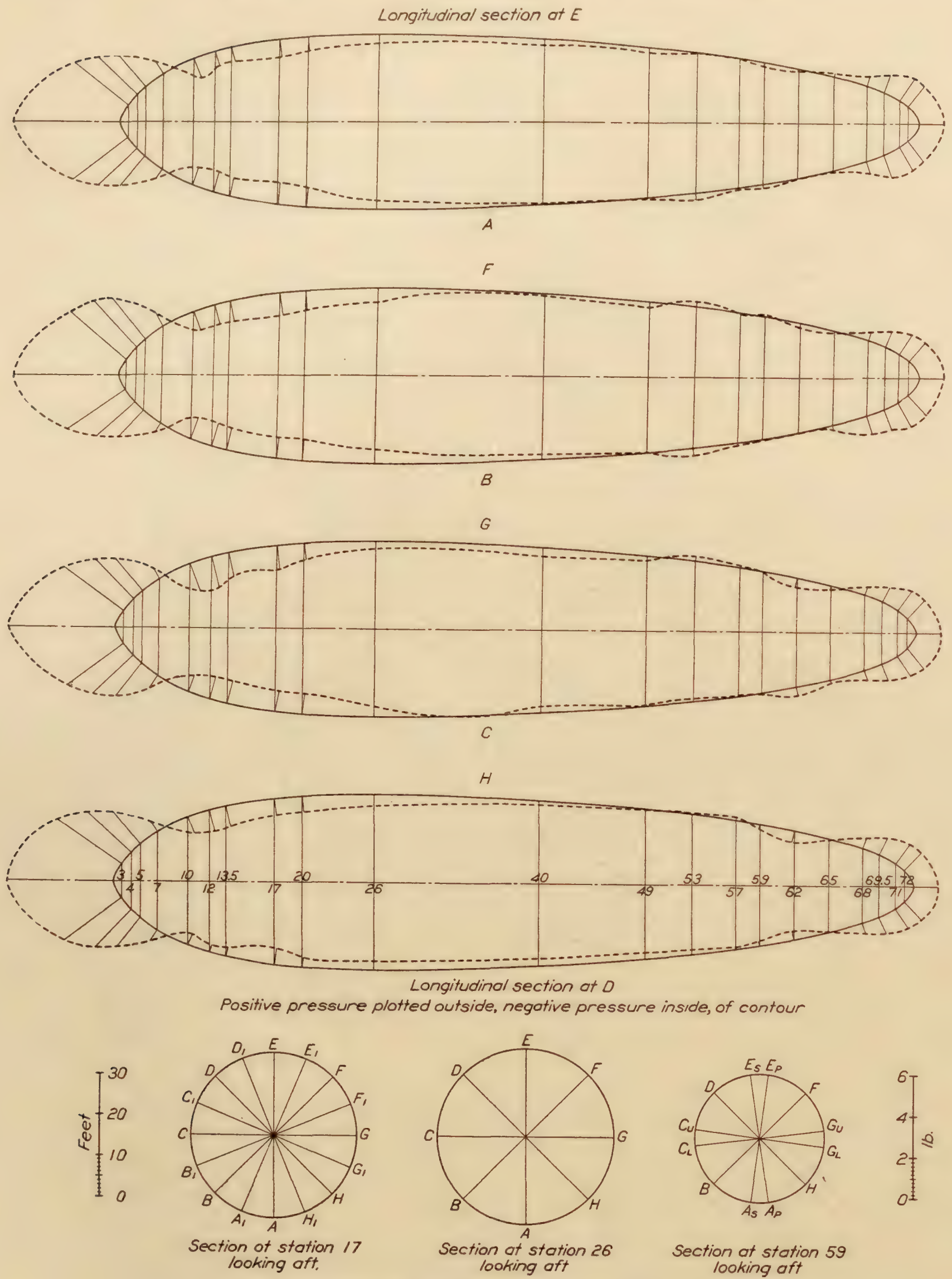
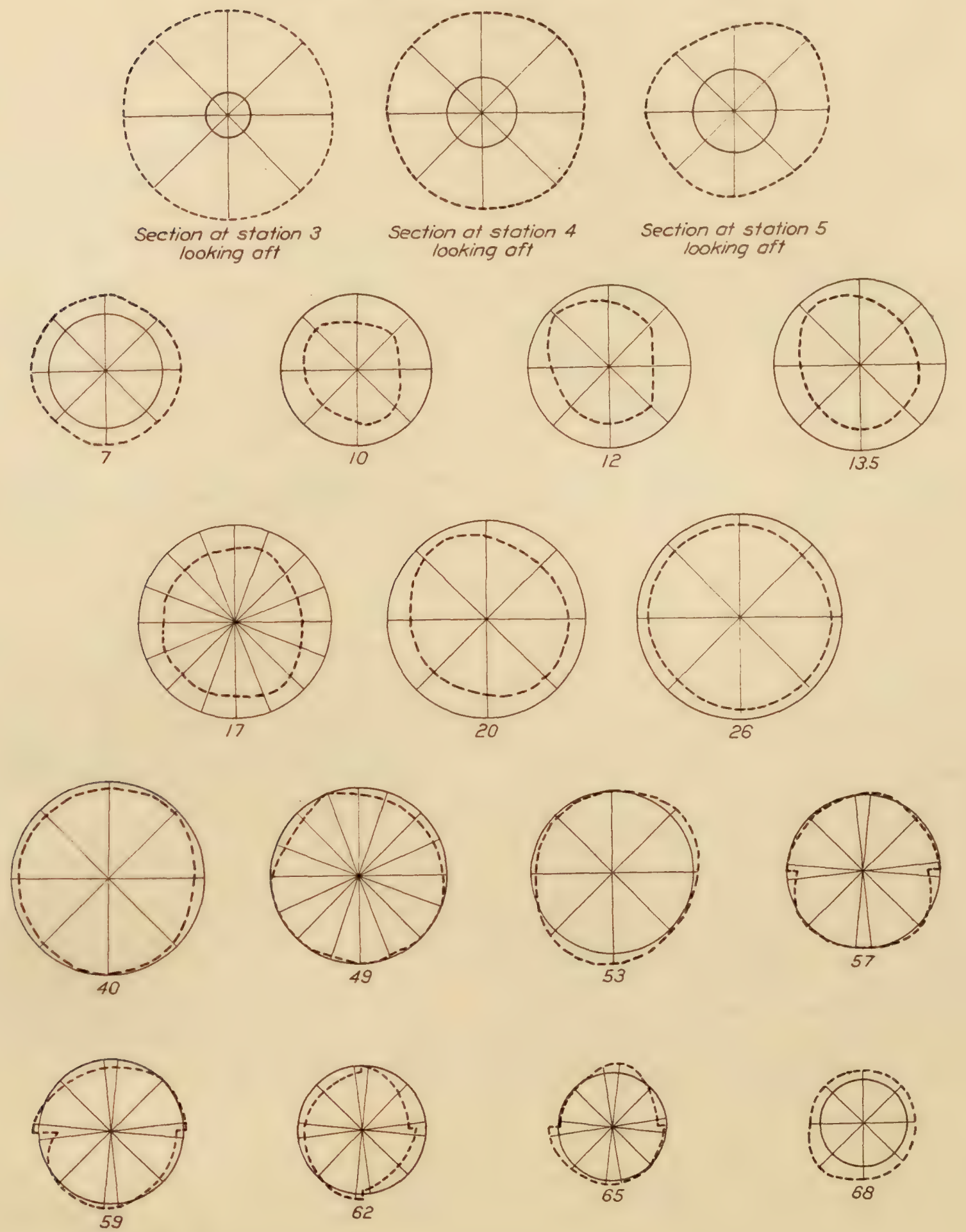


FIG. 23.—Pressure distribution on envelope. Run 28, bump. 1,250 R. P. M.



Positive pressure plotted outside, negative pressure inside, of circumference



FIG. 24.—Circumferential pressure distribution on envelope. Run 28, bump. 1,250 R. P. M.

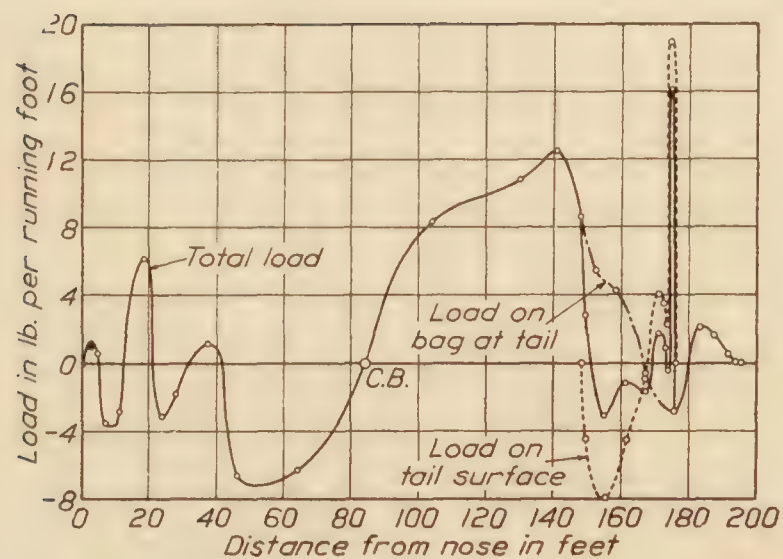


FIG. 25a.—Vertical loads. Run 27b, reversal. Rudder angle 24° left to 18° right. 1,250 R. P. M. Positive loads acting upward. (NOTE.—The moment of the resultant aerodynamic forces on the horizontal tail surfaces about the C. B. = 2,270 lb./ft. clockwise)

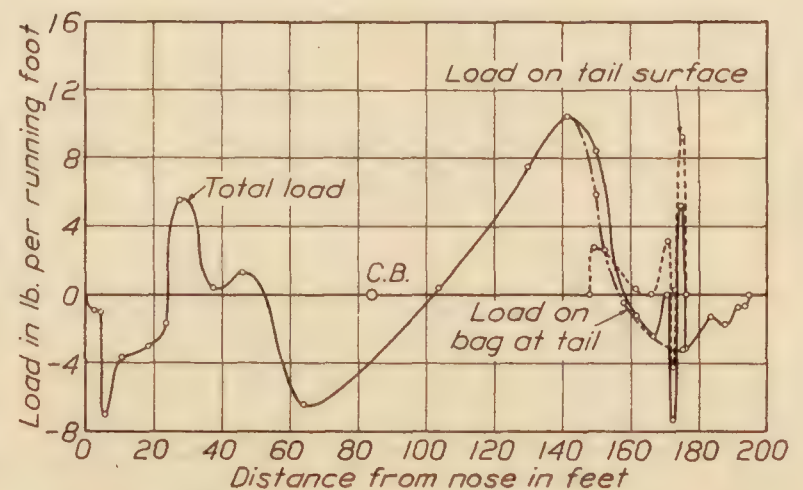


FIG. 26a.—Vertical loads. Run 4, steady circle. Rudder angle 8° right. 1,250 R. P. M. Positive loads acting upward. (NOTE.—The moment of the resultant aerodynamic forces on the horizontal tail surfaces about the C. B. = 3,735 lb./ft. counterclockwise)

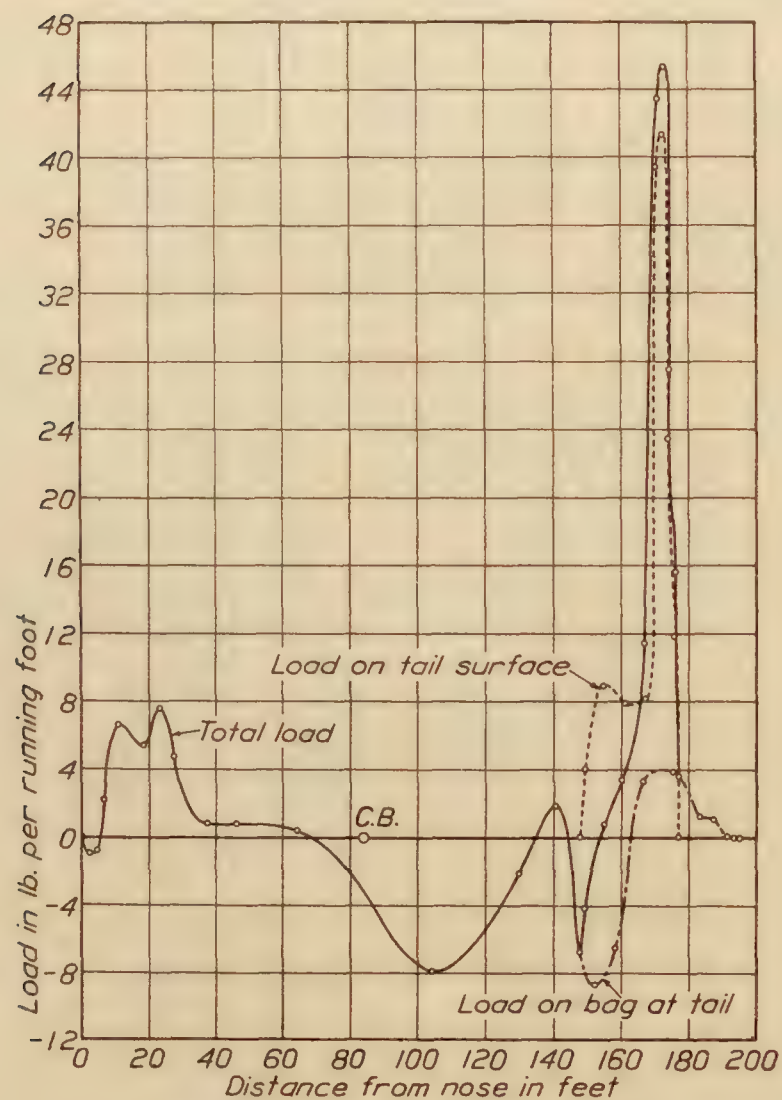


FIG. 25b.—Horizontal loads. Run 27b, reversal. Rudder angle 24° left to 18° right. 1,250 R. P. M. Positive loads acting to port. (NOTE.—The moment of the resultant aerodynamic forces on the vertical tail surfaces about the C. B. = 35,100 lb./ft. clockwise)

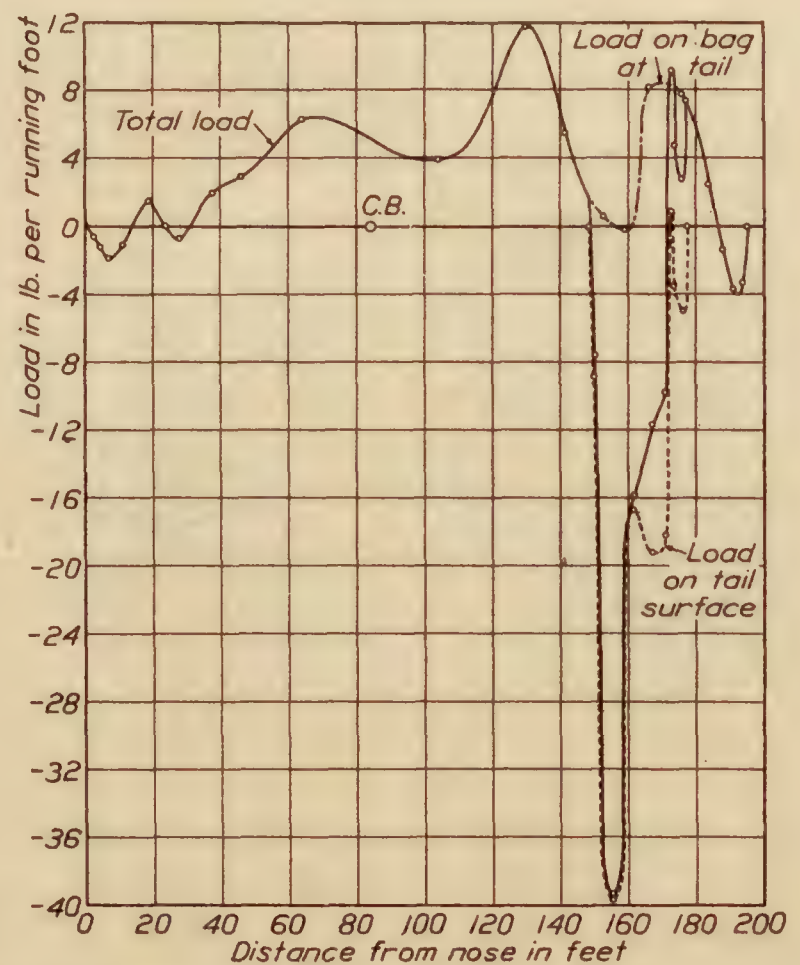


FIG. 26b.—Horizontal loads. Run 4, steady circle. Rudder angle 8° right. 1,250 R. P. M. Positive loads acting to port. (NOTE.—The moment of the resultant aerodynamic forces on the vertical tail surfaces about the C. B. = 37,200 lb./ft. counterclockwise)

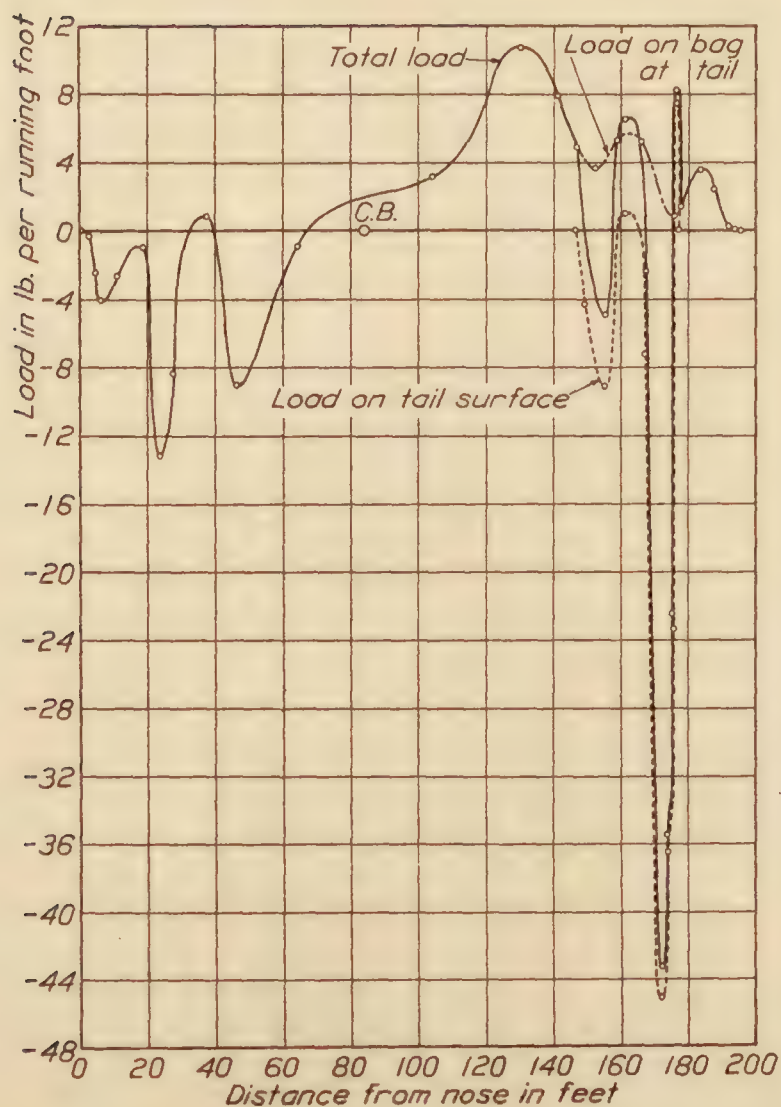


FIG. 27a.—Vertical loads. Run 28, bump. 1,250 R. P. M. Positive load acting upward. (NOTE.—The moment of the resultant aerodynamic forces on the horizontal tail surfaces about the C. B. = 27,440 lb./ft. clockwise)

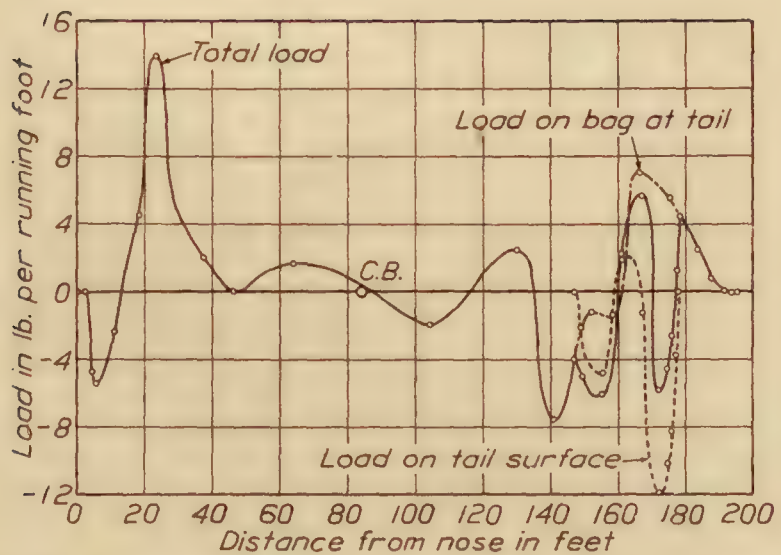


FIG. 27b.—Horizontal loads. Run 28, bump. 1,250 R. P. M. Positive load acting to port. (NOTE.—The moment of the resultant aerodynamic forces on the vertical tail surfaces about the C. B. = 9,095 lb./ft. counterclockwise)

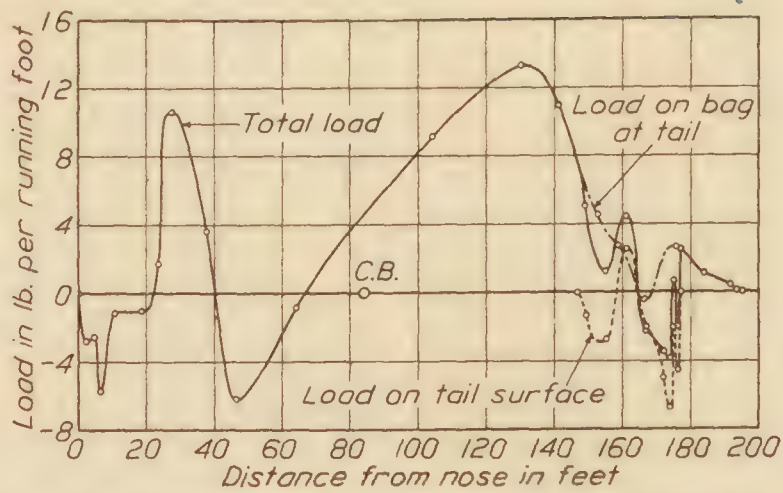


FIG. 28a.—Vertical loads. Run 9b, start circle. Rudder angle 44° right. 1,250 R. P. M. Positive load acting upward. (NOTE.—The moment of the resultant aerodynamic forces on the horizontal tail surfaces about the C. B. = 5,058 lb./ft. clockwise)

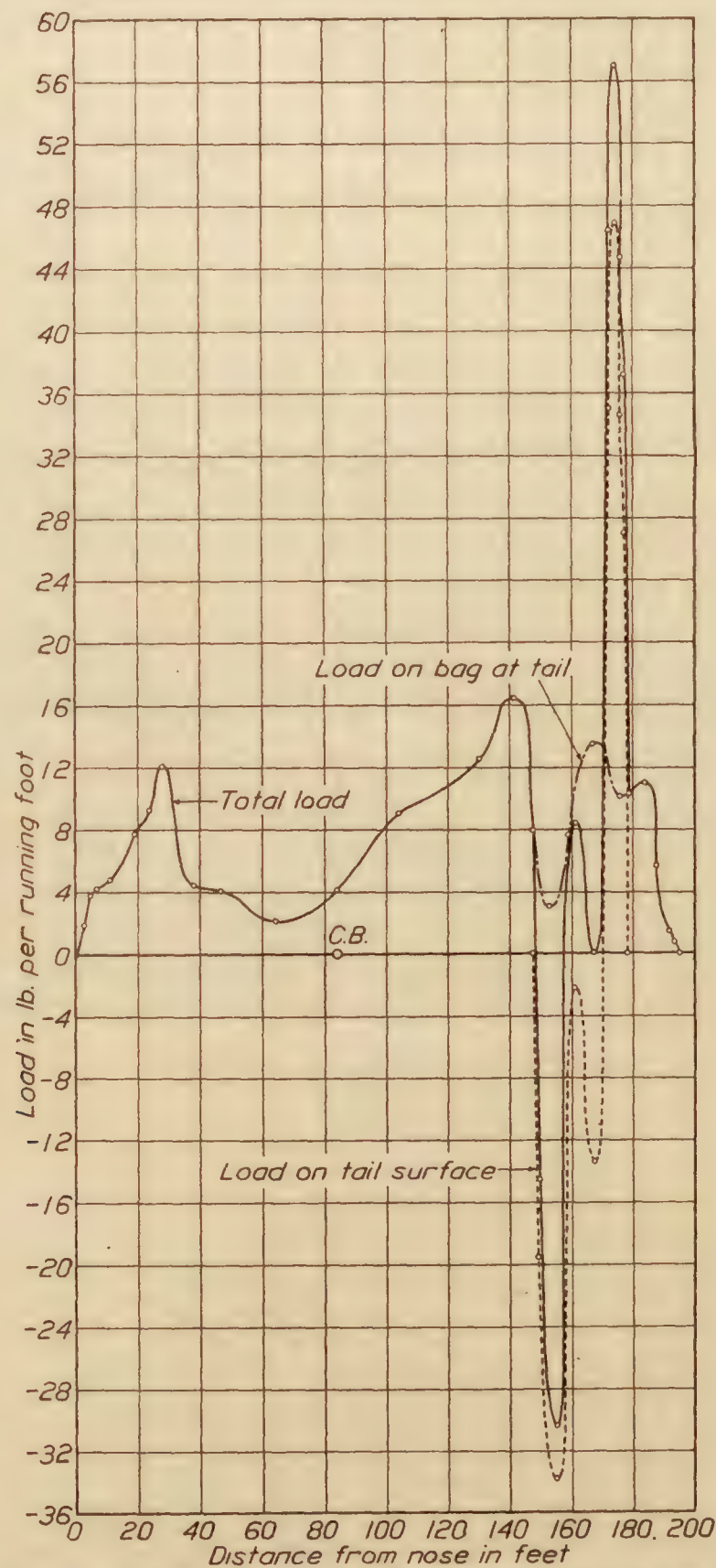


FIG. 28b.—Horizontal loads. Run 9b, start circle. Rudder angle 44° right. 1,250 R. P. M. Positive load acting to port. (NOTE.—The moment of the resultant aerodynamic forces on the vertical tail surfaces about the C. B. = 2,940 lb./ft. clockwise)

REPORT No. 224

AN INVESTIGATION OF THE COEFFICIENT OF DISCHARGE OF LIQUIDS THROUGH SMALL ROUND ORIFICES

By W. F. JOACHIM

Langley Memorial Aeronautical Laboratory

REPORT No. 224

AN INVESTIGATION OF THE COEFFICIENT OF DISCHARGE OF LIQUIDS THROUGH SMALL ROUND ORIFICES

By W. F. JOACHIM

SUMMARY

The work covered by this report was undertaken in connection with a general investigation of fuel injection engine principles as applied to engines for aircraft propulsion, the specific purpose being to obtain information on the coefficient of discharge of small round orifices suitable for use as fuel injection nozzles.

Flow of the liquids tested under high pressure was obtained with an intensifier consisting of a 5-inch piston driving a direct connected $\frac{3}{4}$ -inch hydraulic plunger. The large piston was operated by compressed air and the time required for the displacement of a definite volume by the hydraulic plunger was measured with an electrically operated stop watch. The coefficients were determined as the ratio of the actual to the theoretical rate of flow where the theoretical flow was obtained by the usual simple formula for the discharge of liquids through orifices.

Values for the coefficient were determined for the more important conditions of engine service such as discharge under pressures up to 8,000 pounds per square inch, at temperatures between 80° and 180° F. and into air compressed to pressures up to 1,000 pounds per square inch. The results show that the coefficient ranges between 0.62 and 0.88 for the different test conditions between 1,000 and 8,000 pounds per square inch hydraulic pressure. At lower pressures the coefficient increases materially.

It is concluded that within the range of these tests and for hydraulic pressures above 1,000 pounds per square inch the coefficient does not change materially with pressure or temperature; that it depends considerably upon the liquid, decreases with increase in orifice size, and increases in the case of discharge into compressed air until the compressed-air pressure equals approximately three-tenths of the hydraulic pressure, beyond which pressure ratio it remains practically constant.

INTRODUCTION

As far as is known, no data has been published giving the coefficient of discharge for liquid fuels discharged under high pressures through small orifices. It has been necessary therefore, in the design of an injection valve, to assume a value for the coefficient in order to find approximately the orifice size capable of discharging enough fuel, under the pressure employed, to meet the engine requirements. This research was undertaken in order to determine, for various conditions similar to those met in engine service, the coefficient of discharge of orifices suitable for use in fuel injection valves.

In order to determine the effects of pressure, temperature, and back air pressure upon the coefficient of discharge the work was arranged so that each of these influences could be varied independently. The pressure tests determined the coefficient of discharge for pressures up to 8,000 pounds per square inch, the liquids being discharged at 80° F. into air at atmospheric pressure. Coefficients were obtained for Diesel engine fuel oil discharged through orifices having diameters of 0.015 inch, 0.020 inch and 0.025 inch and for gasoline and water discharged through a 0.020-inch orifice. The temperature tests determined the coefficient at 80° F., 110° F., and 180° F. for Diesel engine fuel oil discharged through a 0.020-inch orifice. Pressures up to 8,000 pounds per square inch were used, the fuel being discharged into air at atmospheric pressure. The tests on the effect of back air pressure determined the coefficient

for the discharge of Diesel engine fuel oil at 80° F. into air at pressures up to 1,000 pounds per square inch using a 0.020-inch orifice. Two air chambers were used in order to determine the effect of a change in chamber size. In the tests with the small air chamber, hydraulic pressures up to 8,000 pounds per square inch and compressed air pressures up to 750 pounds per square inch were used. For the large air chamber hydraulic pressures up to 2,045 pounds per square inch and compressed air pressures up to 1,000 pounds per square inch were used.

METHODS AND APPARATUS

The method employed in the determination of all coefficients consisted in timing the flow of a known volume of liquid and determining the coefficients as the ratio of the actual to the theoretical rate of flow. Photographs of the discharge apparatus are shown in Figures 1 and 2.

In order to obtain a continuous flow of liquid under high pressure and of sufficient quantity to permit reasonably accurate timing, an intensifier operated by compressed air was used. This apparatus consisted primarily of an air cylinder 5 inches in diameter in axial alignment with a hydraulic cylinder three-fourths inch in diameter, the air cylinder piston being connected directly to the hydraulic plunger. By using air pressures up to 195 pounds per square inch in the air cylinder, working hydraulic pressures up to 8,000 pounds per square inch were obtained. The air cylinder and piston were standard Liberty engine parts, the cylinder being mounted on a casting so as to permit a working stroke of 9½ inches. The hydraulic plunger and cylinder were of hardened and ground tool steel, each separately lapped to obtain highly polished working surfaces. The fit between these two parts was such that when thoroughly lubricated a force of about 5 pounds was required to maintain relative movement. The orifices through which the liquids were discharged were also of hardened and ground tool steel. The holes were lapped to a high polish and means employed to secure sharp entering and exit edges.

The timed volume of the liquid discharged was 3.485 cubic inches less the leakage past the hydraulic plunger. This leakage was determined by a separate test for all liquids, pressures, and temperatures and though found to be practically negligible, in most cases considerably less than 1 per cent, was included in the coefficient calculations. The discharge time of this quantity of liquid was obtained with an electrically operated one-hundredth-second stop watch. Starting and stopping of the watch was controlled by an electric contactor located between the air and hydraulic cylinders. The contactor was operated, through a follower, by two shallow notches on the hydraulic plunger. Thus, as the hydraulic plunger descended and the follower moved into the first notch, the contactor closed the electric circuit and started the stop watch. As the follower moved out of the notch, the circuit was broken and the watch stem permitted to return. The stopping of the watch at the completion of the timed discharge volume was accomplished in like manner by the second notch. It may be noted that the watch was operated by two successive "makes" of the circuit, thus giving the same electrical action at the start and finish of the timed stroke. Since the liquids to be discharged were at rest at the beginning of the plunger movement and uniform flow was desired during the timed discharge, about 12 per cent of the total liquid volume was permitted to be discharged before starting the stop watch. Tests showed that this predischage was more than ample for the apparatus used.

Heating of the liquids was controlled in all tests by inclosing the liquid reservoir and discharge apparatus in a cabinet and circulating hot air around all parts until the test temperature was reached. This temperature was then maintained by control of the air temperature which was read from thermometers through glass windows in the cabinet door. The temperature of the liquids was obtained by thermocouples and a potentiometer. Figures 1 and 2 show the arrangement of the apparatus except for the electric heating elements and circulating fan in the back of the cabinet.

The pressure in the compressed air supply tank was raised at the beginning of a test to the maximum value required and the hydraulic pressure controlled by successively lowering the air pressure. The pressure in the air chamber into which the liquids were discharged was maintained at atmospheric pressure in all tests except those discharging into compressed air.

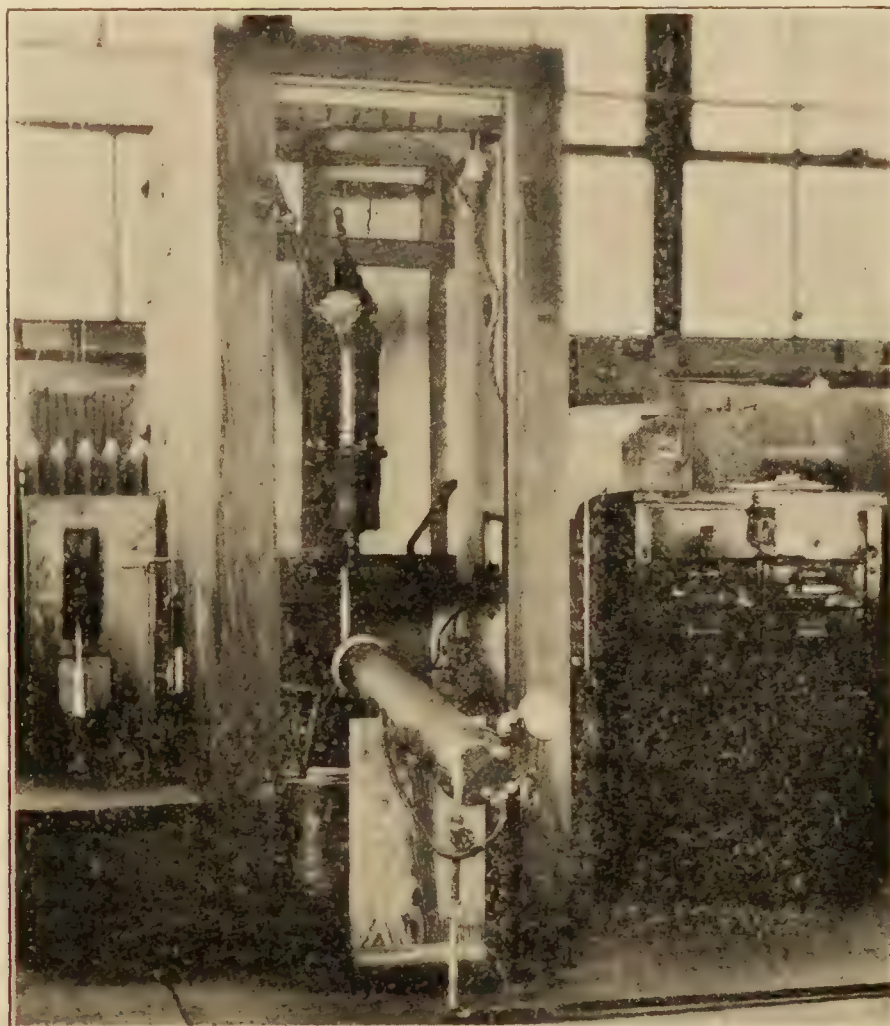


FIG. 1.—Coefficient of discharge apparatus showing arrangement of working parts

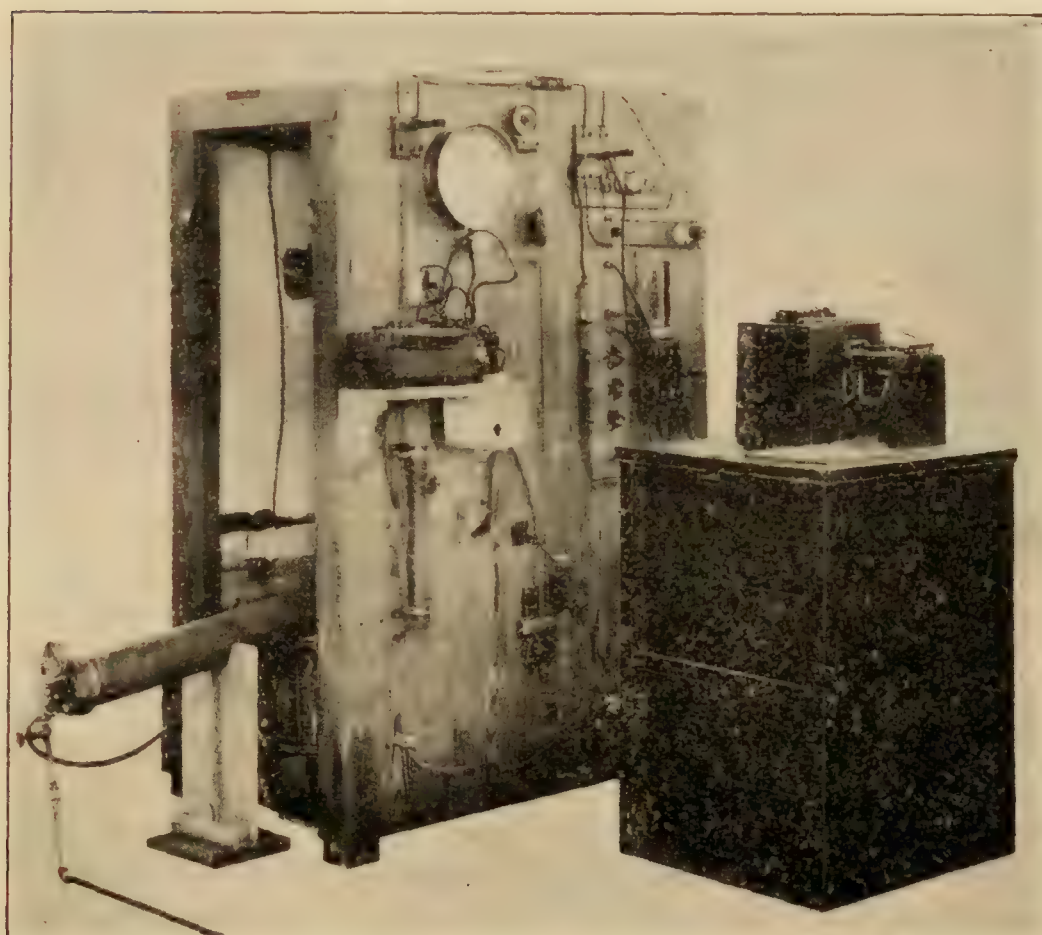


FIG. 2.—Coefficient of discharge apparatus showing controls and instruments

The test procedure, after the desired working conditions had been obtained, was as follows. A valve control, which operated the hydraulic needle valves, was first raised to its limit of travel. This simultaneously opened the inlet valve and closed the discharge valve. The liquid under test was then pumped by hand from the reservoir into the hydraulic cylinder, thus raising the plunger and piston against the air pressure. When the plunger and piston reached the top of their stroke the stop watch switch was closed and the valve control brought rapidly to its lower limit of travel. This simultaneously closed the inlet valve and opened the discharge valve thus discharging the liquid through the orifice and into the air chamber. The hydraulic pressure obtained during the timed portion of the test was read from the hydraulic gage and the time of discharge obtained automatically as previously described.

RESULTS

The greater part of the data obtained in this investigation is given in Figures 3 to 8, inclusive. The data obtained in part range check tests covering certain pressure and temperature effects are not given because these are practically the same as those presented. Considerable data covering high pressure discharge into compressed air are also not given because they duplicate, within the limit of experimental error, that for high pressure discharge into air at atmospheric pressure.

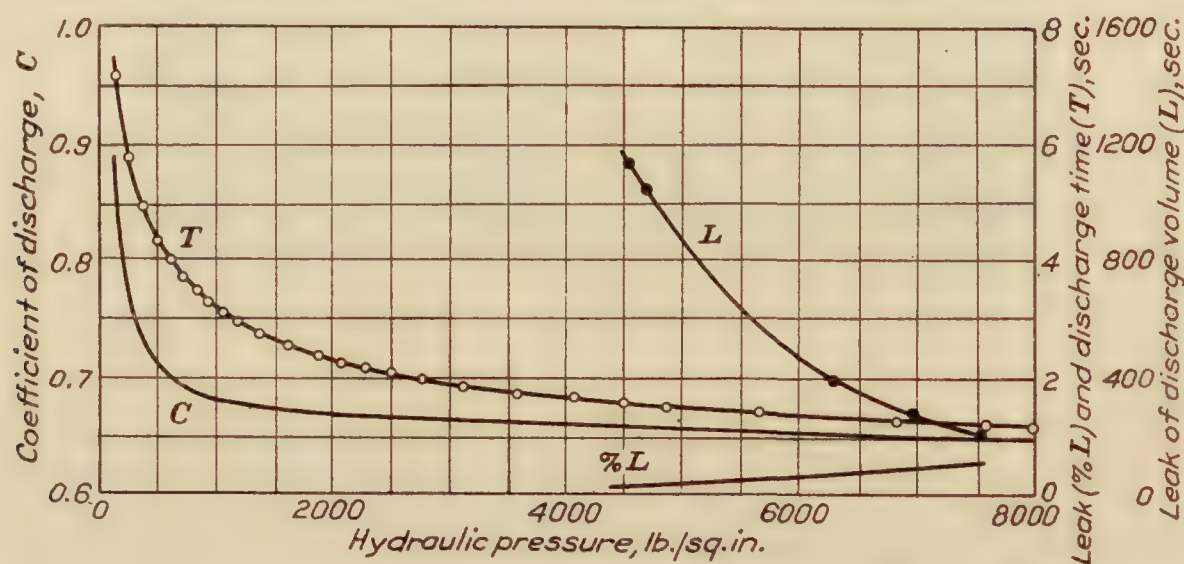


FIG. 3.—Experimental data for a 0.020-inch orifice. Diesel engine fuel oil at 80° F. discharged into air at atmospheric pressure

$$C = \frac{K(1 - \frac{\%L}{100})}{t \sqrt{P}}$$

$$K = 68.57$$

$$Q = \text{cat} \sqrt{2gh}$$

In order to present the data in a form that could be used to calculate discharge quantities and velocities without unnecessary complication, the effects of the compressibility of the liquid and its change of specific gravity with pressure are included in the coefficients. When these variables are taken into account in the calculations, the coefficient of discharge is found to be the same at the lower discharge pressures and to depart uniformly as the pressures increase until at 8,000 pounds per square inch it is about 4 per cent higher than the coefficient based on simple computation.

Pressure tests.—The results of the pressure tests are given in Figures 3, 4, and 5. The data presented in Figure 3 are the experimental and computed results of a test of Diesel engine fuel oil at 80° F. discharged through a 0.020-inch orifice into air at atmospheric pressure. The observed hydraulic pressures and recorded times are plotted as obtained during the test. The times required for the discharge volume to leak past the hydraulic plunger at various pressures are also plotted as obtained. These two curves give the experimental data from which the per cent of leak taking place during the test and the coefficient of discharge are calculated. The per cent of leak at any hydraulic pressure is calculated as the ratio of the discharge time to the

leak time, multiplied by 100. The coefficient of discharge is calculated as the ratio of the actual to the theoretical rate of flow. The actual rate of flow is calculated from the experimental data and the theoretical rate by means of the usual hydraulic formula,

$$v = \sqrt{2gh}$$

The effects of orifice size and of different liquids are given in Figures 4 and 5, the data for these tests being obtained and computed in the same way as that for Figure 3. Three orifice sizes were tested, the diameters and lengths being 0.015 by 0.050 inch, 0.020 by 0.060 inch, and 0.025 by 0.060 inch. The data presented in Figure 4 is for Diesel engine fuel oil at 80° F.

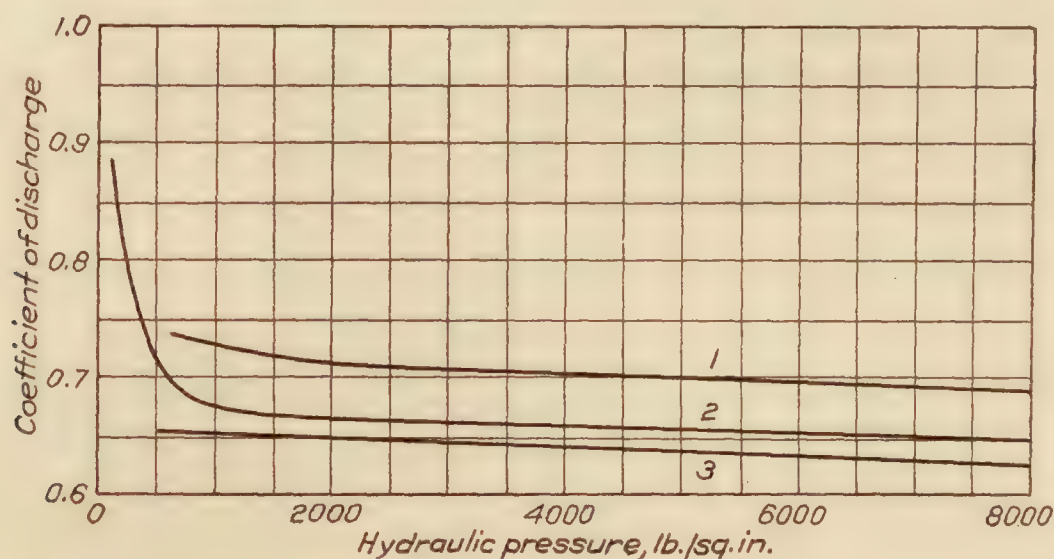


FIG. 4.—Effect of orifice size. Diesel engine fuel oil at 80° F. discharged into air at atmospheric pressure. Orifice size: Curve 1, 0.015 inch by 0.050 inch; curve 2, 0.020 inch by 0.060 inch; curve 3, 0.025 inch by 0.060 inch

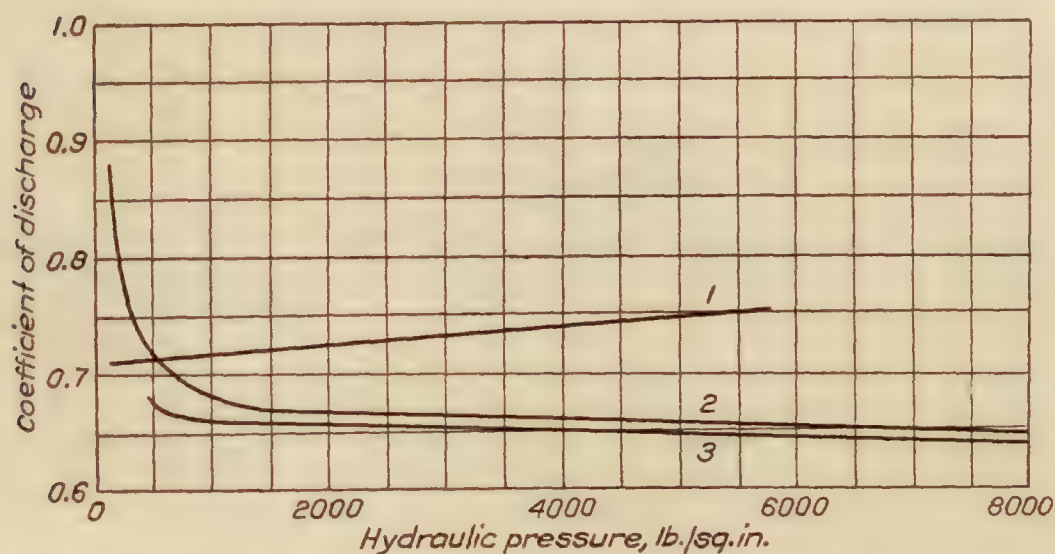


FIG. 5.—Effect of different liquids. Liquids at 80° F. discharged through a 0.020 by 0.060 inch orifice into air at atmospheric pressure. Liquids: Curve 1, water; curve 2, Diesel engine fuel oil; curve 3, gasoline

discharged under pressures up to 8,000 pounds per square inch into air at atmospheric pressure. The parallelism between the curves and the practical constancy of the coefficients for discharge pressures above 1,000 pounds per square inch are worthy of note.

The data on the effect of different liquids, Figure 5, are for Diesel engine fuel oil, gasoline and water discharged through a 0.020-inch orifice, the test temperature and pressures being the same as for Figure 4. The parallelism and proximity of the curves for gasoline and Diesel engine fuel oil are noteworthy and probably indicate that the effect of the lesser density of the gasoline is nearly counteracted by its lesser viscosity.

Temperature tests.—The effect of temperature on the coefficient of discharge was determined for Diesel engine fuel oil discharged through a 0.020-inch orifice into air at atmospheric pressure.

Tests were made at 80°, 110° and 180° F. with hydraulic pressures up to 8,000 pounds per square inch. The coefficient was uniformly lower with the higher temperatures but over the range of these tests the difference was less than 2 per cent.

Tests on discharge into compressed air.—The results of the work on low-pressure discharge into compressed air are given in Figures 6, 7, and 8, the results for high pressure discharge being omitted because they duplicated the results for high pressure discharge into air at atmospheric pressure as previously mentioned. It was also found that the results obtained for discharge into the two sizes of air chambers tested were the same. It was noted during the preliminary tests on discharge into compressed air that the coefficient of the orifice used had increased 0.06 for the case of discharge into air at atmospheric pressure. Microscopic examination of the orifice showed that its entering edge had been rounded. This was probably caused by the flow of unstrained liquid through the orifice, the high pressure strainers having failed during extraneous work. Since all conditions in these tests were the same as those for the pressure tests it is concluded that the increase in the coefficient was due to the change in the orifice edge.

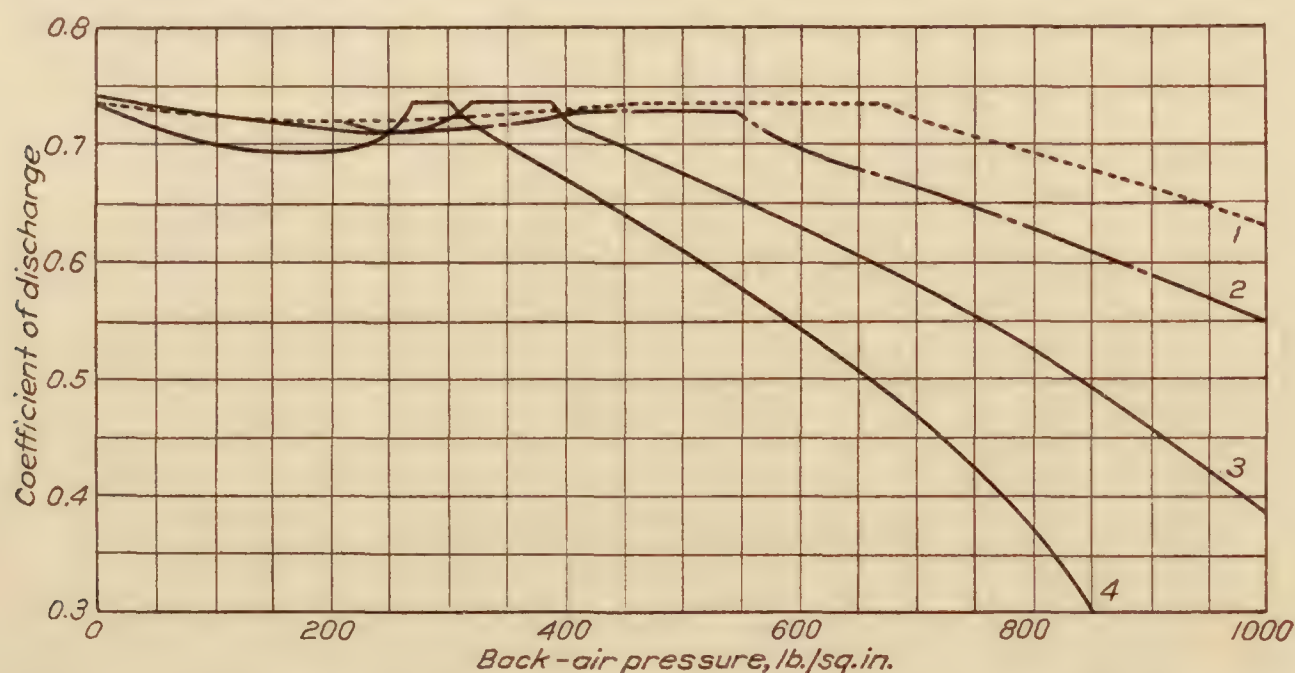


FIG. 6.—Coefficient of discharge versus back-air pressure. Diesel engine fuel oil at 80° F. discharged through a 0.020-inch orifice into air at various pressures. Hydraulic pressures: Curve 1, 2,045 pounds per square inch; curve 2, 1,645 pounds per square inch; curve 3, 1,255 pounds per square inch; curve 4, 1,005 pounds per square inch

$$Q = \text{cat} \sqrt{2gh}$$

In the work with low hydraulic pressures data was obtained for discharge into compressed air ranging in pressure up to 1,000 pounds per square inch, the pressure on the liquid during a test being maintained constant. Four hydraulic pressures, namely, 1,005, 1,255, 1,645, and 2,045 pounds per square inch were used. The data are for Diesel engine fuel oil at 80° F. discharged through a 0.020-inch orifice and are presented in three ways. In Figure 6 the coefficients are calculated in the same way as those for discharge into air at atmospheric pressure and do not take into account in the calculations any decrease in the effective hydraulic pressure due to the increased back air pressure. The coefficients are plotted against the back air pressures. The data plotted from simple computation as above are convenient to use in practice and show clearly the effect of increased back air pressure. It may be noted that the coefficient does not change materially below compressed air pressures approximately three-tenths of the hydraulic pressure and that the deviation within this range decreases with increase in hydraulic pressure. This deviation entirely disappears with higher hydraulic pressures, since in the work on high pressure discharge into compressed air no deviation of the coefficient was noted below the critical pressure ratio of three-tenths. Above this point the coefficient and rate of discharge decrease uniformly with increase in compressed air pressure.

In order to determine the coefficient at the critical point as accurately as possible several check tests were made for each hydraulic pressure. The experimental data giving the back air pressures and corresponding discharge times for the 1,005 pounds per square inch hydraulic pressure, curve 4 of Figure 6, are plotted over a range covering the critical point in Figure 7.

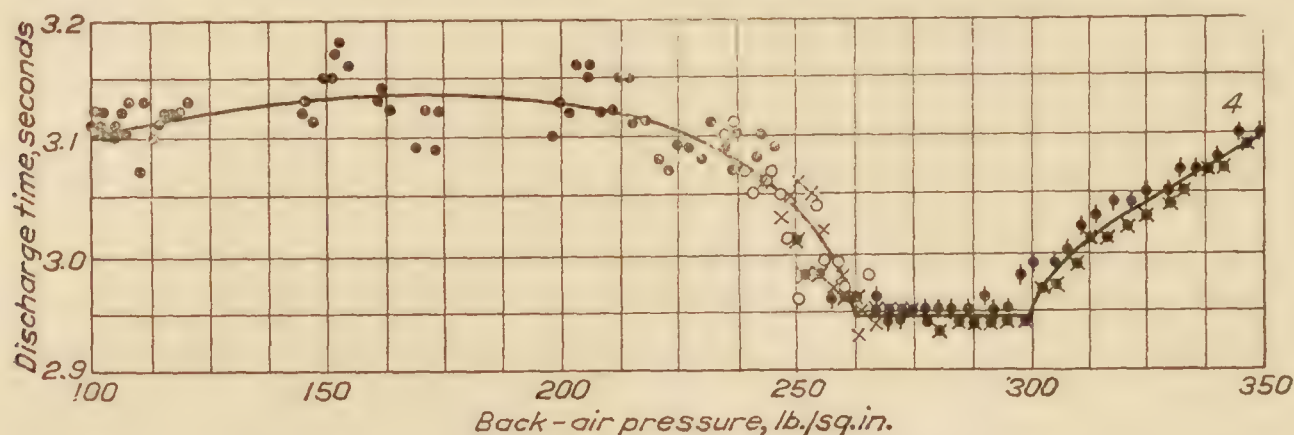


FIG. 7.—Discharge time versus back-air pressure. Diesel engine fuel oil at 80° F. discharged through a 0.020-inch orifice into air at various pressures. Hydraulic pressure: Curve 4, 1,005 pounds per square inch

These data are plotted to enlarged scales and show the degree of check obtained for several runs.

The data for discharge into compressed air has also been computed on the basis that the compressed air pressure reduces the effective hydraulic pressure on the liquid. The theoretical rate of flow was calculated in this case by means of the hydraulic formula

$$V = \sqrt{2g(h - h_A)}$$

in which h is the hydraulic pressure head and h_A the back air pressure head. The coefficients as thus calculated are plotted against the ratio of the back air pressure to the hydraulic pressure in Figure 8. It may be noted that the coefficients for all four curves, calculated on the above

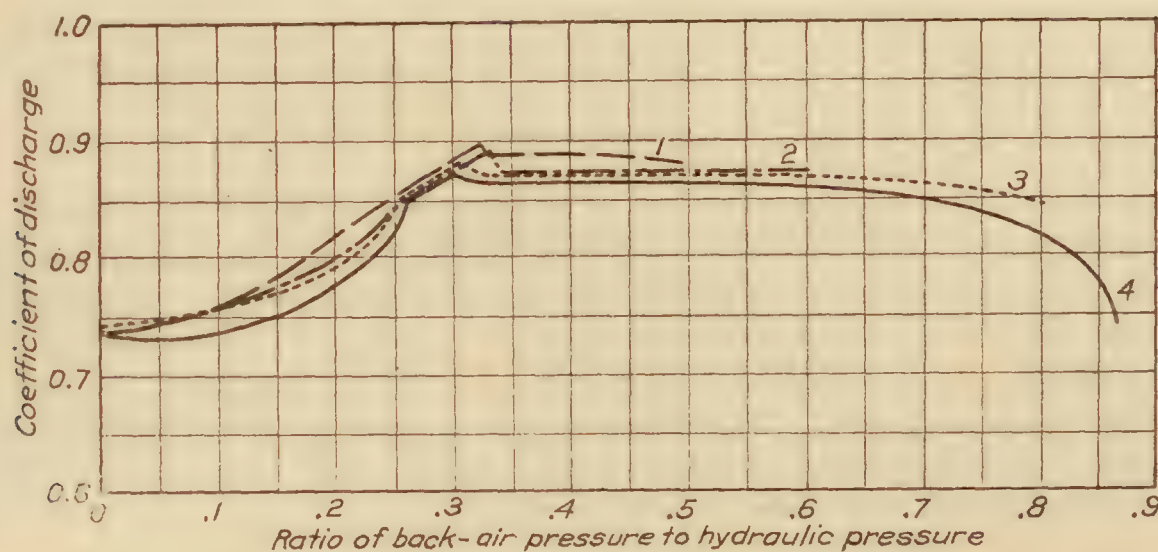


FIG. 8.—Coefficient of discharge versus ratio of back-air pressure to hydraulic pressure. Diesel engine fuel oil at 80° F. discharge through a 0.020-inch orifice into air at various pressures. Hydraulic pressures: Curve 1, 2,045 pounds per square inch; curve 2, 1,645 pounds per square inch; curve 3, 1,255 pounds per square inch; curve 4, 1,005 pounds per square inch
 $Q = \text{cat } \sqrt{2g(h - h_A)}$

basis, increase from about 0.74 at a pressure ratio of zero up to about 0.88 at a pressure ratio of approximately three-tenths. Beyond this ratio or the critical point, the coefficients are practically constant. A decrease in the coefficient at the higher ratios of back air pressure to hydraulic pressure may also be noted, this decrease being considerably smaller in degree for the higher discharge pressures.

Since the work on discharge into compressed air was limited to the use of only one size and proportion of orifice, it is thought that at present no general conclusions on the results may be drawn.

Application.—The accuracy of the results obtained in this investigation depended upon the accuracy with which the hydraulic pressures were observed, the accuracy of the stop watches and of the measurement of a number of constants. The hydraulic pressures were read in general from a 10,000-pound hydraulic test gage which was calibrated by means of a dead weight gage tester. It is believed that the error of the pressure readings did not exceed 5 pounds. Two one-hundredth second stop watches were used, a National Park and a Meylan. The running performance of these stop watches was determined by photographing their indicated times with those of two watches having known errors. The running error was negligible. The starting and stopping errors were not investigated, but in many hundred observations it was noted that where all test conditions were maintained constant for the purpose of checking previous data or determining reproducibility the variation in the recorded times was generally not more than one-hundredth of a second. However, in some cases of discharge into compressed air below the critical point the variation in the recorded times was greater. Figure 7 represents the worst case in this respect. The more important constants measured were the orifice diameters and lengths, specific gravities of the liquids, and the displacement of the hydraulic plunger. At the test temperatures of 80°, 110°, and 180° F. the specific gravity of the Diesel engine fuel oil used was 0.846, 0.833, and 0.802, the corresponding Saybolt Universal viscosity being 39.0, 35.3, and 31.5 seconds. The gravitational constant, g , was calculated as 32.15 for the location of the Laboratory of the National Advisory Committee for Aeronautics at Langley Field, Va. The displacement of the hydraulic plunger and lengths of the orifices were calculated from micrometer measurements, specific gravities were determined with a Westphal balance, and the diameters of the orifices measured on a dividing engine. Wherever practicable several check measurements and test observations were made and the limits of probable error calculated. The total limit of probable error ranged between 1 and 2½ per cent, and was greatest for the low pressures and the smallest orifice.

The results of this work are, in general, applicable to cases of continuous discharge having the same or similar conditions of operation. Intermittent discharge and the flow of other liquids through orifices of the same or different form would probably result in appreciable differences in the coefficient. For such cases the data presented herewith may only be used as an indication.

CONCLUSION

From the results of discharge into air at atmospheric pressure it is concluded that for hydraulic pressures above approximately 1,000 pounds per square inch the coefficient for a given orifice and liquid does not change materially with pressure or temperature, within the limits of these tests, but that for pressures below 1,000 pounds per square inch it trends in general toward unity. The coefficient for gasoline and Diesel engine fuel oil are practically the same, but for water it is considerably higher. An increase in orifice size within the range of this investigation consistently decreased the coefficient. A slight accidental rounding of the entering edge of an orifice in one instance caused an increase in the value of the coefficient.

From the work on discharge into compressed air it was found that the rate of discharge for Diesel engine fuel oil at 80° F. and a 0.020-inch orifice was not materially affected by discharge into dense air at pressures less than approximately three tenths of the hydraulic pressure, but that at higher air pressures it decreased rapidly in agreement with the resulting effective hydraulic pressures.

REPORT No. 225

**THE AIR FORCES ON A MODEL OF THE
SPERRY MESSENGER AIRPLANE
WITHOUT PROPELLER**

By MAX M. MUNK
National Advisory Committee for Aeronautics

and

WALTER S. DIEHL
Bureau of Aeronautics, Navy Department

REPORT No. 225

THE AIR FORCES ON A MODEL OF THE SPERRY MESSENGER AIR-PLANE WITHOUT PROPELLER

By MAX M. MUNK and WALTER S. DIEHL

SUMMARY

This is a report on a scale-effect research which was made in the variable density wind tunnel of the National Advisory Committee for Aeronautics at the request of the Army Air Service. A 1/10 scale model of the Sperry Messenger airplane with USA-5 wings was tested without a propeller at various Reynolds Numbers up to the full scale value. Two series of tests were made: The first on the original model which was of the usual simplified construction, and the second on a modified model embodying a great amount of detail.

While the present report is of a preliminary nature, the work has progressed far enough to show that the scale effect is almost entirely confined to the drag. In the tests so far conducted, the drag at any given angle of attack within the normal flying range is found to vary as $\left(\frac{Vl}{\nu}\right)^n$. The exponent n is constant for any one angle of attack, and ranges from -0.045 at large angles of attack to -0.17 at small angles.

It was also found that the model should be geometrically similar to the full-scale airplane if the test data are to be directly applicable to full scale. If the condition of geometric similarity be fulfilled, the data obtained at a full-scale value of Reynolds Number agree very closely with free-flight data. The variable density wind tunnel therefore appears to be a very promising instrument for procuring test data free from scale effect. It is also admirably suited for studying the scale effect and obtaining information which is necessary in an interpretation of the results obtained in atmospheric wind tunnels at low values of the Reynolds Number.

INTRODUCTION

Until recently the only method of increasing the Reynolds Number $\left(\frac{Vl}{\nu}\right)$ in a wind-tunnel test was to increase either V or l or both together, but the maximum practicable value of $\left(\frac{Vl}{\nu}\right)$ thus obtainable is far below that corresponding to the average airplane in free flight. The variable density wind tunnel of the National Advisory Committee for Aeronautics, using models of normal size and employing moderate speeds, while varying the kinematic viscosity $\nu \left(= \frac{\mu}{\rho}\right)$ by changing the density, supplies a means for bridging the entire gap between a conventional wind-tunnel test and full scale.

Owing to the interest attached to the results of the variable-density tests on account of their novel nature and their probable value to the designer, it has been considered advisable to make available immediately a preliminary report on the first complete series of tests. The

tests with which this preliminary report is concerned are the part of an extensive free-flight and wind-tunnel research conducted by the National Advisory Committee for Aeronautics for the Army Air Service on the Sperry Messenger airplane.

In a new field of research such as that opened by this report, it is to be expected that the test data will show some inconsistencies, partially due to the personal elements, or to the newness of the work, or possibly to some unknown and unsuspected physical law. There are certain inconsistencies to be observed in the data in this report, but time has not been sufficient to investigate them more fully and ascertain the cause or causes. It is expected that the present report will prove instructive both as to the nature of scale effect and as to the probable value of the variable density wind tunnel in further testing.

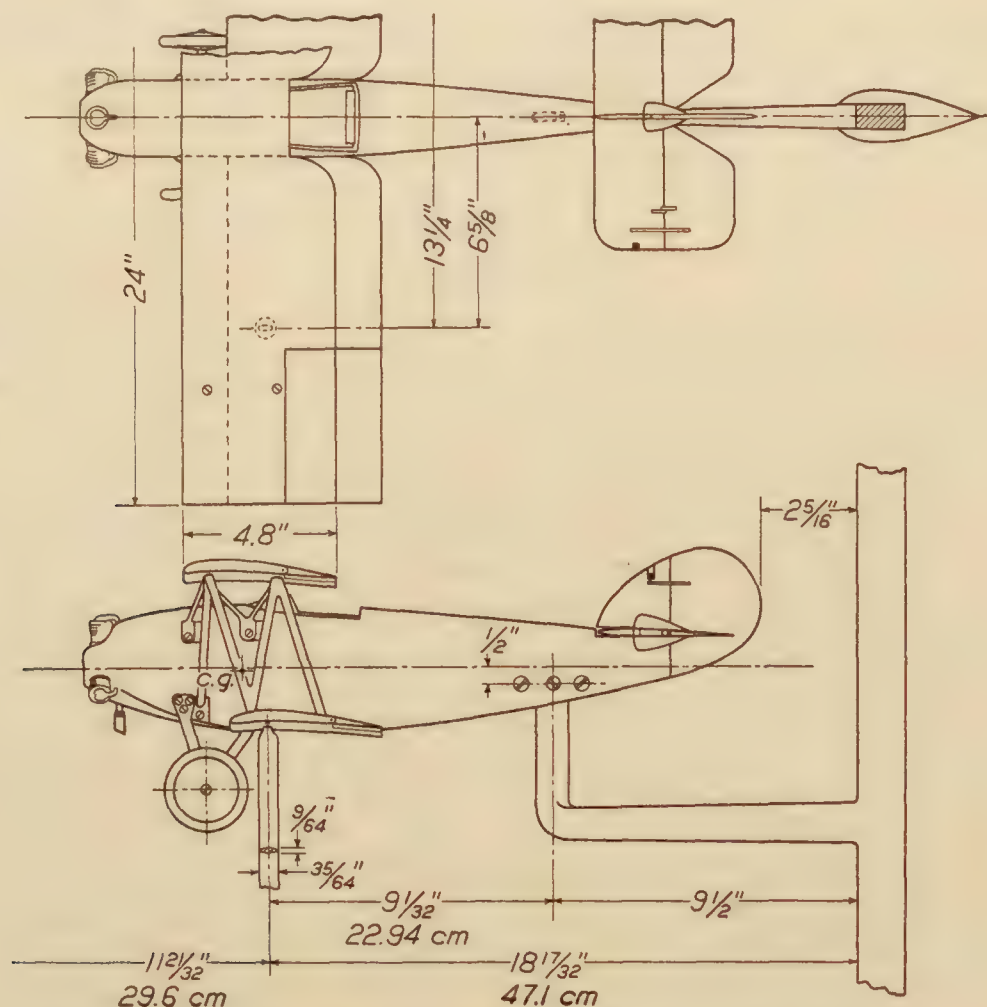


FIG. 1.—Original Sperry Messenger model set up in variable density wind tunnel

METHOD OF TESTING

The original model of the Sperry Messenger as supplied by the Army Air Service was a geometrically similar replica of the airplane so far as the main dimensions were concerned, but many minor parts and details, including the propeller, were omitted in order to simplify the model construction. The original model, therefore, fairly represented the average wind-tunnel model in the amount of detail used.

During the tests the model was attached to the balance in the variable density wind tunnel by means of two vertical "stilts" of ordinary stream-line wire which were hinged at their upper ends to the wings and rigidly connected at their lower ends to the balance. The model was also connected to a vertical shielded balance bar on the down-stream side by means of a short skid which was hinged at the fuselage and rigidly attached to the bar. This arrangement allows the angle of attack to be changed readily. (Figs. 1 and 2.)

During a test run the tank pressure was held constant, and readings of the air forces and moments taken for various angles of attack. The drag and interference corrections for the attachments were determined by separate runs.

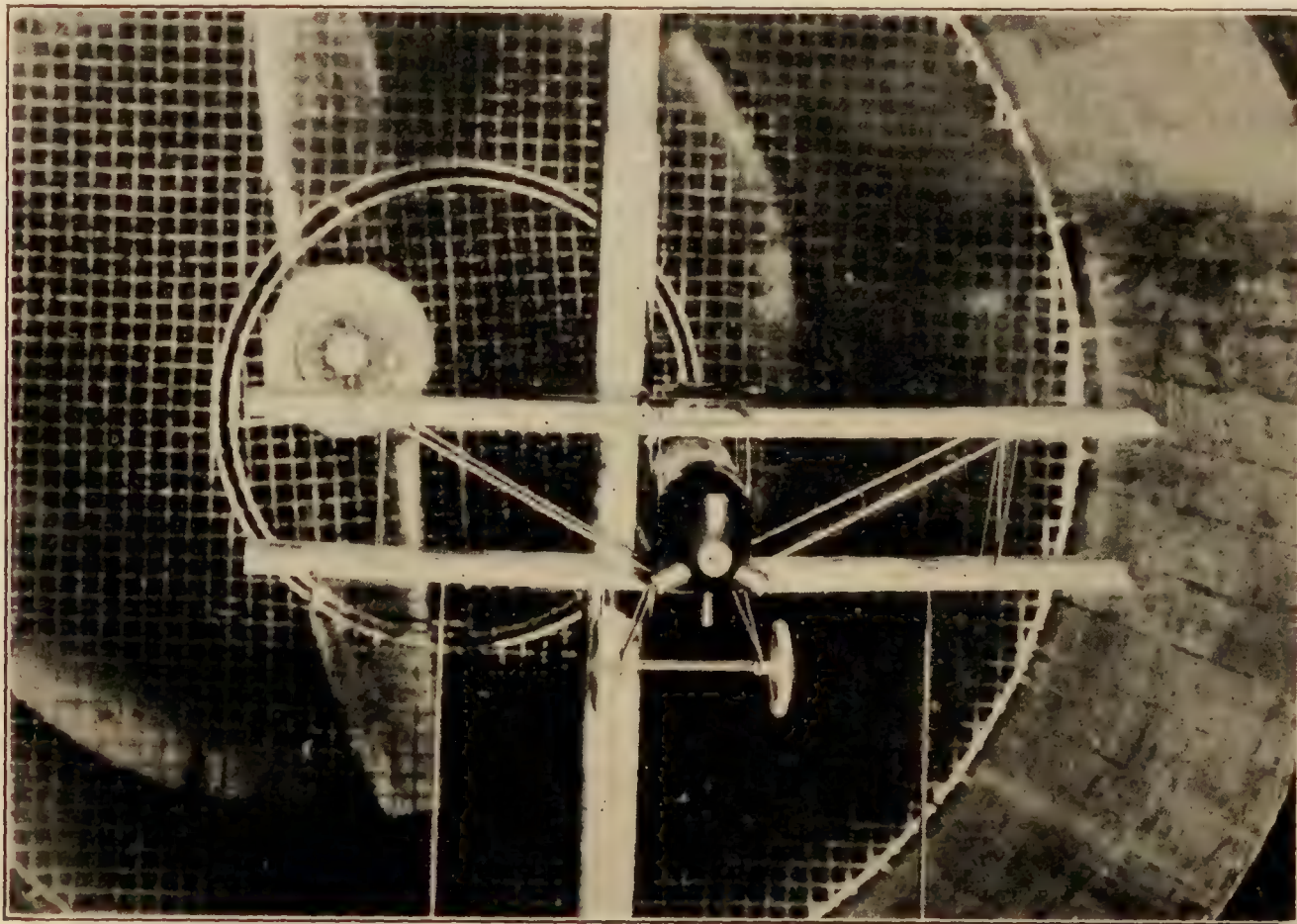


FIG. 2.—Method of supporting model

RESULTS OF THE TESTS

After completing a series of five runs on the original model it was decided to add to it as much detail as practicable in order to get a more exact geometrical similarity. Accordingly 31 changes were made as follows (figs. 3 and 4):

1. New air intake added to carbureter.
2. Oil filler cap added.
3. Fuel tank drain cock added.
4. Oil valve and drain cock added.
5. Pan built up on under side of fuselage.
6. Brass plates added to the sides and bottom of fuselage to approximate bomb rack supports.
7. Chain and sprockets added to side of fuselage.
8. Strips added along top longeron of fuselage.
9. Control cables, horns, and wires added to horizontal tail surfaces.
10. Hole made in under side of fuselage near tail skid.
11. Holes made in stabilizer for control wires.
12. Small fin removed from rudder and fin.
13. Aileron horns and inter aileron struts added with wires running into wing.
14. Cross wires and shock absorbers added to landing gear.
15. Cross wires added in center section above fuselage.
16. Pilot tube added on outer strut.
17. Trailing edge of upper wing altered at center section and hand holes added.
18. Edges of wing changed from round to straight at center section.
19. Angle of attack bomb and cable with rack for bomb added.
20. New engine constructed with fins and valve gear.
21. Length of cockpit changed and hollowed out.
22. Height of wind shield changed.
23. Bump added on top of the fuselage forward as in the full-size airplane.
24. Groove added in ailerons at top and bottom for hinge gap.
25. Wires added to fuselage sides near nose to approximate hinges on cowling.
26. Nose of fuselage hollowed out behind the propeller.
27. Ball bearing propeller hub added.
28. Ailerons fastened in position with screws at ends.
29. Ends of tie struts beveled off at fuselage.
30. Brace wires added between stabilizer and fin.
31. Turnbuckles on all wires approximated by twisting the ends.

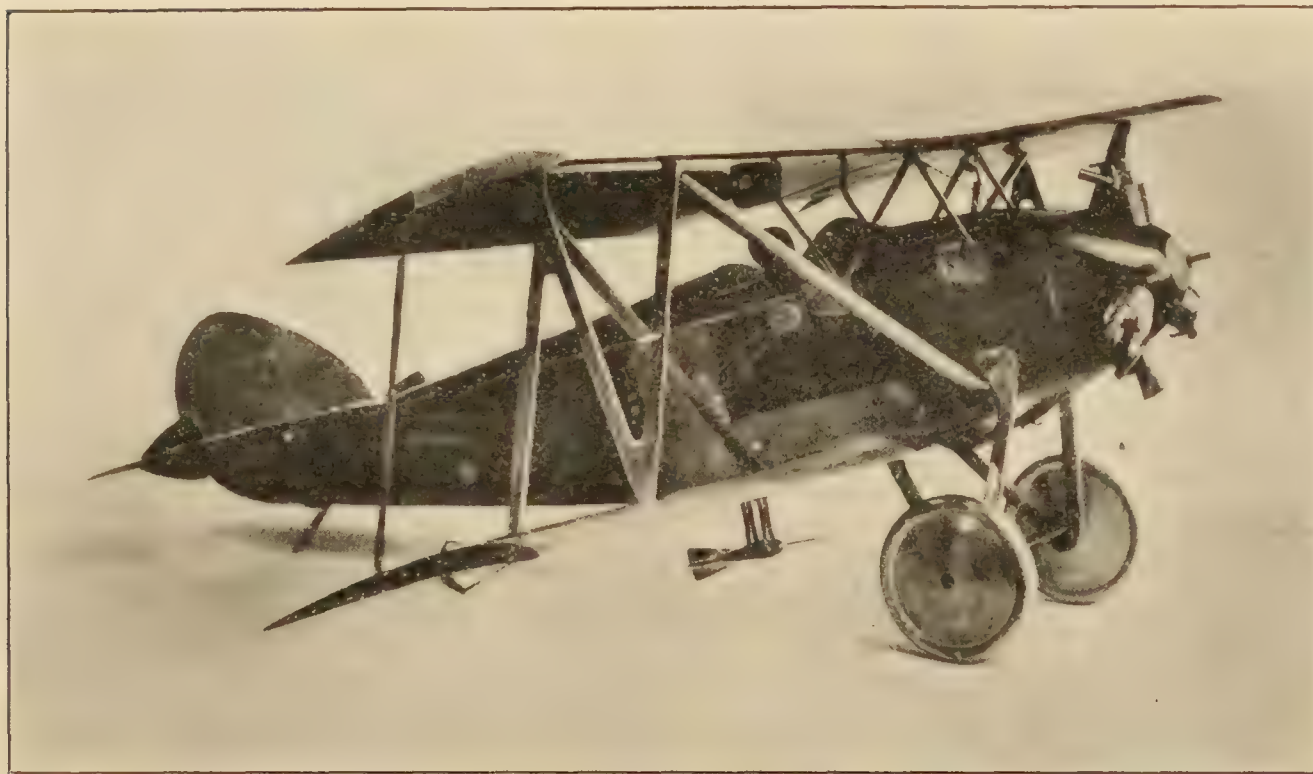


FIG. 3.—View of modified model



FIG. 4.—Three-quarter rear view of model

Upon completion of these changes a series of three runs was made on the modified model. The results of the two series of tests are given in Tables I to VIII and on Figures 5, 6, and 7. The lift coefficient C_L and the drag coefficient C_D are computed by dividing the measured lift or drag by the wing area and the dynamic pressure. The moment coefficient is computed by

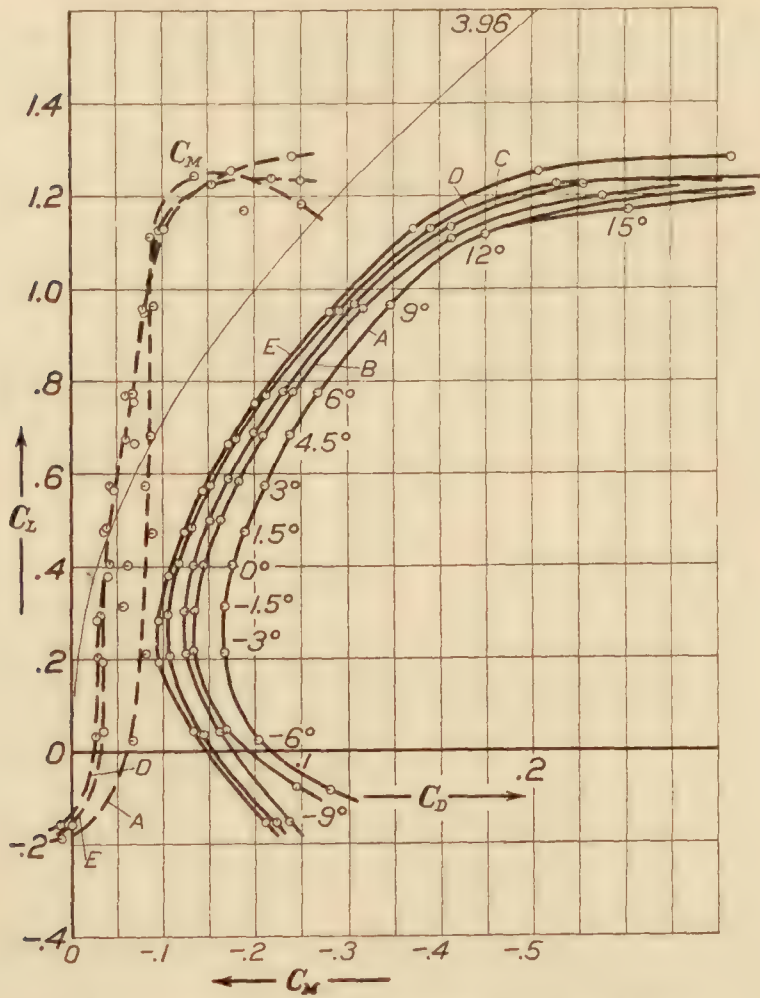


FIG. 5.—Sperry Messenger Original, U. S. A. 5 wings

	Tank pres- sure atmos- phere	Dynamic pressure $q = \text{kg/m}^2$	Reynolds Number
Curve A	1.00	27.9	189,000
Curve B	2.82	80.5	482,000
Curve C	4.83	140.0	820,000
Curve D	10.00	297.0	1,670,000
Curve E	19.86	619.0	3,400,000

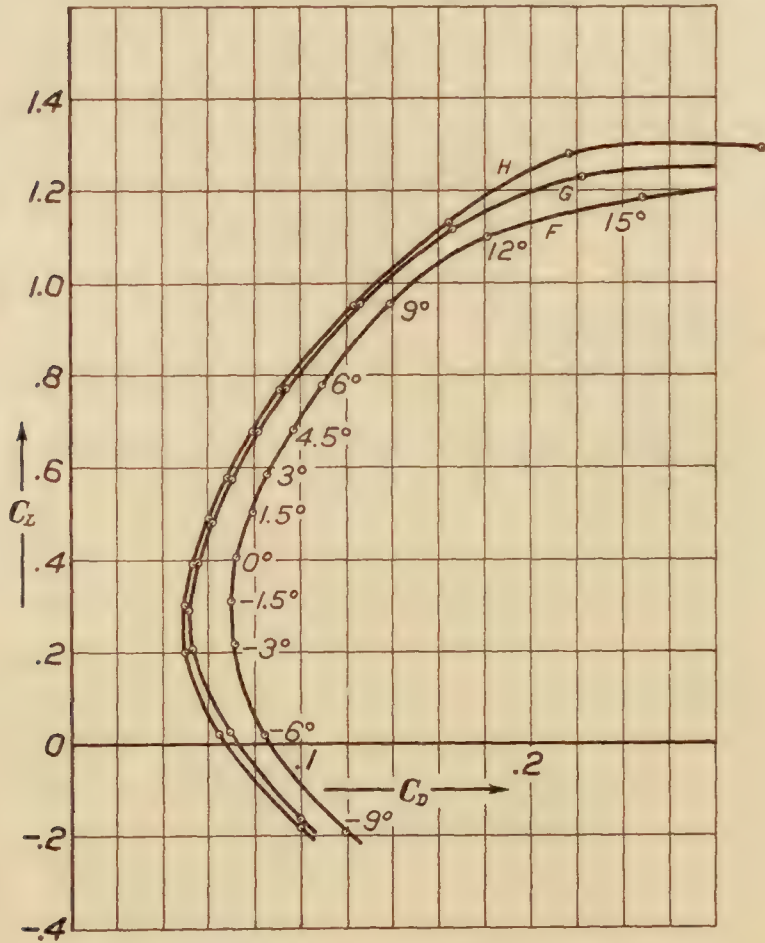


FIG. 6.—Sperry Messenger, modified, U. S. A. 5 wings

	Tank pres- sure atmos- pheres	Dynamic pressure $q = \text{kg/m}^2$	Reynolds Number
Curve F	1.00	26.85	165,000
Curve G	10.30	290.00	1,600,000
Curve H	20.80	637.00	3,450,000

dividing the observed pitching moment about the specified center of gravity by the product of the wing area, the dynamic pressure and the wing chord. That is,

$$C_L = \frac{L}{qS}, \quad C_D = \frac{D}{qS}, \quad \text{and} \quad C_M = \frac{M_{c.g.}}{qCS}$$

The angle of attack is measured from the line of thrust. The Reynolds Number has been computed in the usual way, taking the wing chord as the characteristic length of the model.

An inspection of the test data shows that the scale effect on lift is negligible everywhere except at and near the maximum lift, the maximum effect being of the order of a 4 per cent increase in lift in passing from the Reynolds Number of an ordinary wind tunnel test to the full scale value.

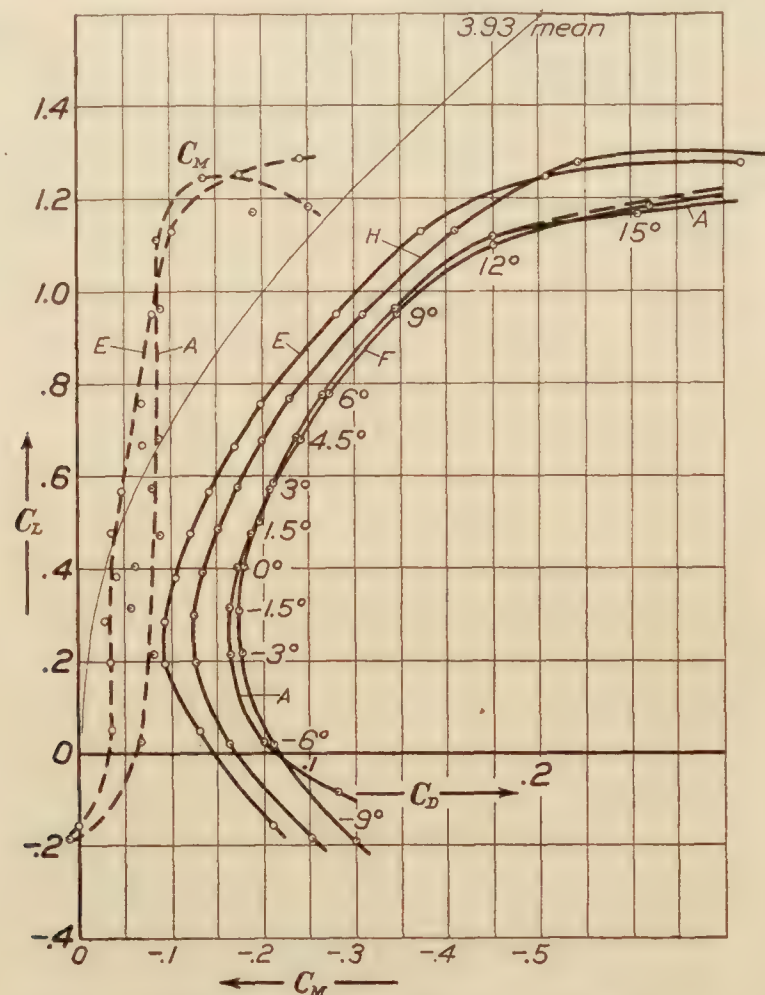


FIG. 7.--Sperry Messenger, U. S. A. 5 wings

		Tank pressure atmosphere	Dynamic pressure $q = \text{kg/m}^2$	Reynolds Number
Curve A	original	1.00	27.90	189,000
Curve E		19.86	619.00	3,400,000
Curve F	modified	1.00	26.85	165,000
Curve H		20.80	637.00	3,450,000

Figure 8 has been prepared to bring out the effect of scale on drag by plotting logarithmically the drag coefficient at a given angle of attack against Reynolds Number. In each case, for the original model, it is found that the experimental points lie on a straight line, showing that the drag varies as $\left(\frac{Vl}{\nu}\right)^n$. For the modified model only three points are available at each angle of attack, but these points also lie on straight lines, which appear to be justified by the more complete data in the first series. The value of the exponent n varies with angle of attack as follows:

Angle of attack α	Original model n	Modified model n
-6°	-0.17	-0.10
0°	-.15	-.09
6°	-.11	-.06
12°	-.07	-.045
18°	-.07	-.045

The absolute decrease in drag in passing from the lowest to the highest Reynolds Number appears to be substantially independent of angle of attack except at the highest angle -18° . These differences are as follows:

Angle of attack α	Original model			Modified model		
	C_D at		ΔC_D	C_D at		ΔC_D
	R. N. = 189,000	R. N. = 3,400,000		R. N. = 165,000	R. N. = 3,450,000	
-6°	0.0811	0.0530	0.0281	0.0846	0.0648	0.0198
0°	.0701	.0423	.0278	.0725	.0539	.0186
$+6^\circ$.1075	.0800	.0275	.1088	.0916	.0172
12°	.1800	.1495	.0305	.1808	.1635	.0173
18°	.3551	.2875	.0676	.3434	.3002	.0432

The great increase at 18° is no doubt due to the change in type of flow which is beginning to occur at this angle. At lower angles the scale effect apparently agrees very closely in form with that predicted by Diehl (Reference 1) from his study of test data at low Reynolds Numbers.

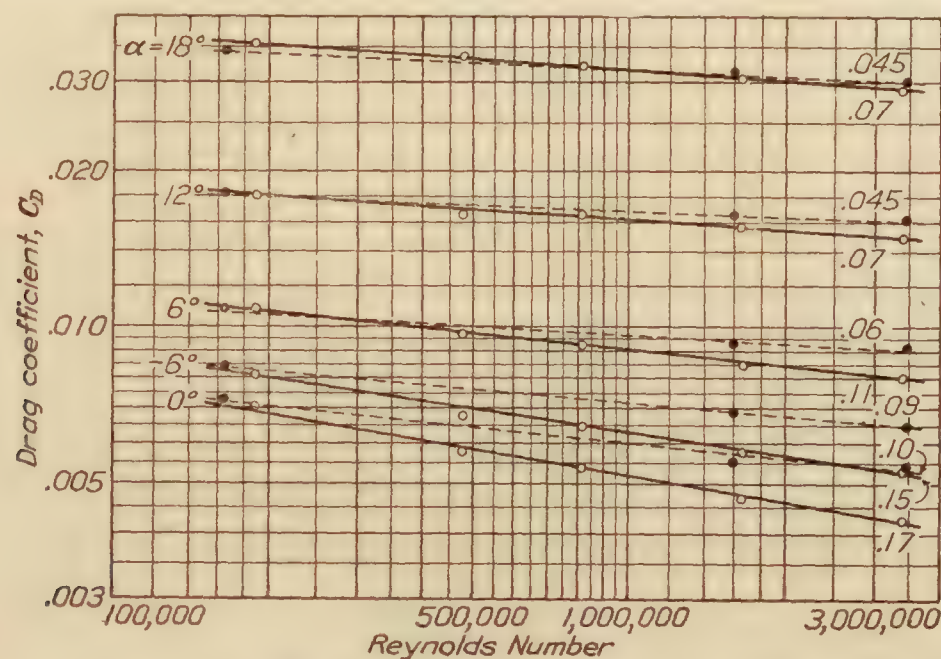


FIG. 8.—Variation of drag coefficient with Reynolds Number for Sperry Messenger model. Variable Density Wind Tunnel

The differences between the absolute drags and the exponents for the original and modified models can not be entirely accounted for at this time. A study of the list of changes will show that while some tend to increase the drag and others reduce it, there is a preponderance in favor of an increase in drag. It is possible, of course, that the drag of some of the added parts, when measured on the model with the mutual interferences present, may increase more rapidly than the square of the Reynolds Number. The curves of the drag coefficient against Reynolds Number for such parts could slope upward to the right on the logarithmic plot, and partially explain not only the lower exponents for the modified model but also close agreement between the drag of the two models at low Reynolds Number.

The research on the Sperry Messenger airplane has not progressed far enough to make possible a complete comparison between the model and full scale data. Based on the free flight data at hand the conclusion is reached that the modified model gives results which are not only substantially correct and in better agreement with free flight than those given by the original model but that the differences are in the same direction. That is, it would appear that the more exact a model is made the more nearly will the test data obtained in the variable density wind tunnel agree with full scale.

These results have a direct bearing on the tests of airplane models made at low values of Reynolds Number in atmospheric wind tunnels, in that they show the common practice of using

simplified models to be unjustified and the test data without meaning unless corrections are applied not only for the omitted parts but also for the scale effect. At present the scale effect correction is rather uncertain, but the variable density wind tunnel will be able eventually to supply the necessary information. A preliminary study indicates that a large part of the scale effect may be due to the model struts and wires, in which case a partial scale effect correction may be readily applied with data now available. Too much emphasis can not be laid on the unsoundness of the assumption that test data obtained on a simplified model can be used without corrections to predict full-scale performance.

CONCLUSIONS

Owing to the preliminary nature of this report, it is impractical to draw any but the most general conclusions, as follows:

1. The scale effect on lift appears negligible except at the maximum lift where a 4 per cent increase was obtained by a twenty-fold increase in Reynolds Number. This effect probably varies with the wing section and arrangement.

2. The scale effect on drag is represented by an exponential variation with Reynolds Number. That is, $C_D \propto \left(\frac{Vl}{\nu}\right)^n$ where the exponent n is probably of the order of -0.10 .

3. A model must represent the full size airplane as accurately as possible if the data obtained from tests in the variable density wind tunnel are to be valid.

4. The test data appear to justify the principle of the variable density wind tunnel, which now offers an extremely valuable means not only of supplying data free from scale effect but also of studying scale effect and similar design problems.

5. The common assumption that data obtained on simplified airplane models at low Reynolds Numbers can be used without corrections to predict full scale performance is unsound and may lead to absurd results in certain cases.

More test data are required along the lines covered by this report before final conclusions can be drawn. It is recommended in particular that the effect of the major changes made on the original Sperry Messenger model be investigated one at a time in order to find the cause or causes for the very slight effect of the changes at low Vl . It is also recommended that a similar research be made on another airplane of a different type, for example, a bomber or a very simple monoplane.

BIBLIOGRAPHY

1. Diehl, W. S. The Variation of Aerofoil Lift and Drag Coefficients with Changes in Size and Speed. 1921. N. A. C. A. Technical Report No. 111.

TABLE I

SPERRY MESSENGER MODEL (ORIGINAL)

Span, 24 inches (61 cm); area, 0.139 m².
Chord, 4.8 inches (12.2 cm); U. S. A. 5 airfoil.

Angle of attack, degrees	Dynamic pressure, $q = \text{kg/m}^2$	Lift coefficient, C_L	Drag coefficient, C_D	Moment coefficient, C_M	$\frac{C_L}{C_D}$
-9.0	27.8	-0.186	0.1121	+0.012	-1.66
-6.0	28.0	.023	.0811	-.066	2.84
-3.0	28.2	.212	.0667	-.083	3.17
-1.5	27.8	.313	.0668	-.057	4.68
0.0	27.8	.406	.0701	-.062	5.79
1.5	28.2	.472	.0757	-.088	6.23
3.0	28.0	.572	.0840	-.081	6.80
4.5	28.0	.683	.0952	-.087	7.17
6.0	28.0	.775	.1075	-.067	7.21
9.0	28.1	.962	.1393	-.090	6.90
12.0	28.0	1.115	.1800	-.086	6.20
15.0	28.1	1.168	.2424	-.184	4.82
18.0	27.8	1.244	.3551	-.136	3.50
21.0	27.4	1.181	.4572	-.250	2.58

¹ Moments taken about the center of gravity.

Average temperature, 20° C.; average tank pressure, 1 atmosphere; average Reynolds Number, 189,000.

TABLE II

SPERRY MESSENGER MODEL (ORIGINAL)

Span, 24 inches (61 cm); area, 0.139 m².
Chord, 4.8 inches (12.2 cm); U. S. A. 5 airfoil.

Angle of attack, degrees	Dynamic pressure, $q = \text{kg/m}^2$	Lift coefficient, C_L	Drag coefficient, C_D	$\frac{C_L}{C_D}$
-9.0	79.7	-0.139	0.0978	-1.42
-6.0	80.0	+.048	.0675	0.71
-3.0	80.6	.219	.0535	4.08
-1.5	80.6	.305	.0540	5.64
0.0	81.3	.402	.0579	6.93
1.5	81.0	.498	.0653	7.62
3.0	81.0	.583	.0735	7.93
4.5	81.5	.681	.0839	8.11
6.0	81.5	.775	.0965	8.03
9.0	81.5	.957	.1272	7.51
12.0	81.5	1.107	.1657	6.68
15.0	81.4	1.197	.2308	5.18
18.0	79.8	1.225	.3357	3.65
21.0	79.8	1.191	.4380	2.72

Average temperature, 23° C.; average tank pressure, 2.82 atmospheres; average Reynolds Number, 482,000.

TABLE III

SPERRY MESSENGER MODEL (ORIGINAL)

Span, 24 inches (61 cm); area, 0.139 m².
Chord, 4.8 inches (12.2 cm); U. S. A. 5 airfoil.

Angle of attack, degrees	Dynamic pressure, $q = \text{kg/m}^2$	Lift coefficient C_L	Drag coefficient C_D	Moment coefficient ¹ C_M	$\frac{C_L}{C_D}$
-9.0	140	-0.151	0.0943	-0.007	-1.60
-6.0	140	+.041	.0646	-.015	0.63
-3.0	140	.213	.0500	-.043	4.26
-1.5	142	.306	.0492	-.049	6.21
0.0	140	.402	.0535	-.055	7.48
1.5	140	.498	.0602	-.055	8.28
3.0	142	.590	.0684	-.077	8.62
4.5	141	.690	.0799	-.069	8.62
6.0	140	.779	.0922	-.097	8.45
9.0	139	.966	.1234	-.075	7.76
12.0	139	1.134	.1651	-.075	6.87
15.0	138	1.224	.2223	-.161	5.52
18.0	138	1.220	.3222	-.187	3.79
21.0	136	1.189	.4272	-.238	2.78

¹ Moments taken about the center of gravity.

Average temperature, 26° C.; average tank pressure, 4.83 atmospheres; average Reynolds Number, 820,000.

TABLE IV

SPERRY MESSENGER MODEL (ORIGINAL)

Span, 24 inches (61 cm); area, 0.139 m².
Chord, 4.8 inches (12.2 cm); U. S. A. 5 airfoil.

Angle of attack, degrees	Dynamic pressure, $q = \text{kg/m}^2$	Lift coefficient C_L	Drag coefficient C_D	Moment coefficient ¹ C_M	$\frac{C_L}{C_D}$
-9.0	292	-0.158	0.0888	+0.013	-1.78
-6.0	298	+.035	.0573	-.026	+0.61
-3.0	295	.207	.0428	-.029	4.83
-1.5	298	.297	.0421	-.032	7.05
0.0	293	.409	.0468	-.042	8.75
1.5	298	.487	.0529	-.038	9.20
3.0	298	.575	.0608	-.043	9.45
4.5	298	.676	.0719	-.060	9.39
6.0	298	.770	.0849	-.061	9.07
9.0	299	.952	.1166	-.078	8.17
12.0	298	1.127	.1562	-.096	7.22
15.0	298	1.225	.2112	-.154	5.81
18.0	298	1.237	.3023	-.219	4.09
21.0	293	1.233	.4148	-.250	2.97

¹ Moments taken about the center of gravity.

Average temperature, 34° C.; average tank pressure, 10 atmospheres; average Reynolds Number, 1,670,000.

TABLE V

SPERRY MESSENGER MODEL (ORIGINAL)

Span, 24 inches (61 cm); area, 0.139 m².
Chord, 4.8 inches (12.2 cm); U. S. A. 5 airfoil.

Angle of attack, degrees	Dynamic pressure, $q = \text{kg/m}^2$	Lift coefficient C_L	Drag coefficient C_D	Moment coefficient ¹ C_M	$\frac{C_L}{C_D}$
-9.0	616	-0.158	0.0841	+0.001	-1.88
-6.0	617	.024	.0530	-.034	+0.45
-3.0	621	.193	.0380	-.034	5.08
-1.5	619	.284	.0380	-.028	7.47
0.0	622	.380	.0423	-.041	8.98
1.5	621	.475	.0490	-.036	9.71
3.0	621	.563	.0573	-.047	9.83
4.5	622	.664	.0684	-.068	9.71
6.0	623	.754	.0800	-.069	9.42
9.0	621	.949	.1124	-.080	8.44
12.0	619	1.130	.1495	-.102	7.57
15.0	619	1.253	.2033	-.175	5.68
18.0	611	1.285	.2875	-.241	4.47

¹ Moments taken about the center of gravity of full scale airplane.

Average temperature, 35° C.; average tank pressure, 19.86 atmospheres; average Reynolds Number, 3,400,000.

TABLE VI

SPERRY MESSENGER MODEL (MODIFIED)

Span, 24 inches (61 cm); area, 0.1377 m².
Chord, 4.8 inches (12.2 cm); U. S. A. 5 airfoil.

Angle of attack, degrees	Dynamic pressure, $q = \text{kg/m}^2$	Lift coefficient C_L	Drag coefficient C_D	$\frac{C_L}{C_D}$
-9.0	26.6	-0.191	0.1203	-1.59
-6.0	26.7	.019	.0846	0.22
-3.0	26.9	.216	.0707	3.05
-1.5	26.9	.310	.0699	4.43
0.0	26.9	.405	.0725	5.74
1.5	26.9	.500	.0787	6.35
3.0	26.7	.582	.0850	6.85
4.5	26.8	.679	.0967	7.01
6.0	26.8	.776	.1088	7.14
9.0	26.8	.952	.1393	6.83
12.0	26.8	1.098	.1808	6.08
15.0	26.8	1.184	.2478	4.78
18.0	26.8	1.225	.3434	3.57
21.0	26.7	1.238	.4528	2.73

Average temperature, 25° C.; average tank pressure, 1 atmosphere; average Reynolds Number, 165,000.

TABLE VII

SPERRY MESSENGER MODEL (MODIFIED)

Span, 24 inches (61 cm); area, 0.1377 m².
Chord, 4.8 inches (12.2 cm); U. S. A. 5 airfoil.

Angle of attack, degrees	Dynamic pressure, $q = \text{kg/m}^2$	Lift coefficient C_L	Drag coefficient C_D	$\frac{C_L}{C_D}$
-9.0	290	-0.167	0.1001	-1.67
-6.0	293	+0.024	.0687	+0.35
-3.0	292	.204	.0526	3.78
-1.5	291	.293	.0509	5.76
0.0	290	.396	.0550	7.19
1.5	290	.486	.0614	7.91
3.0	290	.575	.0698	8.23
4.5	290	.679	.0808	8.40
6.0	290	.773	.0930	8.31
9.0	290	.954	.1251	7.75
12.0	290	1.114	.1651	6.75
15.0	290	1.228	.2214	5.55
18.0	286	1.244	.3144	3.96
21.0	285	1.223	.4216	2.90

Average temperature, 44° C.; average tank pressure, 10.3 atmospheres; average Reynolds Number, 1,600,000.

TABLE VIII

SPERRY MESSENGER MODEL (MODIFIED)

Span, 24 inches (61 cm); area, 0.1377 m².
Chord, 4.8 inches (12.2 cm); U. S. A. 5 airfoil.

Angle of attack, degrees	Dynamic pressure, $q = \text{kg/m}^2$	Lift coefficient C_L	Drag coefficient C_D	$\frac{C_L}{C_D}$
-9.0	628	-0.183	0.1005	-1.82
-6.0	634	+0.019	.0648	+0.29
-3.0	637	.196	.0504	3.88
-1.5	637	.300	.0501	5.99
0.0	634	.390	.0539	7.24
1.5	639	.487	.0610	7.98
3.0	635	.575	.0689	8.34
4.5	644	.675	.0796	8.48
6.0	643	.767	.0916	8.36
9.0	648	.951	.1236	7.71
12.0	638	1.128	.1635	6.90
15.0	630	1.279	.2166	5.92
18.0	632	1.293	.3002	4.31

Average temperature, 39° C.; average tank pressure, 20.8 atmospheres; average Reynolds Number, 2,450,000.

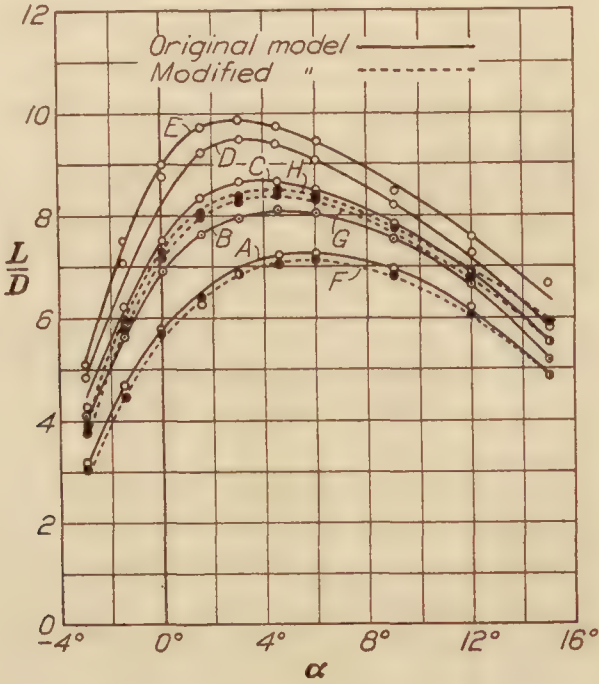


FIG. 9.—Variation of L/D with Reynolds Number

	Tank pressure atmospheres	Reynolds Number
A.....	1.00	189,000
B.....	2.82	482,000
C.....	4.83	820,000
D.....	10.00	1,670,000
E.....	19.86	3,400,000
F.....	1.00	165,000
G.....	10.30	1,600,000
H.....	20.80	3,450,000

REPORT No. 226

CHARACTERISTICS OF A BOAT TYPE SEAPLANE DURING TAKE-OFF

By J. W. CROWLEY, Jr., and K. M. RONAN
Langley Memorial Aeronautical Laboratory

REPORT No. 226

CHARACTERISTICS OF A BOAT TYPE SEAPLANE DURING TAKE-OFF

By J. W. CROWLEY, Jr., and K. M. RONAN

SUMMARY

This report, on the planing and get-away characteristics of the *F-5-L*, gives the results of the second of a series of take-off tests on three different seaplanes conducted by the National Advisory Committee for Aeronautics at the suggestion of the Bureau of Aeronautics, Navy Department. The single-float seaplane was the first tested (Reference 1) and the twin-float seaplane is to be the third.

The characteristics of the boat type were found to be similar to the single float, the main difference being the increased sluggishness and the relatively larger planing resistance of the larger seaplane. At a water speed of 15 miles per hour the seaplane trims aft to about 12° and remains in this angular position while plowing. At 22.5 miles per hour the planing stage is started and the planing angle is immediately lowered to about 10° . As the velocity increases the longitudinal control becomes more effective but overcontrol will produce instability. At the get-away the range of angle of attack is 19° to 11° with velocities from the stalling speed through about 25 per cent of the speed range.

INTRODUCTION

Seaplanes with a hull of the boat type are generally used for weight-carrying purposes. They usually have large wing and power loadings and a small reserve power. The water resistance of a hull while carrying a major portion of the seaplane's weight will necessarily be large and as the efficiency of the propeller is then low the reserve thrust at the peak resistance is seldom large. If, therefore, the planing characteristics of a new design are inferior the boat-type seaplane will require an excessively long run or may even be unable to get away under unfavorable conditions. It is believed that the information contained in this report will prove of considerable value in aiding the designer in the testing and selecting of a suitable seaplane hull.

The seaworthiness of the *F-5-L* makes it admirably fitted for a planing test as it is certainly better to be able to study the characteristics without discounting for objectional serviceable features. The *F-5-L* will weather and get away in as rough a sea as any other seaplane of its size; it will not dive at low speeds nor porpoise at high speeds. In fact, one believes it is probably even a little too statically stable than compatible with ease in breaking loose from smooth water when heavily loaded and it is too sluggish for damping the pitching set up by waves, although this might also be attributed to the inefficient unbalanced elevators, the effective use of which requires a large force. In general the more recent weight-carrying seaplanes have smaller power loadings and larger wing and float loadings. The effect of the large power loading of the *F-5-L* is favorable for amplifying its characteristics (see appendix) while the effect of a greater weight for the same wing and float area is usually to require an increase in the water speed for the various stages.

As will be explained later, the test is not as truly characteristic of the *F-5-L* as was desired and if compared specifically with model tests of the *F-5-L*, judgment should be exercised in formulating any criteria in the relations of model tests to the full scale. However, it is believed that the results as noted with reservations are quite representative.

METHODS AND APPARATUS

A synchronized time-history record of air speed, water speed, and planing angles was obtained for as varied take-off conditions as possible. Before the desired number of check runs and addi-

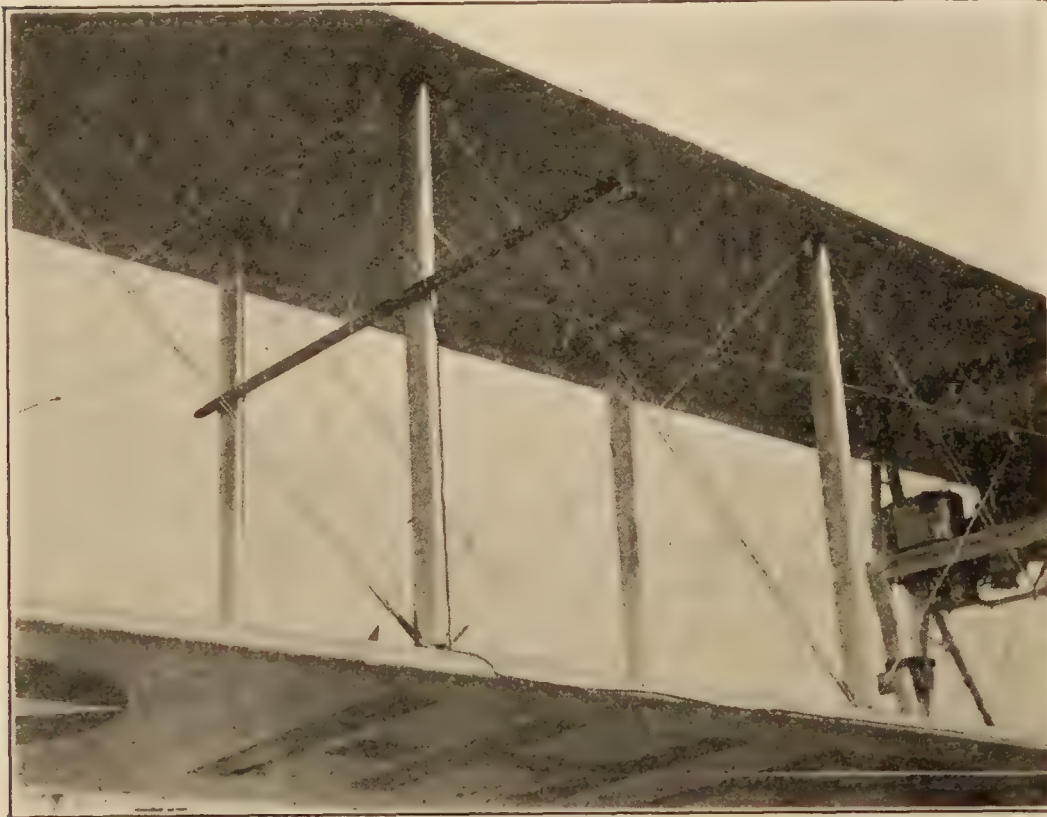


FIG. 1.—Mounting of vane for determining planing angle

The planing angles were obtained by a vane, mounted on a boom extending ahead of the wings (fig. 1), which was free to align itself with the relative wind. The position of the vane was recorded by a special galvanometer, (Reference 3) mounted in the cockpit, to which the vane was electrically connected.

The water speed was measured by a Pitot tube extended through a breather hole aft of the rear step (fig. 2). This was lowered into position after the seaplane was on the water. Due to the sharp V bottom the tube had to be extended 2 feet below the breather hole to be below the keel. Even when the tube was made of $\frac{1}{4}$ -inch hydraulic tubing it was permanently deflected by the landing impact, so that it had to be braced by a cable from the front breather hole. The resistance of the tube and cable was considerable at high speeds. This was emphasized on a calm day, when with a total weight of 14,200 pounds (1,200 pounds overload) the seaplane could not get off with the water speed apparatus lowered. From previous and subsequent experience it has been found that a short Pitot tube extended below the keel makes the best type of water speed head. On the *F-5-L* the use of such a tube fixed on the keel was impossible, due to launching difficulties, while a tube which could be lowered



FIG. 2.—Water speed head lowered into position

tional water speed and angle of attack calibrations were obtained the seaplane threw a propeller and damaged the wings to such an extent that it was necessary to dismantle it. It was not deemed worth while to reinstall the apparatus in another seaplane, nor was this possible as there was not another one available at that time.

The air speed was indicated by a Baden double-Venturi meter and a N. A. C. A. air speed recorder. (Reference 2.) The indicating accuracy of the Venturi head is not as good as that of a Pitot-static head, but due to the larger pressure difference given by it the accuracy of reading low speeds is considerably increased.

through the keel after launching was impracticable because of the structural work necessary, so that the breather hole was used as previously mentioned. Two low-speed points on the water speed calibration curve were obtained by taxiing over a measured course. These showed the indicated water speed to be slightly high. It was assumed that this effect would be lessened as the float raised in the water and the results are corrected accordingly.

To ascertain the natural characteristics, the amount of controllability, and the effects of different control moments, four piloting methods were used. These are designated on the curves as control free, control forward, control back, and normal. Nearly every pilot has a slightly different method of making a take-off, which is also subject to some change depending upon the conditions of load, water, wind, etc. It is therefore very difficult to describe what may be considered a universal method of making a normal take-off. The following description of a normal take-off was made by a pilot of wide experience in naval aeronautics, but as will be noted later this is not entirely similar to the normal method used by the pilots on this investigation: "Give the engine full throttle, hold some up elevator until headway is on, then pull up the elevator until the bow wave moves back to the pilot's seat. The seaplane should now have started planing. As soon as this is appreciably noticeable ease forward on the control, and as planing increases force the nose forward to break the step clear, then ease back on the control, and as the speed increases pull back, harder and harder, and the seaplane should fly off. If the drag is too great, or the seaplane unusually heavy, it may be necessary to flip the nose up, and ease the control forward, but do not rock. Several pulls may be necessary, but each will result in an increase of speed."

PRECISION

The precision to be expected is as follows:

Air speed.....	± 1 mile per hour.
Water speed.....	± 1.5 miles per hour.
Angle.....	$\pm 1^\circ$.
Time synchronization.....	± 0.5 second.

RESULTS

The time consumed for passing through the different stages and the time comparison of the different take-off methods have not been stressed because of the additional drag imposed in measuring the water speed and also, as previously mentioned, because of the inability to obtain sufficient check runs. The records have been studied with the idea of ascertaining general planing characteristics, such as the variation in angle and stability with velocity and control and a few evident resistance characteristics.

The results are contained in Figures 3 to 14. Figures 3 to 12 are records of the individual runs, and Figures 13 and 14 are summaries from the original. The point (*a*) where the water lift begins to become rapidly dynamic rather than buoyant, and thus starts the float to rise out of the water, and the point (*b*) where this process is nearly completed and the planing begins are noted by the terms "rising to step" and "planing on step," respectively. The point (*c*) where the float clears the water is noted as "take-off." The condition "planing on step" is not as well defined in the boat type seaplane as it is in the single-float type. It is believed that this is the effect of the more acute V bottom, necessitating immersing the lower part of the V in order to obtain the required lift, and thus preventing the clean planing characteristics of a flatter bottom (Reference 4). In this connection it was noticed that an unusually large turbulent wave of water at right angles to the front step was carried along throughout both the plowing and planing stages. This does not refer to the thin blister or spray of water thrown up from under the chine which is characteristic of all V bottoms. The disturbance in this region must cause considerable resistance.

Figures 3 and 4 show runs made with the control free. The angle assumed by a seaplane is determined by the combination of the planing balance and the air balance. The *F-5-L* does not have an adjustable stabilizer so that it is balanced for normal flying angles. If a seaplane's weights are adjusted correctly so that it will plane stably it is quite likely to align itself along a line parallel to the line of the two steps, which on the *F-5-L* is about $7\frac{1}{2}^\circ$ to the longitudinal axis. This angle is slightly greater than the cruising air balance and smaller than the

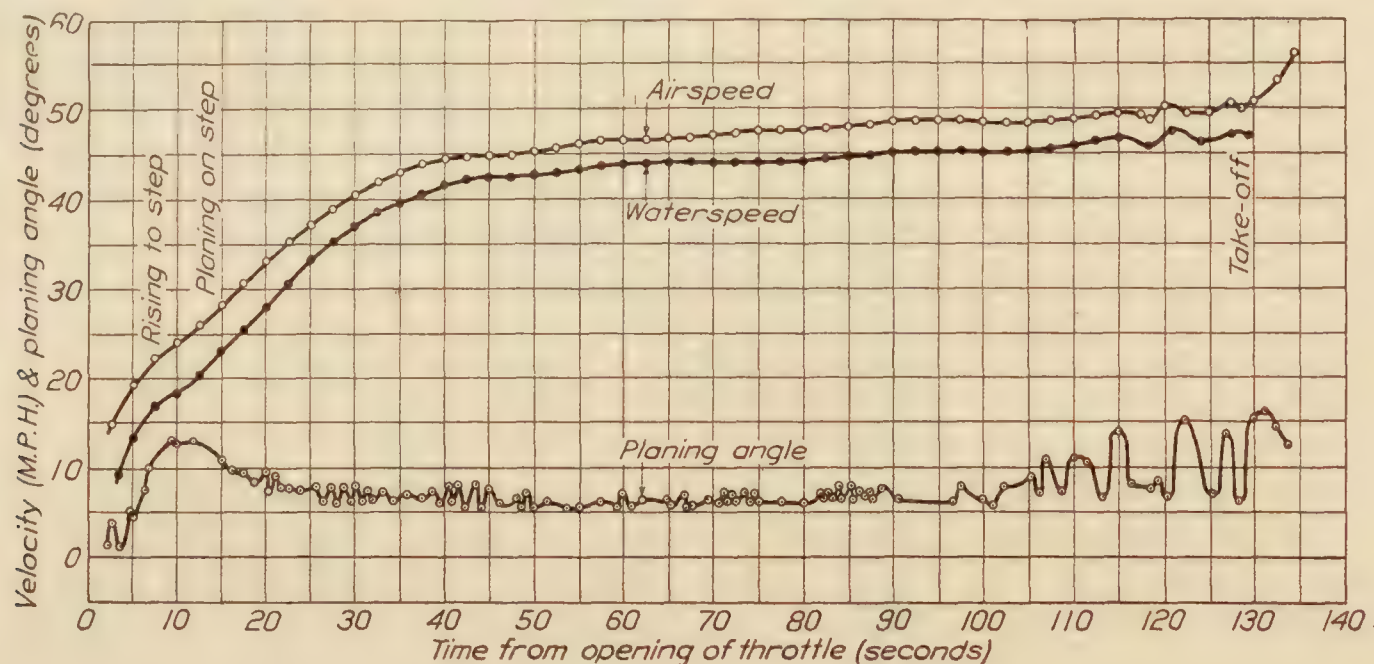


FIG. 3.—Method—Control free
(NOTE.—Pilot had to rock seaplane to get off)

average get-away angle. The run shown in Figure 3 made on smooth water shows that the *F-5-L* planes stably at about 7° . Oscillations are shown to build up slightly and then damp out. It is reasonable to suppose that the hull alone is slightly unstable while planing in smooth water but that the tail surfaces and wings counteract this instability. This feature, however, is not present on slightly rippled water, as is shown in Figure 4, and a slightly lower mean planing angle is maintained. These two characteristics were also evident on the single-float type. This instability is a favorable characteristic, as a float that is slightly unstable is liable to require a smaller moment to change the trim than a stable one. As shown in Figure 3, the pilot first

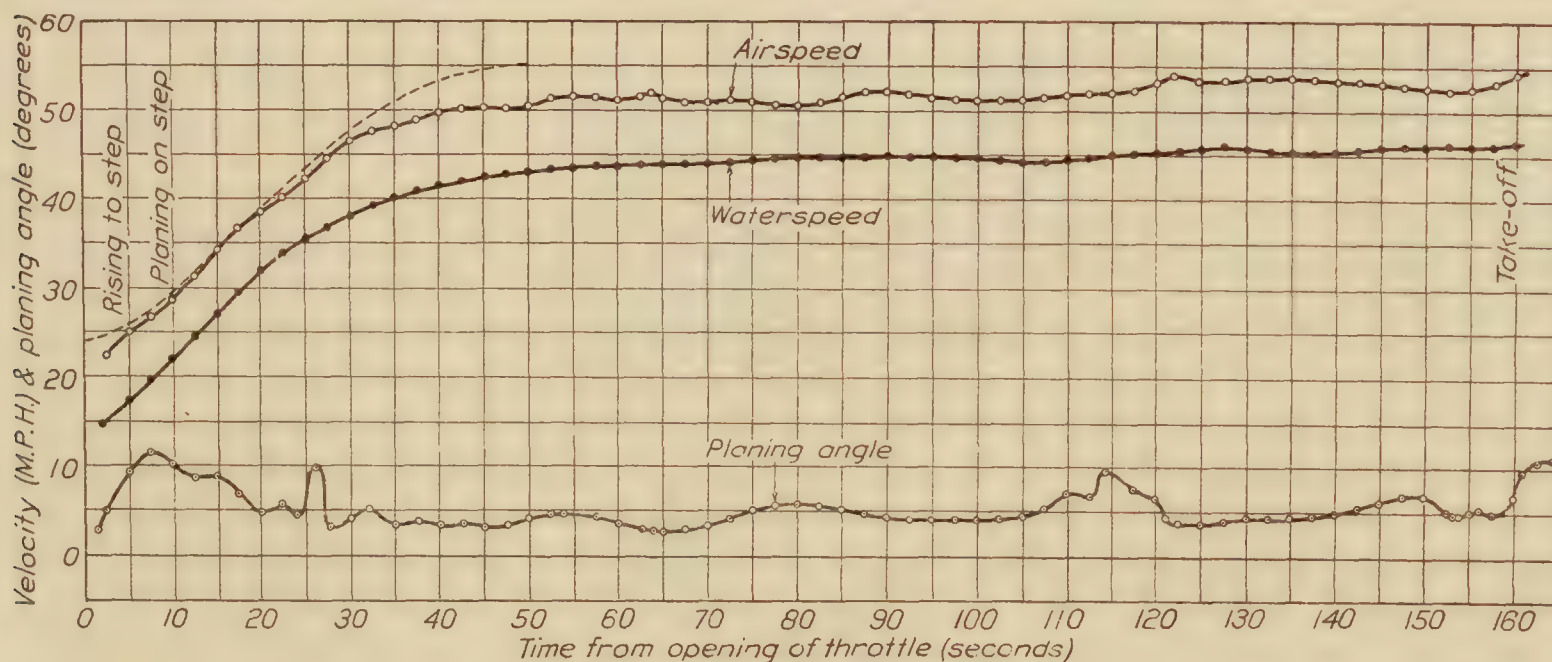


FIG. 4.—Method—Control free
(NOTE.—Pilot had to "pull seaplane off")

pulled the control back, but could not bring it to a high enough angle to get off, and then resorted to rocking. This inability to get off easily when heavily loaded on smooth water may be due, it has been suggested, to the insufficient curvature aft of the rear step. The amplitude of these oscillations shows clearly the ability to rock this seaplane through a large angular range. In the run shown in Figure 4 the increased air speed enabled a get-away to be made by pulling back on the control. It is noted that the seaplane rose to the step on smooth water even with

full load as quickly as if it had been assisted by "rocking." This was not true of the single-float seaplane.

One would think that if a seaplane would not get off with control free it would not do so by pushing the control forward. But Figure 5 shows this to be possible. In this particular run as soon as planing started large damped oscillations were set up, which became so violent toward the end that the pilot pulled back on the control and took off. It is quite probable

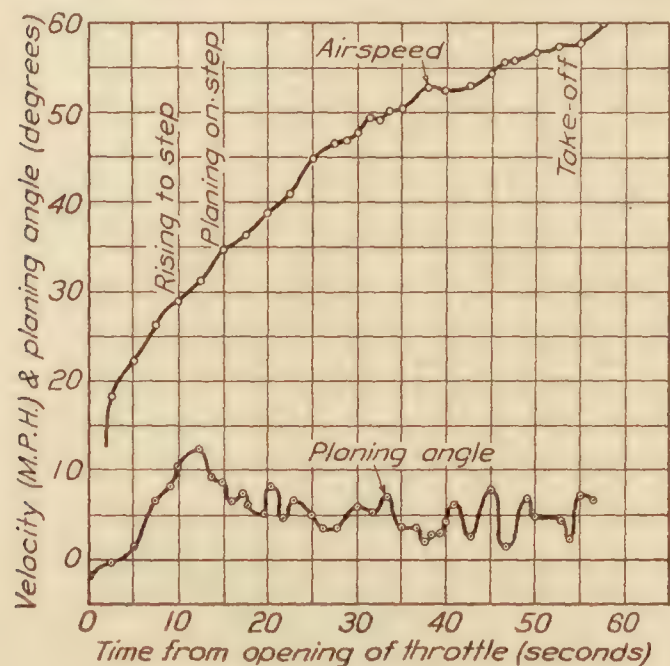


FIG. 5.—Method—Control forward
(NOTE.—Pilot "pulled seaplane off")

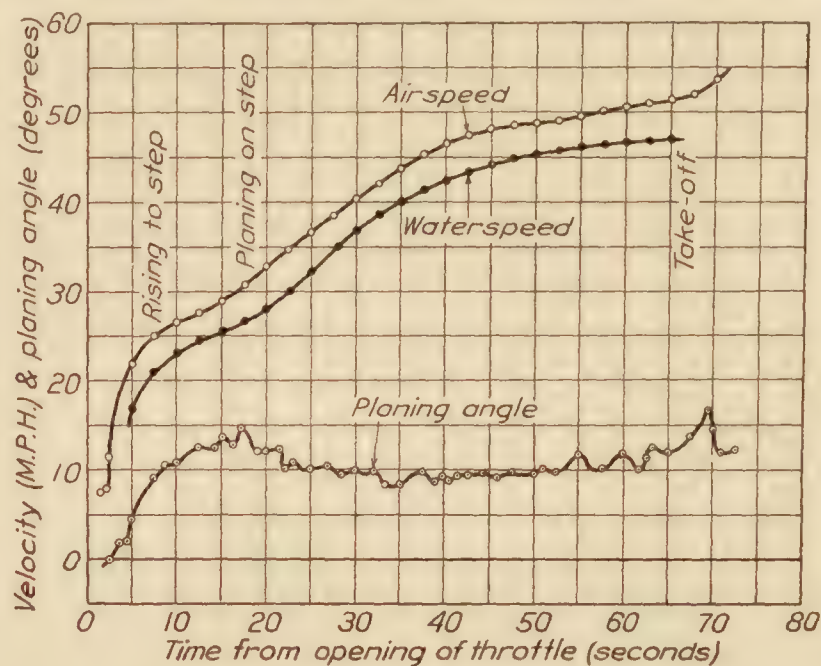


FIG. 6.—Method—Control back

that if he had kept the control forward the seaplane would have jumped out of the water during its oscillations. This is an example of porpoising often occurring in some seaplanes at high planing speeds, which is caused, as in this run, by the bow being held on the water. The inherent porpoising may be attributed to the same condition, but is brought about either by the center of gravity being located too far from the step or by a poor float form. Such was the case with an amphibian boat which has a tail skid extending below the keel aft of the rear step. This seaplane porpoised badly and it is believed that it was mainly due to the tail skid's tendency to hold the bow deeper in the water than it normally would have planed. Again noticing the

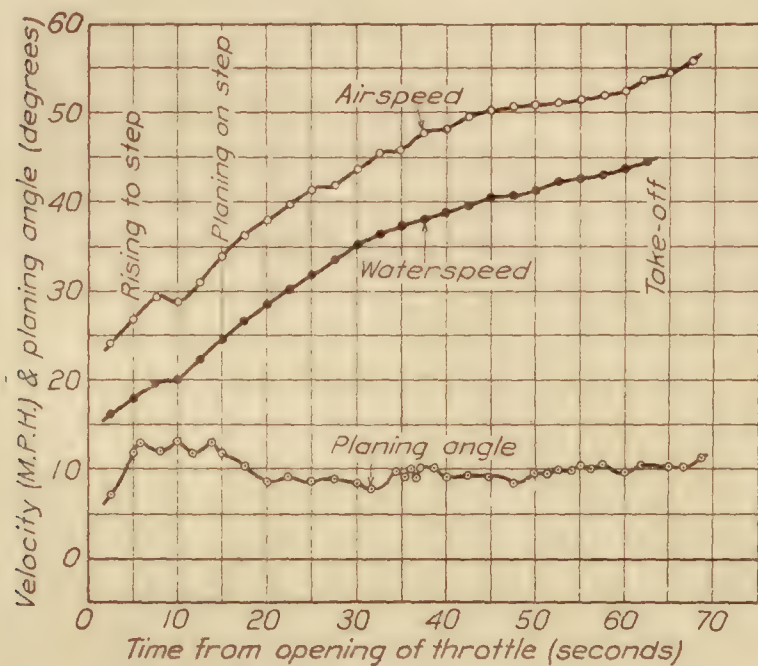


FIG. 7.—Method—Control back

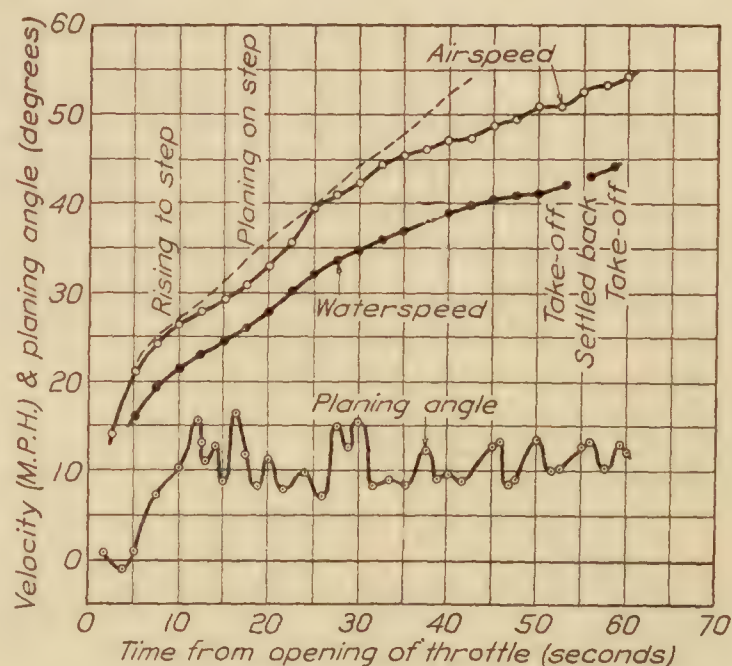


FIG. 8.—Method—Control back

curves of Figure 5, it will be seen that the *F-5-L* rose to the step without reaching as high an angle as by the other methods, and although the "start to rise" point was perhaps somewhat delayed it passed through this transient stage to the planing condition in about the same time. The water speed was not secured on this run.

In Figures 6, 7, and 8 curves of runs made with the control held back are plotted. The run pictured in Figure 6 was made on very smooth glassy water. A high angle was maintained

throughout without any appreciable oscillations until a water speed of 45 miles per hour was reached. Figure 7 shows another rather similar run taken on rippled water. In Figure 8 is shown a run made on smooth water which has large oscillations throughout. Other tests have shown that holding the control back is quite likely to bring porpoising at a lowered speed, as in Figure 6, but not to cause it at all speeds. It is therefore believed that there was a misunderstanding between the pilot and the observer concerning this run and that this is in reality a normal take-off. Discounting Figure 8, it is seen that this method gives a smooth run with a slight porpoising at get-away speeds. It is again evident that rocking is not necessary to get on the step.

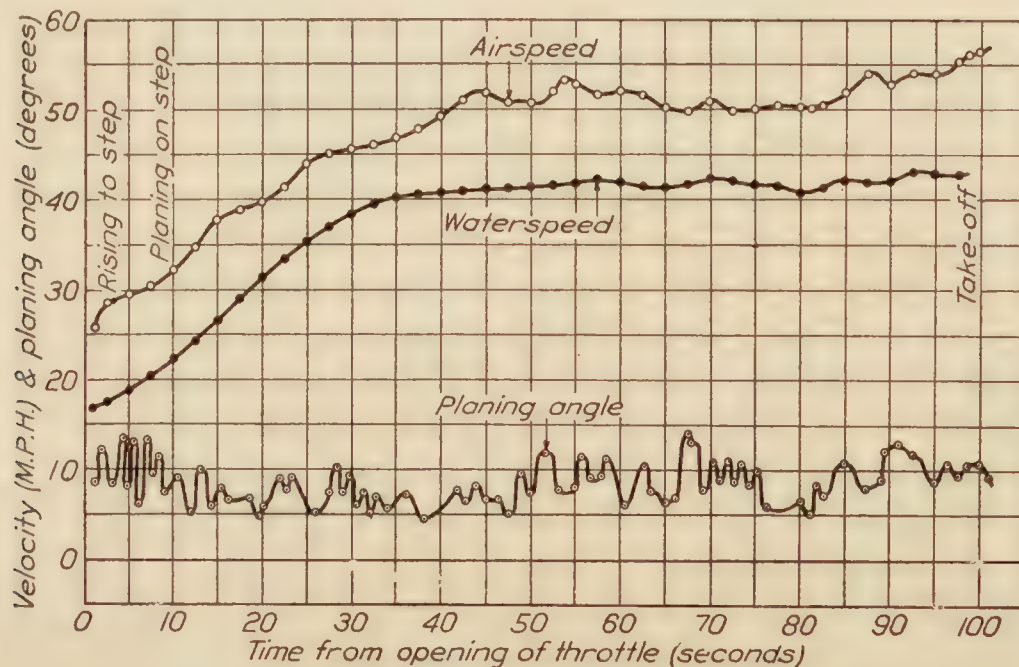


FIG. 9.—Method—Normal

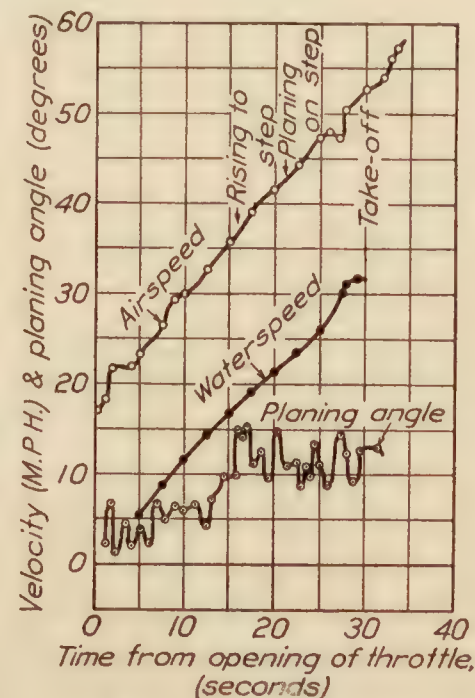


FIG. 10.—Method—Normal

The curves of the normal method shown in Figures 9, 10, 11, and 12 have few similarities. The load on the run shown in Figure 9 was 14,200 pounds and the pilot had extreme difficulty in getting off, and it appears that he rocked the seaplane throughout. Figure 10 shows a normal run taken in choppy water, and it is recalled that the oscillations are more due to the waves than to the controls. In this run "rising to step" and "planing on step" occur at the usual water speeds of 17 and 22 miles per hour, while the air speeds are nearly 20 miles per hour higher. This shows clearly that the attitude of the seaplane is dependent on the water speed until a planing stage is reached. In Figures 11 and 12 are pictured take-offs quite common in the service. The procedure is rocking to get on the step, the amplitude depending on the water conditions and on the success of the pilot in synchronizing with the natural period, pushing the control slightly forward until flying speed is obtained, and then pulling the control back, or if necessary rocking the seaplane to help lift it and decrease the planing resistance.

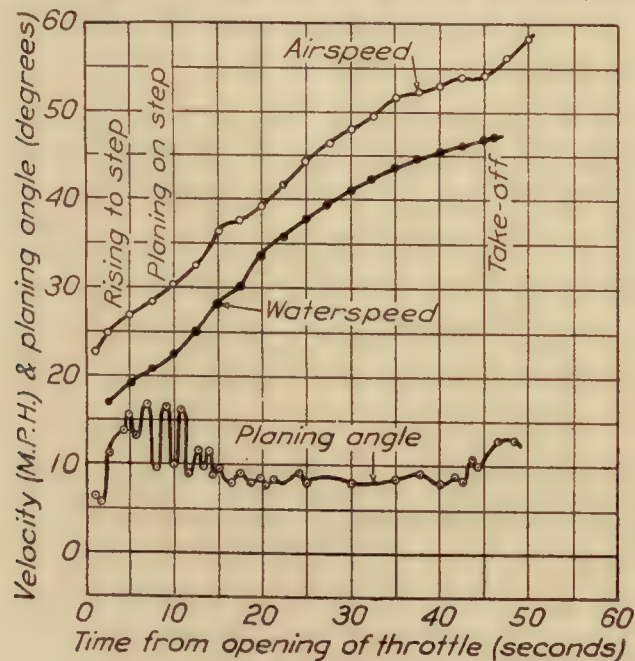


FIG. 11.—Method—Normal

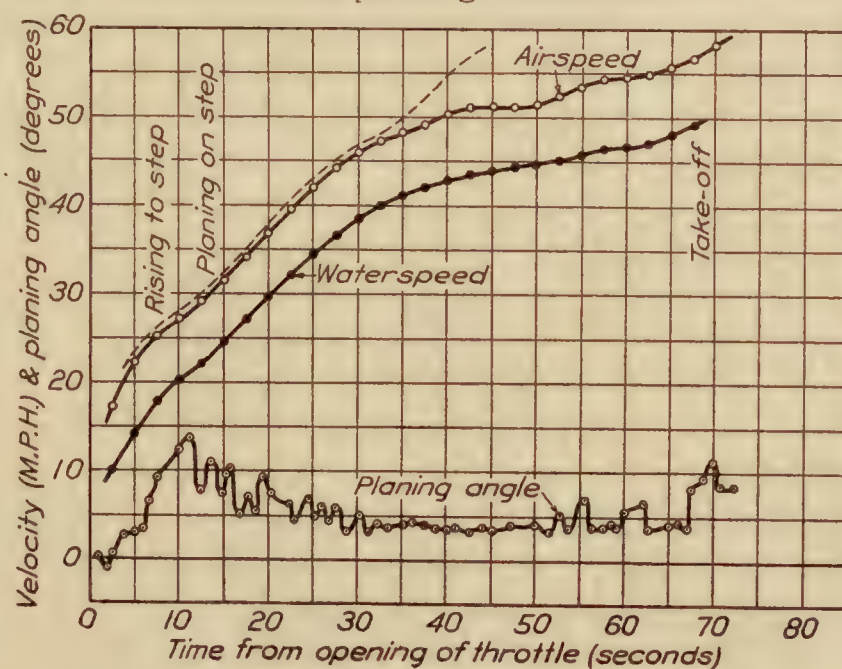


FIG. 12.—Method—Normal

In Figures 4, 8, and 12 are dotted-line curves of air speed taken on similar runs without the water speed apparatus. It is noticeable on these that the slopes of the curves are nearly the same throughout a run, showing only a little flattening out at hump speed. This point of minimum acceleration or maximum resistance occurs between the water speeds of 17.5 and 22.5 miles per hour. The acceleration through this transient stage is fairly good but the pick-up thereafter is poor. As mentioned before, it is believed that this planing quality is due to the high resistance of the ∇ bottom. (Reference 5.) A compromise between the shock-absorbing qualities of the sharp ∇ bottom and the planing and taxiing advantages of the flat bottom has been advanced. (See Reference 4.) This consists in flattening the keel line of the conventional ∇ bottom. If this compromise is unsatisfactory, it seems possible that the shock-absorbing qualities of the sharp ∇ could be replaced by some mechanical means. For obtaining quickly a knowledge of the planing performance, a take-off history of the angle and air speed will give the desired information. Due to the mechanical difficulties involved, with this type of hull, the securing of water speed is not worth while except for extensive research.

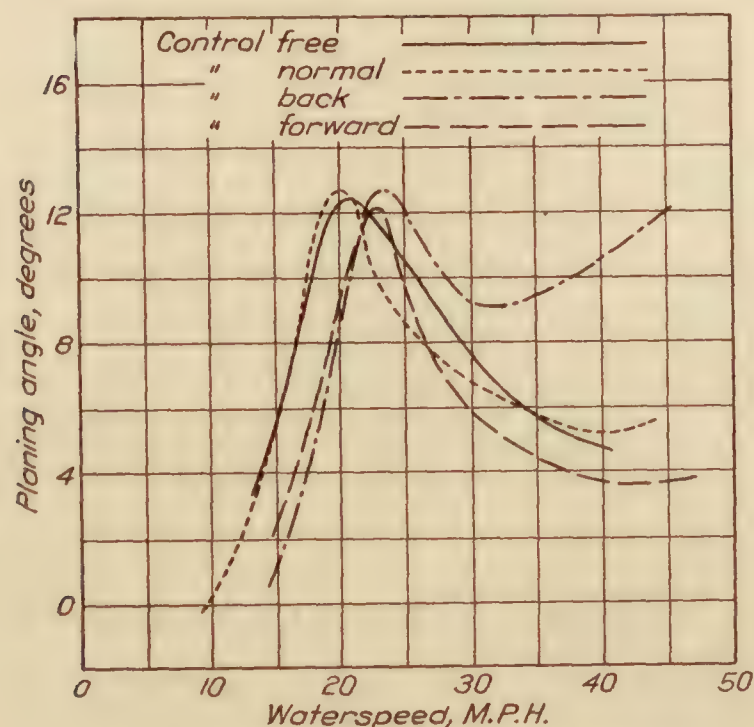


FIG. 13.—Variation in planing angle with water speed

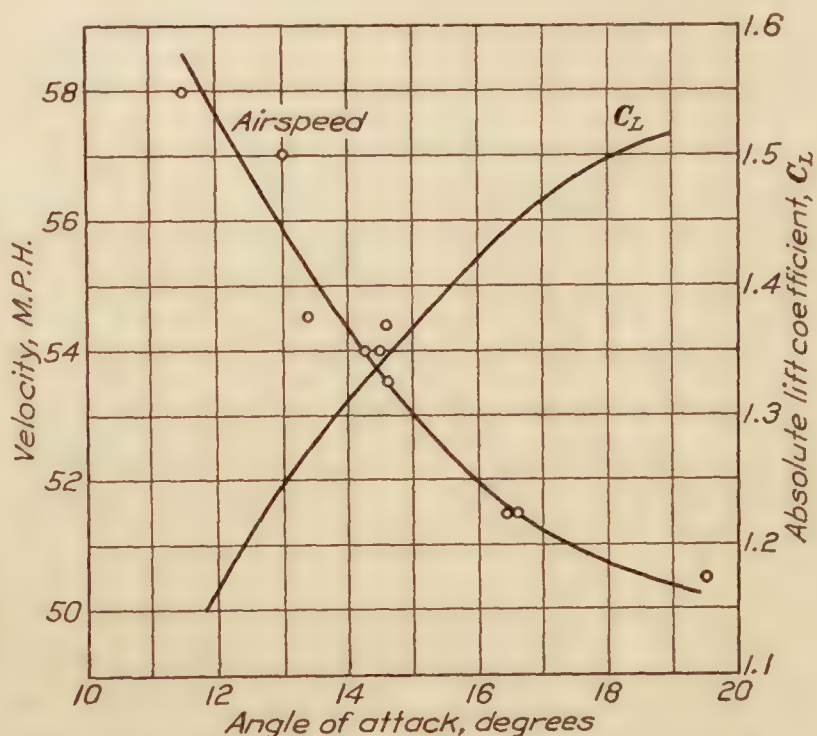


FIG. 14.—Velocity and lift coefficient at various angles of take-off

A comparison of the four methods of take-off shows that it is not necessary to rock the *F-5-L* to get on the step and little or no time is gained thereby, but rocking may be required to get off. The ability of the *F-5-L* to rise to the step when heavily loaded, regardless of the control method or water conditions, shows that it has a sufficient water-lifting area when all of the sponson or "planing fins" are immersed. The apparent necessity of rocking it on smooth waters to get away indicates that the form of its after body could be improved. It is quite desirable with a large military seaplane and very necessary with a commercial seaplane to be able to take off smoothly, as rocking is very disagreeable to passengers and it necessitates fastening everything very rigidly. The control should be used to dampen the pitching caused by waves, rather than to produce pitching. For this reason, and also to be able to raise the nose high enough to get away, a large seaplane should be provided with large horizontal control surfaces and well-balanced elevators.

The average planing angle at each water speed by the different control methods is shown in Figure 13. These curves are found from points on the original curves, but as there were only two or three runs of each condition they may not represent a true average, as the trim is somewhat affected by the water condition. It will be noticed that the peak resistance of the control back method is deferred. In the single-float tests the peaks were practically the same except for control forward. The peak resistance of the hull occurs during the high-angle period or between the water speeds of 17.5 and 22.5 miles per hour.

In Figure 14 are shown the velocities and angles of attack at the get-away. The lift curve, C_L , is derived from this curve by assuming this to be a level flight condition, although ground interference may cause it to be slightly in error. It shows that the angle of attack at the get-away varies from 11° to 19° , with velocities of 58 to 51 miles per hour. Assuming the maximum speed to be 80 miles per hour, the get-away speed range is therefore about 25 per cent of the flying speed range.

CONCLUSIONS

The maximum resistance occurring at a water speed of 17.5 to 22.5 miles per hour and at a planing angle of about 16° is only slightly greater than that occurring at lower and higher speeds. It is believed that this is due to high planing resistance rather than especially low plowing resistance. It seems desirable to reduce the planing resistance by improving the form of the middle body perhaps by flattening of the bottom ahead of the front step.

The seaplane is very stable longitudinally in water calmer than choppy water of a depth between the crest and trough of a foot. However, it is not too stable as to be uncontrollable, so that pitching caused by a rough sea can be somewhat dampened. The *F-5-L* under all conditions will get on the step and under average conditions get away as quickly as when rocking is resorted to. Its get-away speeds are 51 to 58 miles per hour at angles of attack of 19° to 11° .

The fixed stabilizer, which precludes the possibility of trimming for both get-away and cruising angles and the carrying of an unbalanced load, is an undesirable feature. In the design of the empennage on a large flying boat equal consideration should be given to the controllability on the water and in the air. For taking off, large horizontal tail surfaces with efficient well-balanced elevators are desirable, especially on a commercial seaplane.

The securing of a water speed record, without the imposition of considerable drag, on a large acute *V* bottom boat offers such mechanical difficulties that it is not worth while except in an extensive research. To obtain the most important planing characteristics quickly and easily a time-history of the air speed and planing angle is sufficient.

BIBLIOGRAPHY

- Reference 1. CROWLEY, J. W., Jr., and RONAN, K. M., "Characteristics of a Single-Float Seaplane During Take-Off." N. A. C. A. Technical Report No. 209, 1925.
- Reference 2. NORTON, F. H., "N. A. C. A. Recording Air Speed Meter." N. A. C. A. Technical Note No. 64, 1921.
- Reference 3. REID, H. J. E., "The N. A. C. A. Recording Tachometer and Angle of Attack Recorder." N. A. C. A. Technical Note No. 156, 1923.
- Reference 4. MAGALDI, GIULIO, "Hulls for Large Seaplanes," from "La Technique Aeronautique," October 15, 1925. N. A. C. A. Technical Memorandum No. 295, 1925.
- Reference 5. BAKER, G. S. and KEARY, E. M., "Experiments with Models of Flying Boat Hull (16th Series)." British Advisory Committee for Aeronautics R. & M. No. 472, 1918.
- RICHARDSON, H. C., "Airplane and Seaplane Engineering." Bureau of Aeronautics Technical Note No. 59, 1923.
- BAKER, G. S., and KEARY, E. M., "Experiments with Model Flying Boat Hulls and Seaplane Floats (19th Series)." British Advisory Committee for Aeronautics R. & M. No. 655, 1920.
- BAKER and KEARY, "Experiments with Full-Sized Machines (1st Series)." British Advisory Committee for Aeronautics R. & M. No. 473, 1918.

APPENDIX¹

Characteristics of the F-5-L Seaplanes

Type.....	Boat type twin-engine biplane.
Wing area.....	1,397 square feet.
Angle of incidence of wings.....	4°.
Weight, average as tested.....	13,700 pounds. Run No. 9, 14,200 pounds.
Engines.....	2 Libertys, 2 x 360 HP. at 1,650 revolutions per minute.
Wing loading.....	9.8 pounds/square foot.
Power loading.....	19 pounds/B. HP.

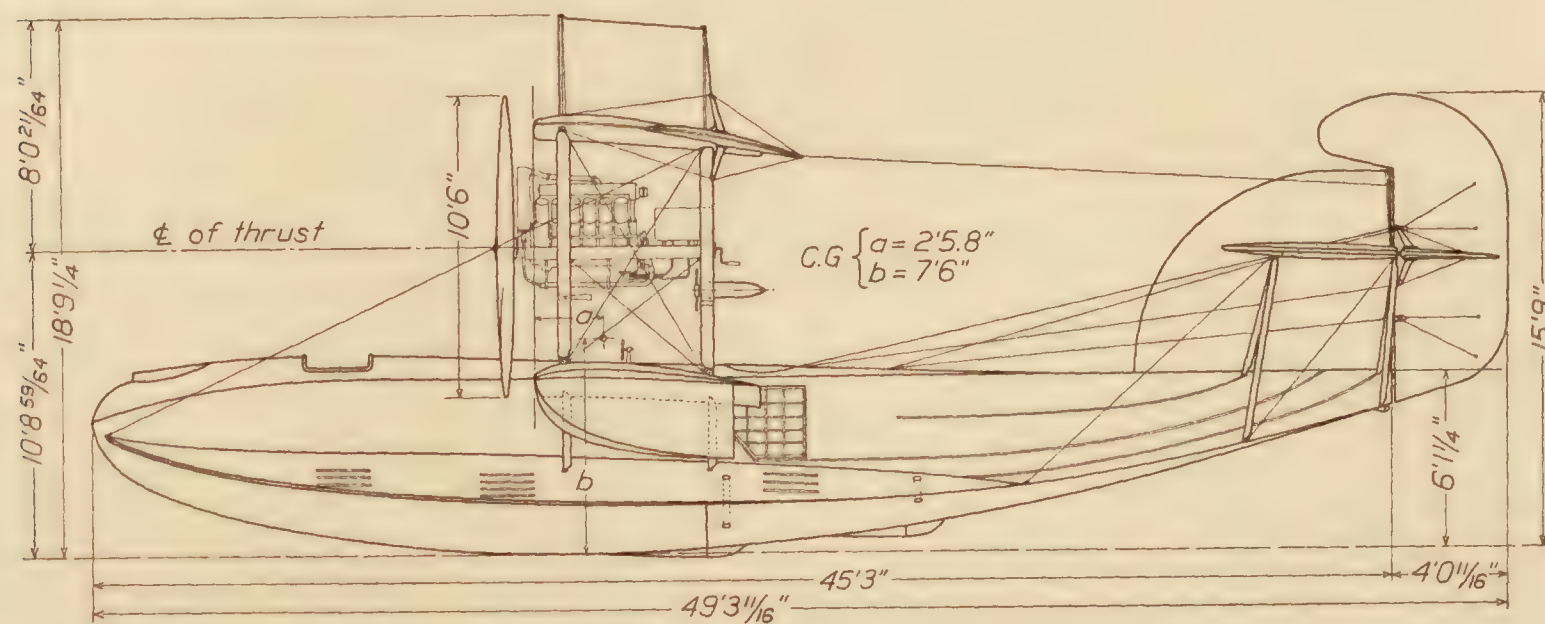


FIG. 15.—F-5-L seaplane

¹ Taken from Bureau of Aeronautics, United States Navy, performance chart.

REPORT No. 227

**THE VARIABLE DENSITY WIND TUNNEL OF THE
NATIONAL ADVISORY COMMITTEE FOR
AERONAUTICS**

**By MAX M. MUNK and ELTON W. MILLER
Langley Memorial Aeronautical Laboratory**

REPORT No. 227

THE VARIABLE DENSITY WIND TUNNEL OF THE NATIONAL ADVISORY COMMITTEE FOR AERONAUTICS

By MAX M. MUNK and ELTON W. MILLER

SUMMARY

This report contains a discussion of the novel features of this tunnel and a general description thereof.

PART I

FUNDAMENTAL PRINCIPLES

By MAX M. MUNK

All the novel features of the new variable density wind tunnel of the National Advisory Committee for Aeronautics were adopted in order to eliminate the scale effect. The leading feature adopted was the use, as the working fluid, of highly compressed air rather than air under normal conditions.

It is not at once obvious that the substitution of compressed air eliminates the scale effect with aerodynamic model tests, although the necessary theoretical discussion has been available for some years. The idea of using compressed air must have occurred, in all probability, to many. It was not, however, till early in 1920 that the thought came to the writer; and in what follows is given his own line of reasoning, expressed in as simple language as possible.

In a paper entitled "Similarity of Motion in Relation to the Surface Friction of Fluids," by T. E. Stanton and J. R. Pannell, *Philosophical Transactions A*, volume 214, pages 199-224, 1914, will be found an excellent treatment of the subject, with references to the earlier discussions by Newton, Helmholtz, and Rayleigh.

Proceeding at once to the motion of a rigid body immersed in a fluid, the aim of the investigation is to obtain information concerning the fluid forces on such a body. Everything in connection with the problem has to be studied to that end, and has to be included in the investigation, whether this latter be analytical or, as we suppose now, experimental. There are the properties of the immersed body, its shape, its direction of motion, eventually the character of its surface. Even more important is the action of the fluid brought into play by these properties. Every detail of the motion of the fluid, together with the physical properties of the fluid, is immediately connected with the kind and magnitude of the forces created. We can only attain to a full knowledge of the forces created by regarding their cause, the fluid motion. All velocity components at all points of the flow are important and characteristic details of the cause of the forces on the body immersed in the fluid.

Then, why do investigators think that they can learn about what will occur on a large scale by observing what occurs on a small scale? Not from any intuitive feeling, inexpressible in words because devoid of thought; not from any vague metaphysical argument difficult to explain. There is a definite, extremely sound, and simple reason why we expect to obtain reliable information from model tests. It is because we expect the two cases when compared with each other will perfectly, at all points, conform to each other, point by point. We do not mentally confine the geometrical similarity to the bodies immersed and to the dimensions of the entire arrangement, leaving as an unsolved and uninteresting question what the fluid does in the two cases. We do not expect that, for some mysterious reason; the fluid forces will correspond to each

other in accordance with some simple rule. On the contrary, we include the flow patterns in our conception of "model." Any two corresponding portions of the flow, however small, are supposed to be similar with respect to shape and direction of the streamlines and with respect to the magnitude of velocities. The ratio of the lengths of a pair of corresponding portions of a streamline is supposed to be constant throughout the flow, and so is the ratio of two velocities corresponding to each other. We are under the impression that with respect to every detail the entire small-scale experiment is an exact replica of what occurs on a large scale, and we believe that the smallest quantity, whatever it is, occurs in a numerically corresponding way with the same conversion factor throughout the entire flow. In such a case, and only then, are we entitled to expect a simple relation between the fluid forces of the model test and those on the large-scale experiment. Such forces are the integrals of the elementary forces, and hence they stand in a constant ratio if the elementary forces do. This constant ratio can furthermore be expected to be a simple algebraic expression of the ratios between the characteristic quantities of the two arrangements.

Not only the model but the entire flow is the replica. There is a good illustration. It sometimes occurs in aerodynamics that the same body moved in the same way in the same fluid gives rise to different configurations of flow. The air forces are then also different.

The question, "Can we learn from aerodynamic model tests?" is thus reduced to the equivalent question, "Can flow patterns be geometrically similar?" If so the boundaries of the flow in general, and the immersed bodies in particular, have to be similar, but this alone is no sufficient reason why the similarity should extend to every streamline. The question whether a test is really a model test in the strict meaning, the question whether the small-scale flow is similar to the large-scale flow, requires a special examination. This examination will decide whether we can obtain reliable information from the test. If the flows are not exactly similar, but only approximately, the information also will only be approximately correct and not wholly reliable. There will exist a "scale effect."

Two configurations of aerodynamic flow are created in different fluids under conditions geometrically similar. We wish to know whether the flow patterns are geometrically similar. We imagine a small-scale flow to exist exactly similar to the large-scale flow really existing, and we ask whether this imagined small-scale flow is compatible with the general laws of mechanics and hence identical with the actual small-scale flow. More particularly, we examine whether each particle of the imagined small-scale flow is in equilibrium, remembering that the corresponding particle of the large-scale flow is.

We assume first that no physical properties of the fluids, nor differences of such properties, have any influence on the shape of the flow pattern or on the fluid forces, except the density of the fluids. We dismiss also any external influence, like that of gravity. Then the only type of force brought into action by the motion of the fluid is the mass force of all the particles, and they are equalized by means of a variable pressure. The pressure distribution is only the natural reaction against changes of mutual positions of all the fluid particles, which changes must be compatible with the continuity conditions of the fluid. Each particle has the natural tendency to move straight ahead with constant velocity. This tendency is in conflict with the other tendency of each fluid particle to claim its own space, not to share its space with any other particle. These two conflicting tendencies lead to a distribution of varying pressure and to mass forces on the particles due to their motion along curved paths and with varying velocities. The pressure distribution gives rise to an elementary force on each particle, and the flow arranges itself in such a configuration that this pressure force is in equilibrium with the mass force.

Let us consider now the case when the linear dimensions are diminished in the ratio $\frac{l_2}{l_1}$, all velocities diminished in the ratio $\frac{V_2}{V_1}$, and the density ρ_2 bears the ratio $\frac{\rho_2}{\rho_1}$ to the original density.

The mass forces are expressed mathematically by a type of term occurring in Euler's¹ or Bernouilli's² equation. Per unit volume, they are of the type

$$\frac{\text{Density} \times \text{Velocity}^2}{\text{Length}}$$

and hence resultant mass forces of corresponding portions of the flow are of the type

$$(1) \quad \text{Density} \times \text{Length}^2 \times \text{Velocity}^2$$

Such forces are in equilibrium with the pressure forces, and this determines the latter. Hence a change of density, scale, and velocity gives rise to a change of all elementary forces and hence of all resultant forces in the ratio

$$\frac{\rho_2 l_2^2 V_2^2}{\rho_1 l_1^2 V_1^2}$$

The equilibrium of the particles remains unimpaired by the change of scale, and we conclude that corresponding flow patterns are necessarily similar. Hence, if the density of the fluid were the only property influencing the fluid paths and hence the fluid forces, all aerodynamic model tests would be interpreted correctly by the application of the so-called "square law." Corresponding fluid forces would be proportional to the fluid density, to the square of the velocity, and to the square of the linear scale. Accordingly, the absolute coefficients generally in use for expressing the magnitude of fluid forces would not only be absolute, but also constant for similar shapes and arrangements.

Experience has shown that the "square law" does not strictly hold, but that the air-force coefficients vary, sometimes slightly and sometimes in a very pronounced way. This is due to the influence of other properties of fluid, neglected before. There arises the question which other property of air is the principal cause of variations of flow patterns under conditions otherwise geometrically similar. All men who have devoted much thought to this problem agree that viscosity has such an effect, greatly in excess of that of other properties. The point is that the forces taken care of by the introduction of such properties of the fluid are very small when compared with the mass forces, which latter alone are governed by the "square law." This holds true at all points of the flow and with respect to all fluid properties, except with viscosity, where it only holds at most points. Viscous forces are proportional to the rate of sliding of adjacent layers of fluid, and are expressed by terms of the type,³

$$(2) \quad \mu \frac{\partial u}{\partial y} dx dz$$

Here the constant quantity μ is called the modulus of viscosity. u , a velocity, is at right angles to y , a Cartesian coordinate, together with x and z . Hence $\frac{\partial u}{\partial y}$ has the physical dimension of an angular velocity, $\frac{1}{\text{Time}}$. Now, this rate of sliding is small throughout an aerodynamic flow except near the boundary. There it may assume a very large magnitude. So, in spite of the small value of the modulus of friction of air, μ , the friction $\mu \frac{\partial u}{\partial y}$ can assume a very large value

¹Euler's equation:

$$\begin{aligned} \frac{\partial u}{\partial t} + u \frac{\partial u}{\partial x} + v \frac{\partial u}{\partial y} + w \frac{\partial u}{\partial z} &= X - \frac{1}{\rho} \frac{\partial p}{\partial x} \\ \frac{\partial v}{\partial t} + u \frac{\partial v}{\partial x} + v \frac{\partial v}{\partial y} + w \frac{\partial v}{\partial z} &= Y - \frac{1}{\rho} \frac{\partial p}{\partial y} \\ \frac{\partial w}{\partial t} + u \frac{\partial w}{\partial x} + v \frac{\partial w}{\partial y} + w \frac{\partial w}{\partial z} &= Z - \frac{1}{\rho} \frac{\partial p}{\partial z} \end{aligned}$$

Lamb, 4th edition, article 6.

²Bernouilli's equation:

$$\frac{p}{\rho} = \frac{P}{\rho} + gz - \frac{1}{2} V^2$$

Lamb, 4th edition, article 24.

³Friction per unit area

$$\text{pxy} = \mu \left(\frac{\partial v}{\partial x} + \frac{\partial u}{\partial y} \right)$$

Lamb, 4th edition, article 326, equation 6.

and can become dominating at certain points of the flow. It can then produce essential changes of the entire flow pattern. Very little in detail is known about these things, and it seems useless to carry the discussion on at this point. Experience has shown that proper attention to the viscosity brings system and regularity into results of tests otherwise obscure and contradictory. It is for this reason that the elimination of the effect of viscosity for many years was thought desirable in the first place as a fundamental improvement of aerodynamic model tests, resulting in the elimination of the scale effect.

There has been some controversy as to whether these arguments are sufficient for the final decision that viscosity is the all-important fluid property. No arguments whatsoever will definitely decide that, but only final success. The separation of the physical effects to be taken into consideration for any practical purpose from those which may be neglected is a mental step which can not be accomplished by mere logics.

Granted, now, that viscosity is of practical importance, the question arises, Are similar flows possible in viscous fluids; and if so, under what conditions will the flows be similar? It is understood now that the arrangements are geometrically similar, that only the density ρ and viscosity μ of the fluid have to be considered in addition to the linear scales of the arrangement and the ratio of the velocities.

The answer to the last question depends again upon the result of the examination whether each particle of an imagined small-scale flow, similar to an actual large-scale flow, is in equilibrium or not. Now, in viscous fluids the mass forces are not in equilibrium with the pressure forces, but in equilibrium with the combination of both the pressure forces and the viscosity forces. We have now three types of forces in equilibrium with each other, and that gives rise to a variety of possibilities. Two forces in equilibrium are, of necessity, numerically equal, hence if one of them be changed in a given ratio the other will too. With three forces, all three may be changed in a different ratio and still the equilibrium maintained.

The criterion for the similarity of flows is, therefore, that two of the three forces be changed in the same ratio. Then the third, in equilibrium with the two, will be changed in this same ratio and needs no special examination.

We compare the ratio of change of the mass forces and of the viscosity forces with each other. We have seen already (1) that the mass forces are changed in the ratio $\frac{\rho_2 V_2^2 l_2^2}{\rho_1 V_1^2 l_1^2}$. The viscous forces being of the type $\mu \frac{\partial u}{\partial y} dx dz$, are seen to be changed in the ratio $\frac{\mu_2 V_2 l_2}{\mu_1 V_1 l_1}$. Now, the two flow patterns will be similar and the test will be a strict model test only if the mass forces and the viscosity forces are changed in the same ratio. Hence we obtain, as the condition of an exact model test,

$$\frac{\rho_2 V_2^2 l_2^2}{\rho_1 V_1^2 l_1^2} = \frac{\mu_2 V_2 l_2}{\mu_1 V_1 l_1}$$

or, written in a different way,

$$(3) \quad \frac{V_1 l_1 \rho_1}{\mu_1} = \frac{V_2 l_2 \rho_2}{\mu_2}$$

The expressions on either side of equation (3) are generally called "Reynolds Numbers," from Osborne Reynolds, who was the first to emphasize their importance. Since V and l are certain velocities and lengths in the two flows, corresponding to each other, but otherwise arbitrarily chosen as "characteristic" velocity or length, the value of one special Reynolds Number in one single case has as little meaning as the scale of one single object. The equality of the Reynolds Numbers of two arrangements, different but geometrically similar, expresses the dynamic equivalence of the two flows compared.

If the ratio of the two Reynolds Numbers is different from unity the value of this ratio can be considered as a kind of relative scale between these two tests, not of the geometric scale but one which may be called dynamic scale. The ratio of the Reynolds Numbers indicates differences in the relative importance of the mass forces and of the viscosity forces. A single Reynolds

Number, together with the definition of the characteristic velocity and length, is only an identification number, not much more than the street number of a house. Comparison of Reynolds Numbers of flows where the conditions are not geometrically similar have hardly any meaning.

The preceding discussion has led us to the condition under which a wind tunnel will have no scale effect due to viscosity, and probably not any scale effect of practical importance. This condition is not equal velocity in model test and in flight. Full velocity is only of value for investigating certain original airplane parts and original flight instruments. The test with a model of diminished scale but at the velocity of flight is by no way distinguished from tests at other wind-tunnel velocities. On the other hand, if there is no scale effect expected, the Reynolds Number being equal in both model test and free flight, the dynamic scale being 1, and if there are still arguments raised doubting the validity of such tests, such arguments hold with equal right or wrong against all other model tests, more particularly against such tests in ordinary atmospheric wind tunnels. For the principal difference between the variable density tunnel and atmospheric tunnels is the elimination of one source of error, of the one moreover, which is believed by most experts to be the most serious.

The fact is, then, that in general model tests in atmospheric wind tunnels are made at a Reynolds Number smaller than in free flight. The linear dimensions of the model are largely diminished, and nothing is done to make up for this; the velocity is at best the same as in flight and the ratio μ/ρ is the same, the same fluid being used in test and in flight.

It is neither practical nor sound to make up for the diminution of the model by correspondingly increasing the velocity so as to obtain the original value of the product Vl as required in equation (3). It is not practical because such a wind tunnel would consume an excessively high horsepower, and because the air forces on the model would become excessive to such an extent as to make the test practically impossible. Such a method would also be unsound. For the differences in air pressure, which amount only to little more than 1 per cent in flight and in ordinary wind tunnels, would increase rapidly with velocities approaching the velocity of sound. Thereby the influence of the compressibility would be rapidly increased, and thus another error, now negligible, would make the results unsuitable for the desired purpose.

There remains then only the diminution of the ratio $\frac{\mu}{\rho}$ often denoted by ν , in order to make up for the diminution of l in equation (3). This means the choice of another fluid. The use of water instead of air has been seriously proposed. With water $\nu = \frac{\mu}{\rho}$ is indeed seven times as small as with air. The problem of the large power consumption could eventually be solved, either by using a natural stream or by towing the model. However, water is about 800 times as dense as air, and hence the forces produced at the same velocity are 800 times as large, giving rise to stresses 800 times enlarged. It is practically impossible to make ordinary model tests with forces on the model 800 times as large as they are now.

What we need is a fluid which may be denser than atmospheric air at sea level, but only so to a moderate degree. Its dynamic viscosity modulus $\nu = \mu/\rho$ should be distinctly smaller than that of air, in order to make up for the scale of the model and eventually for the diminished velocity necessary for bringing down the pressure on the model and the absorbed horsepower. No such fluid is known under ordinary atmospheric conditions. Further consideration showed that a high pressure transforms air (or another gas) into a fluid suitable for wind-tunnel work giving results without scale effect. This fact depends on the physical property of air of keeping the same viscosity modulus μ under all variations of pressure. This has been confirmed by experiments and is mentioned in treatises on physics. It is in keeping with the molecular theory, with denser air the average free paths are proportionally shorter. The viscosity modulus μ remains the same, but the density increases when the pressure increases.

Hence the ratio $\nu = \frac{\mu}{\rho}$ varies inversely with the pressure (the temperature remaining unchanged).

Hence we have

$$\begin{aligned}\text{Kinematic viscosity} &\sim \text{Pressure}^{-1} \\ \text{Model pressure} &\sim \text{Pressure} \times \text{Velocity}^2 \\ \text{Absorbed horsepower} &\sim \text{Pressure} \times \text{Velocity}^3\end{aligned}$$

Assuming a model scale of say 10, we want a kinematic viscosity at least 10 times as small as with air. With pressure of 20 atmospheres we could get

Test velocity = $\frac{1}{2}$ flight velocity.

Resultant model pressure = $20 (\frac{1}{2})^2$, 5 times actual pressure.

Horsepower consumption of the tunnel = $20 (\frac{1}{2})^3$, 2.5 that of an atmospheric tunnel of the same size and operating at full scale velocity.

Reynolds Number = Reynolds Number in free flight. These figures seemed practical. On them the design of the variable density wind tunnel of the National Advisory Committee for Aeronautics has been based.

More generally it can be seen that the principle of compressing the air allows any Reynolds Number, even with a small model, if only the pressure can be produced and maintained. For keeping the Reynolds Number constant and increasing the pressure in the ratio A , decreases the resultant pressure on the model as A^{-1} and the required horsepower as A^{-2} .

The throat diameter of 5 feet was chosen in order to be able to use the same models as in the atmospheric wind tunnel of the National Advisory Committee for Aeronautics. A small diameter would require smaller models, and it becomes increasingly difficult to construct such models accurate enough.

Furthermore, 5 feet is the smallest diameter for a closed tunnel where a man can walk and work without exceeding discomfort. The choice of the smallest diameter suitable was necessary in view of the large costs and difficulties for procuring a large enough housing strong enough to withstand an internal pressure of 25 atmospheres.

The same restriction of space decided the choice of a closed (not free jet) type of tunnel.

All other novel features can be traced back to the particular features of this tunnel, the large inside pressure and the larger resultant force on the model. They are described in the second part of this paper.

REPORT No. 227

THE VARIABLE DENSITY WIND TUNNEL OF THE NATIONAL ADVISORY COMMITTEE FOR AERONAUTICS

PART II

DESCRIPTION OF TUNNEL

By ELTON W. MILLER

In the pages which follow a description is given in some detail of the tunnel and the methods of operation. The purpose in preparing this report is to make clear the testing methods employed, in order that the technical reports now in preparation may be better understood. The building of this tunnel was first suggested by Dr. Max M. Munk in 1921 (Reference 1). The writer has assisted Doctor Munk and Mr. David L. Bacon in the design and development of the mechanical features of the tunnel.

The tunnel is shown in sectional elevation in Figure 1, and consists briefly in an experiment

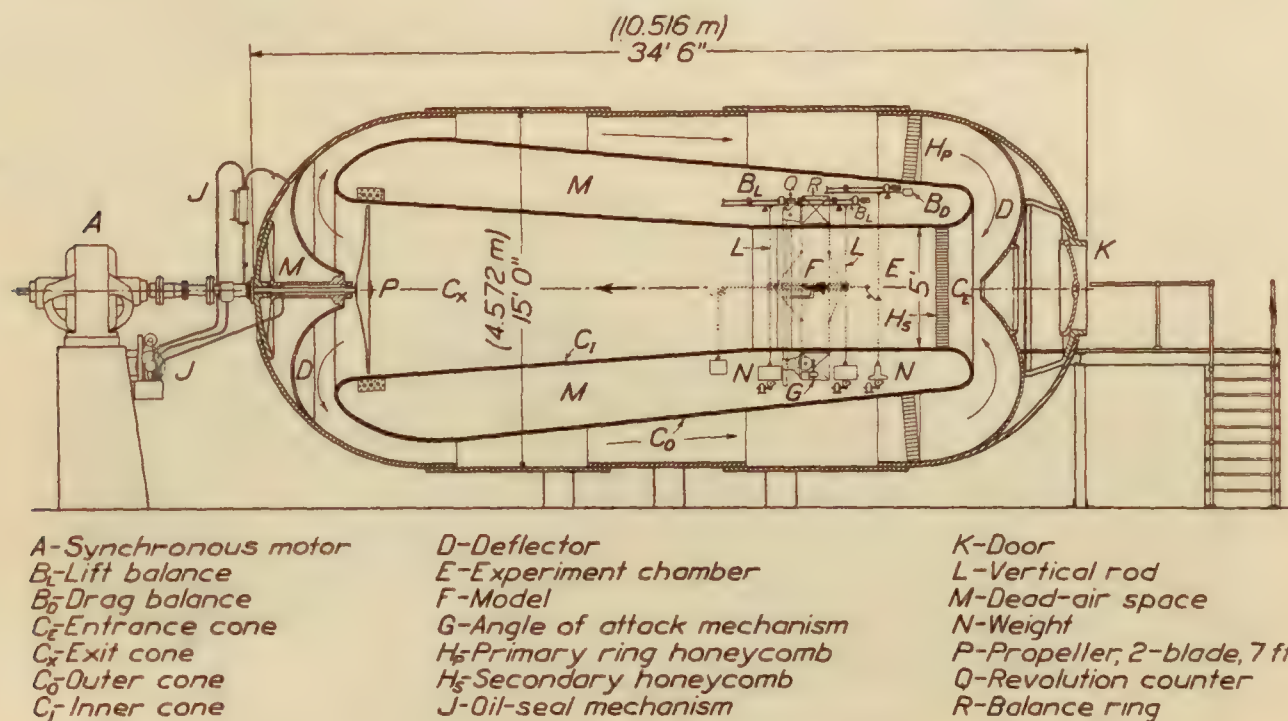


FIG. 1.—Sectional elevation of variable density wind tunnel

section, E, 5 feet (1.52 meters) in diameter, with entrance and exit cones housed within a steel tank 15 feet (4.57 meters) in diameter and 34 feet 6 inches (10.52 meters) long. The air is circulated by a two-blade propeller, returning from the propeller to the entrance cone through the annular space between the walls of the tank and an outer cone, C_o. The balance, which is of novel construction, is mounted in the dead, or noncirculating, air space between the walls of the experiment section and the outer cone. The balance is operated electrically, and readings are taken through peepholes in the shell of the tank. Figures 2 and 3 are general views of the tunnel. Figure 4 is a plan of the building showing the tunnel and compressors.

The tank, which was built by the Newport News Shipbuilding & Dry Dock Co., of Newport News, Va., is capable of withstanding a working pressure of 21 atmospheres. It is built of steel plates lapped and riveted according to the usual practice in steam boiler construction, although,

because of the size of the tank and the high working pressure, the construction is unusually heavy. There is a cylindrical body portion of $2\frac{1}{8}$ -inch (53.98 millimeters) steel plate with hemispherical ends $1\frac{1}{4}$ inches (31.75 millimeters) in thickness. Entrance to the tank is gained

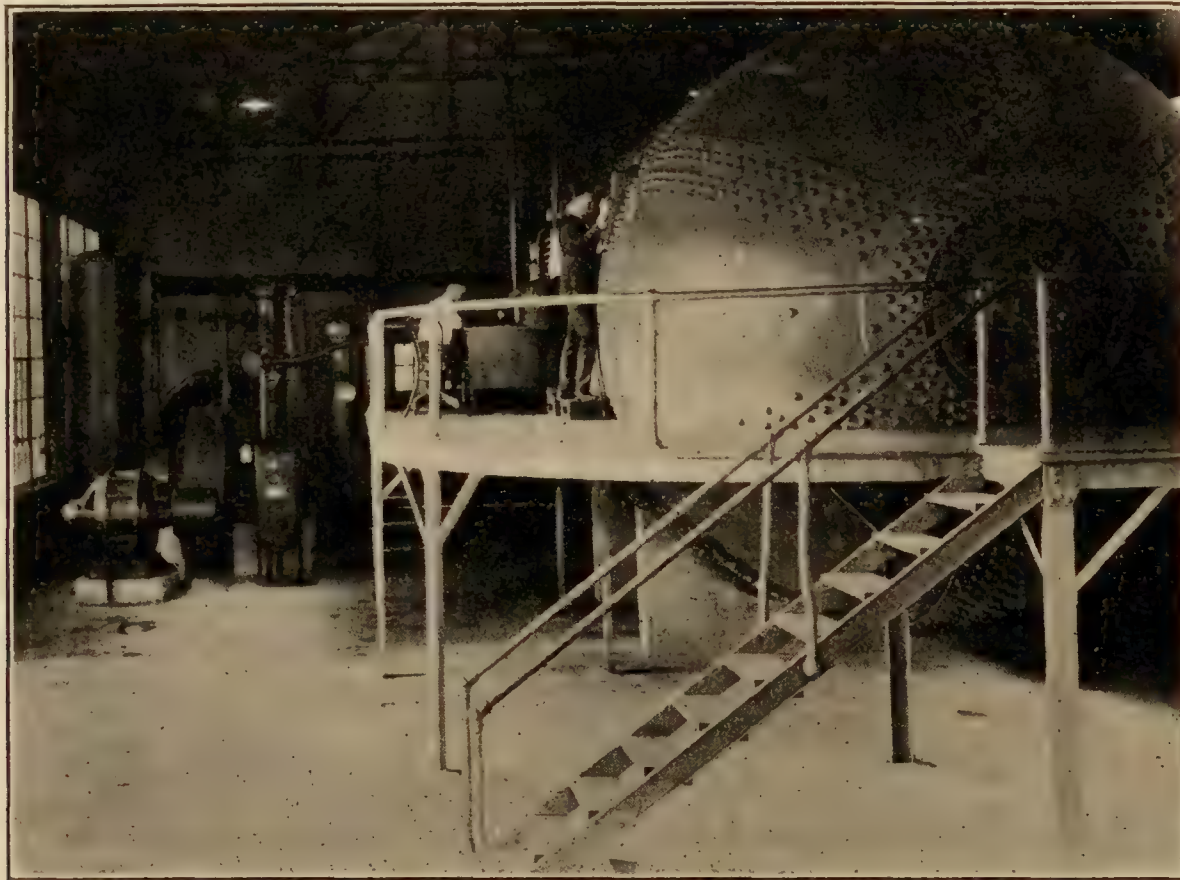


FIG. 2.—General view of tunnel looking west

by an elliptical door K 36 inches (914 millimeters) wide by 42 inches (1,066 millimeters) high. The tank, which with its contents weighs about 100 tons (90.7 metric tons), is supported by a foundation of reinforced concrete.

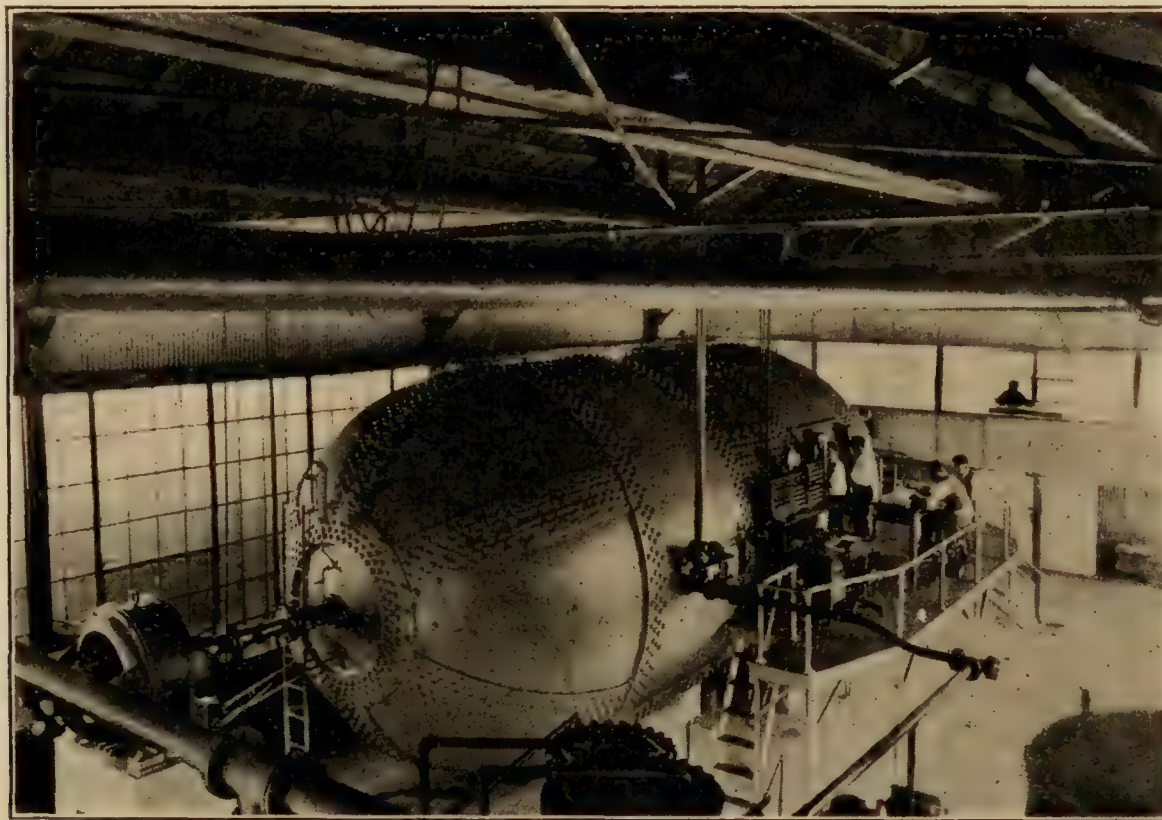


FIG. 3.—General view of tunnel looking east

The walls of the experiment section and cones are of wood; those of the experiment section consist of a series of doors which may be unbolted and removed to gain access to the balance. The cross-sectional area at the large end of the exit cone is substantially twice that

of the experiment section, and the cross-sectional area of the return passage at its largest part is about five times that of the experiment section. Two honeycombs, H_P and H_S , are provided for straightening the air flow. Honeycomb H_P is of 2-inch (50.8 millimeters) round cells, while honeycomb H_S is of 1¼-inch (31.75 millimeters) square cells. The latter honey-

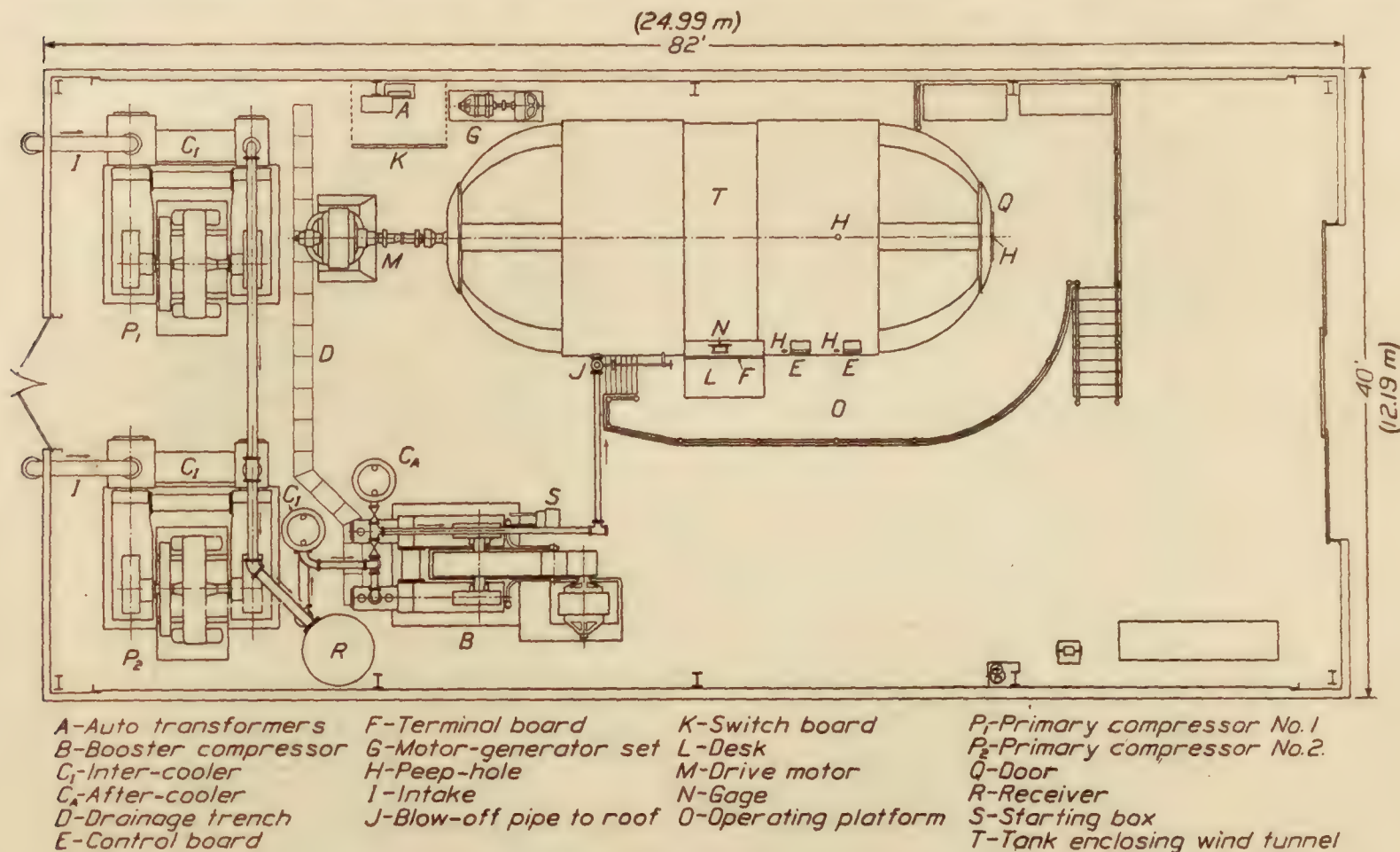


FIG. 4.—Floor plan of variable density wind tunnel and equipment

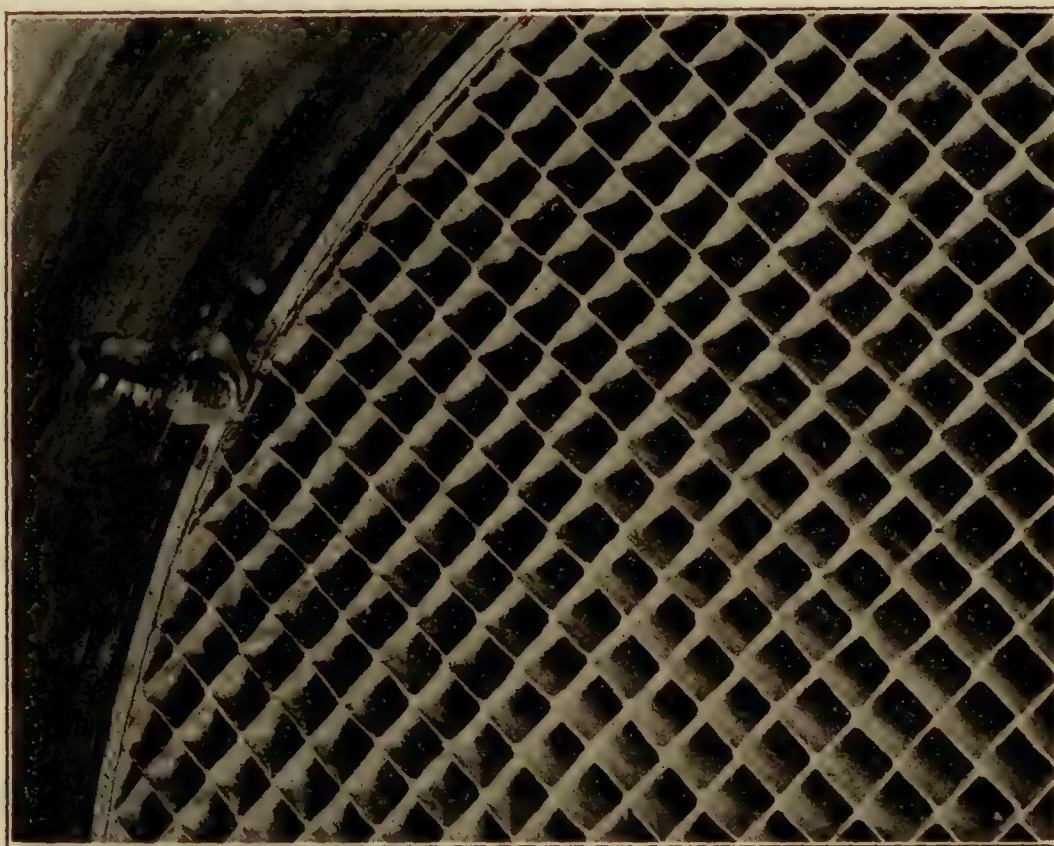


FIG. 5.—Honeycomb (H_S) showing locking device

comb is made removable to permit access to the experiment section; it is suspended from a removable trolley track by which it may be rolled to one side of the entrance cone. In order that the honeycomb may be returned to exactly the same place each time, it is made to seat on three conical points where it may be securely locked. Arrangements have also been made for adjusting the position of the honeycomb, as shown in Figure 5.

The propeller is driven directly by a synchronous motor of 250 horsepower (253.5 metric horsepower), which runs at a speed of 900 revolutions per minute. The synchronous motor has an advantage over the usual direct-current motor in that no complicated devices are neces-

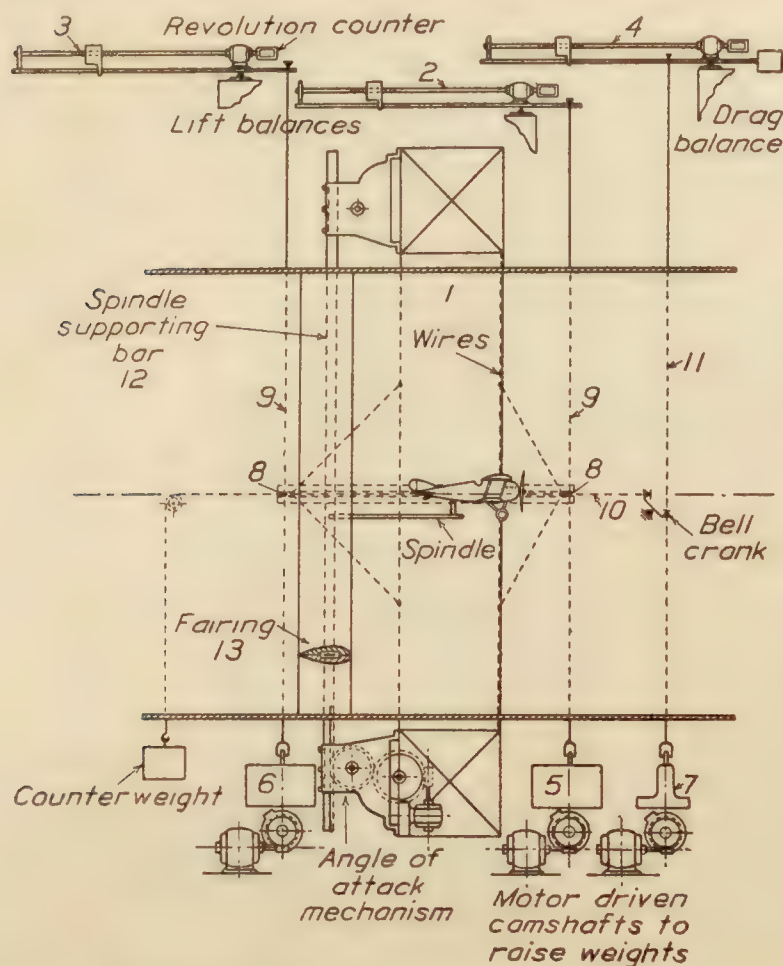


FIG. 6.—Diagrammatic drawing of variable density wind tunnel balance

Air compressors for filling the tank with air are shown in Figure 4. The air is compressed in two or three stages, according to the terminal pressure in the tank. A two-stage primary compressor is used up to a terminal pressure of about seven atmospheres. For pressures above this a booster compressor is used in conjunction with the primary compressor. The booster compressor may be used also as an exhaustor when it is desired to operate the tunnel at pressures below that of the atmosphere. The primary compressors are driven by 250-horsepower synchronous motors and the booster compressor by a 150-horsepower squirrel-cage induction motor.

A diagrammatic drawing of the balance is shown in Figure 6. It consists essentially in a structural aluminum ring (1) which encircles the experiment section, two lever balances (2) and (3) for measuring lift, and a third lever balance (4) for measuring drag. The ring as it looked before assembly in the tunnel is shown in Figure 7. An assembly view in the tunnel is seen in Figure 8. The doors which surround the experiment section have here been removed, exposing the balance to view. The model is attached to the ring by wires or other means, and all forces are transmitted to the ring and thence to the lever balances. The ring is suspended from lever balances (2) and (3), Figure 6, by the vertical members (9), of which there are four, two on

sary for maintaining a constant speed of revolution. Such variations in dynamic pressure as are made in the ordinary atmospheric tunnel by changing the air velocity are here made by changing the density of the air. It is therefore not necessary to vary the air velocity. Fluctuations of a fraction of a percent occur, due to variations in the frequency of the electric current supplied to the motor; otherwise the velocity is constant for a given tank pressure. There is a slight increase in air velocity with an increase in tank pressure, as shown in Figure 16, but this is not objectionable.

The propeller, which is 7 feet (2.14 meters) in diameter, is mounted on a ball-bearing shaft which passes through one end of the tank. The stuffing box through which this shaft passes is only loosely packed, and air leakage is reduced to a minimum by means of oil which is fed by gravity from a reservoir above. The oil which is carried through the stuffing box is returned to the reservoir by a motor-driven pump.

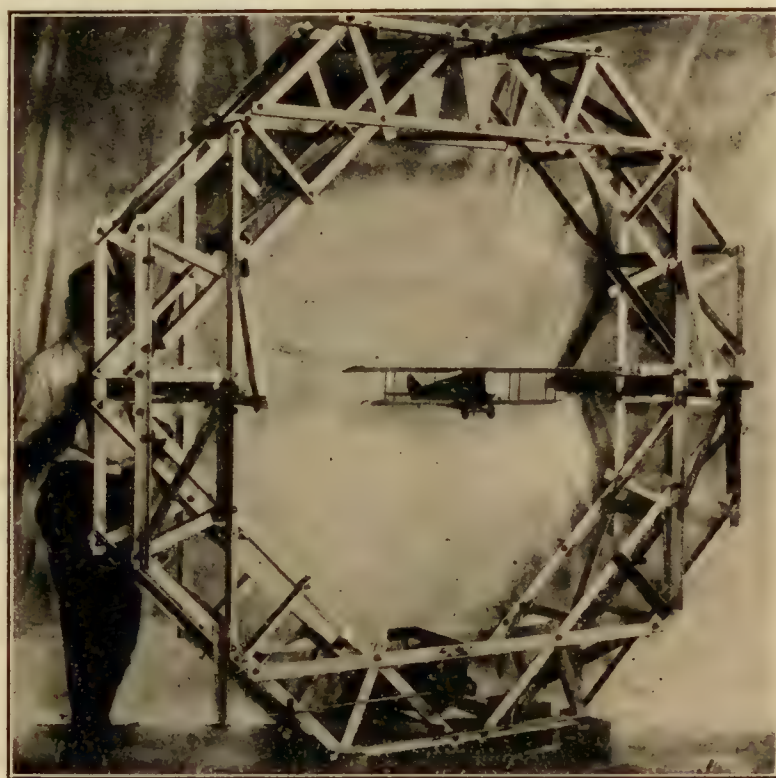


FIG. 7.—Balance ring before assembly in tunnel

each side. Cross shafts and levers are employed in order to carry the full weight of the ring to the two lever balances. The drag forces are transmitted by horizontal members (10) to bell cranks and thence by vertical members (11) to lever balance (4). Hanging from the ring are bridges which carry coarse weights (5) and (6). Any desired number of coarse weights may be added or removed by means of motor-driven cam shafts. A similar bridge carrying coarse weights (7) is hung from lever balance (4).

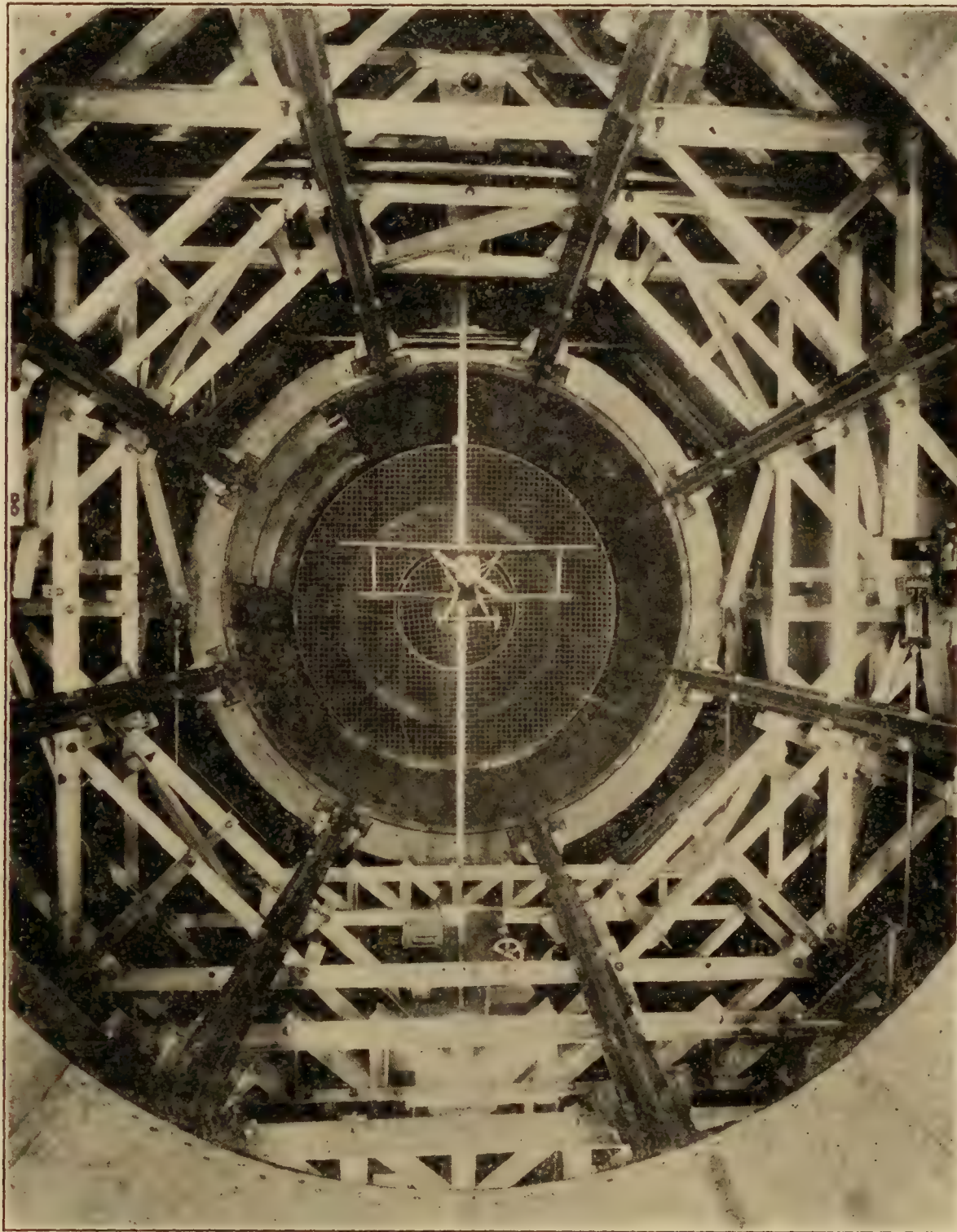


FIG. 8.—Balance with doors of experiment section removed

The sliding weights are moved by motor-driven screws to which are geared revolution counters; these may be read through peepholes in the shell of the tank. At the end of each beam is a pair of electrical contact points by which the beam may be made to balance automatically. The sliding weights may also be controlled by a manually operated switch. The lift balances are sensitive to plus or minus 10 grams and the drag balance to plus or minus 1 gram.

It is possible with this balance to measure any three components; for instance, lift, drag, and pitching moments. The lift is first approximately counterbalanced by increasing or decreasing the number of coarse weights hanging from the two weight bridges. The remainder is then counterbalanced by moving the sliding weights on the two lever balances. The drag is

measured similarly. The total lift is the sum of the readings of the two lift balances; the pitching moment is the algebraic sum of the three balance readings multiplied by their respective lever arms.

The model may be supported in the tunnel by wires only, or by a combination of wires or

struts and a spindle. In the latter case the spindle is attached to a vertical bar (12) which may be raised or lowered by appropriate gearing, thus changing the angle of attack of the model. The angle of attack is indicated by an electrically controlled dial on the outside of the tank. The vertical bar (12) is protected from the air flow by a fairing (13).

Round wires of about 0.040 inch (1 millimeter) diameter have been used for supporting models, this much larger diameter being necessary because of the large

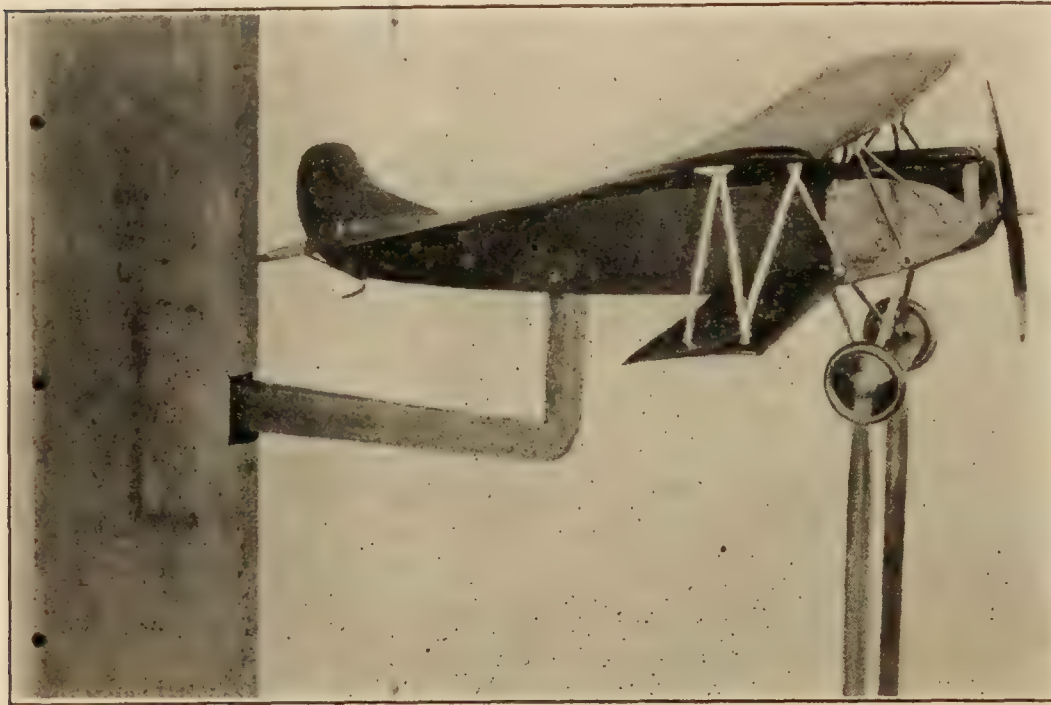


FIG. 9.—Method of supporting Fokker D-VII Model

forces, but streamlined wires of much larger section have been found preferable. These wires are attached to the balance ring below and to the model above, thus serving as struts or free columns to support the weight of the model when the air stream is not on. The struts may be attached to the wheels of the model as shown in Figure 9 or to threaded plugs screwed into the wings as in Figures 10 and 11. The advantage of the streamline wires over the round wires is illustrated in Figure 12. The wire and spindle drag for two airfoils and one airplane model have been reduced to a percentage of the gross minimum drag of the model with wires and plotted against Reynolds Number.

All the various operations required within the tunnel while running, such as the shifting of balance weights and the setting of the manometers, are performed by small electric motors. It has been necessary, therefore, to carry a large number of electric wires through the shell of the tank. These wires pass through a suitable packing gland and are attached to terminal boards inside and out. The outside terminal board may be seen in Figure 3.

The airspeed is measured by static plates, one of which is located in the wall of the experiment section and the other in the wall of the other cone. The static plates are calibrated against Pilot tubes placed in the experiment section. A micromanometer designed especially for use in this tunnel is shown in Figure 13. Alcohol is the liquid used, and a head up to 1 meter may be measured. This manometer is similar in principle to that described in National Advisory Committee for Aeronautics Technical Note No. 81, but is different in that the index

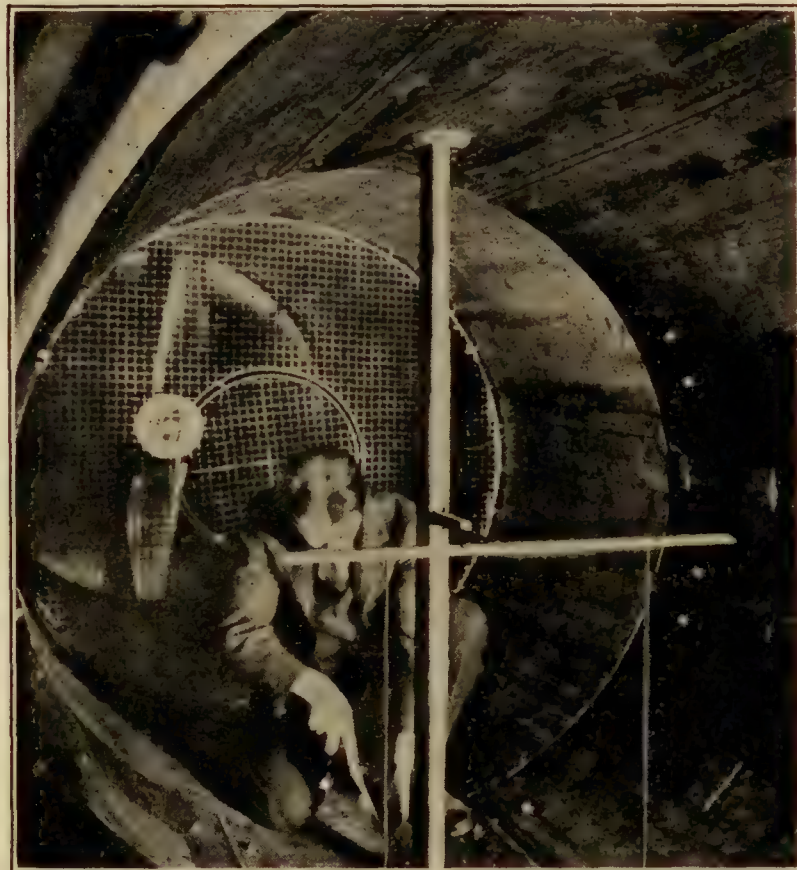


FIG. 10.—Airfoil set-up.

tube is stationary and the reservoir is raised or lowered by a motor-driven screw. A revolution counter geared to the motor indicates the head to 0.1 millimeter. It is possible to determine the dynamic pressure to an accuracy of plus or minus 0.2 per cent.

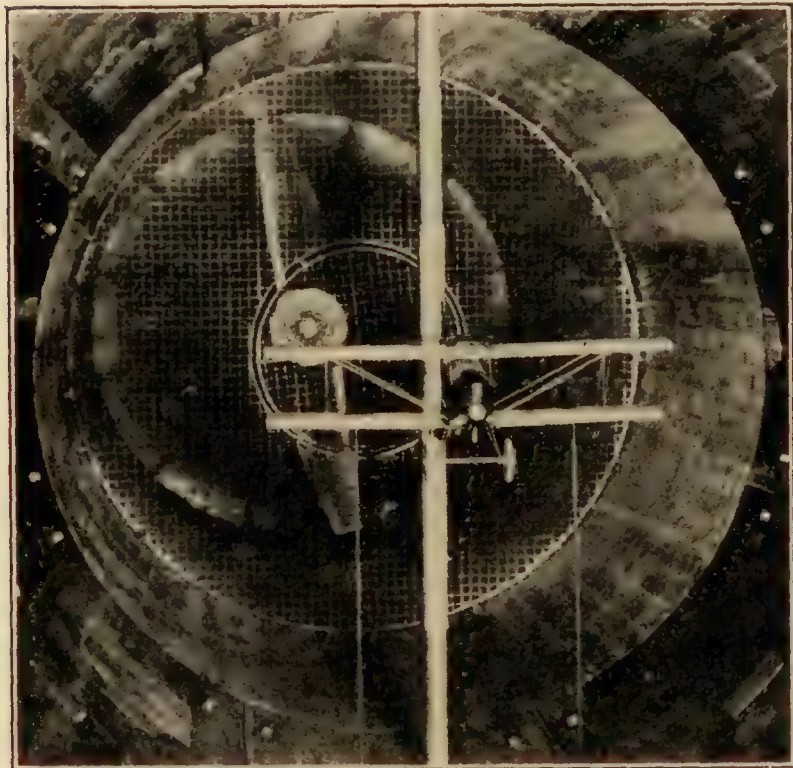


FIG. 11.—Method of supporting Sperry messenger model

could be revolved in the tunnel. Observations were thus made at a large number of points. The dynamic pressure will be seen to vary in the region occupied by the model within a range of plus or minus 2 per cent. This survey was made at one and two atmospheres only. We know from check runs that the same flow condition holds for other pressures. The horizontal static pressure gradient in the tunnel at various pressures is shown in Figure 15. Pressures are given with reference to a static plate located in the wall of the experiment section. It will be noted that the curves which are plotted on semilog paper are parallel, indicating that the pressure gradient is proportional to the density. Operating data of general interest, as the time required for raising pressure in the tank, the time required to exhaust the tank, the power consumption of the compressors and drive motor, are shown in Figure 16. The velocity change with change of tank pressure is also shown. The energy ratio of the tunnel for various tank pressures is shown in Figure 17.

The building of this tunnel and the development of its various mechanical devices to a point where routine testing may be done has required the solution of a number of mechanical problems. This development period has passed, and the results now being obtained in the tunnel are believed to be as consistent and reliable as those obtained in any other wind tunnel. Two airplane models and thirty-seven airfoils have so far been tested. Tests of a Sperry Messenger airplane model provided with eight different sets of wings are now in progress.

The variation of the aerodynamic characteristics of an airplane model with change of scale is shown in Figure 18. This figure gives the polar curves of the Fokker D-7 airplane model tested at various tank pressures. The minimum drag and the lift/drag ratio for this model, and also for a Sperry Messenger model, are plotted against Reynolds Number in Figure 19.

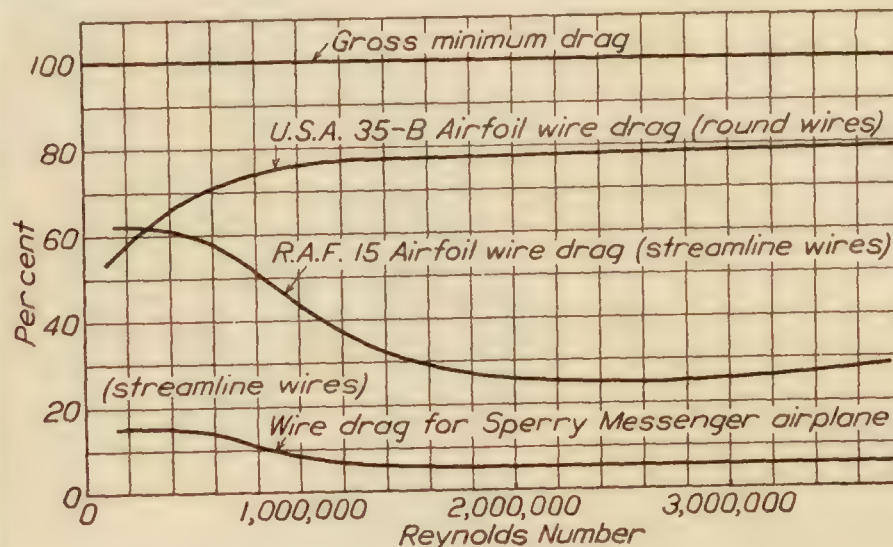


FIG. 12.—Drag of streamline wires as compared with round wires for holding model

The dynamic pressure distribution in the experiment section is represented by contour lines in Figure 14. This survey was made by using a number of Pitot tubes mounted on a bar which



FIG. 13.—Micromanometer

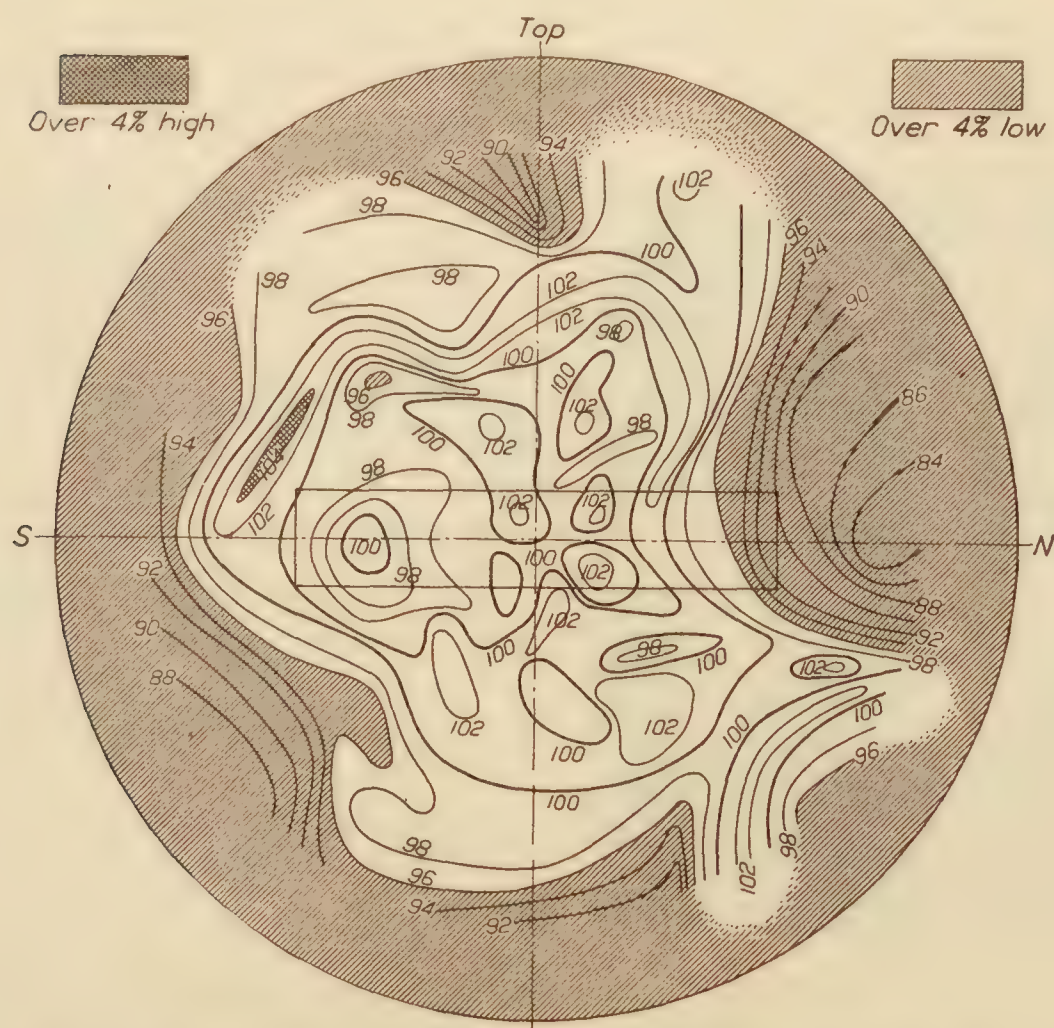


FIG. 14.—Variable density wind tunnel dynamic pressure survey. Observations taken at 161 different points. Pressures are in per cent of arbitrary reference point. Plane of survey —49.5" in rear of honeycomb. Rectangle at center indicates approximate position of airfoil

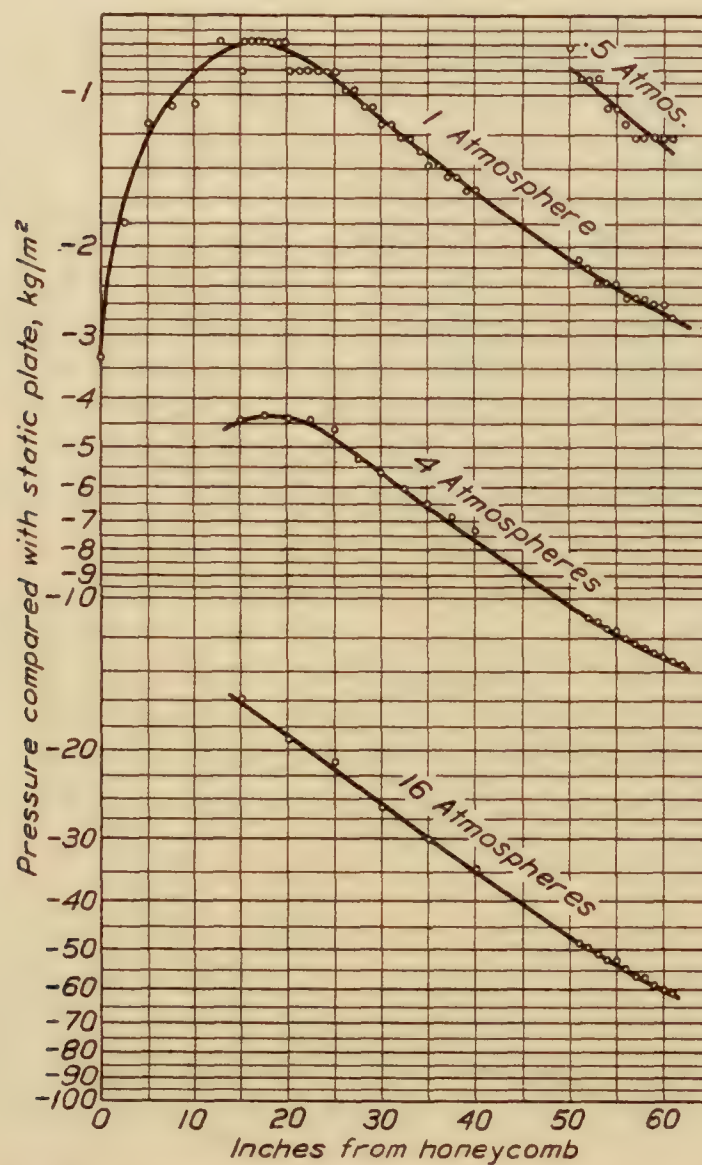


FIG. 15.—Horizontal static pressure gradient for various tank pressures

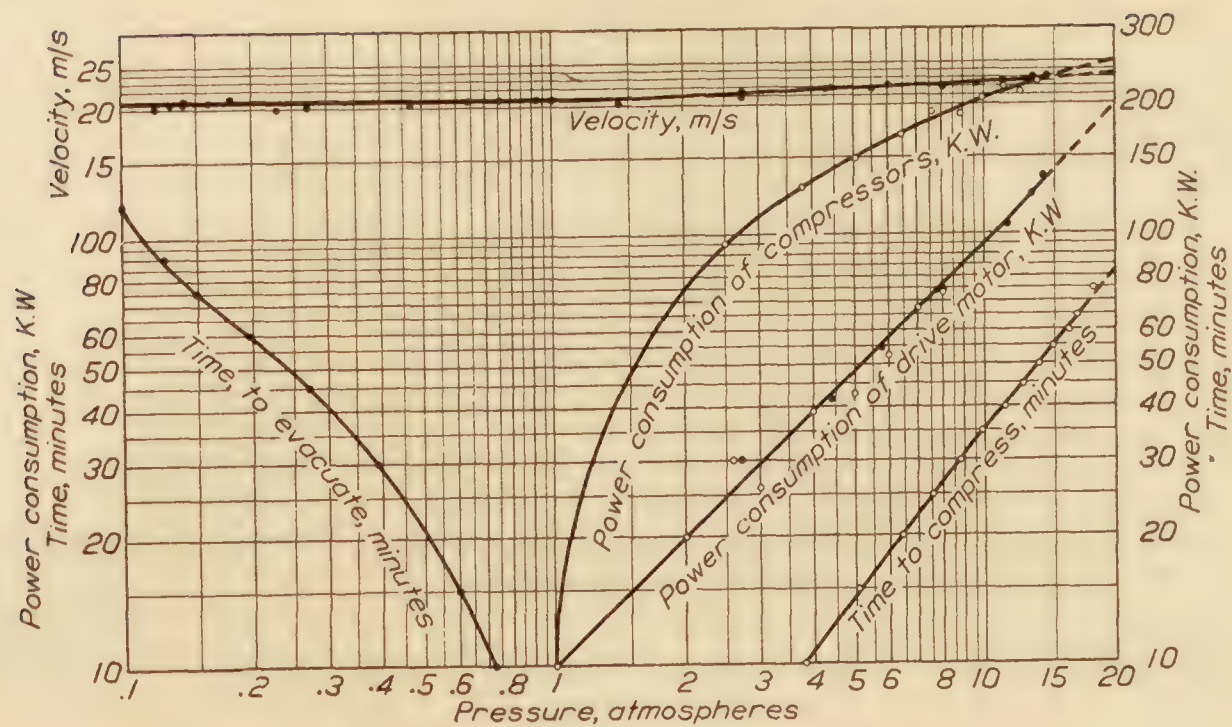


FIG. 16.—Variable density wind tunnel power plant data

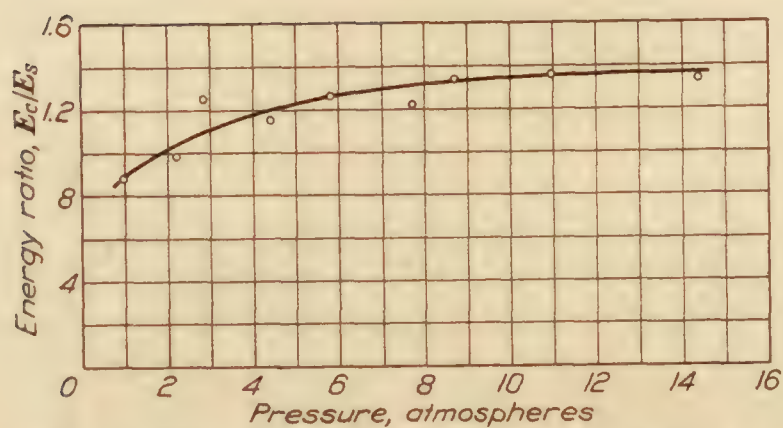
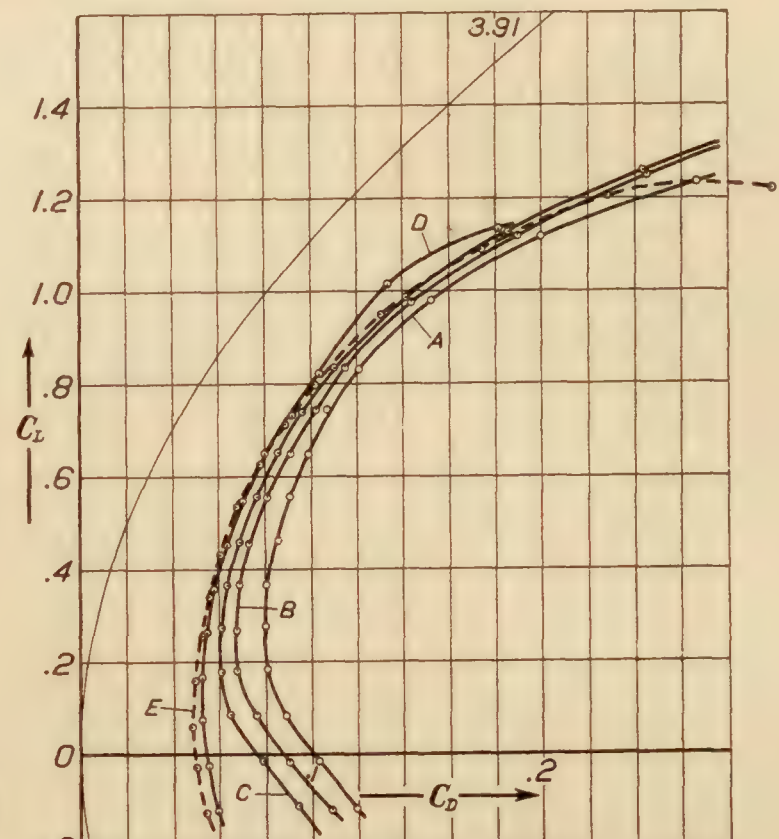
FIG. 17.—Variable density wind tunnel, energy ratio E_c/E_s .
 E_c —Kinetic energy in throat, kg/m/s., E_s —Energy input to motor, including exciting energy

FIG. 18.—Fokker D VII airplane model

	Tank pressure atmosphere	Dynamic pressure $q = \text{kg/m}^2$	Reynolds Number
Curve A	1.00	27.5	135,000
Curve B	2.64	75.6	358,000
Curve C	5.17	149.0	695,000
Curve D	10.14	293.0	1,330,000
Curve E	20.10	625.0	2,720,000

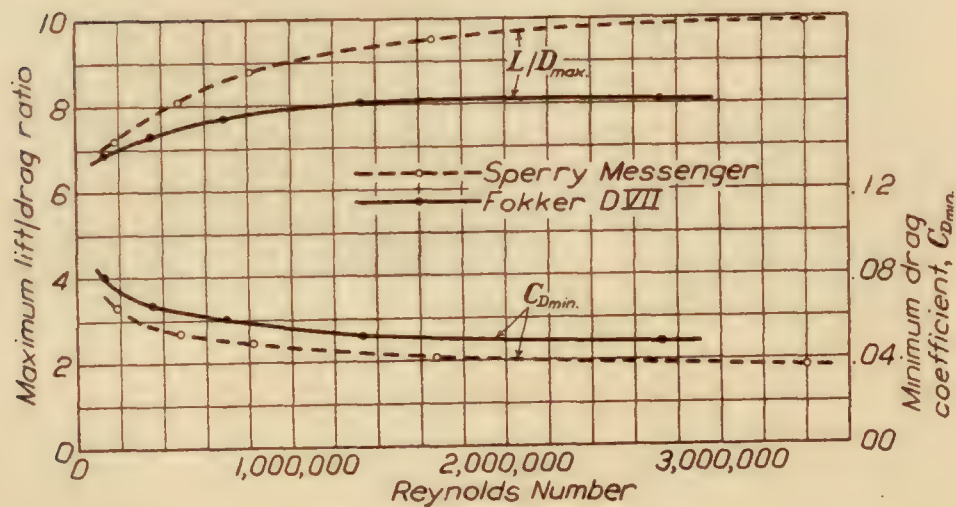


FIG. 19.—Scale effect on airplane models

CONCLUSIONS

The underlying theory of the variable density tunnel has been discussed, the mechanical construction of the tunnel has been described, and some typical results obtained on an airplane model have been given. The tunnel is in continuous operation, and there is every reason to believe that the results obtained at the higher densities are truly representative of full-scale conditions.

REFERENCES

- Reference 1.—“On a New Type of Wind Tunnel,” by Dr. Max M. Munk. N. A. C. A. Technical Note No. 60
“Abriss der Lehre von der Flüssigkeits und Gasbewegung,” by Dr. L. Prandtl. Handwörterbuch der Naturwissenschaften, vol. 4.
“Experimental Investigations,” by O. Reynolds, Phil. Trans. 174 (1883), and “On the Dynamic Theory of Viscous Fluids,” Phil. Trans. A. 186 (1894).
“Similarity of Motion in Relation to the Surface Friction of Fluids,” by T. E. Stanton and J. R. Pannell, Phil. Trans. A, vol. 214, pp. 199–224, 1914.

REPORT No. 228

A STUDY OF THE EFFECT OF A DIVING START ON AIRPLANE SPEED

By WALTER S. DIEHL
Bureau of Aeronautics, Navy Department

REPORT No. 228

A STUDY OF THE EFFECT OF A DIVING START ON AIRPLANE SPEED

By WALTER S. DIEHL

SUMMARY

Equations for instantaneous velocity and distance flown are derived for an airplane which crosses the starting line of a speed course at a speed higher than that which can normally be maintained in horizontal flight. A specific case is assumed and calculations made for five initial velocities. Curves of velocity, average velocity, and distance flown are plotted against time for each case and analyzed. It is shown that the increase in average velocity due to a diving start may be very large for short-speed courses.

INTRODUCTION

In attempts to establish airplane speed records when the method of approach to the speed course is not specified, pilots often dive in order to enter the course at a speed greater than that which can normally be maintained in horizontal flight. The flight over the course is then made at a speed which asymptotically approaches the normal horizontal speed as the excess kinetic energy is absorbed. The increase in average speed thus obtained for courses of varying length should be of considerable interest to pilots and to the officials in charge of contests.

So far as the writer has been able to ascertain, no analysis of this problem has previously been made. In the present analysis, assumptions have been made so as to simplify the problem as much as practicable without seriously affecting the validity of the final results.

ASSUMPTIONS

In order to obtain a simple and reasonably exact solution of the problem the following assumptions have been made:

- (1) Propeller thrust is constant,
- (2) Flight over the course is horizontal,
- (3) The resistance varies as V^2 .

The first assumption is a simplifying approximation only. If the brake horsepower and propeller efficiency were to remain constant then the thrust must vary inversely as the velocity. Actually the engine speeds up and delivers an appreciable increase in power when the flight speed is increased, while the propeller efficiency remains substantially constant. The net result is a thrust which neither remains constant nor varies inversely as the velocity. Since the assumption of constant thrust is simpler than that of variable thrust, it has been adopted.

The second and third assumptions are fully justified. One of the requirements always made in speed runs is horizontal or substantially horizontal flight. The change in angle of attack required to maintain horizontal flight is very small under the conditions assumed. Consequently the drag coefficient will be constant and the drag will vary as V^2 .

DERIVATION OF EQUATION FOR VELOCITY

The horizontal forces acting on the airplane are thrust and resistance. The equation of motion is

$$F = (T - R) = \frac{W}{g} \frac{dV}{dt} \quad (1)$$

R may be replaced by its equivalent KV^2 , the value of K being taken for R in pounds and V in feet per second, in order to obtain consistent units. Substituting KV^2 for R and rearranging equation (1) gives

$$\frac{dV}{T - KV^2} = \frac{g}{W} dt \quad (1a)$$

which upon integration becomes

$$\frac{2g\sqrt{TK}}{W} t = \log_e \frac{(T - V_o\sqrt{TK}) + V(\sqrt{TK} - KV_o)}{(T + V_o\sqrt{TK}) - V(\sqrt{TK} + KV_o)} \quad (2)$$

or

$$e^{\frac{2g\sqrt{TK}}{W} t} = \frac{(T - V_o\sqrt{TK}) + V(\sqrt{TK} - KV_o)}{(T + V_o\sqrt{TK}) - V(\sqrt{TK} + KV_o)} \quad (2a)$$

from which

$$V = \frac{(T + V_o\sqrt{TK}) e^{\frac{2g\sqrt{TK}}{W} t} + (V_o\sqrt{TK} - T)}{(\sqrt{TK} + KV_o) e^{\frac{2g\sqrt{TK}}{W} t} + (\sqrt{TK} - KV_o)} \quad (3)$$

In these equations T is the thrust in pounds, t the time in seconds measured from the time of crossing the starting or base line, V_o the velocity in feet per second when $t=0$, V the instantaneous velocity in feet per second, and K the resistance coefficient previously defined.

For simplicity equation (3) may be written in the form

$$V = \frac{C_1 e^{at} + C_2}{C_3 e^{at} + C_4} \quad (3a)$$

where

$$\begin{aligned} C_1 &= (T + V_o\sqrt{TK}) \\ C_2 &= (V_o\sqrt{TK} - T) \\ C_3 &= (\sqrt{TK} + KV_o) \\ C_4 &= (\sqrt{TK} - KV_o) \\ a &= \frac{2g\sqrt{TK}}{W} \end{aligned}$$

DERIVATION OF EQUATION FOR DISTANCE

The distance flown in a given time may readily be obtained by integrating equation (3a).

$$S = \int V dt = \int_{t_o}^{t_1} \left[\frac{C_1 e^{at} + C_2}{C_3 e^{at} + C_4} \right] dt \quad (4)$$

$$S = \frac{C_1}{aC_3} \log_e (C_3 e^{at} + C_4) + \frac{C_2}{aC_4} [at - \log_e (C_3 e^{at} + C_4)] + C. \quad (5)$$

Equation (5) may now be very much simplified by returning to the original terms, since

$$\frac{C_1}{aC_3} = \frac{(T + V_o\sqrt{TK})}{\frac{2g\sqrt{TK}}{W} (\sqrt{TK} + KV_o)} = + \frac{W}{2gK} \quad (6)$$

$$\frac{C_2}{aC_4} = \frac{V_o\sqrt{TK} - T}{\frac{2g\sqrt{TK}}{W} (\sqrt{TK} - KV_o)} = - \frac{W}{2gK} \quad (7)$$

$$\frac{C_2}{C_4} = \frac{(V_o\sqrt{TK} - T)}{(\sqrt{TK} - KV_o)} = - \sqrt{\frac{T}{K}} = -V_o \quad (8)$$

substituting (6), (7) and (8) into (5) gives

$$S = \frac{W}{gK} \log_e(C_3 e^{at} + C_4) - V_o t + C \quad (5a)$$

When $t=0$, $S=0$. Therefore

$$\begin{aligned} C &= -\frac{W}{gK} \log_e(C_3 + C_4) \\ &= -\frac{W}{gK} \log_e(2\sqrt{TK}) \end{aligned}$$

from which

$$S = \frac{W}{gK} \log_e(C_3 e^{at} + C_4) - V_o t - \frac{W}{gK} \log_e(2\sqrt{TK}) \quad (9)$$

APPLICATION OF EQUATIONS TO A SPECIFIC PROBLEM

In order to study the effects of a diving start, a fictitious airplane having characteristics similar to the recent racing designs will be assumed:

Let $W = 2,100$ lbs.

$V = 250$ M. P. H. $= 366.67$ f. p. s.

and $T = R = 600$ lbs.

Then $K = 600/(366.67)^2 = .0044628$

$$\sqrt{K} = .0668$$

$$\sqrt{T} = 24.4949$$

$$\sqrt{TK} = 1.63636$$

$$\frac{W}{gK} = 14615.335$$

The equations for velocity and distance may now be written for any initial velocity V_o . Table I contains the evaluation of the constants for five values of V_o : 260, 270, 280, 290, and 300 miles per hour. The resulting equations are:

I. $V_o = 260$ M. P. H. $= 381.333$ f. p. s.

$$\text{Velocity} \quad V = \frac{1224 e^{.05014t} + 24}{3.33818 e^{.05014t} - .06545} \quad (10)$$

$$\text{Distance flown} \quad S = 14615.34 \log_e(3.33818 e^{.05014t} - .06545) - 366.67 t - 17328.30 \quad (11)$$

II. $V_o = 270$ M. P. H. $= 396.00$ f. p. s.

$$V = \frac{1248 e^{.05014t} + 48}{3.40364 e^{.05014t} - .13091} \quad (12)$$

$$S = 14615.34 \log_e(3.40364 e^{.05014t} - .13091) - 366.67 t - 17328.30 \quad (13)$$

III. $V_o = 280$ M. P. H. $= 410.66$ f. p. s.

$$V = \frac{1272 e^{.05014t} + 72}{3.46909 e^{.05014t} - .19636} \quad (14)$$

$$S = 14615.34 \log_e(3.46909 e^{.05014t} - .19636) - 366.67 t - 17328.30 \quad (15)$$

IV. $V_o = 290$ M. P. H. $= 425.33$ f. p. s.

$$V = \frac{1296 e^{.05014t} + 96}{3.53455 e^{.05014t} - .26182} \quad (16)$$

$$S = 14615.34 \log_e(3.53455 e^{.05014t} - .26182) - 366.67 t - 17328.30 \quad (17)$$

V. $V_o = 300$ M. P. H. $= 440$ f. p. s.

$$V = \frac{1320 e^{.05014t} + 120}{3.60000 e^{.05014t} - .32727} \quad (18)$$

$$S = 14615.34 \log_e(3.60000 e^{.05014t} - .32727) - 366.67 t - 17328.30 \quad (19)$$

Velocities, distances, and average velocities have been calculated from equations (10) to (19), inclusive, and are given in Tables II and III and plotted in Figures 1 to 5, inclusive. A summary of these data is given in Table IV and plotted in Figure 6.

CONCLUSIONS

From a study of the figures and the summary in Table IV, the following conclusions may be drawn:

1. The effect of a dive before crossing the starting line is to increase the average velocity over the speed course by an amount which is directly proportional to the increase in initial velocity relative to the normal horizontal velocity.

2. A 10 per cent increase in initial velocity gives an increase in average velocity of 7.1 per cent over a 1-mile course, 5.2 per cent over a 2-mile course, 4 per cent over a 3-mile course, and 3.1 per cent over a 4-mile course for the specific case investigated.

3. The effect of an increase in initial velocity persists for a longer time than would be expected. At the end of one minute the velocity is still appreciably above normal.

4. Speed records made over courses of different lengths are not comparable when a diving start is taken.

TABLE I

EVALUATION OF CONSTANTS IN THE EQUATIONS FOR VELOCITY AND DISTANCE FLOWN

	$W=2,100$ lbs.	$V=250$ M. P. H.		$R=600$ lbs.	
V_o M. P. H.-----	260	270	280	290	300
V_o f. p. s.-----	381.33	396.0	410.66	425.33	440.0
$V_o \sqrt{TK}$ -----	624.0000	648.0000	672.0000	696.0000	720.0000
$C_1 = (T + V_o \sqrt{TK})$ -----	1,224.00	1,248.00	1,272.00	1,296.00	1,320.00
$C_2 = (V_o \sqrt{TK} - T)$ -----	24.00	48.00	72.00	96.00	120.00
$K V_o$ -----	1.70181818	1.76727272	1.83272727	1.89818181	1.96363636
$C_3 = (\sqrt{TK} + K V_o)$ -----	3.33818181	3.40363636	3.46909090	3.53454545	3.60000000
$C_4 = (\sqrt{TK} - K V_o)$ -----	-.0654545	-.130909	-.1963636	-.261818	-.3272727
$a = \frac{2g \sqrt{TK}}{W}$ -----	.050141	.050141	.050141	.050141	.050141

$$\begin{aligned} T &= 600 & \sqrt{T} &= 24.4949 \\ K &= .0044628 & \sqrt{K} &= .06680 \\ \sqrt{TK} &= 1.636363 \end{aligned}$$

TABLE II
CALCULATED VELOCITIES
W=2,100 lbs. V=250 M. P. H. R=600 lbs

Time <i>t</i> sec.	Velocities—M. P. H.				
	V ₀ =260	V ₀ =270	V ₀ =280	V ₀ =290	V ₀ =300
0	260.00	270.00	280.00	290.00	300.00
2	259.03	268.02	276.98	285.92	294.80
4	258.15	266.24	274.28	282.27	290.18
6	257.37	264.65	271.86	279.01	286.07
8	256.65	263.22	269.69	276.10	282.41
10	256.01	261.93	267.74	273.49	278.89
15	254.67	259.23	263.70	268.10	272.39
20	253.62	257.15	260.60	263.97	267.25
25	252.81	255.55	258.21	260.81	263.32
30	252.19	254.31	256.37	258.37	260.30
40	251.32	252.60	253.83	255.04	256.19
50	250.80	251.57	252.32	253.04	253.42
60	250.49	250.95	251.40	251.84	252.25

TABLE III
CALCULATED DISTANCES AND AVERAGE VELOCITIES
W=2,100 lbs. V=250 M. P. H. R=600 lbs.

Time <i>t</i> sec.	V ₀ =260		V ₀ =270		V ₀ =280		V ₀ =290		V ₀ =300	
	Distance flown	Average velocity	Distance flown	Average velocity	Distance flown	Average velocity	Distance flown	Average velocity	Distance flown	Average velocity
	Miles	M. P. H.	Miles	M. P. H.	Miles	M. P. H.	Miles	M. P. H.	Miles	M. P. H.
0	0	260.00	0	270.00	0	280.00	0	290.00	0	300.00
2	.144	259.23	.149	268.71	.155	278.18	.160	287.46	.165	297.05
4	.288	258.70	.298	267.71	.307	276.68	.317	285.55	.327	294.50
6	.431	258.38	.445	266.95	.459	275.46	.473	283.90	.487	292.38
8	.573	257.84	.591	266.00	.609	274.10	.627	282.12	.645	290.13
10	.715	257.51	.737	265.28	.758	272.98	.780	280.60	.801	288.22
15	1.069	256.64	1.098	263.56	1.127	270.41	1.155	277.15	1.183	283.88
20	1.422	255.93	1.456	262.12	1.490	268.23	1.524	274.26	1.557	280.24
25	1.773	255.31	1.812	260.88	1.850	266.38	1.888	271.80	1.925	277.16
30	2.123	254.78	2.165	259.84	2.207	264.67	2.249	269.67	2.288	274.54
40	2.822	253.75	2.868	258.13	2.914	262.26	2.959	266.32	3.004	270.33
50	3.518	253.28	3.567	256.84	3.616	260.35	3.664	263.78	3.714	267.42
60	4.213	252.79	4.364	255.85	4.315	258.87	4.364	261.88	4.412	264.74

TABLE IV
SUMMARY OF CALCULATIONS

Length of course	Initial velocity M. P. H.		260	270	280	290	300
	Ratio $\frac{\text{initial velocity}}{\text{normal velocity}}$		1.04	1.08	1.12	1.16	1.20
1 mile	Time, seconds		14.02	13.64	13.28	12.94	12.61
	Final velocity, M. P. H.		254.8	259.8	265.1	270.0	275.1
	Average velocity, M. P. H.		256.8	264.0	271.3	278.4	285.8
	Ratio $\frac{\text{average velocity}}{\text{normal velocity}}$		1.027	1.056	1.085	1.113	1.143
2 miles	Time, seconds		28.25	27.66	27.10	26.56	26.03
	Final velocity, M. P. H.		252.4	254.8	257.3	260.1	262.6
	Average velocity, M. P. H.		255.0	260.3	265.6	270.5	276.6
	Ratio $\frac{\text{average velocity}}{\text{normal velocity}}$		1.020	1.041	1.062	1.082	1.106
3 miles	Time, seconds		42.56	41.88	41.22	40.58	39.95
	Final velocity, M. P. H.		251.2	252.5	253.7	255.0	256.2
	Average velocity, M. P. H.		253.8	257.9	262.0	266.1	270.4
	Ratio $\frac{\text{average velocity}}{\text{normal velocity}}$		1.015	1.032	1.048	1.064	1.082
4 miles	Time, seconds		56.93	56.21	55.50	54.80	54.09
	Final velocity, M. P. H.		250.6	251.2	251.7	252.3	252.8
	Average velocity, M. P. H.		252.9	256.2	259.5	262.7	266.2
	Ratio $\frac{\text{average velocity}}{\text{normal velocity}}$		1.012	1.025	1.038	1.051	1.065

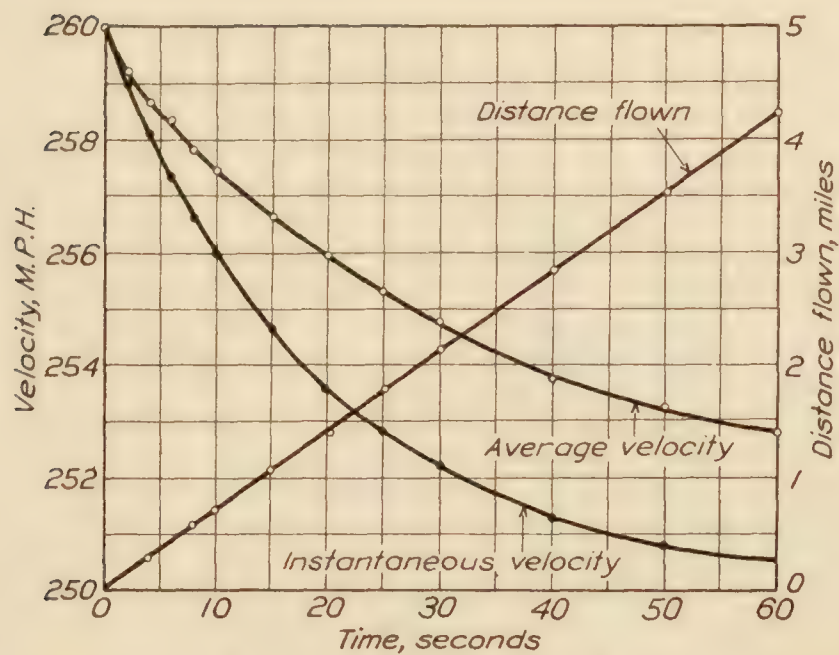


FIG. 1.—Initial velocity 260 M. P. H.

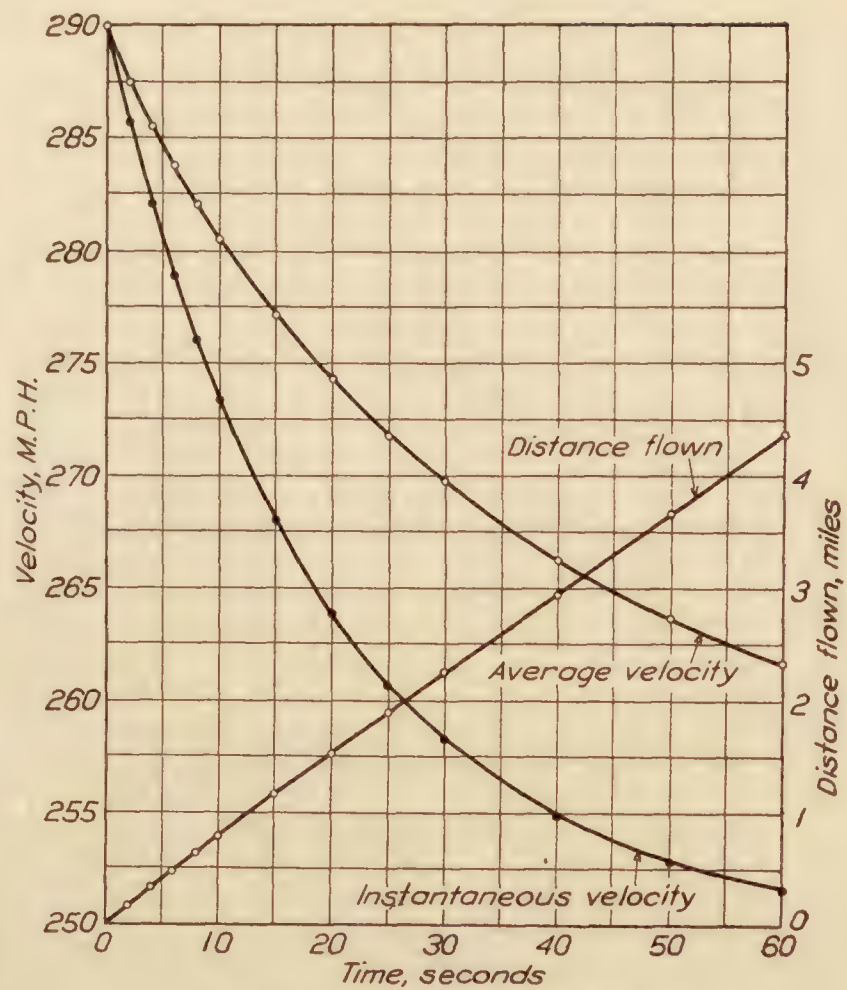


FIG. 4.—Initial velocity 290 M. P. H.

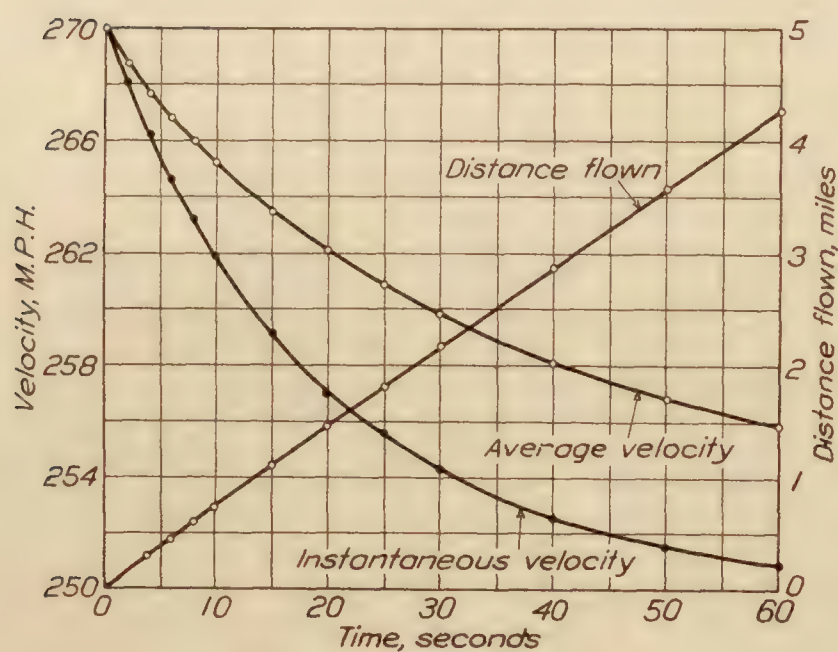


FIG. 2.—Initial velocity 270 M. P. H.

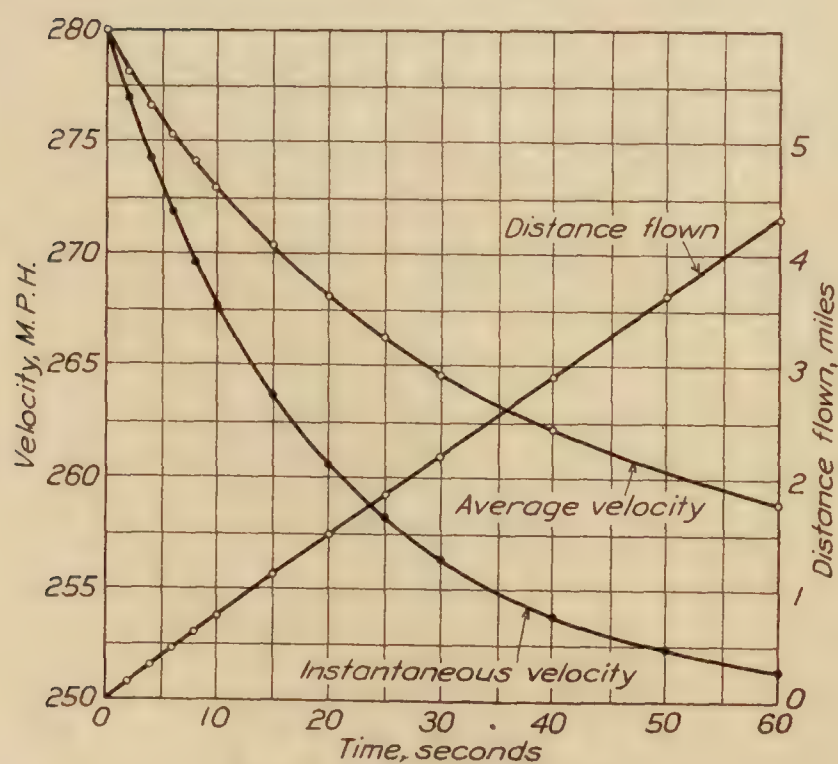


FIG. 3.—Initial velocity 280 M. P. H.

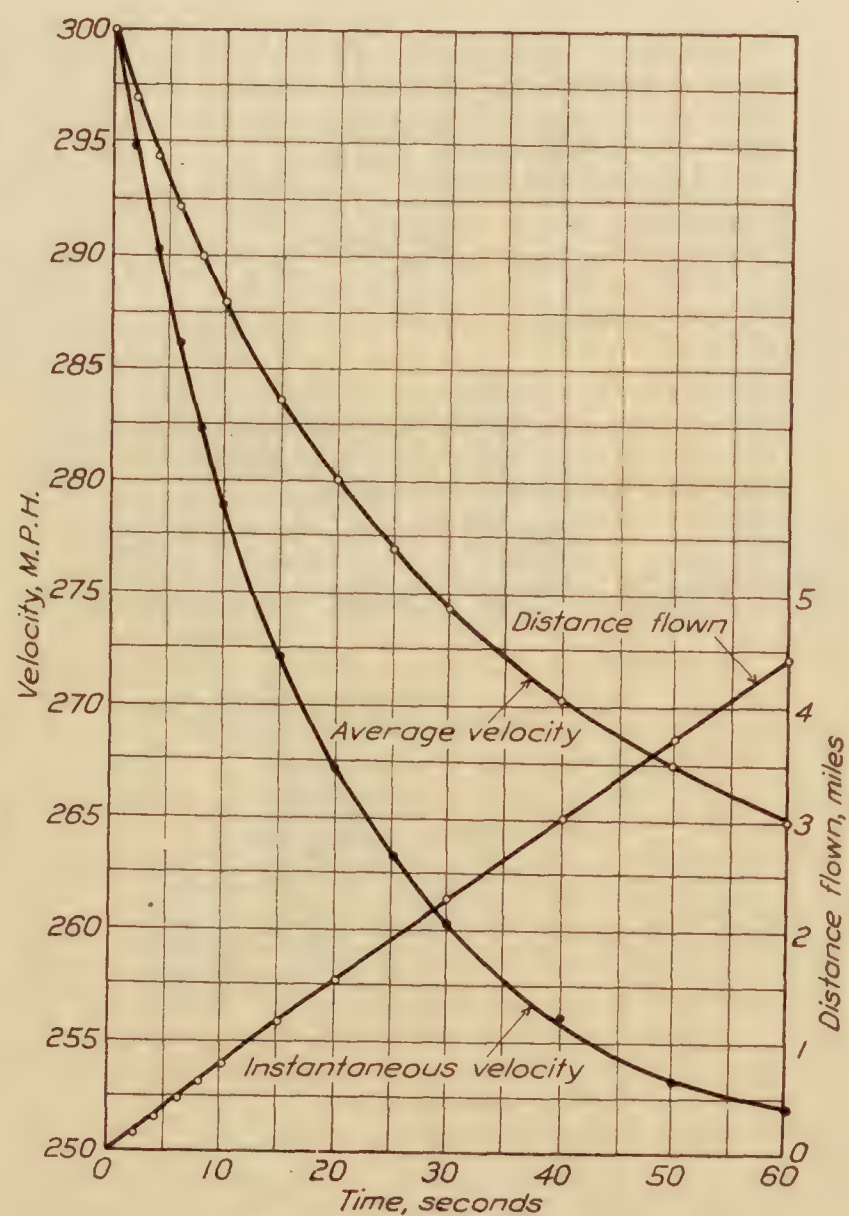


FIG. 5.—Initial velocity 300 M. P. H.

Effect of a diving start—
Normal velocity 250 M. P. H. $W=2,100$ lb. $T=600$ lb.

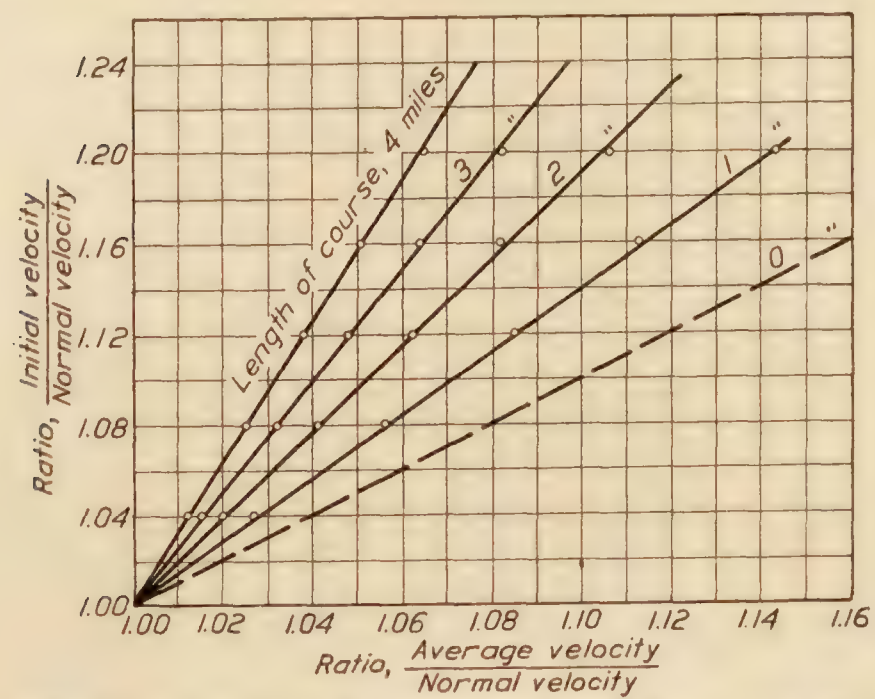


FIG. 6.—The effect of a diving start on average velocity. (High speed racing type airplanes.)

REPORT No. 229

PRESSURE DISTRIBUTION OVER THICK TAPERED AIRFOILS, N. A. C. A. 81, U. S. A. 27 C MODIFIED AND U. S. A. 35

By ELLIOTT G. REID
Langley Memorial Aeronautical Laboratory

REPORT No. 229

PRESSURE DISTRIBUTION OVER THICK TAPERED AIRFOILS, N. A. C. A. 81, U. S. A. 27 C MODIFIED, AND U. S. A. 35

By ELLIOTT G. REID

SUMMARY

At the request of the United States Army Air Service, the tests reported herein were conducted in the 5-foot atmospheric wind tunnel of the Langley Memorial Aeronautical Laboratory. The object was the measurement of pressures over three representative thick, tapered airfoils which are being used on existing or forthcoming Army airplanes. The results are presented in the form of pressure maps, cross-span load and normal force coefficient curves and load contours.

The pressure distribution along the chord was found very similar to that for thin wings, but with a tendency toward greater negative pressures. The characteristics of the loading across the span of the U. S. A. 27 C modified are inferior to those of the other two wings; in the latter, the distribution is almost exactly elliptical throughout the usual range of flying angles.

The form of tip incorporated in these models is not completely satisfactory and a modification is recommended.

INTRODUCTION

In the light of recent studies of accelerations in flight and some unexpected structural failures in the air, the schedule of required load factors for Army airplanes has been made much more severe than that formerly used. Consequently the design of wing cellules and the proper loading of wings in static test have become more serious problems than ever before. This is particularly true of pure or semi cantilever construction which involves the use of thick, tapered wings.

Determinations of the magnitude and disposition of the air loads imposed upon representative wings of this type have therefore been carried out.

METHODS AND APPARATUS

The pressure distribution measurements described below were made on half-span models of the following airfoils: N. A. C. A. 81, U. S. A. 27 C modified, and U. S. A. 35. The first is a double convex section of small mean camber; it is linearly tapered both in thickness and plan form. The second is also doubly convex but of larger camber; it is of constant section for about a chord length at midspan and is tapered linearly in plan form and thickness from this section to a tip which is washed out 1.5 degrees. The third airfoil has a slightly concave lower surface and the greatest camber of the group; its taper is linear in plan form and thickness.

Models.—The models were built of mahogany laminations and inlaid with soft brass tubes of 0.050 inch (1.27 millimeters) outside diameter. The N. A. C. A. 81 and a sample lamination are shown in Figure 1. Details of the models, location of orifices, etc., are given in Figures 2, 3, and 4.

Into each model were built between 70 and 80 tubes which had their open ends distributed along the 6 chosen chords of the semispan. The portion of each lamination to be included within the finished model was laid out and the tube grooves made within these limits. Tubes were then cut to extend slightly beyond the model surface and well beyond the wing butt. Glue and dowel pins were used to build up the laminations into complete wing blanks.



FIG. 1.—N. A. C. A. 81 model and sample lamination with tube in place



FIG. 5.—Model assembled in supporting pedestal

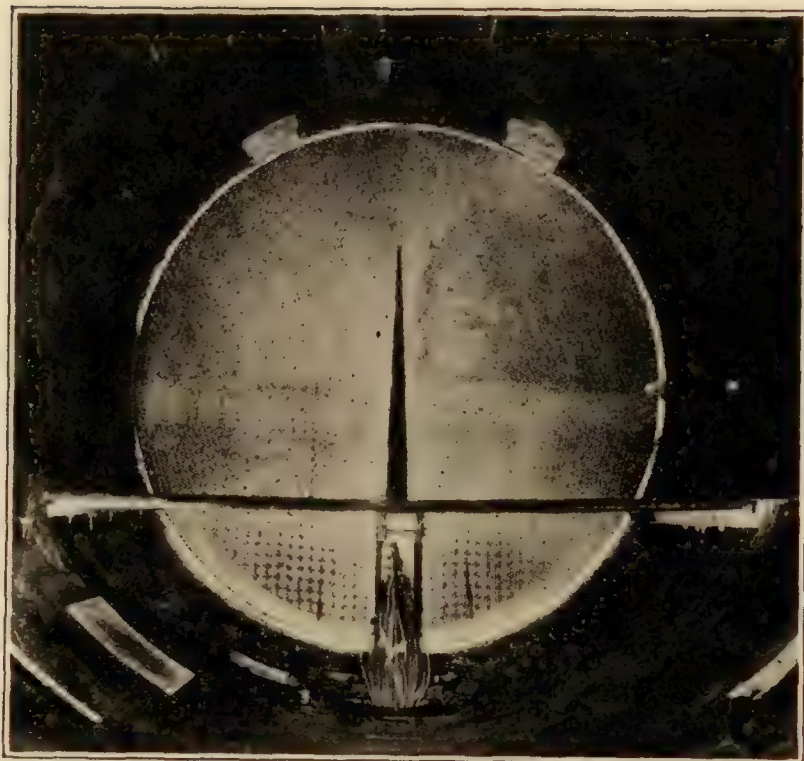


FIG. 6.—View upstream in tunnel before inclosing pedestal

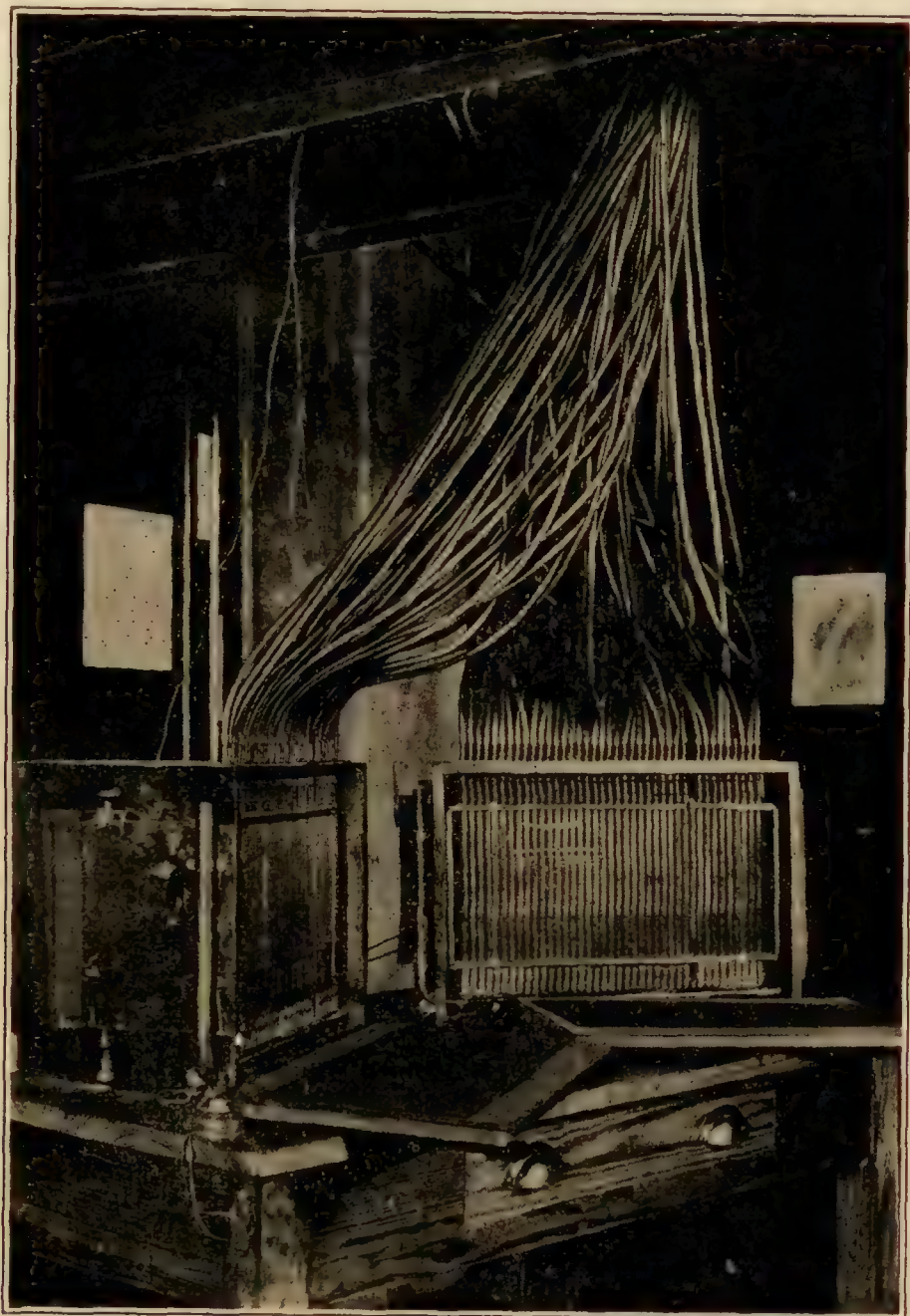


FIG. 7.—Manometer installation

square tip, and the surface faired down to this line. A form approximating that of the leading edge was maintained well around the front corner; the radius was then gradually reduced to give a smooth transition into the sharp trailing edge. The resulting mutilations of the original surface extended inward to a maximum distance of 10–15 per cent of the original tip chord; the actual contours of the sections close to the tip were obtained from plaster casts taken after completion of the tests and are represented, to true scale, in Figures 2, 3, and 4.

Apparatus.—The models were supported in a heavy cast-iron pedestal, or bracket, which could be rotated on a base affixed to the bottom of the tunnel. A sheet-metal “plane of symmetry,” which extended clear across the tunnel, was used to replace, in effect, the other half of the wing by its reflecting or “mirror” action.

Out of this plane was cut a disk and a disk of very slightly smaller diameter was fitted to the wing and carried on bosses on the supporting bracket, as shown in Figure 5. The small gap between disk and plane was sealed by a sheet-metal ring attached to the under side of the disk. The reflecting plane extended 38.5 inches (978 millimeters) upstream and 40.5 inches

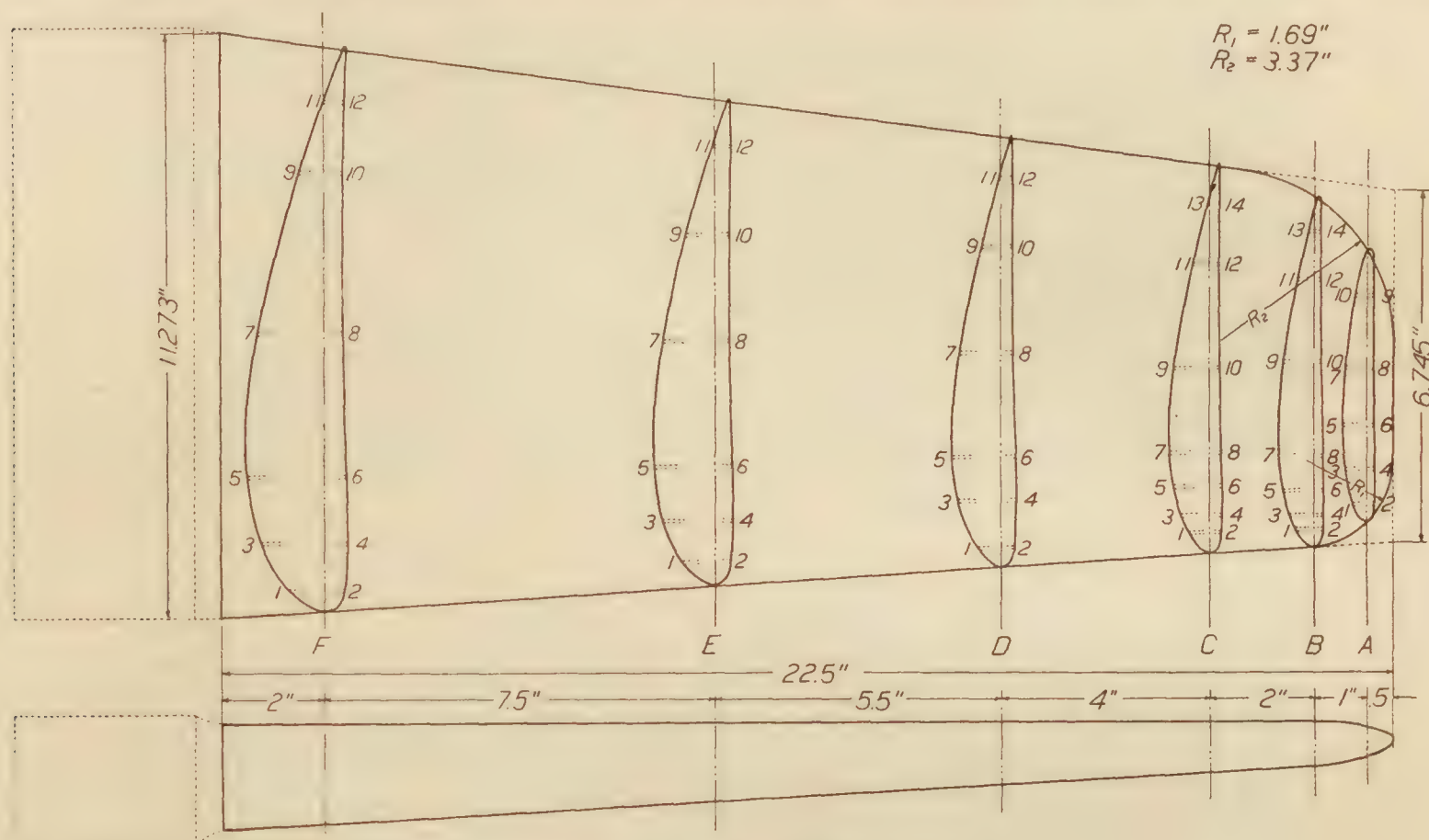


FIG. 4.—U. S. A. 35 model

(1,030 millimeters) downstream from the axis of the supporting bracket. The installation is shown in Figure 6; this photograph is incomplete as a fixed, sheet-metal streamline entirely inclosed the bracket and tubes during testing. It will be noted that wing tip and dividing plane are equidistant, respectively, from top and bottom of the tunnel.

Rubber tubes were led from the wing butt to the two recording multiple manometers which were placed on a table directly below the model (see fig. 7). All upper surface tubes were connected to one manometer and lowers to the other; tubes from adjacent stations were connected to corresponding manometer tubes so that pressure maps could be observed directly in the manometers. This arrangement was very convenient in the location of the angles of attack of zero and maximum normal force. The end tubes of each manometer were connected to a static orifice on the tunnel wall above and just forward of the wing tip. This pressure was used as the reference from which positive and negative pressures were measured.

Small electric bulbs in the backs of the manometers furnished the illumination for exposure of the record blanks of sensitized paper. Blanks were held in contact with the tubes so that direct prints were made, thus eliminating any scaling factor. A sample record is shown in Figure 8.

Procedure.—Before any records were taken, a velocity survey was made directly in front of the model. It was found that the velocity close to the plane was considerably higher than that in the free stream above it. This was quite evidently due to the restriction of the flow beneath the plane by the large stream line required to inclose the bracket.

To remedy this condition, the leading edge of the reflecting plane was slightly elevated. A new velocity survey showed an improved condition and by a series of trials a position giving a very uniform velocity distribution across the span was found. All these preliminary trials were made with the wing at approximately the angle of zero normal force. A satisfactory distribution having been found for this condition, the wing was turned to a large angle and another survey made. To eliminate possible yaw effects on the exploring Pitot, the instrument was turned to parallelism with a silk thread held just above its nose.

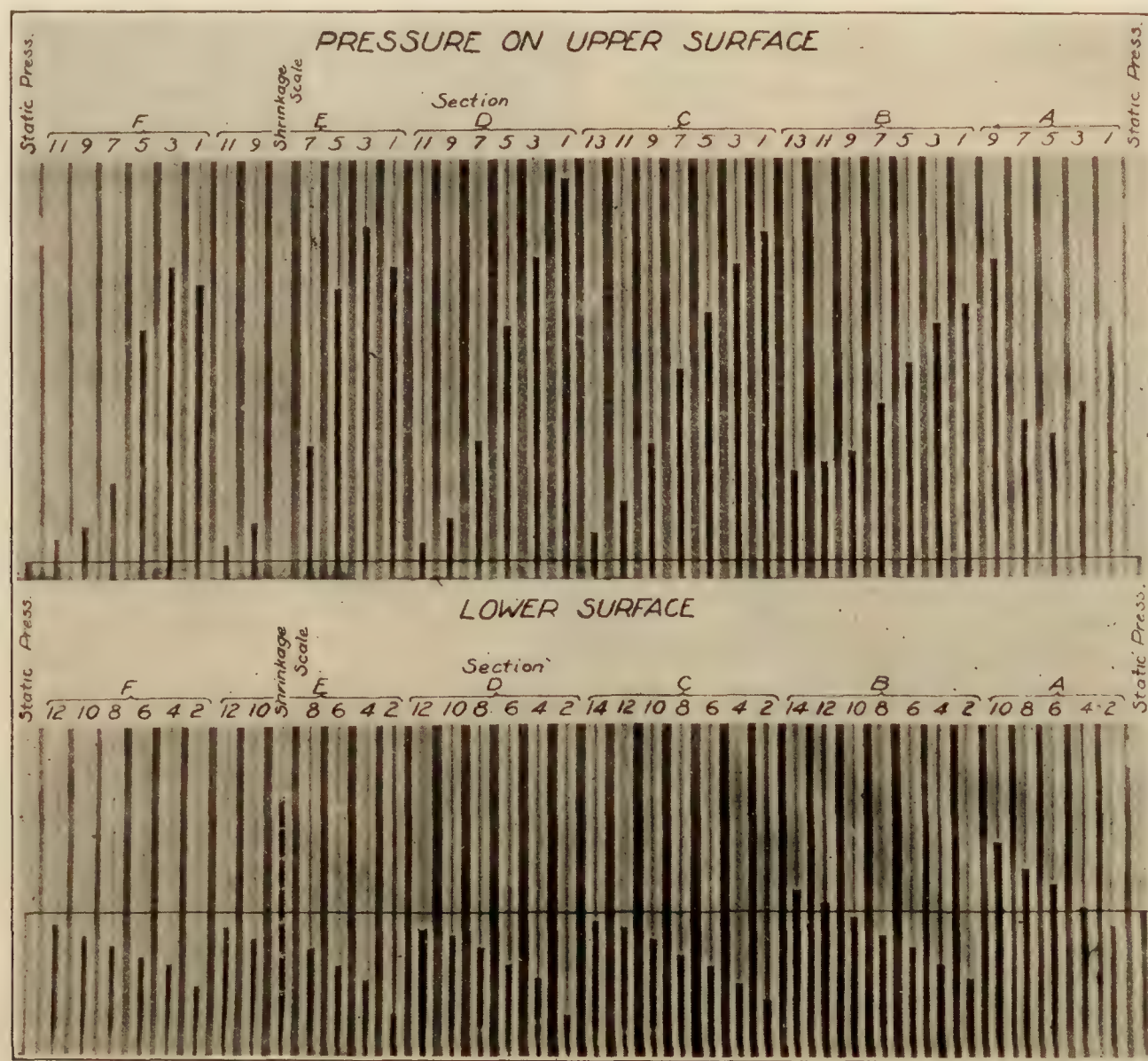


FIG. 8.—Sample manometer record

Results of the two velocity surveys, for the final position of the leading edge of the plane, are given in Figure 9. The dynamic head used in computations was the average of the integrated means of these values. (In the integration, only values between a point 2 inches (50.8 millimeters) above the plane and the wing tip were used.)

Following the establishment of a satisfactory velocity distribution, preliminary runs were made to determine the range of angles to be covered and to make sure that the pressures encountered were within the range of the manometers.

It was found possible to test two of the models at 25 m/s (82.0 ft./s.) but the negative pressures on the U. S. A. 35 were so large that the speed had to be reduced to 22.5 m/s (73.9 ft./s.).

During the taking of records, air speed was maintained constant according to the regular "service Pitot," which is located upstream from the fine honeycomb marking the forward end of the straight throat section of the tunnel.

The actual taking of records was a very short, direct process. The angle of attack was set by means of a vernier on the supporting bracket, the air speed adjusted to the proper value, and the manometers loaded. A few seconds were allowed to elapse for the establishment of steady conditions and then an exposure of about one-half second was made.

Accuracy.—Models were constructed to a maximum tolerance of one-tenth of 1 per cent of the average chord.

After connection with the manometers, each line was checked for leakage and sluggishness. During the tests there were no fluctuations of liquid level sufficiently large or rapid to give indistinct records. The consistency of the method was proved by repeating a run at a high angle of attack several days after the original had been made. Areas of the pressure maps from the two runs were imperceptibly different.

Records were carefully scaled for possible shrinkage of the paper but this was found to be negligible. Planimetering of the pressure maps was held well within an accuracy of 1 per cent except in the smallest diagrams. The faring of curves was susceptible to errors of possibly 2 to 3 per cent. It seems probable that the final curves are accurate to within ± 2 per cent.

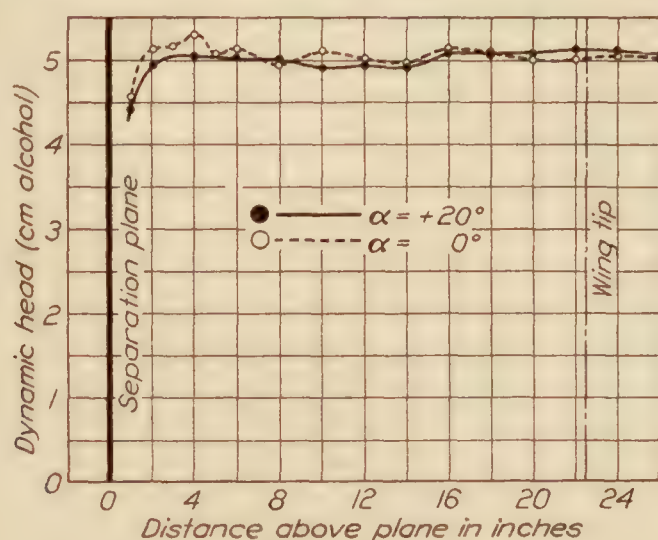


FIG. 9.—Velocity survey above separation plane

ADVANTAGES OF THE METHOD

The present method has three important advantages over those previously used in airfoil pressure distribution work. They are: Attainment of large Vl product by use of large models, elimination of the interference effects of supporting apparatus and pressure leads, and uniformity of results through simultaneous recording of pressures at all points of the wing's surface.

The question of tunnel wall interference might be of large importance, with models of the present size, if we were concerned with drag. However, the effect of drag variation upon normal force is small. If any serious effect upon the "apparent aspect ratio" were present, one would expect to find a considerable difference between the slopes of the curves of normal force versus angle of attack for these large models and for small ones. This does not seem to be the case.

Measurements of pressure taken very close to the dividing plane might be open to criticism as we know that there is a very sharp reduction of velocity in this region. The results obtained for loading across the span, however, seem to be altogether consistent and it is concluded that the closest station was sufficiently removed from the dividing plane to escape this influence.

RESULTS AND DISCUSSION

Pressure maps for the individual stations along the span are given in Figure 10 for the N. A. C. A. 81, in Figure 11 for the U. S. A. 27 C modified, and in Figure 12 for the U. S. A. 35. The contour charts, Figures 13 to 15, were made directly from these maps and represent the total pressure differences between upper and lower surfaces.

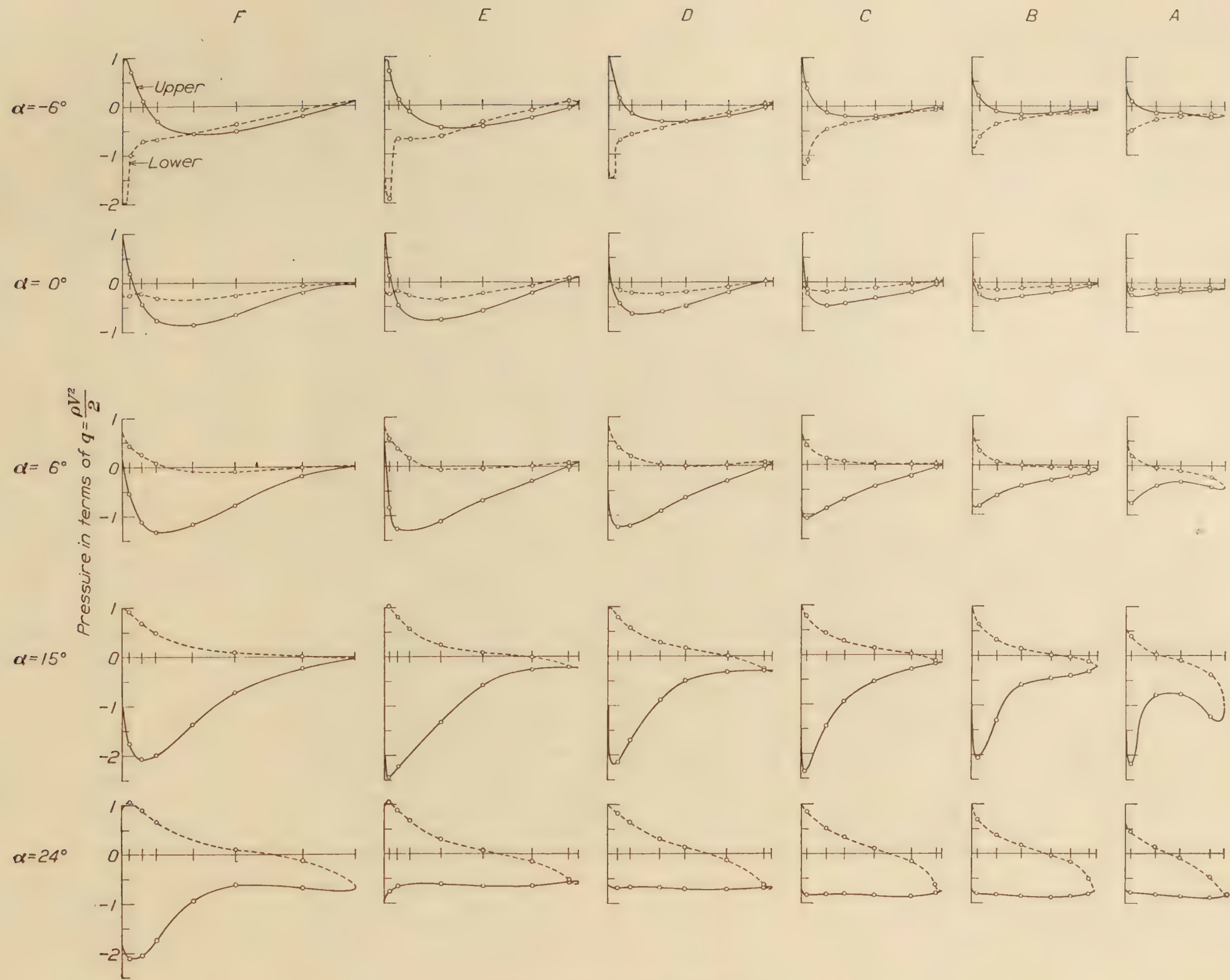


FIG. 10.—N. A. C. A. 81 pressure maps

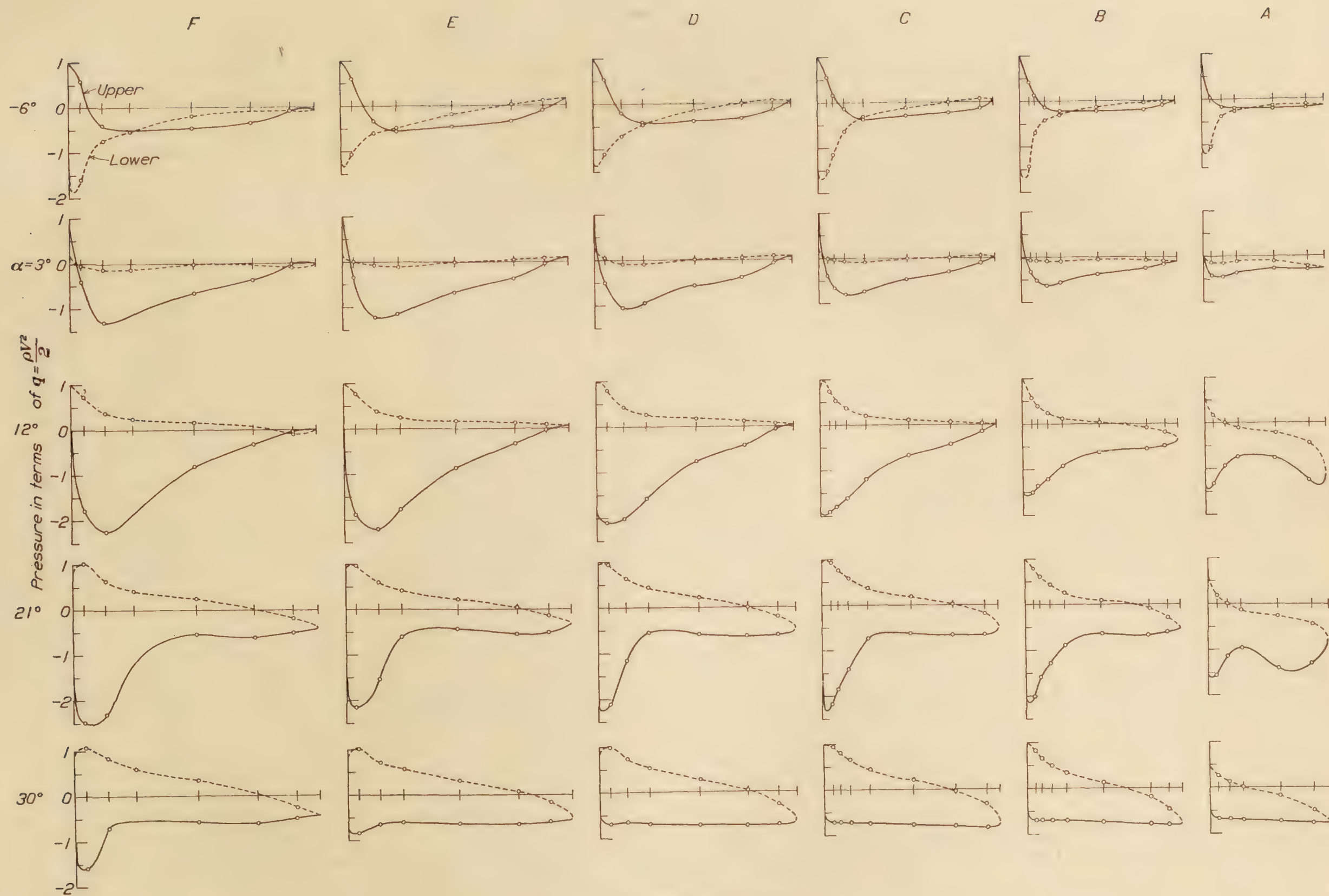


FIG. 11.—U. S. A. 27 C modified pressure maps

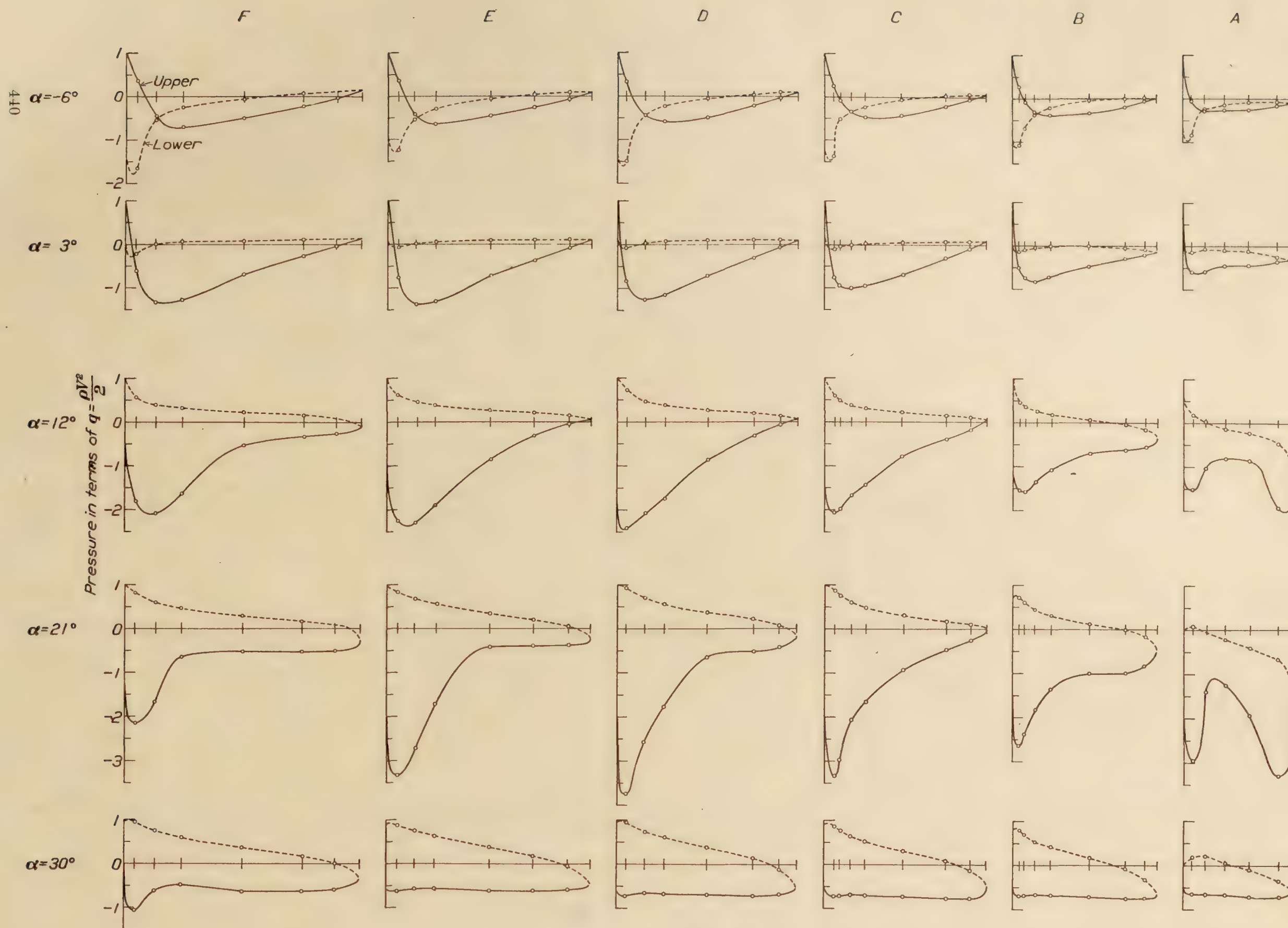


FIG. 12.—U. S. A. 35 pressure maps

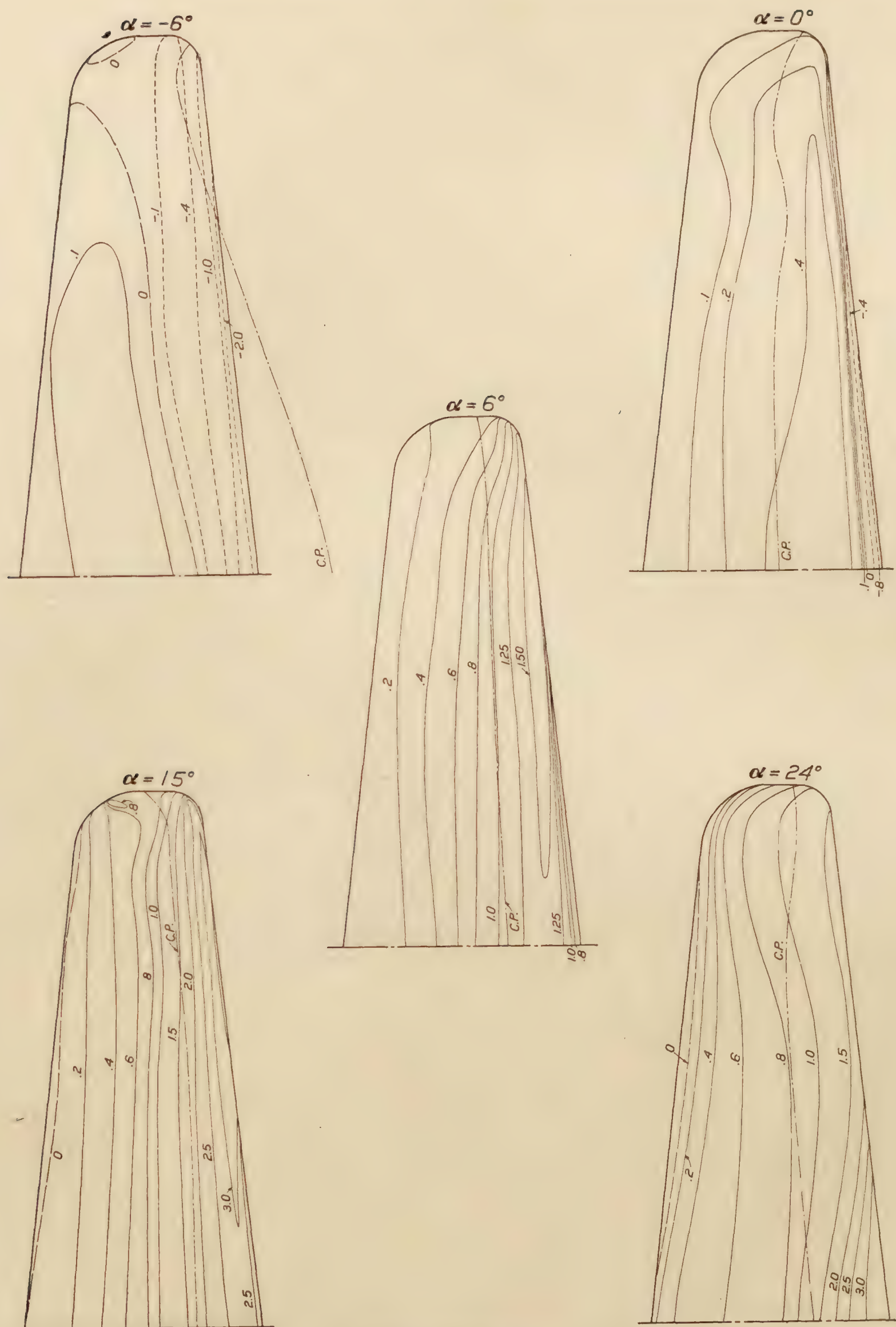


FIG. 13.—Contours of normal pressure—N. A. C. A. 81
(In terms of $q = \frac{\rho V^2}{2}$)

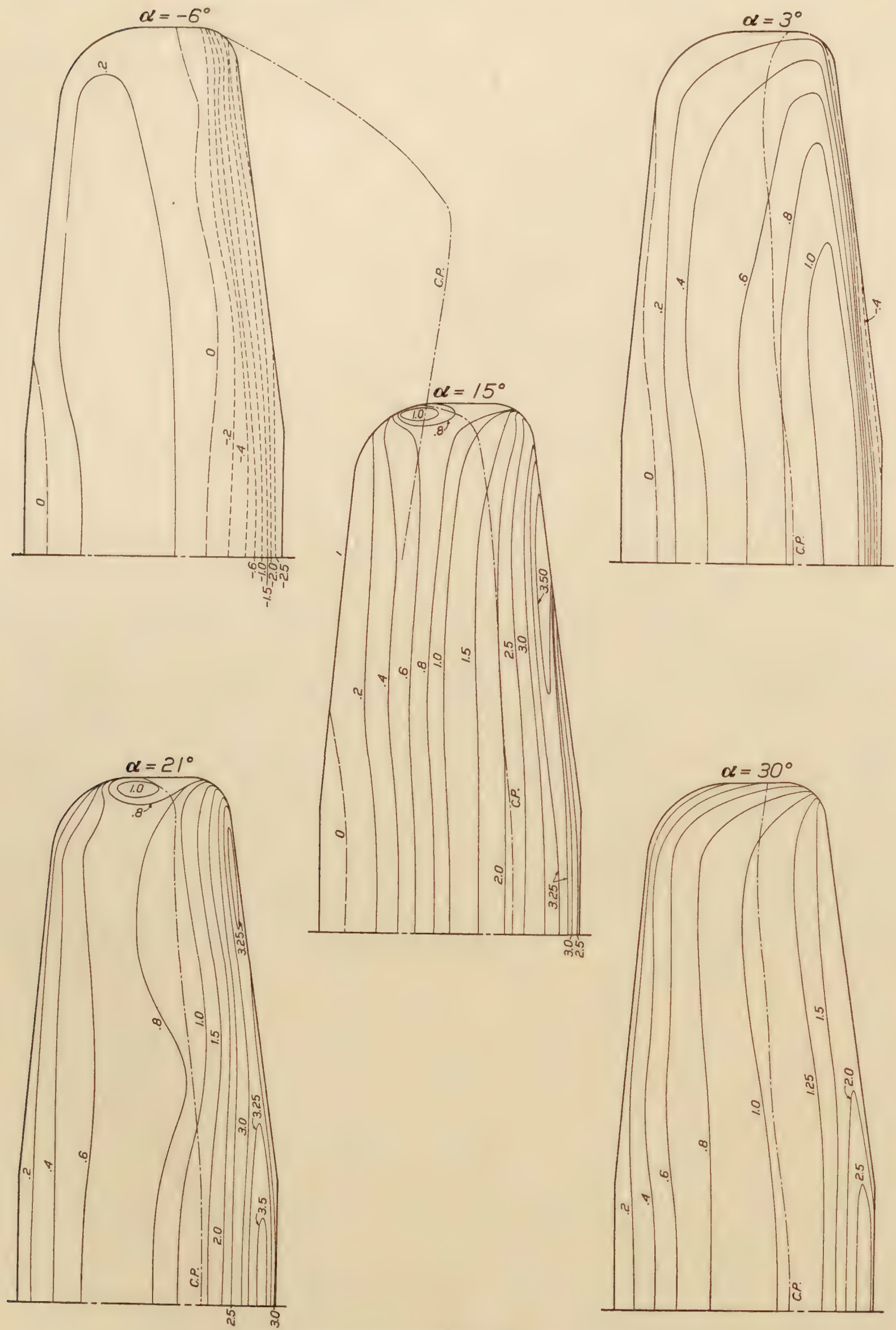


FIG. 14.—Contours of normal pressure—U. S. A. 27 C modified
(In terms of $q = \frac{\rho V^2}{2}$)

The load curves, Figures 16 to 18, have ordinates which are proportional to the areas of the corresponding pressure maps; a nondimensional ordinate has been introduced to avoid confusion in computations involving the varying chord. The coefficient K is equal to C_N times (chord/span); hence, K times q times span equals load per unit span.

From each load, the corresponding normal force coefficient C_N has been calculated and these values are plotted against the span as Figures 19, 20, and 21.

The areas under these curves have been integrated and divided by the semispan to give the values of C_N for the whole wing; the final plots of C_N versus angle of attack are given in Figures 22, 23 and 24.

The individual pressure maps are very similar to those for thin wings. The one outstanding effect of large thickness seems to be a depression of the front and middle portions of the diagrams, i. e., for the same pressure difference between upper and lower surfaces, the absolute pressures on both surfaces are lower for a thick than a thin wing. As zero lift is approached, this effect appears as a downward tilting of the pressure map toward the leading edge. Convexity of the lower surface accentuates this condition very noticeably, as was pointed out in Reference 2.

In general, the loading across the span on all three airfoils is satisfactory. The two main objectives of obtaining small moments about the spar roots and approximately elliptical lift distribution have been attained in all three wings.

Through the angles of the usual flying range, the loadings across the spans of the N. A. C. A. 81 and U. S. A. 35 approach the elliptic form very closely. From this point of view, there is little choice between them, unless it is that the moments about the spar roots are slightly greater for the latter. The load curves for the U. S. A. 27 C modified, however, droop toward midspan and consequently make this airfoil inferior to the other two.

In the high speed or diving range, the inferiority of the U. S. A. 27 C modified is very marked. From the load curves it may be seen that at zero lift the loading changes sign twice in the semispan, that is, there is positive lift at the quarter span point and negative lift at the tips and center. This would stress the spars excessively at the quarter points and probably give rise to uncertain stability and tricky control in a dive, as the airflow in such a condition is bound to be highly unstable.

It will be seen that on both the other wings, to obtain zero lift over the whole wing, the tip must be at negative lift. The condition indicates an excessive washout. Though neither of these wings has any "geometric washout," the aerodynamic characteristic is present to quite a large degree; the washout referred to here is the difference between the angles of zero lift of root and tip sections. This is considered an undesirable quality, particularly in its application to cantilever construction. It could easily be remedied by the use of a slight geometric washin which should not seriously detract from the good characteristics of the positive lift range.

The distribution of load at maximum lift is of considerable importance in the consideration of accelerated flight and, for this reason, the lateral centers of pressure have been calculated from the load curves for this condition. They were found to lie at the following percentages of the semispan, as measured from the center: N. A. C. A. 81, 41.9; U. S. A. 27 C modified, 44.3; U. S. A. 35, 45.5.

It will be noticed that while the sections midway between root and tip burble first in the N. A. C. A. 81 and U. S. A. 27 C modified, the U. S. A. 35 behaves quite differently. When this airfoil reaches maximum lift, the loads at the center of the span begin to decrease, then there is a more or less uniform reduction across the entire span and this is followed by an abrupt drop which attains its greatest value at about the quarter-span point.

The maximum intensity of load found along the leading edges of these wings would indicate that shape of the forward portion of the airfoil is more important than camber, for the order of maxima does not agree with the order of cambers. The highest loads recorded were N. A. C. A. 81, 4.0 q ; U. S. A. 27 C modified, 3.5 q ; and U. S. A. 35, 4.7 q .

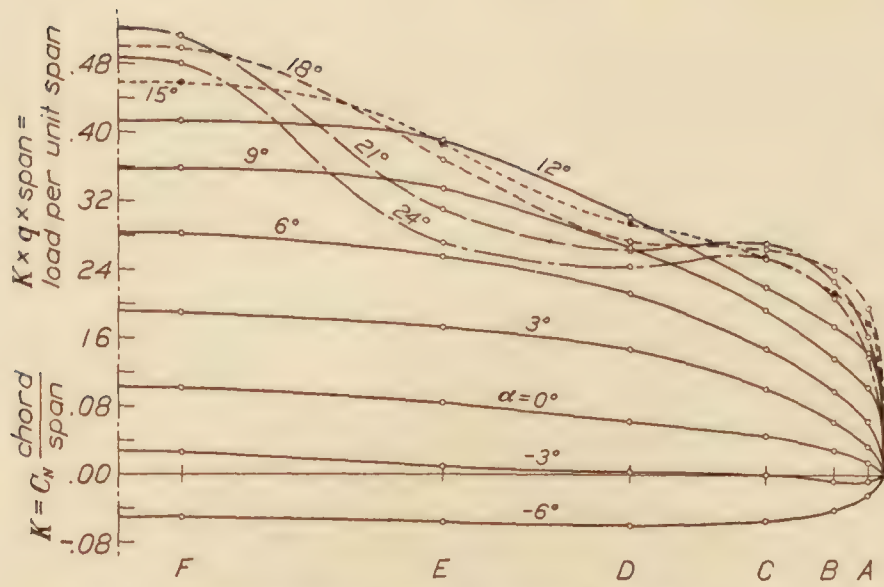


FIG. 16.—Loads on semi-span; N. A. C. A. 81

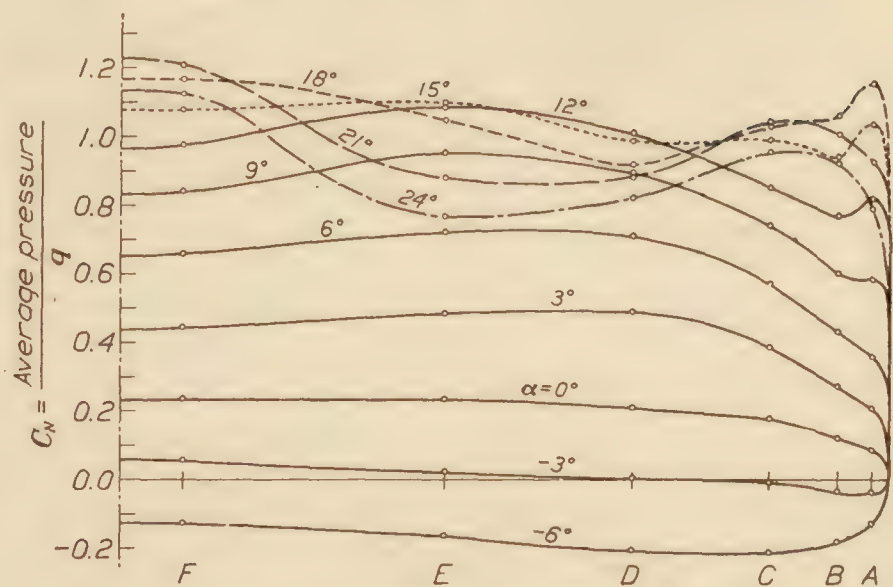


FIG. 19.—Normal force coefficients—N. A. C. A. 81

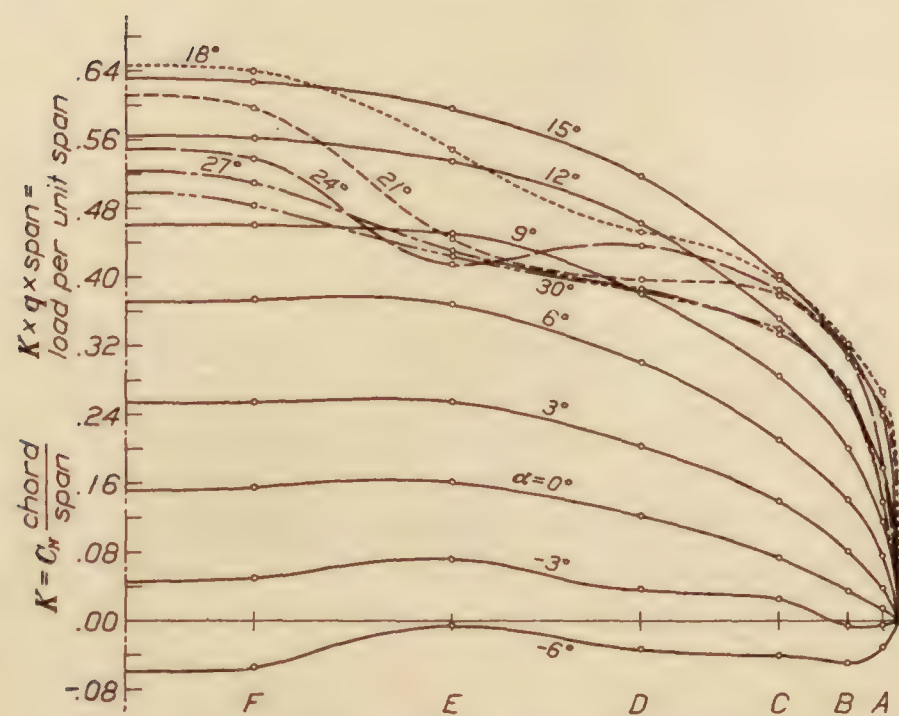


FIG. 17.—Loads on semi-span; U. S. A. 27 C modified

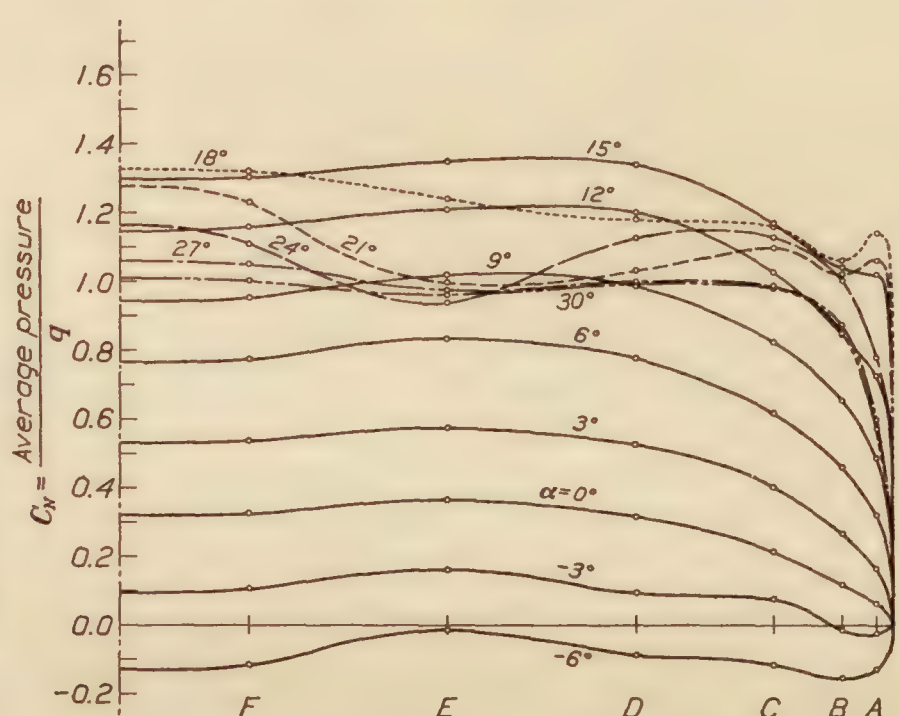


FIG. 20.—Normal force coefficients—U. S. A. 27 C modified

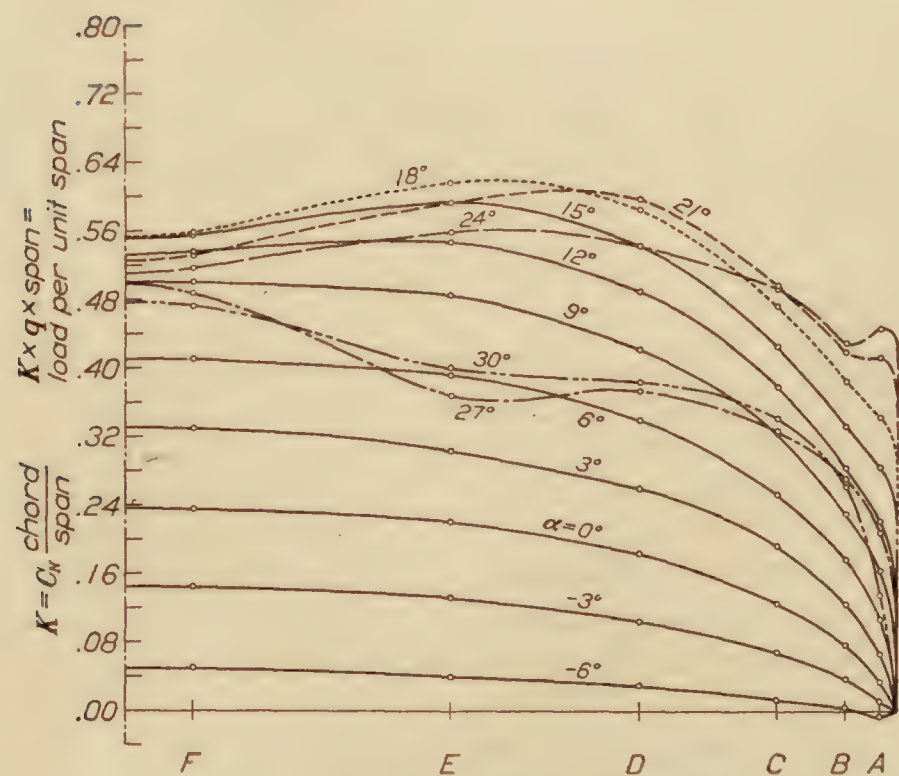


FIG. 18.—Loads on semi-span; U. S. A. 35

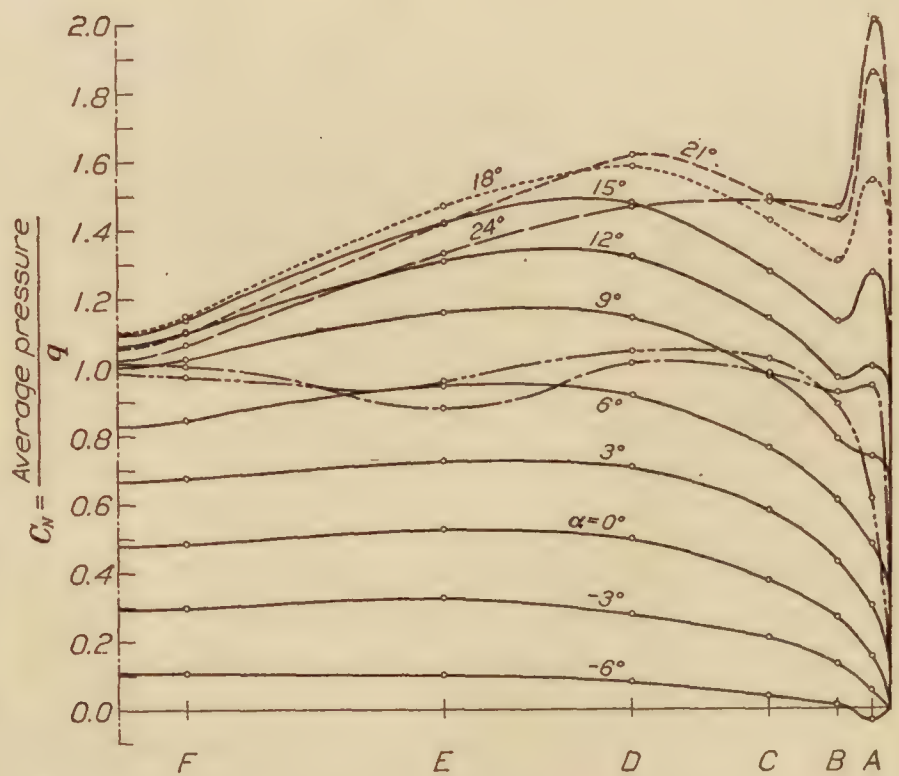


FIG. 21.—Normal force coefficients—U. S. A. 35

The pressures over the tips of these airfoils are of particular interest from both structural and aerodynamic standpoints. It was hoped, when this plan form was laid out, to obtain contours somewhat approximating those of the negatively raked and elliptically tipped wings. The contours show that the results fell short of expectations.

On the N. A. C. A. 81, the tip loading is not really severe, but a small secondary pressure peak does appear at high lifts. This high local pressure is forward of the limits of a normal

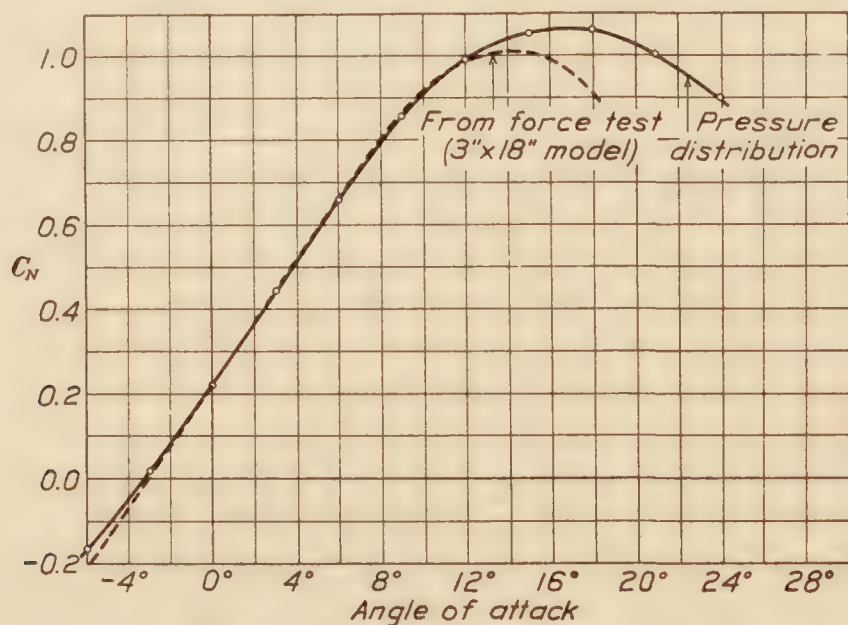


FIG. 22.—Total normal force—N. A. C. A. 81

aileron but might move easily back onto the aileron if the surface were given a large down angle. The maximum load found in the secondary peak has an intensity of $0.8 q$. The condition on the U. S. A. 27 C modified was similar to that of the N. A. C. A. 81, reaching a maximum value of $1.0 q$ and having approximately the same location.

In the case of the higher cambered U. S. A. 35, however, this secondary peak reached alarming proportions. Its maximum intensity was $2.6 q$ and it extended so far forward as to nearly

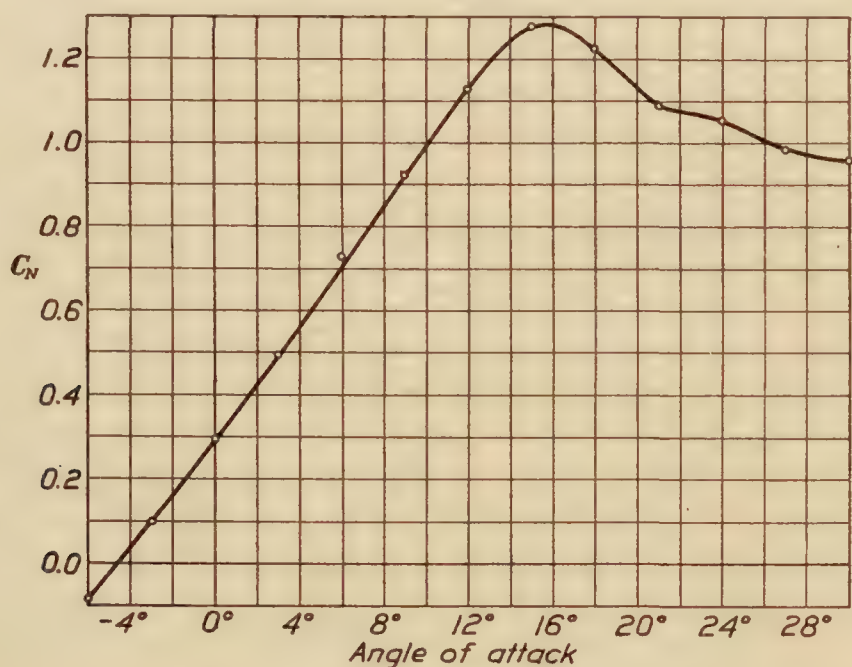


FIG. 23.—Total normal force—U. S. A. 27 C modified

join the high pressure region along the leading edge. The cross-span load curve actually shows a small peak at the outer station whereas the curves for the other wings drop rapidly in this region. It is certain that operation of a normal aileron would not be satisfactory with a tip of this kind on the U. S. A. 35 airfoil.

The peculiar form of pressure distribution found on these tips seems to demand some explanation. The contours resemble both those for rectangular and elliptical tips (Reference 1)

in some details. The high pressure region along the leading edge swings back, as on the elliptical tip, and the secondary peak appears as in the rectangular one. Almost the same condition will be found on the wing No. 59, previously tested. (Reference 2.) It is thought that if this wing had been tested at the angle of maximum lift, the secondary peak would have been even higher than that on the U. S. A. 35 because of its greater camber. It appears that the reduction of chord close to the wing tip plays a part nearly as important as does the distribution of area with respect to the leading edge. The shape of tip used in these tests gives less reduction of chord close to the tip than do the elliptical or raked tips shown in Reference 1, and the close resemblance to the rectangular tip is blamed for the unsatisfactory distribution. In Figure 25, chord is plotted against span for the three shapes of tip; the curve for a suggested form is added. The latter would be laid out by inscribing arcs of 0.25 and 1 tip chord radii within the tip plan form.

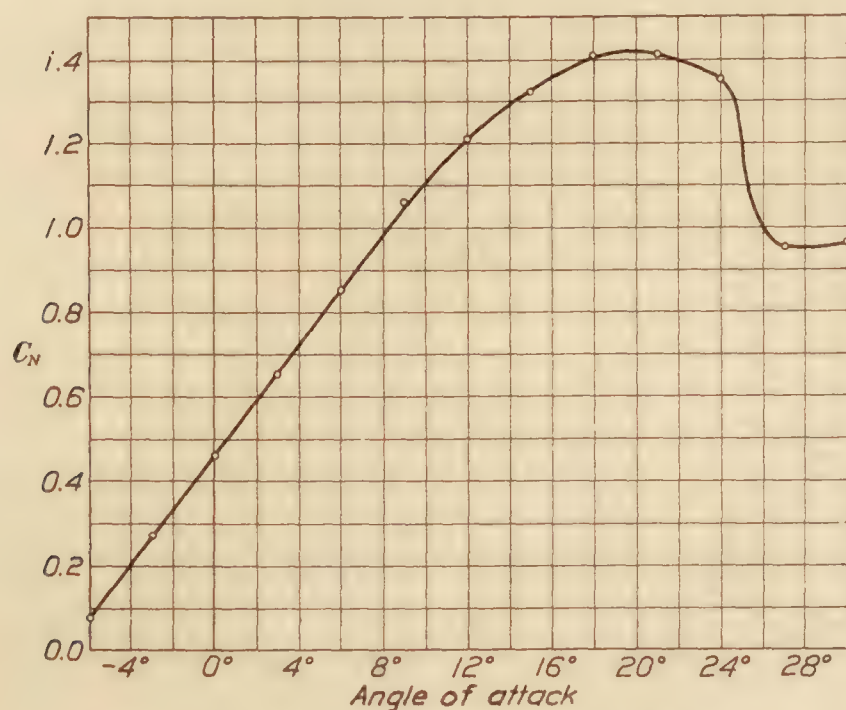


FIG. 24.—Total normal force—U. S. A. 35

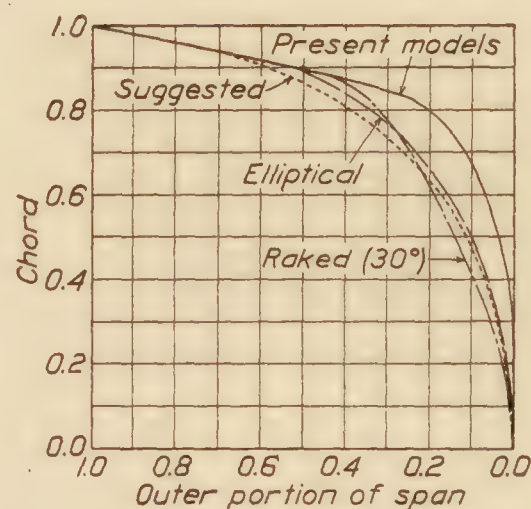


FIG. 25.—Wing tip forms

CONCLUSIONS

The distribution of pressure along the chords of these airfoils is very similar to that on thin airfoils; a greater portion of the surface experiences negative pressure at zero lift in thick sections than thin ones.

The distribution of load across the span of airfoils tapered as are the N. A. C. A. 81 and U. S. A. 35 and having a good form of wing tip is almost ideal from the aerodynamic point of view and is easily dealt with structurally.

While the tip form used on these wings would probably be easier to construct than one involving spars of unequal length, it is seen that a greater reduction of chord should be made close to the tip. Either the elliptical form or the shape suggested in the discussion is recommended.

To improve the distribution of load along the span, particularly at negative and small positive lifts, the wing should be twisted so that all sections will be at zero lift simultaneously.

The plan form used in the U. S. A. 27 C modified seems to have no apparent advantage, either structure or aerodynamic, over the straight tapered wings; in fact, it seems inferior from every point of view.

TABLE 1.—Wing Section Ordinates in Per Cent of Chord; Stations in Per Cent of Chord from L. E.

ROOT SECTION ORDINATES						
Station	N. A. C. A. 81		U. S. A. 27 C modified		U. S. A. 35	
	U.	L.	U.	L.	U.	L.
0	+2.00	+2.00	+9.21	+9.21	+4.33	+4.33
1.25	4.50	-0.27	11.80	7.60	8.09	1.62
2.5	5.75	-0.90	13.32	7.03	9.58	0.96
5	7.80	-1.67	15.80	6.51	11.83	0.42
7.5	9.60	-2.33	17.45	6.02	13.58	0.22
10	11.07	-3.00	18.88	5.64	14.88	0.10
15	13.08	-4.13	20.68	5.05	16.60	0.00
20	14.33	-5.03	21.61	4.77	17.72	0.08
30	15.73	-6.05	22.40	4.72	18.43	0.25
40	15.73	-6.05	21.90	5.07	17.86	0.44
50	14.85	-5.70	20.85	5.48	16.16	0.60
60	13.15	-5.00	19.28	5.87	13.91	0.67
70	10.95	-4.05	17.40	6.25	11.12	0.65
80	8.40	-2.90	14.99	6.67	7.88	0.55
90	5.50	-1.50	11.65	7.10	4.33	0.32
95	3.95	-0.75	9.80	7.30	2.39	0.19
100	1.15	+1.15	7.75	7.75	0.22	0.22
L. E.						
			R=2.06		R _U =5.45	
					R _L =3.24	
T. E. Sharp.			R=0.25		R =0.24	

TIP SECTION ORDINATES						
Station	N. A. C. A. 81		U. S. A. 27 C modified		U. S. A. 35	
	U.	L.	U.	L.	U.	L.
0	+0.50	+0.50	+11.86	+11.86	+2.76	+2.76
1.25	1.12	-0.06	13.05	11.15	5.15	1.03
2.5	1.44	-0.22	13.75	10.80	6.10	0.61
5	1.95	-0.42	15.00	10.54	7.53	0.27
7.5	2.40	-0.58	15.75	10.30	8.65	0.14
10	2.77	-0.75	16.38	10.12	9.47	0.06
15	3.27	-1.03	17.30	9.89	10.57	0.00
20	3.58	-1.26	17.80	9.72	11.28	0.05
30	3.94	-1.51	18.20	9.83	11.74	0.16
40	3.94	-1.51	18.00	10.90	11.37	0.28
50	3.71	-1.43	17.40	10.15	10.29	0.38
60	3.28	-1.25	16.70	10.30	8.85	0.43
70	2.73	-1.01	15.80	10.40	7.08	0.41
80	2.10	-0.72	14.50	10.58	5.02	0.35
90	1.37	-0.38	12.90	10.75	2.76	0.21
95	0.99	-0.19	12.02	10.86	1.52	0.12
100	0.29	+0.29	11.08	11.08	0.14	0.14
L. E.						
			R=0.68		R _U =3.47	
					R _L =2.06	
T. E. Sharp.			R=0.11		R =0.15	
Washed out 1.5°.						

REFERENCES

Reference 1.—BACON, DAVID L., "The Distribution of Lift over Wing Tips and Ailerons." N. A. C. A. Technical Report No. 161, 1923.

Reference 2.—NORTON, F. H. and BACON, D. L., "Pressure Distribution over Thick Airfoils—Model Tests." N. A. C. A. Technical Report No. 150, 1922.

REPORT No. 230

**DESCRIPTION AND LABORATORY TESTS OF A
ROOTS TYPE AIRCRAFT ENGINE
SUPERCHARGER**

**By MARSDEN WARE
Langley Memorial Aeronautical Laboratory**

REPORT No. 230

DESCRIPTION AND LABORATORY TESTS OF A ROOTS TYPE AIRCRAFT ENGINE SUPERCHARGER

By MARSDEN WARE

SUMMARY

This report describes a Roots type aircraft engine supercharger and presents the results of some tests made with it at the Langley Field laboratories of the National Advisory Committee for Aeronautics. The supercharger used in these tests was constructed largely of aluminum, weighed 88 pounds and was arranged to be operated from the rear of a standard aircraft engine at a speed of $1\frac{1}{2}$ engine crankshaft speed. The rotors of the supercharger were cycloidal in form and were 11 inches long and $9\frac{1}{2}$ inches in diameter. The displacement of the supercharger was 0.51 cubic feet of air per revolution of the rotors.

The supercharger was tested in the laboratory, independently and in combination with a Liberty-12 aircraft engine, under simulated altitude pressure conditions in order to obtain information on its operation and performance. During an investigation of the influence on the operation of the engine of various types of air-duct connections between the supercharger and the engine, the supercharger was subjected to considerable rough treatment, which it endured very well, so that it seems apparent that the supercharger could well endure service handling. By the proper proportioning of the air-duct system, the engine would operate at all speeds as smoothly and free from vibration as the normal engine.

From these tests it seems evident that the Roots blower compares favorably with other compressor types used as aircraft engine superchargers and that it has several features that make it particularly attractive for such use.

INTRODUCTION

Since the density of the atmosphere decreases continuously with increase in altitude, the power developed by the normal aircraft engine decreases as its altitude of operation is increased to such an extent that the power developed at 20,000 feet is less than 50 per cent of that developed at sea level. Analyses have shown that this diminution in power can be prevented or at least reduced materially by supercharging, and applications of superchargers to service airplanes have resulted in marked increases in airplane performances. For any given service requirement, the results obtained by supercharging will be influenced by the type of the supercharger selected. Therefore, in order to permit intelligent selection to be made, the characteristics of the different types should be known.

Centrifugal air compressors operating at high rotative speeds have been employed as aircraft engine superchargers both in this country and abroad. Rotor speeds ranging from 6,000 to about 40,000 revolutions per minute have been employed in the various designs and multi-staging has been used in some cases. The turbo-compressor supercharger developed by the Engineering Division of the Air Service is an excellent example of the application of this type of compressor for supercharging duty in this country. The positive-displacement types of compressors have not had such extensive trial. A reciprocating compressor and a rotating vane type have been tried but have mechanical limitations which militate against their utility for aircraft superchargers. The British made some trials with a supercharger patterned after the Roots blower, but the results have not been published. The Roots type has attractive

features and seems to have promise for use as an aircraft engine supercharger as indicated by tests that have been conducted upon the N. A. C. A. Roots type supercharger described in this report. Methods for driving these various types of compressors have included; direct-connected exhaust gas turbines, mechanical drives from the engine by belt and gears and a gasoline engine having the compressor for its sole load.

DESCRIPTION OF THE N. A. C. A. ROOTS TYPE SUPERCHARGER

The National Advisory Committee for Aeronautics constructed a Roots type supercharger from designs made by the Clarke Thomson Research at the time the facilities of this research were placed under the direction of the National Advisory Committee for Aeronautics; G. W. Lewis, as engineer in charge of the Clarke Thomson Research, directed the making of the designs. The construction of the Roots supercharger is considerably different from that of the commercial Roots blowers, since for a supercharger having a given capacity it is necessary that the weight be a minimum compatible with the necessary strength. As a consequence, light alloy castings and alloy steels form the chief constructional materials for the supercharger. The speed of rotation of the rotors is increased considerably over that used in commercial practice in order to obtain greater capacity for a given displacement.

Consideration of the possible synchronization of the pulsating pressure of the air delivered by the supercharger with the pulsating pressure induced by the engine determined the relation of rotor speed to engine speed. With a 12-cylinder engine operating on the four-stroke cycle, there will be six inductions per revolution. With the Roots supercharger, there are two periods of delivery per revolution of each rotor, resulting in four pressure impulses per revolution of the two rotors. Therefore, in order that the frequencies of the pulsations produced by the supercharger and the engine may be equal, the supercharger rotor speed must be 1.5 times the engine speed.

If the intervals between inductions for the different cylinders of the engine were equal, this would give an opportunity to realize some benefit from the synchronization of the pressure impulses produced by the supercharger with the induction periods of the engine. While the pressure fluctuations produced by the supercharger presumably occur at equal intervals, the induction periods with the Liberty 12-cylinder engine do not, since the angle between the two banks of six cylinders is 45° . Furthermore, the character of pressure waves in the two cases may be quite different so that the maximum effects of synchronization probably can not be realized by this particular combination.

The N. A. C. A. Roots supercharger was designed originally to be mounted directly on the rear of a Liberty engine and to be supported solely by the engine. This mounting was not used, however, and in all of the tests, the supercharger was supported by the engine bearers extended, and was driven from the engine through a flexible coupling. With these changes, the liability of damage due to misalignment was reduced. An idea of the construction of the supercharger can be obtained from Figure 1.

The housing is made of aluminum castings, all of the castings being ribbed to provide strength and rigidity with minimum weight, as can be seen from Figure 1. A steel plate separates the rotor chamber from the gear compartment.

The supercharger rotors are shown in Figures 2 and 3. They are hollow castings, having a wall thickness of about three-sixteenths inch and are 11 inches long by $9\frac{5}{8}$ inches in diameter. The contour of the rotors is cycloidal, except for a narrow portion of the tips, which is concentric with the axis of rotation, and a narrow flat portion near the hub; shallow clearance grooves are cut at the junctions of these surfaces with the cycloidal surfaces. The rotors are fitted with rectangular steel driving flanges which fit in machined recesses in the ends of the rotors and are fastened by machine screws. The driving flanges have internally splined hubs which fit on splines on the rotor shaft.

The rotor was constructed originally of an ordinary aluminum casting alloy. After approximately 100 hours of operation, they were replaced with rotors made of another aluminum alloy having a higher specific gravity and a greater tensile strength than that used at first.

Figure 4 shows the gears that drive the rotors. A gear operated at crankshaft speed meshes with a pinion forming an integral part of one rotor shaft, the ratio of these gears determining the rotor speed for a given engine speed. The rotor shafts are connected together by another pair of gears which serves to maintain proper relation between the rotors as well as to transmit torque from one rotor shaft to the other.

In the original design, contact between the ends of the rotors and the housing was limited to a narrow ring near the shaft by a slight projection on the rotor ends formed on the flanged hubs. In most of the work, all contact at the ends of the rotors was prevented by locating the rotors definitely in the housing by distance pieces inserted between the outer races of the rotor shaft ball bearings and the bearing coverplates.

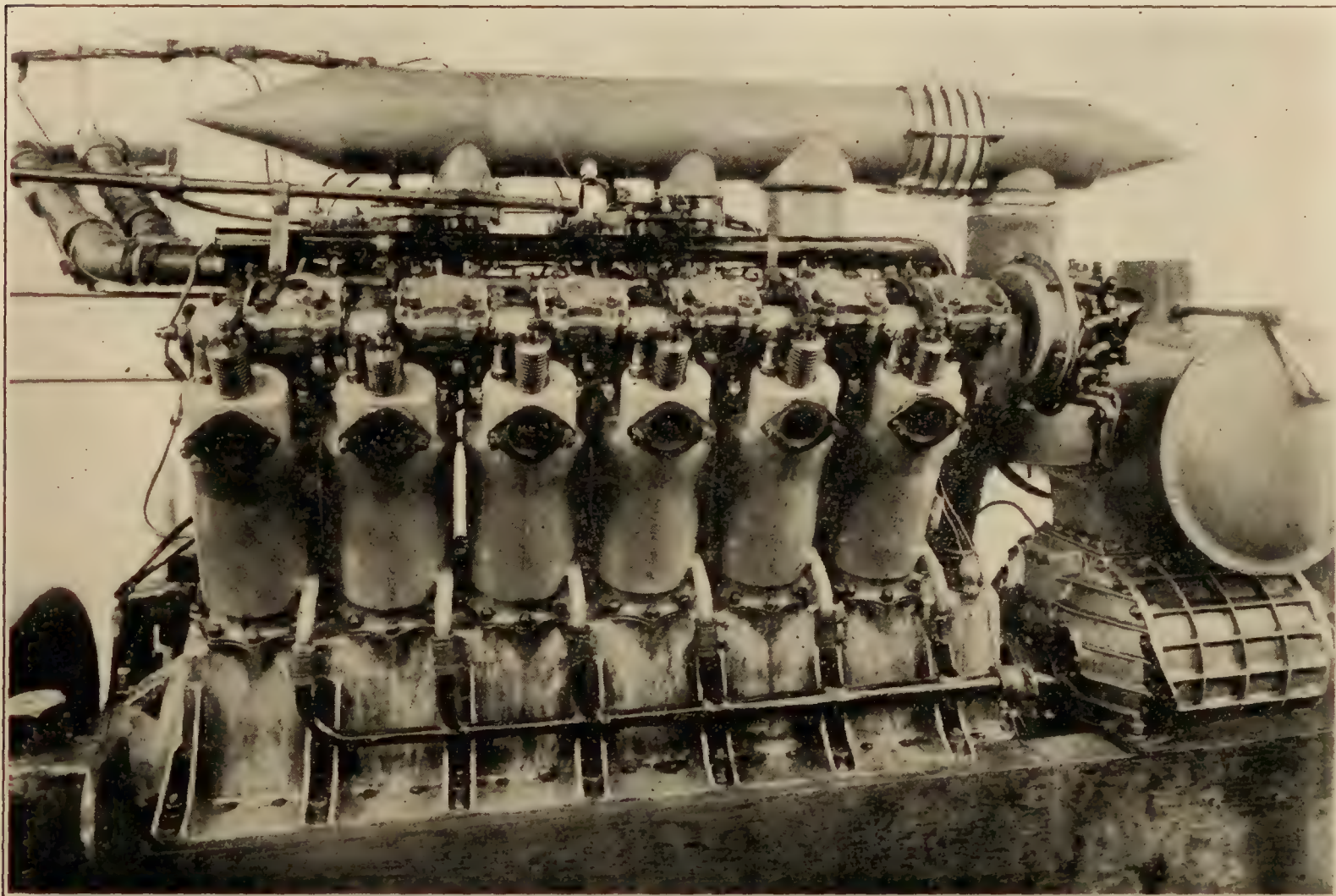


FIG. 1.—N. A. C. A. Roots type supercharger with Liberty-12 engine

It was originally intended that lubrication would be furnished from the main oil pressure system of the engine. During the tests of the supercharger alone, however, it was found that a metering orifice, about No. 70 drill, had to be provided in the oil line to prevent overoiling. During the tests of the engine-supercharger unit, the method of lubricating from the engine pressure system was discarded in favor of a hand lubricator connected to the supercharger gear case which gave greater assurance that proper lubrication of the supercharger would be maintained.

The air ducts provided with the original machine were made of cast aluminum, and were intended for use with standard Zenith carbureters. A single casting connected the two carbureters together at the bottom. From the rear carbureter a Y-shaped casting divided the duct system in order to pass around the Delco generator. Two arrangements were provided for connecting these ducts to the delivery side of the supercharger, one being an aluminum casting giving a direct connection with little volume and the other a sheet steel tank of 1.8 cubic feet capacity. The design of the air connection was changed, however, to that shown in Figure 1, using inverted Stromberg carbureters with the original steel supercharger tank. The new parts were built chiefly of welded sheet steel.

A hand controlled butterfly valve, located in the short pipe shown in Figure 1 on the top of the supercharger tank, served to by-pass directly to the atmosphere all air not required by the engine and forms the sole supercharger control.

An automatic inlet valve, located in the air duct immediately in back of the rear carbureter, was introduced to permit the engine to draw air directly from the atmosphere in case the supercharger should fail. This was a poppet valve, 5 inches in diameter, which was normally held

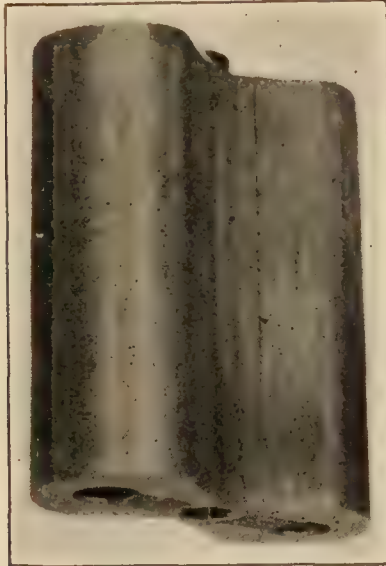


FIG. 2.—Aluminum rotor with steel driving flanges

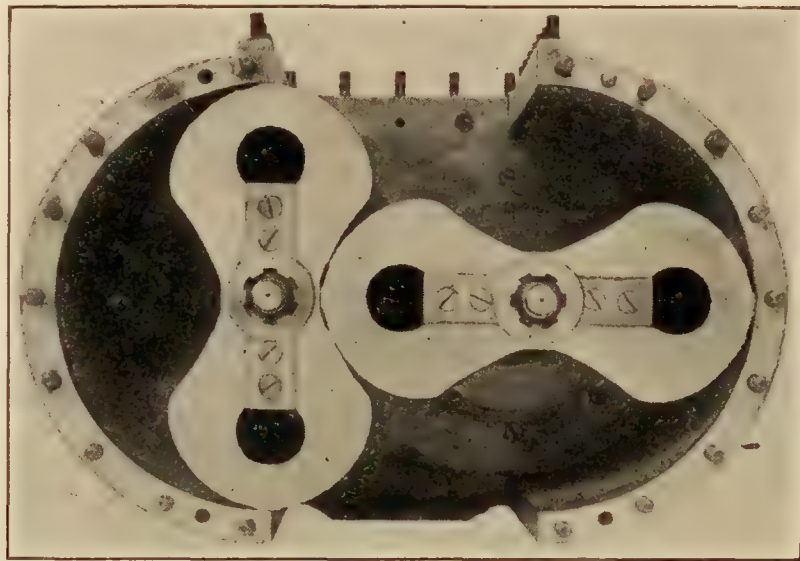


FIG. 3.—Supercharger with rear end plate removed

closed by its own weight and by the pressure in the air duct; the suction from the engine opening it if the supercharge air supply fails. In back of this valve there were four baffle plates made of 0.035-inch sheet steel, in each of which are drilled 30 holes, three-fourths inch in diameter. The holes in successive plates were staggered.

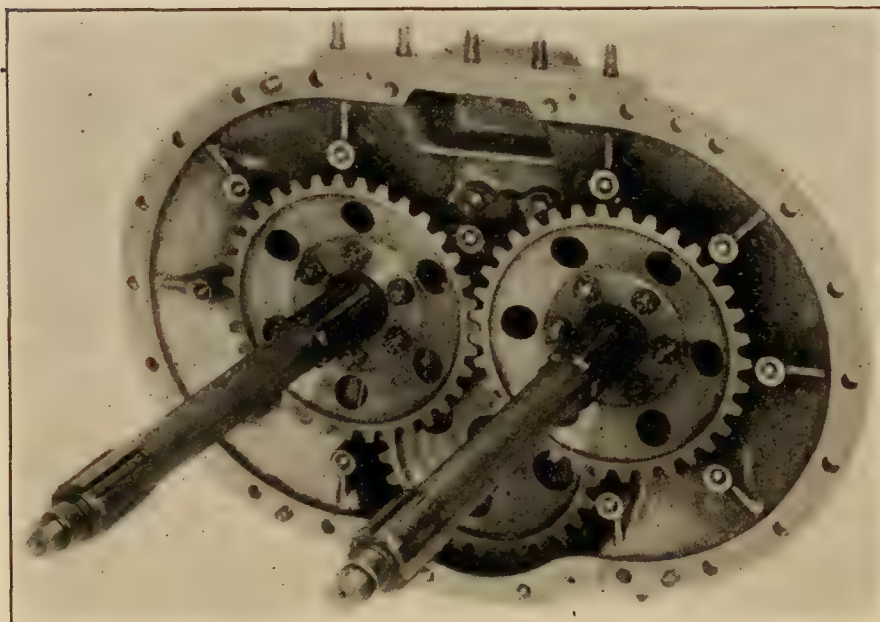


FIG. 4.—Gear case, gears, and rotor shafts

The supercharger complete with rotors made of the heavier aluminum alloy, coupling, and redesigned air ducts weighs 151 pounds. The main component weights are as follows:

	Pounds
Supercharger.....	88
Coupling.....	10
Supercharger tank.....	24
Air ducts.....	29

In making the alterations to the original design mentioned, minimum weight was not given much consideration so that the changes involved an increase in over-all weight of about 30 pounds.

LABORATORY TESTS OF THE SUPERCHARGER

Tests of the supercharger as an independent unit were made with the supercharger connected to a 50–75 horsepower Sprague electric dynamometer. The inlet to the supercharger was throttled to simulate service pressure conditions. The air quantities were measured with thin-plate orifices patterned after those calibrated by R. J. Durley and reported in Volume 27 of Transactions of the American Society of Mechanical Engineers. Provision was made to use two orifices in parallel, so that sizes no larger than those calibrated by Durley would be required. Temperatures were observed by means of chemical mercury thermometers, and pressures by mercury, water and alcohol manometers. A special screw adjustment type alcohol

manometer was used to measure the drop across the metering orifices, which enabled the head to be read easily to within 0.005 inch. The scheme of the apparatus set up is shown in Figure 5, manometers and thermometers being indicated at the points of their introduction into the system.

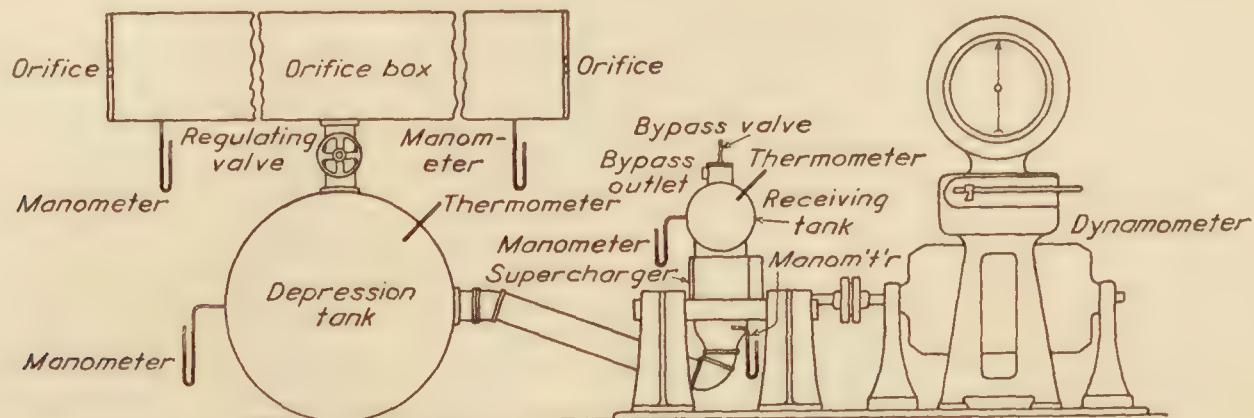


FIG. 5.—Arrangement of apparatus for laboratory test of supercharger

Measurements of power required and weight of air handled were made over a range of ratios of supercharger discharge to inlet pressures from 1.0 to 2.2 and for speeds up to 1,800 revolutions per minute. The various pressure ratios were obtained by varying the inlet pressure, the discharge pressure being held nearly constant. The actual runs were made at constant weights of air handled, the desired pressure ratios being obtained by varying the speed of rotation and the opening of the inlet gate valve.

The following methods were used in working up the plotted results for weight of air handled. The absolute pressure of the different parts of the system were obtained from the barometer and the different manometer observations. The following formula, given by Durley, was used in determining the weight of air handled:

$$W = C.630 d^2 \sqrt{i/T}$$

where

W = weight of air in pounds per second.

C = coefficient of discharge for the orifice.

d = diameter of orifice in inches.

i = head over orifice in inches of water.

T = absolute temperature of air, Fahrenheit.

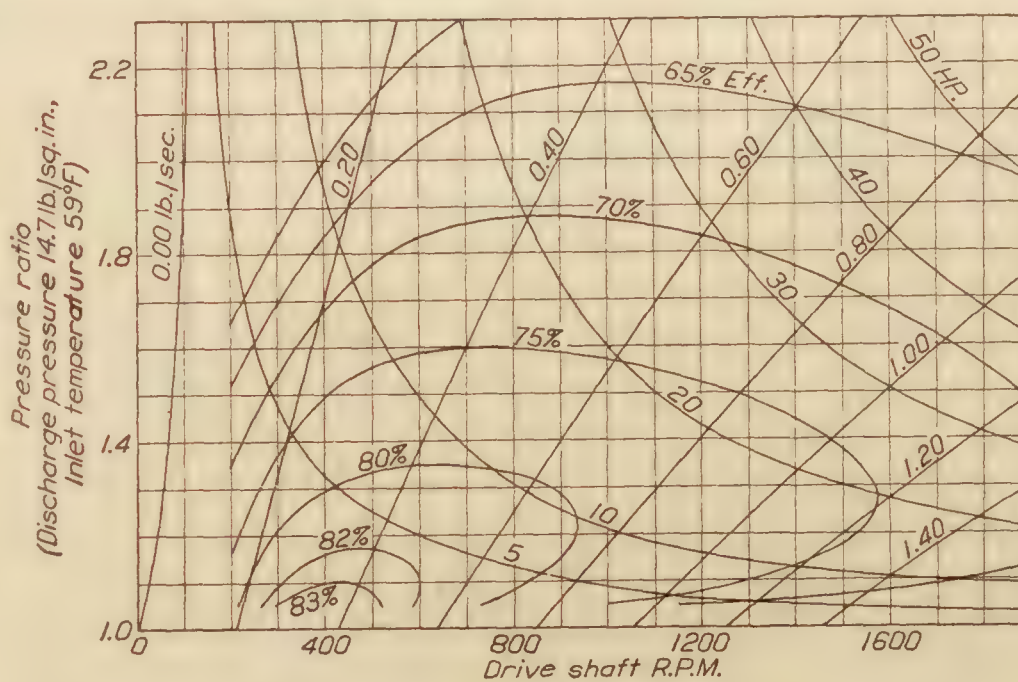


FIG. 6.—Power, efficiency, and air delivery

The coefficient used was that given by Durley, but modified as indicated by a series of experiments made to determine the effect on the orifice coefficient of causing the flow to take place in the reverse direction from that for which the orifice was originally calibrated. The effect of such reversal was insignificant for the purpose of these tests. The volume of air handled in unit time was determined from the density of the air at the supercharger inlet and the weight measured by the orifice meter. From this and the geometrical displacement, the volumetric efficiency of the blower was obtained.

Brake horsepower during the test was determined from the dynamometer torque scale and revolution counter readings. While the runs were so made that very nearly constant air weights were obtained, still there were small differences in air weights between the runs, so that the speed, power, and air volumes were reduced to the same mean weight basis by straight propor-

tion. The amount of such reduction was at all times quite small. The horsepower theoretically required to adiabatically compress and deliver 1 pound of air per second is given by the following formula:

$$\text{HP.} = \frac{RT}{550} \frac{k}{k-1} (r^{\frac{k-1}{k}} - 1) = .336 T (r^{.289} - 1)$$

This power divided by the observed brake horsepower was designated the overall efficiency.

Figure 6 is a plot of the results, the curves having been faired by successive cross-plotting. In Figure 7 constant speed curves of efficiency plotted against pressure ratio are shown for four interesting speeds. The power required to operate the blower with free inlet and discharge is about 3 horsepower at 1,800 revolutions per minute. Figure 8 gives the volumetric efficiency obtained.

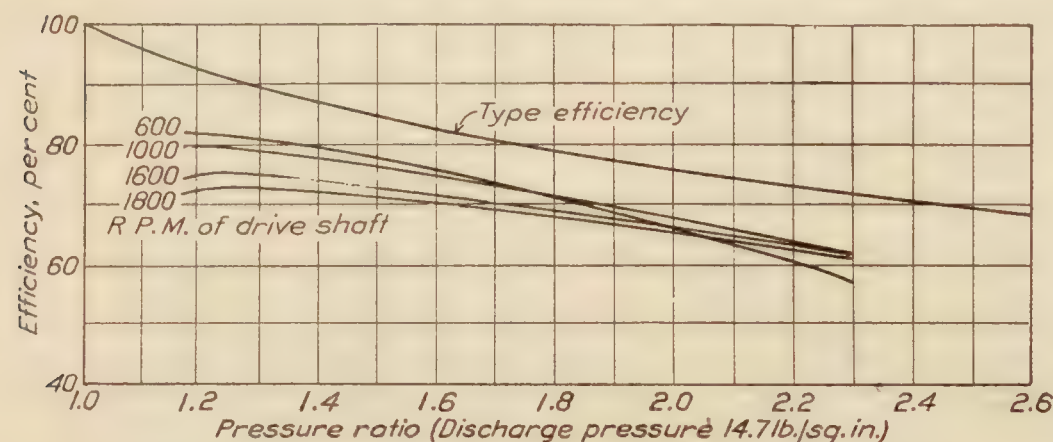


FIG. 7.—Theoretical and test efficiencies

drawn to represent the test results. This curve is closely approximated by another which is determined by the equation, $\frac{T_2}{T_1} = \left(\frac{P_2}{P_1}\right)^{\frac{n-1}{n}}$ with "n" taken as 1.53. A curve showing the relations of these quantities for adiabatic compression, "n" taken as 1.4, is given also on this figure.

Slip speeds were obtained by blocking off entirely the inlet to the supercharger and, observing the speed required to maintain specified pressure ratios up to 2.2 with no discharge, the pressure on the discharge side being atmospheric. The slip speed will be affected considerably by the lubrication conditions and by the clearances between the two rotors and between each rotor and the housing. The slip speeds obtained in these tests are given in Figure 10. A greater amount of lubricant was used during these tests than was found desirable later in actual use of the machine. No tests were made to determine the effect of differences in lubrication and clearances upon these performance characteristics, but the effect may be appreciable.

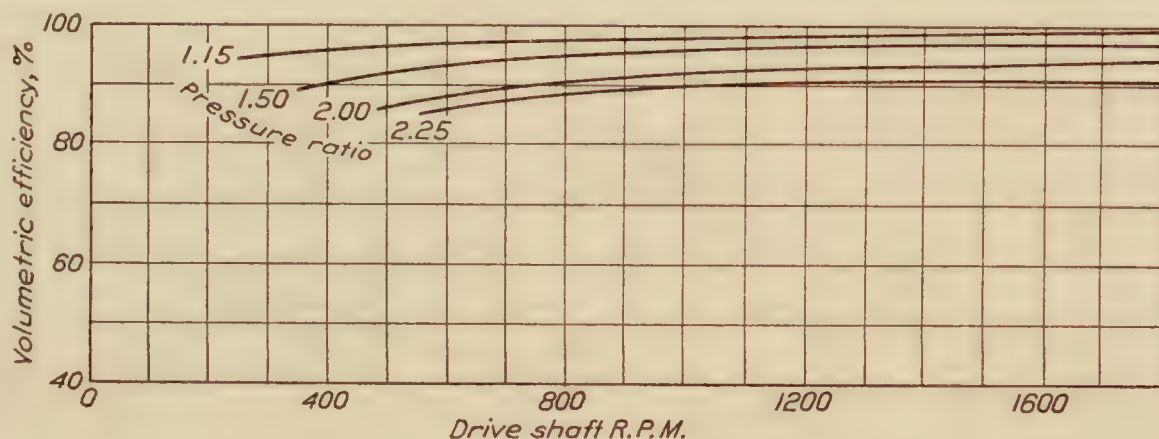


FIG. 8.—Volumetric efficiency

In order to obtain an indication of the mechanical limitations of the type, tests were made to determine the speed at which the rotor would burst when rotating by itself in free air. An aluminum alloy rotor failed at 9,600 R. P. M., while a magnesium alloy rotor made subsequently to these performance tests but similar in design to the aluminum rotor failed at 13,500 R. P. M. The speed of rotation of the supercharger rotors depends upon the speed of the engine and the gear ratio selected. The tests described in this report were made with a gear ratio of 1.5:1 so that with an engine speed of 1,700 R. P. M. the rotor speed is 2,550 R. P. M. During flight tests that were made later than the tests reported here, the gear ratio was increased to 1.94:1 giving a rotor speed of over 3,200 R. P. M. for an engine speed of 1,700 R. P. M. The machine was used considerably with this higher drive ratio and there was no evidence that such high rotor speeds imposed any important limitations.

It is interesting to note that commercial Roots blowers having the same displacement as the N. A. C. A. Roots supercharger, namely, one-half cubic foot per revolution of the rotor, have normal operating speeds of about 500 R. P. M. as against the supercharger speed of 3,200 R. P. M. with the higher gear ratio.

THEORETICAL EFFICIENCY OF ROOTS BLOWER

Figure 7 shows a curve marked "Type efficiency." This efficiency is the ratio of the area for the theoretical adiabatic card for a reciprocating compressor to the area of a rectangular card using the same pressures and inlet volumes. The rectangular card represents approximately the power required by a Roots blower.

Referring to the diagrammatic outline of a Roots blower

in Figure 11, it will be seen that the action of the impeller is to transfer a fixed volume of air "A" from the inlet side and at the inlet pressure to the delivery side, ignoring all losses due to leakage, and that this volume of air "A" is subjected to the full delivery pressure at "B" when a sufficient area has been opened at point "C" by the rotation of the impeller. At this moment

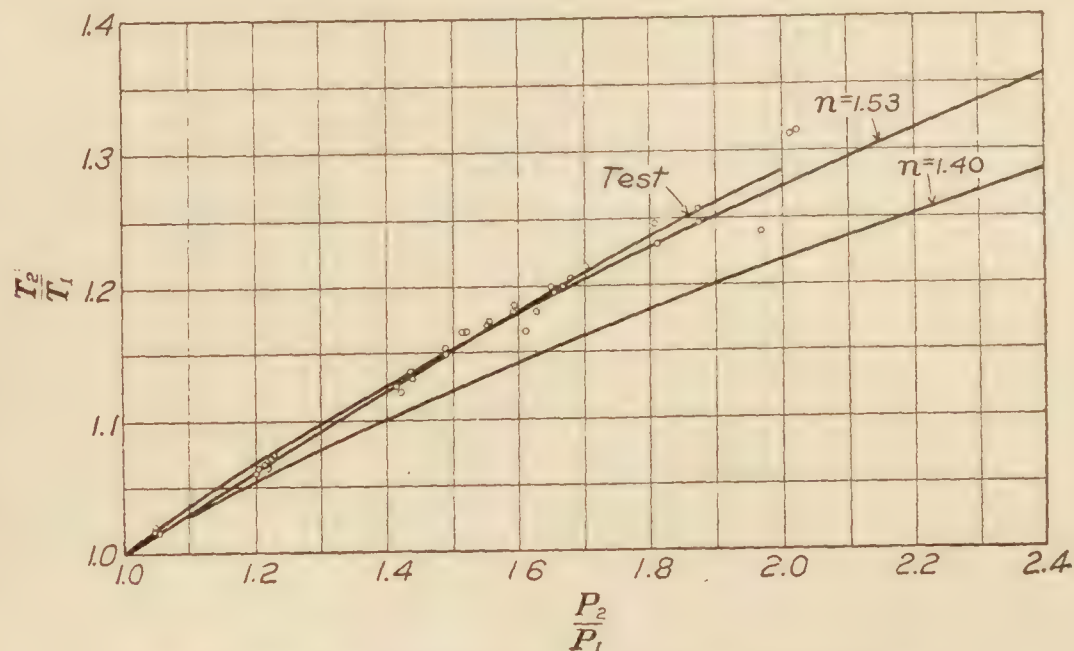


FIG. 9.—Temperature-pressure relations of air handled by supercharger

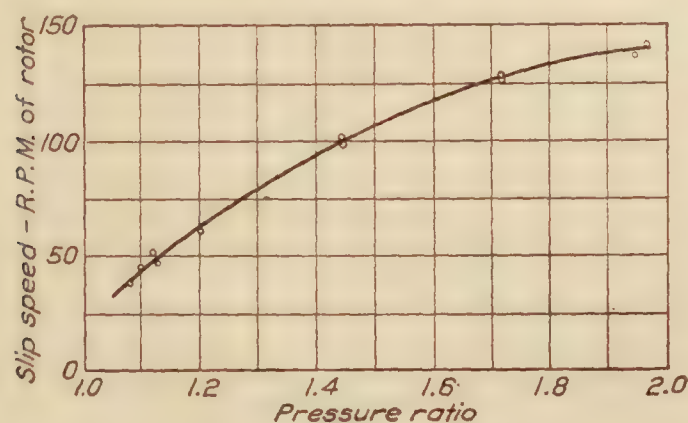


FIG. 10.—Slip speed

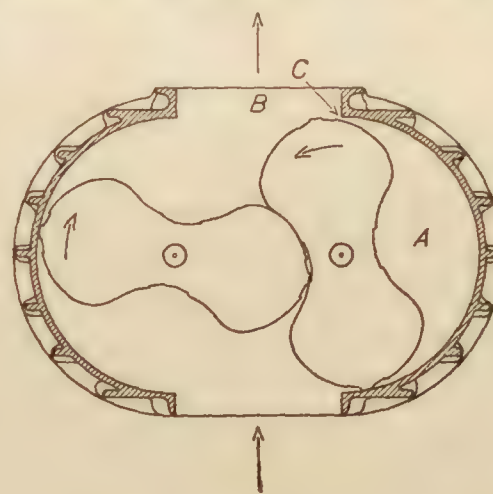


FIG. 11.—Diagrammatic cross section of Roots compressor

the air at "A" is suddenly compressed to the full delivery pressure, and the rotor then works against the delivery pressure during practically the whole movement required to displace the volume "A."

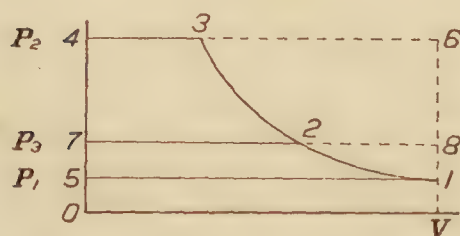


FIG. 12.— P - V relations of Roots and reciprocating compressors

The pressure-volume relation for this condition of operation is shown in Figure 12, where the area 1-2-3-4-5 represents the work required to compress adiabatically and deliver 1 pound of air from the pressure P_1 to the pressure P_2 , a form of indicator card which is given approximately by piston compressors. The area 1-6-4-5 represents the work required to compress and deliver the same unit weight by the method of operation of the Roots blower. The area between the line of instantaneous pressure rise along 1-6 and the adiabatic pressure rise along 1-2-3 represents the extra work done in the Roots type blower. It is apparent that this extra work is small as compared to the total work at low compression ratios but becomes a greater proportion of the total work as the compression ratio increases.

Numerical values of type efficiency can be obtained from simple mathematical treatment of the case. The work required to compress adiabatically and to deliver 1 pound of air, as shown by the area 1-2-3-4-5 in Figure 11 is

$$W_a = \frac{k}{k-1} P_1 V 144 \left(r^{\frac{k-1}{k}} - 1 \right)$$

The work of compression and delivery of 1 pound of air, according to the hydraulic card area 1-6-4-5 in Figure 11, is

$$W_h = V (P_2 - P_1) 144$$

where

P_1 and P_2 = initial and final pressures in lb./sq. in.

$r = \frac{P_2}{P_1}$ = the ratio of compression.

E = theoretical efficiency of Roots blower.

k = ratio of specific heats.

V = the volume of 1 pound of air at initial pressure and temperature conditions.

but

$$P_2 - P_1 = P_1 (r - 1)$$

so that

$$W_h = V P_1 (r - 1) 144$$

The theoretical type efficiency is evidently the ratio between these work areas, or:

$$E = \frac{W_a}{W_h} = \frac{k}{k-1} \left(r^{\frac{k-1}{k}} - 1 \right)$$

For air $K = 1.406$, so that

$$E = \frac{3.463 (r^{.289} - 1)}{r - 1}$$

Computed values of E for pressure ratios up to 3.0 determine the curve marked "Type efficiency" given in Figure 7.

Several methods have been considered for counteracting this characteristic reduction in compressing efficiency with increase of pressure ratio. For instance, the slow-speed commercial Roots blower has been provided with a Venturi restriction at the outlet of the blower for use with pressure differences somewhat above five pounds per square inch, which is intended to give higher efficiencies than would be obtained with the ordinary blower under these conditions. Brief trials were made with a Venturi discharge fixture and with well-rounded orifices, having orifice discharge coefficients for the two directions of flow of approximately 0.95 and 0.60, but no improvement was obtained. The installation of valves above the rotors would tend to reduce the back flow of air, so that the cycle would then approach more nearly that of the piston compressor. Several such valve mechanisms were studied briefly in the laboratory, but all of them imposed so great a pressure drop in passing the air through the valve that no benefit could be expected by their use.

LABORATORY TESTS OF ENGINE-SUPERCHARGER UNIT

After the tests of the supercharger as an independent machine were completed, it was connected to a 12-cylinder Liberty engine and subjected to further tests with a 300-400 horsepower Sprague electric dynamometer, in order to study the action of the unit under simulated altitude pressure conditions for the supercharger and to obtain some performance data under these conditions. The same arrangement of orifice box and depression tank was used as in the previous tests, but the delivery side of the supercharger was connected to the engine carbureters.

When using the original air-duct system and standard Zenith carbureters, very rough running was encountered over a wide range of speeds. Between 600 and 1,400 R. P. M., this

rough running was accompanied by violent back-firing in the carbureter and momentary cutting out of the entire engine. At 1,600 R. P. M., however, the operation was satisfactory. The rough operation noted was definitely attributed to the air-duct system.

A number of radically different systems of air ducts were tried, using Stromberg inverted and standard Zenith carbureters. These systems involved the use of various sizes and arrangements of receivers and pipes and various restrictions and baffles. With these different arrangements, improved operation took the form of narrowing the speed range over which the rough running was encountered. Satisfactory operation throughout the complete speed range was obtained by imposing considerable restriction in direct pipe connections, by using large receivers, or by giving careful attention to the proportions and forms of the various parts of the duct system.

The system adopted for flight test, shown in Figure 1, involved the use of the original receiver, having a volume of 1.8 cubic feet, at the discharge of the supercharger. When using the air-duct system over the carbureter, as shown in this figure, no attempt was made to reduce the size of the supercharger receiver. Recent tests made with another engine, however, have indicated that considerable reduction in size may be possible.

With the Stromberg inverted carbureters mixture adjustment is effected by means of an air leak from the atmosphere to the carbureter float chambers, controlled by a valve located outside of the carbureter and connected to the float chambers by a tube. In the supercharger installation this tube can not be left open to the atmosphere, but must be connected to the supercharger air duct system in order to have the fuel flow through the carbureter jets. With the present installation this was accomplished by inserting a short tube and a control valve for mixture adjustment between each carbureter float chamber and the air duct over the carbureters.

The conditions of operation in these tests were different from flight conditions in several respects. Of these conditions two were radically different; first, in the laboratory tests the engine exhausted into air at approximately sea-level pressure for all supercharger inlet air pressures, and second, the temperature of the air entering the supercharger remained practically constant with changes in pressure instead of decreasing with pressure as in flight. The results were reduced to flight conditions by the use of rational reduction factors. The error introduced by the method of taking into account the differences in engine exhaust pressure has been shown to be relatively unimportant by tests that have been made since at the Bureau of Standards and reported in N. A. C. A. Technical Note No. 210. The method of taking into account the differences in temperature, however, has not been substantiated by test. Since the errors involved in the methods of making the reductions are quite uncertain, the estimated power of the unit for flight conditions as obtained from these laboratory tests are not given.

The following extract from the data serves to illustrate the character of the test conditions:

Supercharger inlet pressure=16.5 in. Hg. absolute.

Supercharger inlet temperature=80° F.

Carbureter pressure=29.8 in. Hg. absolute.

Carbureter temperature=175° F.

Crankshaft speed=1,600 R. P. M.

Brake power of unit=326 H. P.

By taking into account the differences between test and flight temperatures and pressures as referred to in the preceding paragraph, much greater power of the unit is obtained.

A brief study was made of the effects of varying the timing of the pressure pulsations produced by the supercharger with the pressure pulsations induced by the engine. With a large air-duct system that gave smooth operation of the engine no differences in engine operation or power were noted. With the smallest air-duct system used, rough operation was obtained with all adjustments and fair power comparisons could not be made. This study was not extended further, since it was evident that but little could be gained with this combination.

CONTROL METHODS

By supercharging aircraft engines it is intended to prevent or at least to reduce materially the diminution in power suffered by the normal aircraft engine as its altitude of operation is increased. It is necessary, therefore, that the rate of air delivery to the engine when supercharging at considerable altitude above the ground, be roughly the same as the consumption of the normal engine when operating at ground level. At a fixed speed, the Roots supercharger delivers air at a constantly decreasing rate as the altitude of operation is increased, since for this type of machine, the rate of air delivery with 100 per cent volumetric efficiency varies directly with the density of the air at the inlet to the machine and its speed of rotation. Some control means must be provided, therefore, in order to obtain the desired end.

The necessary control may be secured in several ways; first, by operating the supercharger at a fixed engine-supercharger speed ratio, with the inlet side of the supercharger open to take air at the density of the operating altitude and returning to the atmosphere all air in excess of that required by the engine; second, by operating the supercharger at a fixed engine-supercharger speed ratio but with the inlet of the supercharger throttled at low altitudes, so that the density of the air handled by the supercharger will be practically constant; third, by continuously changing the engine-supercharger speed ratio, so that the supercharger will deliver air at just the rate required by the engine. The power required to operate the supercharger by each of the control methods for a constant engine speed, as estimated for flight conditions and using the laboratory tests as a basis, is shown by Figure 13. The three curves intersect at the point where the speed of the supercharger with the method involving speed change is

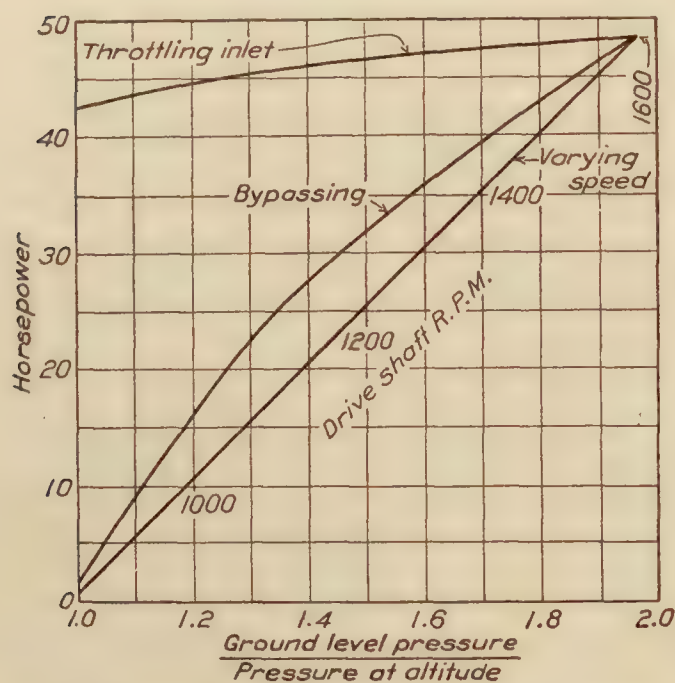


FIG. 13.—Effect of method of control on power required

the same as in the other methods, and the by-pass valve is fully closed and the inlet valve is opened fully for the methods involving these types of controls. The weight of the fixtures for the first and second methods would be about the same, but the method requiring speed change would probably involve a much greater weight because of the mechanism required. The second method involves no more complication than the first, but does take considerably more power at lower altitudes and always delivers air having an absolute temperature at a nearly constant ratio to the absolute temperature of the inlet air, due to the fact that the supercharger itself is operating with nearly the same pressure ratio all the time. With this method, then, the supercharger discharge air temperatures will be excessive near the ground and some method of cooling the air delivered to the engine probably would be necessary.

The first method of control was used in the tests of this supercharger. With this method the temperature rise through the supercharger is a minimum. The power required approaches very close to the minimum as obtained by the variable speed ratio method and does not entail the complication of control, and probably results in quicker response to the control than the latter method. The weight of the fixtures for the first method also is favorable to its selection.

POSSIBILITIES OF THE ROOTS TYPE SUPERCHARGER

These tests indicate that the Roots blower as a type has several features that make its use as an aircraft engine supercharger attractive, although they can not show either the extent or the degree of its value. The machine used in these tests was the first to be built from this design and endured over 100 hours of operation without requiring the replacement of any important parts. Since during a large part of the time the supercharger was subjected to abnormally rough treatment and since the design embodies many features that are a radical departure from commercial practice for this type of machine, this performance indicates that the type is well adapted for aircraft engine supercharging from a durability viewpoint. While the reciprocating

compressor is attractive when the power for the actual compression and delivery of the air alone is considered, mechanical friction losses, together with mechanical limitations, make it unsuitable for very broad application to aircraft engine supercharging. For many applications in this field the Roots type supercharger has power requirement characteristics that are the equal if not the superior of other common types.

While speeds of rotor operation much in excess of those employed in commercial service were involved in these tests, the tests have shown that this condition is no handicap to the use of this machine and indicate, moreover, that still higher speeds could be used as far as structural characteristics are concerned. The use of higher speeds for a given capacity would permit a direct reduction in the weight of the supercharger and by virtue of the increase in the frequency and the reduction of the amplitude of the pressure pulsations, would permit smaller air ducts with further economies in weight of the complete unit. Actual experience is necessary to determine what could be realized in this respect. While it may be thought that inertia stresses may impose the most serious limitation, there have been no indications from work done on this machine that this condition has been even approached. While the pressure pulsation conditions were stated to be improved with increase in speed of operation, experiences encountered in these tests show that the pulsation conditions existing in the present tests could be readily handled so that engine operation would not be affected adversely.

The centrifugal compressor has received far more attention to date than any other type for use as an aircraft engine supercharger. This type of compressor has had considerable use as an exhaust gas driven supercharger. In this case both turbine and compressor are essentially very high speed machines, and their combination forms an admirable unit for certain purposes. The position of the centrifugal compressor is not as favorable, however, when it is used as a mechanically driven machine.

If a centrifugal compressor is driven at a speed bearing a fixed ratio to the engine speed, the ratio of absolute temperatures at the inlet and discharge of the supercharger will not change much with change in altitude at all altitudes up to that at which the supercharger capacity is just sufficient to maintain ground-level pressure at the carbureters. Then, the carbureter temperature at ground level will exceed considerably the atmospheric temperature which is already sufficiently high under most conditions. If the equipment were designed to maintain ground-level pressure at any but very moderate altitudes, the carbureter temperature at the ground level would surely be prohibitive unless elaborate cooling means are provided. In contrast to this condition the Roots type as utilized in these tests compresses the air almost imperceptibly at the ground, and the carbureter temperature is but little in excess of the ambient atmospheric temperature.

Because of the characteristics of the centrifugal compressor, the power required to drive it at ground level at a speed having a fixed relation to the engine speed will differ but little from the power required at the altitude at which the supercharger has just sufficient capacity to maintain ground-level pressure. In contrast to this condition the Roots type, even though it handles a large quantity of air, requires comparatively very little power at ground level since the amount of compression of the air is practically imperceptible.

The exhaust gas turbine driven supercharger will not respond instantaneously to the supercharger control, while, on the other hand, any mechanically driven supercharger can be arranged readily to give instantaneous response to the control. The Roots type, in addition, has more favorable power and air temperature conditions than any other compressor that has yet been seriously considered. Maintenance of mechanical clearances which would seem to be a handicap of the Roots type have not proved troublesome in these or later tests.

CONCLUSIONS

The tests reported herein serve to indicate that the Roots type blower is well adapted for use as an aircraft engine supercharger. From considerations of durability, low power requirements, control, and heating of the air handled, it appears especially well suited for many service requirements.

REPORT No. 231

INVESTIGATION OF TURBULENCE IN WIND TUNNELS BY A STUDY OF THE FLOW ABOUT CYLINDERS

By H. L. DRYDEN and R. H. HEALD
Bureau of Standards

REPORT No. 231

INVESTIGATION OF TURBULENCE IN WIND TUNNELS BY A STUDY OF THE FLOW ABOUT CYLINDERS

By H. L. DRYDEN and R. H. HEALD

INTRODUCTION

With the assistance and cooperation of the National Advisory Committee for Aeronautics the Bureau of Standards has been engaged for the past year in an investigation of turbulence in wind tunnels, especially in so far as turbulence affects the results of measurements in different wind tunnels. At the beginning of the year the research was outlined in some detail by the members of the technical staff of the committee, and so far as has been practicable this outline has been followed. The following pages constitute a report to the committee on the results obtained.

The investigation was planned along two lines, the problem of turbulence being attacked in two directions. In the first place the ultimate effect of turbulence, in which we are interested in practice, is its effect on the measured force on objects subjected to test. Certain types of bodies have been found to be very sensitive to changes of turbulence and have been suggested as indicators of the degree of turbulence present. Spheres and cylinders are the bodies most frequently suggested. Spheres having been already studied at Langley Field and elsewhere, cylinders were proposed as the indicating bodies in the present investigation. The behavior of eight cylinders ranging in diameter from 0.0085 inch to 3 inches has been studied for four turbulence conditions, and the 3-inch cylinder has been studied for a variety of other conditions. As a result of these experiments it has been shown that large effects are produced near the critical region of the Reynolds Number when the air passing near the surface of the cylinder is subjected to disturbance.

From a more fundamental point of view we can never be satisfied until we know more definitely the nature of turbulence; in other words, its cause and the exact manner in which it manifests itself as changes in the air speed, direction, and pressure. We can, as a result of our work along this line, report progress and point out the nature of the difficulties encountered. We believe that we have reliable methods of measuring changes in static pressure, and we have obtained one positive result, namely, that although as shown by measurements with a Taylor yaw-head there seems to be no twist of the air stream produced by the propeller, there is a definite pattern of pressure changes produced by the blades of the propeller and following it in its revolution. The changes in static pressure are of the order of 2 or 3 per cent of the velocity pressure. With impact tubes we have so far not been able to eliminate variations characteristic of the measuring instrument, and on this account the more difficult problem of studying changes of direction by means of a recording yaw meter has not been attacked.

This in brief is a summary of the lines along which we have been working. The following sections describe in detail the more important results obtained.

PART I
FORCE MEASUREMENTS ON CYLINDERS
WIND TUNNEL

The measurements of the resistance of cylinders were carried out in the 54-inch wind tunnel of the Bureau of Standards. This tunnel is of the room return type and consists of a faired entrance 4.3 feet long, a straight section 25.3 feet long, and an exit cone 15.1 feet long. The straight section is of octagonal cross section, the distance between opposite faces being 54 inches. The diameter at the exit end is 9 feet. Two honeycombs are installed within the tunnel, one at each end of the straight section. The front honeycomb is of hexagonal cells, 3.25 inches between opposite faces and 18 inches long. The metal of which the honeycomb is made is 0.03 inch thick. The rear honeycomb is made by piling 12-inch sections of 3-inch sheet-metal tubing against a grid of retaining wires. The experimental station at which the cylinders were placed is 9.6 feet downstream from the front honeycomb.

The room in which the tunnel is centrally located is 68.5 feet long, 28.3 feet wide, 18 feet high. One room honeycomb made up of 1-inch mailing tubes, 4 inches long, piled between retaining screens, is installed in the plane of the propeller.

SPEED MEASUREMENT

Air speeds are ordinarily measured by means of a static plate 4.5 feet upstream from the experimental station, standardized in terms of the readings of a Pitot tube placed at the position to be occupied by the model. When screens are used close to the experimental station, it is usually difficult to obtain a satisfactory calibration because of the nonuniform distribution of velocity across the tunnel. We feel that it is better to measure the average speed ahead of the screen at a place where the speed is nearly constant over the cross section. Since the average speed at all sections of the tunnel must be approximately the same, this procedure gives a close approximation to the average speed at the cylinder. There is one source of error, namely, the possibility that the distribution near the wall may be greatly modified, so that although the average speed over the entire cross section remains constant the average speed over the central part of the tunnel may be changed. The results seem to indicate that this effect is not present to any appreciable extent.

Our standard for speed measurement in the measurements here reported was a Pitot tube mounted on wires 2 feet ahead of the screen, where screens are used, and midway between the axis of the tunnel and the wall. In measurements with no screens present the tube was placed 2 feet 8 inches ahead of the balance axis. Speeds ranged from 20 to 80 feet per second and occasionally to 100 feet per second when the steadiness of the balance permitted.

CYLINDERS

Eight cylinders were used, ranging in diameter from 0.0085 inch to 3 inches. The exact diameters were as follows: 0.0085 inch, 0.063 inch, 0.156 inch, 0.250 inch, 0.500 inch, 0.983 inch, 2.001 inches, and 3.149 inches. The smallest cylinder was a piece of ordinary steel wire; the next four were drill rods, and the last three were pieces of brass tubing. On the curve sheets the cylinders are designated by their approximate diameters 0.0085 inch, $\frac{1}{16}$ inch, $\frac{5}{32}$ inch, $\frac{1}{4}$ inch, $\frac{1}{2}$ inch, 1 inch, 2 inches, 3 inches. The length actually subject to the force of the air stream was about 30 inches, but the conditions approximated those of two-dimensional flow as explained in the section on balances.

SCREENS

Two screens were used as sources of artificial turbulence, one a screen of $\frac{1}{16}$ -inch mesh, the individual wires being 0.011 inch in diameter, the other a screen of $\frac{1}{2}$ -inch mesh, the individ-

ual wires being 0.047 inch in diameter. The $\frac{1}{2}$ -inch mesh screen was formed of wires soldered together and the junction points were somewhat enlarged. The screens were used at two distances, namely, 36 inches and 8 inches from the balance axis.

ARRANGEMENT FOR MEASURING FORCES

The sketch in Figure 1 shows the two methods used for force measurements. In both methods the supports for the wires or cylinders were inclosed within wind shields (see fig. 1), the wind shields being long enough to extend outside the region of reduced speed near the walls. This method of approximating two dimensional flow was used in preference to guards in order that similar methods might be used for all cylinders. Measurements on the 1-inch cylinder mounted in a horizontal position with end guards checked the measurements on the set-up finally adopted within 2 per cent.

In the case of the two smallest cylinders (figs. 1A and 1B) the air force was determined by measuring the deflection. The wires were kept under a known tension by means of a weight applied at the lower end, and end constraints were eliminated by the use of short sections of fine wire at the top support and over a pulley at the bottom. The drag equals eight times the product of tension by deflection at the center, divided by the length if the deflection is small.¹

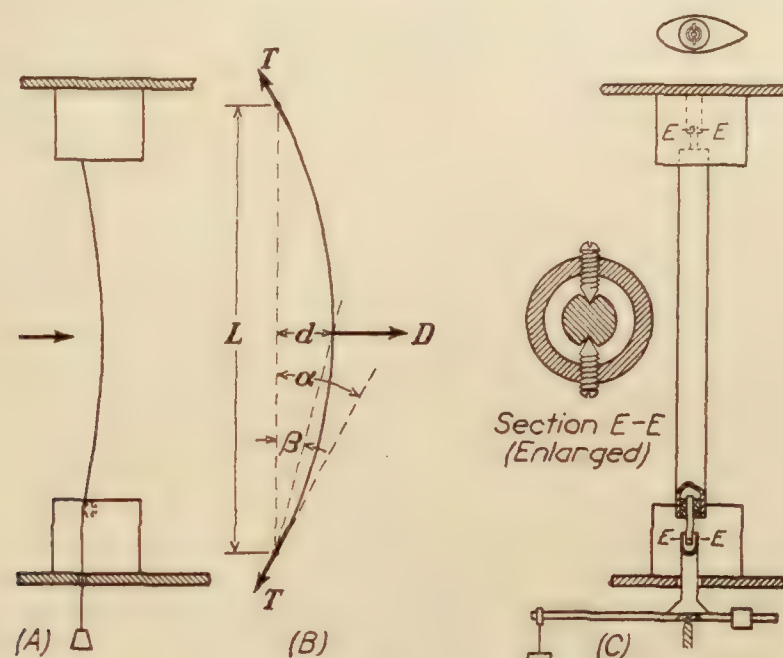


FIG. 1

The larger cylinders were supported from the tunnel roof on two pivot bearings (fig. 1C) in such a manner as to be free to rotate about the line of the pivots in a plane parallel to the wind direction. The lower end was attached to the top of the N. P. L. type balance by a similar connection. Only a part of the force acting on the cylinder is communicated to the balance. Direct calibrations by loads applied horizontally at the centers of the cylinders gave values of the ratio of balance reading to applied load checking the computed value 0.188 within 1 per cent. It was found possible to adjust the sensitivity of the N. P. L. type balance to values satisfactory for the six large cylinders, although the forces varied from about 0.03 pound to over 5 pounds.

¹ In the sketch (fig. 1B) in the condition of equilibrium

$$D = 2T \sin \alpha$$

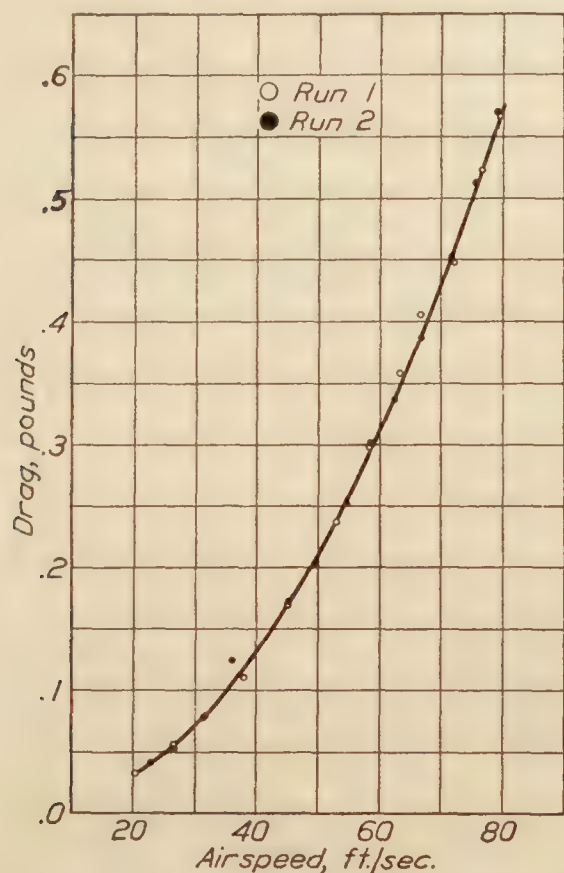
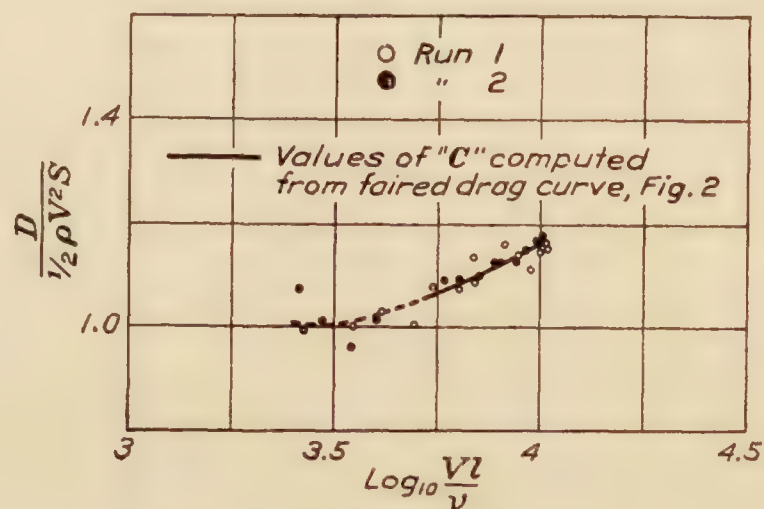
where D is the total drag on the wire, T is the tension, and α the angle of the tangent at the end, made small by using a sufficiently high tension so that $\sin \alpha$ equals α very closely. With a small deflection the wire may be assumed to take a circular form in which case $\alpha = 2\beta$ where $\beta = \frac{d}{L/2}$ d being the deflection at the center and L the chord length. Hence

$$D = \frac{8Td}{L}$$

Closer analysis shows that the term neglected in assuming α small and a circular form is of the order $16 \frac{d^2}{L^2}$ as compared with 1.

RESULTS OF TESTS

The results are expressed in the form of nondimensional coefficients plotted against the common logarithm of the Reynolds Number. The coefficient is defined by the relation $D = CSq$, D being the drag on the cylinder, S the product of cylinder diameter by the length exposed to the wind stream, q the velocity pressure $\frac{1}{2}\rho V^2$ and C the coefficient. The Reynolds Number is defined as $\frac{Vl\rho}{\mu}$ where V is the wind speed, l the cylinder diameter, ρ the density of the air, and μ the viscosity of the air.

FIG. 2.—Resistance of $\frac{1}{4}$ -inch cylinder, open tunnelFIG. 3.— $\frac{1}{4}$ -inch cylinder, open tunnel

The curves shown in Figures 4, 5, 6, and 7 are each computed from average curves representing the force measurements plotted against wind speed. A typical curve of this type is shown in Figure 2. Each individual observation has been represented by plotting the coefficient against the Reynolds Number in Figure 3. It will be noticed that individual observations depart from the mean curve by a maximum of 3 per cent. This is true for all cylinders, and the example shown is typical. Results for speeds below 40 feet per second are less accurate than those for speeds above 40 feet per second and are indicated by dotted curves.

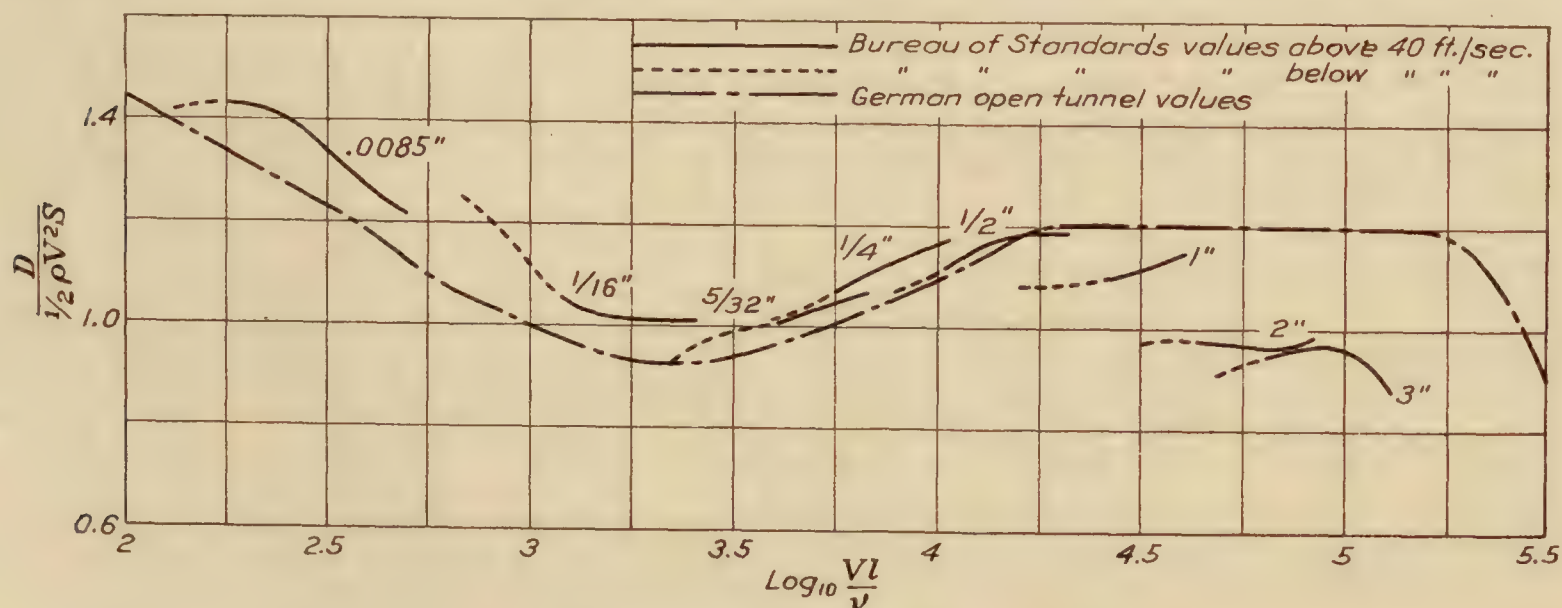
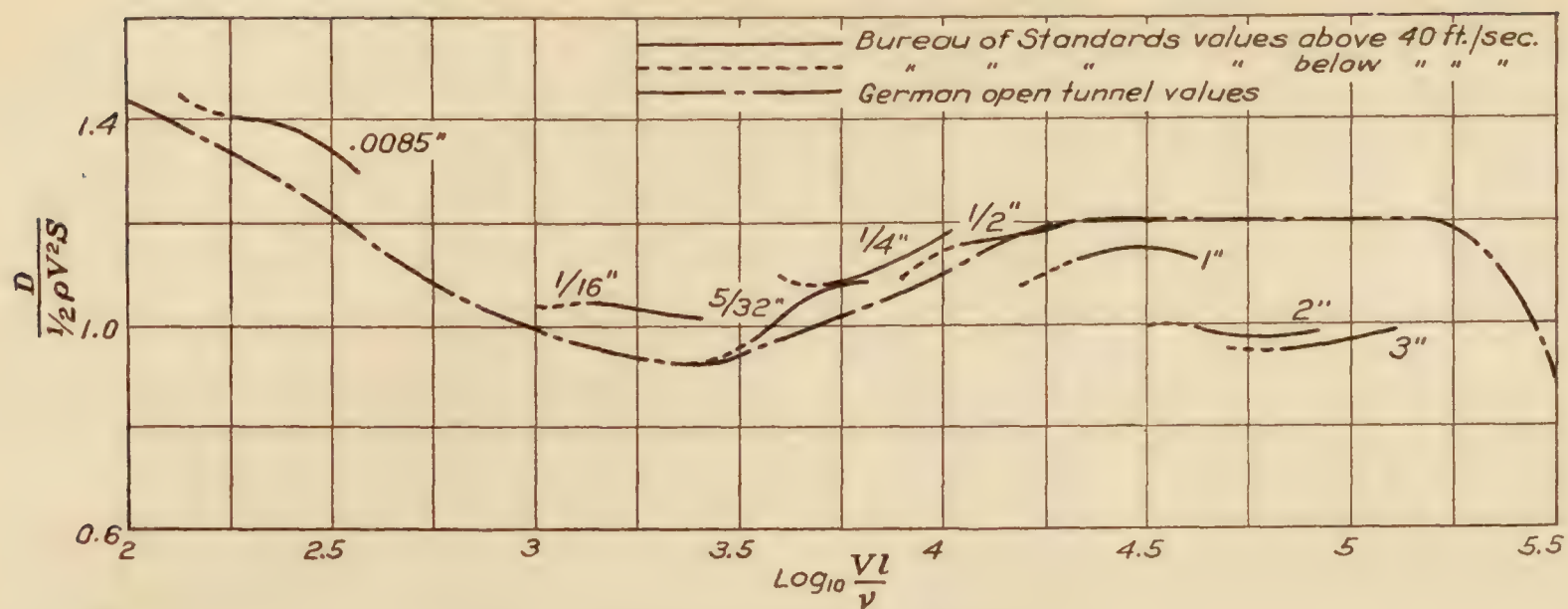
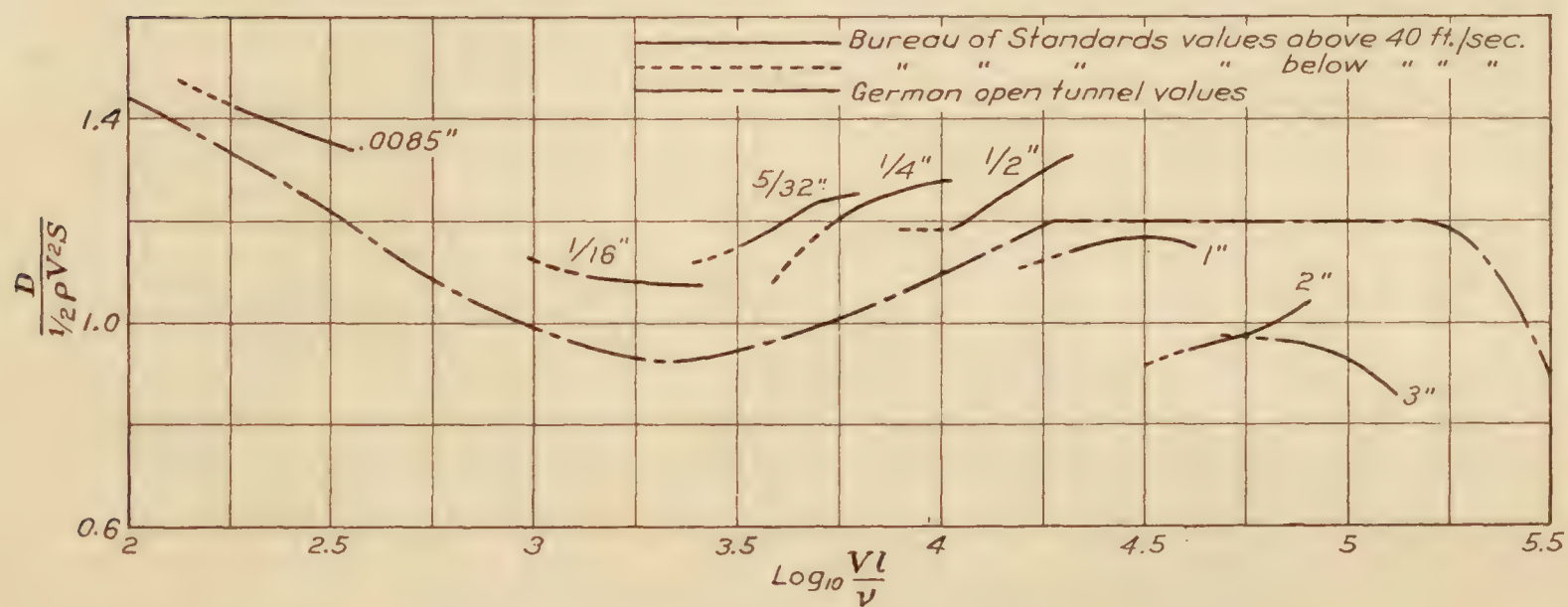
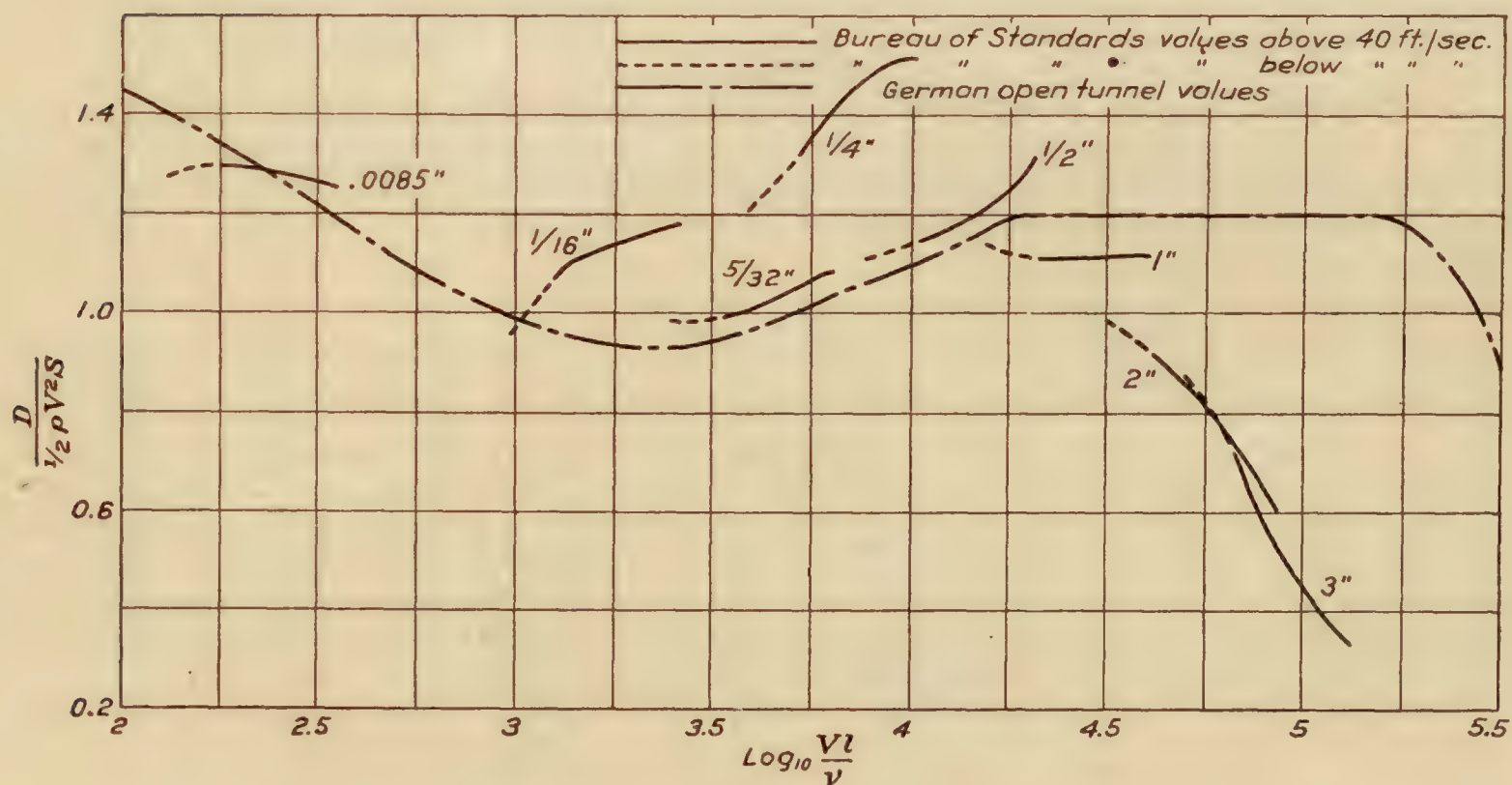


FIG. 4.—Cylinders in open tunnel


 FIG. 5.—Cylinders 3 feet behind $\frac{1}{8}$ -inch mesh screen

 FIG. 6.—Cylinders 8 inches behind $\frac{1}{8}$ -inch mesh screen

 FIG. 7.—Cylinders 8 inches behind $\frac{1}{2}$ -inch mesh screen

The average results for the open tunnel are shown in Figure 4, the curve given by Wieselsberger (Reference 1) being inserted for comparison. A smooth curve could be drawn through our results for the 0.0085-inch, $\frac{1}{16}$ -inch, $\frac{5}{32}$ -inch, and $\frac{1}{4}$ -inch cylinders, lying about 7 per cent higher than Wieselsberger's curve. We shall discuss the reason for this under discussion of the results. The larger cylinders show values falling more and more below this curve, the results being analogous to those obtained previously by one of the authors (Reference 2). It is believed that this is in some way an effect of the tunnel walls. Passing by further discussion for the present, these results are the standards of comparison to be used in discussing the effects of the artificial turbulence produced by the screens.

Figure 5 shows the results with the $\frac{1}{16}$ -inch mesh screen 3 feet ahead of the balance axis. The curves are essentially identical with those for the open tunnel, differing from them by more than 3 per cent at only a few places. The downward trend present in the curve for the 3-inch cylinder in the open tunnel is absent with the screen, but it is doubtful whether this slight change is of any great significance.

When the $\frac{1}{16}$ -inch mesh screen is moved closer to the balance axis the results in Figure 6 are obtained. The 0.0085-inch, 2-inch, and 3-inch cylinders are unaffected. The values for

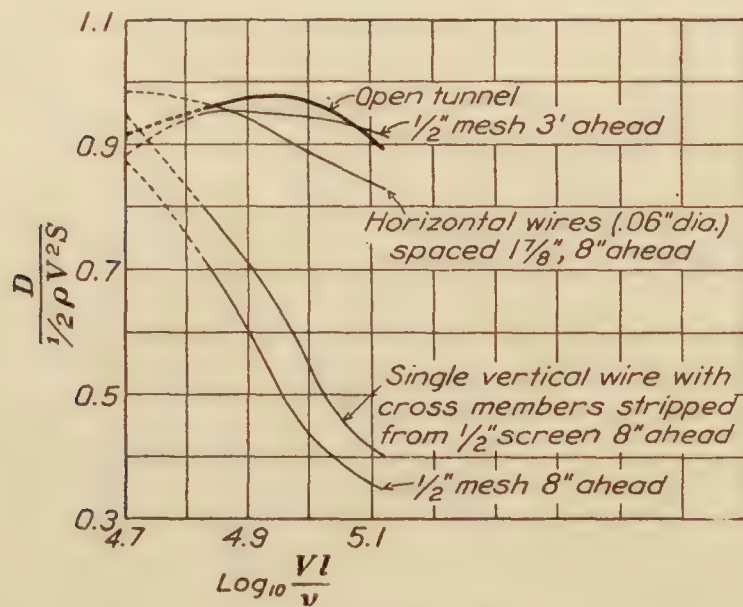


FIG. 8.—3-inch cylinder

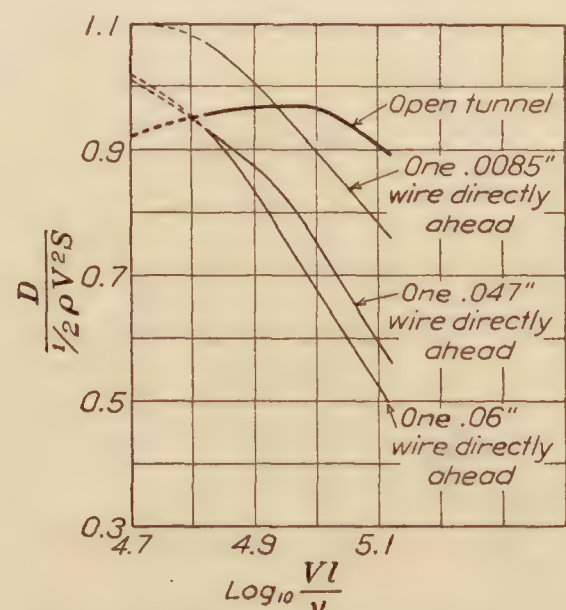


FIG. 9.—3 inch cylinder; wires 8 inches ahead

the other cylinders are higher by about 6 per cent for the $\frac{1}{16}$ -inch and 1-inch cylinders, 8 per cent for the $\frac{1}{2}$ -inch cylinder, 14 per cent for the $\frac{1}{4}$ -inch cylinder, and 20 per cent for the $\frac{5}{32}$ -inch cylinder. We have no explanation for this effect at present.

The results for the $\frac{1}{2}$ -inch mesh screen 8 inches ahead of the balance axis are shown in Figure 7. The $\frac{1}{2}$ -inch and 1-inch cylinders show little effect, the $\frac{1}{4}$ -inch is very high, the $\frac{5}{32}$ -inch shows little effect, the $\frac{1}{16}$ -inch is high, and the 0.0085-inch is low. We believe the erratic nature of the results for the small cylinders to be due to the accidental location of the cylinder with reference to the individual wires of the screen, which are 0.047 inch in diameter. Marked shielding effects probably occur at the distance of 8 inches.

The 2-inch and 3-inch cylinders show coefficients rapidly decreasing as the Reynolds Number increases, indicating that the critical region found by Wieselsberger at a value of $\log_{10} \frac{Vl\rho}{\mu}$ of approximately 5.5 has been shifted to a value of $\log_{10} \frac{Vl\rho}{\mu}$ of approximately 4.7.

A number of experiments were made on the 3-inch cylinder to study the effects of component parts of the screen and of single wires. These results are shown in Figures 8 to 12. Figure 8 shows the effects of a single vertical wire with short sections of the cross members cut from the $\frac{1}{2}$ -inch screen, and of a series of horizontal wires. The curves indicate that the largest part of the effect of the screen may be produced by a single vertical wire.

As a result of this observation a fairly complete study was made of the effects of single wires in various positions. Figure 9 shows the effect of varying the wire diameter, large diameter wires producing the largest effect. At low Reynolds Numbers, however, the wire increases the resistance. Figure 10 shows the results of a traverse along a line perpendicular to the plane of cylinder axis and wind direction. The effect practically disappears when the wire is moved one-half inch from a position directly ahead. Figure 11 shows the results of a longitudinal traverse. The effect is greatest at distances of 8 to 14 inches from the cylinder axis. The decreasing effect at smaller distances is presumably due to the decrease in the intensity of the disturbance in the region of reduced speed near the cylinder. The group of curves indicates that the critical region is shifted when the air passing close to the surface of the cylinder is affected, and if there is no disturbance of this air the effects are small.

Figure 12 shows that similar results are obtained when the boundary layer is disturbed by small projections on the surface of the cylinder and that effects may be produced at distances much greater than 8 inches by increasing the intensity of the disturbance, as, for example, by allowing small tags to flutter in the wind stream.

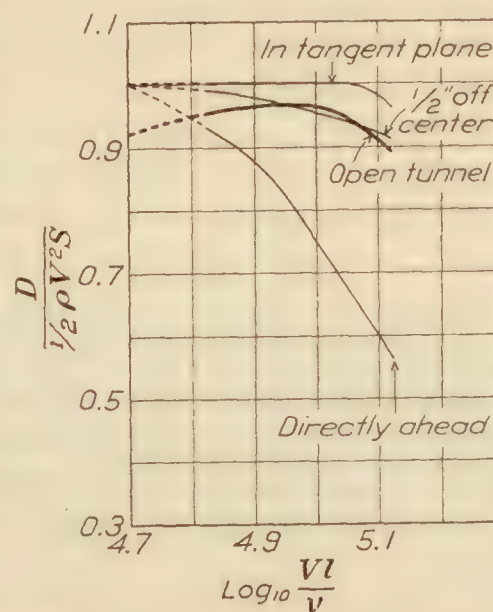


FIG. 10.—3-inch cylinder. Single .047-inch vertical wire 8 inches ahead

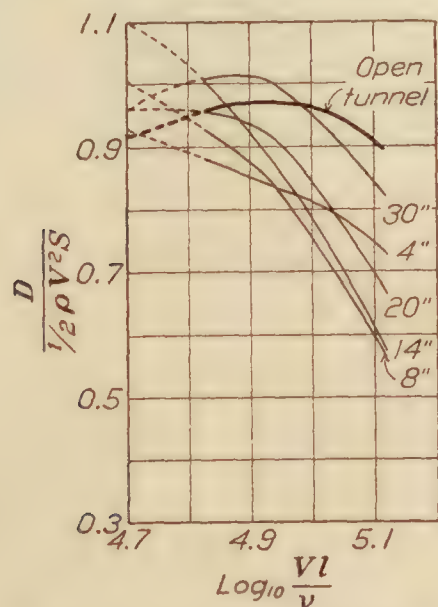


FIG. 11.—3-inch cylinder. Single .047-inch wire directly ahead

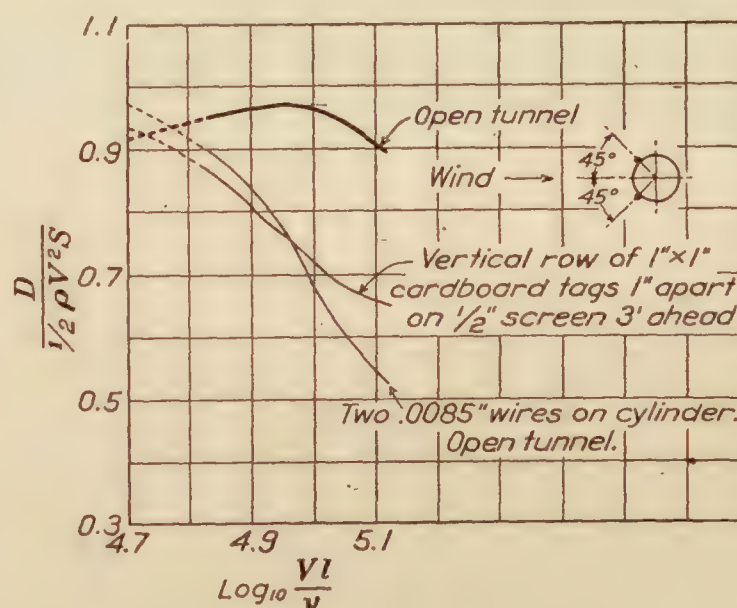


FIG. 12.—3-inch cylinder

DISCUSSION OF THE OBSERVED CYLINDER DRAG

We have called attention to the fact that our results for the smaller cylinders are about 7 per cent higher than those of Wieselsberger. The results of Relf (Reference 3) are in general about 3 per cent higher than those of Wieselsberger. We believe that the differences are due to the differences in the methods used to obtain two-dimensional flow. In Relf's experiments a correction was made for the effect of the ends of the wires by taking the measured force as applying to a wire four diameters shorter than the actual wire tested. For the smallest wires a number of wires were mounted in a rectangular frame, in which case a fairly large correction was necessary for the resistance of the frame, and its effect in modifying the flow is unknown. In Wieselsberger's experiments cylinders less than 0.3-inch in diameter were hung on a long wire from the ceiling of the experimental chamber² and stretched across the air stream, being kept in tension by a weight below. The resistance was computed from the deflection of the system as a pendulum. The length exposed to the stream was somewhat indefinite because of the velocity

² In the Gottingen tunnel the air stream is not inclosed at the experimental chamber.

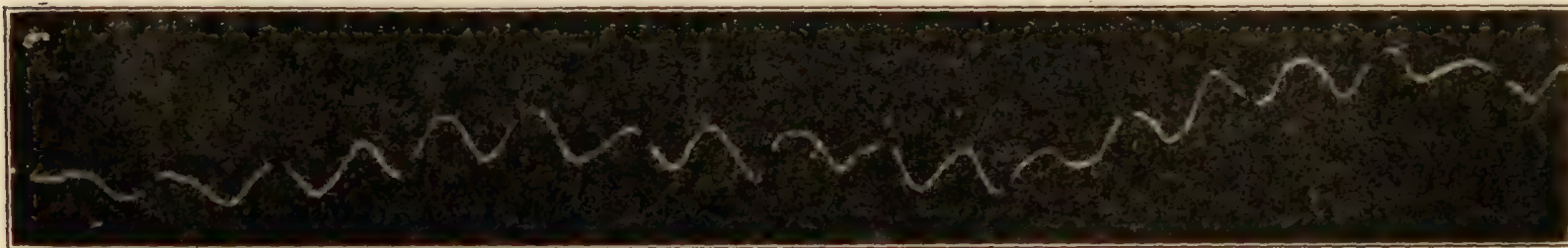
changes near the boundary of the stream. In our own experiments we have shielded the cylinders in the region of decreased velocity near the wall, but there remains the possibility of disturbances due to the wind shields. The resistance of small wires under conditions of two-dimensional flow is therefore uncertain by about ± 3 per cent.

If the models and their mountings were geometrically similar and if there were no effect of the tunnel walls, the values for all the cylinders would be expected to lie on a smooth curve. In the case of the larger cylinders the departures from such a smooth curve are very marked. It is quite possible that the departure is due to an effect of the walls of the tunnel, since the 1-inch cylinder, for example, blocks off about 2 per cent of the tunnel area, but it is difficult to understand why some such effect in the opposite direction was not found in Wieselsberger's experiments in an open-air stream, for he found the law of similarity to hold even when the cylinder occupied as much as 15 per cent of the area of the wind stream. Relf also obtained consistent results when the cylinder diameter was about 3 per cent of the length of the side of his square tunnel, although the ratio of the area occupied by the cylinder to the area of the wind stream was much less because a short cylinder was used.

PART II

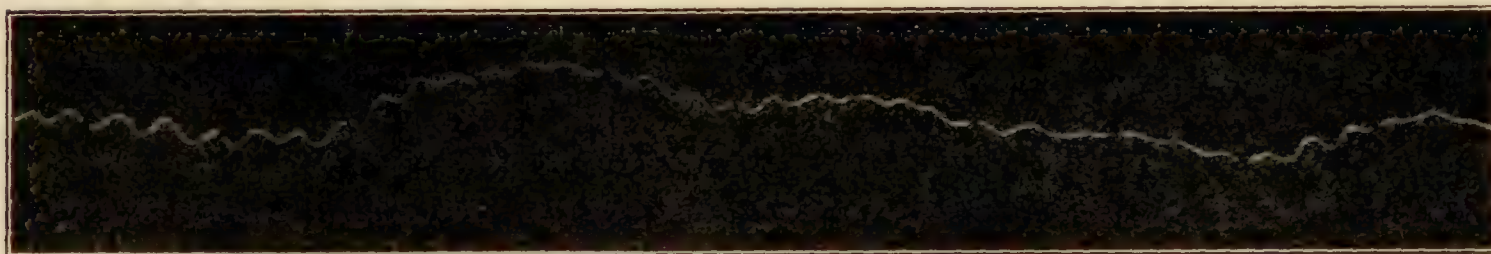
MEASUREMENTS OF EDDY FREQUENCY BEHIND CYLINDERS

It was shown by Karman (Reference 4) that vortices break off fairly regularly behind a circular cylinder in the range of Reynolds Numbers here studied, and the frequency with which they break off has recently been measured by Relf and Simmons (Reference 5). In order to measure the frequency in their experiments, a short platinum wire heated to redness was mounted



A. Pressure variation due to eddies behind 3.15-inch cylinder, no screen Air speed, 65.5 ft./sec. Time between breaks, 0.0296 seconds.
Frequency, 47.3 per second. $\frac{\sim D}{V} = 0.19$

$\text{Log}_{10} R = 5.033$



B. Pressure variation due to eddies behind 3.15-inch cylinder, $\frac{1}{2}$ -inch mesh screen 8 inches ahead. Air speed, 78.2 ft./sec Time between breaks, 0.0308 sec
Frequency, 97.5 per second. $\frac{\sim D}{V} = 0.327$

$\text{Log}_{10} R = 5.11$

FIG. 13

behind the cylinder and the heating circuit coupled by means of a transformer to a circuit in which a string galvanometer was placed. The galvanometer was tuned to resonance with the oscillations of the heating current produced by the velocity changes near the hot wire. The galvanometer was then connected to a single-phase alternator and the speed of rotation of the alternator varied until resonance was again obtained. The alternator speed gave the eddy frequency directly. The most striking feature of their results was the occurrence of a rapid rise in frequency as the critical region of Reynolds Number (where the resistance coefficient falls very rapidly) was reached.

We made a few measurements of eddy frequency to check the occurrence of this rise in frequency when the critical region is artificially displaced, and, as would be expected, found the rise to take place. The experimental arrangement was quite simple. A standard Pitot tube was placed about one diameter behind the cylinder and slightly inside the shadow of the cylinder. The static openings of the Pitot tube were connected to the diaphragm pressure gauge described in Part III of this report and the pressure variations observed photographically. Typical records are shown in Figure 13 A and B, the upper record under conditions of flow corresponding to Reynolds numbers below the critical region, the lower under conditions of flow

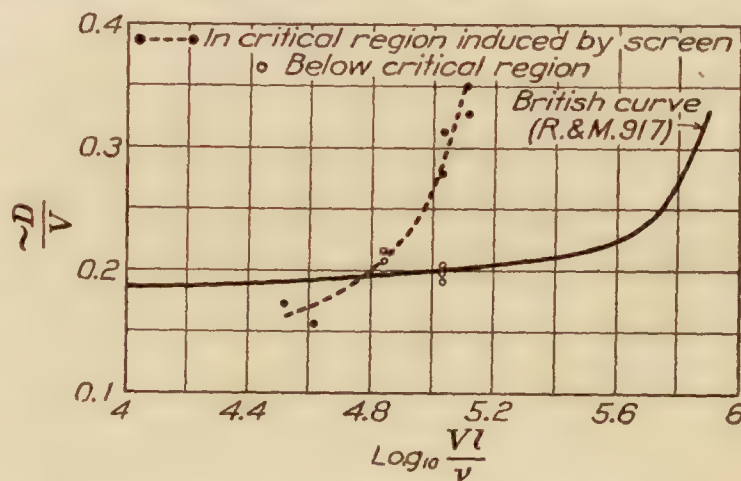


FIG. 14.—Frequency of eddies behind circular cylinders

corresponding to Reynolds Numbers above the critical region, obtained by the use of the $\frac{1}{2}$ -inch-mesh screen 8 inches ahead. The photographic records show that the eddies come off periodically for short-time intervals, but disturbances in the regular course are quite marked, especially when the flow is critical. Figure 14 shows a comparison of our results with those obtained by Relf and Simmons. The points marked as being below the critical region were obtained in the tunnel with the usual honeycombs; those marked as in the critical region, behind the $\frac{1}{2}$ -inch-mesh screen 8 inches ahead. The presence of this screen induces the critical flow at a Reynolds Number lower than normal

PART III

MEASUREMENT OF PRESSURE VARIATIONS

INTRODUCTION

The departures of the air streams of our wind tunnels from the ideal condition of steady and uniform flow, which we group under the name of turbulence, are resolvable ultimately in terms of variations of speed, direction, and static pressure. The direct measurement of turbulence requires the measurement of these variations, a task to which some attention has been given. All of the measurements reduce ultimately to measurements of pressure variations, so that a desirable instrument is a sensitive high-frequency pressure gauge.

The frequencies with which we are concerned are high compared with the frequency of the balance used for force measurements; in other words, of the order of 10 per second and higher. An upper limit is rather hard to fix, but we have attempted to study the range from about 5 per second to 100 per second.

DESCRIPTION OF GAUGE

The fluctuation is rather small, amounting to less than 5 per cent of the velocity pressure; in other words, to less than one-eighth of an inch of water at an air speed of 100 feet per second. The gauge must therefore be rather sensitive, and we have used a diaphragm of rolled aluminum 0.001 inch in thickness and 4 inches in diameter. The motion of the diaphragm is magnified by the arrangement shown in Figure 15. A ribbon attached to the center of the diaphragm passes over a shaft and is kept taut by a spring. The shaft carries a mirror whose motion may be recorded photographically. The necessity for sensitiveness, leading to a system of low stiffness, reduces the natural frequency of the system, but there is no difficulty in obtaining a natural frequency of about 500 per second as shown by actual measurement.

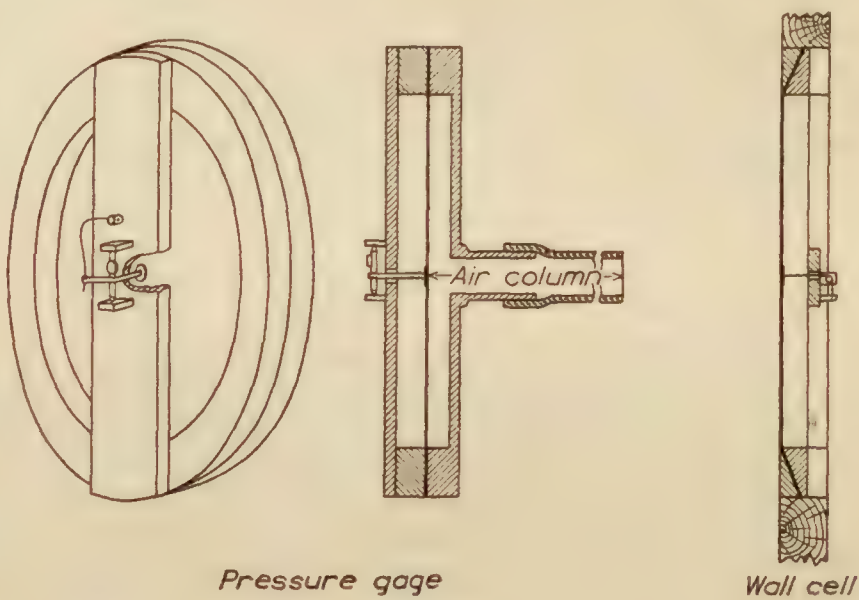


FIG. 15

CHARACTERISTICS OF GAUGE SYSTEM

However, to measure the pressure at the static opening of a Pitot tube, the gauge is necessarily placed some distance away, and a connection must be made by rubber tubing. It was found very early in our work that when $\frac{1}{4}$ -inch tubing was used no disturbance of high frequency was transmitted through the tubing. We were thus led to the use of $\frac{1}{2}$ -inch tubing and in some special experiments to connections of diameter as large as $1\frac{1}{2}$ inches. After many records had been taken in the 54-inch tunnel the equipment was moved to the 10-foot outdoor tunnel and a number of records taken there. The records were so similar in character as to indicate that they were due to the measuring instrument rather than to the tunnel, and further experiment showed that the character of the record depended primarily on the length and diameter of tubing connecting the tube to the gauge.

We had, in some preliminary work, tested the system for resonance by connecting the gauge to a chamber in which a piston was moved back and forth and noting the amplitude shown by the gauge. Further investigation showed that this procedure gave misleading results because of the modification of the end of the air column at the pump. (Fig. 16.) More

reliable results were obtained by inducing the vibration through a T connection, the gauge being connected to the leg of the T, and the pump to one of the arms, the other arm being left open.

By this method the curve shown in figure 17 was obtained. With 39.4 inches of $\frac{1}{2}$ -inch

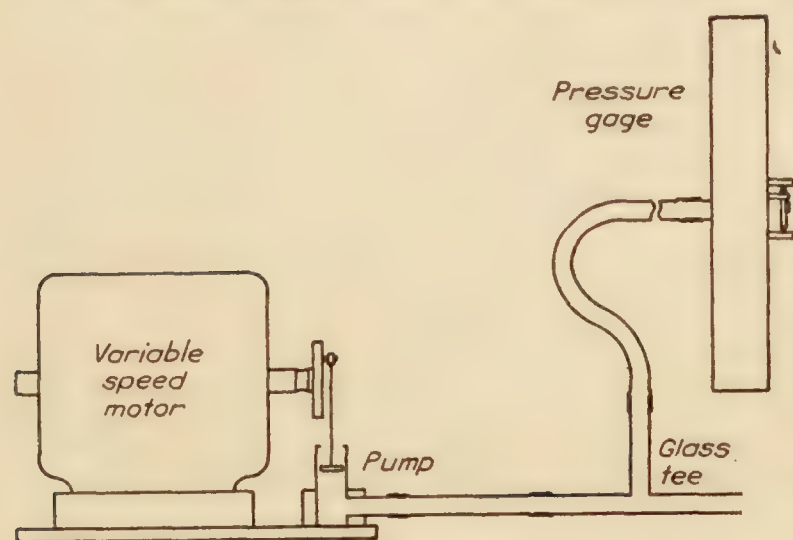


FIG. 16.—Apparatus for measurement of resonance frequencies

tubing the natural frequency of the air column is 20 per second. It will be seen that the frequency varies with the length according to the law

$$\frac{1}{n^2} - \frac{1}{n_0^2} = 0.000064L$$

where $n_0 = 84.6$, n being the frequency and L the length. As nearly as can be judged by ear n_0 is of the order of magnitude of the frequency of the gauge box as a resonator. Our gauge system forms a type of resonator whose frequency depends on the conductance of the outlet (Reference 6), and the conductance in turn is approximately proportional to the re-

ciprocal of the length of the attached tubing, when the length is large in comparison with the diameter of the tubing.

Unfortunately this range of frequency is exactly the range in which we are interested, for the frequency with which a propeller blade passes a fixed point lies within this range for all air speeds. The gauge system, therefore, as a whole is not very suitable for the investigation of disturbances in this frequency range.

Systems of this type have been investigated in some detail by L. F. Simmons and F. C. Johansen at the National Physical Laboratory (Reference 7). A similar variation of resonance frequency with length of tubing was found.

WALL CELL

Having no success in getting a system of satisfactory sensitiveness and high natural frequency we then constructed a gauge suitable for measuring static pressure at the wall of the wind tunnel directly. This consisted (fig. 15) of a diaphragm placed flush with the tunnel wall, the clamping ring being let into the wall so that there were no projections to disturb the flow. The mirror system was arranged as in the other gauge and the diaphragm left without air chambers on either side. We have every reason to believe that this wall cell, as we have called it, gives an accurate reproduction of the changes in static pressure at the wall of the tunnel. Figures 18 A, B, and C show records obtained with this cell. The amplitude shown represents about 2 to 3 per cent of the velocity pressure. The frequencies are as indicated.

The records shown were obtained by reflecting a beam of light from the mirror of the gauge through a lens to a camera. Motion-picture film was used and was moved past the open shutter at a suitable rate. The beam of light was cut off periodically by a sector on the shaft of a motor and the speed of this timing motor observed by a direct connected tachometer.

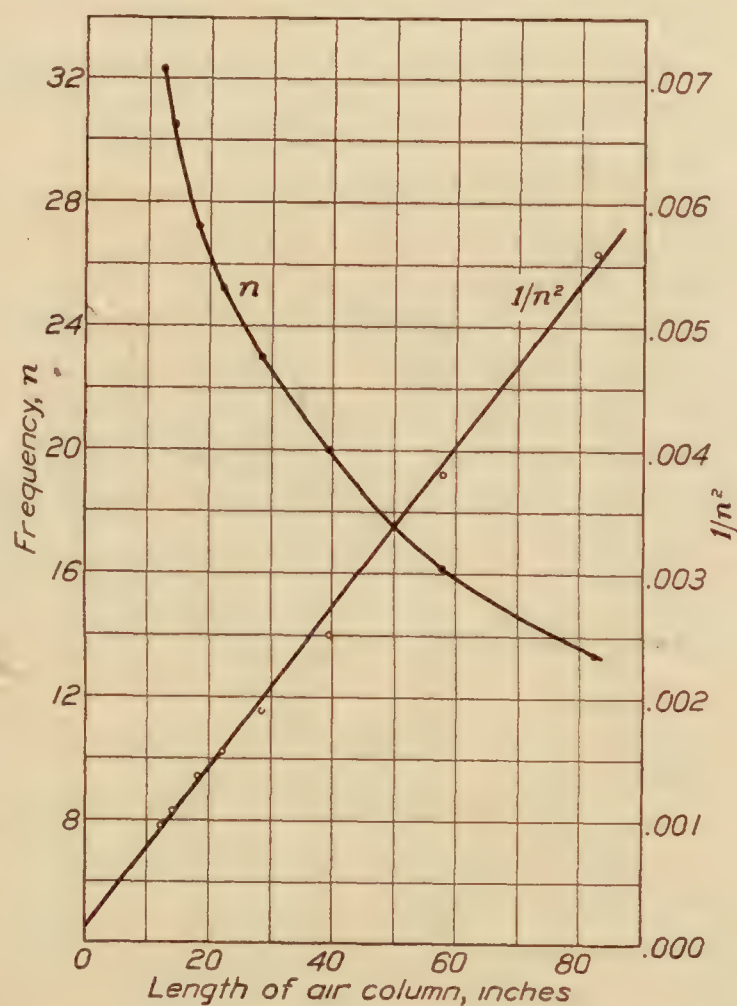
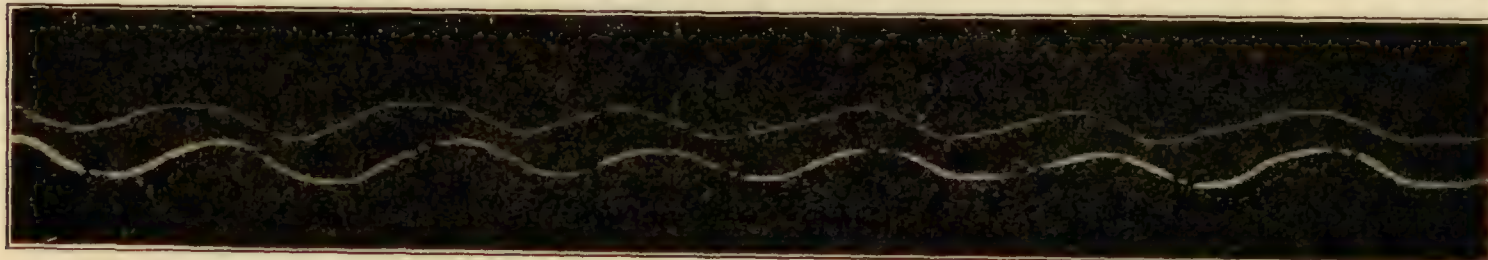


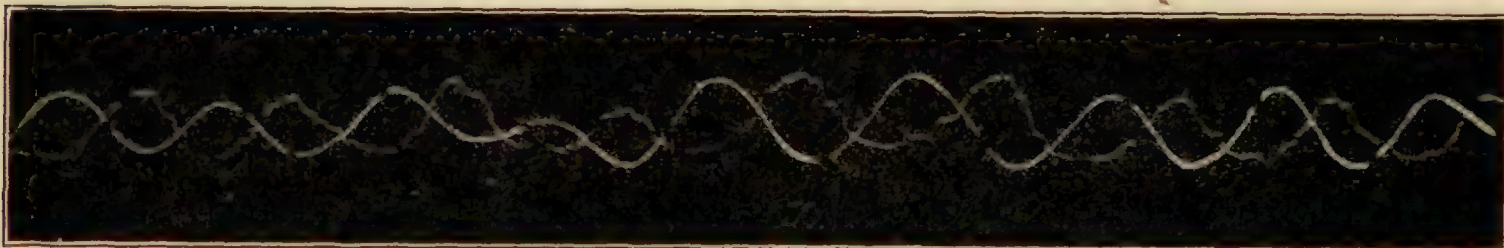
FIG. 17.—Resonance frequencies of gauge and attached tubing

STATIC PLATE RECORDS

The second trace on the records shown in figure 18 was made by a system consisting of the gauge first described connected to a static plate mounted just below the wall cell. A comparison of the records shows the behavior of the gauge system. The predominant frequency observed is that at which a propeller blade passes a fixed point. The four-blade propeller, which draws air through the tunnel, exerts the greatest pull just behind the blades, and each time a blade passes there is an impulse given to the air behind it. These are the impulses recorded. These pressure variations set up forced oscillations in the gauge system, and the



A. Comparison of wall cell (fainter record) and wall plate. Air speed, 40 ft./sec. Time breaks, 0.034 sec. apart. Wind tunnel motor, 300 revolutions per minute. Frequency of blade impulses, 20 per second. Length of air column on wall plate, 19.3 inches; natural frequency, 26.8 per second



B. Comparison of wall cell (fainter record) and wall plate. Air speed, 53.3 ft./sec. Time breaks, 0.03 sec. apart. Wind tunnel motor, 400 revolutions per minute. Frequency of blade impulses, 26.6 per second. Length of air column on wall plate, 19.3 inches; natural frequency, 26.8 per second



C. Comparison of wall cell (fainter record) and wall plate. Air speed, 60 ft./sec. Time breaks, 0.03 sec. apart. Wind tunnel motor, 450 revolutions per minute. Frequency of blade impulses, 30 per second. Length of air column on wall plate 19.3 inches; natural frequency, 26.8 per second.

Note the relative phase change on passing through resonance frequency.

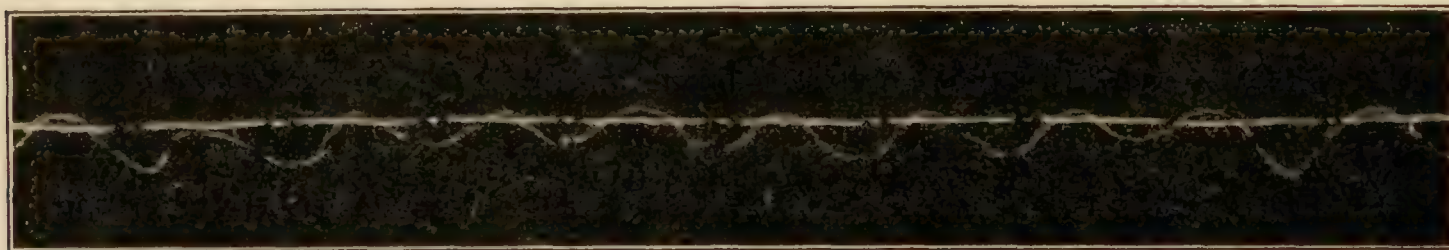
FIG. 18

well-known behavior of such a system near its natural frequency is shown. The gauge system is only one-third as sensitive as the wall-cell system, because of differences in path of the light beams and the presence of an additional reflection in the path of the wall-cell beam, yet the gauge system shows as large an amplitude on the record as the wall cell. Furthermore, when the impressed frequency is lower than the natural frequency of the gauge system the oscillations are in phase; when equal to the natural frequency the records differ in phase by one-quarter period, and when above the natural frequency they are in opposite phase. (Reference 8.) We may remark parenthetically that the small amplitude of the pressure variations produced by eddies, shown on the record in Figure 13, is due to the fact that the eddy frequency is near 100 as compared with a natural frequency of the gauge system of about 10.

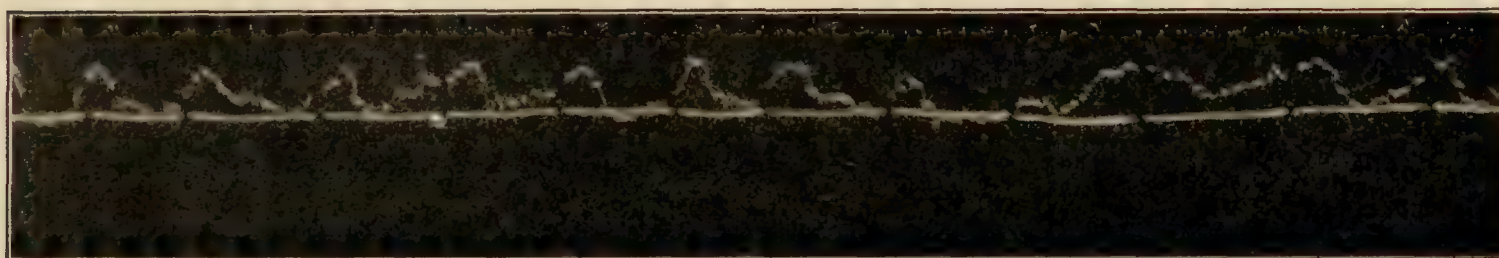
PITOT TUBE RECORDS

When attempts were made to use Pitot tubes placed in the air stream, especially when impact openings were used, a more serious difficulty arose. This was the vibration of the air column with its own natural frequency, induced by the air flow around the tube. When the

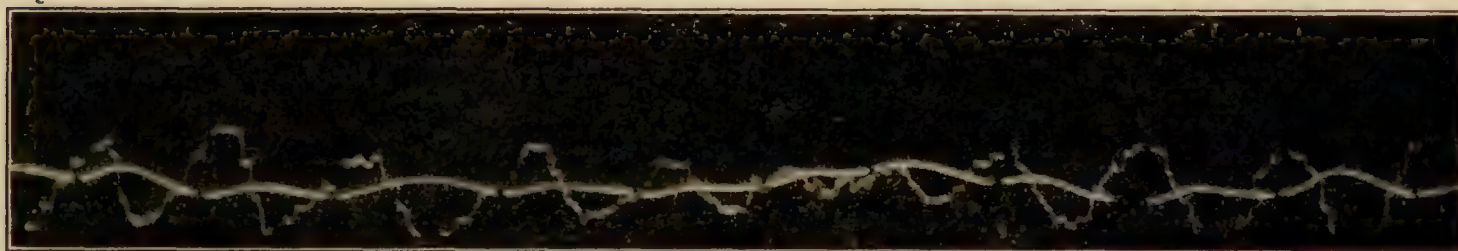
static of the standard Pitot tube is used, the effects were not evident, but as shown in figure 19 A and B nothing of high frequency was transmitted. The damping was large, and the natural frequency very low. When a larger Pitot tube was used with $\frac{1}{2}$ -inch connections, we found at low and moderate speeds the blade impulses coming through, accompanied by an oscillation of frequency near 11 per second. At high speeds this low frequency alone (fig. 19 D) was recorded with very large amplitude. This frequency is lower than that shown by figure 17, probably because of the additional resistance of the small static openings of the tube. We have not as



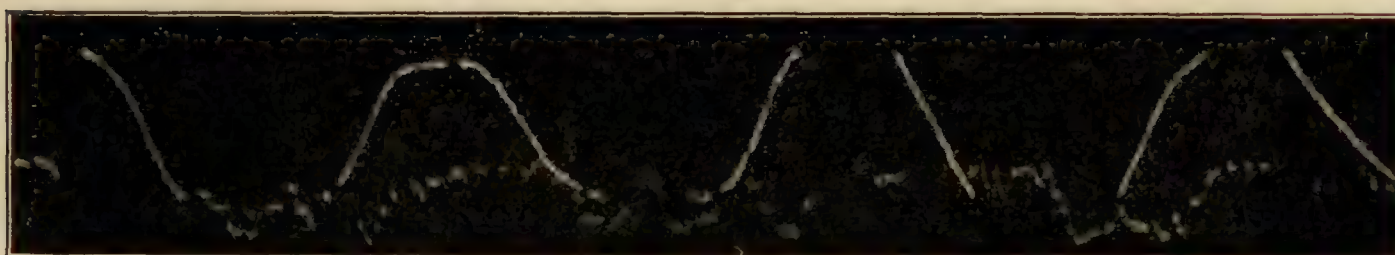
A. Comparison of static of standard Pitot tube and wall cell; 43.3 inches of $\frac{1}{4}$ -inch tubing; 60 ft./sec. Time breaks, 0.034 sec. apart. Wind tunnel motor, 450 revolutions per minute. Frequency of blade impulses, 30 per second. Compare with Fig. 18C



B. Comparison of static of standard Pitot tube and wall cell; 43.3 inches of $\frac{1}{4}$ -inch tubing; 66 ft./sec. Time breaks, 0.03 sec. apart. Wind tunnel motor, 495 revolutions per minute. Frequency of blade impulses, 33 per second



C. Comparison of static of large Pitot tube and wall cell; 43.3 inches of $\frac{1}{2}$ -inch tubing; 66 ft./sec. Time breaks, 0.03 sec. apart. Wind tunnel motor, 495 revolutions per minute. Frequency of blade impulses, 33 per second



D. Comparison of static of large Pitot tube and wall cell; 43.3 inches of $\frac{1}{2}$ -inch tubing; 93 ft./sec. Time breaks, 0.03 sec. apart. Wind tunnel motor, 695 revolutions per minute. Frequency of blade impulses, 46.3 per second

FIG. 19

yet been able to eliminate this oscillation, which entirely masks any pressure variation in the tunnel air stream.

This action is very pronounced even at low speeds when the damping is made small by using an impact opening. There seems to be a valvelike action of the gauge system, an impulse causing air to flow in; the impulse is transmitted to the gauge, reflected, and causes air to flow out. Owing to inertia there is an overshooting and the oscillation builds up and maintains itself.

A careful measurement of the wall cell record shows that there is an oscillation of small amplitude of a frequency of this order of magnitude, but we do not know its source.

SUMMARY

Two methods of making studies of turbulence are described in this report, together with the results of their use in the 54-inch wind tunnel of the Bureau of Standards. The first method consists in measuring the drag of circular cylinders; the second, in measuring the static pressure at some fixed point. Both methods show that the flow is not entirely free from irregularities.

We have shown that the main fluctuations of static pressure in our 54-inch wind tunnel are associated with the unequal driving force over the tunnel mouth. There is a pattern of static pressure changes accompanying the propeller in its revolution. We have pointed out the difficulties encountered in attempting to make measurements by means of a Pitot tube connected to a sensitive gauge.

BIBLIOGRAPHY AND REFERENCES

- Reference 1. *Ergeb. Aerodyn. Versuchsanstalt Gottingen I*, 1923, p. 24.
- Reference 2. Scientific Paper 394. By H. L. Dryden. Bureau of Standards, Sept., 1920.
- Reference 3. British Advisory Committee for Aeronautics, Reports and Memoranda No. 102—Discussion of the Results of Measurements of the Resistance of Wires, with Some Additional Tests on the Resistance of Wires of Small Diameter.
- Reference 4. *Physik. Zeitschrift*, Jan. 15, 1912. Karman.
- Reference 5. British Advisory Committee for Aeronautics, Reports and Memoranda No. 917—The Frequency of the Eddies Generated by the Motion of Circular Cylinders Through a Fluid. By E. F. Relf & L. F. G. Simmons. June, 1924.
- Reference 6. Rayleigh—*Theory of Sound*, chap. 16.
- Reference 7. On the Transmission of Air Waves Through Pipes. L. F. G. Simmons and F. C. Johansen. *Phil. Mag. S. 6*. Vol. 50. No. 297. Sept. 1925.
- Reference 8. Rayleigh—*Theory of Sound*, chap. 3—for mathematical theory.

REPORT No. 232

FUELS FOR HIGH-COMPRESSION ENGINES

By STANWOOD W. SPARROW
Bureau of Standards

REPORT No. 232

FUELS FOR HIGH-COMPRESSION ENGINES

By STANWOOD W. SPARROW ¹

SUMMARY

This report is based very largely on results of tests made at the Bureau of Standards during 1922, 1923, and 1924 under research authorization of the National Advisory Committee for Aeronautics.

From theoretical considerations one would expect an increase in power and thermal efficiency to result from increasing the compression ratio of an internal-combustion engine. In reality it is upon the expansion ratio that the power and thermal efficiency depend, but, since in conventional engines this is equal to the compression ratio, it is generally understood that a change in one ratio is accompanied by an equal change in the other. Tests over a wide range of compression ratios (extending to ratios as high as 14:1) have shown that ordinarily an increase in power and thermal efficiency is obtained as expected provided serious detonation or preignition does not result from the increase in ratio.

There are marked differences between fuels as regards the conditions under which they detonate or preignite. It follows that the employment of a high-compression ratio is contingent upon securing a fuel which is suitable in its resistance to preignition and detonation, and which at the same time possesses the other qualities essential to a satisfactory engine fuel.

This report emphasizes the fact that there may be a difference between a fuel's ability to resist detonation and its ability to resist preignition. Although this report is primarily a general discussion of the properties essential to a satisfactory fuel for high-compression engines, certain fuels, benzol and alcohol in particular, are discussed in some detail.

INTRODUCTION

During the World War the Bureau of Standards conducted an extensive investigation of fuels for aircraft engines. Results were published in Report No. 47 of the National Advisory Committee for Aeronautics entitled "Power Characteristics of Fuels for Aircraft Engines." That this report (No. 47) does not mention detonation or preignition is significant as indicating that at that time the importance of these phenomena was not generally appreciated.

As aviation developed, attempts to use high-compression ratios became more frequent, and in consequence preignition and detonation were encountered more frequently. Ricardo in Great Britain and Midgley in the United States were among the first to draw attention to the seriousness of detonation. The first work at the Bureau of Standards distinctly devoted to fuels for high-compression engines is discussed in Reports 89 and 90 of the National Advisory Committee for Aeronautics. It consisted of tests of two fuels, Alcogas and Hecter, in an aviation engine of 7.2 compression ratio. Subsequently a more general study of fuels for high-compression engines was authorized by the National Advisory Committee for Aeronautics and from time to time the performance of special fuels has been measured for the Bureau of Aeronautics of the Navy Department.

While a single-cylinder engine has been employed extensively in this research, results have been checked frequently by means of multicylinder aviation engines. In some cases the immediate problem has been to select the most suitable fuel for an engine of a given compression ratio, whereas in other cases it has been to determine the best combination of compression ratio

¹ The late S. M. Lee and Messrs. Brooks, Bender, Paul, and Ragsdale have had a major share in the obtaining of the information contained in this report.

and fuel for a given purpose. While the number of fuels investigated has not been large, it is believed that sufficient information has been obtained to form a satisfactory basis for discussing the characteristics of a fuel which determine its suitability for use in high-compression engines.

As already mentioned, the characteristics of a fuel with reference to preignition and detonation are of the utmost importance in determining how high a compression ratio can be used satisfactorily. Hence these two phenomena will be discussed first.

PREIGNITION—DEFINITION AND DESCRIPTION

"Preignition" as used in this paper is defined as ignition from any source prior to the time at which ignition is desired. The term "autoignition" ordinarily is used with reference to an engine such as the Diesel, in which ignition is effected by the generation of heat within the engine cylinder. Preignition usually is a special case of autoignition. If an engine continues to fire after the ignition switches are opened, it is an evidence of autoignition, but not necessarily of preignition. The autoignition may occur when the piston is nearly at top center, somewhat after the time at which the igniting spark would occur in normal operation. The operation of the engine may be uninfluenced by the fact that had the spark not occurred autoignition would have taken place. However, when an engine gives evidence of autoignition, preignition may reasonably be expected to follow as soon as conditions become slightly more severe.

The usual consequences of serious preignition are a decrease in engine power and abnormally high pressures and temperatures of the working fluid. Evidence that preignition is occurring is usually furnished by a decrease in power and high-heat dissipation to the jacket water. Evidence that preignition *has* occurred may be furnished by melted spark-plug electrodes, burned valves, fractured or melted portions of piston heads, etc. Similar effects sometimes result from detonation, as will be discussed later.

WHY PREIGNITION CAUSES HIGH PRESSURES, TEMPERATURES, AND LOSS OF POWER

To understand why preignition causes an increase in maximum temperature two facts should be borne in mind. The first is that the increase in temperature produced by combustion is practically independent of the temperature before combustion, and hence is practically the same regardless of whether the charge is ignited at the normal point in the cycle or earlier, as is the case when the engine preignites. The second is that the ratio between the absolute temperature after compression and that before compression is (1) independent of the temperature before compression and (2) always greater than one. For purposes of illustration, assume

M = increase in mixture temperature due to combustion,

t = mixture temperature at the beginning of compression,

a = ratio between absolute temperatures at end and beginning of compression stroke,

then, in light of the foregoing statements, if combustion occurs at the end of the compression stroke the maximum temperature will be $(at + M)$. If under conditions of severe preignition combustion occurs at the beginning of the compression stroke, then the temperature at the beginning of the compression stroke will be $(t + M)$ and the maximum temperature will be $a(t + M) = at + aM$. In this case the increase in maximum temperature due to preignition will be $(at + aM) - (at + M) = M(a - 1)$. Ordinarily preignition occurs during the compression stroke rather than at the very beginning, and the ratio to which the mixture is compressed after combustion is less than the compression ratio of the engine. The increase in temperature due to preignition will, therefore, depend upon the ratio to which the mixture is compressed after combustion and will be somewhat less than $M(a - 1)$.

Preignition will increase the pressure at the end of the compression stroke in approximately the same ratio that it does the absolute temperature. This is a consequence of the fact that preignition does not alter appreciably the amount of charge which enters the engine in unit time and that at constant volume pressure is directly proportional to the absolute temperature.

The effects of preignition may be small or large, depending upon the severity of the phenomenon. If the preignition is slight the sole consequence may be a small reduction in engine power and economy comparable to what would result from a too far advanced spark. Mild preignition, however, is very apt to develop into that which is severe. A probable sequence of events is as follows: The first occurrence of preignition, even though it is slight, causes an increase in the average temperature of the cycle. This causes the phenomenon to take place earlier in the succeeding cycle. The process continues until eventually the fresh charge is ignited as it enters the cylinder and no power is developed. Figure 1 shows an actual indicator card taken with an engine preigniting. The power developed in the preigniting cylinder was negative, that is to say, a portion of the power developed by the other cylinders was employed in overcoming the resistance which it offered.

CAUSE OF PREIGNITION

Preignition, as contrasted with ignition from an electric spark, is the result of heating a portion of the charge to such a temperature that it ignites. There are many factors which influence the temperature reached by portions of the charge prior to ignition. These include the temperature of the air entering the carburetor, the amount of heat supplied to the charge in its passage to the cylinder, the compression ratio, the amount and temperature of the exhaust gases in the clearance space, and the amount and rate of heat transfer to the charge from various hot portions of the combustion chamber.

In most instances the source of preignition is some portion of the combustion chamber whose temperature normally is much higher than that of other portions of the combustion chamber or of the charge itself. In such cases preignition depends upon the temperature of the hot point, the temperature of the charge, and the rate at which the charge passes the hot point.

There are reasons to believe that slight preignition may often exist without being recognized as such and without causing any appreciable harm. This is possible if the actual amount burned before the charge is ignited from its normal source is sufficiently small. Engine speed may

be important in its effect upon the time available per cycle during which the slight preignition may reach serious proportions. That such is the case is suggested by the fact that engines which operate at normal speeds without any sign of preignition or autoignition will continue to fire after the ignition circuit has been opened and the engine speed has dropped to a very low value. There is no apparent reason why any portion of the combustion chamber under these conditions should be hotter than or even as hot as at normal speed and full load. The probable explanation is that at low speeds the time interval corresponding to a few degrees of crank motion is sufficient to permit a hot portion of the combustion chamber to ignite the charge. At normal engine speeds the time interval corresponding to the same number of degrees might be too short to permit ignition.

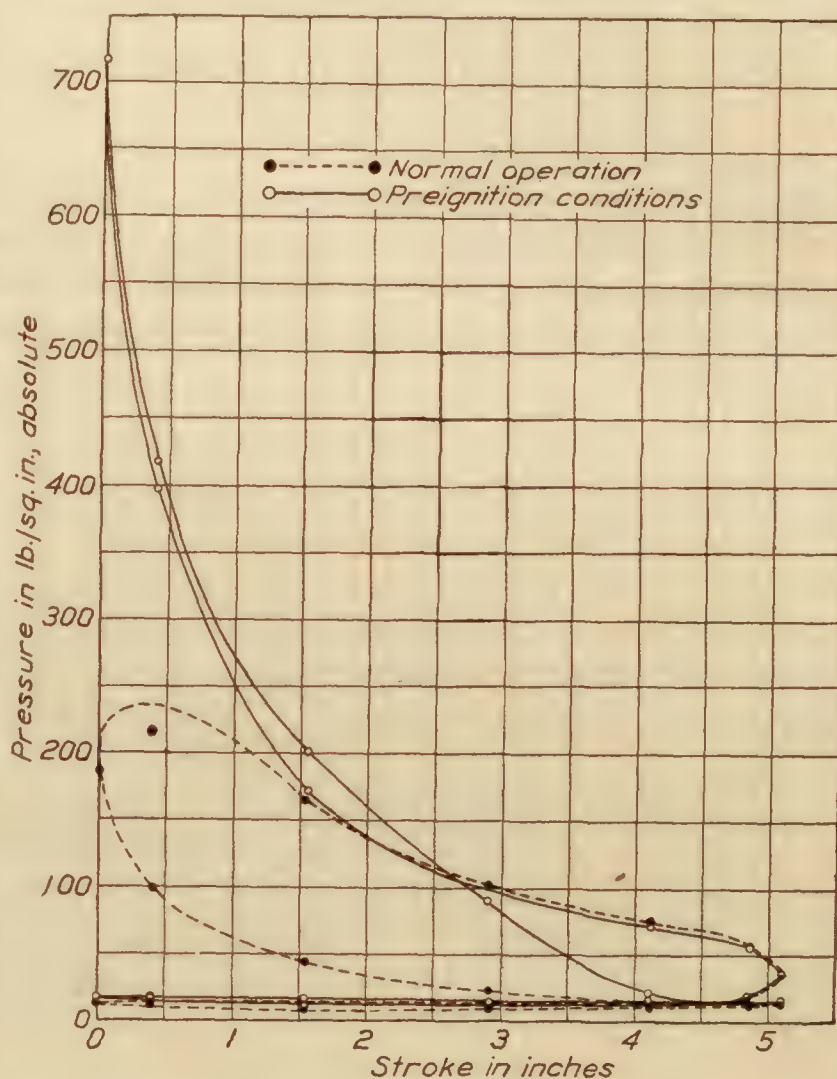


FIG. 1.—Altitude, 7,000 feet. Barometer, 57.8 cm Hg. Compression ratio, 8.3. R. P. M., 1,600

The velocity with which the charge flows to the engine has an influence upon the consequences of preignition. If this velocity is greater than the velocity with which flame is propagated, even though preignition in one cylinder of a multicylinder engine may be so severe that the charge is ignited as it enters, there may be no external evidence other than a loss in power. At lower charge velocities, however, the flame may rush back and cause explosions in manifold and carburetor. Either condition is likely to be encountered in the normal range of engine speeds.

COMPRESSION RATIO AND PREIGNITION ²

It is generally—and in so far as is now known correctly—believed that the likelihood of preignition increases with the compression ratio of an engine. Not all of the changes which accompany an increase in compression ratio, however, increase the engine's tendency to preignite. For this reason an increase in ratio often increases troubles due to preignition to a much less extent than anticipated. As has been shown the ratio between the temperature at the end and at the beginning of the compression stroke increases with increase in ratio. Hence, charge temperatures during the compression stroke are higher the higher the compression ratio. This to be sure increases the tendency for the engine to preignite. On the other hand, because of the decrease in clearance volume with increase in ratio and the decrease in temperature of the exhaust gases, less heating will result from the mixing of the fresh charge with the gases remaining in the clearance space. This tends to decrease the temperature of the charge during the compression stroke and consequently the engine's tendency to preignite. Because of the increase in expansion ratio (expansion and compression ratios are equal in conventional engines) the average temperature during the cycle decreases with increase in compression ratio. Hence, the temperature of spark-plug electrodes, valves, etc., will be correspondingly decreased and likewise the probability that they will cause preignition.

COMPARING FUELS WITH RESPECT TO PREIGNITION

It is not altogether certain by what characteristics of a fuel its tendency to preignite can best be gauged. At present the so-called spontaneous ignition temperatures appear to form the most satisfactory basis for estimating the *relative* ability of various fuels to resist preignition. Spontaneous ignition temperatures, however, can not be taken as indicating the temperatures at which ignition will take place in the engine cylinder and, in fact, values obtained by various investigators differ considerably. This can be attributed to differences in methods of measurement.

A rather brief but nevertheless fairly complete review of work on the spontaneous ignition temperatures of liquid fuels is given by Moore in "The Automobile Engineer" of May, 1920. He defines the temperature of spontaneous ignition as "the temperature at which a substance surrounded by oxygen or air at the same temperature will burst into flame without the application of any spark or other local high temperature." Such a condition may exist when starting an engine of the Diesel type, as the charge in such case is likely to be at a temperature which is nearly uniform throughout and considerably higher than the temperature of surrounding metal parts. In the normal operation of most engines some portion of the combustion chamber is hotter than the charge, so that the condition of "no local high temperature" is not met.³

Moore, in the article previously referred to, discusses the spontaneous ignition temperatures of blended fuels and draws attention to the very interesting condition shown graphically in Figure 2. In this figure, which is typical of all the blends tested by Moore, the spontaneous ignition temperature of the blend is shown to be very nearly the same as that of the constituent which has the lower ignition temperature except when this constituent forms only a small proportion of the blend. The spontaneous ignition temperature then becomes nearly the same as that of the constituent having the higher ignition temperature. This change of spontaneous ignition temperature is brought about by a rather small change of blend proportions. It is rather to be expected that this characteristic will be somewhat less marked in actual engine

² For a more detailed discussion, see Report No. 205 of the National Advisory Committee for Aeronautics, entitled "The Effect of Changes in Compression Ratio upon Engine Performance."

³ See also "The Self-Ignition Temperature of Fuels" by H. T. Tizard. The Automobile Engineer, May, 1923.

operation for the reason that preignition often results from the high temperatures due to detonation and detonation varies much more uniformly with change of blend proportions than do spontaneous ignition temperatures.

At the present time the Bureau of Standards is developing an instrument for use in comparing fuels with respect to preignition. A description of the instrument in its present form will serve to illustrate the objects sought and probable method of use even though the instrument as finally developed may be radically different. As will be noted in the sketch, Figure 3, the instrument consists of a housing which may be screwed into the engine cylinder and plugs of various cross section and lengths which may be clamped in this housing.⁴ Essentially the device is a definite artificially constructed hot spot whose high temperature is attained by exposing a large amount of metal to the burning charge while preventing, so far as is feasible, the conduction of heat from this metal.

There are two general methods by which this instrument may be used in comparing fuels. The first method consists in determining for each fuel which of the various plugs can be used

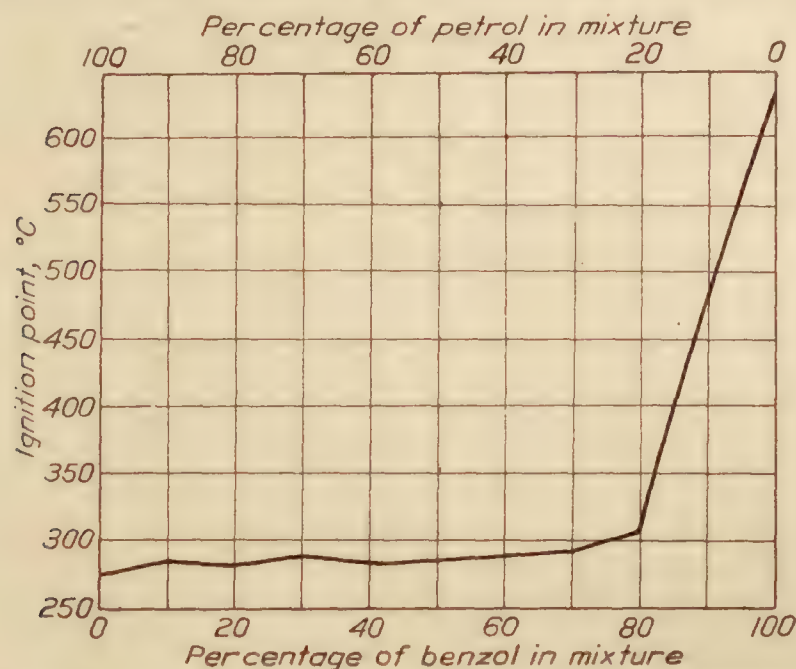


FIG. 2.—Ignition points of mixtures of benzol (crystallizable) and petrol. (From "Spontaneous Ignition-Temperatures of Liquid Fuels" by Harold Moore. "The Automobile Engine," May, 1920.)

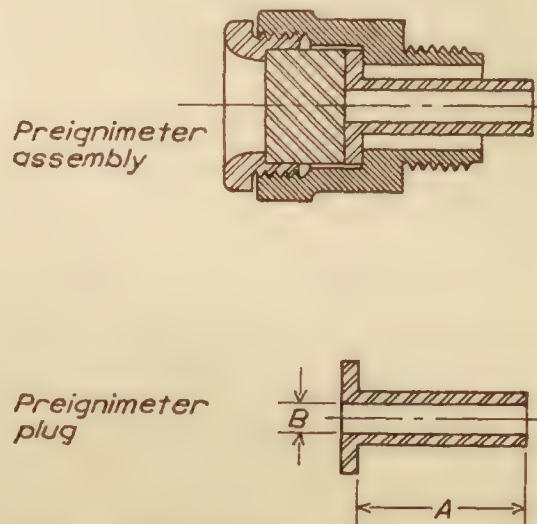


FIG. 3.—(Plugs differing in their tendencies to cause preignition are obtained by varying dimensions A and B.)

without causing preignition. Comparisons are made under certain fixed conditions of engine speed, load, and compression ratio. In the second method the same plug is used with both fuels and the comparison is based upon the relative loads or compression ratios with which satisfactory operation is obtained.

It is to be expected that the relative grouping of fuels as regards preignition will be the same with either method of test. If it is not it suggests that the relative merits of these fuels may not be the same for different types of engines. When fuels are compared on the basis of permissible load or compression ratio but without using a preignimeter, there is no assurance as to what is the hottest portion of the combustion chamber or as to its constancy. The preignimeter to a great extent overcomes this difficulty and should make it possible to obtain measurements of greater reliability.

DETONATION—DEFINITION AND DESCRIPTION

Detonation may be defined as a combustion phenomenon whose best recognized manifestation is the ringing sound which sometimes accompanies a too far advanced spark. In the motor-car engine the noise itself is objectionable, whereas in aviation engines detonation is to be feared because of the extremely high pressure and temperatures which it causes. Serious detonation, aside from its destructive effects, is objectionable in that it results in a decrease in power and an increase in the amount of heat rejected to the jacket water which, in turn, necessitates greater radiator capacity.

⁴ Another possibility is to use a single plug electrically heated. The temperature could then be changed at will and the amount of change could be estimated rather closely from electrical measurements.

DETONATION—METHODS OF MEASUREMENT

Ricardo rates fuels by what he calls "toluene values." He defines the toluene value as "the tendency of a fuel to detonate in terms of its equivalent toluene content, taking standard aromatic free gasoline as having zero toluene value and toluene as having a value of 100." It should be noted that toluene values are not independent of the method of measurement. Ricardo used both a variable compression and a supercharging stratified charge engine. In one instance a toluene value of 28 was obtained with one engine and a value of 18 with the other. For another fuel the value obtained with one engine was 35 and with the other 24. Ricardo made tests of a large number of fuels and assigned to them toluene values. This work is described at length in the *Automobile Engineer* of February to August, 1921, and in *Automotive Industries* of April to September, 1921.

Midgley rates detonation by means of what he terms a "bouncing pin."⁵ The instrument is screwed into the cylinder and is so constructed that a portion of it forms what is essentially a small thin-walled section of the combustion chamber. One end of the bouncing pin rests upon this wall. The pin is so guided that its motion is perpendicular to this wall and motion in this direction is resisted by a spring which when sufficiently deflected closes an electric circuit. As long as the circuit remains closed current flows through a solution of 10 per cent sulphuric acid. As a result gas is evolved and this is collected and measured. The amount of gas evolved in unit time serves as a basis for rating the detonation.

As has been stated, in so far as aviation engines are concerned, the seriousness of detonation lies in its destructive effect. Direct comparisons of this effect have been made by noting the time required to rupture a diaphragm of given thickness when the diaphragm is exposed

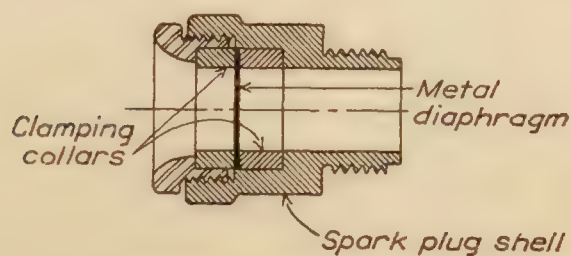


FIG. 4.—Device for comparing maximum pressures

to the pressures in the engine cylinder. The device used at the Bureau of Standards is shown in Figure 4, and is described in Technical Note No. 101 of the National Advisory Committee for Aeronautics. In this device the metal disk which serves as a diaphragm is mounted between two metal washers in a spark-plug shell. The thickness is selected so that when the disk is subjected to the explosion pressure of the engine the exposed

portion will be sheared from the rim in a comparatively short time. Aluminum disks ranging in thickness from 0.010 inch to 0.040 inch have been used for the most part.

Characteristics of fuels with respect to detonation may also be compared by means of an engine having a compression ratio so high that satisfactory full throttle operation is not possible with any of the fuels under comparison. For each fuel the maximum throttle opening at which the engine can operate with no detonation or with no serious detonation is determined and the indicated horsepower developed under these conditions is measured. The comparison of the fuels is based upon the measurements of horsepower thus obtained. It will be noted that this method requires for its application an independent method for determining the presence of detonation or of "serious" detonation.

DIFFICULTIES IN DISTINGUISHING BETWEEN PREIGNITION AND DETONATION

The chief difficulty in measuring preignition and detonation lies in the fact that although these are distinct phenomena each may produce, and often is accompanied by, the other. It is important, however, to distinguish between the two phenomena when rating fuels, as the value of a fuel in one type of engine may be dependent upon its resistance to preignition and in another type upon its resistance to detonation.

Both preignition and detonation are affected by spark advance, fuel-air ratio, and general engine condition. The usual requirement that comparisons be made under the same conditions is applicable, but this does not mean necessarily with the same spark advance or the same fuel-air ratio. It usually means with the fuel-air ratio giving maximum power or some definite

⁵ *Journal of the Society of Automotive Engineers*, January, 1922.

percentage of maximum power and with the spark advance giving the maximum power with this ratio. If there are large differences between the rates of flame spread of two fuels, then there will be large differences in the spark advances at which the two fuels should be compared. This discussion of the difficulties in measuring preignition and detonation has not been introduced with any thought that these difficulties are insurmountable but rather to emphasize the fact that a necessary preliminary to such measurements is often a rather complete series of tests at various throttle openings, fuel-air ratios, and spark advances.

From the foregoing it is evident that the ability of an engine to operate at a certain compression ratio and compression pressure does not prove that another type engine will operate satisfactorily with the same fuel at the same ratio and pressure. Usually, however, if two fuels are compared in engine A and the performance of one of these fuels in engine B is known, it is possible to estimate rather closely the performance of the other fuel in engine B.

Before considering specific fuels it seems advisable to discuss briefly some of the other factors which affect the value of a fuel for use in internal-combustion engines. No attempt will be made to list these factors in the order of their importance as this depends upon the service to which the engine is devoted. Availability, price, calorific value, explosive range, distillation range, latent heat of evaporation, freezing point, separation, viscosity, corrosiveness, specific gravity, chemical composition, and rate of flame propagation are to be discussed.

AVAILABILITY

An aviation engine is to a considerable extent built to "fit" its fuel. Its compression ratio is as high as is considered safe for this particular fuel, its carburetor jets are of the size which will meter the proper amounts of this fuel. It is essential, therefore, that this or a fuel which can be used equally satisfactorily in the same equipment be available wherever the airplane is likely to land.

From a military standpoint it is essential to know to what extent a fuel will be available in time of war. Some European countries import the bulk of their fuel. In the event of war this source of supply might be entirely cut off. Benzol, xylol, and toluol possess desirable antiknock properties, but the objection is frequently raised that in the event of war the output of toluol, at least, might be required for the manufacture of explosives.

PRICE

An airplane permits more rapid transportation than is possible by other means. The higher its speed the more desirable for this purpose it becomes.

Any increase in engine power which does not involve an increase in the over-all weight of the airplane makes possible an increase in speed. Obviously, if one fuel permits an engine to develop more power than another, it will command a much higher price as the cost of fuel is but a small percentage of the total cost of operating an airplane. No argument is necessary as to the value of any changes in fuel characteristics which increase the reliability of the power plant. In the case of a combat airplane differences in fuel characteristics are of the utmost importance. The lack of a few horsepower may cause the death of the pilot and the destruction of the airplane. For these reasons it does not now appear probable that the selection of fuel on the basis of price is likely, except when the fuels under consideration are of nearly equal merit.

CALORIFIC VALUE

Goodenough⁶ defines calorific power as follows: "The union of a combustible with oxygen produces heat, and the heat thus generated when 1 pound of combustible is completely burned is called the heating value or calorific power of the combustible." When not otherwise specified, calorific power is understood to be based on unit weight. It is equally important, however, to know the calorific power of a fuel per unit volume and per unit volume of combustible mixture.

⁶ See Marks' Mechanical Engineers Handbook, footnote on p. 363

For aviation engines it is desirable that the fuel be of high calorific power per unit weight as minimum weight is one of the chief aims of both the engine and airplane designer. High calorific power per unit volume is also desirable as it permits the use of a small fuel tank with a consequent low weight and wind resistance. Probably the most important value, however, is that based on unit volume of combustible mixture. Upon this value the power obtainable from a given engine depends. The fuel ordinarily constitutes a small proportion of the total volume of the charge. As the volume of charge received by the engine in unit time is but slightly dependent upon the fuel used, then it follows that the power developed by the engine will be almost directly proportional to the calorific value of the fuel per unit volume of combustible mixture.⁷ Ricardo, from his investigations,⁸ concluded that the total energy obtainable per unit volume of combustible mixture differs by less than 3 per cent for mixtures of air and hexane, heptane, benzene, toluene, xylene, or ethyl alcohol.

Hydrogen furnishes a rather good illustration of the necessity for specifying whether calorific values are based upon unit weight, unit volume, or unit volume of combustible mixture. The calorific value of hydrogen per pound is nearly three times as great as that of gasoline, whereas the calorific power of a cubic foot of combustible mixture of gasoline and air is between 10 per cent and 20 per cent greater than that of a cubic foot of combustible mixture of hydrogen and air.

EXPLOSIVE RANGE

The term "explosive range" refers to the limits between which the fuel vapor-air mixture is combustible. Narrowing this range increases the difficulty of engine operation. Much of the data which are available on the explosive range of mixtures of gasoline vapor and air have been derived from laboratory experiments with glass bombs in which conditions were considerably different from those which exist in the engine cylinder, both as regards the rate of heat dissipation, turbulence, and amount of inert gas present. Obviously such measurements are not directly applicable to engine operation. It is reasonable to expect, however, that a fuel shown by such tests to possess a greater explosive range than another will have a greater range than the other when used in the engine.

DISTILLATION RANGE

Distillation characteristics of a fuel are ordinarily shown by curves in which temperatures are plotted against "per cent distilled." These curves are valuable as a means of identifying fuels and indicating their suitability for a given type of service.

It is quite generally believed that the more volatile a fuel the more suitable it is for aviation work. To a certain extent this is true, inasmuch as the more readily a fuel vaporizes the more easily is it distributed and prepared for combustion. It is somewhat less generally appreciated that a fuel may be objectionable from the standpoint of being too volatile. The objection to such a fuel arises from the fact that it vaporizes in the carburetor and fuel lines, thus restricting the flow of fuel and interfering with the metering characteristics of the carburetor. This condition is commonly known as "vapor lock." What makes this trouble particularly serious is the difficulty of detecting it. Vapor may form in a fuel line and restrict the flow to such an extent as to cause the performance of the engine to be extremely erratic, and yet this vapor may entirely disappear before an examination of carburetor and fuel lines can be made.

In 1924 the United States Government had two specifications for aviation gasoline. The more volatile fuel was termed "fighting grade" and was intended to be used "as a fuel for fighting airplanes where the highest efficiency is required." The superiority of this fuel to the "domestic grade" for military purposes is questionable in the light of present knowledge as to the seriousness of this trouble from vapor lock. Combat airplanes are capable of climbing very rapidly. As a result there is a considerable reduction in the absolute pressure on the fuel system before

⁷ It is assumed throughout the discussion that the combustible mixture consists of fuel and air. If the mixture consists of fuel and oxygen its calorific value per unit volume of combustible mixture will be much higher.

⁸ See *Automotive Industries*, July 7, 1921. Certain investigators, however, report having found an increase in volumetric efficiency to result from the use of alcohol and they have attributed this increase to the high latent heat of evaporation of the alcohol.

the temperature of the fuel drops in accordance with the low temperatures which prevail at high altitudes. This is the condition most likely to produce trouble from vapor lock and the more volatile the fuel the more easily is such trouble produced.

Extremely high volatility is also undesirable in a fuel because of the resultant waste from evaporation in storage and because of the fire hazard. To minimize the danger from fire repeated attempts have been made to adopt Diesel or other engines using heavy oils instead of gasoline to aviation uses. The ignition temperature of such fuels may be even lower than that of gasoline but the possibility of explosions or of the extremely rapid spread of fire is much less since less vapor is present.

LATENT HEAT OF EVAPORATION

The latent heat of evaporation of a fuel at a given temperature is the amount of heat required to vaporize a unit weight at that temperature. A low latent heat is a desirable characteristic in so far as it reduces the amount of heating of the charge necessary to secure adequate vaporization. Ricardo, in certain experiments with alcohol,⁹ found that power increased as the richness of mixture was increased until the mixture had been enriched to a far greater extent than would appear necessary from the chemical characteristics of the fuel. This he attributed to an increase in volumetric efficiency brought about by the large amount of heat abstracted from the charge in the vaporization of the alcohol. This amount would increase with enrichment of the mixture. This is an instance where high latent heat might be considered of value inasmuch as it permits the development of higher power than would otherwise be possible.

It may be well at this time to mention an extremely undesirable effect which may result from the drop in temperature due to the vaporization which takes place in the intake system of an engine. The effect referred to is the formation of snow. This snow is very apt to collect around the engine throttle although it may cling to any portion of the intake system. Two conditions are necessary for its formation, (1) the air entering the carburetor must contain a considerable amount of moisture, and (2) the vaporization must cause the temperature of the charge or of a portion of the charge to drop below the freezing point of water. Obviously the remedy is to supply sufficient heat to prevent such a temperature drop. An amount of heat equal to the latent heat of evaporation should be adequate for this purpose.

The effect of this snow formation upon engine operation is very serious. It throttles and thus decreases the power of the engine. This may eventually force the airplane to the ground because of insufficient power. When the changes in power take place suddenly, conditions are most serious. This occurs when a considerable quantity of snow collects, and subsequently becomes dislodged due to vibration of the engine, or movement of the throttle, or a change in manifold suction. The effect is that of an uncontrolled and rapidly fluctuating throttle. Needless to say, flight under such conditions is extremely dangerous.

FREEZING POINT

If a fuel freezes at any of the temperatures encountered in normal service, this fact constitutes a serious objection to its use. Most fuels satisfactory in other respects are satisfactory in this also. Benzol is an exception, freezing at temperatures normally prevailing at moderately high altitudes. Fuel sold under the designation "motor benzol" ordinarily contains sufficient toluol to lower the freezing point materially.

SEPARATION

There may be some conditions under which one constituent of a blended fuel separates from the remainder. These will be discussed later in more detail in relation to certain of the more common blends. The merits of a blended fuel disappear when the fuel ceases to be a blend. An unusually serious situation results when one of the constituents of the blend is an anti-knock agent. The use of the fuel from which the antiknock constituent has separated is likely to result not only in poor operation but in engine destruction.

⁹ See *Automotive Industries*, July 7, 1921.

VISCOSITY

So long as a fuel can be metered satisfactorily in the conventional type of carburetor, its actual viscosity is of minor importance. Information should be available, however, as to the extent to which viscosity is affected by temperature and if a change in fuels is to be made the differences in their viscosities should be known. The magnitude of the influence of changes in viscosity upon the rate of fuel flow depends upon the design of the fuel-metering device. If the design is such that viscosity materially affects the rate of fuel flow, then when a change in fuels is made the change in carburetor jet sizes must be governed by the differences in viscosity as well as in the density of the fuel and its combining proportions.

CORROSIVENESS AND TENDENCY TO FORM GUMS

Engine failure is more likely to prove disastrous in the case of the airplane than in other types of automotive transportation. Hence the tendency of a fuel to cause corrosion or to form gums is more objectionable when the fuel is to be used for aviation than when it is to be used for other purposes. Unfortunately some of the fuels which have desirable antiknock characteristics seem to be rather unsatisfactory with respect to corrosiveness and the tendency to form gums. It is believed that in many cases this condition could be remedied by further refining if the demand were sufficient to warrant it.

SPECIFIC GRAVITY

Mention is made of specific gravity merely to call attention to the fact that it is not a reliable indication of the value of a fuel although at one time it was much used for that purpose. Provided the comparison is made between hydrocarbon fuels of the same series an idea as to the relative volatility of such fuels may be obtained from their specific gravities. This is not true when the fuels are not of the same series. Benzol, for example, has a higher specific gravity than the usual grade of motor-car gasoline but it is much more volatile. At the present time distillation data have replaced measurements of specific gravity almost entirely as a means for comparing fuels.

A change of specific gravity will change the metering characteristics of the carburetor. This influence is ordinarily considered in connection with the change of viscosity, which also results from a change of fuel.

CHEMICAL COMPOSITION

By ultimate analysis and other chemical and physical tests it is usually possible to determine the chemical composition of a fuel, its proportion of aromatics, etc. This information may be of scientific interest and is an aid in predicting the fuel's performance. Usually, however, it is easier to measure performance directly than to make a determination of chemical composition. Hence complete chemical analyses are not ordinarily made in the examination of a fuel to determine its suitability for use in high-compression engines. Nevertheless measurements of acidity, unsaturated compounds, and sulphur frequently form a part of acceptance tests.

RATE OF FLAME PROPAGATION

This property has received a great deal of attention at the hands of those studying the properties of fuels. Measurements usually have been made by means of tubes or bombs of the constant pressure or constant volume types. Unquestionably such measurements have furnished a great deal of valuable information as to the nature of combustion and of such phenomena as preignition and detonation. With respect to efficiency, however, Ricardo arrived at the following conclusion: "No fuel has yet been found whose rate of burning is too low to permit of maximum efficiency being obtained in the highest-speed engine yet tested." This statement should not be taken as indicating that the rate of burning never has an appreciable influence on efficiency, for there certainly have been cases where the limit of operating leanness has been that at which the charge was ignited in the manifold by flame rushing back from the cylinder. This occurred because the charge had not been completely burned by the end of the expansion stroke. A more rapid rate of burning would have made possible operation with leaner mixtures and hence better economy.

"MOTOR BENZOL"

Perhaps one of the best known fuels for high-compression engines is "motor benzol," which ordinarily contains not only benzol but also xylol and toluol. This fuel was employed satisfactorily long before its antiknock properties were appreciated or the desirability of such properties understood. Both the Bureau of Aeronautics of the Navy Department and the National Advisory Committee for Aeronautics have supported the tests of this fuel which have been made at the Bureau of Standards. Since the proportions of the various constituents which compose motor benzol are not fixed, the characteristics of each lot of fuel might be expected to be different. Fortunately the properties of the constituents are similar and differences between the products of several refiners proved to be rather small.

The fact that benzol had been used extensively as a fuel for internal-combustion engines rendered unnecessary an examination of all the properties of a fuel which have been mentioned. Hence the following discussion will confine itself very largely to such information as was derived from the above-mentioned study of the suitability of benzol as a fuel for high-compression engines.

In 1923 the question of availability was taken up with the Bureau of Mines and some of the large producers of motor benzol. There was fairly general agreement that at least 50,000,000 gallons of motor benzol were annually available for fuel. Not all of this benzol, however, is as free from corrosive effects as is aviation gasoline. Moreover, the belief is rather widespread that in the event of war the entire production of motor benzol would be required for the manufacture of explosives. At that time a rather careful analysis of the facts seemed to indicate that this fear was not well grounded. Nevertheless it is shared by many who have given considerable thought to the subject. It is undoubtedly true that in the event of war large quantities of toluol would be employed in the manufacture of explosives. If, as a result, the motor benzol available contained less toluol, its freezing point would be higher. This raising of the freezing point would be extremely objectionable in so far as the use of the fuel in aircraft is concerned.

Figure 5 shows some of the results obtained with the single-cylinder engine, indicated mean effective pressures and specific fuel consumptions in pounds per indicated horsepower-hour being plotted against pounds of fuel per hour. The general procedure was to use the single-cylinder engine as far as possible, checking the conclusions by means of tests of multicylinder engines. In most cases the data given in Figure 5 were obtained with blends containing the smallest amount of benzol which would permit satisfactory (free from severe preignition or detonation) operation at the given compression ratio. The curves of Figure 6 are derived from those of Figure 5. The upper curve of specific fuel consumption in Figure 6 is based upon a constant fuel-air ratio, the ratio being approximately that giving maximum power. The lower is based upon a mixture leaned until the power is 99 per cent of maximum. In previous work this 99 per cent value has proved to be a satisfactory basis for comparisons of specific fuel consumption. These curves were plotted originally to show the changes in power and specific fuel consumption which result from changes in compression ratio. They are included in this report as evidence that the fuels used at each ratio were satisfactory in preventing serious preignition and detonation. Had such not been the case the curves probably would have shown abrupt changes in curvature.

Figure 7 shows the percentage of motor benzol required at various compression ratios, based upon the results of this particular group of tests. With another benzol or another type of engine or under different conditions the percentages of benzol required very probably would be different. Nevertheless the figure gives a general idea of the changes in benzol content that are likely to be necessitated by a given change in compression ratio. No attempt was made to use a blend with the 11.5 ratio, but it is evident from the figure that a blend containing a small amount of gasoline would have been satisfactory.

The amount of power developed when using benzol, gasoline, or a blend of the two is very nearly the same, provided there is in no case serious preignition or detonation. One would expect a slight increase in specific fuel consumption with each increase in the benzol content

of the blend inasmuch as the calorific value of motor benzol is somewhat less than that of gasoline. While some of the multicylinder-engine tests have shown tendencies in this direction, the differences have been small. No evidence of this tendency was noted in the single-cylinder engine tests whose results are given in Figures 5, 6, and 7.

From the results of these tests and from such other information as is available it appears that blends of motor benzol and gasoline are reasonably satisfactory with respect to distillation

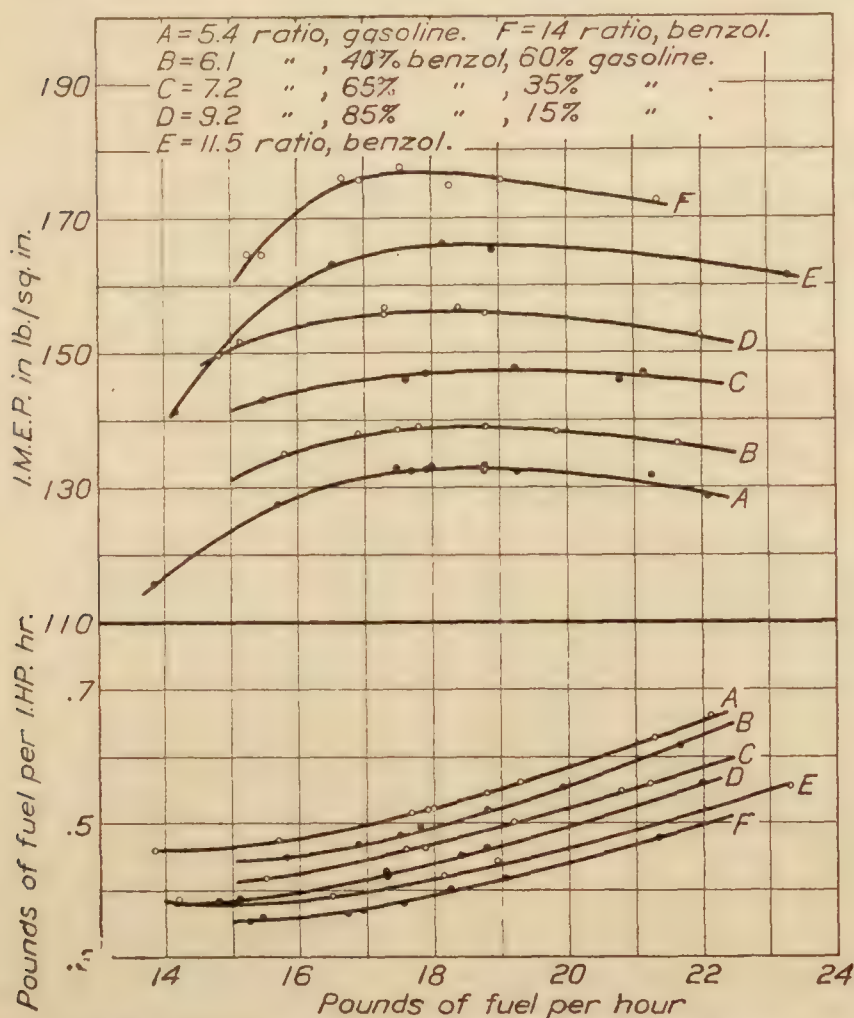


FIG. 5.—Power and fuel consumption at various compression ratios

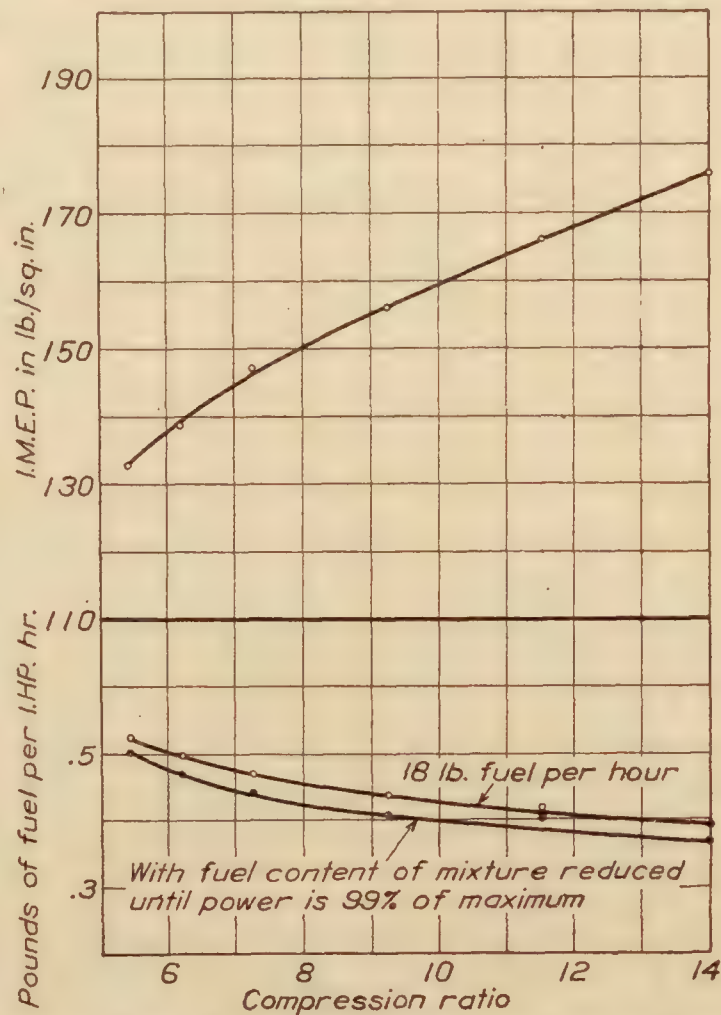


FIG. 6.—Effect of compression ratio on power and fuel consumption (benzol-gasoline blends)

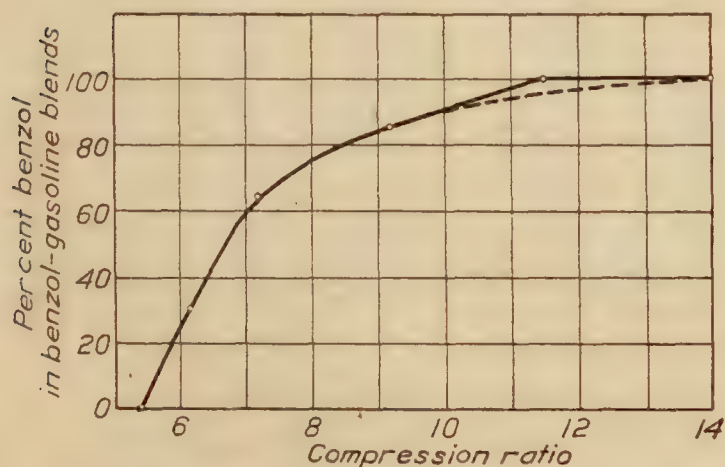


FIG. 7.—Percentages of "Motor Benzol" in benzol-gasoline blends
One-cylinder engine. Bore, 5 inches. Stroke, 7 inches. R. P. M., 1,500. (Percentages will be different for other types of engines.)

range, latent heat of evaporation, viscosity, and rate of flame propagation. Maximum power was obtained with approximately the same spark advance regardless of whether the fuel employed was gasoline, benzol, or a blend of the two. This indicates that under engine conditions the rate of flame propagation is about the same for benzol as for gasoline.

Some of the motor benzol which is now being marketed is less satisfactory from the standpoint of corrosive action than aviation gasoline. This may be due to the lack of sufficient demand for benzol of this quality rather than to any

serious difficulty involved in getting rid of the offending constituents. In this connection it is well to note that benzol is a solvent for certain substances which are unaffected by gasoline. One of the first consequences of its use in a system in which gasoline has been used previously may be to rid the system of certain accumulated deposits. This sometimes clogs fuel lines and carburetor jets and causes the engine operator to believe that the fuel is highly corrosive, whereas the products are in reality the result of the cleaning action of the benzol.

Probably the chief objections to the use of motor benzol or blends of motor benzol and gasoline are that freezing points and separation temperatures are rather high. As these depend

upon the grade of gasoline and the composition of the benzol, measurements made with one lot of motor benzol may not be even approximately correct for another lot, the constituents of which are in different proportions. The following data were obtained from measurements of several blends. Motor benzol A was obtained from a different refiner than motor benzol B. The X gasoline conforms to Government specifications for domestic aviation gasoline and the same grade was used in all the blends.

TABLE 1

40 per cent benzol A; 60 per cent gasoline X: -11° C., slightly milky. -23° C., more milky. -35° C., formation of solid.	40 per cent benzol B; 60 per cent gasoline X: -1° C., milky. -27° C., very milky. -29° C., formation of solid.
30 per cent benzol A; 70 per cent gasoline X: -12° C., slightly milky. -32° C., milky. -42° C., formation of solid.	30 per cent benzol B; 70 per cent gasoline X: +1° C., milky. -34° C., formation of solid.
20 per cent benzol A; 80 per cent gasoline X: -20° C., slightly milky. -45° C., formation of solid.	20 per cent benzol B; 80 per cent gasoline X: -24° C., slightly milky. -43° C., formation of solid.

It is difficult to determine definitely what degree of "miliness" is serious. Certain it is that a pilot would be reluctant to operate under conditions such that the blended fuel gave any indications of being abnormal in appearance or performance.

ETHYL ALCOHOL

The possibility of the extensive use of ethyl alcohol as a fuel for internal-combustion engines has been frequently discussed. Its attractiveness consists in what might be termed its "potential availability." In an emergency it could be produced in practically unlimited quantities, inasmuch as it is not dependent upon an exhaustible source of supply as are petroleum products. Such a course, however, would reduce the amount of food products and its economic soundness is open to question.

It has also been known for a long time that ethyl alcohol can be employed satisfactorily with compression ratios much higher than are permissible with gasoline as a fuel. Its low calorific value and consequent high specific fuel consumption, however, have tended to prevent its adoption for aviation work. Another objection to its use is that starting is more difficult than when gasoline is the fuel. These objections are met to some extent by blending with gasoline, using only as much alcohol as is necessary to give the desired antiknock value. If alcohol is to be blended with gasoline its water content must be very low unless an additional blending agent is used, and until a few years ago the cost of large quantities of alcohol of the desired freedom from water would have been prohibitive.

Figures 8, 9, and 10 show results of tests made at the Bureau of Standards. These received support from the same sources as the benzol tests and were conducted in much the same fashion. Ordinarily the amount of alcohol in the blend was just sufficient to prevent serious detonation. Alcohol alone, however, was used in one group of runs at the 5.4 compression ratio. A comparison of this group of runs with those made with gasoline as a fuel shows the high specific fuel consumption which the use of alcohol entails. Figure 9 is based upon the data given in Figure 8 and shows that a minimum specific fuel consumption is obtained at a compression ratio of about 7. At higher ratios the amount of alcohol which it is necessary to use in the blend in order to obtain satisfactory operation is so great that its low calorific value overbalances the decrease in specific fuel consumption in pounds per horsepower-hour which results from the increase in expansion ratio.¹⁰ It should be observed that the indicated mean effective pressure continues to increase with increase in ratio up to the highest ratio employed. For this reason it might prove desirable for certain classes of service, in short flights, for example, to employ a high-compression ratio and use alcohol as a fuel in spite of the high specific fuel consumption which would be entailed. Before leaving Figure 9 in should be pointed out that this figure

¹⁰ In conventional engines compression ratio and expansion ratio are equal.

does not show the effect of a change in compression ratio alone but this effect superimposed upon the effect of a change in blend proportions. Had alcohol alone been used as fuel there would have been a decrease in specific fuel consumption with each increase in ratio.

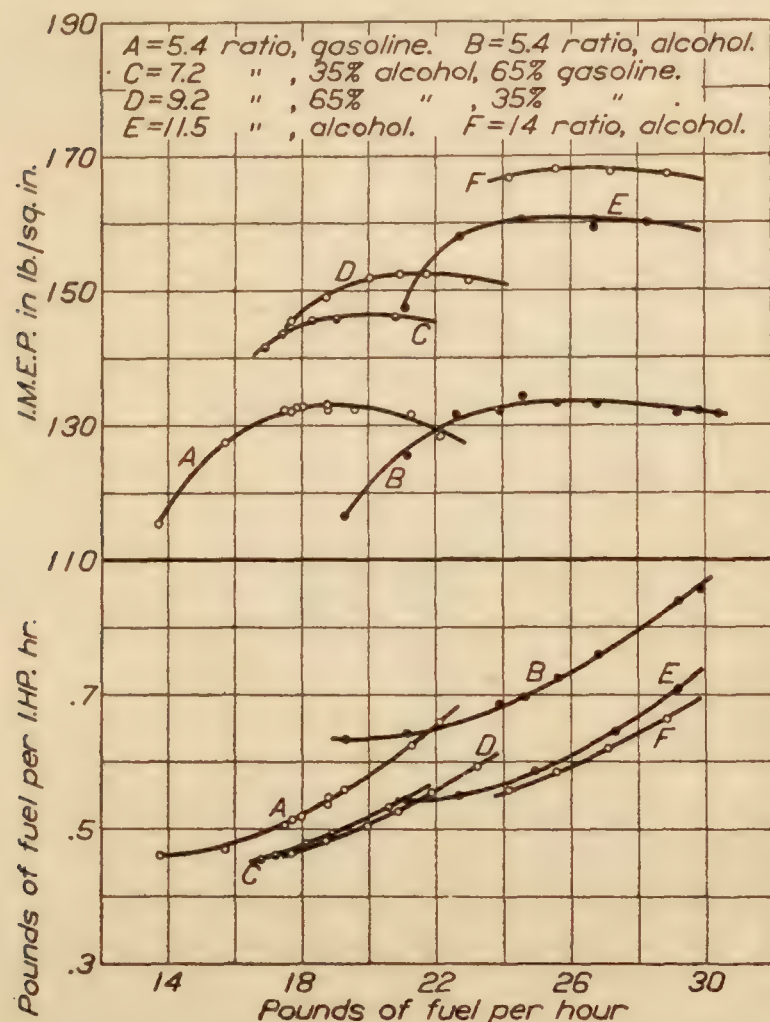


FIG. 8.—Power and fuel consumption at various compression ratios.

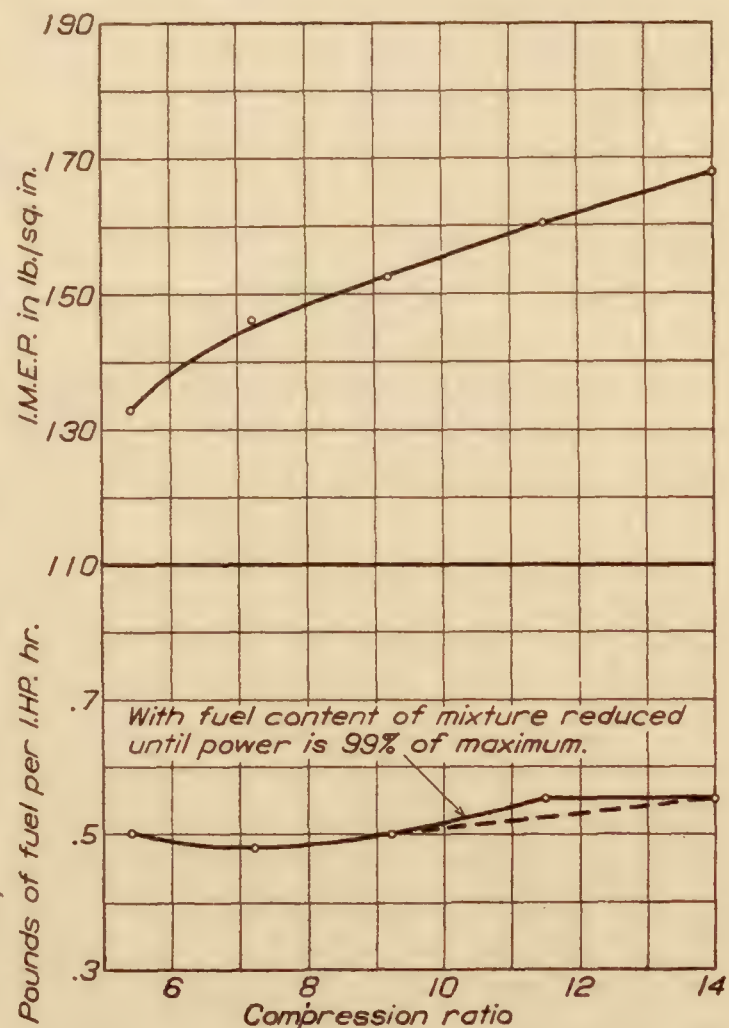


FIG. 9.—Effect of compression ratio on power and fuel consumption (alcohol-gasoline blends). One-cylinder engine. R. P. M., 1,500. Bore, 5 inches. Stroke, 7 inches.

Figure 10 shows the percentages of alcohol required under the conditions of these tests. As was mentioned in the discussion of the benzol-gasoline blends, somewhat different percentages are likely to be required with engines of other types or under different conditions of operation.

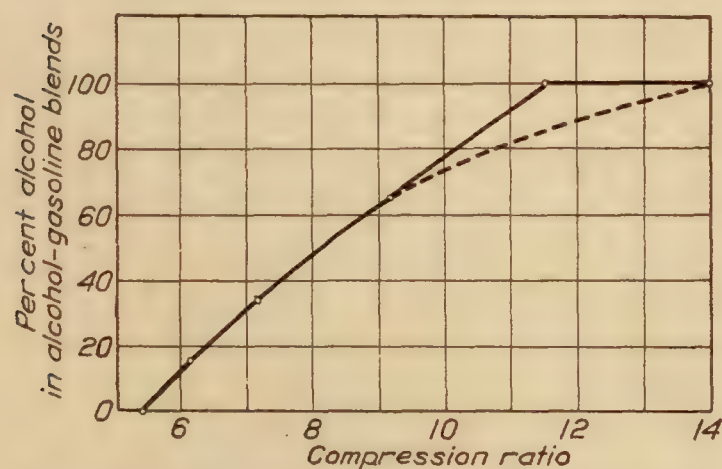


FIG. 10.—Percentage of alcohol in alcohol-gasoline blends. One-cylinder engine. Bore, 5 inches. Stroke, 7 inches. R. P. M., 1,500. (Percentages will be different for other types of engines.)

Nevertheless the figure gives a general idea of the change in alcohol content likely to be necessitated by a given change in ratio.

In these tests some difficulty was experienced in starting the engine when alcohol alone was used as a fuel. This was probably due to the absence of low boiling-point constituents, the boiling point of alcohol being about 78° C. No such difficulty was encountered in the use of the alcohol-gasoline blends and the alcohol itself was entirely satisfactory after the engine had been in operation a few minutes.

Inasmuch as the latent heat of evaporation of alcohol is much higher than that of gasoline, it would probably prove desirable to heat the charge to a greater extent when using alcohol than when using gasoline. Ricardo¹¹ emphasizes the influence which the high latent heat of evaporation has upon the volumetric efficiency of an engine. As has been stated, he found that with alcohol enrichment of the mixture far beyond the point at which maximum power

¹¹ "Recent Research Work on the Internal Combustion Engine," by H. R. Ricardo, Transactions of the Society of Automotive Engineers, vol 17, 1922, part 1, p. 1.

would normally be expected gave an increase in power. This he attributed to an increase of volumetric efficiency brought about by an increase in the amount of heat withdrawn from the charge in the vaporization of the alcohol. No such effect, however, was noted in the tests discussed in this report.

There were no indications of excessive corrosion due to the use of the alcohol, but the tests were not sufficiently extensive to give conclusive evidence in this respect. As is the case with benzol, alcohol acts as a solvent for certain substances not affected by gasoline. When employed in a system previously used for gasoline, foreign matter may be dislodged and clog fuel lines or strainers. This occasionally is attributed to the corrosive action of the alcohol, when in reality it is a result of its cleaning action.

With alcohol a somewhat greater spark advance was required than with aviation gasoline. This would indicate that the ignition velocity of alcohol is somewhat less than that of gasoline. The difference, however, is probably too slight to influence the performance appreciably.

The freezing point of alcohol is below -100°C ., well below any temperature likely to be encountered in flight. With blends of alcohol and gasoline the situation is much less attractive, although these would offer no difficulty if the alcohol were free from water and remained so. Unfortunately, however, alcohol has a strong tendency to absorb water from its surroundings and its miscibility with gasoline decreases with such absorption. After a study of the various factors influencing the stability of gasoline-alcohol-water mixtures, it was concluded that the minimum temperature of complete solubility increases—

- (1) With increasing water content,
- (2) With increasing gasoline content,
- (3) With increasing gravity of gasoline.

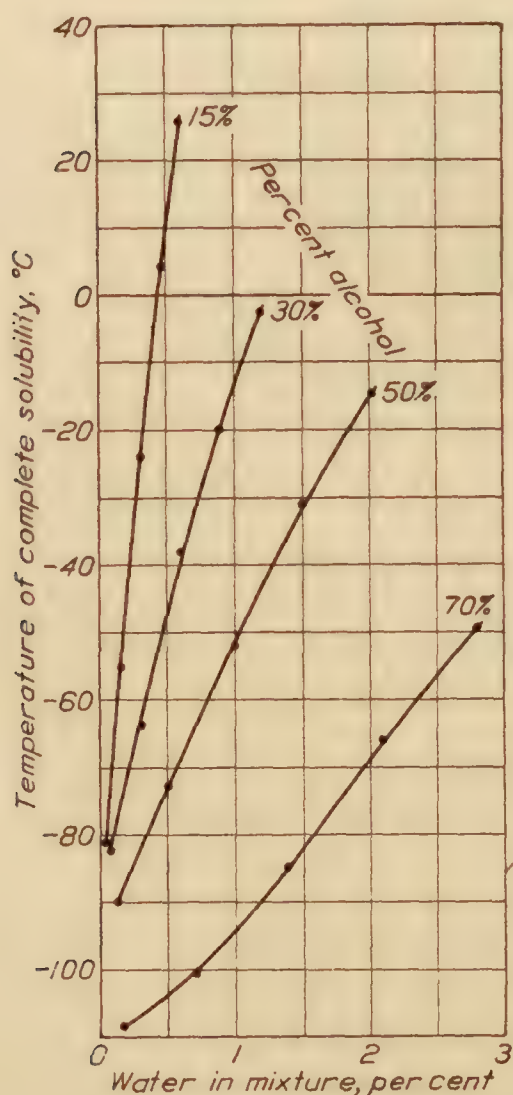


FIG. 11

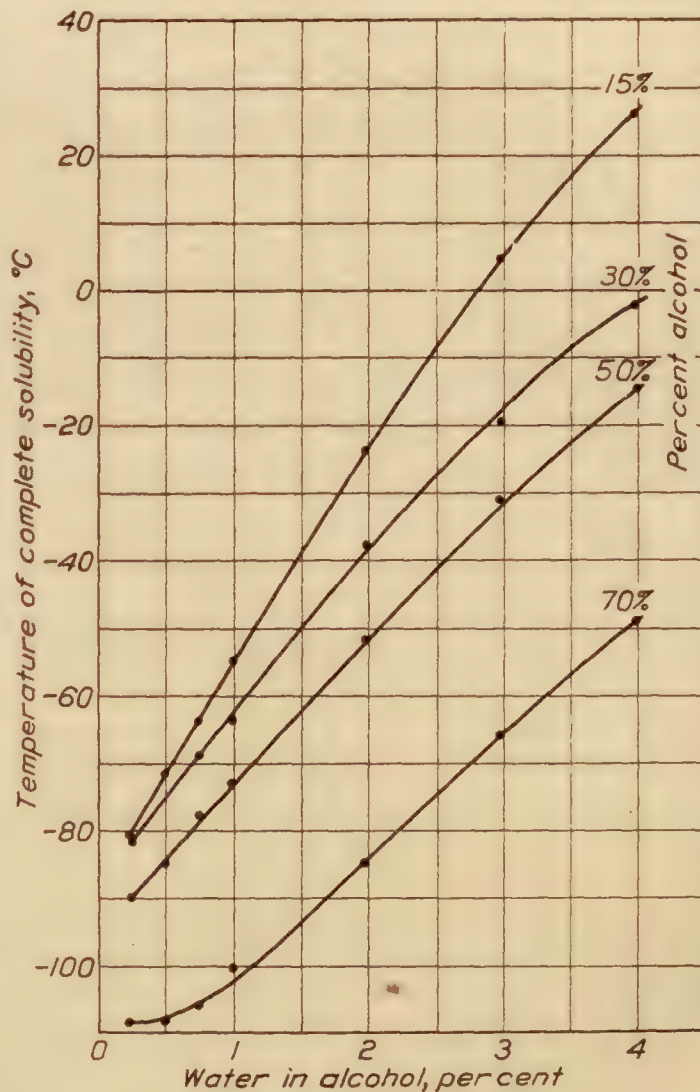


FIG. 12

Solubility curves of alcohol-X gasoline mixtures

Other investigators have found it possible to diminish materially the minimum temperature of complete solubility by adding small percentages of certain substances such as benzol and ether.

Tests on the rate of absorption of water by gasoline-alcohol-water mixtures indicate that this rate increases—

- (1) With decreasing water content of mixture,
- (2) With increasing alcohol content of mixture,
- (3) With increasing humidity.

Results of miscibility tests are shown in Figures 11 and 12. The alcohol as originally received was 99.9 per cent, the gasoline, an aviation gasoline whose distillation characteristics are given in Figure 13. Figures 11 and 12 are both based upon the same data, the abscissæ in one being the percentage of water in the mixture and in the other the percentage of water in the alcohol. Obviously when alcohol-gasoline blends are employed, special precautions should be taken to keep the fuel free from water. This unquestionably is an objection to the use of these blends. If, however, they should be employed extensively it is probable that little difficulty would be experienced in effecting a considerable reduction in the amount of water that ordinarily finds its way into storage and service tanks.

Separation of the blend constituents is most likely to take place at high altitudes because of the low temperatures which prevail there. When separation does take place, alcohol, being the heaviest constituent, will be used first. As the alcohol is the antiknock constituent, serious consequences are likely to result when the airplane reaches low altitudes if the alcohol content of the blend has been reduced. Even at high altitudes considerable difficulty might be experienced in engine operation since for operation with alcohol alone the fuel orifice should be larger than for operation with alcohol-gasoline blends.

SPECIAL ANTIKNOCK CONSTITUENTS

From time to time it has been claimed that material changes in the performance of gasoline would result from the addition of small percentages of certain substances. Very frequently these claims have proved to be unwarranted. It is known, however, that there are certain substances which when added to gasoline materially decrease its tendency to detonate even though they constitute but one or two per cent of the mixture.

Mention of this type of antiknock agent is made primarily to call attention to their apparent decrease in efficacy when it becomes necessary to use them in rather high percentages in order to meet the demands of extremely high-compression ratios. The following table which is based on the work of Midgley,¹² will serve as an illustration:

TABLE 2
ALCOHOL-KEROSENE BLEND

Alcohol, by volume	Kerosene, by volume	Determined equivalent; xylydine in kerosene, by volume
<i>Per cent</i>	<i>Per cent</i>	<i>Per cent</i>
15	85	2.30
25	75	4.60
35	65	7.20
50	50	12.60

The last column shows the percentage of xylydine which must be added to kerosene to give the same antiknock characteristics as are obtained by the addition of the percentages of alcohol which are shown in the left-hand column. One might expect that if 2.30 parts of xylydine gives kerosene the same antiknock value as 15 parts of alcohol, then $\frac{2.30}{15} \times 50$ parts xylydine should give the same antiknock characteristics as 50 parts of alcohol. $\frac{2.30}{15} \times 50 = 7.7$,

¹² Journal of the Society of Automotive Engineers, June, 1922.

whereas the table shows 12.6 parts of xylydine to be necessary. This can be explained partially by the fact that with the alcohol-kerosene blend when the percentage of the knock-suppressing constituent has been increased from 15 to 50, then there is only $\frac{50}{85}$ or 59 per cent as much of the constituent whose knock is to be suppressed. With the xylydine-kerosene mixture there is $\frac{87.3}{97.4}$ or 90 per cent as much of the constituent whose knock is to be suppressed. It is evident that one should guard against overoptimism in estimating the probable performance of an antiknock agent of this type in an engine of extremely high-compression ratio.

One example will serve to illustrate the great value of an antiknock agent of the type described. At the present time most aviation engines employ a compression ratio which permits full throttle operation with aviation gasoline without serious detonation. Occasionally a pilot finds himself where aviation gasoline is not available and is forced to use the grade ordinarily supplied to motor cars. This is likely to result in severe detonation and its consequences may prove serious. It is entirely feasible, however, for the pilot to carry a small amount of one of these very effective antiknock agents and be prepared for such an emergency.

CONCLUSIONS

Much progress has been made in the development of fuels for high-compression engines. In further efforts along this line it should be borne in mind that freedom from detonation does not necessarily give freedom from preignition. It moreover should be realized that, although a fuel possesses satisfactory characteristics from the standpoint of preignition and detonation, it is not a suitable fuel for high-compression engines unless it is satisfactory with respect to the other qualities which have been discussed.

BIBLIOGRAPHY

- Influence of Various Fuels on Engine Performance. By H. R. Ricardo. *The Automobile Engineer*, February, 1921, to August, 1921. *Automotive Industries*, April, 1921, to September, 1921.
- The Character of Various Fuels for Internal-Combustion Engines. By H. T. Tizard and D. R. Pye. *The Automobile Engineer*, February, 1921, to April, 1921.
- Recent Research Work on the Internal-Combustion Engine. By H. R. Ricardo. *Transactions of the Society of Automotive Engineers*, vol. 17, 1922, part 1, page 1.
- Internal-Combustion-Engine Fuels. By C. A. Norman. *Transactions of the Society of Automotive Engineers*, vol. 17, 1922, part 1, page 141.
- Comparison of Alcogas Aviation Fuel with Export Aviation Gasoline. By V. R. Gage, S. W. Sparrow, and D. R. Harper, 3d. Report 89 of National Advisory Committee for Aeronautics, 1920.
- Comparison of Hecter Fuel with Export Aviation Gasoline. By H. C. Dickinson, V. R. Gage, and S. W. Sparrow. Report 90 of National Advisory Committee for Aeronautics, 1920.
- Researches on Alcohol as a Motor Fuel. By H. B. Dixon. Report of Imperial Motor Transport Council, October, 1920.
- Alcohol as Fuel. By J. L. Chaloner. *The Automobile Engineer*, April, 1920.
- Detonation Characteristics of Blended Motor Fuels. By Thomas Midgley, jr., and T. A. Boyd. *Transactions of Society of Automotive Engineers*, vol. 17, 1922, part 2, page 39.

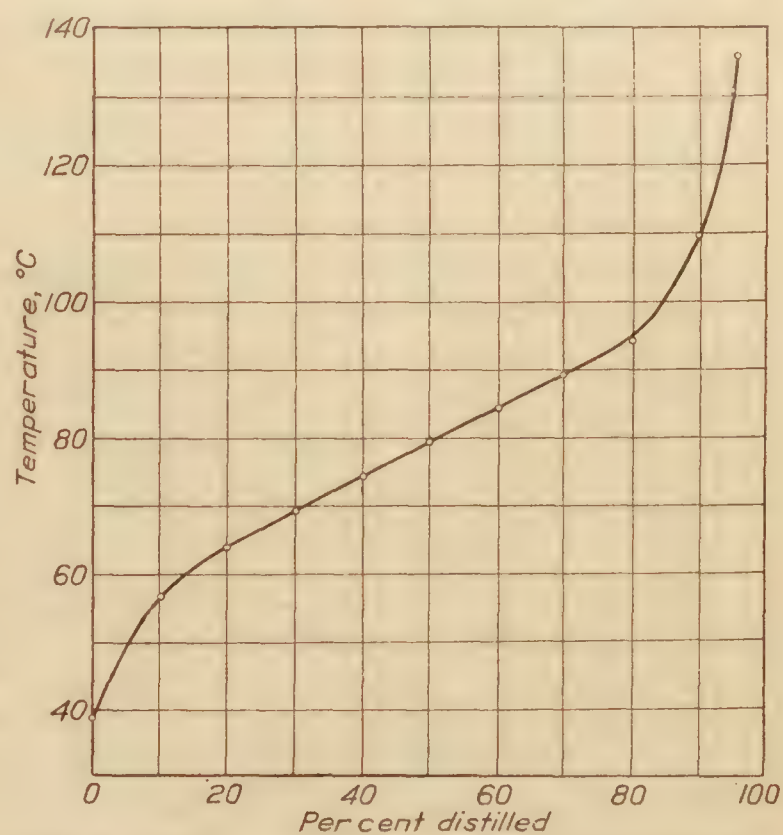


FIG. 13.—Distillation curves of X-gasoline used in alcohol-gasoline solubility tests

- The Problem of Fuel for Aviation Engines. By Prof. Kutzbach. Technical Note No. 62 of National Advisory Committee for Aeronautics, 1921.
- The Problem of Liquid Fuels (for Aircraft Engines). By Prof. Gino Gallo. Technical Memorandum No. 270 of National Advisory Committee for Aeronautics, 1924.
- Fuel for Automotive Apparatus. By E. W. Dean. Transactions of Society of Automotive Engineers, vol. 13, 1918, part 1, page 143.
- The Physical Properties of Motor Fuels. By W. R. Ormandy and E. C. Craven. The Automobile Engineer, March, 1922.
- Spontaneous Ignition Temperatures of Liquid Fuels. By Harold Moore. The Automobile Engineer, May, 1920.
- The Self-Ignition Temperatures of Fuels. By H. T. Tizard. The Automobile Engineer, May, 1923.
- Increase in Maximum Pressures Produced by Preignition in Internal-Combustion Engines. By S. W. Sparrow. Technical Note No. 14 of National Advisory Committee for Aeronautics, 1920.
- Methods of Measuring Detonation in Engines. By Thomas Midgley, jr., and T. A. Boyd. Transactions of Society of Automotive Engineers, vol. 17, 1922, part 1, page 126.
- Comparing Maximum Pressures in Internal-Combustion Engines. By S. W. Sparrow and S. M. Lee. Technical Note No. 101 of National Advisory Committee for Aeronautics, 1922.
- The Background of Detonation. By S. W. Sparrow. Technical Note No. 93 of National Advisory Committee for Aeronautics, 1922.
- Testing Fuels for High-Compression Engines. By S. M. Lee and S. W. Sparrow. Journal of Society of Automotive Engineers, January, 1923.
- The Testing of Motor Fuels. By T. A. Boyd. Automotive Industries, October 13 and 20, 1921.
- The Effect of Changes in Compression Ratio upon Engine Performance. By S. W. Sparrow. Report No. 205 of National Advisory Committee for Aeronautics, 1925.
- The Economical Utilization of Liquid Fuel. By Carl A. Norman. Bulletin No. 19 of Engineering Experiment Station of the Ohio State University, 1921.
- Preignition and Spark Plugs. By S. W. Sparrow. Transactions of Society of Automotive Engineers, vol. 15, 1920, part 1, page 412.
- More Efficient Utilization of Fuel. By C. F. Kettering. Transactions of Society of Automotive Engineers, vol. 14, 1919, part 1, page 201.
- Combustion of Fuels in Internal-Combustion Engines. By C. F. Kettering. Transactions of Society of Automotive Engineers, vol. 15, 1920, part 2, page 453.
- Combustion of Fuels. By Thomas Midgley, jr. Transactions of Society of Automotive Engineers, vol. 15, 1920, part 2, page 659.
- Bureau of Standards Fuel Study. By H. C. Dickinson. Transactions of Society of Automotive Engineers, vol. 16, 1921, part 1, page 111.
- Turbulence. By H. L. Horning. Transactions of Society of Automotive Engineers, vol. 16, 1921, part 2, page 93.
- Elements of Automobile Fuel Economy. By W. S. James. Transactions of Society of Automotive Engineers, vol. 16, 1921, part 2, page 191.
- Condensation Temperatures of Gasoline and Kerosene-Air Mixtures. By Robert E. Wilson and Daniel P. Barnard, 4th. Journal of Society of Automotive Engineers, November, 1921.
- Further Data on the Effective Volatility of Motor Fuels. By Robert E. Wilson and Daniel P. Barnard, 4th. Journal of Society of Automotive Engineers, March, 1923.
- Effect of Doped Fuels on the Fuel System. (From Report of Engineering Div. of Air Service.) Automotive Industries, March 23, 1922.
- Is There Any Available Source of Heat Energy Lighter than Gasoline? By P. Meyer. Technical Note No. 136 of National Advisory Committee for Aeronautics, 1923.
- "Airplane Crashes: Engine Trouble." A Possible Explanation. By S. W. Sparrow. Technical Note No. 55 of National Advisory Committee for Aeronautics, 1921.
- Disturbing Effect of Free Hydrogen on Fuel Combustion in Internal-Combustion Engines. By A. Riedler. Technical Note No. 133 of National Advisory Committee for Aeronautics, 1923.





SMITHSONIAN LIBRARIES



3 9088 01800 8037